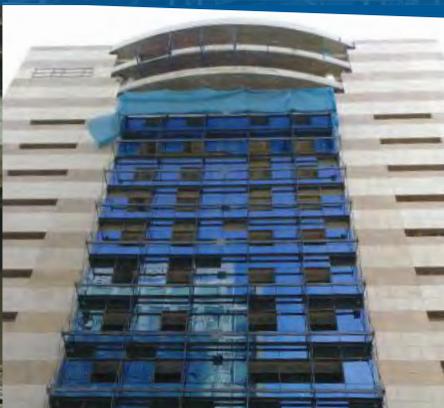# Concrete Buildings in Seismic Regions

George G. Penelis and Gregory G. Penelis

Concrete Buildings in
Seismic Regions

Concrete Buildings in Seismic Regions

George G. Penelis and Gregory G. Penelis

Contents

Preface

This book is addressed primarily to postgraduate students in earthquake engineering and to practising structural engineers specialising in the design of R/C seismic-resistant buildings.

The following basic aims have guided the composition of the material of this book:

1. The presentation of the content should be characterised by integrity, clarity and simplicity, particularly for the design procedure of new R/C buildings or assessment and retrofitting of existing ones. In this respect it should constitute integrated knowledge for a student. The long experience of the first of the authors in teaching undergraduate and postgraduate students about R/C earthquake-resistant structures augurs well for the achievement of this aim.

2. The presentation of the scientific background of each subject should be made in a concise form with all the necessary—but at the same time, limited—references to the sources so that enough of an open field is available for a rigorous and systematic approach to the implementation of the scientific background in design procedure. In this context, this book would be valuable for practising engineers who want to have in-depth knowledge of the background on which the code rules are based. The extensive experience of both authors in the seismic design of new R/C buildings and in the assessment and retrofitting of existing ones, together with the wide experience of the first in posts of responsibility in seismic risk management in Greece, contribute to a balanced merging of the scientific background with practical design issues. At the same time, the numerical examples that are interspersed in the various chapters also intend to serve this aim.

3. For furtherance of the above aims, all of the material of the book has been adjusted to fit a modern Seismic Code of broad application, namely, EN1998/2004-5 (EC8/2004-5), so that quantitative values useful for the practice are presented. At the same time, comparative references are made to the American Standards in effect for seismic design. It is obvious that this choice covers the design requirements for Europe. At the same time, the comparative references to the American Standards enable an easy adjustment of the content to the American framework of codes.

In closing, we express our thanks to the following collaborators for their contributions to the preparation of this book.

- *Professor Andreas Kappos*, co-author with G. Penelis of the book titled, *Earthquake Resistant Concrete Structures* (1997). We are grateful for his consent to reproduce a number of illustrations and some parts of the text from the abovementioned book.
- *Dr. Georgia Thermou,* lecturer in engineering at AUTH and *John Papargyriou* MSc-DIC for their contributions in the elaboration of the numerical examples.

- *Dr. Phil Holland* for correction and improvement of the language of the text.
- *Panayiotis Savas* for the elaboration of the figures.
- *Evaggelia Dara* for the typewritten preparation of the text.
- *Dr. Kostas Paschalidis* for the critical reading and correction of the text.
- *Tony Moore*, senior editor of Spon Press for his efforts in coordinating the publication of the book.

George Gr. Penelis
Gregory G. Penelis

Abbreviations

ACI	American Concrete Institute
ADRS	Acceleration Displacement Response Spectra
AEL	Annualised Earthquake Loss
AELR	Annualised Earthquake Loss Ratio
AFRP	Aramid Fibres
ASCE	American Society of Civil Engineers
ATC	Applied Technology Council
AUTH	Aristotle University of Thessaloniki
B/C	Benefit/Cost
BI	Bilinear Form
BTM	Building Typology Matrix
CEB	Comité Euro-International du Béton
CEN	European Committee for Standardization
CF	Confidence Factor
CFRP	Carbon Fibres
CQC	Complete Quadratic Combination
DBD	Displacement-Based Design
DCH	Ductility Class High
DCL	Ductility Class Low
DCM	Ductility Class Medium
DDBD	Direct Displacement-Based Design
DIN	Deutsches Institut für Normung
DL	Damage Limitation
DLS	Damage Limitation State
DPM	Damage Probability Matrix
DSA	Design Seismic Action
DT	Destructive Test
EERI	Earthquake Engineering Research Institute
ELOT	Greek Organization for Standardization
EMS-98 scale	European Macroseismic
EN1990-1999	Eurocodes EC0-EC9
ENV1990-1999	Eurocodes EC8-EC9 (voluntarily)
EPP	Elastic-Perfectly Plastic
EUROCODES (EC-CODES)	European Standards
FEM	Finite Element Method
FEMA	Federal Emergency Management Agency
FIB	International Federation for Structural Concrete
FRP	Fiber-Reinforced Plastic

GFRP	Glass Fibres
GIS	Geographic Information System
GMPW	Greek Ministry of Public Works
GNP	Gross National Product
HAZUS-MH	Hazards US-Multi Hazard
ICSSC	Interagency Committee on Seismic Safety in Construction
IDA	Inelastic Dynamic Analysis
JBDPA	Japan Building Disaster Prevention Association
LS	Limit State
MDOF	Multi-Degree-of-Freedom
MEP	Mechanical Electrical Plumping
MM scale	Modified Mercalli scale
MRF	Moment Resisting Frames
MSK scale	Medvedev, Sponheuer, Karnik scale
NAD	National Application Document
NC	Near Collapse
NDT	Non-Destructive Test
NIBS	National Institute of Buildings Sciences
NTU	National Technical University of Greece
NZS	New Zealand Code
OASP	Seismic Risk Management Agency of Greece
OCR	Over Consolidation Ratio
PESH	Potential Earth-Science Hazard
PGA	Peak Ground Acceleration
PGD	Peak Ground Displacement
PGV	Peak Ground Velocity
PSV	Pseudovelocity Spectra
R/C	Reinforced Concrete
RILEM	International Union of Laboratories and Experts in construction materials
RISK-UE	Risk-Union European
RVSP	Rapid Visual Screening Procedure
SD	Significant Damage
SDOF	Single-Degree-of-Freedom
SEAOC	Structural Engineers Association of California
SI	Seismic Intensity
SIA	Schweizerische Normenvereinigung
SRSS	Square Root of the Sum of the Squares
TR	Torsionally Restrained System
TUR	Torsionally Unrestrained System
ULS	Ultimate Limit State
UNDP	United Nations Development Programme
UNIDO	United Nations Industrial Development Organization

Chapter 1

Introduction

1.1 HISTORICAL NOTES

Earthquake engineering is an independent scientific discipline that has come into being along with engineering seismology over the past 100 years and is therefore still evolving, as happens in every new scientific field.

It started as a framework of codified rules for the seismic design of buildings at the beginning of the twentieth century, after the catastrophic San Francisco earthquake of 1906. This design procedure was based, on one hand, on a framework of empirical rules for avoiding seismic damage observed in previous earthquakes, and on the other, on the simulation of the seismic action on a set of lateral forces equal to a percentage of the gravity loads of the building. This loading pattern constituted one additional load case, the *'seismic loading'*. The above simulation was based on the fact that the acceleration of the masses of a building due to earthquake causes inertial lateral forces proportional to the masses of the building, and in this respect proportional to the gravity loads. The proportion of lateral seismic loads H_{seism} to gravity loads W resulted from the ratio of the peak ground acceleration (PGA) to the gravity acceleration g ($\varepsilon = PGA/g = H_{seism}/W$).

A critical point in the above procedure was the assessment of the PGA of an earthquake that should be taken into account for the determination of the seismic lateral loading, since for many years up to 1940 there were no instruments capable of determining the PGA (strong motion instruments). Therefore, for a period of almost 35 years after the San Francisco earthquake, qualitative observations were used, like the overturning of heavy objects located at ground level for the quantitative estimate of the PGA as a percentage of g (gravity acceleration). These values were introduced as seismic coefficients in the various Seismic Codes in effect and ranged usually from $\varepsilon = 0.04$ to 0.16, depending on the seismic hazard of each region.

At the same time, it was realised that the vibration of the superstructure of a building caused by seismic actions does not coincide with that of its foundation, particularly in the case of tall buildings, which are flexible. Thus, the first steps in structural dynamics were made early on, particularly for one degree of freedom systems, that is, single-storey buildings simulated by a concentrated mass and connected to their base by an elastic spring and a damper. The aim of these first steps was the determination of the time history of the mass motion in relation to its base for a given time history of motion at the base. The problem of the *resonance* of the vibrating mass was one of the basic points of interest, since such a resonance resulted in an *amplification* of the acceleration of the mass in relation to that of the base motion. These research activities were carried out for simple forms of vibration of the base, for example, sinusoidal or ramp excitations, since these were functions that could easily be integrated without computer facilities.

In 1940, the first accelerograph (strong motion instrument) installed at El Centro in California was activated by a strong earthquake. This was the first time-history acceleration record (Derecho and Findel, 1974) known as the El Centro earthquake record. This was the first big step in earthquake engineering, since an objective method was invented for recording strong ground motions. Nowadays there are thousands of such instruments installed all over the world in seismically sensitive regions, enriching the collection of records of strong earthquakes.

The next big step was made 15 years later (in about 1955) with the development of computational techniques for obtaining *acceleration, velocity* and *displacement elastic response spectra* for a given time history acceleration record. The use of acceleration response spectra enabled the easy and direct determination of the maximum acceleration that develops in the mass of a building of a given fundamental period for a seismic spectrum under consideration. The above step must be attributed mainly to the introduction of computer facilities in engineering (Housner et al., 1953).

The above research activities resulted in the conclusion that the *amplification factor* of the PGA in the case of resonance was very high for elastic structural systems. In this context the peak accelerations of mass were many times higher than those for which the analysis of the buildings had been carried out for many decades according to the Codes then in effect. Therefore, in the case of strong earthquakes, extended collapses were to be expected even of earthquake-resistant buildings. However, while many buildings exhibited extensive damage, collapses were limited. Due to this fact it was concluded that the inelastic behaviour of the structural system, which resulted in damages, led to a reduction of the peak acceleration of mass. So, in the 1960s the energy balance theory of the structure under seismic action was born (Blume, 1960; Park and Paulay, 1975). According to this theory, a seismic action causes the transfer of a certain amount of kinetic energy from the foundation to the structural system. This energy is converted into potential energy, stored in the structural system in the form of strain energy, and then partly dissipated during the successive cycles of vibration in the form of heat or other irrecoverable forms of energy. This cyclic conversion of energy may be accomplished either in the elastic range of a structure through viscous damping by the development of high internal forces accompanied by low strains (below yield), therefore producing no damage at all, or in the inelastic range, in the case of a structure with limited load-carrying capacity, by the development of inertial forces limited to its capacity and large strains beyond the yield point, therefore accompanied by damage or collapse, depending on the inelastic displacement capacities of the structural system. The above theory was the third big step in earthquake engineering.

The above three steps have provided the main core of modern seismic design and technology for the past 40 years. This may be summarised by the following concepts

- Structural systems must resist low-intensity earthquakes without any structural damage.
- Structures should withstand a rare earthquake of moderate intensity (design earthquake) with light and repairable damage in the structural elements.
- Structures should withstand a very rare high-intensity earthquake without collapsing.

Although the acceptance of damages under the design earthquake meant an inelastic response of the structure, the core of the structural analysis procedure for seismic actions continued to be based on the linear theory. So, in order to solve this apparent discrepancy, two new concepts were introduced:

- The *ductility* coefficient
- The *capacity design* procedure

The former allows the reduction of seismic loading by a factor of about 1.5–5.0 times, having as prerequisite *the suitable reinforcing* of the structural elements so that the required inelastic deformation capacities are ensured. The latter readjusts the values of the internal forces due to seismic actions so that the risk of unexpected brittle local failures of structural elements is avoided. The above framework formulated the main body of the modern seismic philosophy known as *'force-based design'* and constitutes the core of all modern Codes in effect. It should be noted here that while structures under the 'design earthquake' respond inelastically, the use of inelastic dynamic analysis was avoided, on purpose, by introducing the ductility coefficients and the capacity design due to computational difficulties, on one hand, and to difficulties for interpretation of the results on the other. So, the procedure of *inelastic dynamic analysis* remained a valuable tool for evaluating other simplified methods like the 'force-based design' and the 'displacement-based design' (see below).

While the force-based design procedure has been proven to be a reliable method for the design of new buildings, or structural systems in general, its implementation in the assessment and rehabilitation of existing buildings runs into many difficulties. Since the design of these buildings does not comply with the rules of the modern Codes in effect, *their capacities* for plastic deformation must be explicitly defined and compared to the *demands* of plastic deformations due to the design earthquake. Therefore, the force-based design is not proper anymore. Instead, the *displacement-based design* may be implemented. This procedure has been developed in the last 20 years and is based, on one hand, on the *'capacity curve'* of the structural system generated by a static lateral loading of the structure up to failure *(push-over analysis)* and on the determination of the *'target displacement'* of the structural system corresponding to the design earthquake, using *energy balance criteria*. Thus, the efficiency of an existing structural system is obtained by displacement verifications. In the last 10 years successful efforts have been made for a *direct displacement-based design method for application in the case of new buildings*. At the same time, the development of the displacement-based design method enabled the introduction of *'the performance based design'* approach in the late 1990s, permitting the establishment of a clear relation matrix between well-defined up-to-collapse *damage levels* to the *return period* of the seismic action.

It should also be noted here that the basic theory of elastic or inelastic vibration had been previously developed for other scientific disciplines. However, its implementation in structural dynamics had encountered impassable obstacles due to the high degree of their redundancy and the random form of time-history seismic records. These two parameters made the numerical treatment of the relevant differential equations impossible. The rapid development of computers in the past 50 years enabled this obstacle to be overcome. It is important to note that until recently the above difficulties did not allow the adoption of even the *'modal response spectrum analysis',* which is a method of dynamic analysis for linear structural systems, as the *'reference method'* in Codes of Practice. Instead, Codes continued to have as a reference method the *'lateral force method of analysis',* which, as was mentioned earlier, simulates the dynamic response of the structure with a laterally loaded static system. Eurocode EC8-1/2004 is the first to have made this step forward to introduce the modal response spectrum analysis as a reference method.

In closing this short historical note on the development of earthquake engineering, reference should be made to the successful efforts for the development of alternative design techniques and devices for special types of buildings, namely the 'base isolation systems' and the 'dissipative devices'.

1.2 STRUCTURE OF THIS BOOK

The considerations of earthquake engineering briefly presented above will be adapted and applied in the forthcoming chapters to buildings with a structural system made of reinforced concrete, which constitute the major part of the building stock of the built environment in developed countries. The material of this book has been formulated into three main parts:

In the first part, seismic demand issues are examined (Chapters 2 through 6). More particularly, this part includes at the outset a short overview of basic issues of structural dynamics, which have been considered of special importance for the comprehension of the material of subsequent chapters. It also includes the procedure for the determination of the seismic actions and the ductility coefficients. The description of the acceptable methods for seismic analysis, and the application of the capacity design rules to the seismic effects (internal forces) are included in this part as well. Finally, the conceptual design of building structural systems is also examined in detail, and guidelines are given for the proper structural system for various types of buildings.

In the second part of the book (Chapters 7 through 10), the capacity of structural systems to withstand seismic effects in terms of strength and deformation (local ductility) is examined in detail. At the same time, design methods are developed that ensure the safety verification of the structural members. More particularly, detailed reference is made to the behaviour of the basic materials (concrete-steel) and their bonding under cyclic loading. Further, a detailed presentation is made of the seismic capacity of the basic structural members of an R/C building, namely of beams, columns, joints, walls, diaphragms and foundations.

Finally, the third part is devoted to existing R/C buildings under seismic action (Chapters 11 through 16). More particularly, a detailed presentation is made of seismic pathology, post-earthquake emergency measures, assessment and rehabilitation procedures, the materials and techniques of repair and strengthening and, finally, seismic risk management.

It should be noted that the book has been adjusted to fit the European Codes and particularly to EN 1998 (Eurocode EC8/2004), with parallel extended references to the American Standards in cases that this has been considered necessary for comparisons.

From this point on, the reader him- or herself will judge if the structure of the extended material of this book fulfills its main aim of providing an integrated, comprehensible, and clear presentation suitable for design practice.

Chapter 2

An overview of structural dynamics

2.1 GENERAL

The structural design of buildings was based for centuries, and even today for the greater part of the world, on the assumption that loading is not time-dependent, with only some special exceptions where cyclically moving masses cause vibrations. In this respect, for centuries and even today the core of the education of the structural engineer has been based on statics and strength of materials. Therefore, it can be easily understood why the first efforts for quantitative evaluation of the seismic actions on buildings, at the beginning of twentieth century and for many decades since, have been based on a simulation with static loads of the time-dependent inertial forces due to seismic vibrations. Even today, the American Codes of Practice for earthquake-resistant structures (ASCE 7-05) has *as reference method of analysis* the 'lateral force method of analysis', where, of course, many of the consequences of dynamic behaviour of structures have been incorporated.

For many decades, the lateral inertial forces induced by an earthquake were calculated as the product of building mass times the maximum ground acceleration due to seismic action (Figure 2.1). In this respect, seismic actions were taken into account as additional static loading.

This approach was based implicitly on the assumption that the relative displacement of the structural system in relation to the foundation during the seismic action may be considered zero, and therefore the inertial forces on the storeys above depend only on the maximum ground acceleration $\ddot{x}_o$ and their mass. This assumption is acceptable to a degree for massive buildings, that is, low-rise buildings (1–3 storeys) with thick walls and small compartments, but not for the buildings of which contemporary cities are composed.

Since the 1950s, *structural dynamics has gradually become the core of the analysis and design of earthquake-resistant structures*. In the beginning, linear models with *viscous damping* were introduced, but soon, steps were made toward models of inelastic behaviour with *hysteretic* damping, aiming at a more realistic approach to the response of structures to strong seismic motions, which cause damage.

This development was not at all easy, mainly due to computational difficulties. In spite of this, progress was accelerated by the need for higher seismic protection of modern cities with high-rise buildings built in seismic regions, where the consequences from a strong earthquake are many times greater than those of small towns. At the same time, the rapid development of computational means enabled the implementation in structural dynamics of knowledge that had been developed in the theory of vibration of simple systems for other scientific branches (e.g., electromagnetics, etc.).

Nowadays, structural dynamics is an autonomous branch of the 'theory of structures'. Therefore, a systematic approach to it is beyond the scope of this book. However, it was considered as a prerequisite to include an overview of the key issues of structural dynamics to

$$\frac{H}{G} = \tan \theta_{max} = \varepsilon$$

$$\frac{M\ddot{x}_o}{Mg} = \frac{\ddot{x}_o}{g} = \tan \theta_{max} = \varepsilon$$

$$H = \varepsilon \, G$$
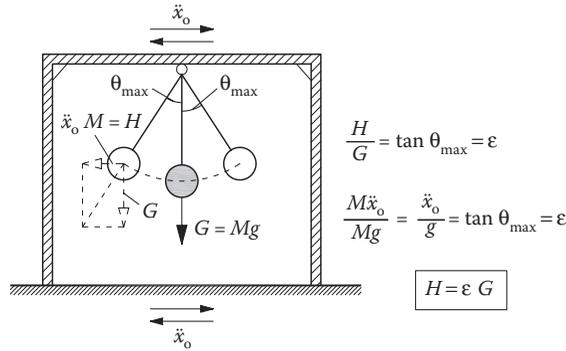
Figure 2.1 Seismic loads of old seismic codes.

which references will be made in subsequent chapters, since, as was noted before, today structural dynamics lies at the core of the analysis and design of earthquake-resistant structures.

2.2 DYNAMIC ANALYSIS OF ELASTIC SINGLE-DEGREE-OF-FREEDOM SYSTEMS

2.2.1 Equations of motion

The simplest structural system induced to seismic excitation of its base is the one shown in Figure 2.2. At the same time, the understanding of the response of this simple system, which has only one degree of freedom in the horizontal direction, is of substantial importance for structural dynamics in general, as will be presented next.

This system comprises one mass M on a spring in the form of two columns, which remain in the elastic range ($V_{el} = Ku$) during the vibration. The vibration is induced by the seismic excitation $x_o(t)$ of the base of the system. At the same time, the vibrating mass is connected to the base of the system with a dash pot ($V_d = c\dot{u}$), which simulates the damping resistance of the oscillator to the vibration due to the internal friction of the structure.

The constant c will be defined later (see Subsection 2.3.2).
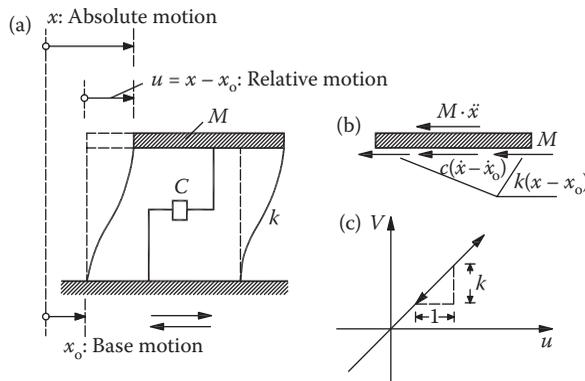
Figure 2.2 Single-degree-of freedom (SDOF) system excited by the base motion: (a) response of the system; (b) dynamic equilibrium condition; (c) shear force versus relative displacement diagram for the columns.

The motion parameters, which are lateral displacement, velocity, and acceleration of the mass of the oscillator, are given by the following expressions (functions of time):

$$x = x_o + u$$
$$\dot{x} = \dot{x}_o + \dot{u} \qquad \text{(2.1a–c)}$$
$$\ddot{x} = \ddot{x}_o + \ddot{u}$$

The notation of the above symbols is given in Figure 2.2.

The implementation of d'Alembert's concept for the equilibrium of the vibrating mass results in the following equation of vibration of the single-degree-of freedom (SDOF) system

$$M\ddot{x} + c\dot{u} + Ku = 0 \qquad \text{(2.2)}$$

or

$$\boxed{M\ddot{u} + c\dot{u} + Ku = -M\ddot{x}_o(t).} \qquad \text{(2.3)}$$

Equation 2.3 shows that the most important parameter in relation to the seismic excitation for the description of the vibration response is the acceleration time history of the base of the SDOF system. It is well known that since 1939 networks of special instruments known as *accelerographs* or *strong motion instruments* that record the time history of ground acceleration have been developed (Figure 2.3). These networks were developed first in the United States but they were later extended to seismic regions all over the world. These instruments are adjusted in advance so that they are triggered every time the ground acceleration exceeds the predefined limit. These instruments record the time history of the ground acceleration in a form that may be used as an input in Equation 2.3, and in this respect these records make possible the determination of the time-history response of the SDOF system to the recorded seismic action.

2.2.2 Free vibration

If during oscillation the exciting force becomes zero ($\ddot{x}_o(t) = 0$), the system continues to vibrate freely. In this case and for zero damping ($c = 0$) the equation of motion (2.3) takes the form:

$$M\ddot{u} + Ku = 0 \qquad \text{(2.3a)}$$

that is, it takes the form of a homogeneous dif. equation of second order. The general solution of this equation has the form:

$$\boxed{u = u_o \cos\omega t + \frac{\dot{u}_o}{\omega} \sin\omega t} \qquad \text{(2.4)}$$

where

$$\boxed{\omega = \frac{2\pi}{T_o} = \sqrt{\frac{K}{M}}} \qquad \text{(2.4a)}$$
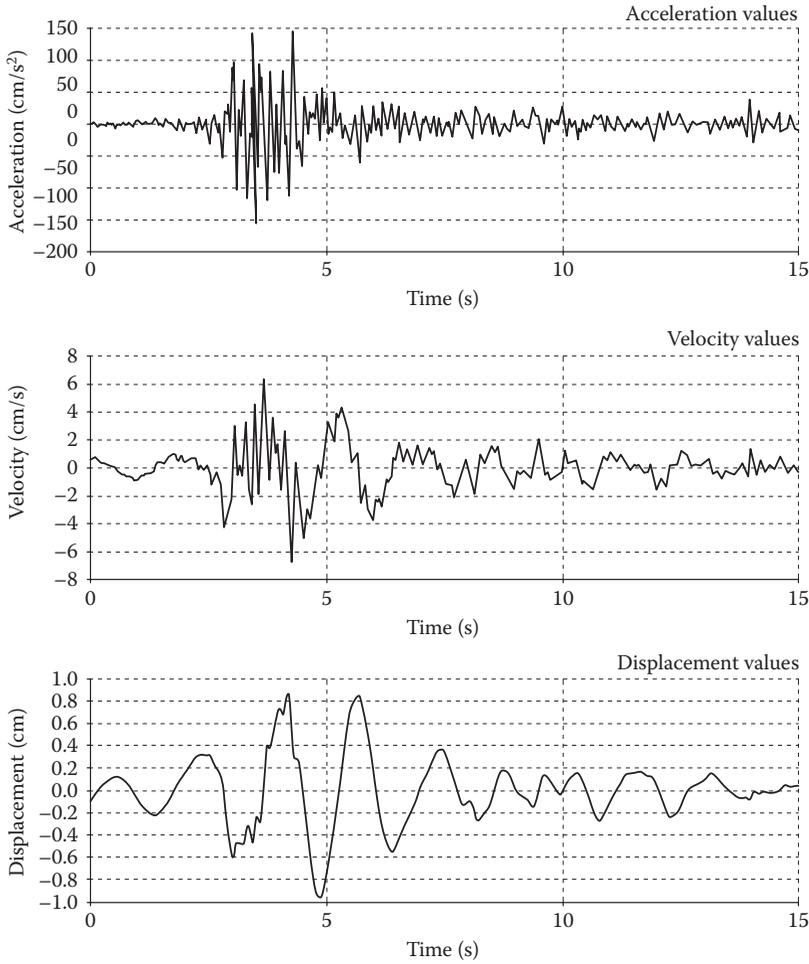
Figure 2.3 Accelerogram of the Athens earthquake of 7 September 1999 (N–S): components and derived diagrams of velocity and displacement. (Adapted from IESEE (Institute of Engineering Seismology and Earthquake Engineering, Greece) 2003. *Strong Motion Data Base of Greece 1978–2003*, Thessaloniki, Greece.)

is the *natural circular frequency* (in rad/s) and

$$T_{\mathrm{o}} = 2\pi\sqrt{\frac{M}{K}} \tag{2.4b}$$

is the *natural period* of the system.

The constant coefficients of Equation 2.4 are determined taking into account the following initial conditions:

For $t = 0$ the initial relative displacement u is supposed to be $u = u_{\mathrm{o}}$, while the initial velocity for $t = 0$ is supposed to be $\dot{u} = \dot{u}_{\mathrm{o}}$, that is, u_{o} and $\dot{u}_{\mathrm{o}}$ are input data (Figure 2.4; Georganopoulou, 1982).

The natural period T_{o} is the dynamic constant of the system, the characteristics of which, the mass M and the spring stiffness K, have been incorporated into it. *Natural period T_{o} expresses the period of the free vibration of the system.*
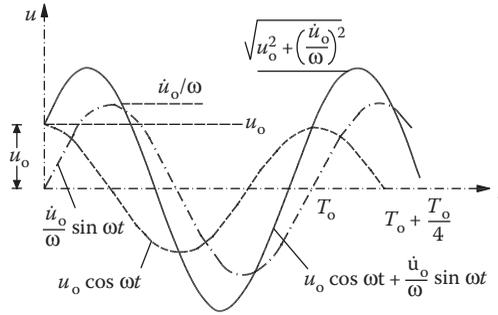
Figure 2.4 Diagram of the free vibration relative displacement of Equation 2.4 for input data: initial displacement $u = u_o$ and initial velocity $\dot{u} = \dot{u}_o$.

When damping is not zero ($c \neq 0$) the homogeneous equation of motion (2.3a) takes the form:

$$M\ddot{u} + c\dot{u} + Ku = 0 \tag{2.3b}$$

The general solution of this equation has the form:

$$u = u_o e^{-\frac{ct}{2M}}(A\sin\gamma t + B\cos\gamma t) \tag{2.5}$$

where

$$\gamma = \sqrt{\frac{K}{M} - \left(\frac{c}{2M}\right)^2} \tag{2.6}$$

For $\gamma = 0$, that is,

$$\boxed{c = c_{cr} = 2\sqrt{MK}} \tag{2.6a}$$

the free vibration is transformed into an attenuation curve (Figure 2.5b). Setting $\zeta = c/c_{cr}$ (*critical damping ratio*), Equation 2.5 becomes

$$\boxed{u = u_o e^{-\zeta\omega t}(A\sin\omega_D t + B\cos\omega_D t)} \tag{2.7}$$

where

$$\omega_D = \omega\sqrt{1 - \zeta^2} = \gamma \tag{2.8}$$

and

$$T_D = \frac{T_o}{(1 - \zeta^2)^{1/2}}. \tag{2.9}$$
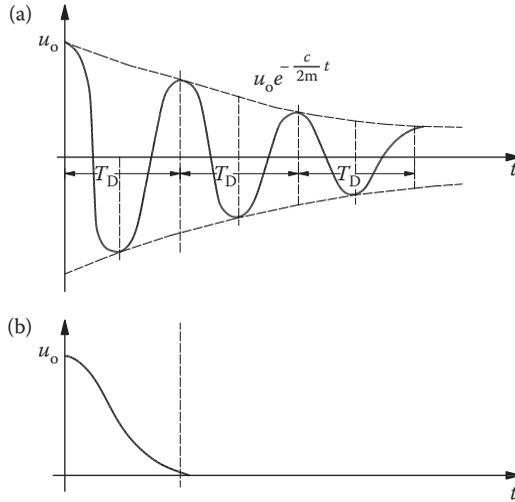
Figure 2.5 Free vibration with damping: (a) initial relative displacement u_o; (b) initial displacement in case of critical damping. (From Biggs, J.M. 1964. *Introduction to Structural Dynamics*. McGraw-Hill, New York. With permission.)

For values of $\zeta < 0.15$, the natural period T_D of the oscillating system is close to that of the undamped system T_o.

The constants A and B are defined by the initial conditions of the initial displacement u_o and the initial velocity $\dot{u}_o$, that is,

$$A = \frac{\dot{u}_o + \gamma u_o}{u_o w_o}, \quad B = 1.0$$

2.2.3 Forced vibration

In the case of a ground excitation $(\ddot{x}_o(t) \neq 0)$, the particular integral of Equation 2.3 must be added to the general integral (Equation 2.7).

In the case of an artificial steady-state excitation in the form of a sinusoidal function (Figure 2.6; Georganopoulou, 1982), that is,

$$\ddot{x}_o(t) = \ddot{x}_{o\max} \sin \Omega t \tag{2.10}$$

the particular integral of the undamped forced vibration takes the form

$$u_p = \frac{\ddot{x}_{o\max}}{K/m} \frac{1}{1 - \beta^2} \sin \Omega t \tag{2.11}$$

where

$$\beta = \frac{\Omega}{\omega} \tag{2.12}$$
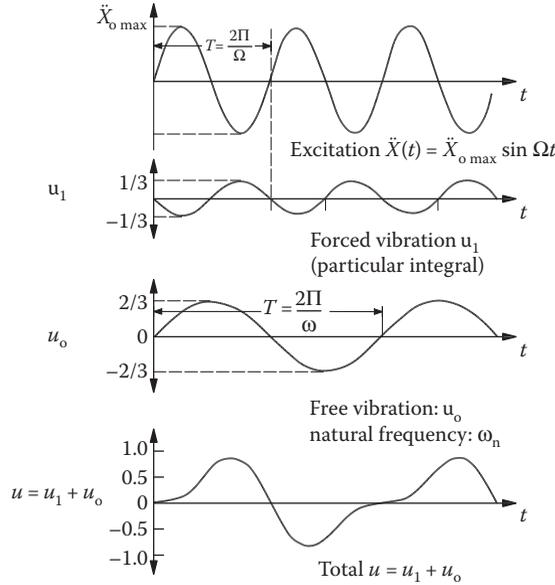
Figure 2.6 Forced vibration of an SDOF system excited by a sinusoidal base acceleration for $\Omega/\omega = 2$.

and in this respect the damped forced vibration takes the form:

$$u_{pd} = \frac{M\ddot{x}_{o\,max}/K}{\sqrt{(1 - \beta^2)^2 + (2\zeta\beta)^2}} \sin\left(\Omega t - \arctan\frac{2\zeta\beta}{1 - \beta^2}\right). \tag{2.13}$$

It is important to note that in the case that

$$\beta = \frac{\Omega}{\omega} = 1$$

which means that the frequency Ω of the excitation coincides with the natural frequency (ω) of the SDOF system, the maximum value of u_p becomes (Figure 2.7):

$$u_{p\,max} = \infty \quad \text{for an undamped system and}$$

$$u_{pd\,max} = \frac{\ddot{x}_{o\,max} \cdot M}{2K\zeta} \tag{2.13a}$$

for a damped one.

It is obvious that in this case *resonance* of the vibrating system takes place due to the coincidence of the natural period of the vibrating system and that of the exciting agent. As a result, the vibrating system *amplifies the ground maximum acceleration and displacement.*

In the case of a transient chaotic seismic excitation, the above process for the determination of the partial integral of Equation 2.3 must be modified radically since it is not possible
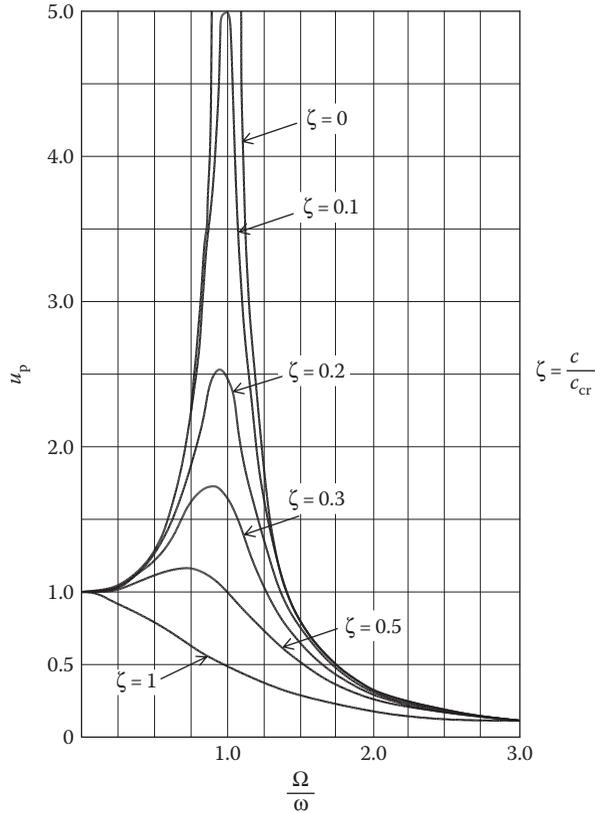
Figure 2.7 Maximum relative displacement u_p of an SDOF system activated by a sinusoidal forced vibration diagram of u_p versus natural frequencies ratio Ω/ω for various values of ζ (critical damping ratio). (From Biggs, J.M. 1964. *Introduction to Structural Dynamics.* McGraw-Hill, New York. With permission.)

to find a closed form of the partial integral. So, the function of the ground acceleration $\ddot{x}_o(t)$ is divided into successive, very short-duration impulses, as shown in Figure 2.8.

$$dP = \ddot{x}_o(\tau) \cdot M \cdot d\tau \tag{2.14}$$

Consider now one of these impulses, which end at time τ after the beginning of the ground motion (Equation 2.14). This impulse in turn causes an initial velocity on the vibrating system:

$$d\dot{u}_o(\tau) = \ddot{x}_o(\tau)d\tau \tag{2.15a}$$

while the initial displacement is

$$du_o(\tau) = 0 \tag{2.15b}$$

Substituting Equation 2.15a,b into Equation 2.4 (undamped vibration), we have

$$du = \frac{\ddot{x}_o(\tau)}{\omega} \sin \omega(t - \tau)d\tau \tag{2.16}$$
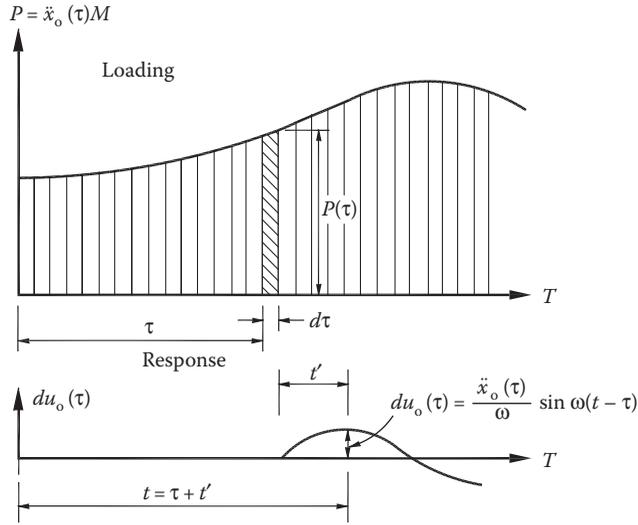
Figure 2.8 Response $u_o(t)$ of an SDOF system to a differential impulse.

In the above expression du is the displacement at time t due to the input ground acceleration $\ddot{x}_o(\tau)$ acting during the time differential $d\tau$. So,

$$u(t) = \frac{1}{\omega}\int_0^t \ddot{x}_o(\tau)\sin\omega(t-\tau)d\tau \qquad (2.17)$$

This is the Duhamel integral, well known in structural dynamics. In the case of damped vibration, Equation 2.17 takes the form:

$$u(t) = \frac{1}{\omega}\int_0^t \ddot{x}_o(\tau)e^{-\zeta\omega(t-\tau)}\sin\omega_D(t-\tau)d\tau \qquad (2.17a)$$

The above Equations 2.17 and 2.17a give the displacement $u(t)$ during the ground motion at any moment t, that is, the time history of the response of the system. It is obvious that the integral in the above equations can be quantified only by using numerical methods, and therefore only the introduction of computers in structural dynamics after 1949 made possible the application of Equations 2.17 and 2.17a for real case studies of seismic input. It should also be mentioned that in this case a strong amplification of the response is observed for natural periods of the vibrating system near to the predominant period of the excitation. This will by clarified in detail in the next subsection.

2.2.4 Elastic response spectra

2.2.4.1 Definition: Generation

The time history of the oscillation phenomenon is not always needed in practice in its entirety, as it suffices to know the maximum amplitude of the relative displacement, the relative velocity, and the absolute acceleration developed during a seismic excitation. This is because from these values the maximum stress and strain state of the system can be

determined. For this reason the concept of the *response spectrum* has been introduced. The response spectrum of an earthquake is a diagram in which ordinates present the maximum amplitude of one of the response parameters (e.g., relative displacement, relative velocity and acceleration) as a function of the natural period of the SDOF system.

For any seismic input (accelerogram $\ddot{x}_o(t)$), three elastic response spectra can be produced to generate ordinates that give the maximum amplitude of the relative displacement S_d, relative velocity S_v and absolute acceleration S_a, respectively, of an SDOF system versus its natural period T (Figure 2.9). This means that the elastic response spectrum of a seismic input reflects the behaviour of all elastic SDOF systems with natural period T between $\varnothing$ and ∞ during that specific excitation. The first elastic response spectra were produced experimentally by Biot in 1935 on a shaking table with SDOF oscillators and a natural period between 0 and 2.4 s (Figure 2.9).

After the introduction of computational means in structural dynamics, Housner and Kahn produced the first elastic response spectra analytically (Housner et al., 1953; Polyakov, 1974) using the Duhamel integral of (Equation 2.18),
that is,

$$
S_d = [u(t)]_{max} = \frac{1}{\omega} \left[\int_0^t \ddot{x}_o(\tau) e^{-\zeta\omega(t-\tau)} \sin \omega_D(t-\tau) d\tau \right]_{max} \tag{2.18}
$$

or Newmark Methods for numerical integration.

On the other hand, the maximum velocity S_v can be approximated, assuming harmonic motion, by the expression:

$$
\boxed{S_v = \omega S_d = S_d \left(\frac{2\pi}{T} \right)} \tag{2.19}
$$
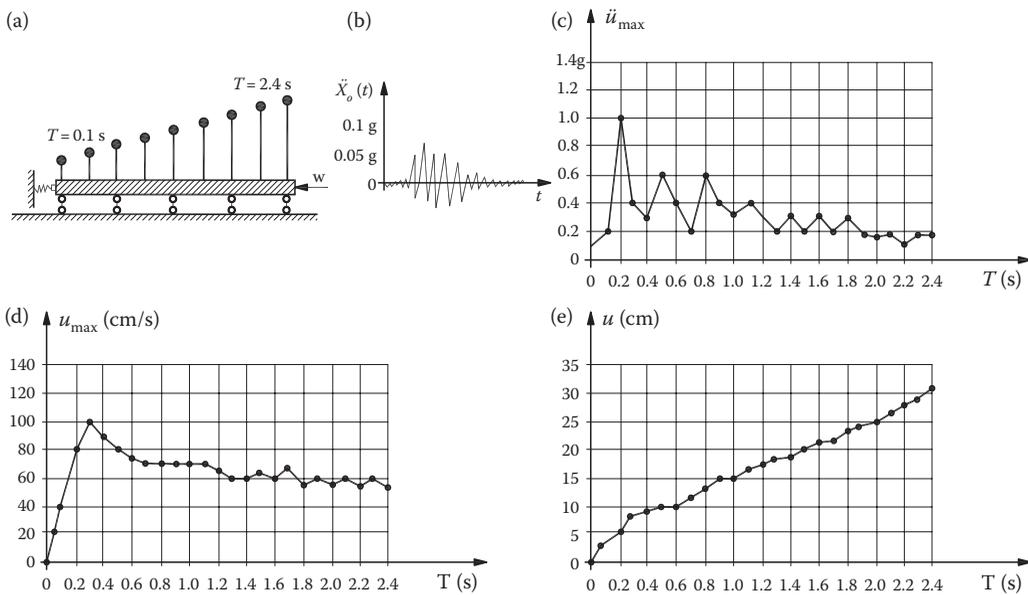
Figure 2.9 Response spectra of SDOF systems: (a) shaking table carrying SDOF systems with $t = 0.1$–2.4 s; (b) accelerogram; (c) acceleration spectrum; (d) velocity spectrum; (e) displacement spectrum.

and the maximum acceleration by the expression:

$$S_{\alpha} = \omega S_{v} = \omega^2 S_{d} = S_{d}\left(\frac{4\pi^2}{T^2}\right). \qquad (2.20)$$

The above assumption is acceptable for values of $\zeta < 0.30$. In reality, the maximum restoring force peaks display just before the point of the maximum displacement. Therefore, S_a in Equation 2.20 is slightly less than the true peak acceleration during an earthquake. Strictly speaking, S_a should be called '*pseudospectral acceleration*' and S_v '*pseudospectral velocity*'. However, for ζ less than 0.15 there is no significance in the above remark.

Thus, the velocity and acceleration spectra are derived by multiplying each ordinate of the displacement spectrum by ω, $(2\pi/T)$, and ω^2, $(4\pi^2/T^2)$, respectively.

From Equation 2.18 it can be seen that *as damping ζ increases, the spectral ordinates decrease* (Figure 2.10; IESEE, 2003). For high values of damping the spectra become smooth. In practice, for reinforced concrete structures ζ is assumed equal to 0.05.
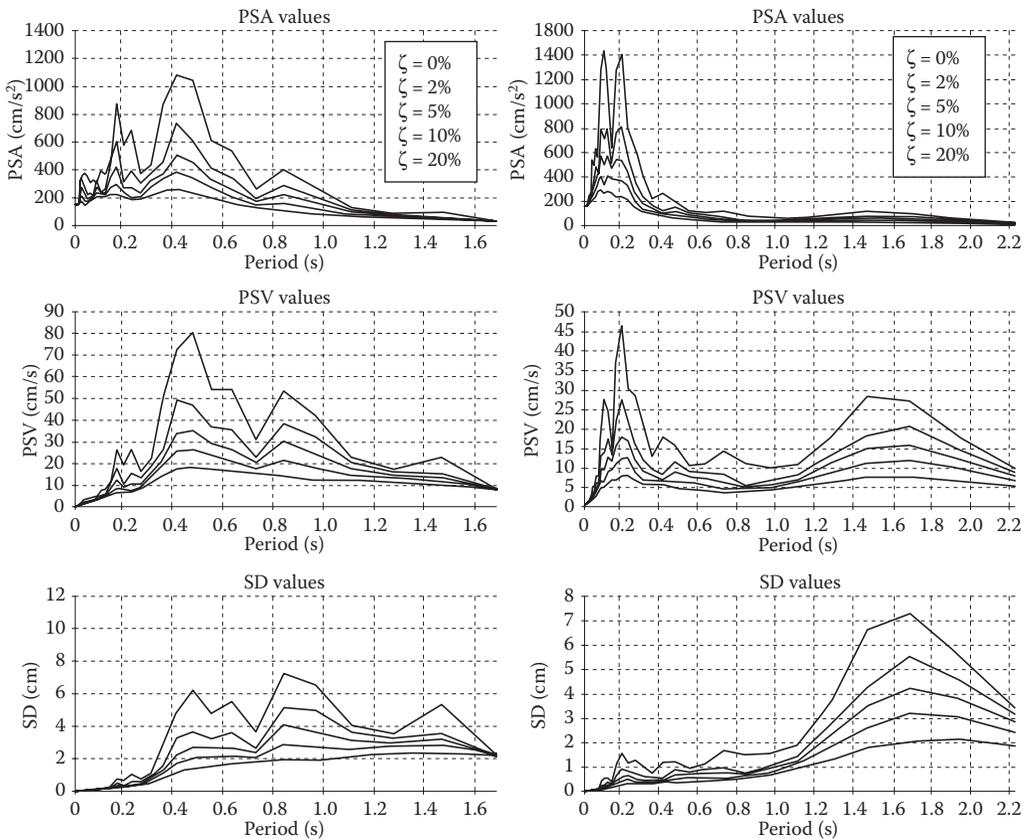
Figure 2.10 Elastic response spectra for 1999 Parnitha (Athens, Greece; right) and for 1978 Thessaloniki (Volvi, Greece; left) earthquakes for various damping values: acceleration (top) velocity (middle) and displacement (bottom). (Adapted from I.E.S.E.E. (Institute of Engineering Seismology and Earthquake Engineering, Greece) 2003. *Strong Motion Data Base of Greece 1978–2003*, Thessaloniki, Greece.)

Practically, the computational procedure for the derivation of elastic response spectra can be summarised as follows (Elnashai and Di Sarno, 2008):

1. Select a digitised form of the selected accelerogram from an available database.
2. For a given value of ζ and for successive values of T between 0.01 and 5.0 s calculate successive values of S_d using one of the existing computing codes, which are based on digitisation of the Duhamel integral Equation 2.18 or other relevant methods.
3. Repeat the procedure of item (ii) for successive values of ζ ranging between 0% and 20%.
4. Compute the velocity S_v and acceleration S_a using Equations 2.19 and 2.20, respectively.
5. Plot S_d, S_v, S_a spectra versus the natural period for the damping values selected.

2.2.4.2 Acceleration response spectra

The acceleration response spectra are of fundamental importance for the seismic design of buildings because they relate to the maximum inertial forces that develop during the earthquake. In this respect they constitute the basis for the force-based design on which all modern Codes of Practice for a seismic design are based (see Subsection 3.4.3).

Therefore, a comprehensive examination of the acceleration response spectra will follow:

1. For $T = 0$, that is, for a completely rigid structure, the maximum acceleration of the system is equal to the *Peak Ground Acceleration (PGA)* $\ddot{x}_o(t)_{max}$.
2. With the increase of the natural period T, the absolute acceleration S_a of the system increases as well, and, for a natural period near to the predominant period T_{predom} of the accelerogram $(\ddot{x}_o(t))$, S_a reaches its maximum value, which tends to be *two* to *three* times the PGA for a 5% damping level. In this case, the system is *in resonance* with the seismic excitation (see Subsection 2.2.3).
3. For systems with natural period T longer than T_{predom}, S_a begins to decrease, since the system again goes out of phase. These are generally flexible systems.
4. Earthquakes occurring at small depths (up to 60 km) in the earth are the most frequent. These earthquakes have a predominant period on the order of 0.2–0.4 s, therefore SDOF systems with a natural period within this range experience the highest acceleration. This natural period corresponds generally to the fundamental period of two to four-storey buildings (see Subsection 5.6.4).
5. For deep, strong earthquakes (70–300 km in depth), which are rarer (1977 Bucharest earthquake, 1985 Mexico City earthquake), the high frequencies of motion are absorbed by the lithosphere, so only long-period motions reach at the ground surface. In this case, the predominant period appears to be 1.0–2.0 s; therefore, systems with a natural period within these limits experience the largest acceleration. Such a natural period generally corresponds to the fundamental period of 10- to 20-storey buildings (Figure 2.11).
6. Soft soils shift the maximum of the acceleration spectrum to the right of the diagram, as the predominant period of the soil is long. On the other hand, firm soils shift the maximum of the acceleration spectrum to the left (short predominant period). So flexible when (high-rise) buildings with a long fundamental period are vulnerable to earthquakes when founded on soft soils, while stiff (low-rise) buildings appear to be vulnerable to earthquakes when they are founded on firm soil (Richart et al., 1970). A good example is the Mexico City earthquake (1985), where the accelerograms recorded in four different locations (Figure 2.12a) have given the acceleration response spectra depicted in Figure 2.12b (Penelis and Kappos, 1997).
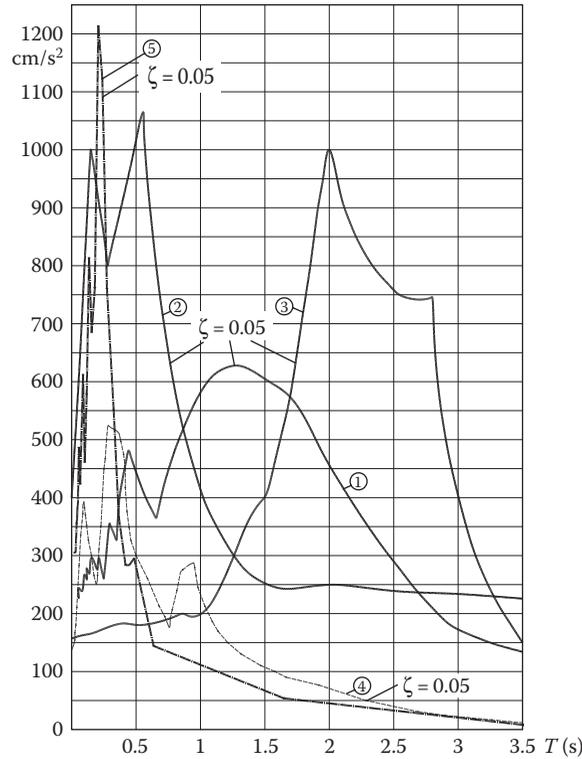
Figure 2.11 Characteristic acceleration spectra of strong earthquakes: (1) Bucharest earthquake 4.3.1977 N–S; (2) El Centro earthquake 18.5.1940 N–S; (3) Mexico City earthquake 19.9.1985 E–W SCl; (4) Thessaloniki earthquake 20.6.1988 E–W 'City' hotel; (5) Athens earthquake 07.09.1999.

7. Acceleration spectra allow an overall picture of the response of a large range of structures to an excitation. At the same time, they allow a static consideration of the seismic excitation, although it is a thoroughly dynamic phenomenon. This offers significant advantages to the structural engineer whose education is mainly focused on statics. Indeed, the relation between the inertial forces and the restoring ones (Figure 2.2b) has the following form:

$$V = K(x - x_o) = Ku = -(c\dot{u} + M\ddot{x}) \tag{2.21}$$

The maximum *base shear* develops when the relative displacement u reaches its maximum value, and therefore the relative velocity $\dot{u}$ takes a value equal to zero.
So,

$$V_{max} = Ku_{max} = MS_a$$

or

$$\boxed{V_{max} = KS_d = MS_a} \tag{2.22}$$
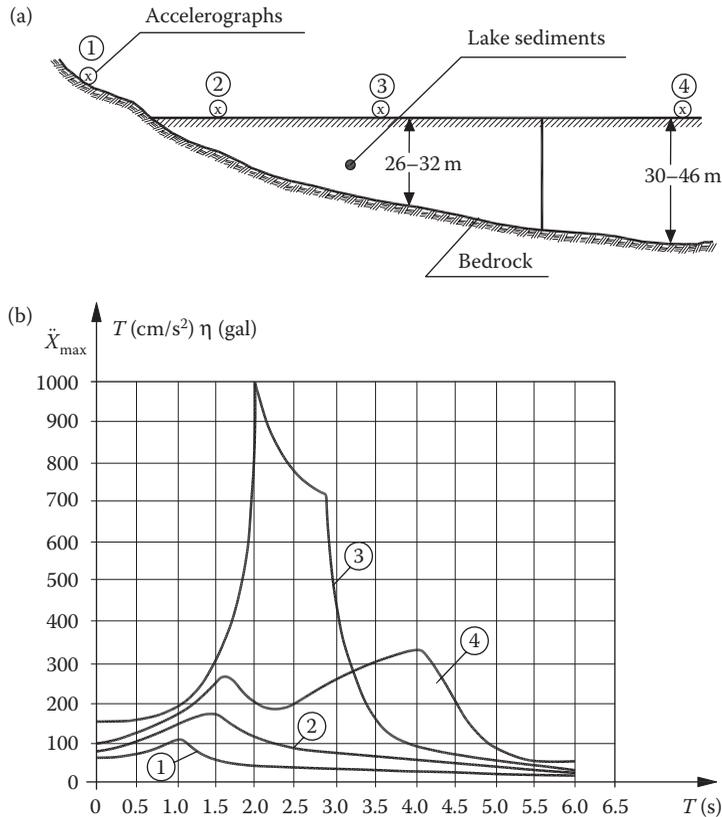
Figure 2.12 Mexico City earthquake 19.9.1985: (a) the ground stratification of Mexico City and (b) acceleration response spectra at points (1), (2), (3) and (4).

If we express V_{max} as a function of the weight W of the structure, the following expression results:

$$\boxed{\frac{V_{max}}{W} = \frac{MS_a}{W} = \frac{MS_a}{Mg} = \frac{S_a}{g} = \varepsilon}$$

(2.23)

The above relation means that in order for the maximum stress and strain of an SDOF system to be determined, the system can be loaded with a horizontal force V equal to the weight W multiplied by *the seismic coefficient* ε, resulting from the acceleration response spectrum of the specific earthquake scaled to g (Figure 2.13). It should be noted that the above conclusion is very close to the approach to the problem of base shear that was followed in the past, up until the early 1950s (see Figure 2.1). The only difference is that ε *is not a constant but it is a value dependent on the natural period T_o of the structure.*

8. It should be noted that the acceleration response spectrum is the main tool for the 'modal response spectrum analysis' of multi-degree of freedom (MDOF) elastic systems (see Subsection 2.4.3 and Chapter 5.5.1).
9. Finally, reference should be made to *the vertical component of the ground motion*, which has generally been ignored for many years. This has changed gradually in the last 20 years due to the increased number of near-source records combined with field observations confirming the destructive effects of high vertical vibrations (Papazoglou
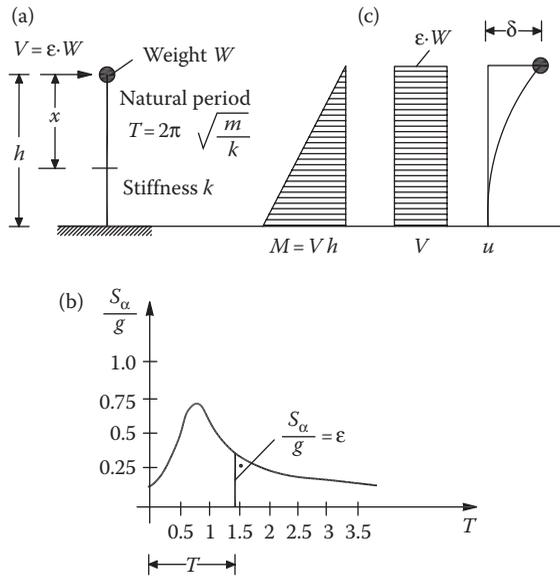
Figure 2.13 Transition from the dynamic to static response: (a) an SDOF system; (b) acceleration response spectrum; (c) maximum response of the structure.

and Elnashai, 1996). The commonly used approach of taking the vertical spectrum as two-thirds of the horizontal one without a change in fundamental period content is now being abandoned (Elnashai and Papazoglou, 1997; Collier and Elnashai, 2001). For example, EC 8-1/2004 introduces forms for vertical elastic acceleration response spectra that are independent of those of the horizontal ones.

2.2.4.3 Displacement response spectra

These spectra have begun to gain interest in the last 15 years due to their direct application in the *displacement-based design (DBD) method*, which has been introduced recently for the assessment and redesign of existing buildings (EC8-1 and 3/2004-5).

As was explained in Paragraph 2.2.4.1, there is a linear relation between S_a and S_d (Equation 2.20) for damping levels below 0.30. However, even for values of $\zeta = 0.05$ but for natural periods longer than 2.0 s, the resulting elastic displacement response spectra from Equation 2.20 have proven to be unreliable (Figure 2.14). The reason is that for many years accelerograms were generated using analogue accelerographs with filters at 3.0 s to cut off noise frequency. However, as various researchers have shown, the elastic response spectra are unreliable for fundamental periods longer than two-thirds of the filter cut-off period, that is, longer than 2 s.

So, in the last few years, extended research has been carried out for the generation of reliable elastic (and inelastic) displacement response spectra based on digital accelerograms for use in the DBD method, where longer than 2 s equivalent periods T_{eq} and higher than 15% equivalent damping coefficients appear due to the degradation of the structural system in the postelastic region (see also Chapter 14.2; Ambraseys et al., 1996; Bommer and Elnashai, 1999; Tolis and Faccioli, 1999). In conclusion, it is important to make the following remarks (Figure 2.14):

 1. Spectral ordinates for all damping coefficients increase with the period from zero to a zone of maximum values and then decrease to converge at the peak ground displacement (PGD) for long periods.
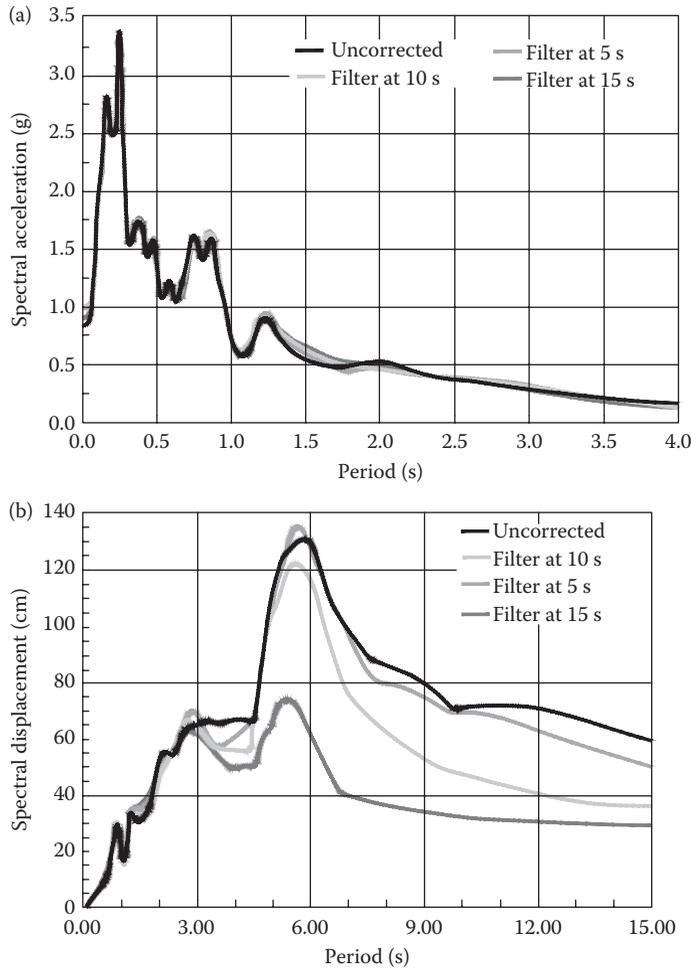
Figure 2.14 The 1978 Tabas (Iran) record filtered at 5, 10 and 15 s cutoff as well as baseline correction only: (a) acceleration spectra; (b) displacement spectra. (Adapted from Elnashai, A.S. and Di Sarno, L. 2008. *Fundamentals of Earthquake Engineering*, Wiley, West Sussex, UK.)

2. This means that for long natural periods, much longer than the predominant period of the seismic motion, the mass of the structural system remains unaffected. The ground vibrates while the mass remains motionless, and so u_{max} (relative displacement) converges at the PGD (PGD $= x_{omax}$).

2.2.4.4 Velocity response spectra

Velocity response spectra are of importance in seismic design because they are an index of the energy transmitted by the ground into the oscillator. Indeed, the energy transmitted into a vibrating mass is

$$E_{max} = \frac{1}{2} M\dot{u}_{max}^2 = \frac{1}{2} MS_v^2 \tag{2.24}$$

In this respect, velocity spectra allow quantitative evaluation of the total seismic excitation, and therefore motions of different amplitude can be scaled (normalised) *to the same*

Table 2.1 Values (in mm) and normalisation factors for the first 10 s of a series of accelerograms

Accelerogram		SI (mm)			Factor
		$\zeta = 0\%$	$\zeta = 5\%$	$\zeta = 10\%$	
El Centro	S00E	2334	1479	1230	1.00
Taft	N21E	1021	651	555	2.24
Taft	S29E	1176	749	605	2.00
Cal Tech	S90W	634	414	338	3.60
Pacoima	S16E	5876	3910	3316	0.37
Thessaloniki	N30E	721	555	484	2.61
Thessaloniki	N60E	698	517	457	2.78

level of intensity. This can be accomplished with the following integral, which was originally defined by Housner (Wiegel, 1970) *as spectrum intensity:*

$$SI = \int_{T_1}^{T_2} S_v(T,\zeta)dT \tag{2.24a}$$

with integration limits $T_1 = 0.15$ and $T_2 = 2.55$. The above integral represents the area under the velocity spectrum for a given damping coefficient ζ, between the limits T_1 and T_2, and it is expressed in units of length. Table 2.1 gives some characteristic SI values (in mm) of several accelerograms, as well as the resulting normalisation factors with regard to the El Centro spectrum (Penelis and Kappos, 1997). The reliability of the scaling factors can be checked by studying the response of multi-storey structures for several accelerograms normalised to the same level of spectrum intensity. Such a response is shown in Figures 2.50, 2.54 and 2.55 (Kappos, 1990; Penelis and Kappos, 1997). It can be seen there that although the accelerograms are normalised, the differences in response are significant. Since that time, many efforts have been carried out by various researchers to improve the reliability of what is denoted as 'spectrum intensity SI' (Nau and Hall, 1984; Kappos, 1990; Matsumura, 1992; Martinez Rueda, 1997; Elnashai, 1998). For more information see Paragraph 5.7.6.1.

2.2.4.5 Acceleration-displacement response spectra

These spectra are generated by plotting spectral acceleration directly against spectral displacement (Mahaney et al., 1993). This can be done by the implementation of Equation 2.20.

$$S_d = \frac{T^2}{4\pi^2} S_a \tag{2.25}$$

Additionally, Equation 2.25 can be rearranged in the form:

$$T = 2\pi\sqrt{\frac{S_d}{S_a}} \tag{2.26}$$

Figure 2.15 presents an ADRS spectrum. It is obvious that each curve refers to a predefined damping level. These spectra have been developed for the application of the Capacity-Spectrum technique in the displacement-based design method (see Subsection 14.2.2).
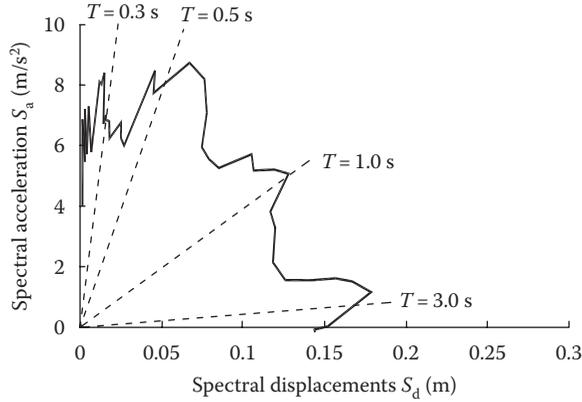
Figure 2.15 Capacity displacement spectrum (ADRS).

2.3 DYNAMIC ANALYSIS OF INELASTIC SDOF SYSTEMS

2.3.1 Introduction

After the introduction of the concept of the response spectrum in earthquake engineering and the development of the first elastic spectra by Housner in 1949 (Housner et al., 1953), it was noticed that the maximum acceleration of the vibrating masses in structures close to resonance with the seismic motion was 2–3 times higher than the PGA. Thus, for $\ddot{x}_{\mathrm{omax}}/g = 0.17$, that is, for a seismic motion of moderate destructiveness, the seismic coefficient ε reached the value of 0.35–0.50. On the other hand, all the existing engineered structures of the past were designed for ε values between 0.04 and 0.16, according to seismic codes then in effect. However, the damage to these structures due to earthquakes that occurred in the meantime was not always destructive.

The difference was so great that it could not be attributed to the existing overstrength in the structures or to calculation errors. A more precise approach to the problem showed that this fact could be explained by taking into account the inelastic behaviour of the structures, which accompanied the structural damage. This behaviour led to the dissipation of a large percentage of the system's kinetic energy through damping.

2.3.2 Viscous damping

Up until now the damping phenomenon of actual structures in the elastic range has been studied using the Kelvin–Voigt model (Figure 2.16). This model consists of a spring and a dashpot acting as a damper connected in parallel with the spring (Housner et al., 1953). Thus, the total force P required for the displacement u of the system is the sum of the restoring force P_e of the spring and the resistance P_d of the damper:

$$P = P_e + P_d = Ku + c\dot{u} \tag{2.27}$$

In this viscoelastic model of Kelvin–Voigt the viscous damping is proportional to the *deformation velocity*. In real structural systems, however, springs and dampers are incorporated into elastic members that connect the masses to each other and to the ground. It is therefore important to evaluate at least qualitatively whether the introduced value for P_d in Equation 2.27 expresses with sufficient accuracy the viscoelastic damping in structures.
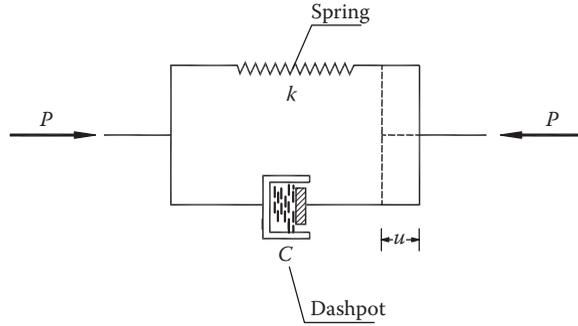
Figure 2.16 The Kelvin–Voigt viscoelastic model.

It is known from material testing that the response of a material to an external loading depends on the rate of loading. The higher the rate of loading, the larger the force required for the same deformation (Figure 2.17).

$$P = P_e + \Delta P = P_e + P_d \tag{2.28}$$

As Figure 2.17 shows, the viscous part of the loading is a complicated function of the deformation rate $\dot{u}$. However, if this function is expanded in a polynomial series of $\dot{u}$ and only the first term is retained, P_d takes the approximate form:

$$P_d = c\dot{u} \tag{2.29}$$

The above approximation, as we have seen, has made possible the linearisation of the dynamic analysis problem of SDOF and MDOF systems, as we will see next.

It is of great interest to present graphically the total restoring force:

$$P = P_e + P_d = Ku + c\dot{u}. \tag{2.30}$$

If the system of Figure 2.2 is subjected to a vibration in the form:

$$u = u_o \sin \omega t \tag{2.31}$$
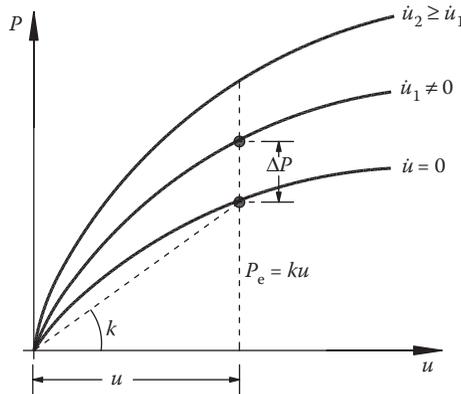
Figure 2.17 Qualitative diagrams of the axial force *P* versus normal strain *u* for various loading rates.

then the relation (2.30) takes the form:

$$P = Ku_\text{o} \sin \omega t + c\omega u_\text{o} \cos \omega t \tag{2.32}$$

Equations 2.31 and 2.32 define a P–u function, which describes an ellipse (Figure 2.18). The area of the shaded loop (area of ellipse) represents the dissipated energy due to the viscoelastic damping. The area of this ellipse is equal to

$$\Delta W = \int\limits_{T}^{T+2\pi/\omega} P(t)\frac{du}{dt}\,dt = \pi c\omega u_\text{o}^2. \tag{2.33}$$

On the other hand, the maximum potential energy U of the system is equal to

$$U_\text{e} = \frac{1}{2} K u_\text{o}^2. \tag{2.34}$$

Therefore,

$$\frac{\Delta W}{U_\text{e}} = \frac{2\pi c\omega}{K}. \tag{2.35}$$

Combining Equations 2.4a, 2.4b and 2.6a results in

$$c = \zeta_\text{el} \cdot c_\text{cr} = \zeta_\text{el}(2\sqrt{MK}) = \zeta_\text{el}(2\omega M). \tag{2.36}$$

Substituting 2.36 into 2.35, ζ_el takes the form:

$$\boxed{\zeta_\text{el} = \frac{1}{4\pi}\frac{\Delta W}{U_\text{e}} = \frac{1}{4\pi}\frac{A_\text{ellipse}}{U_\text{e}}.} \tag{2.37}$$

That is, the viscous damping ratio ζ_el is defined by the ratio of the loop area of Figure 2.18 divided by the maximum elastic strain energy equal to the area of the triangle OAB (Figure 2.18).
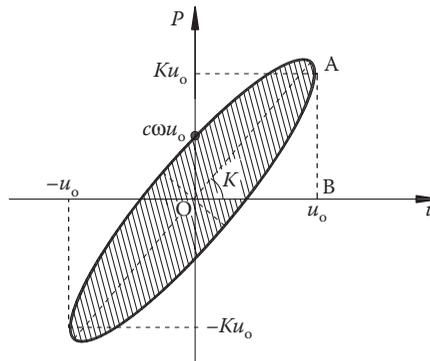
Figure 2.18 Diagram of the restoring force P versus relative displacement u for an excitation $u = u_\text{o} \sin \omega t$ of an SDOF with damping c.

2.3.3 Hysteretic damping

In addition to the viscoelastic behaviour of materials, there are other factors that lead to damping. The most significant, particularly in the case of inelastic deformations due to earthquakes, is '*the hysteretic behaviour of materials*'. The stress–strain diagram of a material or a structural member under cyclic loading has the form of Figure 2.19, with several variations depending on special characteristics of the material or the member and the loading (see also Subsection 14.2.2). The area of the shaded loop of the above figure represents the energy that is dissipated in every loading cycle, due to the plastic behaviour of the *material*. It is obvious that the larger the area of the hysteresis loop, that is, the higher the plastic strain level of the material or of the structural member, the larger the dissipated energy and the damping.

Comparing now Figures 2.18 and 2.19, it is evident that the hysteretic damping may be expressed approximately in the form of viscous damping using a hysteretic damping ratio (Jacobsen, 1960):

$$\boxed{\zeta_{\text{hyst}} = \frac{1}{4\pi} \frac{\Delta W_{\text{hyst}}}{U_{\text{el}}}} \tag{2.38}$$

where

ΔW_{hyst} is the area of the hysteresis loop of Figure 2.19
U_{el} is the area of the triangle OAB of Figure 2.19 equal to $(1/2)K_{\text{ef}}u_{\text{u}}^2$
u_{u} is the ultimate inelastic deformation

In this respect, the equivalent viscous damping is equal to

$$\boxed{\zeta_{\text{eq}} = \zeta_{\text{el}} + \zeta_{\text{hyst}}.} \tag{2.39}$$

Equation 2.38 is a basis for the qualitative understanding of the phenomenon of hysteretic damping and a good indicator of dissipation per cycle of loading. Furthermore, it allows the application of the linear theory in structures exhibiting dissipative behaviour (see also Subsection 14.2.2) by introducing ζ_{eq}, if it does not exceed values of 0.15–0.28. Last but
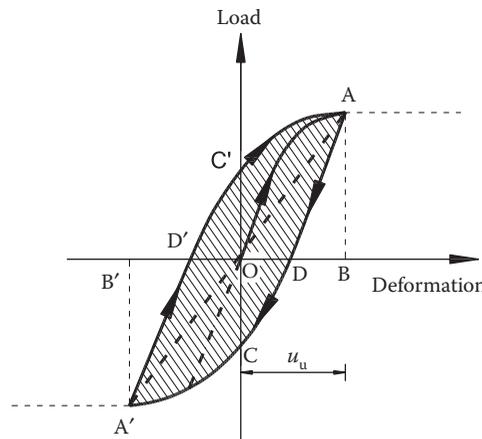
Figure 2.19 A typical hysteresis loop.

not least, it is a very useful tool for displacement-based design (see Subsection 14.2.2), as it makes possible the formulation of relations between *hysteretic damping* ζ_{hyst} and ductility μ ($\mu = (u_p/u_y)$) (see below).

Case study

Below we will determine the relation between ζ_{hyst} and μ in the case of a system with an elastic perfectly plastic (EPP) stress–strain diagram (Figure 2.20)

$$\Delta W_{hyst} = 2(u_p - u_y)2f_y = 4(u_p - u_y)f_y = 4f_y\left(\frac{u_p}{u_y} - 1\right)u_y \tag{2.40}$$

If we denote *ductility*, the ratio u_p/u_y, that is,

$$\boxed{\mu = \frac{u_p}{u_y}} \tag{2.41}$$

and we introduce Equation 2.41 into Equation 2.40, this equation takes the form:

$$\Delta W_{hyst} = 4f_y(\mu - 1)u_y. \tag{2.42}$$

The maximum potential energy of the system is given by the expression

$$U_e = \frac{1}{2}f_y u_p = \frac{1}{2}f_y\frac{u_p}{u_y}u_y = \frac{1}{2}f_y u_y \mu. \tag{2.43}$$

The introduction of Equations 2.42 and 2.43 into Equation 2.38 results in the following expression (Dwairi and Kowalsky, 2007):

$$\zeta_{hyst} = \frac{1}{4\pi}\frac{4f_y u_y(\mu - 1)}{(1/2)f_y u_y\mu}$$

$$\boxed{\zeta_{hyst} = \frac{2}{\pi}\left(1 - \frac{1}{\mu}\right)} \tag{2.44}$$
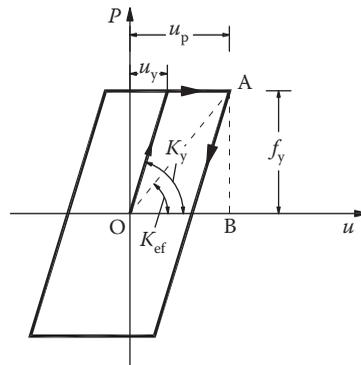
Figure 2.20 Relation between hysteretic damping ζ_{hyst} and ductility μ.
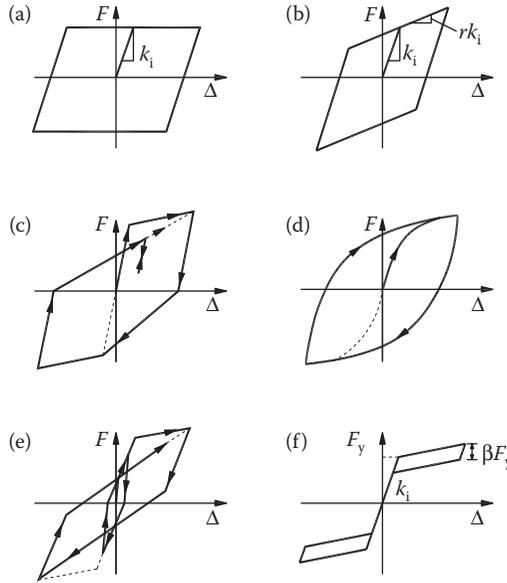
Figure 2.21 Hysteresis rules considered in inelastic time-history analysis. (a) Elastolastic (EPP); (b) bilinear, r = 0.2 (BI); (c) modified clough model; (d) Ramberg–Osgood model; (e) trilinear stiffness-degrading; (f) flag shaped (FS).

The above authors represented ζ_{hyst} in their study in the generalised form:

$$\zeta_{hyst} = \frac{C}{\pi}\left(1 - \frac{1}{\mu}\right) \tag{2.45}$$

where the coefficient C depends on the hysteresis rule (Priestley et al. 2007). In Figure 2.21, various hysteresis rules considered in inelastic analysis are depicted, while in Figure 2.22 (Penelis and Kappos, 1997; Priestley et al., 2007) the hysteretic component of equivalent viscous damping versus displacement ductility μ of two independent studies is given (Grant et al., 2005; Dwari et al., 2007).

2.3.4 Energy dissipation and ductility

The effects of inelastic behaviour on the response of structures to strong seismic motions may be clarified by studying the SDOF system.

Consider two SDOF systems with the same mass M and the same spring stiffness K, and without damping (Figure 2.23). Suppose that both systems vibrate freely and that when they pass through their original equilibrium position they both have the same velocity $\dot{u}_{max} = v_{max}$ (Park and Paulay, 1975). Suppose also that the first one has an elastic connection of ultimate strength V_{1u}, while the second has a strength V_{2u}, which is much lower than V_{1u} (Figure 2.24).

The mass of the first system is subjected to a displacement u_{o1} such that the potential energy stored in the form of strain energy, represented by the area of the triangle OBF, is equal to the kinetic energy of the system:

$$\frac{1}{2}Mv_{max}^2 = \frac{1}{2}Ku_{o1}^2. \tag{2.46}$$
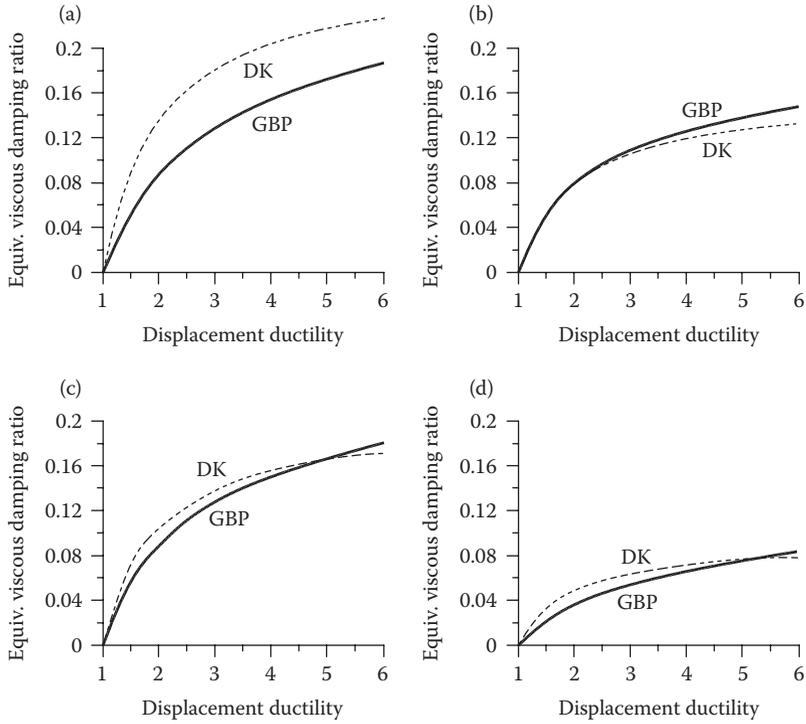
Figure 2.22 Hysteretic component of equivalent viscous damping from two independent studies. (DK indicates Dwairi and Kowalsko, 2007, GBP indicates Grant, D.N. et al. 2005.) (a) Elastoplastic; (b) thin takeda; (c) flat takeda; (d) flag, β = 0.35.
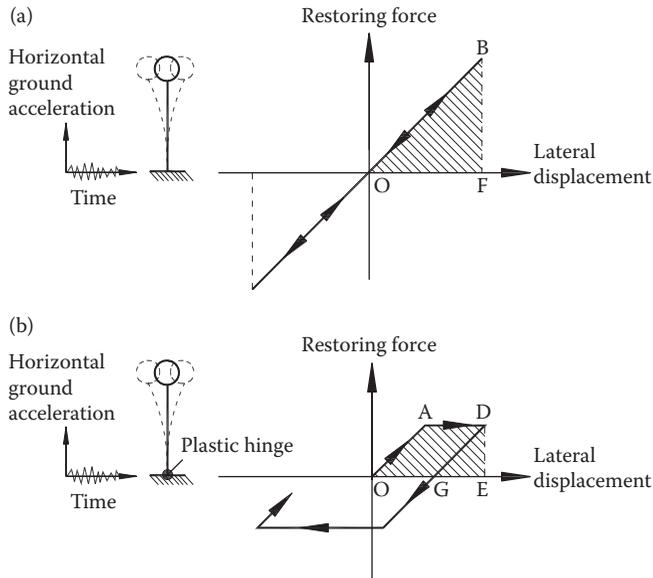
Figure 2.23 Response of SDOF systems to seismic action: (a) elastic response; (b) elastoplastic response.
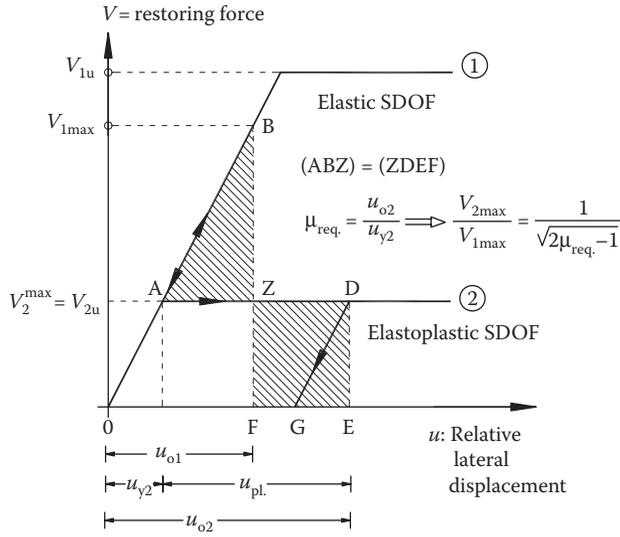
Figure 2.24 Quantitative relation between elastic and elastoplastic response of an SDOF system to an earthquake.

Therefore,

$$u_{01} = \left(\frac{M}{K}\right)^{\frac{1}{2}} v_{max}. \tag{2.47}$$

In this case, a maximum restoring force is developed in the elastic spring, equal to $V_{1max} < V_{1u}$, which coincides with the maximum inertial force $M\ddot{x}_{max}$. Given the fact that the velocity becomes zero, this restoring force starts to accelerate the system in the opposite direction, thus causing oscillations of constant amplitude, since viscous damping has been taken as zero.

The second system, unable to develop a restoring force equal to the first one, is led to the creation of a plastic hinge at the base, with maximum restoring force V_{2u} and maximum displacement u_{o2} such that the area of the trapezoid OADE is equal to the kinetic energy of the system. Thus,

$$\frac{1}{2} M v_{max}^2 = \frac{1}{2} V_{2u} u_{y2} + V_{2u} u_{pl}. \tag{2.48}$$

Therefore,

$$u_{pl} = \frac{1}{2V_{2u}} \left(M v_{max}^2 - V_{2u} u_{y2}\right) \tag{2.49}$$

and the total displacement of the second system is equal to

$$u_{o2} = u_{y2} + u_{pl}. \tag{2.50}$$

For a displacement equal to u_{o2} the system has consumed all its kinetic energy; therefore, under the influence of V_{2u} it begins to move toward its original position. At the moment when V_2 becomes zero, the potential energy that has been transformed into kinetic energy is represented by the area of the triangle EDG because the energy represented by the parallelogram OADG has been dissipated by the plastic hinge in the form of heat and other irrecoverable forms of energy.

From the above it is obvious that, while in the elastic system there is a successive interchange between kinetic and potential energy, which results in a cumulative effect of the successive execution cycles without damping, in the elastoplastic system only part of the kinetic energy is transformed into potential energy from cycle to cycle, a fact that results in a quick hysteretic damping. This means that the displacement u_{o2} as defined above is an upper limit for the elastoplastic system.

From the above discussion it can be concluded that the seismic action on an oscillating system can be resisted either via large restoring forces and oscillation within the elastic range or smaller restoring forces and exploitation of the ability of the system to resist plastic deformations. This ability of the system is characterised as *ductility* and is a property of paramount importance for earthquake-resistant structures because it gives the designer the choice to design the structure for much lower forces than those of the elastic system.

Ductility may be defined either as *ductility demand* or *ductility supply*. The first refers to the ductility requirement for predefined yield strength of the structure under an earthquake action. Speaking in quantitative terms, ductility demand refers to the ductility requirement for a predefined reduction of the restoring force of an inelastic system under a seismic action. The second (ductility supply) refers to the maximum ductility that a structure can develop without collapse or other failure modes.

The ductility supply factor is defined as the ratio of the ultimate deformation at failure to the yield deformation δ_u/δ_y (Figure 2.25). The ultimate deformation at failure is defined for design purposes as the deformation for which the material or the structural element loses only a small predefined percentage of its ultimate strength (e.g., 15% for concrete). The larger the ductility supply factor of a structural element, the larger the safety margins of the element against an earthquake in terms of displacements.

Of particular interest is the determination of the *ductility demand factor* μ_D of a structure for a given ratio of reduction R_μ of the elastic restoring force. Consider an elastoplastic system of mass M, stiffness coefficient K and damping ζ subjected to a seismic action of a given elastic
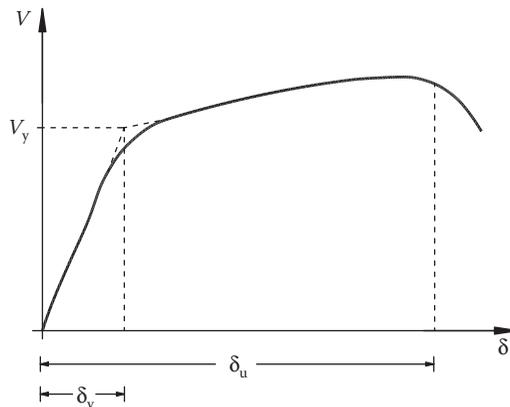
Figure 2.25 Definition of the ductility supply factor.

response spectrum. Under the assumption of fully elastic behaviour, the maximum restoring force V_{el}, which would act on the system, can be easily found from the above data. Now if the system has an ultimate strength V_u, smaller than V_{el}, then the ductility demand factor μ_D of the system, so that it can resist the same earthquake, results from the equation of the potential energy in the two cases (Figure 2.24). Indeed, setting the area of the triangle ABZ equal to the area of the rectangle EDZF, the force reduction factor R_μ results in the following form:

$$R_\mu = \frac{1}{q_\mu} = \frac{V_u}{V_{el}} = \frac{1}{\sqrt{2\mu_D - 1}} \qquad (2.51)$$

where

R_μ is the reduction coefficient of the spectral value of force and μ_D is the ductility demand for this force reduction.

In Equation 2.51, q_μ is called **the behaviour factor** of the structure and, as we will see later, it is the parameter in use in Eurocode 8/2004 in place of R_μ, which represents the reduction factor in use in the American Codes of Practice.

Up to now, in the preceding paragraph the concept of energy dissipation and ductility was examined only in the first quarter of a loading cycle. Therefore, although the above presentation is very important for understanding the meaning of ductility as a concept, the results presented so far must be considered as just a first approximation. Indeed, detailed analytical studies on the dynamic response of inelastic SDOF systems (see also Section 2.5) have shown that, due to heavy damping, the *maximum displacement demands* of an elastic system and the corresponding inelastic one during the seismic excitation are approximately of the same magnitude (Figure 2.26).

Therefore,

$$\mu = \frac{u_{o2}}{u_{y2}} \quad \text{and} \quad u_{o2} = \mu u_{y2} \qquad (2.52a)$$
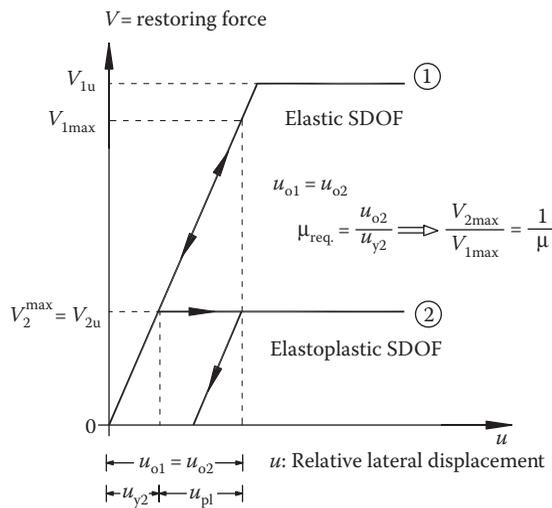
Figure 2.26 An alternative quantitative relation between elastic and elastoplastic response in an SDOF system.

and

$$q_\mu = \mu_D.$$ (2.52b)

In any case, the analytical results so far have shown:

1. SDOF inelastic systems with short fundamental period, that is, systems of high stiffness, present a reduction factor:

$$R_\mu = \frac{1}{q_\mu} = 1.0 \quad \text{for } T < 0.055$$ (2.53)

2. SDOF systems with medium fundamental period, present a reduction factor:

$$R_\mu = \frac{1}{q_\mu} = \frac{1}{\sqrt{2\mu_D - 1}} \quad \text{for } 0.125 < T < 0.5 \text{ s}$$ (2.54)

3. SDOF inelastic systems with a long fundamental period present a reduction factor:

$$R_\mu = \frac{1}{q_\mu} = \frac{1}{\mu_D} \quad \text{for } T > 1.0 \text{ s}$$ (2.55)

For intermediate periods, a linear interpolation is suggested (Newmark and Hall, 1982; Figure 2.27).

The above is the first and simplest formulation used in practice and has been confirmed by other studies. Figure 2.28 shows the two curves described by relationships Equations 2.51 and 2.52 as well as the results of an inelastic analysis of several SDOF systems for the 1940 El Centro earthquake, *N–S* component (Blume, 1967; Wiegel, 1970). Further improvements, however, have been accomplished by many studies since (Krawinkler and Nassar, 1992; Borzi and Elnashai, 2000). The main aim of the above efforts was to incorporate the fundamental period and the stress–strain law in the relation of q_μ and μ_D (Figure 2.27; Elnashai and Di Sarno, 2008).

Eurocode 8-1/2004 has adopted for the relation among behaviour factor q_o, displacement ductility μ_δ and fundamental period T the expressions presented by Vidic et al. (1994), as will be seen in detail in Equation 5.17 found in Paragraph 5.4.4.1.

2.3.5 Physical meaning of the ability for energy absorption (damping)

It is useful to explain here what the term 'ability for energy absorption' means for reinforced concrete structures. Consider the cantilever of Figure 2.29, which is loaded at the top with a horizontal force *V*. By increasing *V*, the cantilever reaches an ultimate limit state. Failure can occur in two ways, either by yielding of reinforcement in normally reinforced sections, or by crushing of concrete in over-reinforced sections, where the strength of the compressive zone is lower than the yield strength of the reinforcement.

In the first case, for a very small increase of *V* above yielding, the displacement δ exhibits considerable values (Figure 2.29g), and this is accomplished through opening of the cracks on the tensile side of concrete due to yielding of reinforcement. After successive steps and
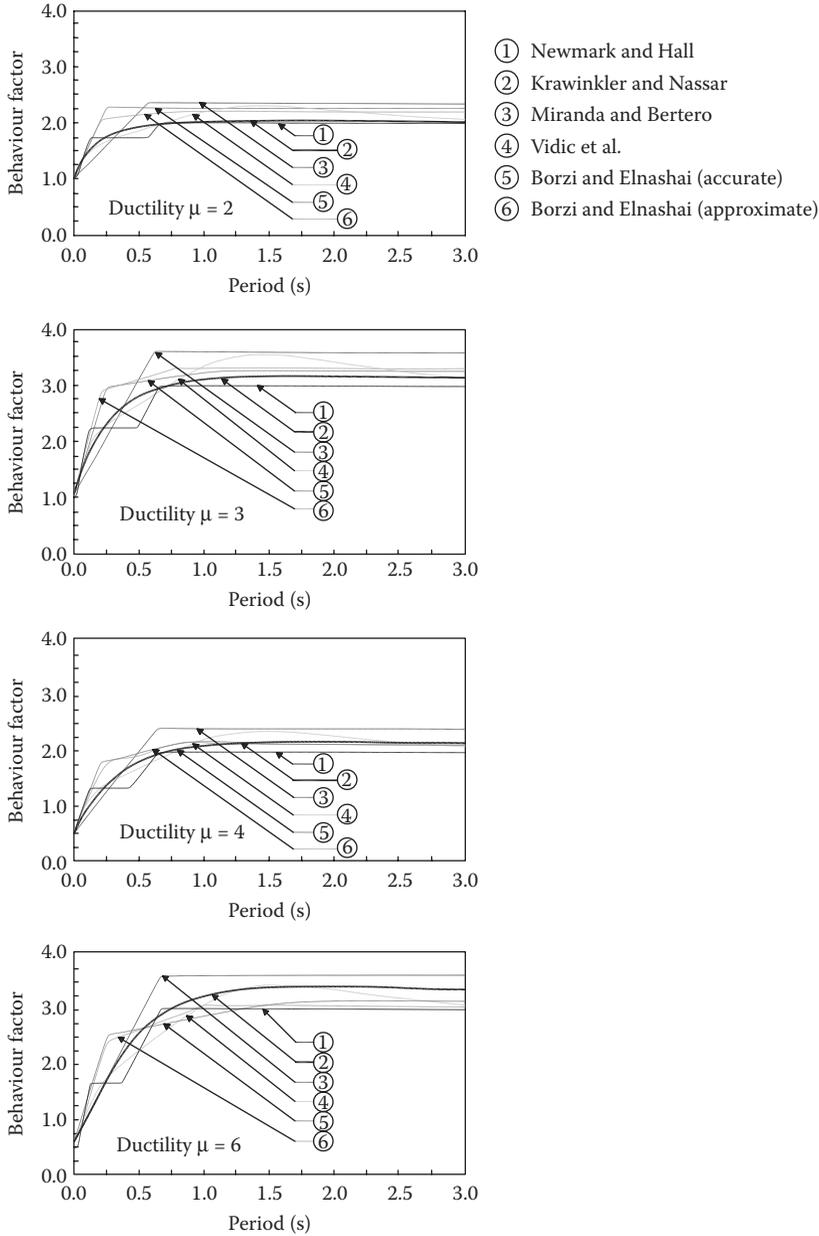
Figure 2.27 Comparison of (demand) derived by using different expressions for elastic—perfectly plastic systems on rock site; values of ductility μ: 2, 3, 4 and 6. (From Elnashai, A.S. and Di Sarno, L. *Fundamentals of Earthquake Engineering*, 2008. Copyright Wiley-VCH Verlag GmbH & Co. KGaA. Reproduced with permission.)

when large plastic deformations of steel in the tensile side have been developed, because of the increasing of the width of the cracks, the depth of the compression zone is substantially decreased and the concrete at the compression side is crushed. Beyond this point there is a rapid deterioration of the structural system and a steep descending branch on the V–δ diagram (Figure 2.29g curve 1). In the second case (fracture of the compression zone without
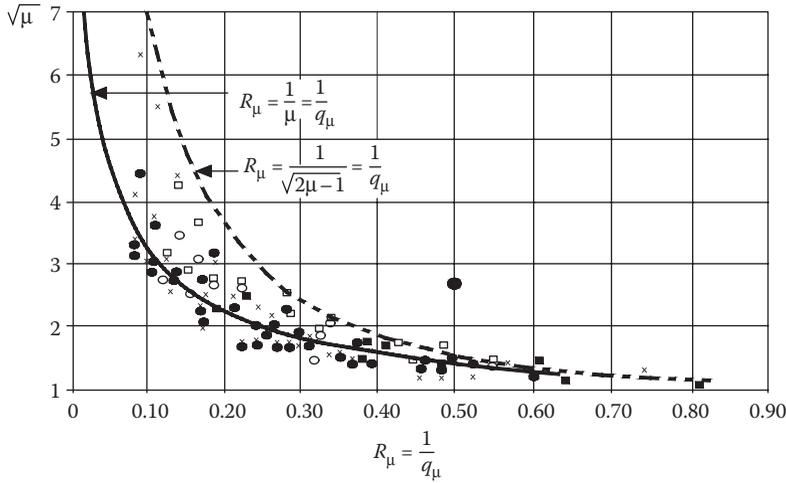
Figure 2.28 Force reduction factor R_μ or $(1/q_\mu)$ versus $\sqrt{\mu}$.

yielding of the reinforcement), there is a brittle failure (Figure 2.29g curve 2) and a steep descending branch on the P–δ diagram, without the development of plastic deformations.

In the first case there is a large amount of available ductility (supply); however, in order to make use of it, some yielding zones in the structure must be tolerated, which of course implies accepting *some degree of damage due to the appearance of wide cracks*. In the second case, the available ductility is very small. Therefore, over-reinforced systems present low ductility. The design and detailing of R/C structural elements and buildings as a whole will be discussed in detail in Chapters 8, 9 and 10.

At this point it will be useful to approach the concept of the ductility factor (supply) and the way it is defined in some detail. So far, the ductility factor has been defined in terms of displacement for the SDOF system, that is,

$$\mu_\delta = \frac{\delta_u}{\delta_y}.$$
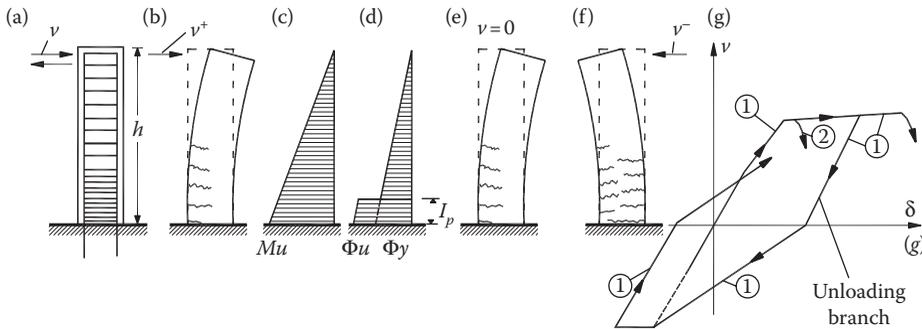
Figure 2.29 Inelastic response of a cantilever R/C beam under cyclic loading: (a) arrangement of cantilever loading; (b) loading with V^+ beyond yielding; (c) ultimate failure moment diagram; (d) distribution of curvature φ-plastic hinge zone l_p; (e) unloading $V = 0$; (f) loading with V^- beyond yielding; (g) V–δ diagram for normally reinforced (1) and over-reinforced (2) cantilever.

However, the ductility factor may be defined in terms of plastic rotations of structural members at plastic hinges, that is,

$$\mu_\theta = \frac{\theta_u}{\theta_y}$$

and at the end of yielding sections in terms of curvatures:

$$\mu_\varphi = \frac{\varphi_u}{\varphi_y}.$$

It is known from the theory of strength of materials that there are well-defined relations among $\mu_\varphi - \mu_\theta - \mu_\delta$. In Subsection 5.4.4 it will be presented in detail how one can go from the level of the section curvature to the level of the member rotations, and finally to the level of the displacement structural system as a whole.

At this point it can only be noted that for a given ductility factor in terms of displacements, the ductility factor in terms of rotations is larger, while the ductility factor in terms of curvatures is much larger:

$$\mu_{\delta supl} \leq \mu_{\theta supl} < \mu_{\varphi supl} \tag{2.56}$$

2.3.6 Inelastic response spectra

2.3.6.1 Inelastic acceleration response spectra

The main problem in the development of an inelastic response spectrum is the solution of the differential equation of motion of an SDOF inelastic system.

$$\boxed{M\ddot{u} + c\dot{u} + K(t)u = -M\ddot{x}_o(t)} \tag{2.57}$$

This equation is identical to Equation 2.3 except that the stiffness K is not a constant but a function of time, or better, a function of u, which is a function of time. Therefore, Equation 2.57 is not a linear differential equation anymore and, as a consequence, this equation can be integrated using only numerical methods. Various methods have been developed so far for this integration (e.g., Newmark methods); however, the presentation of this integration is beyond the scope of this book (Biggs, 1964; Clough and Penzien, 1975; Chopra, 2001).

However, what should be noted here is that the integration of Equation 2.57 can be done only if the constitutive law ($V–u$ diagram) of the SDOF inelastic system (e.g., Figure 2.30) is known. So, as the linear response spectrum gives the maximum response of the elastic system of a given viscous damping for a given accelerogram, in the same way the inelastic response spectrum gives the maximum response of the inelastic system of a given ductility demand, $\mu_D = (u_{max}/u_y)$ for a given accelerogram.

In Figure 2.31 the inelastic acceleration response spectra of the Kalamata, Greece earthquake of 1985, component $N\ 10^0W$ are shown for various ductility demand factors $\mu_D(\mu_D = 1, 2, 4, 6)$ and for the Clough–Riddel–Newmark hysteresis model (Clough and Johnston, 1966; Riddel and Newmark, 1979), which has been widely used for reinforced concrete.

It is evident that the development of inelastic acceleration response spectra directly from Equation 2.57 is a time-consuming and painful exercise. That is why extended studies have been carried out for years for the determination of relationships between R or q_μ and μ_D (see Subsection 2.3.4, Equations 2.51, 2.52). So, *the inelastic acceleration response spectrum*

$$V_{el} = K_o\, u_y$$
$$V_{el} = K_o\, u_{el}$$
$$\mu_D = \frac{u_{max}}{u_y}$$
$$R_\mu = \frac{V_y}{V_{el}} = \frac{1}{q_\mu}$$
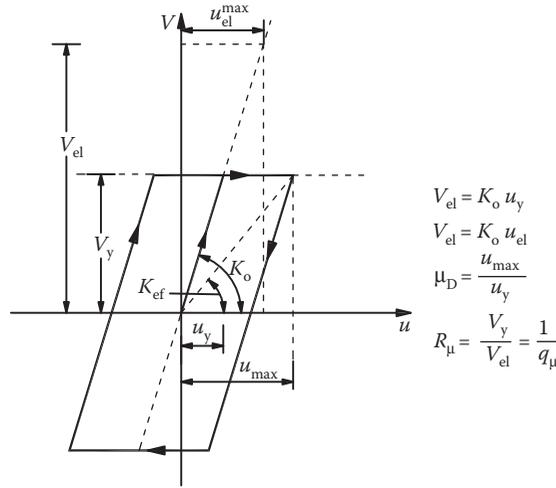
Figure 2.30 V–u diagram for an elastoplastic constitutive law of an SDOF system.

for a given ductility demand factor μ_D can easily be determined with a good approximation from the elastic one by reducing its ordinates by the reduction factors R of Equations 2.53, 2.54 and 2.55, or other similar ones proposed by other authors (see Figure 2.27).

The reduction of the elastic spectra by employing *R*-factors given above is the simplest and most popular approach to derive inelastic acceleration spectra and *is employed in most modern Codes of Practice for force-based design* (see Subsection 3.4.3).

2.3.6.2 *Inelastic displacement response spectra*

Inelastic displacement response spectra are similar to the elastic ones. Maximum displacements are obtained either as ordinates of equal damping coefficient curves or as ordinates
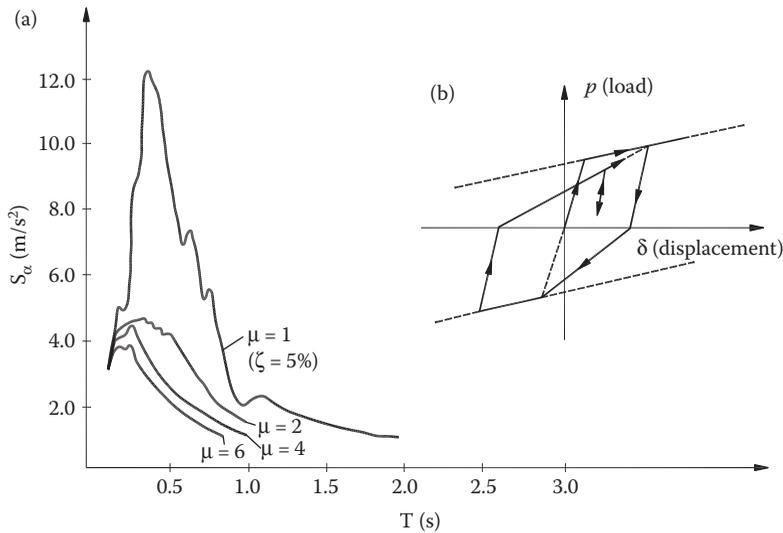
Figure 2.31 (a) Inelastic spectra of the Kalamata (1986), Greece, earthquake components N10⁰W, for various ductility factors μ; (b) Clough–Riddel–Newmark hysteresis model.
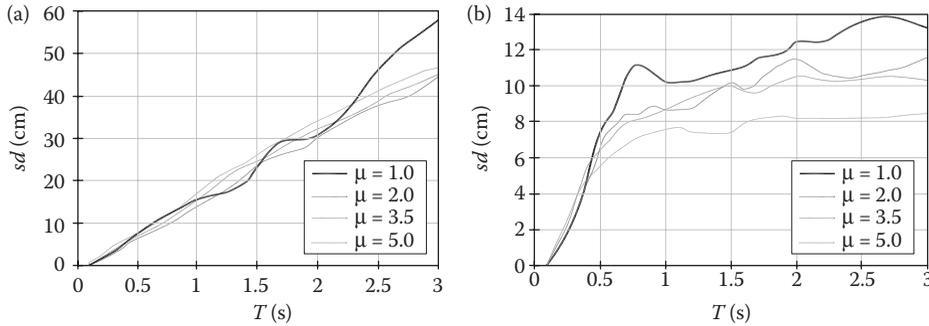
Figure 2.32 Inelastic displacement response spectra for mean alluvial ground layers in the United States (a) and in Greece (b). (Adapted from Kappos, A.J. and Kyriakakis, P. 2001. *Soil Dynamics and Earthquake Engineering*, 20, 111–123.)

of equal ductility demand versus natural periods, since these two options are equivalent according to Equations 2.44 and 2.45 (Figure 2.32). They have the same characteristics as the elastic ones with damping.

It is important to note that for periods up to 1.0 s. the maximum displacements are not much affected by the ductility factor.

2.4 DYNAMIC ANALYSIS OF MDOF ELASTIC SYSTEMS

2.4.1 Introduction

The scope of this book does not allow a detailed approach to the dynamic analysis of systems with more than one degree of freedom. Standard textbooks on structural dynamics (Biggs, 1964; Clough and Penzien, 1975; Warburton, 1976; Anastasiadis, 1989; Chopra, 2001) allow a detailed approach to the subject. However, since the elastic dynamic analysis of MDOF systems is the *reference method of analysis* for modern Codes and particularly EC8-1/2004, it was decided that some major issues should also be presented here, for a better understanding of the main parts of this book.

2.4.2 Equations of motion of plane systems

The number of degrees of freedom of a lumped-mass system is determined by the minimum number of independent displacements and rotations of the lumped masses whereby their geometric position can be defined at a given moment. Thus, in a plane frame, with the mass concentrated in the beams of the storeys and with large axial stiffness of the beams, which are both very realistic assumptions for typical R/C structures, the degrees of freedom are determined by the number of storeys, while the independent variables of motion are their horizontal displacements u relative to the base (Figure 2.33).

The motion of the plane frame of Figure 2.33 is expressed by a system of n linear differential equations with constant coefficients, which can easily be generated. Indeed, the equation of motion of a storey (Figure 2.33) as in the case of the SDOF system (Subsection 2.2.1), can be generated using the dynamic equilibrium equation of d'Alembert, that is,

$$P_{si}(t) + P_{di}(t) + m_i \ddot{x}_i(t) = 0 \tag{2.58}$$
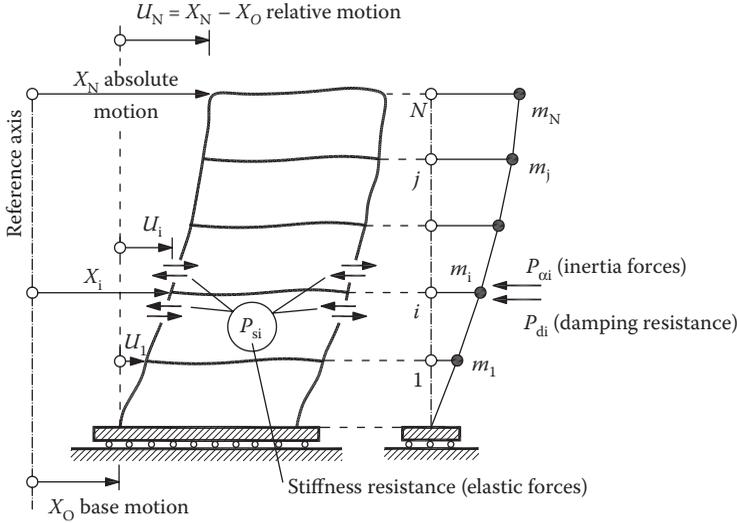
Figure 2.33 Dynamic equilibrium of elastic, damping, and inertial forces at the level of a storey (d'Alembert equation).

or, keeping in mind that

$$P_{si}(t) = \kappa_{i1}u_1(t) + \kappa_{i2}u_2(t) + \cdots + \kappa_{ii}u_i(t) + \cdots + \kappa_{in}u_N(t)$$
$$P_{di}(t) = c_{i1}\dot{u}_1(t) + c_{i2}\dot{u}_2(t) + \cdots + c_{ii}\dot{u}_i(t) + \cdots + c_{in}\dot{u}_N(t)$$
$$m_i\ddot{x}(t) = m_i\ddot{x}_o(t) + m_i\ddot{u}_i(t)$$

the above equation of motion takes the form:

$$m_i\ddot{u}_i(t) + \left(c_{i1}\dot{u}_1(t) + c_{i2}\dot{u}_2(t) + \cdots + c_{in}\dot{u}_{1N}(t)\right) +$$
$$+ \left(\kappa_{i1}u_1(t) + \kappa_{i2}u_2(t) + \cdots + \kappa_{in}u_N(t)\right) = -m_i\ddot{x}_o(t). \tag{2.58a}$$

So, the system of equations of motion takes the form:

$$\boxed{\mathbf{M}\ddot{\mathbf{u}}(t) + \mathbf{C}\dot{\mathbf{u}}(t) + \mathbf{K}\mathbf{u}(t) = \mathbf{M}[d]\ddot{x}_o(t)} \tag{2.58b}$$

where

$$\mathbf{x}(t) = \mathbf{u}(t) + [d]x_o(t)$$

$$\mathbf{M} = \begin{pmatrix} m_1 & & \\ & m_2 & \\ & & m_n \end{pmatrix}, \quad \mathbf{C} = \begin{pmatrix} c_{11} & c_{12} & \cdots & c_{1N} \\ c_{21} & c_{22} & \cdots & c_{2N} \\ & & \vdots & \\ c_{N1} & c_{N2} & \cdots & c_{NN} \end{pmatrix}$$

$$\mathbf{K} = \begin{pmatrix} K_{11} & K_{12} & \cdots & K_{1N} \\ K_{21} & K_{22} & \cdots & K_{2N} \\ & & \vdots & \\ K_{N1} & K_{N2} & \cdots & K_{NN} \end{pmatrix}, \quad \mathbf{u} = \begin{pmatrix} u_1 \\ u_2 \\ \vdots \\ u_N \end{pmatrix}, \quad \mathbf{d} = \begin{pmatrix} 1 \\ 1 \\ \vdots \\ 1 \end{pmatrix}$$

The notation of the above equations is given in Figures 2.33 and 2.34.

The free vibration behaviour of a plane frame is expressed by the above equation of motion (2.58a or b), taking into account that in this case the damping matrix $\mathbf{C}$ and the applied excitation vector $\mathbf{M}[1]\ddot{x}_o(t)$ are both zero. So,

$$\boxed{\mathbf{M}\ddot{u}(t) + \mathbf{K}\mathbf{u}(t) = 0.}$$

(2.59)

Comparing Equation 2.59 with Equation 2.3a of a free vibration of the SDOF system, one can easily assume that the displacement vector $\mathbf{u}$ may be expressed in the form:

$$\mathbf{u} = \bar{\mathbf{u}}\sin\omega t$$

(2.60)

and

$$\ddot{u} = -\omega^2\bar{\mathbf{u}}\sin\omega t$$

(2.61)

where $\bar{\mathbf{u}}$ represents the amplitude of the vibratory motion and ω is the circular frequency. Introducing Equations 2.60 and 2.61 into Equation 2.59 we obtain:

$$\left(-\omega^2\mathbf{M}\bar{\mathbf{u}} + \mathbf{K}\bar{\mathbf{u}}\right)\sin\omega t = 0$$

(2.62)

Taking into account that in Equation 2.62 $\sin\omega t \neq 0$, it may be concluded that

$$\boxed{-\omega^2\mathbf{M}\bar{\mathbf{u}} + \mathbf{K}\bar{\mathbf{u}} = 0.}$$

(2.63a)

That is, a system of linear homogeneous equations for which it is known that in order for a solution for $\bar{\mathbf{u}}$ other than zero to exist, the determinant must be equal to zero, that is,

$$\mathrm{Det}\left|-\omega^2\mathbf{M} + K\right| = 0.$$

(2.63b)
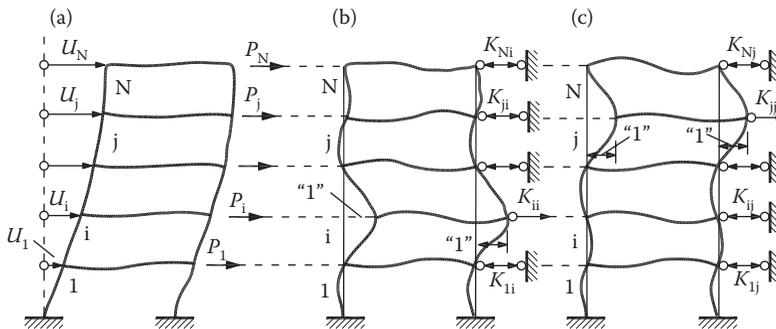
Figure 2.34 Determination of the vectors of the stiffness matrix K (K_i and K_j).

Equation 2.63a, b represents *a classic eigenvalue problem*. Its solution may be carried out by a variety of procedures. Standard digital computer codes are available for providing automatic solutions.

The solution of the eigenvalue equation of a plane frame system having *n* degrees of freedom provides, for each of its *n* modes of vibration, called *normal* or *natural* modes of vibration, the following output:

- The vibration frequency ω_i (or period $T_i = (2\pi/\omega_i)$)
- The vibration shape $j_i^T = \left[\varphi_{1i}, \varphi_{2i}, \cdots \varphi_{ii} \cdots \varphi_{ni}\right]$

The conclusions from the above analysis may be summarised as follows:

1. *The normal or natural modes* are the free, undamped periodic oscillations within which linear combinations represent the position of the system at every moment.
2. For every such normal mode all the masses of the system oscillate *in phase*, that is, at every moment the ratio of the displacements of the damped masses remains constant. As a result, all masses go through rest position and reach maximum amplitude simultaneously.
3. The number *n* of normal modes is equal to the number of degrees of freedom. Every normal mode is related to a natural frequency or period of vibration known as the *natural period*. The normal mode with the longest natural period is by definition the *first or fundamental normal mode*.

Figure 2.35 shows the three normal modes of a three-storey frame. Note that the curves intersect the vertical axis at a number of points (including the one at the base), which coincide
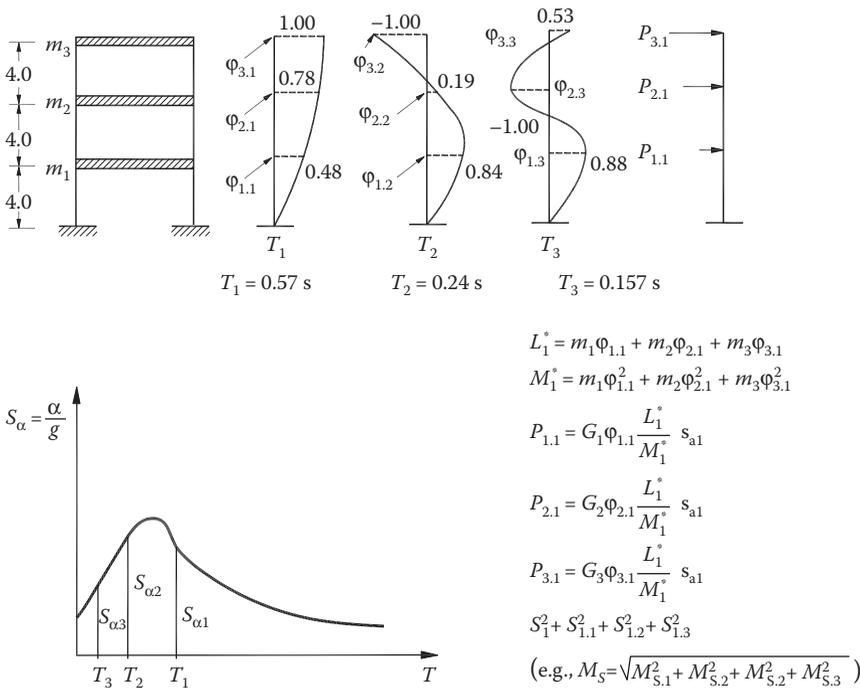
Figure 2.35 A three-storey plane frame analysed according to spectral modal analysis.

with the order of the natural mode. The amplitudes of each natural mode are normalised. Figure 2.35 shows the typical normal modes that correspond to the three-storey building of the figure. The eigen vectors of these modes are

$$j_1 = \begin{pmatrix} 1.00 \\ 0.78 \\ 0.45 \end{pmatrix}, \quad j_2 = \begin{pmatrix} -1.00 \\ 0.19 \\ 0.84 \end{pmatrix}, \quad j_3 = \begin{pmatrix} 0.53 \\ -1.00 \\ 0.88 \end{pmatrix}$$

while the eigen periods are given below:

$T_1 = 0.57$ s, $T_2 = 0.24$ s, $T_3 = 0.157$ s.

It is important to note again that the ratio of the displacements at any moment is constant for each normal mode.

In the next paragraph the two methods for the dynamic analysis of elastic MDOF plane systems, which make use of the above presented modal analysis, will be presented.

2.4.3 Modal response spectrum analysis versus time–history analysis

2.4.3.1 General

1. The term 'dynamic analysis of multidegree of freedom (MDOF) systems' refers to two analytical approaches slightly different from each other. The first, known as *modal response spectrum analysis*, approximates the values of the maximum response parameters (e.g., displacements, bending moments) as a combination of the maximum responses that correspond to every mode. Every contributing eigenmode behaves as an independent SDOF system with a certain characteristic natural period, and the maximum response for this specific natural mode can result from the corresponding spectrum for an SDOF system.

   There are several methods of combining modal contributions, taking into account that the maxima of the different modes do not occur at the same time. The most common method takes *the square root of the sum of the squares* of the maximum modal amplitudes, treating them as random quantities (SRSS method). In the case where the natural periods are only slightly different from each other (closely coupled modes), the square root of the sum of the squares underestimates the expected final value. Therefore, more reliable combination techniques are used, as it will be discussed later. Usually, only the contribution of the first few modes is taken into account, since they contribute the largest portion of the response.

2. Modal response spectrum analysis is the most widely used method for the design of structures and it is the reference method for the analysis of buildings according to EC 8-1/2004. Normalised spectra, based on a number of seismic records and scaled to typical reference intensity, are used as response spectra. The use of normalised spectra provides a simple tool for studying the variation of the response to different seismic inputs. In the following chapters, frequent reference will be made to normalised response spectra.

3. The second method, known as *time-history analysis*, produces the response of the model of the structure over time, when it is subjected to a base acceleration. Either superposition of the normal modes or direct numerical integration of the equations of motion is used for the analysis. In both cases, the total response of the system is calculated at the end of a very small time step, and the analysis proceeds stepwise, using the end conditions of the previous step as initial conditions for the next one.

2.4.3.2 Modal response spectrum analysis

The analysis of multi-storey plane structures using this method is commonly performed with the aid of a proper computer code. The procedure is the following:

1. First, the natural periods and normal modes are determined, that is,

$$
j_1 = \overset{T_1}{\begin{pmatrix} \varphi_{1,1} \\ \varphi_{2,1} \\ \vdots \\ \varphi_{i,1} \\ \vdots \\ \varphi_{n,1} \end{pmatrix}}, \quad
j_2 = \overset{T_2}{\begin{pmatrix} \varphi_{1,2} \\ \varphi_{2,2} \\ \vdots \\ \varphi_{i,2} \\ \vdots \\ \varphi_{n,2} \end{pmatrix}}, \quad
j_i = \overset{T_i}{\begin{pmatrix} \varphi_{1,i} \\ \varphi_{2,i} \\ \vdots \\ \varphi_{i,i} \\ \vdots \\ \varphi_{n,i} \end{pmatrix}}, \quad
j_n = \overset{T_n}{\begin{pmatrix} \varphi_{1,n} \\ \varphi_{2,n} \\ \vdots \\ \varphi_{i,n} \\ \vdots \\ \varphi_{n,n} \end{pmatrix}}
$$

2. From each normal mode the effective:
    a. Modal mass M_i^*
    b. Modal excitation factor L_i^*
    c. Modal participation factor (L_i^*/M_i^*), and
    d. Modal maximum inertial forces P_{ij}
    are determined, as follows:

$$
\left.\begin{aligned}
L_1^* &= m_1\varphi_{1,1} + m_2\varphi_{2,1} + \cdots + m_i\varphi_{i,1} + \cdots + m_n\varphi_{n,1} \\
M_1^* &= m_1\varphi_{1,1}^2 + m_2\varphi_{2,1}^2 + \cdots + m_i\varphi_{i,1}^2 + \cdots + m_n\varphi_{n,1}^2 \\
&\text{participation factor}: \frac{L_1^*}{M_1^*} \\
P_{1,1} &= G_1\varphi_{1,1}\frac{L_1^*}{M_1^*}S_{a,1} \\
P_{2,1} &= G_2\varphi_{2,1}\frac{L_1^*}{M_1^*}S_{a,1} \\
P_{i,1} &= G_i\varphi_{i,1}\frac{L_1^*}{M_1^*}S_{a,1} \\
&\quad\vdots \\
P_{n,1} &= G_n\varphi_{n,1}\frac{L_1^*}{M_1^*}S_{a,1}
\end{aligned}\right\} \text{1st mode}
$$

$$
\left.\begin{aligned}
L_2^* &= m_1\varphi_{1,2} + m_2\varphi_{2,2} + \cdots + m_i\varphi_{i,2} + \cdots + m_n\varphi_{n,2} \\
M_2^* &= m_1\varphi_{1,2}^2 + m_2\varphi_{2,2}^2 + \cdots + m_i\varphi_{i,2}^2 + \cdots + m_n\varphi_{n,2}^2 \\
&\text{participation factor}: \frac{L_2^*}{M_2^*} \\
P_{1,2} &= G_1\varphi_{1,2}\frac{L_2^*}{M_2^*}S_{a,2} \\
P_{2,2} &= G_2\varphi_{2,2}\frac{L_2^*}{M_2^*}S_{a,2} \\
&\quad\vdots \\
P_{i,2} &= G_i\varphi_{i,2}\frac{L_2^*}{M_2^*}S_{a,2} \\
&\quad\vdots \\
P_{n,2} &= G_n\varphi_{n,2}\frac{L_2^*}{M_2^*}S_{a,2}
\end{aligned}\right\} \text{2nd mode}
$$

$$L_i^* = m_1\varphi_{1,i} + m_2\varphi_{2,i} + \cdots + m_i\varphi_{i,i} + \cdots + m_n\varphi_{n,i}$$

$$M_i^* = m_1\varphi_{1,i}^2 + m_2\varphi_{2,i}^2 + \cdots + m_i\varphi_{i,i}^2 + \cdots + m_n\varphi_{n,i}^2$$

$$\text{participation factor} : \frac{L_i^*}{M_i^*}$$

$$P_{1,i} = G_1\varphi_{1,i} \frac{L_i^*}{M_i^*} S_{a,i}$$

$$P_{2,i} = G_2\varphi_{2,i} \frac{L_i^*}{M_i^*} S_{a,i}$$

$$\vdots$$

$$P_{i,i} = G_i\varphi_{i,i} \frac{L_i^*}{M_i^*} S_{a,i}$$

$$\vdots$$

$$P_{n,i} = G_n\varphi_{n,i} \frac{L_i^*}{M_i^*} S_{a,i}$$

ith mode

$$L_n^* = m_1\varphi_{1,n} + m_2\varphi_{2,n} + \cdots + m_i\varphi_{i,n} + \cdots + m_n\varphi_{n,n}$$

$$M_n^* = m_1\varphi_{1,n}^2 + m_2\varphi_{2,n}^2 + \cdots + m_i\varphi_{i,n}^2 + \cdots + m_n\varphi_{n,n}^2$$

$$\text{participation factor} : \frac{L_n^*}{M_n^*}$$

$$P_{1,n} = G_1\varphi_{1,n} \frac{L_n^*}{M_n^*} S_{a,n}$$

$$P_{2,n} = G_2\varphi_{2,n} \frac{L_n^*}{M_n^*} S_{a,n}$$

$$\vdots$$

$$P_{i,n} = G_i\varphi_{i,n} \frac{L_n^*}{M_n^*} S_{a,n}$$

$$\vdots$$

$$P_{n,n} = G_n\varphi_{n,n} \frac{L_n^*}{M_n^*} S_{a,n}$$

nth mode

In the above expressions:

G_i is the gravity load in (kN)

or the respective mass $(G_i/10)(\text{KN/m/s}^2)$

S_{ai} is the seismic motion pseudo-acceleration corresponding to the normal period T_i (Figure 2.35), expressed in the first case as a percentage of g ($g \cong 10$ m/s^2) or in the second one in natural value (m/s^2).

It should be noted that:

a. The sum of all modal participation factors (L_i^*/M_i^*) is equal to unity
b. The participation factors diminish in parallel with the shortening of the normal periods
c. Consequently, for plane or symmetric pseudo-spatial systems, the first 2 to 3 eigenvalues are enough to cover the dynamic excitation of a very large percentage of the mass of the system (more than 90%)

3. For the maximum inertial forces of each normal mode, the probable maximum values of the response parameters (moments, shears, displacements, etc.) are determined through a classic static analysis. It should be noted that the superposition of SRSS should never be implemented in any case for the maximum inertial forces (e.g. $\sqrt{P_{1,2}^2 + P_{2,2}^2 + P_{2,3}^2}$ in Figure 2.35). If a procedure of this type is followed, *erroneous results* are derived for the various response parameters of the structure.

4. The above response quantities for the modes under consideration are superimposed by taking the square root of the sum of their squares (SRSS), that is,

$$S_1 = \sqrt{S_{1,1}^2 + S_{1,2}^2 + S_{1,3}^2 + \cdots + S_{1,n}^2} \tag{2.64}$$

Therefore, for the bending moments, for example, the above relation takes the form

$$M_s = \sqrt{M_{s,1}^2 + M_{s,2}^2 + M_{s,3}^2 + \cdots + M_{s,n}^2}. \tag{2.65}$$

Thus, the superposition is based on the concept that all modes do not reach their maximum simultaneously and that the responses in the vibration modes may be considered independent of each other. Therefore, according to probability theory (Clough, 1970), their most probable maximum value results through the SRSS.

It is evident that the results of this procedure may have either a plus or minus sign and, therefore, in all following calculations they must be introduced with both signs. When the values of the natural period of any successive modes are very close, the above postulated independence does not apply. So, the concept of mode independence according to EC8-1 (CEN 1998-1, 2004) is considered to be fulfilled if

$$T_j \leq 0.9 T_i \quad (i < j) \tag{2.66}$$

where T_i, T_j are the natural periods of any two successive modes of vibration taken into account for the determination of seismic effects.

If Equation 2.66 is not satisfied, a more accurate procedure, the 'complete quadratic combination' (CQC) must be adopted (Wilson and Burton, 1982; Chopra, 2001), that is,

$$S_1 \cong \left(\sum_{n=1}^{n} S_{1n}^2 + \underbrace{\sum_{i=1}^{n} \sum_{n=1}^{n}}_{i \neq n} \rho_{in} S_{1i} S_{1n} \right)^{1/2} \tag{2.67}$$

and

$$\rho_{in} = \frac{8\zeta^2 (1 + \beta_{in}) \beta_{in}^{3/2}}{\left(1 - \beta_{in}^2\right)^2 + 4\zeta^2 \beta_{in} (1 + \beta_{in})^2} \tag{2.68}$$

where

$$\beta_{in} = \frac{\omega_i}{\omega_n}$$
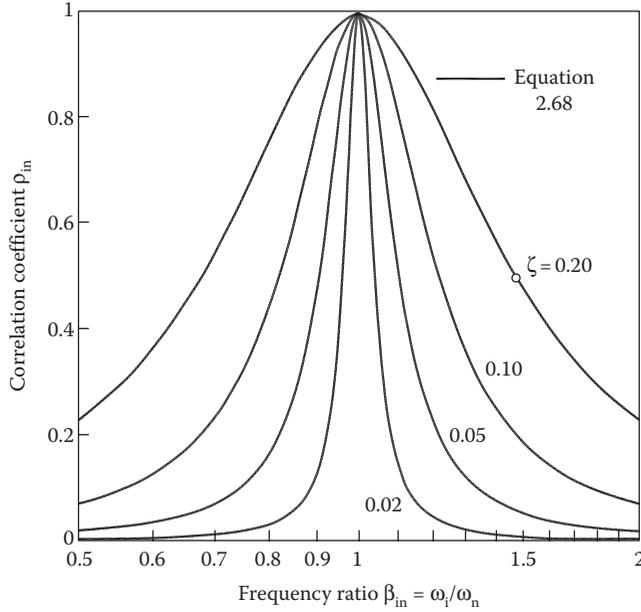
Figure 2.36 Variation of correlation coefficient p_{in} given by Equation 2.68. (Adapted from Chopra, A.K. 2001. *Dynamics of Structures: Theory and Application in Earthquake Engineering*, 2nd Edition. Prentice-Hall, New Jersey.)

This equation (Der Kiureghian, 1981) implies that

$$\rho_{in} = \rho_{ni} \quad \text{for} \quad i \neq n$$
$$\rho_{in} = 1 \quad \text{for} \quad i = n$$

In Figure 2.36 the coefficient ρ_{in} is plotted as a function of $\beta_{in} = \omega_i/\omega_n$ according to Equation 2.68. It is apparent that this coefficient is reduced rapidly, as the two natural frequencies ω_i and ω_n move apart.

2.4.3.3 Time-history analysis

For time-history analysis, two different procedures may be followed: modal analysis or direct numerical integration.

When the modal analysis procedure is chosen and the normal modes of the system are found, the displacement $u_i(t)$ of the mass of an MDOF system with n degrees of freedom can be expressed as the linear combination of the characteristic modal displacements and a function of time $q_j(t)$:

$$u_i(t) = \sum_{j=1}^{n} \varphi_{ij} q_j(t) \tag{2.69}$$

where j is the order of the normal mode. In matrix form, this relation is expressed as follows:

$$\mathbf{u}(t) = F\,\mathbf{q}(t)$$

where Φ is the $(n \times n)$ modal matrix, each column of which represents the modal displacements φ_j (eigen vectors) of mode j, and $\mathbf{q}(t)$ the vector of time functions, each element $q_j(t)$ of which represents the time function of the oscillation at the jth mode, for an inertial load:

$$\frac{\varphi_j^T \mathbf{M} \mathbf{i}}{\varphi_j^T \mathbf{M} \varphi_j} \ddot{x}_o(t) \tag{2.70}$$

where $\mathbf{M}$ is the $(n \times n)$ diagonal mass matrix and $\ddot{x}_o(t)$ is the time history of the base acceleration.

The modal analysis briefly described above allows for a significant reduction in computing time, since the determination of the normal modes and natural periods is done only once. The rest of the calculations deal with the determination of the response of the SDOF systems.

If the method of direct numerical integration is chosen, the system of differential equations for every time step is transformed into a system of algebraic equations involving the displacements. The known terms of the system are found using a certain assumption for the variation of the base acceleration during the integration interval (e.g., linear variation).

No matter which of the two procedures is chosen, the system must be analysed for a series of base accelerograms (typically three to five) scaled to a common level of spectrum intensity, so that the results of this method are sufficiently reliable.

The implementation of time-history analysis, even for a typical multi-storey building, requires too much computational time. Thus, the use of this method can only be justified in special cases. For all other cases, if a dynamic analysis is chosen, it can be performed with the aid of *modal response spectrum analysis*.

2.4.4 Pseudospatial structural single-storey system

2.4.4.1 General

The pseudospatial structural system is the most common model in use for the analysis and design of multi-storey buildings. Its extended use in recent decades must be attributed to the tremendous development in computer-aided structural analysis (Figure 2.37). This progress
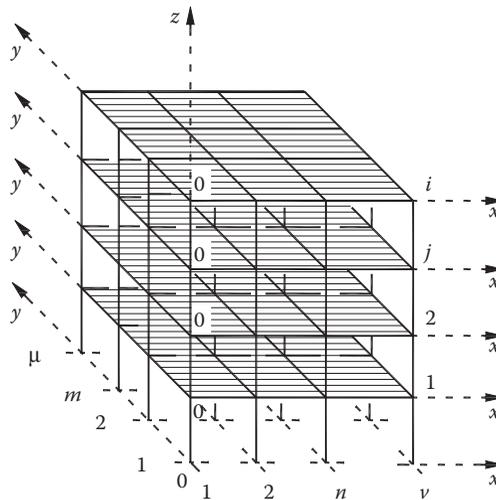
Figure 2.37 The geometry of a pseudospatial frame.

of the last 40 years has made it possible for the structural engineer to approach the structural system of buildings as a space structure without being obliged to analyse it in simpler plane systems, no matter if static or dynamic analysis is used. Even so, the assumption of considering the floors of buildings as rigid diaphragms in their plane simplifies the problem and diminishes the required computer capacity and computing time as well, because it leads to a drastic reduction in the number of unknown 'displacements' in application of the direct stiffness method.

In R/C buildings, the in-plane stiffness of the floors in usually large enough in comparison to the lateral stiffness of the vertical structural elements that the displacement and rotation of any joint in-plane of the floor can be expressed as a linear function of two displacements, u_{mx} and u_{my}, of the centre of mass and a rotation ϕ_{mz} in respect to z-axis ('displacements' of the rigid disc). Thus, the independent deformations of every joint i are limited to two rotations φ_{xi} and φ_{yi} in respect to x–x and y–y axes and a vertical displacement u_{zi}. This system is known as a '*pseudospatial structural system*'.

In this system, if the strains of all columns to axial deformation are assumed to be equal, resulting from the reasonable assumption of equal 'stressing', and the torsional stiffness of the beams is assumed to be zero, which is a very reasonable assumption given that the torsional stiffness of a cracked structural member is very low compared to its flexural stiffness (Figure 2.38), then the structure may be simplified further and be broken into a number of separate plane frames in each of the two main directions, whose stiffnesses are coupled to form a system of $3n$ equations equal to the number of the independent displacements and rotations of the η storey diaphragms.

The purpose of this section is the presentation of some important properties of the response of multi-storey 3D systems subjected to static or dynamic excitation. These properties, like '*centre of stiffness*', '*torsional radius*', '*radius of gyration*' and so forth, will be met many times in subsequent chapters. So, it was decided to present a thorough *static* and *dynamic* analysis of the *single-storey pseudospatial system* here, where each of these properties will be introduced in the simplest form, since the single-storey system is the simplest form of this type of structure. Later, in Chapter 4, *the general static analysis* of the multi-storey pseudo spatial system will also be presented in detail.
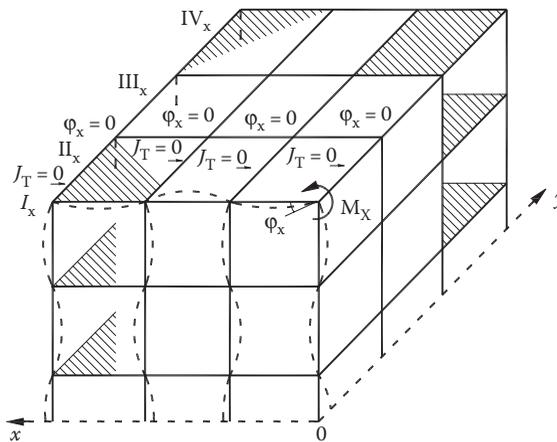
Figure 2.38 Pseudospatial system with parallel plane frames with no strain interaction between them due to the zero torsional stiffness of the connecting beams.

2.4.4.2 Static response of the single-storey 3D system

Consider the pseudospatial single-storey structure of Figure 2.39, which is loaded at the level of the diaphragm with two horizontal seismic forces H_x and H_y passing through the centre of mass m of the diaphragm and a torque M_z. According to what has been discussed in the previous paragraph, the displacement of every point of the diaphragm caused by the horizontal seismic forces and the torque may be determined by the displacement u_{mx} and u_{my} of the centre of mass M and the in-plane rotation of the diaphragm φ.

So, the displacement of the top of a column i (Figure 2.39) results from the relations:

$$\left. \begin{array}{l} u_{ix} = u_{mx} - y_i \varphi \\ u_{iy} = u_{my} + x_i \varphi \end{array} \right\} \tag{2.71}$$

If we now call the stiffness of a frame i of $x–x$ direction K_{ix} and the stiffness of a frame j of $y–y$ direction K_{jy}, this stiffness expresses the required horizontal resistance (shear force) of the frame for the development of a relative displacement equal to '1' (Figure 2.40). As a result, each of the frames i and j develops, respectively, the following horizontal shear forces (reactions) for the displacements of Equation 2.71.

$$\left. \begin{array}{l} V_{ix} = K_{ix} u_{mx} - y_i K_{ix} \varphi \\ V_{jy} = K_{jy} u_{my} + x_j K_{jy} \varphi \end{array} \right\}. \tag{2.72}$$
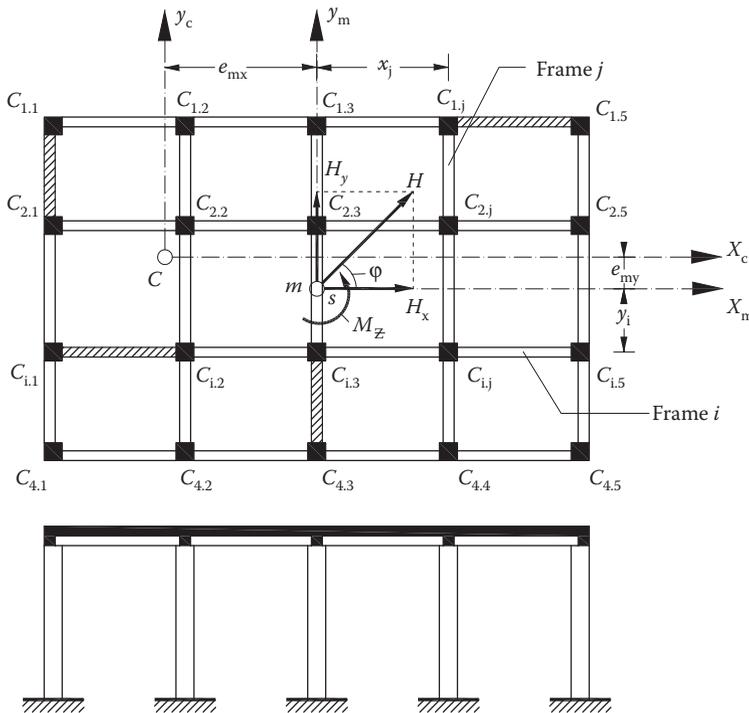
Figure 2.39 Plan and elevation of a single-storey pseudospatial structural system.
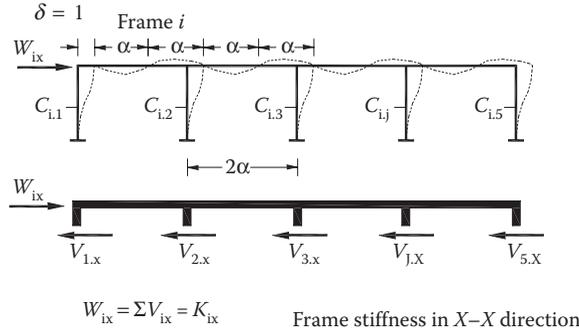
Figure 2.40 Definition of the stiffness K_{ix} of a frame *i* parallel to the *x–x* direction.

The three equilibrium conditions for the floor result in the following equations:

$$
\left.
\begin{aligned}
\sum_{i=1}^{n} V_{ix} &= H_x \\
\sum_{j=1}^{m} V_{jy} &= H_y \\
\sum_{j=1}^{m} x_j V_{jy} - \sum_{i=1}^{i=n} y_i V_{ix} + \sum T_i &= M_z
\end{aligned}
\right\}
\tag{2.73}
$$

where

ΣT_i the sum of the torsional moments developing at the columns due to φ ($T_i = K_{ip}\varphi$).

If Equations 2.72 are incorporated into Equation 2.73, the following system results:

$$
\left.
\begin{aligned}
\left(\sum_{i=1}^{n} K_{ix}\right)u_{mx} + {}+0+{} -\left(\sum_{i=1}^{n} y_i K_{ix}\right)\varphi &= H_x \\
0+ {}+\left(\sum_{j=1}^{j=m} K_{jy}\right)u_{my} + {}+\left(\sum_{j=1}^{m} x_j K_{jy}\right)\varphi &= H_y \\
-\left(\sum_{i=1}^{n} y_i K_{ix}\right)u_{mx} + \left(\sum_{j=1}^{m} x_j K_{jy}\right)u_{my} + \left(\sum_{j=1}^{m} K_{jy} x_j^2 + \sum_{i=1}^{n} K_{ix} y_i^2 + \sum K_{ip}\right)\varphi &= M_z
\end{aligned}
\right\}
\tag{2.74}
$$

System (2.74) allows the determination of the unknown 'displacements' u_{mx}, u_{my}, and φ. From this point on, for reasons of simplicity, the sum ΣT_i will be considered zero, since the torsional stiffness of the columns is very small compared to their bending stiffness.

The system (2.74) may be reduced to a system of three uncoupled equations, if the reference point of the coordinate system is transferred from the *centre of mass* to another point C called *centre of stiffness* (see Sections 5.2 and 5.3), such that the non-diagonal coefficients of the system (2.74) take zero values, that is,

$$\left. \begin{array}{l} \sum_{i=1}^{i=n} y_{ic} K_{ix} = 0 \\[2mm] \sum_{j=1}^{j=m} x_{jc} K_{jy} = 0 \end{array} \right\} \tag{2.75}$$

It must be noted that point C, for which the above equations are in effect, is the centre of static moments of the fictitious forces K_{ix} and K_{iy}, respectively. So, the coordinates of C in relation to the centre of mass M are given by the following expressions (Figure 2.39):

$$\left. \begin{array}{l} e_{mx} = \dfrac{\sum_{j=1}^{j=m} x_j K_{jy}}{\sum_{j=1}^{j=m} K_{jx}} \\[6mm] e_{my} = \dfrac{\sum_{i=1}^{i=n} y_i K_{iy}}{\sum_{i=1}^{i=n} K_{ix}} \end{array} \right\} \tag{2.76}$$

Taking Equations 2.75 and 2.76 into account, the system (2.74) is transformed as follows:

$$\left. \begin{array}{l} \left(\sum_{i=1}^{i=n} K_{ix} \right) u_{cx} + 0 + 0 = H_x \\[5mm] 0 + \left(\sum_{j=1}^{j=m} K_{jy} \right) u_{cy} + 0 = H_y \\[5mm] 0 + 0 + \left(\sum_{j=1}^{j=m} K_{jy} x_{jc}^2 + \sum_{i=1}^{i=n} K_{ix} y_{ic}^2 \right) \varphi = M_c \end{array} \right\} \tag{2.77}$$

where

$$\left. \begin{array}{l} x_{jc} = x_{mj} - e_{mx} \\ y_{ic} = y_{mi} - e_{my} \\ M_c = H_y e_{mx} - H_x e_{my} + M_z \end{array} \right\} \tag{2.78}$$

It should be noted that according to Equation 2.78, frame coordinates and loading system (H_x, H_y, M_z) refer from that point on to the *centre of stiffness* instead of the *centre of mass*. The expression:

$$\boxed{J_{TC} = \sum_{j=1}^{j=m} K_{jy} x_{jc}^2 + \sum_{i=1}^{n} K_{ix} y_{ic}^2} \tag{2.79}$$

is called *torsional stiffness* with respect to the *centre of stiffness*, and its meaning will be examined later (see Section 5.3).

By introducing the notation:

$$
\left.\begin{aligned}
K_x &= \sum_{i=1}^{i=n} K_{ix} \ : \text{storey stiffness } x\text{–}x \\
K_y &= \sum_{j=1}^{j=m} K_{jy} \ : \text{storey stiffness } y\text{–}y \\
J_{TC} &= \sum_{j=1}^{j=m} K_{jy} x_{jc}^2 + \sum_{i=1}^{i=n} K_{ix} y_{ic}^2 \ : \text{torsional stiffness}
\end{aligned}\right\}
\tag{2.80}
$$

in system (2.74) it takes the following form:

$$
\left.\begin{aligned}
K_x u_{mx} + 0 - e_y K_x \varphi &= H_x \\
0 + K_y u_{my} + e_x K_y \varphi &= H_y \\
-e_y K_x u_{mx} + e_x K_y u_{my} + J_{TM} \varphi &= M_z
\end{aligned}\right\}
\tag{2.81}
$$

where

$$
\boxed{J_{TM} = J_{TC} + e_x^2 K_y + e_y^2 K_x}
\tag{2.82}
$$

J_{TM} is called *torsional stiffness* with respect to the *centre of mass*. Its meaning will be discussed later, in Section 5.3.

Now system 2.77 may be rearranged as follows:

$$
\left.\begin{aligned}
K_x u_{cx} + 0 + 0 &= H_x \\
0 + K_y u_{cy} + 0 &= H_y \\
0 + 0 + J_{TC} \varphi &= M_c
\end{aligned}\right\}
\tag{2.83}
$$

From the preceding discussion the following conclusions may be drawn:

1. When $e_{mx} = e_{my} = 0$, that is, the centre of stiffness C coincides with the centre of mass and if torque M_z is zero, M_c in the system (2.77) takes a zero value (Equations 2.78). Therefore, the pseudospatial structure exhibits only *translational* displacements, that is, when the centre of stiffness coincides with the centre of mass and the horizontal loading passes through the centre of mass (inertial forces), the system exhibits translational displacements.

2. If a structural system is symmetric about the x–x axis and is loaded only with H_y passing through the centre of mass, this system exhibits a translational motion u_{cy} parallel to the y–y axis and a torsional deformation φ, that is,

$$
u_{cy} = \frac{H_y}{\sum_{j=1}^{m} K_{jy}}
\tag{2.84a}
$$

$$
\varphi = \frac{e_{mx} H_y}{J_{TC}}.
\tag{2.84b}
$$

From Equation 2.84b it can be seen that the torsional effect is proportional to the distance e_{mx} between M and C, and inversely proportional to the torsional stiffness of the system.

3. The relation:

$$r_x = \sqrt{\frac{J_{TC}}{\sum_{j=1}^{m} K_{jy}}}$$

(2.85)

is called the *torsional radius*, and its meaning will be examined later (Chapters 5.2 and 5.3).

4. In case of a pure *frame resisting* system or *pure shear wall system*, the stiffness K_{ix} or K_{jy} of the structural elements is approximately proportional to the moments of inertia of the cross-section of the columns or the walls. In this case, the equations above may take the following approximate form:

a. Coordinates of *centre of stiffness C* in relation to the *centre of mass M*:

$$\left. \begin{aligned} e_{mx} &= \frac{\sum_{j=1}^{j=m} x_j J_{jx}}{\sum_{j=1}^{j=m} J_{jx}} \\ e_{my} &= \frac{\sum_{i=1}^{i=n} y_i J_{iy}}{\sum_{i=1}^{i=n} J_{iy}} \end{aligned} \right\}$$

(2.86)

b. *Torsional stiffness* with respect to the *centre of stiffness*:

$$\boxed{\overline{J}_{TC} = \sum_{j=1}^{j=m} J_{jx} x_{jc}^2 + \sum_{i=1}^{n} J_{iy} y_{ic}^2}$$

(2.87)

c. *Torsional stiffness* with respect to the *centre of mass*:

$$\boxed{\overline{J}_{TM} = J_{TC} + e_x^2 \left(\sum_{j=1}^{j=m} J_{jx} \right) + e_y^2 \left(\sum_{i=1}^{n} J_{iy} \right)}$$

(2.88)

In case of a system symmetric to both axes x–x and y–y, the torsional deformation φ due to a torsional moment (torque) M_z is derived from Equation 2.84b as

$$\varphi = \frac{M_z}{J_{TC}}.$$

(2.89)

It is obvious that the value of J_{TC} depends mainly on the existence of elements with high flexural stiffness (i.e., structural walls) at the perimeter of the structure and parallel to it (Figure 2.41).

(a) $J_\rho^{wall} \cong \phi$ (b) $\bar{J}_\rho^{wall} = 2J_m \left(\frac{L_y}{2}\right)^2 + 2J_n \left(\frac{L_x}{2}\right)^2$
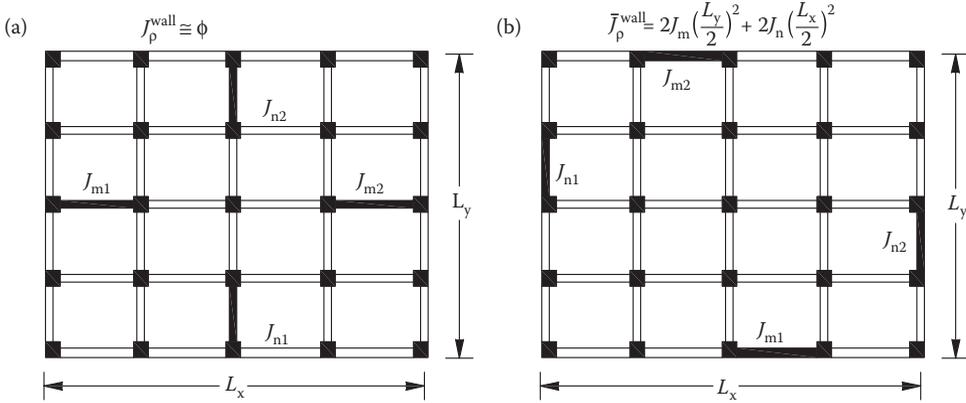
Figure 2.41 Effect of the arrangement of the structural walls on the torsional stiffness of the system: (a) system with low torsional stiffness; (b) system with high torsional stiffness.

d. *Torsional radius* with respect to the *centre of stiffness* C:

$$r_{xc} = \sqrt{\frac{\bar{J}_{TC}}{\sum_{j=1}^{m} J_{jx}}} \tag{2.90}$$

e. *Torsional radius* with respect to the *centre of mass*:

$$r_{xm} = \sqrt{\frac{\bar{J}_{TM}}{\sum_{j=1}^{m} J_{jx}}}. \tag{2.91}$$

5. It should be noted that in case of a space system consisting of *coupled frames* and *walls*, the above approximate equations cannot be used. In this case, taking into account that computer-aided analysis is available, the following procedure may be followed for the determination of the above values e_{mx}, e_{my}, J_{TC}, J_{TM}, r_{xc}, r_{xm}.
   a. The system is loaded with a torque M_z
   b. Taking into account Equation 2.83, one may easily conclude that u_{cx} and u_{cy} are zero since H_x and H_y are zero too. Therefore, from the displacements of two counter-pairs of columns at the perimeter of the system, the position of the centre of stiffness can be determined geometrically, that is, the values e_{mx} and e_{my} are defined (Figure 2.42). Likewise, the torsional deformation φ_z of the system is determined by the relations:

$$\varphi_z = \frac{u_{x1} - u_{x2}}{l_y} = \frac{u_{y3} - u_{y4}}{l_x}. \tag{2.92}$$

   c. From the third equation of 2.83, the value J_{TC} can be easily determined. In fact,

$$J_{TC} = \sum_{j=1}^{j=m} K_{jy} x_{jc}^2 + \sum_{j=1}^{j=m} K_{ix} y_{ic}^2 = \frac{M_z}{\varphi_z} \tag{2.93}$$
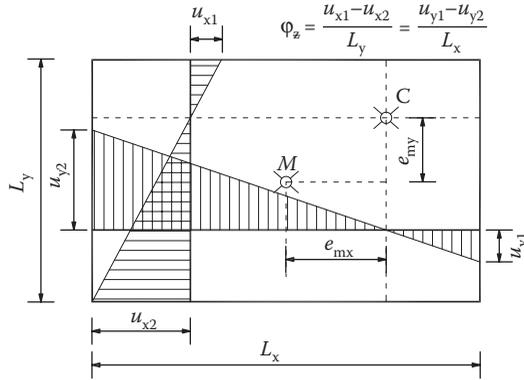
Figure 2.42 Determination of the centre of stiffness and the torsional rigidity with respect to the centre of stiffness, using a computer-aided procedure.

d. Then, the system is loaded with a horizontal force H in the x–x and y–y direction successively at its already determined centre of stiffness. The system will exhibit a translational displacement in the x–x and y–y directions, with u_{cx} and u_{cy} displacements respectively resulting from the analysis. By applying the first two equations of 2.83, the stiffness of the system in the x–x and y–y direction becomes

$$K_x = \sum_{i=1}^{i=n} K_{ix} = \frac{H}{u_{cx}}$$

$$K_y = \sum_{j=1}^{j=m} K_{jy} = \frac{H}{u_{cy}}$$

(2.94)

e. Therefore, by combining Equations 2.93 and 2.94, the values of r_x, r_y and J_{TM} may be easily calculated.

2.4.4.3 Dynamic response of a single-storey 3D system

With regard that equations of motion of plane systems under seismic excitation (Equations 2.58b and 2.59) have been generated by the application of d'Alembert's equations for dynamic equilibrium, it is reasonable, also, to repeat the procedure here, although the motion of the system is not only *translational* but also *rotational*. In this respect, it should be remembered that Newton's second law of translational motion, that is,

$$F = m\ddot{x}$$

(2.95)

should be replaced in case of rotational motion by the equation (Figure 2.43):

$$T_{mz} = J_d\ddot{\varphi}$$

(2.96)

where
   F is the acting force
   m is the total mass of the floor
   $\ddot{x}$ is the absolute translational acceleration of the floor mass
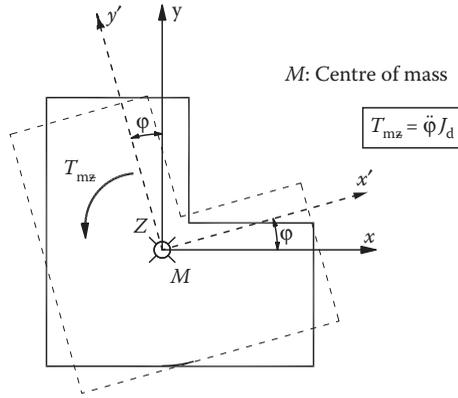
Figure 2.43 Torsional excitation of a pseudospatial single-storey system activated by a torque $T_{mz}(t)$.

T_{mz} is the torsional moment of the rotating system with respect to the centre of mass of the floor

$\ddot{\varphi}$ is the angular acceleration of the floor with respect to the centre of mass

J_d is the polar moment of inertia of the floor mass in plan with respect to the centre of mass of the floor. In case of a rectangular floor $b \times d$ with uniformly distributed mass, J_d is given by the expression:

$$J_d = m\frac{b^2 + d^2}{12}. \tag{2.97}$$

For simplicity, we assume that the system is damping-free, that is $c = 0$ (Equations 2.58b and 2.59).

Now the pseudospatial single-storey system of Figure 2.44, in which excitation at the ground level is determined by an accelerogram:

$$\ddot{x}_o(t) = \begin{bmatrix} \cos\theta \\ \sin\theta \end{bmatrix} \ddot{x}_o(t) = [\delta]\ddot{x}_o(t) \tag{2.98}$$

M: Centre of mass
θ: Direction of excitation
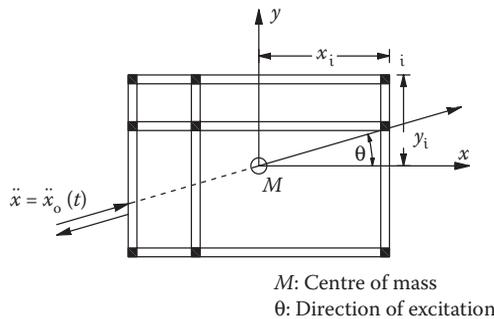
Figure 2.44 Pseudospatial single-storey system excited by an accelerogram $\ddot{x}_o(t)$ in the direction of angle θ with respect to the x–x axis.

where θ is the angle of input motion to the x–x axis of the system. The motion of the system is expressed by two translational and one rotational motion of the centre of mass of the floor relative to the ground, that is,

$u_{mx}(t)$ is displacement, parallel to the x-axis
$u_{my}(t)$ is displacement, parallel to the y-axis
$\phi(t)$ is in-plane rotation about the z-axis, passing through the *centre of mass*

The time-dependent motion of the top of a column i (Figure 2.44) results from the relations (see Equation 2.71):

$$\left.\begin{array}{l} u_{ix}(t) = u_{mx}(t) - y_i\varphi(t) \\ u_{iy}(t) = u_{my}(t) + x_i\varphi(t) \end{array}\right\} \tag{2.99}$$

According to Equation 2.72, each of the frames i and j parallel to the x-axis and y-axis, respectively, develops the following horizontal restoring forces for the relative displacements of Equation 2.99.

$$\left.\begin{array}{l} V_{ix}(t) = K_{ix}u_{mx}(t) - y_iK_{ix}\varphi(t) \\ V_{jy}(t) = K_{jy}u_{my}(t) + x_jK_{jy}\varphi(t) \end{array}\right\} \tag{2.100}$$

At the same time, due to the dynamic character of motion, the developing inertial forces are expressed as follows:

$$\left.\begin{array}{l} f_{mx}(t) = m\ddot{x}_m(t) = m\left[\ddot{x}_o(\cos\theta) + \ddot{u}_{mx}(t)\right] \\ f_{my}(t) = m\ddot{y}_m(t) = m\left[\ddot{x}_o(\sin\theta) + \ddot{u}_{my}(t)\right] \\ T_{mz} = J_d(\ddot{\varphi}(t) + \ddot{\varphi}_o(t)) = J_d\ddot{\varphi}(t) \end{array}\right\} \tag{2.101}$$

The value $\ddot{\varphi}_o(t)$ is taken to be equal to zero due to the fact that the usual types of accelerograms refer only to translational motion of the ground.

The three equilibrium equations of the floor (see Equation 2.73):

$$\left.\begin{array}{l} \displaystyle\sum_{i=1}^{n} V_{ix}(t) + f_{mx}(t) = 0 \\[2em] \displaystyle\sum_{j=1}^{n} V_{jy}(t) + f_{my}(t) = 0 \\[2em] \displaystyle\sum_{j=1}^{n} x_j V_{jy}(t) - \sum_{i=1}^{n} y_i V_{ix}(t) + T_{mz} = 0 \end{array}\right\} \tag{2.102}$$

result in the following linear system of differential equations:

$$
\left.
\begin{aligned}
&\ddot{u}_{mx}(t)m + \left(\sum_{i=1}^{n} K_{ix}\right) u_{mx}(t) + \cdots + 0 + \cdots - \left(\sum_{i=1}^{n} y_i K_{ix}\right) \varphi(t) = -m\ddot{x}_o(t)(\cos\theta) \\
&\ddot{u}_{my}(t)m + 0 + \left(\sum_{j=1}^{j=m} K_{jy}\right) u_{my}(t) + \cdots + \left(\sum_{j=1}^{m} x_j K_{jy}\right) \varphi(t) = -m\ddot{x}_o(t)(\sin\theta) \\
&\ddot{\varphi}(t)J_d - \left(\sum_{i=1}^{n} y_i K_{ix}\right) u_{mx}(t) + \left(\sum_{j=1}^{m} x_j K_{jy}\right) u_{my}(t) + \left[\left(\sum_{j=1}^{m} K_{jy} x_j^2\right) + \left(\sum_{i=1}^{n} K_{ix} y_i^2\right)\right] \varphi(t) = 0
\end{aligned}
\right\}
\tag{2.103}
$$

or in matrix form:

$$
\begin{aligned}
&\begin{pmatrix} m & & \\ & m & \\ & & J_d \end{pmatrix} \begin{pmatrix} \ddot{u}_{mx} \\ \ddot{u}_{my} \\ \ddot{\varphi}_m \end{pmatrix} + \begin{pmatrix} K_x & 0 & -e_{my}K_x \\ 0 & K_y & e_{mx}K_y \\ -e_{my}K_x & e_{mx}K_y & K_{m\varphi} \end{pmatrix} \begin{pmatrix} u_{mx} \\ u_{my} \\ \varphi_m \end{pmatrix} \\
&= -\begin{pmatrix} m & & \\ & m & \\ & & J_d \end{pmatrix} \begin{pmatrix} \cos\theta \\ \sin\theta \\ 0 \end{pmatrix} \ddot{x}_o(t)
\end{aligned}
\tag{2.104}
$$

where

$$
\left.
\begin{aligned}
e_{mx} &= \frac{\sum_{j=1}^{m} x_j K_{jy}}{\sum_{j=1}^{m} K_{jy}} \\
e_{my} &= \frac{\sum_{i=1}^{n} y_i K_{ix}}{\sum_{i=1}^{n} K_{ix}}
\end{aligned}
\right\}
\tag{2.105}
$$

are the coordinates of the *centre of stiffness* (Equations 2.76) and

$$
\left.
\begin{aligned}
K_x &= \sum_{i=1}^{n} K_{ix} \\
K_y &= \sum_{j=1}^{m} K_{jy} \\
K_{m\varphi} &= J_{Tm}
\end{aligned}
\right\}
\tag{2.106}
$$

System (2.104) may be rewritten in a more concise form, as follows:

$$\boxed{\mathbf{M}\ddot{\mathbf{u}}(t) + \mathbf{K}\mathbf{u}(t) = -\mathbf{M}\mathrm{d}\ddot{x}_\mathrm{o}(t)}$$

(2.107)

We see that the seismic motion of 3D structures obeys the same differential equations as with plane structures. The only difference is the meaning of the corresponding matrices and vectors. Therefore, from this point on the procedure for integration is the same as the method developed in Sections 2.4.2 and 2.4.3. However, it is important to make some additional remarks here that will help later on (Section 5.3) with the clarification of issues of 'torsional flexibility'.

2.4.4.4 Concluding remarks

1. The three differential equations in Equation 2.103 or Equation 2.104 governing the three degrees of freedom – u_{mx}, u_{my} and φ – are coupled through the stiffness matrix because this matrix is not diagonal, since, in general, the *stiffness centre C* does not *coincide with the mass centre M*. Any thought of transferring the origin of coordinates from *M* to *C* must be abandoned because, in this case, of course, u_x, u_y and φ would be uncoupled through the transformation of the coupling stiffness matrix to a diagonal one (see Equation 2.83), but at the same time, $\ddot{u}_x, \ddot{u}_y, \ddot{\varphi}$ would be coupled through the transformation of the mass matrix from diagonal to a normal (coupling) one. This is quite reasonable, since the change of the origin of the coordinate system cannot change its dynamic properties. So, it can be concluded that each of the three eigen modes $[\phi_1]$, $[\phi_2]$, $[\phi_3]$ of free vibration represents combined motion of *translation* and *rotation*. It is well known from 'kinetics' that such a motion may be replaced by a rotational motion about three poles (Figure 2.45) – 0_1, 0_2, 0_3 – one for each mode. This problem will be analysed further in a next paragraph.

2. If the system is symmetrical in both directions, the *stiffness centre C* coincides with the *mass centre M*. In this case, e_{mx} and e_{my} in Equation 2.105 are zero and, therefore, the three equations of motion (2.103) become uncoupled and take the following form:

$$\left.\begin{aligned} m\ddot{u}_{\mathrm{mx}} + K_x u_{\mathrm{mx}} &= -m(\cos\theta)\ddot{x}_\mathrm{o} \\ m\ddot{u}_{\mathrm{my}} + K_y u_{\mathrm{my}} &= -m(\sin\theta)\ddot{x}_\mathrm{o} \\ J_\mathrm{d}\ddot{\varphi}_\mathrm{m} + J_{\mathrm{TC}}\varphi_\mathrm{m} &= 0 \end{aligned}\right\}$$

(2.108)

The three uncoupled eigen frequencies are given by the following expressions (see Equation 2.4a:

$$\left.\begin{aligned} \omega_{\mathrm{ux}} &= \sqrt{\frac{K_x}{m}} \\ \omega_{\mathrm{uy}} &= \sqrt{\frac{K_y}{m}} \\ \omega_\varphi &= \sqrt{\frac{J_{\mathrm{TC}}}{J_\mathrm{d}}} \end{aligned}\right\}$$

(2.109)

If the rotational eigen frequency ω_φ is the shortest one, it means that the *rotational mode is the fundamental one*.
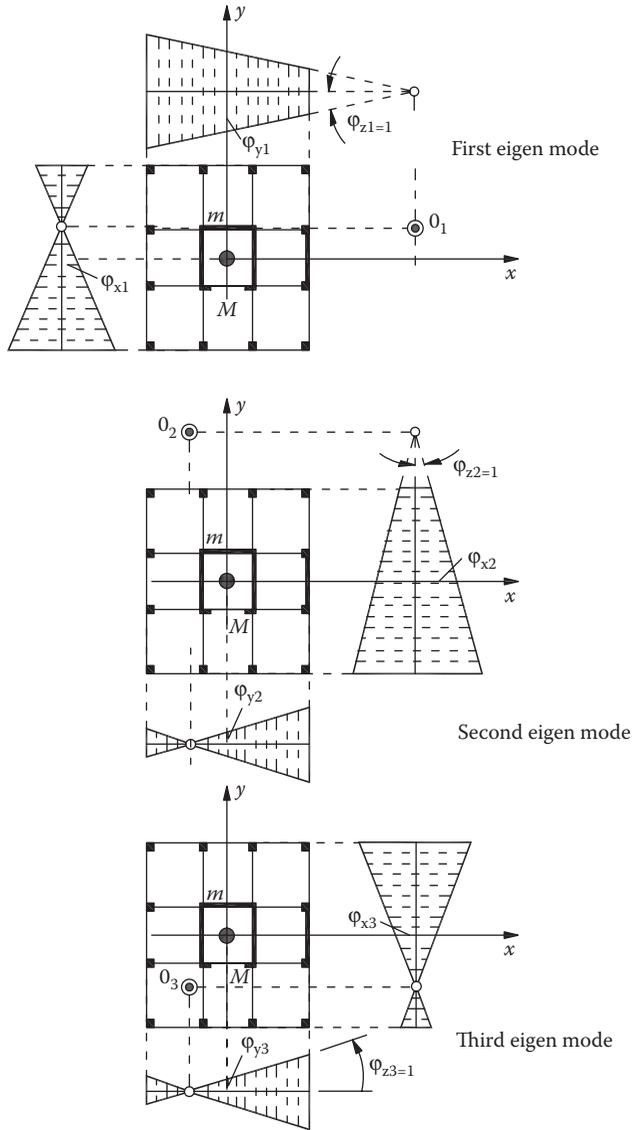
Figure 2.45 The three eigen modes of vibration of a single-storey pseudospatial structure.

In this case:

$$\left.\begin{array}{l} \omega_\varphi < \omega_{ux} \\ \omega_\varphi < \omega_{uy} \end{array}\right\} \tag{2.110}$$

By introducing Equation 2.109 into Equation 2.110, the following expressions may be obtained:

$$\sqrt{\frac{J_{TC}}{J_d}} < \sqrt{\frac{K_x}{m}} \quad \text{and} \quad \sqrt{\frac{K_y}{m}} \tag{2.111}$$

or

$$\sqrt{\frac{J_d}{m}} > \sqrt{\frac{J_{TC}}{K_x}} \quad \text{and} \quad \sqrt{\frac{J_{TC}}{K_y}} \tag{2.112}$$

Keeping in mind that

$$\sqrt{\frac{J_{TC}}{K_x}} \quad \text{and} \quad \sqrt{\frac{J_{TC}}{K_y}}$$

are the torsional radius r_{xc} and r_{yc} in the x–x and y–y directions:
and that

$$\sqrt{\frac{J_d}{m}} = l_s \tag{2.113}$$

is the polar radius of inertia, it may be concluded from Equation 2.112 that if

$$\boxed{l_s > r_{xc} \quad \text{and} \quad r_{yc}} \tag{2.114}$$

then the torsional eigen frequency is the shortest one, and in this respect *the rotational mode is the fundamental one.* In this context, the modal participation factor (Paragraph 2.4.3.2) (L_φ^*/M_φ^*) corresponding to torsional vibration is larger, and therefore the system must be considered 'torsionally flexible' with a lot of consequences for a building belonging to this category, as will be shown later (see Section 5.3).

At the same time, in the case of a symmetric system in two directions, since $e_{mx} = e_{my} = 0$, it may be concluded that

a. $J_{TC} = J_{TM}$ (2.115)
b.   Ground motion in the x-direction causes only u_x displacements. The same also holds true for the y-direction.
c.   The system does not experience any torsional effect unless the base includes rotation about a vertical axis (torsional base acceleration $\ddot{\varphi}_o$) or the mass presents excidental eccentricities (Chopra, 2001).

3. For a structural system symmetric only about the x–x axis, the stiffness centre C lies on the x–x axis of symmetry, that is, $e_y = o$. Now, if the ground excitation acts only in the y–y direction, the system (2.104) takes the form:

$$
\begin{pmatrix} m & & \\ & m & \\ & & J_d \end{pmatrix}
\begin{pmatrix} \ddot{u}_{mx} \\ \ddot{u}_{my} \\ \ddot{\varphi}_m \end{pmatrix}
+
\begin{pmatrix} K_x & 0 & 0 \\ 0 & K_y & e_{mx}K_y \\ 0 & e_{mx}K_y & J_{TC} + e_{mx}^2 K_y \end{pmatrix}
\begin{pmatrix} u_{mx} \\ u_{my} \\ \varphi_m \end{pmatrix}
$$
$$
= -\begin{pmatrix} m & & \\ & m & \\ & & J_d \end{pmatrix}
\begin{pmatrix} 0 \\ 1 \\ 0 \end{pmatrix} \ddot{x}_o(t)
\tag{2.116}
$$

This means that the motion u_x is uncoupled from the other two, and since there is no ground excitation in the $x–x$ direction, there is no displacement in this direction. However, the eigen frequency is

$$\omega_{ux} = \sqrt{\frac{K_x}{m}} \tag{2.117}$$

and the corresponding eigen mode is a pure $x–x$ displacement (Figure 2.46), that is,

$$\varphi_{ux} = 1, \quad \varphi_{uy} = 0, \quad \varphi_{uz} = 0 \tag{2.118}$$

In case of free vibration, the other two equations take the following form:

$$\begin{pmatrix} m & \\ & J_d \end{pmatrix}\begin{pmatrix} \ddot{u}_{my} \\ \ddot{\varphi}_m \end{pmatrix} + \begin{pmatrix} K_{yy} & e_{mx}K_{yy} \\ e_{mx}K_{yy} & J_{TC} + e_{mx}^2 K_{yy} \end{pmatrix}\begin{pmatrix} u_{my} \\ \varphi_m \end{pmatrix} = 0 \tag{2.119}$$

Applying the procedure developed in Chapter 2.4.2, we find

$$\begin{pmatrix} K_{yy} - \omega^2 m & e_{mx}K_{yy} \\ e_{mx}K_{yy} & (J_{TC} + e_{mx}^2 K_{yy}) - \omega^2 J_d \end{pmatrix}\begin{pmatrix} \varphi_y \\ \varphi_z \end{pmatrix} = \begin{pmatrix} 0 \\ 0 \end{pmatrix} \tag{2.120}$$

In this respect, ω^2 results from the following equation:

$$\text{Det}\begin{vmatrix} K_{yy} - \omega^2 m & e_{mx}K_{yy} \\ e_{mx}K_{yy} & \left(J_{TC} + e_x^2 K_{yy}\right) - \omega^2 J_d \end{vmatrix} = 0 \tag{2.121}$$
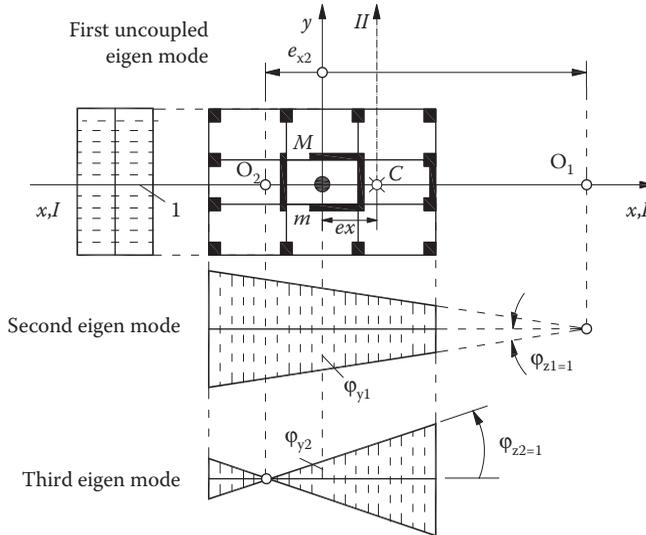
Figure 2.46 Eigen modes of vibration of a single-storey pseudospatial structure, symmetric about the *x–x* axis.

- It is evident that the two values of ω^2 (eigen frequencies) depend on the geometrical and dynamic values of the system, that is,

$$m, J_d, K_{yy}, e_{mx} \quad \text{and} \quad J_{TC}$$

- It is also evident that each of the two coupled eigen modes of motion has a coupled form of a displacement u_{my} and a rotation ϕ_m (Figure 2.46), which correspond to a rotation about two constant poles O_1 and O_2 on the x–x axis (Papapetrou, 1934). If the pole of the *shortest eigen frequency* lies within the boundaries of the floor (O_1 in Figure 2.46), the system is '*torsionally flexible*' with all consequences resulting therefrom.
- The criterion for 'torsional flexibility' results from the analysis of Equation 2.121 (Anastasiadis, 1989; Anastasiadis and Athanatopoulou, 1996) and is

$$\boxed{r_{xc}^2 + e_{mx}^2 < l_s^2} \tag{2.122}$$

where

$$r_{xc} = \sqrt{\frac{J_{TC}}{K_{yy}}} \quad \text{the torsional radius}$$

$$l_s = \sqrt{\frac{J_d}{m}} \quad \text{the polar radius of inertia}$$

- In the case that $e_{mx} = 0$ (system symmetric in both directions), Equation 2.122 is reduced to Equation 2.114.

2.5 DYNAMIC ANALYSIS OF MDOF INELASTIC SYSTEMS

2.5.1 Introduction

The dynamic analysis of MDOF inelastic systems is performed using direct step-by-step integration for small successive time steps. This method considers the response of the inelastic system within every integration time interval as linear. The value of the stiffness during the integration interval is taken to be equal to the slope of the local tangent to the load–deflection curve. Thus, while yielding occurs in some members and the stiffness of the structure changes, the response of the non-linear system is considered to be the response of successive linear systems with different stiffnesses. Every change in the stiffness of a member, which could occur either during its yielding or during its unloading from the yielding branch, theoretically changes the stiffness of the whole system. Therefore, dynamic inelastic analysis, even for plane multi-storey systems, requires excessive computational time.

The various computer codes for dynamic inelastic analysis of multi-storey buildings developed mainly after 1970 (Kanaan and Powell, 1973) offer the possibility of obtaining significant output parameters, such as maximum strains and corresponding internal forces at all critical sections, ductility demand and time histories of strains or displacements at specific points of the structure.

Of course, there are many reservations on the reliability of inelastic analysis deriving from various uncertainties, for example,

- Results may be critically dependent on small variations of input parameters without any obvious explanation.
- Lack of simple, stable and reliable load–strain inelastic models for columns and walls of 3D analysis.
- Simulation of wall members by means of linear members.
- Difficulty of taking into account automatically shear effects on the load strain models introduced in the analysis.

In any case, it is hoped that research and progress in this area will soon enable a reduction in the above reservations.

Finally, it should be noted that in parallel to the research-oriented computer codes, a number of reasonably user-friendly commercial ones have been developed in the last 15 years.

Next, an overview of the methodology of inelastic dynamic analysis applied on plane systems will be presented shortly.

2.5.2 Methodology for inelastic dynamic analysis of MDOF plane systems

Consider the plane dual system of Figure 2.47 and the plane frame system of Figure 2.48. These systems are discretised into structural elements forming the structural model as shown in the above figures. For the analysis, the direct stiffness method is used, according to which the stiffness matrix $\mathbf{K}_T$ of the system is derived by appropriately adding the elements of the stiffness matrices of the individual members.
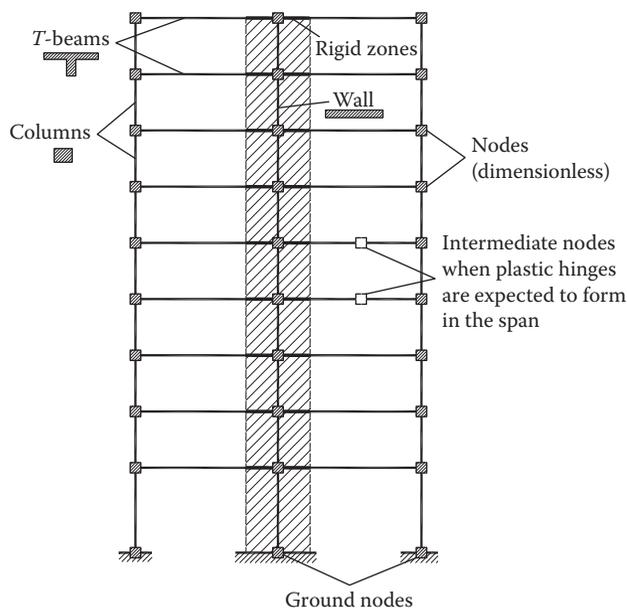
Figure 2.47 Discretisation of a reinforced concrete plane structure.
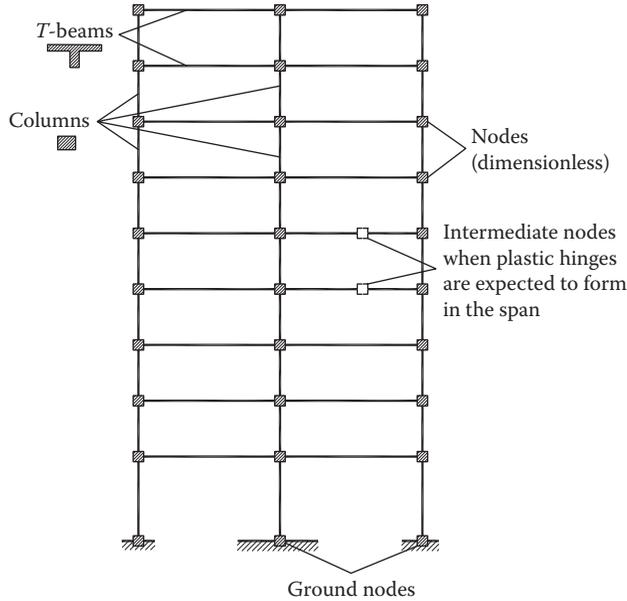
Figure 2.48 Discretisation of a reinforced concrete frame system.

The basic equation of dynamic equilibrium of the discretised system, which is subjected to a base seismic acceleration, is given in incremental (time stepping) form by the equation (Clough and Penzien, 1975; Chopra, 2001):

$$\mathbf{M}\Delta\ddot{\mathbf{u}} + \mathbf{C}_T(u)\Delta\dot{\mathbf{u}} + \mathbf{K}_T(u)\Delta\mathbf{u} = -\mathbf{M}[\mathsf{d}]\mathsf{D}\ddot{\mathbf{x}}_o(t) \tag{2.123}$$

(see Equation 2.58b) where $\mathbf{M}$ is the diagonal mass matrix of the system, $\mathbf{C}_T(u)$ is the tangent damping matrix, and $\mathbf{K}_T(u)$ is the tangent stiffness matrix of the system: they both change every time one or more elements goes from the elastic to the inelastic phase or vice versa. $\Delta\mathbf{u}$, $\Delta\dot{\mathbf{u}}$, $\Delta\ddot{\mathbf{u}}$ are the vectors of incremental changes of relative displacements, velocities and accelerations of the joints of the system, during the time step. Δt of the numerical integration δ is a unit vector and $\mathsf{D}\ddot{\mathbf{x}}_o(t)$ is the incremental change in base seismic acceleration during the time interval Δt.

For the solution of the matrix second-order differential equation (Equation 2.123), either the Newmark $\beta = 1/4$ method is used (method of constant acceleration for every integration time step; Kappos, 1990) or the Wilson's θ method, which is an unconditionally stable method with linearly changing acceleration. It should be noted that in order to avoid pitfalls in the integrations, the time stepping should be very short (1/200 to 1/50 s) and should coincide with the time digitisation intervals of the base accelerogram.

At the same time, the assumption is made that the damping matrix $\mathbf{C}_T$ is given by the relationship:

$$\mathbf{C}_T = a\mathbf{M} + \beta_T\mathbf{K}_T + \beta_o\mathbf{K}_o \tag{2.124}$$

where $\mathbf{K}_o$ is the initial stiffness matrix and a, β_T, β_o are damping coefficients proportional to the damping ratio ζ ($\zeta = 0.02$–0.05).
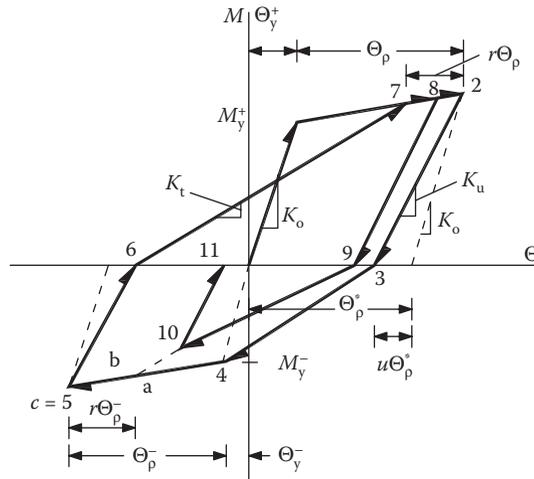
Figure 2.49 The modified Takeda model.

The inelastic strains of members in most methods and computer codes in use are supposed to be concentrated at *plastic hinges at the ends of the members in the form of plastic rotations* θ (DRAIN-2D/90, SAP2000 NL, etc.). However, more refined methods in use for research allow the extension of the inelastic strains to all member lengths (ZEUS, Seismostruct, etc).

The inelastic behaviour of R/C members is taken into consideration with the adoption of appropriate models for the moment (M)–rotation (θ) diagram at those ends. The M–θ diagram of Figure 2.49 is a modification of the well-known Takeda model (Takeda et al., 1970) proposed by Otani and Sozen (1972), and is used in the example of Figure 2.50. In Figure 2.51, a simplified model M–θ is plotted (Wilson, 2002), which has been used in the example of Figure 2.52 (Penelis et al., 2000).

Both models represent with adequate reliability the inelastic response of R/C members with predominantly flexural deformation to cyclic loading.

For the quantitative estimation of the model parameters, for each structural element the cross section geometry, its reinforcement, and the characteristics of the construction materials are needed. This means that the structural system must have been analysed and designed previously using conventional (elastic) seismic design procedures, that is, the method may be used either for research or verification or assessment reasons.

Specifically, the necessary inputs for the inelastic dynamic analysis of a plane R/C structure are the following:

1. The geometry of the system (see Figures 2.50 and 2.52)
2. The yield moments of the structural members defined as a function of the axial force
3. The softening law of the plastic branch as a percentage of original stiffness
4. The original modulus of elasticity E_o of concrete
5. The mass typically assumed to be concentrated at every floor level
6. The viscous damping ratio ζ
7. A digitised time history of acceleration at the base of the structure at time intervals of 1/200 to 1/50 s

The computer code using the above-listed input data (1)–(7) (Figure 2.50) first produces the moment–rotation diagrams for every structural member; mass, stiffness and damping
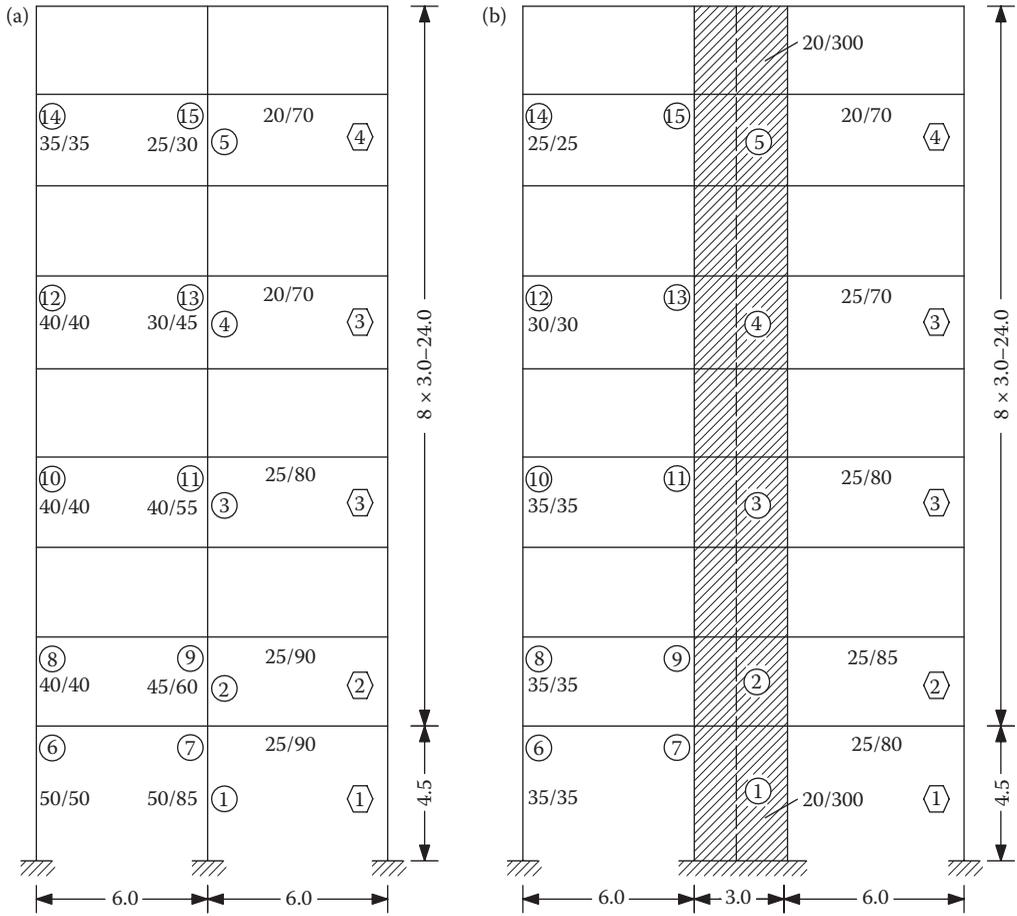
Figure 2.50 Geometric characteristics of two systems for which inelastic analysis was performed: (a) GRFR8 and (b) GRFW8. (Adapted from Kappos, A.J. 1991. *Earthquake Engineering and Structural Dynamics*, 20(2), 167–176.)
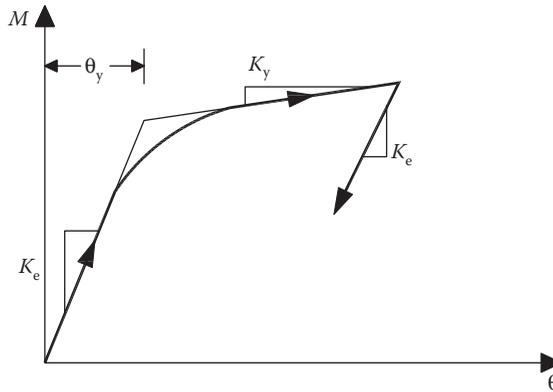
Figure 2.51 Fundamental behaviour of plasticity element (Wilson 2001).
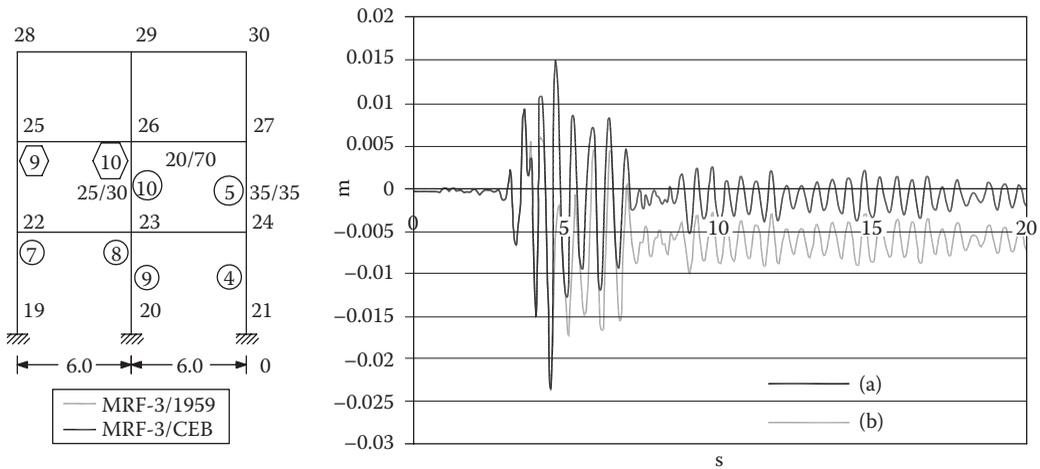
Figure 2.52 Time history of top displacement in a 3-storey frame under the seismic action of 1999 Athens earthquake designed: (a) according to Greek Code of 1959 and (b) according to EC 8-1/2004.

matrices; as well as the excitation vector. Once more it is emphasised that the stiffness and the damping matrices change from time step to time step of the numerical integration, while the mass matrix remains constant throughout the integration procedure.

In light of the above, it would be interesting to stay for a while with the results of such an analysis. It should be noted that the inelastic analysis can give for every critical section the time history response of

- Internal forces *M*, *N*, *V*
- Relative displacements
- Rotations θ of the nodes
- Relative displacements between the floors (inter-storey drifts), and so on. Given that the integration is carried out for very short time steps (1/200 to 1/50 s), calculation results are huge in number and their evaluation is difficult. Thus, every computer program is equipped with a series of post-processors to facilitate evaluation of the results

For example, some of the outputs produced by such post-processors are the following:

- Time history of relative displacements *u* (Figure 2.52)
- *M*–θ response diagram of cyclic loading during the time-history analysis (Figure 2.53)
- Maximum floor displacements *u* (Figure 2.54a)
- Maximum inter-storey drift ratio (deflection of columns from their vertical axis; Figure 2.54b)
- Maximum column and beam ductility demand (Figure 2.54c,d)
- Points where plastic hinges are formed during the excitation (Figure 2.55a–f)

The most critical indicators of the above information for the expected damage to the system are

- The maximum inter-storey drift ratios
- The points where plastic hinges are formed (risk for formation of an inverted pendulum)
- The ratio of ductility demand to ductility supply
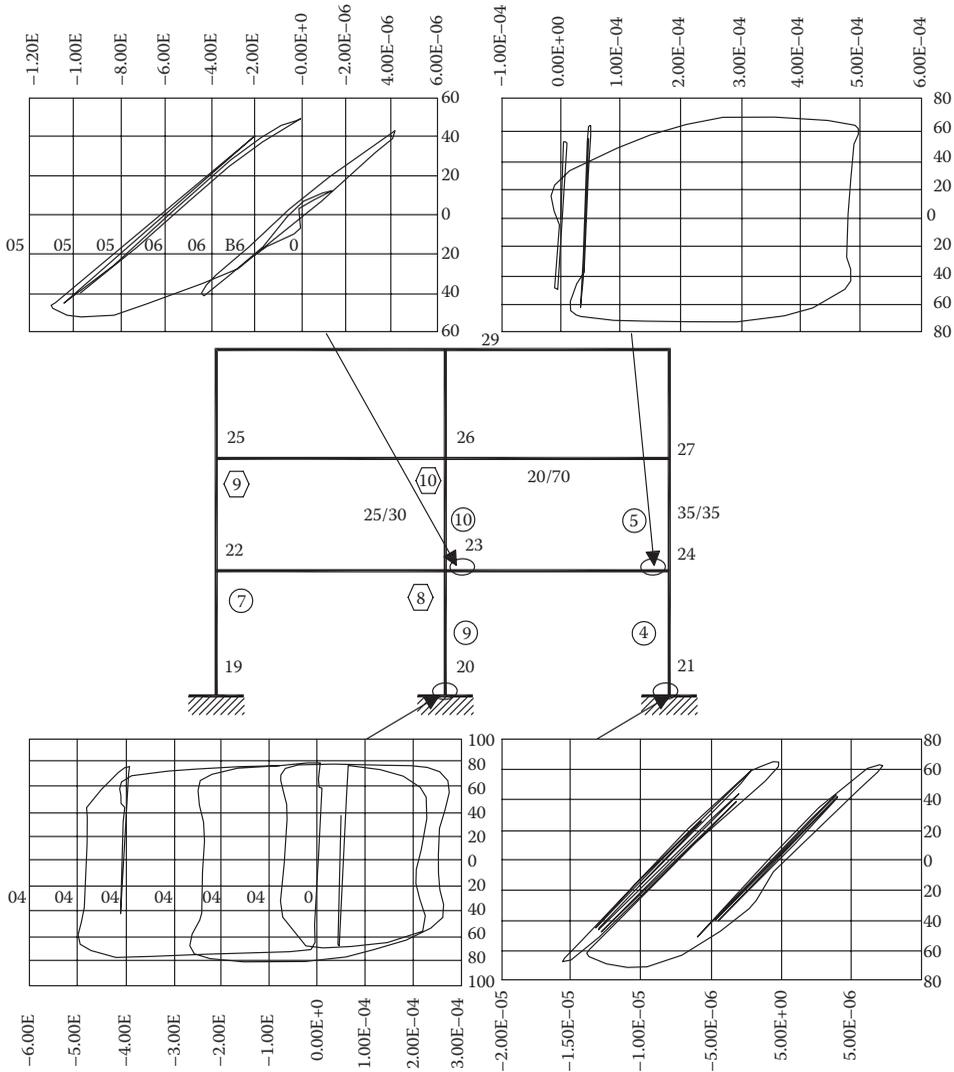
Figure 2.53 M–θ diagrams at critical sections of the 3-storey frame of Figure 2.52 designed according to the Greek Code of 1959.

It should be noted here that the maximum demand of rotation ductility,

$$\mu_\theta = \frac{\theta_y + \theta_p}{\theta_y} = 1 + \frac{\theta_p}{\theta_y}, \tag{2.125}$$

results from the inelastic analysis of the system and is different for different base excitation inputs. Conversely, the ductility supply depends on the geometrical properties (span, cross-section) of the structural member, the reinforcement, the quality of the construction materials, the level of axial loading, and the degree of confinement (see Chapters 8 through 10).
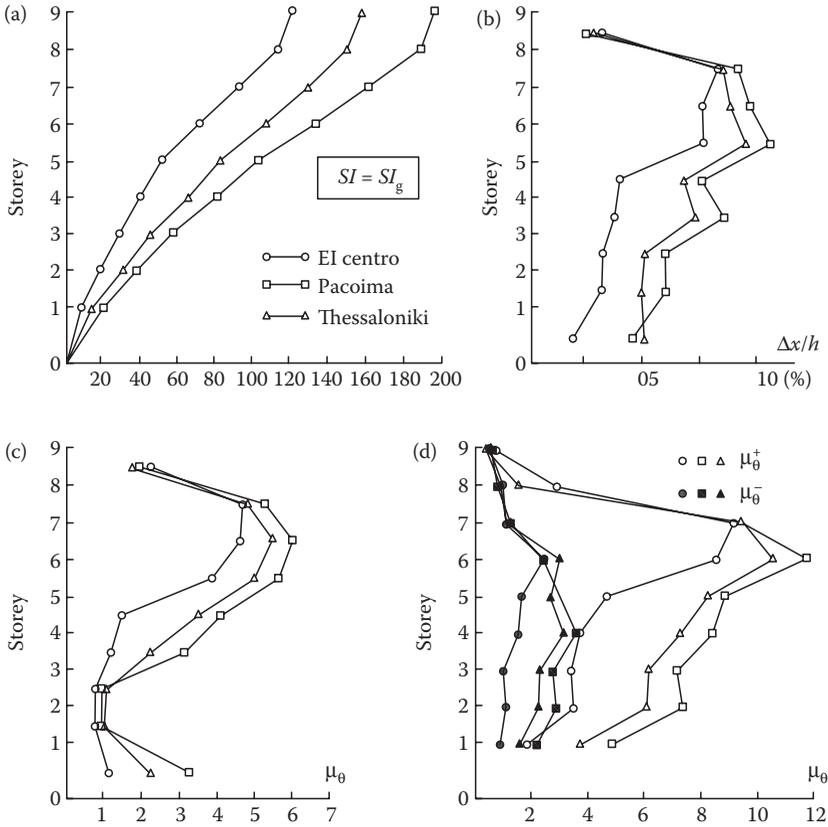
Figure 2.54 Maximum response parameters of a frame system (GRFR8) subjected to a seismic excitation with SI = 1.0 SI_0 for the El Centro x 1.0, Pacoima x 0.4, and Thessaloniki x 2.6 earthquakes: (a) floor displacements; (b) inter-storey drifts $\Delta x/h$; (c) required column ductilities; (d) required beam ductilities.

2.5.3 Concluding remarks

From all of the above, the following conclusions may be drawn:

- Dynamic non-linear analysis constitutes a powerful tool for the study of the seismic response of structures. It is the main tool for the evaluation of the reliability of the results of elastic modal spectral analysis using elastic response spectra reduced by a ductility (reduction) factor (see Paragraph 2.3.5.1). At the same time, it is considered a useful tool for the improvement of the reduction (behaviour) factors used in Codes of Practice (see Subsection 5.4.3).
- For the time being, non-linear seismic analysis is still seen as a non-routine technique in the design practice, used only in special cases such as:
  - Buildings of particular interest
  - Seismically isolated building by simulating isolation bearings with inelastic elements
  - Buildings with dissipative devices also by simulating them with viscous plastic elements
  - Yielding of reinforcement at one side
  - Yielding of reinforcement at both sides
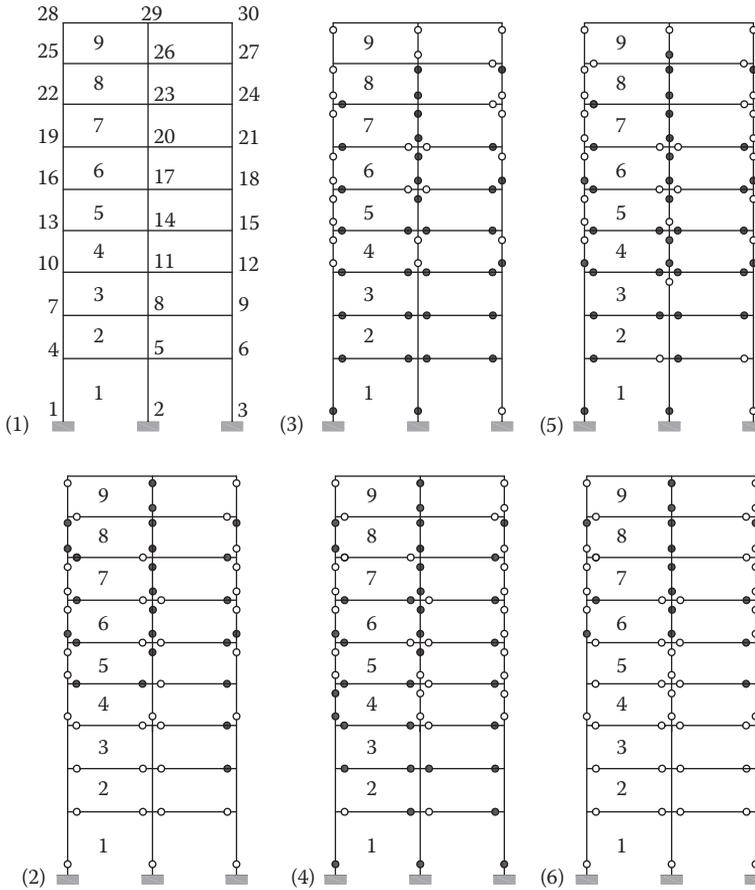
Figure 2.55 Frame system GRFR8: (1) numbering of nodes and floors. Formation of plastic hinges during an excitation from the following earthquakes: (2) El Centro x 1; (3) Pacoima x 1; (4) El Centro x 1.5 (5) Thessaloniki x 2.6; (6) El Centro x 0.75.

- The existing reservations on the reliability of inelastic analysis presented in Subsection 2.5.1 limit in practice, for the time being, the role of the method to that of a supplemental tool for the verification and improvement of the design of a structure that has already been analysed and designed using methods accepted by Codes of Practice.
- Finally, it should be noted that in the last 15 years an extended use has been made of the *static inelastic analysis*, known as '*pushover analysis*', for the determination of inelastic strains (θp, u_{p}, etc) of a structure. This method replaces dynamic inelastic analysis to a degree, giving more stable and reliable results. Detailed reference will be made to its implementation in practice in Chapter 5.

2.6 APPLICATION EXAMPLE

The response characteristics of three variations of a single-storey RC building are examined here, following both the static and the dynamic analysis approach described in Paragraphs 2.4.4.2 and 2.4.4.3.

2.6.1 Building description

The buildings are rectangular in plan with dimensions $b = 30$ m in the horizontal x axis and $d = 25$ m in the horizontal y axis. They consist of six frames in both the x–x and y–y directions, each having five bays, with constant bay lengths equal to 6 and 5 m², respectively (Figure 2.56). The storey height is $H = 5$ m. The first building (Building A) is a frame building, whereas the other two buildings (Buildings B and C) are differentiated as per the addition of RC walls on the perimeter of the building, along the y–y direction, as shown in Figure 2.56. All columns have a 40 cm square cross section. Both interior and exterior beams have a width of $b_w = 30$ cm and a height of $b_b = 60$ cm. The slab thickness is $h_f = 18$ cm. The walls have a thickness $b_t = 25$ cm and a length $l_w = 5$ m.

2.6.2 Design specifications

The factored distributed load at the floor area is taken to be 12 kN/m² for the $(g + \psi_2 q)$ load combination, $\psi_2 = 0.30$.

- Concrete quality is C25/30 with a modulus of elasticity $E_c = 31$ GPa. Steel quality is B500C
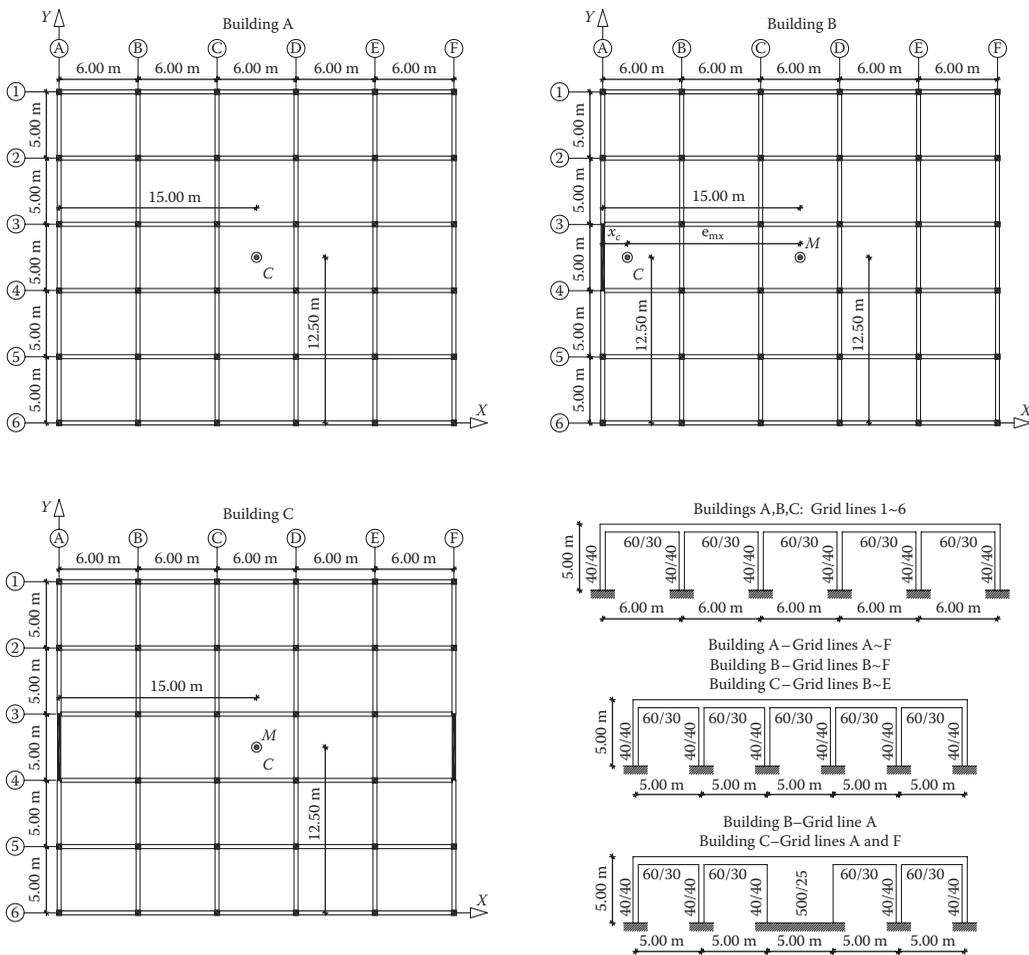
Figure 2.56 Plan view and typical frame arrangements of the buildings.

- The PGA is $a_g = 0.16$ g
- Seismic demand is defined for the EC8 Type I spectrum on ground C. The importance class is II.

2.6.3 Modelling assumptions

The stiffness of the vertical members is estimated by considering representative 2D frames (Paragraph 2.4.4.2). The 3D systems are broken into three types of frames as depicted in Figure 2.56. A unit displacement is applied at the roof level and the sum of the reactions of the vertical members corresponds to the stiffness of each frame.

- The stiffness of the concrete elements is taken to be equal to one-half (50%) of the corresponding stiffness of the uncracked elements, according to EC8 par. 4.3.1(7) (2004).
- Although the behaviour factor of the three building cases differs, for comparison reasons it is taken to be equal to $q = 4$. Thus, a unique response spectrum is defined for all the buildings.
- The centre of mass lies at the intersection point of the symmetry axes of the building.

2.6.4 Static response

The stiffnesses of the three types of frames as depicted in Figure 2.56 are

1. For the frame in the x–x direction $K_{f,x} = 17422.90$ kN/m
2. For the frame in the y–y direction $K_{f,y} = 17575.41$ kN/m
3. For the frame with the wall at the mid-bay $K_{wf,y} = 764001.30$ kN/m

   The individual frames at each direction are considered to function as a sequence of springs in parallel. The total stiffness in each direction is given as the sum of the stiffnesses of the individual frames:

Building A
   x–x axis: $K_x = 6 \cdot K_{f,x} = 6 \cdot 17422.90 = 104537.40$ kN/m
   y–y axis: $K_y = 6 \cdot K_{f,x} = 6 \cdot 17575.41 = 105452.46$ kN/m

Building B
   x–x axis: $K_x = 6 \cdot K_{f,x} = 6 \cdot 17422.90 = 104537.40$ kN/m
   y–y axis: $K_y = 5 \cdot K_{f,y} + K_{wf,y} = 5 \cdot 17575.41 + 764001.30 = 851878.35$ kN/m

Building C
   x–x axis: $K_x = 6 \cdot K_{f,x} = 6 \cdot 17422.90 = 104537.40$ kN/m
   y–y axis: $K_y = 4 \cdot K_{f,y} + K_{wf,y} = 4 \cdot 17575.41 + 2 \cdot 764001.30 = 1598304.24$ kN/m

2.6.5 Hand calculation for the centre of stiffness

The centre of stiffness for Buildings *A* and *C* coincides with the centre of mass, whereas in Building B it is differentiated due to the existence of the 5 m RC wall in the mid-bay of the external frame along the y–y direction (Figure 2.56). The ordinates of the centre of stiffness are

$$x_C = \frac{K_{f,y} \cdot (6 + 12 + 18 + 24 + 30) + K_{wf,y} \cdot 0}{K_y} \Leftrightarrow$$

$$x_C = \frac{17575.41 \cdot (6 + 12 + 18 + 24 + 30) + 764001.30 \cdot 0}{851878.50} 35 = 1.86 \text{ m}$$

$$y_C = \frac{K_{f,x} \cdot (0 + 5 + 10 + 15 + 20 + 25)}{K_x} \Leftrightarrow$$

$$y_C = \frac{17422.90 \cdot (0 + 5 + 10 + 15 + 20 + 25)}{104537.40} = 12.50 \text{ m}$$

The eccentricities are estimated as

$$e_{mx} = x_M - x_C = 15.0 - 1.86 = 13.14 \text{ m}$$

$$e_{my} = y_M - y_C = 12.5 - 12.5 = 0.00 \text{ m}$$

2.6.6 Mass calculation

The total weight of each building is $W = 12 \cdot b \cdot d = 12 \cdot 25 \cdot 30 = 9000$ kN
The total mass of each building is: $M = W/g = 9000/9.81 = 917.43$ t

2.6.7 Base shear calculation

The design spectrum of EC8 (2004) for $S = 1.15$, $q = 4$ (Figure 2.57) is utilised for defining the base shear.

Building A

$$T_x = 2\pi\sqrt{\frac{M}{K_x}} = 2\pi\sqrt{\frac{917.43}{104537.40}} = 0.59 \text{ s} \rightarrow a_g = 0.115g, \quad V_{b,x} = 0.115 \cdot 9000 = 1035 \text{ kN}$$

$$T_y = 2\pi\sqrt{\frac{M}{K_y}} = 2\pi\sqrt{\frac{917.43}{105452.46}} = 0.59 \text{ s} \rightarrow a_g = 0.115g, \quad V_{b,x} = 0.115 \cdot 9000 = 1035 \text{kN}$$
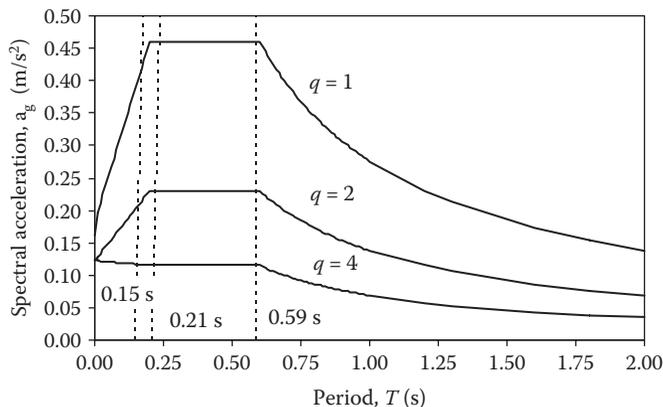
Figure 2.57 Design spectrum of EC8 (2004).

Building B

$$T_x = 2\pi\sqrt{\frac{M}{K_x}} = 2\pi\sqrt{\frac{917.43}{104537.40}} = 0.59\,\text{s} \rightarrow a_g = 0.115\text{g}, \quad V_{b,x} = 0.115 \cdot 9000 = 1035\,\text{kN}$$

$$T_y = 2\pi\sqrt{\frac{M}{K_y}} = 2\pi\sqrt{\frac{917.43}{851878.35}} = 0.21\,\text{s} \rightarrow a_g = 0.116\text{g}, \quad V_{b,y} = 0.116 \cdot 9000 = 1035\,\text{kN}$$

It may be noted that the estimated value of T_y for Building B is not accurate, since motion in the $y–y$ direction is coupled.

Building C

$$T_x = 2\pi\sqrt{\frac{M}{K_x}} = 2\pi\sqrt{\frac{917.43}{104537.40}} = 0.59\,\text{s} \rightarrow a_g = 0.115\text{g}, \quad V_{b,x} = 0.115 \cdot 9000 = 1035\,\text{kN}$$

$$T_y = 2\pi\sqrt{\frac{M}{K_y}} = 2\pi\sqrt{\frac{917.43}{1598304.24}} = 0.15\,\text{s} \rightarrow a_g = 0.117\text{g}, \quad V_{b,y} = 0.117 \cdot 9000 = 1053\,\text{kN}$$

Despite the fact that the addition of walls substantially reduces the period in the $y–y$ axis for Buildings B and C, as expected, this is not reflected in the estimated base shear values, since the estimated periods are either very close to or lie on the plateau of the spectrum.

The torsional stiffness with respect to the centre of stiffness, J_{TC}, and the torsional stiffness with respect to the centre of mass, J_{TM}, are calculated according to Equations 2.79 and 2.82, respectively, and presented in Table 2.2. In the same table, the torsional deformation ϕ_z, estimated according to Equation 2.89, as well as the horizontal displacements of the centre of mass and stiffness, appear. Additionally, the torsional radii with respect to the centre of stiffness in both directions, r_x and r_y, are calculated (Equation 2.90). The analytical estimations are quoted for the case of Building B.

Building B

The torque is:

$$M_z = V_{b,y} \cdot e_{mx} = 1035 \cdot 13.14 = 13603.19\ \text{kNm/rad}$$

Table 2.2 Calculation of parameters J_{TC}, J_{TM}, ϕ_z, u_m, v_m, r_x, r_y

Building	J_{TC}^a (kN m/rad)	J_{TM}^a (kN m/rad)	ϕ_z^b (rad)	x–x		y–y		r_x (m)	r_y (m)
				u_{mx} (mm)	v_{mx} (mm)	u_{my} (mm)	v_{my} (mm)		
A	18.69	18.69	0	9.90	0	0	9.81	13.3	13.4
B	39.44	186.60	3.45	10.20	0	0	1.22	6.8	19.4
C	354.51	354.51	0	10.50	0	0	0.66	14.9	59.9

a $\times10^6$.
b $\times10^{-4}$.

The torsional stiffness with respect to the centre of stiffness is

$$
\begin{aligned}
J_{TC} &= \sum_{j=1}^{j=m} K_{jy} x_{jc}^2 + n \sum_{i=1}^{i=m} K_{ix} y_{ic}^2 = K_{f,x} \cdot 2 \cdot (2.50^2 + 7.50^2 + 12.50^2) \\
&+ K_{f,y} \cdot (4.14^2 + 10.14^2 + 16.14^2 + 22.14^2 + 28.14^2) + K_{wf,y} \cdot 1.86^2 \\
&= 39.44 \cdot 10^6 \text{ kN m/rad}
\end{aligned}
$$

The torsional deformation is defined as

$$
\varphi_z = \frac{M_z}{J_{TC}} = \frac{1035 \cdot 13.14}{39.44 \cdot 10^6} = 3.45 \times 10^{-4} \text{ rad}
$$

The torsional stiffness with respect to the centre of mass is

$$
\begin{aligned}
J_{TM} &= J_{TC} + e_x^2 \left(\sum_{i=1}^{i=n} K_{iy} \right) + e_y^2 \left(\sum_{j=1}^{j=m} K_{ix} \right) = 39.44 \times 10^6 + 13.14^2 \cdot 851878.35 + 0 \\
&= 186.60 \times 10^6 \text{ kN m/rad}
\end{aligned}
$$

The torsional radii with respect to the centre of stiffness are (Equation 2.85):

$$
r_x = \sqrt{\frac{J_{TC}}{K_y}} = \sqrt{\frac{39.44 \times 10^6}{851878.35}} = 6.8 \text{ m}, \quad r_y = \sqrt{\frac{J_{TC}}{K_x}} = \sqrt{\frac{39.44 \times 10^6}{104361.84}} = 19.4 \text{ m}
$$

The displacements of the centre of mass are
  x–x axis: $u_{mx} = 10.2$ mm, $v_{mx} = 0$ m
  y–y axis: $u_{my} = 0$ mm, $v_{my} = 1.21$ mm

The maximum and minimum displacements of the corner columns are
  x–x axis: $u_x = 10.2$ mm, $v_x = 0$ m
  y–y axis: min: $u_{y,min} = 4.31$ mm, $v_{y,min} = 1.86$ mm
  max: $u_{y,max} = 4.31$ mm, $v_{y,max} = 8.48$ mm

Comparison of the response parameters of Buildings A, B and C leads to the following conclusions:

- The addition of a single wall (Building B) increases J_{TC} by 2.1 times and the addition of the two walls (Building C) by 19.0 times compared to the stiffness of the planar frame building (Building A). This has a direct effect on the displacements of the system along the horizontal y–y axis, which are reduced substantially.
- In order to check the torsional rigidity of the three buildings, the radius of gyration of the floor mass in plan is estimated according to Equation 2.122 after substituting Equation 2.97:

$$
l_s = \sqrt{\frac{b^2 + d^2}{12}} = \sqrt{\frac{30^2 + 25^2}{12}} = 11.27 \text{ m}
$$
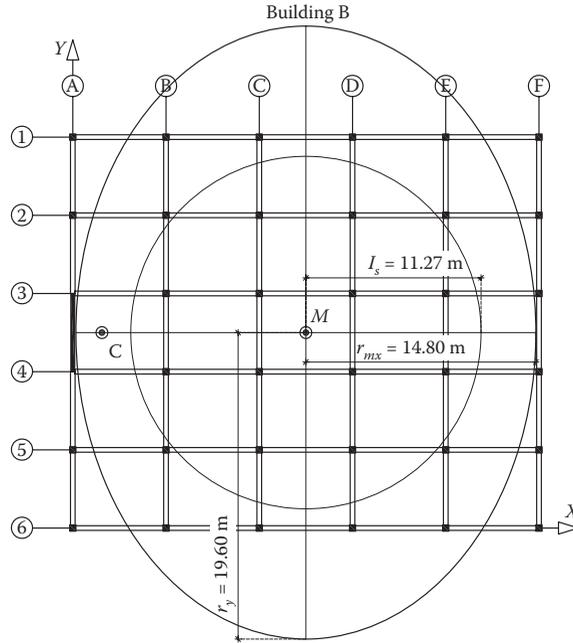
Figure 2.58 Definition of torsional rigidity in Building B.

Building A

$$l_s = 11.27\,\text{m} < r_x = 13.3\,\text{m}; \quad r_y = 13.4\,\text{m}$$

Building B (Figure 2.58)
   x–x axis: Due to eccentricity along the *x–x* axis Equation 2.122 applies:

$$l_s = 11.27\,\text{m} < r_{mx} = \sqrt{r_x^2 + e_{mx}^2} = \sqrt{6.80^2 + 13.14^2} = 14.8\,\text{m}$$

y–y axis:

$$l_s = 11.27\,\text{m} < r_y = 19.4\,\text{m}$$

Building C
   x–x axis: $l_s = 11.27\,\text{m} < r_x = 14.9\,\text{m}$
   y–y axis: $l_s = 11.27\,\text{m} < r_y = 59.9\,\text{m}$

From the above it follows that all the buildings have sufficient torsional rigidity, thus the fundamental translational periods in the two horizontal directions are longer than the torsional period (Tables 2.4 through 2.6).

2.6.8 Computer-aided calculation for the centre of stiffness

The methodology presented in Paragraph 2.4.4.2 (conclusion 5) is implemented for the determination of parameters ϕ_z, J_{TC}, e_{mx}, K_x, K_y, r_x, r_y for Buildings A, B and C. The steps followed are

1. The centre of mass is loaded with a torque $M_z = 10,000$ kN m.
2. The displacements of two counterpairs of columns at the perimeter of the buildings are estimated in order to define ϕ_z and J_{TC} (Equations 2.92 and 2.93 apply):

Building A

$$u_{x1} = 6.61 \text{ mm}, \quad u_{x2} = -6.61 \text{ mm}, \quad u_{y1} = 7.94 \text{ mm}, \quad u_{y2} = -7.94 \text{ mm}$$

$$\varphi_z = \frac{u_{x1} - u_{x2}}{d} = \frac{u_{y1} - u_{y2}}{b} = \frac{6.61 + 6.61}{25,000} = \frac{7.94 + 7.94}{30,000} = 5.29 \times 10^{-4} \text{ rad}$$

$$J_{TC} = \frac{M_z}{\varphi_z} = \frac{10,000}{5.29 \times 10^{-4}} = 18.90 \times 10^6 \text{ kN m/rad}$$

Building B

$$u_{x1} = 3.16 \text{ mm}, \quad u_{x2} = -3.16 \text{ mm}, \quad u_{y1} = 0.47 \text{ mm}, \quad u_{y2} = -7.10 \text{ mm}$$

$$\varphi_z = \frac{u_{x1} - u_{x2}}{d} = \frac{u_{y1} - u_{y2}}{b} = \frac{3.16 + 3.16}{25,000} = \frac{0.47 + 7.10}{30,000} = 2.53 \times 10^{-4} \text{ rad}$$

$$J_{TC} = \frac{M_z}{\varphi_z} = \frac{10,000}{2.53 \times 10^{-4}} = 39.60 \times 10^6 \text{ kN m/rad}$$

Building C

$$u_{x1} = 0.36 \text{ mm}, \quad u_{x2} = -0.36 \text{ mm}, \quad u_{y1} = 0.43 \text{ mm}, \quad u_{y2} = -0.43 \text{ mm}$$

$$\varphi_z = \frac{u_{x1} - u_{x2}}{d} = \frac{u_{y1} - u_{y2}}{b} = \frac{0.36 + 0.36}{25,000} = \frac{0.43 + 0.43}{30,000} = 2.85 \times 10^{-4} \text{ rad}$$

$$J_{TC} = \frac{M_z}{\varphi_z} = \frac{10,000}{2.85 \times 10^{-4}} = 350.38 \times 10^6 \text{ kN m/rad}$$

3. The centre of stiffness is geometrically estimated:
   Buildings A, C: there is no eccentricity

Building B

$$x_c = \frac{u_{y1} \cdot b}{(u_{y1} + u_{y2})} = \frac{0.47 \cdot 30,000}{(0.47 + 7.10)} = 1.86 \text{ m}$$

Hence,

$$e_{mx} = x_M - x_C = 15.0 - 1.86 = 13.14 \text{ m}$$

$$e_{my} = 0.00 \text{ m}$$

4. The centre of stiffness of each building is loaded by a horizontal force, $H = 10,000$ kN, in both the x and y axis. Having estimated the translational displacements u_{cx} and u_{cy} in the x–x and y–y directions, respectively, the corresponding stiffness is calculated according to Equation 2.94.

Building A

$$x\text{–}x \text{ axis: } u_{cx} = 0.0961 \text{ m} \rightarrow K_x = \frac{H}{u_{cx}} = \frac{10,000}{0.0961} = 104058.27 \text{ kN/m}$$

$$y\text{–}y \text{ axis: } u_{cy} = 0.0952 \text{ m} \rightarrow K_y = \frac{H}{u_{cy}} = \frac{10,000}{0.0952} = 105042.02 \text{ kN/m}$$

Building B

$$x\text{–}x \text{ axis: } u_{cx} = 0.0991 \text{ m} \rightarrow K_x = \frac{H}{u_{cx}} = \frac{10,000}{0.0991} = 100908.17 \text{ kN/m}$$

$$y\text{–}y \text{ axis: } u_{cy} = 0.0119 \text{ m} \rightarrow K_y = \frac{H}{u_{cy}} = \frac{10,000}{0.0119} = 840336.13 \text{ kN/m}$$

Building C

$$x\text{–}x \text{ axis: } u_{cx} = 0.0969 \text{ m} \rightarrow K_x = \frac{H}{u_{cx}} = \frac{10,000}{0.0969} = 103199.17 \text{ kN/m}$$

$$y\text{–}y \text{ axis: } u_{cy} = 0.0063 \text{ m} \rightarrow K_y = \frac{H}{u_{cy}} = \frac{10,000}{0.0063} = 1587301.58 \text{ kN/m}$$

5. The torsional radii with respect to the centre of stiffness are estimated as (Equation 2.85):

Building A

$$r_x = \sqrt{\frac{J_{TC}}{K_y}} = \sqrt{\frac{18.90 \times 10^6}{105042.02}} = 13.4 \text{ m}, \quad r_y = \sqrt{\frac{J_{TC}}{K_x}} = \sqrt{\frac{18.90 \times 10^6}{104058.27}} = 13.5 \text{ m}$$

Building B

$$r_x = \sqrt{\frac{J_{TC}}{K_y}} = \sqrt{\frac{39.60 \times 10^6}{840336.13}} = 6.9 \text{ m}, \quad r_y = \sqrt{\frac{J_{TC}}{K_x}} = \sqrt{\frac{39.60 \times 10^6}{100908.17}} = 19.8 \text{ m}$$

Building C

$$r_x = \sqrt{\frac{J_{TC}}{K_y}} = \sqrt{\frac{350.38 \times 10^6}{1587301.58}} = 14.9 \text{ m},$$

$$r_y = \sqrt{\frac{J_{TC}}{K_x}} = \sqrt{\frac{350.38 \times 10^6}{103199.17}} = 58.3 \text{ m}$$

Table 2.3 Comparison of parameters J_{TC}, e_{xm}, r_x, r_y estimated by hand calculations (static analysis) and by computer-aided analysis

	Static analysis				Computer-aided analysis			
Building	J^a_{TC} (kN m/rad)	e_{xm}(m)	r_x (m)	r_y (m)	J^a_{TC}(kN m/rad)	e_{xm}(m)	r_x(m)	r_y (m)
A	18.69	0	13.3	13.4	18.90	0	13.4	13.4
B	39.44	13.16	6.8	19.4	39.60	13.14	6.9	19.8
C	354.51	0	14.9	59.9	350.38	0	14.9	58.3

a $\times 10^6$.

Comparing the values of the response parameters (J_{TC}, e_{mx}, r_x, r_y) estimated by hand calculations to those derived with computer-aided analysis in Table 2.3, it may be concluded that the hand calculation procedure is sufficiently accurate for the type of buildings examined here.

2.6.9 Dynamic response

Eigenvalue *analysis* is performed for all the buildings. The eigen periods and mass participation factors appear in Tables 2.4 through 2.6.

The displacements and rotations of the centre of mass and the corner columns of all the buildings for the first three modes are presented in Tables 2.7 and 2.8, respectively.

2.6.10 Estimation of poles of rotation for building B

Building B is symmetric along the x–x direction, thus the centre of stiffness C and mass M lie on the x–x axis ($e_y = 0$). The motion is uncoupled in the x–x direction, and Equation 2.117 applies for calculating eigen frequency ω_x. The other two eigenmodes are coupled (coupled form of a displacement along the x–x axis, u_{my}, and rotation φ_z) and are estimated according to Equation 2.121. The poles of rotation O_1 and O_2 are estimated below (Figure 2.59):

The uncoupled eigen frequency in the y–y direction is given as

$$\omega_y^2 = \frac{K_y}{m} = \frac{840336.13}{917.74} = 915.66 \text{ s}^{-2}$$

The eigen frequencies of the system are (coupled modes):

$$\text{Mode 2: } T_2 = 0.56 \text{ s} \rightarrow \omega_2^2 = \left(\frac{2\pi}{T_2}\right)^2 = \left(\frac{2\pi}{0.56}\right)^2 = 125.90 \text{ s}^{-2}$$

Table 2.4 Eigen periods and mass participation factors for building A

				Mass participation factors (%)								
	Eigen periods (s)			UX			UY			UZ		
Building	T_1	T_2	T_3	$\varepsilon_{1,UX}$	$\varepsilon_{2,UX}$	$\varepsilon_{3,UX}$	$\varepsilon_{1,UY}$	$\varepsilon_{2,UY}$	$\varepsilon_{3,UY}$	$\varepsilon_{1,UZ}$	$\varepsilon_{2,UZ}$	$\varepsilon_{3,UZ}$
A	0.69	0.69	0.33	100	0	0	0	100	0	0	0	0
					RX			RY			RZ	
				$\varepsilon_{1,RX}$	$\varepsilon_{2,RX}$	$\varepsilon_{3,RX}$	$\varepsilon_{1,RY}$	$\varepsilon_{2,RY}$	$\varepsilon_{3,RY}$	$\varepsilon_{1,RZ}$	$\varepsilon_{2,RZ}$	$\varepsilon_{3,RZ}$
				0	59	0	50	0	0	0	0	100

Table 2.5 Eigen periods and mass participation factors for building B

	Eigen periods (s)			Mass participation factors (%)								
				UX			UY			UZ		
Building	T_1	T_2	T_3	$\varepsilon_{1,UX}$	$\varepsilon_{2,UX}$	$\varepsilon_{3,UX}$	$\varepsilon_{1,UY}$	$\varepsilon_{2,UY}$	$\varepsilon_{3,UY}$	$\varepsilon_{1,UZ}$	$\varepsilon_{2,UZ}$	$\varepsilon_{3,UZ}$
B	0.69	0.56	0.10	100	0	0	0	86	14	0	0	0
				RX			RY			RZ		
				$\varepsilon_{1,RX}$	$\varepsilon_{2,RX}$	$\varepsilon_{3,RX}$	$\varepsilon_{1,RY}$	$\varepsilon_{2,RY}$	$\varepsilon_{3,RY}$	$\varepsilon_{1,RZ}$	$\varepsilon_{2,RZ}$	$\varepsilon_{3,RZ}$
				0	51	0	50	0	0	0	13	85

Table 2.6 Eigen periods and mass participation factors for building C

	Eigen periods (s)			Mass participation factors (%)								
				UX			UY			UZ		
Building	T_1	T_2	T_3	$\varepsilon_{1,UX}$	$\varepsilon_{2,UX}$	$\varepsilon_{3,UX}$	$\varepsilon_{1,UY}$	$\varepsilon_{2,UY}$	$\varepsilon_{3,UY}$	$\varepsilon_{1,UZ}$	$\varepsilon_{2,UZ}$	$\varepsilon_{3,UZ}$
C	0.69	0.18	0.08	100	0	0	0	100	0	0	0	0
				RX			RY			RZ		
				$\varepsilon_{1,RX}$	$\varepsilon_{2,RX}$	$\varepsilon_{3,RX}$	$\varepsilon_{1,RY}$	$\varepsilon_{2,RY}$	$\varepsilon_{3,RY}$	$\varepsilon_{1,RZ}$	$\varepsilon_{2,RZ}$	$\varepsilon_{3,RZ}$
				0	60	0	49	0	0	0	0	97

Table 2.7 Displacements and rotations of the centre of mass

	Building A			Building B			Building C		
Modes	u_{mx} (mm)	u_{my} (mm)	φ_z^a (rad)	u_{mx} (mm)	u_{my} (mm)	φ_z^a (rad)	u_{mx} (mm)	u_{my} (mm)	φ_z^a (rad)
1	28.1	0	0	28.1	0	0	28.1	0	0
2	0	28.1	0	0	26.1	1.62	0	27.9	0
3	0	0	4.37	0	10.1	3.97	0	0	4.21

a $\times 10^{-3}$.

Table 2.8 Displacements and rotations of the corner columns

	Building A			Building B			Building C		
Modes	u_x (mm)	u_y (mm)	φ_z^a (rad)	u_x (mm)	u_y (mm)	φ_z^a (rad)	u_x (mm)	u_y (mm)	φ_z^a (rad)
1	28.1	0	0	28.1	0	0	28.1	0	0
2	0	28.1	0	20.2	1.8	1.62	0	27.9	0
					50.4				
3	54.7	65.6	4.37	49.7	49.5	3.97	52.6	63.1	4.21
					69.7				

a $\times 10^{-3}$.
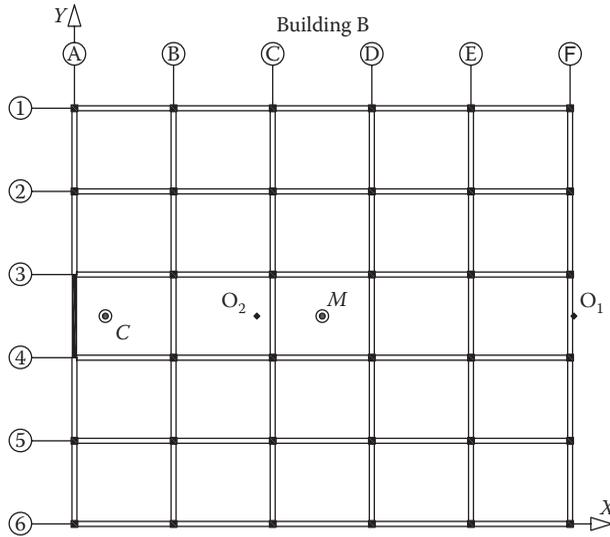
Figure 2.59 Poles of rotation in Building B.

Mode 3: $T_3 = 0.10$ s $\rightarrow \omega_3^2 = \left(\dfrac{2\pi}{T_3}\right)^2 = \left(\dfrac{2\pi}{0.10}\right)^2 = 3947.84$ s^{-2}

The above data are used for the calculation of the ordinates of the poles of rotation relative to the centre of mass (Anastasiadis, 2001):

Coupled mode 2:

$$O_1: e_{x2} = e_{xm}\frac{\omega_y^2}{\omega_y^2 - \omega_2^2} = 13.14\frac{915.66}{915.66 - 125.90} = 15.23 \text{ m}, e_{y2} = 0 \text{ m}$$

Coupled mode 3:

$$O_2: e_{x3} = e_{xm}\frac{\omega_y^2}{\omega_y^2 - \omega_3^2} = 13.14\frac{915.66}{915.66 - 3947.84} = -3.96 \text{ m}, e_{y3} = 0 \text{ m}.$$

This may also be derived by geometrically plotting the eigen vector displacements as may be seen in Subsection 5.9.6, Table 5.14.

Chapter 3

Design principles, seismic actions, performance requirements, compliance criteria

3.1 INTRODUCTION

The performance of a building in response to seismic actions is influenced mainly by three parameters:

1. The *seismic action*
2. The *level of damage* that is acceptable to society in the case of a strong earthquake and therefore is accepted by the legal framework in effect
3. The *quality* of the structural system of the building

The seismic action is a load case with the following characteristics, which differ drastically from all other loading types:

1. It is of high uncertainty in relation to the peak ground acceleration (PGA) $\ddot{x}_{omax}$, but also to its frequency content. This uncertainty is magnified by the fact that the existing strong motion records (accelerograms) cover only the period of the last 70 years.
2. Seismic actions in a region do not have a *reliable ceiling* as far as the expected PGA. This ceiling also depends on the *preselected return period of occurrence*, as will be shown later.
3. It has a short duration (a few seconds) in the form of vibration. In this respect, the induced 'strain energy' is limited in duration but causes high inelastic cyclic strains.

Limits of social acceptance of damages for seismic action of moderate and higher intensity are included in all modern Seismic Codes and were stated first in the SEAOC in 1978 (SEAOC, 1978) in the form of the following *principles*:

1. Structures should resist low-intensity earthquakes *without any structural damage*. Thus, during small and frequent earthquakes all structural components forming the structure should remain in the elastic range.
2. Structures should resist an earthquake of moderate intensity ('design earthquake') with light and repairable damage at some structural members as well as at infill elements, which *do not put human life at risk*.
3. Structures should withstand high-intensity earthquakes with a return period much longer than their design life *without collapsing*.

In this respect, the transition of the structural system *to the inelastic range*, in case of a moderate or higher intensity earthquake, which entails the display of structural damage, must be considered *a basic social concession*.

Finally, the quality of the structural system is a parameter of controlled reliability, since it depends on the structural system layout, design, detailing and quality control of the construction.

In the sections that follow, a detailed presentation will be made of

- The principles of seismic design on the basis of *'energy balance'*
- The *seismic actions*
- The *performance-based design* and the relevant compliance criteria

The building and its design parameters will be examined in the next chapters.

3.2 CONCEPTUAL FRAMEWORK OF SEISMIC DESIGN: ENERGY BALANCE

3.2.1 General

From what has been presented so far, it is obvious that there is a substantial difference between conventional load cases (gravity loads, earth pressure, wind, hydrostatic pressure, etc.) and seismic action.

In the first category, where the actions are either permanent or variable and induced for a period of time, if the *structural resistance* R_κ is bigger than the *action effects* E_κ (internal forces) by a specified percentage (safety factor), the structure is considered safe. This means that if

$$\frac{[R_\kappa]}{[E_\kappa]} \geq \gamma_f \cdot \gamma_m = \gamma_F \qquad (3.1a)$$

and

$$\boxed{\frac{[R_\kappa]}{\gamma_m} \geq \gamma_f \cdot [E_k]} \qquad (3.1b)$$

then the structure is covered by a safety factor:

$$\gamma_F = \gamma_f \cdot \gamma_m \qquad (3.2)$$

In the above equations, the meaning of the notation in use is the following:

$[R_\kappa]$ is the characteristic strength of the structure
$[E_\kappa]$ is the characteristic action effect on the structure
γ_f , γ_m are partial safety factors for loads and materials (both greater than unity)

The above considerations are deemed to ensure the safety of the structure to an acceptable level of probability.

In the second category, the seismic action is introduced at the base of the structure in the form of a vibration of high frequency and short duration (a few seconds). Consequently, a limited amount of kinetic energy is introduced to the mass of the structure via the elastic

or inelastic links of the mass to the foundation ground as long as the seismic motion lasts. Of course, if the mass of the structure is linked loosely to the ground via 'seismic isolators' (see Subsection 3.2.4), which have in parallel the ability to dissipate energy, the transfer of a considerable amount of kinetic energy to the mass of the structure is avoided. Therefore, in this case, the response of the structure to the seismic action is drastically reduced.

If the structure is in a position to transform the induced kinetic energy into potential strain energy without failure and then to dissipate a considerable percentage of this during its cyclic vibration in the form of hysteretic damping, then the structure must be considered safe.

Therefore, if

$$\frac{\left[W^u_{supply}\right]}{\left[W_{demand}\right]} \geq \gamma_w \cdot \gamma_m = \gamma_d \qquad (3.3a)$$

or

$$\boxed{\frac{\left[W^u_{supply}\right]}{\gamma_m} \geq \gamma_w \cdot \left[W_{demand}\right]} \qquad (3.3b)$$

In which

W^u_{supply} is the strain energy that the structure can absorb until failure
W_{demand} is the kinetic energy that is induced to the structure during the vibration
γ_w is the safety factor with respect to energy absorption

then the structure can undergo the earthquake motion with a safety factor:

$$\gamma_d = \gamma_w \cdot \gamma_m \qquad (3.4)$$

It is worth reviewing the preceding remarks on the diagrams of Figures 3.1 and 3.2.

Consider the building of Figure 3.1, which is loaded by permanent gravity loads and a constantly increasing lateral load p_i, which in turn causes a *base shear* V_i, also continuously increasing until *failure.*

$$V_i = \int_o^h P_i \, dh$$
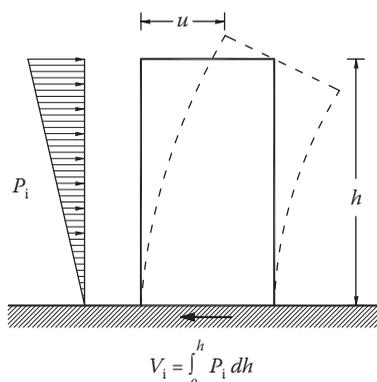
Figure 3.1 Lateral load P_i of a building developing base shear V_i and respective top horizontal displacement u.
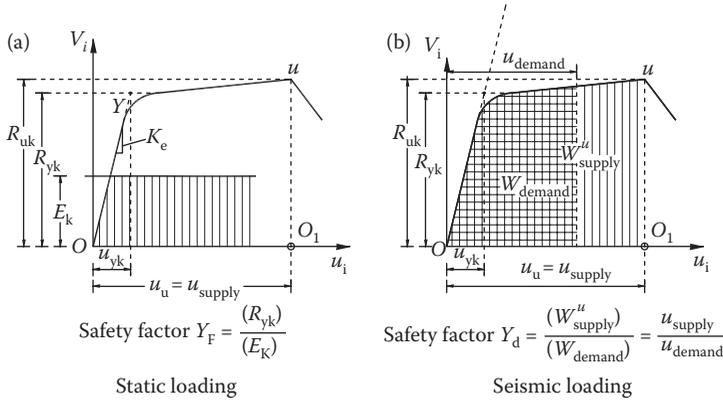
Figure 3.2 The main concept for safety verifications for (a) static loads, and (b) seismic loads.

This lateral loading results in a displacement of the top of the building relative to its base equal to *u*. If the successive steps of $V_i - u_i$ are recorded in a diagram, a curve will be formed known as the *capacity curve of the structure* (Figure 3.2a).

This curve has the following characteristic properties:

- It has a first *almost linear* branch of high slope (stiffness $K_e = \tan \theta$).
- At the end of this branch there is the *yielding point Y*, where the slope of this branch is reduced drastically. The coordinates of this point are known as the *yield strength* ($R_{y\kappa} = V_{y\kappa}$) and the *yield strain* ($u_{y\kappa}$) of the structure.
- The second branch of the diagram starts from the yield point *Y* with a very small slope (strain hardening) and continues up to a point U_u with coordinates $R_{u\kappa} \cong (1.05 \div 1.20 R_{y\kappa})$ known as strength at failure and u_u (strain at failure), at which point *collapse takes place*, that is, an abrupt loss of strength capacity for small additional displacement. The area (W_{supply}) of the surface under the capacity curve of the structure (OY_uO_1) represents the potential strain energy that can be accumulated in the structure for monotonous lateral loading up to collapse.

The above characteristics of the capacity curve have also been examined for the case of an RC cantilever beam in Subsection 2.3.5 (Figure 2.29).

For almost three centuries, but even nowadays, the structural design for almost all types of loading, *except seismic actions*, has been based on the *basic requirement* that action effects (E_κ) should not exceed a percentage of the yield strength ($R_{y\kappa}$) of the structure (Equations 3.1a,b; Figure 3.2a). The reasoning behind this basic concept is that since loading is not instantaneous and acts permanently (static loadings), if it exceeds the yield capacity $R_{y\kappa}$ the structure fails and collapses. Therefore, the safety margin must be based on strength capacity and inequalities (3.1a,b) must be used.

In case of seismic action (Figure 3.2b), the vibration of the mass of the structure is the result of the kinetic energy W_{demand} that has passed from the foundation ground to the vibrating mass through the elastic or inelastic links between ground and mass. This energy (W_{demand}) *is limited*, due to the fact that the seismic duration is limited. Therefore it is displayed in the form of a number of displacement reversals. In this context it is accepted that in the case that yield strength ($R_{y\kappa}$) is exhausted, it would be enough that the displacement (u_{demand}) demand corresponding to the energy demand (W_{demand}) does not exceed a specified percentage of

the displacement capacity at failure u_u, and therefore a percentage of the energy dissipation capacity W_{supply}^u, that is,

$$u_u = u_{supply}$$

$$W_u = W_{supply}$$

The above reasoning is displayed in Equation 3.3.
Taking now into account that

$$\left[W_{supply}^u \right] \cong u_{supply} \left[R_{yк} \right] \tag{3.5a}$$

and

$$\left[W_{demand} \right] \cong u_{demand} \left[R_{yк} \right] \tag{3.5b}$$

it is concluded that

$$\frac{\left[W_{supply}^u \right]}{\left[W_{demand} \right]} \cong \frac{u_{supply}}{u_{demand}} \geq \gamma_w \cdot \gamma_m = \gamma_d \tag{3.6}$$

Now introducing Equation 2.52a, from Chapter 2.3.4, into Equation 3.6 the equivalent:

$$u_{supply} = \mu_{supply} u_y \tag{3.7a}$$

$$u_{demand} = \mu_{demand} u_y \tag{3.7b}$$

the following equation may be obtained:

$$\frac{\left[W_{supply}^u \right]}{\left[W_{demand} \right]} \cong \frac{u_{supply}}{u_{demand}} = \frac{\mu_{supply}}{\mu_{demand}} \geq \gamma_w \cdot \gamma_m = \gamma_d \tag{3.8}$$

where γ_w is the safety factor referring to displacements.
From the above analysis, the following conclusions may be drawn:

1. For seismic actions, *and only for these*, it is accepted that during the earthquake the yield resistance [$R_{yк}$] of the structure may be completely exhausted, that is, it is accepted that due to seismic action the structure may pass into the inelastic range of the capacity curve.
2. For seismic actions, *and only for these*, it is accepted that the safety factor *may be satisfied on a displacement basis*, that is, the maximum displacement [u_{demand}] must not exceed a specified percentage of [u_{supply}] (Equations 3.6 and 3.8).
3. The above considerations in relation to those that have been presented in Subsections 2.3.4 and 2.3.6 constitute the core of the modern philosophy of seismic design, either as it is carried out in the form of *displacement-based design* or in the form of the *force-based design*.

3.2.2 Displacement-based design

3.2.2.1 Inelastic dynamic analysis and design

Taking into account the acceptance of inelastic response of the structure during an earthquake in the inelastic range, which means the acceptance of a specified level of damage, the direct approach to the problem of the analysis and design of seismic-resistant structures includes the following steps:

1. Determination of the capacity curve of the structural system.
2. Dynamic inelastic analysis of the structure for a series of normalised accelerograms to a Code-specified Intensity S.I.
3. Comparison of u_{supply} of the capacity curve with u_{demand}^{max} derived from the dynamic inelastic analysis of the structures (Figure 3.3).

The above procedure should include verifications for all crucial parameters as they have been presented in Section 2.5. As has been explained in the previous chapter, for the time being this procedure is used only in research and in special design cases (e.g., base-isolated systems).

3.2.2.2 Inelastic static analysis and design

This method has been developed in the last 15 years and is implemented basically for the assessment, verification and retrofitting of existing buildings.

A conceptual approach to this method will be given here for the SDOF system depicted in Figure 3.4a.
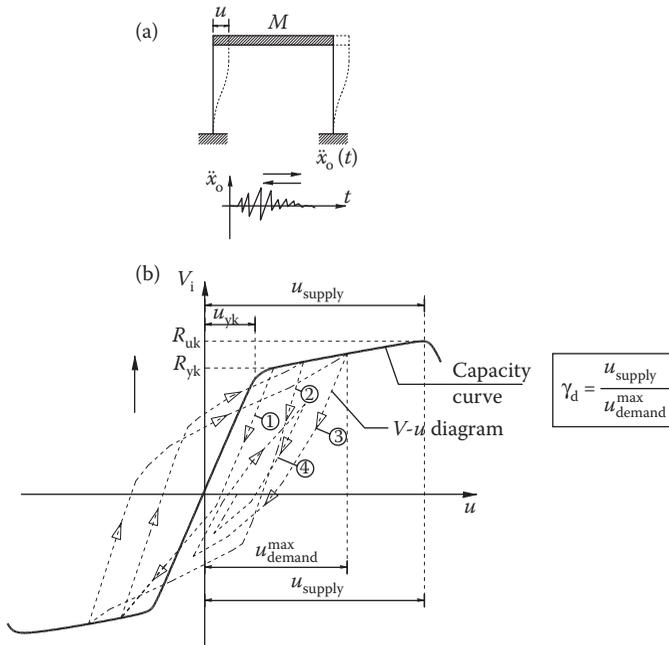
Figure 3.3 Displacement-based design based on inelastic dynamic analysis. (a) The structural system under seismic excitation; (b) $V_i - U_i$ curve for seismic loads and capacity curve of the structure.
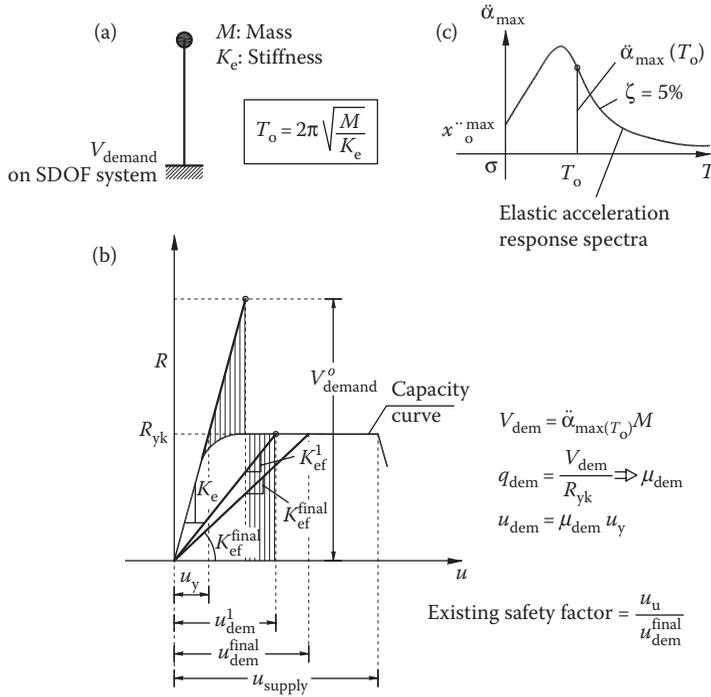
Figure 3.4 Displacement-based design based on inelastic static analysis (a push-over analysis). (a) Structural system; (b) capacity design curve and successive steps for the determination of *u* demand; (c) elastic acceleration response spectrum.

Step 1: Calculation and plotting of the capacity curve of the system (Figure 3.4b). This procedure assumes the implementation of an inelastic static step-by-step analysis of the system for an increasing lateral force ('*push-over analysis*').

Step 2: Determination of the fundamental period T_o, assuming linear elastic response $T_o = 2\pi\sqrt{M/K_e}$·

Step 3: Determination of the base shear of the system V^o_{demand}, assuming linear elastic response, using the elastic acceleration response spectrum (Figure 3.4c), that is,

$$V^o_{demand} = \ddot{\alpha}_{max(T_o)} \cdot M \tag{3.9}$$

Step 4: Determination of the behaviour factor q_{demand} equal to

$$q_{demand} = \frac{V^o_{demand}}{R_{y\kappa}} \tag{3.10}$$

From q_{demand} using Equations 2.53 through 2.55 (see Subsection 2.3.4), μ^1_{demand} is determined.

Step 5: Using the relation:

$$u^1_{demand} = \mu^1_{demand} u_y \tag{3.11}$$

u^1_{demand} is determined (Figure 3.4b).

Step 6: Determination of the new effective stiffness K_{ef}^1 equal to (Figure 3.4b)

$$K_{ef}^1 = \frac{R_{y\kappa}}{u_{demand}^1}$$ (3.12)

Step 7: For this new stiffness, K_{ef}^1 steps 2 through 6 are repeated until successive iteration steps result in very close values for K_{ef}.

Step 8: For the final u_{demand}^{final} (Figure 3.4b), the existing safety factor is determined and compared with a codified safety factor, that is,

$$\frac{u_{supply}}{u_{demand}^{final}} = \gamma_{existing} \geq \gamma_d$$ (3.13)

The above inequality constitutes the safety verification according to *displacement-based design*. Notation in use in the above presentation is given in Figure 3.4.

This method will be presented in detail in Chapters 5 and 14. It should be noted that in this method the inelastic static analysis requires the elaboration of the capacity curve of the system following a monotonous increasing of the lateral loading (*pushover analysis*).

It is obvious that for the elaboration of the capacity curve it is necessary to know

- The material properties of the structure
- Its geometry
- The reinforcement detailing

This means that the structure has been previously designed, and in this respect this method for the time being is used basically for the analysis, safety verification, and retrofitting of *existing buildings*.

Recently, successful efforts have been in progress for the introduction of the above procedure in the analysis and design of new buildings in the form of a *Direct Displacement-Based Design* (DDBD) method (Priestley et al., 2007).

3.2.3 Force-based design

This method is implemented according to Codes in effect *for the analysis and design of new buildings* and it is considered nowadays to be the reference method for the seismic design.

In this method the following procedure is followed:

1. The acceleration and, therefore, the *design base shear*, which results from the linear acceleration response spectrum, is reduced by the *behaviour factor q* ranging between 1.5 and 5.0. This *reduction factor* is specified by the Code of Practice, and its value depends on the structural type (Figure 3.5). For these reduced values of inertial forces the structural system is analysed *under the assumption of linear behaviour.*

2. Based on the combination of load effects that have resulted from these inertial forces reduced by q and from the gravity loads wherein masses have been taken into account for the determination of the inertial forces, using *partial load safety factors* $\gamma_f = 1.0$, the dimensioning and safety verification of the structure is carried out for the ULS (ultimate limit state), that is,
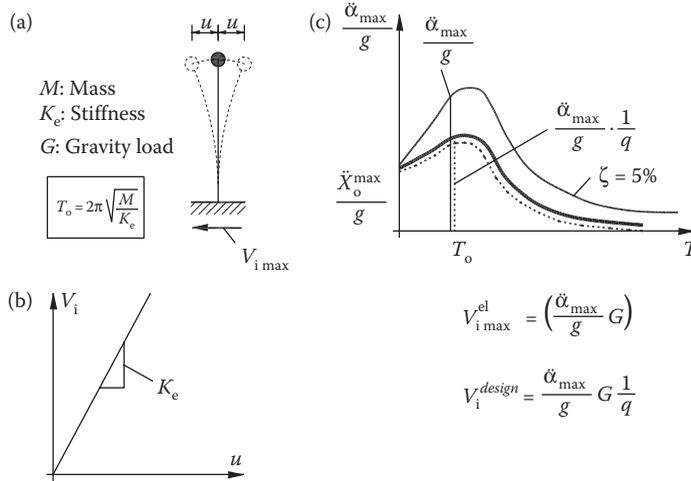
Figure 3.5 Force-based design based on 'model response spectrum analysis' or on 'lateral force method of analysis': (a) structural system under seismic action; (b) $V_i - U_i$ diagram; (c) relation between elastic and design acceleration response spectrum.

$$[E_d] \leq \frac{[R_\kappa]}{\gamma_m} \tag{3.14}$$

3. Based on the codified value of q and on the fundamental period of the structure T, ductility demand μ_{Dem} may be obtained from Equations 2.53 through 2.55 (Subsection 2.3.4).

   Then from equation:

$$\mu_{supply} \geq \gamma_d \mu_{demand} \tag{3.15}$$

μ_{supply} is defined. Thereafter, the structural system is designed and detailed in such a way that its ductility μ_{supply} fulfills Equation 3.15. It is obvious that as the behaviour factor q increases, the value of μ_{demand} increases also, and therefore *the structure must be more ductile*. It should be noted that for the implementation of the procedure of this step, the capacity curve of the structure is needed, and in this respect the *inelastic static analysis* (push-over analysis) of the structure should be carried out.

4. In order to avoid inelastic static analysis, the safeguarding of the necessary ductility of the structure according to all modern Codes is covered by a series of *rules* that are characterised by increasing demands in parallel with the increase of behaviour factor q. In this respect, *the elaboration of the capacity curve of the structure as a whole and of its individual critical regions is avoided*. Only in specific critical regions and for high values of q is *local ductility* verified by calculations, according to rules explicitly stated in Codes.

5. However, it is not certain that the above procedure ensures the required ductility (Figure 3.6) of all structural members, since the structural analysis, either static or dynamic, is carried out in the elastic range. Therefore, a second series of rules is specified by Codes that ensure a desirable hierarchy in the sequence of the breakdown of the chain of resistance of the structure. In this way, the risk of early failure due to the formation of a collapse mechanism (e.g. inverted pendulum, etc.) is reduced and the
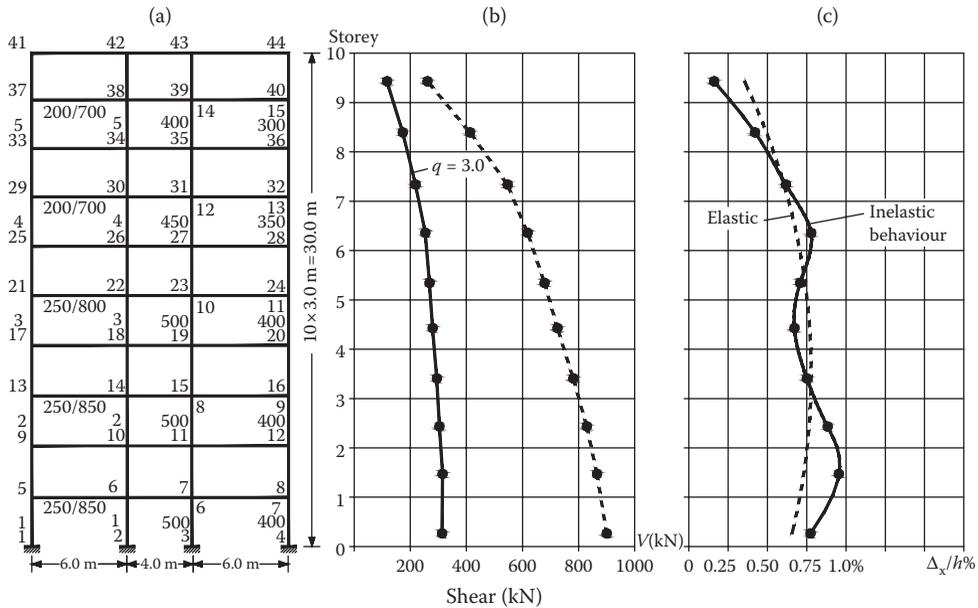
Figure 3.6 Comparison of shear forces and drifts ratios (interstorey deflections/storey height) of inelastic and elastic response at a typical ten-storey building: (a) structural system; (b) shear forces; (c) drift-ratios. (Adapted from Penelis, G.G. and Kappos, A.J. 1997. *Earthquake-Resistant Concrete Structures*. SPON E&FN (Chapman & Hall), London.)

structure may sustain catastrophic earthquakes much stronger than the 'design earth-quake' (see Section 3.1), with extensive damages but without collapse. These rules constitute what it is called *capacity design*, and they will be examined thoroughly in the following chapters (see Chapter 6).

Based on what has been presented above it can easily be understood why

- The partial load safety factor for the seismic combination is $\gamma_f = 1.0$, and
- At the same time the inertial forces derived through a linear analysis are reduced by a *q*-factor ranging between 1.50 and 5.0

The above considerations appear unreasonable to someone who uncritically implements a modern Seismic Code.

3.2.4 Concluding remarks

From what has been presented in this section so far, the following conclusions may be drawn.

1. The energy balance, that is, the balance between the kinetic energy input (demand) in the mass and the potential strain energy storage (supply) in the structure, must be considered the core for seismic design, either for *force-based design* or for *displacement-based design*. Even for alternative design methods that are *base isolation systems* or *passive systems of energy dissipation*, the consideration of energy balance is of paramount importance.
2. *The force-based design method* will be the main issue in the major part of this book, since nowadays it constitutes the basis of all modern Codes for the analysis and design of new buildings. In this method, *strength* and *ductility* remain in a kind of

(a) Conventional structure

Amplification of forces

Significant storey drifts
predetermined forces

(b) Base-isolated structure

Negligible interstorey drifts

Base isolation pads
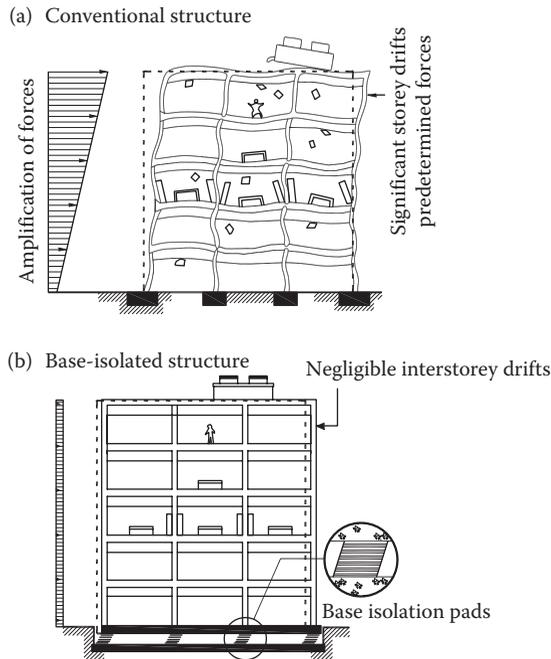
Figure 3.7 Comparative response to seismic action (a) of a conventional earthquake-resistant building; (b) of a building with seismic isolation.

counter-balance, that is, the *reduction* of the '*seismic design force*' and therefore of the '*strength*' $R_{y\kappa}$ of the structure due to a higher *q*-factor result in the need for a *ductility increase* of the structure so that the strength reduction can be counter-balanced.

3. *The displacement-based design method* will be examined in Chapter 5, where the calculation of the capacity curve will be presented, and in Chapter 14, where the assessment of the seismic capacity and retrofitting of existing R/C buildings will be presented. However, it should be noted that there is a high probability for the displacement-based design method to also be adopted by Codes for the design of new buildings in the near future (Priestley et al., 2007).

4. In the alternative design method of seismic base isolation, isolators are introduced between foundation and superstructure. This drastically reduces the kinetic energy input due to the increase of the fundamental period of the new system by removing the relevant ordinate on the elastic acceleration response spectrum to the right. In parallel, most of the kinetic energy input in this case is absorbed and dissipated at the isolators (Figure 3.7), leaving the superstructure almost free of strains.

5. The alternative design method of arranging *passive systems of energy dissipation* in some spans of frame systems protects the structure from damage due to drastic absorption and dissipation of the kinetic energy input by the dissipative devices (Figure 3.8).

3.3 EARTHQUAKE INPUT

3.3.1 Definitions

Earthquakes are ground vibrations that are caused mainly by the fracture of the crust of the earth or by sudden movement along an already *existing fault* (tectonic earthquakes), which
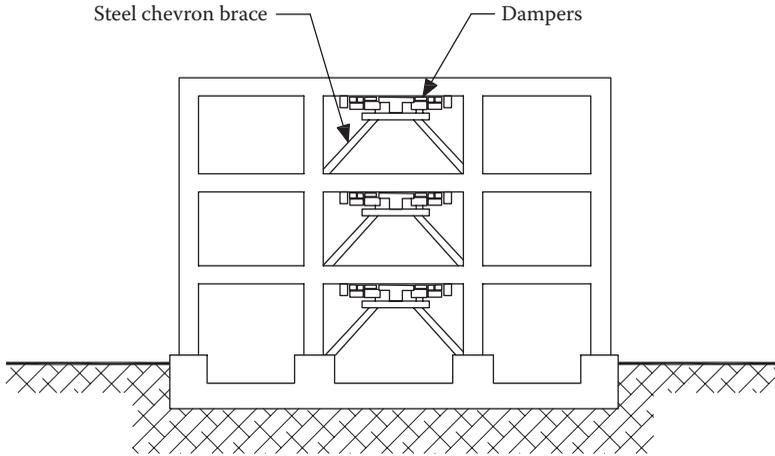
Figure 3.8 Passive energy dissipators (dampers) in a building.

is caused by the sudden release of elastic strain energy in the form of kinetic energy along the length of the fault ('elastic rebound theory'; Reid, 1911). Very rarely, earthquakes can be caused by volcanic eruptions. This energy accumulation can be explained by the theory of motion of *lithospheric plates*, into which the crust of the earth is divided (Figures 3.9 and 3.10; Strobach and Heck, 1980; Papazachos, 1986). Figure 3.11 shows some characteristic terms that are related to the phenomenon of earthquakes.

The quantification of seismic motion is achieved with the use of two types of instruments, namely, *seismographs* and *accelerographs*. The first ones record displacements of the ground as a function of time and operate on a continuous real-time basis. Their recordings are of interest mainly to seismologists. The second ones record the acceleration of the ground as a function of time. They are adjusted to start operating whenever a certain ground acceleration is exceeded (strong motion instruments).

Figure 3.9 Motion of the lithospheric plates.
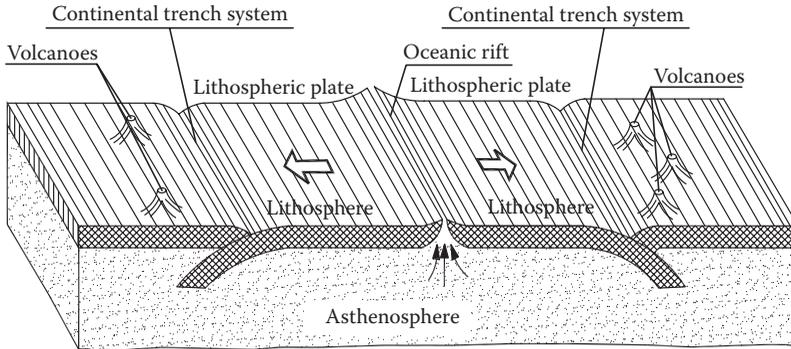
Figure 3.10 Motion system of lithospheric plates.

They are of paramount importance in earthquake engineering since, as we have seen, they provide *the seismic* input for static or dynamic analysis of structures.

The *magnitude* of an earthquake is a measure of this phenomenon in *terms of energy* released in the form of seismic waves *at the point of origin*. It is measured on various scales (Richter scale, M_L; body wave scale, m_b; surface wave scale, M_s; and moment scale, M_w).

The magnitude of any of the above scales is provided by using the relevant seismograms. Energy released at an activated fault may be expressed by the following semi-empirical relation (Richter, 1958):

$$\log E = 11.80 + 1.50\,M_s(\mathrm{erg}) \qquad\qquad (3.16)$$

As the magnitude increases by one unit, the energy release increases by a factor of $10^{1.5} = 31.6$.

The *intensity* of an earthquake is an index of the consequences that this earthquake has on the population and the structures of a certain area. It is obvious that it is impossible to measure the damage due to an earthquake using a single-quantity system. Therefore, the damage is usually estimated qualitatively using *empirical intensity scales*. The most common macro-seismic scales in use today are the Modified Mercalli (MM) scale (Table 3.1), the Medvedev, Sponeur, Karnik (MSK) scale (Table 3.2), and the European Macroseismic (EMS) Scale. All have 12 intensity grades. Figure 3.12 shows the division of Greece into seismic zones (Papaioannou et al., 1994) according to the MM scale. It should be stressed
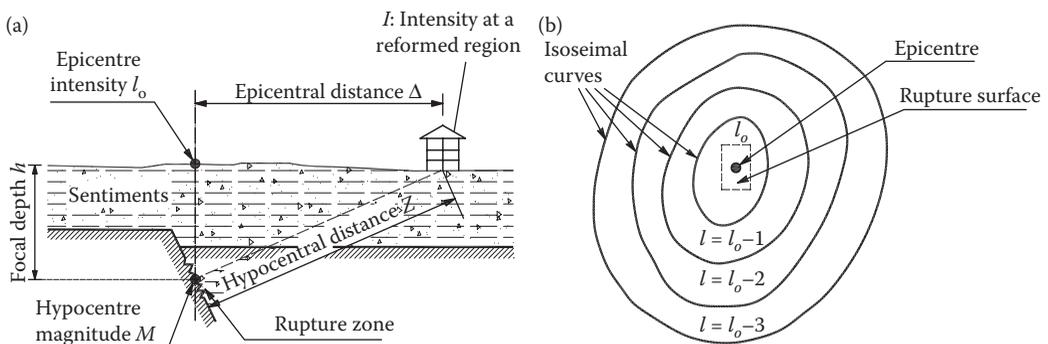
Figure 3.11 Terminology related to earthquakes (a) generation and propagation; (b) isoseismic curves.

Table 3.1 The modified Mercalli scale

		Ground acceleration α	
		cm/s	a/g
I	Not felt except by very few under especially favourable circumstances.		
II	Felt only by a few persons at rest, especially on upper floors of buildings. Delicately suspended objects may swing.	2	
		3	
III	Felt quite noticeably indoors, especially on upper floors of buildings, but many people do not recognise it as an earthquake.	4	
	Standing motor cars may rock slightly. Vibration like passing	5	0.005 g
	truck. Duration estimated.	6	
IV	During the day, felt indoors by many, outdoors by few. At night some	7	
	awakened. Dishes, windows, doors disturbed: walls make creaking	8	
	sound. Sensation like heavy truck striking building. Standing motor	9	
	cars rock noticeably.	10	0.01 g
V	Felt by nearly everyone, many awakened. Some dishes, windows, etc., broken: a few instances of cracked plaster, unstable objects		
	overturned. Disturbances of trees, poles and other tall objects	20	
	sometimes noticed. Pendulum clocks may stop.	30	
VI	Felt by all; many frightened and run outdoors. Some heavy	40	
	furniture moved: a few instances of fallen plaster or damaged	50	0.05 g
	chimneys. Damage slight.	60	
VII	Everybody runs outdoors. Damage negligible in buildings of good	70	
	design and construction: slight to moderate in well-built ordinary	80	
	structures: considerable in poorly built or badly designed structures:	90	
	some chimneys broken. Noticed by persons driving motor cars.	100	0.1 g
VIII	Damage slight in specially designed structures: considerable in ordinary substantial buildings, with partial collapse: great in poorly		
	built structures. Panel walls thrown out of frame structures. Fall	200	
	of chimneys, factory stacks, columns, monuments, walls. Heavy		
	furniture overturned. Sand and mud ejected in small amounts. Changes in well water. Disturbs persons driving motor cars.	300	
IX	Damage considerable in specially designed structures: well-designed		
	frame structures thrown out of plumb: great in substantial buildings,	400	
	with partial collapse. Buildings shifted off foundations. Ground	500	0.5 g
	cracked conspicuously. Underground pipes broken.	600	
X	Some well-built, wooden structures destroyed: most masonry and	700	
	frame structures destroyed with foundations: ground badly cracked.	800	
	Rails bent. Landslides considerable from river banks and steep	900	
	slopes. Shifted sand and mud. Water splashed over banks.	1000	1 g
XI	Few, if any, masonry structures remain standing. Bridges destroyed. Broad fissures in ground. Underground, pipelines completely out of		
	service. Earth slumps and landslips in soft ground. Rails bent greatly.	2000	
		3000	
XII	Damage total. Waves seen on ground surfaces. Lines of sight	4000	
	and level distorted. Objects thrown upward into the air.	5000	5 g
		6000	

Source: Derecho, A. and Fintel, M. 1974. Earthquake-resistant structures, *Handbook of concrete Engineering*, Chapter 12, Van Nostrand Reinhold Co, New York.

Table 3.2 The MSK intensity scale

Degree	Intensity	Effect		
		On people	On structures	On the environment
1	Insignificant	Not felt		
2	Very light	Slightly felt		
3	Light	Felt mainly by people at rest		
4	Somewhat strong	Felt by people indoors	Trembling of glass Windows	
5	Almost strong	Felt indoors and outdoors, awakening of sleeping people	Oscillation of suspended objects, displacement of pictures on walls	
6	Strong	Many people are frightened	Light damage to structures, fine cracks in plaster	Very few cracks on wet soil
7	Very strong	Many people run outdoors	Considerable damage to structures, cracks in plaster, walls and chimneys	Landslides of steep slopes
8	Damaging	Everybody is frightened	Damage to buildings, large cracks in masonry, collapse of parapets and pediments	Changes in well-water Landslips of road Embankments
9	Very damaging	Panic	General damage to buildings, collapse of walls and roofs	Cracks on the ground, landslides
10	Extremely damaging	General panic	General destruction of buildings, collapse of many buildings	Changes on the surface of the ground, appearance of new water wells
11	Destructive	General panic	Serious damage to well-built structures	
12	General destruction	General panic	Total collapse of buildings and other civil engineering Structures	Changes on the surface of the ground, appearance of new water wells

that an earthquake *has only one magnitude* but different intensities from one place to the other.

The intensity generally *attenuates* as the distance from the epicenter increases. The soil conditions have a significant effect on the distribution of structural damage. If the points of equal intensity are connected on a map, the resulting curves are called *isoseismic contours* (Figure 3.11). From the design point of view, the intensity as it has been defined above is not of great interest.
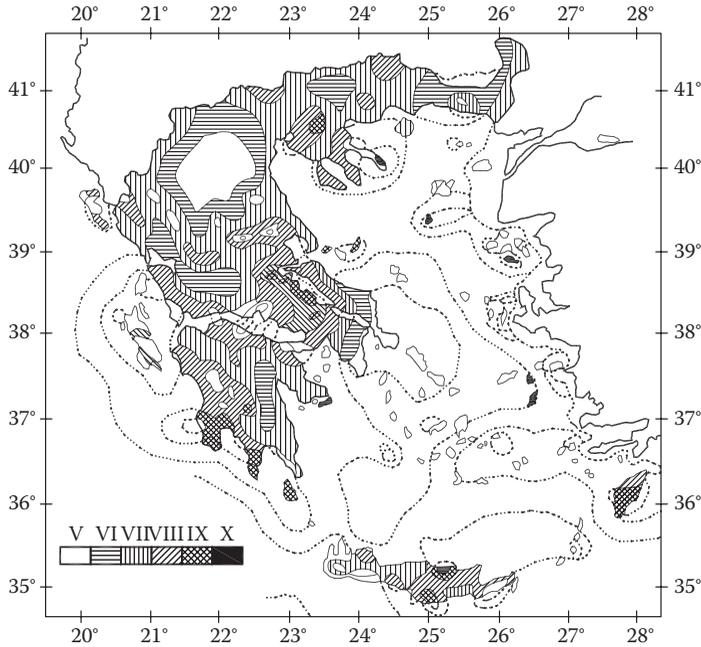
Figure 3.12 Maximum observed intensities in Greece between 1700 and 1981 on the MM scale.

The reason is that, on one hand, it does not provide any quantitative information about the parameters that are related to the ground motion (e.g., peak ground acceleration (PGA), peak ground displacement (PGD), peak ground velocity (PGV), predominant period, duration). On the other hand, it is because it is not an objective procedure since it evaluates the exciting force (the earthquake) using the response of the excited medium (structure), which depends on a series of variables such as strength, natural period, and so forth, independent of the cause of damage.

However, considering that seismological records (from seismographs) do not exist for periods before mid-nineteenth century, that strong motion records do not exist for periods prior to 1939, and that the number of the latter in most seismic regions is limited even today, it is obvious that there is no other way but the one that combines the limited strong motion records with records based on qualitative intensity scales like that of the MM. Indeed, despite their subjective character, these macro-seismic scales allow:

- The use of the seismic history of a region
- The correlation of the maximum expected intensity in a certain period with existing records of strong motions in the same or even other areas and adoption of appropriate response spectra

Of course, it is not unusual for this kind of extrapolation to lead to serious mistakes, which make zoning revisions necessary after catastrophic earthquakes with unexpected spectral characteristics.

3.3.2 Seismicity and seismic hazard

For the seismic design of structures it is essential to know the expected ground motion due to earthquakes. An earthquake, however, is a stochastic phenomenon with a random

distribution of magnitude and intensity in time and space. Therefore, even for cases in which there are long-term seismic records, statistical processing of the latter is necessary for *the design earthquake* to be chosen with a preselected *probability of occurrence* in a certain period of time (e.g., 50 years, which is the design life of conventional buildings). For this reason, two concepts have been introduced: *seismicity* and *seismic hazard*.

3.3.2.1 Seismicity

Seismicity is a parameter that increases both with magnitude and with the frequency of occurrence of earthquakes in an area. This parameter is expressed by the frequency of earthquakes (number of earthquakes per year), which exceed a predefined magnitude *M*. Seismicity is expressed by the statistical law of Gutenberg and Richter (1956), as follows (Figure 3.13):

$$\boxed{\ln N_m = a - bM}$$ (3.17)

where N_m is the frequency per year of earthquakes with magnitude *M* or larger and *a* and *b* are constants that are derived from statistical processing of the seismic records.

   For example, for the area of Greece and for the period of 1901–1983, for a logarithmic basis of 10 instead of *e*, the values of *a* and *b* are (Papazachos, 1986):

$$a = 5.99, \quad b = 0.94$$

   It is evident that parameters *a* and *b* mainly describe the seismicity of an area.
   The above Equation 3.17 is used in many instances for the statistical evaluations of many seismic parameters for everyday use in the seismic design of buildings. So,

   The number of earthquakes per year with a magnitude greater than *M* is deduced from Equation 3.17:

$$\boxed{N = \frac{e^a}{e^{bM}}}$$ (3.18)
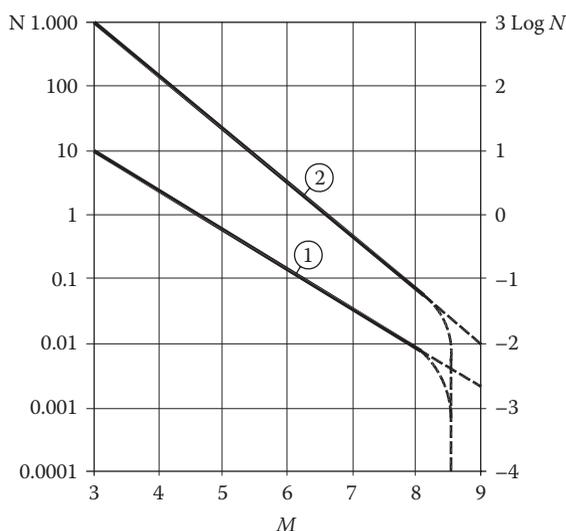
Figure 3.13 Cumulative function of earthquakes in (1) northern Greece; (2) Greece.

The corresponding *return period* T_R (the average time between two earthquakes of magnitude M or larger) is

$$T_R = \frac{1}{N} = e^{-(a-bM)} \tag{3.19}$$

Using Poisson's distribution in combination with Equation 3.17, it is easy to estimate *the probability of exceedance P_r(%)* during a period of t_r years (period of reference):

$$\ln(1 - P_r) = -\frac{t_r}{T_R} \tag{3.20a}$$

The period t_r is called the *reference period* and usually has to do with the estimated lifetime of the buildings.

For example, a 475-year return period (T_R) corresponds to a probability of exceedance in a 50-year building life (t_r):

$$\ln(1 - P_r) = -\frac{50}{475}$$

$$P_r = 10\%$$

The above example corresponds to *the seismic design input* for conventional buildings according to modern seismic codes (reference PGA a_{gR}; see Subsection 3.4.2).

3.3.2.2 Seismic hazard

According to the EERI glossary (EERI Committee on Seismic Risk, 1984; Dowric, 2005), '*Seismic hazard* is any physical phenomenon associated with an earthquake that may produce adverse effects on human activities'.

Usually the seismic hazard in an area is expressed quantitatively by the value of PGA (a_{gR}) or intensity I, for which the probability of exceedance of this value in a certain period of time (building lifetime) corresponds to a predefined value.

It has already been mentioned that the intensity I or the PGA (α_{gR}) generally decrease as the distance from the epicentre increases. The statistical evaluation of a large number of earthquakes has produced some *empirical attenuation laws*, which relate the maximum intensity I or PGA (a_{gR}) to the magnitude of the earthquake M and the distance Δ from the epicentre. For Europe, the following attenuation law for PGA (a_{gR}) has been proposed by Ambraseys and Bommer (1991):

$$\log a_{gR} = -0.87 + 0.217\,M_s - \log r + 0.00117r + 0.26P \tag{3.21}$$

where

$$r = \sqrt{\Delta^2 + h^2}$$

with Δ the source distance and h the focal depth.

In Equation 3.21, P is zero for 50th percentile values and one for 84th percentile values. For Greece, which is a region of very high seismicity, the following attenuation laws for I and PGA (a_{gR}) have been proposed (Papazachos, 1986; Papaioannou et al., 1994):

$$I = 6.362 + 1.20M_L - 4.402\log(\Delta + 15) \tag{3.22}$$

$$\log a_{gR} = 3.775 + 0.38M_L - 2.370\log(\Delta + 13) \tag{3.23}$$

Over the last 20 years, extended research in engineering seismology has been in process all over the world, with interesting results in refining the above equations by introducing many other parameters (e.g. Takahashi et al., 2000; Ambraseys et al., 2005; Boore, 2005).

The scope of this book does not allow any further extension on the subject of attenuation. At this point it is interesting to make use of Equations 3.18 through 3.20 for the probabilistic evaluation of PGA (a_{gR}) at various hazard levels (EC8-1/2004, par. 2.1(4), FEMA 356/2000: par. 1.6.1.3).

1. If a_{gR} is the PGA with a probability of exceedance P_r during a reference period of t_r years (reference lifetime of building), the following values may be defined:
   a. The corresponding return period T_r (the time between two earthquakes of equal or higher value than a_{gR}) results from Equation 3.20.

$$\boxed{T_r = -\frac{t_r}{\ln(1 - P_r)}} \tag{3.24}$$

   b. The number of earthquakes per year of equal or higher value than a_{gR} results from Equation 3.19.

$$N_r = \frac{1}{T_r} \tag{3.25}$$

2. If a_g is required for the same probability of exceedance as in item 1, but for a reference period of t_L years different from t_r (lifetime of a building), this value based on Poisson's assumption results from Equation 3.24.

$$\gamma_1 = \frac{a_g}{a_{gR}} \cong \left(\frac{t_L}{t_r}\right)^{\frac{1}{\kappa}} \tag{3.26}$$

   where
   $\kappa \cong 3$ for $t_L > t_r$
   $\kappa \cong 2$ for $t_L < t_r$
   α_{gR} is the PGA for the reference period (life time of the building) t_r.
   a_g is the PGA for the reference period t_L.

3. If a_g is required for the same reference period of t_r years as in item 1 (reference lifetime of the building), but for a given period of occurrence T longer or shorter than T_r, this value results for the same reason as in item 2 from the equations below:

$$\boxed{\ln(1 - P) = -\frac{t_r}{T} \Rightarrow P} \tag{3.20b}$$

Table 3.3 Values of maximum expected intensities *I* and accelerations α_g in 10 Greek cities for an 80-year reference period

Town	I (MM)	α_g/g
Rhodes	8.0	0.38
Larissa	7.8	0.37
Patra	7.6	0.37
Mitilini	7.6	0.30
Thessaloniki	7.3	0.26
Kalamata	7.2	0.24
Iraklion	7.1	0.23
Ioannina	7.1	0.20
Athens	6.7	0.17
Kavala	6.5	0.11

or

$$\gamma_1 = \frac{a_g}{a_{gR}} \cong \left(\frac{P_r}{P}\right)^{\frac{1}{\kappa}} \qquad (3.27)$$

In the above equations, γ_1 is called the *importance factor* (see Paragraph 3.4.2.2).

The knowledge of the seismicity of a region together with attenuation laws enables the preparation of *seismic hazard tables and maps*, for example, Table 3.3 (Papaioannou et al., 1994) and Figure 3.14 (Drakopoulos and Makropoulos, 1983). Based on this information, *zonation maps* are issued by the national authorities of countries with high seismic hazard (Figure 3.15) and are incorporated in their seismic codes.

Such maps constitute for the time being the main contribution of engineering seismology to structural design as they provide, in effect, the seismic input.

However, the designer should not overlook the paramount importance of other seismic motion characteristics that are not included in the hazard maps, such as frequency content, earthquake duration and so on. These parameters are incorporated, to a degree, in *the design spectra*. These will be presented in the next section.

3.3.3 Concluding remarks

Summarising the material presented above, we should focus on the following points:

1. Earthquakes constitute a hazard primarily for human beings, for buildings and for structures in general.
2. Magnitude is a measure of the event in terms of energy release at the point of origin. Therefore, the destructiveness of an earthquake, although directly related to its magnitude, is also a function of many other parameters such as the focal depth, the distance from the epicentre, the soil conditions, and the mechanical properties of the structures.
3. The intensity of an earthquake is an index of the consequences of an earthquake on the population and the buildings of a certain region. For many years only qualitative macroseismic intensity scales have been used for the damage estimate.
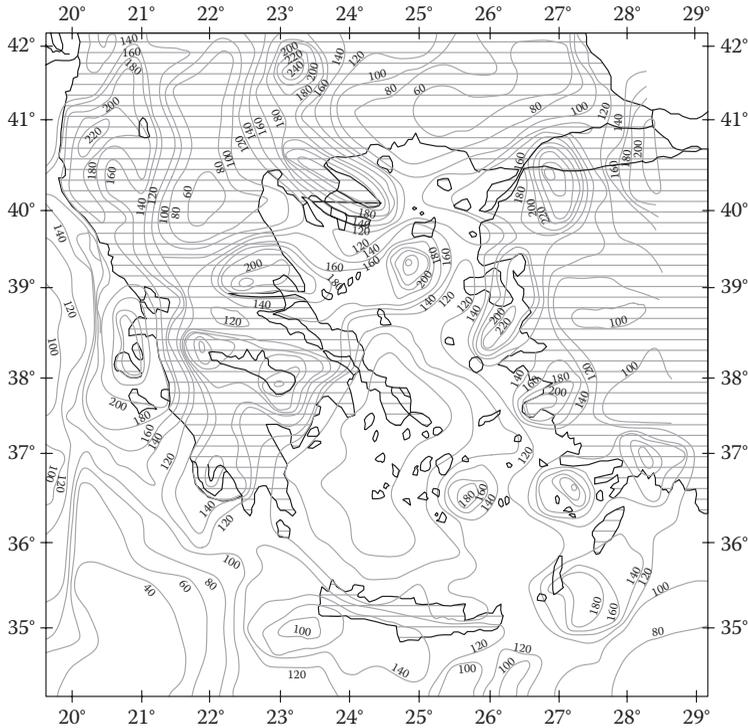
Figure 3.14 Maximum accelerations in gal (1000 gal = g) with a 90% probability to not be exceeded in 25 years reference period (Greece).

4. The assessment of the seismic hazard of a region is a complicated procedure based on the statistical analysis of existing strong motion records of the last few decades, together with the historical information on intensity that goes back to the past. Therefore, the result of this combination presented on hazard maps is information of limited credibility, but of crucial importance for design. That is why every now and then major changes are introduced by the national authorities in the hazard maps.

3.4 GROUND CONDITIONS AND DESIGN SEISMIC ACTIONS

3.4.1 General

Recalling from Subsection 2.4.1 that the *usual method* of analysis in most modern Codes is the *elastic modal response spectrum analysis* and that the seismic motion input in this analysis is an *elastic acceleration response spectrum*, it is evident that Seismic Codes specify this spectrum in detail.

Elastic or inelastic response spectra (see Subsections 2.2.4 and 2.3.6) for a real seismic record give useful information for the assessment of the response of existing structures at the location where the seismic motion was recorded.
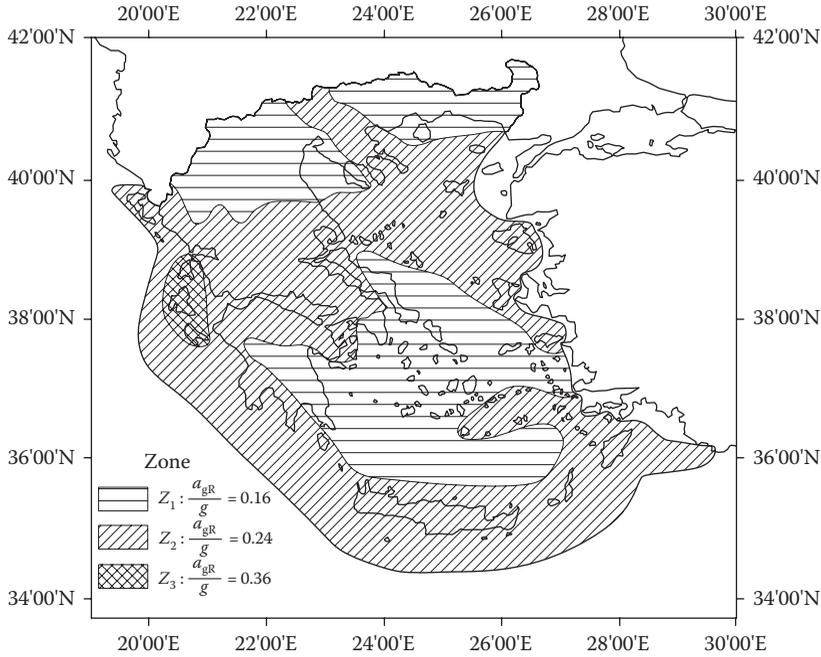
Figure 3.15 The zonation of Greece according to the National Annex (N.A.) of Greece attached to EC8-1/2004.

For design purposes, however, *the design spectrum* must be based on *a probabilistic pre-diction* based on various parameters, that is,

- Reference PGA a_{gR} with a given probability P_r of exceedance during a reference period t_r of years (reference lifetime of a building)
- Soil conditions
- Frequency content of the seismic motion
- The damping factor ζ
- The importance factor γ_1
- The behaviour factor q

So, the design spectra are *codified diagrams* based on a multi-functional evaluation of elastic and inelastic response spectra of past earthquakes combined with provisions that prevent non-conservative estimates for design actions. In this respect, *the design spectra do not correspond to any real earthquake of the past*. They are simply codified design tools with the following main characteristics:

- They are the averaged output, smoothed and normalised by a_{gR}, of real response spectra obtained from records of similar characteristics and a damping factor $\zeta = 5\%$.
- They have a generic form that is adjusted to the local conditions by introducing the proper values of the above mentioned parameters.

In the next subsections the formulation of seismic actions according to EC8-1/2004 will be explained in detail.

3.4.2 Ground conditions

3.4.2.1 Introduction

The seismic response of buildings is substantially influenced by the underlying soil conditions. It must be clear that there is an important distinction between the earthquake influence on ground cyclic motion and a series of other implications of the earthquake for the ground like ground rupture, slope instability and permanent settlements caused by liquefaction or densification. This category of consequences may dramatically affect the building behaviour in response to the earthquake on a geological scale and, therefore, a geological and geotechnical investigation is required in order to make sure that the area is free of this kind of risk. If, however, the ground is susceptible to liquefaction or other types of failure, special geotechnical studies must be carried out for the proper design of the building. At the same time, depending on the importance of the structure, site investigation and laboratory tests must be carried out for the determination of the ground conditions in accordance with EC 8-1/2004.

3.4.2.2 Identification of ground types

Ground types are classified according to EC8-1/2004, in five categories labeled with letters A–E, and are presented in Table 3.4.

They are described by the stratigraphic profiles and are quantitatively characterised by the following parameters:

- Average shear wave velocity ($V_{s,30}$)
- Number of blows (N_{SPT})
- Undrained shear strength (c_u)

The characterisation of the ground type may be based on any one of the above parameters that is available.

In Table 3.4 two other ground types are included, namely, S_1 and S_2. These ground types are susceptible to liquefaction (S_2) and to anomalous site amplification (S_1). Therefore, a special geotechnical study should be carried out and special measures should be taken for soils of these categories so that the implications of ground failure for the building are diminished.

As we will see in the next section, the category in which the ground of a location is classified plays a paramount role for design seismic actions.

3.4.3 Seismic action in the form of response spectra

3.4.3.1 Seismic zones

As has been previously noted, it is necessary for the formation of the elastic response spectrum to know the reference PGA a_{gR}. In this context, national territories are divided by national authorities into *seismic zones* depending on the local hazard level, usually described in terms of the value a_{gR} *in rock or firm soil*. This acceleration corresponds to a reference return period of occurrence T_r of 475 years and coincides with the reference PGA a_{gR} with a 10% probability of exceedance during a reference period t_r of 50 years (lifetime of a building).

Then, the reference PGA a_{gR} is multiplied with an importance factor γ_I *to produce the design ground acceleration:*

$$\boxed{a_g = \gamma_I a_{gR}}$$

(3.28)

Table 3.4 Ground types

Ground types	A	B	C	D	E	S1	S2
$V_{s,30}$(m/s)	>800	360⊠800	180⊠360	<180	⊠	<100 (indicative)	⊠
N_{SPT} blows/30 cm	⊠	>50	15⊠50	<15	⊠	⊠	⊠
c_u(kPa)	⊠	>250	70⊠250	<70	⊠	10⊠20	⊠

Description of stratigraphic profile:

A: Rock or other rock-like geological formation, including at most 5 m of weaker material at the surface.

B: Deposits of very dense sand, gravel, or very stiff clay, at least several tens of metres in thickness, characterised by a gradual increase of mechanical properties with depth.

C: Deep deposits of dense or medium-dense sand, gravel or stiff clay with thickness from several tens to many hundreds of metres.

D: Deposits of loose-to-medium cohesionless soil (with or without some soft cohesive layers), or of predominantly soft-to-firm cohesive soil.

E: A soil profile consisting of a surface alluvium layer with v_s values of type C or D and thickness varying between about 5 m and 20 m, underlain by stiffer material with v_s > 800 m/s.

S$_1$:   Deposits consisting, or containing a layer at least 10 m thick, of soft clays/silts with a high plasticity index (PI > 40) and high water content.

S$_2$:   Deposits of liquefiable soils, of sensitive clays, or any other soil profile not included in types A–E or S1.

The importance factor γ_1 for conventional buildings is equal to 1.0, and it will be examined in more detail in the next section.

Seismic zones with design ground acceleration not greater than 0.08 g are characterised as *low seismicity zones*, for which reduced or simplified seismic design procedures for certain types or categories of structures may be used. *The provisions of seismic codes need not be considered in seismic zones with design ground acceleration a_g not greater than 0.04 g.*

The selection of the categories of structures, ground types and seismic zones in a country for which low seismicity or very low seismicity characterisation is given is the responsibility of the national authorities, and they are included in the National Annexes of EC8-1/2004.

3.4.3.2 Importance factor

As was clarified in the previous paragraph, the reference PGA a_{gR} included in seismic zones corresponds to a reference return period of occurrence T_r of 475 years and coincides with an a_{gR} with a 10% probability of exceedance during a reference period of 50 years, which is considered to be the design lifetime of normal buildings.

It is obvious that for different types of buildings different hazard levels are established by the national authorities on the basis of the consequences of their failure. This reliability differentiation is implemented by classifying structures into different importance classes. *An importance factor γ_1 is assigned to each class category, which reflects a higher or a lower value of the return period of occurrence T of the seismic event. Detailed guidance on the importance classes and the corresponding importance factors according to EC8-1/2004 is given below.*

Buildings are classified into four importance classes depending on the size of the building, its value, its importance for public safety, and the probability of human losses in case of collapse. The recommended values for the importance factor γ_1 are 0.8, 1.0, 1.2 and 1.4 for importance classes I, II, III and IV, respectively (Table 3.5).

It is important to note that in the case that a hazard level different from that assigned in Table 3.5 is specified, the importance factor γ_1 may be determined easily using Equations 3.26, 3.20 and 3.27.

EXAMPLE 3.1

If the design lifetime of an important building is specified as 100 years, then the importance factor γ_1 results from Equation 3.26, that is,

$$\gamma_1 = \frac{a_g}{a_{gR}} = \left(\frac{t_L}{t_r}\right)^{\frac{1}{k}} \cong \left(\frac{100}{50}\right)^{\frac{1}{3}} = 1.25$$

For this building and for a probability of exceedance $P = 0.10$, the return period of occurrence results from Equation 3.20, that is,

$$l_n(1 - P) = -\frac{t_r}{T}$$

$$l_n(1 - 0.10) = -\frac{100}{T}$$

$$T = \frac{100}{0.11} = 949\,\text{years}$$

EXAMPLE 3.2

If the lifetime of the building is 50 years (reference lifetime $(t_L = t_r)$ but the building must be designed for a return period of occurrence $T = 2.000$ years, then from Equation 3.20 it may be obtained:

$$l_n(1 - P) = -\frac{t_r}{T} = -\frac{50}{2000} = -0.025$$

$$1 - P = e^{-0.025} \Rightarrow P = 0.02$$

Table 3.5 Importance classes of buildings and importance factors according to EC8-1/2004

Importance class	Buildings	Importance factor γ_I
I	Buildings of minor importance for public safety, for example, agricultural buildings, etc.	0.8
II	Ordinary buildings, not belonging in the other categories.	1.0
III	Buildings with a seismic resistance of importance in view of the consequences associated with a collapse, for example, schools, assembly halls, cultural institutions, etc.	1.2
IV	Buildings with integrity during earthquakes that is of vital importance for civil protection, for example, hospitals, fire stations, power plants, etc.	1.4

Note: Importance classes I, II and III or IV correspond roughly to consequences classes CC1, CC2 and CC3, respectively, defined in EN 1990:2002, Annex B.

Introducing $P = 0.02$ into Equation 3.27 we obtain:

$$\gamma_1 = \frac{a_g}{a_{gR}} \cong \left(\frac{0.10}{0.02}\right)^{\frac{1}{3}} = 1.70$$

EXAMPLE 3.3

If the reference time for damage limitation is $t_L = 10$ years, then the importance factor γ_1 results from Equation 3.26, that is,

$$\nu = \frac{a_g}{a_{gR}} = \left(\frac{t_L}{t_r}\right)^{\frac{1}{k}} \cong \left(\frac{10}{50}\right)^{\frac{1}{2}} \cong 0.44$$

For this hazard level and for probability of exceedance $P = 0.10$, the return period of occurrence results from Equation 3.20, that is,

$$l_n(1 - P) = -\frac{t_r}{T}$$

$$l_n(1 - 0.10) = -\frac{10}{T}$$

$$T = \frac{10}{0.11} = 91 \, \text{years}$$

3.4.3.3 Basic representation of seismic action in the form of a response spectrum

The *generic* form of the seismic action that is the generic acceleration response spectrum, henceforward called an *'elastic response spectrum'*, is presented in Figure 3.16. This form is the same for horizontal and vertical elastic response spectra as well. They are used for the ULS design seismic action and for the damage limitation state (see subsection 3.5.3).

The abscissa of the corner points T_B, T_C, T_D (in seconds) and the parameter S for each ground type are given in Tables 3.6 and 3.7.

It must be noted that the *elastic response spectra* are grouped in two main categories. The first is characterised as Type 1 spectra and the second as Type 2 spectra. Values for Type 1 spectra are given in Table 3.6 and are recommended for regions affected mainly by earthquakes with a surface-wave magnitude M_s *greater than 5.5*. Values of Type 2 spectra are given in Table 3.7 and are recommended for regions affected mainly by earthquakes with a surface-wave magnitude M_s *not greater than 5.5*.

It should be noted that earthquakes of high magnitudes (>5.5) are deeper and excite a bigger earth mass. Therefore, the high-frequency content is filtered to a degree, so the maxima of the elastic spectra (the plateau area) are displaced to the right of the diagram (longer periods; Figure 3.17).

Conversely, earthquakes of lower magnitude (<5.5) are shallow ones, and therefore the high-frequency content is not filtered. Therefore, the elastic spectra have their maxima (the plateau area) displaced to the left of the diagram (shorter periods; Figure 3.18).
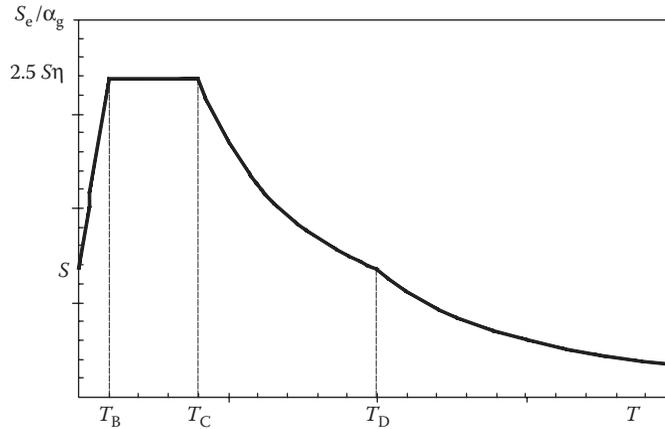
Figure 3.16 Generic shape of the elastic response spectrum. (From E.C.8-1/EN1998-1. 2004. *Design of Structures for Earthquake Resistance: General Rules, Seismic Actions and Rules for Buildings*. CEN, Brussels, Belgium. With permission of the British Standards Institution (BSI, CEN).)

Table 3.6 Values of the parameters describing the recommended Type 1 elastic response spectra

Ground type	S	T_B (S)	T_C (S)	T_D (S)
A	1.0	0.15	0.4	2.0
B	1.2	0.15	0.5	2.0
C	1.15	0.20	0.6	2.0
D	1.35	0.20	0.8	2.0
E	1.4	0.15	0.5	2.0

Table 3.7 Values of the parameters describing the recommended Type 2 elastic response spectra

Ground type	S	T_B (S)	T_C (S)	T_D (S)
A	1.0	0.05	0.25	1.2
B	1.35	0.05	0.25	1.2
C	1.5	0.10	0.25	1.2
D	1.8	0.10	0.30	1.2
E	1.6	0.05	0.25	1.2

It should also be noted that soft soils according to the diagrams of Figures 3.17 and 3.18 amplify the maxima of spectral diagrams more strongly than firm ones (Figure 3.19). This is discussed in more detail in Chapter 2 (see Subsection 2.2.4).

3.4.3.4 Horizontal elastic response spectrum

For the horizontal components of the seismic action, the elastic response spectrum $S_e(T)$ is defined by the following expressions (Figures 3.17 and 3.18):

$$0 \leq T \leq T_B : S_e(T) = a_g \cdot S \cdot \left[1 + \frac{T}{T_B}(\eta \cdot 2.5 - 1)\right] \tag{3.29}$$
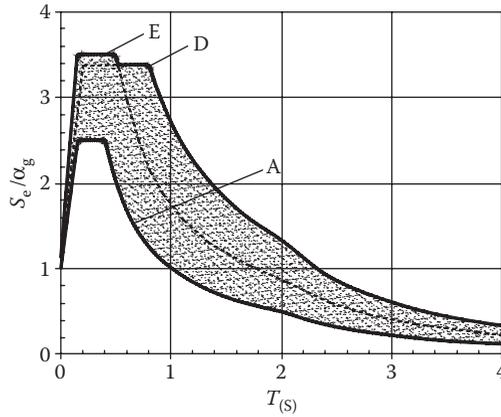
Figure 3.17 Recommended Type 1 elastic response spectra for ground types A–E (5% damping). (From E.C.8-1/EN1998-1. 2004. *Design of Structures for Earthquake Resistance: General Rules, Seismic Actions and Rules for Buildings.* CEN, Brussels, Belgium. With permission of the British Standards Institution (BSI, CEN).)
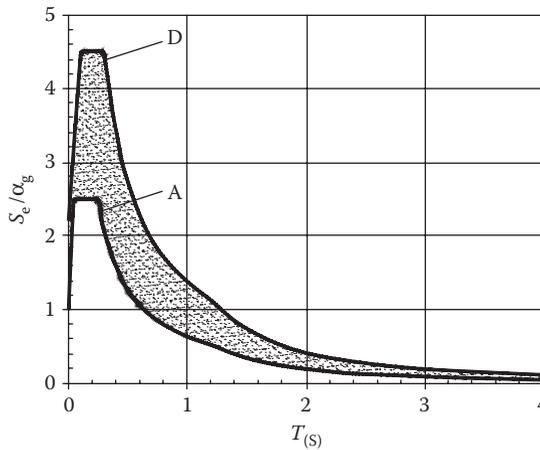
Figure 3.18 Recommended Type 2 elastic response spectra for ground A–E (5% damping). (From E.C.8-1/ EN1998-1. 2004. *Design of Structures for Earthquake Resistance: General Rules, Seismic Actions and Rules for Buildings.* CEN, Brussels, Belgium. With permission of the British Standards Institution (BSI, CEN).)

$$T_{\mathrm{B}} \leq T \leq T_{\mathrm{C}} : S_{\mathrm{e}}(T) = a_{\mathrm{g}} \cdot S \cdot \eta \cdot 2.5 \tag{3.30}$$

$$T_{\mathrm{C}} \leq T \leq T_{\mathrm{D}} : S_{\mathrm{e}}(T) = a_{\mathrm{g}} \cdot S \cdot \eta \cdot 2.5 \left[\frac{T_{\mathrm{C}}}{T} \right] \tag{3.31}$$

$$T_{\mathrm{D}} \leq T \leq 4s : S_{\mathrm{e}}(T) = a_{\mathrm{g}} \cdot S \cdot \eta \cdot 2.5 \left[\frac{T_{\mathrm{C}} T_{\mathrm{D}}}{T^2} \right] \tag{3.32}$$

where
  $S_{\mathrm{e}}(T)$ is the elastic response spectrum.
  T is the vibration period of a linear single-degree-of-freedom system.
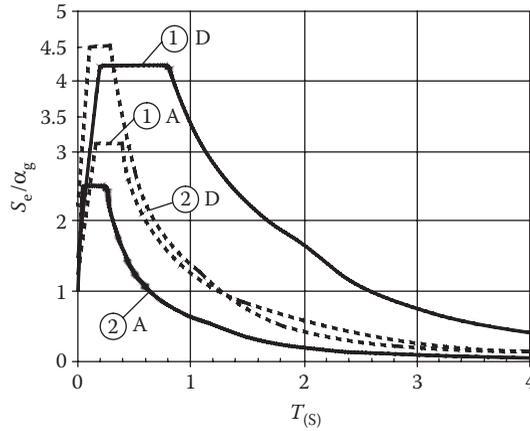
Figure 3.19 Soft soils (D) amplify the maxima of spectral diagrams more strongly than firm ones (A).

a_g is the design ground acceleration on type A ground ($a_g = \gamma_1 \cdot a_{gR}$).

T_B is the lower limit of the period of the constant spectral acceleration branch.

T_C is the upper limit of the period of the constant spectral acceleration branch.

T_D is the value defining the beginning of the constant acceleration response range of the spectrum.

S is the soil factor.

η is the damping correction factor with a reference value of $\eta = 1$ for 5% viscous damping.

The value of the damping correction factor *n* may be determined by the expression:

$$\boxed{n = \sqrt{\frac{10}{5 + \zeta}} \geq 0.55} \tag{3.33}$$

where ζ is the viscous damping ratio of the structure (see Chapter 2). From Equation 3.33 it can be seen that the elastic response spectra are credible for ζ values up to

$$\boxed{\zeta \leq 28\%} \tag{3.34}$$

It should be noted that for *concrete structures* in the elastic range, ζ has a value of 5% and therefore *n* = 1.0.

The horizontal seismic actions are described by two orthogonal components considered independent and represented by the same response spectrum (Penzien and Watabe, 1974; Rosenblueth and Contreras, 1977).

3.4.3.5 *Vertical elastic response spectrum*

The commonly used approach in the past, of taking the vertical spectrum as two-thirds of the horizontal one without a change in frequency content, has been abandoned (Elnashai and Papazaglou, 1997; Colier and Elnashai, 2001). In this context, EC8-1/2004 has introduced

the following equations for the vertical elastic response spectrum $S_{ve}(T)$ based again on the generic form of par. 3.4.3.3.

$$0 \leq T \leq T_B : S_{ve}(T) = a_{vg}\left[1 + \frac{T}{T_B}(\eta \cdot 3.0 - 1)\right] \tag{3.35}$$

$$T_B \leq T \leq T_C : S_{ve}(T) = a_{vg} \cdot \eta \cdot 3.0 \tag{3.36}$$

$$T_C \leq T \leq T_D : S_{ve}(T) = a_{vg} \cdot \eta \cdot 3.0\left[\frac{T_C}{T}\right] \tag{3.37}$$

$$T_D \leq T \leq 4s : S_{ve}(T) = a_{vg} \cdot \eta \cdot 3.0\left[\frac{T_C T_D}{T^2}\right] \tag{3.38}$$

The values of T_B, T_C, T_D and a_{vg} for each Type 1 or 2 of vertical spectra recommended by EC8-1/2004, as they have been defined in par. 3.4.3.3, are given in Table 3.8.

It should be noted that these spectra are independent of the ground type ($S = 1$).

It is also important to note that the frequency content at high frequencies for the vertical component of the earthquake is higher than that of the horizontal ones (see Subsection 2.2.4). This explains the displacement of the plateau with the maximum values in the vertical response spectra diagram on the left, in relation to the corresponding diagram of horizontal response spectra.

It should also be noted here that usually only horizontal seismic actions are taken into account when designing a building. However, for the design of certain structures the vertical component of the seismic action needs to be considered. According EC8-1/2004, these structures are

- Pre-stressed beams
- Beams supporting columns
- Cantilever beams longer than 5.0 m
- Beams with spans over 20.0 m
- Base isolated structures

3.4.3.6 Elastic displacement response spectrum

The elastic displacement response spectrum $S_{De}(T)$ of the relative displacement u is obtained for a period T up to 4.0 s directly from the elastic acceleration response spectrum $S_e(T)$ using Equation 2.20 (Chapter 2).

$$\boxed{S_{De}(T) = S_e(T)\left(\frac{T}{2\pi}\right)^2} \tag{3.39}$$

Table 3.8 Recommended values of parameters describing the vertical elastic response spectra

Spectrum	α_{vg}/α_g	T_B (S)	T_C (S)	T_D (S)
Type 1	0.90	0.05	0.15	1.0
Type 2	0.45	0.05	0.15	1.0
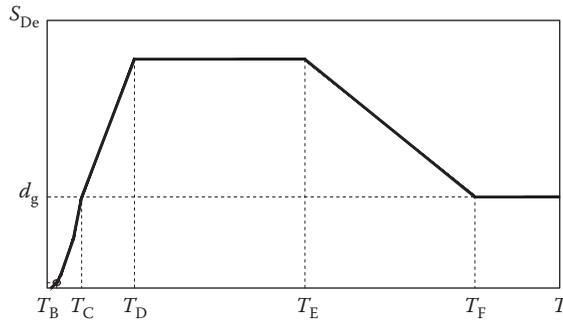
Figure 3.20 Elastic displacement response spectra. (From E.C.8-1/EN1998-1. 2004. *Design of Structures for Earthquake Resistance: General Rules, Seismic Actions and Rules for Buildings.* CEN, Brussels, Belgium. With permission of the British Standards Institution (BSI, CEN).)

Table 3.9 Additional control periods for Type 1 displacement spectrum

Ground type	T_E (S)	T_F (S)
A	4.5	10.0
B	5.0	10.0
C	6.0	10.0
D	6.0	10.0
E	6.0	10.0

This part of $S_{De}(T)$ is codified by EC8-1/2004. For values of T longer than 4.0 s the expressions below (3.40) and (3.41) are proposed (Figure 3.20; EC8-1/2004, Annex A [informative]).

$$T_E \leq T \leq T_F : S_{De}(T) = 0.025 \cdot a_g \cdot S \cdot T_C \cdot T_D \cdot \left[2.5n + \left(\frac{T - T_E}{T_F - T_E} \right)(1 - 2.5\,n) \right] \quad (3.40)$$

$$T \geq T_F : S_{De}(T) = 0.025 \cdot a_g \cdot S \cdot T_C \cdot T_D = d_g \quad (3.41)$$

The control periods T_E and T_F are presented in Table 3.9 (EC8-1/2004, Annex A).
Value d_g in Equation 3.41 represents the *design ground displacement* (DGD) corresponding to the design ground acceleration, according to EC8-1/2004.

A reference to Paragraphs 2.2.4.3 and 2.3.6.2 should be made here in order to recall the scientific background of the codified expressions presented above.

3.4.3.7 Design spectrum for elastic analysis

As has been already discussed in detail (see Section 3.2), the capacity of structural systems of buildings to resist seismic actions in their nonlinear range permits their design for forces smaller than those corresponding to a linear elastic response.

To avoid explicit nonlinear analysis, the energy dissipation capacity of the structure is taken into account by performing a linear analysis based on a reduced response spectrum, henceforth called *design spectrum for elastic analysis*. This reduction is accomplished by introducing the *behaviour factor q*.

The design spectrum $S_d(T)$ for horizontal components and for the reference return period of 475 years, which is normalised by the gravity acceleration g, is defined (for $\zeta = 5\%$) in EC8-1/2004 by the following expressions:

$$0 \leq T \leq T_B : S_d(T) = a_g \cdot S \cdot \left[\frac{2}{3} + \frac{T}{T_B} \left(\frac{2.5}{q} - \frac{2}{3} \right) \right] \tag{3.42}$$

$$T_B \leq T \leq T_C : S_d(T) = a_g \cdot S \cdot \frac{2.5}{q} \tag{3.43}$$

$$T_C \leq T \leq T_D : S_d(T) \begin{cases} a_g \cdot S \cdot \dfrac{2.5}{q} \left[\dfrac{T_C}{T} \right] \\ \geq \beta \cdot a_g \end{cases} \tag{3.44}$$

$$T_D \leq T : S_d(T) \begin{cases} a_{vg} \cdot S \cdot \dfrac{2.5}{q} \left[\dfrac{T_C T_D}{T^2} \right] \\ \geq \beta \cdot a_g \end{cases} \tag{3.45}$$

where

a_g, S, T_C, T_D are as defined in par. 3.4.3.4
$S_d(T)$ is the design spectrum
q is the behaviour factor
β is the lower bound factor for the horizontal design spectrum

The value to be ascribed to β for use in a country can be found in its National Annex. The recommended value for β is 0.2.
The values of q for horizontal components will be discussed in detail in Subsection 5.4.3, as they are related to the ductility and overstrength of the various R/C building types.

Comparing Equations 3.42 through 3.45 with the relevant ones of the horizontal elastic response spectrum, we can make the following remarks:

1. In design spectra the value of n is equal to 1 as any additional damping is incorporated in the q factor (see Chapter 2).
2. In Equation 3.42 (first branch of design spectrum) there is a term equal to two-thirds instead of 1 (first branch of elastic response spectrum). This change covers the introduction of a q factor equal to 1.50 for structures of high stiffness (natural period equal to zero) due to the overstrength of structures of this type.
3. In design spectra, a minimum value has been introduced ($\beta = 0.20$) so that non-conservative estimates are prevented.

For the vertical component of the seismic action, the design action is given by the following expressions:

$$0 \leq T \leq T_B : S_{vd}(T) = a_{vg} \left[\frac{2}{3} + \frac{T}{T_B} \left(\frac{2.5}{q} - \frac{2}{3} \right) \right] \tag{3.46}$$

$$T_B \leq T \leq T_C : S_{vd}(T) = a_{vg} \cdot \frac{2.5}{q} \tag{3.47}$$

$$T_C \leq T \leq T_D : S_{vd}(T) \begin{cases} a_{vg} \cdot \dfrac{2.5}{q}\left[\dfrac{T_C}{T}\right] \\ \geq \beta \cdot a_{vg} \end{cases} \tag{3.48}$$

$$T_D \leq T : S_{vd}(T) \begin{cases} a_{vg} \cdot \dfrac{2.5}{q}\left[\dfrac{T_C T_D}{T^2}\right] \\ \geq \beta \cdot a_{vg} \end{cases} \tag{3.49}$$

where

a_{vg} is the design ground acceleration for the vertical spectral component

β is the lower bound factor for the vertical design spectrum (recommended value $\beta = 0.20$)

q is the behaviour factor for the vertical spectrum component not greater than $q = 1.50$

For the displacement-based design method where a design displacement response spectrum is needed, the ductility demand is introduced in the elastic displacement response spectrum in the form of equivalent damping ζ and therefore in the form of an equivalent n (see Section 14.2).

3.4.4 Alternative representation of the seismic action

3.4.4.1 General

It has already been noted (see Chapter 2.5) that for the inelastic analysis of earthquakes the time-history procedure is inevitable. In this context, the input seismic motion must be introduced in the form of a digitised accelerogram. EC8-1/2004, like all the other modern Codes of Practice (BSSC 2003, SEAOC 1999, ASCE 2007, etc.), foresees a well-defined procedure similar to those of other internationally known seismic codes for the generation of credible design accelerograms.

The specified procedures are the following:

- Generation of artificial accelerograms
- Recorded or simulated accelerograms

In case of a structural 3D model, the seismic motion must consist of three simultaneously acting accelerograms. The two horizontal ones may not be identical.

3.4.4.2 Artificial accelerograms

Artificial accelerograms are mathematical functions generated through random vibration theory. The most usual procedure is to generate a random signal similar to an accelerogram record, with an elastic response spectrum for 5% viscous damping that fits the codified elastic spectrum with a predefined accuracy, say 3–5% (Clough and Penzien, 1993). It must be noted that this method is an iterative one. Therefore, the output can fit as much as we like by employing more cycles of iteration. The scope of this book does not allow

for extended treatment of the subject. Much more information on the generation procedure may be found in more specific textbooks on engineering seismology (Elnashai and Di Sarno, 2008).

EC8-1/2004 specifies a series of requirements for such an accelerogram, namely:

1. The duration of the accelerograms must comply with the earthquake magnitude and the relevant seismological information (e.g. distance and depth of the source) that were taken into account for the determination of a_{gR}.
2. The stationary part of the accelerogram, in the case that the seismological information on this issue is limited, must not be shorter than 10 s.
3. The suite of the artificial accelerograms should obey the following rules:
   a. At least three accelerograms are required for analysis.
   b. The mean value of PGA of these accelerograms must not be less than a_{gR} of the elastic design spectrum.
   c. The mean values of the 5% viscous damping elastic spectra of the above accelerograms must not be less than 90% of the elastic design spectrum in the period's region between $0.2T_1$ and $2T_1$, where T_1 is the fundamental period of the structure.

Various computer programs have been developed that are proper for the generation of artificial accelerograms, for example, the SIMQKE-1 platform (Gasparini and Vanmarke, 1976), or ASING (Figure 3.21; Sextos et al., 2003).

The main disadvantage of the artificial accelerograms is that, many times, although all of them comply with the above-presented requirements, they present serious discrepancies among them as far as the response strains they cause to the structures. Additionally, very often they have a greater number of cycles of high amplitude than the natural accelerograms, a fact that leads to overly conservative response demands of the structure.

3.4.4.3 Recorded or simulated accelerograms

The use of natural records, and particularly those recorded at the reference region for which the accelerograms must be developed, constitutes theoretically the best procedure for obtaining this type of accelerogram by scaling them to the codified elastic acceleration spectrum. However, the requirements of EC8-1/2004 for the identical suite for both recorded and artificial ones make the procedure difficult. The reason is that many times the scaling to PGA leads to spectra not compatible with the codified ones and vice versa. So, very often, analysts have to run to various data banks and try many natural records of other regions with seismological characteristics similar to the reference location until the proper records are found that are compatible with the Code specifications (e.g. European Commission project site http://www.isesd.cv.ic.ac.uk/esd; Elnashai and Di Sarno, 2008).

The same holds for the simulated accelerograms that are generated through a physical simulation of the earthquake source, the wave path, and the soil conditions. In conclusion, it should be mentioned that for many years extended research has been carried out for the generation of more reliable criteria based on quantitative intensity scales (see Chapter 2) for a comparative evaluation of the natural records instead of the requirements specified by modern Codes (Housner, 1953; Nau and Hall, 1984; Kappos, 1991; Matsumura, 1992; Martinez-Rueda, 1997; Elnashai, 1998).
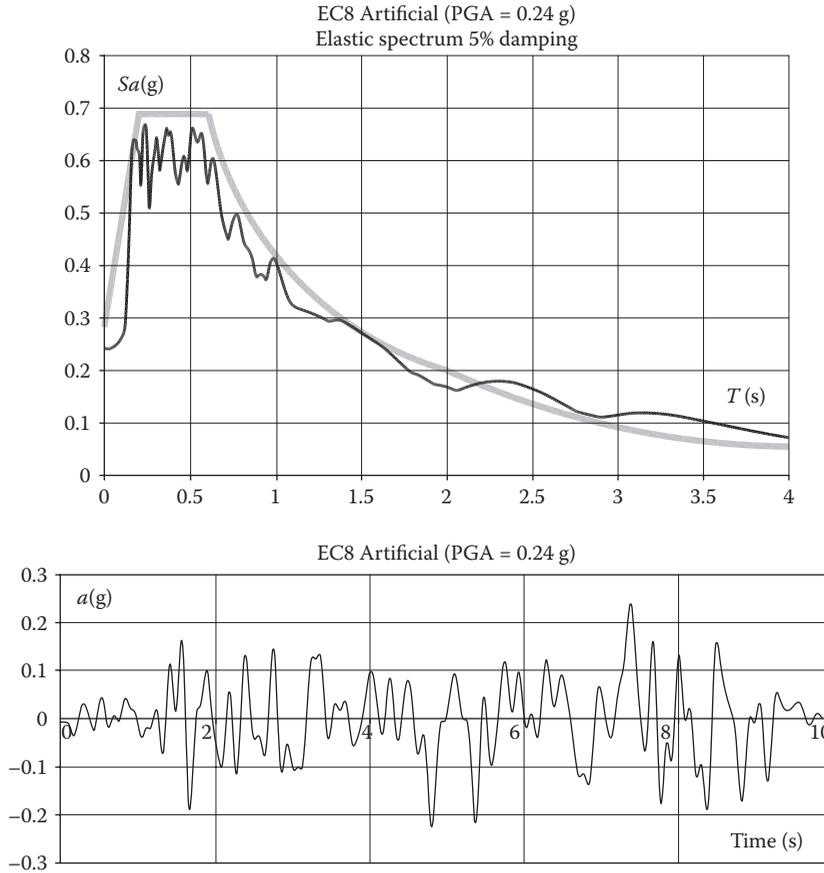
Figure 3.21 Artificial accelerogram for PGA = 0.24 g. (After Sextos, A., Pitilakis, K. and Kappos, A. 2003. *Earthquake Engineering and Structural Dynamics*, V, 32(4), 607–627.)

3.4.5 Combination of seismic action with other actions

The design values E_d of the various action effects in the seismic design combination are determined according to EC8-1/2004 by combining the values of the relevant actions as follows:

$$\sum G_{\kappa j}\,'+'\,A_{Ed}\,'+'\,P_{\kappa}\,'+'\,\sum \psi_{Ei}Q_{\kappa i} \tag{3.50}$$

where '+' implies 'combined with', Σ implies 'the combined effect of', $G_{\kappa j}$ is the characteristic value of permanent actions j (dead loads), A_{Ed} is the design value of the seismic action including the importance factor γ_1, P_{κ} is the characteristic value of pre-stressing action, ψ_{Ei} is the combination coefficient for the variable action i, and $Q_{\kappa i}$ is the characteristic value of variable action i.

The combination coefficient ψ_{Ei} is given according to EC8-1/2004 by the expression:

$$\psi_{Ei} = \varphi\,\psi_{2i}$$

where

  ψ_{2i} is the combination coefficient for the quasi-permanent value of variable action $Q_{\kappa i}$.
  φ is a reduction factor ranging between 1.0 and 0.5 depending on the type of variable action.

The combination actions given in expression (3.50) are used for both the *ULS* and the *damage limitation state* (see subsection 3.5.3).

The effects of the seismic action are defined by considering that all gravity loads and consequently the relevant masses appearing in the following combination of actions are present:

$$\boxed{\sum G_{\kappa j}\, {}'+{}'\, \sum \psi_{Ei} Q_{\kappa i}}$$

(3.51)

where ψ_{Ei} is a combination coefficient for the variable action *i* presented above. Expressions (3.50) and (3.51) will be discussed in detail in Subsection 5.8.1.

3.5 PERFORMANCE REQUIREMENTS AND COMPLIANCE CRITERIA

3.5.1 Introduction

During the last 15 years, in the United States there has been an increasing interest in defining design objectives based on the performance of the building (performance-based design). The term *performance levels* refers to *damage states* associated with the post-earthquake disposition of the buildings that are important to the building users.

It is important to note that the performance levels may be based on socioeconomic losses or on nonstructural or structural building damage. Since the objective of this book is the structural design of R/C buildings in seismic regions, the discussion will be focused on structural performance levels.

In the document Vision 2.000 (SEAOC, 1995), which has exercised a strong influence on the formation of recent seismic design philosophy, four performance levels are defined. These levels, as they were later formulated by FEMA (FEMA 273, 274, 1997), are presented below:

- *Level 1*: *Fully operational* – The building continues to operate with insignificant damage.
- *Level 2*: *Immediate occupancy* – Damage is relatively limited. The structure retains a significant portion of its original stiffness and most or all of its original strength.
- *Level 3*: *Life safety* – Substantial damage has occurred to the structure and it may have lost a significant amount of its original stiffness. However, a substantial margin remains for additional lateral deformation before collapse would occur. In this respect, *life is protected*.
- *Level 4*: *Collapse prevention* – The building has experienced extreme damage. *Life is at risk*. If it is laterally deformed beyond this point due to post-earthquake action, the structure can experience instability and collapse.

It is obvious that the above descriptive definition of the performance levels must be given in an engineering form so that they may be expressed quantitatively. Figure 3.22a presents a typical capacity curve of a ductile building, where the various performance levels have been depicted, while Figure 3.22b presents the same curve for a 'brittle' building.
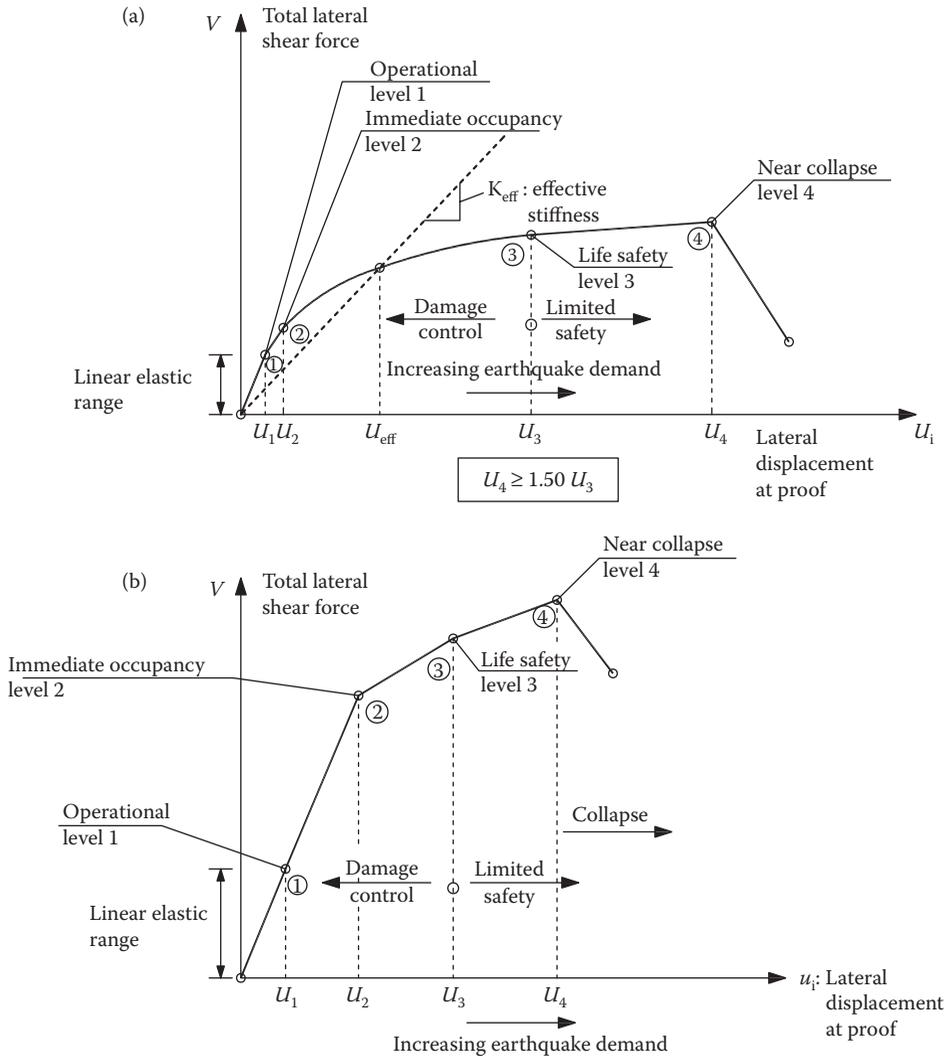
Figure 3.22 Typical capacity curve of an R/C building with the characteristic performance levels: (a) building with a ductile behaviour; (b) building with a brittle behaviour. (Adapted from FEMA 273, 274. 1997. *NEHPR Guidelines for the Seismic Rehabilitation of Buildings*, FEMA, Washington, DC.)

It should be noted that the structure should be designed and constructed to satisfy the specified performance levels. This constitutes one of the main objectives of the seismic design. It should also be noted that the compliance of the structural response with a specified performance level on the general capacity curve of the structure (Figure 3.22) does not ensure the satisfaction of the relevant performance level locally in the various elements of the structure. Seismic design has as a basic objective the assurance of the specified performance level for both *the structural elements and the structure as a whole*.

The above four performance levels are coupled through the matrix of Figure 3.23 with the followings four levels of seismic excitation, which were introduced by FEMA (FEMA 273; 274, 1997).
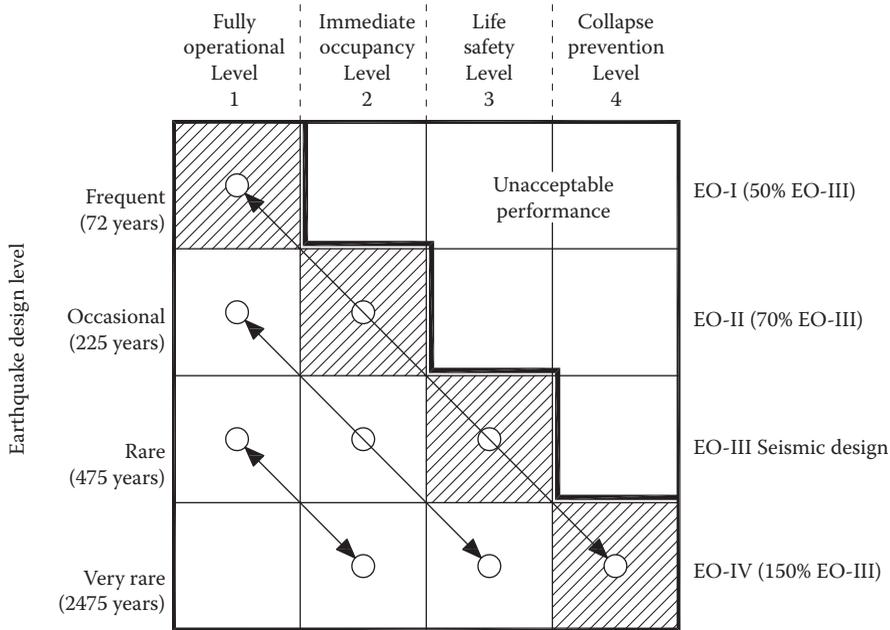
Figure 3.23 Matrix coupling of four performance levels with four levels of seismic excitation. The diagonal corresponds to the basic objectives for normal buildings. (Adapted from FEMA 273, 274. 1997. *NEHPR Guidelines for the Seismic Rehabilitation of Buildings*, FEMA, Washington, DC.)

- EQ-I: 50% probability in 50 years (50% of EQ-III)
  Mean return period 72 years
- EQ-II: 20% probability in 50 years (70% of EQ-III)
  Mean return period 225 years
- EQ-III: 10% probability in 50 years (reference seismic action)
  Mean return period 475 years
- EQ-IV: 2% probability in 50 years (150% of EQ-III)
  Mean return period 2,475 years

The matrix diagonal corresponds to the basic objectives for normal buildings. This means that all diagonal combinations must be fulfilled.

It is evident that as the performance moves to higher levels the relevant seismic action for which the structure must be analysed and designed is also higher.

3.5.2 Performance requirements according to EC 8-1/2004

In Europe, the performance levels have a long history, beginning in 1970 (CEB, 1970; Rowe, 1970) in the form of '*limit states*'. These are states 'beyond which the structure no longer fulfils the relevant design criteria' (EN 1990, 2002). The whole structure of Eurocodes is based on the concept of 'limit states' for all structural materials and all loadings. These are given below:

- Ultimate limit state (ULS)
- Serviceability limit state (SLS)

The first has to do with life safety and the second with comfort during operation. It is evident that the first is combined with higher loading (higher partial safety factor for loading) than the second one.

For seismic design, a proper transformation has been made by EC8-1/2004 in order for the system to comply with the philosophy of seismic design presented in Section 3.2. So, *the performance requirements* introduced are two, namely:

- *Non-(local) collapse requirement*

According to this requirement the structure must be designed and constructed to withstand the design seismic action coupled to this requirement without *local* or *global collapse* retaining its structural integrity and a residual load-bearing capacity after the seismic event.

- *Damage limitation requirement*

The structure should be designed and constructed to withstand a seismic action that has a larger probability of occurrence than the design seismic action without sustaining damage that could impose any limitation on the use of the structure.

The above two performance requirements are coupled through the matrix of Figure 3.24 with the following two levels of seismic excitation:

- EQ-III: The reference seismic action a_{gR} associated with a reference probability of exceedance $P_{NCR} = 10\%$ in 50 years or a reference return period $T_{NCR} = 475$ years multiplied by the importance factor γ_1, that is, $a_g = \gamma_1 a_{gR}$ (recommended values for γ_1; see subsection 3.4.3).
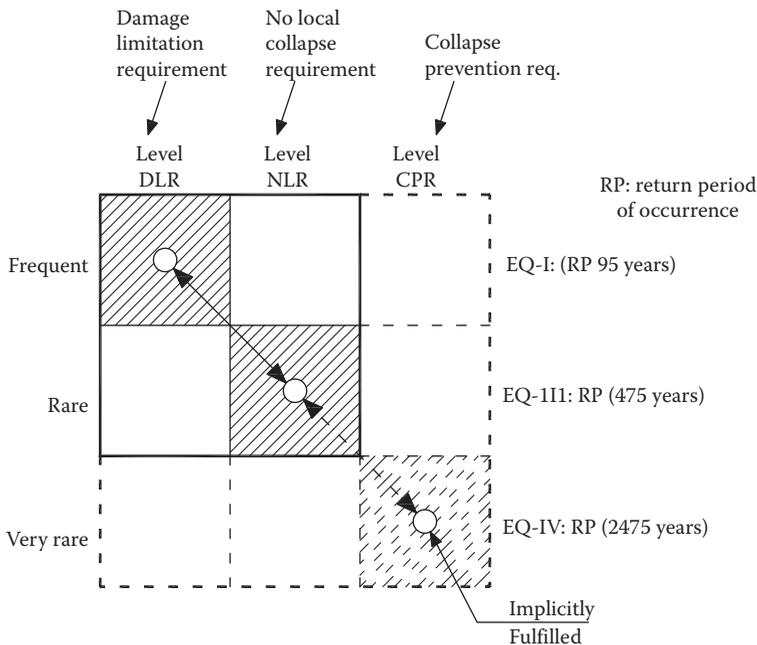
Figure 3.24 Matrix coupling of three performance levels with three levels of seismic excitation for new buildings according to EC8-1/2004.

- EQ-I: The seismic action a_{gp} associated with a probability of exceedance $P_{DLR} = 10\%$ in 10 years or a reference return period $T_{DLR} = 95$ years, that is, $a_{gP} = \nu a_{gR}$ where $\nu = 0.5$ for importance classes I and II, and $\nu = 0.4$ for importance classes III and IV. The above values are recommended by EC8-1/2004. Different values for use in each E.U. member state may be found in its National Annex.

From what has been presented so far it seems that the performance requirements specified by EC 8-1/2004 do not agree with those of FEMA (Figure 3.23), since they do not include the basic concept presented in Section 3.1, according to which in case of a high-intensity earthquake with a return period much longer than that of the design earthquake the building should withstand it without collapse. This lack of agreement is rather superficial. Indeed, although no additional performance requirement for collapse prevention under a very rare seismic motion (e.g. mean return period of 2,475 years) is explicitly stated, it is considered that a series of provisions of EC 8-1/2004 for proper energy dissipation abilities of the structure together with the capacity design approach (see Chapter 6) implicitly ensure this third performance requirement (Figure 3.20 dashed part).

3.5.3 Compliance criteria

3.5.3.1 General

For the satisfaction of the above-mentioned performance requirements, the following two limit states shall be checked:

- ULS
- Damage limitation state (DLS)

The first is associated with local collapse or other forms of failure, which might *endanger life safety.*
The second is associated with damage beyond which *the service ability* of the building is degraded.
In order to ensure the protection of the building against collapse under seismic actions much more severe than the design ones, a number of *specific measures* must be taken. This last principle of EC8-1/2004 is the first answer to the remarks of the last paragraph of Subsection 3.5.2.

3.5.3.2 Ultimate limit state

Two parameters must be verified for the ULS:

- Sufficient strength
- Corresponding sufficient ductility

These two parameters are closely related, as there is a counter-balance between strength and ductility during seismic excitation. This issue has been discussed extensively in previous sections (see Section 3.2). Design for the ULS is *a force-based procedure*, as it was explained in Section 3.2, although the combination of strength and ductility is a matter of energy absorption and dissipation by the structure, which is finally expressed in the form of inelastic displacements. As it has already been noted over and over again, if this displacement demand is less than displacement supply scaled by a safety factor, the structure can withstand the

seismic motion sufficiently. However, for the design of the ULS for new buildings, the *force-based design* method has been adopted in all modern Codes.

According to this procedure:

1. The structure is analysed for gravity loads and seismic motion using *linear elastic–static* or linear *dynamic methods*. For the seismic motion, the codified elastic acceleration response spectrum is reduced by the *behaviour factor q*, ranging between 1.5 and 5.0 of its elastic values (design spectrum) depending on the ductility level of the structure (*q*-factor).
2. Then the structure is designed for a linear combination of internal forces (action effects) caused by gravity loads and reduced by *q* seismic actions. The dimensioning is carried out as for all other load cases implemented in the case of Eurocodes EC 2-1-1/2004, that is,

$$[E_d] \leq [R_d] \tag{3.52}$$

where
  $[E_d]$ is the design internal forces (action effects) for load combinations of gravity loads and design seismic actions.
  $[R_d]$ is the design resistance of each cross-section calculated according to the rules of the relevant Codes in effect for all the other load cases.

3. In this way, it is obvious that the structure indirectly enters the post-elastic range, since it has been designed for reduced seismic actions by *q* = 1.5–5.0. Therefore, this reduced strength must be combined with measures for *sufficient ductility*. These measures are based on dimensioning and detailing rules. These rules are specified in Seismic Codes, and as the codified ductility demand becomes higher so these rules become stricter. All these rules will be presented, analysed, explained and discussed in Chapters 8 through 10. *The safety factor ensured in this way seems to be in terms of displacements between 1.50 and 2.00 (see* Figure 3.22*)*.

Summarising the procedure presented in the above three items, *it* can be said that the *benefit* due to seismic force reduction is partially balanced by the *cost* for higher ductility. Indeed, the results of extended cost–benefit analyses on this issue have shown that the choice to reduce forces and improve ductility is cost beneficial. What is more important, *it is much easier to improve ductility in order to withstand unexpected very rare severe earthquakes than to improve strength*.

In conclusion, it would be interesting to discuss the reasons for which the force-based design method has been adopted by modern Codes for the design of new buildings. This must be attributed to the following reasons:

1. The structure is analysed using linear methods that are simpler and much more reliable than the inelastic ones, which are necessary for a displacement-based design (generation of the capacity curve).
2. Under these conditions, *analysis and design* for seismic actions is carried out as for all other loadings, and therefore the usual superposition procedures can be adopted.
3. *Analysis and dimensioning are separated*. The analysis precedes and dimensioning follows based on the results of the analysis, while in the case of inelastic procedure the dimensioning must proceed based on approximate methods. In other words, the procedure of the displacement-based design is a procedure for *assessment and verification*.

In the next chapters (Chapters 5, 8 and 9), a detailed discussion will be carried out on quantitative procedures for the relation between the overall ductility demand of the structure in the form of q-factor and ductility demand μ_D at the level of the structural elements (local ductility). In this respect, structural members will be either designed for ensuring local ductility supply in critical regions, for which there are relevant Code requirements, or will be detailed according to rules specified by Code.

3.5.3.3 Damage limitation state

This limit state protects the structure mainly from non-structural damage (in-fill walls, plasters, window glass, etc.) caused by frequent earthquakes. For these earthquakes (EQ-I subsection 3.5.2), the structure must present deformation (interstorey drifts) that satisfy the deformation limits defined by the Code, so that the building is safe against unacceptable damage.

3.5.3.4 Specific measures

As it was noted at the beginning of this subsection, a series of specific measures is foreseen in all modern Codes for prevention of the collapse of the building in case of an unexpected, very rare and more severe earthquake than the design earthquake. These measures specified by EC8-1/2004 refer to:

- Design
- Foundations
- Quality system plan

Specifically, for R/C buildings, additional measures are imposed to cover:

- Resistance uncertainties.
- Ductility uncertainties.
- General configuration of the building. The design measures specify rules and principles for regularity in plan and elevation, for ensuring a hierarchy in the loss of resistance of the structural members by means of *capacity design procedures*, so that premature failure may be avoided, and for taking into account soil deformability and adjacent structures in the formation of structural models.
- For the foundation, the Code imposes the basic principle for overstrength design of the foundation so that failure is limited to the super-structure.
- For the quality system plan the Code specifies a series of obligations that should be taken into account during the preparation of drawings, technical reports, and technical specifications for the design of the building.
- For resistance uncertainties in R/C buildings, the Code provides minimum dimensions and special detailing of the structural members.
- For ductility uncertainties in R/C buildings, minimum–maximum reinforcement limits are foreseen at the critical regions and limited normalised axial forces at the vertical R/C members (columns, structural walls).

In the chapters that follow, the implementation of the preceding principles presented in this section (Section 3.5) will be presented in detail.

Configuration of earthquake-resistant R/C structural systems

Structural behaviour

4.1 GENERAL

One of the basic factors contributing to the proper seismic behaviour of a building is a rational conceptual design of the structural system in a way that lateral seismic actions (inertia-forces) are transferred to the ground without excessive rotations of the building and in a ductile manner. This cannot be achieved only through mandatory requirements of the Code. Therefore, there are also some general principles that can lead to the desirable result when they are followed. The guidelines that should govern a conceptual design against seismic hazard according to EC8-1/2004 are:

- Structural simplicity
- Uniformity and symmetry
- Redundancy
- Bidirectional resistance and stiffness
- Torsional resistance and stiffness
- Diaphragmatic action at storey levels
- Adequate foundation

It should be mentioned that after a thorough examination of the 103 most badly damaged or collapsed R/C buildings in Athens after the earthquake of Parnitha (7-9-1999), it was found that 29 of these buildings had failed mainly due to their poor configuration (OASP, 2000). This was attributed mainly to the absence of collaboration between the architect and the structural engineer at the early stages of planning when a satisfactory compromise could have been reached. Of course, this is a usual situation only in small- and medium-sized buildings where there are not distinct stages of a preliminary design, predesign, and final design where this collaboration is consolidated.

It should also be remembered (see Subsection 3.4.2) that in the case of big projects, geotechnical site investigations should be carried out and a geotechnical report should be prepared by an expert in soil mechanics to include all necessary information about:

- The stratification profile
- The mechanical properties of the soil
- The ground type (see Paragraph 3.4.2.2)
- The water table
- The presence of liquefiable soils
- The proposal on the type of foundation (shallow or deep)

It must be noted that even in case of small projects it is necessary that soil investigation be carried out if there is no relevant information from buildings existing in the neighbourhood.

In the next section, a discussion will be presented on the guidelines stated above.

4.2 BASIC PRINCIPLES OF CONCEPTUAL DESIGN

4.2.1 Structural simplicity

The existence of simple structural systems with easily identified load paths for the transmission of gravity and seismic loads from the structural members to the foundation must be a basic objective of the conceptual design. It must be noted that in the case of a simple structural system the results of analysis and design are much more credible than those of a complicated one. In Figure 4.1 some simple structural systems are given in a plan.

4.2.2 Structural regularity in plan and elevation

Buildings regular in plan and in elevation, without re-entrant corners and discontinuities in transferring the vertical loads to the ground, display good seismic behaviour. The presence of irregularities in plan leads to stress concentrations dangerous to the structure. In this case, if necessary, the entire building with re-entrant corners in plan may be subdivided by seismic joints into independent seismic compact parts (Figures 4.2 and 4.4).

Uniformity in elevation in mass and stiffness distribution is of essential importance for good seismic behaviour. Discontinuities in load transfer to the foundation with walls or columns 'planted on' beams and discontinued below, or discontinuities in deck diaphragms or building aspects with re-entrant corners are bad signs for the behaviour of the building in case of a strong earthquake (Figures 4.4 and 4.5). Although the symmetrical arrangement of stiffness elements is not always possible due to architectural constraints, there should be a special concern in this direction so that torsionally flexible or asymmetric structures, which can cause failures to the corner columns and the walls at the perimeter, will be avoided (Figures 4.2 through 4.5; Baden Württenderg Innenministerium, 1985; see also Sections 2.4 and 5.3).
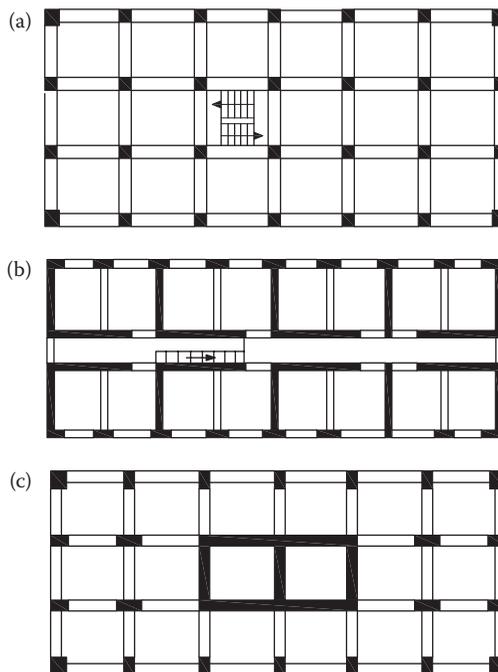
Figure 4.1 Structural systems characterised by simplicity: (a) a typical form of a frame system; (b) a typical configuration of an R/C shear wall system; (c) a dual system with an R/C core and frames.
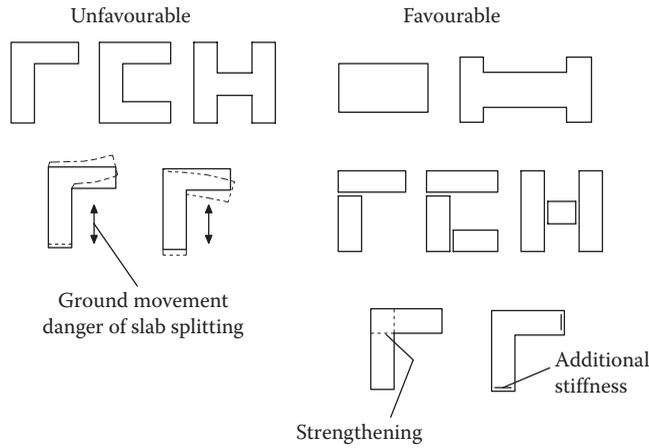
Figure 4.2 Unfavourable and favourable geometric configuration in plan.

4.2.3 Form of structural walls

In the case that they span voids between adjacent R/C columns, R/C structural walls should span the whole distance between them. In this way, the stiffness, strength, and ductility of the structure are improved (Figure 4.6).
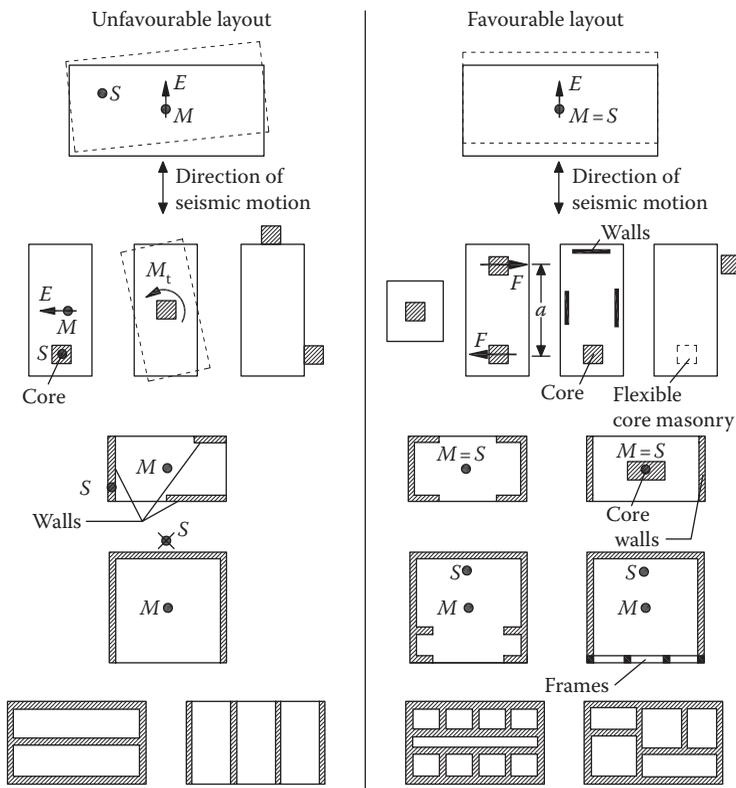
Figure 4.3 Distribution of mass and stiffness in plan.
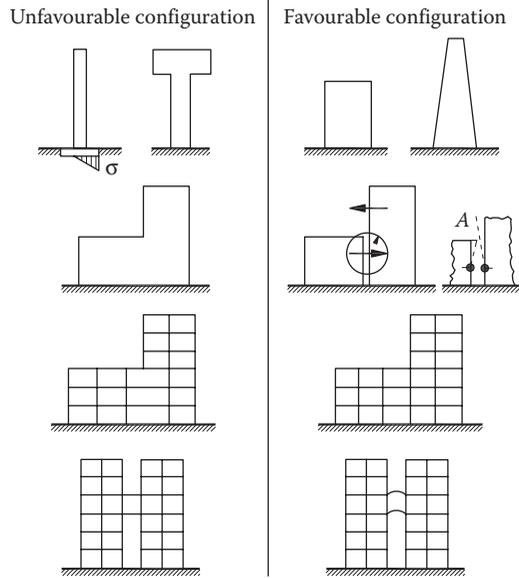
Figure 4.4 Unfavourable and favourable configuration in elevation.
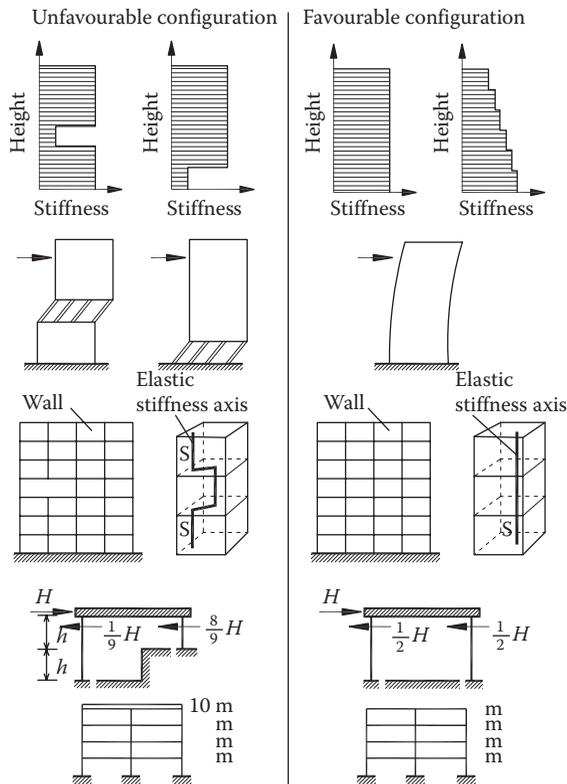
Figure 4.5 Distribution of mass and stiffness in elevation.
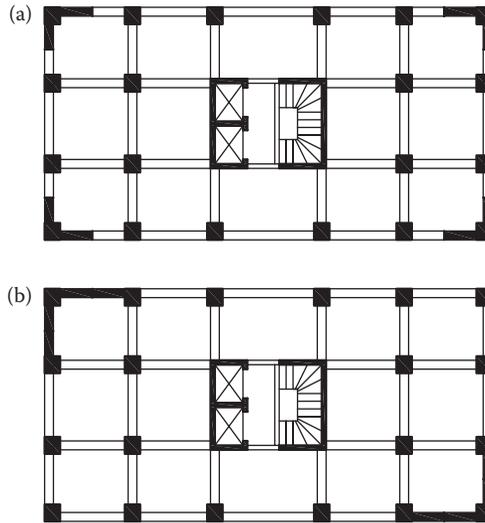
Figure 4.6 Layout of shear walls at the perimeter (a) acceptable arrangement, (b) improved arrangement.

4.2.4 Structural redundancy

All the structural elements, including the foundation, should be well interconnected to build a monolithic, robust structure with high redundancy. High stiffness cores (staircases-shafts) lying in the perimeter of the building may be easily separated during an earthquake from the diaphragmatic system, leading the structure to unexpected response (Figure 4.7).

4.2.5 Avoidance of short columns

Short columns resulting from the presence of mezzanines or stiff masonry or R/C parapets below the windows should be avoided. If such arrangements cannot be avoided, their effect on the behaviour of the structure should be taken into account as far as the load effects, ductility, and shear capacity are concerned (see Subsection 8.3.6; Figures 4.8 and 4.9).
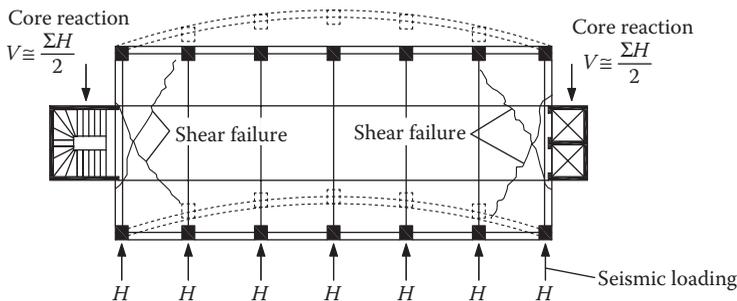
Figure 4.7 Unfavourable core arrangement; diaphragm at risk due to shear failure at the connections to the cores.
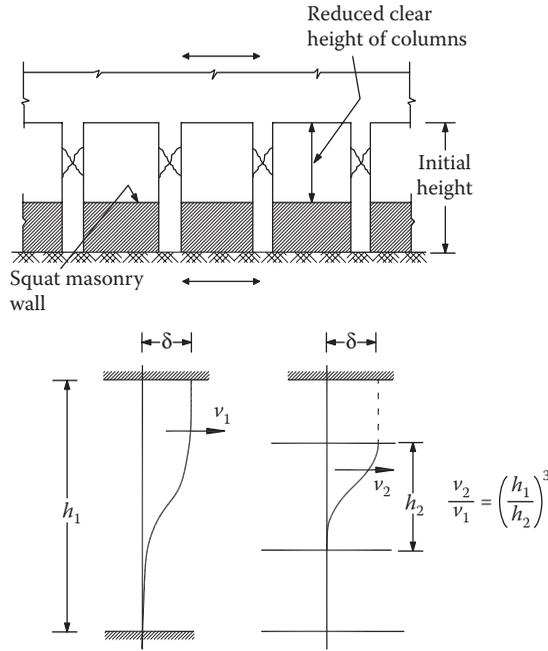
Figure 4.8 Concentration of large shear forces on short columns at the perimeter of the building.

4.2.6 Avoidance of using flat slab frames as main structural systems

Flat slab systems (Figure 4.10) without beams, although quite attractive in construction due to the low cost for formwork and the free space at storey for the arrangement of E/M ducts, should be avoided, as they are not covered completely by EC8-1/2004. *This does not mean*
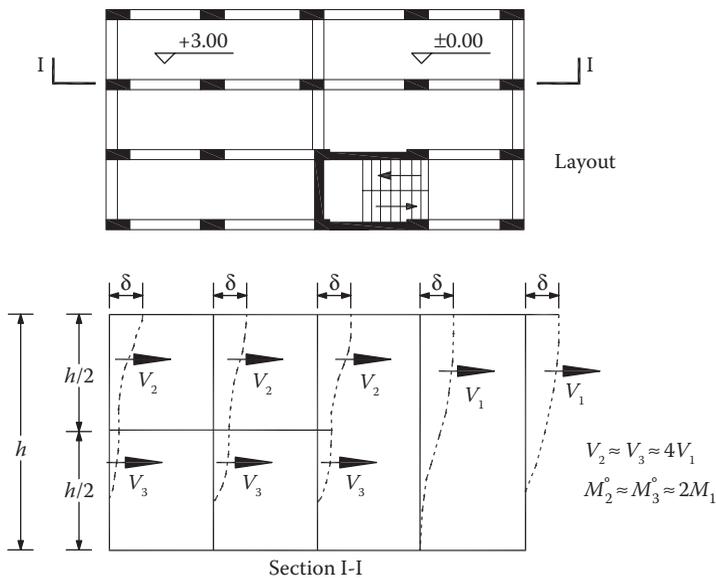
Figure 4.9 Concentration of large shear forces on short mezzanine columns.
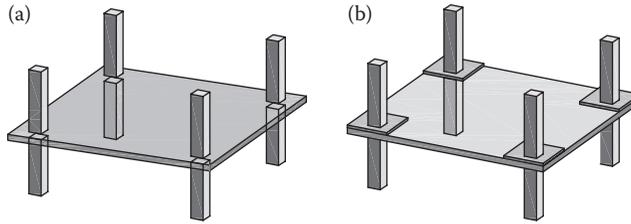
Figure 4.10 Flat slab systems; (a) slab directly on columns, (b) slab with drop panels.

that they cannot be combined with structural walls or cores and frames capable of carrying the seismic actions (Figures 4.11 and 4.12).

4.2.7 Avoidance of a soft storey

Large discontinuities in the infill system in elevation (such as open-ground storeys) should be avoided (Figure 4.5). A stiffness discontinuity of this type generates a soft storey mechanism, which is very susceptible to collapse.

   In the case that this type of structure cannot be avoided, as it happens in most Mediterranean countries where the General Building Code imposes an open storey at the ground level (Pilotis system), special measures should be taken in analysis and detailing of the structural walls and the columns.

4.2.8 Diaphragmatic behaviour

The system of the floors and roof of a multistorey building constitutes the basic mechanism for transfer of inertial seismic forces from the slabs of the building where the masses are distributed to the vertical structural members (columns and structural walls) and thereby to the foundation. In parallel, the system of the slabs, particularly of cast in situ R/C buildings, ensures the behaviour of each storey deck as a rigid disc in plane, that is, as a horizontal diaphragm, but that is flexible in the vertical direction. In this way the storey diaphragms contribute to increasing the system's redundancy. It is evident that the creation of this 3D structure with high redundancy can be generated very easily in case of R/C buildings cast in situ.

   When an R/C building has a compact form in plan it is obvious that there is not any risk for structural failure of the diaphragms. However, when the structural system includes R/C cores of high stiffness at the limit of its perimeter (Figure 4.7) or in case of the existence of re-entrant corners in plan (Figure 4.2) or very large floor openings (Figures 4.13, 4.14 and 4.15), the diaphragmatic function may fail, and therefore special attention must be given to the analysis and design of the diaphragm itself (i.e., the analysis and design of the slab as a disc in-plane under the action of the inertial forces and the shear reactions of the vertical structural members on the disc).

4.2.9 Bi-directional resistance and stiffness

The structural elements should be arranged in an orthogonal in-plan structural pattern ensuring similar resistance, stiffness, and ductility in both main directions (bi-directional function) since the seismic action may have any direction, and in this context the structure must be in a position to withstand any excitation with its two orthogonal components.
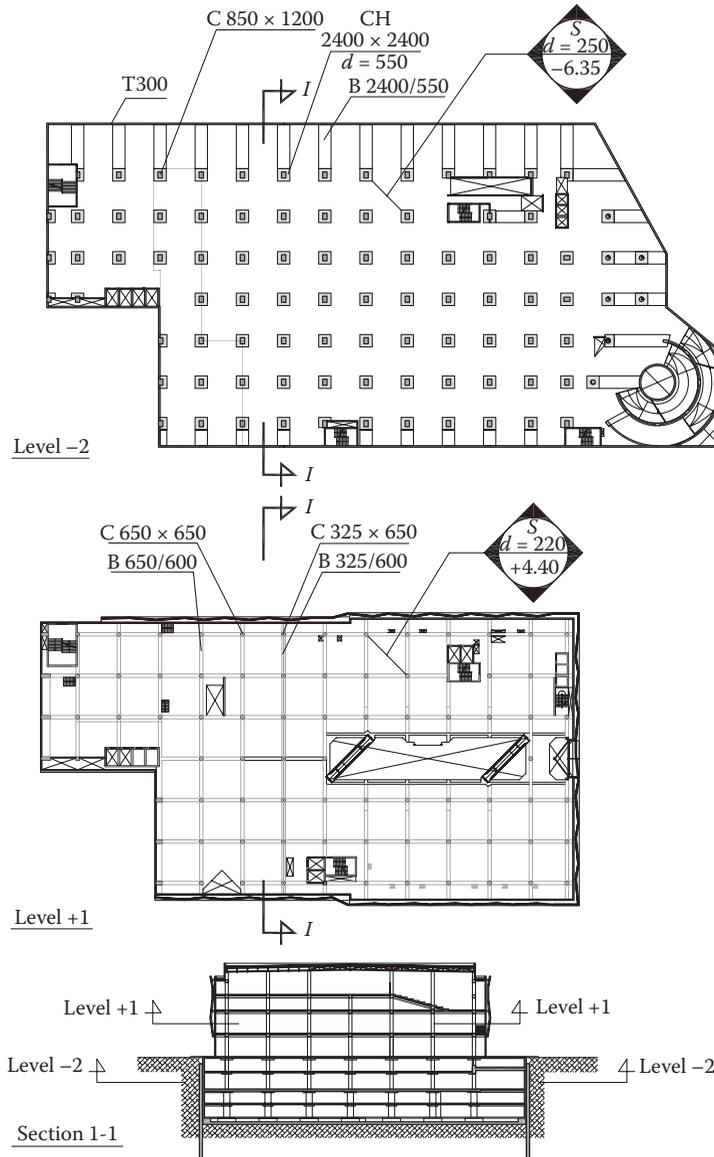
Figure 4.11 VRBANI, Zagreb mall; basements with flat slab frames and walls at the perimeter; frame system at the superstructure with limited shear walls.

4.2.10 Strong columns–weak beams

Structures have to be composed of strong columns and weak beams for capacity design reasons. In Chapter 6 this recommendation will be discussed in detail.

4.2.11 Provision of a second line of defense

It is recommended to include in the structural system in parallel to shear walls a second line of defense formed by *ductile frames*. Thus, the dual system (structural walls combined with
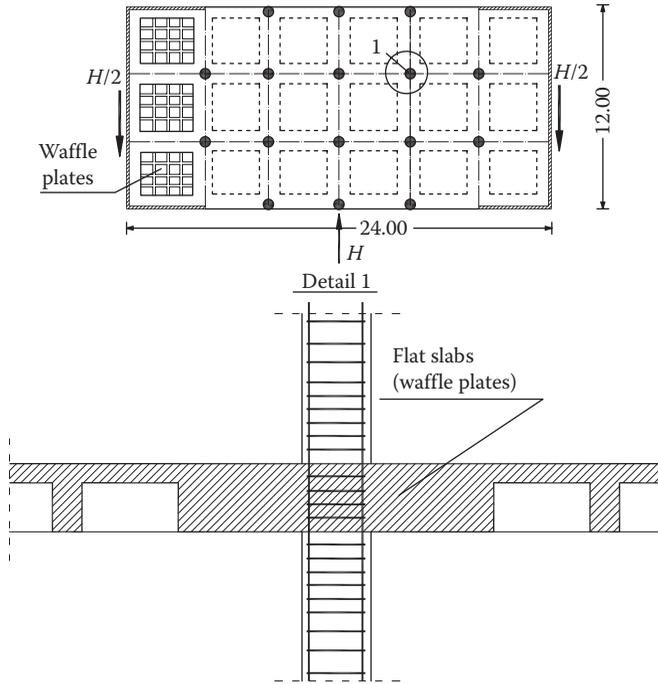
Figure 4.12 Flat slab frames combined with shear (ductile) walls.

ductile frames) seems to be the most appropriate for resisting seismic action. ASCE 7-05 requires that, independent of the results of the analysis, 25% of the earthquake actions have to be carried by these frames. It should be noted that EC8-1/2004 does not impose such an obligation; instead, in the case that the frames resist for more than 35% of the base shear, the structural system is upgraded as far as its behaviour factory is concerned.

Longitudinal section
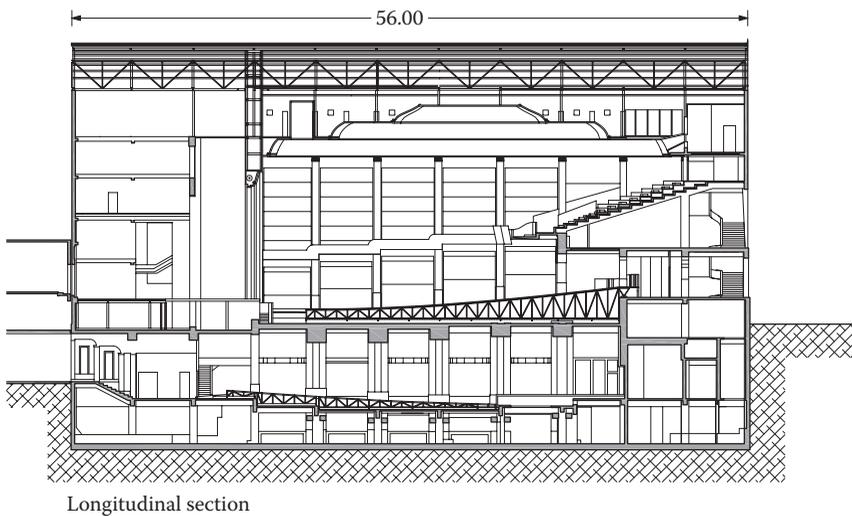
Figure 4.13 Palace-Aliki theaters, Athens, Greece; Elevation.
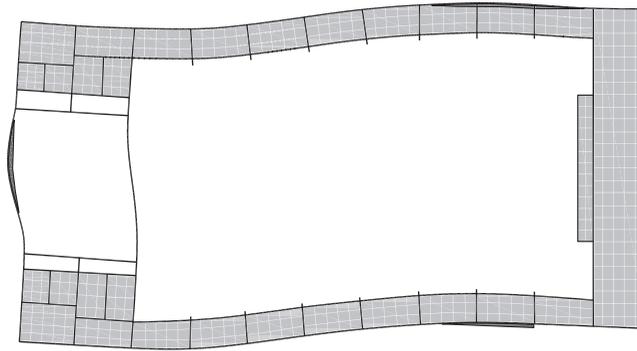
Figure 4.14 Palace—Aliki theaters, Athens, Greece 3rd eigen mode of the structure at the level of balconies (FEM elastic modal spectrum analysis).
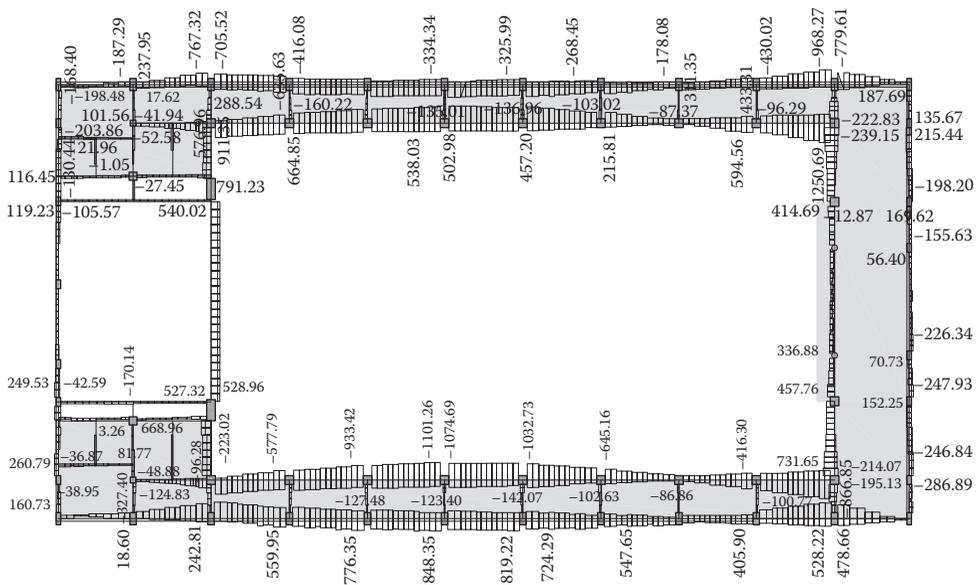
Figure 4.15 Palace—Aliki theaters, Athens, Greece. Axial forces of beams at the level of balconies due to seismic combination in the *y-y* direction.

4.2.12 Adequate foundation system

The foundation plays a crucial role in the behaviour of the building in response to seismic actions. It should be noted that no matter what material is used for the superstructure, R/C is used almost exclusively for the foundation. The following recommendations should be kept in mind as far as the foundation is concerned:

- The site where the building will be constructed must be free of risks of soil rupture, slope instability, and permanent settling caused by liquefaction or densification in the event of an earthquake (see also Subsections 3.4.2 and 10.2.3).
- In the case of shallow foundations, the recommended system is a mat foundation or a grid of foundation beams or at least a grid of tie beams between the independent pads in case of firm soil or bedrock.
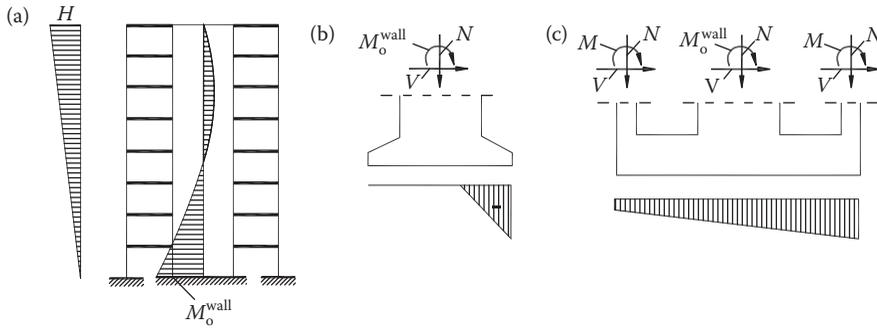
Figure 4.16 Foundation issues of shear (ductile) walls (a) wall response in a dual system under lateral loading; its behaviour maybe simulated to a one end fixed cantilever supported by a spring at the other end (b) wall foundation on a pad; overturning risk; (c) connections of the wall with the external columns with a foundation beam: diminishing of the risk of overturning due to enhancement of the total axial force and broadening of the foundation basis.

- In the case of deep foundations (piles), the use of a foundation slab or tie-beams between pile caps in both main directions is recommended.
- The existence of a basement with one or more underground storeys is a very good opportunity for the formation of an underground box structure. This box structure consists or a foundation mat or a grillage of foundation beams, a perimetric R/C wall system acting in parallel as a retaining wall for earth pressure, vertical structural members (columns, structural walls) in the basement space, and the ground slab of the building. This box acts as a solid structure that safeguards the synchronous vibration of all vertical structural members at the level of the foundation (Figure 10.4), and in parallel it diminishes the overturning risk that exists in the case of eventual independent footings of the walls (Figure 4.16).
- It is evident that all recommendations for foundations so far, except for the first one, have as their main objective making sure that all vertical elements have a synchronous excitation during a seismic motion, which is a basic design principle (see Subsection 2.4.4). Indeed, it should not be forgotten that the seismic actions reach the foundation in the form of waves (Figure 4.17). Thus, if footings are not well interconnected, each of them experiences an asynchronous vibration.
- Finally, it is recommended that all footings rest, if possible, on the same horizontal level (Figure 4.18).
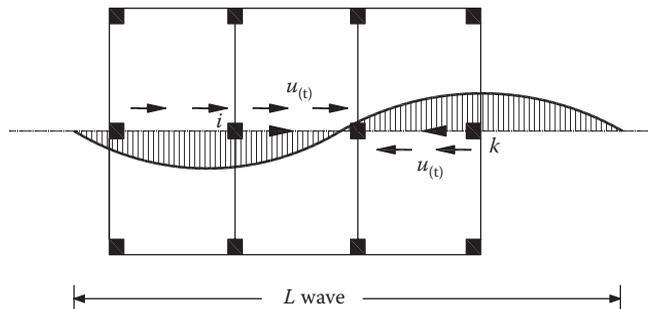
Figure 4.17 Relative displacement of the footings of columns *i* and *k* of a phase difference of the ground motion at points *i* and *k*.
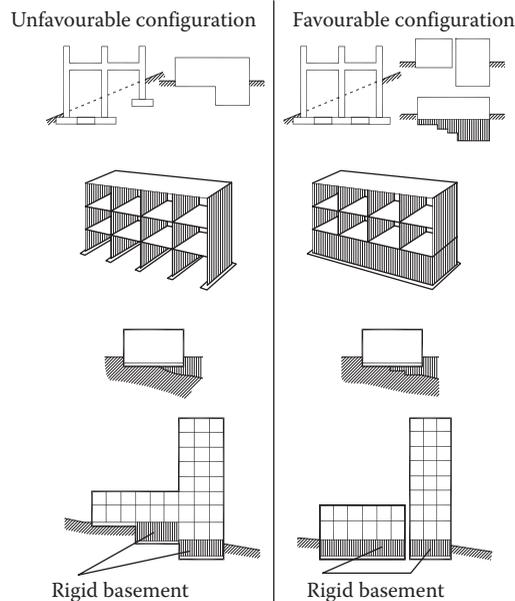
Figure 4.18 Unfavourable and favourable configuration of the foundation and the basement.

4.3 PRIMARY AND SECONDARY SEISMIC MEMBERS

EC8-1/2004 allows flexibility to the designer to characterise a number of structural members (beams and/or columns) as *'secondary'* seismic members not forming part of the seismic action system of the building. This means that these elements will be introduced in the structural model as elements of zero bending stiffness. The reasoning behind this flexibility is that the designer might combine in the same building members that are not covered by the Code, like flat slab systems, together with others that are in accordance with the regulations, like ductile frames and/or walls. In this case the ductile members constitute the *'primary seismic system'* while the secondary ones are used for carrying *only gravity loads*.

   The Code specifies some restrictions in order to allow this procedure in analysis and design, that is:

   1. The total contribution to lateral stiffness of all secondary seismic members should not exceed 15% of that of all primary seismic members. This can be checked by comparing the displacements of the centre of mass at the top storey for a horizontal loading in the two main orthogonal directions of the building, once taking into account the stiffness of all structural members, and another taking into account the stiffness of the primary members only. In particular, in the case of a flat slab system, a band of the slab (effective width) equal to the width of the columns plus two times the thickness of the slab should be taken into account (ACI 318 M-2011, EAK 2000) for the framing of the columns.
   2. The design of the secondary R/C members should take into account, in addition to the action effects of gravity loads, the bending moments and shear forces that develop for the displacements at their ends (first- and second-order effects) due to the seismic action on the primary system. Taking into account that the stiffness of the secondary members is not higher than 15% of the primary ones, and that computer-aided

analysis and design run very fast, it can be said that the above requirement can be fulfilled approximately by analysing the system again with all its elements, primary and secondary ones in the same model, and proceeding to the dimensioning of the secondary members for the action effects due to gravity loads and seismic loading, but without any 'capacity design' considerations.

3. The dimensioning of the secondary seismic members is carried out as in non-seismic regions (e.g., EC2-1/2002), that is, without taking into account the regulations of EC8-1 for R/C primary seismic members.

4.4 STRUCTURAL R/C TYPES COVERED BY SEISMIC CODES

The structural system should preferably be composed of frames either alone or coupled with structural walls in two directions, so that a clearly defined flow of lateral forces is achieved. The structural walls in this case might be either independent plane members (discs) or combined plane members to form in plan *L*, *T*, *C*, *Z* sections or tubes. The structural systems covered by EC8-1/2004 should belong to one of the following structural types according to their behaviour under horizontal seismic actions:

- *Frame system:* A structural system in which both the vertical and lateral loads are mainly resisted by 3D ductile frames with a base shear that exceeds 65% of the total shear resistance of the whole structural system (Figure 4.1a).
- *Ductile wall system:* Structural systems in which vertical and lateral actions are mainly resisted by vertical structural ductile walls, either coupled or uncoupled, with a shear resistance at the building base that exceeds 65% of the total shear resistance of the whole structural system (Figure 4.1b). The percentage of shear resistance may be replaced approximately by the percentage of the shear action effects developed at the walls under lateral loading.
- *Dual system (frame or wall equivalent):* A structural system in which support for the vertical loads is mainly provided by a 3D frame system and resistance to lateral loads is covered in part by the frame system and in part by coupled or uncoupled structural walls (Figure 4.1c). From the structural point of view these systems must be classified in two different categories, that is:
  - *Frame-equivalent dual systems,* in which the shear resistance of the frame system at the building base is greater than 50% of the total shear resistance of the whole structural system, and
  - *Wall-equivalent dual systems,* in which the shear resistance of the walls at the building base is higher than 50% of the total seismic resistance of the whole structural system.

    For the above classification the percentage of the shear resistance may be replaced approximately by the percentage of the shear action effects developed at the walls under lateral loading.

    The above three structural systems, that is:
    – Frame systems
    – Wall systems
    – Dual systems

    are the main structural systems in use in earthquake-resistant R/C buildings. In Table 4.1 an overview is given of these systems together with their corresponding base shear resistance.

Table 4.1 Main structural systems for earthquake resisting R/C buildings

Type of structural system	Percentage of base shear resisted by the system	
Frame system	>65%	Resisted by frames
Wall system	>65%	Resisted by walls
Dual system		
Frame equivalent	>50%	Resisted by frames
Wall equivalent	>50%	Resisted by walls

The quantitative classification of a structure in one of the above categories according to the percentage of their shear resistance at the base of the building in relation to the total shear resistance is considered a safe index for the type of failure mode of the building that is likely to appear under a strong seismic action. Therefore, it is a good criterion for the evaluation of the *'behaviour factor'* of the building, as we will see in the next chapter.

The simplification of the Code to allow the substitution of the 'shear capacity' of the vertical structural members at the base of the building by 'the demand' in estimating the percentage of shear participation of frames or walls *is a very useful approach for design practice.*

Indeed, for the determination of shear capacity of the structural members, the procedure of design must be integrated by dimensioning and detailing of the structural members. However, it is necessary to know the behaviour factor *q* at the beginning for the quantification of the design spectrum (see Subsection 3.4.3). This means that a time-consuming iterative procedure should be established until the correct *q* factor is determined. The introduction of the above 'simplification' allows the determination of the shear percentages of the structural elements in each main direction by applying a horizontal static loading at the rigidity centre of each storey (see Subsections 2.4.4 and 4.5.3) and determining the shear force at the base of the vertical structural elements. This can be done at the beginning after the preparation of the formwork drawings and the analytical model (geometry) of the structure before any analysis or design.

- *Torsionally flexible systems:* Another crucial point for the above structural systems is their *torsional rigidity*. According to the Code, there must be a distinction between *'torsionally flexible'* and *'torsionally rigid'* structural systems. Simply speaking, a 'torsionally flexible system' is a structural system wherein small eccentricities of the seismic horizontal forces cause large torsional deformations to the storey diaphragms and therefore excessive drifts at the perimeter columns of the system, disproportionate to those caused by the translational displacements (see Subsection 2.4.4; Figure 4.3).

This distinction will be discussed in detail in Chapter 5. For the time being it must be noted only that in the case that the above systems fall into the category of the 'torsionally flexible', they continue to be accepted as systems covered by EC8-1/2004. However, a series of implications is activated. These implications have to do with the values of the *q*-factor of the system and its regularity in plan, which has an influence on the accepted methods of analysis for the system.

In addition to the four main structural systems presented above, two other less usual systems are covered by EC8-1/2004. These systems are the following:

- *System of large lightly reinforced walls:* This is a type of R/C building with the main structural system consisting of large R/C walls, which carry a large part of the gravity

loads and the seismic action as well. According to EC8-1/2004, **a wall system** is classified as a system of large, lightly reinforced walls if in each of the two orthogonal directions it includes at least two walls with a horizontal dimension of not less than 4.00 m or $2h_w/3$ (h_w is the height of the wall), whichever is less. These walls in each main direction collectively must support at least 20% of the total gravity load, that is, 40% of the gravity loads must be carried by walls in both orthogonal directions. Additionally, the fundamental period T_1 of the building, assuming fixed walls at the foundation, must be less than 0.5 s. These systems are considered to belong to 'wall family systems'. 'Behaviour factor' issues of this type of structural system will be discussed together with all other types in Chapter 5.

In the case that the system is torsionally flexible, it moves from the category of walls to the category of the torsionally flexible systems, like the main three systems described in the previous paragraphs.

- *Inverted pendulum system:* A system in which 50% or more of the mass is in the upper third of the height of the structure, such as with water or TV towers, is classified as an inverted pendulum system. In the same category structural systems in which the dissipation of energy takes place mainly at the base of a single building element should be included, like a main shaft for elevators, stairs, and E/M installations combined with few columns.

One-storey buildings—that is, buildings extended horizontally like industrial installations, covered stadia, cultural halls, auditoria, and so on—*are excluded from the category of the inverted pendulum* if the normalised axial load ν_d (see Subsection 8.3.4) does not exceed the value of 0.30.

It must be noted here again (see Section 4.2) that concrete buildings with *flat slab frames* used as primary seismic elements *are not covered* by EC8-1/2004.

4.5 RESPONSE OF STRUCTURAL SYSTEMS TO LATERAL LOADING

4.5.1 General

From the discussion so far, it can easily be concluded that even a multimodal response spectrum analysis results in a series of inertial horizontal loadings, one for each mode (see Subsection 2.4.3). The final result is in general a load pattern of horizontal forces at the level of the storey decks parallel to the two main directions of the structure. Therefore, thorough discussion on the behaviour of the structural systems in use for earthquake-resistant R/C buildings under horizontal loading is considered to be of major importance. In this respect, knowledge of the structural behaviour of pseudospatial systems, like R/C buildings, under horizontal loads turns out to be a useful tool for:

- The conceptual Design of the Structure
- Qualitative evaluations of the computational output of the analysis of the seismic loading, no matter which method has been used.

4.5.2 Plane structural systems

As already stated in Section 4.4, the R/C structural systems mainly used in earthquake-resistant structures are:

- Frame systems
- Wall systems (ductile walls)
- Dual systems

Usually plane systems of the above type arranged in the two main orthogonal directions of a building compose through the storey diaphragms a pseudospatial structural system (see Sections 2.4.4 and 4.6) suitable for an R/C earthquake-resistant building. Therefore, before any reference to the behaviour of pseudospatial systems, it is interesting to study the above systems in their plane configuration.

4.5.2.1 Moment-resisting frames

Frames with rigid girders subjected to lateral forces (Figure 4.19) exhibit zero moments at the mid-height of the columns, shear distribution at each storey proportional to the moments of inertia of the cross sections of its columns, and relative displacements (or inter-storey drifts) proportional to the storey shear:

$$u_i = \left[\sum_j V_{ij} \right] \frac{h^3}{12E \sum_j J_{ij}} = \left[\sum_{i=i}^{i=n} H_i \right] \frac{h^3}{12E \sum_j J_{ij}} \tag{4.1}$$

and

$$V_{ij} = \left(\sum_{i=i}^{i=n} H_i \right) \frac{J_{ij}}{\sum_j J_{ij}} \tag{4.2}$$

From Equation 4.1 it may be concluded that the relative displacements are proportional to the storey shear; this is the reason why these systems are also called *'shear systems'*. It should be noted that the ability of these systems to resist horizontal forces derives from the moment resistance of their joints. The deformation of these systems is such that they display a concave form on the side of the loading. In conventional frames, due to their *T* section, the girders exhibit in general much greater stiffness compared to that of columns. Therefore, their behaviour is very similar to the behaviour of 'shear systems'.
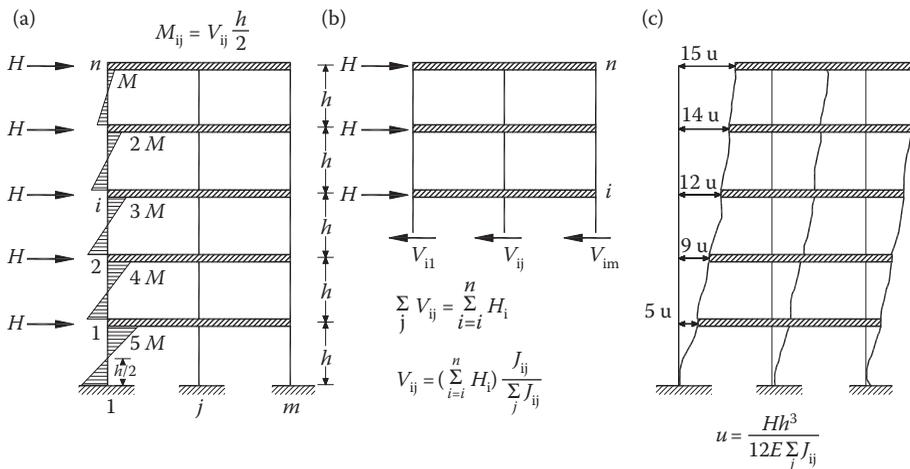
Figure 4.19 Action effects on shear frames under lateral loading; (a) *M* – diagram; (b) equilibrium between shear and lateral loads; (c) storey displacements.
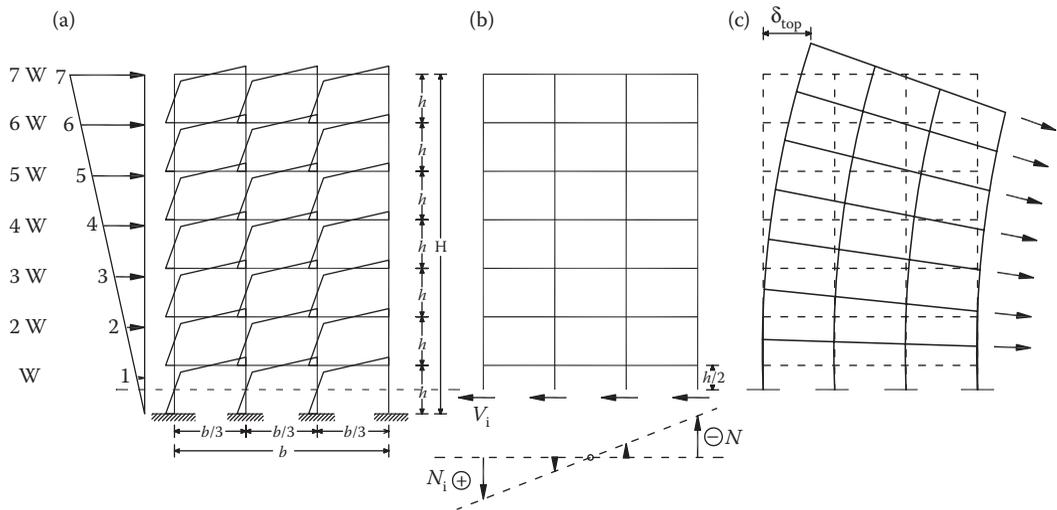
Figure 4.20 Frame system under lateral loading. (a) Moment diagram; (b) axial forces at the columns (opposite sign); (c) displacements due to axial strain of columns.

From the form of the moment diagrams (Figure 4.20) it can be easily concluded that the areas of potential plastic hinges in the moment-resisting frames are around the joints of the frame.

At the same time, these systems develop axial forces at the columns as a counter-balance to the action of the pattern of the horizontal loading (see Figure 4.20b). Consequently, in addition to the shear action they present a bending deformation due to the compression and tensile forces of the columns (Figure 4.20c); so the system for its bending behaviour presents a convex form on the side of the loading. However, the displacements due to bending are limited to 15–20% of those of shear action and therefore shear behaviour prevails.

4.5.2.2 Wall systems or flexural systems

Walls coupled with beams of low-flexural stiffness behave under the action of lateral forces as cantilevers (Figure 4.21). They are also called *shear or ductile walls* due to the fact that in structural systems these walls, due to their high stiffness, carry the major part of the base shear of the structure caused by horizontal loading.
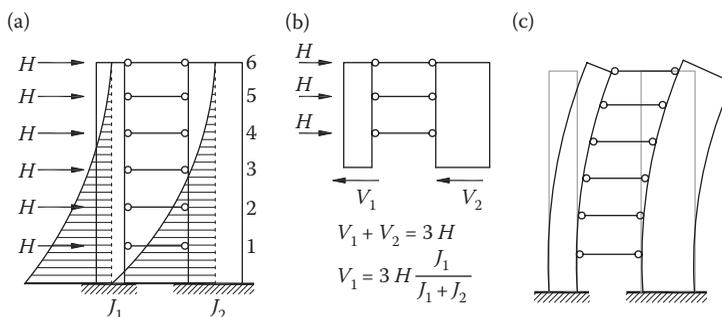
Figure 4.21 Action effects of shear (ductile) wall system under lateral loading (a) M – diagram; (b) equilibrium between shear and lateral loads; (c) storey displacements.

The shear distribution is approximately proportional to the moments of inertia of the cross-sections of the walls. The relative displacements of the storeys result mainly from bending deformation of the walls and therefore they present a convex form of the side of the loading. Taking into consideration that the bending moments of shear walls present their maximum value at the base of the walls, it can easily be concluded that the *critical region of these structural members where a plastic hinge could be formed in case of a strong earthquake is likely to be at its base.*

4.5.2.3 Coupled shear walls

When shear walls are arranged at the perimeter of the building, very often they have the form of coupled walls with spandrels arranged above door or window openings at the façade of the building (Figure 4.22).

Moment diagrams of these systems are depicted in Figure 4.22. The main characteristic of these diagrams is that the end moment at the base of each of the two walls is smaller than the half of the end moment that would be developed in the case that the stiffness of the spandrels is zero. This reduction of the end-moment at the base of the walls is attributable to the function of the spandrels. In fact, as their stiffness increases, the end-moment of the walls diminishes, to the limit form of Figure 4.22g.
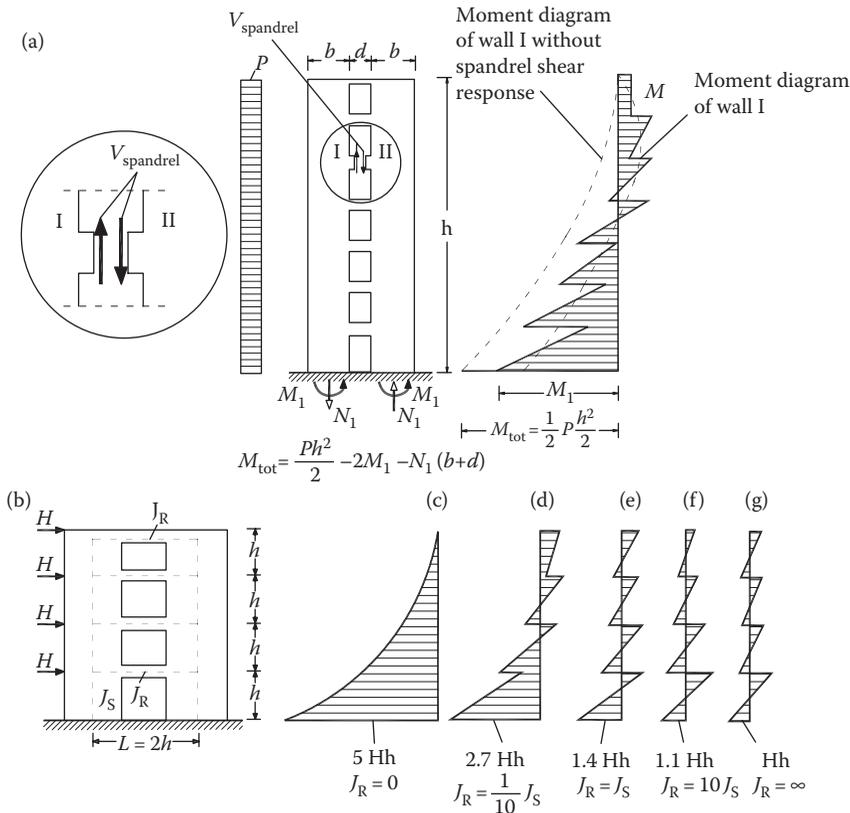
Figure 4.22 (a) Response of coupled shear walls under lateral loading; (b) to (g) the influence of the spandrel stiffness on the moment diagrams of the walls.

This is attributable to the fact that a percentage of the external total moment of the horizontal loading pattern is carried by a couple of internal axial forces N at the base of the two coupled walls. These axial forces are caused by the shear forces of the spandrels (Figure 4.22a). The shear forces of the spandrels take high and alternative values due to the cyclic seismic motion. This, together with their ability to dissipate energy, will be discussed in a later chapter (see Subsection 9.2.4).

4.5.2.4 Dual systems

The coupling of ductile frames and shear walls into a dual system under lateral loading results in such interaction forces that alter the moment and shear diagrams of both the frame and the wall (Figure 4.23). This is attributable to the completely different deformation shape of the individual components. The characteristic of this combination is that at the lower storeys the wall retains the frame while at the upper floors the frame inhibits the large displacements of the wall. As a result, the frame exhibits a small variation in storey shear V between the first and the last floor. Therefore, the moment diagram of the columns is antisymmetric, with small variation from storey to storey. This observation allows the simulation of the dual system with the frame and the wall coupled only at the top of the building (Figure 4.24; Macleod, 1970).

The basic conclusion of the analysis of the dual system is that the function of the wall resembles a beam that is fixed at the bottom and has an elastic support at the top, and therefore the fixed-end moment is sufficiently large but less than the fixed-end moment of a cantilever. These models may be considered realistic if the wall is completely fixed at the ground level through a robust foundation (e.g., mat-foundation, piles with pile cup, and tie beams, etc.). Otherwise, the fixed-end moment of the wall is further reduced without any significant reduction of the shear forces while the moments of the beams coupling the wall increase. The diagrams of Figure (4.25a–d) correspond to 100%, 50% and 25% rotational restraint of the fixed end. The fact that shear wall failures in the past due to strong earthquakes were almost always x-shaped-type-shear failures (x-shaped cracks at the base) and seldom flexural-type-failures (horizontal cracks or crushing of the wall edges at the base) should be attributed to the elastic rotation of the wall foundation.
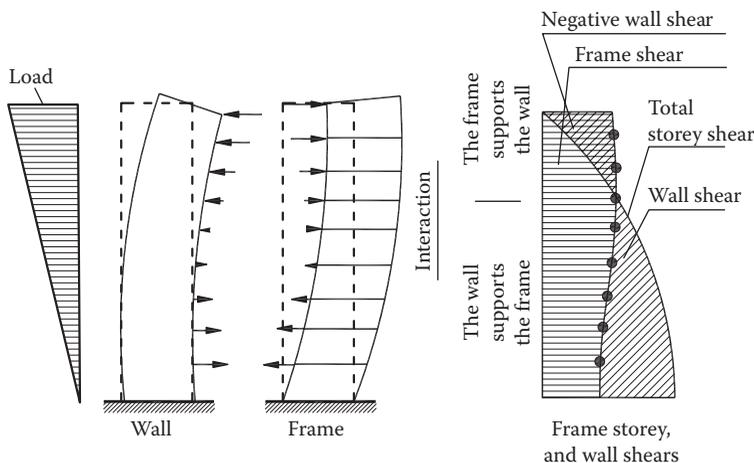
Figure 4.23 Interaction between frame and shear wall in a dual system under lateral loading.
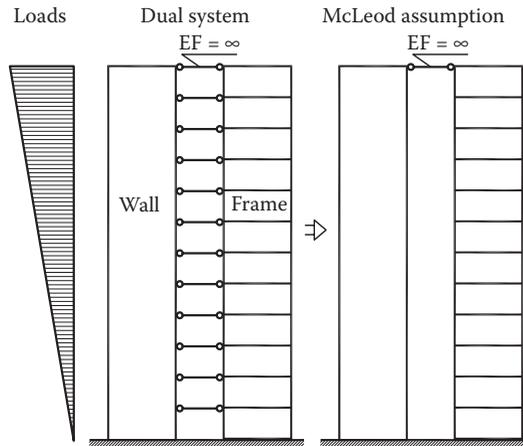
Figure 4.24 Simulation of coupling between frame and shear wall in a dual system with only one coupling bar at the top.

4.5.3 Pseudospatial multistorey structural system

Single-storey pseudospatial systems have been analysed already for static and dynamic excitation in Subsection 2.4.4. Here, the response of a multi-storey pseudospatial system to static lateral loading will be presented, aiming at the integration of the picture of the qualitative response of 3D structural systems in use in seismic design of R/C buildings.

Consider the system of Figure 2.47 (Roussopoulos, 1956; Penelis, 1971). Under the action of lateral forces each floor sustains a relative displacement with respect to the floor below, which can be described by three independent variables, the horizontal relative displacements u_{oj} and v_{oj} of the origin coordinate system and the rotation ω_j of the floor (see Subsection 2.4.4). Thus, the relative displacement of the frame m along the x-axis on the floor j is determined by the relationship:

$$u_{jm} = u_{jo} - \omega_j y_m \tag{4.3}$$

while the relative displacement of a frame n along the y-axis on the same floor by the relationship:

$$u_{jn} = u_{jo} + \omega_j x_n \tag{4.4}$$

The above relationships determine the displacements of the joint n, m of the floor j. In matrix form they can be written as follows:

$$\begin{aligned} \boldsymbol{u}_m &= \mathbf{u}_o - w\, y_m \\ \boldsymbol{v}_n &= \mathbf{v}_o + w\, x_n \end{aligned} \tag{4.5}$$

Next, the lateral stiffness of the plane frames will be defined, taking into account what has been discussed in Subsection 2.4.4. Consider the frame of Figure 4.26, which is loaded
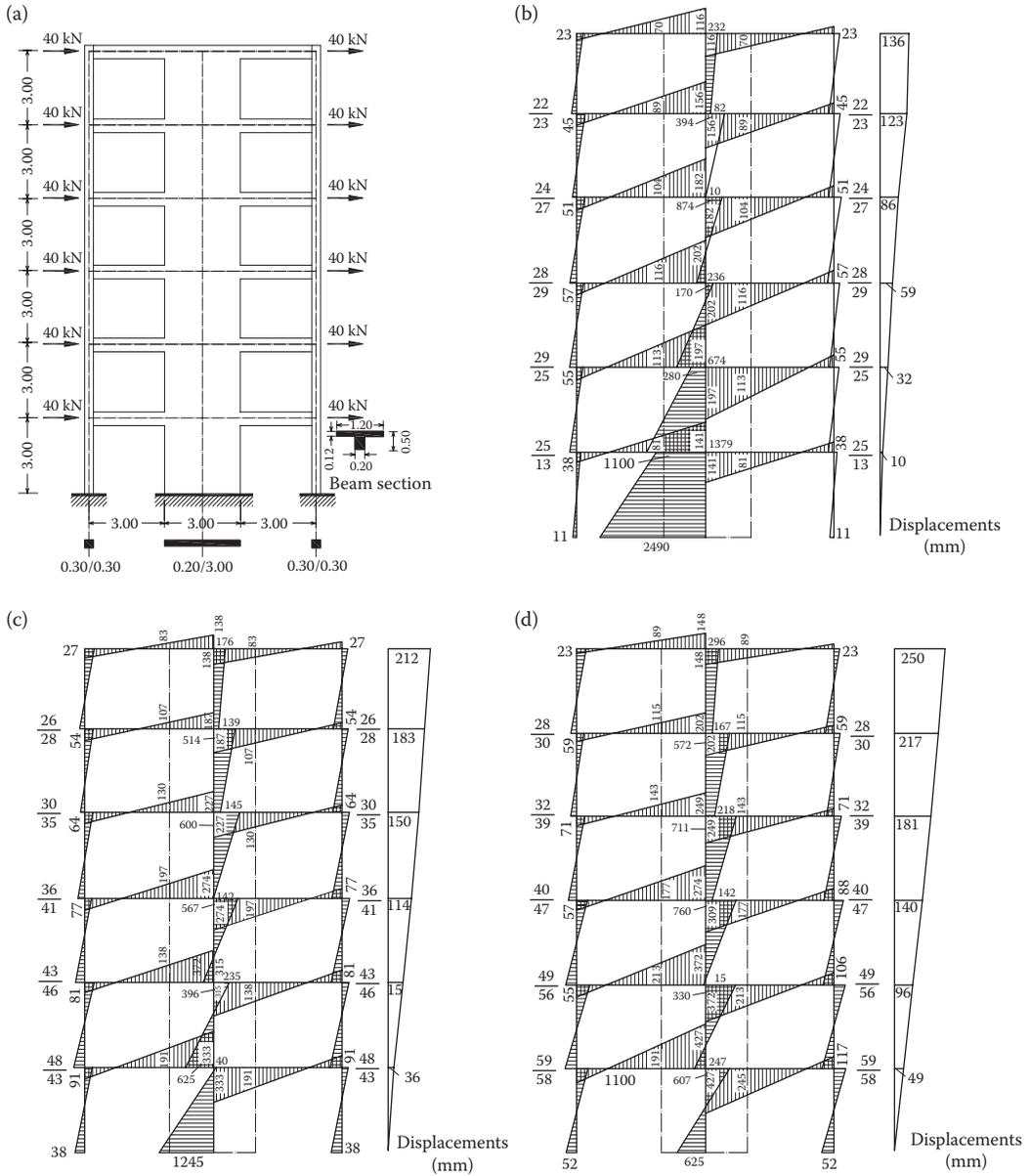
Figure 4.25 Moment diagrams of a dual system under lateral loading for various degrees of wall base restraint. (a) Dual frame–wall structure, (b) wall fully fixed on the ground, (c) wall flexibly supported on the ground (50% fixity) and (d) wall flexibly supported on the ground (25% fixity).

with horizontal forces H_j. *Storey shear V_j* is called the sum of the shears of the columns of storey j, that is:

$$V_j = \sum_{j=j}^{j=i} H_j \qquad (4.6)$$
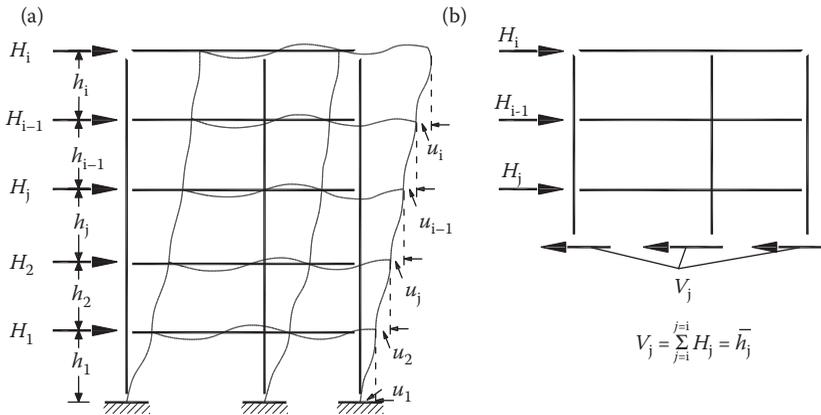
Figure 4.26 Displacement patterns of a plane frame under lateral loading (a) notation; (b) equilibrium of horizontal forces.

If u_1, u_2, ..., u_j, ..., u_i are the relative displacements of the floors due to the action of H_j, then the shear of the storey j is related to the u_j through the relationship:

$$V_j = K_{j1}u_1 + K_{j2}u_2 + \cdots + K_{jj}u_j + \cdots + K_{ji}u_i \tag{4.7}$$

or in matrix form:

$$V = K \cdot u \tag{4.8}$$

The above relationship, for $u_{oj} = 1$ and $u_1 = u_2 = \cdots = u_{j-1} = u_{j+1} = u_i = 0$ (Figure 4.27) results in:

$$V_1 = K_{1j}, \quad V_2 = K_{2j}, ... V_i = K_{ij} \tag{4.9}$$

which means that the elements of the matrix K can be considered as the storey shears for a unit relative displacement of the storey. In the case of rigid girders and $s \neq i$, K_{sj} are zero, and the matrix K becomes diagonal.

From the equilibrium conditions of the shear forces of each storey toward the lateral forces that act on the floor under consideration, $3i$ equations with $3i$ unknowns derive, from which the relative displacements u, v and ω of the floors can be determined.

Indeed, for every storey three equilibrium conditions are set forth, that is:

$$\left.\begin{aligned}
\sum V_{mj} &= \sum H_{xj} = \bar{h}_{xj} \\
\sum V_{nj} &= \sum H_{yj} = \bar{h}_{yj} \\
\sum V_{nj}x_n - \sum V_{mj}y_m &= \bar{h}_{yj}x_G - \bar{h}_{xj}y_G
\end{aligned}\right\} \tag{4.10}$$

$$V_{1,j} = K_{1,j} = \sum_{1}^{i} H_{i,j}$$
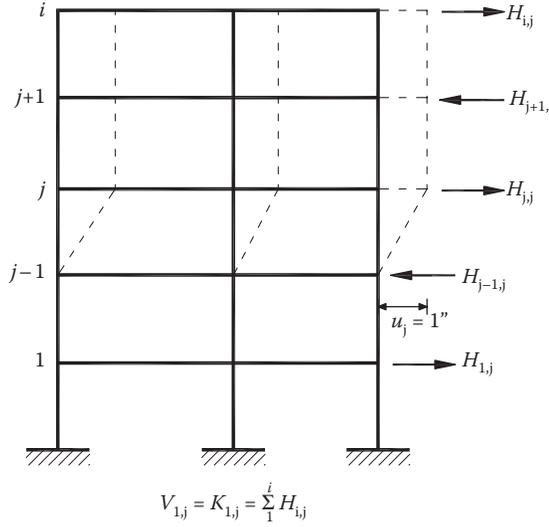
Figure 4.27 Structural interpretation of the elements of matrix *K*.

where x_G and y_G are the coordinates of the centre of mass, or in matrix form:

$$\left.\begin{array}{l} \sum V_m = \bar{\mathbf{h}}_x \\[2mm] \sum V_n = \bar{\mathbf{h}}_y \\[2mm] \sum V_n x_n - \sum V_m y_m = \bar{\mathbf{h}}_y x_G - \bar{\mathbf{h}}_x y_G \end{array}\right\} \tag{4.11}$$

Substituting Equations 4.5 and 4.8 into Equation 4.11 we obtain:

$$\left.\begin{array}{l} \left(\sum K_m\right)\mathbf{u}_o + 0 \qquad\quad - \left(\sum K_m y_m\right)\mathbf{w} \qquad\qquad = \bar{\mathbf{h}}_x \\[2mm] \qquad 0 + \left(\sum K_n\right)\mathbf{v}_o \quad + \left(\sum K_n x_n\right)\mathbf{w} \qquad\qquad = \bar{\mathbf{h}}_y \\[2mm] -\left(\sum K_m y_m\right)\mathbf{u}_o + \left(\sum K_n y_n\right)\mathbf{v}_o + \left(\sum K_n x_n^2 + \sum K_m y_m^2\right)\mathbf{w} = \bar{\mathbf{h}}_y x_G - \bar{\mathbf{h}}_x y_G \end{array}\right\} \tag{4.12}$$

These equations allow the calculation of the relative displacements and rotation of the floors in their plane, and consequently the load effects of the horizontal forces on the system. From the above presentation it is obvious that for an efficient treatment of a pseudospatial system, even with the simplifications mentioned above under horizontal loadings, strong computational aid is needed.

If the origin of the coordinate system at every floor is replaced by a new point (see Subsection 2.4.4) such that the following relationships are fulfilled:

$$\sum_m K_m y_m = 0, \quad \sum_n K_n x_n = 0 \tag{4.13}$$

then Equations 4.12 take the following form:

$$
\left.\begin{aligned}
\left(\sum K_m\right)\bar{u}_o &= \bar{h}_x \\
\left(\sum K_n\right)\bar{v}_o &= \bar{h}_y \\
\left(\sum K_n \bar{x}_n^2 + \sum K_m \bar{y}_m^2\right)\bar{\omega} &= h_y \bar{x}_G - h_x \bar{y}_G
\end{aligned}\right\}
\qquad(4.14)
$$

That is, the unknown $\bar{u}_o$, $\bar{v}_o$ $\bar{w}$ and are not coupled anymore.

All coordinates refer to the new systems of coordinates, which are in general *different at each floor*. The coordinates of the origin of these new systems with respect to the original one derive from the following relationships:

$$
x_{cj} = \frac{\sum K_n^j x_n}{\sum K_n^j}, \quad y_{cj} = \frac{\sum K_m^i y_m}{\sum K_m^i}
\qquad(4.15)
$$

Keeping in mind the analysis of one- storey pseudospatial systems (Subsection 2.4.4) it may be concluded that the points with coordinates x_{cj} and y_{cj} with respect to the original system are the *centres of stiffness* of the successive storeys. These points in general *are not located on a vertical axis*. Only in case of a symmetric system with respect to both axes do the centres of stiffness of the successive storeys lie on a vertical axis passing through the centre of symmetry of the system.

In case of pseudospatial systems consisting only of frames or only of walls, the values of V_j in Equations 4.6 may be considered approximately as linear relations of the moments of inertia J_j of the columns or the walls under consideration. Therefore, in this case the centre of stiffness for all storeys may be defined by the relations:

$$
x_c = \frac{\sum J_n^1 x_n}{\sum J_n^1}, \quad y_c = \frac{\sum J_m^1 y_m}{\sum J_m^1}
\qquad(4.16)
$$

applied for the columns or the walls, say, at the ground floor. Thereafter, values of J_{TC}, T_{MT}, r_x, r_y may be defined by the Equations (2.78c, d) and (2.81b), which are valid for one-storey pseudospatial systems.

This simplification *cannot be applied in case of dual systems*, that is, systems of coupled frames and ductile walls (see Subsection 4.5.2) since the response of such a system differs from the response of its constituent elements. In this case, which is the most common in practice, EC8-1/2004 allows the national authorities to adopt documented rules in their national Annex that might provide computational procedures for the determination of a conventional centre of stiffness and of the torsional radius in multi-storey buildings.

In Greece, the Seismic Code in effect from 2000 until recently had adopted the following procedure (EAK 2000) (Figure 4.28):

- Load the successive storeys with a torque proportional to the storey height z:
    $$T_z = G \cdot z$$
    G being the dead load of each storey
- Taking into account Equation 4.14 it may easily be concluded that $\bar{u}_o$ and $\bar{v}_o$ are zero since $\bar{h}_x$ and $\bar{h}_y$ are also zero. Therefore, from the values of the displacements of
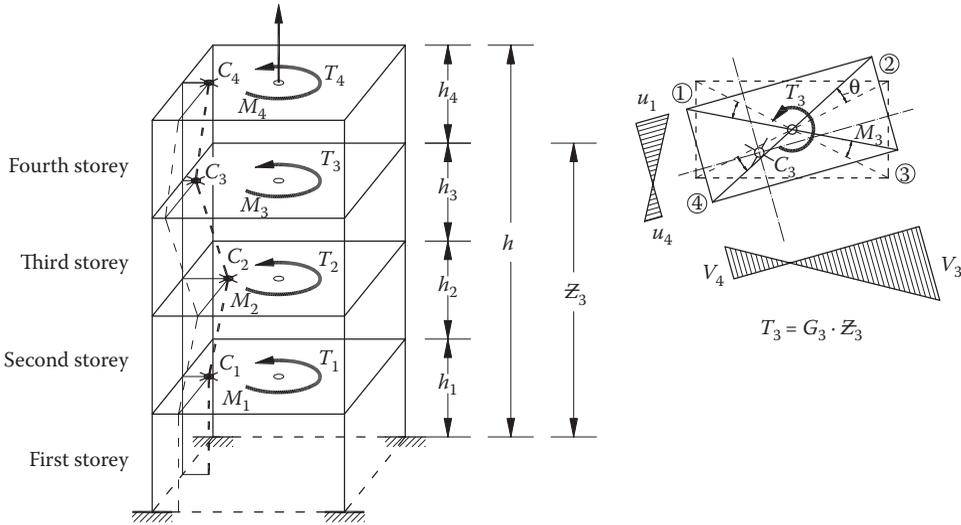
Figure 4.28 Determination of the 'plasmatic' axial of centre of stiffness *C*.

two counter pairs of columns on the perimeter of the system at each storey, the position of the centre of stiffness can be determined geometrically, that is, the values x_{cj} and y_{cj} can be determined. From all these successive centres of stiffness *only one is considered as the conventional centre of stiffness,* that is, the centre of stiffness of a storey which is nearest at a level $\cong 0.80\ h$ where h is the total height of the building. It has been proven (Anastasiadis, 1997; Makarios, 1997) that if the centres of stiffness of the successive storeys are considered as lying on a vertical axis passing through this point called *the 'plasmatic axis of centres of stiffness'*, then the sum of the squares $\Sigma_j \omega_j^2$ of the twists of the successive floors for horizontal loads

$$H = G \cdot z$$

passing through the centre of stiffness of each storey, is minimum (least-squares method).

In parallel the torsional deformation $\omega_{0.8H}$ at height 0.8 h is determined by the relations:

$$\omega_{0.8\,H} = \frac{u_1 - u_2}{l_y} = \frac{v_3 - v_4}{l_x} \tag{4.17}$$

where u and v are the displacements of two counter pairs of columns at the perimeter of the storey near 0.80 h.

J_{TC} results from the relation:

$$J_{TC} = \frac{\sum_{j=1}^{j=i} T_{jz}}{\omega_{0.8\,H}} \tag{4.18}$$

where

$\sum_{j=1}^{j=i} T_{jz}$: the sum of the torques from storey 1 to storey *i* (last storey)

- Load the system with a pattern of horizontal forces in *x-x* and *y-y* directions successively. This pattern must have the form:

$$H_{jx} = G \cdot z_j, \quad H_{jy} = G \cdot z_j \qquad (4.19)$$

and it must pass through the centres of stiffness lying on the 'plasmatic axis of centres of rigidity'. The system will exhibit translational – or almost translational displacements in the *x-x* and *y-y* direction with $u_{c,0.80H}$ and $v_{c,0.80H}$ resulting from the analysis at storey with level near to 0.8H. The stiffness of the system in the *x-x* and *y-y* direction results from by the following equations:

$$\left.\begin{array}{l} K_x = \dfrac{\sum\limits_{j=1}^{j=i} H_{jx}}{u_{c,0.8H}} \\[4mm] K_y = \dfrac{\sum\limits_{j=1}^{j=i} H_{jy}}{v_{c,0.8H}} \end{array}\right\} \qquad (4.20)$$

Therefore, by combining Equations 4.18 and 4.20 the 'plasmatic' values of r_x, r_y and J_{MT} may be easily determined.

In the case of a unisymmetric system (for example along the *x*-axis) both in geometry and loading, the stiffness centres are on the symmetry plane along which the loading $\bar{\mathbf{h}}_x$ also acts. Consequently, Equations 4.14 take the form:

$$\left.\begin{array}{l} \left(\sum K_m\right)\bar{u}_o = \bar{h}_x \\[2mm] \left(\sum K_n\right)\bar{v}_o = 0 \\[2mm] \omega\left[\sum K_n \bar{x}_n^{-2} + \sum K_m \bar{y}_m^{-2}\right] = 0 \end{array}\right\} \qquad (4.21)$$

That is, v_o and ω are equal to zero and the system is subjected to a translational displacement u_o only, so the problem is simplified into a plane one. (Figure 4.29, see Subsection 2.4.4).

In case that the system is symmetric in both its main directions, the axis of centres of stiffness coincides with the axis of symmetry. Therefore, for loading in each of these two main directions passing through the centre of symmetry, uncoupled translational patterns of displacements appear in *x-x* and *y-y* directions. So, the system may be replaced by two plane systems in the *x-x* and *y-y* directions.

4.6 STRUCTURAL CONFIGURATION OF MULTI-STOREY R/C BUILDINGS

4.6.1 General

The architectural form and the internal 'anatomy' of a building are governed by parameters of *'aesthetics'* and *'functioning'*. These parameters constitute for the owner the main criteria for his choice of the architectural design for his project, and therefore even of the team of designers to whom he will award the next steps of the project. Therefore, the structural system of the building must comply with the basic options for the above two parameters, and for this reason cooperation of the structural and MEP engineer with the architect of the project must be established from the early stages of design.
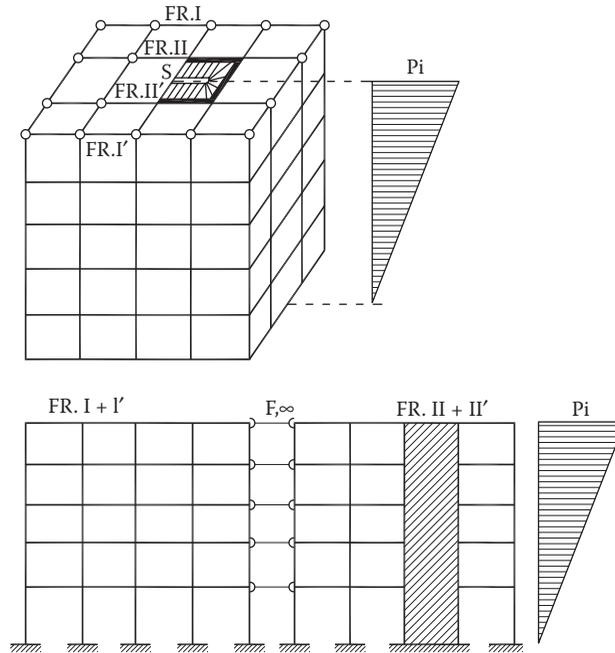
Figure 4.29 Analysis of a symmetric system.

In this way, after mutual compromises the requirements for:

- The structural system
- The air conditioning
- The elevators for persons and goods
- The MEP storeys.

will be incorporated in the final proposal for the project. Buildings may be classified into the following main categories:

1. *Multi-storey buildings*

   In this category the following types of buildings may be included:

   Residential buildings, Office buildings, Malls, Parking garages, Hotels, etc.

   The majority of these buildings are constructed in the centre of cities and are subjected to numerous consequences because of their vicinity to existing buildings with foundations at various levels.

   The basic characteristics of these buildings may be summarised as follows:

   a. They usually have small (4.00–5.00 m) or medium size (7.00–8.00 m) spans and a high number of storeys.

   b. They have high gravity loads per plan unit at the foundation level due to the successive storeys.

   c. The centre of their mass is higher as the number of storeys increases.

       The above three characteristics have a series of consequences for multi-storey buildings, that is:

   d. They present serious foundation problems due to the successive storeys and to their closeness to existing buildings in the case that the existing buildings have foundations at shallower level than the new ones.

e. They need large column cross sections, particularly at the lower storeys. Therefore, a significant percentage of useful space on the ground floor and in basements is lost. For this reason, in the last few years, high-quality concrete, up to C90, has been used in Europe for high-rise buildings.

f. The seismic horizontal loads are very high due to the large mass of the building. At the same time, the result of these forces is applied at a considerable height (at about two-thirds of the height of the building). Therefore, under this loading, the columns and the structural walls develop at their base high bending moments, shear forces, and antisymmetric axial forces (tension-compression), and therefore they are exposed to a high risk of overturning.

g. For buildings with increased number of storeys, the 'damage limitation state' from seismic action becomes critical for either the form of the structural system or its dimensioning.

2. *Buildings developed horizontally*

In this category the following types of buildings may be included

a. Industrial buildings, warehouses, malls, etc.

These buildings are usually one-storey buildings with considerable storey height. Therefore, their gravity load per unit plan is limited. They usually have large spans (20.00-80.00 m) and are arranged in modular form. The above two characteristics have the following consequences for their structural behaviour:

b. Basically, the critical load combination is that of gravity loads. In the analysis and design of these buildings the main concern is focused on girders (R/C or P/C beams, arches, shells, folded plates etc.) under gravity loads.

c. The operational requirements for open plan spaces exclude almost completely the use of structural walls. So, the horizontal seismic forces are resisted usually by bending frames or cantilever columns in both directions.

d. Due to the small masses of the buildings and their low position in relation to the base of the building the seismic action is not a critical issue for the design options. Many times it is *less important than wind loading*.

3. *Buildings for special use*

In this category the following types of buildings may be included:

a. Stadiums, cultural centres, silos, water towers, water tanks, museums, etc.

Each of the above types of buildings exhibits special problems related to its basic function. Therefore, it is evident that the characteristics of the above buildings cannot be classified easily into categories. Each of them is confronted by the structural engineer who is responsible for the design as a special case for which he mobilises his knowledge, his experience, and mainly his talent.

From what has been presented so far it emerges that the most critical category for seismic design is that of multi-storey buildings, both in the stage of preliminary design and in the stage of the final design. Therefore, our interest will next be focused on the multi-storey building.

4.6.2 Historical overview of the development of R/C multi-storey buildings

Since its early steps in history, mankind has tried to express its magnificence by building mega-structures in height and extent (e.g., the Pyramids, the Tower of Babel, Hagia Sofia, Gothic cathedrals, etc.). The main materials that were used for centuries in the past were masonry and timber. These materials did not allow the design and construction of high-rise

buildings with many storeys. At the same time, the operation of these buildings without the existence of elevators was out of the question for residential use.

The industrialisation of the nineteenth century and the subsequent explosion of the population of big cities have led to the extension of the cities upward. Steel, the main new industrial material of that period exhibiting high strength and ductility, has constituted the basic material for the structural system of multi-storey buildings and has dominated up to our days. In parallel, the development of elevators operated by electric power solved the problem of vertical transportation of humans and goods. Some buildings of the past with steel structural systems are mentioned below as examples. (Findel, 1974; König and Liphardt, 1990).

- Home Insurance Building in Chicago, 1883. A 10-storey steel skeleton building
- Woolworth building in Manhattan, 1913. A 60-storeystorey steel skeleton building
- Chrysler Building in New York, 1920-1930. A 72-storeystorey steel skeleton building
- The Empire State Building, New York, 1929. A 102-storeystorey steel skeleton building

In many skyscrapers of this period the foundations and the floor slabs were constructed with concrete (composite structures).

After World War I (1918), *multi-storey R/C buildings* from 10 to 12 storeys began to appear sporadically. The structural type in use was an imitation of the steel skeleton system, that is, the traditional beam column frame system combined with R/C slabs, providing in this way a robust structure with diaphragmatic action at the level of the storeys (Figure 4.1a).

In the early 1950 s the introduction of *shear wall type of construction* extended the use of the R/C structural system to buildings of up to 30 storeys (Figure 4.1b).

In the same period the combination of flat slab frames with shear wall structural systems, due to the low cost of construction and to the flexibility of decks without beams in passing E/M ducts, helped to spread the use of this R/C structural system to a large number of residential and office buildings of up to 20 storeys (Figures 4.11 and 4.12).

The development of the *frame tube* structural system in the 1960s, that is, a perforated tube in the form of a moment-resisting frame at the perimeter of the building with closely
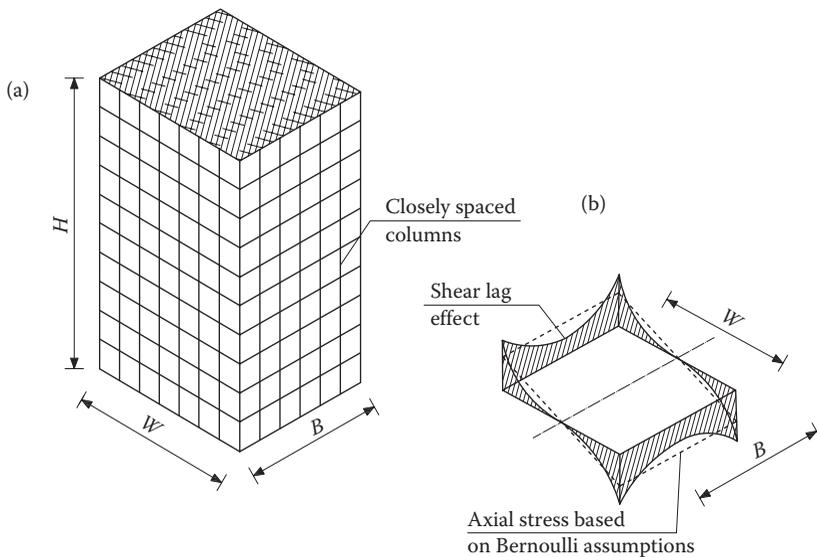
Figure 4.30 Framed system: (a) perspective view; (b) stress distribution under lateral loads. (Adapted from Elnashai, A.S. and Di Sarno, L. 2008. *Fundamentals of Earthquake Engineering*, Wiley, West Sussex, UK.)
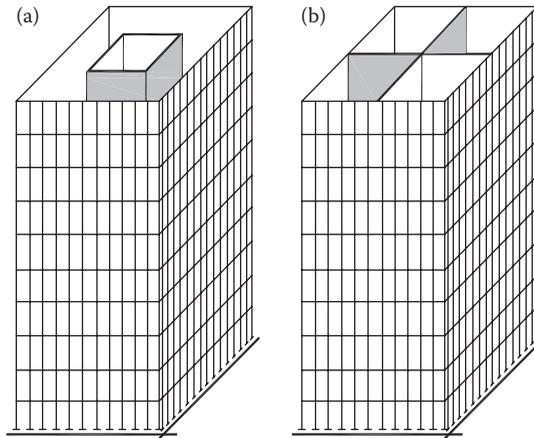
Figure 4.31 Dual system (a) Tube-in-tube system; (b) external tube combined with shear walls. (From König, G. and Liphardt, S. 1990. *Hochhäuser aus Stahlbeton*, Beton Kalender, Teil II, 457–539. Copyright Wiley-VCH Verlag GmbH & Co. KGaA. Reproduced with permission.)

spaced columns, allowed the extension of R/C buildings up to 40 to 50 storeys (e.g., the 30-storey CBS building in New York, 1965; Figure 4.30).

The development of the *tube-in-tube system,* that is, internal large cores of shear walls used as service shafts (staircases-lifts-air ducts) in combination with an external framed tube-type structure, increased resistance and stiffness and allowed the development of high-rise concrete buildings of up to 162 floors (Burj Dubai, 818 m high, 2009; Taranath, 2010; Figures 4.31 and 4.32).

The tube type and the tube-in-tube type structural systems fitted absolutely with the architectural style of the 1960s that *Mies van der Rohe* had imposed, that is, high-rise buildings of prismatic form with an orthogonal, hexagonal, or multicell plan (Figure 4.33). It can be said that these systems were the outcome of the close cooperation of architecture with structural engineering for confronting the aesthetic, operational, and resistance problems of high-rise buildings.

Contemporary post-modern architecture after the Mies van der Rohe period has transformed the prismatic form of high-rise buildings into more plastic shapes. As the building is extended upward its plan is transformed. Therefore, the tube-type structural systems can no longer fit post-modern plastic architectural forms. So, the external tube has been replaced by 'mega columns.' In Figure 4.34 the structural systems in use for R/C buildings

Section   Floor plan
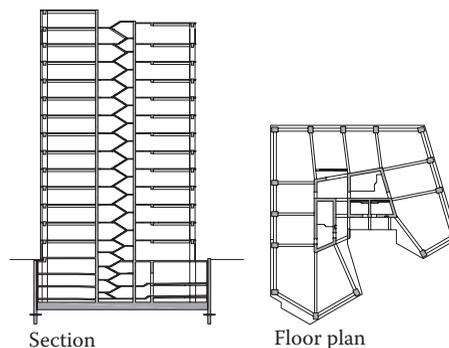
Figure 4.32 Olympia tower, Bucharest, Romania; tube-in-tube system.

Flat slab $d = 20$ cm
with drop panels
at the columns
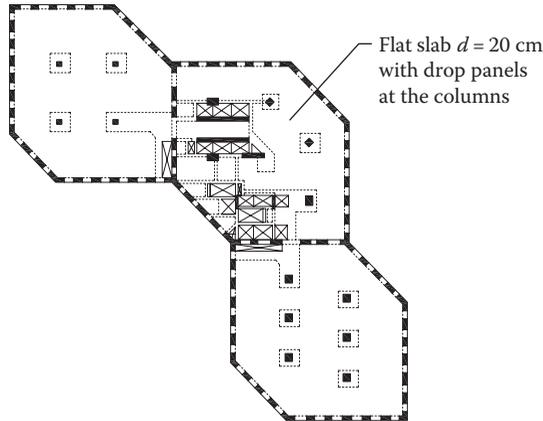
Figure 4.33 One Magnificent Mile; tube system with flat slabs and a hexagonal multicell floor plan. (From König, G. and Liphardt, S. 1990. *Hochhäuser aus Stahlbeton*, Beton Kalender, Teil II, 457–539. Copyright Wiley-VCH Verlag GmbH & Co. KGaA. Reproduced with permission.)

with various numbers of storeys are depicted, while in Figure 4.35 the aspect of several of the world's tallest buildings is displayed.

The development of reinforced concrete multi-storey building construction must be attributed mainly to the development of:

- High-strength materials
- New design concepts
- New structural systems
- New construction methods

No.	System	Number of Stories	Ultra-tall Buildings
		0 10 20 30 40 50 60 70 80 90 100 110	120–200 stories
1.	Flat slab and columns		
2.	Flat slab and shear walls		
3.	Flat slab, shear walls and columns		
4.	Coupled shear walls and beams		
5.	Rigid frame		
6.	Widely spaced perimeter tube		
7.	Rigid frame with haunch girders		
8.	Core supported structures		
9.	Shear wall frame		
10.	Shear wall haunch girder frame		
11.	Closely spaced perimeter tube		
12.	Perimeter tube and interior core walls		
13.	Exterior diagonal tube		
14.	Modular tubes and spine wall systems with outrigger and belt walls		

Figure 4.34 Structural system categories. (Adapted from Taranath, B.S. 2010. *Reinforced Concrete Design of Tall Buildings*, CRC Press (Taylor & Francis Group).)
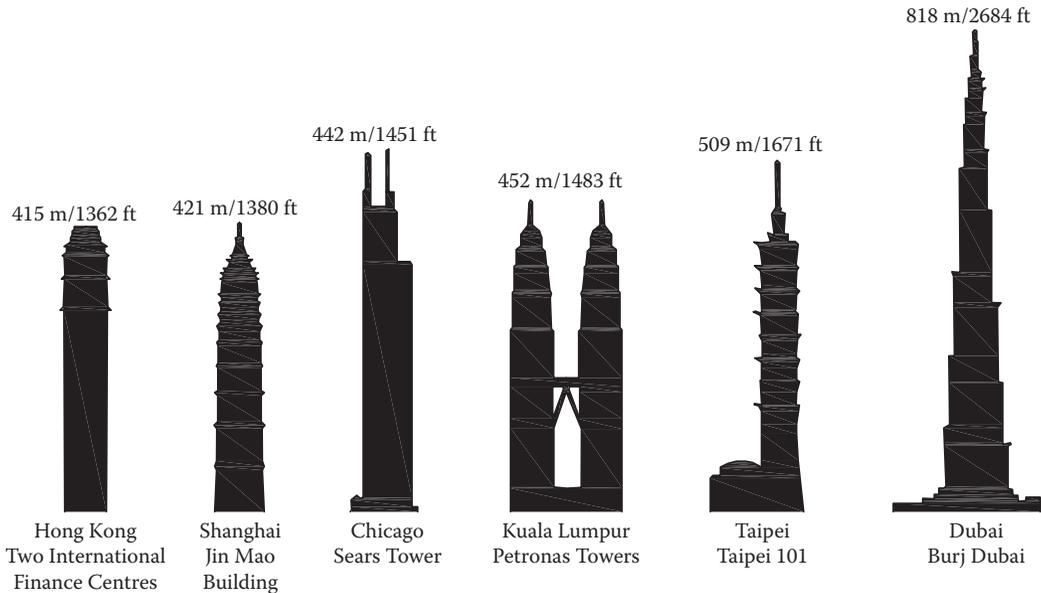
Figure 4.35 Comparative heights of some of the world's tallest buildings. (Adapted from Taranath, B.S. 2010. *Reinforced Concrete Design of Tall buildings*, CRC Press (Taylor & Francis Group).)

4.6.3 Structural system and its main characteristics

4.6.3.1 General

The main structural systems in use in multi-storey buildings may be summarised as follows:

- Moment resisting frames
- Shear wall systems
- Frame-wall or dual systems
- Flat slabs combined with shear walls and frames
- Tube systems
- Tube-in-tube systems
- Core-mega column systems

The above systems are covered completely by EC8-1/2004.

In the following paragraphs a short overview of these systems and their structural characteristics will be made.

4.6.3.2 Buildings with moment-resisting frames

1. These systems consist of plane frames arranged in two orthogonal directions on a modular shaped plan (Figure 4.1a). The spans usually range between 4.00 and 8.00 m. Span-to-storey height ratio usually ranges between 1.50 and 2.50. Due to the gravity loads, larger spans result in greater beam depths, and therefore in limited free storey height.
2. The system presents high redundancy, regularity, adequate torsional rigidity, and structural ability to resist horizontal forces in any direction.
3. The values of moment, shear, and axial force diagrams increase gradually from the top storeys to the fixed base (Figure 4.20). As a result, the demands for the cross-sections of columns and beams increase at the lower storeys as the number of storeys increases.

4. The displacement at the top of the system results from the bending deformation of the beams, with the bending deformation of the columns both constituting the shear racking of the rectangles formed by the beams and columns and the axial deformation of the columns (see Figures 4.19 and 4.20). Thus, the total displacement of a moment-resisting frame comprises:
   a. Cantilever behaviour of the building (column axial forces): 15% to 20%.
   b. Frame shear type displacement (shear racking) due to bending of beams: 50% to 60%.
   c. Frame shear type displacement (shear racking) due to bending of columns: 20% to 30%.
5. Due to the low stiffness of moment-resisting frame systems, they present high inter-story drifts. Therefore, after a number of storeys the building design is governed by the 'damage limitation state'.
6. The high flexibility described above detunes the system from a short predominant period earthquake, particularly in the case of stiff soil.
7. For reasons discussed in the above item, as well as in item 5, this type of structural system is used in buildings of up to 20 storeys. Generally speaking, an acceptable aspect ratio (height to width) of these buildings must be less than 4.
8. Keeping in mind the M, V and N diagrams of a moment-resisting frame due to seismic action, it can easily be concluded that the critical regions that contribute mainly to seismic force resistance are the joints and a small region of the beams and columns joining there. Therefore, the strength and ductility of these regions are crucial for the seismic behaviour of the system, and special care should be taken for their design and detailing. Even so, if there is a feeling that, due to the absence of skilled craftmanship, the construction of a frame system might be poor, this type of structure should be replaced by others (e.g. dual-system or wall system), because in case of failure, soft storeys are formed, with catastrophic consequences for the building, leading it many times to 'pancake' collapses (Booth and Key, 2006).

4.6.3.3 Buildings with wall systems

1. According to seismic codes in force, the vertical structural members with a ratio of cross-section dimensions greater than 4 are defined as *'walls'*.
2. These members are characterised by their high stiffness in relation to columns with equivalent cross section. For example, the moment of inertia of a wall 0.20×2.5 m compared to that of a column 0.70×0.70 m with the same cross-section area is about 14 times more. Consequently, R/C walls constitute the most effective tool for the radical reduction of interstory drifts and the displacements of the storeys. At the same time, when walls and columns participate together in the resisting system of a building, walls with a total area equal to that of the columns undertake the main part of the base shear due to seismic motion. This justifies their definition as *structural walls* or *shear walls* in various English-speaking countries. As already noted, these walls are characterised as *ductile walls* by EC 8-1/2004.
3. At the same time, shear walls appear to be more effective than columns in undertaking bending moments. In fact, it is known that the bending resistance of an R/C section results approximately from the relation:

$$\boxed{M_u = z f_{yd} A_s \cong 0.90 d f_{yd} A_s}$$ (4.22)

where

z is the lever arm of internal forces.
d is the structural height of a section.
A_s is the area of the reinforcement.
f_{yd} is the design value of the yield strength of steel.

Therefore, given the same reinforcement the ratio of bending resistance from the wall to the column, in the example above, is:

$$\lambda = \frac{2.15}{0.65} \cong 3.30 \tag{4.23}$$

In conclusion, it should be remembered that both walls and columns with equal cross-section area have almost the same shear capacity.

4. In this context, structural walls seem to respond very effectively to horizontal forces as far as strength and displacements are concerned. Of course, at first glance the above spectacularly better behaviour of walls in relation to columns is to a degree superficial, because it should not be forgotten that columns are not independent cantilevers in space, but that they are coupled with beams and slabs in frame structural systems. Columns with beams compose resisting frame systems with reduced bending moments at the columns compared to those of free cantilevers (shear system, see Paragraph 4.5.2.1), due to their counter flexure deformation within the height of each storey. On the other hand, the walls respond like free cantilevers with coupled displacements at the levels of the floors (see Paragraph 4.5.2.2), due to the low out of plane stiffness of the diaphragms. So, the remarkable difference of behaviour between columns and walls observed above is reduced to a degree in conventional structures (Figure 4.36).

5. According to EC8-1/2004, the structural system of a building is characterised as a *'wall system'* in the case that the walls carry at least 65% of the horizontal loading. Since the walls are coupled at the level of the floors in relation to displacements

(a)

$V_{base} = \Sigma H = 21H$

$\Sigma M_{base} \cong 4\,(\Sigma H)\,\dfrac{h}{2} = 42Hh$

(b)

$V_{base} = \Sigma H = 21H$

$\Sigma M_{base} = (\Sigma H)\,\dfrac{2}{3}\,6\,h = 84Hh$
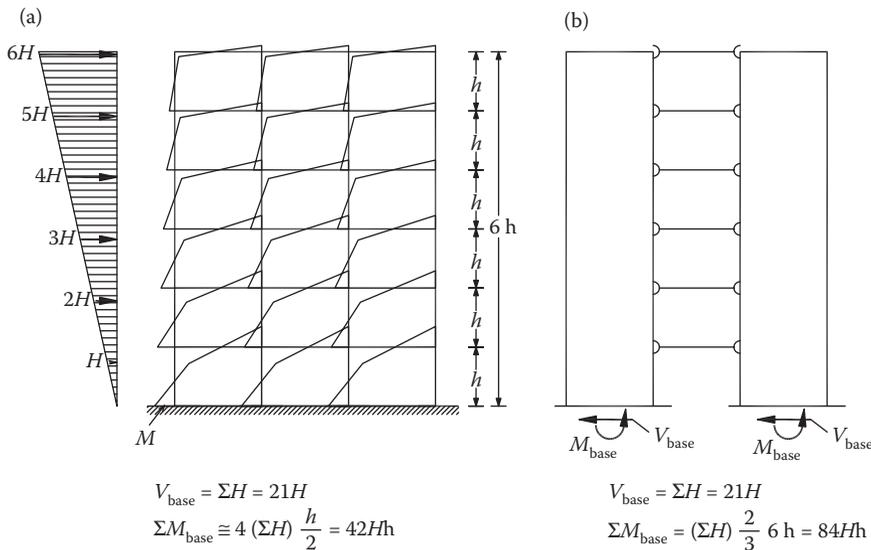
Figure 4.36 Comparison of the response of a frame to the response of a wall system under the same lateral loads: (a) Frame response; (b) wall system response.

only (diaphragmatic action), they respond like cantilevers (see Subsection 4.5.3). As a result, if these structural walls were reinforced adequately so that they failed first to bending and not to shear, this failure would happen at their base, where the bending moment caused by horizontal loading displays its maximum value. At this critical region, if the wall is adequately reinforced, plastic deformations may develop a plastic hinge. Consequently, the energy-dissipating zones in structural walls develop at their bases (Figure 9.14).

6. In the case that the coupling of the shear walls is strong enough with *spandrels,* these systems, according to EC8-1/2004, are classified as *coupled walls,* a fact that has serious consequences for their analysis and design, as will become apparent in the following chapters (see Section 9.3). As was explained in Paragraph 4.5.2.3, Figure 4.22, the bending moments at the base of these walls are reduced significantly due to the development of strong shear forces at their spandrels. At the same time, keeping in mind that the failure of the spandrels under horizontal loading precedes the failure at the base of the walls due to high shear, it may easily be concluded that these systems give an additional first line of defense to seismic action at their spandrels, where the failure precedes that of the plastic hinges at their bases. For this reason, EC8-1/2004 classifies coupled walls in a higher 'behaviour' category than independent walls (see Subsection 5.4.3).

7. In the category of wall systems also belong the systems of *large lightly reinforced walls,* for which a first approach has been made in Section 4.4.

8. Of course, it should be noted that in order for a plastic hinge to develop at the base of a wall before its shear failure, the aspect ratio of the wall must be greater than 2 (see Subsection 9.4.4), that is:

$$\frac{H}{l_w} \geq 2.0 \tag{4.24}$$

In the case that this relation is not fulfilled, as we will see in the next chapter, the 'behaviour factor' of the building, which is related directly to its structural ductility, is reduced drastically, according to EC8-1/2004.

At the same time, in order for shear walls to fulfil their main objective, which is the reinforcement of buildings with high stiffness, according to design practice they must have an aspect ratio not smaller than 7, that is:

$$\boxed{\frac{H}{l_w} \leq 7.0} \tag{4.25}$$

From the above two expressions it may be concluded that a reasonable length l_w of the wall must range between:

$$\boxed{0.15H < l_w \leq 0.50H} \tag{4.26}$$

9. Wall systems are highly suitable for buildings up to *about 20 storeys.* For higher buildings, due to the quasicantilever behaviour of the structural system, the interstorey drifts at the upper storeys of buildings begin to be critical at 'damage limitation state.' Therefore, the wall system must be assisted by moment-resisting frames coupled with the walls, which operate as retaining systems for the upper floors (see Paragraph 4.5.2.4).

10. From what has been discussed so far it can be concluded that the main advantages of wall systems may be summarised as follows:
    a. They provide high strength and stiffness at low cost.
    b. Their structural behaviour to past strong earthquakes has proven to be excellent. The creation of plastic hinges only at the base of the walls does not allow the formation of an inverted pendulum system as happens in frames, and therefore excludes collapses of the pancake type that can flatten frames.
    c. The constructability of the walls is much better than that of frames where quality control might be easily lost at hundreds of joints, which are the critical regions of frames.
    d. They provide a very effective system for limited storey drifts in case of frequent small- or medium-sized earthquakes, and in this way they protect the non-structural elements, that have a value much higher than that of the structural system.
11. At the same time, some disadvantages must be noted:
    a. The redundancy of the system is lower than that of a framed one.
    b. The walls present large moments at their base, which usually cause an uplift of independent footings even if the wall carries high axial loading. Therefore, their foundation must be well connected with the foundation of the rest of the structural elements, preferably in a box foundation system (Figures 4.16 and 10.4).
    c. Walls are, in general, undesirable elements in architectural design, since they put obstacles in the way of free communication from space to space at the floor level of the building.

4.6.3.4 Buildings with dual systems

1. In Paragraphs 4.6.3.2 and 4.6.3.3 above the characteristics of moment-resisting frame systems and of structural walls have been presented in detail. From the analysis so far, it can be concluded that the coupling of shear walls with frame systems can provide the building with the advantages of both and diminish their disadvantages. This combination of structural walls with moment-resisting frames is defined as a *dual system*.
2. In these systems, structural walls are usually arranged at the centre of the building around staircases, lifts, air ducts, etc., in the form of a core, while the frames are arranged at the perimeter of the building. So, a tube-in-tube system is generated. Not seldom, when the core is eccentric to the centre of mass of the building in plan, additional walls are arranged at the perimeter of the buildings so that the stiffness of the core is balanced. Many times beams are arranged connecting the cores with the perimeter columns. Such an arrangement enhances the bearing capacity of slabs for the gravity loads and in parallel increases the stiffness of the system by carrying a remarkable percentage of the overturning moment at the base of the building in the form of a pair of controversial axial forces acting at the columns of the perimeter. So, the displacements of the storeys due to seismic action diminish (Figure 4.25b). However, it should be noted that the clear height of the storeys below the beam becomes shorter. Sometimes, in tube-in-tube buildings with more than 50 storeys, outrigger beams are arranged at some storeys, aiming at the diminishing of storey displacements, particularly in the 'damage limitation state'. This system (tube-in-tube with outriggers or tube-in-tube with outriggers and mega columns) constitutes the predominant one for buildings with a very great number of storeys (more than 100 Figure 4.37).
3. In these systems, as has been explained in Paragraph 4.5.2.4, walls retain the frames at the lower storeys, while at the upper floors, the frames inhibit the large displacements and large interstorey drifts of the walls.
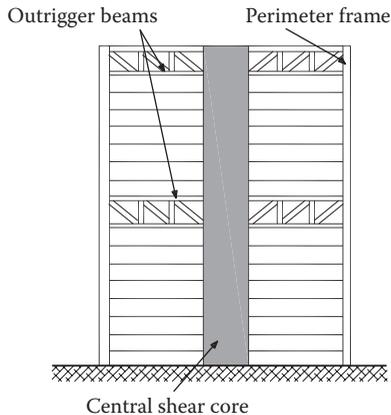
Figure 4.37 Outriggers in a shear core combined with perimeter frame (tube). (Adapted from Booth, E. and Key, D. 2006. *Earthquake Design Practice for Buildings*, Thomas Telford Ltd.)

4. The above response has the following consequences:
    a. For small intermediate and frequent earthquakes, the building exhibits limited interstorey drifts, and consequently the damage limitation state is easily accomplished, even in very high buildings.
    b. In case of a strong earthquake, the first line of defense appears at the base of the walls in the form of plastic hinges, which begin to dissipate energy before the yield of the frames at their joints. Therefore, the risk for generation of a soft storey and for a pancake collapse is drastically diminished.
    c. The moment-resisting frames constitute a second line of defense for a building, which is activated after the generation of the plastic hinges at the base of the walls. In this phase, the building has lost a part of its stiffness due to the plastic hinges of the walls and therefore is detuned with a subsequent diminishing of the inertial horizontal forces. ASCE 7-05 required that the moment-resisting frames in dual systems should have a resisting capacity at least equal to 25% of the base shear of the system. EC8-1/2004 does not impose such an obligation. Instead, in the case that the frame resistance is higher than 35% of the base shear, the Code upgrades the behaviour factor of the system, that is, EC8-1/2004 gives incentives instead of imposing mandatory requirements.
5. The combination of moment-resisting frames with shear walls provides the building with a structural system of high redundancy.
6. In the case of outrigger beams, a special concern is necessary to exclude brittle failure of external columns due to axial overloading. In this context the outriggers should be designed as ductile members that fail prior to column failure.

4.6.3.5 *Buildings with flat slab frames, shear walls and moment-resisting frames*

1. These systems constitute a very common and attractive type of structural system for multi-storey buildings of up to 10 storeys. The structural system consists of flat two-way slabs on columns with or without column capitals, shear walls at the core and/or at the perimeter of the building, and moment-resisting frames at the perimeter.

2. In this system, according to EC8-1/2004, the flat slab frames consisting of columns and slab strips in both directions are not considered suitable for earthquake loading, due to the low ductility of the column-slab joints. So, the flat slab frames in such a system should be considered as a secondary structural system, proper only for gravity loads (see Subsection 4.2.6, Figure 4.11, Figure 4.12).
3. These systems are very attractive in construction due to:
   a. The simple and low-cost formwork
   b. The larger clear storey height
   c. The free passage for the E/M installations

4.6.3.6 Buildings with tube systems

1. In Paragraph 4.6.3.2 it was already made very clear that in the case of high-rise buildings, the beams of the bending resisting frame systems need to be deep enough so that the beams at the lower storeys are in position to carry moments and shears due to an earthquake. However, if the internal columns are omitted or if a flat slab system is arranged in the tube, then the columns of the frames at the perimeter of the building may be arranged as closely as necessary, while the beams could take the form of deep spandrels. In this respect, the tube at the perimeter can be a stiff-framed system capable of carrying the lateral seismic loading.
2. In practice, these systems are used in buildings of up to 50 to 55 storeys.
3. The columns are spaced close enough (1.50–3.0 m), while spandrels have a depth of about 0.60 m.
4. It is important to note that this structural system has the behaviour of a perforated tube in response to horizontal actions. When the holes are circular, small, and limited in number, it behaves like a closed tube and, if the Bernoulli concept holds (aspect ratio H/l greater than 2), the bending moment at the base is carried by normal forces with almost linear distribution. If the number of holes increases and they take rectangular form, a large part of the horizontal forces is transferred to the base by the shear behaviour of the frames parallel to the load direction, that is, through 'shear lag effect' (Elnashai and Di Sarno, 2008; Figure 4.30).
5. Many times the tubes are hexagonal or multicell (Figure 4.33).
6. When the above-described system is combined with a core in its centre, it is transformed to a tube-in-tube system proper for very high-rise buildings (over 100 storeys), especially if it is combined with outrigger beams every number of storeys. From the structural point of view, as we have seen before, this system is also characterised as a dual system.

Analysis of the structural system

5.1 GENERAL

For the analysis of a structural system for seismic actions, a set of properties of the system must be taken into account in advance, since according to EC8-1/2004 these properties influence:

- Design actions
- Structural model
- Method of analysis
- Capacity design of columns

These properties are:

- The structural regularity of the building
- Its torsional flexibility
- The ductility level of the structure

Most modern Codes for the above properties specify quantitative criteria with which the analysis must comply. The above issues will be examined in detail in the subsequent sections.

5.2 STRUCTURAL REGULARITY

5.2.1 Introduction

For many years up to 1988, the regularity of the building was a qualitative parameter that had to be taken into account in the preliminary structural design and was given as a recommendation of the Code. Since then, for the purpose of design, building structures in all modern Codes are separated into two categories:

- Regular buildings
- Non-regular buildings

This distinction has implications for the structural model, the method of analysis, and the value of the behaviour factor q, which is decreased for buildings that are non-regular in elevation. More particularly, according to EC8-1/2004:

- The structural model can be either a simplified plane or a spatial one
- The method of analysis can be either a simplified lateral force or a modal analysis

Table 5.1 Consequences of structural regularity on seismic analysis

Regularity		Allowed simplification		Behaviour factor
Plan	Elevation	Model	Linear-elastic analysis	For linear analysis
Yes	Yes	Planar	Lateral force	Reference value
Yes	No	Planar	Modal	Decreased value
No	Yes	Spatial	Lateral force	Reference value
No	No	Spatial	Modal	Decreased value

- The reference value of the behaviour factor q_o given in Table 5.2 is decreased for build-ings that are non-regular in elevation. Table 5.1 describes the implications for struc-tural regularity on the design according to EC8-1/2004.

5.2.2 Criteria for regularity in plan

Buildings regular in plan must fulfill all the following requirements:

- The structural system of the building with respect to lateral stiffness and mass distri-bution must be approximately symmetric in plan in two orthogonal directions. It is obvious that in this case the *centre of stiffness* is very near to the *centre of mass*.
- The plan configuration must be compact, with re-entrant corners not affecting the area of the convex envelope of the floor more than 5% (Figure 5.1).
- The floor must provide an efficient diaphragmatic action effect, that is, large in-plane stiffness compared to the stiffness of the vertical members.
- The slenderness

$$\lambda = L_{max}/L_{min}$$

of the building in plan must not be higher than 4, where L_{max} and L_{min} are the orthogo-nal dimensions in plan of the building.

At each level and for each direction x and y, the structural eccentricity e_m and the tor-sional radius r_c must be in accordance with the two conditions below:

$$(A_1) = \frac{\alpha.b}{2} \leq 0.05 \; lx \; ly$$
$$\leq 0.05 \; A$$

$$0.35 \; lx \geq \alpha$$

$$0.35 \; ly \geq b$$

Area of ABCEFA : A
Area of CDE   : A_1 } regularity condition: $\frac{(A_1)}{(A)} \leq 5\%$
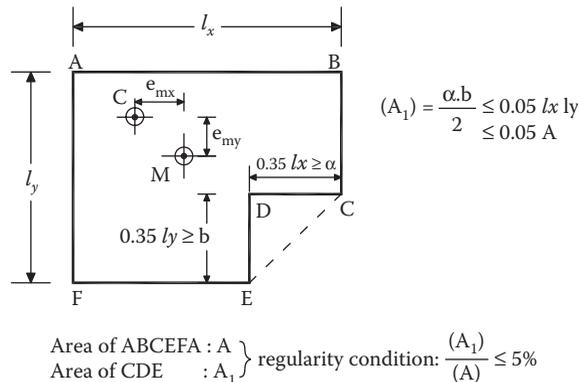
Figure 5.1 Condition of regularity at the re-entrant corner.

$$\boxed{\begin{aligned} e_{mx} &\leq 0.30 r_{xc} \\ e_{my} &\leq 0.30 r_{yc} \end{aligned}}$$

(5.1a)

and

$$\boxed{\begin{aligned} r_{xc} &\geq l_{ms} \\ r_{yc} &\geq l_{ms} \end{aligned}}$$

(5.1b)

where:

e_{mx}/e_{my} is the distance between the *centre of stiffness* C and the *centre of mass* M measured along the *x/y* direction, which is normal to the direction of analysis under consideration (Figure 5.1).

r_{xc}/r_{yc} is the '*torsional radius*' with respect to the centre of stiffness, which is the square root of the ratio of torsional stiffness with respect to the centre of stiffness to the lateral stiffness in the *y/x* direction, respectively.

l_{ms} *the radius of gyration of the floor mass* in plan with respect to the *centre of mass* M.

The definition of the above parameters e_{mx}, e_{my}, r_{cx}, r_{cy}, l_{ms} together with r_{mx} and r_{my} has been given in Subsections 2.4.4 and 4.5.3. At the same time, in the same subsections their structural meaning has been clarified in detail together with various simplifications acceptable to EC8-1/2004 for the calculation of their values. For the sake of convenience, the results of the analysis in the above subsections are also summarised below:

1. In the case of pseudospatial systems consisting only of *frames* or only of *walls*, the centres of stiffness C for all storeys lie approximately on a nearly perpendicular axis passing from a point at the plan of the 1st floor with coordinates with respect to the centre of mass given by Equation 2.86:

$$e_{mx} = \frac{\sum_{j=1}^{j=m} x_j j_{jx}}{\sum_{j=1}^{j=m} j_{jx}}, \quad e_{my} = \frac{\sum_{i=1}^{i=n} y_i j_{iy}}{\sum_{i=1}^{i=n} j_{iy}}$$

2. *Torsional stiffness* with respect to the *centre of stiffness* C is given by Equation 2.87

$$\bar{J}_{TC} = \sum_{j=1}^{j=m} j_{jx} x_{jc}^2 + \sum_{i=1}^{i=m} j_{iy} y_{ic}^2$$

3. *Torsional stiffness* $\bar{J}_{TM}$ with respect to the *centre of mass* M is given by Equation 2.88:

$$\bar{J}_{TM} = \bar{J}_{TC} + e_{mx}^2 \left(\sum_{j=1}^{m} j_{jx} \right) + e_{my}^2 \left(\sum_{i=1}^{n} j_{ix} \right)$$

4. *Torsional radius* with respect to the *centre of stiffness* is given by Equation 2.90

$$r_{xc} = \sqrt{\frac{\bar{J}_{TC}}{\sum_{j=1}^{m} j_{jx}}}$$

5. *Torsional radius* with respect to the *centre of mass* is given by Equation 2.91

$$r_{xm} = \sqrt{\frac{\bar{J}_{TM}}{\sum_{j=1}^{m} j_{jx}}}$$

6. *Radius of gyration* with respect to the *centre of mass* (orthogonal plan) is given by Equation 2.113:

$$l_{sm} = \sqrt{\frac{J_d}{m}} = \sqrt{\frac{b^2 + d^2}{12}}$$

7. In the case of a pseudospatial system consisting of *dual systems*, the methodology of '*plasmatic axis*' of centres of stiffness may be followed (Subsection 4.5.3).

5.2.3 Criteria for regularity in elevation

Buildings regular in elevation must fulfill the following requirements:

- All lateral resisting systems must run without interruption from their foundation to the top of the building.
- In *framed buildings*, the ratio of the actual storey capacity to the demand required by the analysis should not vary disproportionately between adjacent storeys. Special concern must be given to masonry infilled frames (see Paragraph 8.5.3.2).
- Both the lateral stiffness and the mass of the individual storeys must remain constant or diminish gradually from the base to the top of the building.
- Special consideration must be given in the case that setbacks are present.

In the case that any one of the above requirements is not fulfilled, the structural system is considered non-regular in elevation, and therefore the reference values of behaviour factors given in Table 5.2 are decreased to 0.80 of their value.

5.2.4 Conclusions

1. The criteria for regularity in plan are mainly qualitative and can be checked very easily at the beginning of the analytical procedure. Only the last one, the verification of Equations 5.1a and 5.1b, needs complicated calculations. However, acceptance by EC8-1/2004 of simplified procedures for the determination of the parameters included in Equations 5.1a and 5.1b, as was explained in Subsection 5.2.2, makes the whole procedure a little bit easier, and allows the decision making for regularity in plan at the beginning of the analysis.
2. Having in mind that non-regularity in plan does not have any computational implications for the structure except that of not allowing the introduction in the analysis of planar models together with some consequences of secondary importance for behaviour factor q_o (see Section 5.5), and that modern computational means have devalued the Code permit of using planar models and static seismic loadings, it seems that the requirements of Equations 5.1a and 5.1b are no longer of importance for the successive steps of analysis. Indeed, if the structural system is modelled as a pseudospatial system and the modal response spectrum analysis is used, which is the common practice

Table 5.2 Basic values for the determination of *q*-factors

Structural type	K_w	K_R^{el} Yes	No	K_R^{over} Yes	No	QSP Yes	No	q_o DCM	DCH
1 Frame system	1	1	0.8	$\dfrac{a_u}{a_l}$	$\dfrac{1+(a_u/a_l)}{2}$	1.2	1	3.0	4.5
2 Frame-equivalent dual system	1	1	0.8	$\dfrac{a_u}{a_l}$	$\dfrac{1+(a_u/a_l)}{2}$	1.2	1	3.0	4.5
3 Wall-equivalent dual system	$0.5 < (1+a_o)/3 \le 1$	1	0.8	$\dfrac{a_u}{a_l}$	$\dfrac{1+(a_u/a_l)}{2}$	1.2	1	3.0	4.5
4 Coupled wall system	$0.5 < (1+a_o)/3 \le 1$	1	0.8	$\dfrac{a_u}{a_l}$	$\dfrac{1+(a_u/a_l)}{2}$	1.2	1	3.0	4.5
5 Uncoupled wall system	$0.5 < (1+a_o)/3 \le 1$	1	0.8	1	1	1.2	1	3.0	$4.5\left(\dfrac{a_u}{a_l}\right)$ or $\dfrac{1+(a_u/a_l)}{2}$
6 Large lightly reinforced walls	$0.5 < (1+a_o)/3 \le 1$	1	0.8	1	1	1.2	1	3.0	—
7 Torsionally flexible system	$0.5 < (1+a_o)/3 \le 1$	1	0.8	1	1	1.2	1	2.0	3.0
8 Inverted pendulum	1	1	1.0	1	1	1.2	1	1.5	2.0

nowadays, the regularity criteria in plan and elevation become insignificant for the analytical procedure.

3. The only serious consequence for the successive steps of analysis is non-regularity in elevation, which imposes a decrease of the reference factor to 0.8 of its value. The check of regularity in elevation can be carried out very easily, without complicated calculations, at the preliminary stage of design.
4. The above requirement for decrease of the q_o factor has as its main aim a response to increased ductility demands at the level of soft storeys. Indeed, a modal response spectrum elastic analysis does not reveal the local ductility demands in case of a soft storey. The decrease of the value of the q_o factor, together with special measures taken at the areas of soft storey (capacity design, etc.), offer sufficient resistance in the critical areas (e.g. column joints) of the system.

5.3 TORSIONAL FLEXIBILITY

As was explained in Section 4.4, a 'torsionally flexible system' is a structural system where small eccentricities of the seismic horizontal forces cause large rotational deformations to the storey diaphragms and, therefore, excessive drifts at the columns of the perimeter, disproportional to those caused by the relevant translational displacements. This behaviour under special circumstances is amplified in case of dynamic excitation of the system, causing

in many cases uncontrollable storey drifts. The above qualitative approach to the problem will be quantified in the next paragraph.

According to EC8-1/2004, a structural system is torsionally flexible if (see subsection 5.2.2):

$$\boxed{\begin{aligned} r_{xc} &\leq l_{ms} \\ r_{yc} &\leq l_{ms} \end{aligned}} \tag{5.1c}$$

From the analysis of Paragraph 2.4.4.4 it may be concluded (Equation 2.109) that *in the case of a double symmetric system*, the fulfilment of Equation 5.1c means that the three *uncoupled* eigen frequencies of an one-storey pseudospatial system are arranged as follows:

$$\boxed{\omega_{ux}, \omega_{ux} > \omega_{\varphi}} \tag{5.2}$$

that is, the greater eigen frequencies are translational ones and consequently the vibration of the system is dominated by the rotational vibration. In the above relation (5.1c), the right-side term expresses the lever arm of the inertial forces due to an eventual dynamic (seismic) excitation, while the term on the left side r_{xc} or r_{yc} expresses the lever arm of the restoring forces. So, in the case that r_{xc} and r_{yc} are smaller than l_{ms} at every moment, the developing restoring forces are smaller than the inertial ones and the torsional mode prevails.

The above physical interpretation is expressed quantitatively by the fact that the first eigen mode is rotational, and in this respect the greater part of the mass of the system is activated in a rotational motion.

Conversely, if

$$r_{xc} \text{ and } r_{yc} \geq l_{ms} \tag{5.3}$$

the translational excitations in x and y direction are the predominant ones and therefore only limited drifts due to rotational vibration may develop.

In the case of a non-symmetric system, the fulfilment of Equation 5.1c as a criterion for torsional rigidity lies on the safe side. Indeed, from the analysis of Paragraph 2.4.4.4 (Equation 2.122) it may be concluded that in the case of a non-symmetric system Equations 5.1c are transformed to:

$$\boxed{\begin{aligned} r_{xm} &\leq l_{ms} \\ r_{ym} &\leq l_{ms} \end{aligned}} \tag{5.1d}$$

where:

r_{xm} and r_{ym} are given by Equation 2.91:

$$r_{xm} = \sqrt{\frac{\bar{J}_{TM}}{\sum_{j=1}^{m} J_{jx}}}$$

Since $\bar{J}_{TM} > \bar{J}_{TC}$ (see Equations 2.87 and 2.88), it is obvious that in the case that the centre of stiffness does not coincide with the centre of mass, the criterion for flexural flexibility established by Equation 5.1c is on the safe side.

In the case of a system with torsional flexibility, EC8-1/2004 specifies a considerable reduction in the values of the q_o-factors (Table 5.2) ranging from 0.66 to 0.75. At the same time, the structural system is not qualified for any release from joint capacity design, no matter if it is a wall system (more than 65% wall shear capacity) or a wall-equivalent dual system (more than 50% wall shear capacity).

It is important to know the degree of protection offered to structures that abide by the criteria for structural regularity and torsional rigidity of EC8-1/2004, expressed by Equations 5.1b and 5.1c. In this context it is interesting to comment on Figure 5.2 as developed by Cosenza et al. (2000). In this figure the behaviour of various one-storey pseudo-spatial systems designed according to various Codes and re-analysed as inelastic systems under dynamic excitation is presented by markers of various designation. Systems of good and satisfactory inelastic behaviour are designated as white and grey (increase of 10–20% in ductility demands), while systems of poor inelastic behaviour are designated as black (ductility demands greater than 50% compared to their torsionally balanced system). On this plot the requirements for regularity and torsional rigidity of EC8-1/2004 are also plotted, that is, Equations 5.1b and 5.1c. Area ABCD corresponds to the area where the regularity criteria are fulfilled, while area AEFD corresponds to the area where the torsional rigidity criteria are fulfilled. From this figure it can easily be concluded that most of the case studies that fulfil the above-mentioned criteria present a good to satisfactory inelastic behaviour. The same conclusion can be drawn from Figure 5.3, which corresponds to multi-storey pseudospatial structural systems.

From the discussion above it may be concluded that the torsional flexibility of the structure must be determined in advance, at the beginning of the analysis procedure, so that a
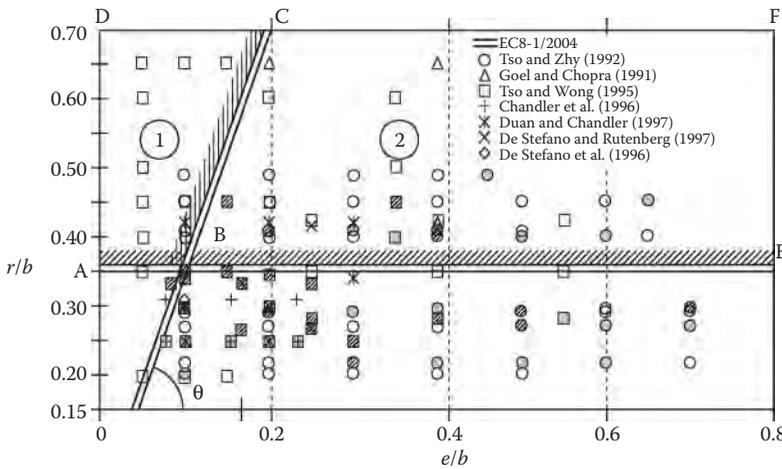
① ABCD: Structural regularity

② AEFD: Torsional rigidity

Remark:
Grey and stripped markers represent poor inelastic response

Equation (5.1a): $\dfrac{e}{b} \le 0.30 \dfrac{r}{b} => \tan \theta = 3.33$

Equation (5.1b): $\dfrac{r}{b} \ge = \dfrac{l_s}{b} \quad 0.30 \div 0.40 \cong 0.35$

Figure 5.2 Evaluation of the structural regularity and torsional rigidity criteria in a one-storey structure. (Adapted from Cosenza, E., Munfredi, G. and Realfonzo, R. 2000. Torsional effects and regularity conditions in R/C buildings. *Proceedings of the 12th World Conference on Earthquake Engineering*, Auckland.)
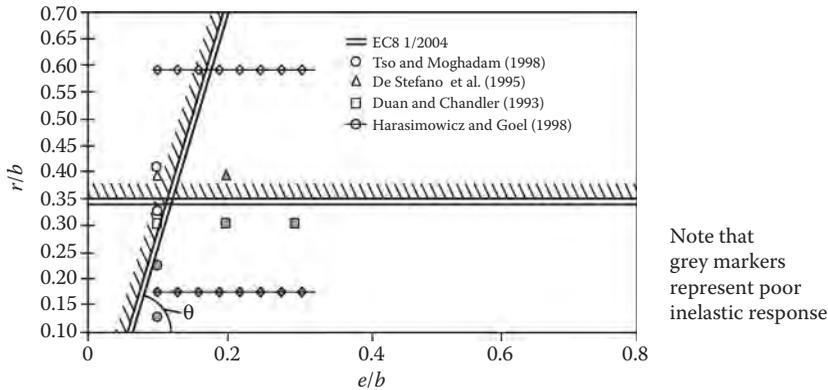
Figure 5.3 Results for regularity and torsional rigidity of multi-storey building models. (Adapted from Cosenza, E., Munfredi, G. and Realfonzo, R. 2000. Torsional effects and regularity conditions in R/C buildings. *Proceedings of the 12th World Conference on Earthquake Engineering*, Auckland.)

decision can be made on *q factor* and *capacity* design issues from the beginning. For this decision to be made the following procedure can be followed:

1. In the case of a frame system or wall system for the definition of e_{mx}, e_{my}, $\bar{J}_{TC}$, r_{cx}, r_{yc}, l_{ms}, Equations 2.86, 2.87, 2.88, 2.113 may be used.
2. In the case of a dual system, the method of the 'plasmatic axis' of centres of rigidity may be followed (subsection 4.5.3).
3. If the lower few eigen modes are determined together with their poles of rotation on each storey in case of a response spectrum 3-D analysis, these eigen modes may be used directly for checking the flexural rigidity. In fact, if the pole of the shortest eigen frequency lies in the boundaries of the floor, at any floor of the system this system is '*torsionally flexible*' (see Paragraph 2.4.4.3), with all consequences resulting therein. It should be noted here that this procedure precedes the analysis of the system. In fact, after the elaboration of the analytical model and geometric, material, and mass properties, the eigen modal analysis is executed, and there of the decision on torsional flexibility may be taken.

5.4 DUCTILITY CLASSES AND BEHAVIOUR FACTORS

5.4.1 General

As was explained in Subsections 2.3.4, 3.2.1 and 3.4.3.7 the action effects (internal forces) due to seismic actions are defined in the force-based design method by taking into account that the structural system is in a position to dissipate seismic energy. Therefore, seismic actions are reduced by a factor *q*, which was called there the 'behaviour factor'. This factor is directly related to the ductility demand of the structure (Section 3.2). The reduced load effects resulting in this way from the analysis, *taking into account the behaviour factor* that has been introduced in the seismic actions, constitute the *demand* for the structural type under consideration and its structural members.

This *demand* must be covered by the capacity of the structure as a whole and of its structural members in strength and ductility (*supply*). Strength requirements are considered to be fulfilled if for all critical regions of the structural members the following relation is verified:

$$E_d \leq R_d$$ (5.4)

where

E_d is the action effect due to reduced seismic action combined with gravity loads.

R_d is the strength calculated by applying R/C mechanics supplemented by some additional rules, which will be presented in the next chapters.

On the other hand, ductility requirements are covered mainly by a series of rules specified by the Code in each case and in special cases by local ductility analytical verifications also specified by the Code. These rules and computational procedures for local ductility verifications will also be examined in detail in subsequent chapters.

5.4.2 Ductility classes

EC8-1/2004 classifies concrete structures into three ductility classes:

1. *Ductility class 'L'* (DCL – low ductility): corresponds to structures designed according to EC2-1-1/2004 (Eurocode for R/C structures) supplemented by rules enhancing available ductility. For all types of structures of this class the specified value of the '*q*' factor is

$$q = 1.5$$ (5.5)

2. *Ductility class 'M'* (DCM – medium ductility): corresponds to structures designed, dimensioned and detailed according to specific earthquake-resistance provisions, enabling the structure to enter well into the inelastic range under repeated reversal loading without suffering considerable loss of strength or brittle failures endangering the local or overall stability of the structure.
3. *Ductility class 'H'* (DCH-high ductility): corresponds to structures for which the design, dimensioning and detailing provisions are such as to ensure, in response to the seismic excitation, the development of a stable mechanism associated with large hysteretic energy dissipation, which has been chosen in advance and is under control during the excitation (capacity design).

In principle, the designer might choose any of the above three ductility classes for an earthquake-resistant structural system, since there is a trade-off between design seismic loading (relevant '*q*' factor) and required ductility (μ_D) (Figure 5.4). However, modern Codes (e.g. EC8-1/2004 ASCE 7-05), taking into account the fact that it is easier to attain high ductility than high strength, put restrictions on the choice of ductility class, relating this choice to the seismicity of the region where the building is located. So, EC8-1/2004 allows the design according to DCL class *only* for buildings in regions of *low seismicity*. The selection of the categories of structure, ground types and seismic zones in a country for which provisions of low seismicity apply is found in the National Annex of each country. EC8-1/2004 recommends considering as low seismicity cases either those in which the design ground acceleration of type A soil, a_g, is not greater than 0.08 g, or those where the product $a_g S$ is not greater than 0.1 g. It can easily be concluded that buildings of DCL are designed without any particular provision for energy dissipation and ductility. Indeed, these buildings are designed according to EC2-1/2004 for load safety factors in earthquakes equal to 1.0, since earthquake action is considered accidental loading. The introduction of behaviour factor $q = 1.5$ is attributable to the overstrength of the structure due
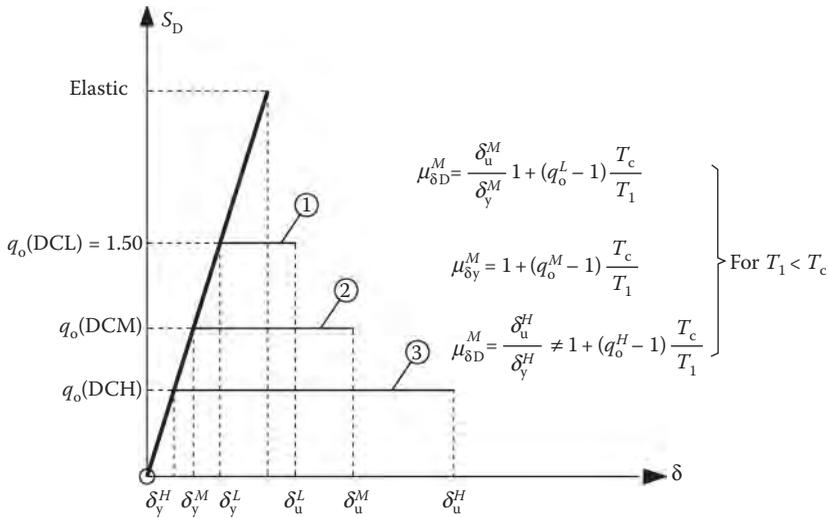
Figure 5.4 Relation between design force and ductility demand at the plateau of the design spectrum (see Chapter 3.2) for fundamental period $T_1 < T_c$ (Equation 5.17).

to material (steel-concrete) overstrength, structural redundancy, minimum reinforcement requirements and so on.

On the other hand, in the case of *very low seismicity*, EC8-1/2004 exempts the structures from any obligation for earthquake design. The cases of very low seismicity are also defined by the National Annex of each country. EC8-1/2004 recommends considering as very low seismicity cases either those in which the design ground acceleration on type A soil, a_g, is not greater than 0.04 g or those where the product a_gS is not greater than 0.05 g.

Coming now to the other two ductility classes, DCM and DCH, it should be noted that according to EC8-1/2004 these two classes must be considered equivalent. However, Eurocode gives the option to country members of the EU to specify geographical limitations on the use of ductility classes M and H in their relevant National Annexes.

5.4.3 Behaviour factors for horizontal seismic actions

The upper-limit value of the behaviour factor q introduced (see Subsection 3.2.3) to account for energy dissipation capacity must be derived for each design direction, according to EC8-1/2004, as the result of a multifunctional relationship of the following form:

$$\boxed{q = K_w \cdot K_R^{el} \cdot K_R^{over} \cdot K_Q \cdot q_o \geq 1.50}$$

(5.6)

where

q_o is the basic value of the behaviour factor, dependent on the type of the structural system, related with its redundancy, its ability to dissipate energy, the number of regions where energy can be dissipated and so on.

K_R^{over} is the factor reflecting the *overstrength and regularity in plan* of the building.

K_w is the factor reflecting the prevailing failure mode in structural systems with walls.

K_R^{el} is the factor reflecting the *regularity* or *irregularity* of the building in *elevation*.

K_Q is the factor reflecting the application or not of a Quality System Plan to the design, procurement and construction.

The values of the above factors are summarised in Table 5.2. The above factors will be examined in detail in the following chapters.

1. For buildings irregular in elevation, factor K_{reg}^{el} is reduced to 0.80, while for buildings regular in elevation its value is 1.0.
2. The factor K_w reflects the prevailing failure mode in structural systems with walls. If the failure mode is of flexural ductile type with formation of plastic hinges in critical regions,

$$K_w = 1.0 \qquad (5.7a)$$

This is the case of frames, frame-equivalent dual systems, and of flexural structural walls, that is, walls with an aspect ratio a_o (h_{wi}/l_{wi}: height/length) greater than 2. In the case that the aspect ratio of walls, wall-equivalent systems and torsionally flexible systems are less than 2, it may be concluded that the shear mode of failure (x-type failure) prevails and precedes that of a flexural failure. Therefore, ductility and the q-factor must be reduced. So, K_w takes the following values (see Table 5.2):

$$K_w = \begin{cases} 1.00, \text{ for frame and frame-equivalent dual systems} \\ (1 + a_o)/3 \le 1, \text{ but not less than } 0.5 \\ \text{for wall, wall-equvalent and torsionally} \\ \text{flexible systems} \end{cases} \qquad (5.7b)$$

In the case of the existence of many walls in the structural system, the prevailing aspect ratio a_o may be determined from the following relation:

$$a_o = \sum h_{wi} \Big/ \sum l_{wi} \qquad (5.8)$$

where
h_{wi} is the height of wall i, and
l_{wi} is the length of the same wall
3. The factor:

$$\boxed{K_R^{over} = a_u/a_1} \qquad (5.9)$$

in Table 5.2 presents the reflection of the overstrength of a regular in-plan system on q-factor. Factors a_u and a_1 in Equation 5.9 are defined below:
a_1 is the value by which the horizontal seismic design action must be multiplied so that at least one member of the structure exhausts its flexural resistance while all other design actions participating in the 'seismic combination' remain constant.
a_u is the value by which the horizontal seismic design action must be multiplied so that plastic hinges are formed in a number of critical regions sufficient for the development of a mechanism, while all other design actions participating in the 'seismic combination' remain constant.
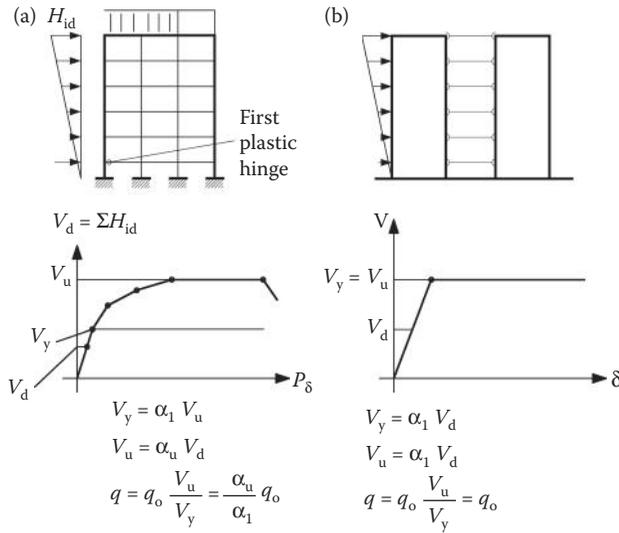
Figure 5.5 Justification of the magnifier factor a_u/a_1 introduced in the q_o-factors of frame or frame-equivalent systems: (a) frame system; (b) shear wall system.

To clarify the above definitions and relations, let us consider two structural systems, one with high redundancy (Frame system) and the other with low redundancy (Wall system) loaded with constant gravity loads and design seismic actions H_{id} in the form of an inverted triangle (Figure 5.5). The V–δ diagram (pushover curve) of the first system is depicted in Figure 5.5a. As V_d increases, one of the structural elements reaches at its critical region its yielding strength in bending and, therefore, at this point the first plastic hinge is formed. The horizontal seismic action at this level is

$$V_{yd} = a_1 V_d \tag{5.10}$$

Therefore, from this point on, the stiffness of the system decreases and consequently the first knee appears in the diagram. Also, as V_d increases, new plastic hinges are generated, accompanied by new knees on the diagram until the structure collapses. The horizontal seismic action at this level is

$$V_u = a_u V_d \tag{5.11}$$

It is evident that the system presents an overstrength:

$$\boxed{K^{ov} = \frac{V_u}{V_{yd}} = \frac{a_u}{a_1}} \tag{5.12}$$

Therefore, since there is a trade-off between strength and ductility, the q_o factor must increase by the factor (a_u/a_1).

Let us come now to the system of low redundancy (two uncoupled walls; Figure 5.5b). Since the two walls have the same cross-section, the plastic hinges are generated at both of them simultaneously.

Therefore,

$$V_{yd} = V_u \tag{5.13}$$

and

$$\boxed{\frac{a_u}{a_1} = 1.00} \tag{5.14}$$

In other words, for structural systems of low redundancy, the factor K^{ov} is equal to 1.00 (see Table 5.2). In this respect, according to EC 8-1/2004, q_o is multiplied by K^{ov}, which is either 1.00 or a_u/a_i. In order to evaluate a_u/a_i, a static inelastic analysis for constant gravity loads and successively increasing horizontal seismic loads must be carried out (pushover analysis; Figure 5.5a) so that a_u and a_1 may be defined. It is obvious that this type of analysis assumes that the structural system has already been analysed elastically and designed properly. So, while a_u/a_i is included in the required data for the evaluation of the seismic actions for the elastic initial analysis, it appears to be the output of an additional and extended inelastic analysis that should precede the elastic analysis and design of the system. To overcome this contradiction, EC 8-1/20004 for the determination of a_u/a_i gives the option to the designer to use either a pushover analysis or to use an approximate conservative value for a_u/a_i specified by the Code.

In the case of a pushover analysis, a_u/a_i must not exceed the value of 1.50 no matter what the output of the analysis. According to EC8-1/2004, the approximate values of a_u/a_i that might be introduced for the determination of the q factor are the following:

a. Frames or frame-equivalent dual system
    i. One-storey building: $a_u/a_i = 1.1$
    ii. Multi-storey one bay frames: $a_u/a_i = 1.2$
    iii. Multi-storey, multi-bay frames or frame-equivalent dual systems $a_u/a_i = 1.3$
b. Wall or wall-equivalent dual systems
    i. Wall systems with only two uncoupled walls per horizontal direction: $a_u/a_i = 1.0$
    ii. Other uncoupled wall systems: $a_u/a_i = 1.1$
    iii. Wall-equivalent or coupled wall systems: $a_u/a_i = 1.2$

The above values $K_R^{ov} = \alpha_u/\alpha_i$ correspond to buildings regular in plan. In the case of irregular buildings, in plan the factor a_u/a_i is reduced to

$$\boxed{K_R^{plan} = \left(1 + \frac{a_u}{a_1}\right)\Big/2} \tag{5.15}$$

4. The factor K_Q reflects the application or not of a Quality System plan to the design, procurement and construction. The value of this factor is defined in the National Annex of the country members. This value is allowed to range between 1.0 and 1.20.
5. The basic value q_o of the behaviour factor is dependent on the type of structural system. Its values have been determined explicitly by the Code and are related to the redundancy of the system's capacity for energy dissipation, the degree of distribution of plastic hinges and so forth. A thorough examination of this subject will be presented in the next subsection.

For inverted pendulum systems, q_o values for R/C buildings in EC8-1/2004 are in disagreement with relevant values of EC8-2/2004 for bridges with R/C single piers, which

are in fact also inverted pendulum systems. In fact, q factors for these piers are specified as equal to 3.50. To overcome this discrepancy, EC8-1/2004 allows the adoption of increased values for the q-factor for inverted pendulum systems, provided that it is shown that correspondingly higher energy dissipation is ensured at the base of the pendulum. This means that a higher value of q is allowed to be introduced in the elastic analysis if after the analysis and design has been finalised a 'pushover' inelastic analysis is carried out and from the capacity curve of the system a new q value is determined, taking into account also a displacement safety factor γ_d (see Subsection 3.2.3) of the order of 1.50. This new q-factor may be introduced in an elastic re-analysis and redesign of the pendulum.

It should also be recalled that the q factor for vertical seismic excitation must be

$$\boxed{q_{vert} \leq 1.5} \tag{5.16}$$

unless a greater value is justified through an appropriate analysis.

6. Finally, it should be noted that in contrast to older European National Codes or even to ACI 318-11, the determination of the behaviour factor is related to an initial structural analysis at least for the characterization of the structural system (frame-equivalent/wall-equivalent), thus making the determination of the q-factor an 'iterative' procedure.

5.4.4 Quantitative relations between the Q-factor and ductility

5.4.4.1 General

A crucial question emerging from the previous subsection concerns the method that has been followed for the definition of q_o-factors that were introduced by EC8-1/2004 in Table 5.2. It is also important to clarify how these values that have been introduced into the Code influence the rules of dimensioning and detailing of structural elements so that these elements are in a position to grant the structural system the global ductility demand and the relevant q_o-factor that has been taken into account for the determination of seismic loading. In other words, it is necessary now to open the 'black box' of the relation between the q_o-factor and the inelastic deformations (plastic curvatures ϕ_u) of the critical areas of the structural members that constitute the ultimate regions where the energy dissipation takes place.

According to what has been presented so far, the value of the q-factor is directly related to the global ductility factor of the structure *expressed in horizontal displacements* at the top of the structure. The relations between the q_o-factor and the displacement ductility μ_δ that have been adopted by EC8-1/2004 have the following form (Vidic et al., 1994; see Chapter 2.3.4):

$$\boxed{\begin{aligned} \mu_\delta &= q_o & \text{if } T \geq T_c \\ \mu_\delta &= 1 + (q_o - 1)\frac{T_c}{T} & \text{if } T < T_c \end{aligned}} \tag{5.17}$$

The value of μ_δ, as already known, is a multi-parametric function of geometry and of elastic as well inelastic properties of the structural members of the system. More precisely, inelastic displacements of a structure at its top are related to inelastic deformations of its structural members. At structural member level, inelastic deformations appear at two subsequent stages, that is, *as inelastic rotations* θ_{in} and as *inelastic curvatures* φ_{in}, which constitute the final (end) state, where plasticity is expressed.

The figure shows four stacked diagrams relating $M(x)$, $\delta(x)$, $\theta(x)$, and $\varphi(x)$ versus x, with the following relations:

$$\theta_{(x)} = \frac{d\delta_{(x)}}{dx}$$

$$\varphi_{(x)} = \frac{d^2\delta_{(x)}}{dx^2} = \frac{d\theta_{(x)}}{dx} = \frac{M_{(x)}}{E_o J_{ef}}$$
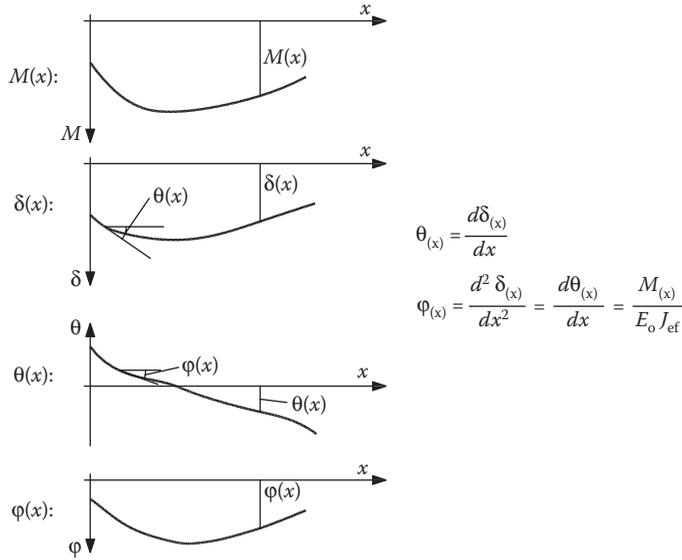
Figure 5.6 Differential relations between bending moment $M(x)$, curvature $\varphi(x)$, rotation $\theta(x)$, and displacement $\delta(x)$ established first by Mohr.

The aim of this subsection is the establishment of simple *generic* relationships among the q_o-factor, displacement ductility μ_δ, the structure-rotational ductility μ_θ of its members, and the curvature ductility μ_φ of member sections. Having established relations among

$$q_o - \mu_\delta - \mu_\theta - \mu_\varphi$$

it is obvious that:

1. For given values of q_o, values of μ_φ may be defined in all critical member sections, and therefore simplified rules for design and detailing may also be established and codified.
2. For limit values of μ_φ (μ_φ-supply), values of q_o-factors (q_o-demand) may be defined and codified properly (Table 5.2).

It is important to remember here from Mechanics the differential relations among bending moment M, curvature φ, rotation θ and displacement δ established first by Mohr in the nineteenth century. These relations are summarised in Figure 5.6.

5.4.4.2 M–φ relation for R/C members under plain bending

5.4.4.2.1 Curvature φy at yield

Consider a rectangular beam section loaded by a bending moment M. Before steel yielding, the relation between curvature φ and bending moment M is (Nitsiotas, 1960)

$$\varphi = \frac{M}{E_b J_{ef}} \tag{5.18}$$

where
$E_b J_{ef}$ is the effective stiffness of the member, which is considered constant up to steel yielding. Effective stiffness is defined below.

When bending moment increases at the level of steel yielding, curvature ϕ_y and bending moment M_y take the following form (Figure 5.7a):

$$\varphi_y = \frac{\varepsilon_c}{x_y} = \frac{\varepsilon_{sy}}{d - x} = \frac{\varepsilon_c + \varepsilon_{sy}}{d} \tag{5.19}$$

$$x_y \cong \frac{D_c}{0.8 f_{cu}} \cong \frac{A_s f_{sy}}{0.8 f_{cu}} \tag{5.20}$$

$$M_y = A_s f_{sy} z \cong 0.87 d A_s f_{sy} \tag{5.21}$$

and

$$EJ_{ef} = \frac{M_y}{\varphi_y} \tag{5.22}$$

where
ε_c is the concrete strain $\leq \varepsilon_{cu}$.
ε_{cu} is the ultimate concrete strain.
ε_y is the steel strain at yield.
f_{sy} is the steel strength at yield.
D_c is the concrete compression at the stage of steel yield.
A_s is the steel area.

The rest of the symbols are depicted in Figure 5.7.
It is obvious that, if the geometry of the cross-section and material properties are known, M_y, ϕ_y and EJ_{ef} may be easily calculated.
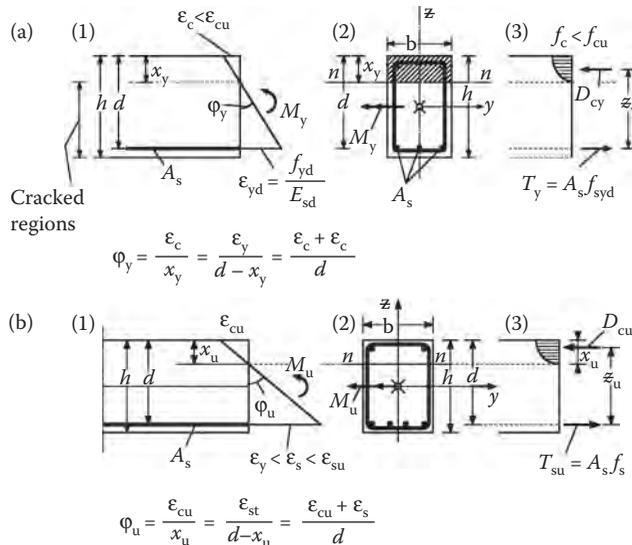
Figure 5.7 (a) Curvature ϕ_y at yield for R/C members under bending: (1) strain pattern at yield plane; (2) cross-section at yield; (3) internal force pattern. (b) Curvature ϕ_u at failure for R/C members under plane bending: (1) strain pattern at failure; (2) cross-section at failure; (3) internal forces at failure.

5.4.4.2.2 Curvature φ_u at failure

As is well known, for a regularly reinforced R/C member, for small steps of increase of bending moment, steel strains increase disproportionally after yield. Compression zone x also decreases, so that, for small moment increase beyond M_y, φ increases disproportionally and the member fails due to concrete crash caused mainly by the decrease of compressive zone x (see Subsection 2.3; Figure 5.7b). In this case,

$$\varphi_u = \frac{\varepsilon_{cu}}{x_u} = \frac{\varepsilon_s}{d - x_u} = \frac{\varepsilon_{cu} + \varepsilon_s}{d} \tag{5.23}$$

$$x_s \cong \frac{D_{cu}}{0.8 f_{cu}} \cong \frac{A_s f_s}{0.8 f_{cu}} \tag{5.24}$$

$$M_s = A_s f_s z_u \cong 0.9 d A_s f_s \tag{5.25}$$

and

$$E_b J_{inel} = \frac{M_u - M_y}{\varphi_u - \varphi_y} \tag{5.26}$$

where

ε_s is the steel strain at failure $< \varepsilon_{su}$.
ε_{su} is the ultimate elongation of reinforcing steel.
D_{cu} is the concrete compression at failure (crush).
EJ_{inel} is the mean stiffness in inelastic region.

It is obvious that for a given geometry of the cross-section and material properties, M_u, φ_u and EJ_{inel} may be easily calculated. It should be noted that the relation $M-\varphi$ from yield to failure stops being linear. However, in this region it is also considered that the relation is approximately linear with inelastic stiffness that of Equation 5.26.

So, taking these into account,

- For M values from zero to M_y, the relation $M-\varphi$ is given by Equation 5.18

$$\varphi = \frac{M}{E_b J_{ef}}$$

- For M values form M_y to M_u, the relation $M-\varphi$ is given by the relation:

$$\varphi = \frac{M - M_y}{E_b J_{inel}} \tag{5.27}$$

Based on the above considerations, the $M-\varphi$ diagram is depicted in Figure 5.8.
Section curvature ductility is defined as follows:

$$\mu_\varphi = \frac{\varphi_u}{\varphi_y} = \frac{\varepsilon_{cu} + \varepsilon_s}{\varepsilon_c + \varepsilon_y} \tag{5.28}$$

A detailed quantitative procedure will be given in Chapters 8 and 9 for the determination of $\varphi_y - M_y$, $\varphi_u - M_u$ and μ_φ of beams, columns and walls.
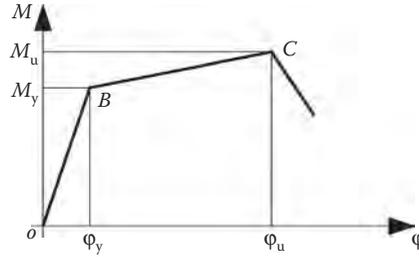
Figure 5.8 Moment–curvature diagram of a ductile R/C member under bending.

5.4.4.3 Moment–curvature–displacement diagrams of R/C cantilever beams

Consider now the cantilever R/C beam of Figure 5.9, loaded at the top with a horizontal load H, which is in position to cause steel yielding (H_y) at first step, and at second step failure (H_u). Curvatures developed along the length l of the cantilever due to loads H_y and H_u (Figure 5.9a), according to the presentation of the previous paragraph (Figure 5.8), have the form of Figure 5.9b. In order to simplify the calculations, the trapezium 0'022' in Figure 5.9b is replaced by an equivalent orthogonal. The area of this orthogonal:

$$\theta_p = l_{pl} \cdot \varphi_u \tag{5.29}$$

represents the concentrated plastic rotation θ_p of the cantilever at a length l_{p1}, which is the *ideal length* of the *plastic hinge*.

Considering now successively, as for elastic loads, the curvatures ϕ_y and ϕ_u and implementing Mohr's theory, we define for δ_y and δ_u the following values:

$$\delta_y = \frac{\varphi_y}{3} l^2 \tag{5.30}$$
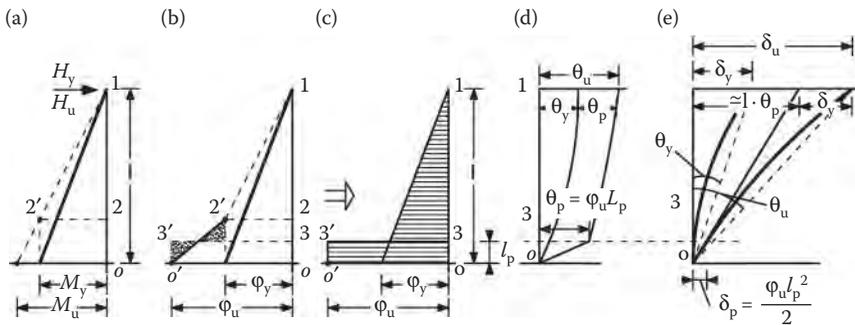
Figure 5.9 Moment–curvature displacement diagrams of an R/C cantilever beam: (a) loading pattern at yield and failure; (b) curvature diagram at yield and failure; (c) definition of the plastic rotation at the fixed end; (d) rotation of the plastic rotation at the fixed end; (d) rotation diagram at yield and failure; (e) displacement diagram at yield and failure.

and

$$\delta_u = \frac{\varphi_y}{3} l^2 + (\varphi_u - \varphi_y) l_{pl} \left(l - \frac{l_{pl}}{2} \right)$$

(5.31)

Consequently,

$$\mu_\delta = \frac{\delta_u}{\delta_y} = 1 + \frac{3l_{pl}}{l} (\mu_\varphi - 1) \left(1 - 0.5 \frac{l_{pl}}{l} \right)$$

(5.32)

The chord rotations are given by the following expressions:

$$\theta_y = \frac{\delta_y}{l}, \qquad \theta_u = \frac{\delta_u}{l}$$

(5.33)

and therefore,

$$\mu_\theta = \frac{\theta_u}{\theta_y} = \mu_\delta$$

(5.34)

The determination of the ideal length l_{p1} of the plastic hinge has been the object of extended research for many years. The value that has been adopted by EC8-3-ANNEX A/2005 has the following form:

$$l_{pl} = 0.1l + 0.17h + 0.24 \frac{d_{bl} f_y (\text{MPa})}{\sqrt{f_{cu} (\text{MPa})}}$$

(5.35)

where
   h is the depth of the member.
   d_{b1} is the mean diameter of the tension reinforcement.
   f_y is the steel stress at yield.
   f_{cu} is the concrete compressive strength.

For a range of usual values of the parameters included in Equation 5.35, the length of plastic hinges varies between the following limits (Fardis et al., 2005):

$$\left. \begin{array}{l} \text{Columns} \begin{cases} 0.35l \\ 0.45l \end{cases} \text{mean value: } 0.40l \\ \text{Beams} \begin{cases} 0.25l \\ 0.35l \end{cases} \text{mean value: } 0.30l \\ \text{Walls} \begin{cases} 0.18l \\ 0.24l \end{cases} \text{mean value: } 0.22l \end{array} \right\}$$

(5.36)

where
   l is the length of a cantilever loaded horizontally at the top or the distance of joints to zero-moment points of beams or columns of a frame loaded with horizontal loads at the storeys (shear span M/V). This length usually corresponds to the half-span or half-height of beams or columns, respectively.

5.4.4.4 Moment–curvature–displacement diagrams of R/C frames

Consider the closed frame of Figure 5.10, which is the basic unit of multi-storey multibeam frames. Consider also a horizontal loading H at the top beam, which is in position to cause steel yielding (H_y) at a first step, and at a second step failure (H_u). For the mode of failure of this frame two options exist:

1. In the case of strong beams – weak columns: formation of plastic hinges at the column ends (Figure 5.10a)
2. In the case of strong columns – weak beams: formation of plastic hinges at the beam ends (Figure 5.11a)

If the procedure for the cantilever is repeated for the frame of Figure 5.10, the following results are derived:

- Frame with strong beams – weak columns (Figure 5.10a–d)

$$\delta_y = 2\frac{\varphi_y}{3}(l_c')^2 \tag{5.37}$$

$$\delta_u = 2\frac{\varphi_y}{3}(l_c')^2 + 2l_{pl}'(\varphi_u - \varphi_y)\left(l_c' - \frac{l_{pl}'}{2}\right) \tag{5.38}$$

$$\boxed{\mu_\delta = \frac{\delta_u}{\delta_y} = 1 + 3\frac{l_{pl}'}{l_c'}(\mu_\varphi - 1)\left(1 - 0.5\frac{l_{pl}'}{l_c'}\right)} \tag{5.39}$$

$$\theta_s = \frac{\delta_y}{b}, \qquad \theta_u = \frac{\delta_u}{b} \tag{5.40}$$
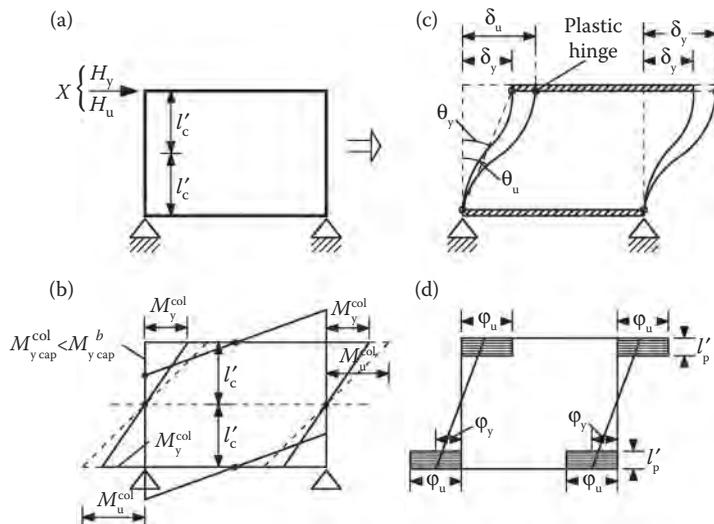
Figure 5.10 Moment–curvature displacement diagrams for R/C frames with strong beams–weak columns: (a) geometry; (b) moment diagrams at yield and failure; (c) displacement diagrams at yield and failure; (d) curvature diagrams at yield and failure.
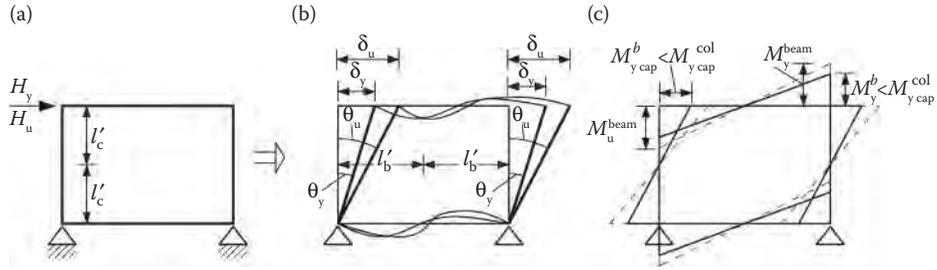
Figure 5.11 Moment–curvature displacement diagrams of R/C frames with strong columns–weak I_y beams: (a) geometry; (b) displacement diagrams at yield and failure; (c) moment diagrams at yield and failure.

$$\mu_\theta = \frac{\theta_u}{\theta_y} = \mu_\delta \qquad (5.41)$$

- Frame with strong columns – weak beams (Figure 5.11a–d)

$$\theta_y^{beam} = 2\left(\frac{\varphi_y l_b'}{2}\right)\left(\frac{2}{3}l_b'\right)\frac{1}{2l_b'} = \frac{1}{3}\varphi_y l_b' \qquad (5.42)$$

$$\delta_y = h\theta_y^{beam} = \frac{1}{3}\varphi_y l_b' h \qquad (5.43)$$

$$\theta_u^{beam} = \frac{1}{3}\varphi_y l_b' + 2(\varphi_u - \varphi_y)l_{pl}'\left(l_b' - \frac{l_{pl}'}{2}\right)\frac{1}{2l_b'} \qquad (5.44)$$

$$\delta_u = \theta_u^{beam} h$$

$$\mu_\delta = \frac{\delta_u}{\delta_y} = 1 + 3\frac{l_{pl}'}{l_b'}(\mu_\varphi - 1)\left(1 - 0.5\frac{l_{pl}'}{l_b'}\right) \qquad (5.45)$$

$$\mu_\theta = \frac{\theta_u^{beam}}{\theta_y^{beam}} = \frac{\delta_u/h}{\delta_y/h} = \mu_\delta \qquad (5.46)$$

5.4.4.5 Conclusions

From the above analysis the following conclusions may be drawn:

1. For the basic forms of a structural system, that is, a cantilever (free standing wall) or a frame system, the relation between μ_θ and μ_φ has the same generic form, that is (Equations 5.32, 5.39, 5.45).

$$\mu_\delta = \mu_\theta = 1 + \frac{3l_{pl}}{l}(\mu_\varphi - 1)\left(1 - 0.5\frac{l_{pl}}{l}\right) \qquad (5.47)$$

where

l is the shear span (M/V), or, more simply, the length from the end of the structural member to the zero-point of the bending moment diagram.

l_{pl} is the ideal length of the plastic hinge (Equation 5.35).

Consequently, if Equation 5.47 is introduced in Equation 5.17, the following relationships are derived:

$$1 + \frac{3l_{pl}}{l}(\mu_\varphi - 1)\left(1 - 0.5\frac{l_{pl}}{l}\right) = q_o \quad \text{if } T \geq T_c \tag{5.48}$$

and

$$1 + \frac{3l_{pl}}{l}(\mu_\varphi - 1)\left(1 - 0.5\frac{l_{pl}}{l}\right) = 1 + (q_o - 1)\frac{T}{T_c} \quad \text{if } T < T_c \tag{5.49}$$

In this way, a direct relation *of generic type* is established between q_o and μ_ϕ for every structural type, that is, between the global q_o-factor of the structure and the curvature ductility at the ends of its structural members.

2. In EC8-1/2004, for reasons of simplicity and continuity with ENV edition (EN1998-1-3; Fardis et al., 2005), the following simpler expressions have been introduced in place of Equation 5.47, that is,

$$\mu_\delta = \mu_\theta = 1 + 0.5(\mu_\varphi - 1) \tag{5.50}$$

or

$$\mu_\varphi = 2\mu_\theta - 1 \tag{5.51}$$

Consequently, introducing Equation 5.51 into Equation 5.17, the following relationships are drawn:

$$\mu_\varphi = 2q_o - 1 \qquad \text{if } T \geq T_c \tag{5.52a}$$

and

$$\mu_\varphi = 1 + 2(q_o - 1)\frac{T_c}{T} \qquad \text{if } T < T_c \tag{5.52b}$$

3. The simplified relation (5.51) is on the safe side. In fact, from the statistical analysis of μ_ϕ values, for the three types of structural members (beams, columns and walls) and for the full range of DCH and DCM buildings, taking into account usual l_{pl} values (Equation 5.36, the following mean safety factors have been derived:

for columns: 1.65
for beams: 1.35   (5.52c)
for walls: 1.10
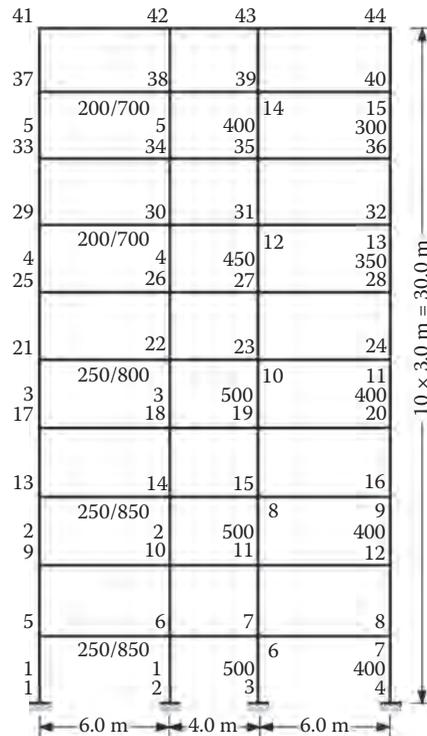
Figure 5.12 Ten-storey R/C frame designed to EC8. (From Penelis, G.G. and Kappos, A.J. 1997. *Earthquake-Resistant Concrete Structures*. SPON E&FN (Chapman & Hall), London.)

4. In all above relations, according to EC8-1/2004 instead of final *q*-factors, *the basic ones, q*$_o$, are introduced, because *q*-factors generally present reduced values due to various penalties that are imposed on the procedure of analysis (design spectrum) to overcome various irregularities of the structure. It is not prudent to introduce this reduction of *q*$_o$-factors into Equations 5.48, 5.49 or 5.52 because it would result in a decrease of μ_ϕ-safety factors.
5. The above rationally concrete framework of relations between $q_o - \mu_\delta - \mu_\theta - \mu_\varphi$ has been verified through extensive prenormative analytical trials on real buildings. Indeed, a series of buildings was designed according to EC8-1/2004 in early prenormative stage and then these buildings were evaluated through static or dynamic inelastic analysis. The conclusions of all these trials are that the conceptual basis of analysis and design established by EC8-1/2004 is sound and safe.

The results of some of these trials are depicted in Figures 5.12 through 5.15 (Kappos, 1991; Kappos and Penelis, 1986, 1997).

5.4.5 Critical regions

From what has been presented in the previous subsection, the energy-dissipating zones of a structure are localised at the regions of the structural elements where plastic hinges might form. From the previous discussion it can easily be concluded that these regions are located
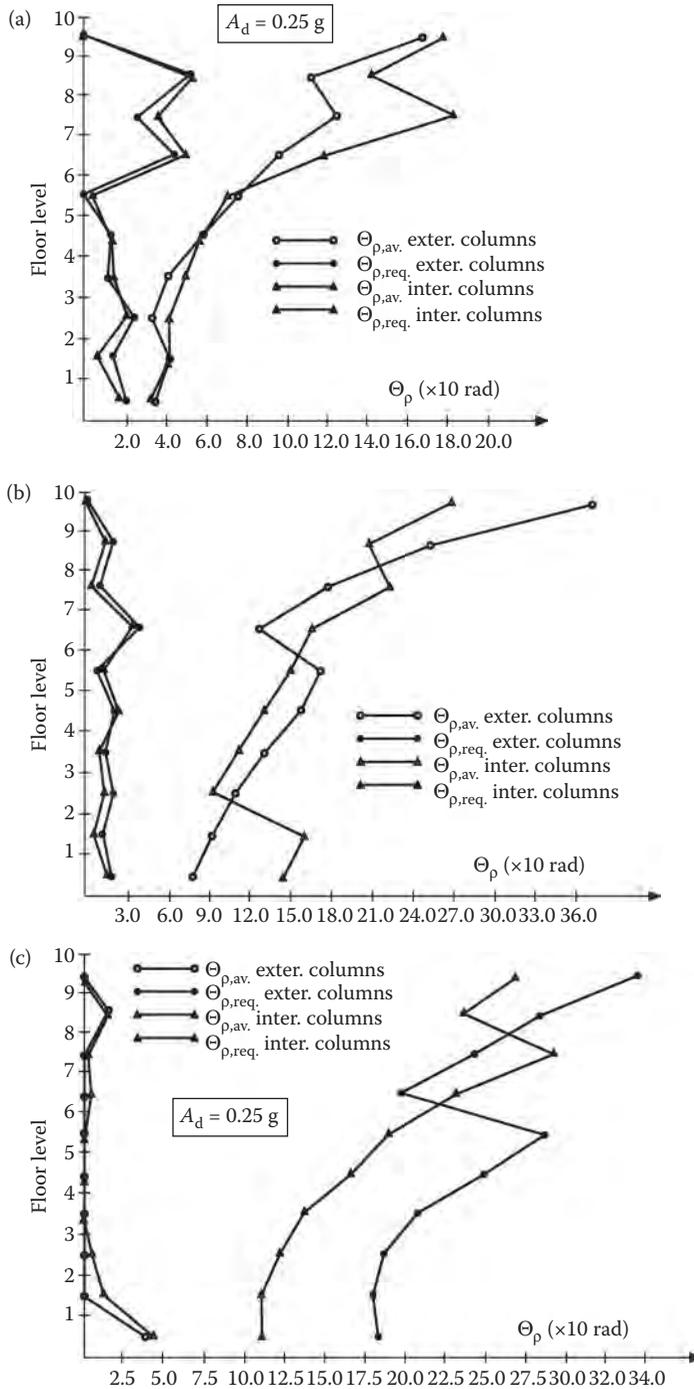
Figure 5.13 Required (demand) available (supply) rotational capacities in 10-storey R/C frame designed for different ductility levels: (a) DCL; (b) DCM; (c) DCH. (From Penelis, G.G. and Kappos, A.J. 1997. *Earthquake-Resistant Concrete Structures*. SPON E&FN (Chapman & Hall), London.)
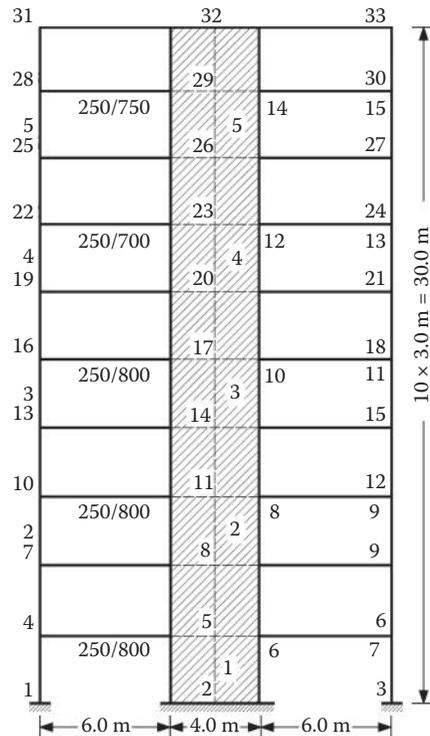
Figure 5.14 Ten-storey dual R/C system designed to EC8. (From Penelis, G.G. and Kappos, A.J. 1997. *Earthquake-Resistant Concrete Structures*. SPON E&FN (Chapman & Hall), London.)

at the areas where the most adverse combinations of action effects occur (M, N, V, T). These regions of the primary seismic elements are defined as *critical regions*. Critical zones are located at the ends of beams and columns in R/C frames and at the bottom of R/C structural walls. The length of these regions is defined for each type of structural element by Codes. Having in mind that the plastic hinges undergo reversal cyclic rotations θ_{p1} during an earthquake, it is evident that the critical regions should be designed and reinforced properly. Length, reinforcement and detailing of critical regions will be discussed in detail in Chapters 8, 9 and 10 for each structural element separately.

5.5 ANALYSIS METHODS

5.5.1 Available methods of analysis for R/C buildings

Over the years the computational capacity has increased (doubles every 18 months according to Moore's law; Moore, 1965) thus rendering the use of extremely advanced and detailed analysis of structures feasible. This, however, should not shift practicing structural engineers necessarily toward those methods, as their complexity creates several issues regarding input parameters that are not available, modelling approaches that are extremely complex and interpretation of results that is diverse and not straight forward. All these issues will be further discussed and tackled in the following paragraphs.
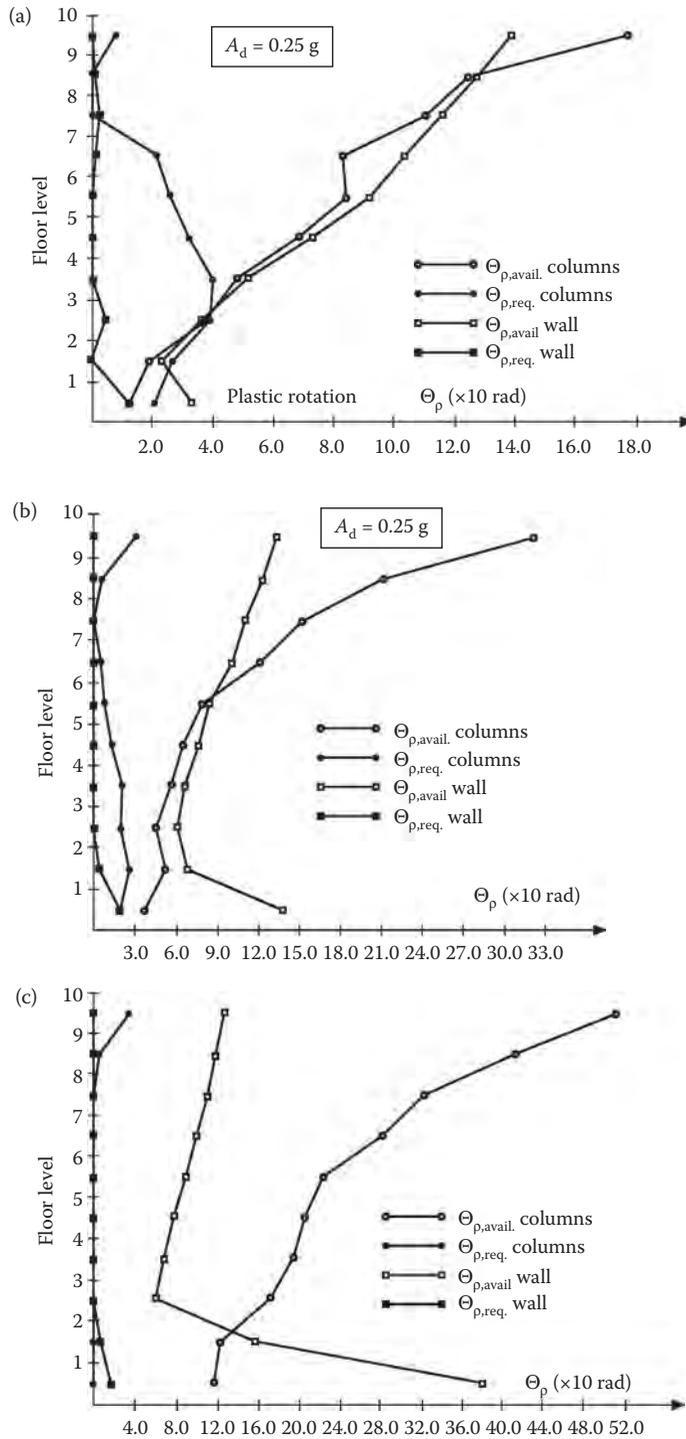
Figure 5.15 Required (demand) and available (supply) rotational capacities in a 10-storey dual structure designed for different ductility levels: (a) DCL; (b) DCM; (c) DCH. (From Penelis, G.G. and Kappos, A.J. 1997. *Earthquake-Resistant Concrete Structures*. SPON E&FN (Chapman & Hall), London.)

The most commonly used methods of analysis or R/C buildings under seismic actions are:

- Equivalent static elastic analysis, called 'lateral force method of analysis'
- Modal spectral elastic analysis, called 'modal response spectrum analysis'
- Equivalent static inelastic (nonlinear) analysis, called 'pushover analysis'
- Time history (*t-h*) inelastic (nonlinear) analysis (*t-h* linear analysis is not frequently used for buildings)

Of those, the reference method for EN1998-1/2004 is *the modal response spectrum analysis*, while for US codes (ACI318.11, IBC2012, SEAOC 09) the reference method *is the lateral force method of analysis*. This difference is significant as the two methods have very distinct advantages and disadvantages summarised at the following:

- *The modal response spectrum analysis* accurately depicts the dynamic behaviour of the structure by identifying the several important modes of vibration and using them in the calculation of the lateral forces at each level, but produces unsigned results for displacements, internal forces and stresses.
- *The lateral force method* uses the fundamental mode to calculate those forces but produces signed results for internal loads and stresses; the sign makes the results more comprehensive and more clear with regard to several aspects, such as the combination of dynamic and static load cases, the biaxial bending with axial load of columns, the integration of stresses of non-rectangular cross-section walls and cores and so forth.

Having in mind the above, there are elements of EN1998-1/2004 like the participation of walls shear in the total storey shear that actually require the execution of an equivalent static analysis (see Sections 4.5 and 5.2), an issue solved by current analysis software by either using such an analysis or producing signed modal results (a notion theoretically wrong) according to a selected mode of vibration.

Of course all these issues are increased exponentially when dealing with the nonlinear approaches, which have the very serious distinction between the point hinge approach and the fibre approach (distributed plasticity over the cross-section). These two approaches also have very distinct advantages and disadvantages, mainly summarised at the following:

- *The point hinge approach* is codified (through available $M-\theta$ diagrams) and easily applied in available commercial software, and produces controlled results ideal for performance base design/assessment. However, it is impossible to model shear walls and cores with 2-D shell elements, thus creating the need for a linear finite element approach, with uncertainties in the connectivity and the $M-\theta$ diagram of the complex section.
- *The fibre model provides* a more accurate solution on the element plasticity and also deals with the issue of complex section walls and cores, as their plasticity is inherently inserted in the modelling of the element. However, this accuracy requires a very deep knowledge of material properties of concrete, rebars, and stirrups and their interface, which makes such a modelling approach extremely risky for practicing engineers not familiar with nonlinear analysis. It should also be noted that this modelling approach increases the instability of the nonlinear analysis and the possibility for errors.

Available commercial software provide solutions based on the point hinge approach with some fibre model capabilities for shell elements (walls) in order to overcome the obvious problems of the former method, and there is very reliable free academic software that provides solutions for the complete fibre model approach.

Finally, there is the distinction between *static* and *dynamic nonlinear analysis*, both of which are available tools in modern codes, and both of them also have advantages and disadvantages.

- *The static nonlinear analysis* provides a straightforward procedure for the input of the seismic forces as constantly increasing lateral loads (or displacements), requires 'simple' constitutive laws for point hinges or even fibre approaches and produces very comprehensive results as the capacity curve and the status of the elements of the building at each loading step. However, there are uncertainties on the lateral loads shape, the lateral loads point of application and the transformation of the building force–displacement curve (P–δ) to an equivalent SDOF capacity curve.
- *The dynamic t-h nonlinear analysis* is considered the most accurate and sophisticated analysis approach (for buildings) available, especially when the fibre approach is utilised. It produces results that have inherently taken into account the torsional effects, the seismic load distribution and the displacements, which do not require a transformation to an equivalent SDOF oscillator. On the other hand this type of analysis is very sensitive to the selection of appropriate accellerograms (recorded, artificial, hybrid), the hysteretic behaviour of concrete and rebars, the distribution of masses and the interpretation of the results on an element (section) level (peak values, peak values within a time frame, effective values, etc.).

The current trend in academia is to try to combine the static nonlinear analysis with the dynamic modal analysis, either by producing a series of modal pushover analyses then combining them (Chopra and Goel, 2002), or by using the adaptive pushover approach, which detects the changes in the stiffness matrix, calculates new modes and accordingly modifies the lateral load value and shape at each step (Elnashai and Mwafy, 2000; Antoniou and Pinho, 2002). This approach, although very promising, is neither codified nor suggested for practicing engineers at the moment. Instead, EUROCODE EC8-1/2004 introduces two different lateral load patterns for which the static inelastic analysis is carried out.

All the aforementioned issues are elaborated in the following sections.

5.6 ELASTIC ANALYSIS METHODS

5.6.1 General

As has been mentioned in previous chapters, there are several elastic analysis methods available that are usually called 'linear' although they might include geometric nonlinearity approaches (buckling), thus making the use of the term "elastic" more accurate. As explained previously these methods are:

- Equivalent static elastic analysis, called 'Lateral force method of analysis'
- Modal spectral elastic analysis, called 'Modal response spectrum analysis'
- Time history (*t-h*) elastic analysis

5.6.2 Modelling of buildings for elastic analysis and BIM concepts

For either static or dynamic approaches, the modelling of three-dimensional structures in modern FE software packages has reached a level where all geometric features of a building
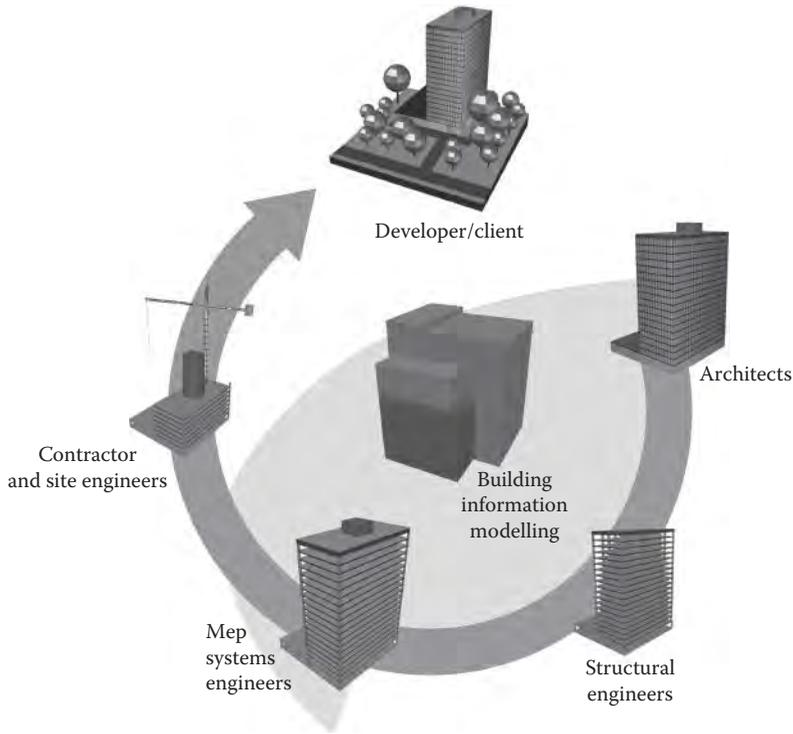
Figure 5.16 BIM concept: interoperability among engineering disciplines.

may be accurately modelled. Especially with the introduction of Building Information Modelling (BIM), the FE model of the building is an actual 3-D representation of the structure, which includes all structural and nonstructural elements, MEP installations, loads and boundary conditions, which are then automatically exported to a structural analysis software that can perform the analysis, calculate the required reinforcement and feed it back to the BIM model.

This is graphically shown in Figure 5.16, as an example application from the new opera in Athens in Figure 5.17. It is, however, important for all structural engineers to be aware that these interfaces are only used, to date, for clash detection between architectural, structural and MEP design, while the structural modelling is done independently either from scratch or by using the BIM output as a reference model to be modified and verified by the structural engineer.

5.6.3 Specific modelling issues

The main problems of a full 3-D FE model of an actual building are the following:

- Simulation of walls, cores and openings
- Simulation of T- and Γ-shaped beams
- Diaphragm constraint
- Application of eccentricity of seismic loads
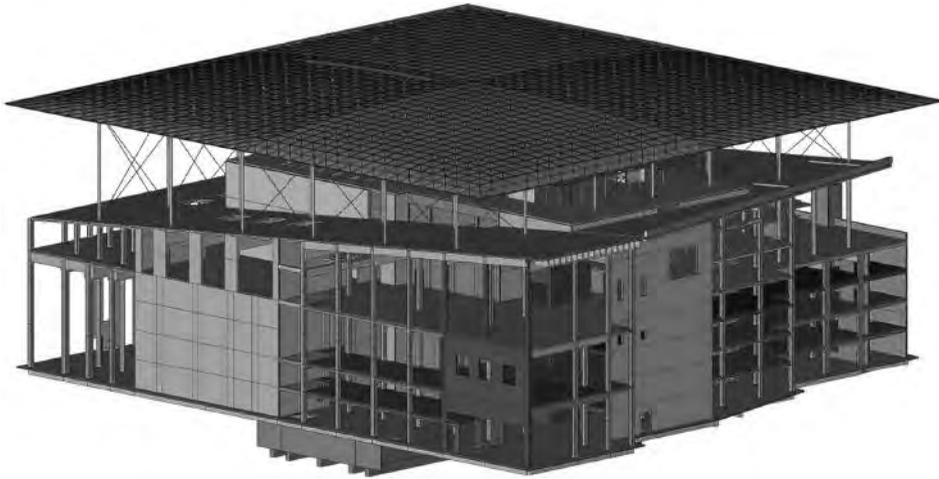
Figure 5.17 BIM application for the Athens Opera House (SNFCC) using Nemetschek Scia Engineer.

5.6.3.1 Walls and cores modelling

The modelling of walls and especially cores is available in most modern software packages through the use of planar (shell) finite elements, which reduce the requirements for modelling of rigid connections and equivalent stiffness, as was the case in the past for all types of analyses and remains to-date for nonlinear analysis. The accurate modelling of cores in medium-rise and high-rise buildings is crucial, as it affects the total response and plays a significant role in the final architectural layout of these buildings.

However, another key issue is the design of these complex section elements, which, although modelled accurately for the analysis, are sometimes treated as individual rectangular sections (legs) for the design, thus underestimating their flexural capacity up to 25% (ECtools, 2013).

Finally, a very important issue for the design of walls is the accurate modelling of the openings, or, more precisely, the spandrels (connection beams) that are created. Unless properly modelled, these elements might elude the checking of the general concrete wall and remain poorly reinforced, while all the checks elaborated in the relevant chapters should be applied.

5.6.3.2 T- and Γ-shaped beams

As it is very well known, all modern codes require an effective flange length to be taken into account in the design of beams that are directly under slabs, thus resulting in a *T* section (where the slab is on both sides of the beam) or a Γ section (where the slab is on one side of the beam). There lies the risk of actually taking into account twice the part of slab that coincides with the part of the beam section, both regarding stiffness and self-weight.

Some modern commercial software packages allow the modelling of the hanging part of the beam (rib) separately while the modelling of the flange is done with the slab shell elements. Then the section of the beam is comprised by the two parts and the section forces are the combination of the integrated stresses of the required part of the slab and the section forces of the rib, as is shown in Figure 5.18:
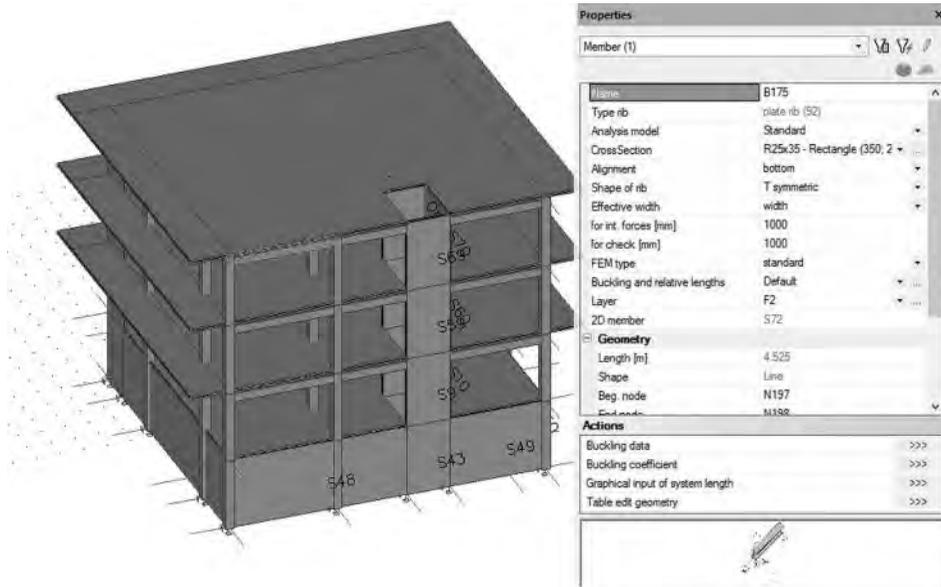
Figure 5.18 Modelling of ribs with 1-dimension finite element (1-DFE) and of effective flange width from slab 2-dimension finite element(2-DFE).

However, other general purpose software packages do not provide this option; hence, the engineer has to follow one of the two options below:

- Model the beams as T or Γ sections and reduce their self-weigh and stiffness accordingly (through property modifiers) so that the total building self-weight and stiffness are correct
- Model the beams as rectangular section, place them under the shell elements of the slab and then manually integrate the results (combining stresses from shell elements and section forces from the rectangular section) and calculate the required reinforcement for the actual T or Γ section.

It is crucial to avoid modelling the flanges twice (as slab and as a beam section), as this seriously affects the stiffness, the mass and the resulting dynamic characteristics of the building.

5.6.3.3 Diaphragm constraint

All modern seismic codes for buildings have checks and verifications that have the inherent notion of a storey (storey forces, interstorey drifts, etc.). In the past two decades, when computational power was significantly lower it was important to seriously reduce the stiffness and mass matrices of finite element models of buildings, and for this main reason the diaphragm constraint had been introduced, which essentially defines one master joint in the centre mass of a storey and connects all other nodes of the storey (as slave nodes) with rigid-body in-plane motion relative to that master joint. This allowed the use of a condensed stiffness and mass matrix and all results were actually then extrapolated to all the connected slave nodes through shape functions (see Subsections 2.4.4 and 4.5.3).

It is obvious that nowadays, for normal buildings, the significance of the reduction of required computation force has been minimised; however, there are other issues that make the use of a diaphragm constraint a suggested option:

- Elimination of secondary eigen modes
- Application of the equivalent static analysis in a straightforward way (by applying the forces on the master node)
- Application of accidental eccentricities in the equivalent static or spectral dynamic analysis
- Easily checked interstorey drifts and storey displacements
- The philosophy of analysis and design of all modern Codes, which is based on the notion of diaphragm constrain

However, there are cases where the diaphragm constraint should or must be avoided:

- Buildings that have storeys with large openings (i.e. atriums)
- Buildings that after a height, have twin towers
- Buildings with very flexible floors

All modern software packages foresee the following options:

- Rigid diaphragms
- Flexible diaphragms
- No diaphragms

It is clear that for most common buildings the use of the diaphragm constraint is suggested, while in complex buildings it is up to the structural engineer to decide upon using a flexible diaphragm or no diaphragm constraint at all. EN1998-1/2004 (EC8-1) notes that, 'the diaphragm is taken as being rigid, if, when it is modelled with its actual in-plane flexibility, its horizontal displacements nowhere exceed those resulting from the rigid diaphragm assumption by more than 10% of the corresponding absolute horizontal displacements in the seismic design situation'.

5.6.3.4 Eccentricity

The issue of the required eccentricity in the application of the seismic loads in either the equivalent static or the spectral analysis has been elaborated in a previous chapter. However, the modelling of this eccentricity is a tricky issue, as one has the following options, depending on the modelling assumptions that have been adopted:

- Introduce the resulting torsion at the master joint when a diaphragm exists (for both static and spectral analysis)
- Divide the resulting torsion at all the nodes of the storey when a diaphragm does not exist (for both static and spectral analysis)
- Place either the lumped mass (for the case of modal spectral analysis) or the horizontal forces (for the case of equivalent static analysis) at 4 offset positions from the centre of mass, provided that a diaphragm constraint can be applied. This option, which conceptually is the most accurate, significantly increases the seismic lateral load cases from two (EX and EY) to four and the load combinations accordingly (exponentially). Some software codes perform this offset automatically and the envelope results; which, however, is not easily verified by the engineer.

It should be noted that according to EC8-1/2004, in order to account for uncertainties in the location of masses, the calculated centre of mass at each floor i shall be considered as being displaced in each direction by an accidental eccentricity:

$$e_{ai} = \pm 0.05 \cdot L_i \tag{5.67}$$

where
   e_{ai} is the accidental eccentricity of storey mass *i*.
   L_i is the floor-dimension perpendicular to the direction of the seismic action.

5.6.3.5 *Stiffness*

As has already been elaborated, the stiffness in elastic analysis plays a significant role, especially in the modal spectral analysis as it affects the dynamic characteristics of the structure. Different codes provide different information of the effective stiffness of structural elements, using the basic notion that all elements, except columns that have a high axial load, are at stage II, that is, cracked, when an earthquake occurs, hence beams and walls have a reduced effective stiffness of 50–70% of the uncracked one.

However, there are cases where this assumption creates misleading results for the gravity load combination, in the cases where this is critical. A very indicative example on the matter is for buildings with seismic isolation and the effect of the stiffness modifiers on the load distributions to each isolation unit.

5.6.4 Lateral force method of analysis

This method, for both main directions of the building, takes into account only the fundamental mode of vibration. Based on the above modes of vibration, the respective fundamental periods T_{1x}, T_{1y}, and the relevant design spectrum, modified by the importance factor, the total inertia forces in the two main directions and their contribution along the height of the structure are defined (Subsection 3.2.3). For these loads, a static analysis of the structural system is carried out. In this context this method might be characterised as an equivalent static analysis. From the above presentation it is concluded that this type of analysis can only be applied to buildings in which the first two eigen modes are translational and response is not expected to have any essential contribution from higher modes of vibration.

EC8-1/2004 (par. 4.3.3.2.1) defines the following conditions for such an analysis to be used, in buildings that:
Condition 1
The fundamental periods of vibration T1 in two main directions are less than the following values:

$$T_1 \le \begin{cases} 4T_C \\ 2.0s \end{cases} \tag{5.53}$$

where T_c is the upper limit of the period of the constant spectral acceleration branch (plateau).
Condition 2
Meet the criteria for regularity in elevation given in subsections 4.2.2 and 5.2.3.

5.6.4.1 Base shear forces

The seismic base shear force V_B, for each horizontal direction in which the building is analysed, shall be determined using the following expression:

$$V_B = S_d(T_1) \cdot m \cdot \lambda \tag{5.54}$$

where
$S_d\,(T_1)$ is the ordinate of the design spectrum at period T_1.
T_1 is the fundamental period of vibration of the building for lateral motion in the direction considered.
m is the total mass of the building, above the foundation or above the top of a rigid basement.
λ is the correction factor, the value of which is equal to: $\lambda = 0.85$ if $T_1 < 2\ T_C$ and the building has more than two storeys, or $\lambda = 1.0$ otherwise.

5.6.4.2 Distribution along the height

The base shear is distributed among the storeys in the same proportion as the inertia forces that correspond to the fundamental period of the structural system, which is homologous to the characteristic shape of the fundamental mode. Given the fact that the first mode of a multi-storey, multi-column system, with a limited number of storeys and sufficient lateral stiffness, appears to be linear (Figure 5.19; Biggs, 1964; Polyakov, 1974), the following relationships apply:

$$\varphi_{i1} = \frac{h_i}{h_n} \tag{5.55}$$

$$H_i = \lambda\gamma_1 \frac{L_1^*}{M_1^*} m_i S_d \varphi_{i1} \tag{5.56}$$

and

$$\sum_i H_i = V_B = \lambda\gamma_1 \frac{L_1^*}{M_1^*} S_d \sum_i m_i \varphi_{i1} \tag{5.57}$$
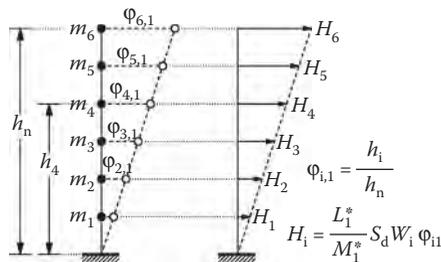
Figure 5.19 The fundamental mode of a multi-storey system and the corresponding inertial forces.

Therefore,

$$\lambda \gamma_1 \frac{L_1^*}{M_1^*} S_d = V_B / \sum_i m_i \varphi_{i1} \tag{5.58}$$

Substituting Equations 5.55 and 5.58 into Equation 5.56 the following expressions are obtained:

$$H_i = \frac{m_i \varphi_{i1}}{\sum m_i \varphi_{i1}} V_B \tag{5.59}$$

or

$$\boxed{H_i = \frac{m_i h_i}{\sum m_i h_i} V_B} \tag{5.60}$$

where
  h_i is the height of storey i from ground.

On the basis of this theoretical background, EC8 (par. 4.3.3.2.3) requires a distribution of forces as per the fundamental mode shape displacement at each storey level that is according to Equations 5.60.

This equation for constant values of m_i; and storey heights h yields

$$H_i = \frac{m h_i}{m \Sigma h_i} V_B \tag{5.61}$$

or

$$H_i = (n_i / \sum_i n_i) V_B \tag{5.62}$$

where
  n_i is the number of the storey at the level of which the lateral force H_i is induced.

Equation 5.62 yields a *triangular distribution of seismic loading.*

It should be noted however that all advanced software packages provide the option to distribute the base shear linearly, uniformly or under any mode shape, thus allowing a different distribution of forces along they height for each direction of analysis.

5.6.4.3 Estimation of the fundamental period

The estimation of the fundamental period may be done either by approximate methods or by applying modal analysis to the building, as it is available to most engineering software. However, even in those cases, the following approximations provide a measure to check the accuracy of the modelling of the building.

For buildings with heights of up to 40 m, the value of T_1 (in s) may be approximated by the following expression:

$$T_1 = C_t \cdot H^{3/4} \tag{5.63}$$

where
> C_t is 0.085 for moment resistant space steel frames, 0.075 for moment resistant.
>   space concrete frames and 0.050 for all other structures;
> H is the height of the building, in m, from the foundation or from the top of a rigid
>   basement.

Alternatively, for structures with concrete shear walls the value C_t may be taken as being:

$$C_t = \frac{0.007}{\sqrt{A_c}} \tag{5.64}$$

where

$$A_c = \sum \left[A_i \cdot (0.2 + (l_{wi}/H))^2 \right]$$

and
> A_c is the total effective area of the shear walls in the first storey of the building, in m^2.
> A_i is the effective cross-sectional area of shear wall i in the direction considered in the
>   first storey of the building, in m^2.
> L_{wi} is the length of the shear wall i in the first storey in the direction parallel to the
>   applied forces, in m, with the restriction that l_{wi}/H should not exceed 0.9.

The estimation of T_1 (in s) may also be made by using the following expression:

$$T_1 = 2\pi \cdot \sqrt{d} \tag{5.65}$$

where
> d is the lateral elastic displacement of the top of the building, in m, due to the gravity
>   loads applied in the horizontal direction.

For the determination of the fundamental period of vibration period T_1 (in s) of the building, expressions based on methods of structural dynamics may be used. For example, the Rayleigh method may be properly adapted:

$$T_1 = 2\pi \left(\sqrt{\frac{1}{g} \frac{\sum W_i \delta_i^2}{\sum H_i \delta_i}} \right) \tag{5.66}$$

where H_i ($i = 1,2\ldots,N$) is a group of forces at the level of the floors, with a triangular distribution, δ_i ($i = 1,2,\ldots,N$) is the corresponding displacements of the floors and W_i ($i = 1,2, \ldots,N$) is the vertical loads at each storey i. For $N = 1$, from Equation 5.66 the previous Equation 5.65 can be derived.

5.6.4.4 Torsional effects

In the case of systems regular in plan and in elevation, as these properties have been defined in Section 5.1, the torsional effects taken into account in the 'simplified modal analysis' are only those related to an accidental eccentricity equal to (par. 5.6.3-D):

$$e_{ai} = \pm 0.05 \cdot L_i \tag{5.67}$$
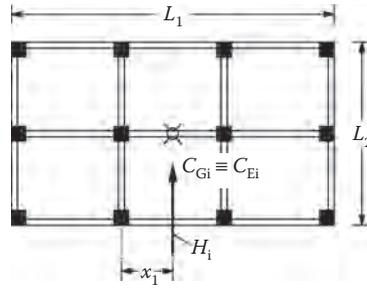
Figure 5.20 Evaluation of the torsional effects on a symmetric system with the aid of an amplification factor.

In this case, EC8 allows the torsional effects to be taken into account by amplifying the action effects on the individual load-resisting plane elements parallel to the seismic action using an amplification factor δ equal to (Figure 5.20):

$$\delta = 1 + 0.6\frac{x_i}{L_i} \leq 1.30 \tag{5.68}$$

If the analysis is performed using two planar models, one for each main horizontal direction, torsional effects may be determined by doubling the accidental eccentricity e_{ai}

$$2e_{ai} = \pm 0.10 L_i \tag{5.69}$$

which results in the following amplification factor δ:

$$\delta = 1 + 1.2\frac{x_i}{L_i} \leq 1.60 \tag{5.70}$$

It is obvious that such approaches are related to this type of simplified analysis, and whenever torsional sensitivity is considered an issue by the designer, at least a modal analysis should be executed.

It should be noted, again, that codes that promote (use as reference method of analysis) this type of static–elastic analysis, suggest procedures that the dynamic characteristics of the building are determined through modal analysis. In that way most of the drawbacks are eliminated while the main advantage, which is comprehensive and physically meaningful *signed results*, is preserved.

5.6.5 Modal response spectrum analysis

As already mentioned, this type of analysis is the reference analysis method according to EC8-1/2004. It may be applied to all types of buildings, even those that do not satisfy the conditions for applying the lateral force method of analysis.

For buildings complying with the criteria of regularity in plan but not in elevation, the analysis can be performed using two plane models, one for each main direction. Otherwise, the system must be analysed using a spatial model. Whenever a spatial model is used, the design seismic action will be applied along its two main directions determined by the resisting elements of the system. Otherwise, the design seismic action will be applied along all relevant horizontal directions and their orthogonal horizontal axes.

5.6.5.1 Modal participation

In a multimodal analysis the responses of all modes of vibration contributing significantly to the global response are taken into account (Clough and Penzien, 1975). This may be satisfied by either of the following:

- Demonstrating that the sum of the effective modal masses for the modes considered, amounts to at least 90% of the total mass of the structure, that is

$$\sum_{i=1}^{k} \frac{L_i^{*2}}{M_i^*} \geq 0.9 \sum_{i=1}^{n} M_i \tag{5.71}$$

  where k is the number of modes considered and n the number of masses.
- Demonstrating that all modes with effective modal masses greater than 5% of the total mass are considered, that is

$$\frac{L_j^{*2}}{M_j^*} \leq 0.05 \sum_{i=1}^{n} M_i \tag{5.72}$$

  where j is the index of the modes not considered.

In the case of a spatial model the above conditions must be verified for each main direction.

In buildings with a significant contribution from torsional modes, if the above conditions cannot be satisfied the minimum number of modes k to be considered in a spatial analysis should satisfy the following condition (EN1998-1/2004):

$$k \geq 3 \cdot \sqrt{n}$$

and

$$T_k \leq 0.20 \, s$$

where T_k is the period of vibration of mode k.

Here it should only be added that whenever a spatial model is used,

- The floor masses will be considered as either lumped masses concentrated at the centre of gravity of each floor or distributed depending on the diaphragm modelling approach adopted, as has been elaborated in Paragraph 5.6.4.3.
- The accidental torsional effects may be determined using the appropriate modelling approach, which has been elaborated in the previous Paragraph 5.6.4.4.

5.6.5.2 Storey and wall shears

To evaluate the percentage of the storey shear that the walls receive (compared to the total), equivalent static analyses are utilised. This is necessary because the seismic modal analyses produce results that are unsigned, thus making them useless for such an evaluation. It should be noted that in dual systems this percentage in the upper storeys can be negative, since the response of the wall differs from that of the frame.

This has been evident since the 1960s in the application of the Mc Leod method, as is shown in Figures 4.23 and 4.25.

5.6.5.3 *Ritz vector analysis*

Although eigen vectors have been used extensively in modal analysis, in recent years an approximate approach, called the Ritz vector analysis, has been utilised in buildings that have a very complex geometry. This analysis allows the identification of significant modes of vibration (excluding minor modes), as it uses as a starting point vectors defined by the engineer (the first vector is the displacement vector obtained from a static analysis) using the spatial distribution of the dynamic load vector as input. As has been demonstrated by Wilson (1985), dynamic analyses based on a unique set of Ritz vectors yield more accurate results than the use of the same number of exact mode shapes. It is considered beyond the scope of this chapter to further elaborate on this approach, which proves useful in dealing with complex spatial structures.

5.6.6 Time–history elastic analysis

The time history elastic analysis is used only at specific cases of analysis where the exact response of the building through the duration of a set of excitations is required. Such requirements arise in the following types of buildings:

- Buildings with seismic isolation
- Buildings with damping devices
- Buildings with active mass systems

In all the above cases the modelling approaches analysed in the previous paragraphs are applicable, with the exception of the seismic devices which require modelling with additional data, such as:

- Effective (elastic) Stiffness
- Effective damping

These parameters are initially determined by the designing engineer and are then provided/confirmed by the selected manufacturer.

The *t-h* analysis can provide, in such cases, information about the modification of the dynamic characteristics of the building, which are only approximated when using the previous types of analysis (i.e. torsional effects, participation of higher modes due to additional damping of first mode, etc.).

The selection of the excitation, scaling and interpretation of the results are issues that are elaborated in the relevant section for the nonlinear *t-h* analysis.

5.7 INELASTIC ANALYSIS METHODS

5.7.1 General

As is widely known, the design of new buildings is based on elastic methods (static or dynamic); however, buildings often sustain damage during an earthquake and thus develop some degree of nonlinear inelastic behaviour depending on the extent of damage. This behaviour is introduced into the design by modern codes by the use of a reduction factor for the seismic forces (*q*-factor, *R*-factor, etc.). On the other hand, for the assessment of the

seismic behaviour of an existing building many modern codes/guidelines suggest the use of a more 'accurate' approach – that of the nonlinear analysis.

Assessing the nonlinear behaviour of a building requires appropriate software, the most advanced case being the nonlinear step-by-step dynamic time-history analysis with a fibre model for the structural elements behaviour. This type of analysis, though very useful for the researcher/engineer, as a benchmark is extremely strenuous and non-design friendly as it requires a bundle of input data (accelerograms, damping values for each element, stress–strain laws for each material with a cyclic behaviour, etc.) and produces unclear results for design purposes (stress–strain over time steps, maximum–minimum values at different time steps, absorbed energy, etc.).

5.7.2 Modelling in nonlinear analysis

It is well known that the software available for nonlinear analysis can be generally divided into three different categories:

- Linear finite element point hinge models
- Linear finite element distributed nonlinearity (fibre) models
- Planar (shell) or spatial finite element nonlinear models (continuous or discrete)

It is obvious that the methods are presented with increasing demand in modelling complexity and computational power. From these, only the first two are used for the analysis of complete structures while the latter are used mainly for substructures.

The point hinge approach concentrates the nonlinearity of the structural elements in nonlinear rotational springs at the ends of each element, the moment rotation curve of which corresponds to nonlinear behaviour of each element (see Subsections 2.3.5, 2.5.2 and 5.4.4).

The fibre model utilises nonlinear material laws for concrete and reinforcement, and by dividing each element into sections and each section into regions (fibres), calculates, by section analysis, the moment–curvature for each load step for each section and then integrates along the length of the element, thus producing the nonlinear behaviour for each load step.

Modelling a building for nonlinear analysis requires different approaches than that of the modelling for linear analysis, specifically with regard to the following aspects:

- Slab and transfer of loads
- Diaphragm constraint
- Foundation
- R/C wall and cores
- fibre or point hinge modelling
- Use of safety factors

5.7.2.1 Slab modelling and transfer of loads

Slabs in most modern commercial software packages are modelled by the use of some type of elastic shell element that transfers the gravity loads to the beams, facilitates the slab design itself and applies the diaphragm constraint. However, in nonlinear analysis the shell elements for slab must not be present, as they will act elastically, thus interfering with the nonlinear behaviour of the *T*-beams. Therefore, two different problems arise: (i) the transfer of loads from slabs to beams; (ii) the modelling of the diaphragm constraint.
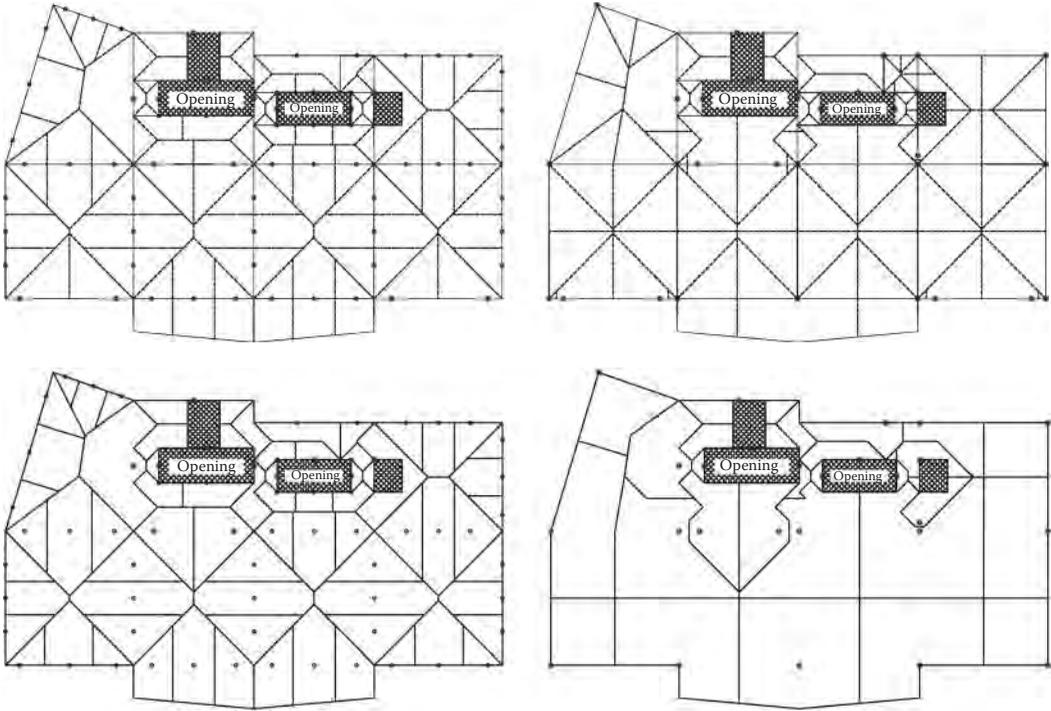
Figure 5.21 Gravity load distribution (left) and mass distribution (right).

Regarding the first issue (i), some software packages include a macro element for slabs that only transfers the loads at an 'initial step' and then set the slab stiffness matrix to zero [0] in order to perform nonlinear analysis for gravity and lateral loads. In the cases where this option is not present, as in most current NL software packages, the loads are transferred manually using a triangulation approach, at the thirds of each beam, as shown in the following figures from a 16-storey actual building presented in the examples of this chapter.

It should also be noted, for the case of *t-h* nonlinear analysis, that the additional masses corresponding to the slab self-weight and gravity loads (mass combination) should be transferred directly to the nodes of each vertical element per storey to facilitate the nonlinear analysis. These concepts are shown graphically in Figure 5.21 for the typical storey of an actual building.

5.7.2.2 Diaphragm constraint

Regarding the issue of the diaphragm constraint there are also nonlinear software packages that allow the use of a rigid diaphragm constraint in selected nodes; however, in cases where this option is not available the engineer must manually add *x*-braces with numerically rigid elements (elastic material with $E_{\mathrm{Rigid}} = 10 \cdot E_{\mathrm{s}}$ and 1.0×1.0 m cross-section) and end releases, as shown in Figure 5.22.

5.7.2.3 R/C walls and cores

As in the case with slabs, R/C walls and cores in most modern commercial software packages are modelled with elastic shell elements, an approach that has simplified the
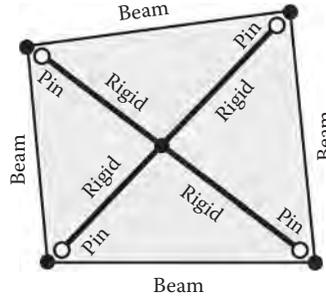
Figure 5.22 Rigid diaphragm modelling (plan view).

modelling of these elements to the average engineer and has essentially transformed the elastic structural modelling of a building to a 3-D BIM-type approach. Unfortunately, this simplification is not available, and not recommended even if available, for the non-linear structural modelling as all elements should be simulated using 1-D elements either in point hinge or fibre model approaches. Therefore, the R/C walls and cores have to be modelled following the 'old' rules used in the 1990 s for modelling such elements (then elastically).

Rectangular R/C walls should be modelled using one 1-D element corresponding to the dimensions, material properties and reinforcement of the wall itself. This element must be connected to the beams through the use of numerically rigid elements (elastic material with $E_{\text{Rigid}} = 10 \cdot E_s$ and 1.0×1.0 m cross-section).

R/C cores of arbitrary geometry represent a higher challenge, as they have to follow different modelling approaches for point hinge models and fibre models. In the case of the point hinge model the core must be modelled using one element placed at the centre of stiffness (shear centre) with the geometrical properties of the core section and a biaxial moment–rotation diagram (with axial force interaction) that corresponds to the nonlinear behaviour of the core. As this is not available by any standard, a detailed section analysis should be performed in order to define this set of curves. In the case of the fibre model, each leg of the core should be modelled as one 1-D element at the centre of stiffness of the leg with geometrical properties, material properties and reinforcement corresponding to this leg. In both cases, the 1-D elements are connected to the geometrical extremities of the core using numerically rigid elements (Figure 5.23).

It should be noted that if the proposed arrangement for the fibre model is applied in the point hinge model for the nonlinear simulation of cores, it will lead to a *significant uncon-servative error*, as the moment capacity of the set of 1-D elements will be governed by their axial load–deformation curve, which in most approaches is elastic, thus giving the core infinite yield moment capacity.
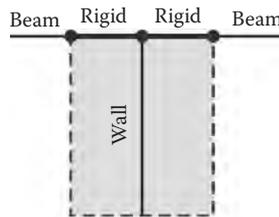
Figure 5.23 Wall modelling (left, elevation view).

5.7.2.4 Foundation

It is suggested that the building is modelled as fixed at the level where it is laterally restrained (i.e. foundation box). This approach reduces the size of the nonlinear model and eliminates possibility of mistakes. Cases in which soil–structure interaction or foundation design is required should opt for simpler models of the superstructure and use geotechnical nonlinear software (e.g. Plaxis, 2012).

5.7.2.5 Point hinge versus fibre modelling

Two of the key issues in the point hinge modelling are the initial stiffness and the ultimate available rotation of each structural element. As the approach is approximate, these two assumptions seriously affect the results and their credibility. Usually the fibre model approach is used as a benchmark.

5.7.2.5.1 Initial stiffness

In U.S. guidelines such as FEMA356 or ATC40 the aforementioned modelling problems are dealt with in a, more or less, straightforward fashion. As far as reinforced concrete members elastic stiffness (second level) is concerned, the values defined in Table 6-5 of FEMA 356 where the beams are modelled with 50% of their uncracked flexural rigidity while columns with 50–70% of their uncracked flexural rigidity (Table 5.3) are proposed.

EC8-1/2004 suggests the use of cracked sections as defined in its Subsection 4.3.1, that is, 50% of the gross section for all elements. On the other hand, in text books (Leonhardt, 1977) the rigidity is modelled as a function of the flexural reinforcement ratio and varies from 25% to 50% of the uncracked rigidity (Figure 5.24).

One should be very careful when defining the initial stiffness in a point hinge model, as in most software the initial elastic behaviour is defined by the elastic properties of the element while the point hinge is activated at the yield moment, thus requiring a rigid–plastic point hinge model, instead of elastic-plastic one (that is prescribed in the codes), while the initial stiffness must be introduced in the general properties (by section modifiers or reduced E modulus) and not in the point hinge modelling.

5.7.2.5.2 Ultimate rotation

As far as member ductility is concerned, a very precise bilinear diagram is proposed, shown in principle in Figure 5.25 of the FEMA356, while the values for this diagram are derived from tables as a function of the axial and shear stress of the element (Table 5.4).

Table 5.3 FEMA 356 cracked flexural and shear rigidity

Component	Flexural rigidity	Shear rigidity
Beams – nonprestressed	$0.5E_cI_g$	$0.4E_cA_w$
Beams – prestressed	E_cI_g	$0.4E_cA_w$
Columns with compression due to design gravity loads $\geq 0.5\ A_gf_c$	$0.7E_cI_g$	$0.4E_cA_w$
Columns with compression due to design gravity loads $\leq 0.3\ A_gf_c$ or with tension	$0.5E_cI_g$	$0.4E_cA_w$
Walls – uncracked (on inspection)	$0.8E_cI_g$	$0.4E_cA_w$
Walls – cracked	$0.5E_cI_g$	$0.4E_cA_w$
Flat slabs – nonprestressed	See FEMA 356/6.5.4.2	$0.4E_cA_g$
Flat slab – prestressed	See FEMA 356/6.5.4.2	$0.4E_cA_g$
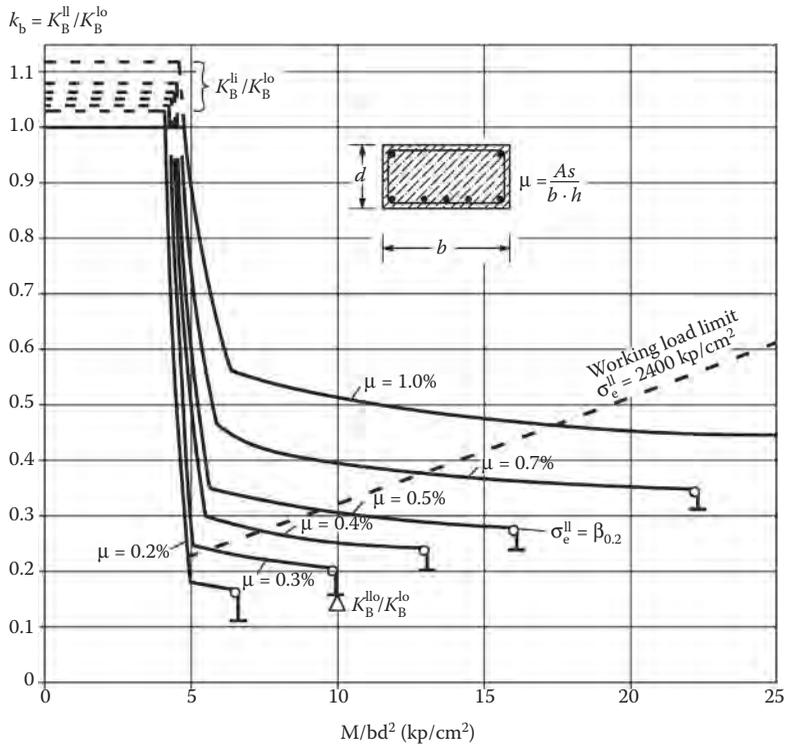
Figure 5.24 Ratio of cracked over uncracked rigidity as a function of reinforcement percentage.
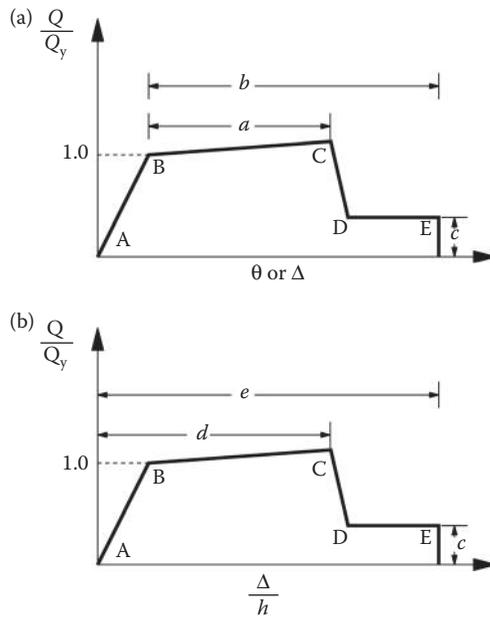
Figure 5.25 Point hinge constitutive law suggested by U.S. guidelines. (a) Deformation; (b) deformation ratio.

Table 5.4 Adaptation of the values for the point Hinge diagram of columns (FEMA 356, Tables 5.6 through 5.8) to SI units and eurocode notation

Conditions — Columns controlled by flexure			Modelling parameters			Acceptance criteria — Plastic rotation angle (rad) — Performance level — Component type				
			Plastic rotation angle (rad)		Residual strength ratio	Primary			Secondary	
$\dfrac{N_{sd}}{b \cdot d \cdot f_{ck}}$	Stirrups	$\dfrac{V_{sd}}{b_w \cdot d \cdot \sqrt{f_{ck}}}$	a	b	c	IO	LS	CP	LS	CP
≤0.1	C	≤0.25	0.02	0.03	0.2	0.005	0.015	0.02	0.02	0.03
≤0.1	C	≥0.5	0.016	0.024	0.2	0.005	0.012	0.016	0.016	0.024
≥0.4	C	≤0.25	0.015	0.025	0.2	0.003	0.012	0.015	0.018	0.025
≥0.4	C	≥0.5	0.012	0.02	0.2	0.003	0.01	0.012	0.013	0.02
≤0.1	NC	≤0.25	0.006	0.015	0.2	0.005	0.005	0.006	0.01	0.015
≤0.1	NC	≥0.5	0.005	0.012	0.2	0.005	0.004	0.005	0.008	0.012
≥0.4	NC	≤0.25	0.003	0.01	0.2	0.002	0.002	0.003	0.006	0.01
≥ 0.4	NC	≥ 0.5	0.002	0.008	0.2	0.002	0.002	0.002	0.005	0.008

EN1998-3, on the other hand, provides very detailed equations for the derivation of these values, and thus renders the whole approach very cumbersome and prone to errors.

The problem with all these data is that no analytical simulations of experimentally tested structures have been provided, making the user quite sceptic of their accuracy. This exercise, on the contrary, has been performed for some of the analytical nonlinear software packages used by academia and the results have been very encouraging (ICONS project using Adaptic, 2012; Seismostruct, 2013; Elnashai et al. (ZEUS), 2002–2005).

5.7.2.6 Safety factors

Amongst the several parameters that affect the results of nonlinear analysis is the proper use of safety factors, local and global. More specifically of interest are, for local values, the material properties safety factors and the loads safety factors, as well as the global safety factor of the structure. Indicatively, FEMA356 uses the reliability of the material factor ($k = 0.75$–1.00) and characteristic values are used for gravity loads and mean values for deformation values without any additional safety factor. The safety factors are introduced in the end results, that is, the rotational capacity of structural elements that are clearly conservative (yet quantified), and the required over available ductility that ATC40 introduces a factor of 2.50.

For EC8-3/2005 the use of safety factors depends on several aspects, as is shown in Table 5.5.

It is mainly up to the designing engineer to decide upon the safety factors introduced, and since the analysis is nonlinear and the analogy between input and output, which exists in linear analysis, is not guaranteed it indeed makes sense to use unfactored values and opt for a global safety factor in terms of ductility or displacements. However, it is suggested that in design applications (not assessment) the use of design material properties is adopted in order to safeguard against possible legal implications, thus obviously reducing the global safety factor opted for.

Table 5.5 Values of material properties and criteria for analysis and safety verifications

Type of element or mechanism (e/m)		Linear model (LM)		Nonlinear model		q-Factor approach	
		Demand	Capacity	Demand	Capacity	Demand	Capacity
	Ductile	Acceptability of Linear Model (for checking of $\rho_i = D_i/C_i$ values): From analysis. Use mean values of properties in model. Verification (if LM accepted): From analysis.	In terms of strength. Use mean values of properties. In terms of deformation. Use mean values of properties divided by CF.	From analysis. Use mean values of properties in model.	In terms of strength. Use mean values of properties divided by CF and by partial factor.	From analysis	In terms of strength. Use mean values of properties divided by CF and by partial factor.
	Brittle	Verification (if LM accepted): If $\rho_i \leq 1$: from analysis. If $\rho_i > 1$: from equilibruum with strength of ductile e/m. Use mean values of properties multiplied by CF.	In terms of strength. Use mean values of properties divided by CF and by partial factor.		In terms of strength. Use mean values of properties divided by CF and by partial factor.	In accordance with the relevant Section of EN1998-1:2004.	

5.7.3 Pushover analysis

Taking into account all the issues raised previously regarding static and dynamic nonlinear analysis currently, the nonlinear method used for design purposes (FEMA 356, ATC40, EC8-1/2004) is the static nonlinear analysis, widely known as 'pushover'. According to EC8-1/2004 it is defined as 'a non-linear static analysis carried out under conditions of constant gravity loads and monotonically increasing horizontal loads'.

The static nonlinear analysis produces as a basic result the *P*–δ curve of the building, which demonstrates the capacity of the building to lateral loads (depicts the base shear capacity over lateral displacement). This curve corresponds to the multi-degree-of-freedom (MDOF) system, which with appropriate coefficients is transformed to the curve of the equivalent single-degree-of-freedom (SDOF) system oscillator called capacity spectrum (Figure 5.26).

Additionally, the displacement pattern and condition (level of developed nonlinearity) of each structural element is produced for each time step.

Three key points are defined on the capacity spectrum of a building:

- Yield capacity: Corresponds to the base shear which limits the linear-elastic behaviour of the building.
- Design capacity: Correspond to the design base shear, which should be less than the yield base shear as safety factor for materials are used, as well as construction guidelines (minimum reinforcement, stirrups, capacity rules, etc.), which increase the actual base shear capacity.
- Ultimate capacity: Correspond to the maximum base shear when the building has been fully plasticised.

The following approximate relations connect those key points:

$$YC\ (V_y, \Delta_y)\text{: } V_y\ =\ \gamma C_s \qquad \Delta_y\ =\ \frac{V_y}{4\pi^2} T^2 \tag{5.73}$$

$$UC\ (V_u, \Delta_u)\text{: } V_u\ =\ \lambda V_y\ =\ \lambda\gamma C_s \quad \Delta_u\ =\ \lambda\mu V_y\ =\ \lambda\mu\gamma C_s \frac{T^2}{4\pi^2} \tag{5.74}$$
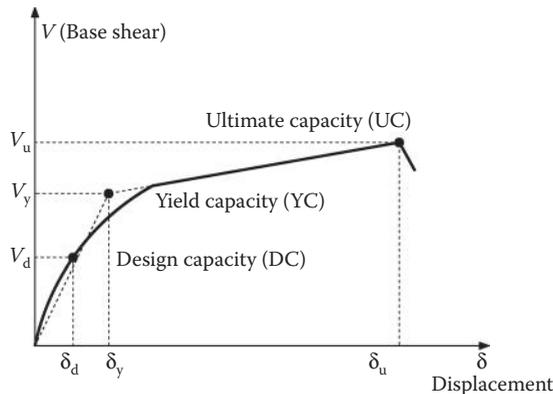
Figure 5.26 Capacity spectrum.

where

C_s is the seismic coefficient (percentage of building effective weight).

T is the elastic fundamental period of the building.

γ is the design overstrength factor (yield base shear/design base shear).

λ is the actual overstrength factor (ultimate base shear/yield base shear).

μ is the total ductility factor $= \delta_u/\delta_y$.

From the above relations the building behaviour factor (q) may be defined as

$$q = q_{os} \cdot q_\zeta \cdot q_\mu$$

where

q_{os} is the overstrength behaviour factor $q_{os} = 0.50(V_u + V_y)/V_d.$

q_ζ is the damping behaviour factor $= 1.0$ for R/C buildings.

$$q_\mu: \begin{cases} \text{Ductility behaviour factor} = \mu & \text{for } T > 0.50 \text{ s} \\ \text{Ductility behaviour factor} = 1/\sqrt{2\mu - 1} & \text{for } T < 0.50 \text{ s} \end{cases}$$

as shown in Subsection 2.3.4.

5.7.4 Pros and cons of pushover analysis

Static nonlinear analysis facilitates the assessment of the behaviour of a structure by calculating the available strength capacity of the structural elements and the corresponding deformations (ductilities) and comparing them to the corresponding demands as defined for the design earthquake. The assessment is based on several parameters of structural behaviour as total drift, interstorey drifts, required ductilities versus available ductility, node loads and element loads. The key benefit in using pushover analysis is that the designer has an estimate of the developed forces and deformations as the building enters the nonlinear range, taking into account the changes in the stiffness of the individual members and the redistribution of forces that take place.

The basic data that result from a pushover analysis, and not from an elastic static or dynamic analysis, are the following:

- Realistic values of forces on brittle elements such as short columns, coupling beams or high-depth beams and so on.
- Estimate of the total (inelastic) deformations that must develop at critical parts of structural elements so that the structure can dissipate the seismic energy.
- Effect of the yield or failure of a structural element on the overall behaviour of the structure and the redistribution of forces.
- Pinpointing of the critical areas of elements that require high available ductility.
- Highlighting of structural asymmetries in plan or along height, resulting from the plasticisation of critical elements that affect the structural and dynamic behaviour of the building (torsional effects, infill walls, soft storeys).
- Soft storey identification, either due to abrupt changes in stiffness, or more importantly due to abrupt changes in strength, along the height.
- Capability of modelling and assessing the effect of infills, which when distributed unevenly seriously alter the desired behaviour of a building.

The accuracy and validity of all of the aforementioned results depends highly on the assumptions and modelling approaches used during the analysis, especially regarding hysteretic behaviour of materials or whole elements, the load pattern and/or the corresponding displacement pattern and so on. Useful for the better understanding of the limits and capabilities of the pushover analysis is the following brief demonstration of principles upon which the method is based.

Pushover analysis and the assessment of buildings based upon it rely on the following two assumptions:

1. The response of a MDOF system that can be accurately represented by an equivalent SDOF system even in post-elastic range.
2. The behaviour is guided by a modeshape that remains constant during the duration of the excitation.

It is obvious that both assumptions are not entirely accurate; however, several parametric studies have shown that the estimate of the maximum seismic response of MDOF systems is acceptable provided that the behaviour is indeed guided by one modeshape (Figure 5.27; Fajfar and Fischinger, 1994; Saiidi and Sozen, 1981).

Regarding the second assumption, the works of Elnashai (2000) and Antoniou et al. (2002) demonstrate an extended pushover analysis, called adaptive pushover, which takes into account the following:

1. The changes (shifts) of the eigen modes, as several elements yield and cause a change in the stiffness matrix (K) of the structure, are taken into account by performing an eigenmode analysis at every 'significant' change of the stiffness matrix.
2. Higher significant eigen modes are taken into account corresponding to their participation mass ratio, as it results from the eigen analysis.
3. Use of the spectra of the specific excitations considered, from which the participating ratios are weighted.

Results based on this type of analysis, of buildings sensitive to pushover analysis, are extremely close to ones by nonlinear time-history dynamic analysis for different levels of excitation. Indicative application of the method on an eight-storey non-symmetric moment resisting frame (MRF), a 12-storey symmetric MRF and an eight-storey dual system have been presented in the work of Antoniou et al. (2002). Figure 5.28 shows the accuracy of the method compared to the nonlinear *t-h* analysis and the triangular and uniform distribution of loads for pushover analysis.

$$m^* = \Sigma m_i \, \Phi_i$$

$$k^* = F_y^*/D_y^*$$

$$T^* = 2\pi \sqrt{m^*/k^*}$$
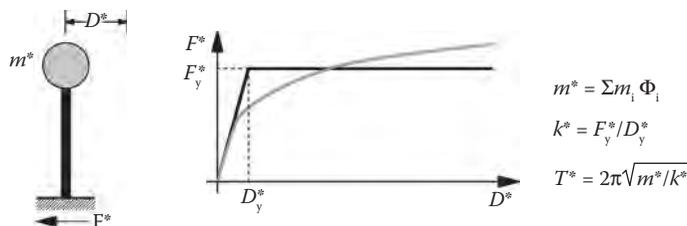
Figure 5.27 Equivalent SDOF system. (From Fajfar, P. and Dolsek, M. 2000. A transparent nonlinear method for seismic performance evaluation. *3rd Workshop of the Japan-UK Seismic Risk Forum, Proceedings*, Imperial College Press, 2000.)
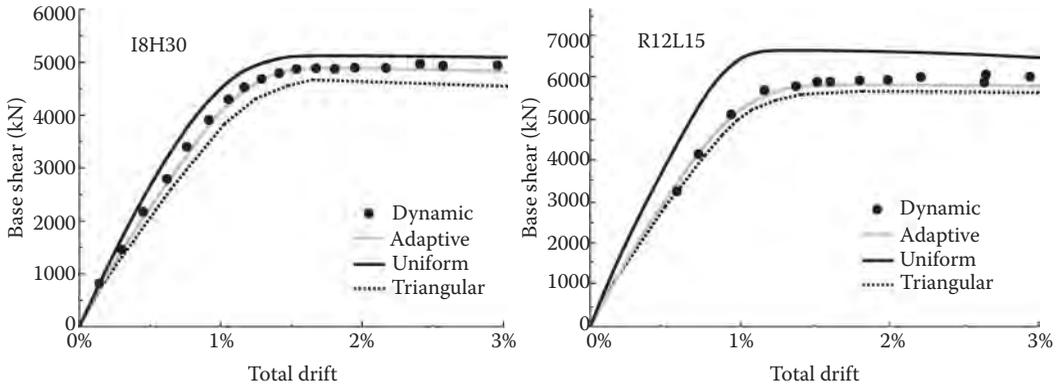
Figure 5.28 Adaptive pushover, pushover and nonlinear *T-h*: (a) asymmetric system of high ductility; (b) symmetric system of low ductility.

5.7.5 Equivalent SDOF systems

In modern earthquake engineering the seismic excitation is either defined by design spectra or accelerograms; however, in codified design the input is always defined, or at least correlated to spectra, which provide information about the acceleration and/or displacement of SDOF systems. Therefore, it is essential to correlate the results of the pushover analysis, which corresponds the MDOF system to the properties of an equivalent SDOF system, taking into account the nonlinearity of the response both in terms of forces (base shear) and deformations. This is tackled by the use of an equivalent SDOF oscillator, a version of which is presented in the following two paragraphs, the first referring to the typical translational case, while the latter in the case of translational and rotational (torsional) behaviour.

5.7.5.1 Equivalent SDOF for torsionally restrained buildings

Several different approaches for the definition of the equivalent SDOF oscillator are available in literature, yet all start using the basic assumption that the deformation of the MDOF system may be described by a deformation vector $[\Phi]$, which remains constant through the loading time-history, regardless of the magnitude of the applied deformation.

In this paragraph the well-known methodology for the definition of the SDOF oscillator for translational behaviour of spatial (3-D) structures, which was developed in the early work of Saiidi and Sozen, 1981 (Krauwinkler and Nassar, 1992) is presented, while in the next paragraph, an adaptation for translational and torsional deformation (asymmetric buildings) will be presented.

The equation describing the dynamic elastic response of the system (Figure 5.29) to excitation in vector form is

$$[M][\ddot{u}(t)] + [C][\dot{u}(t)] + [P(t)] = -[M][1]\ddot{u}_\mathrm{o}(t) \tag{5.75}$$

By eliminating the damping terms from Equation 5.75 $[C][\dot{u}(t)]$, Equation 5.76 results:

$$[M][\ddot{u}(t)] + [P(t)] = -[M][1]\ddot{u}_\mathrm{o}(t) \tag{5.76}$$
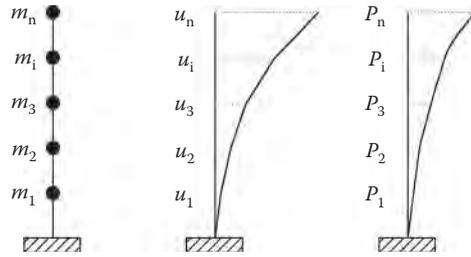
Figure 5.29 Modal deformation of a torsionally insensitive (translational) MDOF system.

where:

$$[M] = \begin{bmatrix} m_1 & 0 & - & 0 \\ 0 & m_2 & - & 0 \\ - & - & - & - \\ 0 & 0 & - & m_n \end{bmatrix}_n \quad \text{is the mass matrix}$$

$$[u] = \begin{bmatrix} u_1 \\ u_2 \\ - \\ u_n \end{bmatrix}, \text{ displacement vector}$$

$$[P] = \begin{bmatrix} P_1 \\ P_2 \\ - \\ P_n \end{bmatrix}, \text{ restoring force (internal) vector}$$

It is assumed that the displacement $[u]$ and the restoring force $[P]$ of the elastic MDOF system can be correlated to the corresponding parameters of the equivalent SDOF nonlinear oscillator u_n and P_n as a function of two vectors $[\Phi]$ and $[\Psi]$:

$$[u(t)] = [\Phi]u_n(t) = \begin{bmatrix} \varphi_1 \\ \varphi_2 \\ - \\ \varphi_n \end{bmatrix} u_n(t) \tag{5.77}$$

$$[P] = [\Psi]P_n(t) = \begin{bmatrix} \psi_1 \\ \psi_2 \\ - \\ \psi_n \end{bmatrix} P_n(t) \tag{5.78}$$

Therefore, using these transformations, the equation of vibration of the MDOF system becomes, in vector form:

$$[M][\Phi]\ddot{u}_n(t) + [\psi]P_n(t) = -[M][1]\ddot{u}_o(t) \qquad (5.79a)$$

And in algebraic form

$$\left. \begin{array}{l} m_1\varphi_1\ddot{u}_n(t) + \psi_1 P_n = -m_1\ddot{u}_o(t) \\ m_2\varphi_2\ddot{u}_n(t) + \psi_2 P_n = -m_2\ddot{u}_o(t) \\ \text{----------------------------------} \\ m_n\varphi_n\ddot{u}_n(t) + \psi_n P_n = -m_n\ddot{u}_o(t) \end{array} \right\} \qquad (5.79b)$$

By multiplying Equation (5.79a) times $[\Phi]^T$:

$$[\Phi]^T[M][\Phi]\ddot{u}_n(t) + [\Phi]^T[\Psi]P_n(t) = -[\Phi]^T[M]\{1\}\ddot{u}_o(t) \qquad (5.80)$$

and by transforming the first term:

$$[\Phi]^T[M][\Phi]\frac{[\Phi]^T[M]\{1\}}{[\Phi]^T[M]\{1\}}\ddot{u}_n(t) + [\Phi]^T[\Psi]P_n(t) = -[\Phi]^T[M]\{1\}\ddot{u}_o(t) \qquad (5.81a)$$

or

$$[\Phi]^T[M]\{1\}\frac{[\Phi]^T[M][\Phi]}{[\Phi]^T[M]\{1\}}\ddot{u}_n(t) + [\Phi]^T[\Psi]P_n(t) = -[\Phi]^T[M]\{1\}\ddot{u}_o(t) \qquad (5.81b)$$

We define

$$u^* = \frac{[\Phi]^T[M][\Phi]}{[\Phi]^T[M]\{1\}}u_n(t) \qquad (5.82a)$$

$$m^* = [\Phi]^T[M]\{1\} \qquad (5.82b)$$

so, Equation 5.81a becomes in vector form:

$$m^*\ddot{u}^*(t) + [\Phi]^T[\Psi][P_n(t)] = -m^*\ddot{u}_o(t) \qquad (5.83)$$

While Equations 5.82a and 5.82b are in algebraic form:

$$m^* = m_1\varphi_1 + m_2\varphi_2 + \cdots + m_n\varphi_n = \sum_1^n m_i\varphi_i$$

$$[\Phi]^T[M][\Phi] = m_1\varphi_1^2 + m_2\varphi_2^2 + \cdots + m_n\varphi_n^2 = \sum_1^n m_i\varphi_i^2$$

$$[\Phi]^T[\Psi] = \sum_1^n \psi_i\varphi_i$$

meaning

$$m^* = \sum_1^n m_i \varphi_i \tag{5.84a}$$

$$u_n^*(t) = \frac{\sum_1^n m_i \varphi_i^2}{\sum_1^n m_i \varphi_i} u_n(t) \tag{5.84b}$$

$$[\Phi]^T[\Psi] = \sum_1^n \psi_i \varphi_i \tag{5.84c}$$

Equation 5.83 by introducing Equations 5.84a through 5.84c is transformed to

$$\left[\sum_1^n m_i \varphi_i \right] \ddot{u}^*(t) + \left[\sum_1^n m_i \psi_i \right] P_n(t) = -\left[\sum_1^n m_i \varphi_i \right] \ddot{u}_o(t) \tag{5.85a}$$

Taking into account that,

$$\left[\sum_1^n m_i \psi_i \right] P_n(t) = V(t) \quad \text{or} \quad P_n(t) = \frac{V(t)}{\left[\sum_1^n m_i \psi_i \right]} \tag{5.86}$$

where V is the base shear of the MDOF excited system

Equation 5.85a may be re-written as

$$m^* \ddot{u}^*(t) + \frac{\sum_1^n \varphi_i \psi_i}{\sum_1^n \psi_i} V(t) = -m^* \ddot{u}_o(t) \tag{5.85b}$$

This corresponds to an SDOF system, which has defined the following properties:

$$m^* = [\Phi]^T[M]\{1\} = \sum_1^n m_i \varphi_i$$

(see Equation 5.84a)

$$V^*(t) = \frac{[\Phi]^T[\Psi]}{\{1\}^T[\Psi]} V(t) = \frac{\sum_1^n \varphi_i \psi_i}{\sum_1^n \psi_i} V(t) \tag{5.87}$$

where $m^*, u^*(t), V^*$ are the mass, displacement and base shear of the equivalent SDOF oscillator.

The equation of vibration under excitation for this SDOF system is

$$m^* \ddot{u}^*(t) + V^*(t) = -m^* \ddot{u}_o(t) \tag{5.88}$$

having

$$u^*(t) = \Gamma_1 u(t) \tag{5.89a}$$

$$V^*(t) = \Gamma_2 V(t) \tag{5.89b}$$

$$\Gamma_1 = \frac{[\Phi]^T[M][\Phi]}{[\Phi]^T[M]\{1\}} = \frac{\sum_1^n m_i \varphi_i^2}{\sum_1^n m_i \varphi_i} \tag{5.89c}$$

$$\Gamma_2 = \frac{[\Phi]^T[\Psi]}{\{1\}^T[\Psi]} = \frac{\sum_1^n \varphi_i \psi_i}{\sum_1^n \psi_i} \tag{5.89d}$$

By introducing

$$\psi_i = \varphi_i$$

one gets

$$\Gamma_2 = \frac{\sum_1^n \varphi_i^2}{\sum_1^n \varphi_i} \tag{5.90a}$$

and for $m_i = m = $ constant

$$\Gamma_1 = \frac{\sum_1^n m_i \varphi_i^2}{\sum_1^n m_i \varphi_i} = \frac{m \sum_1^n \varphi_i^2}{m \sum_1^n \varphi_i} = \Gamma_2 \tag{5.90b}$$

so in the end one factor Γ is used, with

$$\Gamma = \frac{\sum_1^n \varphi_i^2}{\sum_1^n \varphi_i} \tag{5.91}$$

This transformation factor is denoted as Γ in the Annex B of EC8-1/2004, Equation B3:

$$\Gamma = \frac{m^*}{\sum_1^n m_i \varphi_i^2} = \frac{\sum_1^n m_i \varphi_i}{\sum_1^n m_i \varphi_i^2} \tag{5.92}$$

5.7.5.2 Equivalent SDOF for torsionally unrestrained buildings

This approach uses for the definition of the response quantities a generalised equivalent SDOF system with both translational and torsional response, by extending the methodology

presented in the previous paragraph, wherein only the translational characteristics were accounted for.

Consider a multi-storey monosymmetric (i.e. stiffness symmetric with respect to one axis only, in the case of Figure 5.30, the horizontal axis) building (Pauley, 1996, 1997). The centre of mass is denoted as CM and the centre of resistance as CR. The equations describing the dynamic elastic response of the system to excitation in one direction (here, the y-direction) for an undamped system are (Chopra, 1995):

1st storey

$$m_1 \ddot{u}_{y1}(t) + \sum_{j=1}^{n} u_{yj}(t) \cdot \sum_{1}^{i} k_{yi1j} + \sum_{j=1}^{n} \theta_{z1} \cdot \sum_{1}^{i} k_{yi1j}\alpha_{xi1} = -m_1 \ddot{u}_{oy}(t)$$

$$m_1 r_1^2 \ddot{\theta}_{z1}(t) + \sum_{j=1}^{n} u_y(t) \sum_{1}^{i} \alpha_{xi1} k_{yi1j} + \sum_{j=1}^{n} \theta_{zj}(t)\left(\sum_i k_{t1j} + \sum_i \alpha_{yi1}^2 k_{xi1j} + \sum_i \alpha_{xi1}^2 k_{yi1}\right) = 0$$

jth storey

$$m_j \ddot{u}_{yj}(t) + \sum_{j=1}^{n} u_{yj}(t) \cdot \sum_{1}^{i} k_{yijj} + \sum_{j=1}^{n} \theta_{zj} \cdot \sum_{1}^{i} k_{yijj}\alpha_{xij} = -m_j \ddot{u}_{oy}(t)$$

(5.93a)

$$m_j r_j^2 \ddot{\theta}_{zj}(t) + \sum_{j=1}^{n} u_{yj}(t) \sum_{1}^{i} \alpha_{xij} k_{yijj} + \sum_{j=1}^{n} \theta_{zj}(t)\left(\sum_i k_{tij} + \sum_i \alpha_{yij}^2 k_{xijj} + \sum_i \alpha_{xij}^2 k_{yij}\right) = 0$$

nth storey

$$m_n \ddot{u}_{yn}(t) + \sum_{j=1}^{n} u_{yj}(t) \cdot \sum_{1}^{i} k_{yinj} + \sum_{j=1}^{n} \theta_{zn} \cdot \sum_{1}^{i} k_{yinj}\alpha_{xin} = -m_n \ddot{u}_{oy}(t)$$

$$m_n r_n^2 \ddot{\theta}_{zn}(t) + \sum_{j=1}^{n} u_y(t) \sum_{1}^{i} \alpha_{xin} k_{yinj} + \sum_{j=1}^{n} \theta_{zj}(t)\left(\sum_i k_{tnj} + \sum_i \alpha_{yin}^2 k_{xinj} + \sum_i \alpha_{xin}^2 k_{yin}\right) = 0$$
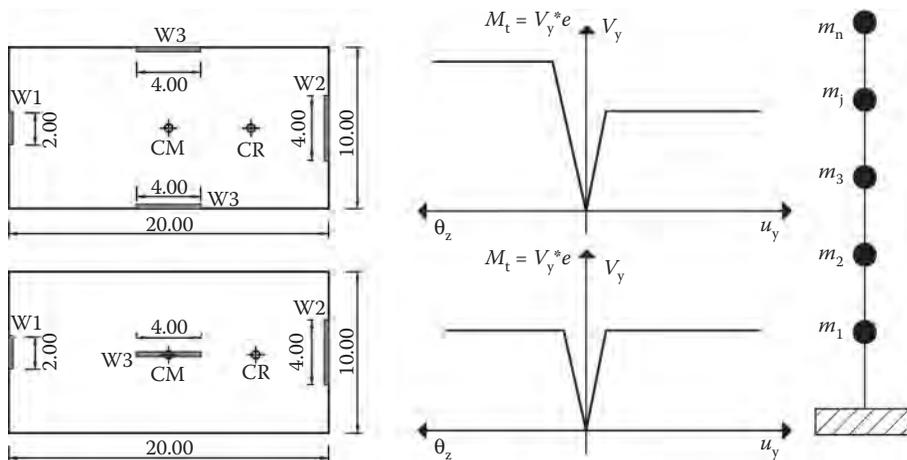
Figure 5.30 Torsionally restrained (TR-top) and torsionally unrestrained (TUR-bottom) multi-storey buildings.

or, in vector notation

$$\{M\}\{\ddot{u}\} + \{K\}\{u\} = \{M\}\{\delta\}\ddot{u}_{oy}(t) \tag{5.93b}$$

where

$$
M = \begin{bmatrix}
m_1 & 0 & \dots & 0 & 0 & \dots & 0 & 0 \\
0 & m_1 r_1^2 & 0 & 0 & 0 & 0 & 0 & 0 \\
0 & 0 & 0 & 0 & 0 & 0 & 0 & 0 \\
0 & 0 & \dots & m_j & 0 & \dots & 0 & 0 \\
0 & 0 & 0 & 0 & m_j r_j^2 & 0 & 0 & 0 \\
0 & 0 & \dots & 0 & 0 & \dots & 0 & 0 \\
0 & 0 & 0 & & 0 & 0 & m_n & \\
0 & 0 & \dots & 0 & 0 & \dots & 0 & m_n r_n^2
\end{bmatrix}
$$

$$
K = \begin{bmatrix}
K_{11} & K_{12} & \dots & K_{1,2\cdot j-1} & K_{1,2\cdot j} & \dots & K_{1,n-1} & K_{1,2\cdot n} \\
K_{21} & K_{22} & \dots & K_{2,2\cdot j-1} & K_{2,2\cdot j} & \dots & K_{2,n-1} & K_{2,2\cdot n} \\
\vdots & \vdots & \vdots & \vdots & \vdots & \vdots & \vdots & \vdots \\
K_{2\cdot j-1,1} & K_{2\cdot j-1,2} & \dots & K_{2\cdot j-1,2\cdot j-1} & K_{2\cdot j-1,2\cdot j} & \dots & K_{2\cdot j-1,2\cdot n-1} & K_{2\cdot j-1,2\cdot n} \\
K_{2\cdot j,1} & K_{2\cdot j,2} & \dots & K_{2\cdot j,2\cdot j-1} & K_{2\cdot j,2\cdot j} & \dots & K_{2\cdot j,2\cdot n-1} & K_{2\cdot j,2\cdot n} \\
\vdots & \vdots & \vdots & \vdots & \vdots & \vdots & \vdots & \vdots \\
K_{2\cdot n-1,1} & K_{2\cdot n-1,2} & \dots & K_{2\cdot n-1,2\cdot j-1} & K_{2\cdot n-1,2\cdot j} & \dots & K_{2\cdot n-1,2\cdot n-1} & K_{2\cdot n-1,2\cdot n} \\
K_{2\cdot n,1} & K_{2\cdot n,2} & \dots & K_{2\cdot n,2\cdot j-1} & K_{2\cdot n,2\cdot j} & \dots & K_{2\cdot n,2\cdot n-1} & K_{2\cdot n,2\cdot n}
\end{bmatrix}
$$

$$
\{\delta\} = \begin{bmatrix} 1 \\ 0 \\ \vdots \\ 1 \\ 0 \\ \vdots \\ 1 \\ 0 \end{bmatrix}
\{\ddot{u}\} = \begin{bmatrix} \ddot{u}_{y1} \\ \ddot{\theta}_{z1} \\ \vdots \\ \ddot{u}_{yj} \\ \ddot{\theta}_{zj} \\ \vdots \\ \ddot{u}_{yn} \\ \ddot{\theta}_{zn} \end{bmatrix},
\{u\} = \begin{bmatrix} u_{y1} \\ \theta_{z1} \\ \vdots \\ u_{yj} \\ \theta_{zj} \\ \vdots \\ u_{yn} \\ \theta_{zn} \end{bmatrix}
$$

and

$$K_{11} = \sum_1^i k_{yi1,1} \quad K_{12} = \sum_1^i k_{yi1,1}\alpha_{xi1}$$

$$K_{21} = \sum_1^i k_{yi1,1}\alpha_{xi1} \quad K_{22} = \sum_1^i k_{ti1,1} + \sum_1^i \alpha_{yi1}^2 k_{xi1,1} + \sum_1^i \alpha_{xi1}^2 k_{yi1,1}$$

....

$$K_{2j-1,2j-1} = \sum_1^i k_{yij,j} \quad K_{2j-1,2j} = \sum_1^i k_{yij,j}e_{xij}$$

$$K_{2j,2j-1} = \sum_{1}^{i} k_{yij,j}\alpha_{xij} \quad K_{2j,2j} = \sum_{1}^{i} k_{tij,j} + \sum_{1}^{i} \alpha_{yij}^2 k_{xij,j} + \sum_{1}^{i} \alpha_{xij}^2 k_{yij,j}$$

....

$$K_{2n-1,2n-1} = \sum_{1}^{i} k_{yin,n} \quad K_{2n-1,2n} = \sum_{1}^{i} k_{yin,n}\alpha_{xin}$$

$$K_{2n,2n-1} = \sum_{1}^{i} k_{yin,n}\alpha_{xin} \quad K_{2n,2n} = \sum_{1}^{i} k_{tin,n} + \sum_{1}^{i} \alpha_{yin}^2 k_{xin,n} + \sum_{1}^{i} \alpha_{xin}^2 k_{yin,n}$$

where

$m_1,\dots m_j,\dots m_n$ are the vibrating masses on storey 1, j and n, respectively.

k_{xi1j}, k_{yi1j} are the translational stiffnesses of individual resisting element (i) in the x- and y-directions, respectively, on storey 1 for unit displacement of storey j.

$k_{ti,1,j}$ are the rotational stiffnesses of individual resisting element (direction zz) on storey 1 for unit rotation of storey j.

α_{xij}, α_{yij} are the distances from individual resisting element i to the centre of mass (C_M) in x and y direction, respectively, on storey j.

$u_{yj}(t)$, $\theta_{zj}(t)$ are the displacement and rotation of the C_M as a function of time, on storey j.

$\ddot{u}_{oy}(t)$ is the excitation acceleration, as a function of time.

$\ddot{u}_{yj}(t), \ddot{\theta}_{zj}(t)$ are the second derivatives of $u_y(t)$ and $\theta_z(t)$ with respect to time (translational and angular accelerations) on storey j.

In order to approximate the inelastic dynamic vibration of the system with an equivalent static one, by analogy to the case of translational multi-DOF system (presented in the previous paragraph), the following assumption is adopted:

$$\{u\} = \begin{bmatrix} u_{y1} \\ \theta_{z1} \\ \vdots \\ u_{yj} \\ \theta_{zj} \\ \vdots \\ u_{yn} \\ \theta_{zn} \end{bmatrix} = \begin{bmatrix} \varphi_{yo1} \\ \varphi_{z02} \\ \vdots \\ \varphi_{y0j} \\ \varphi_{z0j} \\ \vdots \\ \varphi_{y0n} \\ \varphi_{z0n} \end{bmatrix} \cdot \bar{u}_y(t) \quad \text{or} \quad \{u\} = \{\varphi_0\}\bar{u}_y(t) \tag{5.94}$$

and

$$\{p\} = \begin{bmatrix} V_{y1} \\ M_{t1} \\ \vdots \\ V_{yj} \\ M_{tj} \\ \vdots \\ V_{yn} \\ M_{tn} \end{bmatrix} = \begin{bmatrix} \psi_{Po1} \\ \psi_{Mo1} \\ \vdots \\ \psi_{P0j} \\ \psi_{M0j} \\ \vdots \\ \psi_{P0n} \\ \psi_{M0n} \end{bmatrix} \cdot \bar{p}(t) \quad \text{or} \quad \{p\} = \{\psi_o\}\bar{p}(t) \tag{5.95}$$

where

V_{yj}, M_{tj} are the generalised lateral force and torque at the CM of storey j.

$\bar{u}_y(t), \bar{p}(t)$ are the 'dummy' time functions of displacement and force, respectively.

Hence, the assumption made is that the storey displacements (u_{yi}, θ_{zi}), as well as the story forces, are expressed as a function of time using the preselected vectors φ_o (normalised spectral modal displacements u_{ymax}, θ_{ymax}) and ψ_o (normalised spectral modal loads V_{max}, M_{max}), and corresponding dummy functions that will be eliminated at the end of the procedure, hence need no explicit definition.

Referring to Equation 5.93a, the term

$$\sum_{j=1}^{n} u_{yj}(t) \cdot \sum_{1}^{i} k_{yijj} + \sum_{j=1}^{n} \theta_{zj} \cdot \sum_{1}^{i} k_{yijj} e_{xij}$$

expresses the generalised lateral restoring force for storey j, $\psi_{poj}\bar{p}(t)$,

$$\sum_{j=1}^{n} u_{yj}(t) \cdot \sum_{1}^{i} k_{yijj} + \sum_{j=1}^{n} \theta_{zj} \cdot \sum_{1}^{i} k_{yijj} e_{xij} = \psi_{poj}\bar{p}(t) \tag{5.96a}$$

while the term

$$\sum_{j=1}^{n} u_y(t) \sum_{1}^{i} e_{xi1} k_{yi1j} + \sum_{j=1}^{n} \theta_{zj}(t) \left(\sum_i k_{t1j} + \sum_i e_{yi1}^2 k_{xi1j} + \sum_i e_{xi1}^2 k_{yi1} \right)$$

expresses the generalised restoring torque for storey j, $\psi_{Moj}\bar{p}(t)$.

$$\sum_{j=1}^{n} u_y(t) \sum_{1}^{i} e_{xi1} k_{yi1j} + \sum_{j=1}^{n} \theta_{zj}(t) \left(\sum_i k_{t1j} + \sum_i e_{yi1}^2 k_{xi1j} + \sum_i e_{xi1}^2 k_{yi1} \right) = \psi_{Moj}\bar{p}(t) \tag{5.96b}$$

In the previous definitions the terms expressing the restoring forces of the elastic MDOF system have been replaced by the forces calculated for the inelastic SDOF system.

Using these definitions, Equations 5.93a and 5.93b are reduced to the following:

1st storey

$m_1 \varphi_{y01} \ddot{\bar{u}}_y(t) + \psi_{P01}\bar{p}(t) = -m_1 \ddot{u}_{oy}(t)$

$m_1 r_1^2 \varphi_{z01} \ddot{\bar{u}}_y(t) + \psi_{M01}\bar{p}(t) = 0$

jth storey

$m_j \varphi_{y0j} \ddot{\bar{u}}_y(t) + \psi_{P0j}\bar{p}(t) = -m_j \ddot{u}_{oy}(t)$ $\qquad$ (5.97a)

$m_j r_j^2 \varphi_{z0j} \ddot{\bar{u}}_y(t) + \psi_{M0j}\bar{p}(t) = 0$

nth storey

$m_n \varphi_{y0n} \ddot{\bar{u}}_y(t) + \psi_{P0n}\bar{p}(t) = -m_n \ddot{u}_{oy}(t)$

$m_n r_n^2 \varphi_{z0n} \ddot{\bar{u}}_y(t) + \psi_{M0n}\bar{p}(t) = 0$

or, in vector notation

$$\{M\}\{\varphi_0\}\ddot{\bar{u}}_y + \{\psi_o\}\bar{p}(t) = -\{M\}\{\delta\}\ddot{u}_{oy}(t) \tag{5.97b}$$

Pre-multiplying 5.97b by $\{\varphi_o\}^T$, the following equation is derived:

$$\{\varphi\}^T\{M\}\{\varphi_0\}\ddot{\bar{u}}_y + \{\varphi_0\}^T\{\psi_o\}\bar{p}(t) = -\{\varphi_0\}^T\{M\}\{\delta\}\ddot{u}_{oy}(t) \tag{5.98}$$

Taking into account that the lateral storey force (storey shear) can be defined as

$$V_y(t) = \{\delta\}\{h\} = \{\delta\}\{\psi_o\}\bar{p}(t) = \sum_{j=1}^n \psi_{P0j} \cdot \bar{p}(t) \tag{5.99a}$$

it follows that

$$\bar{p}(t) = \frac{V_y(t)}{\{\delta\}^T\{\psi_0\}} = \frac{V_y(t)}{\displaystyle\sum_{j=1}^n \psi_{P0j}} \tag{5.99b}$$

Equation 5.98 can be transformed as follows:

$$\boxed{\{\varphi_0\}^T\{M\}\{\varphi_0\}\ddot{\bar{u}}_y + \frac{\{\varphi_0\}^T\{\psi_o\}V_y(t)}{\{\delta\}^T\{\psi_0\}} = -\{\varphi_0\}^T\{M\}\{\delta\}\ddot{u}_{oy}(t)} \tag{5.100}$$

In order to proceed, the following notation is adopted

$$m^* = \{\varphi_0\}^T\{M\}\{\delta\} = \sum_{j=1}^n m_j\varphi_{y0j} \tag{5.101a}$$

$$u_y^*(t) = \Gamma_1\bar{u}_y(t) \tag{5.101b}$$

$$V_y^*(t) = \Gamma_2 V_y(t) \tag{5.101c}$$

where

$$\Gamma_1 = \frac{\{\varphi_o\}^T\{M\}\{\varphi_o\}}{m^*} = \frac{\displaystyle\sum_{j=1}^n m(\varphi_{yoj}^2 + r^2\varphi_{zoj}^2)}{\displaystyle\sum_{j=1}^n m_j\varphi_{yoj}} \tag{5.102a}$$

$$\Gamma_2 = \frac{\{\varphi_o\}^T\{\psi_o\}}{\{\delta\}^T\{\psi_0\}} = \frac{\displaystyle\sum_{j=1}^n (\varphi_{yoj}\psi_{poj} + \varphi_{zoj}\psi_{Moj})}{\displaystyle\sum_{j=1}^n \psi_{P0j}} \tag{5.102b}$$

$m^*, u_y^*(t), V_y^*$: are the mass, displacement and base shear of the equivalent SDOF oscillator, respectively.

Introducing the foregoing notation into Equation 5.100 the following expression is obtained:

$$m^* \ddot{u}_y^*(t) + V_y^*(t) = -m^* \ddot{u}_{oy}(t) \tag{5.103}$$

Equation 5.103 describes the inelastic response of the equivalent SDOF oscillator, while Equations 5.101 and 5.102 describe the relationship between the multi-storey 3-D building (modelled as an MDOF system) and the equivalent SDOF oscillator.

For the case of a single storey building, Equations 5.101 and 5.102 are simplified as follows:

$$m^* = \{\varphi\}^T \{M\}\{\delta\} = m\varphi_{yo} \tag{5.101a'}$$

$$u_y^*(t) = \Gamma_1 \bar{u}_y(t) \tag{5.101b'}$$

$$V_y^*(t) = \Gamma_2 V_y(t) \tag{5.101c'}$$

where

$$\Gamma_1 = \frac{\{\varphi_o\}^T \{M\}\{\varphi_o\}}{m^*} = \frac{m\varphi_{yo}^2 + mr^2\varphi_{zo}^2}{m\varphi_{yo}} \tag{5.102a'}$$

$$\Gamma_2 = \frac{\{\varphi\}^T \{\psi_o\}}{\psi_{po}} = \frac{\varphi_{yo}\psi_{po} + \varphi_{zo}\psi_{Mo}}{\psi_{po}} \tag{5.102b'}$$

For the application of the methodology it is proposed that a single pushover analysis is used. The load vector is the set of storey forces causing the elastic spectral modal displacements of the building. As one may observe, this vector is slightly different from the spectral modal loads. The spectral modal displacements are a vector resulting by applying the SRSS rule at the displacement caused by the contribution of each mode, while the spectral modal loads are a vector resulting by applying the SRSS rule on each mode base shear contribution. The required vector may be correctly obtained as the storey shears, when applying the spectral modal displacement vector as a displacement constraint.

This methodology has been applied by Penelis and Kappos (2005) in single- and multi-storey buildings. For the single-storey buildings (Figure 5.30), Table 5.6 summarises the results for four different sets of accelerograms (3–10 excitations each), where the target displacements and rotations vary around 10% from the corresponding dynamic *t-h* results.

For the multi-storey buildings (Figure 5.31), Table 5.7 summarises the results for four different sets of accelerograms (3–10 excitations each), where the target displacements and rotations vary around 20% from the corresponding dynamic *t-h* results.

Indicative graphical representation, in Figures 5.32 and 5.33, which show the *t-h* results using inelastic dynamic analysis (IDA) and the corresponding pushover for the cases of torsionally restrained (TR) and torsionally unrestrained (TUR) single-storey buildings, and in Figure 5.34 for a multi-storey building, confirms the validity of the method.

It is useful to note here that, torsionally, unrestrained buildings demonstrated significant scatter in the resulting torsional rotations, even for inelastic dynamic analysis, as it is evident

Table 5.6 Proposed pushover response versus *t–h* nonlinear analysis

	Dynamic		Static	
Torsionally restrained single-storey building				
Q1 set	Mean	c.o.v.	Pushover	Diff.%
uy (cm)	0.792	12.86%	0.824	4.02%
Θz (rad)	4.96E–02	14.93%	5.30E–04	6.90%
Q2 set	Mean	c.o.v.	Pushover	Diff.%
uy (cm)	0.799	1.38%	0.783	2.06%
Θz (rad)	4.69E–04	0.73%	5.30E–04	4.94%
Q3 set	Mean	c.o.v.	Pushover	Diff.%
uy (cm)	1.034	32.54%	0.954	7.70%
Θz (rad)	4.90E–04	33.61%	4.41E–04	10.17%
Q4 set	Mean	c.o.v.	Pushover	Diff.%
uy (cm)	1.0709263	50.11%	1.041	2.78%
Θz (rad)	9.02E–04	60.96%	6.00E–04	33.48%
Q4 set pga	Mean	c.o.v.	Pushover	Diff.%
uy (cm)	2.255035	37.92%	1.822	19.20%
Θz (rad)	1.11E–03	43.88%	8.90E–04	19.84%
Torsionally unrestrained single-storey building				
Q1 set	Mean	c.o.v.	Pushover	Diff.%
uy (cm)	0.062	15.27%	0.765	13.61%
Θz (rad)	6.18E–04	23.68%	7.60E–04	23.05%
Q2 set	Mean	c.o.v.	Pushover	Diff.%
uy (cm)	0.128	24.82%	1.150	17.21%
Θz (rad)	1.28E–03	26.05%	1.10E–03	14.00%
Q3 set	Mean	c.o.v.	Pushover	Diff.%
uy (cm)	1.463	21.21%	1.531	4.66%
Θz (rad)	1.22E–03	22.54%	1.30E–03	6.95%
Q4 set	Mean	c.o.v.	Pushover	Diff.%
uy (cm)	5.834	66.11%	7.654	31.20%
Θz (rad)	5.15E–03	72.76%	4.30E–03	16.57%
Q4 set pga	Mean	c.o.v.	Pushover	Diff.%
uy (cm)	5.837	63.88%	5.640	3.37%
Θz (rad)	5.19E–03	69.34%	4.50E–03	13.27%

from Table 5.5. This high scatter may be explained in the case of torsionally unrestrained buildings (Figure 5.30, bottom) as yielding of one of the lateral resisting elements practically renders the building as pinned, for the torsional degree of freedom, rotating 'freely' around the remaining lateral resisting element (with the exception of the torsional rigidity of the element itself). This obviously represents an upper-bound for the scatter of the torsional response and corresponds to a theoretical case, *as actual buildings always have some degree of torsional restraint provided by the existence of more than two lateral resisting elements in both principal directions.*

Obviously, one can also use other approaches, such as the Modal Pushover Analysis presented by Chopra (2002) or the modified N2 method by Fajfar et al. (2005), as the issue of pushover analysis of torsionally sensitive buildings is currently an ongoing research issue.

Figure 5.31 Torsionally unrestrained four-storey and eight-storey buildings.

5.7.6 Time–history nonlinear analysis

Time-history nonlinear dynamic analysis is considered to be the most accurate approach in the evaluation of the performance of a building under earthquake excitation, provided that all modelling approaches and input parameters have been introduced correctly. Its complexity has mainly limited this type of analysis to academic use, where it is often the benchmark approach for buildings, while it has application in the field by practicing engineers, on the modelling of seismically isolated buildings, where, however, the nonlinearity is limited to the isolator devices while the rest of the building is modelled elastically.

5.7.6.1 Input motion-scaling of accelerograms

The input motion in the *t-h* nonlinear analysis is always a set of accelerograms. There are several types of accelerograms:

- Recorded accelerograms of previous earthquakes
- Artificial accelerograms compiled manually or using algorithms to match a spectra
- Hybrid accelerograms, resulting from the modification of a recorded one in order to match a selected spectra type

Although intuitively an engineer would tend toward using actual recorded accelerograms, which include a more representative frequency content, the code specifications that require the use of a number of accelerograms with a spectra close to the code elastic spectra render the use of artificial or hybrid accelerograms almost mandatory for practical applications. This has already been elaborated in Subsection 3.4.4.

The scaling of accelerograms has several different available techniques, the most common of which are:

Table 5.7 Proposed pushover response versus *t–h* nonlinear analysis

	Dynamic		Static	
Torsionally unrestrained four-storey building				
Q1 set	Mean	c.o.v.	Pushover	Diff.%
uy (cm)	7.169	31.76%	5.741	19.91%
Θz (rad)	9.55E–03	27.27%	7.70E–03	19.34%
Q2 set	Mean	c.o.v.	Pushover	Diff.%
uy (cm)	15.499	21.61%	13.748	11.29%
Θz (rad)	1.63E–02	19.38%	1.80E–02	10.43%
Q3 set	Mean	c.o.v.	Pushover	Diff.%
uy (cm)	13.847	31.93%	10.949	20.93%
Θz (rad)	1.86E–02	28.83%	7.00E–03	19.32%
Q4 set	Mean	c.o.v.	Pushover	Diff.%
uy (cm)	13.041	63.53%	10.902	16.40%
Θz (rad)	1.71E–02	63.22%	1.30E–02	23.90%
Torsionally unrestrained eight-storey building				
Q1 set	Mean	c.o.v.	Pushover	Diff.%
uy (cm)	24.999	74.76%	18.804	24.78%
Θz (rad)	1.34E–02	90.00%	1.50E–02	11.56%
Q2 set	Mean	c.o.v.	Pushover	Diff.%
uy (cm)	13.916	24.86%	11.364	18.34%
Θz (rad)	7.37E–03	20.09%	7.40E–03	0.45%
Q3 set	Mean	c.o.v.	Pushover	Diff.%
uy (cm)	21.061	31.65%	15.626	25.80%
Θz (rad)	1.10E–02	31.44%	1.10E–02	14.61%
Q4 set	Mean	c.o.v.	Pushover	Diff.%
uy (cm)	35.913	94.82%	31.767	11.55%
Θz (rad)	2.50E–02	88.40%	2.50E–02	22.34%

- Scaling according to maximum peak ground acceleration (PGA) target
- Scaling according to maximum velocity peak ground velocity (PGV)
- Scaling according to Arias or Housner intensity

Although for unidirectional or bidirectional excitation in elastic analysis the aforementioned procedures do not result in serious differences, in the case of inelastic analysis this selection results in significant differences.

The Housner Intensity is described by the following expression, which in essence is the area under the Pseudovelocity Spectra PSV over the period (see Chapter 2.2.4.4):

$$\text{SI} = \int_{0.1}^{2.5} PSV(t)\,dt \tag{5.104}$$

Proposals to modify this intensity by using a smaller period domain for the integration, that is, a time window close to the fundamental period of the building has been considered and well documented for research purposes (Kappos and Kyriakakis, 2000).
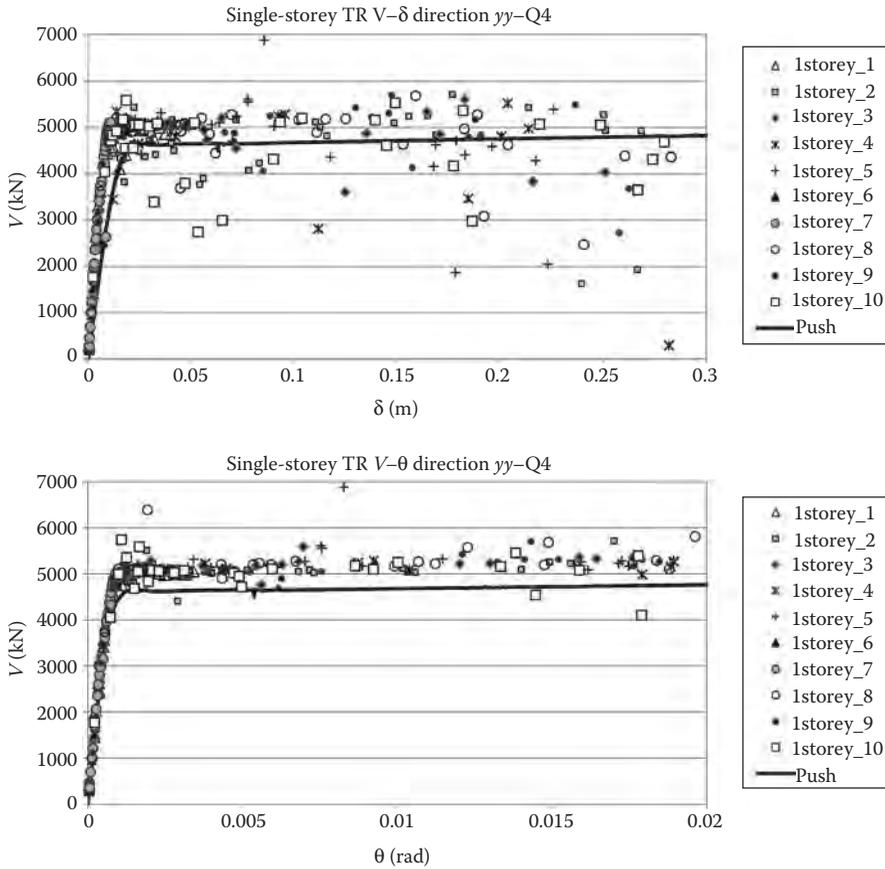
Figure 5.32 Torsionally restrained single-storey building *V*–δ and *V*–θ.

The ARIAS intensity is described by the following integral:

$$AI = \int_t a^2(t)dt \qquad (5.105)$$

where *a*(*t*) is the acceleration.

For the *t-h* inelastic analysis of a building, the scaling of the total energy of each excitation is critical, therefore it is suggested that the ARIAS (or Housner) intensity is scaled for the sum of the energies of both directions, as can be shown in Table 5.8, which includes three accelerograms from the European Strong Motion Database (Ambraseys, 2000).

5.7.6.2 *Incremental dynamic analysis IDA*

The incremental dynamic analysis (IDA) is a procedure to define the capacity curve of a building by using a set of *t-h* inelastic analyses with an increasing intensity. Plotting the results of this analysis in the form of base shear-top displacement results in a trendline of points that includes the capacity curve of the building. An indicative IDA curve is shown Figure 5.35, which refers to a 3-D eight-storey MRF both in terms of base shear-displacement and base shear-rotation (torsion).
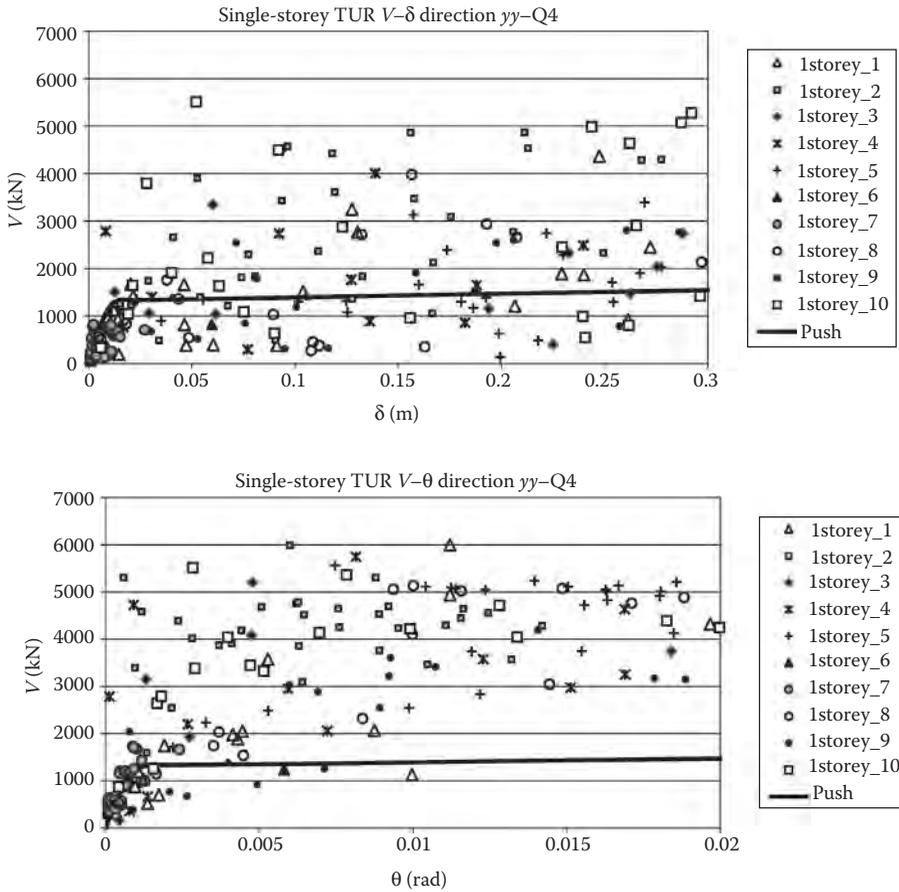
Figure 5.33 Torsionally unrestrained single-storey building *V*–δ and *V*–θ.

This procedure has been extensively investigated by Vamvatsikos and Cornel (2002), and has also been used in 2-D research approaches.

In the case of 3-D analysis with torsional effects, the procedure requires additional attention to the selection of corresponding values for plotting this curve. There are several options that are summarised herein:

- Selecting the maximum responses for base shear and displacement (maxBS–maxD approach)
- Selecting the maximum top displacement and corresponding to this time (t_1) step base shear (maxD approach)
- Selecting the maximum base shear and corresponding to this time step (t_2) displacement (maxBS approach)
- Introducing a time window to the maxD and maxBS approaches as follows:

  maxD(t_1), maxBS$\{t_1 \boxtimes \Delta t, t_1, t_1 + \Delta t\}$

  maxBs(t_2), maxD$\{t_2 \boxtimes \Delta t, t_2, t_2 + \Delta t\}$

All these are shown in the graphical representation of Figure 5.36.

Eight-storey TUR P–δ direction yy–Q3

Eight-storey TUR P–θ direction yy–Q3
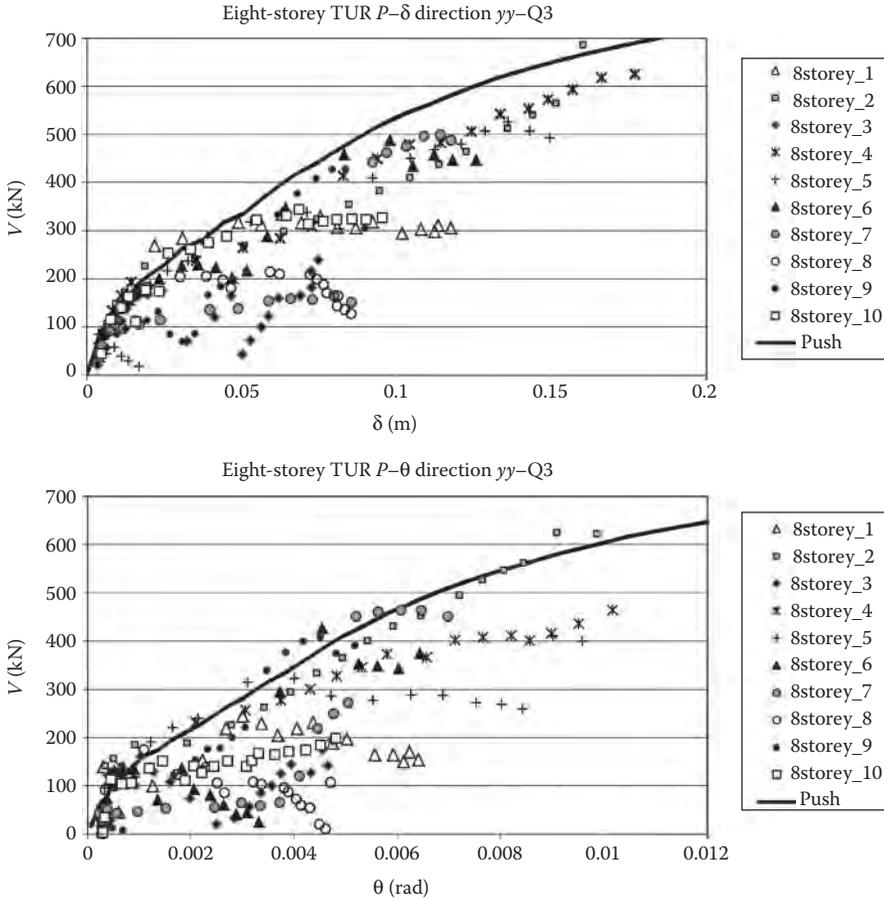
Figure 5.34 Torsionally unrestrained single-storey building V–δ and V–θ.

Table 5.8 Scaling of accelerograms

Scaling factors for bidirectional t-h inelastic analysis					
Event	Direction	Arias I.	Total I.	Target intensity	Target/recorded (scale factor)
TABAS, IRAN (16/09/78 Ms = 7.3)	EW	11.21	23.17	9.71	0.65
	NS	11.97			
Friuli, IT (15/09/76 Ms = 6.0)	EW	1.09	1.82		2.31
	NS	0.73			
Gazli, UZB (17/05/76 Ms = 7.0)	EW	4.95	9.71		1.00
	NS	4.76			

As has been theoretically explained by Penelis and Kappos 2005, the suggested approach is the maxD with a time window of one time step, which produces the most accurate results compared to the theoretical solution elaborated for the single-storey torsionally unrestrained system shown in Figure 5.37. In this figure the left chart shows the results of *t-h* inelastic analysis using all of the aforementioned matching pairs (red for maxD, blue

Eight-storey TUR P–δ direction yy–Q3

Eight-storey TUR P–θ direction yy–Q3
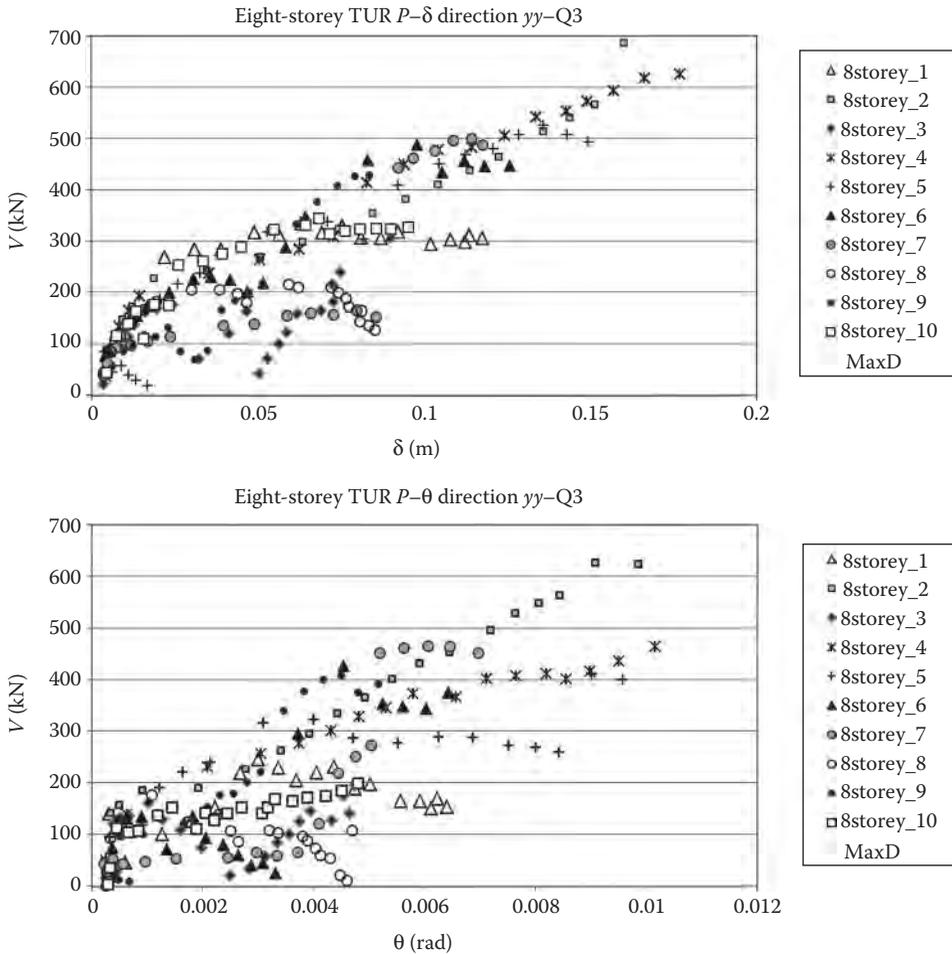
Figure 5.35 IDA of an eight-storey torsionally unrestrained MRF (V–δ and V–θ charts).

for maxD–maxBS and black for maxBS) and the resulting trendlines, while the right chart shows the theoretical solution for torsionally restrained and torsionally unrestrained buildings of Figure 5.30.

5.8 COMBINATION OF THE COMPONENTS OF GRAVITY LOADS AND SEISMIC ACTION

5.8.1 General

Coming back to the linear methods of analysis it should be noted that, no matter which one of the two procedures presented above has been used, that is, 'the modal response spectrum analysis', or the lateral force method, the horizontal components of the seismic action should be considered, according to EC8-1/2004, as acting simultaneously in the two main directions. These two components may also be considered to have equal and uncorrelated intensities (Rosenblueth and Contreras, 1977).
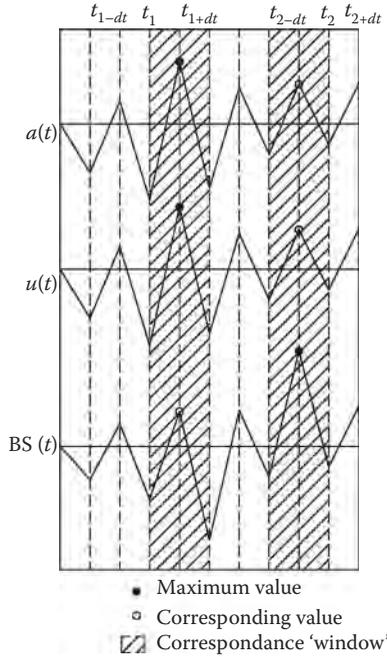
Figure 5.36 DA of an eight-storey torsionally unrestrained MRF.

The combination of these two horizontal components for the determination of maximum seismic effects and, subsequently, their combination with the permanent gravity loads, may be carried out as follows:

1. At first the structural response to each horizontal component shall be computed by means of the combination rules for modal responses given in subsection 2.4.3.1 or by means of lateral force method of analysis (subsection 5.6.4).
2. Then the maximum value of each action effect on the structure due to the two horizontal components of the seismic action may be estimated by the square root of the sum of the squared responses to each component of the seismic action, that is:

$$E_{max} = \pm\sqrt{E_x^2 + E_y^2}$$ (5.106)

where

E_{max} is the maximum action effects (M_x, M_y, M_z, V_x, V_y, N) due to the simultaneous action of the earthquake in both main directions.

E_x is the maximum action effects due to the application of the seismic action along the horizontal axis $x–x$ of the structure.

E_y is the maximum action effects due to the application of the seismic action along the horizontal axis $y–y$ of the structure.

In the case of a vertical element (column or wall) subjected to bending with axial force, the above are exemplified as follows:

a. For the $x–x$ earthquake component, the following internal forces are derived:

$\pm M_{Exx}$, $\pm M_{Eyx}$, $\pm N_{Ex}$
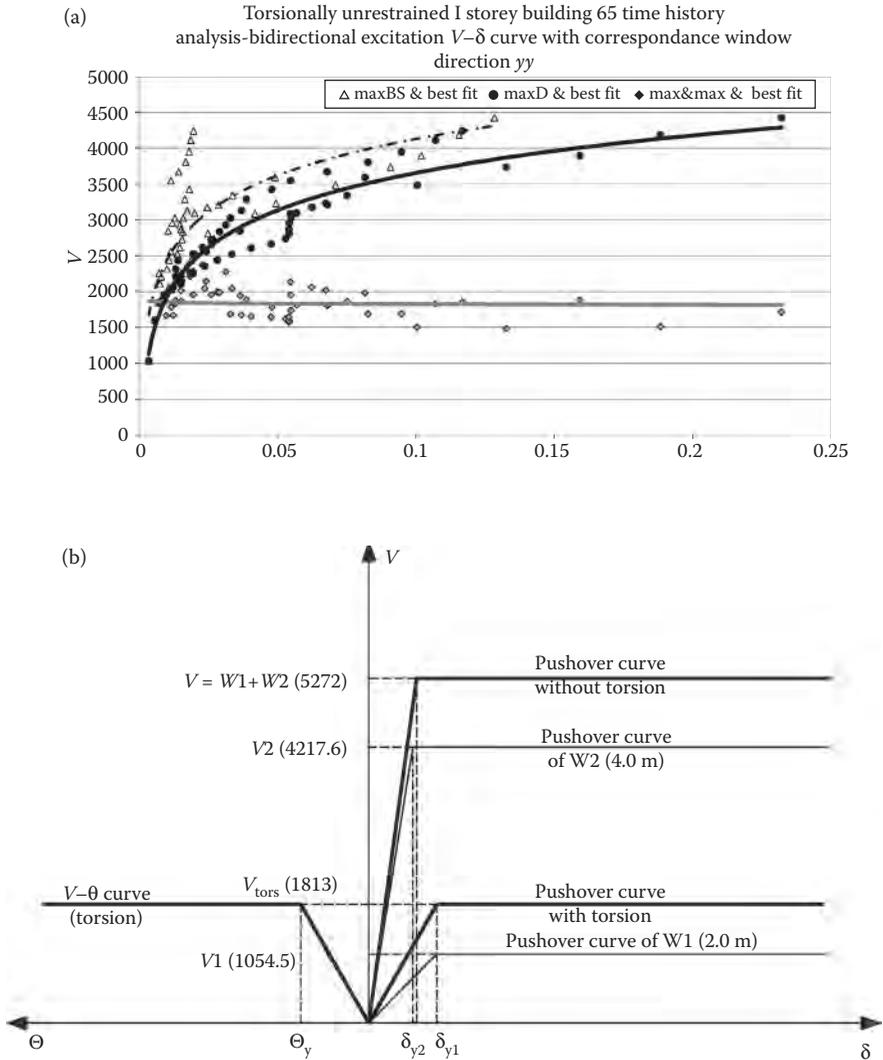
Figure 5.37 IDA curves for a TUR 1-storey building using several approaches for the definitions versus the theoretical solution: (a) IDA curves for 65 time history analysis; (b) the theoretical solution.

b.   For the $y-y$ earthquake component, the following internal forces are derived:

$$\pm M_{\mathrm{Ex}\,y}, \quad \pm M_{\mathrm{Ey}\,y}, \quad \pm N_{\mathrm{Ey}}$$

Therefore, the extreme values of internal forces $\pm M_{\mathrm{Ex\,max}}$, $\pm M_{\mathrm{Ey\,max}}$, $\pm N_{\mathrm{Emax}}$ will have the following form:

$$M_{\mathrm{Ex\,max}} = \pm\sqrt{\left(M_{\mathrm{Ex}\,x}\right)^2 + \left(M_{\mathrm{Ex}\,y}\right)^2}$$

$$M_{\mathrm{Ey\,max}} = \pm\sqrt{\left(M_{\mathrm{Ey}\,y}\right)^2 + \left(M_{\mathrm{Ey}\,x}\right)^2} \qquad (5.107\mathrm{a-c})$$

$$N_{\mathrm{E\,max}} = \pm\sqrt{\left(N_{\mathrm{Ex}}\right)^2 + \left(N_{\mathrm{Ey}}\right)^2}$$

Since the alternative values for each load effect are two ($\pm$) and the number of the internal forces participating in the design of the element are three ($M_{\text{Ex max}}$, $M_{\text{Ey max}}$, N_{E}), it follows that the number of combinations necessary for the design is

$$\lambda = b^n = 2^3 = 8 \tag{5.108}$$

where

n is the number of load effects participating in the design, (in case of biaxial bending with axial load $n = 3$).

b is the number of alternative choices for each load effect (plus-minus ($\pm$) $b = 2$).

3. The seismic action effects must be superimposed on the gravity load effects, that is, on (Subsection 3.4.5, Equations 3.50 and 3.51):

$$E_w = E\left(G \text{ '+' } \psi_{Ei} Q_i\right)$$

Therefore, the final action effects due to gravity loads and earthquake will have the form (Section 3.4.5):

$$\boxed{E_s = E\left(G \text{ '+' } \psi_{Ei} Q_i\right) \text{ '+' } E\left(\gamma_1 S_{dx} \text{ '+' } \gamma_1 S_{dy}\right)} \tag{5.109}$$

where '+' implies 'to be combined with', G are the dead loads, Q_i is the characteristic value of variable action i, $S_{dx,y}$ is the design value of the seismic action parallel to x–x and y–y respectively, γ_1 the importance factor, and ψ_{Ei} is the combination coefficient for the variable action I (see Subsection 3.4.5).

It should be noted that the extreme values of seismic effects ($M_{x,ex}$, $M_{y,ex}$, $M_{z,ex}$, $V_{x,ex}$, $V_{y,ex}$, N_{ex}) determined above do not act simultaneously. Therefore, in the case that more than one load effect is needed for the safety verification at ultimate limit state (i.e. M_x, M_y, N for the cross-section of a column), the combination of the extreme values of all relevant load effects would be, at first glance, conservative.

In the following subsections a theoretical approach to the problem will be presented, so that the reader may have a global view of the approximations involved in various procedures established in practice.

5.8.2 Theoretical background

Let n be the number of the load effects defining the response state of an R/C structural element (i.e. $n = 3$ for a column under M_x, M_y, N). Its response to gravity and earthquake loading acting parallel to the x and y axes simultaneously is defined at an n-dimensional *response space* of the interacting load effects (i.e. M_x, M_y, N) by an ellipsoid (Rosenblueth and Contreras, 1977; Gupta, 1990), with its centre at r_0 (M_{x0}, M_{y0}, N_0) (Figure 5.38), described at a local reference coordinate system by the equation:

$$\bar{\mathbf{x}}^T G^{-1} \bar{\mathbf{x}} = 1$$

where M_{x0}, M_{y0}, N_0 are the responses to gravity loads,

$$\bar{\mathbf{x}}^T = \left\{\bar{X}_c, \bar{Y}_c, \bar{Z}_c\right\} = \left\{\bar{M}_{xc}, \bar{M}_{yc}, \bar{N}_c\right\}$$
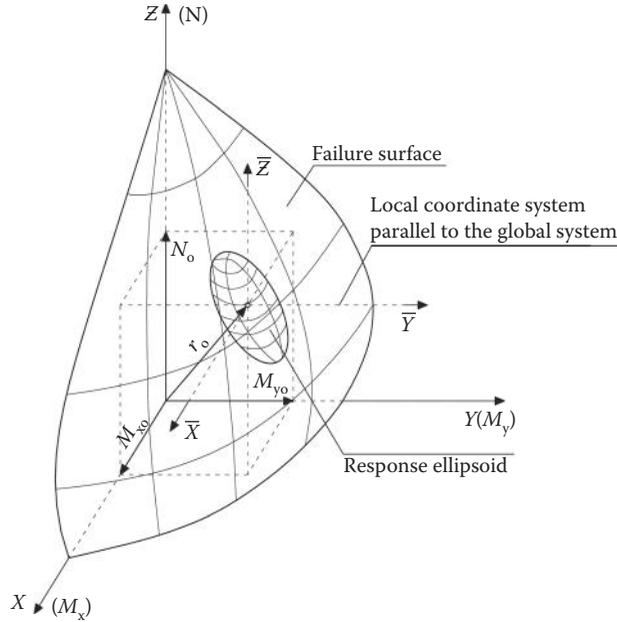
Figure 5.38 Response ellipsoid and failure envelope.

the vector of the most probable simultaneously acting relevant load effects at the local reference system, and

$$\mathbf{G} = \begin{pmatrix} X_{ex}^2 & \rho_{xv} & \rho_{xz} \\ \rho_{yx} & Y_{ex}^2 & \rho_{yz} \\ \rho_{zx} & \rho_{zy} & Z_{ex}^2 \end{pmatrix} = \begin{pmatrix} M_{x_{ex}}^2 & \rho_{xv} & \rho_{xz} \\ \rho_{yx} & M_{y_{ex}}^2 & \rho_{yz} \\ \rho_{zx} & \rho_{zy} & N_{ex}^2 \end{pmatrix} \qquad (5.110)$$

In the above matrix G, quantities X_{ex}, Y_{ex}, Z_{ex} are derived from Equation 5.106, while quantities $\rho_{xy} = \rho_{yx}$, $\rho_{xz} = \rho_{zx}$, $\rho_{yz} = \rho_{zy}$ are derived from the following expressions:

$$\left. \begin{aligned} \rho_{xy} &= \sum_i (X_{i,x}\, Y_{i,x} + X_{i,y}\, Y_{i,y}) = \sum_i (M_{xi,x}\, M_{yi,x} + M_{xi,y}\, M_{yi,y}) \\ \rho_{xz} &= \sum_i (X_{i,x}\, Z_{i,x} + X_{i,y}\, Z_{i,y}) = \sum_i (M_{xi,x}\, N_{i,x} + M_{xi,y}\, N_{i,y}) \\ \rho_{yz} &= \sum_i (Y_{i,x}\, Z_{i,x} + X_{i,y}\, Z_{i,y}) = \sum_i (M_{xi,x}\, N_{i,x} + M_{xi,y}\, N_{i,y}) \end{aligned} \right\} \qquad (5.111)$$

where $X_{i,x}$, $Y_{i,x}$, $Z_{i,x}$ are the response spectrum values of the interacting response in the ith mode of vibration due to the x–x earthquake component ($i = 1, 2\ldots.k$), and $X_{i,y}$, $Y_{i,y}$, $Z_{i,y}$ are the response spectrum values of the interacting response in the ith mode of vibration due to the y–y earthquake component ($i = 1, 2\ldots.k$).

In general, the state of the ellipsoid (or response ellipsoid) that presents the simultaneous variation of the values of the three responses (M_x, M_y, N) to gravity and earthquake loading

(Equation 5.109) has inclined axes, while the failure envelope for M_x, M_y, N of the R/C structural element is not susceptible to simple description. The task of investigating whether the ellipsoid lies entirely within the safe domain, and that of selecting a failure surface that will lie just outside the ellipsoid are excessively complicated for routine design. Consequently, based on the above theoretical background, a series of simplified procedures has been developed.

5.8.3 Simplified procedures

Some of these simplified procedures will be presented here, mainly for a two-dimensional response space (i.e. M and N on the cross-section of an R/C wall), so that a plane schematic presentation of the various approaches can be feasible (Figure 5.39a). In this case the response, or interaction, ellipsoid is reduced to an interaction ellipse defined at the local coordinate system by the following equation (Gupta and Singh, 1977; Panetsos and Anastassiadis, 1994):
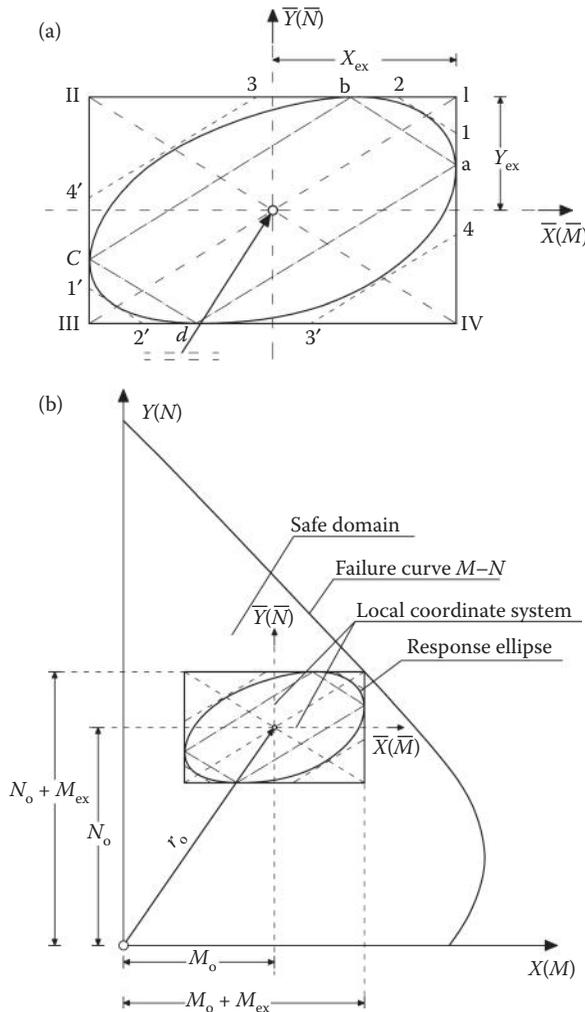
Figure 5.39 Response ellipse and failure envelope: (a) various simplified approaches to the problem; (b) response ellipse in the safe domain of the envelope (bending design).

$$\left.\begin{array}{l} \dfrac{X_c^2}{X_{ex}^2} + \dfrac{Y_c^2}{Y_{ex}^2} - 2\rho_{xy}\dfrac{X_c Y_c}{X_{ex}^2 Y_{ex}^2} = 1 - \left(\dfrac{\rho_{xy}}{X_{ex} Y_{ex}}\right)^2 \\[2mm] \text{or} \\[2mm] \dfrac{M_c^2}{M_{ex}^2} + \dfrac{N_c^2}{N_{ex}^2} - 2\rho_{xy}\dfrac{M_c N_c}{M_{ex}^2 N_{ex}^2} = 1 - \left(\dfrac{\rho_{xy}}{M_{ex} N_{ex}}\right)^2 \end{array}\right\} \qquad (5.112)$$

where

$$\rho_{xy} = \sum_i \left(X_{i,x}\, Y_{i,x} + X_{i,y}\, Y_{i,y}\right)$$

The centre of this ellipse must be placed in the global coordinate system at the point $r_0(X_0 = M_0,\ Y_0 = N_0)$ representing the gravity load effect vector (Figure 5.39b).

5.8.3.1 Combination of the extreme values of the interacting load effects

In the case that for safety verification the maximum values resulting from Equation 5.106 are combined, the ellipse of Equation 5.112 is replaced by the rectangle I, II, III, IV (Figure 5.39). It is obvious that this approach is on the safe side.

In most conventional design procedures, it is implicitly assumed that the maxima occur simultaneously. This assumption introduces an error on the safe side, which can be significant. From various case studies conducted so far (Leblond, 1980; Panetsos and Anastassiadis, 1994; Zararis et al., 1994) it may be concluded that for R/C columns and shear walls this error ranges from 15% to 35%, measured as a percentage of the 'exact' reinforcement of the R/C element.

The number of combinations in this case is four for a two-load effect component interaction.

5.8.3.2 Combination of each extreme load effect with the corresponding values of the interacting ones

In this case the ellipse (Figure 5.39a) is replaced by the parallelogram *a, b, e, d*. It is obvious that this approach is on the unsafe side. The relevant combinations for the load effect components (i.e., *M* and *N*) are listed in Table 5.9 (Gupta and Chu, 1977).

In the case of a three-component interaction problem (i.e., M_x, M_y, N), the simultaneously acting components are given in Table 5.10.

According to the conclusions of various case studies conducted so far, the error for R/C columns and walls ranges from –5% to –10%, measured as a percentage of the exact reinforcement of the R/C element.

Table 5.9 Simultaneously acting X_c, Y_c Values

	Points a, c	Points b, d
X_c	$\pm X_{ex}$ (Equation 5.106)	$\pm\rho_{xy}/X_{ex}$
Y_c	$\pm\rho_{xy}/X_{ex}$	$\pm Y_{ex}$ (Equation 5.106)

Table 5.10 Simultaneously acting X_c, Y_c, Z_c values

	2 points	2 points	2 points
X_c	$\pm X_{ex}$	$\pm \rho_{xy}/Y_{ex}$	$\pm \rho_{xz}/Z_{ex}$
Y_c	$\pm \rho_{yx}/X_{ex}$	$\pm Y_{ex}$	$\pm \rho_{yz}/Z_{ex}$
Z_c	$\pm \rho_{zx}/X_{ex}$	$\pm \rho_{zy}/Y_{ex}$	$\pm Z_{ex}$

5.8.3.3 Gupta–Singh procedure

According to this procedure (Gupta and Singh, 1977), the ellipse is approximated by the circumscribed octagon 1, 2, 3, 4, 1′, 2′, 3′, 4′ (Figure 5.39a). It is obvious that this approach is on the safe side, while the error is not as significant as in case (a). The coordinates of the above-designated points are as follows:

Point 1: $X_{1c} = X_{ex}$ $\qquad\qquad$ $Y_{1c} = Y_{ex}(\mu_{xy} - 1)$

Point 2: $X_{2c} = X_{ex}(\mu_{xy} - 1)$ $\qquad$ $Y_{2c} = Y_{ex}$

Point 3: $X_{3c} = X_{ex}(1 - r_{xy})$ $\qquad$ $Y_{3c} = Y_{ex}$

Point 4: $X_{4c} = X_{ex}$ $\qquad\qquad$ $Y_{4c} = Y_{ex}(1 - r_{xy})$

where

$$\mu_{xy} = \left[2\left(1 + \frac{\rho_{xy}}{X_{ex}Y_{ex}}\right)\right]^{1/2} \qquad r_{xy} = \left[2\left(1 - \frac{\rho_{xy}}{X_{ex}Y_{ex}}\right)\right]^{1/2}$$

The other four vertices are symmetric to the previous ones with respect to the centre of the octagon.

In the case of a three-component interaction problem (i.e., M_x, M_y, N), the ellipse is *approximated* by a polyhedron with 24 vertices. Their coordinates are as follows:

Point 1: $\quad X_{1c} = X_{ex}$ $\qquad$ $Y_{1c} = Y_{ex}(\mu_{yz} - 1)$ $\qquad$ $Z_{1c} = Z_{ex}(\mu_{xz} - 1)$

Point 2: $\quad X_{2c} = X_{ex}(\mu_{yz} - 1)$ $\qquad$ $Y_{2c} = Y_{ex}$ $\qquad$ $Z_{2c} = Z_{ex}(\mu_{xy} - 1)$

Point 3: $\quad X_{3c} = X_{ex}(\mu_{zx} - 1)$ $\qquad$ $Y_{3c} = Y_{ex}(\mu_{xy} - 1)$ $\qquad$ $Z_{3c} = Z_{ex}$

Point 4: $\quad X_{4c} = X_{ex}(1 - r_{yz})$ $\qquad$ $Y_{4c} = Y_{ex}$ $\qquad$ $Z_{2c} = Z_{ex}(1 - r_{xy})$

Point 5: $\quad X_{5c} = X_{ex}(1 - r_{xz})$ $\qquad$ $Y_{5c} = Y_{ex}(1 - r_{xy})$ $\qquad$ $Z_{5c} = Z_{ex}$

Point 6: $\quad X_{6c} = X_{ex}$ $\qquad$ $Y_{6c} = Y_{ex}(1 - r_{yz})$ $\qquad$ $Z_{6c} = Z_{ex}(1 - r_{xz})$

Point 7: $\quad X_{7c} = X_{ex}$ $\qquad$ $Y_{7c} = Y_{ex}(\mu_{yz} - 1)$ $\qquad$ $Z_{7c} = Z_{ex}(1 - r_{xz})$

Point 8: $\quad X_{8c} = X_{ex}(1 - r_{yz})$ $\qquad$ $Y_{8c} = Y_{ex}$ $\qquad$ $Z_{8c} = Z_{ex}(\mu_{xy} - 1)$

Point 9: $\quad X_{9c} = X_{ex}(\mu_{xz} - 1)$ $\qquad$ $Y_{9c} = Y_{ex}(1 - r_{xy})$ $\qquad$ $Z_{9c} = Z_{ex}$

Point 10: $\quad X_{10c} = X_{ex}$ $\qquad$ $Y_{10c} = Y_{ex}(1 - r_{yz})$ $\qquad$ $Z_{10c} = Z_{ex}(\mu_{xz} - 1)$

Point 11: $\quad X_{11c} = X_{ex}(\mu_{yz} - 1)$ $\qquad$ $Y_{11c} = Y_{ex}$ $\qquad$ $Z_{11c} = Z_{ex}(1 - r_{xy})$

Point 12: $\quad X_{12c} = X_{ex}(1 - r_{xz})$ $\qquad$ $Y_{12c} = Y_{ex}(\mu_{xy} - 1)$ $\qquad$ $Z_{12c} = Z_{ex}$

where

$$\mu_{xy} = \left[2\left(1 + \frac{\rho_{xy}}{X_{ex}Y_{ex}} \right) \right]^{1/2} \quad r_{xy} = \left[2\left(1 - \frac{\rho_{xy}}{X_{ex}Y_{ex}} \right) \right]^{1/2}$$

$$\mu_{yz} = \left[2\left(1 + \frac{\rho_{yz}}{X_{ex}Y_{ex}} \right) \right]^{1/2} \quad r_{yz} = \left[2\left(1 - \frac{\rho_{yz}}{X_{ex}Y_{ex}} \right) \right]^{1/2}$$

$$\mu_{xz} = \left[2\left(1 + \frac{\rho_{xz}}{X_{ex}Y_{ex}} \right) \right]^{1/2} \quad r_{xz} = \left[2\left(1 - \frac{\rho_{xz}}{X_{ex}Y_{ex}} \right) \right]^{1/2}$$

The other 12 vertices are symmetric to the previous ones with respect to the centre of the polyhedron.

Various case studies (Leblond, 1980; Panetsos and Anastassiadis, 1994) have shown that for R/C columns and walls the error ranges from 2% to 6%, measured as a percentage of the exact reinforcement of the R/C element.

5.8.3.4 Rosenblueth and Contreras procedure

Rosenblueth and Contreras (1977) have replaced the ellipsoid by a vector (Figure 5.40):

$$r_c = r_0 + \alpha_x r_x + \alpha_y r_y \tag{5.113}$$

where r_c is the most probable extreme response vector of the R/C gravity and earthquake loading, r_0 is the response vector of the R/C element to gravity loading only (i.e. M_{x0}, M_{y0},
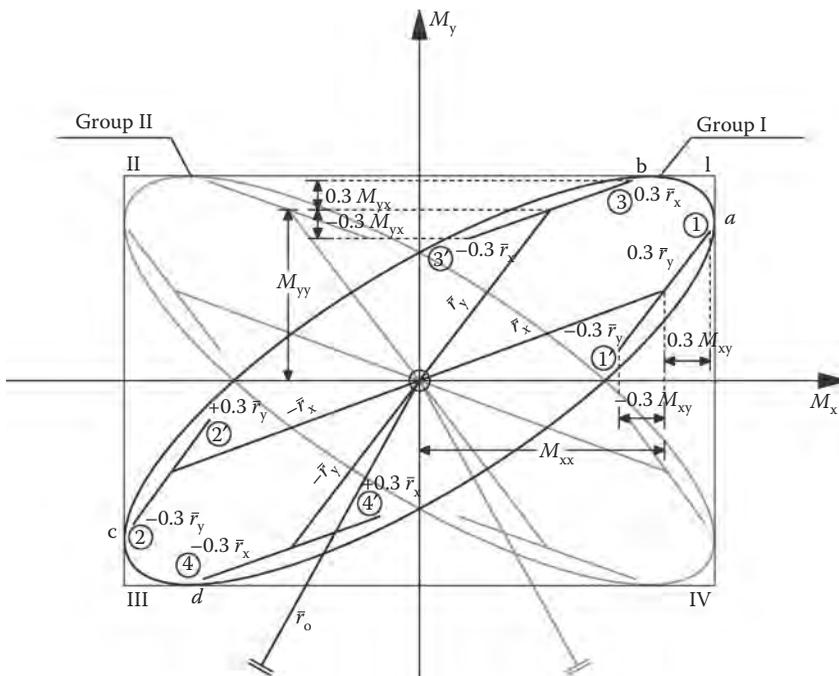
Figure 5.40 The Rosenblueth and Contreras procedure (alternative Code procedure).

N_0), r_x is the most probable extreme response vector of the R/C element to earthquake loading parallel to the x–x axis (i.e. $M_{x,ex,x}$, $M_{y,ex,x}$, $N_{ex,x}$), r_y is the most probable extreme response vector of the R/C element to earthquake loading parallel to the y–y-axis (i.e. $M_{x,ex,y}$, $M_{y,ex,y}$, $N_{ex,y}$) and α_x, α_y are constant coefficients to be determined, so that the probable error on the safe side will be equal to that on the unsafe side. Through this approach it has been concluded that for:

$$\alpha_x = \begin{cases} 1.00 \\ 0.336 \end{cases} \quad \text{and} \quad \alpha_y = \begin{cases} 0.336 \\ 1.00 \end{cases}$$

respectively, the maximum error is ±5.5%. This simplified procedure had also been proposed earlier, in 1975 (with $\alpha_{x,y} = 1.00$ and 0.33), by A.S. Veletsos, and it has served as a basis for Code requirements in the United States (UBC, 1988) and recently in the European Union (EC8-1/2004).

In both Codes the values of α_x, α_y as introduced are the following:

$$\alpha_x = \begin{cases} \pm1.00 \\ \pm0.30 \end{cases} \quad \text{and} \quad \alpha_y = \begin{cases} \pm0.30 \\ \pm1.00 \end{cases}$$

respectively. For these values the maximum error is 4.4% on the safe side and 8.1% on the unsafe side.

In the case of a two-dimensional response space (i.e. M and N on an R/C wall), the ellipsoid is reduced to an interaction ellipse, and Equation 5.113 takes the following algebraic form:

$$\left.\begin{aligned}
M_{1c} &= M_0 + M_{ex,x} + 0.30M_{ex,y}, & N_{1c} &= N_0 + N_{ex,x} + 0.30N_{ex,y} \\
M_{2c} &= M_0 + M_{ex,x} - 0.30M_{ex,y}, & N_{2c} &= N_0 + N_{ex,x} - 0.30N_{ex,y} \\
M_{3c} &= M_0 - M_{ex,x} + 0.30M_{ex,y}, & N_{3c} &= N_0 - N_{ex,x} + 0.30N_{ex,y} \\
M_{4c} &= M_0 - M_{ex,x} - 0.30M_{ex,y}, & N_{4c} &= N_0 - N_{ex,x} - 0.30N_{ex,y}
\end{aligned}\right\} \text{4 combinations}$$

$$\left.\begin{aligned}
M_{5c} &= M_0 + 0.30M_{ex,x} + M_{ex,y}, & N_{5c} &= N_0 + 0.30N_{ex,x} + N_{ex,y} \\
M_{6c} &= M_0 + 0.30M_{ex,x} - M_{ex,y}, & N_{6c} &= N_0 + 0.30N_{ex,x} - N_{ex,y} \\
M_{7c} &= M_0 - 0.30M_{ex,x} + M_{ex,y}, & N_{7c} &= N_0 - 0.30N_{ex,x} + N_{ex,y} \\
M_{8c} &= M_0 - 0.30M_{ex,x} - M_{ex,y}, & N_{8c} &= N_0 - 0.30N_{ex,x} - N_{ex,y}
\end{aligned}\right\} \text{4 combinations}$$

5.8.3.5 Extreme stress procedure

Anastassiadis (1993) has adopted the procedure mainly used for steel structures (Wilson and Button, 1982) for the design of R/C structures. According to this procedure, it is assumed that the cross-section of the R/C element is homogeneous and uncracked. Therefore, the extreme values of the stresses at the vertices of the R/C cross-section may be computed as if it were a steel cross-section. The computed extreme stresses themselves are of no significance but are used only as a vehicle for the determination of the components that should be combined.

5.8.4 Code provisions

5.8.4.1 Suggested procedure for the analysis

Bearing in mind, as already mentioned, that strong computational tools are available at low cost, it is suggested that, in the case that modal response spectrum analysis is applied, a spatial system with diaphragms at floor levels is used. At this case, the most convenient approach to the problem according to the authors' opinion is the following:

- The floor masses will be considered as lumped ones, concentrated at the centre of gravity of each floor.
- The accidental torsional effect ($e_i = \pm 0.05\ L_i$) may be determined as the envelope of the effects resulting from an analysis for static loading consisting of the torsional moments M_i about the vertical axis of the storey i.

$$\mathbf{M}_i = e_{1i} \cdot H_i \tag{5.114}$$

where M_i is the torsional moment of storey i about its vertical axis, e_{1i} is the accidental eccentricity of the storey mass i accounting for the two main directions and H_i is the horizontal force acting at storey i as derived from the application of lateral force method of analysis for the two main directions. The effect of the loading described above is considered, with alternating singes the same for all storeys. Therefore, the structural system will be analysed for the following actions:

- $W = G\text{'+'}\psi_{Ei} \cdot Q_i$ $\}$ gravity load (see Chapters 3.4.5, Equations 3.50 and 3.51)

- Design spectrum (S_{dx})
  modified by the importance
  factor for horizontal excitation x–x seismic action
  parallel to the x–x axis and masses
  at the centre of gravity of the floors
- $M_i = e_{1y} \cdot H_{ix}$ (see Paragraph 5.6.3.4)

- Design spectrum (S_{dy})
  modified by the
  importance factor for
  horizontal excitation y–y seismic action
  parallel to the y–y axis
  and masses at the centre
  of gravity of the floors
- $M_i = \pm e_{1x} \cdot H_{iy}$ (see Paragraph 5.6.3.4)

$$\tag{5.115}$$

The loading effects (E) from the above analysis, for each loading direction, will be obtained as follows (Figure 5.41)
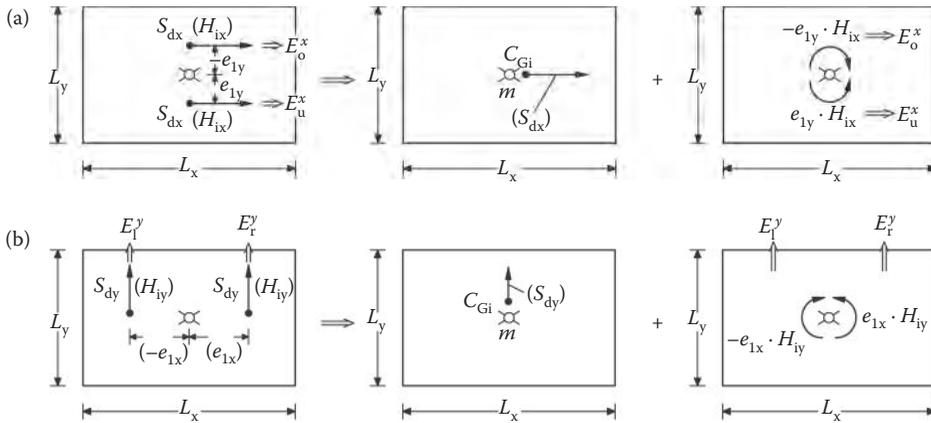
Figure 5.41 Seismic action effects E resulting from a modular response spectrum analysis: (a) seismic action in the x–x direction; (b) seismic action in the y–y direction.

$$
\begin{aligned}
E_w &\Rightarrow G \text{ '+' } \psi_{Ei} \cdot Q_i \qquad \big\} \quad \text{gravity load} \\[4pt]
E_u^x &\Rightarrow S_{dx} \text{ '+'} e_{1y} \cdot H_{ix} \\
E_o^x &\Rightarrow S_{dx} \text{ '+'}(-e_{1y}) \cdot H_{ix}
\end{aligned} \Big\} \quad x\text{–}x \text{ seismic action}
$$

$$
\begin{aligned}
E_r^y &\Rightarrow S_{dy} \text{ '+' } e_{1x} \cdot H_{iy} \\
E_l^y &\Rightarrow S_{dy} \text{ '+' } (-e_{1x}) \cdot H_{iy}
\end{aligned} \Big\} \quad y\text{–}y \text{ seismic action}
$$

(5.116)

where t means 'combined with'.

The notation above is given in Figure 5.41.

The above procedure seems to be the most convenient. All other options, for example, the use of two plane models combined with simplified torsional analysis, are proper only in the case that no efficient computational tools are available.

5.8.4.2 Implementation of the reference method in case of horizontal seismic actions

The reference method of EC8-1/2004 for the calculation of the combinations of the seismic effects that should be taken into account in the design is based on the assumption that the horizontal components of the seismic action (see subsection 5.8.1) are taken as acting simultaneously. This assumption introduces an error on the safe side, from 15% to 35%. In this case, the number of combinations of load effects that should be taken into account for the design of a column or a wall is eight.

In addition, it should be noted that due to the introduction of accidental eccentricities, four different centres of masses must be considered. Therefore, it follows that the total number of combinations for the design of the cross-section of a column is 32 (4×2^3). In fact, substituting Equation 5.116 into Equation 5.106 and superimposing the gravity load effects, the following combinations result:

$$E = E_w \pm \sqrt{\left(E_u^x\right)^2 + \left(E_r^y\right)^2} = \begin{cases} E_{1,I} \\ E_{1,II} \end{cases}$$

$$E = E_w \pm \sqrt{\left(E_u^x\right)^2 + \left(E_l^y\right)^2} = \begin{cases} E_{2,I} \\ E_{2,II} \end{cases}$$

$$E = E_w \pm \sqrt{\left(E_0^x\right)^2 + \left(E_r^y\right)^2} = \begin{cases} E_{3,I} \\ E_{3,II} \end{cases}$$

$$E = E_w \pm \sqrt{\left(E_0^x\right)^2 + \left(E_l^y\right)^2} = \begin{cases} E_{4,I} \\ E_{4,II} \end{cases}$$

that is, eight different combinations for each load effect (M_x, M_y, M_z, V_x, V_y, N).

In the case of a column where three load effects must be considered, that is M_x, M_y and N, the number of combinations is 32:

$$
\begin{array}{lll}
M_x = M_{1,Ix} & M_y = M_{1,Iy} & N = N_{1,I} \\
M_x = M_{1,IIx} & M_y = M_{1,IIy} & N = N_{1,II}
\end{array} \bigg\} \quad \text{8 combinations}
$$

$$
\begin{array}{lll}
M_x = M_{2,Ix} & M_y = M_{2,Iy} & N = N_{2,I} \\
M_x = M_{2,IIx} & M_y = M_{2,IIy} & N = N_{2,II}
\end{array} \bigg\} \quad \text{8 combinations}
$$

$$
\begin{array}{lll}
M_x = M_{3,Ix} & M_y = M_{3,Iy} & N = N_{3,I} \\
M_x = M_{3,IIx} & M_y = M_{3,IIy} & N = N_{3,II}
\end{array} \bigg\} \quad \text{8 combinations}
$$

$$
\begin{array}{lll}
M_x = M_{4,Ix} & M_y = M_{4,Iy} & N = N_{4,I} \\
M_x = M_{4,IIx} & M_y = M_{4,IIy} & N = N_{4,II}
\end{array} \bigg\} \quad \underline{\text{8 combinations}}
$$

Total   32 combinations

5.8.4.3 Implementation of the alternative method in the case of horizontal seismic actions

As was already noted as an alternative to the above procedure, it is permitted according to EC8-1/2004 to compute the action effects due to both components using the following formulae (see Paragraph 5.7.3.4):

$$
\left.
\begin{aligned}
E &= \quad E_x \; '+' \; 0.30E_y \\
E &= 0.30E_x \; '+' \; E_y
\end{aligned}
\right\}
\tag{5.117}
$$

The same formulae have been introduced in the United States by BSSC 2003 and SEAOC 1999.

This assumption introduces a maximum error of 4.4% on the safe side and 8.1% on the unsafe side. In this respect, this alternative results in steel savings in the vertical elements in comparison to the reference method.

However, the implementation of this method requires particular attention in the combination of the partial components of the seismic effects, especially in the case that the modal response spectrum analysis is used. In this case the partial components of the seismic effects result in absolute values for the output of the SRSS or Complete Quadratic Combination (CQC) procedure (see Subsection 2.4.3).

For example, in the case of a vertical element (column or wall) subjected to bending with axial force, according to what has been presented in subsection 5.8.1 the following load vectors develop.

For the x–x earthquake component:

$$\pm M_{Exx}, \quad \pm M_{Ey\,x}, \quad \pm N_{Ex}$$

For the y–y earthquake component:

$$\pm M_{ex\,y}, \quad \pm M_{Eyy}, \quad \pm N_{Ey}$$

Therefore, the extreme values of the internal forces $M_{Ex\,max}$ with the corresponding M_{Ey} and N_E result from the following equations:

$$M_{Ex\,ext} = \pm M_{Exx} \pm 0.30 M_{Exy}, \quad M_{Ey}^{cor} = \pm M_{Ey\,x} \pm 0.30 M_{Eyy}, \quad N_{ex}^{cor} = \pm N_{ex} \pm 0.30 N_{Ey} \quad (5.118)$$

while the extreme values of the internal forces $M_{Ey\,max}$ with the corresponding M_{Ex} and N_E result from the following ones:

$$M_{Ey\,extr} = \pm M_{Eyy} - 0.30 M_{Ey\,x}, \quad M_{Ex}^{cor} = \pm M_{Exy} \pm 0.30 M_{Exx}, \quad N_{Ey}^{cor} = \pm N_{Ey} \pm 0.30 N_{Ex} \quad (5.119)$$

Since the alternative values for each load effect are four ($\pm$ '+' $\pm$) and the numbers of internal forces participating in the design of the element are three (M_x, M_y, N_E), it may be concluded that the number of combinations necessary for the design are

$$\lambda = b^n = 4^3 = 64$$

Additionally, bearing in mind that due to the introduction of accidental eccentricities four different centres of masses must be considered, it follows that the total number of combinations for the design of the cross-section of a vertical element is

$$\lambda' = 4 \times 64 = 256$$

It is apparent that such an enormous number of load effect combinations cannot be afforded, despite the reinforcement savings if it were compared with the 32 load effect combinations required for the reference method. So, a comprehensive examination of the above equations (5.118) and (5.119) should be carried out, combined with some approximations so that this large number of 256 combinations may be diminished.

Consider for a moment that N_E has a given value. The above equations (5.118) and (5.119) may be arranged in two groups (Figure 5.40), that is:

Group (1)

Points $\boxed{1}$ 1.1′: $M_{\text{Ex max}} = +M_{\text{Ex,x}} \pm 0.30M_{\text{Ex,y}}, \quad M_{\text{Ey}}^{\text{cor}} = M_{\text{Ey,x}} \pm 0.30M_{\text{Ey,y}}, \quad N_{\text{ex}}^{\text{cor}} = N_{\text{E}}$

Points $\boxed{1}$ 2.2′: $M_{\text{Ex min}} = -M_{\text{Ex,x}} \pm 0.30M_{\text{Ex,y}}, \quad M_{\text{Ey}}^{\text{cor}} = -M_{\text{Ey,x}} \pm 0.30M_{\text{ey,y}}, \quad N_{\text{Ex}}^{\text{cor}} = N_{\text{E}}$

Points $\boxed{1}$ 3.3′: $M_{\text{Ey max}} = +M_{\text{Ey,y}} \pm 0.30M_{\text{Ey,x}}, \quad M_{\text{ex}}^{\text{cor}} = M_{\text{ex,y}} \pm 0.30M_{\text{Ex,x}}, \quad N_{\text{Ey}}^{\text{cor}} = N_{\text{E}}$

Points $\boxed{1}$ 4.4′: $M_{\text{Ey min}} = -M_{\text{ey,y}} \pm 0.30M_{\text{Ey,x}}, \quad M_{\text{ex}}^{\text{cor}} = -M_{\text{Ey,y}} \pm 0.30M_{\text{Ex,x}}, \quad N_{\text{Ey}}^{\text{cor}} = N_{\text{E}}$

$$(5.120)$$

Group (2)

Points $\boxed{2}$ 1.1′: $M_{\text{Ex max}} = +M_{\text{Ex,x}} = 0.30M_{\text{Ex,y}}, \quad M_{\text{Ey}}^{\text{cor}} = -M_{\text{Ey,x}} \pm 0.30M_{\text{Ey,y}}, \quad N_{\text{ex}}^{\text{cor}} = N_{\text{E}}$

Points $\boxed{2}$ 2.2′: $M_{\text{Ex min}} = -M_{\text{Ex,x}} = 0.30M_{\text{Ex,y}}, \quad M_{\text{Ey}}^{\text{cor}} = +M_{\text{Ey,x}} \pm 0.30M_{\text{Ey,y}}, \quad N_{\text{Ex}}^{\text{cor}} = N_{\text{E}}$

Points $\boxed{2}$ 3.3′: $M_{\text{Ey min}} = -M_{\text{Ey,y}} = 0.30M_{\text{Ey,x}}, \quad M_{\text{Ex}}^{\text{cor}} = M_{\text{Ex,y}} \pm 0.30M_{\text{Ex,x}}, \quad N_{\text{Ey}}^{\text{cor}} = N_{\text{E}}$

Points $\boxed{2}$ 4.4′: $M_{\text{Ey max}} = M_{\text{Ey,y}} = 0.30M_{\text{Ey,x}}, \quad M_{\text{Ex}}^{\text{cor}} = M_{\text{Ex,y}} \pm 0.30M_{\text{Ex,x}}, \quad N_{\text{ey}}^{\text{cor}} = N_{\text{E}}$

$$(5.121)$$

Group (1) corresponds to the eight points 1–4 and 1′–4′, which approximate according to Equation 5.117 ellipse (1) (Figure 5.40), while group (2) corresponds to the eight points 1–4 and 1′–4′ which approximate ellipse (2), that is, the mirror of ellipse (1) (Figure 5.40).

Now, if the envelope of the design strength $M_{\text{xd}} - M_{\text{yd}}$ of a symmetric R/C cross-section (e.g. column) for a given value of $N_{\text{Ed}} = N_{\text{E}}$ is plotted on the same plot with the ellipses (1) and (2) (Figure 5.42), the following cases may appear.
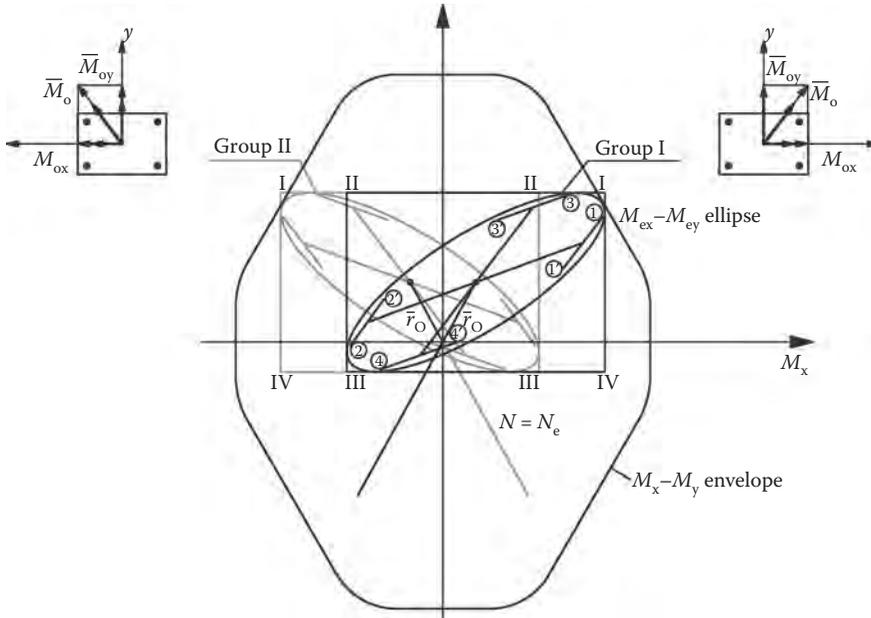
Figure 5.42 Choice of the proper ellipse (group I or group II) in regard to the position of the gravity load effects vector $\overline{r}_0$ in the quarters of the capacity envelope of a symmetric cross-section.
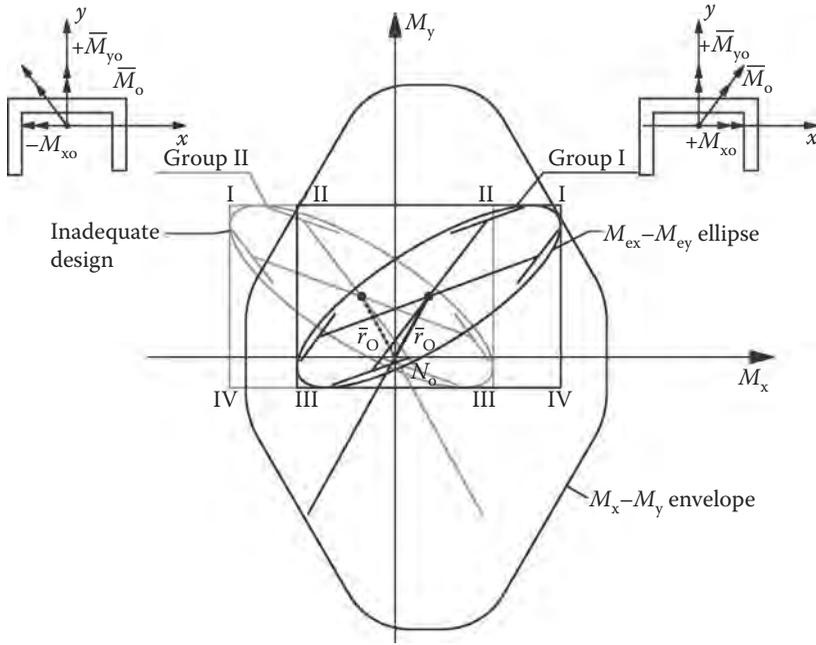
Figure 5.43 Choice of the proper ellipse (group I or group II) in regard to the position of the gravity load effects vector $\overline{r}_0$ in the quarters of the capacity envelope of a unisymmetric cross-section.

Case 1

The vector $\overline{r}_0(M_{ox}, M_{oy})$ due to the gravity loads of seismic design may fall in the first or third quarter of the strength envelope, where M_{ox} M_{oy} have the same sign, either $(+, +)$ or $(-, -)$. In this case, ellipse (1) becomes the crucial one for the dimensioning of the cross-section and in this respect the combinations of group (1) are also the crucial ones for the design.

Case 2

The vector $\overline{r}_0(M_{ox}, M_{oy})$ may fall in the second or fourth quarter of the strength envelope, where M_{ox}, M_{oy} have different sign, either $(+, -)$ or $(-, +)$. In this case, ellipse (2) becomes the crucial one for the dimensioning of the cross-section and in this respect the combinations of group (2) are also crucial for the design.

Case 3

The vector $\overline{r}_0(M_{ox}, M_{oy})$ may fall on one of the main axes x–x or y–y, which means that the stress state due to gravity loads of seismic design is symmetric to one of the two main axes or to both of them. In this case it is indifferent which of the two ellipses and, consequently, the two groups (1) and (2) will be used for the design.

The above considerations also hold for non-symmetric cross-sections (e.g. a cross-section with a *U* form; Figure 5.43).

From all of the above considerations it may be easily concluded that the number of combinations in the case of use of the alternative method for seismic load combinations expressed by Equation 5.117 continues to be 32, as in the case of the reference method expressed by Equation 106.

It should be noted here that in the place of N_E the following values are introduced:
Group (1)

$$
\begin{aligned}
\text{Points } \boxed{1} \quad 1.1': & \ N_{ex}^{cor} = +N_E \pm 0.30 N_{Ey} \\
\text{Points } \boxed{1} \quad 2.2': & \ N_{ex}^{cor} = -N_{Ex} \pm 0.30 N_{Ey} \\
\text{Points } \boxed{1} \quad 3.3': & \ N_{ey}^{cor} = +N_{ey} \pm 0.30 N_{ex} \\
\text{Points } \boxed{1} \quad 4.4': & \ N_{ey}^{cor} = -N_{ey} \pm 0.30 N_{ex}
\end{aligned}
\tag{5.122}
$$

Group (2)

$$
\begin{aligned}
\text{Points } \boxed{2} \quad 1.1': & \ N_{Ex}^{cor} = +N_{Ex} \pm 0.30 N_{Ey} \\
\text{Points } \boxed{2} \quad 2.2': & \ N_{Ex}^{cor} = -N_{Ex} \pm 0.30 N_{Ey} \\
\text{Points } \boxed{2} \quad 3.3': & \ N_{Ey}^{cor} = -N_{Ey} \pm 0.30 N_{Ex} \\
\text{Points } \boxed{2} \quad 4.4': & \ N_{ey}^{cor} = +N_{Ey} \pm 0.30 N_{Ex}
\end{aligned}
\tag{5.123}
$$

The above procedure has been incorporated into the computer platform EC tools.

5.8.4.4 Implementation of the alternative method for horizontal and vertical seismic action

It has been mentioned (Subsection 3.4.3) that the vertical component of the seismic action has to be considered only for certain structures (Luft, 1989). The effects of the vertical component according to EC8-1/2004 need only be taken into account for the elements under consideration and their directly associated supporting elements or substructures.

In the case that the horizontal components of the seismic action are also relevant for these elements, EC8 introduces the following combinations:

$$
\left.
\begin{aligned}
E &= 0.30 E_x \ '+' \ 0.30 E_y \ '+' \ E_z \\
E &= E_x \ '+' \ 0.30 E_y \ '+' \ 0.30 E_z \\
E &= 0.30 E_x \ '+' \ E_y \ '+' \ 0.30 E_z
\end{aligned}
\right\}
\tag{5.124}
$$

where E_z is the action effect due to the application of the vertical component of the design seismic action.

The number of combinations needed for the design of R/C sections is equal to

$$
\lambda = 4 \times 2 \times 2^3 = 64
\tag{5.125}
$$

This number also includes the displacements of the centre of mass due to accidental eccentricities.

5.9 EXAMPLE: MODELLING AND ELASTIC ANALYSIS OF AN EIGHT-STOREY RC BUILDING

5.9.1 Building description

The building under investigation is an eight-storey RC building with one basement storey as shown in Figure 5.44. The total height of the building above the ground level is $H = 26$ m.
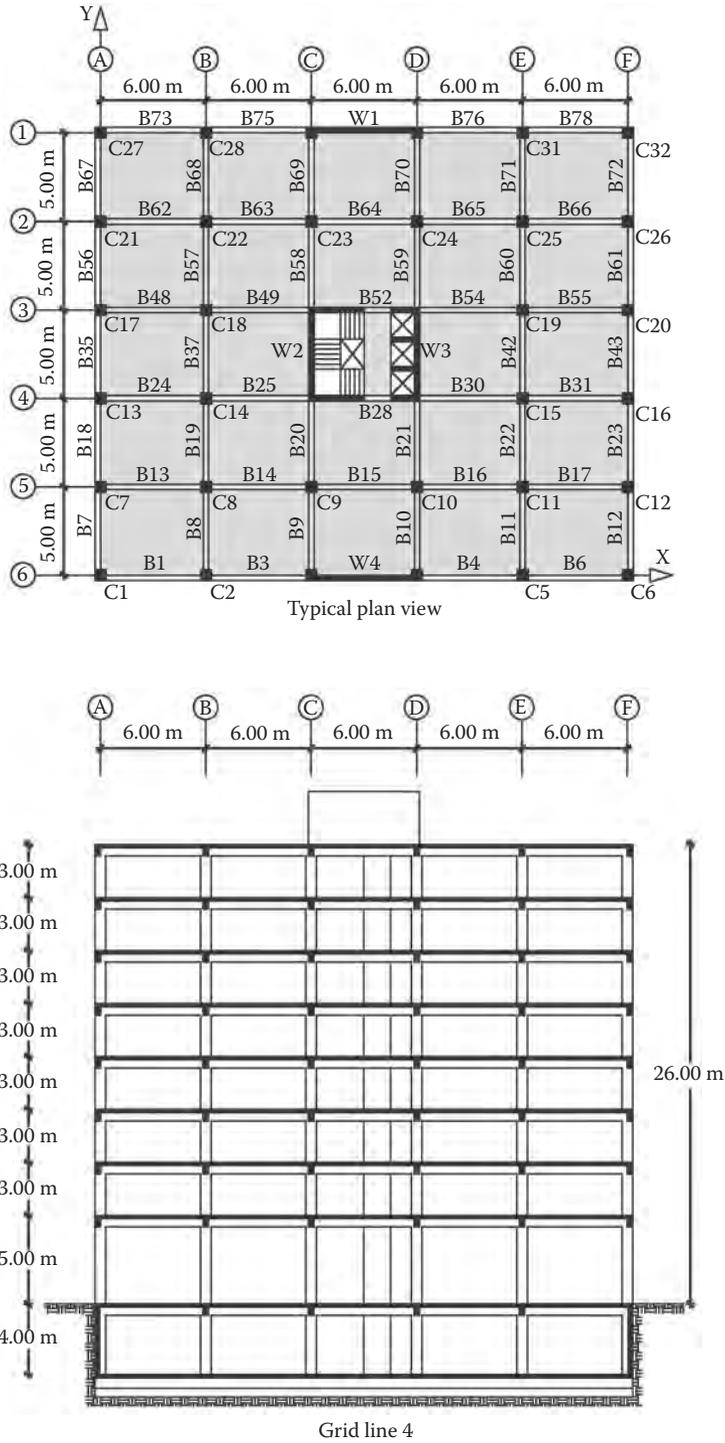
Figure 5.44 Plan and elevation view of the eight-storey building.

The height of a typical storey is 3 m, whereas the height of the first storey and the basement are differentiated to 5 m and 4 m, respectively (Figure 5.44). The building is rectangular in plan, with dimensions of 30 m on the horizontal x axis and 25 m on the horizontal y axis. The structural system consists of walls and frames. All columns have a 60 cm square cross-section. Both interior and exterior beams have a width of $b_w = 30$ cm and a height of $h_b = 65$ cm. The slab thickness is $h_f = 18$ cm. Walls have a thickness of $b_t = 30$ cm, except for the perimeter basement walls, which have a thickness of $b_t = 25$ cm. Details relative to the length of the walls appear in Figure 5.44.

5.9.2 Material properties

- Concrete quality is C25/30, with a modulus of elasticity $E_c = 31$ GPa (EC2 Table 3.1).
- Steel quality is B500C.

5.9.3 Design specifications

- Permanent loads due to floor finishes and suspended ceilings: 2 kN/m²
- Permanent loads due to roof finishes: 3.5 kN/m²
- Permanent loads due to light partition walls: 0.5 kN/m²
- Permanent facade loads: 3.0 kN/m
- Live load (whole building except roof): 5.0 kN/m²
- Live load on the roof: 2.0 kN/m²
- The peak ground acceleration is $a_g = 0.24$ g
- Seismic demand is defined for the EC8-Part I Type I spectrum on ground C. Importance class is II

5.9.4 Definition of the design spectrum

5.9.4.1 Elastic response spectrum (5% damping)

Seismic actions are estimated according to the EC8-Part I elastic response spectrum, Type 1 (EC8-Part I, Section 3.2.2.2(1)P) for ground type C. The values of the periods T_B, T_C, T_D and of the soil factor S for ground type C are defined as: $T_B = 0.2$ s, $T_C = 0.6$ s, $T_D = 2.0$ s and S = 1.15. Peak ground acceleration is considered equal to $a_g = 0.24$ g. The building is classified in importance class II, hence the importance factor is $\gamma_I = 1$ (EC8-Part I, Section 4.2.5, Table 4.3). The elastic response spectrum is derived for 5% damping following the set of equations of EC8-Part I, Section 3.2.2.2(1)P.

5.9.4.2 Design response spectrum

For the definition of the design response spectrum the knowledge of the behaviour factor, q, is necessary. Therefore, the building's structural system has to be classified according to its behaviour under horizontal seismic actions (EC8-Part I, Section 5.2.2.1). Moreover, the regularity in elevation and plan as well as the ductility class need to be taken into account for deriving the value of the behaviour factor. These criteria are examined in Sections 5.2.2 and 5.2.3, where more details appear for the extracted value of q. The design response spectrum (EC8-Part I, Section 3.2.2.5(4) P) utilised for the design of the building examined here is defined for $q = 4.4$ (the detailed procedure for estimation of the behaviour factor appears in Section 5.4.3). Both the elastic and the design response spectra are presented in Figure 5.45.
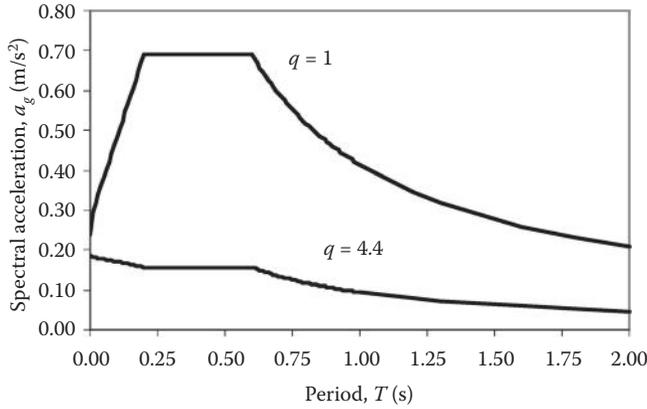
Figure 5.45 Elastic and design response spectrum of EC8-Part I (2004).

5.9.5 Estimation of mass and mass moment of inertia

The total weight of each floor is estimated by considering the combination ($G+0.3Q$) for permanent and live loads. The polar moment of inertia, J_d, is estimated as well (Equation 2.97):

$$J_d = m\frac{b^2 + d^2}{12} = m\frac{30^2 + 25^2}{12} = 127.08\, m$$

The results appear in Table 5.11.

5.9.6 Structural regularity in plan and elevation

5.9.6.1 Criteria for regularity in plan

The regularity criteria in plan that need to be satisfied are (Chapter 5, Subsection 5.2.2):

- The slenderness of the building in plan shall be $\lambda = L_{max}/L_{min} \le 4$
- At each floor, i, and for each direction of analysis, x and y, the structural eccentricity, e_{mx}, e_{my}, and the torsional radius, r_{xc}, r_{yc}, shall meet the following conditions (Equations 5.1):

Table 5.11 Storey weight, storey masses and moments of inertia

Level	Storey weight (kN)	Storey mass (ton)	Moment of inertia (ton·m²)
8th	7946.14	810.00	102880.98
7th	8934.60	910.76	115678.89
6th	8934.60	910.76	115678.89
5th	8934.60	910.76	115678.89
4th	8934.60	910.76	115678.89
3rd	8934.60	910.76	115678.89
2nd	8934.60	910.76	115678.89
1st	9448.53	963.15	122332.84
Total	71002.29	7237.75	919287.17

x–x direction: $e_{mx,i} \leq 0.30 \cdot r_{xc,i}$, $r_{xc,i} \geq l_s$

y–y direction: $e_{my,i} \leq 0.30 \cdot r_{yc,i}$, $r_{yc,i} \geq l_s$

The slenderness of the building is: $\lambda = L_{max}/L_{min} = 30 \text{ m}/25 \text{ m} = 1.2 < 4$

The determination of parameters e_{mx}, e_{my}, r_{xc}, r_{yc}, is carried out following the procedure described in Section 4.5.3.

1. Each floor is loaded at the centre of mass by $T_{zi} = G_i \cdot z_i$ and analysis is performed (G_i is the dead load of each storey, z_i is the storey height; Table 5.12).
2. The plasmatic axis of the centre of stiffness passes through the centre of rotation of floor ℓ (point P_o), being the one that lies closest to the level $z_o = 0.8 \cdot H = 0.8 \cdot 26 = 20.8$ m, which here is the sixth floor. The torsional deformation is (Equation 4.17)

$$\omega_{0.8H} = \frac{+0.1476 - (-0.1476)}{25} = \frac{+0.1792 - (-0.1751)}{30} = 0.0118 \text{ rad}$$

Torsional stiffness with respect to the centre of stiffness (Equation 4.18):

$$J_{TC} = \frac{\sum_{j=1}^{j=i} M_{jz}}{\omega_{0.8H}} = \frac{966428.58}{0.0118} = 81900727.12 \text{ kN m/rad}$$

3. The centre of stiffness of storey ℓ (point P_o) is geometrically estimated:

$$x_c = \frac{u_{y1} \cdot b}{(u_{y1} + u_{y2})} = \frac{0.175 \cdot 30000}{(0.175 + 0.179)} = 14.83 \text{ m}$$

Hence, $e_{mx} = x_M - x_c = 15.00 - 14.83 = 0.17$ m, $e_{my} = 0.00$ m
4. The centre of stiffness of each storey is considered to coincide with the point where the plasmatic axis passes through the structure. A pattern of horizontal forces, $H_{jx} = H_{jy} = G_i \cdot z_i$, is applied to the centre of stiffness of every storey (Equation 4.19, Table 5.13). The translational displacements, $u_{c,0.080\,H}$ and $v_{c,0.80\,H}$, in the x–x and y–y directions, respectively, are estimated and the corresponding stiffnesses are calculated according to Equation 4.20.

Table 5.12 Definition of G_i, z_i and T_{zi} parameters

Storey	G_i	z_i	T_{zi}
8th	7509.49	26.00	195246.80
7th	7842.98	23.00	180388.57
6th	7842.98	20.00	156859.62
5th	7842.98	17.00	133330.68
4th	7842.98	14.00	109801.74
3rd	7842.98	11.00	86272.79
2nd	7842.98	8.00	62743.85
1st	8356.91	5.00	41784.53
Total	62924.29		966428.58

Table 5.13 Definition of parameters G_i, Z_i, H_{jx}, H_{jy}

Storey	G_i	z_i	$H_{jx} = H_{jy}$
8th	7509.49	26.00	195246.80
7th	7842.98	23.00	180388.57
6th	7842.98	20.00	156859.62
5th	7842.98	17.00	133330.68
4th	7842.98	14.00	109801.74
3rf	7842.98	11.00	86272.79
2nd	7842.98	8.00	62743.85
1st	8356.91	5.00	41784.53
Total	62924.29		966428.58

$x–x$ axis:

$$u_{c,0.80H} = 2.2583 \text{ m} \rightarrow K_x = \frac{\sum_{j=1}^{j=1} H_{jx}}{u_{c,0.8H}} = \frac{966428.58}{2.2583} = 427945.17 \text{ kN/m}$$

$y–y$ axis:

$$v_{c,0.80H} = 3.0128 \text{ m} \rightarrow K_y = \frac{\sum_{j=1}^{j=1} H_{jy}}{v_{c,0.8H}} = \frac{966428.58}{3.0128} = 320774.22 \text{ kN/m}$$

5. The torsional radii with respect to the centre of stiffness are estimated as (Equation 2.85)

$$r_{xc} = \sqrt{\frac{J_{TC}}{K_y}} \sqrt{\frac{81900727.12}{320774.22}} = 15.97 \text{ m}, \quad r_{yc} = \sqrt{\frac{J_{TC}}{K_x}} \sqrt{\frac{81900727.12}{427945.17}} = 13.83 \text{ m}$$

The radius of gyration, l_s, is also estimated in order to apply the regularity criteria:

$$l_s = \sqrt{\frac{b^2 + d^2}{12}} = \sqrt{\frac{30^2 + 25^2}{12}} = 11.27 \text{ m}$$

In all cases, $l_s < r_{xc}$, $l_s < r_{xy}$, hence the system has sufficient torsional rigidity (Figure 5.46).

The poles of rotation, O_1 and O_2, as estimated by ECtools (Penelis Software Ltd) for the first two eigenmodes at each floor, appear in Table 5.14. The first two modes may be considered uncoupled in both directions of loading, despite the small eccentricity presented along the $x–x$ axis ($e_{mx} = 0.17$ m) corresponds to 0.56%b where $b = 30$ m). Looking at the ordinates of O_1 and O_2, it may be seen that they are placed practically at an infinite distance from the centre of mass. Pole O_1 (it corresponds to loading in the $y–y$ direction) is closer to the centre of mass compared to pole O_2 due to the small eccentricity presented along the $x–x$ axis.

5.9.6.2 Criteria for regularity in elevation

All the conditions listed in Subsection 5.2.3 are satisfied. Thus, the building is characterised by regularity in elevation.
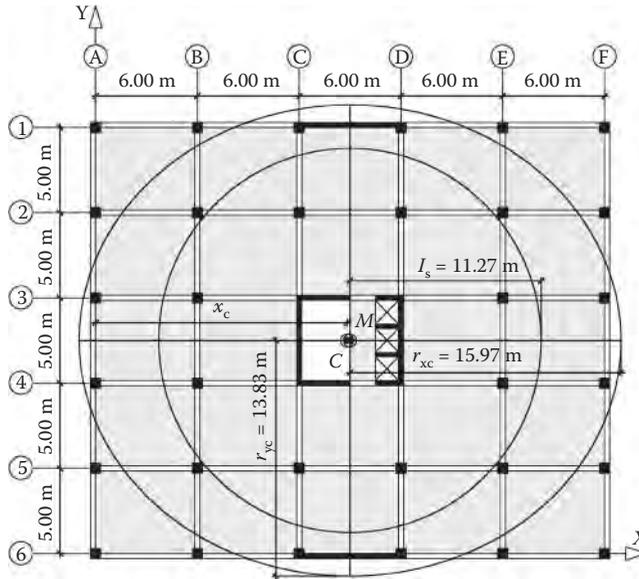
Figure 5.46 Definition of torsional rigidity.

5.9.7 Determination of the behaviour factor *q* (Subsection 5.4.3)

The structural system of the building under investigation can be characterised as an *uncoupled wall system* in both directions. In this case, the shear resistance of the walls at the building base is higher than 65% of the total seismic resistance of the whole structural system. Taking into account the note provided by EC8-Part I (Subsection 5.1.2), where the fraction of shear resistance may be substituted by the fraction of shear forces, the base shear taken by walls is 88.9% and 82.4% in the *x* and *y* directions, respectively. The building is designed for high ductility class (DCH, Subsection 5.4.2).

The upper limit value of the behaviour factor is given by Equation 5.6:

$$q = K_w \cdot K_R^{el} \cdot K_R^{over} \cdot K_Q \cdot q_o$$

with: $K_w = 1$, $K_{reg}^{el} = 1$, $K_Q = 1$ and $q_o = 4.0 \cdot a_u/a_1 = 4.4$ with $a_u/a_1 = 1.1$ for uncoupled wall systems.

Table 5.14 Poles of rotation at each storey

Storey	O_1 (y–y direction)		O_2 (x–x direction)	
	e_{xI} (m)	e_{yI} (m)	e_{xI} (m)	e_{yI} (m)
1st	728.57	0	0	1.00E+100
2nd	626.83	0	0	1.00E+100
3rd	593.81	0	0	1.00E+100
4th	589.17	0	0	1.00E+100
5th	601.44	0	0	1.00E+100
6th	626.64	0	0	1.00E+100
7th	662.83	0	0	1.00E+100
8th	705.56	0	0	1.00E+100

5.9.8 Description of the structural model

Analyses were conducted by the use of ETABS V9.7.4 (Computers and Structures Inc.). The building is idealised as a spatial structural model, comprising beams, columns and walls (Figure 5.47). For the analysis the following modelling assumptions are taken into consideration:

- Beams and columns are modelled with line elements using T and rectangular sections, respectively.
- The walls of the superstructure and the basement perimeter walls are modelled with shell elements.
- The slabs are modelled with shell elements and rigid diaphragm action is considered at each storey.
- The masses and moments of inertia are lumped at the centre of mass of each storey according to EC8-1/2004 (Paragraph 4.3.1(3)), and are evaluated by all gravity loads appearing in the combination of actions $\Sigma G_{k,j} + \Sigma \psi_{E,i} \cdot Q_{k,i}$ (EC8-Part I, Paragraph 3.2.4(2)).
- The foundation, in order to account for soil deformability, is modelled by means of foundation beams on elastic support and its parameter and modelling assumptions will be discussed in more detail in Chapter 10. Line and shell elements are used for this purpose.
- The bottom level of the 1st storey is considered as the base of the building, as far as the distribution of lateral seismic loads is concerned. First, response spectrum analysis is performed, and from the resulting shear forces at each storey the horizontal seismic
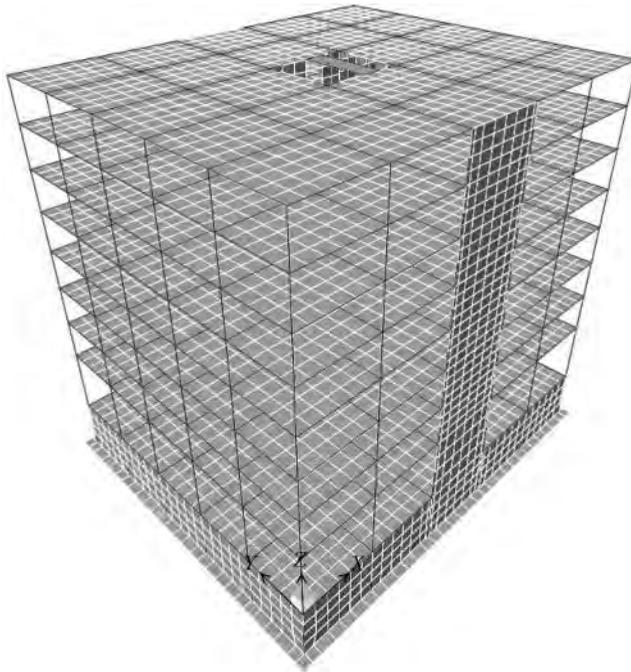
Figure 5.47 Structural model of the eight-storey building.

forces are calculated. These forces are applied to each storey both in the x–x and the y–y directions.

- Cracked concrete is assumed by multiplying the elastic stiffness parameters of the structural elements by 0.5 and the elastic torsional stiffness by 0.1.

Beams are modelled as line elements. The effective width is estimated according to EC2 (Paragraph 5.3.2.1). The code allows taking a constant width over the whole span in structural analysis (Paragraph 5.3.2.1(4)), which is the value of the span section. The effective width is estimated for two internal and two external beams (Figure 5.48). The following equations apply (Equation 5.7, EC8-Part I, Paragraph 5.3.2.1):

$$b_{\text{eff}} = \sum b_{\text{eff}} + b_{\text{w}} \le b, \, b_{\text{eff,i}} = 0.2 \cdot b_{\text{i}} + 0.1 \cdot l_0 \le \min\left(0.2 \cdot l_0; b_{\text{i}}\right) \quad \text{for } l_0 = 0.7 \cdot L$$
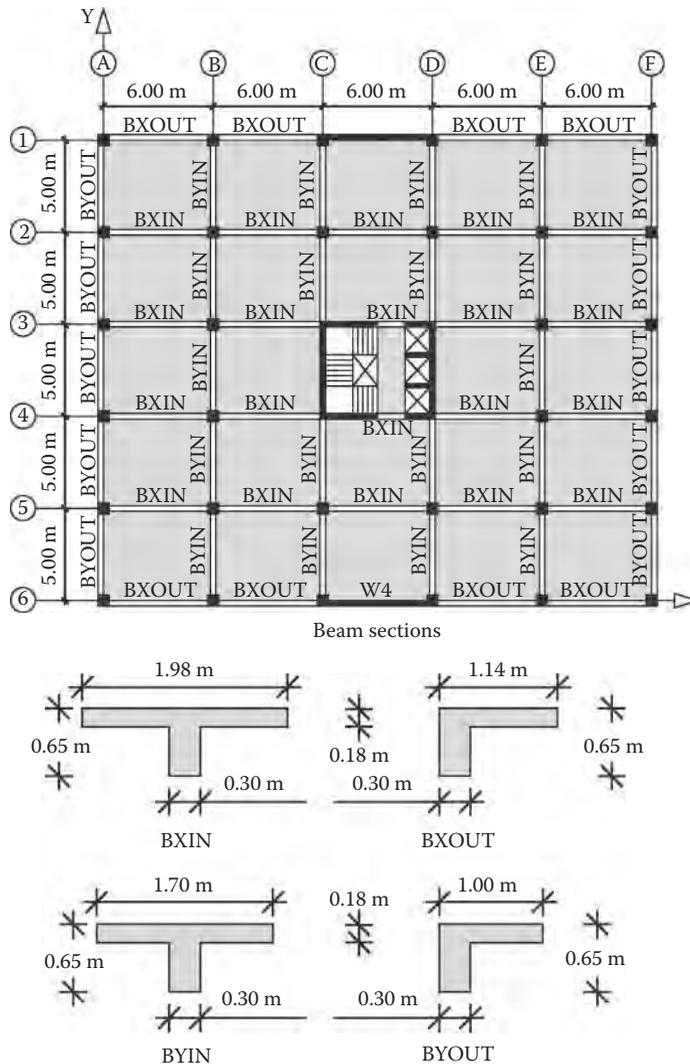
Figure 5.48 Beam sections and effective widths.

x–x direction:

$$b_{\text{eff},1} = b_{\text{eff},2} = 0.2\frac{(5-0.30)}{2} + 0.1(0.7 \cdot 6.0) = 0.89 \, m > \min\left(0.2 \cdot 0.7 \cdot 6.0; \frac{5}{2}\right) = 0.84 \, \text{m}$$

Internal beams (BXIN): $b_{\text{eff,BXIN}} = 0.84 + 0.84 + 0.30 = 1.98 \, \text{m}$

External beams (BXOUT): $b_{\text{eff,BXOUT}} = 0.84 + 0.30 = 1.14 \, \text{m}$

y–y direction:

$$b_{\text{eff},1} = b_{\text{eff},2} = 0.2\frac{(6-0.30)}{2} + 0.1(0.7 \cdot 5.0) = 0.92 \, \text{m} > \min\left(0.2 \cdot 0.7 \cdot 5.0; \frac{6}{2}\right) = 0.70 \, \text{m}$$

Internal beams (BYIN): $b_{\text{eff,BYIN}} = 0.70 + 0.70 + 0.30 = 1.70 \, \text{m}$

External beams (BYOUT): $b_{\text{eff,BYOUT}} = 0.70 + 0.30 = 1.00 \, \text{m}$

5.9.9 Modal response spectrum analysis

Response spectrum analysis is performed in two horizontal directions by considering the design response spectrum of Figure 5.45 ($q = 4.4$). The number of modes taken into account is defined by the sum of the effective modal masses, which has to be equal to at least 90% of the total mass of the structure. The CQC method is used to combine the results of the modes considered, in each direction. These results include the accidental torsional effects as described hereafter.

5.9.9.1 Accidental torsional effects

There are eight (8) basic seismic load combinations which result from $G+0.3 \, Q\pm E_x\pm0.3E_y$ and $G+0.3 \, Q\pm E_y\pm0.3E_x$, where E_x and E_y are the seismic actions applied in the *x–x* and *y–y* directions, respectively. In the case that the centre of mass at each floor is considered to be displaced from each nominal location in each direction by an accidental eccentricity, then the resulting load combinations become 32 in number (8 basic seismic load combinations × 4 locations of mass).

The accidental eccentricity, according to EC8-Part I (Paragraph 4.3.3.3.3), is $e_{\text{ai}} = \pm0.05 \cdot L_i$, where L_i is the floor dimension perpendicular to the direction of the seismic action (EC8-Part I, Equation 4.3).

In the example building studied here, a feature of ETABS is implemented, where the accidental eccentricity for each diaphragm is automatically taken into account for each of the seismic actions in directions *x–x* and *y–y*. This eccentricity displaces the mass along the *x* and *y* axes, causing additional moments, the larger absolute value of which is then applied as torsion about the centre of mass, and the results are added to the response spectrum output. This is considered a conservative approach to the problem, but at the same time it eliminates the need to define a set of 8 combinations for each mass location, since the effect of the eccentricity is already included in the results of the applied seismic actions and E_y, leaving in the end 8 combinations.

In Tables 5.15 and 5.16, the influence of the accidental eccentricity at the response spectrum analysis results is shown for the *x–x* and *y–y* directions, respectively. As may be observed, the accidental eccentricity increases the value of the torsion T_i in both directions.

Table 5.15 Response spectrum analysis for E_x

Storey	V_{xi} (kN)	V_{yi} (kN)	M_{xi} (kN m)	M_{yi} (kN m)	T_i (kN m) $e_{ai} = 0$	T_i (kN m) $e_{ai} = \pm 0.05 \cdot L_i$
8th	1736.61	0.08	0.23	5209.84	21708.37	23874.54
7th	3278.27	0.15	0.67	14943.00	40979.46	45197.69
6th	4592.75	0.22	1.32	28520.13	57410.58	63448.52
5th	5693.97	0.28	2.15	45310.68	71175.77	78884.20
4th	6626.00	0.34	3.15	64765.64	82826.13	92057.79
3rd	7386.06	0.38	4.28	86381.15	92326.83	102961.83
2nd	7980.14	0.42	5.51	109671.82	99752.88	111634.49
1st	8422.90	0.44	7.70	150705.27	105287.36	118341.19

5.9.9.2 Periods, effective masses and modes of vibration

The modal properties are presented in Table 5.17 for the first 27 modes of vibration, which are considered in the response spectrum analysis, since the sum of the effective modal masses is over 90% of the total mass of the structure EC8-Part I (Paragraph 4.3.3.3.1). It is noted that the criterion regarding the sum of the effective modal masses is satisfied in the *x–x* and *y–y* directions by considering the first 11 modes only. The need to comply with that criterion about the vertical axis too imposes the consideration of a larger number of modes. The 27th mode of vibration has a significant impact on the effective mass about the vertical axis.

The first three periods of vibration, considered to be the fundamental ones, are equal to 0.82, 0.71 and 0.60 s. According to the percentage of effective masses, it follows that the first two modes are predominantly translational in the *x–x* and *y–y* direction, whereas the third is predominantly torsional (Figure 5.49).

5.9.9.3 Shear forces per storey

The base shear obtained by response spectrum analysis in the *x–x* and *y–y* directions is $V_{b,x} = 8422.90$ KN and $V_{b,y} = 7252.29$ kN in the first storey. The base shear distribution along the height of the building is shown in Table 5.18.

5.9.9.4 Displacements of the centres of masses

According to Subsection 6.2.3 the displacement d_s due to the design seismic action could be the result of the elastic analysis of the structural system magnified by the behaviour factor q (Equation 6.43):

$$d_s = q \cdot d_e$$

Table 5.16 Response spectrum analysis for E_y

Storey	V_{xi} (kN)	V_{yi} (kN)	M_{xi} (kN m)	M_{yi} (kN m)	T_i (kN m) $e_{ai} = 0$	T_i (kN m) $e_{ai} = \pm 0.05 \cdot L_i$
8th	0.09	1494.34	4483.03	0.27	22929.52	25166.25
7th	0.17	2808.99	12816.05	0.79	42944.08	47292.45
6th	0.25	3915.30	24383.14	1.52	59715.70	65921.25
5th	0.31	4842.32	38629.07	2.43	73742.95	81696.95
4th	0.35	5633.68	55112.33	3.48	85735.69	95294.71
3rd	0.39	6295.14	73443.73	4.64	95788.85	106883.01
2nd	0.42	6830.78	93264.90	5.89	103972.78	116457.88
1st	0.44	7252.29	128392.70	8.07	110455.47	124279.18

Table 5.17 Periods and effective masses

Mode	T (s)	$M_{eff,x}$ (%)	$M_{eff,y}$ (%)	$M_{eff,Mz}$ (%)
1	0.82	0.00	75.36	0.02
2	0.71	73.98	0.00	0.00
3	0.60	0.00	0.02	70.57
4	0.20	0.00	10.76	0.06
5	0.17	11.63	0.00	0.00
6	0.17	0.00	0.09	10.23
7	0.09	0.00	3.26	0.04
8	0.08	3.95	0.00	0.00
9	0.08	0.00	0.04	3.03
10	0.06	0.00	1.70	0.01
11	0.05	2.48	0.00	0.00
12	0.05	0.00	0.02	1.10
13	0.04	0.00	2.78	0.00
14	0.04	0.00	5.19	0.00
15	0.04	4.63	0.00	0.00
16	0.03	0.00	0.02	0.50
17	0.03	0.00	0.51	0.00
18	0.03	2.95	0.00	0.00
19	0.03	0.00	0.05	0.00
20	0.03	0.00	0.00	0.30
21	0.03	0.00	0.00	0.00
22	0.03	0.17	0.00	0.00
23	0.02	0.00	0.00	0.21
24	0.02	0.00	0.00	0.12
25	0.02	0.02	0.00	0.00
26	0.02	0.00	0.00	0.00
27	0.02	0.00	0.00	13.79
$\Sigma M_{eff} =$		99.81	99.81	99.99
		1st mode, T = 0.82 s	2nd mode, T = 0.71 s	3rd mode, T = 0.60 s

The calculations are presented in Table 5.19 for $q = 4.4$. The drift at the eighth storey (roof level) is 0.40% (=0.1043/26) in the $x–x$ direction and 0.45% (=0.1175/26) in the $y–y$ direction.

5.9.9.5 Damage limitations

For buildings having non-structural elements of brittle materials attached to the structure (Equation 6.45):

$$d_{ri} \leq \frac{0.005 \cdot h_i}{r}$$

For buildings having ductile non-structural elements (Equation 6.46):
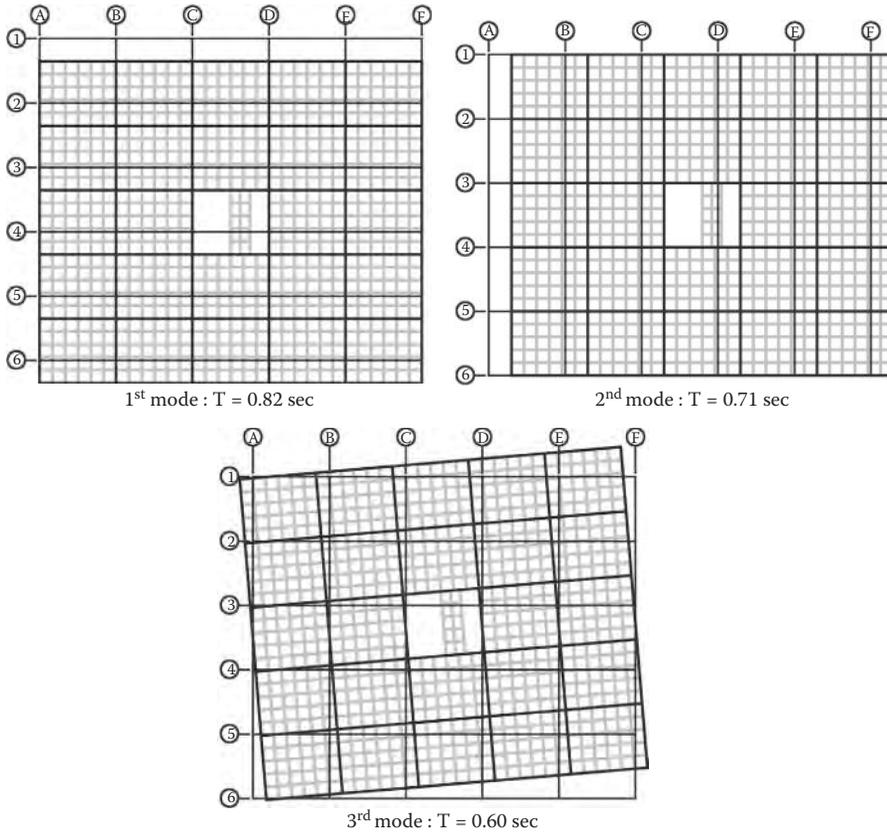
Figure 5.49 Fundamental modes of vibration.

$$d_{ri} \leq \frac{0.0075 \cdot h_i}{r}$$

For buildings having non-structural elements fixed in a way so as not to interfere with structural deformation or without non-structural elements (Equation 6.47):

$$d_{ri} \leq \frac{0.010 \cdot h_i}{r}$$

Table 5.18 Storey shear forces

Storey	$V_{b,x}$	$V_{b,y}$
8th	1736.61	1494.34
7th	3278.27	2808.99
6th	4592.75	3915.30
5th	5693.97	4842.32
4th	6626.00	5633.68
3rd	7386.06	6295.14
2nd	7980.14	6830.78
1st	8422.90	7252.29

Table 5.19 Displacements at the centre of mass along the elevation in both the x–x and y–y directions

Storey	d_e (m)		$d_s = d_e{}^*q$ (m)	
	x–x	y–y	x–x	y–y
8th	0.0237	0.0267	0.1043	0.1175
7th	0.0215	0.0244	0.0946	0.1074
6th	0.0191	0.0218	0.0840	0.0959
5th	0.0165	0.019	0.0726	0.0836
4th	0.0137	0.0159	0.0603	0.0700
3rd	0.0107	0.0127	0.0471	0.0559
2nd	0.0077	0.0094	0.0339	0.0414
1st	0.0048	0.0061	0.0211	0.0268

The reduction factor r is taken to be equal to $r = 0.50$ for importance class II. The design inter-storey drift d_r is evaluated as the difference of the average lateral displacements ds at the top and bottom of the storey under consideration. The centre of mass is considered as the reference point for estimating the lateral displacements of the structural system. It may be noted that EC8-Part I (2004) does not provide a specific procedure for the estimation of the average lateral displacements. The calculations performed appear in Table 5.20. The ratio $(r \cdot d_{ri}/h_i)$ in all storeys is well below the strictest value of $d_{ri} = 0.005$. Hence, no damage is anticipated.

5.9.9.6 Second-order effects

$P-\Delta$ effects need not be taken into account in the case that the inter-storey drift sensitivity coefficient θ_i is (Chapter 6, Subsection 6.2.2, Equation 6.36):

$$\theta_i = \frac{\Delta_{el}^i \cdot q}{h_i} \cdot \frac{W_{tot}^i}{V_{tot}^i} \le 0.10$$

The term $\left(\Delta_{el}^i \cdot q\right)$ is equal to the design inter-storey drift d_{ri}. The sensitivity coefficients of all the storeys appear in Table 5.21. As may be observed, the second-order effects need not be taken into account, since $\theta_i \le 0.10$ in all storeys (Figure 5.50).

Table 5.20 Calculation of the damage limitation index

Storey	d_{ri} (m)		h_i	$r \cdot d_{ri}/h_i$	
	x–x	y–y		x–x	y–y
8th	0.0097	0.0101	3	0.0016	0.0017
7th	0.0106	0.0115	3	0.0018	0.0019
6th	0.0114	0.0123	3	0.0019	0.0021
5th	0.0123	0.0136	3	0.0021	0.0023
4th	0.0132	0.0141	3	0.0022	0.0024
3rd	0.0132	0.0145	3	0.0022	0.0024
2nd	0.0128	0.0146	3	0.0021	0.0024
1st	0.0211	0.0268	5	0.0021	0.0027

Table 5.21 Estimation of the inter-storey drift sensitivity coefficients θ_i of each storey

Storey	$d_{ri}(=\Delta_{el}^i \cdot q)$ (m)		W_{tot}(kN)	V_{tot} (kN)		h_i (m)	θ_i (%)	
	x-x	y–y		x–x	y–y		x–x	y–y
8th	0.0097	0.0101	7946.14	1736.61	1494.34	3	1.48	1.79
7th	0.0106	0.0115	16880.74	3278.27	2808.99	3	1.82	2.30
6th	0.0114	0.0123	25815.34	4592.75	3915.30	3	2.14	2.70
5th	0.0123	0.0136	34749.94	5693.97	4842.32	3	2.50	3.25
4th	0.0132	0.0141	43684.54	6626.00	5633.68	3	2.90	3.64
3rd	0.0132	0.0145	52619.14	7386.06	6295.14	3	3.13	4.04
2nd	0.0128	0.0146	61553.74	7980.14	6830.78	3	3.29	4.39
1st	0.0211	0.0268	71002.27	8422.90	7252.29	5	3.56	5.25

5.9.9.7 Internal forces

In Figures 5.51 through 5.56 the envelope diagram bending moments are presented for the seismic load combinations ($G+0.3Q\pm E_x\pm 0.3E_y$ and $G+0.3Q\pm E_y\pm 0.3E_x$) for the elevation of grid axes B and C. The results at the foundation level are omitted.

5.10 EXAMPLES: APPLICATIONS USING INELASTIC ANALYSIS

5.10.1 Cantilever beam

5.10.1.1 Modelling approaches

A simple cantilever beam shown in Figure 5.57 is modelled using the point hinge and fibre analysis approach. The beam is 10 m high with a rectangular cross-section of 40×40 cm and $6 \times D14$ at each side. The materials used are C16/20 for concrete and B500C for steel, which are used with their characteristic values. It should be noted that this case represents
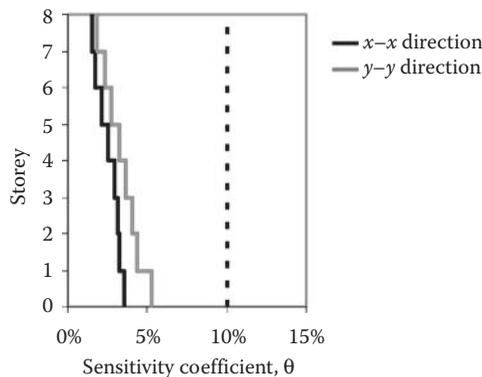
Figure 5.50 Comparison of the calculated inter-storey drift sensitivity coefficients θ_i with the Code upper limit ($\theta_i \leq 0.10$).

−211.30	−355.21	−349.31	−349.33	−355.22	−211.33
−467.56	−685.50	−679.51	−679.53	−685.53	−467.62
−731.78	−1021.57	−1017.53	−1017.56	−1021.61	−731.88
−1004.29	−1360.72	−1361.64	−1361.68	−1360.77	−1004.42
−1283.40	−1704.95	−7712.71	−1712.82	−1705.02	−1283.56
−1566.40	−2055.83	−2070.99	−2071.05	−2055.91	−1566.58
−1849.81	−2414.75	−2435.37	−2435.44	−2414.85	−1850.02
−2138.66	−2803.69	−2831.71	−2831.77	−2803.80	−2138.88
−1119.93					−1120.04
	−3212.86	−3224.57	−3224.63	−3212.98	

Figure 5.51 Envelope of axial forces – Grid axis B.

the simplest structural form and should always be used to validate and check new nonlinear analysis software, as the response can easily be assessed by hand calculations. The analyses have been performed using Etabs (2013) and ECtools (2013) for the point hinge model and Seismostruct (2013) for the fibre model.

For the point hinge approach, a bilinear moment rotation curve (rigid plastic) is used for the plastic part of the rotation, with unlimited deformation capability in order to be able to compare the initial stiffness and the ultimate strength as shown in Figure 5.58.

On the other hand, for the elastic part of the rotation up to yield moment M_y, flexural rigidity is introduced with values varying from 30% to 70% of the uncracked one. The loading is introduced as an incremental lateral load combined with a displacement control approach in order to simulate the post-yield behaviour.

For the distributed nonlinearity approach different material models were used for confined concrete and steel, as shown in Figures 5.59a and 5.59b.

The element used was a cubic linear element discretised into four different elements. The convergence strategy was a mixed one, starting with load control and then shifting to automatic displacement control.

5.10.1.2 Results

The results are presented in the form of a pushover curve in Figure 5.60.

From that, it is derived that both approaches model accurately the strength capacity of a single member. The initial stiffness is modelled accurately, compared to the more detailed fibre model, by introducing the rigidity as 25–35% of the uncracked one, which is different

Figure 5.52 Envelope of shear forces – Grid axis B.

from the FEMA 356 guidelines but in accordance with other publications. As far as the overall ductility of the member, it is obvious that this example is not suitable since the point hinge approach used a perfectly plastic constitutive law without any limit to deformations. This will be investigated in the following case of an MRF.

5.10.2 2-D MRF

5.10.2.1 Modelling approaches

As a second approach, a two storey–two bay 2-D frame designed according to the EC2-1-1/2004 and EC8-1/2004 is modelled. The materials used are C16/20 for concrete and B500C for steel, which are used with their design values. The geometry and the reinforcement of the frame are shown in Figure 5.61. The gravity load is *g* = 20 kN/m at all beams

Figure 5.53 Envelope of bending moments – Grid axis B.

(including self-weight of the whole structure) and $q = 15$ kN/m. The pushover analysis is performed using the seismic combination of $G+0.30Q+E$. This frame is also modelled using both the point hinge and the fibre approach.

For the point hinge approach, bilinear moment rotation curves are used to model the nonlinear behaviour of beams and columns. The yield and ultimate moment capacity of the columns were calculated using the ECtools (2013) post processor using a credible axial load as predicted by linear analysis while the corresponding deformations were derived from the FEMA 356. The member performance criteria were also derived from the FEMA tables using the same post processor. Two of these moment rotation diagrams are shown in Figure 5.62.

The flexural rigidity is introduced with values varying from 30% to 70% of the uncracked one for both beams and columns. The loading is introduced in two phases: a gravity load case with $G+0.3Q$ and seismic load case continuing from the gravity up to failure. A displacement control approach has been selected in order to simulate the post yield behaviour.
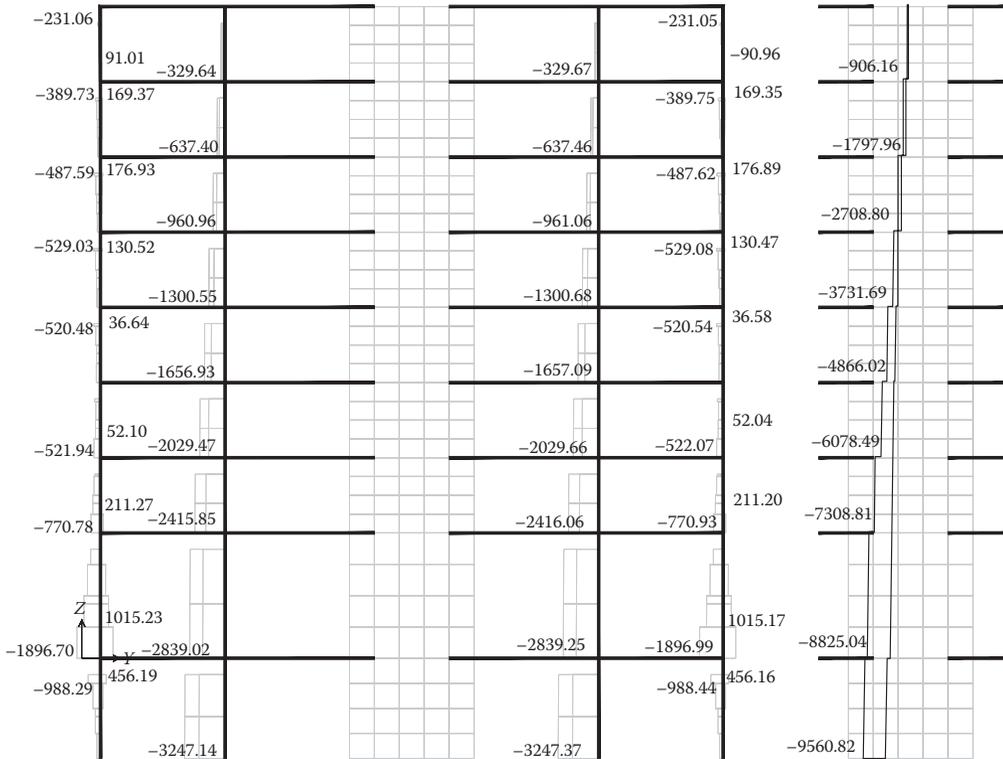
Figure 5.54 Envelope of axial forces – Grid axis C.

For the distributed nonlinearity approach, different material models are used for confined concrete and steel, as shown in Figures 5.63a and 5.63b as they are available in Seismoctruct (2013).

The element used is a cubic linear element discretised into four different elements. The load is introduced in two phases starting with the G+0.3Q as initial loading and continuing with an incremental lateral load pattern. The convergence strategy is a mixed one, starting with load control and then shifting to automatic displacement control.

5.10.2.2 Results

The results are presented in the form of a static pushover curve shown in Figure 5.64. Both approaches model accurately the strength capacity of the structure since they present less than 10% difference (cantilever and frame). The initial stiffness is modelled accurately, as previously elaborated, using 25–35% of the uncracked one. As far as the overall ductility, which presents a significant difference between the two approaches, is attributed to the member ultimate deformations as defined by the FEMA 356 guidelines, which seem to be conservative.

From all of the above it can be derived that by using the simplest static nonlinear approach, which is the point hinge model, the nonlinear behaviour of buildings can be modelled with acceptable accuracy, but only if the engineer has a deep knowledge of the nonlinear behaviour of reinforced concrete as far as initial cracking, post cracking behaviour and modelling are concerned. On the other hand, the ongoing developments in nonlinear software have rendered the fibre approach a viable solution for more accurate modelling, as will be presented in the next paragraph.

Figure 5.55 Envelope of shear forces – Grid axis C.

5.10.3 Sixteen-storey R/C building

5.10.3.1 Modelling approaches

Most of the modelling approaches mentioned this chapter with regard to inelastic analysis are represented in this application. This building is an actual structure in Bucharest, Romania, which has been designed according to EN1992:2004 and EN1998:2004 using the relevant Romanian National Annex. It is a dual R/C system with 16 storeys and four basements.

The plan view and section of the building is shown in Figure 5.65.

The building was initially analysed using Etabs (2013) and ECtools (2013), while for the nonlinear analyses, performed at a later stage and presented herein, the Zeus nonlinear software was used. More details on the modelling and the results may be found in the paper by Penelis and Papanikolaou (2009).

The modelling approach for the nonlinear analysis was the fibre model with linear elements for all structural elements. The finite element modelling is shown in Figures 5.66 and 5.67.

It is obvious that the suggestion to avoid the modelling of basements for the nonlinear analysis has been used.

A very useful tool to assess the accuracy of the NL model is to compare the eigen periods (elastic) to the ones of the elastic model used for design. In the case of the example, these are shown in the following Table 5.22.

Reinforced concrete sections (geometry and detailed reinforcement bar topology) were defined according to the original formwork drawings and were assigned to cubic elastoplastic

Figure 5.56 Envelope of bending moments – Grid axis C.

$$\theta_u = \theta_y + \theta_{pl}$$
$$\delta_u = \delta_y + \delta_{pl}$$
$$= (\theta_y + \theta_{pl})l$$
$$\theta_y = \frac{M_y}{E_{jef}} \cdot l/3$$

$$\theta_{pl} = \frac{\delta_{pl}}{l}$$
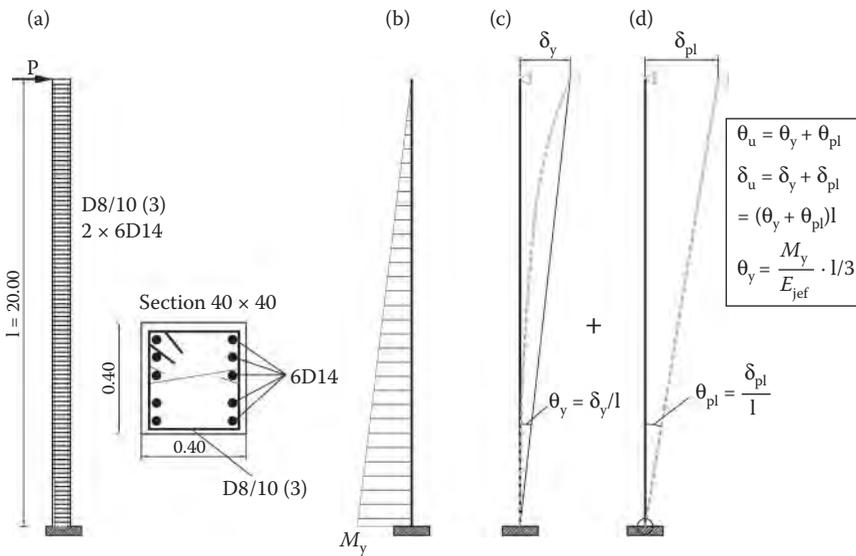
Figure 5.57 Cantilever with lateral loading: (a) geometry; (b) moment diagram at yield; (c) deflexion at yield; (d) post-yield plastic deflexions.

Point	Moment (kNm)	Rotation (rad)
E−	−145	−1
D−	−145	−0.1
C−	−145	−0.05
B−	−145	0
A	0	0
B	145	0
C	145	0.05
D	145	0.1
E	145	1

☑ Hinge is rigid plastic

☑ Symmetric
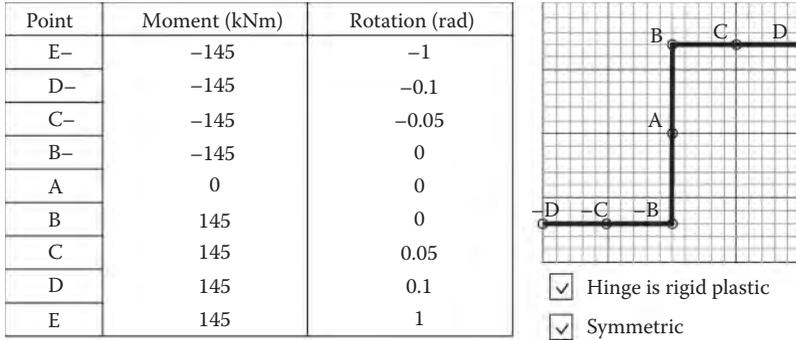
Figure 5.58 Point hinge model for cantilever.

(a)

Initial stiffness (N/mm²) 28,000

Compressive strength (N/mm²) 16

Degradation stiffness (N/mm²) −1000

Residual strength (N/mm²) 2

(b)

Initial stiffness (N/mm²) 2,00,000

Yield strength (N/mm²) 500

Strain-hardening parameter (−) 0.01
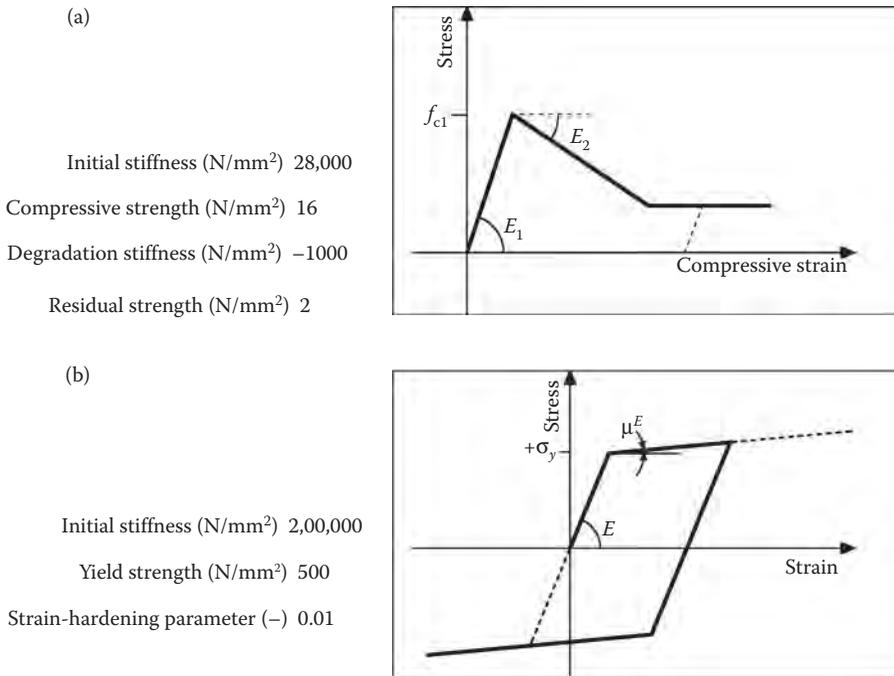
Figure 5.59 Material models (concrete, steel) used for fibre analysis: (a) concrete; (b) steel reinforcement.

frame elements, which have a tangent stiffness matrix that is integrated using second-order Gaussian quadrature (two Gauss points).

Structural walls were modelled using vertical frame elements along the wall mass centre and their horizontal kinematic constraint at storey levels with neighbouring beams was modelled explicitly, using numerically rigid elements (elastic material with $E_{Rigid} = 10 \cdot E_s$ and 1.0×1.0 m cross-section; Figure 5.23).

Rigid diaphragm action was considered at all storey levels. However, numerical treatment using master–slave joint constraints was not available in the current computational platform, and hence an explicit representation was necessary. This was realised using end-pinned, crossed diagonal rigid links on each quadrilateral slab region (Figure 5.22).
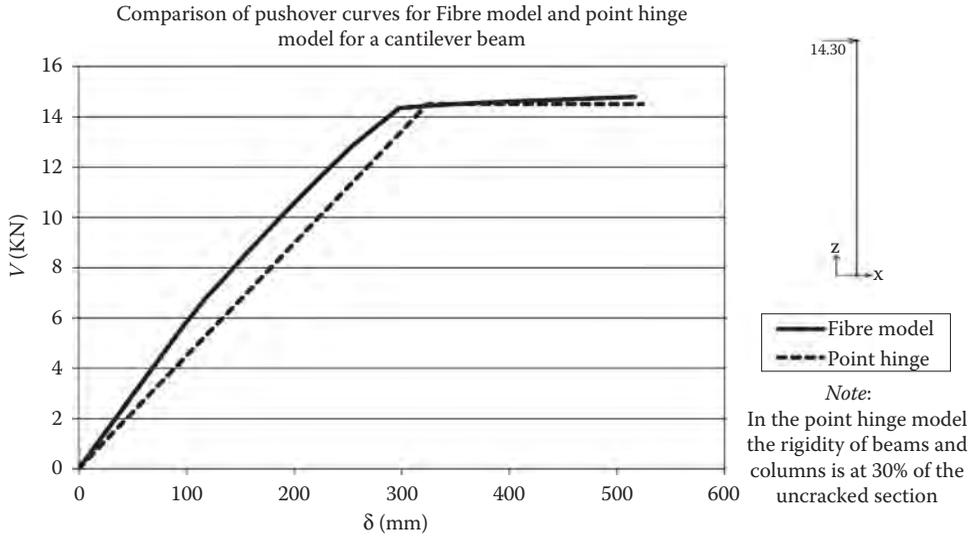
Figure 5.60 Pushover curves from point hinge and fibre model.
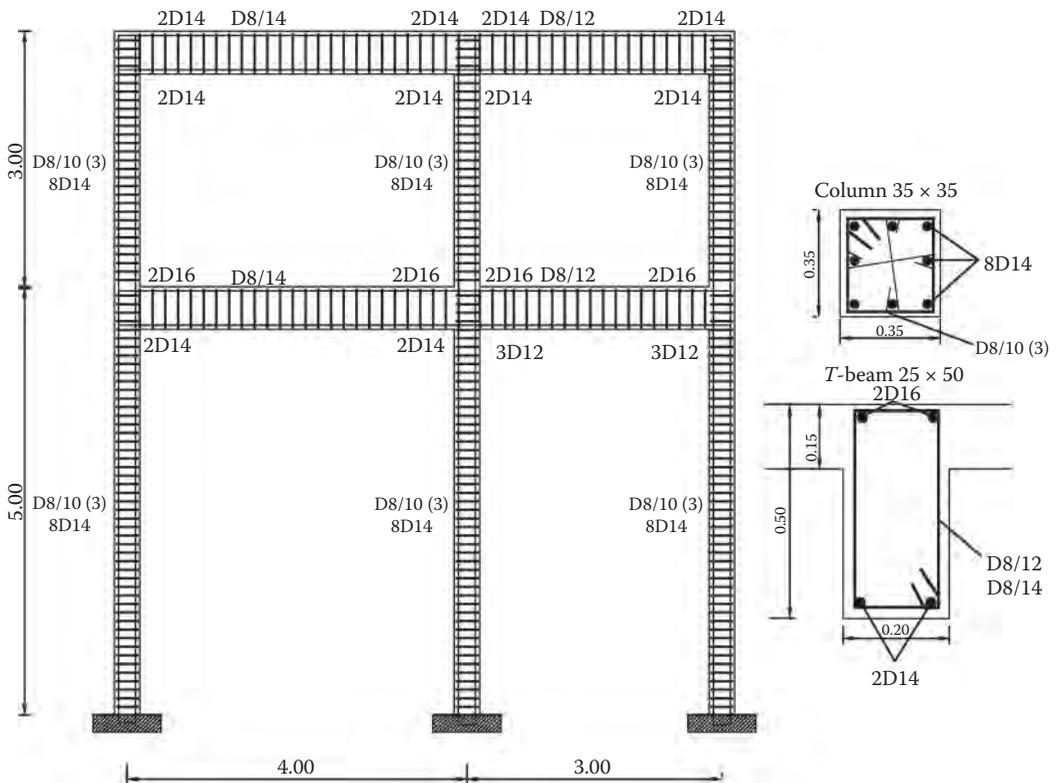
Figure 5.61 Pushover curves from point hinge and fibre model.

Point	Moment (kNm)	Rotation (rad)
E–	–11.63	–0.037
D–	–11.63	–0.019
C–	–58.15	–0.019
B–	–58.15	0
A–	0	0
B	44.7	0
C	44.7	0.02
D	8.94	0.02
E	8.94	0.04

☑ Hinge is rigid plastic
☐ Symmetric

Point	Moment (kNm)	Rotation (rad)
E–	–11.82	–0.03
D–	–11.82	–0.02
C–	–59.12	–0.02
B–	–53.21	0
A	0	0
B	53.21	0
C	59.12	0.02
D	11.82	0.02
E	11.82	0.03

☑ Hinge is rigid plastic
☑ Symmetric
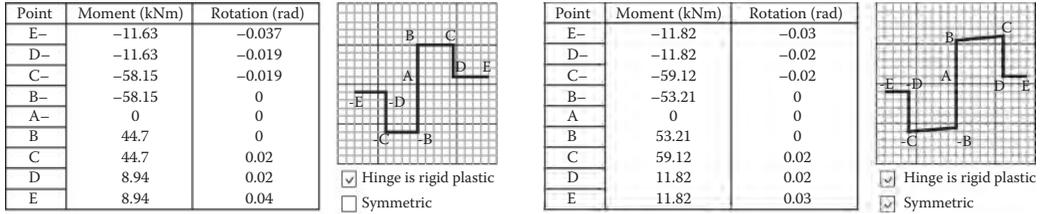
Figure 5.62 Characteristic point hinge models for beams (left) and columns (right).

(a)

Initial stiffness (N/mm^2) 28,000

Compressive strength (N/mm^2) 10.6

Degradation stiffness (N/mm^2) –1000

Residual strength (N/mm^2) 2

(b)

Initial stiffness (N/mm^2) 2,00,000

Yield strength (N/mm^2) 434

Strain-hardening parameter (–) 0.01
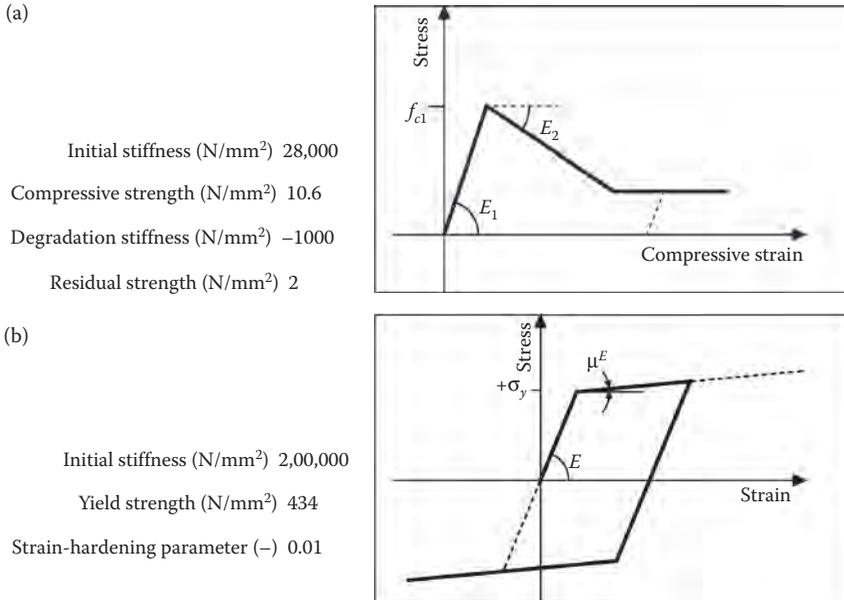
Figure 5.63 Material models (concrete – steel) for fibre analysis: (a) concrete; (b) steel reinforcement.

Comparison of pushover curves for Fibre model and point hinge model for two storey two bay frame

—— Fibre model
- - - Point hinge

Note:
In the point hinge model the rigidity of beams and columns is at 25% of the uncracked section
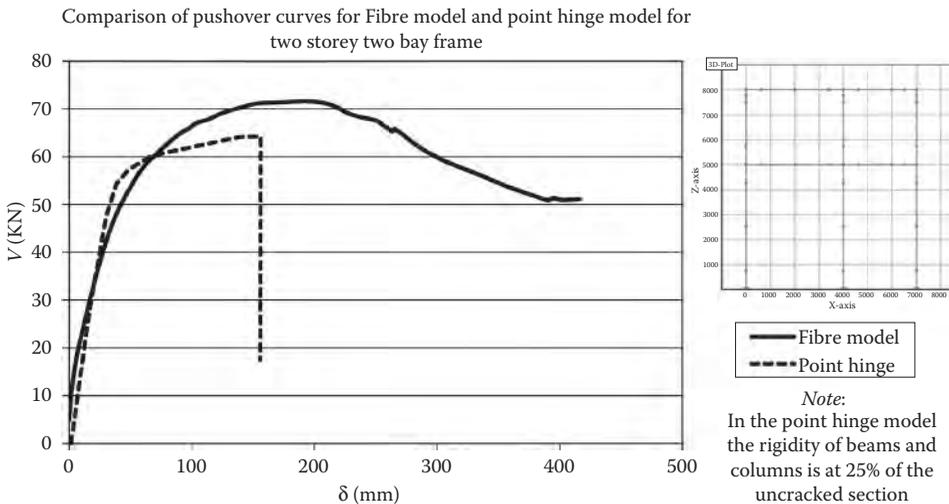
Figure 5.64 Material models (concrete – steel) for fibre analysis.
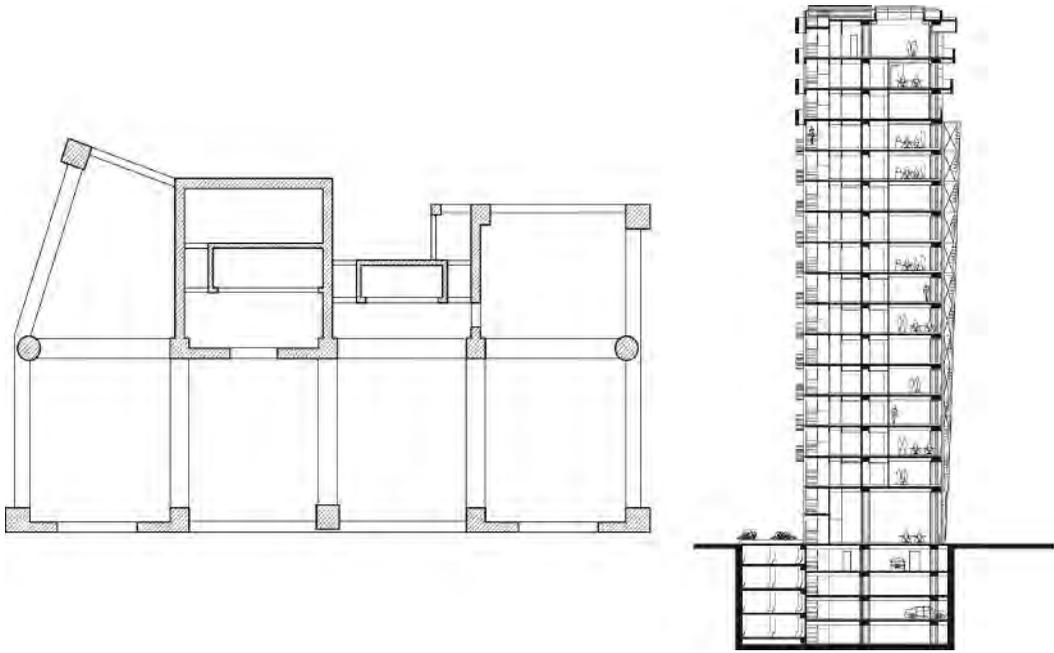
Figure 5.65 Plan view and elevation of a 16-storey building in Bucharest.

Short spandrels connecting walls with openings, which originally included embedded *x*-braces, were explicitly modelled by equivalent column sections and rigid link (Figure 5.68).

The total gravity load for each storey was calculated from the $G+\psi_2 \cdot Q$ seismic load combination of the initial design and was applied to the three beam inner-nodes and wall end-nodes, according to their geometrically derived tributary area.

For dynamic analysis, the total mass of each storey $m = (G+\psi_2 \cdot Q)/g$ was distributed to the end-nodes of all vertical elements (columns and walls), according to their tributary area.

The horizontal loading pattern for inelastic static analysis was applied on the node coincident to the centre of mass (CM, Figure 5.66) of each storey level and, for dynamic analysis, biaxial excitation in both directions x and y (in the form of time–acceleration history) was applied on all base nodes.
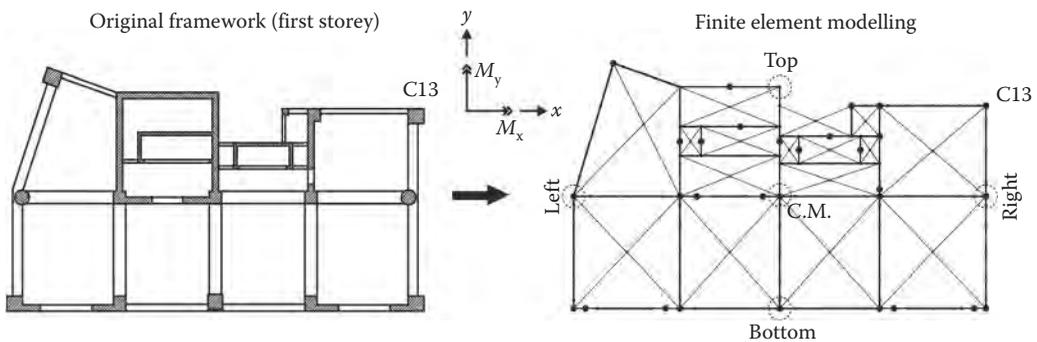
Figure 5.66 Typical storey plan view and modelling.
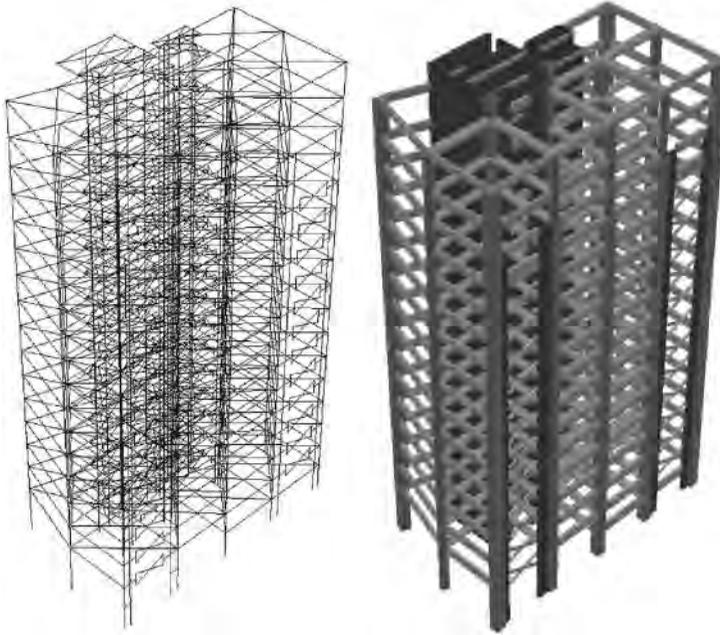
Figure 5.67 Finite element model of the 16-storey building.

Table 5.22 Eigen period from elastic and inelastic model

Mode	Zeus-NL (s)	ETABS (s)
1	1.03	0.98
2	0.81	0.73
3	0.53	0.56
4	0.25	0.22
5	0.21	0.21
6	0.16	0.16
7	0.14	0.12
8	0.13	0.09
9	0.12	0.08
10	0.11	0.08
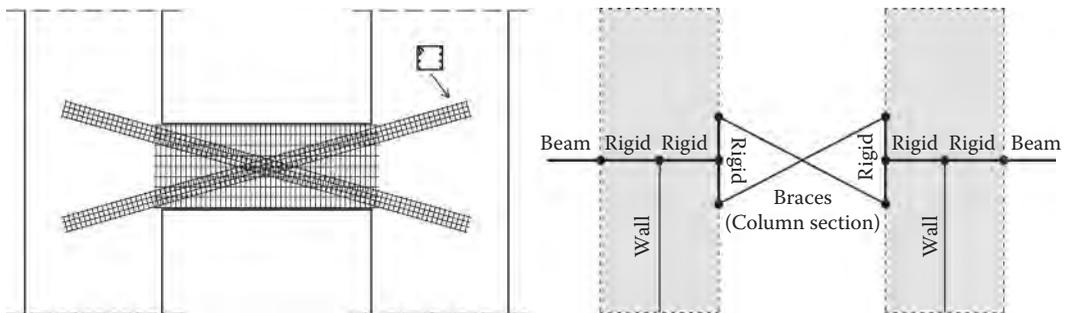
Figure 5.68 Finite element model for the short spandrels of the 16-storey building.
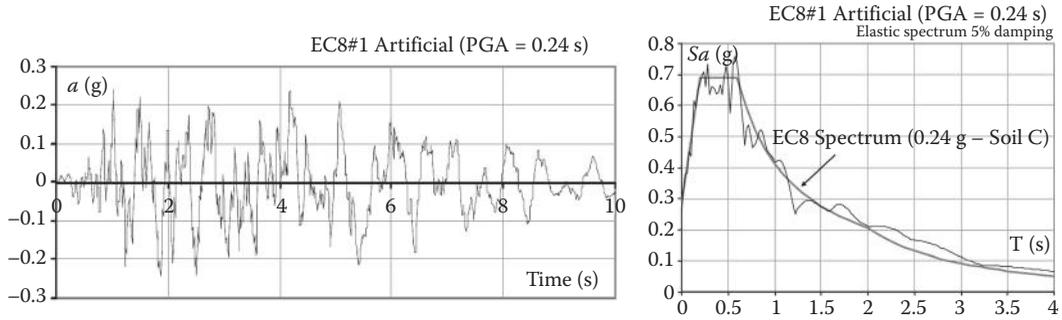
Figure 5.69 EC8 artificial strong motion records (0.24 g and soil C; left) and respective elastic spectra (right).

5.10.3.2 Nonlinear dynamic analysis

The excitations selected were three artificial 10 s strong motion records with an standard EC8-compatible frequency content for $a = 0.24$ g and soil C (Figure 5.69) and the 1977 Vrancea event (NS and EW components) unscaled.

Seven nonlinear time-history dynamic analyses were performed, six using the EC8 artificial records and one using the Vrancea 1977 event as follows:

1. EC8 #1 to #3 records: 100% in the x direction and 30% in the y direction ($x+0.30 \cdot y$)
2. EC8 #1 to #3 records: 30% in the x direction and 100% in the y direction ($0.30 \cdot x+y$)
3. Vrancea NS record in the x direction and EW record in the y direction (x:NS+y:EW)

5.10.3.3 Nonlinear static analysis

The approach presented in Paragraph 5.7.5.2 for torsionally sensitive buildings has been used for the application of the static nonlinear analysis.

Three inelastic static (pushover) analyses were performed, two using EC8-compatible static loads (for $a = 0.24$ g and soil C spectrum, see Figure 5.69) and one using the Vrancea event. The above analyses were performed in both positive and negative directions in order to capture the expected asymmetric structural response.

Specifically:

1. EC8 spectrum: 100% in the x direction and 30% in the y direction $\pm(x+0.30\ y)$
2. EC8 spectrum: 30% in the x direction and 100% in the y direction $\pm(0.30 \cdot x+y)$
3. Vrancea NS in the x direction and Vrancea EW in the y direction $\pm(x$:NS + y:EW)

It is apparent that different loads (lateral and torsional) as well as different modification factors (c_1 and c_2) were derived for each static excitation, depending on the spectral shape. The capacity curves extracted from the analysis were converted into Acceleration-Displacement Response Spectrum (ADRS) and bilinearised using special software (Panagopoulos and Kappos, 2009), employing the equal areas principle (see Paragraph 14.2.2.2).

The target displacement of the SDOF oscillator was in turn determined iteratively using constant ductility capacity spectra, and finally the target displacement of the MDOF building was calculated. The above procedure is schematically depicted in Figure 5.70 (see Paragraph 14.2.2.2).
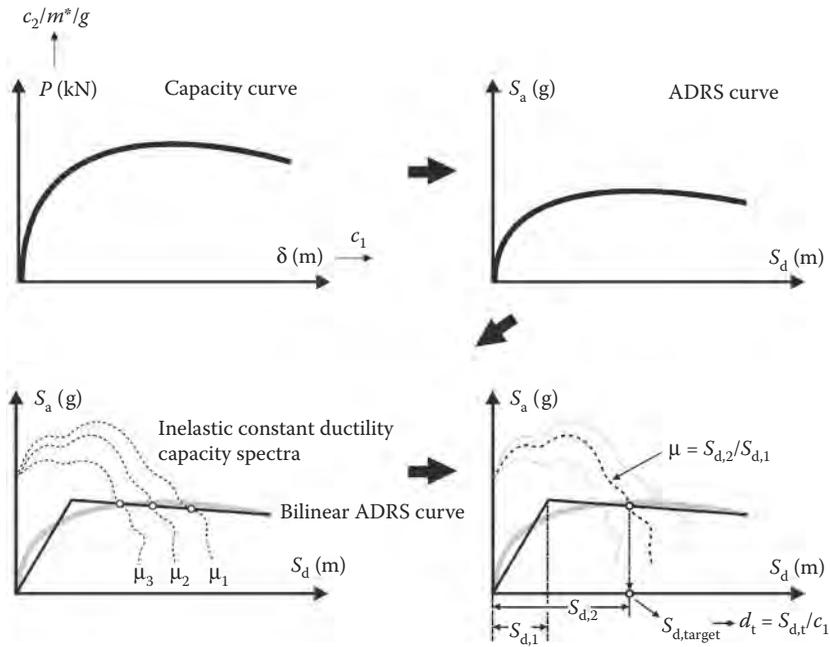
Figure 5.70 Derivation of target displacement from the capacity curve using the ADRS method.

5.10.3.4 Results: Global response

The global response results presented hereinafter for each excitation and analysis type are the following:

1. Static and dynamic capacity curves (P–δ) (Figures 5.71 and 5.72), which demonstrate that there is a close correlation between static and dynamic nonlinear behaviour
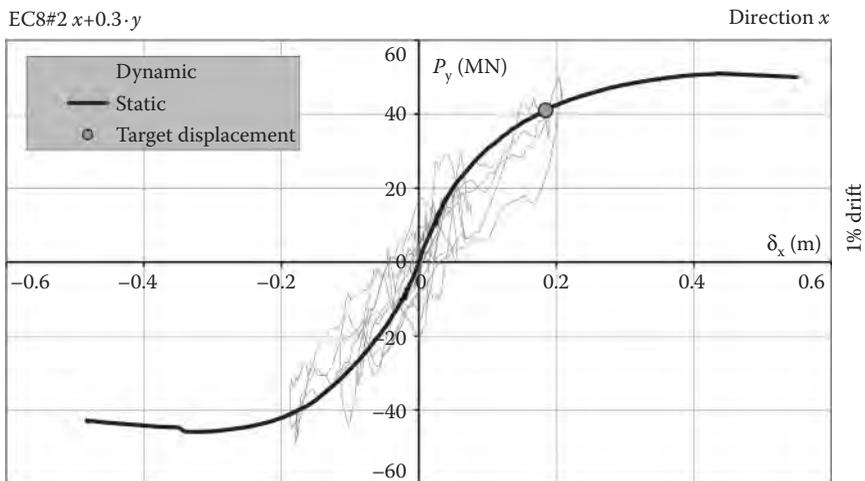
Figure 5.71 Global P–δ comparison between static and dynamic analysis for the EC8#2 x+0.3·y excitation.

Table 5.23 Comparison of top displacements at centre of mass and opposite sides between static and dynamic analysis

Excitation	Dynamic (maximum)	Static (at target disp.)	Difference (%)
Response at centre of mass (CM)			
EC8#1 $x+0.3 \cdot y$ (δ_x)	0.181	0.200	10.6
EC8#2 $x+0.3 \cdot y$ (δ_x)	0.208	0.185	11.2
EC8#3 $x+0.3 \cdot y$ (δ_x)	0.205	0.200	2.5
EC8#1 $0.3 \cdot x+y$ (δ_y)	0.308	0.290	6.0
EC8#2 $0.3 \cdot x+y$ (δ_y)	0.229	0.290	26.7
EC8#3 $0.3 \cdot x+y$ (δ_y)	0.251	0.270	7.6
Vrancea x: NS+y:EW (δ_x)	0.259	0.295	13.8
		Average	11.2
Response at opposite sides			
EC8#1 $x+0.3 \cdot y$ (δ_x)–Top	0.141	0.151	7.3
EC8#1 $x+0.3 \cdot y$ (δ_x)–Bottom	0.222	0.250	12.8
EC8#2 $x+0.3 \cdot y$ (δ_x)–Top	0.177	0.138	22.2
EC8#2 $x+0.3 \cdot y$ (δ_x)–Bottom	0.240	0.232	3.4
EC8#3 $x+0.3 \cdot y$ (δ_x)–Top	0.175	0.151	13.7
EC8#3 $x+0.3 \cdot y$ (δ_x)–Bottom	0.238	0.250	5.1
EC8#1 $0.3 \cdot x+y$ (δ_y)–Left	0.290	0.227	21.8
EC8#1 $0.3 \cdot x+y$ (δ_y)–Right	0.328	0.352	7.3
EC8#2 $0.3 \cdot x+y$ (δ_y)–Left	0.219	0.226	3.1
EC8#2 $0.3 \cdot x+y$ (δ_y)–Right	0.244	0.352	44.6
EC8#3 $0.3 \cdot x+y$ (δ_y)–Left	0.238	0.187	21.4
EC8#3 $0.3 \cdot x+y$ (δ_y)–Right	0.264	0.299	13.0
Vrancea x:NS+y:EW (δ_x)–Top	0.222	0.231	4.2
Vrancea x:NS+y:EW (δ_x)–Bottom	0.300	0.362	20.7
		Average	14.3

and that the building shows asymmetric response due to structural eccentricity. The maximum top displacement from nonlinear dynamic analysis for the EC8-compatible excitations is approximately 20 cm for the x direction and 30 cm for the y direction (Figures 5.71 and 5.72, respectively, and Table 5.23), which renders the estimation of 36 and 68 cm calculated from the elastic design of the building (EC8), respectively, a safe approach. Moreover, the base shear capacity of the building is approximately 50 MN for x direction and 40 MN for y direction, while the base shear design force is approximately 24 MN.

2. The storey displacements in the x and y directions for both sides of the building (x: top and bottom of plan, y: left and right of plan), which demonstrate not only the translational response, but also the rotational (Figure 5.73). In the same figure, the derivation of the target displacement for inelastic static analysis (using the ADRS method) is also shown. The differences between the dynamic and static nonlinear approach regarding the displacement profiles are presented in Table 5.23. It is important that the average difference regarding the response at the centre of mass is about 11%, while the average difference for the sides response (or rotational response) is about 14%.
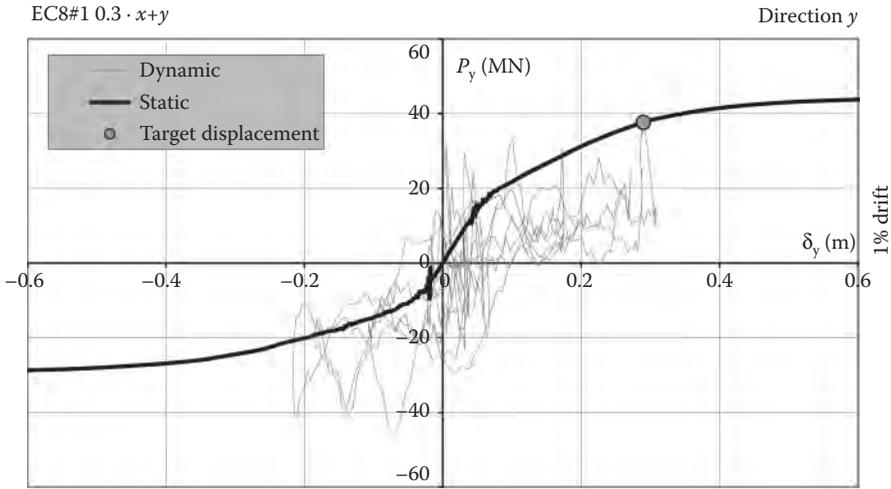
Figure 5.72 Global P–δ comparison between static and dynamic analysis for the EC8#1 0.3·x+y excitation.

5.10.3.5 Results: Local response

The local response results are shown for the corner column C13 (top-right corner of plan) in order to investigate the biaxial nonlinear stress state of the section under a varying axial load. Figure 5.74 shows the moment-chord rotation curves (static and dynamic) as well as the maximum dynamic demand in comparison to the static demand calculated at the target displacement step of the inelastic static analysis. The large difference between moment capacities for x and y directions (shown in Figure 5.74), even though the cross-section is
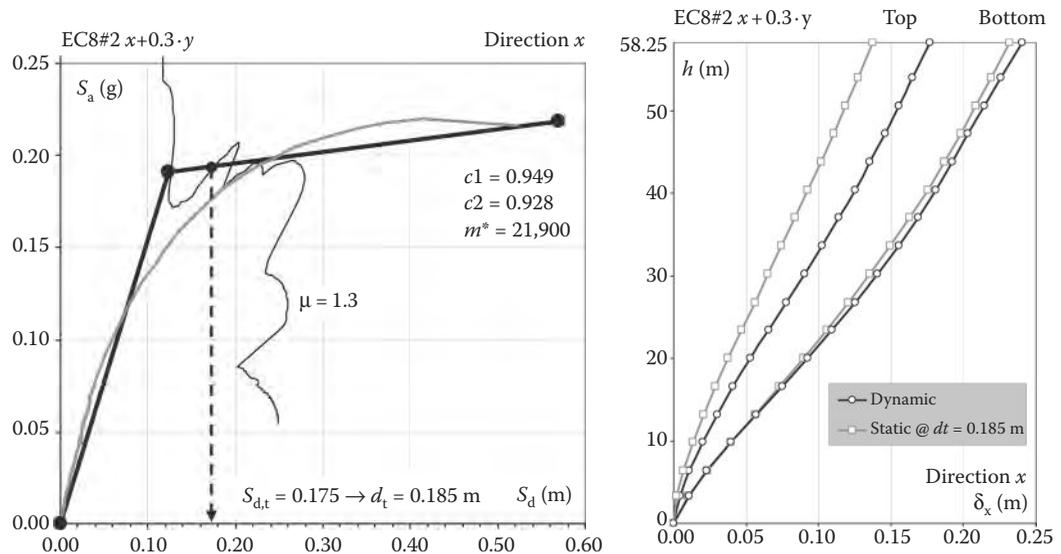
Figure 5.73 Derivation of target displacement and displacement profiles for the EC8#2 $x+0.3·y$ excitation.
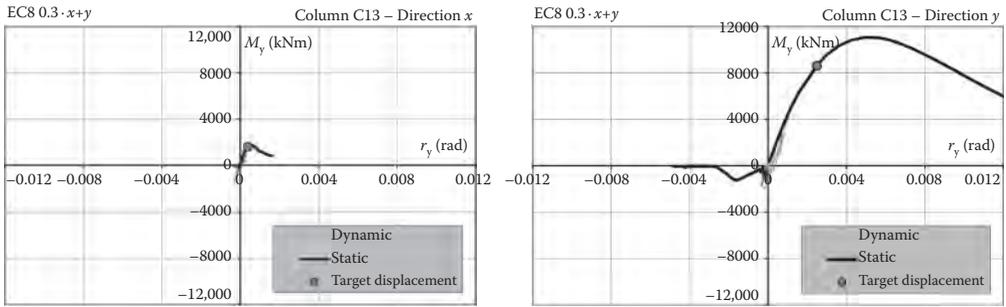
Figure 5.74 Local *M–r* comparison between static and dynamic analysis for the EC8#2 *x*+ 0.3·*y* excitation.

almost symmetrical, are justified if one takes into account the biaxial moment stress of the column with different axial load at different time steps.

The results show an acceptable agreement between dynamic and static approach, considering the different variation of the column axial load between static and dynamic nonlinear analysis. Furthermore, the nonlinear demands (column rotations) are well within the design requirements of EC8.

Capacity design – design action effects – safety verifications

6.1 IMPACT OF CAPACITY DESIGN ON DESIGN ACTION EFFECTS

6.1.1 General

Earthquakes belong to the category of accidental actions, therefore:

- They are not combined with other accidental actions, and
- Earthquake loading is combined with gravity loads with partial safety factors for actions equal to 1.0 (see Chapter 5.8.4).

According to the procedure described in detail in Chapters 3, 4 and 5, the action effects are defined in a deterministic way, as if the loads were statistically reliable and the response of the structure was in the elastic range. These two weak points in the calculation of the action effects make necessary a more reliable approach to the problem, which would ensure the existence of adequate strength and ductility in crucial regions of the structure, so that premature local or general collapse is excluded.

Indeed, since it is impossible to predict with accuracy the characteristics of the seismic motion due to an earthquake larger than the design earthquake, it is impossible to estimate with accuracy the response of an R/C building to this earthquake. However, it is possible to provide the structure with those features that will ensure the resistance shifting of the building in displacement terms beyond life safety limits. In terms of ductility, energy dissipation, damage or failure pattern, this means that the sequence in the breakdown of the chain of resistance of the structure will follow a predefined desirable hierarchy (Park and Paulay, 1975; Penelis and Kappos, 1997; Elnashai and Di Sarno, 2008; Fardis, 2009). In order to ensure a certain sequence in the failure mechanism of the resistance chain, the resistance of every link should be known. This knowledge should not be based on assumptions of disputable reliability, but on quantified strength of the structural elements that will be subjected to very large deformations (due to formation of plastic hinges) during a catastrophic earthquake.

Although the nature of the design actions is probabilistic, the ability to have a semi-deterministic allocation of strength and ductility in the structural members provides an effective tool for ensuring a successful response and prevention of collapse during a catastrophic earthquake.

Such a response may be achieved if the successive regions of energy dissipation are rationally chosen and secured through a proper design procedure, so that the predecided energy dissipation mechanism would hold throughout the seismic action. This design concept is included in a procedure called *capacity design procedure*.

According to this procedure, the structural elements that are designated to dissipate the seismic energy via reversal bending are reinforced accordingly, with a special concern for avoiding brittle failure due to shear in regions out of the plastic hinges. In the same way, all other members are provided with adequate strength reserves, so that it is ensured that the chosen dissipating mechanism will be activated and preserved during a strong earthquake without premature brittle failure of non-ductile regions or members.

This means that the action effects that have resulted from the analysis *serve only as a guide and must be properly modified* in order to accommodate the capacity design of the structure. It is obvious that this modification cannot be based solely on the knowledge and ingenuity of the designer, and it should be formulated in a disciplined procedure with reference to the Code. It is also obvious that this modification of the seismic effects should also be a function of the chosen ductility class.

The aforementioned concepts have been incorporated into all modern Codes for earthquake design and since the early 1980s in EC 8-(ENV).

6.1.2 Design criteria influencing the design action effects

From the design criteria for R/C buildings included in EC8-1/2004, only:

- Local resistance criteria
- Capacity design criteria

influence the determination of the design action effects. All the others refer to dimensioning and detailing of the R/C structural members and will therefore be addressed in Chapters 8 through 10. The design criteria influencing the design action effects are the following, in detail:

1. All critical regions of the structure must exhibit resistance adequately higher than action effects, developed in these regions under the seismic design situation (e.g. minimum reinforcement in tensile zones, minimum reinforcement in compressive zones, etc.)
2. Brittle or other undesirable failure modes, such as:
   a. Shear failure of the structural members
   b. Failure of beam–column joints
   c. Yielding of foundations
   d. Yielding of any other element intended to remain elastic (e.g. structural walls beyond critical zones)

   must be excluded. This can be ensured if the design action effects of purposely selected regions are derived *from equilibrium conditions* when flexural plastic hinges with their potential overstrengths have occurred in adjacent areas.
3. Extensive distribution of plastic hinges should be ensured, avoiding their concentration in any single storey (*'soft storey' mechanism*) and particularly at both ends of a number of columns in the same storey. This can be achieved with sufficient reliability, if it is ensured that plastic hinges develop only in beams and not on columns, except for the unavoidable formation of plastic hinges at the base of the building. (Figure 6.1).

The implementation of these criteria for the determination of the design action effects of the various structural elements of a building is given below.
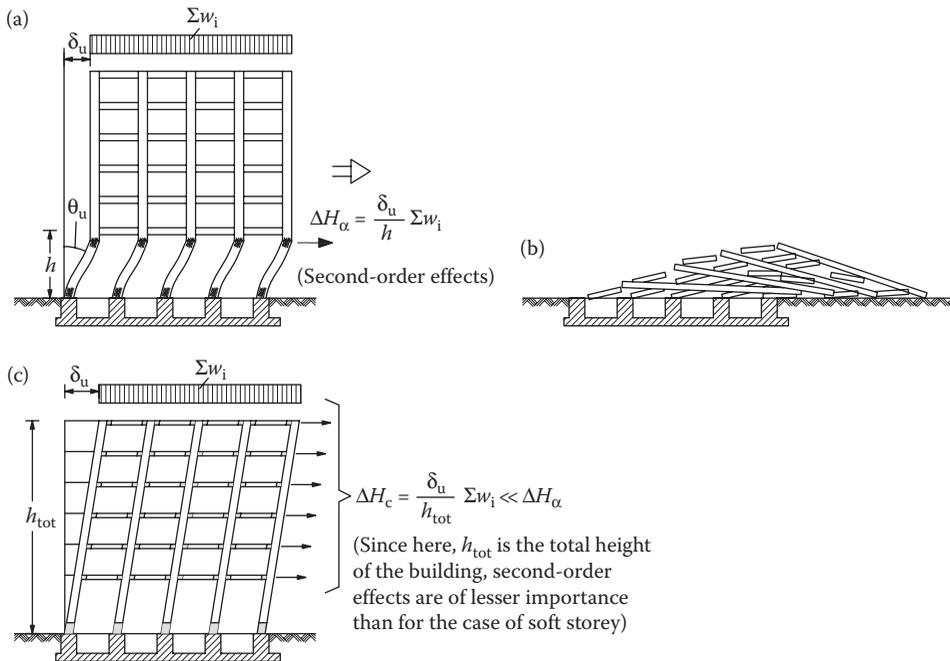
Figure 6.1 Plastic mechanism of a frame system with strong beams – weak columns. (a) Generation of a soft storey. The second order effects lead to an overturning of the formed inverted pendulum; (b) pancake collapse pattern; (c) a frame system with strong columns – weak beams. This ensures the existence of a strong vertical spine preventing collapse.

6.1.3 Capacity design procedure for beams

According to EC8-1/2004, CEB/MC-SD 185 (CEB 1985), ASCE 7-05, NEHRP 2003 and SEAOC 1999, the design values of the bending moments of a beam for all ductility classes are obtained from the analysis of the structure for the seismic loading combinations, as described in detail in Subsection 5.8.4, without any modifications except for a possible redistribution.

However, according to all relevant Codes, beams need an additional compression rein-forcement at their support equal to at least 50% of the corresponding tension reinforcement in order to ensure an adequate local ductility level (Subsection 8.2.5). Based on the capacity design concept, these reinforcement bars are appropriately anchored in concrete, so that they can operate as tension reinforcement in case of moment reversal due to an unexpected severe earthquake. Therefore, the moment resistance envelope of the beams is considerably improved at low cost (the cost of anchorages of the compression reinforcement) no matter what the values are of the design action effects, which have been derived from the analysis (Figure 6.2a).

This means that the beam, as it is designed, can carry much larger moment fluctuations generated by an earthquake than the design action moments. However, in order to ensure this behaviour, the structural element has to be protected from a premature shear fail-ure, because it is well known that shear failure does not present a ductile mode (see also Subsection 8.3.5). Therefore, the design shear for DCM and DCH R/C buildings should not
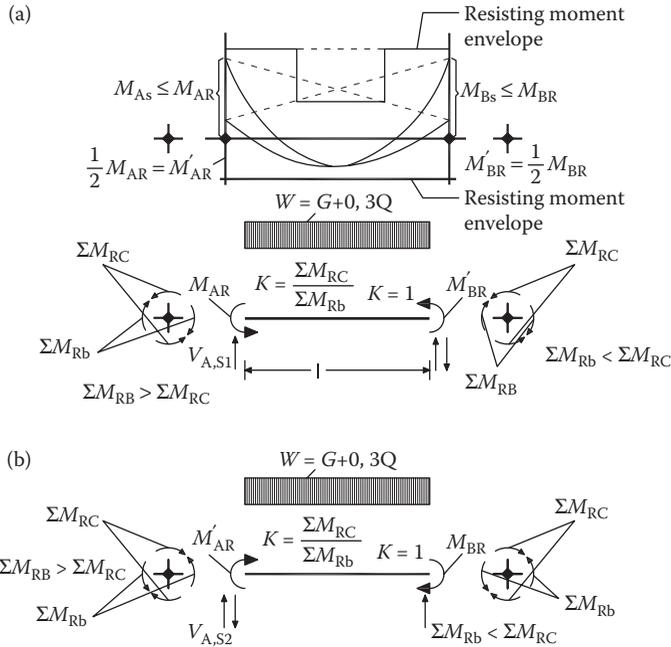
Figure 6.2 Capacity design values of shear forces acting on beams; (a) resisting moment envelope; (b) equilibrium conditions for the determination of shear forces.

be that resulting from the analysis, but the shear corresponding to the equilibrium of the beam under the appropriate gravity load and a rational adverse combination of the actual bending resistances of the cross-sections at the ends of the beam (Figure 6.2b):

$$
\begin{aligned}
V_{AS1} &= \frac{wl}{2} + \gamma_{Rd} \frac{\kappa_A M_{AR} + \kappa_B M'_{BR}}{l} \\
V_{AS2} &= \frac{wl}{2} - \gamma_{Rd} \frac{\kappa_B M_{BR} + \kappa_A M'_{AR}}{l} \\
V_{BS1} &= -\frac{wl}{2} + \gamma_{Rd} \frac{\kappa_A M_{AR} + \kappa_B M'_{BR}}{l} \\
V_{BS2} &= -\frac{wl}{2} - \gamma_{Rd} \frac{\kappa_B M_{BR} + M'_{AB}}{l}
\end{aligned}
\tag{6.1}
$$

where M_{AR}, M'_{AR}, M_{BR}, M'_{BR} are the actual resisting moments at the ends of the beam, accounting for the actual area of the reinforcing steel (all moments positive) and γ_{Rd} an amplification factor due to materials overstrength but also taking into account the reduced probability that all end moments exhaust simultaneously all strength reserves. This γ_{Rd} factor counterbalances the partial safety factor of steel that has been introduced for the fundamental combination (see subsection 6.2.2), as well as for the seismic one, and covers the hardening effects as well. In the absence of more reliable data, according to EC8-1/2004, γ_{Rd} may be taken as

- Ductility class medium: $\gamma_{Rd} = 1.00$
- Ductility class high: $\gamma_{Rd} = 1.20$

$$\tag{6.2}$$

Coefficients κ_A and κ_B have been introduced to respond to the case of strong beams and weak columns. Indeed, in the case that the columns are strong and the beams weak, which is the prevailing condition for earthquake-resistant R/C buildings, the sum of the resisting design bending moments of the columns at the joints, taking into account their axial load effects, is larger than the sum of the resisting design bending moments of the beams framing into the joints, that is, $\Sigma M_{Rc} > \Sigma M_{Rb}$. In this case, plastic hinges are formed at the beam ends. Therefore, coefficient κ is equal to 1.00,

$$\kappa = 1.00 \tag{6.3}$$

since at the beam ends their resisting design bending moments may develop to their highest value.

Conversely, in the case of strong beams and weak columns, the sum of the resisting design bending moments of the beams framing the joints are larger than the sum of the resisting design bending moments of the columns running to the joints, taking into account, of course, their axial load effects, that is, $\Sigma M_{Rb} > \Sigma M_{Rc}$. In this case plastic hinges are likely to form at column ends at the joints. Therefore, coefficient κ must be less 1.00, because at the beam ends their resisting design bending moments cannot develop their highest values, as these are limited by the lower resisting moments of the adjacent columns. In this case, κ should have a reduced value equal to

$$\kappa = \frac{\Sigma M_{Rc}}{\Sigma M_{Rb}} \leq 1 \tag{6.4}$$

In this respect, according to EC8-1/2004, κ should be equal to (Figure 6.2b):

$$\kappa = \min\left(1, \frac{\Sigma M_{Rc}}{\Sigma M_{Rd}}\right) \tag{6.5}$$

The sign of the ratio:

$$\zeta = \frac{V_{AS2}}{V_{AS1}} \quad \text{or} \quad \frac{V_{BS2}}{V_{BS1}} \tag{6.6}$$

has a considerable effect on the shear design of the beams, as will be explained in Chapter 8. The above capacity design procedure, according to EC8-1, applies to DCM and DCH buildings. For DCL buildings the design values of the acting shear forces are obtained from the analysis of the structure for the seismic load combination, as described in detail in Subsection 5.8.4.

6.1.4 Capacity design of columns

6.1.4.1 General

The basic concept in the capacity design of frame or frame-equivalent dual systems is that the failure mechanism must include plastic hinges only at the base of the columns, while all other plastic hinges of the mechanism are distributed at the beams (Figure 6.1c). In this context, a prevailing strong vertical spine is ensured in the building, which could potentially protect the building against the formation of a 'soft storey' (inverted pendulum) and a collapse in a pancake pattern in the case of a strong unexpected earthquake (Figure 6.1b,c;

Chapter 11, Figure 11.44). Of course, this assumes that bending failure, which is dissipative, precedes that of shear, which is brittle.

6.1.4.2 Bending

It has already been noted that the formation of plastic hinges in the columns during the earthquake should be avoided so that the energy is dissipated by the beams only (Park, 1986). The reasons for this requirement, which are very clearly stated in EC8-1/2004 (see Subsection 6.1.2), are the following:

1. Due to axial compression, columns have less available ductility than beams, as will be clarified in Subsection 8.3.2. On the other hand, for the same displacement at the top of the frame (Figure 6.3), that is, for the same global ductility expressed in terms of displacements (see subsection 5.4.4), much larger plastic column rotations are required than beam rotations. Indeed, in the case of plastic hinges at columns, the total required
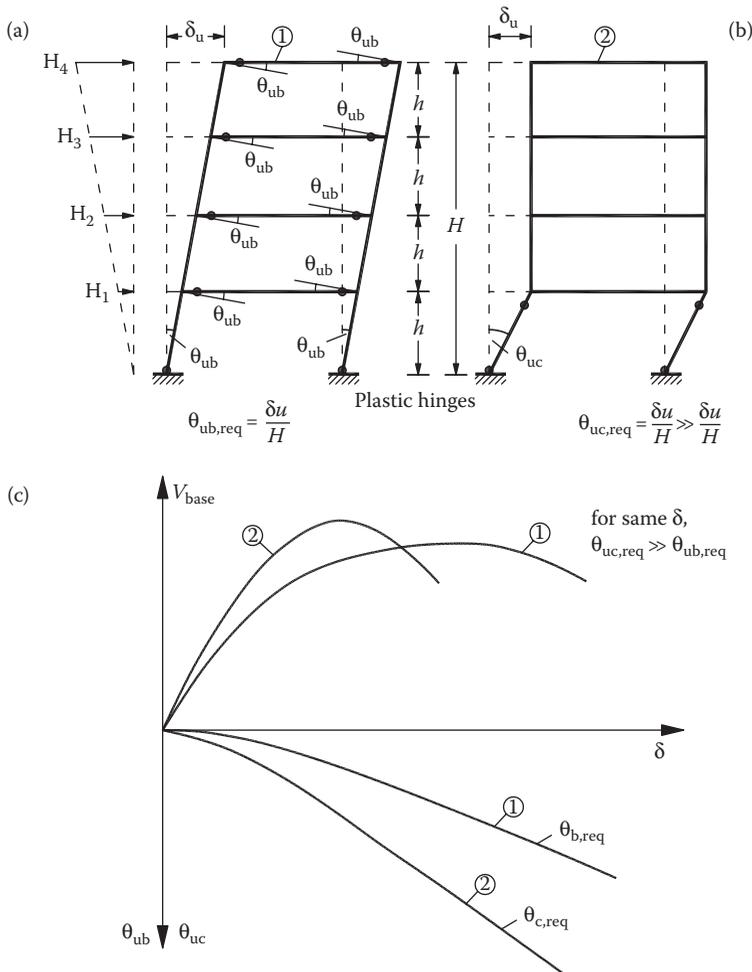
Figure 6.3 Failure mechanism of a frame: (a) Beam mechanism; (b) storey mechanism; (c) interpretation of the vulnerability of a storey mechanism via $V_{base} - \delta - \theta$ diagram.

plastic rotations are developed at the top and bottom of the columns of one storey (soft storey), while in the case of plastic hinges, they develop at the beams and are spread to all storeys of the frame (Figure 6.3). Therefore, for the same global ductility, a larger local column ductility in rotations is required (Figure 6.3a) over local beam ductility. Thus, while (Park and Paulay, 1975)

$$\theta_{uc}^{avail} \leq \theta_{ub}^{avail} \tag{6.7a}$$

for the same δ_{ureq} (i.e., the same μ_{ureq})

$$\theta_{uc}^{required} = \frac{\delta_{ureq}}{h} \geq \theta_{ub}^{required} = \frac{\delta_{ureq}}{H} \tag{6.7b}$$

2. While beam failure exhibits extended cracking only in the tension zones, due to the yielding of the reinforcement, column failure mode presents, in successive steps close to one another, spalling of concrete, breaking of ties, crushing of concrete core and buckling of the longitudinal rebars. This process leads to the creation of a collapse mechanism due to the inability of the columns to carry the axial gravity loads after their failure. Therefore, avoiding column failure is much more crucial for the overall safety of the structure than avoiding beam failure in bending.
3. The formation of plastic hinges in the columns leads to significant inter-storey drifts, so that the relevant second-order effects may lead to a premature collapse of the structure.

In order to decrease the probability of plastic hinge formation in the columns, *frames or frame-equivalent dual systems* (see Subsection 5.4.4) must be designed to have 'strong columns and weak beams' (Park, 1986; Paulay et al., 1990; Priestley and Calvi, 1991; Penelis and Kappos, 1997). This concept is adopted in the requirements of EC8-1 and other relevant Codes. They state that the sum of the resisting design moments of the columns at a joint, taking into account the action of normal force, should be greater than the sum of the resisting design moments of all beams framing the joint for each one of the two orthogonal directions of the building and for both positive of negative action of the seismic motion (Figure 6.4), that is,
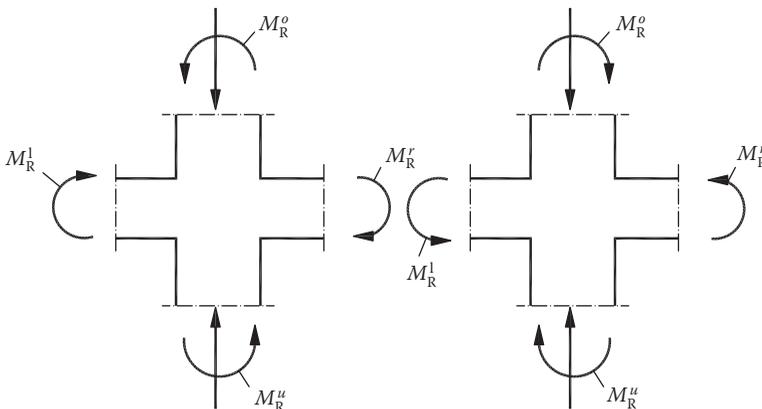
Figure 6.4 Strong columns–weak beams.

$$\left. \begin{array}{l} \left|M_{R,1}^{c,o}\right| + \left|M_{R,1}^{c,u}\right| \geq 1.30\left(\left|M_{R,1}^{b,l}\right| + \left|M_{R,1}^{b,r}\right|\right) \\ \left|M_{R,2}^{c,o}\right| + \left|M_{R,2}^{c,u}\right| \geq 1.30\left(\left|M_{R,2}^{b,l}\right| + \left|M_{R,2}^{b,r}\right|\right) \end{array} \right. \tag{6.8}$$

Factor 1.30 has been introduced in order to take into account the variability of the yield stress f_y of the reinforcement and the probability of strain-hardening effects (overstrength factor).

Therefore, the capacity design is satisfied if the columns are designed for the following moments:

$$\left. \begin{array}{l} M_{S1CD} = a_{CD1}M_{S1} \\ M_{S2CD} = a_{CD2}M_{S2} \end{array} \right\} \tag{6.9}$$

where

$$\left. \begin{array}{l} a_{CD1} = 1.30\dfrac{\left|M_{R,1}^{b,l}\right| + \left|M_{R,1}^{b,r}\right|}{\left|M_{S,1}^{c,o}\right| + \left|M_{S,1}^{c,u}\right|} \\[3ex] a_{CD2} = 1.30\dfrac{\left|M_{R,2}^{b,l}\right| + \left|M_{R,2}^{b,r}\right|}{\left|M_{S,2}^{c,o}\right| + \left|M_{S,2}^{c,u}\right|} \end{array} \right\} \tag{6.10}$$

In the above relationships:

M_S^c is the action effects (bending moments) of the columns derived from the analysis for the seismic combination.

M_R^b is the design resisting moments of the beam derived from the design of the beams, which has already preceded column design.

EC8-1 allows a relaxation of the above capacity design criterion whenever the probability of full reversal of beam end-moment is relatively low (wall-equivalent dual systems, uncoupled wall systems). The following cases are also exempted from the requirements of the above procedure:

- In single-storey R/C buildings and in the top storey of multi-storey buildings
- In one-quarter of the columns of each storey in plane R/C frames with four or more columns
- In two-storey R/C buildings if the value of the normalised axial load v_d at the bottom storey does not exceed 0.3 in any column

In EC8-1/2004 it is clearly stated that the capacity design procedure for columns is implemented *in frame* and *frame-equivalent dual* systems. No reference is made to these systems in the case that they are 'torsionally flexible'. It is the author's opinion that *the torsionally flexible frame or frame-equivalent systems should also comply with the capacity design procedure* because of their additional vulnerability, which is attributable to the torsional behaviour of the system.

Finally, for DCL buildings, the design bending moments of columns are determined from analysis of the structure for the seismic load combination without any application of the capacity design criterion.
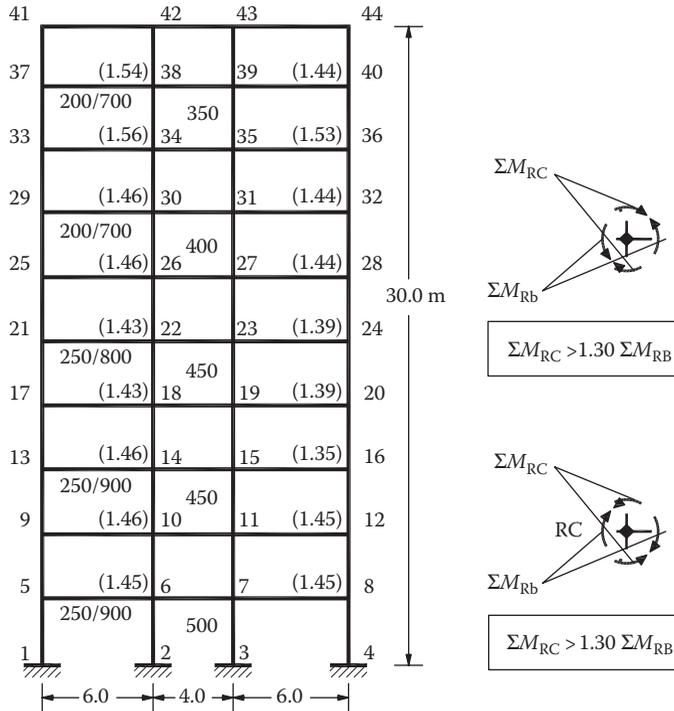
Figure 6.5 Values of the magnification factors α_{CD} for a 10-storey, 4-column R/C frame.

The magnification factor a_{CD} (Equations 6.9 and 6.10) takes rather high values. In the example of Figure 6.5, where a plane frame has been analysed for gravity loads '+' seismic actions, the values of a_{CD} for DC *M* range from 1.35 to 1.56.

6.1.4.3 Shear

According to the capacity design criterion, and following the rationale developed for beams (subsection 6.1.3), shear forces are determined by considering the equilibrium of the column under the actual resisting design moments at its ends (Figure 6.6):

$$V_{sd.CD} = \gamma_{Rd} \frac{\kappa_A M_{AR} + \kappa_B M_{BR}}{l_c} \tag{6.11}$$

where M_{AR} and M_{BR} are the actual resisting moments at the ends of the column, taking into account the axial existing forces and accounting for the actual area of the reinforcing steel (all moments positive), and γ_{Rd} is an amplification factor due to the materials overstraining but also taking into account the reduced probability that all end moments exhaust simultaneously all strength reserves. In the absence of more reliable data, according to EC8-1/2004, γ_{Rd} may be taken as

$$\begin{array}{l} \text{Ductility class medium: } \gamma_{Rd} = 1.10 \\ \text{Ductility class high: } \gamma_{Rd} = 1.30 \end{array} \tag{6.12}$$
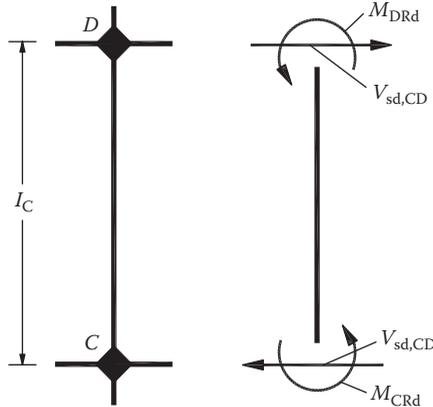
Figure 6.6 Capacity design of shear forces acting on columns derived by equilibrium condition of the column under shear forces and resisting moments M_{Rd}.

Coefficients κ_A and κ_B have been introduced to account for the case of strong columns and weak beams. Indeed, in the case that the beams are strong and the columns weak, the sum of the resisting design bending moments of the beams framing into the joints is larger than the sum of the resisting design bending moments of the columns running to the joints, taking into account their axial load effects, that is: $\Sigma M_{Rc} < \Sigma M_{Rb}$. In this case (Figure 6.6), plastic hinges are formed at column ends. Therefore, the coefficient κ is equal to 1.0,

$$\kappa = 1.00 \tag{6.13}$$

since at the column ends their resisting design bending moments may develop to their highest value.

Conversely, in the case of strong columns and weak beams, the sum of the resisting design moments of the beams framing into the joints are smaller than the sum of the resisting design bending moments of the columns running to the joints, taking into account, of course, their axial load, that is, $\Sigma M_{Rc} > \Sigma M_{Rb}$. In this case (Figure 6.6), plastic hinges are likely to form at the beam ends at the joints. Therefore, the coefficient κ must be less than 1.00 because at the column ends their resisting design bending moments cannot develop their highest values, as these are limited by the lower resisting moments of the adjacent beams. In this case, κ should have a reduced value equal to

$$\kappa = \frac{\sum M_{Rb}}{\sum M_{Rc}} \leq 1.0 \tag{6.14}$$

In this respect, according to EC8-1/2004, κ should be equal to (Figure 6.6)

$$\boxed{\kappa = \min\left(1, \frac{\sum M_{Rb}}{\sum M_{Rc}}\right)} \tag{6.15}$$

Finally, for DCL, the design action shear forces are determined by the analysis of the structure for the seismic load combination without any application of the capacity design criterion.

6.1.5 Capacity design procedure for slender ductile walls

6.1.5.1 General

The basic concept in the capacity design of wall or wall-equivalent dual systems is that the failure mechanism must include plastic hinges only at the base of the walls and of the eventual columns of the system, while all other plastic hinges of the mechanism are distributed at the beams. At the same time, bending failure must precede any shear failure, which is brittle, and in this way it interrupts the dissipative procedure. Likewise, as in the case of a frame or frame-equivalent dual system with strong columns and weak beams, a vertical spine is formed for the building, which shifts its resistance in terms of displacements beyond the life safety limits (see Subsection 6.1.4; Figure 6.7).

6.1.5.2 Bending

The moment diagrams of slender ductile (shear) walls ($h_w/l_w > 2$) under static seismic action have the form of Figure 6.8. However, a dynamic response analysis results in moment diagrams with approximate linear variation (Paulay and Priestley, 1992). Thus, the design moment diagram introduced by EC8-1 has the form of a trapezoid covering the saw-like M-diagram (Paulay, 1986).

The introduction of this M-diagram ensures that the plastic hinge will be generated at the base of the shear wall, while the rest of the wall will remain in elastic region during a strong seismic motion. In this respect, the shear wall will have ductile behaviour so that it may be considered synonymous with a 'ductile wall'.

The value a_1 expresses the tension shift equal to (Figures 6.8 and 6.9):

$$a_1 = z \cot \theta \cong 0.9 l_w \cot \theta \tag{6.16}$$

For the usual case where

$$\theta = 45^0$$
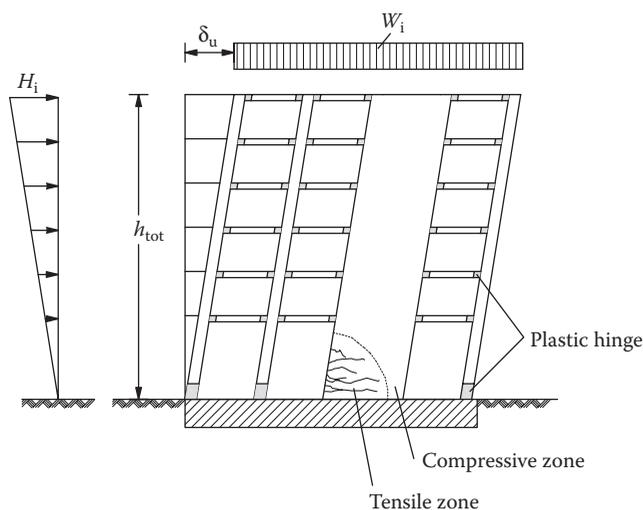
Figure 6.7 Plastic mechanism of a wall-equivalent dual system designed according to capacity design requirements (plastic hinges at beam ends and at the base of the vertical elements).
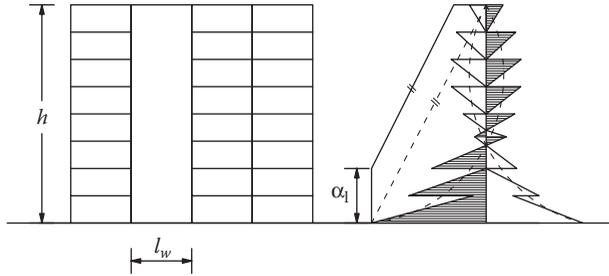
Figure 6.8 Slender ductile wall moment diagram and the capacity design envelope.

$$a_1 \cong 0.9\, l_w \tag{6.17}$$

In addition to the above changes of moment diagrams of ductile walls, Code allows the following redistributions in order to account for uncertainties in analysis and post-elastic dynamic effects.

1. Redistribution of seismic action effects (bending moments, shear forces) up to 30% in all types of ductile walls.
2. In coupled walls, the above redistribution of 30% should be redistributed from the walls, which are under low compression to those which are under high compression. Such redistribution alleviates the shear requirements, as will be seen in the next section. At the same time, redistribution of seismic action effects between coupling beams of different storeys up to 20% is allowed under the assumption that the axial force at the base of the walls is not modified (see Subsection 9.3.2).
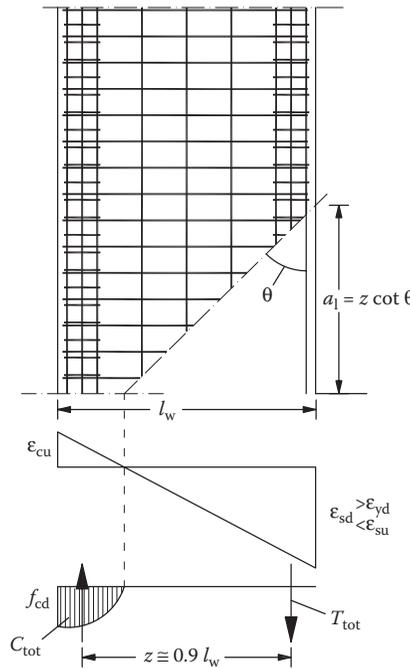
Figure 6.9 Tension T_{tot} shift mechanism in slender ductile walls.

6.1.5.3 Shear

As is well known, the available moment resistance M_{rd} at the base of a ductile wall is usually larger than the moment demand M_{Ed}. Therefore, according to the capacity design criterion, design shear demand derived from the analysis must be magnified by a magnification factor ε so that the above-defined possible moment increase, together with various uncertainties in the analysis and post-elastic dynamic effects, is taken into account.

- *DCM buildings*
  - For ductile walls, the magnification factor ε may be taken as equal to:

$$\boxed{e = 1.50} \tag{6.18}$$

  - For ductile walls in dual systems, a modified design envelope of shear forces is adopted (Figure 6.10). The design envelope of the shear forces along the height of the wall is derived as follows:
    - For $z < 1/3\ h_w$

$$\boxed{V_{Sd} = 1.50 V'_{Sd}} \tag{6.19}$$

    - For $1/3\ h_w < z < h_w$
      V_{Sd} at the top is equal to

$$\boxed{V_{Sd} = \frac{1}{2} V_{Sd}^{base}} \tag{6.20}$$

Variation between $z < 1/3\ h_w$ and $z = h_w$ must be considered linear (see Figure 6.10).
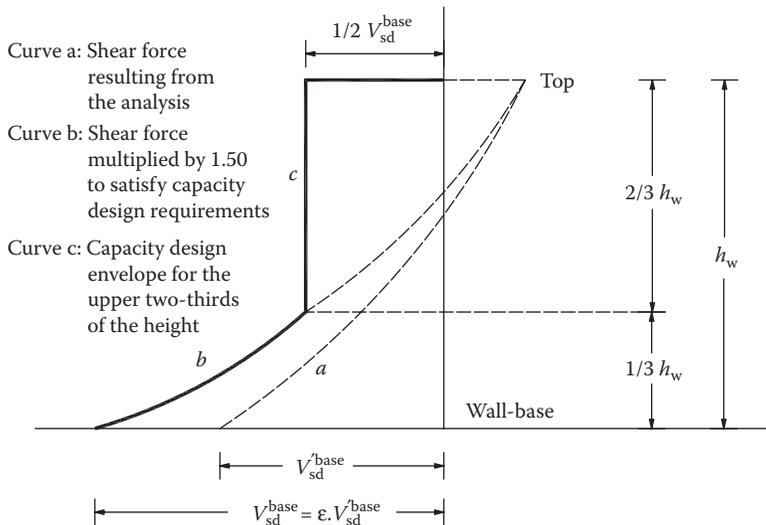
Figure 6.10 Design envelope of the shear forces in the walls of a dual system: Curve a: Shear forces resulting from the analysis. Curve b: Shear forces multiplied by 1.50 to satisfy capacity design requirements. Curve c: Capacity design envelope for the upper 2/3 of the height.

The notation of the above equations is given below:

V'_{Sd} is the shear force along the height of the wall obtained from the analysis

V_{Sd} is the capacity design value

h_w is the height of the ductile wall

z is the reference height measured from the base of the wall

The adoption by EC8-1/2004 of the above envelope of design shear forces for ductile walls in dual systems accounts for the uncertainties of contribution of higher modes. In addition, inelastic analyses performed so far (Eibl and Keintzel, 1988) have shown that the resulting shears are much higher than the shears derived from an elastic response analysis, due to changes of frame reactions on the walls in the post-elastic range.

- **DCH buildings**

For this class of buildings, in the case of slender ($h_w/l_w > 2.0$) ductile walls, the magnification factor ε may be estimated as follows:

$$\varepsilon = q \left[\left(\frac{\gamma_{rd}}{q} \frac{M_{Rd}}{M_{Ed}} \right)^2 + 0.1 \left(\frac{S_e(T_c)}{S_e(T_1)} \right)^2 \right]^{1/2} \leq q \tag{6.21}$$

where

q is the behaviour factor used in the design.

M_{Ed} is the design bending moment at the base of the wall.

M_{Rd} is the design flexural resistance at the base of the wall.

γ_{Rd} is the factor to account for overstrength due to the steel-hardenings recommended value of 1.20.

T_1 is the fundamental period of vibration of the building in the direction of consideration.

T_c is the upper-limit period of the constant spectral acceleration branch (see Subsection 3.4.3).

$S_e(T)$ is the ordinate of the elastic response spectrum.

In any case, the magnification factor ε must be limited between

$$1.5 \leq \varepsilon \leq q \tag{6.22}$$

It should be clarified that the design envelope of the shear forces along the height of the wall in the case of a dual-wall system in DCH buildings has the same form as that of DCM ones (Figure 6.10).

It is recommended that both design moments (M_{Ed}, M_{Rd}) in Equation 6.21 should be calculated for the same design axial force. Otherwise, erroneous results are derived, particularly in the case of coupled walls, where the axial force of gravity loads may even change sign due to the coupled action under horizontal seismic loading (see Subsection 9.3.2, and Paragraph 4.5.2.3, Fig. 4.22). The erroneous results mentioned above tend to be smoothened if moment redistribution is implemented from the walls, which are under low compression to those which are under high compression.

6.1.6 Capacity design procedure for squat walls

As was mentioned before, walls with an aspect ratio $h_w/l_w < 2.0$ are defined as 'squat walls'. Capacity design rules for bending and shear for Ductility Classes M and H are given below.

6.1.6.1 DCH buildings

- In regard to flexure there is no need to modify the *M*-diagrams derived from the analysis.
- The shear force V'_{Ed} from the analysis should be increased as follows:

$$1.50 V'_{Ed} < V_{Ed} = \gamma_{Rd} \left(\frac{M_{Rd}}{M_{Ed}} \right) V'_{Ed} \le q V'_{Ed} \qquad (6.23)$$

The definition and variable values are given in the paragraph above.

6.1.6.2 DCM buildings

- Referring to flexure, there is no need to modify the M-diagrams derived from the analysis.
- The shear force V'_{Ed} from the analysis should be increased as follows:

$$V_{Ed} = 1.50 V'_{Ed} \qquad (6.24)$$

6.1.7 Capacity design of large lightly reinforced walls

- In Chapters 4 and 9, detailed reference is made to this type of structural system and to its structural behaviour, particularly to the procedure of energy dissipation through wall uplifting from the soil or through opening and closing of horizontal cracks.
- The additional dynamic axial forces developed in large walls due to the dissipating mechanisms described above should be taken as being ±50% of the axial force of the wall due to gravity loads, unless they are evaluated using a more precise calculation. Therefore, while bending moments derived by the analysis are not modified, the corresponding axial forces must be modified as follows:

$$N_{Ed} = (1.0 \pm 0.50) N'_{Ed} \qquad (6.25)$$

where
   N'_{Ed} is the axial force from the analysis corresponding to the design bending moment
   N_{Ed} is the modified capacity design value.
   In the case that the behaviour factor *q* of the wall does not exceed 2.0, that is, in the case of an aspect ratio less than 1.0 or a torsionally flexible system, the effect of the dynamic axial force may be neglected.

- In order to ensure that flexural failure precedes shear failure of the wall, the shear force V'_{Ed} from the analysis must be increased at every storey in accordance with the following expression:

$$V_{Ed} = V'_{Ed} \frac{q + 1}{2} \qquad (6.26)$$

where *q* is the behaviour factor of the building.

- It should be noted here that, since the large lightly reinforced walls are characterised as DCM structures, the maximum value of the q-factor can be $q = 3.0$. In this respect, the magnification factor for V'_{Ed} takes a value equal to 2.0, that is, higher than the magnification factor ε imposed on DCM ductile walls.

6.1.8 Capacity design of foundation

It should be remembered here that the exclusive material for the foundation members (pads, tie beams, foundation beams, rafts, piles) is reinforced concrete, no matter if the superstructure is an R/C, steel or composite structural system. It should also be noted from the beginning that by the term 'foundation' reference is made to the structural components (pads, tie beams, foundation beams, rafts, piles) and to the soil. These two components constitute a composite system that might be used for energy dissipation in case of an earthquake (Figures 6.1 and 6.7). However, keeping in mind that the mechanical properties of soil are of limited reliability, particularly in the inelastic range, it would not be reasonable for somebody to rely upon a dissipative mechanism that might extend to the soil.

At the same time, the foundation is a part of the structure buried in the ground, and therefore it cannot be easily examined for eventual damage after an earthquake, and it is more difficult to intervene for retrofitting.

Consequently, it is reasonable for the foundation, that is, structural members and soil, to be kept in elastic range for the design seismic action, and therefore to be designed not for the seismic effects resulting from the analysis for the seismic combination but for the resistance of the vertical members of the superstructure at their joints with foundation members.

The above considerations have formulated the *capacity design* procedure for foundations (structural members and soil) adopted by EC8-1/2004. This procedure is given below:

1. The action effects for the foundation elements shall be derived on the basis of capacity design considerations, taking into account the development of possible overstrength. Of course, this procedure must not result in values of action with an effect greater than those resulting for $q = 1$ (elastic behaviour).
2. If the action effects for the foundation have been determined using the value of the behaviour factor q:

$$\boxed{q = 1.5}$$

applicable to DCL structures, no capacity design considerations in accordance with (i) are required. This might be a convenient simplification in computational procedure. However, for individually founded vertical members or even for a common foundation of all of them (e.g., a raft foundation) in the case of large building aspect ratios (h_w/l_w), such a simplification, due to the decreased value of q, leads to big tensile action effects at the perimeter or at the corner points of the foundation, or to overturning or even sliding instabilities of the whole building considered as a rigid body (Figure 6.11). Therefore, this simplification should be used with much concern for its consequences.
3. For foundations of individual walls or columns the capacity design procedure is considered to be satisfied if the design values of the action effects E_{Fd} on the foundations are derived as follows:

$$\boxed{E_{Fd} = E_{F,G} + \gamma_{Rd}\Omega E_{F,E}} \tag{6.27}$$

$h_w/l_w = 3$ (assumption)

$\dfrac{\varepsilon W}{W} \cdot \dfrac{2}{3} h_w \le \dfrac{l_w}{4}$ (stability condition against overturning)

$\boxed{\varepsilon \le \dfrac{3}{8} \cdot \dfrac{l_w}{h_w} = \dfrac{1}{8} = 0.12}$

Very low value!
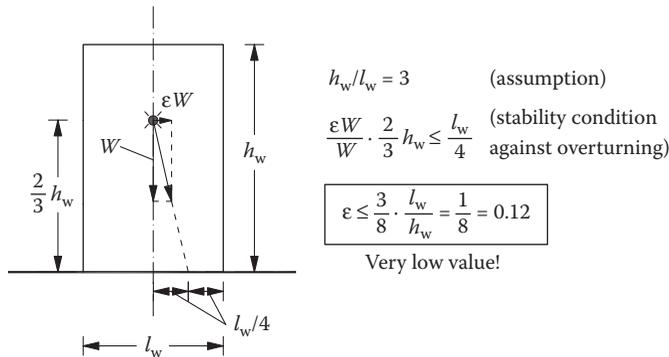
Figure 6.11 Stability condition against overturning.

where

γ_{Rd} is the overstrength factor, taken as being equal to

$$\left.\begin{array}{ll} \gamma_{Rd} = 1 & \text{for } q \le 3 \\ \gamma_{Rd} = 1.2 & \text{for } 3.0 \le q \end{array}\right\} \tag{6.28}$$

$E_{F,G}$ is the action effect due to the non-seismic actions (gravity load effects) included in the seismic combination,

E_{FE} is the action effect from the analysis of the design seismic action, and

Ω is a magnification factor of the element i of the structure, which has the highest influence on the effect E_f under consideration.

4. For foundations of structural walls or columns of moment-resisting frames on individual footings, Ω is the *minimum value* of the ratio M_{Rd}/M_{Ed} in the two orthogonal principal directions at the lowest cross-section where a plastic hinge can form in the vertical element in the seismic design situation. It is self-evident that M_{Rd} is defined taking into account the axial force of the corresponding seismic combination that has resulted M_{Ed}. So,

$$\Omega = \min\left[\left(M_{Rd,x}/M_{Ed,x}\right); \left(M_{Rd,y}/M_{Ed,y}\right)\right] \tag{6.29}$$

It should be remembered (see Chapter 5) that M_{Ed} may have eight different values for each orthogonal direction. So, the computation of 16 Ω values for each individual vertical member and therefore for each independent footing tends to be a tiresome procedure.

5. For common foundations of more than one vertical element (foundation beams, rafts, etc.), Ω used in the expression (6.27) is derived from the vertical element with the largest horizontal shear force in the design seismic situation or, alternatively, by introducing for $\gamma_{Rd}\Omega$ in (6.27) the value:

$$\boxed{\gamma_{Rd}\Omega = 1.40} \tag{6.30}$$

6. Under the above considerations, dimensioning and design of foundation members are carried out according to EN1992-1-1:2004 and to the limited additional rules in use for DCL buildings, since the procedure developed above ensures that the dissipative zones of the building are limited only to the superstructure.

Keeping in mind that the common foundations for almost all vertical elements are the usual cases for earthquake-resistant buildings, it can easily be concluded that, according to Equation 6.30, seismic actions for the foundation are increased by 40% in comparison to those for the superstructure of the building. At this point, Eurocode is very conservative compared to USA codes (DSSC 2003, SEAOC 1999, Booth and Key, 2006), which by contrast reduce the overturning moments at the base from the analysis by 10% to 25% depending on the method in use for the elastic analysis, taking implicitly into account the ability of the foundation soil to dissipate energy to a degree (cf. Figure 6.11).

Finally, it should be noted that EC8-1/2004 allows as an alternative the design action effects for foundation elements to be derived on the basis of the analysis for the seismic design situation without the capacity design consideration presented above. In this case the design of these elements follows the corresponding rules for elements of the superstructure, that is, the rules for DCM or DCH building. The reasoning behind the above alternative approach is based on the assumption that plastic hinges might also be acceptable in the foundation elements (tie beams, foundation beams, etc.; Figure 10b). *However, the above alternative refers only to the structural element of the foundation and not the soil.* The above alternative simplifies the analysis and design of common base foundations and results in more cost-effective solutions.

All above considerations presented here in principle will be examined in detail in Chapter 10.

6.2 SAFETY VERIFICATIONS

6.2.1 General

As already mentioned in Subsection 3.5.3, in order to satisfy the fundamental requirements of *'no (local) collapse'* and *'damage limitation', three compliance criteria* should be considered, namely:

- Ultimate limit state
- Damage limitation
- Specific measures

For buildings of importance classes other than IV (see Paragraph 3.4.3.2), the requirements of earthquake-resistant design may be considered satisfied if the total base shear due to seismic action combination, calculated with a behaviour factor $q = 1.5$ (MCL), is less than that due to other relevant combinations (e.g., wind combination) for which the building is designed on the basis of a linear elastic analysis. This means that in regions of low seismic hazard, where wind or other horizontal loading subject the structure to base shear higher than that caused by the seismic actions (for $q = 1.5$), the design of the structure should be carried out without taking into account the seismic actions. In seismic regions where the preceding conditions are not fulfilled, the following verifications must be considered.

6.2.2 Ultimate limit state

Safety against (local) collapse is considered to be satisfied if the following conditions are met:

- Resistance condition
- Second-order effects
- Ductility condition

- Equilibrium condition
- Resistance of horizontal diaphragms
- Resistance of foundations
- Seismic joint conditions

In the following sections the above conditions will be examined in detail.

6.2.2.1 Resistance condition

The resistance condition is satisfied if for every structural element the following relations are fulfilled:

$$\boxed{\begin{aligned} E_{d1} &\leq R_d \\ E_{d2} &\leq R_d \end{aligned}}$$
(6.31a–b)

where

E_{d1} are the design action effects for the gravity combination (e.g., $E(1.35G \; '+' \; 1.50Q)$,

E_{d2} are the design action effects on the structural element for gravity loads and seismic actions, also taking into consideration the capacity design rules on the seismic action effects, and

R_d is the corresponding design resistance of the same element. For the determination of R_d, the Code for R/C structures is implemented (EC2-1-1/2004) unless additional rules are imposed by the Seismic Code in particular cases (see Chapters 8 through 10).

For the determination of R_d, the partial safety factor – γ_s for steel and γ_c for concrete may be taken from Eurocode EC2-1-1/2004 for the fundamental load combinations, that is,

$$\boxed{\begin{aligned} \gamma_s &= 1.15 \\ \gamma_c &= 1.50 \end{aligned}}$$
(6.32a–b)

The choice of the above values is based on the assumption that, due to the local ductility provisions, the ratio between the residual strength after the seismic degradation of the R/C member and its initial strength is roughly equal to the ratio between γ_m values of accidental and fundamental load combinations. From the above consideration it can be seen that in any case the partial material safety factors for seismic loading should not be those introduced in EC2-1-1/2004 for accidental loading, although seismic action is considered accidental. This must be attributed to the fact that an inelastic cyclic loading results in degradation of the member resistance (see EN 1990/2002) and, therefore, such a reduction of safety factors would be risky.

At the same time, the introduction of the safety factors of the fundamental load combination allows the same value for the design resistance R_d to be used for the gravity combination and for the seismic design situation.

6.2.2.2 Second-order effects

Because of their inelastic response, most structural systems under the action of seismic forces sustain large horizontal displacements, resulting in the creation of large secondary effects (Luft, 1989; Wilson and Habibullah, 1987; Paulay et al., 1990).
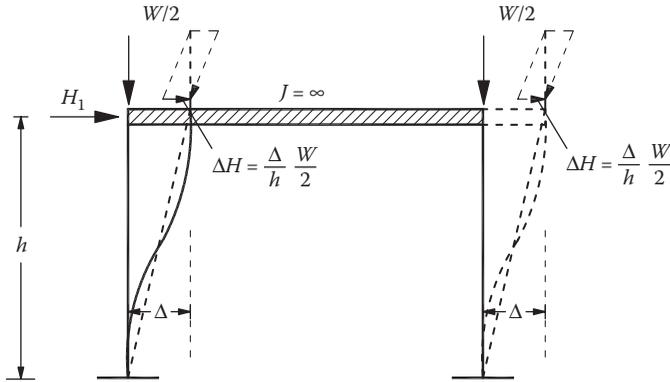
Figure 6.12 Second-order effect on a one-storey, two-column frame.

Consider the frame of Figure 6.12. When this frame for some external reason (an earthquake, in this case) is displaced by Δ, each of the two $W/2$ column loads can be analysed into an axial force on the column with a value approximately $W/2$ and a horizontal one

$$\Delta H_{1,2} \ = \ \frac{\Delta}{h} \cdot \frac{W}{2}$$

Thus the floor is loaded additionally (second-order effect) by a horizontal force equal to

$$\boxed{\Delta H \ = \ \frac{\Delta}{h} W} \tag{6.33}$$

In the case of a seismic action, the displacement Δ according to what has been explained in the chapter about ductility for a fundamental period longer than T_c (corner point C of the acceleration spectrum) is equal to Δ_{el}, which results from the design seismic loading of the Code multiplied by the behaviour factor q of the structure:

$$\Delta \ = \ \Delta_{el} \cdot q \tag{6.34}$$

For simplicity's sake, Eurocode EC8-1/2004 also allows the use of the above expression in the case where $T < T_c$ (see subsection 6.2.3). Therefore, the additional shear force of the storey due to the second-order effect is equal to

$$\boxed{\Delta V \ = \ \frac{\Delta_{el} q}{h} W} \tag{6.35}$$

Eurocode EC8-1/2004 specifies the following procedure for the verification of the influence of second-order effects:

  1. For:

$$\boxed{\theta_i \ = \ \frac{\Delta V}{V} \ = \ \frac{\Delta_{el}^i q}{h} \frac{W_{tot}^i}{V_{tot}^i} \leq 0.10} \tag{6.36}$$

P–Δ effects need not be taken into account. In the above relation the various symbols have the following meaning:

θ_i is the inter-storey drift sensitivity coefficient of each storey

W_{tot}^i is the total gravity load at and above the storey under consideration in the seismic design situation

Δ_{el}^i is the elastic displacement inter-storey drift (difference of displacements between the top and the bottom of the storey under consideration) at the centre of mass for design seismic loading

q is the behaviour factor of the building

V_{tot}^i is the total seismic storey shear

h is the inter-storey height

2. For

$$\boxed{0.10 \leq \theta_i \leq 0.20}$$ (6.37)

the *P*–Δ effects must be taken into account. In this case an acceptable approximation could be to increase the relevant seismic action effects by a factor equal to

$$\boxed{\varphi = \frac{1}{(1-\theta)}}$$ (6.38)

3. For

$$\boxed{0.20 \leq \theta_i \leq 0.30}$$ (6.39)

it is necessary for the *P*–Δ effects to be taken into account in analysis, otherwise the stiffness of the system must be increased, and finally:

4. For

$$\boxed{0.30 \leq \theta_i}$$ (6.40)

the stiffness of the system must be increased, since EC8-1/2004 does not allow such large inter-storey drift sensitivities.

In any case, it is recommended that a high degree of lateral stiffness be provided for the structural system so that at least second-order effects are prevented. This can be easily achieved in R/C buildings, especially in case of dual structural systems.

Finally, it should be noted that *P*–Δ effect verifications should be carried out *at the beginning of the analysis and design,* because at that moment decisions must be made for the type of elastic analysis, that is, for the consideration of *P*–Δ effects or not, and for the eventual increase of load effects (in the case that $0.10 < \theta < 0.20$). Therefore, a preliminary static analysis for seismic loads is usually carried out (see Subsection 5.5.1) so that all the parameters in use in Equation 6.36 are defined in advance.

6.2.2.3 Global and local ductility condition

The ductility condition is satisfied by means of:

- Specific material-related requirements
- Maximum–minimum requirements for the reinforcement for flexure in critical regions of the structural members
- Minimum reinforcement requirements for shear in critical regions

- Minimum reinforcement requirements for confinement of critical regions
- Calculation of the required confinement reinforcement in critical regions of members of major importance for the seismic resistance of the structure (columns-structural walls)
- Appropriate reinforcement detailing
- Application of capacity design procedure

The last requirement has already been examined in detail in the previous section. It is obvious that it is taken into account for the determination of the load effects E_{d2} and therefore in the verification of resistance condition. All the other requirements are closely related to the selected ductility class of the building (ductility demand; see Subsection 5.4.2).

These requirements will be presented and discussed in detail in Chapters 8 through 10 for every type of structural component, together with all necessary experimental and analytical evidence.

6.2.2.4 Equilibrium condition

Equilibrium condition refers to the stability of the building under the set of actions given by the combination rules described in Subsection 5.8.4. It should be noted that *the seismic actions even for the equilibrium condition are introduced with their reduced values due to the behaviour factor q of the building, but also taking into account the capacity design magnification that has been introduced in subsection 6.1.8*. This is a reasonable consequence of the fact that due to the dissipative mechanisms generated in the critical regions of the structure, satisfying the selected *q*-factor, the internal forces that develop in the structural members cannot overcome their resistance, and therefore those of the elastic analysis carried out for the design seismic actions multiplied by the capacity design magnification factors.

In equilibrium conditions, mainly the overturning and sliding of the building as a rigid body is included. It is obvious that these types of verifications refer mainly to buildings with large aspect ratios h_w/l_w (total height to building/small dimension in plan), where overturning problems is critical. They also refer to buildings susceptible to sliding (see Chapter 10).

6.2.2.5 Resistance of horizontal diaphragms

The resistance of horizontal diaphragms refers to their ability to transmit with sufficient overstrength the design seismic action effects to the various lateral load-resisting systems to which they are connected. As already discussed in Chapters 4 and 5, R/C slab diaphragms without re-entrant corners or discontinuities in plan present a high level of diaphragmatic resistance, and therefore in this case safety verification is not needed. In the case, however, that a resistance verification of the diaphragm has been decided, the forces or stresses obtained from the analysis as acting on the diaphragm must be multiplied by an overstrength factor γ_d greater than 1.0. The recommended values by EC8-1/2004 for the relevant resistance verifications are:

- For brittle failure mode (shear)

$$\boxed{\gamma_d = 1.30} \tag{6.41}$$

- For ductile failure mode

$$\boxed{\gamma_d = 1.10} \tag{6.42}$$

Design provisions for R/C diaphragms (analysis-dimensioning-detailing) will be given in Section 9.7.

6.2.2.6 Resistance of foundations

Action effects for foundation design taking into account capacity design rules have been discussed in detail in subsection 6.1.8. Detailed analysis and design issues for foundations will be discussed and presented in Chapter 10.

6.2.2.7 Seismic joint condition

Seismic joint condition is satisfied by means of joints between adjacent buildings or between adjacent statically independent units of the same building. These joints must be wide enough to protect them from earthquake-induced pounding.

For buildings that do not belong to the same property, the distance of the building from the property line must be at least equal to the maximum horizontal displacement d_{smax} resulting from Equation 6.43 (see Subsection 6.2.3).

For adjacent independent units of the same building, the distance between them must not be less than the square root of the sum of the squares (SRSS) of the maximum horizontal displacements of the two units also resulting from Equation 6.43.

Finally, in the case that the floor elevations of the adjacent independent units under design are the same, the minimum distance mentioned above may be reduced by a factor of 0.7.

6.2.3 Damage limitation

The task of damage limitation is to ensure the protection of non-structural elements (masonry, glass panels, tiles, etc.) from premature failure for seismic actions of a higher probability of occurrence than that of the design. The main parameter of seismic action that influences the behaviour of these elements is the ratio of the inter-storey drift d_r to the inter-storey height h, which is induced in them by the adjacent R/C members of the building (Figure 6.13; Uang and Bertero, 1991; Stylianidis, 2012).

The reason for this must be attributed to the fact that masonry and other low-strength brittle materials fail at much lower inter-storey drift d_{ri}/h_i than the surrounding R/C frames (Figure 6.14).

From the above it may be concluded that for the verification of the damage limitation criterion (serviceability limit state), the displacement due to the design seismic actions must be calculated and then be reduced so that a shorter return period is taken into account.
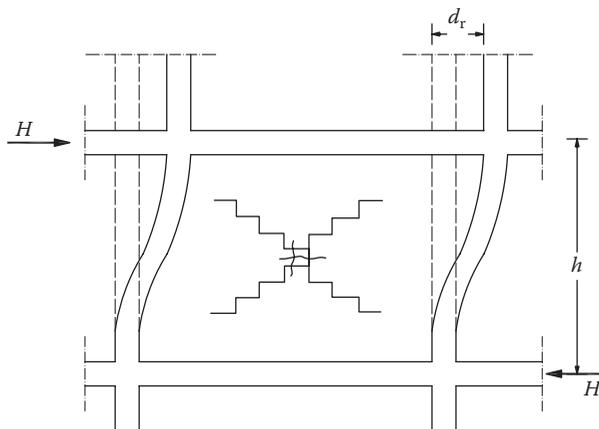
Figure 6.13 Masonry failure with x-shaped cracks due to the R/C frame inter-storey drift d_r.

H (frame shear)

II masonry infilled frame

I bare frame

I

$\theta_u^{ll} \cong 10‰$

$\theta = \dfrac{d_r}{h}$
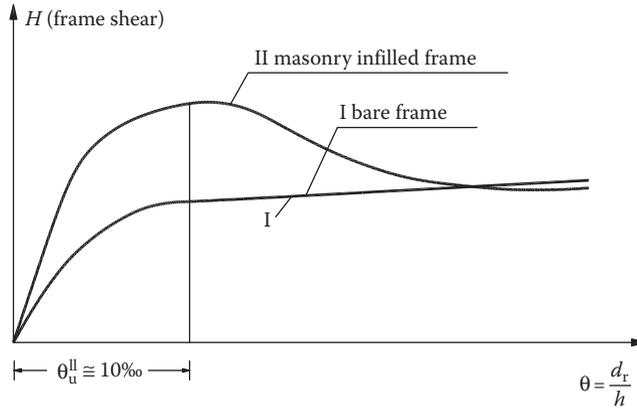
Figure 6.14 $H - \theta$ diagram of a masonry-infilled frame.

The displacement d_s due to the design seismic action could be the result of the elastic analysis of the structural system magnified by the behaviour factor q, since the ordinates of the design response spectrum corresponding to the analysis include a reduction factor q. Consequently,

$$d_s = qd_e \tag{6.43}$$

where

d_s is the displacement of a point of the structural system induced by the design seismic action

q is the q-factor introduced into the analysis of the system

d_e is the displacement of the same point of the structural system as determined by the linear analysis based on the design response spectrum

In this respect the relevant inter-storey drift d_r/h is equal to

$$\frac{d_{ri}}{h_i} = \frac{d_{si} - d_{s(i-1)}}{h_i} \tag{6.44}$$

d_{si} and $d_s(i-1)$ are the displacements of storeys i and $i-1$, respectively, at the reference point, and

h_i is the storey height.

To ensure the damage limitation according to EC8-1/2004, the inter-storey displacement d_{ri} must fulfil the following limits:

1. For buildings having non-structural elements of brittle materials attached to the structure:

$$d_{ri}r \leq 0.005 \, h_i \tag{6.45}$$

2. For buildings having ductile non-structural elements:

$$d_{ri}r \leq 0.0075 \, h_i \tag{6.46}$$
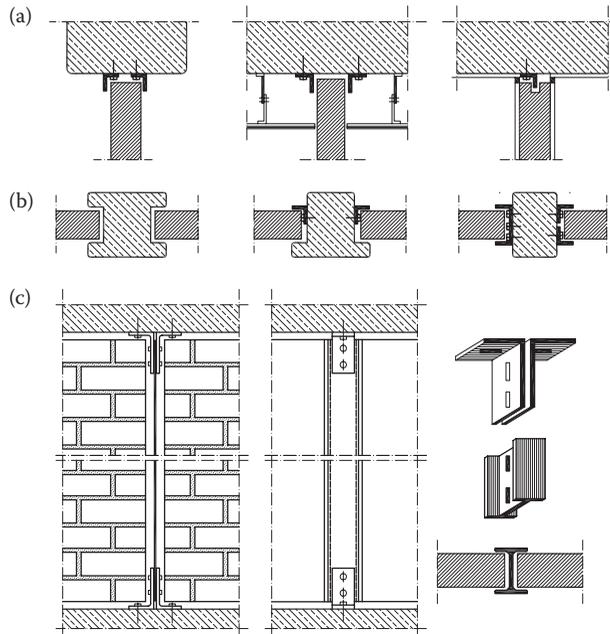
Figure 6.15 Detailing of separation joints between partition walls and R/C frame: (a) upper boundary; (b) lateral boundary; (c) reinforcement for out-of-plane overturning.

3. For buildings having non-structural elements fixed in a way so as not to interfere with structural deformations, or without non-structural elements (Figure 6.15),

$$d_{ri} r \leq 0.010 \, h_i \tag{6.47}$$

The reduction factor r accounts for the consideration of the shorter return period that should be taken into account for the damage limitation in relation to the return period for ULS.

Recommended values by EC8-1/2004 for r are given below:

- For buildings of importance classes
  III and IV: $r = 0.40$
- For buildings of importance classes
  I and II: $r = 0.50$

The above reduction factors correspond to a probability of exceedance $P_{DLR} = 10\%$ in $t_L = 10$ years.

For this hazard level the reference return period of occurrence is reduced from 475 years (ultimate limit state) to 95 years (see Subsection 3.5.2). The exact value for the above conditions results in

$$r = 0.44 \tag{6.48}$$

The small increase of r for classes III and IV in contrast to the small decrease of r for classes I and II must be attributed to the fact that the importance factor γ_1 introduced for classes III and IV has already increased the reference period of occurrence of 475 years to a higher level for these classes, while the importance factor γ_1 introduced into class I has decreased it.

Finally, it should be noted that the damage limitation verification is implicitly based on the assumption that the ordinates of the elastic response spectrum for the 90-year reference period of occurrence *are proportional* to those of the elastic response spectrum for 475 years, which has been used for the ultimate limit state, that is, the same design response spectrum is used in both cases.

6.2.4 Specific measures

It has been noted already in Subsection 3.5.3 that a series of specific measures is foreseen in all modern Codes for the collapse prevention of a building in the case of a very rare earthquake and therefore more severe than the design earthquake. Some of these measures have already been presented in detail in the previous chapters, while others will be presented in Chapters 8 through 10. However, it would be useful to summarise these measures here, so that a global view of the three *compliance criteria* mentioned at the beginning of this section can be obtained. These measures specified by EC8-1/2004, particularly for R/C buildings, refer to:

- Design of the superstructure
- Foundations
- Quality system plan
- Resistance uncertainties
- Ductility uncertainties

6.2.4.1 Design

- Structures should have a simple and regular form in plan and elevation (Subsections 4.2.2, 5.2.2 and 5.2.3).
- In order to ensure an overall ductile behaviour, brittle failure or premature formation of unstable mechanisms must be avoided. For this reason, the capacity design procedure should be adopted (Section 6.2).
- Since the seismic performance of the structure depends on the behaviour of its critical regions, the detailing of these regions must be such that they maintain under cyclic conditions the ability to transmit the necessary forces and to dissipate energy. For this reason, the detailing of connections between structural elements and regions where nonlinear behaviour is foreseeable deserves special care in design (Chapters 8 through 10).
- The analysis must be based on an appropriate structural model (Chapter 5).

6.2.4.2 Foundations

- The stiffness of the foundation must be adequate in terms of transmitting to the ground as uniformly as possible the actions received from the superstructure (Section 6.2, Chapter 10).
- Only one foundation type must in general be used for the same structure (Chapters 4 and 10).

6.2.4.3 Quality system plan

- The choice of materials and construction techniques must be in compliance with the design assumptions. The design documents must indicate structural details, sizes and quality provisions.

- Elements of special structural importance requiring special checking during construction should be identified on the design drawings. In such cases, the checking methods to be used should also be specified.

6.2.4.4 Resistance uncertainties

Important resistance uncertainties could be produced by geometric errors. To avoid these uncertainties, rules referring to the following items should be applied:

- Certain minimum dimensions of structural elements (Chapters 8 through 10)
- Appropriate limitations of column drifts must be provided (Subsection 6.2.2)
- Special detailing rules should be applied in reinforcing R/C elements, so that unpredictable moment reversals and uncertainties related to the position of the inflection point are taken into account (Chapters 8 through 10).

6.2.4.5 Ductility uncertainties

In order to minimise ductility uncertainties, the following rules must be applied:

- An appropriate minimum local ductility is needed in every seismic-resistant part of the structure (Chapters 8 through 10); thus, by enhancing the redistribution capacity of the structure some of the model uncertainties are alleviated.
- Minimum–maximum reinforcement percentages in all critical regions are specified to take into account ductility requirements and to avoid brittle failure upon cracking (Chapters 8 through 10).
- The normalised design axial force values are kept at a low level to avoid decrease of local ductility at the top and bottom of the columns (Chapters 8 through 10).

6.2.5 Concluding remarks

In conclusion, it should be noted that until recently there was no Code providing a direct computational procedure for quantifying the safety level of a new structure designed according to its principles against collapse in the case of a very rare and high-intensity earthquake (e.g., collapse prevention requirement under a seismic motion of a mean return period of 2,475 years). Even today, it is considered that the series of provisions for the design of a structure that have been already presented, such as appropriate configuration in plan and in elevation, correct elastic analysis based on a reliable design spectrum, conformation of the seismic design effects to the capacity design considerations, and design verifications according to the code provisions and so forth, form a reliable set of conditions that ensure *qualitatively* the safety of a structure against collapse under severe unexpected seismic actions.

During the last 20–25 years, numerous attempts have been made to control the collapse requirement quantitatively, using inelastic seismic analysis. In the beginning, inelastic dynamic seismic analysis was used (see Subsection 2.5.2) mainly in research and particularly for the evaluation of the codified design procedure by means of extended parametric analyses (Kanaan and Powel, 1975; Park et al., 1985; Kappos and Penelis, 1986, 1989; Kappos et al., 1991; Michailidis et al., 1995). Many of the principles and rules introduced in modern Codes are owed to the results of this research.

Later, the development of displacement-based design, which has as a core the inelastic static analysis for horizontal loading (push-over analysis), made possible the quantitative evaluation of the structural safety against collapse in everyday practice. Indeed, the

development of the computational power of desktops in the last 15 years and the parallel development of commercial computational codes for push-over analysis enabled the use of displacement-based design for the quantitative follow-up of the post-elastic behaviour of a structure as a whole and of its structural elements up to collapse (see Sections 5.7 and 14.2). EC8-1/2004 is the first Code that has introduced, in case of uncertainties, the redesign of a new building by the push-over analysis for detailed evaluation of the post-elastic performance of the structural system, that is, the early development of plastic hinges and the eventual creation of a soft storey, the brittle failure of structural elements, and, most important, the safety factor of the structure against collapse *in terms of displacements*.

EC8-1/2004 goes one step further, allowing the country members of the EU to make use of a push-over analysis as the prime method (displacement-based design) under well-defined prerequisites instead of the force-based design that has been presented so far and that constitutes the reference method for the design of buildings in seismic regions for all modern Codes.

Finally, it should be noted that for the assessment and retrofitting of existing buildings, EC 8-3/2005 introduces displacement-based design as a method of reference. The above brief remarks on displacement-based design will be elaborated in greater detail in Chapter 14.

Reinforced concrete materials under seismic actions

7.1 INTRODUCTION

It is well known that reinforced concrete is a composite material consisting of *concrete* and *steel* reinforcement. These two materials, *bonded together* due to their physicochemical and mechanical properties, have supplied one of the basic materials for the construction of building structural systems for the past 120 years. The behaviour of reinforced concrete is therefore quite well known under static loading.

Here, reference will be made mainly to its behaviour under seismic loading and only brief reference will be made to its behaviour under static loading, when it is necessary for a comprehensive understanding of its behaviour under cyclic loading.

Static loading is imposed on materials or structural elements in the lab at slow rates, increasing from zero to failure in two different procedures, that is:

- Load-controlled procedure
- Displacement-controlled procedure

According to the first, which was the traditional method for more than one century up to early 1970s, for each successively increasing loading step the corresponding displacement or strain is measured at a reference point of the specimen. So, a diagram of P–δ or σ–ε is platted and known as the *constitutive law of material or the structural element* under consideration. This procedure extends up to P_{max} or σ_{max} and the corresponding displacement or strain. From that point on the experimental procedure 'collapses', since the test set up is load controlled.

Since the late 1960s, new types of testing machines have been developed for the study of the post-elastic behaviour of materials or structural members, as well as study of the descending branch of the diagram P–δ or σ–ε. The main characteristic of these testing machines is that displacement or deformation is controlled. In this case, for each increasing deformation or displacement step imposed, the loading is determined (measured) until the complete disintegration of the material of the structural element. The function of these machines is controlled by servo-electronic valves and is based on a computerised programming of the *deformation* or *displacement path,* which is transformed by means of the servo-electronic valves to an analog signal for the proper operation of the hydraulic jacks of loading.

Seismic action can be simulated by a reversal cyclic loading with a limited number of cycles. The loading frequency is also low, ranging between 0.5 and 10 Hz. Last but not least, it should be noted that according to what has been presented in previous chapters, this reversal cyclic loading is extended in the post-elastic region of the P–δ or σ–ε diagram. In other words, in case of seismic excitation, we have to do with *low cycle fatigue*

to the opposite of what happens in the case of dynamic loaded works in their elastic region as bridges, industrial installations and so forth, where a high-cycle fatigue problem may appear.

For the study of a reversal cyclic loading of a material or a structural element displacement, controlled machines are used, equipped with servo-electronic valves and double-acting loading jacks. A computerised program of the displacement or strain time history is given as input and, as the displacement or the strain is imposed, the corresponding loading is determined (measured) and depicted on a P–δ or σ–ε constitutive diagram.

Main parameters that influence the capacity of a specimen for energy absorption and dissipation are the following:

1. Plastic deformation that may be developed under monotonic loading without serious strength degradation.
2. Relation of the monotonic curve of a load–deformation diagram with that of the envelope of the cyclic loading.
3. Loop area of each cycle of reversal loading.
4. Low cycle fatigue limit.
5. Influence of the strain rate on the envelope of the cyclic loading.

In the past 50 years, extended research has been carried out either in the lab or analytically for the experimental investigation and analytical modelling of the above parameters, as far as material and structural elements are concerned. The basic conclusions of this extended research may be summarised as follows:

1. The envelope of recycling loading does not substantially deviate from the monotonous one.
   Low cycle fatigue, even if the load level exceeds 85–90% of the strength under monotonic action, does not result in failure for a low number of reversals, that is, for seismic action. The cases of *shear* and *bonding-slip* of reinforcement should be exempted, since in these cases the degradation of the strength of structural elements is serious even for a low number of cycles. For this reason a great effort has been made for these types of strains in structural systems to be kept at a low level by means of a capacity design approach.
2. For low cyclic loading strain rates similar to those of earthquake excitation, strength does not substantially exceed the strength of monotonic loading.
3. From all of the above it may be concluded that the energy dissipation capacity of a material or a structural element depends on the following characteristics:
   a. The available inelastic deformation (ductility supply) under monotonic loading
   b. The area of the energy dissipation loop of each cycle, since it is known (see Subsections 2.5.2 and 2.3.3) that this area expresses the dissipated seismic energy for every reversal cycle

In this context, the basic aim of the seismic design of critical regions of a structural system is the provision of satisfactory ductility and 'full' dissipation recycling loops, that is, the avoidance of strength degradation due to *shear* and *bond slip*.

In this chapter and in Chapters 8 through 10, a comprehensive presentation will be made of the techniques and analytical tools that are used in the seismic design of materials and structural elements for qualitative as well as quantitative safeguarding of the ductility demand of the structure.

7.2 PLAIN (UNCONFINED) CONCRETE

7.2.1 General

It is known that concrete presents a rather high compressive strength but a limited and unreliable tensile strength, so that in the design of R/C structures the tensile concrete strength is ignored (cracked tensile zones). It is also a brittle material, like all other stone or stone-like materials. In this context, it is necessary that its use in a seismic design be combined with special measures that mitigate the effects of this property.

7.2.2 Monotonic compressive stress–strain diagrams

The form of this diagram is depicted in Figure 7.1 (Park and Paulay, 1975). It should be noted that as the strength of the material increases, its brittleness also increases. In any case, the maximum compressive strength corresponds to a strain ranging from 2‰ to 1.7‰. Various analytical models have been developed for the simulation of the $\sigma_c - \varepsilon_c$ curve (FIB, 2010).

   The best-known analytical expression for the ascending branch of the diagram is Hognestad's expression (Park and Paulay, 1975):

$$\sigma_c = f_c \left[\frac{2\varepsilon_c}{\varepsilon_{c1}} - \left(\frac{\varepsilon_c}{\varepsilon_{c1}} \right)^2 \right] \tag{7.1}$$

where:

   $\varepsilon_{c1} = \dfrac{2f_c}{E_{co}}$: (see diagram of Figure 7.2)
   E_{co} is the initial tangent modulus of elasticity
   $\varepsilon_{c1} = 2.0‰$
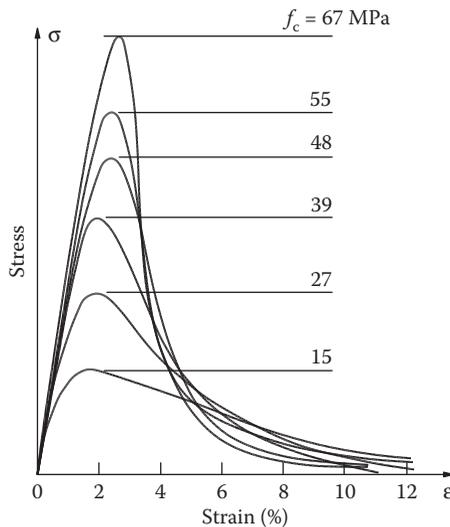
Figure 7.1 Stress–strain curves for various concrete classes under uniaxial compression. (Adapted from CEB. 1993. CEB-FIP Model Code 1990, *Bulletin d'Information*, CEB, 213/214, Lausanne.)
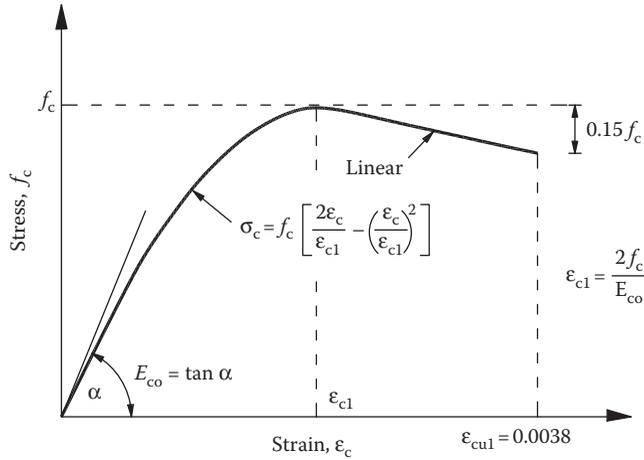
Figure 7.2 Idealised stress–strain curve for concrete under uniaxial compression. (Adapted from Park, R. and Paulay, T. 1975. *Reinforced Concrete Structures.* Copyright Wiley-VCH Verlag GmbH & Co. KGaA. Reproduced with permission.)

For the descending branch, the model of Kent and Park (1971) (Park and Paulay, 1975) may be considered the simplest, as this branch is simulated by a descending straight line presented by the following expression:

$$\sigma_c = f_c[1 - z(\varepsilon_c - \varepsilon_{c1})] \tag{7.2}$$

where

$$z = \frac{0.50}{\varepsilon_{c50} - \varepsilon_{c1}}$$

and

$$\varepsilon_{c50} = \frac{3 + 0.29 f_c}{145 f_c - 1000} \quad (f_c \text{ in MPa}) \tag{7.3}$$

which is an expression obtained by fitting to experimental results.

For large strains, a residual strength equal to $0.20\,f_c$ was introduced by Kent and Park in the above model. Later in this chapter the provisions of EC2-1-1/2004b will be presented for the simulation of the $\sigma_c - \varepsilon_c$ diagram.

7.2.3 Cyclic compressive stress–strain diagram

Such a diagram is depicted in Figure 7.3 (Karsan and Jirsa, 1969). It should be noted that the successive loops are almost in contact with the curve of monotonic loading. From extended experimental work the following results may be drawn:
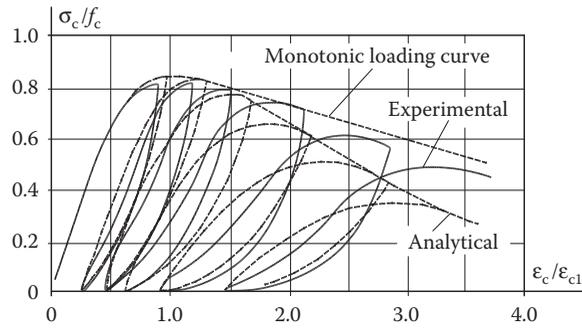
Figure 7.3 Stress–strain diagrams for concrete subjected to repeated uniaxial compression. (Adapted from Karsan, I.D. and Jirsa, J.O. 1969. *Journal of the Structural Division, ASCE* 95(ST 12), 2543–2563.)

1. For high values of strain rate, strength and stiffness are strongly influenced positively (Figure 7.4; Priestley and Wood, 1977). However, in the case of seismic action, which has a strain rate that is rather low, at a range of, $\dot{\varepsilon} = 4 \div 5 \, 10^{-2}/s$, the positive influence is rather small, ranging from 10% to 15%.
   Therefore, this overstrength may be ignored, as it is on the safe side.
2. For successive loading cycles below 85% of the axial compressive strength of monotonic loading and for a large number of reversals (about 200), specimens do not display any sign of failure (low cycle fatigue). If loading exceeds 90% of the compressive strength, 19 to 20 cycles are enough for the strength degradation and failure of the specimen (Figure 7.5; Karsan and Jirsa, 1969; Fardis, 2009). However, keeping in mind that the number n of cycles during a seismic event is limited ($n \cong t/T$ where t is the duration of the event and T the predominant period of the seismic motion) and that only a small number of cycles exhausts the strength limits, it may be concluded that low cycle fatigue does not seriously influence concrete strength during a seismic motion. In any case, in order to take measures against this strength degradation,
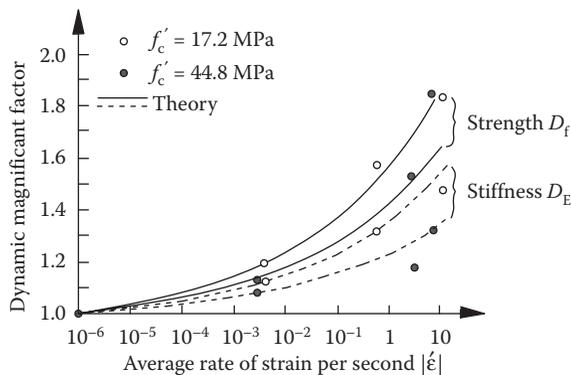
Figure 7.4 Dynamic magnification factors D_f and D_E to allow for strain rate effects on strength and stiffness. (From Priestley, M.J.N. and Wood, J.H. 1977. *Behaviour of a complex prototype box girder bridge. Proceedings of the RILEM International Symposium on Testing In-Situ of Concrete Structures*, Budapest, 1, 140–153. Copyright Wiley-VCH Verlag GmbH & Co. KGaA. Reproduced with permission.)
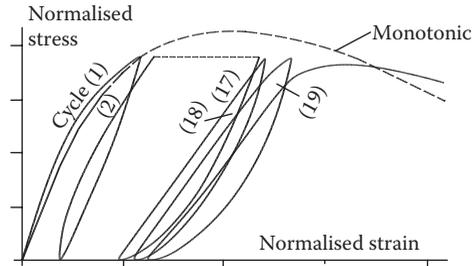
Figure 7.5 σ–ε diagram of concrete under cyclic uniaxial compression. (Adapted from Karsan, I.D. and Jirsa, J.O. 1969. *Journal of the Structural. Division*, ASCE 95(ST 12), 2543–2563.)

EC8-1/2004 recommends the use of material partial factors for seismic design equal to those in force for static loading, although seismic action is considered to be accidental (see Chapter 6).

The above considerations have influenced the formulation of programs for displacement-controlled tests in the laboratory. In fact, two such programs are mainly in use. The first includes one cycle of displacement or strain per step, while the second one includes two to four cycles (Figure 7.6; Stylianidis, 2012).
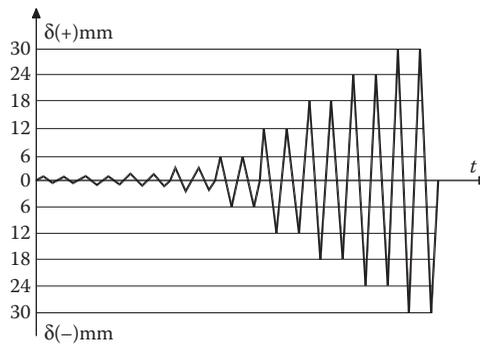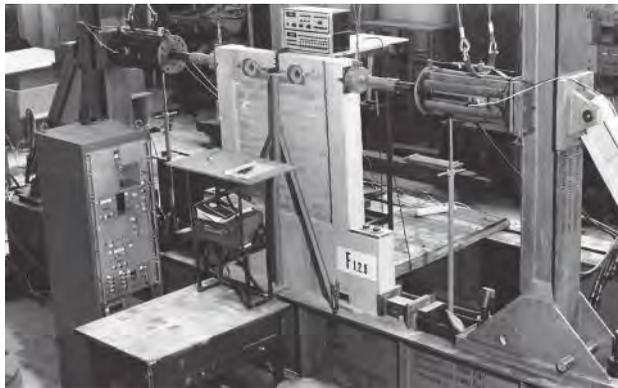
Figure 7.6 Loading program (two cycles per step) for testing of infilled R/C frames. (Adapted from Stylianidis, K. 2012. *The Open Construction and Building Technology Journal*, 6, 194–212.)

7.2.4 Provisions of Eurocodes for plain (not confined) concrete

According to EC8-1/2004, all properties that are specified by EC2-1-1/2004 (R/C structures) for plain concrete are accepted also for earthquake-resistant R/C buildings. A summary of the most important properties is given below:

- **Strength:**
    - For buildings of ductility class medium (DCM): Concrete class may range from C16/20 to C90/105
    - For buildings of ductility class high (DCH): Concrete class may range from C20/25 to C90/105
- **Stress–strain diagram ($\sigma_c - \varepsilon_c$) of monotonic compressive loading for inelastic analysis**
  The constitutive law of $\sigma_c - \varepsilon_c$ is depicted in Figure 7.7 and results from the expression:

$$\frac{\sigma_c}{f_{cm}} = \frac{\kappa n - n^2}{1 + (\kappa - 2)n} \tag{7.4}$$

where

$$n = \frac{\varepsilon_c}{\varepsilon_{c1}} \tag{7.5}$$

$$\kappa = 1.05 \, E_{cm} \left|\varepsilon_{c1}\right| / f_{cm} \tag{7.6}$$

The above expression (7.4) is valid for $0 < |\varepsilon_c| < |\varepsilon_{cu1}|$.
The meaning of the notation in the above expressions is the following:

f_{cm} is the mean compressive strength (MPa)
E_{cm} is the mean modulus of elasticity
ε_{c1} is strain at maximum stress

Values for the various concrete classes may be found in Table 3.1 of EC2-1-1/2004 (Table 7.1 in this Chapter). Equation 7.4 is a generalised form of Hognestad's expression (7.1). In the expression (7.1), κ has a constant value equal to 2, while in Code's expression (7.4) κ varies according to concrete class.

- **Stress–strain diagram ($\sigma_c - \varepsilon_c$) for section design**
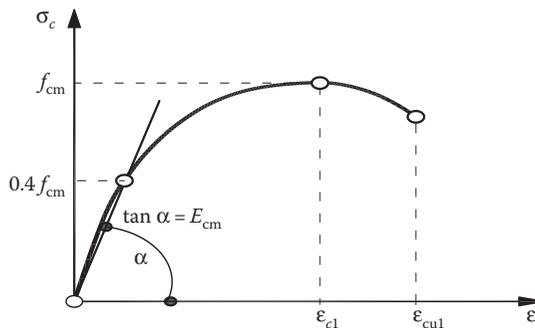
Figure 7.7 Schematic representation of the stress–strain relation of concrete for structural analysis. (Adapted from EC2-1-1/EN1992-1-1. 2004. *Design of Concrete Structures—Part 1-1: General Rules and Rules for Buildings*. BSI, CEN, Brussels, Belgium.)

Table 7.1 Strength and deformation characteristics for concrete

	Strength classes for concrete									
f_{ck} (MPa)	12	16	20	25	30	35	40	45	50	55
$f_{ck,cube}$ (MPa)	15	20	25	30	37	45	50	55	60	67
f_{cm} (MPa)	20	24	28	33	38	43	48	53	58	63
f_{ctm} (MPa)	1.6	1.9	2.2	2.6	2.9	3.2	3.5	3.8	4.1	4.2
$f_{ctk,0.05}$ (MPa)	1.1	1.3	1.5	1.8	2.0	2.2	2.5	2.7	2.9	3.0
$f_{ctk,0.95}$ (MPa)	2.0	2.5	2.9	3.3	3.8	4.2	4.6	4.9	5.3	5.5
E_{cm} (GPa)	27	29	30	31	33	34	35	36	37	38
ε_{c1} (‰)	1.8	1.9	2.0	2.1	2.2	2.25	2.3	2.4	2.45	2.5
ε_{cu1} (‰)					3.5					3.2
ε_{c2} (‰)					2.0					2.2
ε_{cu2} (‰)					3.5					3.1
n					2.0					1.75
ε_{c3} (‰)					1.75					1.8
ε_{cu3} (‰)					3.5					3.1

Source: From EC2-1-1/EN1992-1-1. 2004. Design of Concrete Structures—Part 1-1: General Rules and Rules for Buildings. BSI, CEN, Brussels, Belgium. With permission.

Figure 7.8 Parabola–rectangle diagram for concrete under compression for design. (Adapted from EC2-1-1/EN1992-1-1. 2004. *Design of Concrete Structures—Part 1-1: General Rules and Rules for Buildings*. BSI, CEN, Brussels, Belgium.)

The constitutive law $\sigma_c - \varepsilon_c$ for the design of R/C sections in bending with or without axial load is given in Figure 7.8 and results from the following expressions:

- For $0 \leq \varepsilon_c \leq \varepsilon_{c2}$

$$\sigma_c = f_{cd}\left[1 - \left(1 - \frac{\varepsilon_c}{\varepsilon_{c2}}\right)^n\right] \tag{7.7}$$

- For $\varepsilon_{c2} \leq \varepsilon_c \leq \varepsilon_{cu2}$

$$\sigma_c = f_{cd} \tag{7.8}$$

where

n is an exponent taken from Table 3.1 of EC2-1-1/2004 (Table 7.1)

ε_{c2} is the strain corresponding to the maximum strength according to the above Table 7.1

ε_{cu2} is the strain at failure according also to the above Table 7.1

For simplicity's sake, the compressive strength and the corresponding strain are introduced in the above expressions with a positive sign.

- **Remarks**
  - The exclusion of some low classes of concrete from the earthquake-resistant R/C building aims at an increase of the ductility of the structural system, as we will see later.
  - For concrete classes from C16/20 to C50/60, the values of the above parameters are given below:

    ε_{c1}: 1.9‰–2.45‰

    ε_{cu1}: 3.5‰ (constant)

    ε_{c2}: 2.0‰ (constant)

    ε_{cu2}: 3.5‰ (constant)

    n : 2

    It should be noted that ε_{c2}, ε_{cu1}, ε_{cu2}, n for concrete classes in common use *are constant*.
  - For concrete classes from C55/67 to C90/105, the values of ε_{c1}, ε_{c2} increase successively, while the values of ε_{cu1}, ε_{cu2} decrease with a parallel decrease of the curvature of the ascending branch of the $\sigma_c - \varepsilon_c$ diagram. In other words, this diagram tends

to be linear without a descending or horizontal branch. In effect, as the strength of concrete increases above C50/60, its behaviour tends to be more brittle (Figure 7.1).

- In EC8-1/2004, a bold step was made by introducing high concrete classes above C50/60 and up to C90/105. This step was based on extended research carried out in the last few years, and the objective was to make R/C competitive with steel in the tall building industry. In order to limit the use of high-strength concrete to high-rise buildings, EC2-1-1/2004 recommends that member states decide about such limitations in their National Annexes. Some countries already specify the obligation of the user to obtain a special permit from the relevant national authorities for the use of a concrete class above C50/60.

7.3 STEEL

7.3.1 General

It is well known to every structural engineer that steel is a material with high and reliable tensile strength as well as high ductility. The same properties hold also in compression of steel rebars if they are *secured against buckling.* Therefore, it is the material used in the form of bars for reinforcing all R/C structural members in zones under tension. Similarly, particularly in R/C seismic structures, it is used to confine and to strengthen the structural member or zones under compression because, as will be seen in subsequent chapters, in this way the ductility of the critical regions is increased.

7.3.2 Monotonic stress–strain diagrams

Stress–strain diagrams $\sigma_s - \varepsilon_s$ of various steel grades are given in Figure 7.9, while the forms of hot-rolled and cold-deformed steel are given in Figure 7.10a and b). It should be noted that for hot-rolled steel in use in R/C structures, the stress and strain at failure $\sigma_{uк}$ and $\varepsilon_{uк}$ are in the range of 550 MPa and 75‰, respectively (Table 7.2; see table C.1 EC2-1-1/2004 Annex C).

Keeping in mind that the area of the $\sigma_s - \varepsilon_s$ diagram (Figure 7.11) expresses the energy absorbed up to failure per unit of material volume, and comparing the corresponding areas for steel and concrete, we see that the ratio of energy absorption W_s to W_c of steel to concrete for typical classes of materials is on the order of

$$\frac{W_s}{W_c} = 1000 \div 1200 \tag{7.9}$$

So, even in the case that the volumetric steel percentage of R/C members is on the order of 2% (140–150 kg/m³), the capacity of steel for seismic energy absorption and dissipation is about 20–25 times higher than for that of concrete. From what has been presented above it may be concluded that the capacity for ductile behaviour of R/C members relies basically on steel.

7.3.3 Stress–strain diagram for repeated tensile loading

A typical stress–strain $\sigma_s - \varepsilon_s$ diagram for repeated tensile loading is depicted in Figure 7.12 (Blakeley, 1971; Park, R. 1972). It is important to note that the successive loops are in contact with the curve of the monotonic tensile loading diagram. It is also important to note that the following useful conclusions may be drawn from extended laboratory research:
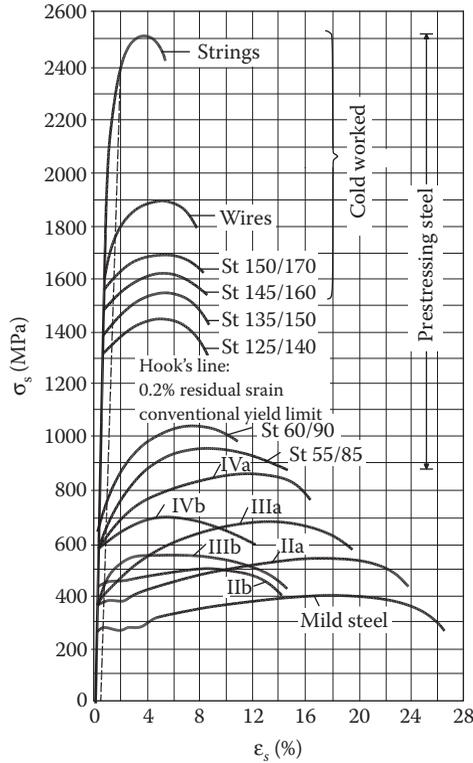
Figure 7.9 Stress–strain diagrams for steel rebars of various grades. (Adapted from Penelis, G.G. and Kappos, A.J. 1997. *Earthquake-Resistant Concrete Structures.* SPON E&FN (Chapman & Hall), London.)

1. For low values of strain rates ($\cong 1.0 10^{-2}$) the yield limit increases 10–20%, with the higher values of increase corresponding to steels of low strength.
2. In the case of a repeated tensile cyclic loading (about 90% of the yield strength) and for a large number of loading cycles (above 1000) under high strain rates (above $10 10^{-2}$/s), the failure load is limited very little in comparison to the failure static loading. In other words, the increase of the yield strength due to the high strain rate is counter-balanced by the fatigue symptom. All the above characteristics are also in effect for compressive axial loading under the assumption that buckling is prohibited.
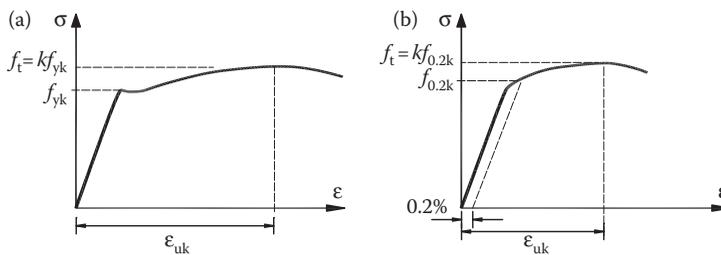
Figure 7.10 Stress–strain diagrams of typical reinforcing steel: (a) hot-rolled steel; (b) cold-rolled steel. (Adapted from EC2-1-1/EN1992-1-1. 2004. *Design of Concrete Structures—Part 1-1: General Rules and Rules for Buildings.* BSI, CEN, Brussels, Belgium.)

Table 7.2 Properties of reinforcement

Product form	Bars and de-coiled rods			Wire fabrics		
Class	A	B	C	A	B	C
Characteristic yield strength f_{yk} or $f_{0.2k}$ (MPa)			400–600			
Minimum value of $k = (f_t/f_y)_k$	≥1.05	≥1.08	≥1.15 <1.35	≥1.05	≥1.08	≥ 1.15 <1.35
Characteristic strain at maximum force, ε_{uk} (%)	≥2.5	≥5.0	≥7.5	≥2.5	≥5.0	≥ 7.5
Bendability		Bend/Rebend test			—	
Shear strength		—		0.3 A f_{yk} (A is area of wire)		

Source: From EC2-1-1/EN1992-1-1. 2004. *Design of Concrete Structures—Part 1-1: General Rules and Rules for Buildings.* BSI, CEN, Brussels, Belgium. With permission.

7.3.4 Stress–strain diagram for reversed cyclic loading

Under reversed cyclic loading the stress–strain properties of steel become quite different from those of purely tensile or compressive stress. This is known as the *Bauschinger effect* and results in a lowering of the reversed yield stress (Figure 7.13; Park, 1972). Once a full loop is integrated, the linear relation between stress–strain (constant E_s) is disrupted for all successive cycles. Many attempts have been made to elaborate reliable analytical models for simulating the stress–strain constitutive law for reversal cyclic loading (Popov, 1977; CEB, 1991). One of the most reliable expressions is that of Ramberg–Osgood, based on curve fitting to available test data (Figure 7.14; Park and Paulay, 1975; Popov, 1977).
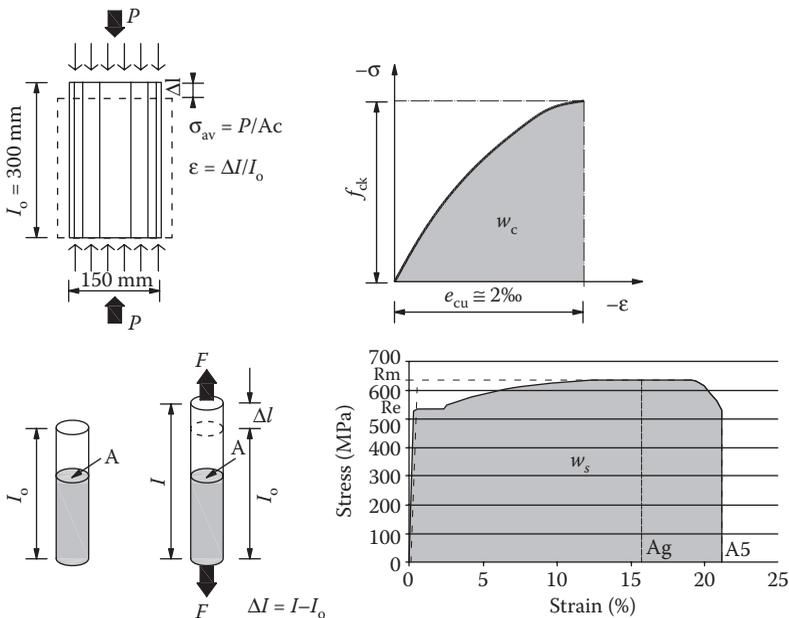
Figure 7.11 Determination of the ratio of strain energy absorbed up to failure per volume unit of steel to concrete.
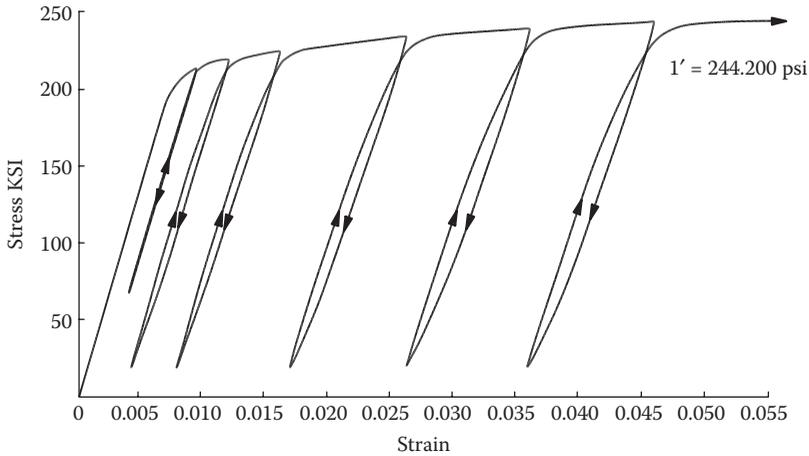
Figure 7.12 Stress–strain curve for steel wire under repeated tensile loading. (Adapted from Sinha, B.P., Gerstle, K.H. and Tulin, L.C. 1964. *Journal of the American Concrete Institute*, Proceedings, 61(8), 1021–1038; Park, R. 1973. Theorization of structural behaviour with a view to defining resistance and ultimate deformability. *Symposium on Resistance and Ultimate Deformability of Structures Acted on by Well-Defined Repeated Loads*. IABSE, Lisboa, 1973. With permission of IABSE.)
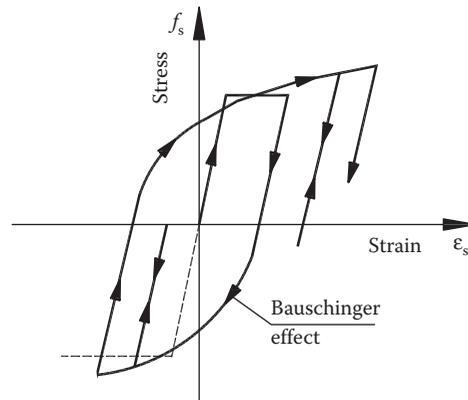
Figure 7.13 Stress–strain diagram for steel under reversed loading (Bauschinger effect). (Park, R. 1973. Theorization of structural behaviour with a view to defining resistance and ultimate deformability. *Symposium on Resistance and Ultimate Deformability of Structures Acted on by Well-Defined Repeated Loads*. IABSE, Lisboa, 1973. With permission of IABSE.)

7.3.5 Provisions of codes for reinforcement steel

Generally, reinforcement steel categories in Europe are specified by EN1992-1-1:2004 and by EN10080 (Table 7.2; Figure 7.15). The various categories are classified into three classes, namely:

- Steel class B (400–600) A
- Steel class B (400–600) B
- Steel class B (400–600) C
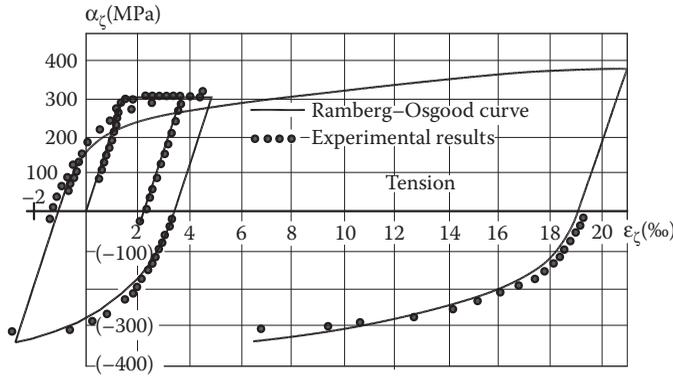
Figure 7.14 Modeling of the cyclic loading of steel bars and comparisons with relevant test data. (From Park, R. and Paulay, T. 1975. *Reinforced Concrete Structures.* Copyright Wiley-VCH Verlag GmbH & Co. KGaA. Reproduced with permission.)
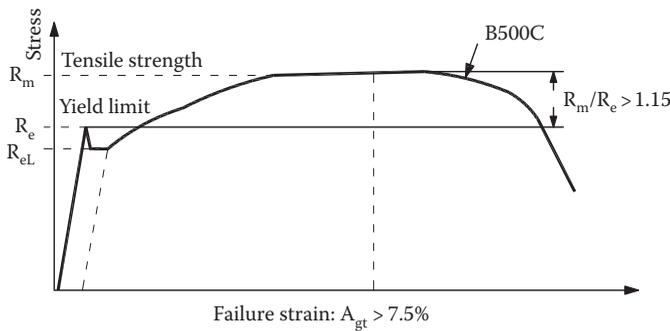
Figure 7.15 Stress–strain diagram of steel B500C (EN 10080).

Class A refers to cold deformed steel bars. *This class is considered to be unsuitable for primary structural members* of seismic-resistant buildings, even for DCL buildings, because of their low strain at failure ε_{su}. For buildings of moderate ductility (DCM buildings), the other two steel classes B and C may be used, while for buildings of behaviour class DCH (high ductility) only steel rebars of class C may be used.

With the exceptions of closed stirrups and ties, *only ribbed bars* may be used as reinforcing steel in primary structural members.

It should be mentioned here that the majority of steel factories in southern Europe, where seismicity is high, produce mainly steel rebars and weldable meshes of class B500C (weldable tempcore steel) in diameters from $d = 6$ to $d = 40$ mm. This steel category is suitable for buildings of all ductility classes. At the same time, they produce steel of class B500A in diameters of $d = 5$ to $d = 8$ mm in the form of welded meshes for non-primary seismic structural members (e.g. in Greece ELOT: EN 1420-2-3).

In Table 7.3, the steel classes that may be used in each ductility class are given together with their main mechanical properties.

7.3.6 Concluding remarks

1. Basic requirements for steel rebars in use for the primary seismic-resistant members are the following:

Table 7.3 Requirements for steel reinforcement bars according to EN1998-1

Magnitude	EN 1998-1/2004 DCM structures		(EUROCODE EC8-1) DCH structures		ELOT: EN 1420-2-3	
	Steel class B	Steel class C	Steel class B	Steel class C	Steel class B500 A	Steel class B500 C
R_m/R_e	≥1.08	≥1.15 <1.35	Ø	≥1.15 <1.35	≥1.05	≥1.15 <1.35
Agt (%)	≥5.0	≥7.5	Ø	≥7.5	>2.5	≥7.5
$R_{e\,act}/R_{e\,nom}$	<1.30	<1.30	Ø	<1.25	Ø	≤1.25
			EC 1992-1			

a. High strength
b. High ductility
c. High bond to concrete

In this respect:

a. Yield stress is about 500 MPa (almost twice the yield stress of classic mild steel)
b. Steel class A with a low value of ε_{su} (2.5%) is excluded from primary seismic members of all ductility classes
c. Steel of class B with a medium value of ε_{su} (≥5.0%) is allowed for use only in buildings of low and moderate ductility (DCL and DCM)
d. Only steel of class C with a high value of ε_{su} (≥7.5%) is allowed for use in buildings of ductility class DCH
e. Ribbed steel rebars are obligatory for ensuring a high bond between rebars, and concrete, hoops, and ties are exempted from the rule. A detailed examination of this issue will be presented in a subsequent paragraph, because rebar slip due to bond disintegration causes a quick degradation of rebar anchorage in concrete.

2. In addition to the above requirements, steel rebars for seismic-resistant primary members must fulfill a requirement for a minimum ratio $\kappa = f_t/f_y$, namely:

$$\kappa = f_t/f_y \begin{cases} \geq 1.05, \text{ for steel of class A} \\ \geq 1.08, \text{ for steel of class B} \\ \geq 1.15, \text{ for steel of class C} \end{cases} \qquad (7.10a\text{--}c)$$

where

f_y is the yield strength
f_t is the tensile strength

The above requirement imposes a minimum level of strain hardening with increasing value from steel class A to steel class C. The reasoning behind this is that the length of the plastic hinge that might be formed in the critical zone of a structural member (Figure 7.16) is closely related to the strain hardening of the reinforcement. Indeed, the plastic rotation capacity θ_u^{avail} of a joint is expressed by the dashed area of the curvature diagram in Figure 7.16. Therefore, the plastic curvatures must extend to a sufficient length of the member l_{p1} known as 'the length of the plastic hinge'. In fact, taking into account that the yield and failure moments M_y and M_u, respectively, at the base
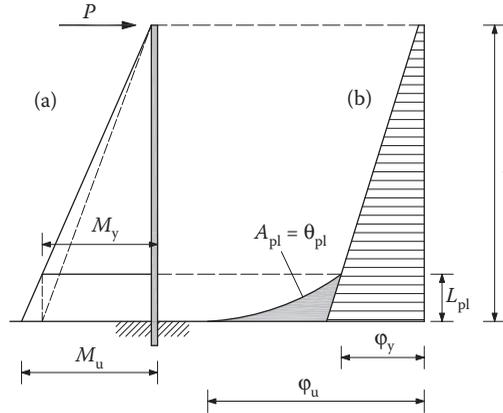
Figure 7.16 Schematic presentation of the reasoning behind the requirement that $f_t/f_y > 1.0$: (a) Moment diagrams yield and failure; (b) curvature diagram: plastic rotation $\theta_{pl} = A_{pl}$. In conclusion, if there is no degree of strain hardening ($f_t > f_y$), there is no plastic hinge.

of the cantilever in Figure 7.16 result with a good degree of approximation from the relations:

$$\left. \begin{array}{l} M_y \cong z_y \cdot f_y \cdot A_s \\ M_u \cong z_u \cdot f_u \cdot A_s \end{array} \right\}$$ (7.11a,b)

where

f_y and f_u are the yield and the tensile strength

z_y and z_u are the lever arms of internal forces at yield and failure and that they might approximately be considered equal

Therefore, the plastic hinge length may be given from the expression below:

$$l_{pl} = l\left(1 - \frac{M_y}{M_u}\right) \cong l\left(1 - \frac{f_y}{f_t}\right)$$ (7.12)

From the above expression it may be concluded that as the ratio f_y/f_t tends to 1.0, the length of the plastic hinge l_{pl} decreases and therefore the capacity of plastic rotation at the hinge also decreases.

3. Finally, according to European Codes, steel of class C, which is suitable for use in high-ductility R/C buildings (DCH), must also have a guaranteed upper limit of tensile strength, that is:

$$\left. \begin{array}{l} \kappa = \dfrac{f_t}{f_y} \leq 1.35 \\ \text{and} \\ \dfrac{f_{y\kappa0.95}}{f_{ynom}} \leq 1.25 \end{array} \right\}$$ (7.13a,b)

where

$f_{y\kappa 0.95}$ is the upper characteristic (95% fractile) of the actual yield strength

$f_{y\text{nom}}$ is the nominal yield strength

The above requirement for high-ductility steel (class C) allows the introduction of reasonable and reliable values of overstrength γ_{Rd} in the determination of capacity design action effects (see Chapter 6).

7.4 CONFINED CONCRETE

7.4.1 General

Since the beginning of the twentieth century it has been clear that concrete under triaxial compressive loading, that is, a predominant axial stress σ_1 and a hydrostatic lateral pressure ($\sigma_2 = \sigma_3 = p$) (Figure 7.17), presents an increase of its axial strength and its ability for plastic deformation. Lateral pressure p is accomplished mainly using circular spirals or narrow spaced hoops. When axial stress exceeds 70% of the axial compressive strength of plain concrete, the lateral reinforcement is activated due to the volume increase of the concrete core laterally. At the same time, the member under compression begins *to spall* little by little. So, finally, the concrete core inside the spiral reinforcement continues to be uncracked, confined by the steel reinforcement, while the cover has been spalled completely. When the axial stress exceeds a critical value, *confinement steel yields first,* while at the same time longitudinal cracks appear in the core parallel to the axial stress, which leads to the failure of the core. From what has been presented so far, the lateral reinforcement, due to its tensile strain, exerts pressure on the concrete core, which confines its lateral extension. For this reason the term 'confined concrete' has been introduced. In Figure 7.18, $\sigma_1 - \varepsilon$ diagrams are presented, showing the influence of the degree of confinement on concrete (Scott et al., 1982).

Recently, FRP warps have been used for the confinement of existing R/C structures. A detailed treatment of this issue will be made in Section 15.5 dealing with the repair and strengthening of R/C members.

In closing, it should be noted that confinement is the most effective tool for increasing the strength of concrete and *mainly for its transformation from a brittle material into a material with sufficient ductility.*
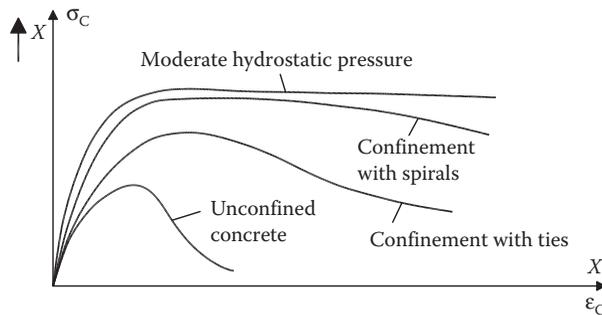
Figure 7.17 Stress–strain diagrams for various types of confinement.
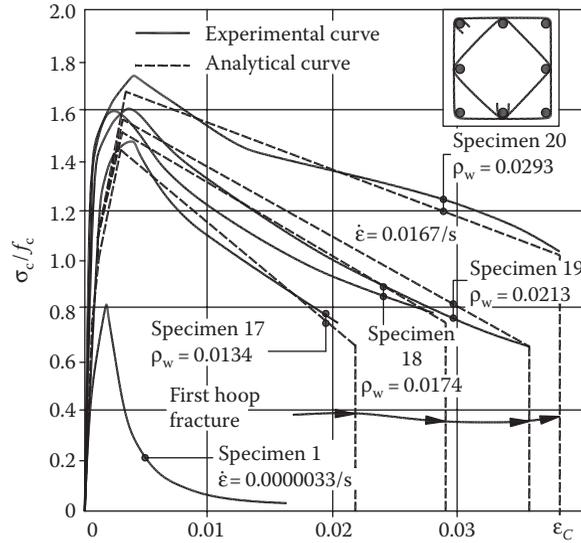
Figure 7.18 Stress–strain diagrams for concrete confined by different numbers of hoops. (Adapted from Scott, B.D., Park, R. and Priestley, M.J.N. 1982. *ACI Structural Journal*, Vol. 79(1), 13–27.)

7.4.2 Factors influencing confinement

Confinement is influenced by the following factors:

1. *The volumetric coefficient of transverse reinforcement ρ_w*
   This coefficient is defined as the ratio of the volume of spiral reinforcement or of hoops to the volume of relevant concrete that is confined by the spiral or hoop reinforcement.
2. *The yield strength of transverse reinforcement f_{yw}*
   It is obvious that this and the previous factor define the maximum possible value of confinement.
3. *The compressive strength f_c of concrete*
   The influence of confinement is more effective on low-strength concrete.
4. *The spacing of hoops or the spiral pitch*
   It is obvious that widely spaced spirals or hoops leave zones of the compressed member unconfined.
5. *The form and the arrangement of the spirals and hoops*
   Cyclic hoops are more effective than orthogonal ones (Figure 7.19). Hoops or ties that penetrate the concrete core are also more effective than orthogonal ones since in this case unconfined zones are limited.
6. *The strain rate $\dot{\varepsilon}$ of axial deformation*
   A high strain rate $\dot{\varepsilon}$ influences the increase of strength and the decrease of plastic deformation, as in the case of plain concrete.
7. *The strain gradient in the cross-section*
   R/C members under compression are likewise affected by bending moments, causing a strain gradient on the affected section. This eccentric loading does not have a serious influence on the confinement of the structural member.
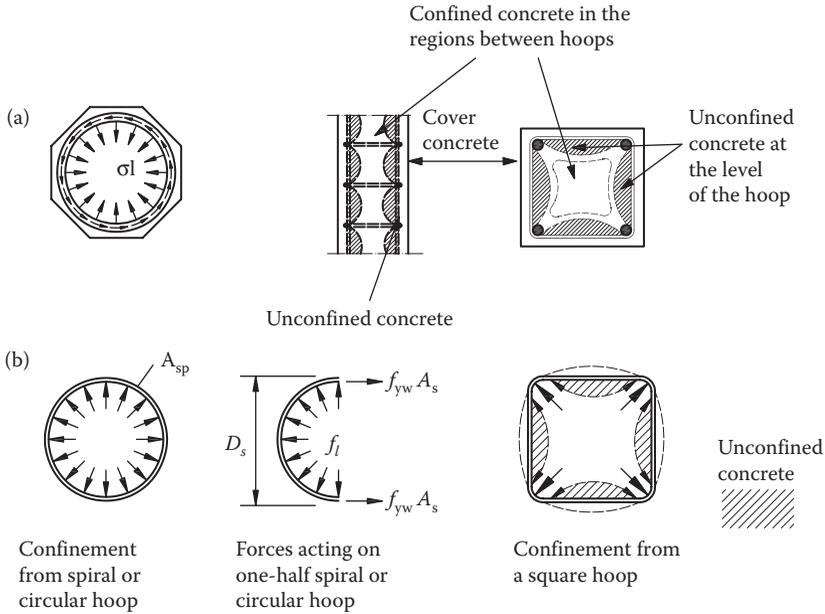
Figure 7.19 Confinement of concrete by circular and square hoops: (a) region confined by hoops; (b) stress pattern due to confinement by hoops. (Adapted from Penelis, G.G. and Kappos, A.J. 1997. *Earthquake-Resistant Concrete Structures.* SPON E&FN (Chapman & Hall), London.)

The above factors have been investigated for many years and have been simulated by analytical models of varying reliability. The scope of this book does not allow an extended treatment of this research. In any case, the results of this research have influenced the Codes of Practice in the dimensioning of members under compression.

A detailed examination of this issue will be made in the following subsections. Here, the presentation will be limited to the changes of the $\sigma_c - \varepsilon_c$ diagram that have been adopted by Codes in effect (EC2-1-1/2004 and EC8-1/2004) in the case of transverse hydrostatic stresses independently of the type of confinement.

7.4.3 Provisions of Eurocodes for confined concrete

7.4.3.1 *Form of the diagram* $\sigma_c - \varepsilon_c$

The diagram $\sigma_c - \varepsilon_c$ of confined concrete that has been adopted by EC2-1-1 and EC8-1 is given in Figure 7.20. The values of $f_{ck,c}$, $\varepsilon_{c2,c}$, and $\varepsilon_{cu2,c}$ are given below:

For $\sigma_2 \leq 0.05 f_{ck}$:

$$f_{ck,c} = f_{ck}(1.0 + 5.0\, \sigma_2/f_{ck}) \tag{7.14a}$$

For $0.05\, f_{ck} \leq \sigma_2$:

$$f_{ck,c} = f_{ck}\left(1.125 + 2.5\, \sigma_2/f_{ck}\right) \tag{7.14b}$$

$$\varepsilon_{c2,c} = \varepsilon_{c2}\left(f_{ckc}/f_{ck}\right)^2 \tag{7.15}$$
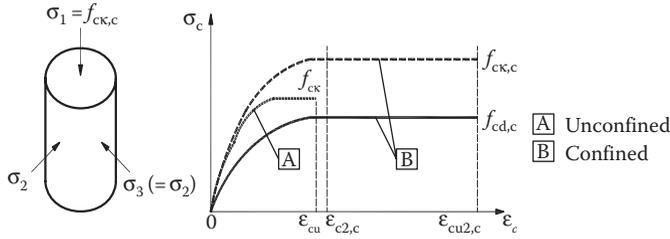
Figure 7.20 Stress–strain diagrams of confined concrete. (Adapted from EC2-1-1/EN1992-1-1. 2004. *Design of Concrete Structures—Part 1-1: General Rules and Rules for Buildings*. BSI, CEN, Brussels, Belgium.)

$$\varepsilon_{cu2,c} = \varepsilon_{cu2} + 0.2\sigma_2/f_{c\kappa} \tag{7.16}$$

Symbols in use are depicted in Figure 7.20. The above relations, that have been adopted first by Model Code 90/CEB/FIP and then by EC2-1-1/2004, underestimate the consequences of confinement in relation to other models of higher reliability, like that of Newman and Newman (1971).

According to this model (Figure 7.21; Fardis, 2009):

$$f_{c\kappa,c} = f_{c\kappa}(1 + \kappa) \tag{7.17}$$

$$\varepsilon_{c2,c} = \varepsilon_{c2}(1 + 5\kappa) \tag{7.18}$$

$$\varepsilon_{cu2,c} = 0.004 + 0.5\frac{\sigma_2}{f_{c\kappa c}} \tag{7.19}$$
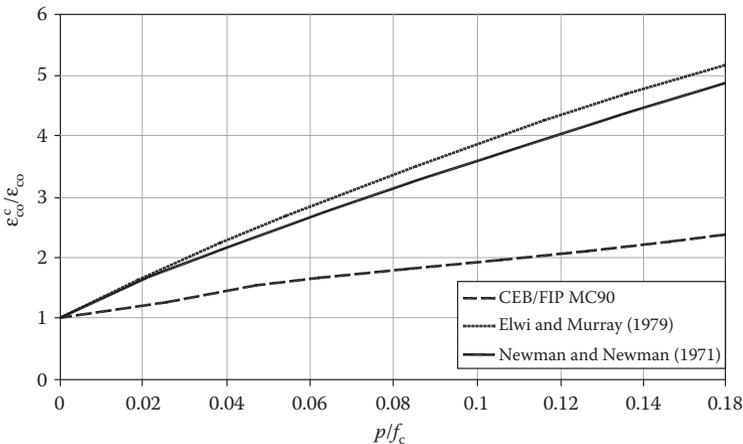
Figure 7.21 Comparison of the predictions of various confinement models for the enhancement of concrete strain at maximum strength; p, confinement stress; ε_{co}, strain at failure of unconfined concrete; ε_{co}^c, strain at failure of confined concrete. (Adapted from Newman, K. and Newman, J.B. 1971. *Failure Theories and Design Criteria for Plain Concrete. Solid Mechanics and Engineering Design*. J. Wiley-Interscience, New York; With kind permission from Springer Science+Business Media: Fardis, M.N. 2009. *Seismic Design, Assessment and Retrofitting of Concrete Buildings*.)

where

$$\kappa \cong 3.7\left(\frac{\sigma_2}{f_{c\kappa}}\right)^{0.86} \tag{7.20}$$

This model has been adopted by EC8-3/2005 for the assessment and strengthening of existing structures.

7.4.3.2 Influence of confinement

According to what has been presented in the previous paragraph, the determination of σ_2 in Equations 7.14 through 7.20 is the basic parameter for confinement consequences. In the case of confinement by means of spirals, hoops, stirrups and ties, the confined concrete core *fails just after the yield of confining reinforcement*. Therefore, the crucial point in the design is the determination of σ_2 at the stage of yielding of the reinforcement of confinement.

Consider first a circular cross-section confined by means of circular spiral reinforcement with a core diameter D_c and a pitch of the spiral s (Figure 7.22). At an advanced stage of axial loading, after spalling of the cover, lateral stresses σ_2 are developed in the form of a hydrostatic pressure. If the spacing of spirals is very small, these stresses may be considered uniformly distributed along the member height. Therefore, according to known expressions from the theory of strength of materials (Figure 7.22):

$$2A_s f_{yw} = \sigma_2 D_c s \tag{7.21}$$
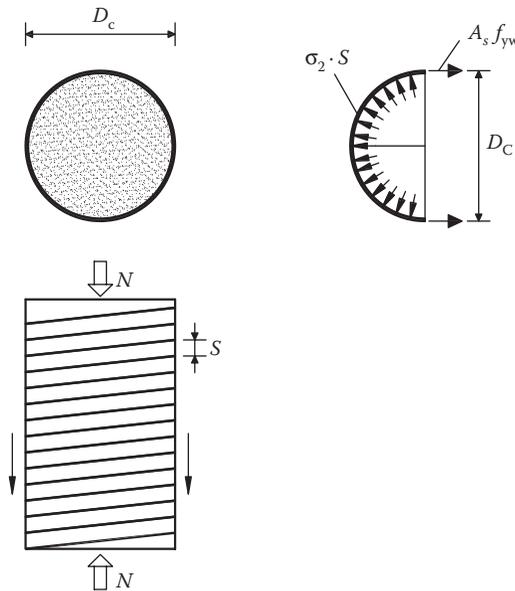
Figure 7.22 Stress pattern for the determination of the confinement degree (σ_2) as a function of the mechanical percentage (ω_w) of spiral confinement on concrete strength (f_{ck}).

and

$$\sigma_2 = \frac{2A_s f_{yw}}{D_c s} \qquad (7.22)$$

Now, taking into account that the mechanical percentage of lateral confining reinforcement is equal to

$$\omega_w = \rho_w \frac{f_{yw}}{f_{cк}} = \frac{A_s \pi D_c}{\pi D_w^2 s/4} \frac{f_{yw}}{f_{cк}} = \frac{4A_s}{D_w s} \frac{f_{yw}}{f_{cк}} \qquad (7.23)$$

and introducing Equation 7.23 into Equation 7.22 we obtain:

$$\sigma_2 = 0.5\omega_w f_{cк} \qquad (7.24)$$

In the above equations the various symbols have the following meaning:

D_c is the core diameter (Figure 7.22).
s is the pitch of the spiral.
A_s is the area of the cross-section of a spiral.
$f_{cк}$ is the characteristic concrete strength.
f_{yw} is the yield strength of the spiral reinforcement.
$\rho_w = \dfrac{4A_s}{D_c s}$ is the volumetric percentage of spiral reinforcement.
$\omega_w = \rho_w \dfrac{f_{yw}}{f_{cк}}$ is the mechanical percentage of spiral reinforcement.

In practice, members under compression are usually neither circular nor laterally reinforced with spirals or hoops in very narrow spacing. Therefore, expression (7.24) must be modified so that the real stress condition is defined with sufficient accuracy. So, in Equation 7.24 a coefficient of reduction factor α must be introduced for the estimation (see 7.4.2) of:

- Spacing of the spirals, hoops or stirrups
- Arrangement of the stirrups and ties in the cross-section
- Longitudinal reinforcement of the member

that is:

$$\boxed{\sigma_2 = 0.5\alpha\omega_w f_{cк}} \qquad (7.25)$$

In this respect, Equations 7.14b and 7.16 take the following form:

$$\boxed{f_{cк,c} = f_{cк}\left(1.0 + 2.5\alpha\omega_w\right)} \qquad (7.26)$$

$$\boxed{f_{cк,c} = f_{cк}\left(1.125 + 1.125\alpha\omega_w\right)} \qquad (7.27)$$

$$\boxed{\varepsilon_{cu2,c} = \varepsilon_{cu2} + 0.10\alpha\omega_w} \qquad (7.28)$$

The mechanical models that have been used for the evaluation of α have taken into account the attenuations of the core confinement in longitudinal and transversal directions
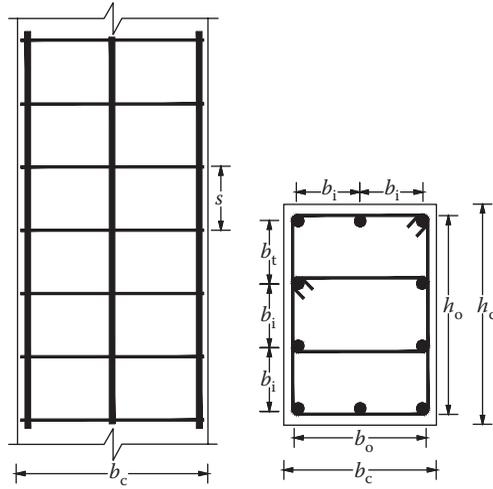
Figure 7.23 Confinement of concrete orthogonal cross-section with hoops.

as well as (Figure 7.23) the form of hoops, stirrups and ties (circular or orthogonal). In this respect, for each type of lateral confinement α is expressed as the product of two factors, α_s and α_n, that is:

$$\alpha = \alpha_s \cdot \alpha_n \tag{7.29}$$

In the above relation, α_s expresses the influence of spiral hoops or stirrups spacing (s), while α_n is the influence of the distance of longitudinal rebars that are engaged by stirrups or ties.

- For orthogonal members under compression and orthogonal stirrups (Figure 7.23), which is the most common case in practice, EC8-1/2004 specifies α_s and α_n as follows:

$$\alpha_s = \left(1 - s/2b_o\right)\left(1 - s/2h_o\right) \tag{7.30}$$

and

$$\alpha_n = 1 - \sum_n b_i^2 / 6 b_o h_o \tag{7.31}$$

where
   n is the number of longitudinal rebars with lateral constraint by stirrups or ties
   b_i is the distance between laterally engaged longitudinal bars by means of stirrups and ties
The rest of the symbols may be found in Figure 7.23.

- For circular cross-sections reinforced with hoops:

$$\alpha_n = 1 \tag{7.32}$$

$$\alpha_s = (1 - s/2D_c)^2 \tag{7.33}$$
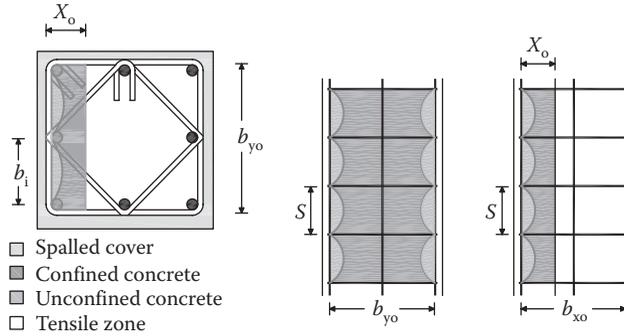
Figure 7.24 Calculation of confinement effectiveness in the compression zone of the confined core of a member in flexure. (With kind permission from Springer Science+Business Media: Fardis, M.N. 2009. *Seismic Design, Assessment and Retrofitting of Concrete Buildings*.)

where

D_c is the core diameter measured between the axes of hoop rebars

s is the spacing of hoops

• In the case of eccentric axial load of an orthogonal cross section (Figure 7.24; Fardis, 2009):

$$a_n = 1 - \frac{\sum b_i^2}{6x_o b_{yo}} \tag{7.34}$$

$$\alpha_s = \left(1 - \frac{s}{2b_{xo}}\right)\left(1 - \frac{s}{4x_o}\right) \tag{7.35}$$

The symbols of Equations 7.34 and 7.35 maybe found in Figure 7.24.

Many researchers have contributed to the development of the above mechanical models in the last 40 years (Park et al., 1982; Sheikh and Uzumeri, 1982; Mander et al., 1988; Kappos, 1991).

At the same time, the output of analytical models has been cross-checked by means of extended laboratory evidence (see reviews in Park and Paulay, 1975; Aoyama and Noguchi, 1979; Sakai and Sheikh, 1989).

The procedure for determination of α_s will be presented as an example in the case of circular hoops. It is assumed that the load path of confinement stresses from hoops to the core follows the form depicted in Figure 7.19. In this respect, the envelope of the confined zone between two hoops is an axisymmetric parabolic surface with a minimum diameter $D_{c\,min}$ at the mid-height of distance s of two successive hoops equal to

$$D_{c\,min} = D_c - \frac{s}{4}2 = D_c - \frac{s}{2} \tag{7.36}$$

Therefore, the area $A_{c\,min}$ of the minimum cross-section of the confined core is

$$A_{c\,min} = \frac{\pi}{4}\left(D_c - \frac{s}{2}\right)^2 \tag{7.37}$$

and finally

$$\alpha_s = \frac{A_{c\,min}}{A_c} = \frac{\left(D_c - \frac{s}{2}\right)^2}{D_c^2} = \left(1 - \frac{s}{2D_c}\right)^2 \tag{7.38}$$

that is, the same expression as that in Equation 7.33 adopted in EC8-1/2004.

7.5 BONDING BETWEEN STEEL AND CONCRETE

7.5.1 General

It is well known from the design of R/C structures under static loading that *bonding* between steel rebars and concrete is of paramount importance for the mechanical behaviour of reinforced concrete. In fact, bonding is a prerequisite for the transfer of any stress of a steel rebar to concrete in the form of shear bond stresses.

Consider Figure 7.25: Equilibrium conditions result in the following expression:

$$\frac{\pi d_s^2}{4} d\sigma_s = \pi d_s \tau_b dx \tag{7.39}$$

or

$$d\sigma_s = \frac{4}{d_s} \tau_b dx \tag{7.40}$$
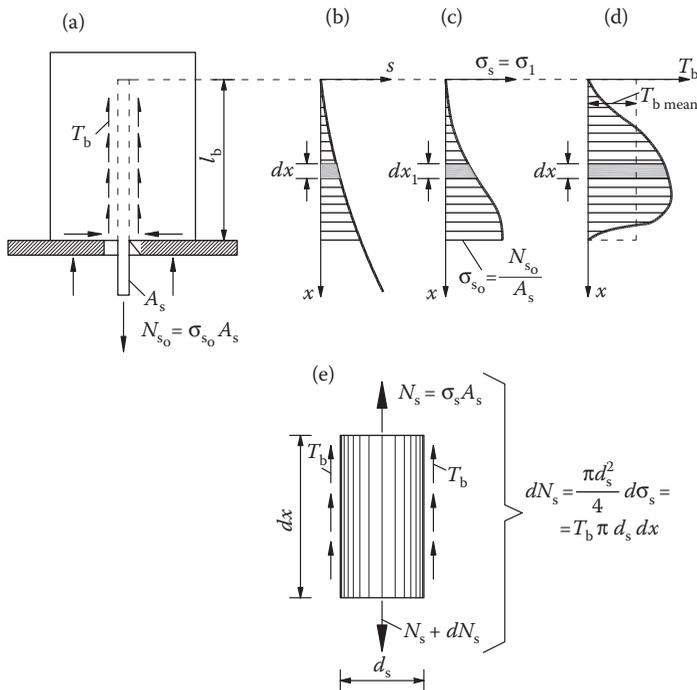
Figure 7.25 Bond shear stress distribution at the pull-out test: (a) experimental layout; (b) rebar slip; (c) tensile stresses at rebar; (d) bond stresses; (e) stress pattern at a differential element d*x* of the rebar.

Integrating Equation 7.40 between two points S_0 and $S_\perp$ in a distance l_b, the following expression is obtained:

$$\sigma_o = \sigma_{S0} - \sigma_{S1} = \frac{4}{d_s} \int_{S_0}^{S_1} \tau_b dx = \frac{4}{d_s} \tau_{b\,mean} l_b \qquad (7.41)$$

The meaning of the above symbols may be found in Figure 7.25.

It may be easily concluded from Equation 7.40 that any change of axial stresses along the rebar results in the development of bond shear stresses τ_b at the interface of steel and concrete, and conversely, *it is impossible for tensile stresses to develop in rebars* without bonding between concrete and reinforcement, that is, if $\tau_{b\,mean} = 0$.

These bond shear stresses are the result of stresses caused by three different transfer mechanisms. These mechanisms may be briefly described as follows:

1. *Chemical adhesion* of the cement paste on the surface of the steel bar. The degree of adhesion depends mainly on the roughness and the cleanness of the steel rebar surface. Its value τ_o ranges from 0.5 to 1.0 MPa (ACI Committee 408, 1991) and is exhausted before any slip δ between steel and concrete.
2. *Bond due to friction*. When the loading of the bar causes a bond shear stress

   $$\tau > \tau_o$$

   adhesion breaks down and bonding is developed *by friction* shear stresses, even *for a very small slip* of the rebar in the concrete. It is known that for the development of shear stresses due to friction a transverse pressure on the steel surface is needed. These pressures may be caused by transverse confinement of concrete, transverse loading, and microscopic anomalies (pitting) of the rebar surface. The friction coefficient μ ranges between 0.30 and 0.60, depending on the roughness of the steel surface. This type of bond is distinct only in the case of smooth rebar surfaces.
3. *Mechanical interlock*. Mechanical interlock is developed in the case of rebars with ribs, and it leads to an imposing enhancement of the total bond shear. In this case, the slip of the rebar in relation to the surrounding concrete is accompanied by internal cracks of concrete at the points of interlock of the ribs (Figure 7.26; Leonhardt, 1973) These cracks display vertically with respect to the main tensile stresses. This means that a slip at failure is accompanied by widening of the concrete circumference around the bar. As a consequence, strong circumferential stresses are developed, which cause splitting failure at the free surface of the concrete (Figure 7.27). At this point the bond to a large degree disintegrates. In this context, bonding is enhanced if there is adequate confinement. Bond strength in the case of deformed bars, according to EC2-1-1/2004, is estimated to be 3.0–7.0 times higher than that of smooth rebars, depending on the position of the bar in the concrete member. This can explain why in earthquake-resistant R/C structures the main rebars must be deformed.

   For the study of bonding, the three load transfer mechanisms presented above are examined together as one in the form of bond shear f_b. In this context, bond shear f_b is defined experimentally using specimens and loading in the form depicted in Figure 7.28 (RILEM/CEB/FIP). The mean values of τ_b for the successive loading steps and the corresponding relative slip between steel and concrete are depicted in a τ–s diagram, which presents the constitutive law of bonding. The conventional value of f_{bd} is defined as the mean bond shear stress for which a slip of 0.1 mm is displayed.

Tensile stress trajectories
-------- Compressive stress trajectories
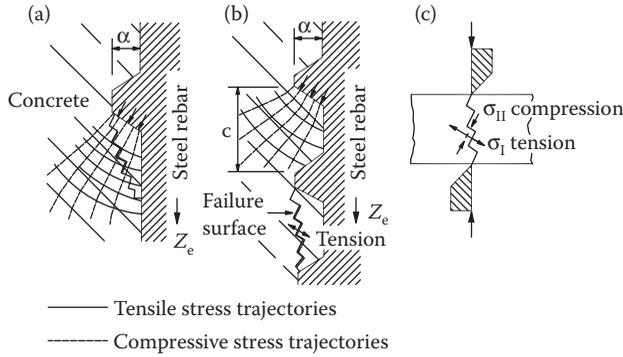
Figure 7.26 Qualitative stress and failure surface distribution of concrete at the ribs of deformed bars: (a) for large rib spacing; (b) for small rib spacing; (c) failure surface at shear (according to E. Morsh). (With kind permission from Springer Science+Business Media: Leonhardt, F. and Mönnig, E. 1973. *Vorlesungen uber Massivbau, Erster Teil.*)
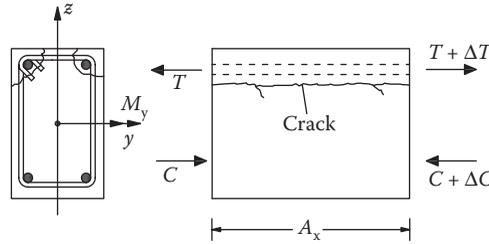
Figure 7.27 Longitudinal cracks due to bonding failure in the case of deformed steel rebars.

The scope of this book does not allow an extended examination of bond issues (anchorage lengths, reinforcement splices, reinforcement overlapping, etc.) for static loading, since all the above belong to the common practise for R/C structures in general. Here, we will focus our interest mainly on the following issues:

a. Monotonic loading up to failure of the bonding mechanism, including the descending branch of the $\tau_b - s$ diagram
b. Reversed cyclic loading up to failure
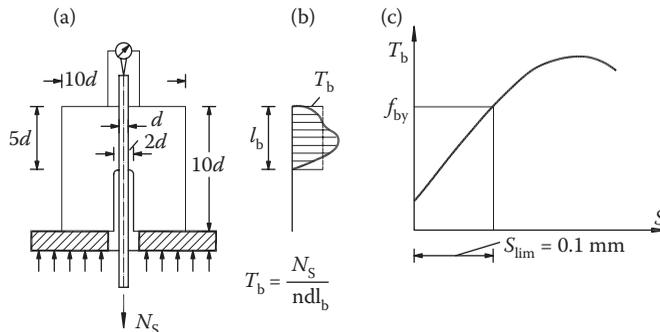
Figure 7.28 Pull-out test: (a) experimental layout; (b) normalised bond stress τ_b; (c) $\tau_b - s$ diagram. (RILEM/ CEB/FIB. With kind permission from Springer Science+Business Media: Leonhardt, F. and Mönnig, E. 1973. *Vorlesungen über Massivbau, I. Teil.*)

The above two parameters, together with those in effect for static loading, govern the bond mechanism in seismic structures and specifically at critical regions like joints, where significant bond stresses develop and sometimes lead to bond failure.

7.5.2 Bond–slip diagram under monotonic loading

Bonding between steel and concrete has been a subject of extended research since the beginning of the twentieth century due to its importance for the behaviour of reinforced concrete. However, the complete diagram of $\tau_b - s$, including also its descending branch up to complete failure of the bond, has been studied in the last 35 years, mainly in relation to the study of seismic-resistant R/C structures in the post-elastic stage.

In Figure 7.29 the idealised form of the diagram $\tau_b - s$ of *deformed bars* is depicted, based on laboratory tests carried out by Eligehausen et al. (1983) for unconfined and confined concrete. In parallel, the mechanical model adopted by Model Code 1990/CEB/FIB, 1993, is given in Figure 7.30. The main characteristics of the above diagrams for bonding of deformed bars under monotonic loading are the following:

1. *Specimens without lateral confinement*
   a. For loading up to a certain level $\tau_b = \tau_o$, no slip s is displayed because bonding of steel and concrete is based on the chemical adhesion. The value of τ_o ranges between 0.5 and 1.0 MPa (ACI Committee 408, 1991).
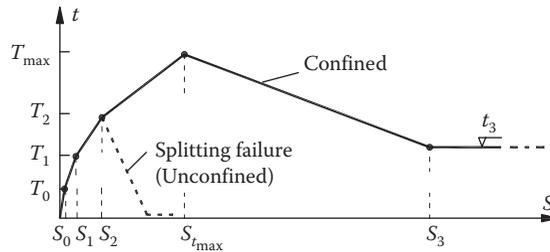
Figure 7.29 Idealised diagram of $\tau_b - s$. (Adapted from Eligehausen, R., Popov, E.P. and Bertero, V.V. 1983. Local bond stress–slip relationships of deformed bars under generalized excitations. *Report EERC-83/23*, Univ. of California, Berkeley; Penelis, G.G. and Kappos, A.J. 1997. *Earthquake-Resistant Concrete Structures*. SPON E&FN (Chapman & Hall), London.)
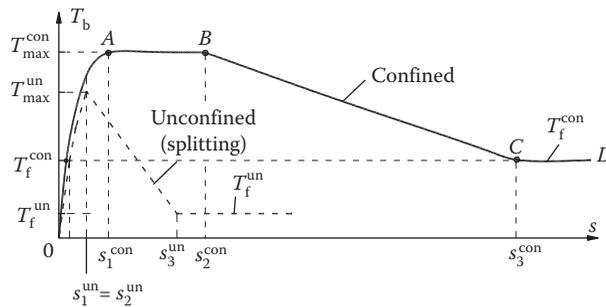
Figure 7.30 Idealised diagram of $\tau_b - s$ according to Model Code 1990. (Adapted from CEB 1993. CEB-FIP Model Code 1990, *Bulletin d'Information*, CEB, 213/214, Lausanne.)

b. For $\tau_o < \tau < \tau_{max}^{un}$, after the rupture of adhesion, friction begins to be activated together with the mechanical interlock of ribs of deformed bars in concrete.

c. For the next loading steps, internal micro cracks appear in concrete at its interface with rebars. As a result, the slip of $\tau_b - s$ diagram begins to decrease.

d. For a value $\tau_b = \tau_{max}^{un}$, splitting is displayed at the concrete surface, accompanied by an abrupt decreasing of τ_b (descending branch in Figure 7.30 of unconfined bonding).

e. The characteristic values of τ_b and s accompanied by analytical expressions for the ascending branch in Figure 7.30 are given in Model Code 1990 of CEB/FIB (1993) and are presented below:

   i. $s_1 = s_2 = 0.6$ mm

   ii. $s_3 = 1.0$ and 2.5 mm: for 'good' and 'poor' bond conditions, respectively

   iii. $\tau_{max} = 2.0\sqrt{f_{ck}}$ and $1.0\sqrt{f_{ck}}$: for 'good' and 'poor' bond conditions, respectively

   iv. $\tau_f = 0.15\tau_{max}$

   v. $\tau = \tau_{max}\left(\dfrac{s}{s_1}\right)^{0.40}$: for the ascending branch

2. *Specimens with lateral confinement*

   a. In the case of lateral confinement caused either by lateral reinforcement or by transversal external pressure, the diagram $\tau_b - s$ (Figure 7.30) has the same form as that of the unconfined specimen with the higher value of τ_{max} as its main characteristic, and a strength plateau at τ_{max}.

   b. After the concrete splitting, a horizontal plateau is displayed in the $\tau_b - s$ diagram due to lateral confinement, and the descending branch then follows, which corresponds to the concrete pulverising between successive ribs.

   c. The characteristic values of τ_b and s accompanied by an analytical expression for the ascending branch in Figure 7.30 are given in Model Code 1990/CEB/FIB, 1993, and are presented below:

   i. $s_1 = 1.0$ mm $= s_f$

   ii. $s_2 = 3.0$ mm

   iii. $s_3 =$ rib spacing

   iv. $\tau_{max} = 2.5\sqrt{f_{cк}}$ and $1.25\sqrt{f_{cк}}$: for 'good' and 'poor' bond conditions, respectively

   v. $\tau_f = 0.4\ \tau_{max}$

   vi. $\tau = \tau_{max}\left(\dfrac{s}{s_f}\right)^{0.40}$: for the ascending branch

The above parameters are in effect for lateral confinement defined below:

$$
\left.\begin{array}{l}
p \geq 7.5\ \text{MPa} \qquad\qquad 7.42a \\[4pt]
\text{or} \\[4pt]
\dfrac{\sum A_{sw}}{(nA_s)} \geq 1 \qquad\qquad 7.42b
\end{array}\right\} \qquad\qquad (7.42)
$$

where

A_s is the area of the cross-section of each bonded rebar

n is the number of bonded bars

ΣA_{sw} is the area of the cross-section of the confining stirrups along the bond length under consideration

For

$$0 \leq p \leq 7.5 \text{ MPa} \qquad \qquad 7.43a$$

or

$$0.25 \leq \sum A_{sw}/(nA_s) \leq 1 \qquad 7.43b$$

$$(7.43)$$

a linear interpolation is recommended between the respective values of unconfined and confined concrete.

3. From extensive laboratory tests it has been verified that the $\tau_b - s$ diagram for bars under compression is identical to that for rebars under tension in the case of lateral confinement.

4. Finally, in the case that steel bars under tension exhaust their yield strength, their respective lateral contraction causes a decrease of bond. The opposite happens in case of rebars under compression.

7.5.3 Bond–slip diagram under cyclic loading

A bond–slip diagram under repeated loading of an embedded bar has as an envelope the monotonic diagram of bond-slip presented in the previous paragraph.

Results of a reversed cyclic loading in conceptual form are depicted in the diagram of Figure 7.31 (Balázs, 1989; Fardis, 2009) and Figure 7.32. In this case it is important to note:

1. Reversal loading leads to a degradation of high order of bonding after a number of cycles.
2. The main characteristic of bond hysteretic loops is that for bond stresses above τ_f the loading reversals are accompanied by horizontal branches at the loops caused by almost free slip of the rebars in the surrounding concrete, due to the disintegration and pulverising of the cement paste between the successive ribs (Figure 7.32). This form of loops results in the loss of a big percentage of the capacity for energy dissipation at the region of bonding. In other words, before the yielding of a rebar by means of which the hysteretic energy dissipation mechanism is activated, the disintegration of the bonding of the rebar with the surrounding concrete leads to the drastic degradation of the
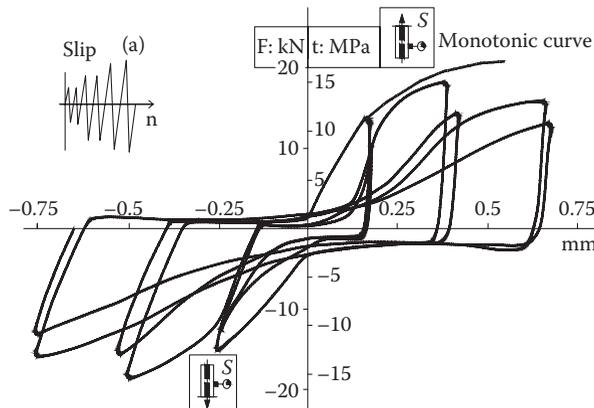
Figure 7.31 Bond stress–slip diagram under cyclic loading with $f_c = 25$ Mpa. (Adapted from Balázs, G.L. 1989. Bond softening under reversed load cycles. *Studie Ricerche, Politecnico di Milano,* No. 11, Milano, 503–524.)
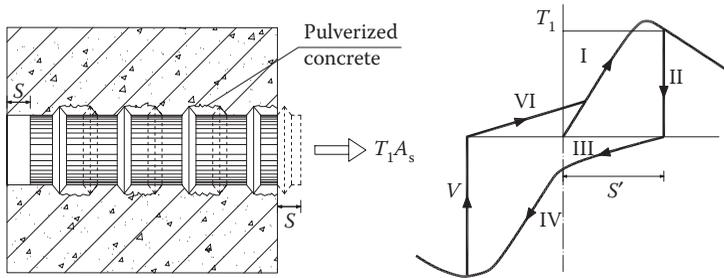
Figure 7.32 Bond stress–slip diagram under cyclic loading in conceptual form (I–VI: diagram branches of one cycle).

ductility of the structure. Consequently, it is of major importance that special measures be taken at the critical regions, for example, joints of seismic-resistant frames, so that this risk may be eliminated or at least be minimised (see Subsection 8.4.3). The most important of these measures in Codes of Practice is the introduction of very low values for f_{db}. In this way, bond zones remain in the elastic domain of the $\tau_b - s$ curve and the degradation of the anchorage action is not significant. However, this requirement for low values for f_{db} leads to considerable lengths of anchorage or splices.

3. The formation of hooks at the end of embedded rebars, usually at right angles, seems to be a very effective measure for improving anchorage. From the extensive laboratory research of Eligehausen et al. (1983) the following remarks may be drawn.

    a. In the $\tau - s$ diagram under monotonic loading after the maximum value of τ has been reached, the descending branch continues to be very stable with a very smooth slope, which means that the bond continues to be stable against large slips. This must be attributed to the resistance of the hook to a pull-out effect, which contributes substantially to the internal forces of the bond.

    b. The $\tau - s$ curve for reversed cyclic loading continues to be very close to the curve of monotonic loading for a large number of reversals.

    c. The above remarks are taken into account very seriously for bar anchorage in joints of frames, particularly at the external columns (see Subsection 8.4.3).

    d. In the last 30 years many analytical models have been formulated that simulate in one way or the other the behaviour of bonds under reversed cyclic loading, as has been presented in experimental research (Tassios, 1979; Eligehausen et al., 1983; Filippou et al., 1983; ACI Committee 408, 1991; CEB Task Group 22, 1991; Soroushian et al., 1991; Darwin et al., 2002a,b; Cairns, 2006; Eligehausen and Lettow, 2007).

7.5.4 Provisions of Eurocodes for bond of steel to concrete

7.5.4.1 Static loading

It should be noted again that, as was explained in Subsection 7.5.1, the basic provisions for bond anchorage lengths, splices and overlaps are specified by Codes of Practice for conventional R/C structures. In Europe, EC2-1-1/2004 covers this issue in detail.

A summary of the main points of these provisions will be presented below:

1. The synergy of the three bonding mechanisms presented in Subsection 7.5.1 is approached by the assumption that constant design bond shear strength f_{db} develops

along the interface of a rebar and concrete. This is defined by the following expressions (Figure 7.25).

a. For deformed steel rebars:

$$\boxed{f_{bd} = 2.25 f_{ctк}/\gamma_c \cong 0.32 f_{cк}^{2/3}}\tag{7.44}$$

where
$f_{ctк}$ is the characteristic tensile strength of concrete (5% fractile)
γ_c is the partial safety factor for concrete equal to 1.5
$f_{cк}$ is the characteristic compressive strength of concrete (5% fractile)

b. Eurocode EC2-1-1/2004 does not make any reference to smooth steel rebars, since this type of reinforcement is excluded from the design of R/C structures.

It should be remembered that the above value of f_{db} corresponds to a slip s relative to concrete equal to 0.1 mm, in contrast to $s_f = 0.6$ mm, which is considered the limit of s, for which τ_b max is developed (see Subsection 7.5.2) in an anchorage without confinement. Therefore, it may be concluded that Codes are very conservative with respect to bond since they are formulated to exclude bond failure at anchorage or splicing zones.

2. As far as the influence of confinement on f_{db} is concerned, an enhancement coefficient equal to the following is specified:

$$\boxed{1/(1 - 0.04p) \le 1.4}\tag{7.45}$$

or

$1/(1 - \kappa\lambda) \le 1.4$

where
p is the confinement due to external pressure along the anchorage length

$\lambda = (\Sigma A_{st} - \Sigma A_{st\ min})/A_s$

ΣA_{st} is the area of transverse reinforcement along the anchorage length
A_S is the area of the cross-section of the anchored rebar with the bigger diameter
ΣA_{stmin} is the area of the minimum transverse reinforcement (0.25 As for beams and zero for slabs)
κ is a coefficient ranging from 0 to 0.1 depending on the arrangement of the transverse reinforcement

3. The above values of f_{bd} refer to a 'good' position of rebars in concrete, for example:
   a. At the bottom of the beams
   b. At least 300 mm below the upper surface of the concrete
   c. At an angle greater than 45° in relation to the horizontal line.

In the case of 'poor' position, the above values of f_{bd} should be reduced to 0.70 of those for 'good' position.

4. As far as the basic anchorage or splicing length l_b, this is defined under the assumption that rebar yields before bond failure. Taking into account Equation 7.41 and introducing there, in place of σ_{so}, the design yield stress f_{yd} of steel, and in place of $\tau_{b\ mean}$ the value f_{bd} that results:

$$f_{yd} \le \frac{4}{d_s} f_{bd} l_b\tag{7.46}$$

or

$$l_b \geq \frac{f_{yd}}{f_{bd}} \frac{d_s}{4}$$ (7.47)

where:

f_{yd}, f_{bd} are design stresses for steel and bond, respectively
d_s is the rebar diameter
l_b is the basic anchorage or splicing length

The above basic length is modified in order to comply with special conditions, for example, the position of the anchorage zone, the existence or not of hooks and so on.

7.5.4.2 Seismic loading

Keeping in mind that the provisions for design anchorage and splice lengths for static loads are based on the assumption that rebar design yield precedes the design bond failure (bond slip, <0.1 mm), it can easily be concluded that these provisions also cover, in general, the requirements for seismic design of bonding, since the provisions for static load *are based on a capacity design concept for bonding.*

So, seismic codes for R/C structures include only some additional requirements, which are summarised below:

1. Only deformed rebars are accepted for main reinforcement due to their high bond strength.
2. Measurement of anchorage length should start some diameters inside the frame joints, so that even if a limited length of bond anchorage is degraded at the beginning of the joint because of load reversals, its influence would be of no significance for the overall behaviour of the anchorage. In fact, the rebar tensile stress diminishes rapidly at a distance of some diameters of the rebar inside the limit of the joint to the beam or the column and, therefore, bond degradation is limited only in this additional anchorage length, which is not taken into account. The above concept imposes special rules on the design of anchorages or splices of R/C members. These rules will be examined in detail in Chapters 8 and 9.
3. Determination of anchorage of splice length should take into account that rebars may be affected in tension or compression, and therefore the most unfavorable situation must be taken into account.
4. Special measures are foreseen is critical zones. There, due to concrete cracking by bending, bonding is vulnerable, and therefore special rules should be implemented in case of steel splicing.
5. All of the above, together with a series of special rules, will be presented in detail in subsequent chapters in the examination of the behaviour of seismic-resistant R/C members.

7.6 BASIC CONCLUSIONS FOR MATERIALS AND THEIR SYNERGY

From what has been presented in the previous subsections, the following conclusions may be drawn.

1. The basic material on which structural ductility is based is steel. In fact, steel has tremendous capacity for absorbing and dissipating seismic energy.

2. Concrete is a brittle material with very limited capacity for absorbing and dissipating seismic energy. However, thanks to its high compressive strength, it allows R/C members under bending to develop high curvature at failure stage, and therefore it allows the steel, which is embedded in the flexural zone, to develop high post-elastic tensile strains and consequently to absorb and dissipate a considerable amount of seismic energy.

3. The strength and ductility of concrete are substantially enhanced by a proper confinement by means of spirals, hoops or stirrups.

4. The bonding of steel and concrete is a crucial parameter for the seismic response of R/C structures. In the case that the slippage of a steel rebars exceeds the design limit (0.1 mm) due to reversal loading, a disintegration of the bond takes place and the hysteretic loops at the post-elastic stage of steel are replaced by the s-shaped loops of bond, which are unstable and 'thin'. In fact, in this case bond degradation takes place before steel yield, and therefore the bond loop prevails.

5. Consequently, R/C structures have the capacity for developing adequate plastic deformations and therefore of absorbing and dissipating seismic energy, under the assumption that they are properly reinforced and designed (capacity design). In the chapters that follow, the design of the main structural members of R/C buildings will be presented in detail.

6. It is important to note the paramount importance of the development of analytical models for monotonic or cyclic loading for the basic materials and their bonds. As we will see later, these models will prove very useful for the design of R/C members. At the same time, they constitute the basis for the formulation of constitutive laws for reversed cyclic loading of R/C members, which are one of the necessary inputs for the nonlinear analysis of R/C structures (see Subsections 2.5.2 and 5.7.2).

7. Last but not least, it should be noted that both materials, concrete and steel, display a stress–strain diagram under monotonic loading, which is with a very good approximation the envelope of cyclic loading for both materials.

The above fact allows the reasonable consideration that in cross-sections of R/C members where axial stresses prevail (bending with axial force), $M–\varphi$ diagrams defined for monotonic loading are also the envelopes for cyclic loading caused by seismic action. In this respect, this curve may be used either in elastic or inelastic dynamic or static analysis for the control of demands in relation to the capacities. Extensive testing of R/C members under prevailing bending has confirmed the above consideration, as we will see in the next chapter.

Chapter 8

Seismic-resistant R/C frames

8.1 GENERAL

It has already been noted in Chapter 4 that seismic-resistant R/C *frames* together with R/C *walls* and *dual systems* constitute the three basic seismic-resistant systems in use for earthquake-resistant buildings. Frame systems are usually 3-D structures consisting of plane frames arranged in two orthogonal directions, usually in the form of pseudo 3-D structure. It is obvious that each of these frames is affected biaxially, at least at its columns, due to the simultaneous seismic actions in both main directions. However, for a better understanding, the plane frame will be examined first and then reference will be made to biaxial loading.

It should be noted from the beginning that the elements of a frame are beams, columns and joints. These elements will be examined in detail in the following sections.

It has been noted already that seismic design is carried out for seismic actions in combination with the gravity loads for which masses have been taken into account for the determination of the inertial seismic forces, no matter if the analysis has been carried out using a linear static or linear dynamic method.

The form of moment diagrams M_{wd} of gravity loads W_{dE}, which participate in seismic load combinations, is given in Figure 8.1. It should be remembered that these diagrams correspond to the combination:

$$\boxed{W_{dE} \; = \; \sum G_{kj} \text{'} + \text{'} \sum \varphi \psi_{2i} Q_i} \tag{8.1}$$

(see Subsection 3.4.5). On the other hand, the relevant forms of moment diagrams of seismic action effects (32 combination cases) E_d are given in Figure 8.2.

It is obvious that in Figure 8.2, for simplicity, only one of the 32 combinations is depicted. It should also be noted that for a reversed seismic action these diagrams change sign.

The combinations of gravity and seismic action effects for beams are given in Figure 8.3, while the relevant diagrams for columns are given in Figures 8.4 and 8.5. The main remarks for the above diagrams are the following:

1. Beams are affected mainly in bending and shear.
2. Columns are affected by normal forces, moments and shear.
3. Action effects in beams and columns increase from the upper to the lower storeys.
4. Axial forces of the external columns *are strongly affected* by the seismic action to such a degree that in the case that the aspect ratio *H/L* of the frame is high they may change sign (Figure 8.6).
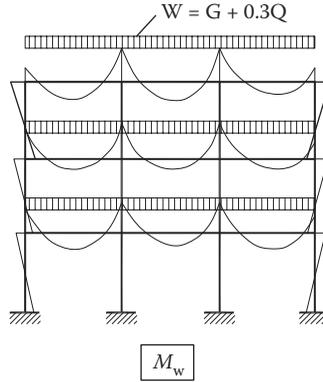
Figure 8.1 Bending moment diagram for gravity loads.

5. The moments of the beams due to seismic action adjacent to a joint have the opposite sign and are counterbalanced by the relevant moments of the adjacent columns framing to the same joint. This means that in the core of the joint very strong changes of moments and shears take place both in the beam as well as in the column direction. As a result, very strong shear and bond stresses develop in the limited area of the joint core. For this reason, as we will see later, *these areas are very vulnerable* to seismic action and need special concern (Figure 8.7).

8.2 DESIGN OF BEAMS

8.2.1 General

For a thorough examination of the action effects of a beam as a component of a ductile frame, the following diagrams of a typical internal beam are depicted in detail.

- In Figures 8.3a and b, typical M_d, V_d diagrams are given for the seismic combination W_{dE} '+' E_d.
- In Figure 8.3c, typical M_d, V_d diagrams are given for the 'basic' combination (i.e. $1.35G$ '+' $1.50Q$).
- In Figure 8.3d, an envelope for the above two cases has been elaborated.
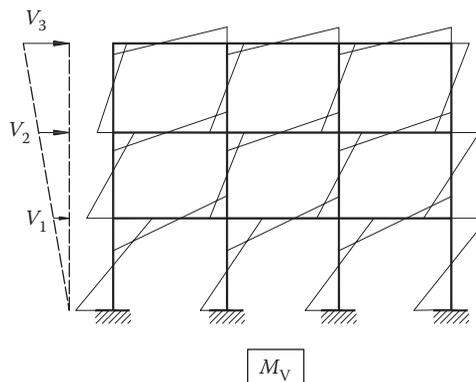
Figure 8.2 Bending moment diagram for horizontal seismic actions.
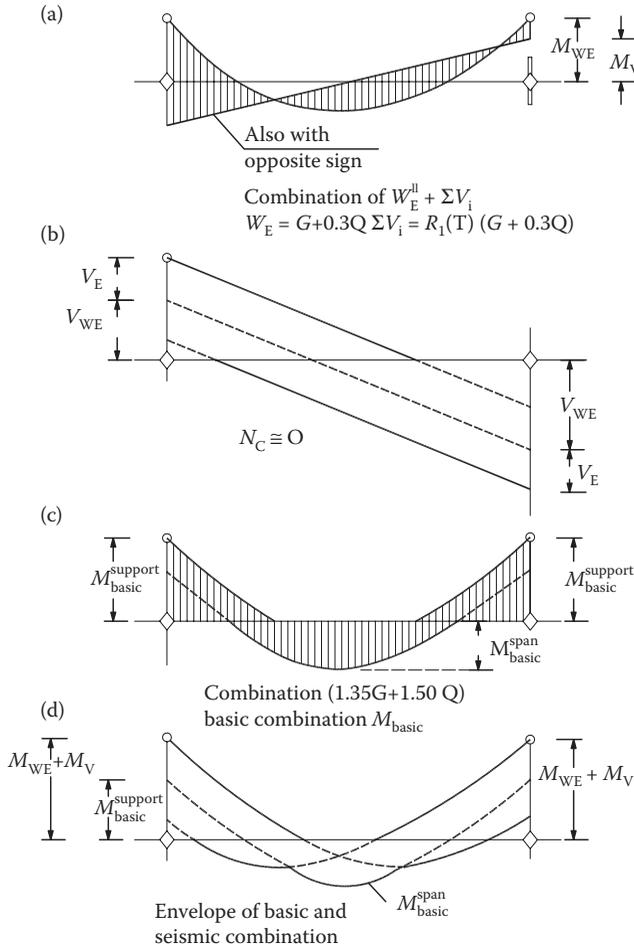
Figure 8.3 Moment diagram of frame beams for various load cases: (a) seismic combination with the corresponding gravity loads; (b) shear diagrams corresponding to load case combination (a); (c) basic load combination (1.35G+1.50Q); (d) Bending moment envelope of basic load combination (c) with seismic load combination (a).
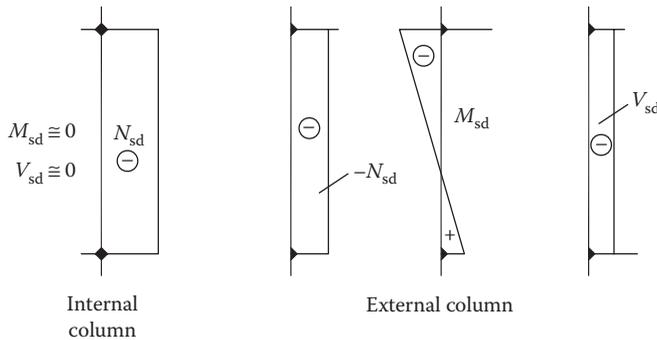
Figure 8.4 M, N, V column diagrams under gravity loads.
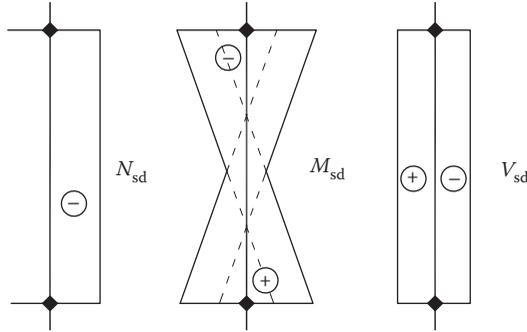
Figure 8.5 M, N, V column diagrams under horizontal seismic and corresponding gravity loads.

$$E = R_d(T)\,[G+03\,Q]$$

$$N_C = N_A \cong \pm \frac{E\,(2/3\,H - h/2)}{L}$$
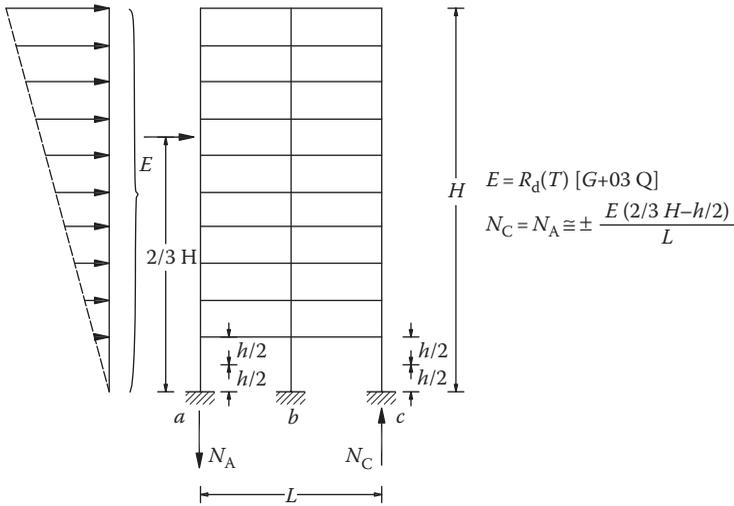
Figure 8.6 Axial reactions at the base of the external columns of a frame due to horizontal seismic action.
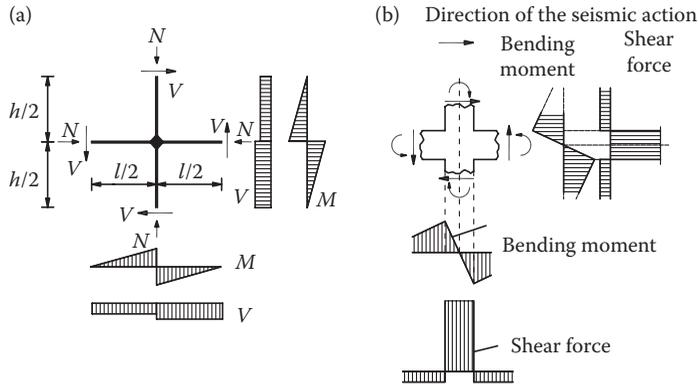
Figure 8.7 (a) M–V diagrams of a frame sub-assemblage due to seismic action (sway); (b) magnification of M–V diagrams in the region of the joint.
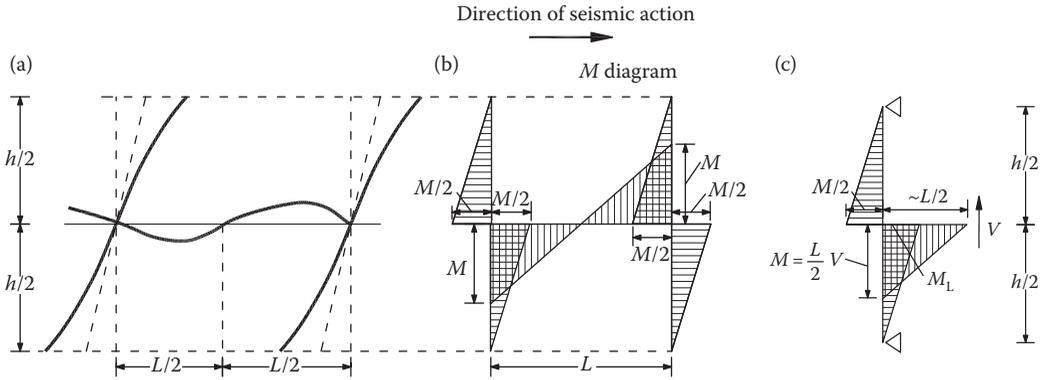
Figure 8.8 Flexural behaviour of a frame sub-assemblage: (a) deformations; (b) moment diagrams; (c) substitute sub-assemblage.

From the examination of the above diagrams the following remarks should be noted:

- Bending and shear prevail while axial forces are of secondary importance for beams.
- The influence of seismic actions increases from the top storeys to the base so that the combination of moment diagrams of seismic action and corresponding gravity loads present reversed sign at the critical zones near joints of lower storeys.
- The same also holds for shear diagrams. However, it should be remembered that design shear forces are determined on the basis of the capacity design procedure developed in Section 6.1.
- Moment diagrams of seismic actions induce contra-flexural deformation of beams (Figure 8.8). In this context each beam behaves like two cantilevers, each with a span equal to about the half of the length of the beam under a reversed loading V_{Ed} at their free end. This behaviour explains why in almost all laboratory tests for beams under seismic cyclic excitation, the model in use is a cantilever imposed on a cyclic loading at its free end.
- The envelope of moment diagrams for 'the basic combination' (gravity design loads) and for the seismic combinations (Figure 8.3d) shows that a beam may be found under tension in almost its entire length at both its flanges (top and bottom) during load reversals, depending on the direction of seismic action and the level of the storey where the beam is located. This is taken into account very seriously by Codes in beam detailing, as it will be presented later.

8.2.2 Beams under bending

8.2.2.1 Main assumptions

The assumptions made for the design of R/C beam sections under bending and for the elaboration of M–φ diagrams are the same as those in use for R/C members under static loading.

These assumptions are the following:

1. Equilibrium conditions are considered for a structure without taking into account its deformations (first-order theory).
2. Concrete cannot carry tensile stresses (stage II).

A	Ultimate strain of steel
B	Ultimate strain of concrete
C	Ultimate strain of concrete under plain compression
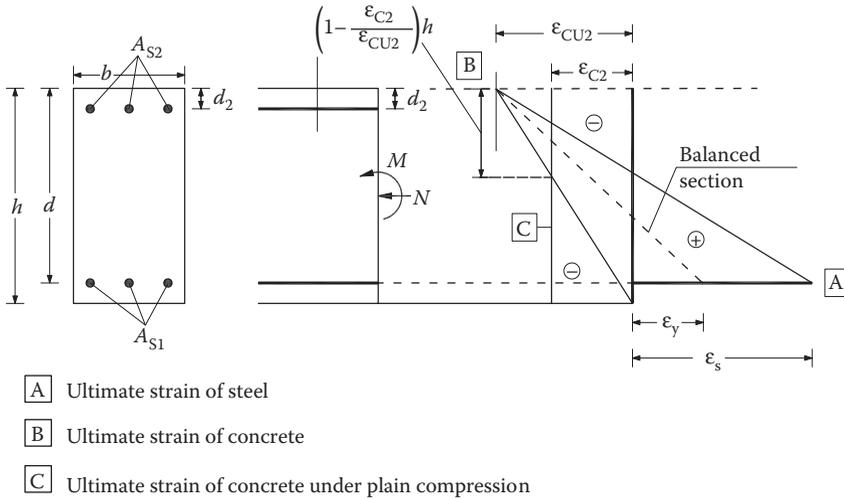
Figure 8.9 Failure criteria in bending with axial force.

3. Plane cross sections vertical to the axis of a beam under bending continue to be plane and vertical to the deformed axis up to failure (Bernoulli concept). In this respect, strain distribution over a cross section continues to be linear up to failure.
4. Stress–strain diagrams of steel and concrete are those given by the Code for stress analysis (see Subsections 7.2.4 and 7.3.5).
5. There is perfect bonding between steel rebars and concrete, that is, strains of concrete and steel at any point of a cross section are identical, that is,

$$\varepsilon_{si} \equiv \varepsilon_{ci} \tag{8.2}$$

In this context for low strains where σ_c may be considered as a linear function of the relevant strain, that is, for $\sigma_c < 0.7\, f_c$, the following expressions are in effect:

$$\varepsilon_{si} = \frac{\sigma_{si}}{E_s}, \quad \varepsilon_{ci} = \frac{\sigma_{ci}}{E_c}$$

and therefore,

$$\sigma_{si} = \sigma_{ci} \frac{E_s}{E_c} = n\sigma_{ci} \tag{8.3}$$

where
  E_s is the modulus of elasticity of steel
  E_c is the modulus of elasticity of concrete
  n is the ratio (E_s/E_c)

6. Failure criterion for bending is the ultimate strain of concrete (Figure 8.9).

8.2.2.2 Characteristic levels of loading to failure (limit states)

Consider the cantilever beam of Figure 8.10, which is loaded by a force V vertically to its axis at its free end. By increasing V from zero to a limit value V_{crack}, tensile and compressive

stresses develop at a cross section near the fixed end, wherein extreme values are given by the expression (Figure 8.10a):

$$\left.\begin{array}{c} \sigma_o \\ \sigma_u \end{array}\right\} \cong \pm \frac{M_A}{bh^2/6} = \pm \frac{lV}{bh^2/6} \le f_{ctm,fl} \tag{8.4}$$

where

$f_{ctm,fl}$ is the mean tensile strength of concrete to flexure; all other symbols may be found in Figure 8.10.

Up to this level an R/C cross section does not display any cracks, and therefore the whole concrete section participates in carrying axial stresses, compressive and tensile. In this context, the curvature of the cross section is given by the well-known expression:

$$\varphi = \frac{M_A}{E_c J} = \frac{lV}{E_c bh^3/12} \tag{8.5}$$
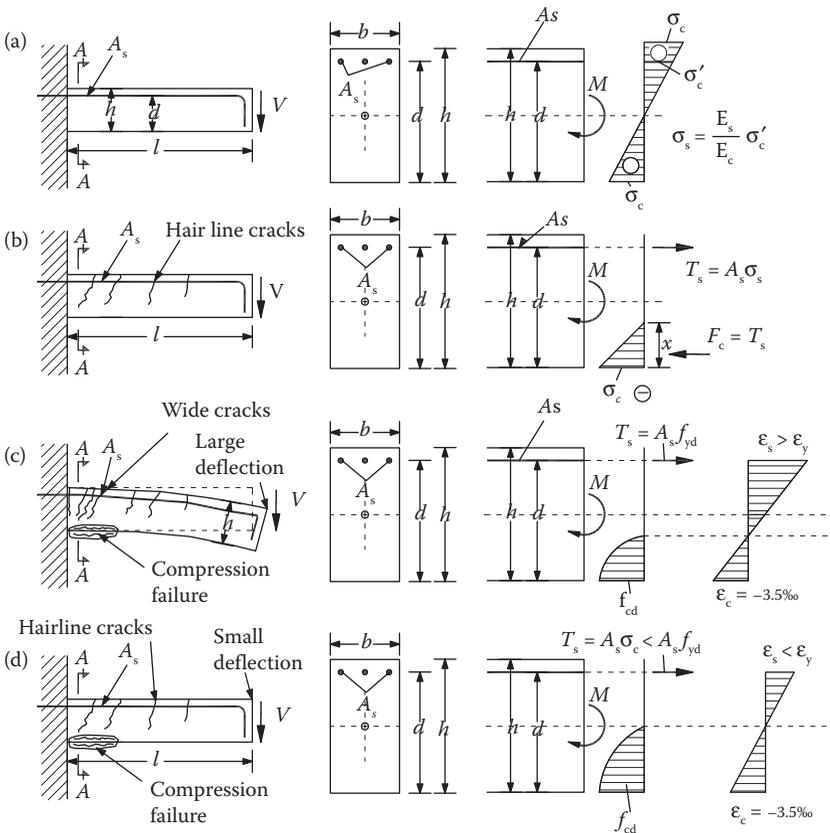
Figure 8.10 Successive steps of loading to failure of a beam under flexure: (a) stage I (uncracked); (b) stage II (cracked tensile zone); (c) failure due to steel yield (normally reinforced beam); (d) failure due to compression failure of concrete before steel yield (over-reinforced beam).

where

E_c is the modulus of elasticity of concrete.

As V gradually increases, tensile stresses σ_o approach $f_{ctm,fl}$; at this stage, when:

$$\sigma_o = f_{ctm,fl} \tag{8.6}$$

concrete in the tension zone cracks. Therefore for

$$M_{cr} = V_{cr} \cdot l = f_{ctm,fl} \frac{bh^2}{6} \tag{8.7}$$

cracks display at the base of the beam vertically to its axis. At this stage the existing reinforcement in the tensile zone must be in position to substitute the tensile forces of concrete that has cracked, otherwise *a brittle collapse will take place* (Figure 8.10b).

Therefore,

$$A_{smin} f_{yk} z \geq M_{cr} = f_{ctm,fl} bh^2/6 \tag{8.8}$$

Taking into account that:

$$z \cong 0.87d = 0.87 \cdot 0.93\,h = 0.81\,h$$

Equation 8.8 takes the form:

$$\boxed{\rho_{min} = \frac{A_{smin}}{bh} = 0.205 \frac{f_{ctm,fl}}{f_{yk}}} \tag{8.9a}$$

At the same time the relation between $f_{ctm,fl}$ and f_{ctm} according to EC2-1-1/2004 is given by the expression:

$$f_{ctm,fl} = \max\{(1.6 - h/1000)f_{ctm}; f_{ctm}\}$$

where

h is the total member depth in mm
f_{ctm} is the mean axial tensile strength of concrete

For a depth of 350–450 mm, the above relation results in

$$f_{ctm,fl} = (1.25 \div 1.15)f_{ctm}$$

Introducing this value in Equation 8.9a we obtain:

$$\boxed{\rho_{min} \cong (0.26 \div 0.24) \frac{f_{ctm}}{f_{yк}}} \tag{8.9b}$$

It should be noted that the recommended value of EC2-1-1/2004 for ρ_{min} is the same as the above, with a coefficient equal to 0.26.

Thereafter, as V continues to increase above V_{cr}, cracks slowly extend deeper, exhibiting a stable situation. Of course, the slope of the moment–curvature diagram becomes smoother (Figure 8.12) due to the fact that the tensile zone of concrete has cracked, and therefore the stiffness of the beam gradually diminishes. This procedure continues until one of the two materials, that is, steel or concrete, fails.

- In the case that the beam is *normally reinforced,* steel yields first, before concrete failure at the compressive zone occurs (Figure 8.10c). As a consequence, for a small additional load, cracks open, the height of the compression zone decreases, due to the deepening of the cracks, and, finally, the compression zone fails due to crushing. At this stage the *beam collapses.* However, between steel yielding and concrete crushing in the compression zone large plastic deformations take place, accompanied by a low-strain 'hardening' of the relevant branch of the moment–curvature diagram (Figure 8.12). Therefore, the available ductility of the beam in terms of moment–curvature diagrams is significant.
- In the case that the beam is over-reinforced before steel yielding (Figure 8.9d), concrete at the compression zone fails due to crushing before the appearance of wide and deep cracks at the tension zone. In fact, since steel has not yielded yet, the width of cracks at the tension zone continues to be small, while the compression zone, if it is not con-fined, fails in *a brittle mode* without any warning. It is obvious that in this case there are not any plastic deformations in terms of curvature (Chapter 2, Figure 2.29).
- The critical point between these two types of failure is the *balanced failure*. In this case, both materials, steel and concrete, fail simultaneously. This means that at this stage steel yields while concrete exceeds its extreme deformation $\varepsilon_c = \varepsilon_{cu2}$ (Figure 8.11). For example, in the case of unconfined concrete of class $\leq C50/60$ and steel of class B500c, a cross section under balanced failure displays the deformation pattern of Figure 8.11, that is,

$$x \cong 0.58d \tag{8.10a}$$

In this context, for an orthogonal cross section, which is simply reinforced, the reinforcement percentage ρ_b at balanced failure is equal to

$$\boxed{\rho_b \cong 0.47 \frac{f_{ck}}{f_{y\kappa}}} \tag{8.10b}$$
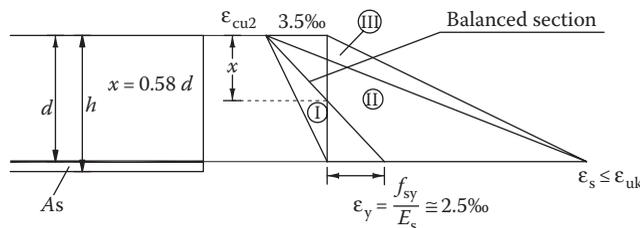
Figure 8.11 Deformation pattern of cross section Region I: brittle failure mode due to over-reinforcement of the section; Region II: ductile failure mode of normally reinforced sections; Region III: brittle failure mode due to under-reinforcement of the section.

or in case of a cross section reinforced also with reinforcement $\rho_2 = A_{s2}/bd$ in its compression zone, ρ_{max}, in the tension zone takes the form:

$$\rho_{max} - \rho_2 = 0.47 \frac{f_{c\kappa}}{f_{y\kappa}} \tag{8.10c}$$

For a ductile type of failure ρ must be less than ρ_b. *In this case, the deformation pattern* of the cross section is located in region II of Figure 8.11. For ρ greater than ρ_b, a compression brittle failure prevails. In this case the deformation pattern of the cross section is located in region I of Figure 8.11. Finally, it should be noted that region III of Figure 8.11 corresponds to $\rho < \rho_{min}$, that is, to tension brittle failure due to inefficient steel reinforcement capable of substituting tensile stresses at the cracking stage.

8.2.2.3 Determination of the characteristic points of M−φ diagram and ductility in terms of curvature for orthogonal cross section

From the presentation so far, three characteristic points have been defined (Figure 8.12):

- Point A: corresponding to cracking stage ($M_{cr} - \varphi_{cr}$)
- Point B: corresponding to steel yield stage ($M_y - \varphi_y$)
- Point C: corresponding to failure stage ($M_u - \varphi_u$)

The cross-section deformation patterns for these three points are given in Figure 8.13.

In the following paragraph, closed expressions will be derived for orthogonal cross sections using some approximations that simplify the procedure. For cross sections of a complex form (e.g. T, U, Z, Γ, etc.), computer platforms have been developed to allow the determination of points A, B and C (e.g. NOUS (2005), RCCOLA-90, etc.).

1. *Point A: $M_{cr} - \varphi_{cr}$*
   From Equations 8.4 and 8.5 it follows that:

$$\boxed{M_{cr} = f_{ctm,fl} b^2 / 6} \tag{8.11a}$$
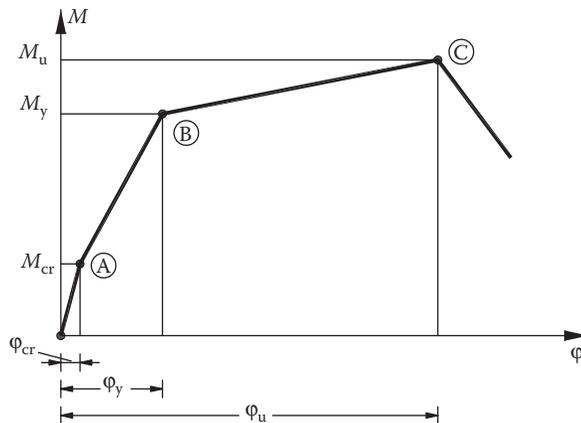
Figure 8.12 M−φ diagram for normally reinforced cross section.
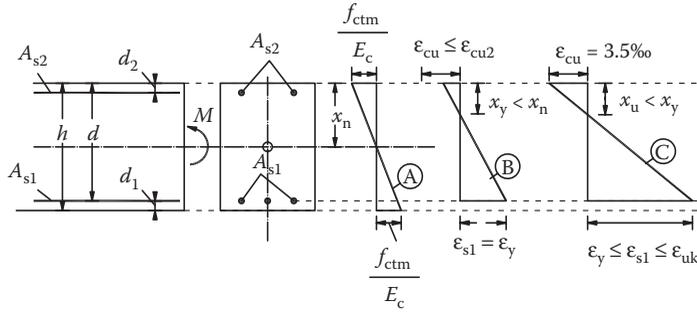
Figure 8.13 Deformation pattern of a cross section: (A) cracking; (B) yield; (C) failure.

$$\varphi_{cr} = \frac{M_{cr}}{E_c bh^3/12}$$

(8.11b)

2. *Point B:* $M_y - \varphi_y$ (Figure 8.14)

Taking into account that the deformation pattern of the cross section for this point of the diagram is depicted in Figure 8.14, it may be concluded that

$$\varphi_y = \frac{\varepsilon_c}{x} = \frac{\varepsilon_{s1y}}{d-x} = \frac{\varepsilon_c + \varepsilon_{s1y}}{d} = \frac{\varepsilon_{s2}}{x - d_2}$$

(8.12a)

or

$$\varphi_y = \frac{\varepsilon_c}{\xi d} = \frac{\varepsilon_{s1}}{d - \xi d} = \frac{\varepsilon_{s2}}{\xi d - d_2} = \frac{\varepsilon_c + \varepsilon_{s1}}{d}$$

(8.12b)

where

$$\xi = \frac{x}{d}$$
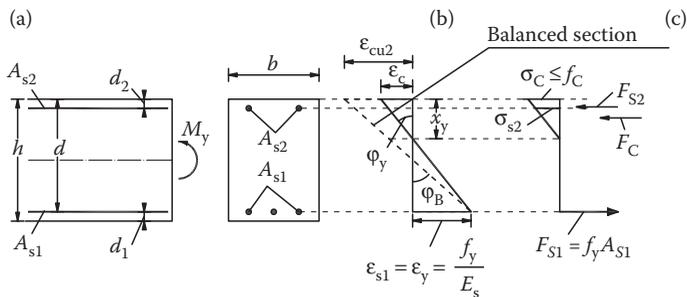
Figure 8.14 Cross section at yield: (a) geometry; (b) deformation pattern; (c) internal forces.

Assuming that the stress distribution in the compression concrete zone is linear, since at this stage usually $\sigma_c < 0.7 f_c$ (Subsection 7.3.2), it can be seen that

$$\varepsilon_c = \frac{\sigma_c}{E_c}, \quad \varepsilon_{s1} = \frac{\sigma_{s1}}{E_s}, \quad \varepsilon_{s2} = \frac{\sigma_{s2}}{E_s} \tag{8.13}$$

Substituting the above expressions in Equation 8.12b, the following values of σ_{s1} and σ_{s2} are determined:

$$\sigma_{s1} = \frac{1 - \xi}{\xi} n\sigma_c \tag{8.14a}$$

$$\sigma_{s2} = \frac{\xi d - d_2}{\xi d} n\sigma_c \tag{8.14b}$$

The equilibrium condition of internal forces of cross section (*Fc*, *Fs*1 and *Fs*2) gives

$$\boxed{F_c + F_{s2} - F_{s1} = 0} \tag{8.15}$$

Substituting into Equation 8.15 the values of σ_{s1} and σ_{s2} of Equation 8.14, and taking into account that the distribution of the compressive stresses of concrete has been assumed to be linear, Equation 8.15 takes the following form:

$$\frac{1}{2} b \xi d \sigma_c + \sigma_{s2} A_{s2} - \sigma_{s1} A_{s1} = 0 \tag{8.16a}$$

$$\frac{1}{2} b \xi d \sigma_c + \frac{\xi d - d_2}{\xi d} n A_{s2} \sigma_c - \frac{1 - \xi}{\xi} n A_{s1} \sigma_c = 0 \tag{8.16b}$$

or

$$\xi^2 + 2n(\rho_1 + \rho_2)\xi - 2n\left(\rho_1 + \frac{d_2}{d}\rho_2\right) = 0 \tag{8.16c}$$

where

$$n = \frac{E_s}{E_c}, \quad \rho_1 = \frac{A_{s1}}{bd}, \quad \rho_2 = \frac{A_{s2}}{bd} \tag{8.17}$$

The solution of Equation 8.16c gives the following results:

$$\boxed{\xi_y = \sqrt{n^2(\rho_1 + \rho_2)^2 + 2n\left(\rho_1 + \frac{d_2}{d}\rho_2\right)} - n(\rho_1 + \rho_2)} \tag{8.18}$$

If $\xi_y = (x/d) \geq 0.58$ (for steel class B500c), brittle collapse prevails due to concrete failure under compression (see par. 8.2.2.2) and the procedure ends, otherwise the procedure continues as follows:

If ξ is introduced from Equation 8.18, in Equation 8.12b the following equation is obtained:

$$\varphi_y = \frac{\varepsilon_{s1}}{d(1 - \xi_y)} = \frac{f_y/E_s}{d(1 - \xi_y)} \tag{8.19}$$

The corresponding value of M_y is equal to the moments of internal forces F_{s2} and F_{s1} about the centroid of the triangle of compression stresses of concrete, that is:

$$M_y = A_{s1}f_y d\left(1 - \frac{\xi}{3}\right) + A_{s2}\sigma_{s2}d\left(\frac{\xi}{3} - \frac{d_2}{d}\right) \tag{8.20}$$

Introducing in Equation 8.14a the value of f_y in place of σ_{s1} and substituting $n\sigma_c$ into Equation 8.14b from Equation 8.14a, we get the following expression for σ_{s2}:

$$\sigma_{s2} = \frac{\left(\xi_y - d_2/d\right)}{\left(1 - \xi_y\right)}f_y \tag{8.21}$$

Introducing now Equation 8.21 into Equation 8.20 we finally get

$$M_y = f_y d\left[A_{s1}\left(1 - \frac{\xi_y}{3}\right) + A_{s2}\frac{\left(\xi_y - d_2/d\right)}{\left(1 - \xi_y\right)}\left(\frac{\xi_y}{3} - \frac{d_2}{d}\right)\right] \tag{8.22}$$

where ξ_y is taken from Equation 8.18. So, Equations 8.18, 8.19 and 8.22 allow the determination of ξ_y, M_y and φ_y.

3. *Point C: $M_u - \varphi_u$ (Figure 8.15)*
   Taking into account that the strain pattern of the cross section at this point of the diagram $M-\varphi$ is depicted in Figure 8.15, it may be concluded that

$$\varphi_u = \frac{\varepsilon_{cu2}}{x} = \frac{\varepsilon_{s1u}}{d - x} = \frac{\varepsilon_{cu2} + \varepsilon_{s1u}}{d} = \frac{\varepsilon_{s2}}{x_u - d_2} \tag{8.23a}$$

or

$$\varphi_u = \frac{\varepsilon_{cu2}}{\xi_u d} = \frac{\varepsilon_{s1u}}{d - \xi_u d} = \frac{\varepsilon_{s2}}{\xi_u d - d_2} = \frac{\varepsilon_{cu2} + \varepsilon_{s1u}}{d} \tag{8.23b}$$
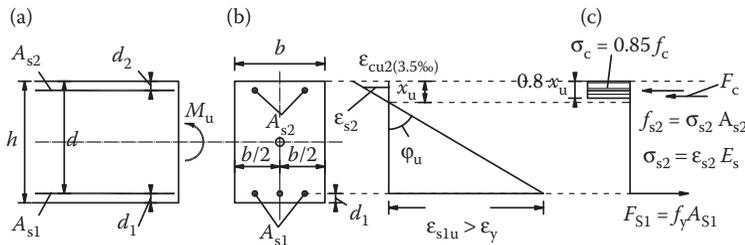
Figure 8.15 Cross section at failure: (a) geometry; (b) deformation pattern; (c) internal forces.

where

$$\xi_u = \frac{x_u}{d}$$

In this case (Figure 8.15), the equilibrium condition (Equation 8.15) may be written as follows:

$$0.8x_u \, bf_c + A_{s2} \, f_y - A_{s1} \, f_y = 0 \tag{8.24}$$

Therefore,

$$x_u = \frac{(A_{s1} - A_{s2})f_y}{0.8f_c b} \tag{8.25}$$

$$\boxed{\xi_u = \frac{x_u}{d} = \frac{(\rho_1 - \rho_2)}{0.8} \cdot \frac{f_y}{f_c}} \tag{8.26}$$

In Equations 8.24 through 8.26 it has been assumed that σ_{s2} is equal to yield stress, and consequently that

$$\varepsilon_{s2} \geq \frac{\sigma_{s2}}{E_s} = \frac{f_y}{E_s} \tag{8.27}$$

According to Figure 8.16 this assumption is fulfilled if

$$\varepsilon_{s2} = \varepsilon_{cu2} \frac{x_u - d_2}{x_u} \geq \frac{f_y}{E_s} \tag{8.28}$$

or

$$\boxed{\bar{\xi}_u \geq \frac{\varepsilon_{cu2} \, d_2/d}{\varepsilon_{cu2} - f_y/E_s}} \tag{8.29}$$

Introducing the value of $\bar{\xi}_u$ from Equation 8.29 into Equation 8.26, we find

$$\boxed{\rho_1 - \rho_2 \geq 0.8\bar{\xi}_u \frac{f_c}{f_y}} \tag{8.30}$$
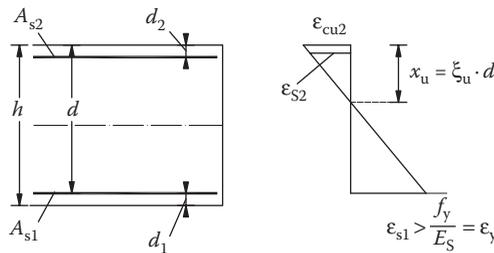
Figure 8.16 Strain pattern for $\varepsilon_{s2} \geq (f_y/E_s) = \varepsilon_y$.

EXAMPLE

For concrete class C20, steel class B500c and $d_2/d = 0.07$ (cross sections with moderate height), according to EC2-1-1/2004 we have

$$\varepsilon_{cu2} = 3.5\text{‰}, \quad f_c = 20 \text{ MP}\alpha, \quad f_y = 500 \text{ MP}\alpha, \quad E_s = 200 \text{ GR}\alpha, \quad \frac{f_y}{E_s} = 2.5\text{‰}$$

Therefore,

$$\bar{\xi}_u = \frac{3.5 \cdot 0.07}{3.5 - 2.5} = 0.245$$

$$\rho_1 - \rho_2 \geq 0.8\,\bar{\xi}_u\,\frac{f_c}{f_y} = 0.8 \cdot 0.245 \cdot \frac{20}{500} = 0.008$$

which means that if ρ_1 and ρ_2 differ by less than 8‰, Equation 8.30 gives erroneous results.

In this context, if ξ_u is introduced from Equation 8.26, φ_u results from Equation 8.23b:

$$\boxed{\varphi_u = \frac{\varepsilon_{cu2}}{\xi_u d}} \tag{8.31}$$

The corresponding value of M_u is equal to the moments of internal forces F_{s2} and F_{s1} about the centroid of the orthogonal of compression stresses of concrete, that is:

$$M_u = A_{s1}f_{y1}(d - 0.4x_u) + A_{s2}f_{y2}(0.4x_u - d_2) \tag{8.32}$$

Introducing Equation 8.26 into 8.32 we get

$$M_u = A_{s1}f_y d\left(1 - \frac{0.4}{0.8}(\rho_1 - \rho_2)\frac{f_y}{f_c}\right) + A_{s2}f_y d\left(\frac{0.4}{0.8}(\rho_1 - \rho_2)\frac{f_y}{f_c} - \frac{d_2}{d}\right) \tag{8.33a}$$

$$M_u = A_{s1}f_y d\left(1 - \frac{(\rho_1 - \rho_2)}{2}\frac{f_y}{f_c}\right) + A_{s2}f_y d\left(\frac{(\rho_1 - \rho_2)}{2}\frac{f_y}{f_c} - \frac{d_2}{d}\right) \tag{8.33b}$$

The above equations are valid under the following assumptions:
- $\sigma-\varepsilon$ diagram of steel is elastoplastic without strain hardening
- A_{s2} has yielded
- A_{s2} has not buckled

4. *Ductility μ_φ in terms of curvature*

Ductility μ_φ in terms of curvature is determined by the following expression:

$$\boxed{\mu_\varphi = \frac{\varphi_u}{\varphi_y}} \tag{8.34a}$$

Introducing φ_n and φ_y in the above expression from Equations 8.19 and 8.31 we get

$$\boxed{\mu_\varphi = \frac{0.80\varepsilon_{cu2} \cdot f_{ck} \cdot E_s}{(\rho_1 - \rho_2)f_{yk}^2}(1 - \xi_y)} \tag{8.34b}$$

It must be noted again that the above expression is in effect in the case that steel under compression yields.

From the above expression the following conclusions may be drawn:

- High concrete strength f_c increases μ_φ since it is included in the numerator of Equation 8.34b.
- Confinement also increases μ_φ since in case of confinement ε_{cu2} is enhanced.
- High-yield strength f_y of steel decreases μ_φ since its square is included in the denominator of Equation 8.34b.
- A high percentage ρ_1 of steel in the tensile zone decreases μ_φ since ρ_1 is included in the denominator. In parallel, ρ_1 contributes to the enhancement of ξ_y (Equation 8.18) and therefore to a decrease of μ_φ.
- Steel in the compressive zone increases μ_φ since its value is subtracted from ρ_1 in the denominator of expression (8.34b).

In the case that $\varepsilon_{s2} < \varepsilon_y = (f_y/E_s)$, μ_φ may be determined from the following expressions (Park and Paulay, 1975):

$$\mu_\varphi = 0.8 E_s \varepsilon_{cu2} (1 - \xi_y) \left(f_y \left\{ \left[\left(\frac{\rho_2 \varepsilon_{cu2} E_s - \rho_1 f_y}{1.7 f_c} \right)^2 + \frac{d_2}{d} \cdot \frac{\rho_2 \varepsilon_{cu2} E_s}{1.25 f_c} \right]^{1/2} - \left(\frac{\rho_2 \varepsilon_{cu2} E_s - \rho_1 f_y}{1.7 f_c} \right) \right\} \right)^{-1} \quad (8.35)$$

The ratio M_u/M_y for simply reinforced cross sections averages around 1.05 while for double reinforced ones this ratio averages a little bit higher (1.07–1.10).

8.2.2.4 Determination of the characteristic points of M–φ diagram and ductility in terms of curvature for a generalised cross section

As was mentioned before, points A, B and C of M–φ diagrams of Figure 5.12 may be determined for any form of the cross section using proper computer codes. In the following paragraphs the method that is in the core of the computer program NOUS will be outlined in brief (Penelis, 1969; EC Tools, 2012). It should be noted that although in the following paragraphs the method is presented for a symmetric cross section, the program can also be used for non-symmetric cross sections either for the design or for the determination of M–φ diagrams (see Paragraph 9.2.2.3).

1. *Point A: $M_{cr} - \varphi_{cr}$*
   Consider the cross section of Figure 8.17 symmetric to the z–z axis. For the determination of M_{cr} and φ_{cr}, the corresponding deformation pattern is defined by two points, the extreme concrete point at tension on the z–z axis, where the strain is

$$\varepsilon_{ctm} = \frac{f_{ctm}}{E_c} \quad (8.36)$$

and the centroid of the composite cross section $\left(A_c + n \sum A_{si} \text{ where } n = E_s/E_c \right)$ where the strain is zero. In fact, since

$$\sigma_{ct} \leq f_{ctm} \quad (8.37)$$
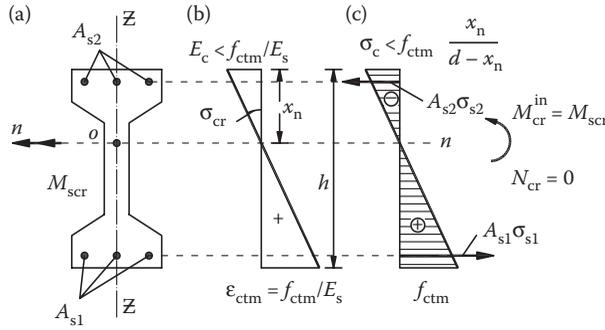
Figure 8.17 Cross section at crack stage: (a) cross section; (b) deformation position at crack stage; (c) corresponding stresses and internal forces.

where

σ_{ct} is the extreme tension stresses of concrete

f_{ctm} is the mean tension strength of concrete at flexure

the cross section is not yet cracked, for this deformation pattern.

In this context φ_{cr} is equal to

$$\varphi_{cr} = \frac{\varepsilon_{ctm}}{h - x_n} = \frac{f_{ctm}}{(h - x_n)E_c} \qquad (8.38)$$

where

x_n is the distance of neutral axis n–n from the external point of concrete in compression on the z–z axis.

At the same time, the moment of all internal forces for this deformation pattern about the centroid of the extreme rebar in tension has the moment M_{cr} as an output at the crack.

2. *Point C: $M_u - \varphi_u$*

Consider the cross section of Figure 8.18 symmetric to the z–z axis. For the determination of M_u and φ_u, the deformation pattern of the cross section must be defined.
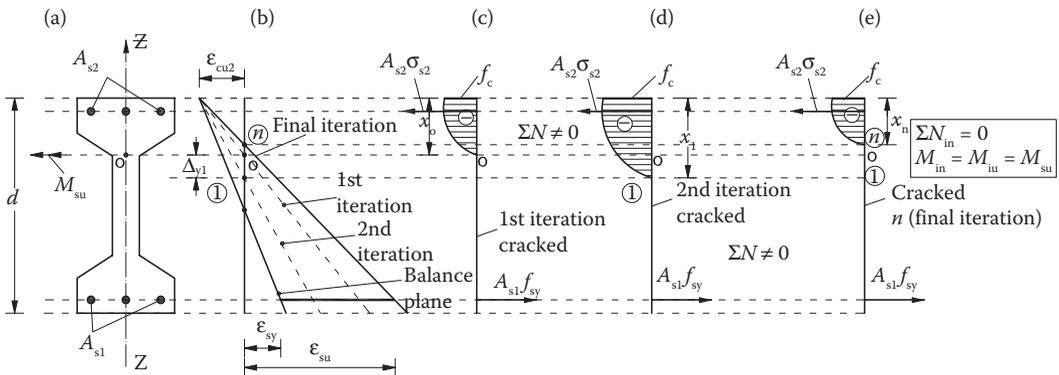
Figure 8.18 Cross section at concrete failure under compression: (a) cross section; (b) deformation pattern at successive iteration cycles 0.1, n; (c) internal forces of iteration (I); (d) internal forces of iteration (2); (e) internal forces of final iteration (n).

This pattern must have an ordinate at the extreme point of concrete under compression equal to ε_{cu2} (Figure 8.18b). Therefore, one point of this straight line is explicitly defined. If this line now intersects the z–z axis at a distance x_n from the extreme point of concrete under compression, then φ_u is determined by the relation:

$$\varphi_u = \frac{\varepsilon_{cu2}}{x_n} \tag{8.39}$$

and M_u results from the sum of the moments of all internal forces corresponding to this deformation pattern about the centroid of the extreme steel bars under tension.

Therefore, the crucial point of the whole procedure is the determination of the position of the neutral axis, that is, the value x_n.

The determination of x_n is based on the condition that the sum of the internal forces corresponding to this deformation pattern is equal to zero ($\Sigma N_{in} = 0$), since the cross section is under plain bending.

It should be noted that the extreme steel strain equal to

$$\varepsilon_{se} = \frac{\varepsilon_{cu2}}{x_n}(d - x_n) \tag{8.40a}$$

must be greater than ε_y, in order for a plastic deformation to exist, that is,

$$\varepsilon_{se} = \frac{\varepsilon_{cu2}}{x_n}(d - x_n) > \varepsilon_{sy} = \frac{f_y}{E_s} \tag{8.40b}$$

Otherwise, the bending member displays a brittle failure before the yielding of steel. In this case the procedure for determining M_y and φ_y has no meaning.

In any case, for the determination of x_n the following procedure is followed:

Step 1: For the determination of a second point of the deformation pattern we suppose that at first position of deformation plane intersects the z–z axis at the centroid 0 of the composite uncracked cross section ($A_c + n\Sigma A_{si}$). This is an arbitrary position, which is considered to be the first iteration.

Step 2: For this position ΣN_{io} is determined as the sum of all internal forces corresponding to the assumed deformation pattern. Obviously this sum is not zero since x_o has been selected arbitrarily.

Step 3: For a small displacement Δy_1 of the neutral axis parallel to its initial position, ΣN_{io} becomes equal to

$$\sum N_{io} + \Delta N_{io} \tag{8.41a}$$

If this displacement is the proper one, the above relation must be equal to zero, that is,

$$\sum N_{io} + \Delta N_{io} = 0 \tag{8.42a}$$

The value of ΔN_{io} is approximately a linear relation of Δy_1, that is, equal to

$$\Delta N_{io} = F_o \, \Delta y_1 \tag{8.43a}$$

where

F_o: is a function of

- The first arbitrary position of the neutral axis n–n (x_o)
- A series of geometrical parameters of the cracked cross section (concrete-steel) related to x_o
- The characteristic strength and deformation of concrete (f_{ck}, ε_{cu2}) and steel (f_{yk}, $\varepsilon_{yk} = f_{yk}/E_s$)

It should be noted that for relatively small displacements Δy, the values of F_o tend to be independent of Δy (Newton–Raphson approach).

Therefore, Equation 8.42a takes the form:

$$\sum N_{io} + F_o \Delta y_1 = 0 \tag{8.44a}$$

or

$$\Delta y_1 = -\frac{\sum N_{io}}{F_o} \tag{8.45a}$$

Step 4: For this new position of the neutral axis ($x_1 = x_o + \Delta y_1$), the new ΣN_{i1} is determined, which continues to be other than zero. Consequently, a new small displacement Δy_2 of the neutral axis n–n is required so that

$$\sum N_{i1} + \Delta N_{i1} = 0 \tag{8.41b}$$

$$\sum N_{i1} + F_1 \Delta y_2 = 0 \tag{8.43b}$$

or

$$\Delta y_2 = -\frac{\sum N_{i1}}{F_1} \tag{8.45b}$$

Step 5: After a small number of iterations, the neutral axis converges very quickly to its final position, for which:

$$\sum N_n \cong 0 \tag{8.46}$$

Step 6: For the final position of the neutral axis ($x = x_n$) the moments of all internal forces, corresponding to the final deformation pattern, about the extreme rebar under tension result in the bending moment M_u at flexure.

The ultimate curvature at section level is given as in paragraph (ii) by the expression:

$$\boxed{\varphi_u = \frac{\varepsilon_{cu2}}{x_n}} \tag{8.47}$$

In the case that

$$\varepsilon_{se} = \frac{\varepsilon_{cu2}}{x_n}(d - x_n) < \varepsilon_y = \frac{f_y}{E_s} \tag{8.48}$$

the failure of concrete to compression precedes steel yield at tension zone.

Therefore, the procedure stops here and what is presented in the next paragraph is in this case meaningless for the procedure. Otherwise, the procedure continues as follows:

3. *Point B:* $M_y - \varphi_y$

Consider the cross section of Figure 8.19 symmetric to the z–z axis. For the determination of M_y and φ_y, the deformation pattern of the cross section must be defined. This pattern must have an ordinate at the extreme rebar under tension equal to ε_y (Figure 8.19b). Therefore, one point of this straight line is explicitly defined. For the time being we consider that this line intersects z–z at a distance x_n from the extreme point of concrete under compression. We recall that this point is located on the neutral axis n–n. The condition for the determination of x_n (the position of the neutral axis n–n) is based again on the requirement that the sum of the internal forces corresponding to this deformation pattern be equal to zero ($\Sigma N_{in} = 0$), since the cross section is under plain bending. If x_n is known, φ_y is determined by the relation:

$$\varphi_y = \frac{\varepsilon_y}{d - x_n} \tag{8.49}$$

while M_y results from the sum of the moments of all internal forces corresponding to this deformation pattern about the centroid of the extreme steel rebar under tension. It should be remembered that the case of having a final extreme strain ε_{cextr} of concrete under compression greater than ε_{cu2} has already been excluded by means of the procedure developed in paragraph (ii).
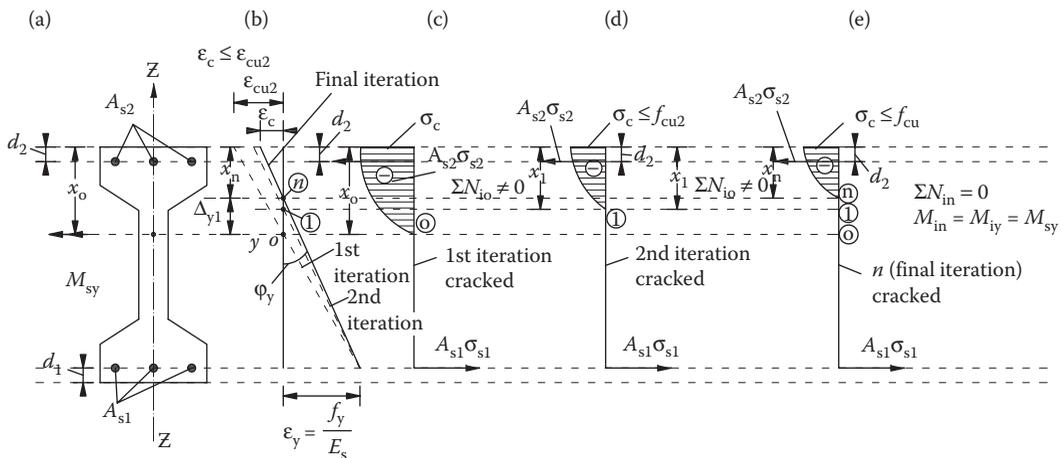
Figure 8.19 Cross section at yield stage (a) cross section; (b) deformation pattern at successive iteration steps 0.1, *n*; (c) internal forces of step (1); (d) internal forces of step (2); (e) internal forces of final step (*n*).

For the determination of x_n the following procedure is followed:

Step 1: For the determination of the position of the strain pattern we suppose first that the straight line of its boundary intersects the z–z axis at the centroid 0 of the composite uncracked cross section. This is an arbitrary position of the strain pattern considered a first iteration to the final position. It should be noted that in the case that the corresponding extreme strain deformation ε_{cext} of concrete under compression exceeds ε_{cu2}, the deformation plane for the first iteration is replaced by the balanced situation (ε_{cu2}, ε_{sy}).

Steps 2, 3, 4, 5: The same procedure is followed as that of the corresponding steps in paragraph (ii).

Step 6: For this final position of x_n of the neutral axis, values M_y and φ_y are determined according to what has been presented at the beginning of this paragraph.

8.2.3 Load–deformation diagrams for bending under cyclic loading

8.2.3.1 General

As has already been noted (Subsection 2.3.3), the notion of ductility capacity should be accompanied by that of energy dissipation, related to moment–curvature or force–displacement loops under cyclic loading. In fact, it has been explained in detail in Subsection 2.3.3 that the capacity of a member to dissipate energy under cyclic loading is expressed by the area of the loops of cyclic loading. The moment–curvature or force–displacement diagram of monotonic loading is assumed to be the envelope of cyclic loading, and this has to be proven by experimental evidence. Figure 8.20 makes apparent the above considerations. Although both diagrams have as a backbone the same M–φ curve, that of Figure 8.20a with spindle-shaped loops displays a much higher capacity for energy dissipation than that of Figure 8.20b with pinched loops. Therefore, it is of paramount importance to comment on moment–curvature or force–deflection diagrams of beams under cyclic loading.

From a review of extensive experimental data, it may be seen that the behaviour of critical regions of beams under cyclic loading should be classified as follows:

- Critical regions where inelastic behaviour is controlled by bending (flexural critical regions)
- Critical regions where inelastic behaviour is controlled by high shear while bending is of secondary importance

In the next paragraph, flexural behaviour under cyclic loading will be examined, while in Subsection 8.2.4 behaviour under prevailing shear will be examined.
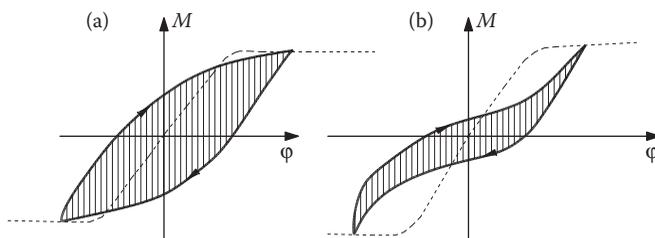
Figure 8.20 M–φ diagrams: (a) spindle-shaped loops when flexure prevails; (b) pinched loops when shear prevails.

8.2.3.2 Flexural behaviour of beams under cyclic loading

From the abundant experimental data, two characteristic cases will be examined below:

1. The case of a cantilever with an orthogonal cross section 406×203 mm reinforced with a reinforcement percentage $\rho_1 = 1.4\%$ and $\rho_2 = 0.74\%$ and a shear span $M/Vd = 4.5$. Nominal shear stress is rather low, $\tau_n = 0.26\sqrt{f_c}$ (Figure 8.21; Bertero and Popov, 1977; Penelis and Kappos, 1997).
2. The case of a cantilever beam T cross section with dimensions also depicted in Figure 8.21, with top reinforcement $\rho_1 = 1.4\%$ while bottom reinforcement $\rho_2 = 0.74\%$.
   In both cases the bottom flange reinforcement is 50% of the reinforcement at the top, which is in accordance with the Seismic Code provisions for the reinforcement of critical regions of T and orthogonal beams. Shear span M/Vd continues to be equal to 4.5 while the nominal shear stress is the same as that of case (i).

From detailed examination of the above diagrams the following remarks may be made:

1. Loops of flexural behaviour are *spindle-shaped* and therefore absorb and dissipate adequate amounts of seismic energy.
2. Cyclic loading *is stable,* having as its envelope the corresponding $M-\varphi$ or $P-\delta$ curve of monotonic loading.
3. No significant stiffness degradation occurs at service levels, in contrast to the behaviour at post-elastic levels, where stiffness is reduced instantaneously after each reversal of moment in which the peak curvature is increased beyond its previous value. This may be mainly attributed to the Bauschinger effect, which influences the steel stress–strain diagram under reversals of loading (see Subsection 7.3.4).
4. Repeated reversals up to the same post-elastic level of deformation show a remarkable strength stiffness and energy dissipation stability.
5. Finally, it should be noted that failure is usually due to buckling of the main reinforcement under compression (Figure 8.22). Factors controlling buckling are:
   - Concrete cover
   - The spacing size and detailing of hoops
   - Strain history of the rebars that may cause rupture of one or more of them.
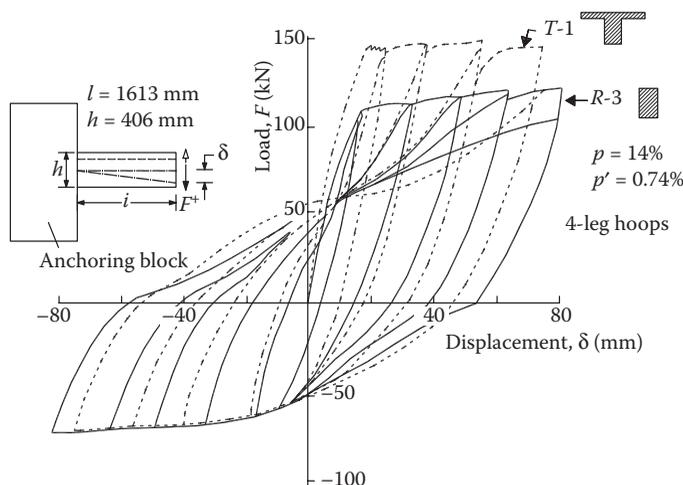
Figure 8.21 Hysteresis loops of R/C members subjected to predominantly flexural cyclic loading.
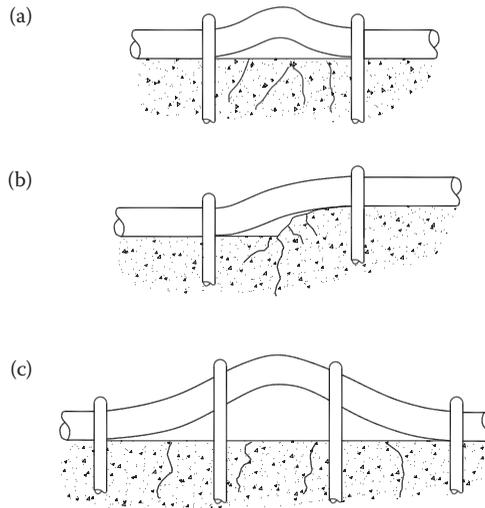
Figure 8.22 Different modes of buckling in reinforcing bars.

8.2.4 Strength and deformation of beams under prevailing shear

8.2.4.1 Static loading

Dimensioning of R/C beams against shear under-static loading is one of the main issues in the design of R/C conventional structures. Therefore, a detailed presentation of this subject is beyond the scope of this work. Here, an overview of the main issues of the problem will be made so that a subsequently easy transition to cyclic loading may be made. Failure under shear of a reinforced beam with *longitudinal rebars and stirrups* in the web may occur by *diagonal tension* (Figure 8.23a; diagonal concrete cracking accompanied by stirrup yield) or *by diagonal compression* (diagonal concrete crush; Figure 8.23b).
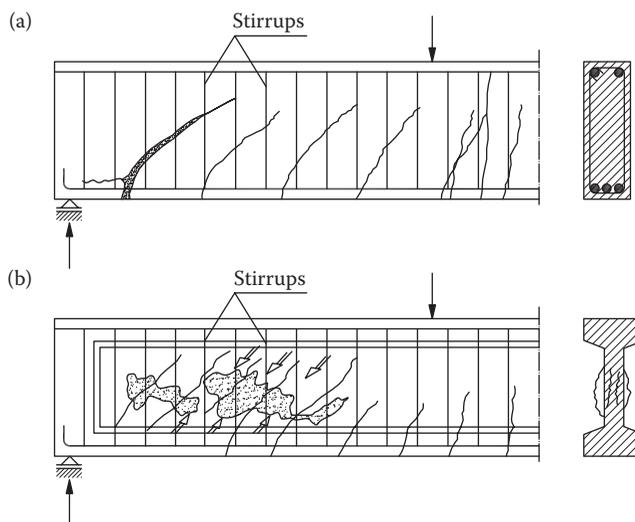
Figure 8.23 Failure of an R/C beam to shear: (a) failure due to diagonal tension; (b) failure due to crushing of the compressive diagonal struts.

8.2.4.1.1 Failure caused by diagonal tension

This type of failure is resisted by two mechanisms, that is:

- Beam action in the shear span without web reinforcement
- Truss mechanism of web reinforcement (stirrups, bent-up rebars)

8.2.4.1.1.1 BEAM ACTION IN THE SHEAR SPAN WITHOUT WEB REINFORCEMENT

This type of failure is governed mainly by concrete tensile strength and the existing tensile flexural reinforcement in the shear span (Figure 8.24).

Extended experimental evidence (Leonhardt and Walther, 1962; Leonhardt and Mönnig, 1973) has shown that shear failure in the form of diagonal cracking exhibits before failure to flexure in the case that the shear span-to-depth ratio:

$$\boxed{\frac{a}{d} = \frac{M_{Eu}}{V_E d}} \tag{8.50}$$

ranges between the following limits (Figure 8.25):

$$\boxed{2.0 \leqq \frac{a}{d} \leqq 7.0} \tag{8.51}$$

The characteristic picture of this failure mode displays diagonal cracks that start up from existing already flexural ones at the shear span. These inclined cracks develop rapidly up to the compression zone, leading to a *brittle* failure.

- Shear strength of compressive zone: V_{Rc}
- Aggregate interlock: V_{Ra}
- Dowel effect: V_{Rd}
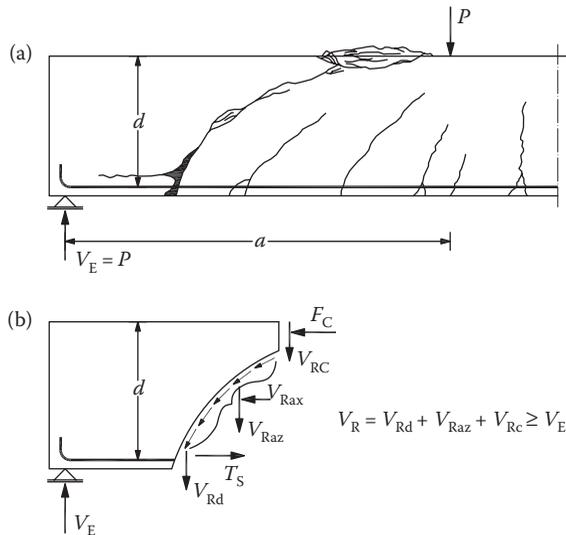
Figure 8.24 Shear failure of a beam without shear reinforcement: (a) failure mode; (b) factors contributing to shear resistance.
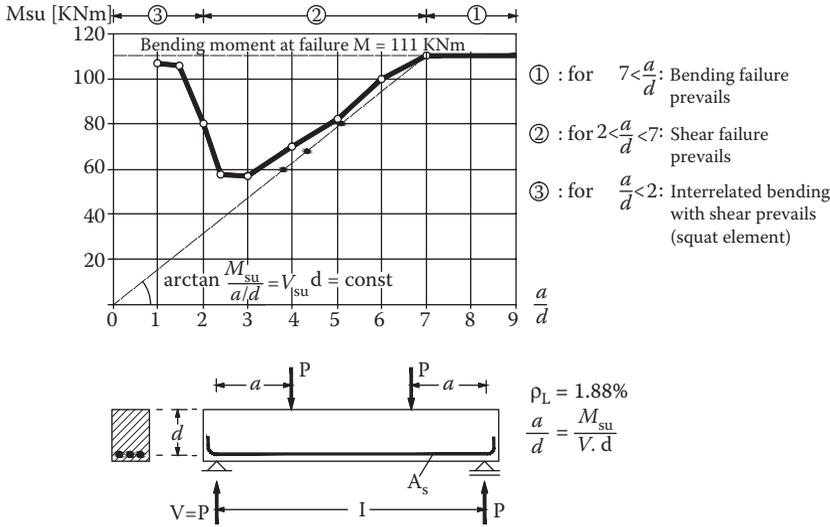
Figure 8.25 The influence of the ratio *a/d* on the shear strength of beams without shear reinforcement. Results of Stuttgart test. Beam with constant cross section and reinforcement ratio at bottom flange $\rho_L = 1.88\%$ $V_{su} = (M_{su}/a)$. (Adapted from Leonhardt, F. and Walther, R. 1962. *Schubversuche an einfeldrigen Stahlbetonbalken mit und ohne Schubbewehrung.* DA für Stahlbeton Heft 151, W. Ernst und Sohn, Berlin; With kind permission from Springer Science+Business Media: Leonhardt, F. 1973. *Vorlesungen uber Massivbau, 1. teil.*)

Therefore, in order to avoid this type of failure, a minimum web reinforcement is foreseen by Codes, even if the dimensioning of the beam to shear does not require it.

More specifically, parameters that contribute to shear strength in this case are (Figure 8.24b):

- The shear strength of the compression zone
- Aggregate interlock
- Dowel effect of tensile longitudinal reinforcement

Shear strength of the uncracked compression zone depends on concrete strength. On the other hand, aggregate interlock and the dowel effect are strongly influenced by the percentage of reinforcement in the tension zone of the beam, since the width of the diagonal cracks is strongly affected by the tensile stress of longitudinal bars and therefore by its percentage. Based on the above remarks it can easily be concluded that the shear strength of a beam without web reinforcement is determined mainly by:

1. The tensile strength of concrete
2. The percentage of tensile reinforcement in the tension zone of the shear span

EUROCODE EC2-1/1991 ENV (CEN, 1992) had quantified shear strength in this case by the expression:

$$V_{Rd,c} = \tau_{Rd} \cdot \kappa \cdot (1.2 + 40\rho_1)b_w \cdot d \tag{8.52}$$

where

b_w is the smallest web width

d is the effective height of the cross section

κ is $1.6-d \not< 1.0$ (in meters) expressing the size effect of the cross section

ρ_l is the longitudinal reinforcement ratio at shear span

$\tau_{Rd} = (f_{ctk}/\gamma_d)\xi$ is the reduced tensile strength of concrete to the height x of the compression zone

$\xi = x/d$ (estimated to $\xi \cong 0.25$)

The influence of the above-mentioned two parameters (concrete tensile strength and percentage of tensile reinforcement at the shear span), together with the size effect of the beams, are displayed with scientific transparency in Equation 8.52. At the same time, this approach complies with the modifications necessary for seismic action effects as we will see in the next paragraph. A similar expression has been adopted for many years by the American Codes (ACI 318-2005, 2008, 2011) as well as by the Codes of many other countries.

Eurocode EC2-1-1/2004 has adopted the following expression for the determination of V_{Rdc}:

$$\boxed{V_{Rd,c} = C_{Rd,c} \cdot \kappa \cdot (100\rho_l f_{c\kappa})^{1/3} b_w \cdot d}$$ (8.53)

This value should not be *less than* ($V_{Rd,cmin}$):

$$\boxed{V_{Rd,cmin} = 0.035\kappa^{3/2} f_{c\kappa}^{1/2} \cdot b_w d}$$ (8.54)

where

$C_{Rd,c}$ is the coefficient derived from tests (recommended value 0.12)

κ is the size effect factor $\kappa = 1 + \sqrt{\dfrac{200}{d}}$ with d in (mm)

ρ_l is the longitudinal reinforcement ratio in tension zone of the shear span (≤ 0.02)

$f_{c\kappa}$ is the characteristic concrete compression strength (MPa)

b_w is the smallest web width (mm)

d is the effective height of the cross section (mm)

$V_{Rd,c}$ (N)

8.2.4.1.1.2 TRUSS MECHANISM OF WEB REINFORCEMENT. ALTERNATIVE (A)

Web reinforcement (stirrups, bent-up rebars) generates for the beam an additional resisting mechanism to shear. This mechanism, according to the well-known Mörsh truss analogy, consists of (Figure 8.26):

- A chord of longitudinal reinforcement under tension at the bottom of the beam
- A chord of the compressive stresses of concrete and of the compressive forces of reinforcement under compression concentrated at the centroid of the compressive zone
- Stirrups and bent-up rebars in the web acting as tension members
- Inclined concrete struts under compression between the successive inclined shear cracks, which are developed after V_{Ed} has exceeded $V_{Rd,c}$. For almost one century and even nowadays, according to the ACI318-2011 the inclination of these struts was considered to be 45°.
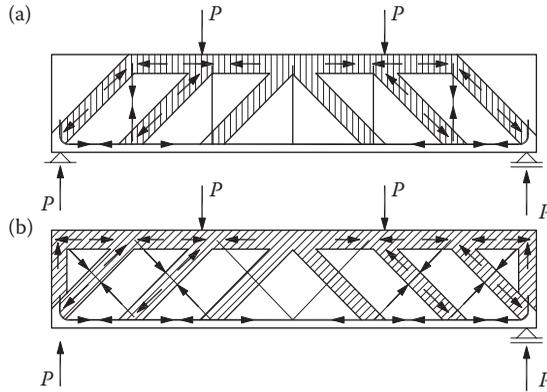
Figure 8.26 Mörsh truss mechanism: (a) stirrups as shear reinforcement; (b) bent-up bars as shear reinforcement.

In this context, shear force V_{wd} resisted by web reinforcement is equal to

$$V_{wd} = \frac{A_{sw}}{s} 0.9d \cdot f_{ywd} \tag{8.55}$$

where
    A_{sw} is the cross-sectional area of web reinforcement
    s is the spacing of the stirrups
    f_{ywd} is the design yield strength of the shear reinforcement
    $0.9d$ is a good approximation for the lever arm z of the internal forces of the beam in
        bending

The same procedure was followed in EC2-1-1/1991 ENV.
It should be noted here that:

1. According to what has been presented so far, a beam with web reinforcement in the form of stirrups comprises two shear-resisting mechanisms to shear failure caused by diagonal tension. At ultimate state both mechanisms must be exhausted. Therefore, the shear strength of the beam to diagonal tension is equal to:

$$V_{Rd} = V_{Rd,c} + V_{Wd} \tag{8.56}$$

2. It is equally important to note that while the beam mechanism without stirrups is *brittle*, the arrangement of web reinforcement stabilises the inclined cracks and their width, until stirrups yield. Therefore, web reinforcement together with the enhancement of the shear strength of the beam improves radically its ductility.
3. Beams should be reinforced at least with a minimum web reinforcement in the form of stirrups even if

$$V_{Ed} \leq V_{Rd,cmin} \tag{8.57}$$

The minimum web reinforcement ratio that is specified by Codes:

$$\rho_w = \frac{A_{sw}}{b_w s} \tag{8.58}$$

covers the concrete (unreinforced) shear resistance $V_{Rd,c}$

8.2.4.1.1.3 TRUSS MECHANISM OF WEB REINFORCEMENT—ALTERNATIVE (B)

A different procedure was followed by EC2-1-1/2004 for failure caused by diagonal tension. In the case that V_{Ed} exceeds the value of $V_{Rd,c}$ given by Equations 8.53 and 8.54, the *truss model analogy with concrete struts of variable inclination is applied* (Figure 8.27).

The only difference of this model from the 'Mörsh truss model' is that the inclination of the cracks and therefore of the compressed concrete struts is considered to be of variable inclination δ, varying between

$$\boxed{21.8° \le \delta \le 45°} \tag{8.59a}$$

or

$$\boxed{2.5 \ge \cot \delta \ge 1.0} \tag{8.59b}$$

In this context, shear force $V_{\omega d}$ resisted by web reinforcement is equal to

$$\boxed{V_{wd} = V_{Rd} = \frac{A_{sw}}{s} 0.9 d f_{ywd} \cot \delta} \tag{8.60}$$

The actual value of δ that should be introduced in Equation 8.60 is defined by the strut inclination for which shear failure due to diagonal tension and diagonal compression occur simultaneously (see next paragraph).

It should be noted here that in contrast to the ENV edition of EC2-1-1/1991 and to ACI318-2011 in the above expression (8.60), both mechanisms of Equations 8.52 and 8.55 are incorporated into one, that is, '*the variable inclination strut*'.
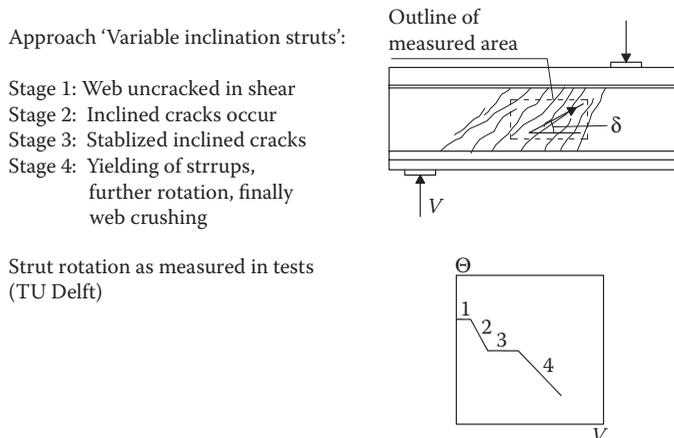
Figure 8.27 The principle of variable truss action. (Adapted from Walraven, J.C. 2002. Delft, University of Technology, Background document for EN1992-1-1. Eurocode 2: Design of Concrete Structures-Chapter 6.2: Shear, Delft.)

The above mechanism is based on extended experimental evidence (Walraven, 2002), according to which shear failure exhibits the following stages:

- For $V_{Ed} \le V_{Rd,c}$ the web remains uncracked to shear.
- For $V_{Rd,c} \le V_{Ed}$, inclined cracks occur at the beginning at an angle in relation to the beam axis at about 45°.
- These cracks remain stable while V_{Ed} increases and while stirrups begin to develop tensile stresses below yielding stress.
- Shear failure occurs when stirrups yield, followed by strut rotation, until finally the web crushes (Figures 8.23b, 8.27).

8.2.4.1.2 Failure caused by diagonal compression

It is apparent that this type of failure does not refer to the beam action without web reinforcement, since in this case tensile diagonal failure prevails due to the very low tensile strength of concrete. Instead, this type of failure may be critical for beams with web reinforcement.

For the determination of shear resistance in the case of *diagonal concrete crushing,* the Mörsh truss model already presented above is used.

According to this model (Figures 8.28a,b):

$$\boxed{V_{Rd,max} = \alpha_{cw} b_w 0.9 \cdot d \, (\nu_1 f_{cd})/2}$$
(8.61)

$$V_{Rd\,max} = \frac{\sqrt{2}}{2} D$$

$$D = b_w \cdot a_s \frac{\sqrt{2}}{2} (f_{cd} \cdot \nu_1)$$

therefore

$$V_{Rd\,max} = \frac{1}{2} (\nu_1 f_{cd}) b_w \cdot 0.9 \, d$$

$$V_{Rd\,max} = D \sin \delta$$

$$D = b_w \cdot a_s \sin \delta \, (f_c \cdot \nu_1)$$

therefore

$$V_{Rd\,max} = 0.9 \, d \, b_w (\nu_1 f_c) \cot \delta/(1 + \cot^2 \delta)$$
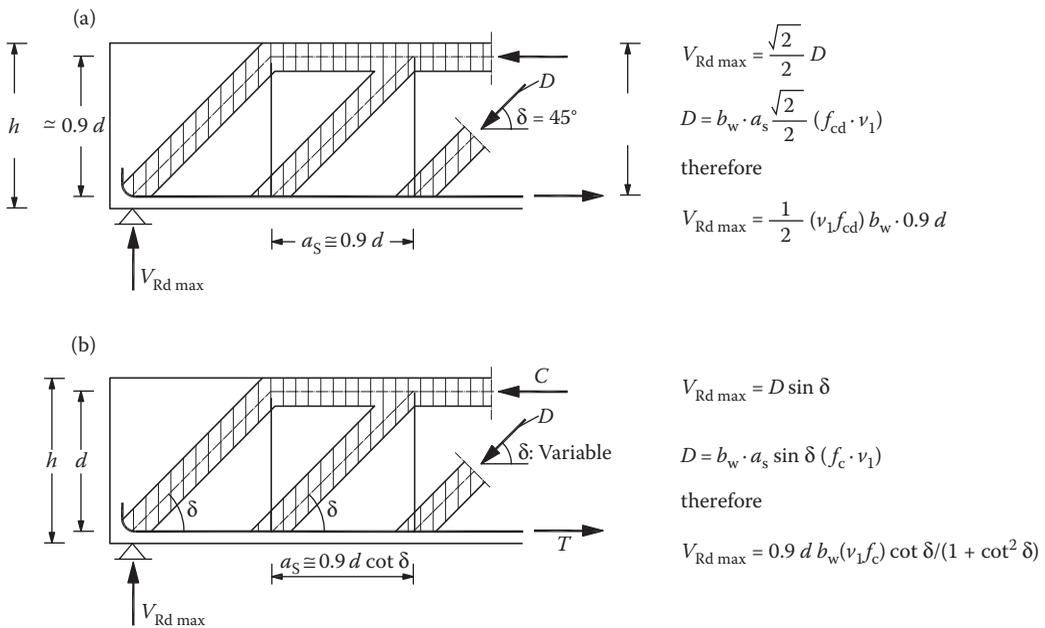
Figure 8.28 Determination of the shear resistance $V_{Rd\,max}$: (a) diagonal compression failure at $\delta = 45°$; (b) variable diagonal compression failure at $21.8° \le \delta \le 45°$. (Adapted from Penelis et al. 1995; Walraven, J.C. 2002. Delft, University of Technology, Background document for EN1992-1-1. Eurocode 2: Design of Concrete Structures-Chapter 6.2: Shear, Delft.)

for $\delta = 45°$ (ACI318-2011), or

$$V_{Rd,max} = \alpha_{cw} b_w 0.9d \, (v_1 f_{cd}) \cdot \cot \delta / (1 + \cot^2 \delta)$$

(8.62)

for δ variable $(21.8° \leq \delta \leq 45°)$ (EC2-1-1/2004),
where

    δ is a variable ranging between $(21.8° \leq \delta \leq 45°)$ (EC2-1-1/2004).
    v_1 is a factor for concrete compressive strength reduction of concrete already cracked
       by shear:

$$v_1 = 0.6 \left[1 - \frac{f_{ck}}{250} \right]$$

(8.63)

    (f_{ck} in (MPa))

    α_{cw} is a coefficient equal to 1.0 for beams without axial loading.

8.2.4.1.3 Design procedure for shear under static loading according to codes

Based on the above presentation, an overview of the design procedure for shear under static loading according to Codes in use would be useful.

- *Step 1*: Determine span-to-depth ratio

$$\frac{a}{d} = \frac{M}{V \cdot d}$$

    if $(a/d) \geq 2.0$ the following procedure will be followed:
- *Step 2*: Shear resistance $V_{Rd,c}$ of the beam without web reinforcement is determined using Equation 8.52 (ENV EC2-1/1991) or using Equations 8.53 and 8.54 (EC2-1-1/2004). If

$$V_{Ed} \leq V_{Rd,c}$$

    web reinforcement is not required. However, *minimum web reinforcement* in the form of stirrups must be foreseen to ensure the beam against a potential brittle shear failure.
- *Step 3*: In the case that

$$V_{Ed} \geq V_{Rd,c}$$

    two different procedures are foreseen, depending on the Code under consideration:
  - In the case that ACI 318-2011 is in effect, design shear for V_{Ed} must be less than the sum of the shear contribution of the concrete $V_{Rd,c}$ and the shear contribution of the web reinforcement V_{wd}, under the assumption that the concrete struts exhibit a constant indication $\delta = 45°$, that is,

$$V_{Ed} \leq V_{Rd,c} + V_{wd}$$

(8.64)

    This expression allows the determination of the required web shear reinforcement.

At the same time, the concrete struts under compression must have a sufficient safety factor from crushing. Therefore, V_{Ed} must also satisfy the following expression:

$$V_{Ed} \leq V_{Rd,max} \quad \text{for } \delta = 45° \tag{8.65}$$

Usually, Equation 8.65 is satisfied without any difficulty unless webs are very thin. In this case, web width or the nominal depth of the cross section must be increased.

- In the case that EC2-1-1/2004 is in effect, design shear force must be covered by the *truss model analogy* with concrete struts of *variable inclination* simultaneously for both the web reinforcement yield and concrete inclined struts trussing, that is,

$$V_{Ed} \leq V_{Rd} = \frac{A_{sw}}{s} 0.9d \cdot f_{ywd} \cot \delta \tag{8.66a}$$

and

$$V_{Ed} \leq V_{Rd,max} = \alpha_{cw} b_w 0.9d(\nu_1 f_{cd}) \cdot \cot \delta/(1 + \cot^2 \delta) \tag{8.66b}$$

with $21.8° \leq \delta \leq 45°$.

The accomplishment of both expressions (8.66a) and (8.66b) is satisfied by successive trials for various values of δ.

- *Step* 4: In the case that the shear span-to-depth ratio (shear-span ratio) is less than or equal to 2.0, that is,

$$\frac{a}{d} \leq 2.0$$

a special procedure must be followed, since in this case the Bernoulli concept for a plane strain pattern over the cross section of the member does not prevail, and therefore a two-dimensional stress state prevails where strong relation among shear and normal stresses exists. This case refers mainly to spandrels between shear walls, to joints of frames and to low shear walls. Therefore, detailed reference will be made to this issue in the relevant chapters (see Subsection. 8.3.6, Section 9.4).

8.2.4.2 Cyclic loading

It has been noted many times thus far that beams of ductile R/C frames display potential plastic hinges at their ends. During a strong seismic action these plastic hinges yield first in one direction and then in the other, as the frames sway to the right and left successively. Under these conditions of cyclic loading of combined bending and shear, if shear prevails ($2 \leq (M/V \cdot d) \leq 7.0$), diagonal cracks progressively develop crosswise in the region of the plastic hinge. These cracks widen from cycle to cycle, since plastic strains of flexural and of shear reinforcement are accumulated (Park and Paulay, 1975; Bertero, 1979; Paulay and Bull, 1979; Scribner and Wight, 1980; Paulay and Priestley, 1992; Penelis and Kappos, 1997; Booth and Key, 2006; Fardis, 2009).This tends to eliminate the aggregate interlock, the dowel effect and the shear strength of the compressive zone, which are the basic parameters that contribute to the beam shear action together with the truss mechanism of web reinforcement. For this reason, Codes of Practice specify that the above contribution to shear (beam shear strength) should be eliminated unless the ductility demand of the building
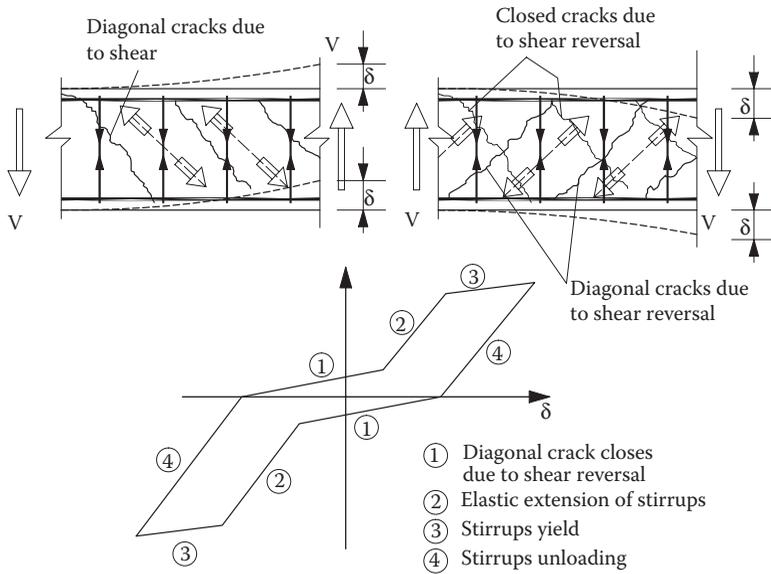
Figure 8.29 Shear deformation in reversing hinge zones: (a) crack pattern; (b) deformation of truss; (c) shear versus deformation in reversing hinge. (Adapted from Booth, E. and Key, D. 2006. *Earthquake Design Practice for Buildings.* Thomas Telford Ltd. With permission.)

is of a limited level. In this context, shear action effect should be resisted *only by the web reinforcement* determined by the 'Mörsh' truss analogy mechanism.

Furthermore, the widening of diagonal cracks in the hinge plastic region lead to a 'pitching effect' on the *V–δ* diagram. In fact, for a diagonal strut under compression, which has been cracked transversally in the previous step to be activated, the transverse cracks must close first. This leads to a situation where there is very little resistance to shear, and therefore stiffness around the midpoint of the loading cycle diminishes gradually from cycle to cycle (Figure 8.29). In this context the capacity of the beam for energy absorption and dissipation in the region of plastic hinge is radically reduced in the case of diagonal shear cracks.

In closing, it should be noted that the cyclic widening and closing of diagonal cracks, in combination with the corresponding widening and closing of the flexural cracks, leads to the degradation of the plastic hinge region and finally to failure in a mode of *sliding shear* (Figure 8.30).

8.2.4.3 Concluding remarks on shear resistance

From what has been presented so far regarding the behaviour of plastic joints in response to shear, the following remarks may be made:

1. The design of the beams for seismic shear effects may be carried out basically like that of conventional static loading.
2. In particular, additional special measures should be taken at the regions of plastic hinges (critical regions). These measures may be summarised as follows:
   a. Enhancement of shear effects based on the capacity design concept (Subsection 6.1.3), so that yield of shear reinforcement at the plastic hinges does not develop during seismic load reversals.
   b. Elimination of the contribution of the beam resistance to shear in case of high-ductility demand.
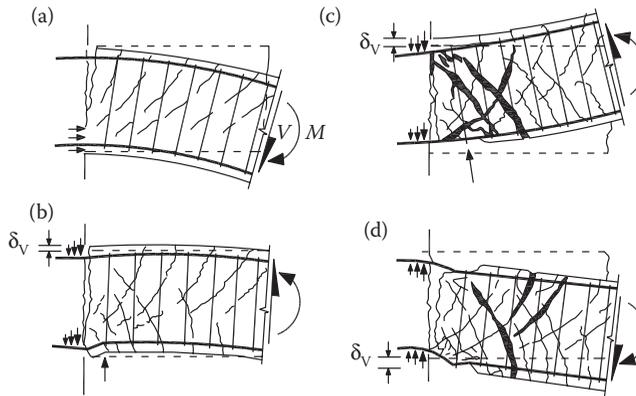
Figure 8.30 Characteristic phases of the response of an R/C beam to reverse cyclic loading: (a) loading downwards; (b) loading upwards up to original position; (c) continuation of the upward loading; (d) reverse loading downwards accompanied with sliding shear.

    c. Arrangement of diagonal reinforcement in the region of plastic hinges in the case that the design shear effects present reversed sign, so that sliding is avoided.

  3. In the case that shear reinforcement yields, adverse consequences are evident at the region of a plastic hinge, that is:

    a. Quick strength degradation of the hinge region

    b. Pinching effects on the P–δ diagram

    c. Shear sliding failure at a position where wide flexural cracks have been developed

  4. It is the author's opinion that the design method for shear of the variable compression strut inclination model, adopted by EC2-1-1/2004, presents some weak points in comparison to that of the constant inclination model adopted by ACI 318-2011.

    a. There is inadequate transparency of the mechanical models behind the design method of EC2-1-1/2004.

    b. In fact, for values of $V_{Ed} \leq V_{Rd,c}$ a beam model is used, where the two factors (concrete shear strength and flexural reinforcement percentage) are not clearly distinct.

    c. Furthermore, in the case that $V_{Ed} \geq V_{Rd,c}$ the beam model is completely abandoned and it is incorporated in the truss model of variable angle strut, without an apparent engineering concept behind it, except the 'best-fitting' statistical concept of extensive experimental results.

    d. Last but not least is the case of buildings of high-ductility demand. A return to the truss model of constant angle (45°) in order to eliminate the beam mechanism contribution appears to be unjustified from the engineering point of view.

  5. For joints, spandrels and deep beams, a special design procedure should be followed for both bending and shear (see Sections 8.4 and 9.4), since bending and shear can no longer be considered two independent strain states.

8.2.5 Code provisions for beams under prevailing seismic action

8.2.5.1 *General*

The design rules of beams under seismic actions according to EC8-1/2004 are given below, together with the required justification in terms of the theory developed in the previous subsections. It should be noted that the design specifications are directly related to the ductility demand under consideration, that is, DCL, DCM and DCH. For higher ductility class,

specifications tend to be stricter in order for a higher local ductility in terms of curvature to be obtained.

Specifications for the design effects, taking into account capacity design procedure, have already been presented in Subsection 6.1.3.

Material issues have also been presented in Subsections 7.2.4, 7.3.5 and 7.5.4 for all ductility classes.

It should be mentioned here that for the design of beams of buildings of class DCL, Code specifications for conventional R/C structures (EC2-1-1/2004) are adopted, except where concrete and steel reinforcement qualities have been specified by EC8-1/2004, as has already been presented in Chapter 7. For this reason, design of beams for DCL buildings will not further occupy our attention in this book. Therefore, in the following paragraphs only the design of beams for DCM and DCH buildings will be presented.

In closing, it should be noted that all rules and specifications of the corresponding Code for conventional R/C structures (EC2-1-1/2004) continue to be in effect, unless they contradict what will be presented below.

8.2.5.2 Design of beams for DCM buildings

1. Geometrical constraints
   a. The eccentricity of a beam axis relative to that of the column with which it is connected should be limited to $b_c/4$, where b_c is the largest cross-sectional dimension of the column normal to the longitudinal axis of the beam, that is (Figure 8.31):

$$e \le b_c/4 \tag{8.67}$$

   In this way, cyclic moments can be transferred safely from the columns to the beams.
   b. The beam width b_w should be (Figure 8.31):

$$b_w \le \min (b_c + h_w, 2b_c) \tag{8.68}$$

   where h_w is the depth of the beam
   In this way, a large percentage of the horizontal bars of the beam pass at the joints through the column and, therefore, take advantage in their bond of the favourable effect of column compression.
2. Resistance in bending and shear
   a. Bending and shear resistance of beams for DCM are determined in accordance with the Code in effect for conventional R/C structures, that is, EC2-1-1/2004. It should also be remembered that the design for shear is not carried out for the design shear effects that result from the analysis but for those from the capacity design procedure (Subsection 6.1.3).
   b. The top reinforcement of the end cross sections with T or Γ-shaped sections should be placed mainly within the width of the web, and only a part of these rebars might
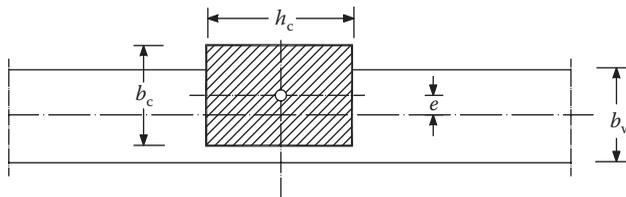
Figure 8.31 Eccentric arranged beam in relation to the supporting column.
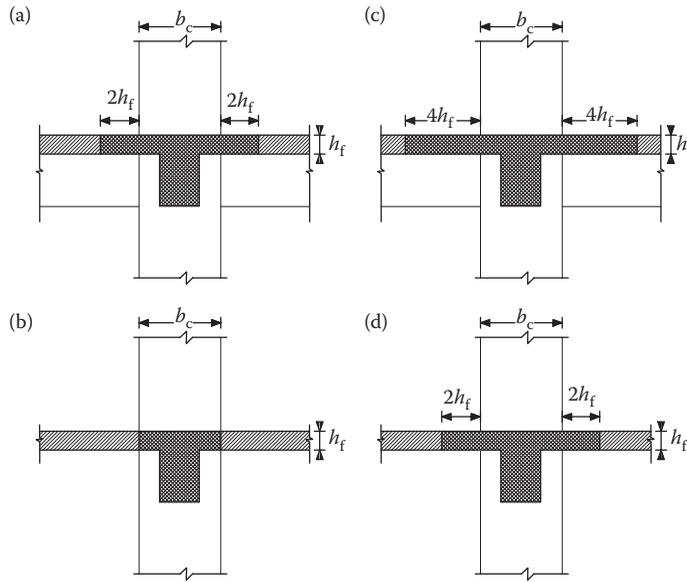
Figure 8.32 Effective flange width b_{eff} for beams framing into columns: (a) exterior column with transverse beam; (b) exterior column without transverse beam; (c) interior column with transverse beam; (d) interior column without transverse beam. (Adapted from E.C.8-1/EN1998-1. 2004. *Design of Structures for Earthquake Resistance: General Rules, Seismic Actions and Rules for Buildings.* CEN, Brussels, Belgium.)

be placed outside the web but within the effective flange width b_{eff}. The effective flange width is depicted in Figure 8.32 for various types of column–beam joints.

3. Detailing for local ductility

a. The *critical regions* of the beam are defined as the regions of a length $l_{cr} = h_w$ (where h_w is the depth of the beam) measured from the two ends of the beam to its span. As was already explained, these are regions of potential yield of steel reinforcement and therefore the positions of potential plastic hinges (Figure 8.33).

b. In beams supporting discontinued (cut-off) vertical elements (Figure 8.33), the regions up to a distance of $2h_w$ on each side of the supported vertical element should also be considered as being critical regions.

c. The value of the curvature ductility demand μ_φ at the critical regions must satisfy Equations 5.52a and 5.52b, that is,

$$\mu_\varphi = 2q_o - 1 \qquad \text{if} \quad T_1 \geq T_c \tag{5.52a}$$

$$\mu_\varphi = 1 + 2(q_o - 1)\frac{T_c}{T_1} \qquad \text{if} \quad T_1 < T_c \tag{5.52b}$$
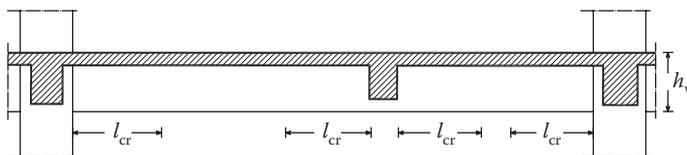
Figure 8.33 Critical regions of beams.

This is deemed to be satisfied if the following conditions are met at both flanges of the beam:

1. At the compression zone, reinforcement equal or greater than half of the reinforcement provided at the tension zone ρ_1 should be placed, in addition to any compression reinforcement computed for the ULS design.
2. The reinforcement ratio ρ_1 in the tension zone should not exceed a value of:

$$\boxed{\rho_{1max} \leq \rho_2 + \frac{0.0018}{\mu_\varphi \cdot \varepsilon_{sy,d}} \frac{f_{cd}}{f_{yd}}} \tag{8.69}$$

where (Figure 8.34):

$$\rho_1 = \frac{A_{s1}}{bd} \tag{8.70a}$$

$$\rho_2 = \frac{A_{s2}}{bd} \tag{8.70b}$$

The above expression results from Equation 8.34b. In fact, if in Equation 8.34b:
$f_{cκ}$, $f_{yκ}$ are replaced by f_{cd}, f_{yd}, and
a. ε_{cu2} is replaced by the conventional value of 0.0035 corresponding to concrete classes C16–C50, and
b. ξ_y is replaced by its mean value equal to 0.34, resulting from Equation 8.18.
Equation 8.34b takes the form:

$$\rho_1 - \rho_2 = \frac{0.8 \cdot 0.0035 \cdot f_{cd} \cdot E_s}{\mu_\varphi \cdot f_{yd} \cdot f_{yd}/E_s} 0.66$$
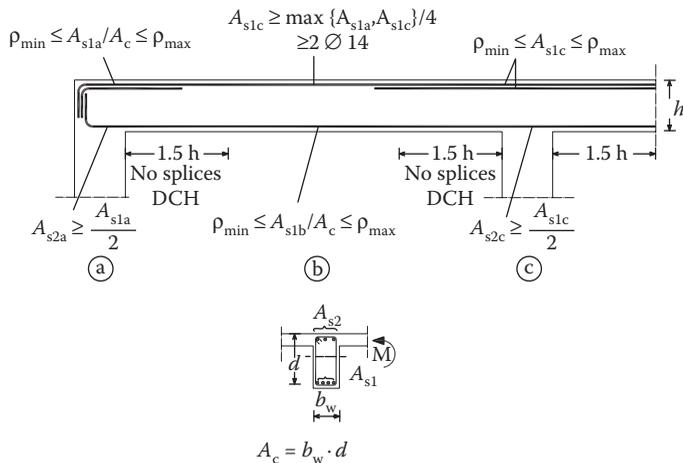
Figure 8.34 Arrangement of longitudinal reinforcement in earthquake-resistant R/C beams.

or

$$\rho_{1\max} \leq \rho_2 + \frac{0.0018}{\mu_\varphi \cdot \varepsilon_{sy,d}} \frac{f_{cd}}{f_{yd}} \qquad (8.69)$$

Keeping in mind that $\mu_{\varphi demand}$ values resulting from Equation 5.52a or 5.52b exhibit a mean safety factor for beams on the order of 1.35 (see Subsection 5.4.4.5) and that the ratio:

$$\frac{f_{cd}}{f_{yd} \cdot \varepsilon_{sy,d}} = \frac{f_{ck} \cdot 1.15^2}{1.5 \cdot f_{yк} \cdot \varepsilon_{sy}} = \frac{1}{1.14} \frac{f_{cк}}{f_{yк} \cdot \varepsilon_{sy}}$$

it may easily be concluded that a safety factor on the order of $1.35 \cdot 1.14 \cong 1.54$ is introduced in terms of curvature ductility by implementing expression 8.69 (see Section 3.2) for determination of $\rho_{1\max}$.

Equation 8.69 is very restrictive for the top reinforcement ρ_1 at beam supports, particularly for DCH buildings for which high values of $\mu_{\varphi demand}$ result (on the order of 10–12). Therefore, the only way to satisfy both requirements, that is:

i. Strength verification:

$$\rho_{1d} \cong \frac{M_{Ed}}{0.9d^2 b f_{yd}} \qquad (8.71)$$

ii. Ductility requirement:

$$\rho_{1\max} \leq \rho_2 + \frac{0.0018}{\mu_{\varphi dem} \cdot \varepsilon_{sy,d}} \frac{f_{cd}}{f_{yd}} \qquad (8.72)$$

is either to change the cross section of the member or to increase the reinforcement percentage ρ_2 at the compression zone, which is the easy way, since the change of cross sections of the members has consequences for the analysis (change of member stiffness) and mainly for the building operation.

Finally, it should be noted that in the case of use of reinforcement steel class B, the curvature ductility factor μ_φ in expression (8.69) should be magnified by a factor 1.5. This requirement results in the enhancement of steel reinforcement ρ_2 under compression, and in this respect in the dissuasion of the designer from using class B steel reinforcement instead of class C.

In Table 8.1, the maximum reinforcement ratio $\rho_{1\max}$ (‰) may be found for various concrete classes, for steel reinforcement class B500c, for $\rho_2 = (1/2)\rho_1$ and for ductility classes DCM and DCH (Ignatakis, 2011).

Table 8.1 Maximum per mil (‰) of tensile reinforcement at l_{cr}: $\rho_{L,max} = A_{s,max}/(b \cdot d)$ (Steel Class B500c)

Materials		C16	C20	C25	C30	C35	C40	C45	C50	C55	C60
$P_{L,max}$ (‰)	DCM	5.97	7.47	9.34	11.20	13.07	14.94	16.80	18.67	20.54	22.40
	DCH	3.80	4.75	5.93	7.12	8.31	9.49	10.68	11.87	13.05	14.24

Assumption: $\rho' = \rho_{L,max}/2$, $\varepsilon_{sy,d} \approx 2.174‰$, $\mu_\varphi = 6.8$(DCM) or 10.7(DCH), μ_φ = Steel Class B500c: $C(f_{yd} = 500/1.15$ MPa).

Table 8.2 Minimum per mil (‰) of tensile reinforcement at tensile zones: $\rho_{L,min} = A_{s,min}/(b \cdot d)$ (Steel Class B500c)

Materials	C16	C20	C25	C30	C35	C40	C45	C50	C55	C60	C70	C80	C90
$\rho_{L,min}$ (‰)	1.90	2.20	2.60	2.90	3.20	3.50	3.80	4.10	4.20	4.40	4.60	4.80	5.00

Steel Class B 500c: $f_{yk} = 500$ MPa.

3. The reinforcement ratio of the tension zone at any point along the beam must not be less than the following minimum value ρ_{min}:

$$\rho_{min} = 0.50\left(\frac{f_{ctm}}{f_{yк}}\right) \tag{8.73}$$

so that pre-emptive brittle failure due to concrete tension cracks is avoided.

This quantity is almost twice as high as that recommended by EC2-1-1/2004 for conventional R/C structures (see Equation 8.9). This discrepancy must be attributed to the fact that Equation 8.73, although based on the same concept as Equation 8.9, refers to T-shaped beams, which are the usual case in R/C buildings. In fact, the part of the web under tension of a T beam (in uncracked stage) is much larger – almost double – than that of the orthogonal section where the tension zone is limited to the mid-height of the web. The output of Equation 8.73 is much closer to those of the relevant requirements of the American Code ACI 318-2011. In any case, it is the author's opinion that in the next revision of Eurocodes this discrepancy should be clarified.

Finally, it should be noted that in Equation 8.73 a safety factor of at least 1.15 is included, since steel overstrength for steel class C is $f_{ut}/f_{yк} \geq 1.15$.

In Table 8.2 the minimum reinforcement ratio ρ_{min} (‰) may be found for various concrete classes and for steel reinforcement class B500c (Ignatakis, 2011).

4. Within the critical regions, hoops satisfying the following conditions should be provided:
   a. The diameter d_{bw} of the hoops should not be less than 6 mm
   b. The spacing, s, of hoops (in mm) should not exceed

$$s = \min\left(h_w/4;\ 24d_{bw};\ 225\ \text{mm};\ 8d_{bL}\right) \tag{8.74}$$

where
d_{bL} is the minimum diameter of longitudinal bars (in mm)
h_w is the beam depth (in mm)

   c. The first hoop should be placed at a distance not more than 50 mm from the adjacent face of the column (Figure 8.35).

8.2.5.3 Design of beams for DCH buildings

8.2.5.3.1 Geometrical constraints

In addition to the rules for DCM buildings, the following rules should be implemented for DCH buildings:

1. The width of beams must not be less than 200 mm
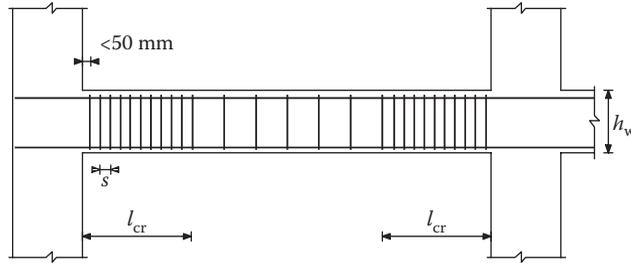
Figure 8.35 Transverse reinforcement in critical regions of beams. (Adapted from E.C.8-1/EN1998-1. 2004. *Design of Structures for Earthquake Resistance: General Rules, Seismic Actions and Rules for Buildings.* CEN, Brussels, Belgium.)

2. The height-to-width ratio of the web should satisfy the following expressions:

$$\frac{l_{ot}}{b} \leq \frac{70}{(h/b)^{1/3}} \quad \text{and} \quad \frac{h}{b} \leq 3.5 \tag{8.75}$$

where

l_{ot} is the distance between torsional constraints. In the case of beams, l_{ot} may be defined as the clear span between the adjacent columns where the beam is jointed.

h is the beam depth at mid-span, including also the depth of the slab.

b is the width of the flange under compression. For a beam under seismic action b is the width of the web.

Beam safety against lateral stability is deemed to be satisfied by the above expression (8.75).

8.2.5.3.2 Resistance to bending

The rules in effect for beams of DCM buildings in bending also apply for DCH buildings without any exceptions.

8.2.5.3.3 Resistance to shear

- For shear resistance, the Code for conventional R/C buildings (i.e. EC2-1-1/2004) applies, unless otherwise specified below.
- Shear action effects, as has been mentioned before, will derive from capacity design rules (see Subsection 6.1.3), so that brittle shear failure may be prevented.
- In the critical regions *the strut inclination ⌧ in the truss model should be 45°.* This provision aims indirectly at eliminating concrete shear resistance (see Subsection 8.2.4).
- With regard to the arrangement of shear reinforcement within the critical region, the following cases should be distinguished, depending on the algebraic value of the ratio:

$$\boxed{\zeta = V_{Ed,min}/V_{Ed,max}} \tag{8.76}$$

between the minimum and maximum acting shear forces as derived by application of the capacity design rule (see Subsection 6.1.3).

1. If $\zeta \geq -0.5$, the shear resistance provided by the reinforcement should be computed in accordance with the Code for conventional R/C structures, *but for strut inclination δ equal to 45°.*

2. If $\zeta \leq -0.5$, that is, when a reversal of shear forces prevails, then:

a. If

$$|V_E|_{max} \leq (2 + \zeta) \cdot f_{ctd} \cdot b_w \cdot d \tag{8.77}$$

where
f_{ctd} is the design value of concrete tensile strength specified by EC2-1-1/2004,

then the rule of paragraph 1 also applies in this case.

b. If

$$|V_E|_{max} \geq (2 + \zeta) \cdot f_{ctd} \cdot b_w \cdot d \tag{8.78}$$

inclined reinforcement should be provided in two directions, usually at ±45° to the beam axis. X-shaped reinforcement should be capable of resisting half of $|V_E|_{max}$, while the other half should be resisted by stirrups. In this case the verification is carried out by means of the truss analogy (Figure 8.36), that is,

$$\boxed{0.5 V_{E max} \leq 2 A_s \cdot f_{yd} \cdot \frac{\sqrt{2}}{2}} \tag{8.79}$$

where
A_s is the area of the inclined reinforcement in one direction, crossing the potential slid-ing plane (usually the beam end section).

If the angle of the inclined reinforcement differs from 45°, which is the case of short beams (type of spandrel) where the inclined reinforcement follows the two diagonals of the beam in place of ($\sqrt{2}/2$) in Equation 8.79, the value of sin α is introduced, where α is the angle of the diagonals of the beam to its axis (Figure 8.36). The provision for inclined shear reinforcement at the critical regions aims at the avoidance of failure in sliding shear mode (Figure 8.30) to which detailed reference has been made is Paragraph 8.2.4.2.
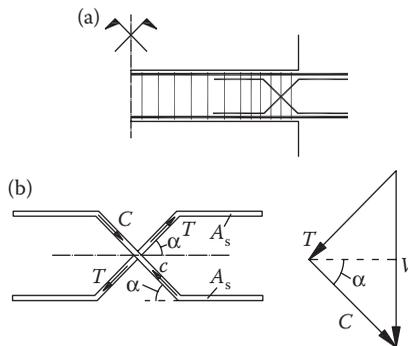
Figure 8.36 X-shaped type of reinforcement for beams with high shear: (a) arrangement of shear reinforce-ment; (b) design of the x-shaped diagonal reinforcement.

8.2.5.3.4 Detailing for local ductility

- Rules for the local ductility of DCM buildings also apply for DCH buildings, unless they contradict the following provisions referring to such buildings.
- The critical regions of a beam of a DCH building are defined as the regions of a length $l_{cr} = 1.50 h_w$ (where h_w is the depth of the beam).
- At least two ribbed bars with $d_{bL} = 14$ mm must be provided, both at the top and the bottom of the beam.
- 1/4 of the maximum top reinforcement at the supports should run along the entire beam length (Figure 8.34). This requirement, in combination with the requirement for a minimum reinforcement in compression zones at the end of the beams, is deemed to secure upper and bottom flanges of the beam from the risk of being found under tension over almost all their length at successive load reversals, depending on the level of the storey where the beam is located.
- The spacing, s, of hoops (in mm) within the critical region in the case of DCH buildings should not exceed:

$$s = \min\,(h_w/4;\ 24 d_{bw};\ 175\ \text{mm};\ 6 d_{bL})$$ (8.80)

8.2.5.4 Anchorage of beam reinforcement in joints

1. For the anchorage of beam reinforcement, all rules specified by the Code for conventional R/C structures (EC2-1-1/2004) are in effect unless otherwise specified in the following paragraphs.
2. The additional rules specified below by EC8-1/2004 are in effect for both DCM and DCH buildings.
3. The part of longitudinal beam reinforcement bent in joints of the frame for anchorage should always be placed inside the corresponding column hoops.
4. The diameter of beam longitudinal reinforcement passing through beam column joints must be in accordance with the following limitations.
   - For interior beam–column joints:

$$\frac{d_{bl}}{h_c} \le \frac{7.5}{\gamma_{Rd}} \cdot \frac{f_{ctm}}{f_{yd}} \cdot \frac{1 + 0.8\nu_d}{1 + 0.75\kappa_D \cdot \rho_2/\rho_{1max}}$$ (8.81)

   - For exterior beam–column joints:

$$\frac{d_{bl}}{h_c} \le \frac{7.5 \cdot f_{ctm}}{\gamma_{Rd} \cdot f_{yd}} \cdot (1 + 0.8\nu_d)$$ (8.82)

where
h_c is the width of the column parallel to the beam
f_{ctm} is the mean value of the tensile strength of concrete
f_{yd} is the design value of the yield strength of steel
ν_d is the normalised minimum design axial force in the column for the seismic design combination ($\nu_d = N_{Ed}/f_{cd} \cdot A_c$)
κ_D is the factor reflecting the ductility class
$\kappa_D = 1.0$ for DCH buildings
$\kappa_D = 0.66$ for DCM buildings
ρ_{1max} is the maximum allowed tension steel ratio in critical regions
ρ_2 is the compression steel ratio

Table 8.3 Maximum diameter sizes for a column width $h_c = 500$ mm.

Concrete				C16	C20	C25	C30	C35	C40	C45	C50	C55	C60
$\varnothing_{L,max}$ (mm)	DCM	$k_D = 2/3$	$+$	17	20	24	26	29	32	35	37	38	40
		$y_{Rd} = 1.0$	$\vdash$	22	25	30	33	36	40	43	47	48	50
	DCH	$k_D = 1.0$	$+$	13	15	18	20	22	24	26	28	29	30
		$y_{Rd} = 1.2$	$\vdash$	18	21	25	28	30	33	36	39	40	42

Steel Class B500c: $f_{yd} = 500/1.15$ MPa, $v_d = 0.40$, $\rho'/\rho_{max} = 0.50$.

> γ_{Rd} is the model uncertainty factor of the design value of resistances, taken as being equal to 1.2 or 1.0 respectively for DCH or DCM

In Table 8.3, the maximum allowed rebar diameters may be found for various concrete classes, for internal and external joints, for steel class B500c, for $\rho_2/\rho_{1max} = 0.50$ and for $v_d = 0.40$ (Ignatakis, 2011).

From the above table it may be concluded that the ratio h_c/d_{bl}, for internal joints, ranges from 38.4 (C16) to 17.8 (C50) for DCH buildings. This means that the requirements imposed by expressions (8.81) and (8.82) are crucial at the prestudy stage for the choice of the dimensions of the columns and the concrete class in relation to the diameters of the rebars that are going to be used in beams. In fact, if the limits of the diameters are small, it will be necessary to have a large number of longitudinal rebars in the beam, closely spaced hoops to avoid buckling and therefore high construction cost together with many problems in concrete casting. In this respect, these requirements appear to have many implications for the design and construction of R/C buildings. However, they have been justified by extensive laboratory tests on interior joints under cyclic loading (Kaku and Asakusa, 1991; Kitayama et al., 1991).

The derivation on the above expressions (8.81) and (8.82) is based on analytical considerations of steel bonding in the joint (Fardis, 2009). These considerations are based mainly on the following assumptions (Figure 8.37):

- Steel bars yield at one face of the joint in tension while at the other face they yield simultaneously in compression (capacity design concept).
- The joint core is confined due to the axial forces of the column.
- Bars are bonded to a length equal to $0.8h_c$.
- In DCH structures the anchorage length of beam or column bars anchored within column–beam joints is measured from a point on the bar at a distance $5d_{bL}$ inside the face of the joint, to take into account the yield penetration due to cyclic inelastic deformations (Figure 8.38a; see Subsection 7.5.4)
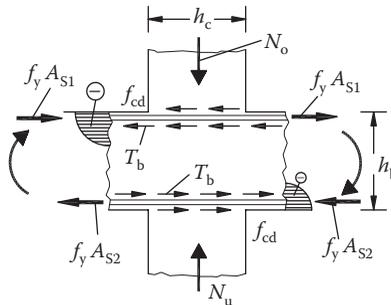
Figure 8.37 Internal force pattern on the bonded rebars in a joint.
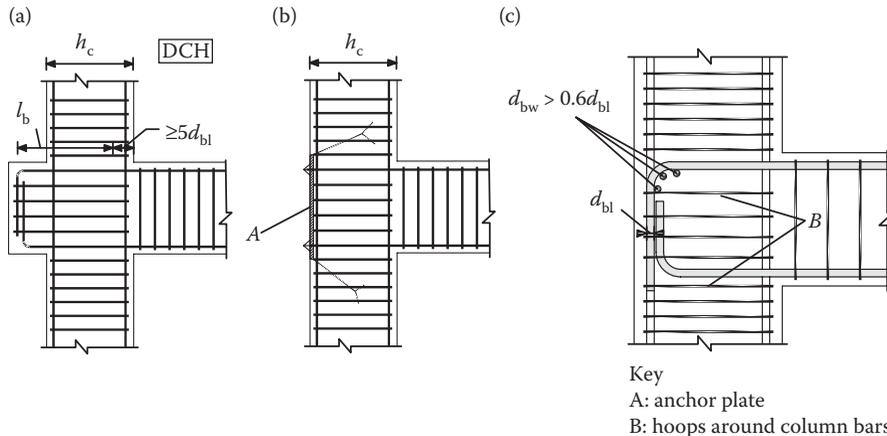
Figure 8.38 Additional measures for anchorage in exterior beam–column joints: (a) beam extension; (b) anchorage plate; (c) bonds and transverse reinforcement. (Adapted from E.C.8-1/EN1998-1. 2004. *Design of Structures for Earthquake Resistance: General Rules, Seismic Actions and Rules for Buildings.* CEN, Brussels, Belgium.)

5. If the requirements of expression (8.82) cannot be satisfied in exterior beam–column joints, because of the limited depth h_c of the column, the following additional measures may be taken to ensure the anchorage of the longitudinal rebars.
   • The beam may be extended horizontally in the form of exterior stubs (Figure 8.38a) if this may be accepted by the architectural design.
   • Headed bars or anchorage plates welded to the end of the bars may be used (Figure 8.38b).
   • Bends with a minimum length of 10 d_{bl} and transverse reinforcement placed tightly inside the bend of the bars may be added (Figure 8.38c). In this case, h_c/d_{bl} may be reduced to 70% of results from expression (8.82). The risk of bond failure for bars under compression in the joint is eliminated due to the closely spaced hoops of the column that encloses the bends.
6. Top and bottom bars passing through joints should terminate in the adjacent beams not less than l_{cr} from the external face of the joint (Figure 8.34).

8.2.5.5 Splicing of bars

1. For splicing of bars, all rules imposed by the Code for conventional R/C structures (EC2-1-1/2004) are in effect, unless it is otherwise specified in the following paragraphs.
2. The additional rules specified below by EC8-1/2004 are in effect for both DCM and DCH buildings.
3. Lap-splicing by welding is prohibited in the critical zones.
4. The following requirements should apply for the transverse reinforcement within the lap length, in addition to the provisions of EC 2-1-1/2004.
   a. If the anchored and the continuing bar are arranged in a plane parallel to the transverse reinforcement, the sum of the area of all spliced bars ΣA_{SL} will be used in the calculation of the transverse reinforcement (Figure 8.39a).
   b. If the splicing is arranged within a plane normal to the transverse reinforcement, the area of the transverse reinforcement will be calculated on the basis of the area of the larger-lapped longitudinal bar A_{SL} (Figure 8.39b).
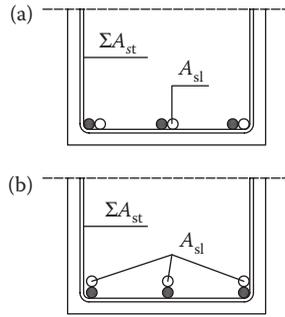
Figure 8.39 Arrangement of slicing bars in relation to the transverse reinforcement: (a) in a plane parallel to the bottom flange of the beams; (b) in planes vertical to the bottom flange.

c.   The spacing s of the transverse reinforcement in the lap zone will not exceed:

$$s = \min\{h/4; 100\}(\text{mm}) \tag{8.83}$$

where h is the minimum cross-sectional dimension.

8.3 DESIGN OF COLUMNS

8.3.1 General

For a thorough examination of the action effects of a column as a component of a seismic-resistant frame, the following diagrams of load effects of a typical internal and a typical external column have been already depicted.

In Figure 8.4, typical M_{Ed}, N_{Ed}, V_{Ed} diagrams are given for the 'basic' combination (i.e. 1.35 G '+' 1.50 Q).

In Figure 8.5, typical M_{Ed}, N_{Ed}, V_{Ed} diagrams are given for the seismic combination W_{dE} '+' E_d.

Based on the examination of the above diagrams, the following remarks should be made:

1. 'Basic' combination 1.35G '+' 1.50Q
   a.   Internal columns exhibit:
      i.   Large axial compressive forces N_{Ed}
      ii. Insignificant bending moments M_{Ed}
      iii. Insignificant shear forces V_{Ed}
   b.   External columns exhibit:
      i.   Large axial compressive forces N_{Ed} but generally smaller than those of the internal columns
      ii. Intermediate bending moments M_{Ed}
      iii. Intermediate shear forces V_{Ed}
2. 'Seismic' combination W_{dE} '+' E_d
   a.   For both internal as well as external columns, axial load effects N_{Ed} exhibit high values, still lower, however, than those corresponding to the 'basic' combination

1.35G '+' 1.50Q, since the partial load coefficients for 'seismic' combination are for gravity loads equal to 1 and for live loads usually equal to $\psi = 0.30$.

b. N_{Ed} exhibits strong variations due to reversals of seismic effect (Figure 8.6), particularly at the external columns of frames with a large aspect ratio H/L.

c. M_{Ed} and V_{Ed} exhibit high values with reversed sign due to the seismic effect reversals.

d. In frame systems, all action effects M_{Ed}, N_{Ed}, V_{Ed} increase from the top to the base of the building (see Paragraph 4.5.2.1).

e. In dual systems, while N_{Ed} of columns increase from the top to the base of the building, M_{Ed} and V_{Ed} do not present serious changes from the top to the base (see Paragraph 4.5.2.4).

3. Concluding remarks

a. Columns are affected by strong axial forces increasing from the top to the base of the building. At the same time, these axial forces exhibit significant variations due to the seismic action reversal.

b. Seismic action also causes large moments and shears increasing from the top to the base of the building, with reversals in sign due to the cyclic character of seismic action.

c. Moment diagrams exhibit their extreme values at the ends of columns, while at their mid-height they are about zero. In this context each column behaves like two cantilevers, each with a span equal to about half of the height of the column, under a cyclic loading $\pm V_{Ed}$ at their free ends and an axial load equal to N_{Ed}.

d. Finally, it should be noted that each column in a frame system belongs to two plane frames orthogonally arranged in the building since the building is a 3-D structure, and in this context columns are induced to biaxial bending with axial loading.

8.3.2 Columns under bending with axial force

8.3.2.1 General

According to most modern Codes of Practice, a linear R/C structural member is characterised as a column when the normalised axial load

$$\boxed{\nu_d = \frac{N_{Ed}}{A_c f_{cd}} \not< 0.10} \tag{8.84}$$

where

N_{Ed} is the normal action effect (compression as positive)

A_c is the area of its cross section

f_{cd} is the design strength of concrete in compression

- The assumptions for the design of R/C column sections under axial load with bending and for the generation of M–φ diagrams are the same as those of R/C beams already presented in Subsection 8.2.2.1.
- Some critical conclusions from the design of orthogonal cross sections under M_{Ed} and N_{Ed} would be useful for the next steps of this chapter, and they are therefore summarised below:
- M–N interaction diagram for an orthogonal symmetrically reinforced cross section under uniaxial bending with axial force in qualitative form is given in Figure 8.40.
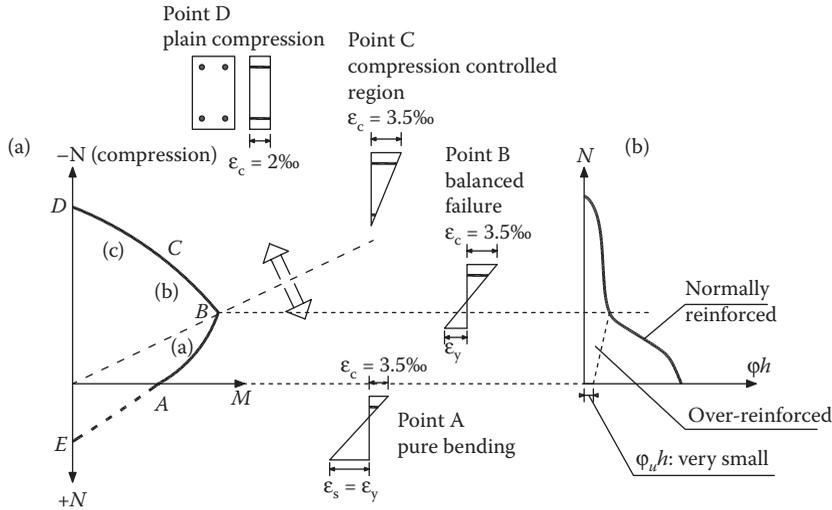
Figure 8.40 (a) $M - N$ interaction diagram for an orthogonal symmetrically reinforced cross section of a column and relevant strain patterns; (b) qualitative presentation of ductility capacity in relation to N. (Adapted from Zararis, P. 2002. *Design Methods of Reinforced Concrete* (in Greek). Kyriakides Bros. Ltd, Thessaloniki.)

- In the same figure, the strain pattern of the cross section is depicted for the three branches (a), (b), (c) of the interaction curve (Figure 8.40b), described below:
  - Branch A–B
    Corresponds to the region (a) of the strain diagram, that is, this branch corresponds to post-yielding strains of steel in tension, and in this context the cross section may develop a post-elastic deformation in terms of curvature.
  - Point B
    Corresponds to *the balanced failure* of the cross section (see Subsection 8.2.2(b)), that is, $\varepsilon_c = \varepsilon_{cu2}$ and $\varepsilon_{s1} = \varepsilon_{y1}$.
  - Branch B–C
    Corresponds to the region (b) of the strain diagram, that is, this branch corresponds to tension steel strains lower than yield.
  - Branch C–D
    Corresponds to the region (c) of the strain diagram, that is, this branch corresponds only to compression concrete strains over the entire cross section.
- The balanced failure (point B) corresponds to a normalised axial load ν ranging between 0.30 and 0.45 (Figure 8.41). This means that for ν greater than or around this value, post-elastic deformations may be achieved either by increasing the strength of concrete so that ν is diminished or by increasing concrete strain at failure through confinement.
- Keeping in mind that for column design the load effects result from a capacity design procedure, according to which potential plastic hinges around the joint develop only at the end of the beams, it is reasonable to consider that ductility supply for the columns is not essential. However, for various reasons the probability of ductility demand at the ends of columns cannot be excluded. Some of these reasons are listed below:
  - The strain hardening of the longitudinal rebars of the beams ranging between 10% and 25% may cause overloading of the beams in terms of bending moments, leading to unacceptable deformations of the ends of the columns
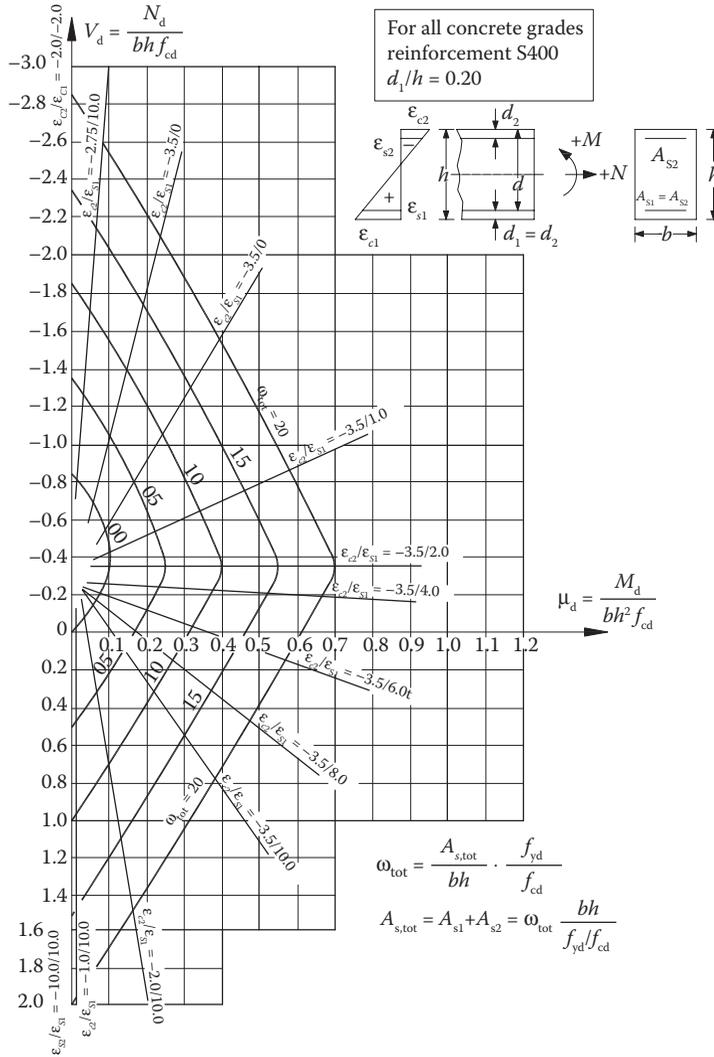
Figure 8.41 Interaction $M - N$ diagrams and the relevant strain patterns at characteristic points. (Adapted from Zararis, P. 2002. *Design Methods of Reinforced Concrete* (in Greek). Kyriakides Bros. Ltd, Thessaloniki.)

in case of non-existence of a controlled capability for post-elastic rotations of their ends (Paulay, 1986).

– As shown in Figure 8.40, the flexural strength of a column is strongly influenced by the axial loading, which is not constant during the seismic action, particularly for columns at the perimeter of the building. This variation of the axial load may easily exceed the values predicted by the analysis, particularly because of unexpected vertical seismic accelerations (Papazoglou and Elnashai, 1996). In this respect, if the column is not in a position to carry the load effects, it is necessary to be in a position of entering into an inelastic range. Therefore, the availability of a quantified ductility capacity should be sought for the columns.

– Dynamic inelastic analysis of multi-storey R/C frames has shown that in order for columns to remain in elastic range all along their height except at their fixed

ends at the foundation, beam overstrength factor γ_{Rd} for the capacity design of the joints should be in the range of 2–2.5, while, as we have seen in Subsection 6.1.4, their codified values, for cost reasons, range between $\gamma_{Rd} \approx 1.10$ and 1.30. Therefore, the need for ductility at the end of columns is again obvious.

– The 3-D functioning of the columns of the frames in a 3-D structure reduces the reliability of the results of the capacity design procedure for the columns (see Subsection 8.3.5).

For these reasons and some others of secondary importance, columns must be designed for axial load and bending as ductile members. In this respect, the inelastic moment–curvature (M–φ) diagram up to failure must be examined as has been done for beams, but taking into account the influence of the axial load, which is based on uniaxial bending considerations.

8.3.2.2 Determination of characteristic points of M–φ diagram and ductility in terms of curvature under axial load for an orthogonal cross-section

From the presentation of beams it is known that three characteristic points must be defined (Figure 8.12):

1. Point A corresponding to cracking stage ($M_{cr} - \varphi_{cr}$)
2. Point B corresponding to steel yield stage ($M_y - \varphi_y$)
3. Point C corresponding to failure stage ($M_u - \varphi_u$)

It is apparent that these three points for the same R/C cross section have different coordinates each time, depending on the axial load.

In the following paragraph, closed expressions will be developed for an orthogonal cross section using some approximations that simplify the whole procedure (Park and Paulay, 1975; Penelis and Kappos, 1997; Fardis, 2009). For cross sections of any complex form and reinforcement, computer platforms have been developed to allow the determination of points A, B and C (e.g. RCCOLA-90, NOUS, 2005 Papanikolaou, 2012). The theoretical background of NOUS (2005) has already been presented for beams and can also be used for columns.

8.3.2.2.1 Point A: $M_{cr} - \phi_{cr}$

Keeping in mind from classic strength of materials that (Figure 8.42):

$$\sigma_{M+N}^{max} = \frac{M}{bh^2/6} - \frac{N}{bh} \leq f_{ctm,fl} \tag{8.85}$$

(+N for compression)

$$\sigma_M = M/bh^2/6 \qquad \sigma_N = \frac{N}{bh} \qquad \sigma_{M+N} \leq f_{ctm,fl}$$
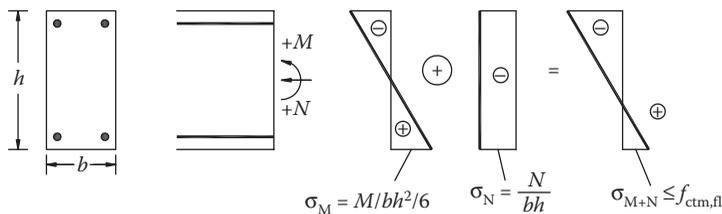
Figure 8.42 Stress pattern of a column under bending M with axial force N before cracking.

the following expressions may be obtained:

$$M_{cr} = f_{ctm,fl} \frac{bh^2}{6} + N\frac{h}{6}$$

$$\varphi_{cr} = \frac{M_{cr}}{E_c bh^3/12}$$

(8.86a–b)

where
$f_{ctm,fl}$ is the mean tensile strength of concrete to flexure
E_c is the modulus of elasticity of concrete

All other symbols are given in Figure 8.42.

It is obvious that for the same cross section the coordinates of point A increase with an increase of axial force N.

8.3.2.2.2 Point B: $M_y – \phi_y$

Consider a column with orthogonal cross section, double-reinforced (Figure 8.43) and loaded by a constant compressive axial load N and a uniaxial bending moment M increasing from M_{cr} to yield of the reinforcement in the tensile zone.

The following normalised parameters will be introduced in the following presentation.

1. Normalised axial force:

$$\nu = \frac{N}{dhf_c}$$

(8.87a)

2. Percentage of reinforcement under tension:

$$\rho_1 = \frac{A_{s1}}{bh}$$

(8.87b)

3. Percentage of reinforcement under compression:

$$\rho_2 = \frac{A_{s2}}{bh}$$

(8.87c)

4. Percentage of web longitudinal reinforcement:

$$\rho_v = \frac{A_{sv}}{bh}$$

(8.87d)
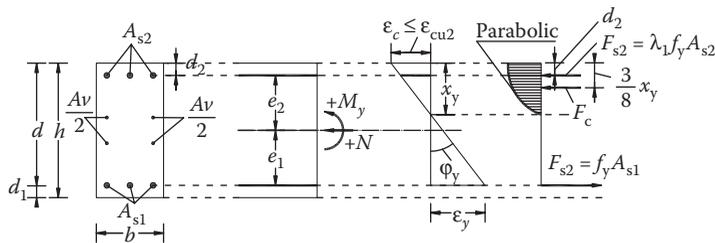
Figure 8.43 Strain and stress pattern of an R/C column at yield.

The following assumptions are taken also into account for the derivation of the main expressions:

- $d \cong 0.9h$
- $\sigma_c \cong f_c$, which is a reasonable approximation for bending with axial load at yield.
- The stress pattern of concrete is parabolic at yield.
- $\sigma_{s2} = \lambda_1 f_y$, where $\lambda_1 \leq 1$ (stress of the reinforcement A_{s2} in the compression zone).

From the strain pattern at yield, depicted in Figure 8.43 and under the above assumptions, the equilibrium between external loading and internal forces gives

$$N = F_c + F_{s2} + F_{sv} - F_{s1} \tag{8.88}$$

or

$$\nu f_c b \cdot h = \frac{2}{3} f_c b \cdot x_y + \lambda_1 f_y \rho_2 b \cdot h + \rho_v f_y b \cdot h - f_y \rho_1 b \cdot h \tag{8.89}$$

$$\nu f_c = \frac{2}{3} f_c \xi_y \frac{d}{h} + \lambda_1 f_y \rho_2 - f_y \rho_1 + \rho_v f_y \tag{8.90}$$

or

$$\boxed{\xi_y = \frac{1}{0.6}\left(\nu + (\rho_1 - \lambda_1 \rho_2 + \rho_v)\frac{f_y}{f_c} \right)} \tag{8.91}$$

Parametric investigations (Tassios, 1989) have led to the following values for λ_1
- For

$$\nu < 0.1 \text{ ('beams') : } \lambda_1 = 0.5 + 18\rho_1 \tag{8.92a}$$

- For

$$\nu = 0.1 : \lambda_1 \cong 2/3 \tag{8.92b}$$

- For

$$\nu = 0.2 : \lambda_1 \cong 0.9 \tag{8.92c}$$

- For

$$\nu > 0.2 : \lambda_1 \cong 1.0 \tag{8.92d}$$

It should be noted that ν usually ranges between 0.20 and 0.60.

The value of ξ_y determined above must be compared to $\xi_b = \frac{x_b}{d} = 0.58$ (for steel class B500c see par. 8.2.2.2), which corresponds to the *balanced failure* of a cross section.

If $\xi_b < 0.58$ failure at yield prevails and the procedure continues as in the following paragraph, or else brittle failure of concrete precedes steel yielding and the procedure ends here.

In the case that $\xi_b < 0.58$, the corresponding bending moment M_y at yield may be determined using the moment equilibrium equation between external loading and internal forces with respect to the reinforcement in tension, that is,

$$M_y = f_{s2}0.9d + \frac{2}{3}f_cbd^2\xi_y\left(1 - \frac{3}{8}\xi_y\right) - Ne_1 \tag{8.93}$$

or

$$M_y = bd^2\left[\lambda_1 f_y\rho_2 + \frac{2}{3}f_c\xi_y\left(1 - \frac{3}{8}\xi_y\right)\right] - Ne_1 \tag{8.94}$$

Remark

The moments of web reinforcement A_v are not taken into account because their influence is very small.

The curvature of the cross section at yield results from the relation:

$$\varphi_y = \frac{\varepsilon_y}{d - x_y} = \frac{\varepsilon_y}{d(1 - \xi_y)} \tag{8.95}$$

Equations 8.91, 8.94 and 8.95 allow the determination point B of the M–φ diagram.

8.3.2.2.3 Point C: $M_u - \phi_u$

Taking into account that the strain pattern of the cross section for this point of the diagram is depicted in Figure 8.44, it may be concluded that

$$x_u = \frac{\varepsilon_{cu2}}{\varepsilon_{cu2} + \varepsilon_s}d \tag{8.96}$$

Assuming that the stress pattern of concrete is orthogonal (Figure 8.44) at failure and that the same expression is in effect for σ_{s2} as at yield, that is, $\sigma_{s2} = \lambda_1 f_y$, the equilibrium equation between internal forces and external loading gives

$$N = F_{cut} + F_{s2u} + F_{svu} - F_{s1u} \tag{8.97}$$

or

$$\nu f_c bh = 0.8f_c bx_u + \lambda_1 f_y\rho_2 bh + \rho_v f_y bh - f_y\rho_1 bh \tag{8.98a}$$
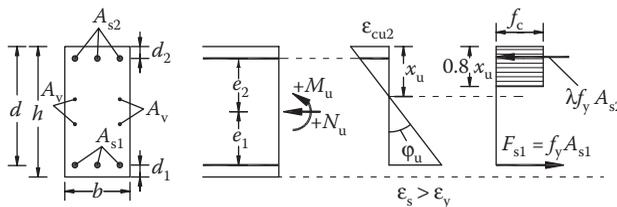
Figure 8.44 Strain and stress pattern of an R/C column at failure.

$$\nu f_{\mathrm{c}} = 0.8 f_{\mathrm{c}} \xi_{\mathrm{u}} \frac{d}{b} + \lambda_1 f_{\mathrm{y}} \rho_2 + \rho_{\mathrm{v}} f_{\mathrm{y}} - f_{\mathrm{y}} \rho_1 \tag{8.98b}$$

$$\xi_{\mathrm{u}} = \frac{1}{0.72}\left(\nu + (\rho_1 - \lambda_1 \rho_2 + \rho_{\mathrm{v}})\frac{f_{\mathrm{y}}}{f_{\mathrm{c}}}\right) \tag{8.99a}$$

Taking into account that for columns under seismic action $\rho_1 = \rho_2$ and that ν is usually greater than 0.20, the above expression takes the following form:

$$\xi_{\mathrm{u}} = \frac{1}{0.72}\left(\nu + \rho_{\mathrm{v}}\frac{f_{\mathrm{y}}}{f_{\mathrm{c}}}\right) = \frac{1}{0.72}(\nu + \omega_{\mathrm{v}}) \tag{8.99b}$$

where

ω_{v} is the mechanical ratio of web reinforcement $\left(\omega_{\mathrm{v}} = \dfrac{A_{\mathrm{sv}}}{bb}\dfrac{f_{\mathrm{y}}}{f_{\mathrm{c}}}\right)$.

The corresponding bending moment M_{u} at failure may be determined using the moment equilibrium equation between external loading and internal forces with respect to the reinforcement at tension, that is,

$$M_{\mathrm{u}} = F_{\mathrm{s2}}0.9d + 0.8x_{\mathrm{u}}f_{\mathrm{c}}b(d - 0.4x_{\mathrm{u}}) - N \cdot e$$

or

$$M_{\mathrm{u}} = bd^2\left[\lambda_1 f_{\mathrm{y}}\rho_2 + 0.8 f_{\mathrm{c}}\xi_{\mathrm{u}}(1 - 0.4\xi_{\mathrm{u}})\right] - N \cdot e \tag{8.100}$$

The curvature of the cross section at failure has the following form:

$$\varphi_{\mathrm{u}} = \frac{\varepsilon_{\mathrm{cu2}}}{x_{\mathrm{u}}} = \frac{\varepsilon_{\mathrm{cu2}}}{\xi_{\mathrm{u}}d} \tag{8.101}$$

Equations 8.99b, 8.100 and 8.101 allow the determination of point C of the M–φ diagram. The above equations are in effect under the following assumptions:

- σ–ε diagram of steel is elastoplastic without strain hardening
- A_{s2} has not buckled

8.3.2.2.4 Ductility μ_{φ} of the column

Ductility μ_{φ} of the column is obtained by the following expression:

$$\mu_{\varphi} = \frac{\varphi_{\mathrm{u}}}{\varphi_{\mathrm{y}}} \tag{8.102}$$

Introducing φ_{u} and φ_{y} into the above expression from Equations 8.95 and 8.101 results in

$$\mu_{\varphi} = \frac{\varepsilon_{\mathrm{cu2}}}{\varepsilon_{\mathrm{y}}}\frac{1 - \xi_{\mathrm{y}}}{\xi_{\mathrm{u}}} \tag{8.103}$$

or

$$\mu_\varphi = 1.2 \frac{\varepsilon_{cu2}}{\varepsilon_y} \left[\frac{0.60}{v + (\rho_1 - \lambda_1 \rho_2 + \rho_v)} - 1 \right]$$

(8.104a)

Taking into account that $\lambda_1 = 1$ and $\rho_1 = \rho_2$, the above expression takes the following form:

$$\mu_\varphi = 1.2 \frac{\varepsilon_{cu2}}{\varepsilon_y} \left[\frac{0.60}{v + \omega_v} - 1 \right]$$

(8.104b)

The above equations (8.104a) and (8.104b), although approximate, offer an effective tool for the study of the parameters that influence the value of μ_φ. In fact, if it is taken into account that:

- For columns under seismic action $\rho_1 = \rho_2$
- v is usually greater than 0.20 and therefore $\lambda_1 = 1$
- For concrete classes between C20 and C50 $\varepsilon_{cu2} = 3.5\text{‰}$
- For conventional steel the reinforcement class is B500c, that is, $\varepsilon_y = \dfrac{500}{200 \cdot 10^3} = 2.5$

μ_φ takes the following form:

$$\mu_\varphi = 1.2 \frac{3.5}{2.5} \left(\frac{0.60}{v + \omega_v} - 1 \right)$$

(8.104c)

where

$\omega_v = \rho_v \dfrac{f_c}{f_y}$ is the mechanical percentage of longitudinal steel in web.

The above expression (8.104c) for $v \geq 0.33$ and $\omega_v \cong 0.00$ results in μ_φ having a value $\mu_\varphi \leq 1$. This conclusion is in agreement with what has been mentioned in Paragraph 8.3.2.1. Even for $v \cong 0.20$, which is a rather low value for v in the design of columns, the above expression results in:

$$\mu_{\varphi\,supl} \cong 1.2 \frac{3.2}{2.5} \left(\frac{0.60}{0.20} - 1 \right) \cong 3.36$$

This is a very low value for $\mu_{\varphi supl}$, even for this low normalised axial load, if it is taken into account that according to Equations 5.52a and 5.52b $\mu_{\varphi demand}$ must be higher than

$$\mu_\varphi = 2q_o - 1 \qquad \text{if} \quad T_1 \geq T_c$$

$$\mu_\varphi = 1 + 2(q_o - 1)\frac{T_c}{T_1} \qquad \text{if} \quad T_1 < T_c$$

In this respect, in order for the expression:

$$\mu_\varphi^{demand} \leq \mu_\varphi^{supply}$$

(8.105)

to be fulfilled, *the only way is the confinement of the critical zones of the columns with hoops* so that ε_{cu2} is increased in Equation 8.104b to the required degree so that the above inequality (8.105) is accomplished.

It should be added here that the expression of μ_φ adopted by EC 8-1/2004 has a different starting point. It is based on the assumption that φ_y may be expressed by the following semi-empirical equation:

$$\varphi_y = \frac{\kappa \varepsilon_y}{h} \tag{8.106}$$

where κ has the following values:

$\kappa = 1.75$ for rectangular beams and columns
$\kappa = 1.44$ for rectangular walls
$\kappa = 1.57$ for T, U or hollow rectangular section

The above semi-empirical expression (8.106) is based on procedures best fitting with experimental results (Biskinis, 2007; Fardis, 2009).

Taking into account the above expressions (8.101) and (8.106), μ_φ takes the form:

$$\mu_\varphi = \frac{\varphi_u}{\varphi_y} = \frac{\varepsilon_{cu2} h}{\xi_u d \cdot \kappa \cdot \varepsilon_y} = \frac{\varepsilon_{cu2}}{\varepsilon_y} \frac{h}{d} \frac{0.72}{(\nu + \omega_v) \cdot \kappa}$$

or

$$\mu_\varphi = \frac{\varepsilon_{cu}}{\varepsilon_y} \frac{0.72}{0.9 \cdot \kappa(\nu + \omega_v)} \cong 0.80 \frac{\varepsilon_{cu}}{\kappa \cdot \varepsilon_y(\nu + \omega_v)} \tag{8.107}$$

This equation will be used in Subsections 8.3.4 and 9.2.4 for the determination of the required confinement reinforcement of the critical regions of columns and ductile walls, according to their ductility class.

8.3.2.3 Behaviour of columns under cyclic loading

- As has already been noted in Paragraphs 4.5.2.1 and 4.6.3.2, column failure in frame or frame-equivalent systems has destructive consequences for the building because of the loss of support for storeys above, and therefore of the risk of a pancake type collapse. So, a special concern should be given to column protection from flexural or shear failure.
- The basic difference between beam and column behaviour under cyclic loading is attributable to the axial compressive load of the column. Extensive laboratory research has focused the influence of the axial loading to column behaviour under cycling bending on the following consequences:
  - Failure to flexure depends significantly on the value of the compressive force N (Figures 8.40 and 8.45). For increasing values of N from zero to N-balance, bending moments also increase with parallel decrease of the capacity of the column for post-elastic deformation. For a further increase of N beyond the balance point, the moment at failure decreases with a parallel drastic diminishing of the post-elastic deformation of the column.
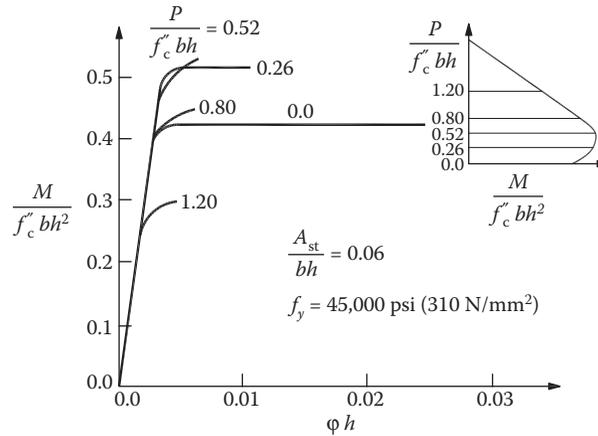
Figure 8.45 Moment—curvature curves for column sections at various levels of axial load. (From Park, R. and Paulay, T. 1975. *Reinforced Concrete Structures.* Copyright Wiley-VCH Verlag GmbH & Co. KGaA. Reproduced with permission.)

- The axial compressive strain caused by axial loading is added to the compressive strain due to bending at the compression zone at each cycle. As a result, concrete degradation accompanied by spalling and crushing in the compressive zone, and therefore also steel rebar buckling, is almost inevitable, unless adequate *confinement* by means of closely spaced hoops in the critical regions is specified.
- Flexural and shear cracks formed in each loading semi-cycle tend to close during the reversing semi-cycle that follows due to axial load. This has as a consequence the diminishing of the pinching effect on the hysteresis loops of cycling loading, which are present in the case of beams. Additionally, concrete disintegration due to shear failure does not prevail, and therefore it is reasonable for axial load favourable contribution to shear to be taken into account in the shear design.
- The change of the axial force N during a cyclic seismic action, caused mainly by the overturning moment of the building (see Paragraph 4.5.2.1) to the columns of the perimeter, leads to asymmetric hysteresis loops (see Figure 8.46) due to the variation of the axial load of the column.
- Axial tension is not impossible in external columns, particularly in buildings with high aspect ratio, *H/L* (see Figure 8.6). In this case the hysteresis loops tend to have zero area, and therefore the capacity of the column for energy dissipation is eliminated.
- Finally, it should be noted that in the case of large inter-storey drifts, second-order effects influence in an adverse way the bending moment at failure.

8.3.3 Strength and deformation of columns under prevailing shear

8.3.3.1 General

Column design to shear follows the same procedure under either static or dynamic loading, as in the case of beams (Subsection 8.2.3), taking into account in the case of columns the beneficial influence of the compressive axial force to shear. *This allows the concrete contribution to shear to be taken into account* for both ductility classes (DCM and MCH). In this respect, x-shaped reinforcement in the critical regions is not obligatory for columns under seismic action.

(a)

(b)
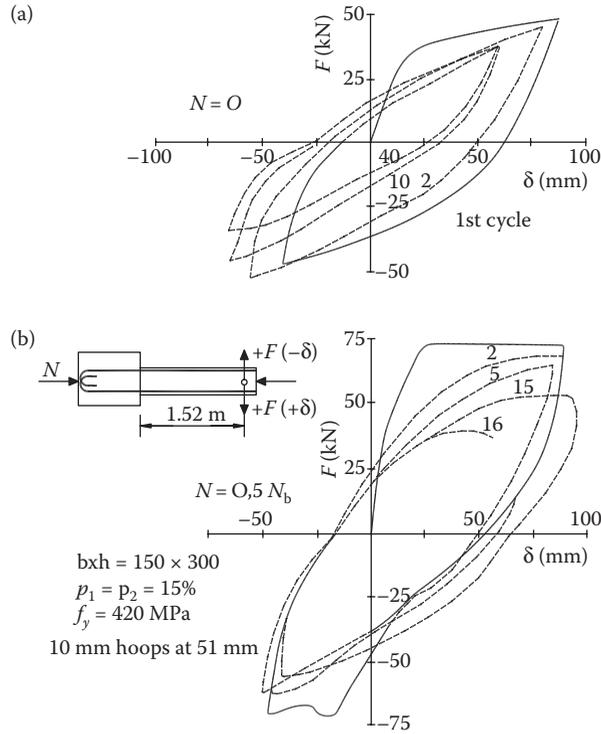
Figure 8.46 Hysteresis loops of elements under flexure and axial loading at various levels: (a) axial load N = 0; (b) axial load N = 0.5 N_b. (Adapted from Jirsa, J.O. 1974. Factors influencing behaviour of reinforced concrete members under cyclic overloads. *Proceed of 5th World Conf. on Earthq. Eng.* June 1973, Rome, Italy, 2 pp. 1198–1204.)

Reference should be made here again to the following remarks from the presentation of beams:

- For shear span-to-depth ratio:

$$\frac{\alpha}{d} = \frac{M_{Eu}}{V_{Eu}d} \geqq 7.0 \tag{8.108}$$

  bending prevails, and in this case bending failure occurs before any shear failure, no matter if shear reinforcement exists or not.
- For shear span-to-depth ratio:

$$2.0 \leqq \frac{\alpha}{d} \leqq 7.0 \tag{8.109}$$

  the failure mode depends on the shear reinforcement of the web. For columns of conventional R/C structures, the main concept of the design is that both shear and bending strengths satisfy the strength inequalities (see Subsection 3.2.1, Equation 3.1a and b) for the corresponding load effects resulting from the analysis. In this respect, bending failure is likely to precede or be simultaneous with shear failure. For columns of earthquake-resistant R/C structures, special concern is given to the requirement that a column must yield at both its ends before shear failure. Therefore, shear effects derive from the capacity design procedure (see Subsection 6.1.4).

- For shear span-to-depth ratio:

$$\frac{\alpha}{d} \leqq 2.0 \tag{8.110}$$

that is, in the case of short R/C columns, a special design procedure must be followed so that an explosive cleavage failure of the short column is avoided (see Subsection 8.3.6).

From the above presentation it may be concluded that in this section only the design of regular R/C columns will be dealt with, that is, columns with shear-span ratio:

$$\frac{\alpha}{d} = \frac{M_{Ed}}{V_{Ed}} \geqq 2.0$$

Short columns will be discussed in detail in Subsection 8.3.6.

8.3.3.2 Shear design of rectangular R/C columns

Failure under shear of a reinforced column with longitudinal rebars on both sides and transverse hoops may occur, as in the case of a beam failing to *diagonal tension* (Figure 8.23a) or *diagonal compression* (Figure 8.23b).

8.3.3.2.1 Failure caused by diagonal tension

As was noted in Subsection 8.2.4 for beams, this type of failure is resisted by two mechanisms, that is:

- Beam action in the shear span without web reinforcement
- Truss mechanism of web reinforcement (stirrups—bent-up rebars)

8.3.3.2.1.1 SHEAR RESISTANCE IN THE SHEAR SPAN WITHOUT REINFORCEMENT

According to EC2-1/1991 ENV, in order for the beneficial influence of a compressive axial force N (N compressive is introduced with positive sign) to be taken into account, an additional term is introduced in Equation 8.52, that is,

$$\boxed{V_{Rdc} = \tau_{Rd} \cdot \kappa(1.20 + 40\rho_1 + 0.15\sigma_{cp})b_w d} \tag{8.111}$$

where

$$\sigma_{cp} = N_{Ed}/A_c \tag{8.112}$$

N_{Ed} is the axial force due to loading or prestress. The meaning of all other symbols may be found in Paragraph 8.2.4.1 for beams.

A similar expression has also been adopted by the American Codes (ACI 318-2005, 2008, 2011), as well as by the Codes of many other countries.

Eurocode EC2-1-1/2004 has adopted for the determination of V_{Rdc} the following expression in the case of existence of an axial load:

$$\boxed{V_{Rdc} = \left[C_{Rd,c} \cdot \kappa(100\rho_1 f_{ck})^{1/3} + \kappa_1 \sigma_{cp} \right] b_w d} \tag{8.113}$$

and not less than ($V_{Rd,c}$ min):

$$\boxed{V_{Rd,c\,min} = (0.035\kappa^{3/2}f_{ck}^{1/2} + \kappa_1\sigma_{cp})b_w d}$$

(8.114)

where
  κ_1 is a coefficient with a recommended value of 0.15
  N_{Ed} is the axial force in section caused by loading or prestress (N)
  A_c is the area of the concrete section (mm²)

$$\boxed{\sigma_{cp} = N_{Ed}/A_c \leq 0.2f_{cd} \quad (MPa)}$$

(8.115)

$V_{Rd,c}$ is in (N).

8.3.3.2.1.2 TRUSS MECHANISM OF WEB REINFORCEMENT—ALTERNATIVE (A)

As was explained in Paragraph 8.2.4.1.1.2 in the beam case, the truss mechanism, according to ACI 318-2005-2011, is based on the concept of concrete strut diagonals with a constant indication of 45°. The same assumption was also in effect in EC2-1-1/1991 ENV. According to this assumption, even in the case of the existence of an axial compressive load, the shear resistance by the column web reinforcement is given by the expression:

$$\boxed{V_{wd} = \frac{A_{sw}}{s}0.9d \cdot f_{ywd}}$$

(8.116)

The meaning of all symbols above has been defined for the relevant equation for beams (8.55).

Taking all the above into account, it may be concluded that, as in the case of columns, shear strength to diagonal tension is equal to

$$V_{Rd} = V_{Rdc} + V_{wd}$$

(8.117)

The beneficial influence of the compressive axial force has been incorporated above in V_{Rdc}.

8.3.3.2.1.3 TRUSS MECHANISM OF WEB REINFORCEMENT—ALTERNATIVE (B)

A different procedure has been followed by EC2-1-1/2004 for failure caused by diagonal tension for both beams and columns. In the case that V_{Ed} exceeds the value of V_{Rdc} given by Equation 8.113 and 8.114, *the truss model analogy with concrete struts of variable inclination is applied.*

In this context, as was explained in the case of beams:

$$\boxed{V_{wd} = V_{Rd} = \frac{A_{sw}}{s}0.9d \cdot f_{ywd} \cot\delta}$$

(8.118)

where (Equation 8.59b):

$$2.5 \geq \cot\delta \geq 1.0$$

It should be remembered that in the above expression (8.118) both mechanisms of Equations 8.113 and 8.116 *are incorporated into one* that is *'the variable inclination strut'*.

The beneficial influence of compressive axial force in this procedure is incorporated into the capacity of cot δ to take values closer to 2.5 (more inclined struts), since, as we will see later, $V_{\text{Rd max}}$ increases due to N_{Ed}.

8.3.3.2.2 Failure caused by diagonal compression

As was explained in the case of beams, for the determination of *diagonal concrete crushing* 'the truss analogy' model is used, taking into account the influence of the axial load, that is:

- For δ = 45° (ACI 318-2011, EC2-1-1/1997 ENV)

$$V_{\text{Rd max}} = \alpha_{\text{cw}} b_{\text{w}} 0.9d(\nu_1 f_{\text{cd}})/2 \tag{8.119}$$

- For 2.5 ≥ cot δ ≥ 1.0 (EC2-1-1/2004)

$$V_{\text{Rd max}} = \alpha_{\text{cw}} b_{\text{w}} 0.9d(\nu_1 f_{\text{cd}}) \cot \delta/(1 + \cot^2 \delta) \tag{8.120}$$

Particularly for columns or prestressed members, according to EC2-1-1/2004, the following values are recommended for α_{cw} (Figure 8.47):

$$\alpha_{\text{cw}} = 1 + \sigma_{\text{cp}}/f_{\text{cd}} \quad \text{for} \quad 0 < \sigma_{\text{cp}} \leq 0.25 f_{\text{cd}} \tag{8.121a}$$

$$\alpha_{\text{cw}} = 1.25 \quad \text{for} \quad 0.25 f_{\text{cd}} < \sigma_{\text{cp}} \leq 0.55 f_{\text{cd}} \tag{8.121b}$$

$$\alpha_{\text{cw}} = 2.50(1 - \sigma_{\text{cp}}/f_{\text{cd}}) \quad \text{for} \quad 0.5 f_{\text{cd}} < \sigma_{\text{cp}} \leq 1.0 f_{\text{cd}} \tag{8.121c}$$

The meaning of the above symbols has been clarified in the relevant Equations 8.61 and 8.62 for beams.

In this context, in case of compressive axial force, $V_{\text{Rd max}}$ increases and therefore the relevant value of cot δ in Equation 8.118 may be higher, leading to a lower requirement for web shear reinforcement.
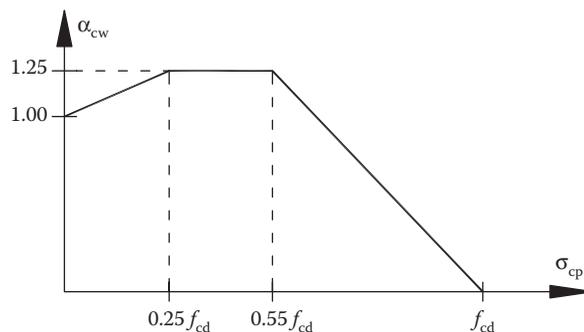
Figure 8.47 Increase of web crushing capacity to shear by axial compression or prestressing. (Adapted from Walraven, J.C. 2002. Delft, University of Technology, Background document for EN1992-1-1. Eurocode 2: Design of Concrete Structures-Chapter 6.2: Shear, Delft.)

8.3.3.2.3 Design procedure for columns under shear

Based on the above presentation, an overview of the design procedure for columns under shear according to Codes in use would be useful.

- *Step 1*: Determine span-to-depth ratio:

$$\frac{\alpha}{d} = \frac{M}{V \cdot d}$$

   If $\frac{\alpha}{d} \cong 2.0$, the following procedure will be followed:
- *Step 2*: Shear resistance V_{Rdc} of the column without web reinforcement is determined using Equation 8.111 (EC2-1/1991 ENV) or using Equation 8.113 (EC2-1-1/2004). If $V_{Ed} \leq V_{Rdc}$, web reinforcement is not required.
   However, minimum web reinforcement in the form of hoops must be foreseen to secure the column form a potential brittle failure to shear.
- *Step 3*: In the case that:

$$V_{Ed} \geq V_{Rdc}$$

   two different procedures are foreseen depending on the Code under consideration:
   - In the case that ACI 318-2011 is in effect, design shear force V_{Ed} must be less than the sum of the shear contribution of the concrete V_{Rdc} (Equation 8.111; beam action) and the shear contribution of the web reinforcement V_{wd} (Equation 8.116), under the assumption that concrete struts exhibit a constant indication $\delta = 45°$, that is (Equation 8.64):

$$\boxed{V_{Ed} \leq V_{Rdc} + V_{wd}}$$

   This expression allows the determination of the required web shear reinforcement. It is obvious that the beneficial influence of a compression axial force is included in V_{Rdc}.
   At the same time, the concrete struts must have a safety factor sufficient to resist crushing. Therefore, V_{Ed} must also satisfy the following expression (Equation 8.65):

$$\boxed{V_{Ed} \leq V_{Rd\,max}}$$

   for $\delta = 45°$
   $V_{Rd\,max}$ is given in Equation 8.119.
   - In the case that EC2-1-1/2004 is in effect, design shear force must be covered by the *truss model analogy* with concrete struts of *variable inclination* simultaneously for both the web reinforcement yield and concrete inclined struts crushing, that is,

$$\boxed{\begin{aligned} V_{Ed} \leq V_{Rd} &= \frac{A_{sw}}{s} 0.9 d f_{ywd} \cot\delta \\ V_{Ed} \leq V_{Rd\,max} &= \alpha_{cw} b_w 0.9 d (\nu_1 f_{cd}) \cot\delta/(1 + \cot^2\delta) \end{aligned}}$$

(8.122a–b)

where

$$21.8° \leq \delta \leq 45°$$

The accomplishment of both expressions (8.122a) and (8.122b) is satisfied by successive trials. It should be noted here that the beneficial influence of N_{Ed} is included in Equation 8.122b and particularly in the coefficient α_{cw}.

• *Step 4*: In the case that the span-to-depth ratio (shear-span ratio) is

$$\frac{\alpha}{d} \leqq 2.0$$

a special procedure must be followed (see Section 8.4).

In closing, it would be worthwhile to repeat here that, thanks to compressive axial load, columns do not exhibit crosswise widening bending and shear cracks from cycle to cycle of seismic loading. This allows the shear strength contribution to be taken into account in the shear design of columns under seismic action. In this context, in the procedure imposed by EC2-1-1/2004, the inclination of concrete struts *also continues to be considered variable* in the case of seismic design for all ductility classes. At the same time, x-shaped reinforcement in the critical regions of the column is not obligatory.

8.3.4 Code provisions for columns under seismic action

8.3.4.1 General

The design rules for columns under seismic actions according to EC8-1/2004 are given below, together with the required justification in terms of the theory developed in the previous subsections. It should be noted that the design specifications, as in the case of beams, are directly related with the class of ductility demand, that is, DCL, DCM and DCH. For higher ductility classes they tend to be stricter in order to obtain a higher local ductility in terms of curvature.

Specifications for the design effects, taking into account capacity design procedure, have already been presented for columns in Subsection 6.1.4.

Material issues have also been presented in Subsections 7.2.4, 7.3.5 and 7.5.4 for all ductility classes. It should also be mentioned here that for the design of columns of buildings of class DCL, Code specifications for conventional R/C structures are applied (EC2-1-1/2004), except that concrete and steel reinforcement qualities are specified by EC 8-1/2004 and have already been presented in Chapter 7. For this reason, design of columns for DCL buildings will not further occupy our attention in this book.

In closing, it should be noted that all rules and specifications of the corresponding Code for conventional R/C structures (EC2-1-1/2004) continue to be in effect unless they contradict what will be presented below.

8.3.4.2 Design of columns for DCM buildings

8.3.4.2.1 Geometrical constraints

Unless $\theta \leq 0.1$ (see Paragraph 6.2.2.2), the cross-sectional dimensions of columns should not be smaller than 1/10 of the larger distance between the point of contra-flexure and the ends of the column.

8.3.4.2.2 Resistance to flexure with axial load and shear

Flexural and shear resistance will be determined in accordance with EC2-1-1/2004, that is, as in the case of conventional R/C buildings, using the value of the axial force from the analysis of the seismic design combination.

- Biaxial bending, which is the usual case, may be simplified by substituting two uniaxial bending situations for it, one for every main direction, introducing a reduction of 30% in the uniaxial bending resistance of the cross section, that is:

$$\boxed{0.7M_{\mathrm{Rid}}(N_{\mathrm{Ed}}) \geq M_{\mathrm{Eid}}\ (i = x,y)}$$

(8.123)

  where
  M_{Eid} is the acting bending moment, in $i = x,\ y$ directions
  N_{Ed} is the most unfavourable axial load resulting from the seismic combination
  M_{Rid} is the bending strength under N_{Eid} in $i = x,\ y$ direction

  The above simplification is insignificant, if it is taken into account that today there are computer platforms that can carry out the biaxial verification very easily and quickly (e.g. NOUS, 2005; RCCOLA-90, FAGUS, 2012).

- In columns of seismic-resistant frames, the value of the normalised axial force ν_{d} should comply with the following expression:

$$\boxed{\nu_{\mathrm{d}} = \frac{N_{\mathrm{Ed}}}{A_{\mathrm{c}}f_{\mathrm{cd}}} \leq 0.65}$$

(8.124a)

  where
  N_{Ed} is the design axial force
  A_{c} is the area of the cross section of the column
  f_{cd} is the design concrete strength

  Taking into account that $f_{\mathrm{cd}} = \dfrac{f_{\mathrm{ck}}}{1.50}$, it may be concluded that:

$$\nu_{\mathrm{d}} = 1.50\ \nu$$

and therefore,

$$\boxed{\nu \leq \frac{0.65}{1.50} \cong 0.43}$$

(8.124b)

  that is, this requirement ensures that ν is very near to ν_{balance} (see par. 8.3.2.1).

8.3.4.2.3 Detailing of columns for local ductility

- *The critical regions* of a column are defined as the regions of a length l_{cr} quantified below and measured from the two ends of the column to its height. As has already been explained, these are regions of potential plastic hinges (Figure 8.48).
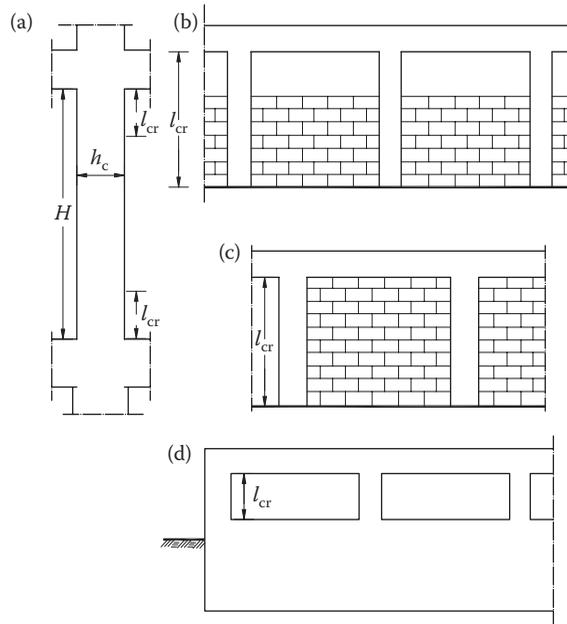
Figure 8.48 Column critical regions.

- *The length of the critical region* l_{cr} (in meters) may be determined from the following expressions:

$$l_{cr} = \max\{h_c; l_c/6; 0.45\} \tag{8.125}$$

where
  h_c is the largest cross-sectional dimension of the column (in meters)
  l_c is the clear length of the column (in meters)

- *If $l_c/h_c < 3$ (short column)*, the entire height of the column should be considered a critical region. This type of column will be examined separately and in detail in the next section.
- *The total longitudinal reinforcement* ρ_l should not be less than 0.01 and not more than 0.04, that is,:

$$0.01 \leq \rho_l \leq 0.04 \tag{8.126}$$

  and should be arranged symmetrically in symmetric cross sections ($\rho_1 = \rho_2$).
- At least one intermediate bar should be provided between corner bars along each column side, to ensure the integrity of the beam–column joints.
- In the critical region *at the base* of the columns, a value of the curvature ductility factor μ_φ should be provided, equal to that given to the critical region of beams (see Paragraph 8.2.5.2.3, Equations 5.52a and 5.52b). In all other critical regions of the columns, the required local ductility is deemed to be covered by the confinement specified in subsequent paragraphs *without quantitative verification*.

- Particularly in the critical region at the base of a column, the above-mentioned requirement will be satisfied by a proper confinement of the critical region by means of hoops, which will allow the enhancement of the strain capacity of concrete from −0.0035 to a higher value, ensuring the development of a quantified post-elastic deformation without concrete spalling. This requirement is deemed to be satisfied if

$$\alpha\,\omega_{wd} \geq 30\mu_\varphi v_d \varepsilon_{syd} \frac{b_c}{b_o} - 0.035 \qquad (8.127)$$

where (Figure 8.49):

ω_{wd} is the mechanical volumetric ratio of confining hoops within the critical region.

$$\left[\omega_{wd} = \frac{\text{volume of confining hoops}}{\text{volume of concrete core}} \cdot \frac{f_{yd}}{f_{cd}} \right] \qquad (8.128)$$

μ_φ is the required value of the curvature ductility factor
v_d is the normalised design axial force ($v_d = N_{Ed}/A_c f_{cd}$)
b_c is the cross-sectional depth
b_o is the depth of the confined core (to the centreline of the hoops)
ε_{syd} is the design value of tension steel strain at yield
b_c is the cross-sectional width
b_o is the width of the confined core (to the centreline of the hoops)

α is the confinement effectiveness factor, equal to

$$\alpha = \alpha_n \cdot \alpha_s \qquad (8.129)$$
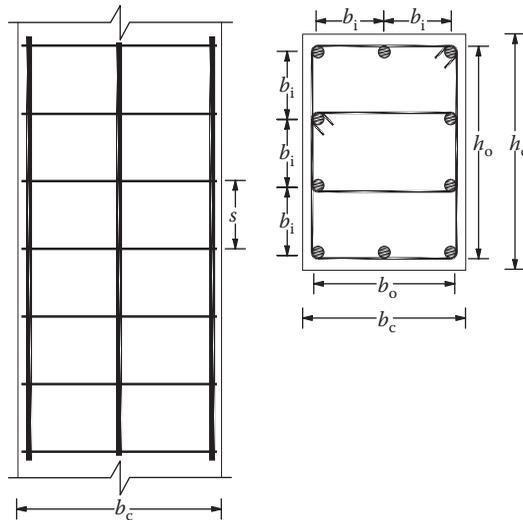
Figure 8.49 Confinement of concrete core.

In the above expression, α_n and α_s take the following values:

1. For rectangular cross sections:

$$\alpha_n = 1 - \sum_n b_i^2 / 6b_o h_o \tag{8.130a}$$

$$\alpha_s = (1 - s/2b_o)(1 - s/2h_o) \tag{8.131a}$$

where
  n is the number of longitudinal bars laterally engaged by hoops or cross ties
  b_i is the distance between consecutive engaged bars (see also Figure 8.49 for b_o, h_o)

2. For circular cross sections with circular hoops and diameter of confined core D_o (to the centreline of hoops):

$$\alpha_n = 1 \tag{8.130b}$$

$$\alpha_s = \left(1 - \frac{s}{2D_o}\right)^2 \tag{8.131b}$$

3. For circular cross sections with spiral hoops:

$$\alpha_n = 1 \tag{8.130c}$$

$$\alpha_s = \left(1 - \frac{s}{2D_o}\right) \tag{8.131c}$$

4. For cross sections of L, T, C and so on, detailed reference will be made in the next chapter, where local ductility issues of shear wall cores will be dealt with.

The derivation of $\alpha = \alpha_n \cdot \alpha_s$ was presented in Paragraph 7.4.3.2 for concrete confinement by means of hoops.

The justification of Equation 8.127 will be presented in the next Paragraph 8.3.4.2.4.

It should be noted here that the relevant American Code of Practice (ACI 318-2008 Chapter 21) specifies semi-empirical formulas for the quantification of confinement reinforcement in all critical regions of columns, justifying this choice by the fact that μ_φ and ν_d are not known with sufficient accuracy. In this way, the design of the local ductility reinforcement in the critical regions is greatly simplified, and the design is carried out either manually or is computer-aided.

- A minimum value of ω_{wd} equal to 0.08 should be provided within the critical region at the base of the columns. This value corresponds in the case of concrete class C25 and steel class B500c to a volumetric percentage of
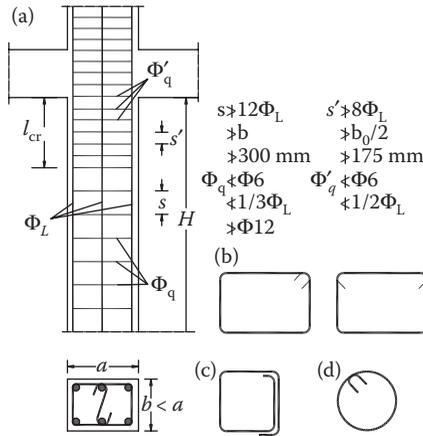
Figure 8.50 Arrangement of column reinforcement: (a) arrangement of hoops; (b) closing of external hoops; (c) closing of internal hoops; (d) closing of cyclic hoops (DCM buildings).

$$\rho_{w,min} = 0.08\frac{25 \cdot 1.15}{500 \cdot 1.5} = 0.003 \quad (3‰$$

- Within the critical regions of columns, hoops and cross-ties with a diameter $\not< 6.00$ mm will be provided at spacing such that a minimum ductility is ensured and local buckling of longitudinal bars is prevented. These requirements are satisfied if the following conditions are taken into account (Figures 8.50 and 8.51).

1. The spacing s of the hoops (in mm) does not exceed:

$$s = \min\{b_o/2; 175\ \text{mm}; 8d_{bl}\} \tag{8.132}$$

where
  b_o is the minimum dimension of the concrete core (in mm)
  d_{bl} is the minimum diameter of the longitudinal bars (in mm)

2. The distance between consecutive longitudinal bars engaged by hoops does not exceed 200 mm.
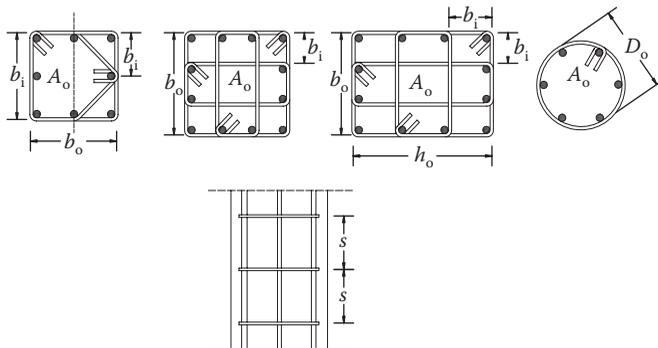
Figure 8.51 Various types of hoop arrangement in orthogonal and circular cross sections of columns, with the required notation for the implementation of expressions (8.130a), (8.131a) and (8.131b).

8.3.4.2.4 Justification of equation 8.127, specified by the code for the calculation of the required confinement reinforcement

Consider the column of Figure 8.52 with the following cross-sectional characteristics:

- h_c, b_c are its cross-sectional dimensions.
- c is the concrete cover of reinforcement.
- d_{bl}, d_{bw} are the diameters of the longitudinal and transverse reinforcements.
- h_o, b_o are the cross-sectional dimensions of the core after surface spalling ($h_o = h_c - (2c + d_{bw})$, $b_o = b_c - (2c + d_{bw})$).
- d is the depth of the column.

$$d_o = d - \left(c + \frac{d_{bw}}{2}\right)$$

$$\rho_1 = \frac{A_{s1}}{h_c b_c}, \quad \rho_1^* = \frac{A_{s1}}{h_o b_o} \quad \omega_{1d} = \rho_1 \frac{f_{yd}}{f_{cd}}, \quad \omega_{1d}^* = \rho_1^* \frac{f_{yd}}{f_{cd}}$$

$$\rho_2 = \frac{A_{s2}}{h_c b_c}, \quad \rho_2^* = \frac{A_{s2}}{h_o b_o} \quad \omega_{2d} = \rho_2 \frac{f_{yd}}{f_{cd}}, \quad \omega_{2d}^* = \rho_2^* \frac{f_{yd}}{f_{cd}}$$

$$\rho_v = \frac{A_{sv}}{h_c b_c}, \quad \rho_v^* = \frac{A_{sv}}{h_o b_o} \quad \omega_{vd} = \rho_v \frac{f_{yd}}{f_{cd}}, \quad \omega_{vd}^* = \rho_v^* \frac{f_{yd}}{f_{cd}}$$

For columns, usually $\rho_1 = \rho_2 = \rho$ and $\rho_v \cong 0$.
N is the compressive axial load:
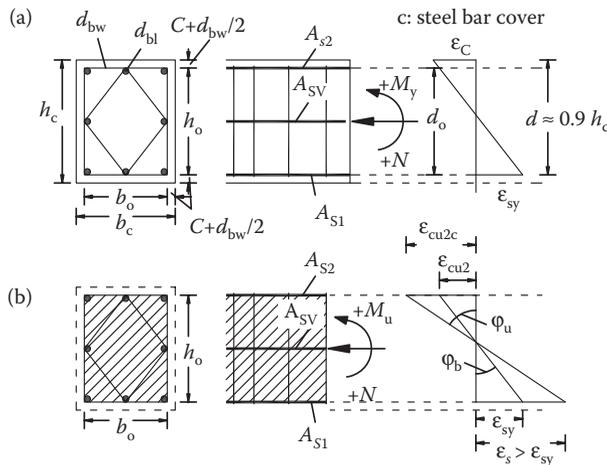
$$(N = \nu \, b_c \, h_c \, f_{ck})$$

Figure 8.52 Confinement for a quantified local ductility in the case of columns: (a) notations of the cross section; (b) notation of the confined core.

ν is the normalised axial force:

$$\nu^* = \frac{N}{b_o h_o f_{c\kappa c}^*} = \frac{\nu b_c h_c f_{c\kappa}}{b_o h_o f_{c\kappa c}^*} = \frac{\nu_d b_c h_c f_{cd}}{b_o h_o f_{c\kappa c}^*}$$

$$\nu_d = \frac{N}{b_c h_c f_{cd}} = \frac{N}{b_c h_c f_{c\kappa}/\gamma_c} = \gamma_c \nu = 1.50\,\nu$$

M_y, M_u are the bending moments at yield and failure, respectively.

The available ductility μ_φ in terms of curvature of the column, as was explained in Paragraph 8.3.2.2.4 Equation 8.104c, is limited due to ν, and therefore the only way to ensure a specified value of μ_φ is to increase $\boxtimes_{cu2}$ by concrete confinement by means of closely spaced hoops and spirals. In this respect, the concrete cover of reinforcement spalls at failure stage, while at the confined core an ultimate strain $\boxtimes_{cu2c}$ develops, capable of providing the required μ_φ. Therefore, the aim of this analysis is the determination of the required confinement reinforcement so that the required μ_φ is ensured.

Taking into account that curvature at yield φ_y refers to the original cross section while curvature at failure φ_u^* refers to the core section, Equations 8.106 and 8.101 take the form:

$$\varphi_y = 1.75\,\varepsilon_y/h_c \tag{8.133}$$

$$\varphi_u^* = \frac{\varepsilon_{cuc}^*}{\xi_u^* d_o} = \frac{\varepsilon_{cuc}^*}{\dfrac{1}{0.72}\left(\nu^* + \rho_v^* \dfrac{f_y}{f_{cc}^*}\right)d_o} \tag{8.134}$$

Therefore,

$$\mu_\varphi = \frac{\varphi_u^*}{\varphi_y} = \frac{0.72}{1.75}\frac{\varepsilon_{cuc}^* h_c}{\left(\nu^* + \rho_v^* \dfrac{f_y}{f_{cc}^*}\right)\varepsilon_y} \tag{8.135}$$

Taking into account that according to Chapter 7.4.3(b) Equations 7.28 and 7.26 ε_{cuc}^* and $f_{c\kappa c}^*$ have the following values:

$$\varepsilon_{cuc}^* = \varepsilon_{cu2} + 0.10\alpha\omega_w \tag{8.136a}$$

$$f_{c\kappa c}^* = f_{c\kappa}(1 + 2.5\alpha\omega_w) = \beta f_{c\kappa} \tag{8.136b}$$

and that the relation between ν and ν^* is given at the beginning of the paragraph, it follows that μ_φ in Equation 8.135 may take the following form:

$$\mu_\varphi = \frac{0.72}{1.75}\frac{\varepsilon_{cuc}^*}{\varepsilon_y}\frac{h_c}{\left(\nu + \rho_v \dfrac{f_y}{f_{c\kappa}}\right)\dfrac{b_c h_c}{b_o h_o}\dfrac{d_o}{\beta}} \tag{8.137}$$

Taking into account that:

$\dfrac{d_o}{b_o} \cong 0.9$ and introducing ε_{cuc}^* from Equation 8.136a), it follows that:

$$\varepsilon_{cuc}^* = \varepsilon_{cu2} + 0.10\alpha\omega_w = \frac{1.58\mu_\varphi}{0.72}\left(\nu + \rho_v \frac{f_y}{f_{c\kappa}}\right)\frac{b_c}{b_o}\beta$$

or

$$\alpha\omega_w = \frac{1.58}{0.72}10.0\mu_\varphi\varepsilon_y(\nu + \omega_v)\frac{b_c}{b_o}\beta - 10\varepsilon_{cu2} \tag{8.138}$$

In the case of columns, ω_v may be considered zero, as ω_v is insignificant compared to ν. Additionally, for concrete classes from C20 to C50, ε_{cu2} is equal to 0.0035. Finally, β may be replaced by its mean value, which has been estimated from parametric analysis to range around 1.15 for a wide range of confinement.

Taking all the above into account, and that:

$$\nu = \frac{\nu_d}{\gamma_c} = \frac{\nu_d}{1.50} \tag{8.139a}$$

and

$$\varepsilon_y = \gamma_s\varepsilon_{yd} = 1.15\varepsilon_{yd} \tag{8.139b}$$

it follows from Equation 8.137:

$$\alpha\omega_w = \frac{1.58}{0.72}10.0 \cdot 1.50 \cdot 1.15\mu_\varphi\varepsilon_{yd}\nu_d \frac{b}{b_o} - 0.035$$

or

$$\boxed{\alpha\omega_{wd} = 16.8\mu_\varphi\varepsilon_{yd}\nu_d \frac{b}{b_o} - 0.035} \tag{8.140}$$

Comparing Equations 8.127 and 8.140, and taking into account that the safety factor of μ_φ derived from Equations 5.52a and 5.52b in relation to q_o is about 1.65 (Equation 5.52c), it is concluded that the imposed confinement by the Code via Equation 8.127 ensures a safety factor for local ductility of columns on the order of:

$$\gamma_{\mu\varphi} \cong 1.65\frac{30}{16.8} = 2.95 \tag{8.141}$$

8.3.4.3 Design of columns for DCH buildings

8.3.4.3.1 Geometrical constraints

In addition to the requirements for columns of DCM buildings, in the case of DCH the minimum cross-sectional dimension should not be less than 250 mm.

8.3.4.3.2 Resistance to flexure with axial load and shear

The rules for DCM are also here in use. The only difference is that:

$$\boxed{\nu_d = \frac{N_{Ed}}{A_c f_{cd}} \leq 0.55} \qquad (8.142)$$

instead of 0.65, which is imposed on DCM buildings. This value of ν_d corresponds to a value for ν equal to

$$\boxed{\nu = \frac{0.55}{1.50} \cong 0.36} \qquad (8.143)$$

that is, this requirement ensures that ν is below $\nu_{balance}$ (see Paragraph 8.3.2.1).

8.3.4.3.3 Detailing of columns for local ductility

- The rules for DCM are also in effect here, unless they contradict what is specified below.
- The length of the critical region l_{cr} may be determined as follows (in meters):

$$\boxed{l_{cr} = \max\{1.5\,h_c;\ l_{cl}/6;\ 0.6\}} \qquad (8.144)$$

where
  h_c is the largest cross-sectional dimension of the column (in meters)
  l_{cl} is the clear length (in meters)

- The detailing of critical regions above the base of the columns should be designed for a minimum value of the curvature ductility factor μ_φ derived from Equations 5.52a and 5.52b for reduced values of q_o to two-thirds of their values that have been taken into account for the determination of the q-factor of the building. In this case, $\alpha\omega_{wd}$ should again be determined by applying Equation 8.127.
- In any case, the minimum value of ω_{wd} should be:
  - In the critical region of the base

$$\boxed{\omega_{wd} \geq 0.12} \qquad (8.145)$$

  - In all other critical regions of the column:

$$\boxed{\omega_{wd} \geq 0.08} \qquad (8.146)$$

  - Within the critical regions of columns, hoops and cross-ties with a diameter

$$\boxed{d_{bw} \geq 0.4 d_{bL\,\max} \sqrt{f_{ydL}/f_{ydw}}} \qquad (8.147)$$

should be provided at a spacing such that a minimum ductility is ensured and local buckling of longitudinal bars is prevented. These requirements are satisfied if the following conditions are fulfilled.

1. The spacing s of the hoops (in mm) does not exceed

$$\boxed{s = \min\{b_o/3; 125\text{mm}; 6d_{bl}\}} \tag{8.148}$$

where
   b_o is the minimum dimension of the concrete core (in mm)
   d_{bl} is the minimum diameter of longitudinal bars (in mm)

2. The distance between consecutive longitudinal bars encaged by hoops does not exceed 150 mm^2.
3. The critical regions in the columns of the two lower storeys should be increased in length by 50%.
4. The amount of longitudinal reinforcement at the base of the columns of the bottom storey should not be less, in any case, than that provided at the top of the columns of this storey.

8.3.4.4 Anchorage of column reinforcement

1. For the anchorage of column reinforcement, all rules specified by the Code for conventional R/C structures (EC2-1-1/2004) are in effect unless otherwise specified in the following paragraphs.
2. The additional rules specified below by EC8-1/2004 are in effect for both DCM and DCH buildings.
3. The anchorage length l_{anc} of column bars within critical regions should be calculated for a ratio of the required area of reinforcement. $A_{s,req}$. to the available area $A_{s,avail}$ equal to 1.0, that is:

$$\boxed{\frac{A_{s,req}}{A_{s,avail}} = 1.0} \tag{8.149}$$

no matter if $A_{s,avail}$ is greater than $A_{s,required}$.
4. If under the seismic design combinations the axial force in the column is tensile, the anchorage lengths should be increased by 50% relative to those specified by EN1992-1-1/2004.

8.3.4.5 Splicing of bars

- In addition to what has been developed in the relevant paragraph for beams (8.2.4(e)), the following rules are specified for columns.
- Mechanical couplers may be used in columns if these devices are covered by appropriate testing documents.
- The required area of transverse reinforcement of columns spliced at the same location could be calculated from the following expression:

$$\boxed{A_{st} = s(d_{bl}/50)(f_{yld}/f_{ywd})} \tag{8.150}$$

where
   A_{st} is the area of one *leg* of the transverse reinforcement
   d_{bL} is the diameter of the spliced bar

s is the spacing of the transverse reinforcement

f_{yld} and f_{ywd} are the design values of the yield strength of the longitudinal and transverse reinforcements, respectively

8.3.5 Columns under axial load and biaxial bending

8.3.5.1 General

So far, column design has been approached as if columns were members of plane frames. Even for the verification at ultimate limit state, Code allows the substitution of biaxial bending by two independent uniaxial states reducing in parallel the design resistance to bending in the direction under consideration by 30%.

For ensuring column ductility the confinement degree has been determined separately in each main orthogonal direction, that is, under a uniaxial consideration in two main directions.

M−θ diagrams under monotonic or cyclic loading, their stability under cyclic loading, and the form of their hysteresis loops have also been examined under uniaxial bending with axial force.

However, as was noted at the beginning of this section, columns in buildings are subjected to a biaxial loading due to seismic action. Therefore, it is important to examine the degree of reliability of all these simplifications that have been introduced by Codes in the analysis and design of columns as 3-D frame members. Unfortunately, the existing test results on axially loaded members under biaxial bending are limited, due to the practical difficulties of such testing (Fardis, 2009).

At the same time, the bidirectional loading history of the column plays a very important role for the results and the relevant conclusions (Figures 8.53 and 8.54).

In any case, taking into account the existing state of the art on the behaviour of columns under biaxial bending, the following issues will be examined:

- Strength
- Yield and failure stages
- Ductility μ_φ at curvature level
- Stability of *M*−θ curve under cyclic loading
- Form of hysteresis loops under biaxial loading

8.3.5.2 Biaxial strength in bending and shear

It is well known from the design of conventional R/C structures that biaxial bending with axial load is depicted by the 3-D envelope of Figure 8.55. In case of an orthogonal, symmetrically reinforced cross section and for a given axial force *N* (compressive is considered positive), the safe region is enclosed by the curve depicted in Figure 8.56a. The form of this curve is related to the percentage of steel reinforcement $\rho_{tot} = \dfrac{A_s}{bh}$ and its class.

If the parameters of the problem are normalised, that is,

$$m_{yRd} = \frac{M_{yRd}}{bh^2 f_{cd}} \tag{8.151a}$$

$$m_{zRd} = \frac{M_{zRd}}{bh^2 f_{cd}} \tag{8.151b}$$
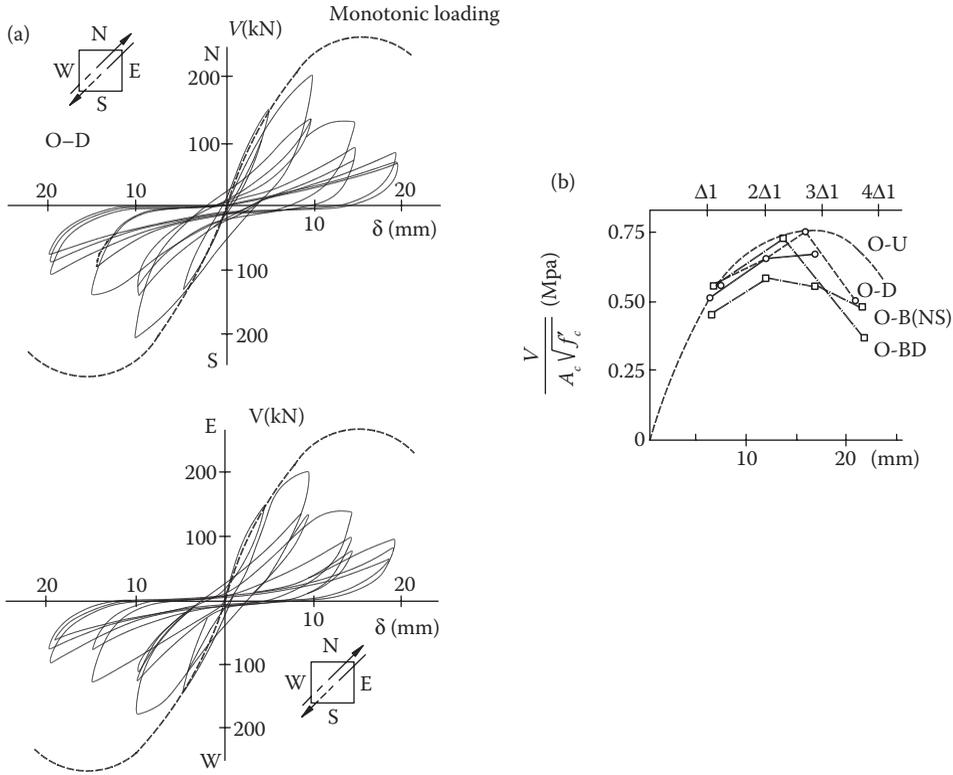
Figure 8.53 Diagonal cyclic loading of columns: (a) hysteresis loops in each direction; (b) envelope of the resultant action. (Adapted from Jirsa, J.O., Maruyama, K. and Ramirez, H. 1980. The influence of load history on the shear behaviour of short RG columns. *Proceedings of the 7th World Conference on Earthquake Engineering*, Istanbul, 6, 339–146.)

$$\omega_{\text{tot}} = \frac{A_{\text{s,tot}}}{bh} \frac{f_{\text{yd}}}{f_{\text{cd}}} = \rho_{\text{tot}} \frac{f_{\text{yd}}}{f_{\text{cd}}} \tag{8.152}$$

$$\nu_{\text{d}} = \frac{N_{\text{Ed}}}{bhf_{\text{cd}}} \tag{8.153}$$

then the curve depicted in Figure 8.56a is transformed into the curve depicted in Figure 8.56b (the various symbols are defined in Figure 8.56), which is expressed by the following equation:

$$\boxed{m_{\text{yd}}^{\alpha} + m_{\text{zd}}^{\alpha} = m_{\text{Rd}}^{\alpha}} \tag{8.154}$$

where

$$m_{\text{Rd}} = m_{\text{yRd}} = m_{\text{zRd}} \tag{8.155}$$

The value of *a*, for reasonable values of ω_{tot}, ν_{d} and steel classes, ranges

$$\alpha = 1.33 - 2.00 \tag{8.156}$$
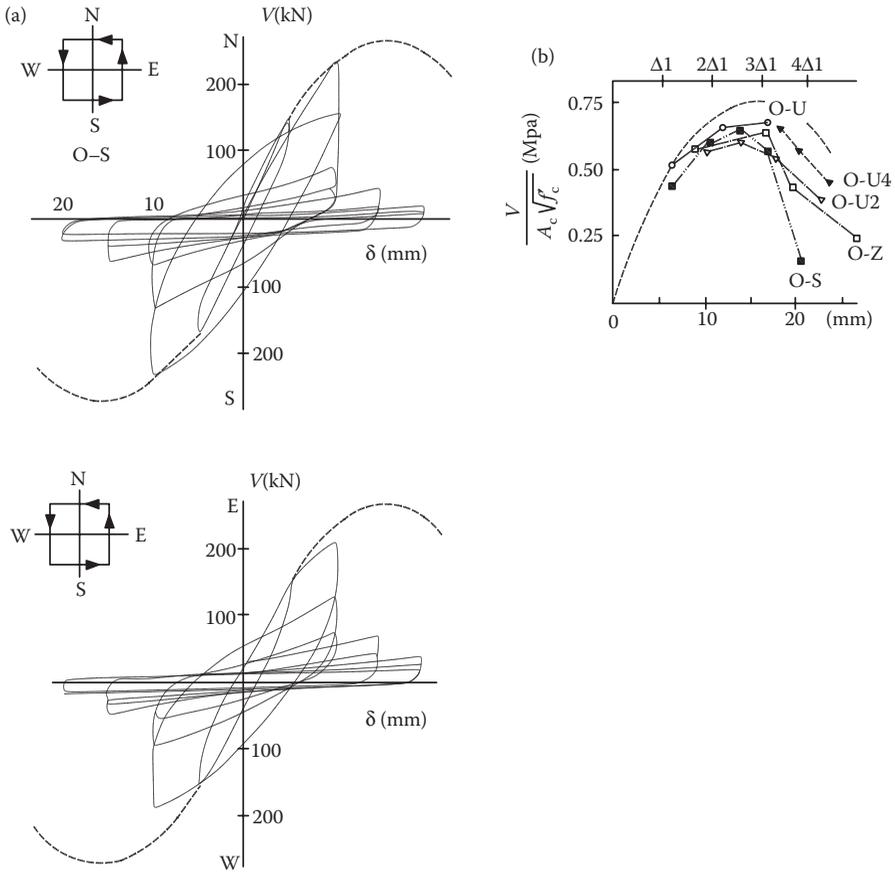
Figure 8.54 Square-like cyclic loading of columns: (a) hysteresis loops in each direction; (b) envelope of the resultant action. (Adapted from Jirsa, J.O., Maruyama, K. and Ramirez, H. 1980. The influence of load history on the shear behaviour of short RG columns. *Proceedings of the 7th World Conference on Earthquake Engineering*, Istanbul, 6, 339–146.)
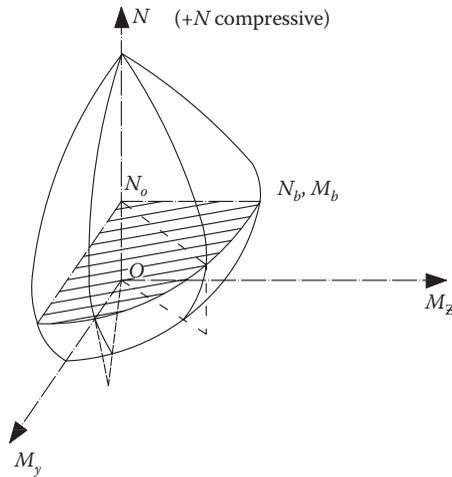
Figure 8.55 Interaction diagram of biaxial bending with axial compressive force.
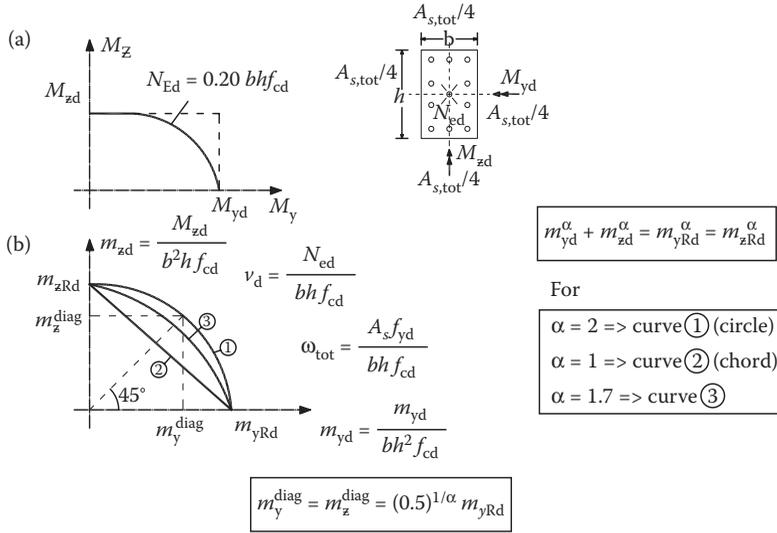
Figure 8.56 $M_y - M_z$ interaction diagrams for a given axial force N (a) $M_y - M_z - N$; (b) normalised diagram of $M_y - M_z - N$.

that is, between a circle and inflated rhombus (Figure 8.56b). This is the basic form of the curves of all charts for the design of R/C orthogonal cross sections under biaxial bending with axial load (Hassoun and Al-Manaseer, 2008).

From the above chart it follows that biaxial loading leads to a strength decrease, since both normalised moments m_{yd} and m_{zd} corresponding to the $m_{zd} - m_{yd}$ envelope are less than m_{Rd} (Figure 8.56). Furthermore, taking into account that the codified loading combination is given by an expression in the form:

$$m_y \ '+' \ 0.30m_z \quad \text{or} \quad m_z \ '+' \ 0.30m_y \tag{8.157}$$

it may be concluded that the corresponding maximum reduction of m_{Rd} that should be introduced in the verification of the substitute uniaxial bending at ULS, is derived from the following expression:

$$\boxed{m_{yd}^{1.33} + m_{zd}^{1.33} \leq m_{Rd}^{1.33}} \tag{8.158}$$

where

$$\frac{m_{zd}}{m_{yd}} \cong 0.30 \quad \text{or} \quad m_{zd} \cong 0.30m_{yd}$$

Therefore,

$$\boxed{m_{yd} \leq 0.78m_{Rd}} \tag{8.159}$$

The above expression (8.159) explains the adoption of a value equal to 0.70 for this reduction in the Code (see par. 8.3.4.2). It should again be pointed out that the above codified

simplification is insignificant nowadays, when commercial computer platforms are in use for the design of any form of R/C cross section under biaxial bending with axial force.

Also, taking into account that capacity design for the joints of frame or frame-equivalent buildings is carried out for the two main orthogonal plane frame directions independently, while strength verification of the columns is carried out in one direction under the capacity design moment values and in the other under the M values resulting from the seismic analysis, it can easily be concluded that in case of an earthquake with effects exceeding the design seismic action it is probable that in both directions the capacity moments might be developed at the ends of a column. In this case, and taking into account what has been presented earlier, columns might be overloaded and fail. Therefore, the case mentioned above constitutes an additional reason for the confinement of the critical regions of the columns, so that plastic deformations are developed in case of overloading, in case the main concept for 'strong columns-weak beams' for unexpected reasons does not function.

In conclusion, it should be pointed out that although test results of columns under cyclic biaxial bending with axial load are very limited (Fardis, 2009), the results on a series of 35 specimens (Bousias et al., 2002; Biskinis, 2007) have given experimental results very close to analytical ones, that is: $M_{yy,\,exp}/M_{yy\,an}$ and $M_{zy,\,exp}/M_{zy\,an}$ are very close to 1.0.

8.3.5.3 *Chord rotation at yield and failure stage: Skew ductility* μ_φ *in terms of curvature*

From the laboratory tests on 35 specimens to which reference was made in the previous paragraph, the following conclusions can be drawn:

- The chord rotation at the yield stage fulfills with reasonable accuracy (7–10% scattering) the following expression:

$$\left(\frac{\theta_{yy\,exp}}{\theta_{yy\,uniax}}\right)^2 + \left(\frac{\theta_{yz\,exp}}{\theta_{yz\,uniax}}\right)^2 = 1 \tag{8.160}$$

  that is, a relation similar to that of Equation 8.154.
- A similar expression is in effect for the failure stage, that is,

$$\left(\frac{\theta_{uy\,exp}}{\theta_{uy\,uniax}}\right)^2 + \left(\frac{\theta_{uz\,exp}}{\theta_{uz\,uniax}}\right)^2 = 1 \tag{8.161}$$

  with a scattering up to 17%.
- Finally, a similar expression is obtained analytically for the skew ductility μ_φ in terms of curvature, that is,

$$\boxed{\frac{(\mu_{\varphi y})^2}{(\mu_{\varphi 1})^2} + \frac{(\mu_{\varphi z})^2}{(\mu_{\varphi 2})^2} = 1} \tag{8.162}$$

This means that for given values of $\mu_{\varphi 1}$ and $\mu_{\varphi 2}$ (capacities of ductility in terms of uniaxial bending), when the seismic action is skew, the available capacity in the main directions

diminishes. For example, in the case of an angle of 45° ($\mu_{\varphi y} = \mu_{\varphi z}$) the available capacity in the main directions takes the form

$$\mu_{\varphi y} = \mu_{\varphi z} = \sqrt{\frac{\mu_{\varphi 1}^2 \mu_{\varphi 2}^2}{\mu_{\varphi 1}^2 + \mu_{\varphi 2}^2}} \qquad (8.163)$$

It is apparent that these values of $\mu_{\varphi y}$ and $\mu_{\varphi z}$ are smaller than the relevant values of $\mu_{\varphi 1}$ and $\mu_{\varphi 2}$. However, this negative consequence of the skew bending on the ductility capacity of the columns is covered by the existing safety factor for their local ductility, which has been estimated to be about 2.95 (see par. 8.3.4.2).

8.3.5.4 Stability of M−θ diagrams under cyclic loading: Form of the hysteresis loops

According to test results of Jirsa et al. (1980) and Umehara and Jirsa (1984) (Figures 8.53 and 8.54) the following conclusions have been drawn:

- For cyclic loading into inelastic range, the biaxial response appears to be inferior of the uniaxial one. Even less favourable conditions arise if a bidirectional loading history such as the square loading history is applied. In this case, the reduction in strength is more pronounced.
- The hysteresis loops of square columns reinforced with closely spaced hoops have shown that their behaviour under biaxial cyclic loading along the diagonal of the cross section is quite satisfactory, characterised by stable hysteresis loops even at ductility levels $\mu_f > 8$ (Priestley and Park, 1987). The same conclusions have been drawn from the laboratory tests on a series of the 35 specimens mentioned before.
- From the above contradictory results to those presented in the diagrams of Figures 8.53 and 8.54, it may be concluded that reliable conclusions on the above issues cannot yet be drawn, as the number of tests is limited.

8.3.5.5 Conclusions

From the presentation above the following concluding remarks may be made. Code provisions for strength, ductility and capacity design, although based on the concept of a plane frame, cover completely the 3-D function of the frame system and particularly its columns, which are subjected to 3-D loading. This is accomplished by the introduction of various safety keys like greater safety factors, local ductility demands and so forth.

8.3.6 Short columns under seismic action

8.3.6.1 General

As has been clarified in previous sections of this chapter, the design procedure for columns presented thus far has referred to regular columns with slenderness (Figure 8.57).

$$\lambda = \frac{L}{h} \geqq 4.00 \qquad (8.164)$$
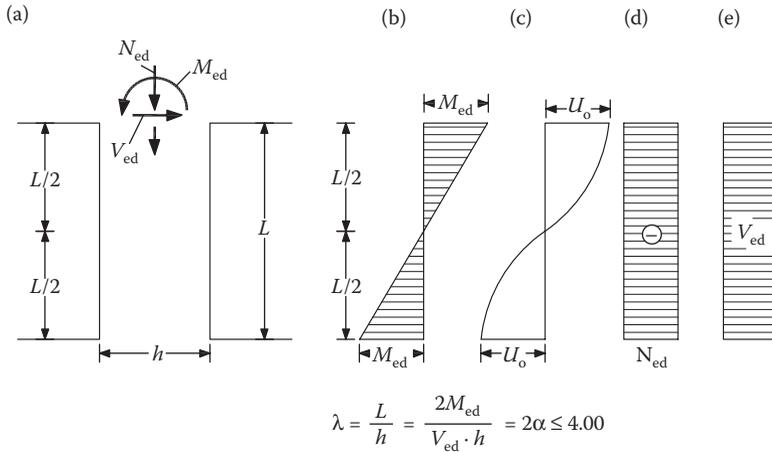
Figure 8.57 Squat column: *M*, *N*, *V* deflection diagrams; (a) geometry; (b) bending moments; (c) deflections; (d) axial forces; (e) shear forces.

or to antisymmetrically loaded columns with a shear span-to-depth ratio:

$$\alpha = \frac{M_{Ed}}{V_E \cdot h} = 0.5\lambda \geqq 2.0 \tag{8.165}$$

Members with $\alpha \leqq 2.0$, reinforced conventionally, have substantially different behaviour under cyclic loading, characterised by a high vulnerability to brittle failure in a mode of x-shaped diagonal splitting of concrete due to a diagonal compressive field leading to a premature *explosive cleavage shear fracture* (Figure 8.58; Minami and Wakabayashi, 1980; Tegos and Penelis, 1988). The inability of the conventional design procedure for columns of regular slenderness to give a reliable solution also for short columns must be attributed to the fact that in the case of short columns the plane strain distribution concept over the cross section of the member stops prevailing. Therefore, a two-dimensional stress field is developed with strong interrelation between shear and normal stresses.

Short columns are often found in industrial or school buildings where continuous masonry infills are used to create openings extending along full spans of R/C frames at the facade of the building. They are also found at the perimeter of elevated underground storeys, with their deck slab one to one-and-a-half meters above the surrounding ground level. Finally, in case of multi-storey buildings with a regular storey height of 3.00–3.20 m, the loads of the columns at the lower storeys require dimensions for the columns more than 0.80×0.80 m, which corresponds to a low slenderness value of $\lambda = \dfrac{3.20}{0.80} = 4.0$. For all of these buildings there are examples of impressive collapses due to a premature explosive cleavage shear fracture exhibited at short columns.

For this reason, extensive laboratory and analytical research has been conducted since the early 1980s aiming at the examination of the behaviour of short columns under cycling horizontal loading with axial load. These research programs have covered the following issues:

- Shear strength—failure mode
- Available ductility
- Stiffness and energy dissipation
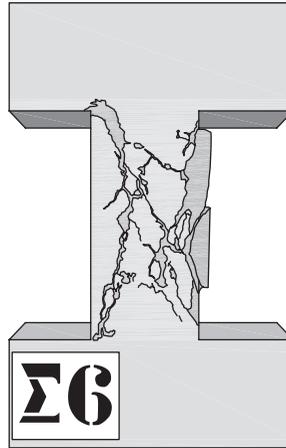
Figure 8.58 Premature explosive cleavage shear fracture of a short column. (Adapted from Tegos, I. 1984. *Contribution to the study and improvement of earthquake-resistant mechanical properties of low slenderness structural elements.* PhD thesis, Aristotle University of Thessaloniki (in Greek).)

The arrangement of the reinforcement that has been examined refers to (Penelis and Kappos, 1997):

- Conventional reinforcement consisting of longitudinal rebars with transverse hoops (Figure 8.59)
- Bidiagonal reinforcement (Figure 8.60)
- Rhombic truss reinforcement (Figure 8.61)

A short overview of the results of these efforts, of the relevant design proposals and of Code provisions as well will be made below.
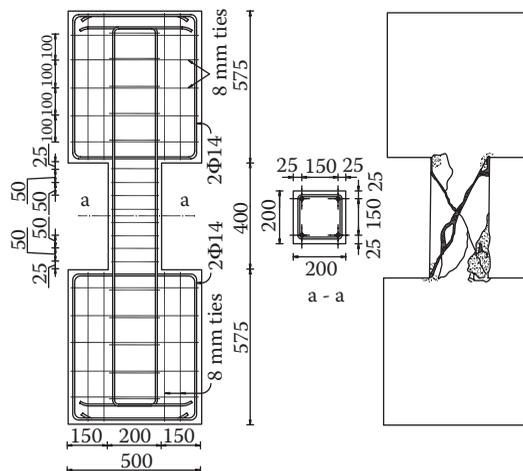
Figure 8.59 Conventional reinforcement of short columns against shear (close spaced ties).
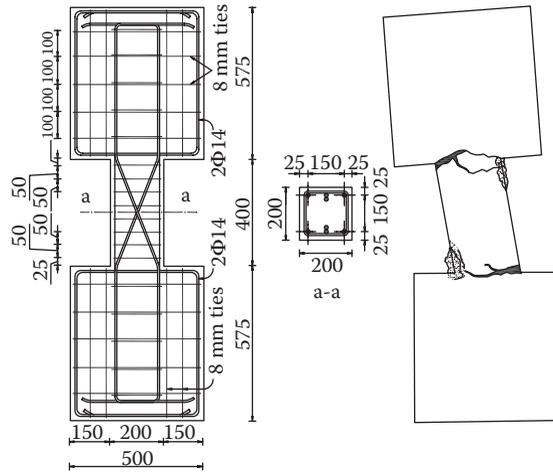
Figure 8.60 Bidiagonal reinforcement and ties of short columns against shear.

8.3.6.2 Shear strength and failure mode of conventionally reinforced squat columns

8.3.6.2.1 Shear failure models

In the early 1980s, Shohara and Kato (1981) had developed a composite model consisting of the conventional truss mechanism with 45° strut inclination and a diagonal strut running from the compression zone of the top end to that of the bottom of the column, combined with the longitudinal outer steel chords acting as ties (Figure 8.62). This model, modified in regard to the truss mechanism by introducing variable strut inclination, has been adopted in the guidelines of the Architectural Institute of Japan (AIJ 1994) for the shear design of R/C members in general. This approach has given a good explanation for M–N envelope modification in the case of short columns (Figure 8.63). The meaning of this modified diagram is that squat columns fail to shear before bending failure.
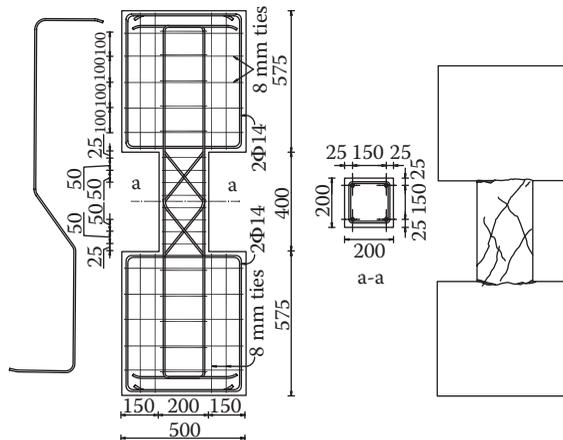
Figure 8.61 Rhombic reinforcement and ties of short columns against shear.

$$\alpha = \frac{bL\rho_w f_{yw}}{2A_s f_y}$$

$$\beta = \frac{2\rho_w f_{yw}}{f_c}$$

Figure 8.62 The superposition of two mechanical models (truss mechanism + diagonal strut mechanism [with tensile chords]) according to Shohara and Kato (1981) for shear design of short columns. (Adapted from Tegos, I. 1984. *Contribution to the study and improvement of earthquake-resistant mechanical properties of low slenderness structural elements*, PhD thesis, Aristotle University of Thessaloniki (in Greek).)

The correlation of the Shohara–Kato method with test results of various researchers on short columns (Tegos, 1984) has proved that the analytical results were on the safe side. However, there was a low correlation between analytical and experimental results (Figure 8.64).

The above model has been modified (Tegos, 1984; Tegos and Penelis, 1988) as follows:

- *The truss model* was modified by introducing *the variable strut inclination mechanism*. This mechanism resists shear loading via web reinforcement strength Z_w (Figure 8.65b).
- The diagonal strut model was replaced by *the diagonal parallelogram model* combined with the longitudinal outer steel chords acting as ties (Figure 8.65). This mechanism resists loading via splitting resistance Z_c (Figure 8.65a).

Figure 8.63 Application for dimensional M–N and V–N of 200 mm square column with four 16 mm bars (CEB, 1996a; Adapted from Fardis, M.N. 2009. *Seismic Design, Assessment and Retrofitting of Concrete Buildings.* Springer, Heidelberg.)

Figure 8.64 Correlation of test results and analytical considerations according the Sohara and Kato method. (Adapted from Tegos, I. 1984. *Contribution to the study and improvement of earthquake-resistant mechanical properties of low slenderness structural elements.* PhD thesis, Aristotle University of Thessaloniki (in Greek).)

The first model (truss mechanism) was studied in detail in Subsection 8.3.4 in regard to regular columns. The second model adequately simulates the load path from one end of the compression zone to the other and makes possible the introduction of the splitting forces Z_c in the relevant equations.

Using these two models and introducing some approximations of low significance, the $N–V$ interaction diagram is obtained in Figure 8.66. In this diagram the following notations have been introduced:

$$v_{Rd} = \frac{V_{Rd}}{bhf_{cd}}, \; v_d = \frac{N_d}{bhf_c}, \; \omega_s = \frac{A_s}{bh}\frac{f_{yd}}{f_{cd}}, \; \omega_w = \frac{A_w}{bt}\frac{f_{yw}}{f_{cd}} \tag{8.166a}$$
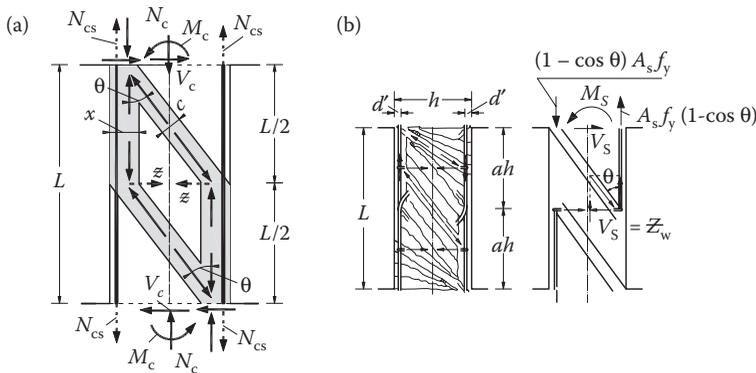
Figure 8.65 (a) The diagonal parallelogram strut model under compression; (b) the truss model with variable inclination struts.
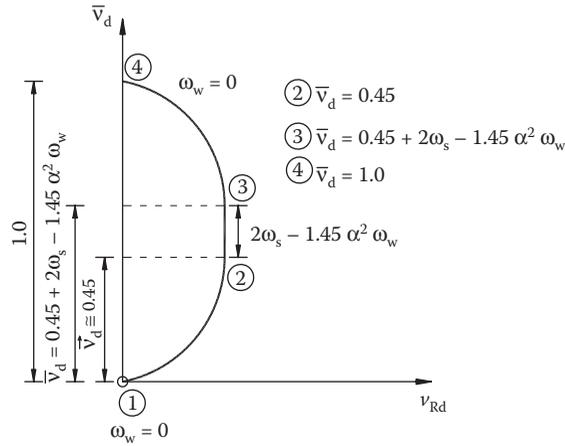
Figure 8.66 $\bar{v}_d - v_{Rd}$ interaction diagram.

$$\bar{v}_d = v_d + 2\omega_s - 1.45\alpha^2\omega_w \qquad (8.166b)$$

where

b, h are the dimensions of cross section of the column.

$$\alpha = \frac{M_{Ed}}{V_{Ed}h} = \frac{L}{2h}$$

L is the length of the column.
t is the spacing between the hoops.
A_s is the area of the steel chord at each bound of the column. $(A_{tot} = 2A_s)$
A_w is the sum of the area of all legs of the hoops at the same level, cutting the column axis transversally.

The value of normalised stress v_{Rd} in relation to v_d, ω_w and α is given by the expression:

$$v_{Rd} = \frac{\alpha(\bar{v}_d + 1.04\alpha^2\omega_w)}{5\bar{v}_d}\left[\sqrt{1 + \frac{5\bar{v}_d}{\alpha^2}\left(1 - \bar{v}_d + \frac{0.96\alpha^2\omega_w}{\bar{v}_d + 1.04\alpha^2\omega_w}\right)} - 1\right] \qquad (8.167)$$

while its maximum value, corresponding to the region 2–3 in the diagram of Figure 8.66, is given by the following expression:

$$v_{Rd\,max} = \frac{\alpha(0.45 + 1.04\alpha^2\omega_w)}{2.25}\left[\sqrt{1 + \frac{2.25}{\alpha^2}\left(0.55 + \frac{0.96\alpha^2\omega_w}{0.45 + 1.04\alpha^2\omega_w}\right)} - 1\right] \qquad (8.168)$$

The main critical question is about *the value of a*, for which bending reinforcement (A_s) and shear reinforcement (A_w) fail simultaneously. In this case, there will be *simultaneous* failure due to bending and shear. It is apparent that for a value of α greater than the above

critical value, the truss mechanism prevails, while for a smaller value than this critical value the diagonal parallelogram mechanism prevails.

In order for this condition to be fulfilled, point 2 in Figure 8.66 must coincide with point 3, that is,

$$\boxed{2\omega_s - 1.45\alpha_{cr}^2\omega_w = 0}$$ (8.169)

or

$$\boxed{\alpha_{cr} \cong 1.152\sqrt{\frac{\omega_s}{\omega_w}}}$$ (8.170)

If

$$\boxed{\alpha \leq \alpha_{cr}}$$ (8.171)

the diagonal parallelogram model fails first. Therefore, brittle failure due to explosive cleavage shear fracture prevails.

If

$$\boxed{\alpha \geq \alpha_{cr}}$$ (8.172)

the variable strut mechanism prevails. Therefore, if the column is reinforced properly with hoops, bending failure prevails. Otherwise, shear failure as in the case of regular column occurs.

EXAMPLE

For an R/C column with orthogonal cross section $h = 0.50$ m, $b = 0.40$ m, concrete class C25 and steel class B500c reinforced with longitudinal reinforcement $\rho_{tot} = 2.0\%$

$(A_{tot} = 40 \text{ cm}^2{:}4\Phi25 + 4\Phi25)$ and hoops $2\Phi10/20$ cm $\left(\rho_\omega = \dfrac{2 \cdot 2 \cdot 0.8}{20 \cdot 40} = 0.4\%\right)$

$$\omega_{tot} = \frac{2}{100} \cdot \frac{500 \cdot 1.5}{1.15 \cdot 25} = 0.52 \quad \omega_s = 0.26$$

$$\omega_w = \frac{4}{1000} \cdot \frac{500 \cdot 1.5}{1.15 \cdot 25} = 0.104$$

$$\alpha_{cr} = 1.15\sqrt{\frac{0.26}{0.104}} \cong 1.80$$

- For $\alpha \geq 1.80$ and proper shear reinforcement, the longitudinal reinforcement yields first, with prevailing horizontal flexural cracks at the top and bottom of the column.
- For $\alpha \leq 1.80$, the shear reinforcement (hoops) yield first, with prevailing diagonal cracks due to splitting forces at the horizontal diagonal of the strut in the form of a parallelogram.

Returning to the diagram of Figure 8.66, the following conclusions may be drawn.

1. In the case that $\alpha \geq \alpha_{cr}$, failure due to *premature explosive cleavage fracture is excluded*. The corresponding value of ν_{Rd} is given by Equation 8.167.
2. In the case that $\alpha \leq \alpha_{cr}$, the following failure modes are expected:
   a. For

$$0.0 \leq \bar{\nu}_d \leq 0.45 \quad \text{(Region 1–2)} \tag{8.173}$$

   bending failure precedes due to yield of longitudinal steel reinforcement, under the assumption that adequate web reinforcement ω_w excludes a failure in the form of diagonal tension. In other words, the short column behaves like the regular column. The corresponding value of ν_{Rd} may be determined by Equation 8.167.
   b. For

$$0.45 < \bar{\nu}_d < 0.45 + 2\omega_s - 1.45\alpha^2\omega_w \quad \text{(Region 2–3)} \tag{8.174}$$

   failure is brittle, taking place by yielding of transverse reinforcement accompanied by diagonal concrete splitting, while all longitudinal reinforcement is still in the elastic range. The corresponding value of ν_{Rd} is given by Equation 8.168.
   c. For

$$0.45 + 2\omega_s - 1.45\alpha^2\omega_w < \bar{\nu}_d \leq 1 \quad \text{(Region 3–4)} \tag{8.175}$$

   concrete failure prevails at the *compression zones at the ends of the column,* accompanied by failure at yield under compression of the longitudinal steel bars and eventual buckling. The corresponding value of ν_{Rd} is given by Equation 8.167.

In conclusion, it should be noted that recently modified expressions have been proposed by Biskinis (2007) based mainly on statistical analysis of experimental results.

8.3.6.2.2 Design procedure

Based on the above presentation, the diagrams of Figures 8.67 through 8.69 have been prepared (Tegos, 1984), which make possible the design in both cases.

- In the case that $\alpha \leq \alpha_{cr} \cong 1.15\sqrt{\dfrac{\omega_s}{\omega_w}}$, the diagram of Figure 8.67 is used.

  This diagram for given values of α, ω_s, ω_w allows the determination of ν_{Rd}.
- In the case that:

$$\alpha \geq \alpha_{cr} \cong 1.15\sqrt{\frac{\omega_s}{\omega_w}} \tag{8.176}$$

  the diagrams of Figures 8.68 and 8.69 are used. The first facilitates the determinations of ω_w for given values of α, ν_d, ω_s, while the second allows the determination of ν_{Rd}. The above procedure has been used (Tegos, 1984) for the analytical determination of shear capacity (ν_t) for 69 case studies, for which experimental results have been
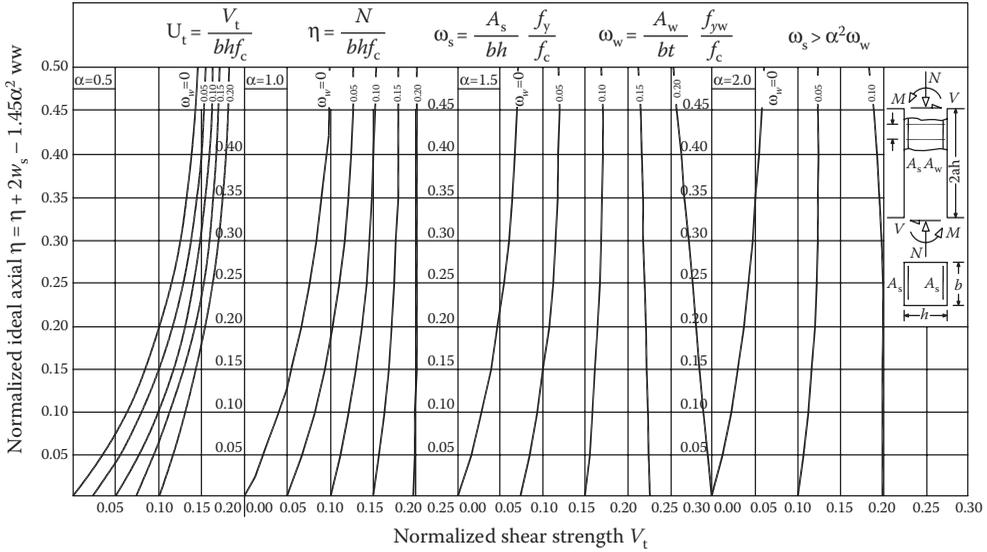
Figure 8.67 Diagrams for the calculation of the shear strength for squat columns ($\lambda < 4$) and $\omega_s > \alpha^2\omega_w$. (Adapted from Tegos, I. 1984. *Contribution to the study and improvement of earthquake-resistant mechanical properties of low slenderness structural elements.* PhD thesis, Aristotle University of Thessaloniki (in Greek).)
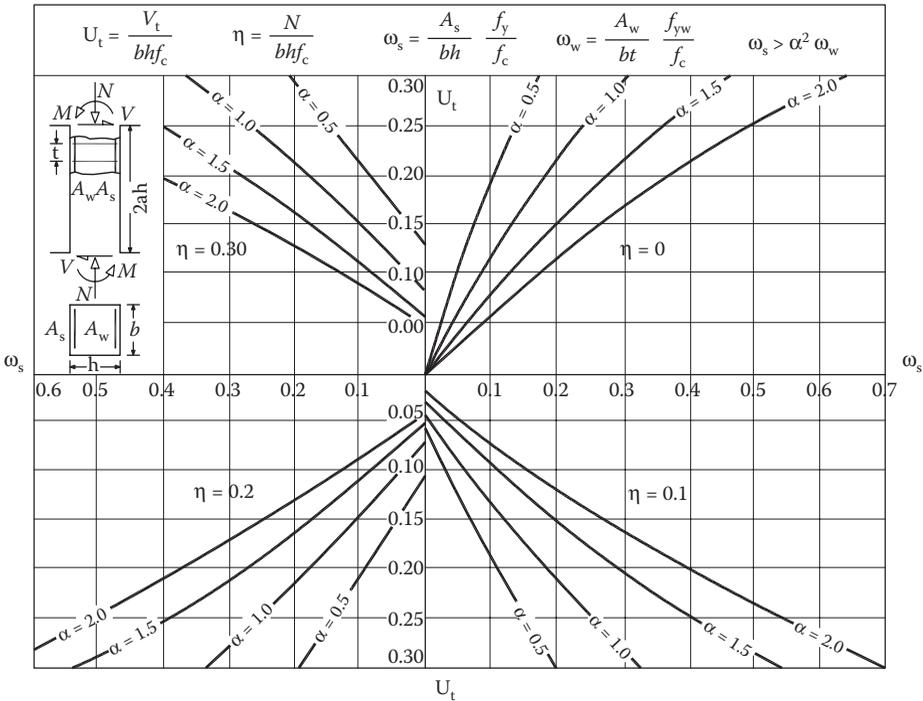
Figure 8.68 Design diagram for the calculation of shear strength in the case that $\alpha = (M/V \cdot h) \leq 2.0$ and $\omega_s > \alpha^2\omega_w$. (Adapted from Tegos, I. 1984. *Contribution to the study and improvement of earthquake-resistant mechanical properties of low slenderness structural elements.* PhD thesis, Aristotle University of Thessaloniki (in Greek).)
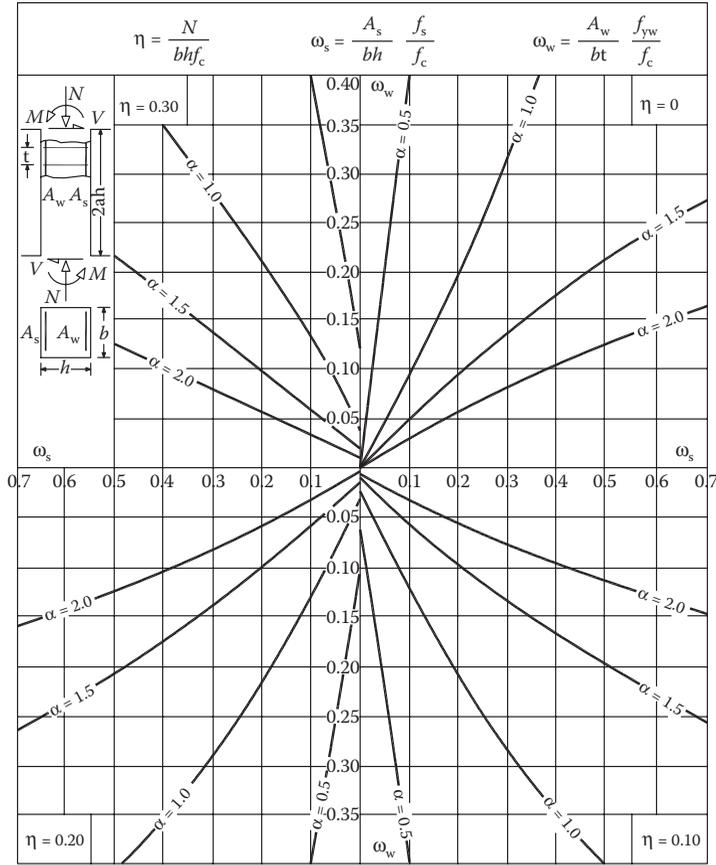
Figure 8.69 Design diagram for the calculation of shear reinforcement (hoops) in the case of $\alpha = (M/V \cdot h) \leq 2.0$. (Adapted from Tegos, I. 1984. *Contribution to the study and improvement of earthquake-resistant mechanical properties of low slenderness structural elements*. PhD thesis, Aristotle University of Thessaloniki (in Greek).)

reported by various researchers r_{xy}. The coefficient of correlation between analytical and experimental results was found to be (Figure 8.70):

$$r_{xy} = 0.97$$

8.3.6.3 Shear strength and failure mode of alternatively reinforced short columns

During the 1980s, alternative arrangements of reinforcement were proposed by various researchers aiming at the improvement of the behaviour of short columns under seismic action and especially aiming at avoiding premature explosive cleavage fracture.

Minami and Wakabayashi (1980) have proposed the use of cross-inclined diagonal bars (*bidiagonal* reinforcement; Figure 8.60), while Tegos and Penelis (1988) have proposed the use of a *rhombic* truss as shown in Figure 8.61. Test results have shown that these alternative reinforcement arrangements lead to an increase in shear capacity, but mainly to an improvement of the failure mode, ductility and energy dissipation capacity. More particularly, failure mode of explosive cleavage shear fracture no longer prevails. Bidiagonal reinforcement is
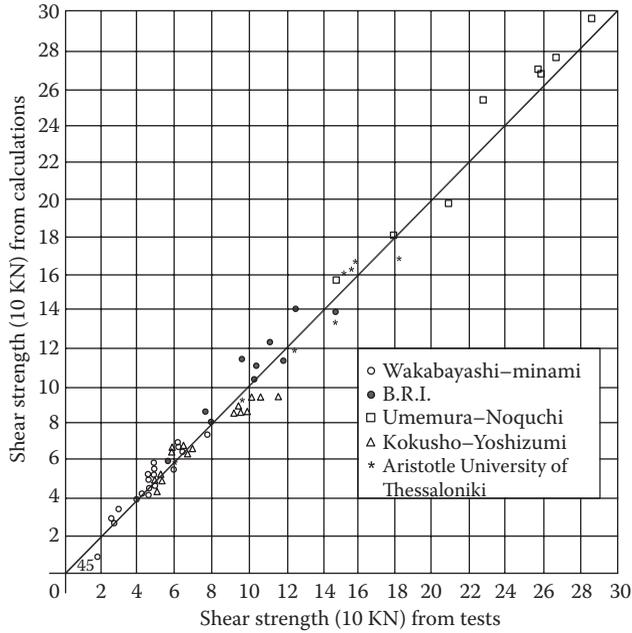
Figure 8.70 Correlation of shear strength results based on tests and on various analytical considerations. (Adapted from Tegos, I. 1984. *Contribution to the study and improvement of earthquake-resistant mechanical properties of low slenderness structural elements.* PhD thesis, Aristotle University of Thessaloniki (in Greek).)

particularly preferable for slenderness $l/h < 2$, while the rhombic reinforcement is preferable for $2.0 \le l/h \le 4.0$.

The shear strength design for the arrangement of rhombic or bidiagonal reinforcement may be carried out as in the case of short columns with conventional reinforcement, by also taking into account an additional third mechanism in the form of a rhombic or an x-formed truss (Figure 8.71). This truss contributes to increasing the shear strength of the column at an amount:

$$V_{id} = 2A_s f_{yd} \sin\theta \tag{8.177}$$
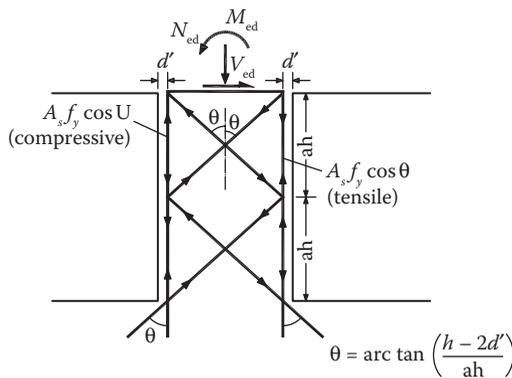
Figure 8.71 The additional mechanism of shear resistance in the case of rhombic reinforcement.

At the same time, a part of the axial strength of the longitudinal reinforcement is exhausted by this action, that is,

$$U_{id} = A_s f_y \cos\theta \tag{8.178}$$

Therefore, the analysis for the other two mechanisms, that is, the diagonal parallelogram and the truss mechanism, will be carried out by introducing in the place of N_s the value ΔN_s

$$\Delta N_s = (1 - \cos\theta)A_s f_y \tag{8.179}$$

and in normalised values:

$$\Delta\omega_s = (1 - \cos\theta)\omega_s \tag{8.180}$$

From this point on the design is carried out as in the case of conventional reinforced short columns, again using the formulas and the diagrams of paragraph (b), that is,

$$\alpha_{cr} \cong 1.15\sqrt{\frac{\Delta\omega_s}{\omega_w}} \tag{8.181}$$

and

$$\bar{V}_{Rd} = V_{Rd} + V_{id} \tag{8.182}$$

where

V_{Rd} is the result from the implementation of the diagrams of Figures 8.67, 8.68 and 8.69.

V_{id} results from Equation 8.177.

$\bar{V}_{Rd}$ is the total shear resistance.

8.3.6.4 Code provisions for short columns

Eurocodes EC2-1/2004 and EC8-1/2004 do not include any special provision for short columns. The only provision is that the critical region of the column should be extended to the total length of its height in the case that $\lambda = L/h$ is less than 3. ACI 318-11 does not include any requirement for short columns either.

However, it should be noted that various authors (Wight and Sozen, 1975) have come to the following conclusions, based on statistical analyses of experimental results:

1. If $\alpha = \dfrac{M}{Vh} \geq 2$, the column does not exhibit diagonal explosive shear failure (splitting).

2. A reasonable minimum value for transverse reinforcement in the form of hoops is ρ_w min $\cong 6\unicode{x2030}$ or ω_w min $\cong 0.16$.

In conclusion, it should be mentioned that some EU Member States, in the framework of their National Annexes for EC8-1/2004 (e.g. Greece), have introduced special rules for short columns, which are based on the analysis presented above but in a very simplified way (National Annex of Greece, 2010).

8.4 BEAM–COLUMN JOINTS

8.4.1 General

Beam–column joints are the most crucial parts of seismic-resistant R/C frames because in their limited volume the stress state field that develops due to seismic action is very high.

Indeed, keeping in mind that the joints are considered for the structural analysis as solid elements, it may be concluded that they must be in a position to sustain in their core:

- High shear stresses acting horizontally and vertically, as well (Figure 8.7).
- High bond stresses acting at the interface of concrete and longitudinal steel bars passing through the joint because of bending at the ends of the beams and the columns framing at the joint (Figure 8.37).

The determination of the stress field in joints is a very difficult and questionable procedure, even in the case of a plane frame, due to the existence of the longitudinal rebars in the joint subjected to high stresses, and also of the contribution of horizontal hoops to the shear resistance of the core of the joint and its confinement. The whole situation becomes more complicated in the case of 3-D joints, which constitute the most usual case (Figure 8.72) due to development of a triaxial stress state. Finally, the existence of a slab acting as a diaphragm makes the stress state even more complicated, due to the confinement that it causes for the joint. Consequently, it is not surprising that there is strong disagreement among various investigators about the design procedure that should be followed for R/C joints. This disagreement is also reflected in the various Seismic Codes for R/C structures. In any case, the main concept of all codes is that in the design procedure *failure should be excluded from the joint region* and be limited to the ends of the beams or at least of the columns framing at the joint.

The failure modes of some basic types of joints are depicted in Figures 11.23, 11.24 and 11.25 (Subsection 11.1.5). The usual types of failure of a joint may be classified as follows:

- *Spalling* of cover concrete at the faces of the joint core (Figure 8.73a).
- *Bond failure* of the longitudinal bars of the beam, which leads to strength deterioration and to a significant stiffness degradation due to fixed-end rotations (Figure 8.73b).
- *Diagonal splitting* caused by shear (Figure 8.73c).
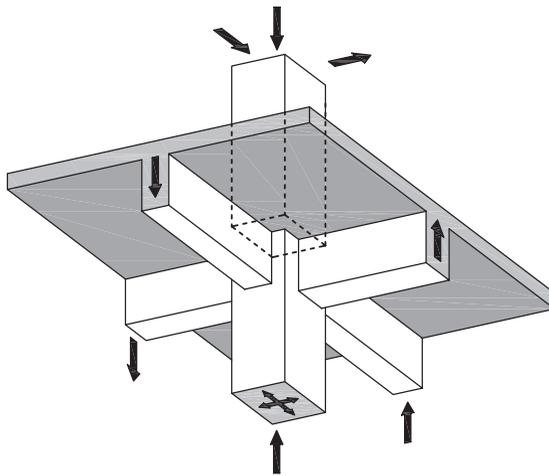
Figure 8.72 Alternative detailing of interior joints. (Adapted from Paulay, T. and Priestley, M.J.N. 1992. *Seismic Design of Reinforced Concrete and Masonry Buildings*. J. Wiley & Sons, New York.)
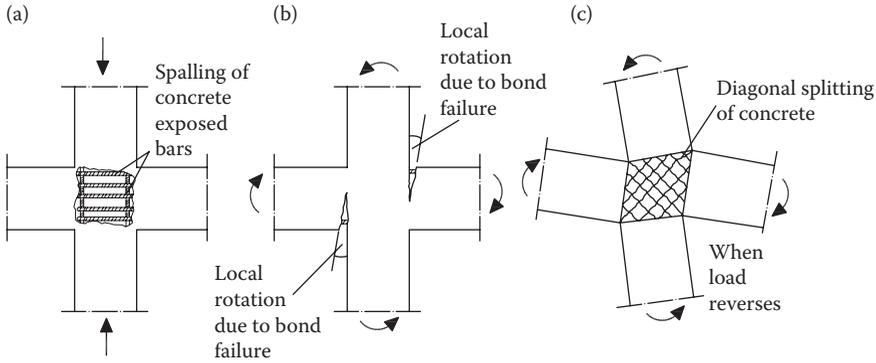
Figure 8.73 Types of failures at beam–column joints: (a) spalling of joint core; (b) anchorage failure of beam bars; (c) shear failure of the joint core.

8.4.2 Design of joints under seismic action

In the following paragraphs a short overview will be presented on the various methods developed for the design of joints under seismic action, and in particular of:

- The design of joints to shear developed by Park and Paulay (1975) and Paulay and Priestley (1992).
- The design method adopted by EC 8-1/2004.
- The design of joints to shear developed by Tsonos (Tsonos et al., 1995; Tsonos, 1999, 2001).

8.4.2.1 Demand for the shear design of joints

The forces acting on the core of an interior joint of a plane frame under seismic action are shown in Figure 8.74. The horizontal joint shear V_{jh} is counterbalanced by $T_{b1} + C_{b2} - V_{col}$, that is,

$$V_{jh} = T_{b1} + C_{b2} - V_{col} \tag{8.183}$$
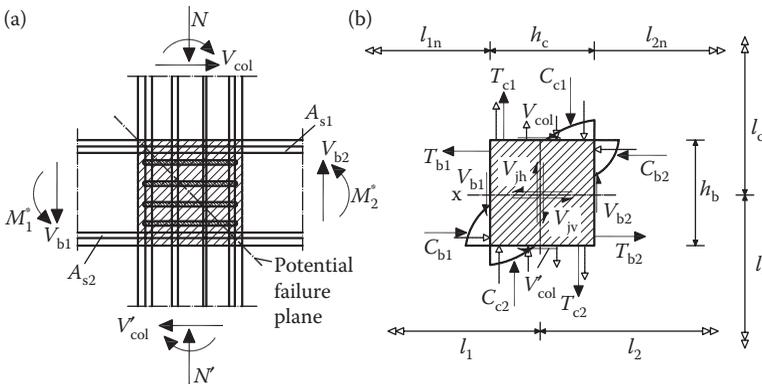
Figure 8.74 (a) Seismic actions in the joint core; (b) internal forces in the joint core (*T* results from tensile forces and *C* results from compressive forces at each face of the joint).

where

T_{b1} is the tensile force of the reinforcement at the top of beam 1 (to the left of the joint).

C_{b2} is the resultant of the compressive stresses at the top of beam 2 (to the right of the joint).

T_{b2} is the tensile force of the reinforcement at the bottom of beam 2 (to the right of the joint).

Taking into account that the axial force in the beam is very small, it may be concluded that:

$$C_{b2} = T_{b2} \tag{8.184}$$

Therefore, Equation 8.183 takes the form:

$$\boxed{V_{jh} = T_{b1} + T_{b2} - V_{col}} \tag{8.185}$$

Assuming that both top and bottom reinforcement of the beam are at yield point, Equation 8.185 takes the following form:

$$\boxed{V_{jh} = \gamma_{Rd} \cdot f_{yd}(A_{s1} + A_{s2}) - V_{col}} \tag{8.186}$$

where

γ_{Rd} is the overstrength due to steel strain hardening. For DCH buildings, γ_{Rd} should not be less than 1.20 ($\gamma_{Rd} \not< 1.20$).

For the determination of V_{col}, the values of bending moments at the top and bottom end of the column above the joint should be known at the yield stage of the beams framing to the joint. These values are difficult to define due to the permanent change of member stiffness in post-elastic stage. Given this, Paulay et al. (1978) suggested a capacity relationship for estimating the column shear V_{col} on the basis of the beam moments at the joint faces (Figure 8.74):

$$V_{col} = \frac{(l_1/l_{1n})M_1^* + (l_2/l_{2n})M_2^*}{(l_c + l_c')/2} \tag{8.187}$$

where

l_1 and l_2 are the beam spans measured from the column centre lines.

l_{1n} and l_{2n} are the corresponding clear spans of the beams.

l_c and l_c' are the column heights.

M_1^* and M_2^* are the capacity design moments of the beams at the joint faces.

Expression (8.187) has been adopted by the New Zealand Code (NZS 3101, 1995) but not by EC8 (see Subsection 8.4.2.1).

The vertical joint shear V_{jv} can be easily derived by applying the Caushy theorem, according to which $v_{jh} = v_{jv}$. Therefore,

$$v_{jh} = \frac{v_{jh}}{b_j h_c} = \frac{v_{jv}}{b_j h_b} = v_{jv} \tag{8.188}$$

or

$$V_{jv} = \frac{b_b}{b_c} V_{jh}$$ (8.189)

The same procedure may be applied for the determination of V_{jh} at an exterior joint (Figure 8.79). Taking into account that there is only one beam, Equation 8.186 takes the form:

$$V_{jh} = \gamma_{Rd} f_y A_{s1} - V_{col}$$ (8.190)

and

$$V_{col} = \frac{(l_2 / l_{2n}) M_2^*}{(l_c + l_c')/2}$$ (8.191)

8.4.2.2 Joint shear strength according to the Paulay and Priestley method

As in the case of short columns, beam column joints resist shear through two mechanisms (Figure 8.75; Paulay and Priestley, 1992):

1. A diagonal concrete strut, which provides a shear resistance V_{ch}.
2. A truss mechanism comprising a diagonal compression field combined with horizontal (hoops) and vertical (longitudinal rebars) reinforcement. This mechanism provides a shear resistance V_{sh}.

The strut shear resistance V_{ch} is caused by the following forces on the faces of the joints:

- The compression forces in concrete C_{cb1}, C_{cc1}, C_{cc2}, C_{cb2}
- The bond forces ΔT_{cb1}, ΔT_{cc1}, ΔT_{cc2}, ΔT_{cb2} transferred by the reinforcement bars within the compression zone
- The beam and column shear forces V_{b1}, V_{col1}, V_{col2}, V_{b2}

These forces acting in two opposite groups at the top left and bottom right corners of the joint, respectively, cause a diagonal compressive force D_c. Therefore,

$$V_{ch} = D_c \cos(\alpha)$$ (8.192a)
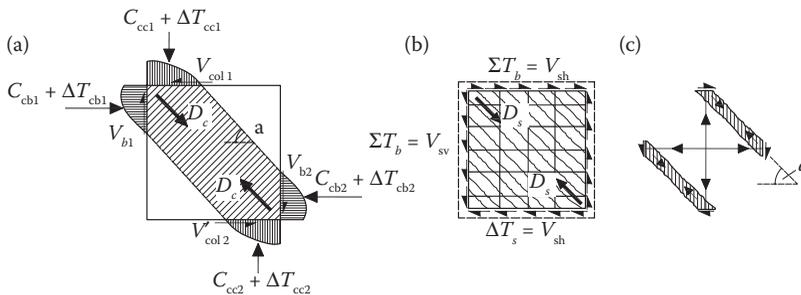
Figure 8.75 Shear transfer mechanism in a joint core: (a) diagonal concrete strut; (b) truss mechanism; (c) typical components of the truss.

$$V_{cv} = D_c \sin(\alpha) \tag{8.192b}$$

where

α is the angle of the diagonal of the joint with respect to the horizontal.

It should be noted that ΔT_c refer to only a part of the bond forces, while the rest of them are introduced along the longitudinal rebars of beams and columns in the core of the joint in the form of bond stresses. It is assumed that these bond stresses which are introduced along the longitudinal bars cause the compression forces D_s (Figure 8.75a) of the truss mechanism. Therefore,

$$V_{sh} = D_s \cos(\alpha) \tag{8.193a}$$

and

$$V_{sv} = D_s \sin(\alpha) \tag{8.193b}$$

The total shear resistance of the joint core can be expressed as the sum of the previously described mechanisms, that is,

$$V_{jh} = V_{ch} + V_{sh} \tag{8.194a}$$

$$V_{jv} = V_{cv} + V_{sv} \tag{8.194b}$$

Making now some reasonable assumptions and approximations (Paulay and Priestley, 1992), the following expressions may result for the factors of the above expressions (8.194(a)) and

$$V_{ch} = \left(1.55\frac{c}{b_c} + \beta - 0.55\right)T - V_{col} \tag{8.195}$$

$$V_{sh} = V_{jh} - V_{ch} = 1.55\left(1 - \frac{c}{b_c}\right)T \tag{8.196}$$

Taking into account that

$$\frac{c}{b_c} \cong 0.25 + 0.85\frac{N_{Ed}}{f_{cd}A_c} \tag{8.197}$$

Equation 8.196 takes the form

$$V_{sh} \cong \left(1.15 - 1.30\frac{N_{Ed}}{f_c'A_c}\right)T \tag{8.198}$$

Therefore, the required horizontal reinforcement in the form of hoops in the core of the joint may be defined as follows:

$$A_{jh} = V_{sh}/f_{ywd} \tag{8.199}$$

or

$$A_{jh} = \left(1.15 - 1.30\frac{N_{Ed}}{f_{cd}A_c}\right)\frac{\gamma_{Rd}f_{yd}}{f_{ywd}}A_{s1}$$

(8.200)

In the above equations, the following notations have been used.

c is the depth of the flexural compression zone of the column.

β is the ratio of compression reinforcement content in beam sections to the corresponding tensile one. $\left(0.5 \leq \beta = \frac{A_{s2}}{A_{s1}} \leq 1.0\right)$

γ_{Rd} is the overstrength factor for steel ranging between $1.2 < \gamma_{Rd} < 1.4$.

T is the tensile force of the steel at the upper flange of the beams $T = \gamma_{Rd}f_{yd}A_{s1}$.

N_{Ed} is the minimum compression force action on the column.

A_c is the area of cross section of the column.

f_{cd} is the design compressive strength of concrete.

f_{yd} is the design yield strength of longitudinal steel bars.

f_{yw} is the design yield strength of transverse steel hoops.

Keeping in mind expression (8.186), according to which:

$$V_{jh} = \gamma_{Rd} \cdot f_{yd}(A_{s1} + A_{s2}) - V_{col} = (1 + \beta)\gamma_{Rd} \cdot f_{yd} \cdot A_{s1} - V_{col}$$

(8.201)

and making the reasonable assumption that:

$$V_{col} \approx 0.15(1 + \beta)T$$

(8.202)

it is concluded that:

$$\frac{V_{sh}}{V_{jh}} = \frac{1.15 - 1.30(N_{Ed}/f_{cd}A_c)}{0.85(1 + \beta)}$$

(8.203)

So, for N_{Ed} min $\approx 0.10 f_{cd} A_c$, the truss mechanism should resist 60–80% of the total horizontal joint shear force. From the above expression it may easily be concluded that as N_{Ed} increases, the ratio V_{sh}/V_{jh} diminishes.

It is also worth noting that for $f_{ywd} = f_{yd}$, $N_{Ed} \cong 0.10 f_{cd} A_c$, $\gamma_{Rd} = 1.25$, the expression (8.200) takes the form:

$$A_{jh} \geq 1.28A_{s1}$$

(8.204)

This reinforcement should be placed in the space within the longitudinal steel (bars) of beams at their upper and lower flange and should comprise horizontal hoops and ties (Figure 8.74), placed normally to column axis.

Finally, for the vertical joint shear reinforcement, the following expression is obtained:

$$A_{jv} = \frac{1}{f_{yd}}[0.50(V_{jv} + V_b) - N_{Ed}]$$

(8.205)

When Equation 8.205 becomes negative, obviously no vertical joint shear reinforcement will be required.

Equations 8.200 and 8.205 ensure the joints against cracking caused by diagonal tension. On the other hand, diagonal compression (Figure 8.75) may cause diagonal crushing. Therefore, the magnitude of the horizontal joint shear stress should be limited to acceptable levels. According to Paulay and Priestley (1992), this limit is given below:

$$\boxed{v_{jh} = \frac{V_{jh}}{b_j h_j} \leq 0.25 f_{cd} \leq 9 \quad (MPa)}$$ (8.206)

The above procedure has been adopted by the New Zealand Code (NZS 3101, 1995).

8.4.2.3 Background for the determination of joint shear resistance according to ACI 318-2011 and EC8-1/2004

The collection and compilation of test results on interior joints (Kitayama et al., 1989, 1991), have caused serious reservations for a number of researchers, including the majority of those in North America, regarding the validity of the joint shear transfer models developed above. In fact, according to the ACI-special publication of Kittayama et al., the ultimate shear strength V_j of Equations 8.186 and 8.189 increases about linearly with the ratio of horizontal reinforcement ρ_{jh} (hoops) up to $\rho_{jh} = 0.4\%$ (Figure 8.76). Above this value of the steel ratio and up to $\rho_{jh} = 2.4\%$, the ultimate joint strength remains independent of ρ_{jh}, while diagonal compressive failure mode always prevails. At the same time, the joint confinement via transverse beams and the slab at their top acting as a diaphragm increases the joint shear strength v_{ju} significantly (Figure 8.77). Thus, the approach to the design of joints adopted by U.S. investigators and by ACI 318-2011 is based on a best-fitting procedure from a large number of available test results, allowing the adoption of a maximum allowable nominal shear strength V_{jh} for each type of joint.
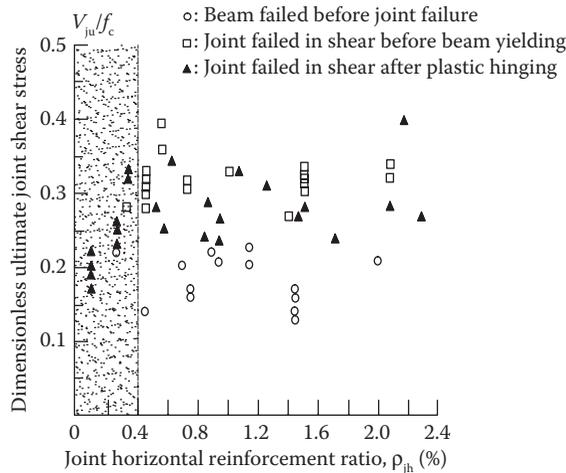
Figure 8.76 Effect of horizontal reinforcement ratio in interior joint ρ_{jh} on joint strength. (Adapted from Kitayama, K., Otani, S. and Aoyama, H. 1991. *Development of Design Criteria for R/C Interior Beam–Column Joints*. ACI Special Publication SP123, American Concrete Institute, Detroit, Michigan, 97–124.)
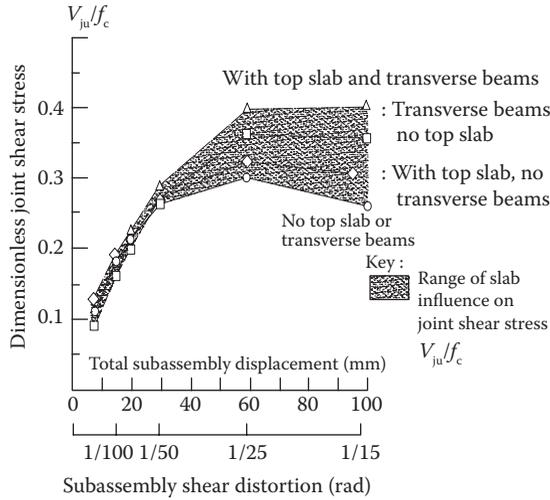
Figure 8.77 Effect of top slab and/or transverse beam on both sides on the ultimate shear strength of interior joints. (Adapted from Kitayama, K., Otani, S. and Aoyama, H. 1991. *Development of design criteria for R/C interior beam-column joints*, ACI Special Publication SP123, American Concrete Institute, Detroit, Michigan, 97–124.)

In view of the above, Eurocode EC8-1/2004 has adopted a homogeneous plane stress field in the core of the joint, depicted in Figure 8.78, for the calculation of joint horizontal reinforcement. This field includes:

1. The shear stress $v_{jh} = v_{jv}$ from Equation 8.188.
2. The vertical normal stress

$$\sigma_y = -N_{Ed}/A_c = -v_d \cdot f_{cd} \tag{8.207}$$
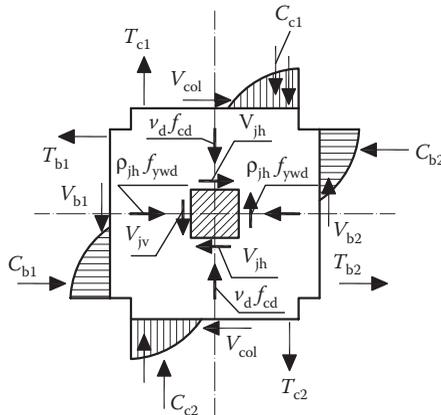
Figure 8.78 The homogeneous stress field in the joint. (Adapted from E.C.8-1/EN1998-1. 2004. *Design of Structures for Earthquake Resistance: General Rules, Seismic Actions and Rules for Buildings.* CEN, Brussels, Belgium.)

3. A smeared horizontal normal stress corresponding to the core reinforcement (transverse hoops)

$$\sigma_x = -\rho_{jh} f_{ywd} \qquad (8.208)$$

which confines the concrete core in a horizontal direction at the yield stage of confinement steel.

The principal stresses σ_I and σ_{II} of this plane stress field at failure stage should be equal to f_{ctd} (design tensile strength of concrete) and $-v_1 f_{cd}$ (design compressive strength of concrete), in inclined concrete struts. Therefore,

$$\left.\begin{matrix} f_{ctd} = \sigma_I \\ -v_1 f_{cd} = \sigma_{II} \end{matrix}\right\rangle \frac{\sigma_x + \sigma_y}{2} \pm \sqrt{\left(\frac{\sigma_x - \sigma_y}{2}\right)^2 + \sigma_{xy}^2} \qquad (8.209a)$$

or

$$\left.\begin{matrix} f_{ctd} \\ -v_1 f_{cd} \end{matrix}\right\rangle - \frac{v_d f_{cd} + \rho_{jh} f_{ywd}}{2} \pm \sqrt{\left(\frac{v_d f_{cd} - \rho_{jh} f_{ywd}}{2}\right)^2 + v_{jh}^2} \qquad (8.209b)$$

From the above equation (8.209b), the following two equations are obtained:

$$\frac{v_{jh}}{f_{cd}} = \sqrt{\left(\frac{f_{ctd}}{f_{cd}} + v_{top}\right)\left(\frac{f_{ctd}}{f_{cd}} + \rho_{jh}\frac{f_{ywd}}{f_{cd}}\right)}$$

or

$$\boxed{\rho_{jh} \cdot f_{ywd} \geq \frac{v_{jh}^2}{f_{ctd} + v_d f_{cd}} - f_{ctd}} \qquad (8.210)$$

and

$$\boxed{\frac{v_{jh\,max}}{f_{cd}} \leq \sqrt{(v_d - v_1)\left(\rho_{jh}\frac{f_{ywd}}{f_{cd}} - v_1\right)}} \qquad (8.211)$$

Equation 8.210 allows the determination of required reinforcement for shear in the core of the joint in the form of hoops and ties, so that diagonal tension cracks are avoided. The second equation (Equation 8.211) gives the upper limit for the nominal shear stress that may develop in the joint without any risk for failure due to diagonal compression.

At the same time, EC8-1/2004 has also adopted an alternative approach based mainly on the Paulay–Priestley model, which has been introduced with some simplifications.

Finally, it should be noted that the basic approach of EC 8-1 2004 to the problem gives reliable results in relation to the statistical evaluation elaborated by Kitayamma et al. (1991) *only for medium–high values of* v_d (around 0.30). These values for columns are the most common (DCM: $v_d \leq 0.65$, DCH $v_d \leq 0.55$).

8.4.2.4 Joint shear strength according to A.G. Tsonos

As in the Paulay and Priestley method (Paragraph 8.4.2b), the shear forces acting in the joint core, according to A.G. Tsonos' model (Tsonos, 1999, 2001), are resisted by two mechanisms (see also the mechanisms for short columns par. 8.3.6.2.1).

1. By a diagonal compression strut (Figure 8.79a).
2. By a truss mechanism formed by horizontal and vertical reinforcement and concrete compression struts. The horizontal and vertical reinforcement is normally provided by horizontal hoops in the joint core and by longitudinal column bars (Figure 8.79a).

Both mechanisms depend on the core concrete strength. Thus, the ultimate concrete strength of the joint core under compression or tension controls the ultimate strength of the joint and is diminished by gradual crushing of concrete along the cross-diagonal cracks (Figure 8.79a).

Consider now the section I-I in the middle of the joint height (Figure 8.79a). In this section the flexural moment is almost zero. The forces acting in the concrete are shown in Figure 8.79b. The forces acting in the longitudinal column bars between the corner bars in the side faces of the column are symbolised by T_i.

These bars compress the joint core by equal and opposite directional forces. Thus, the vertically acting forces are (Figure 8.79b):

$$D_{cy} + (T_1 + \cdots + T_4 + D_{vy}) = D_{cy} + D_{sy} = V_{jv} \tag{8.212}$$

where

D_{cy} is the vertical component of compression strut.
$T_1 + \cdots + T_4 + D_{vy}$ is the vertical component of the truss model.
V_{jv} is the vertical joint shear force.

(see par. 8.4.2.1)
The sum of the horizontally acting forces also gives the horizontal joint shear force as

$$D_{cx} + (D_{1x} + \cdots + D_{vx}) = V_{jh} \tag{8.213}$$

Taking the above relations into account, the vertical normal compressive stress σ and the shear stress τ (homogeneous stress field over the joint) are given by the following equations:

$$\sigma = \frac{D_{cy} + D_{sy}}{h'_c \cdot b'_c} = \frac{V_{jv}}{h'_c \cdot b'_b} \tag{8.214}$$

$$\tau = \frac{V_{jh}}{h'_c \cdot b'_b} \tag{8.215}$$

where

h'_c and b'_b are the length and the width of the joint core, respectively.

Taking now into account Equation 8.189, it can be seen from Equations 8.214 and 8.215 that

$$\sigma = \frac{V_{jv}}{V_{jh}}\tau = \frac{b'_b}{h'_c}\tau = \alpha \cdot \tau \tag{8.216}$$
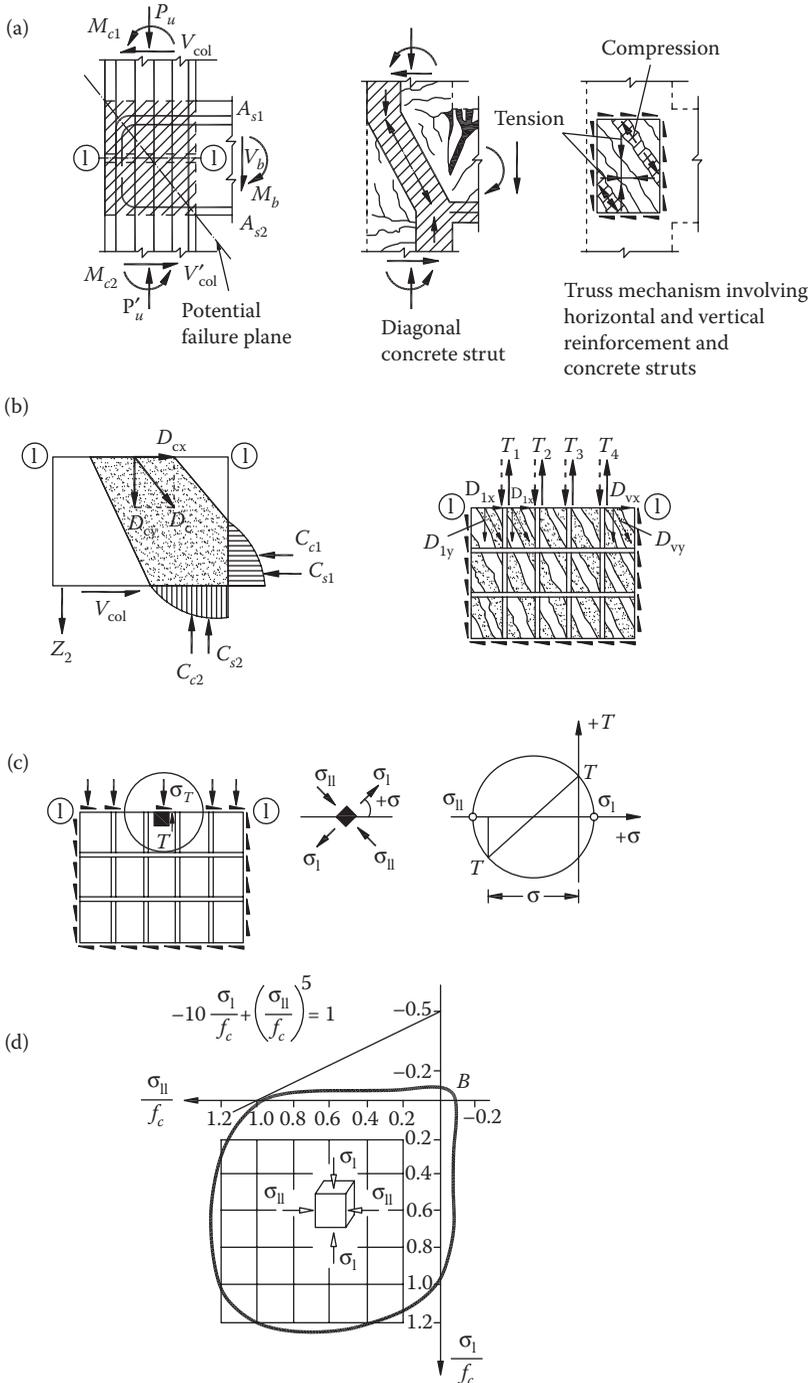
Figure 8.79 (a) External beam–column connection and the two mechanisms of shear transfer (diagonal concrete strut and truss mechanism); (b) forces acting in the joint core concrete through section I-I from the two mechanisms; (c) stress state of element of this studied region; (d) representation of concrete biaxial strength curve by a parabola of the 5th degree. (From Tsonos, A. 1999. Lateral load response of strengthened reinforced concrete beam-to-column joints. *ACI Structural Journal Proceedings*, V 96(1), 46–56. With permission of ACI.)

where
   α is the aspect ratio of the core of the joint.

The maximum principal stresses are given, as known by the following expression (Figure 8.79c) (see par. 8.4.2.3):

$$\sigma_{I,II} = \frac{\sigma}{2} \pm \frac{\sigma}{2}\sqrt{1 + \frac{4\tau^2}{\sigma^2}} \tag{8.217}$$

Keeping in mind that the envelope of concrete (Kupfer and Hilsdorf, 1969) and the branch A–B of this envelope depicted in Figure 8.79c may be approximated by a 5th degree parabola, as was first proposed by Tegos in his research on short columns (Tegos, 1984), the relation between σ_I and σ_{II} may be obtained by the following expression:

$$-10\frac{\sigma_I}{f_{ckc}} + \left(\frac{\sigma_{II}}{f_{ckc}}\right)^5 = 1 \tag{8.218}$$

where
   f_{ckc} is the confined concrete strength.

This strength of concrete is taken from the relation:

$$f_{ckc} = \kappa\, f_{ck} \tag{8.219}$$

In the above expression (8.219), f_{ck} and κ have the following meaning:
   f_{ck} is the characteristic concrete strength.
   κ is a magnifying factor in the joint (see par. 8.3.4.2.4).

Introducing now Equations 8.216 and 8.217 into Equation 8.219 and using the expression:

$$\tau = \gamma\sqrt{f_{ckc}} \tag{8.220}$$

the following expression is obtained:

$$\boxed{\left[\frac{\alpha\gamma}{2\sqrt{f_{ckc}}}\left(1 + \sqrt{1 + \frac{4}{\alpha^2}}\right)\right]^5 + \frac{5\,\alpha\gamma}{\sqrt{f_{ckc}}}\left(\sqrt{1 + \frac{4}{\alpha^2}} - 1\right) = 1} \tag{8.218a}$$

The above expression (8.218a) allows the calculation of γ and therefore the determination of τ_{ult} via Equation 8.220, and consequently the ultimate shear strength of the joint (Equation 8.215).

For simplicity's sake, the presentation of the above method has been made for exterior beam–column joints. The approach is also the same for interior joints.

The validity of the above equation (8.218a) was checked using test data for 38 exterior and interior beam–column sub-assemblages that were tested in the Laboratory of Reinforced Concrete at Aristotle University of Thessaloniki, as well as data from similar tests carried out in the United States. The comparison between the experimental and the predicted result (γ_{cal} to γ_{ex}) is shown in Figure 8.80, where very good correlation is observed.
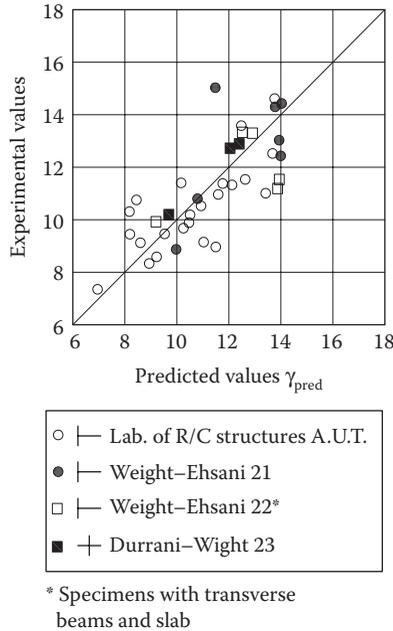
Figure 8.80 Correlation of experimental values and values predicted by the formulation of the strength of beam–column sub-assemblages. (From Tsonos, A. 2001. Seismic retrofit of R/C beam-to-column joints using local three-sided jackets. *Journal of European Association for Earthquake Engineering,* I, 48–64. With permission of ACI.)

8.4.3 Code provisions for the design of joints under seismic action

From what has been presented so far it is apparent that there are deviations from country to country in the Code specifications for the design of R/C joints against seismic action. Thus:

- The New Zealand Seismic Code NZS 3101, 1995, has adopted the Paulay and Priestley (1992) method as it was developed in Paragraphs 8.4.2.1 and 8.4.2.2.
- The U.S. Code ACI 318-2011 has adopted a very simple approach based on statistical evaluations of test results. According to this:
  - Joints must be reinforced by hoops and ties of the same type as the critical regions of the adjacent columns.
  - Nominal shear v_{jh} must be less than

$$v_{jh} \leq 1.7\sqrt{f_{cd}} \quad \text{(MPa)} \text{ for internal joints (beams framing on four faces)} \tag{8.221}$$

$$v_{jh} \leq 1.2\sqrt{f_{cd}} \quad \text{(MPa)} \text{ for external joints (beams framing on three faces)} \tag{8.222}$$

- The European Code EC8-1/2004 is based on the mechanical model presented in Paragraph 8.4.2.3 and specifies in detail the following rules.

8.4.3.1 DCM R/C buildings under seismic loading according to EC 8-1/2004

The Code does not specify any analytical verification. The specified requirements may be summarised as follows:

- The horizontal confinement of the critical regions of the columns must also be extended in the joint.
- If beams frame into all four sides of the joint and their width is at least three-fourths of the parallel cross-sectional dimension of the column, the spacing of the horizontal confinement in the joint may be increased to twice that specified for the critical region of the columns but not greater than 150 mm.
- At least one intermediate vertical bar should be provided between corner bars at each side of the joint.

8.4.3.2 DCH R/C buildings under seismic loading according to EC 8-1/2004

1. Capacity design effects
   a. For the horizontal shear force V_{jhd} acting on the concrete core of the joints, the expressions (8.186) and (8.190) may be used.
   b. The shear force of the column V_{col} above the joint corresponds to the most adverse value resulting from the analysis in the seismic design.
2. ULS verification and detailing
   a. The diagonal compression in the diagonal strut mechanism, taking into account in addition the transverse tensile strains, should not exceed the value $\nu_1 f_{cd}$ (see Equation (8.209b)
   where

$$\nu_1 = 0.6\left[1 - \frac{f_{ck}}{250}\right]$$
(8.223)

(f_{ck} in [MPa])
   The above requirement is deemed to be satisfied if the following rules are in effect:
      i. Interior beam–column joints
Shear demand V_{jhd} should satisfy the following expression:

$$\boxed{V_{jhd} \le \nu_1 f_{cd} \sqrt{1 - \frac{\nu_d}{\nu_1}} \cdot b_j \cdot h_{jc}}$$
(8.224)

   where

$$b_j = \min\{b_c; (b_w + 0.5h_c)\} \quad \text{if } b_c > b_w$$
(8.225)

$$b_j = \min\{b_w; (b_c + 0.5h_c)\} \quad \text{if } b_c < b_w$$
(8.226)

h_{jc} is the distance between extreme layers of column reinforcement.
ν_d is the normalised axial force in the column above the joints.
The above expression (8.224) results from expression (8.211) with the simplification

$$\rho_{jh} = 0$$

which is on the safe side.
The above expression ensures that joints are safe against a diagonal compression failure mode.

 ii. Exterior beam–column joints

At the exterior beam–column joints, V_{jhd} should also satisfy the expression (8.224) with its right-hand term reduced by 0.80.

b. Shear reinforcement of the joint (horizontal reinforcement of hoops and vertical reinforcement of intermediate longitudinal bars) should satisfy the following expression:

$$\frac{A_{sh} \cdot f_{ywd}}{b_j h_{jw}} \geq \frac{\left(\dfrac{V_{jhd}}{b_j \cdot h_{jc}} \right)^2}{f_{ctd} + v_d f_{cd}} - f_{ctd} \tag{8.227}$$

where

A_{sh} is the total area of the horizontal hoops.

V_{jhd} is as defined by expressions (8.186) and (8.190).

h_{jw} is the distance between the top and the bottom reinforcement of the beam.

b_{jc} is the distance between extreme layers of the column reinforcement.

b_j is as defined above in expressions (8.225) and (8.226).

v_d is the normalised design axial force of the column above ($v_d = N_{Ed}/A_c f_{cd}$).

f_{ctd} is the design value of the tensile strength of concrete in accordance with EN 1992-1-1-2004.

The above equation (8.227) results from Equation 8.210 presented in the previous paragraph.

c. As an alternative to the above procedure with number 2, the following equations may be used:

 i. In interior joints:

$$A_{sh} f_{ywd} \geq \gamma_{Rd}(A_{s1} + A_{s2})f_{yd}(1 - 0.8v_d) \tag{8.228}$$

 ii. In exterior joints:

$$A_{sh} f_{ywd} \geq \gamma_{Rd} A_{s2} f_{y1}(1 - 0.8v_d) \tag{8.229}$$

where

$\gamma_{Rd} = 1.20$

v_d refers to the column above the joint in the case of an interior column and to the column below the joint in the case of an exterior column.

A_{s1} is the beam top reinforcement area.

A_{s2} is the beam bottom reinforcement area.

The above equations (8.228) and (8.229) result from Equation 8.200 after the introduction of some additional simplifications. It should be noted that the results of the basic expressions (8.224) and (8.227) differ significantly from those of the alternative expression of (8.228) and (8.229) presented above. It is the author's opinion that the whole issue of the design of column beam joints should be re-examined on the basis of the approach of ACI 318-2011, which, as was explained previously, is based mainly on statistical evaluation of test results, until more reliable expressions are established for the design.

d. Adequate vertical reinforcement of the column passing through the joint should be provided, so that:

$$\boxed{A_{sv,1} \geq 2/3A_{sh}(h_{jc}/h_{jw})} \qquad\qquad (8.230)$$

where

A_{sh} is the required total area of the horizontal hoops in the joint.

$A_{sv,1}$ denotes the total area of the intermediate bars placed in the relevant column sides between corner bars.

e. Rules referring to DCM buildings are in effect also for DCH buildings unless they are covered by the rules set forth above.

8.4.4 Non-conventional reinforcing in the joint core

Park and Paulay (1975) pointed out that the typical shear reinforcement of joint cores, which consists of hoops and vertical bars, may be replaced by cross-inclined bars resulting from bending part of the longitudinal reinforcement of the beam. It is understood that such a detailing causes construction difficulties and it is infeasible to apply it in two orthogonal directions (when beams are framing into all four faces of a joint), hence it has not been applied in practical situations.

On the other hand, the results of tests at the University of Thessaloniki (Tsonos et al., 1995), where use was made of cross-inclined bars resulting form bending of column reinforcement, as shown in Figure 8.81, have shown superior performance of the non-conventionally
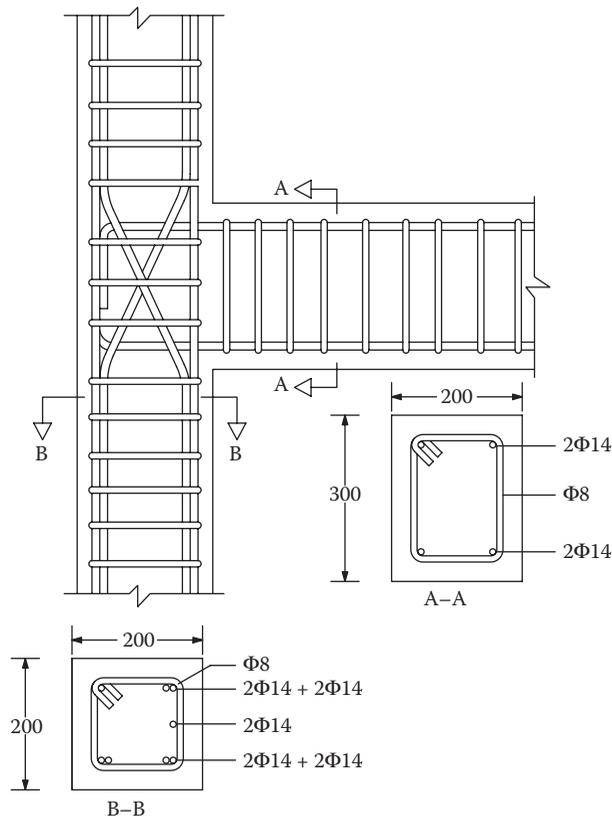
Figure 8.81 Arrangement of x-shaped bars in an exterior joint core.
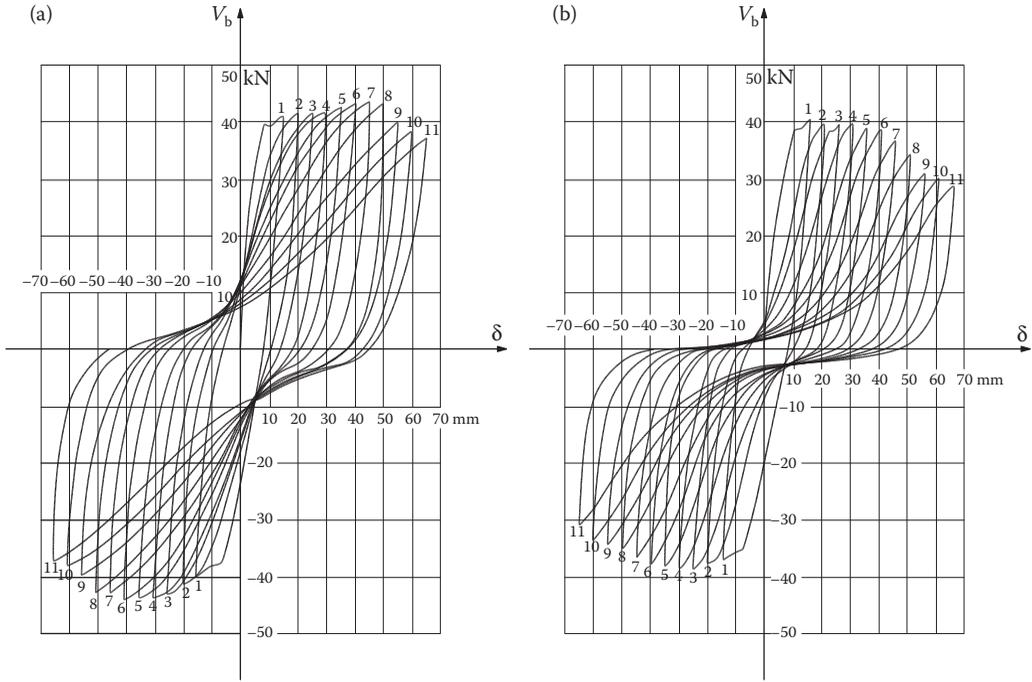
Figure 8.82 Hysteresis loops for exterior beam–column joints: (a) with x-shaped bars; (b) with conventional reinforcement.

reinforced beam–column sub-assemblages compared with similar specimens reinforced only with hoops and vertical straight bars. As shown in Figure 8.82, the hysteresis loops of specimens with cross-inclined column bars were considerably more stable and less pinched than the loops of similar conventionally reinforced specimens. The improvement was attributed mainly to the prevention of slippage of column bars within the joint core and to the increase in shear strength caused by the cross-inclined bars (see also Paragraph 8.3.6.3).

It is also pointed out that for this arrangement of bars the required hoop reinforcement is less than in conventionally reinforced joints. However, the use of cross-inclined column bars in two-way frames presents insurmountable difficulties. A possible way of resolving this problem might be the use of a pair of inclined bars placed along the diagonal of the column section; such a novel reinforcing pattern should, of course, first be studied experimentally to evaluate its efficiency as joint shear reinforcement.

8.5 MASONRY-INFILLED FRAMES

8.5.1 General

The masonry infills under consideration in this section are constructed after hardening of the concrete skeleton, in contact with it, but without special connection to it. In this context they are considered in the first instance as non-structural elements and therefore as gravity loads on the underlying frame beams. This type of masonry infill is very common in southern Europe, where seismicity is very high.

Older versions of codes (Vintzeleou, 1987) provide specific instructions for the design and construction of infilled structures, recommending two alternatives: either an effective isolation of the infills from the surrounding frames (Subsection 6.2.3, Figure 6.15) or a tight placing of the infills so that their interaction with the frames should be properly considered. In the first case the structural system is clear and relatively reliable, but the infills are susceptible to overturning out of plane, in the case of a strong earthquake. In the second case the tight placing seems to improve the seismic behaviour of the building, a fact that counterbalances to a degree the additional inertial seismic forces corresponding to the significant masses of masonry infills.

Given that infills of this type have a considerable strength and stiffness, they provide a remarkable contribution to the seismic response of the structural system. In general, the presence of masonry infills affects the seismic behaviour of buildings in the following ways (Tassios, 1984; Penelis and Kappos, 1997; Dowrick, 2005; Fardis, 2009; Stylianidis, 2012).

- The stiffness of the building increases, while the fundamental period decreases, and therefore the base shear due to seismic action also increases.
- The distribution of the lateral stiffness of the structure in plan and elevation is modified.
- Part of the seismic action is carried by the infills, thus relieving the structural system.
- The ability of the building to dissipate energy increases substantially.

The more flexible the structural system, the more the above effects of the infills is seen on the structural system. Masonry infills have less deformability than the structural system, that is, they are brittle structural elements and, therefore, they fail first, presenting at first stage separations from the frame (see Subsection 11.1.7, Figure 11.30) and then x-shaped diagonal cracks or slide cracks at the mid-height of the panel (Figures 8.86 and 11.32). Thus, infills dissipate significant quantities of seismic energy, acting as a first line of seismic defense for the building. To this contribution of masonry infills must be attributed the limited damage in the structural system of R/C buildings with regular distribution of masonry in plan and elevation (residential buildings without stores at ground level) in cities affected by strong earthquakes like Bucharest in 1977, Thessaloniki in 1978, Athens in 1981, etc.

However, there are many drawbacks in regard to the positive influence of masonry infills on the seismic behaviour of buildings. The early failure of infills under small inter-storey drifts due to their brittle character leads to a decrease in strength and stiffness of the building as a whole, and therefore to a simultaneous load transfer from the infill to the R/C structural system in the form of impulse loading. In this context the load path in the case of a strong earthquake is transformed from one moment to the other with questionable reliability. Therefore, the various analytical models developed so far are complicated, due to the descending branch of the $M-\theta$ diagram, they are sensitive, and in this respect unreliable for the prediction of the inelastic response of the structure to the successive steps of infill failure under a strong seismic motion (Michailidis et al., 1995). On the other hand, the quality control of the masonry infills is also not reliable (brick and mortar strength, brick construction pattern, etc.). Finally, the impulse loading of R/C frames at their diagonally located corners by the infill masonry (Figure 8.84) many times causes shear failure in the case of infill of high strength, as in the case of short columns (see Subsection 8.3.6).

In the subsequent subsections the above advantages and disadvantages will be examined in detail on the basis of experimental evidence carried out for many years in the Lab of R/C structures of Aristotle University of Thessaloniki (Stylianidis, 1985, 2012; Valiasis, 1989; Sarigianis, 1989; Valiasis et al., 1993).At the same time, detailed reference will be made to Code specifications for infill frames as far as modeling, analysis and design.
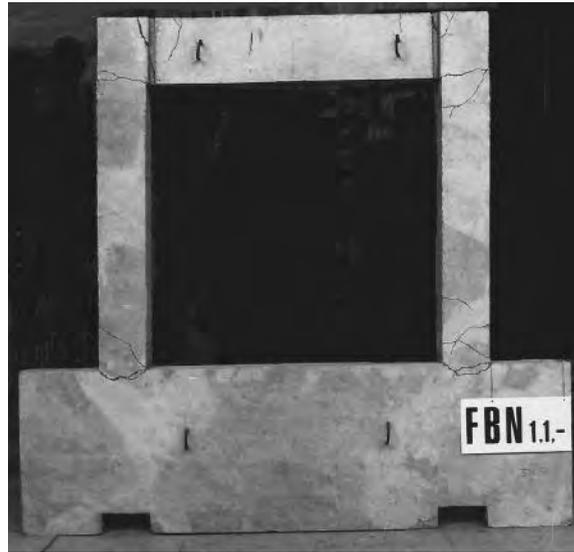
Figure 8.83 Failure modes of bare frame FBN$_{1, 1-}$ with axial load on the columns. (Adapted from Stylianidis, K. 2012. *Journal of O.C.B.T.*, 6, 194–212.)

8.5.2 Structural behaviour of masonry infilled frames under cyclic loading reversals

The main conclusions drawn from experimental results under cyclic loading reversals on one storey-one bay frames are the following (Subsection 7.2.3, Figure 7.6).

- In case of relatively weak infills, the failure modes of the infilled frames are almost the same as those of the corresponding bare frames (Figures 8.84 through 8.86).
- The hysteresis loops of the bare frames are rich, typical for inelastic rotations of plastic hinges (Figure 8.87). Conversely, pinching effects occur at the infilled frames, which are typical to brittle failure of infills (Figure 8.88).
- The load–displacement envelopes of the bare frames are those of an elastoplastic system (Figure 8.87).
- The horizontal branch of H(KN)-γ(‰) appears at an angular distortion of about 12–18‰ where the frame reaches its maximum strength.
- The presence of infills alters the load–displacement envelopes of the infilled frames (Figure 8.88). At the beginning, an almost linear behaviour is displayed due to the composite action of the infilled system. This linear behaviour is terminated for an angular distortion of about 0.2–0.5‰. From there on, an ascending curved branch appears that depicts the separation of the infill from the surrounding frame and cracking of both the frame and the infill. This branch is terminated at an angular distortion of 3–6‰. After this critical value of distortion is reached, *a descending branch follows*, due to the *loss of strength* and integrity of the infill. This branch is relatively smooth and almost linear. It should be noted that the ascending branch of the *H–γ* curve stops for very low distortion (γ = 3–6‰), that is, before the failure capacity of the bare frame (γ ≅ 12–18‰; Figure 8.89).
- The infills offer *strength, stiffness* and *energy dissipation capacity* depending on the strength of the infill in relation to the strength of the frame. However, this contribution is rapidly diminished at high angular distortions (Figures 8.90 through 8.92). So,

Figure 8.84 Failure mode of the strengthened infilled frame FINR. (Adapted from Stylianidis, K. 2012. *Journal of O.C.B.T.* 6, 194–212.)

- *The ratio of the strength* of the infilled frames to the strength of the bare frames for masonry infills common in use in the construction industry is about 2.5–3.0 at distortions of 2‰. At higher displacements the infill gradually degrades but still contributes to the strength of the system. The ratio continues to be about 1.5–1.70 at distortions of 30‰ (Figure 8.90).

Figure 8.85 Failure mode of bare frame FB. (Adapted from Stylianidis, K. 2012. *Journal of O.C.B.T.*, 6, 194–212.)

Figure 8.86 Failure mode of the infilled frame F5. (Adapted from Stylianidis, K. 2012. *Journal of O.C.B.T.*, 6, 194–212.)

- *The initial stiffness* of the infilled frames for a distortion of 0.1‰ is 4.5–5.5 times the stiffness of the bare frames depending on the existence or not of axial loads at the columns (Figure 8.91). This stiffness rapidly diminishes as the distortion increases. Therefore, the fundamental period T_o of the system is unstable, increasing rapidly with the angular distortion.
- *The energy dissipation mechanism* of the infilled frame includes, in addition to the frame dissipative mechanism of plastic hinges, another mechanism due to the friction of the infills across the bounding frame and mainly across the cracks of the infill. This friction-type mechanism is very active at *low distortions* but it tends to disappear at high distortions, *since infill degrades rapidly* with angular distortion.
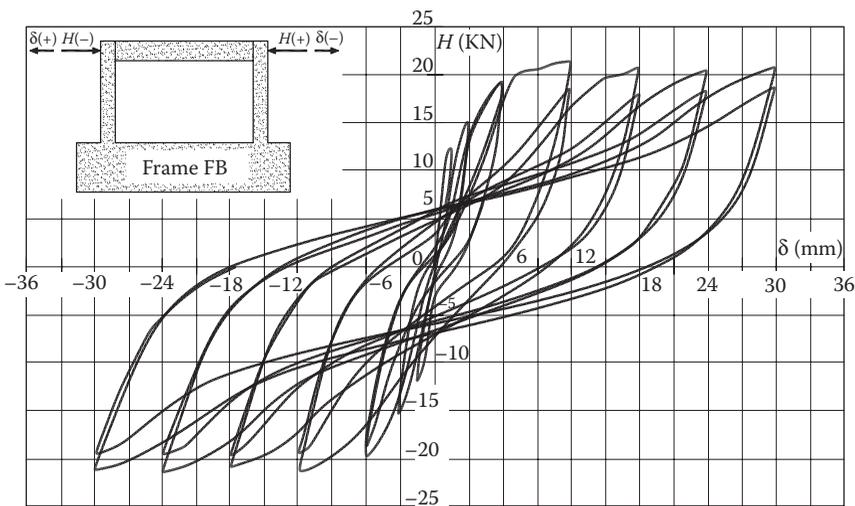
Figure 8.87 Lateral load–displacement loops. Bare frame FB. (Adapted from Stylianidis, K. 2012. *Journal of O.C.B.T.*, 6, 194–212.)
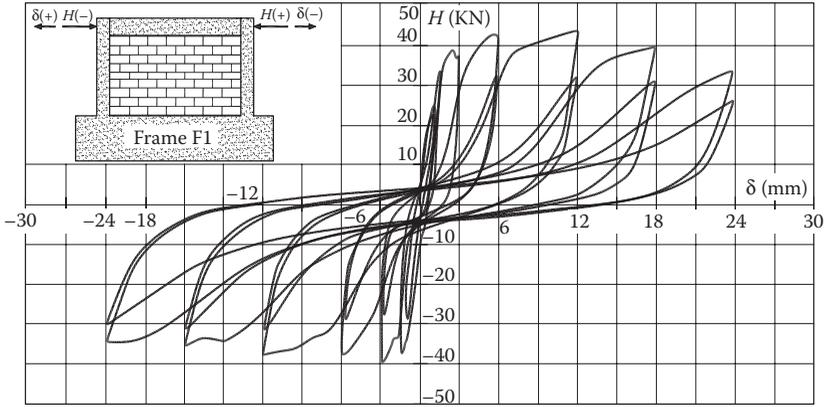
Figure 8.88 Lateral load–displacement loops. Infilled frame F1. (Adapted from Stylianidis, K. 2012. *Journal of O.C.B.T.*, 6, 194–212.)
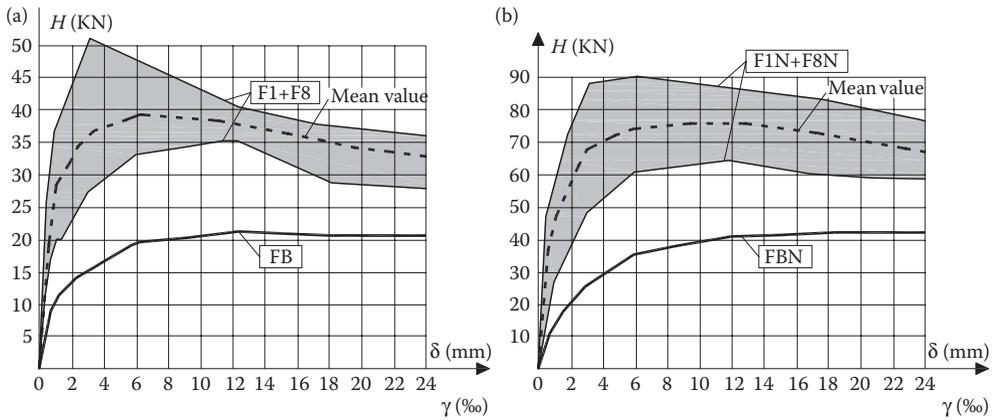
Figure 8.89 Program #1. Lateral load–displacement envelopes: (a) models without axial force; (b) models with axial force. First cycles only. (Adapted from Stylianidis, K. 2012. *Journal of O.C.B.T.*, 6, 194–212.)
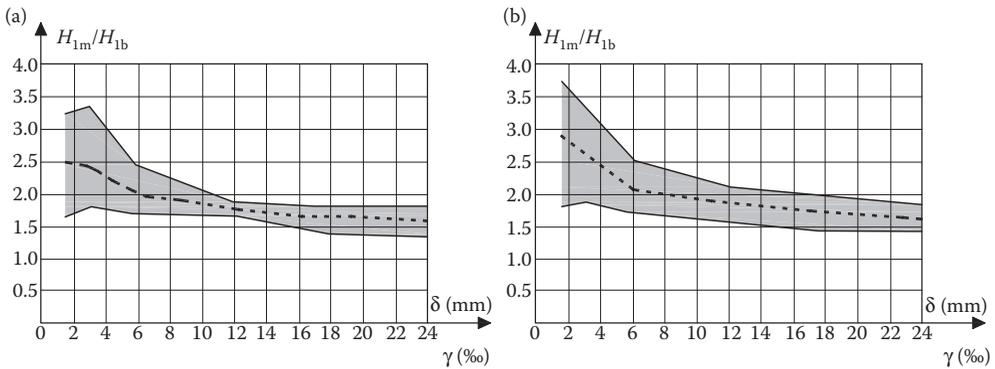
Figure 8.90 Program #1. Ratio of infilled frames to bare frames strength. (a) Models without axial force (b), models with axial force. First cycles only. (Adapted from Stylianidis, K. 2012. *Journal of O.C.B.T.*, 6, 194–212.)
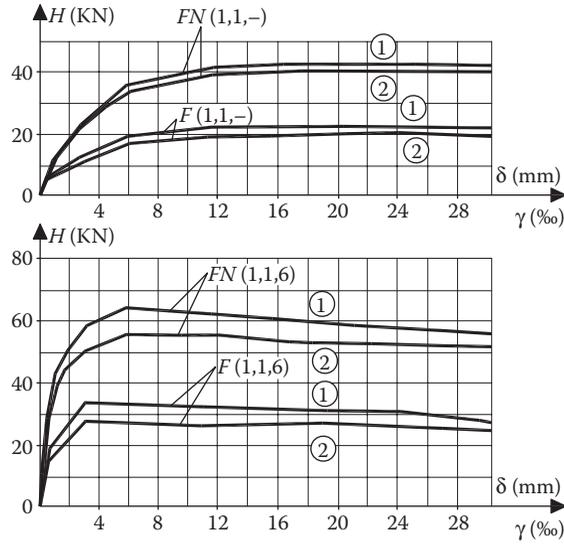
Figure 8.91 Program #2. Lateral load–displacement envelopes of bare frames $F_{1,1,\boxtimes}$, and $FN_{1,1,\boxtimes}$ infilled frames $F_{1,1,6}$ and $FN_{1,1,6}$. (Adapted from Stylianidis, K. 2012. *Journal of O.C.B.T.*, 6, 194–212.)

The maximum ratio of the energy dissipation capacity of the infilled frames to corresponding bare frames *is about 3.0–5.0* at distortions of 2‰ and about 1.3–1.5 at distortions of 30‰ (Figure 8.92).

- *The ductility* of infilled frames is satisfactory, though lower than that of the bare frames. In fact, for $\beta = 0.8–0.9$ (Figure 8.93), ductility of the angular distortion γ ranges between 14.0 and 5.0 with a mean scatter of 30%. However, it should be noted that this ductility in terms of ultimate distortion is not compatible with that of a bare frame. In fact, the ultimate distortion of the bare frame is higher than 30‰ ($H/H_{max} = 0.9$), while the ultimate distortion of an infilled frame is in the range of 8–10‰.
- In case of *high strength infill* compared to bare frame, local shear failures at the joints of the columns may occur due to the diagonal compression of the infill in the form of a strut (Figures 8.84 and 8.94).
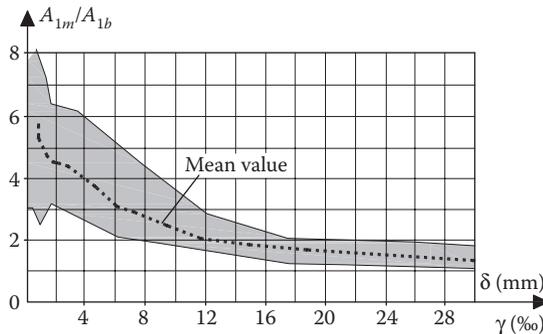
Figure 8.92 Program #2. Mean value and scatter of the ratio of infilled frames to bare frames energy dissipation $A_{1\,m}/A_{1b}$. (Adapted from Stylianidis, K. 2012. *Journal of O.C.B.T.*, 6, 194–212.)
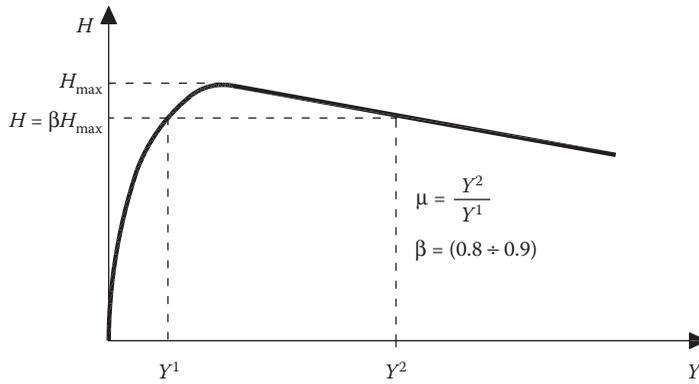
Figure 8.93 Definition of the ductility index. (Adapted from Stylianidis, K. 2012. *Journal of O.C.B.T.*, 6, 194–212.)
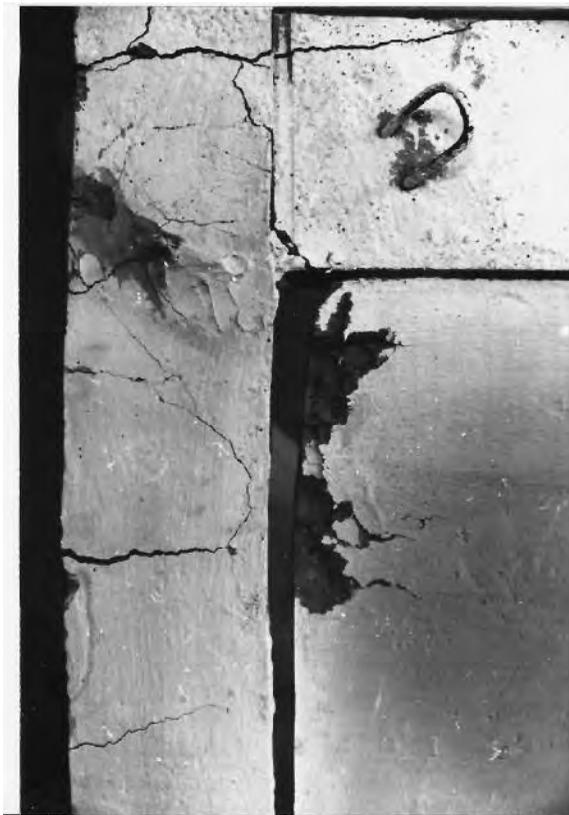
Figure 8.94 Separation of the infill from the frame; local crushing of the infill corners of frame F4R. (Adapted from Stylianidis, K. 2012. *Journal of O.C.B.T.*, 6, 194–212.)

- There is a need for an analytical model to describe the cyclic behaviour of the infill that will be capable of complying with existing inelastic analysis computer platforms. Some efforts have been made thus far (Michailidis et al., 1995), but not enough for a reliable and general approach to the problem.
- The general conclusion is that simple infilling techniques, like the construction of a brick wall with a width of half the width of the adjacent columns can:
  - Double the strength of the system
  - Triple the energy dissipation capacity
  - Give four times higher stiffness at low distortions.

At the same time, the rapid decrease of the above magnitudes with increasing distortions generates strong reservations about the ability of making use of the above capacities in a reliable and controlled analytical procedure.

8.5.3 Code provisions for masonry-infilled frames under seismic action

8.5.3.1 Requirements and criteria

The effects of the infills in analysis and design must be considered together with the high degree of uncertainty related to their behaviour, namely:

- The variability of their mechanical properties and therefore the low reliability in their strength, stiffness and energy dissipation capacities.
- Their wedging condition, that is, how tightly they are connected to the surrounding frame.
- The potential modification of their integrity during the life of the building.
- Their irregular arrangement in plan and elevation in the building.
- The possible adverse local effects due to the frame–infill interaction in critical regions of the frame (e.g. shear-failure of columns under shear forces induced by the diagonal strut action of the infill).

Thus, according to EC 8-1/2004 *the safety of the structure cannot rely, not even partly, upon the infills and only their probable adverse influence is taken into account.*

Because of their high lateral stiffness, a large percentage of the seismic effects would have been transferred to them in the case that they were taken into account as structural elements. However, for increasing distortions, this initial distribution of seismic effects between infills and frames would change rapidly against the frame system. It is obvious that such an approach would be against the structural safety of the system.

So, according to EC 8-1/2004, the seismic analysis, in general, is carried out *on the bare frame system, and only additional measures are taken for an eventual adverse influence* of the masonry infills on the structural system. These measures are given in the following paragraphs and refer *only to frame and frame equivalent dual systems* for DCH buildings. However, they provide criteria for good practice, which may also be useful for DCM and DCL R/C buildings. For all wall or wall-equivalent dual systems, the interaction between the concrete structural system and the infills may be neglected.

It is the author's opinion that the above approach of the Code to the problem is very conservative. Documented capacities in stiffness strength and energy dissipation of masonry infills could be exploited to a degree for low-rise buildings with regular distribution of infills

in plan and elevation, combined with rules that would ensure the quality control of masonry construction. In this way it is expected that a significant cost reduction could be obtained, particularly for low-cost residential blocks of apartments.

8.5.3.2 Irregularities due to masonry infills

1. Irregularities in plan
   a. Strongly irregular, non-symmetric or non-uniform arrangements of infills in plan should be avoided. Of course, this is not always possible due to the architectural constraints imposed on the design. For example, in the case of buildings located at the corner of a building block, with stores on the ground floor, there are infills along two consecutive sides of the building adjacent to the block and there are show windows on the other two. In such a case, the structural system should be analysed again, including in the structural model the infills simulated according to the recommendation presented in the next paragraph (8.5.3.4). It is apparent that the re-analysis should be carried out for a 3-D structural model. In this case, special attention should be paid to the verification of structural elements on the flexible sides of the plan against the effects of any torsional response caused by the infills.
   b. When masonry infills are not regularly distributed, but not in such a way as to constitute a severe irregularity as in the corner building above, these irregularities may be taken into consideration by increasing the effects of the accidental eccentricity imposed by Code with a factor λ equal to 2.0:

$$\lambda = 2.0 \tag{8.231}$$

2. Irregularities in elevation
   a. If there are considerable irregularities in elevation (e.g. in the case of a pilotis-open ground storey imposed by the Building Code, or ground floors used as stores with open space and show windows at the facade), the internal seismic forces in the vertical elements of the respective storey should be increased (penalised).
   b. A simplified procedure for the determination of this magnifying factor η is specified by EC 8-1/2004 and is given below:

$$\eta = \left(1 + \Delta V_{RW} \middle/ \sum V_{Ed}\right) \le q \tag{8.232}$$

where

   ΔV_{RW} is the total reduction of the resistance of masonry infills, in the storey concerned, compared to the more infilled storey above it, and

   ΣV_{Ed} is the sum of the seismic shear forces acting on all vertical primary seismic members of the storey concerned.

   c. If the above-defined magnification factor η is lower than 1.10, there is no need for modification of the seismic action effects.
   d. It should be remembered that the above penalty expressed by the magnifier η, at least for DCH buildings, should be added for the columns of the storey concerned to the penalty imposed on the whole structural system of a 20% reduction of the q-factor for DCM and DCH buildings with significant irregularities in elevation with abrupt changes.

e. It is important to note that for the determination of ΔV_{RW} in Equation 8.232 there is no need for an additional analysis, since V_{RW} refers to the strength capacity of the individual infill panels.

8.5.3.3 Linear modeling of masonry infills

For the linear analysis of structural systems, including masonry infills, particularly in the case of significant irregularities in plan or even in the case of strong irregularities in elevation (e.g. soft ground story), two procedures may be followed.

The most usual one is the simulation of the infill through a compression diagonal strut (Figure 8.95) with the following properties (Michailidis et al., 1995):

- Thickness t of the strut: the thickness of the wall t
- Width of the strut: $w \simeq 0.20d$ where d is the length of the diagonal
- Modulus of elasticity E_w of the strut: the modulus of elasticity of the masonry taken from EC 6

The second procedure, in use in the last decade, simulates the infill panels through shell finite elements (FEM). Taking into account that a rapid degradation of the infill occurs, it should not be forgotten that for the modulus of elasticity of the masonry, a reduction factor equal to 0.5 or less should be introduced.

In the case of perforated walls with more than one opening (e.g. door and window), the infill is disregarded in the model.

8.5.3.4 Design and detailing of masonry-infilled frames

8.5.3.4.1 General

Masonry-infilled frames may have two different forms:

1. Infill panels are separated from the structure and are fixed in the surrounding frame in such a way that they do not interfere with the structural deformation (Chapter 6, Figure 6.15). The main issues for these panels are their stabilisation against out-of-plane overturning in case of a strong earthquake and their heating and sound insulation problem at the gaps with the surrounding frame. This type of infill has no influence on the structural behaviour of the building in response to seismic actions.
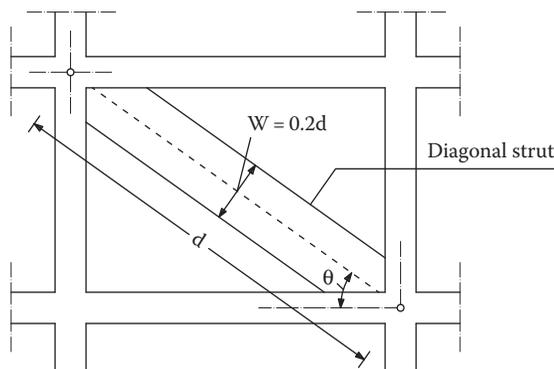
Figure 8.95 Compression diagonal model for the estimation of infill stiffness.

2. Infill panels are integrated with the structural system. They are usually built in the form of masonry infills after concrete hardening, are edged at the surrounding frames, and many times they are connected with them. It is obvious that the presentation so far refers to this type of masonry-infilled structures (Figure 8.48). In any case, for both infill types belonging to all ductility classes DCL, M and H, appropriate measures are taken to avoid brittle failure and premature disintegration of the infill walls. The main measures refer to 'damage limitation' and particularly to *the limitation of inter-storey drifts',* which have been presented in detail in Subsection 6.2.3.

8.5.3.4.2 Masonry infills integrated into the structural system

For these masonry infills, in addition to the 'limitation of interstorey drifts' specified by the Code, the following protective measures should be taken:

1. Particular attention should be paid to masonry panels with a slenderness ratio of >15 (ratio of the smaller of length or height to thickness). The same holds also in case of openings.
2. The measures for the protection of the above masonry walls against out-of-plane over-turning or shear failure x-shaped cracks are the following:
   a. Wall ties fixed to the columns and cast into the bedding planes of the masonry.
   b. Reinforced concrete posts and belts across the panels and through the full thickness of the wall.
   c. if there are large openings or perforations in any of the infill panels, their edges should be trimmed with belts and posts.

8.5.3.4.3 Adverse effects on columns adjacent to masonry infills

- Taking into account the particular vulnerability of the infill walls of ground floors, it is reasonable that, due to partial or total failure of some of these walls, a seismically induced irregularity is to be expected. Appropriate measures should therefore be taken. The simplest approach to the problem, according to EC 8-1/2004, is the extension of the critical region at the columns of the ground floor to their entire length being confined accordingly.
- If the height of the infills is smaller than the clear length of the adjacent columns, the following measures should be taken (Figure 8.48).
  - The entire length of the column is considered a critical region and should be reinforced with the number and pattern of stirrups for critical regions.
  - The consequences of the decrease of the shear span ratio of these columns should be appropriately confronted. In fact, in this case the plastic hinges of the column are likely to be formed at their top, and at the captive point at the top of the masonry wall. Therefore, the capacity design shear force is increased, since the shear span ratio decreases. In this case, the clear length of the column l_{cl} is taken to be equal to the free part of the column, and $M_{i,d}$ at the column section at the top of the infill wall should be taken as being equal to $\gamma_{Rd} M_{Rc,i}$, with $\gamma_{Rd} = 1.1$ for DCM and 1.3 for DCH and $M_{Rc,i}$ the design resistance of the column.
  - The transverse reinforcement resulting above should cover the free part of the column plus a height equal to the dimension of the cross section of the column parallel to the infills in extension to the contact region of the column with the infill.
  - If the length of the free part of the column is less than 1.5 h_c, the shear force should be resisted *by diagonal* reinforcement (see Subsection 8.3.6).

- When the masonry infill extends to the entire height of the columns, but only to one side of it while the other is free (e.g. corner columns), the entire length of the column should be considered a critical region and be reinforced with the number and pattern of stirrups required for critical regions.
  - The length l_c of columns, over which the diagonal strut force of the infill is applied, should be verified in shear for the smaller of the following shear forces:
  - The horizontal component of the strut force of the infill estimated to be equal to the horizontal *shear strength* of the panel, determined on the basis of the shear strength of bed joints;
  - The shear force estimated on the basis of shear capacity design for columns applied to the contact length l_c of the strut to column and with moment resistance at the ends of the contact length l_c, the overstrengthened moment resistance $\gamma_{Rd} M_{Rc,i}$ of the column. In most cases this second value is much higher than the shear strength capacity of the infill along its horizontal joint bed.
- All measures presented above for confronting the adverse effects of masonry infills on the columns hold for both ductility classes, that is, DCM and DCH buildings.

8.5.4 General remarks on masonry-infilled frames

The approach of EC 8-1/2004 to masonry-infilled frames and masonry-infilled frame-equivalent dual systems of DCM and DCH seems to be rather prohibitive, in fact:

- The increase of the accidental eccentricity for DCH by 2, even for buildings with limited irregularities in infill arrangement.
- The increase of the calculated action effects on the bare structure for DCH by a factor η ranging up to 1.70 for irregularities in elevation.
- The re-analysis of buildings with high irregularities in infill arrangement, taking into account their stiffness and redesigning of all structural elements (mainly columns) with an adverse influence on their design action effects due to infills.
- The design rules specified by the Code for the columns in infilled frames drive the designer to avoid the use of masonry infills or to provide separation joints between masonry and the R/C structural system. However, extensive research (Valiasis and Stylianidis, 1989; Stylianidis and Penelis, 1993; Michailidis et al., 1995; Stylianidis, 2012) has shown that masonry infills constitute a highly effective dissipation mechanism. In addition, extended statistical damage evaluation in areas affected by strong earthquakes (Penelis et al., 1989; Fardis, 2009) has in general shown a positive influence of masonry infills on the seismic behaviour of buildings. In this respect, infill masonry walls constitute a first line of defence of the building against earthquakes, acting as a type of damper that protects the R/C skeleton to a significant degree. Therefore, the subject should in the future be reconsidered by the Code so that methods could be developed that will allow on one hand local improvement of the structural elements suffering from the presence of masonry infills, while on the other favouring and promoting the extensive use of masonry infills in building construction.

8.6 EXAMPLE: DETAILED DESIGN OF AN INTERNAL FRAME

The internal frame along the *y–y* direction, grid axis B, of the eight-storey RC building studied in Chapter 5 has been selected for a detailed design (Figure 5.44). Since beams B8 and B19 are symmetrical to B57 and B68, the analytical calculations are performed only
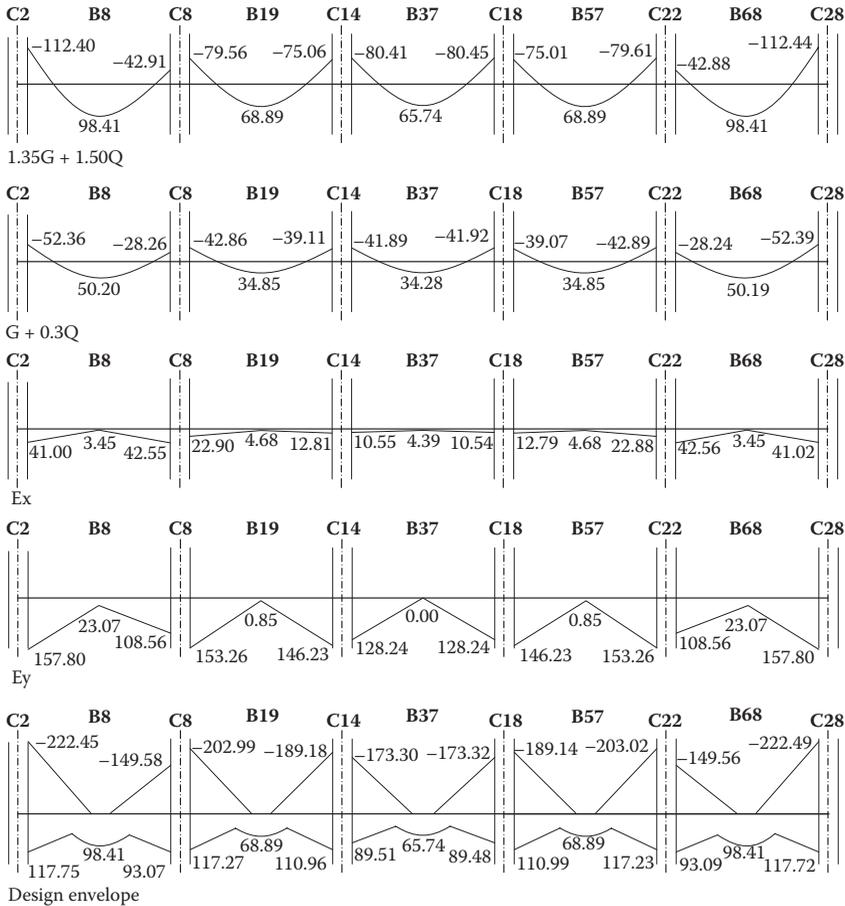
Figure 8.96 Moment diagrams for the various loading cases.

for B8 and B19, whereas beam B37 follows the design of B19. The same applies for columns C2, C8 and C14, which are symmetrical to C28, C22 and C18. In Figures 8.96 and 8.97 the moment and shear diagrams for the various loading cases are shown (it should be recalled that the number of seismic load combinations is limited to 8. Details are provided in Subsection 5.9.1).

8.6.1 Beams: Ultimate limit state in bending

Minimum percentage of longitudinal reinforcement (Equation 8.73):

$$\rho_{min} = 0.5\frac{f_{ctm}}{f_{yk}} = 0.5\frac{2.6}{500} = 0.0026 \rightarrow A_{s,min} = 4.66 \text{ cm}^2$$

8.6.1.1 External supports on C2 and C28 (beam B8-left, B68-right)

Hogging design moment for the top reinforcement: $M_d^- = -222.45$ kN m
   Sagging design moment for the bottom reinforcement: $M_d^+ = 117.75$ kN m
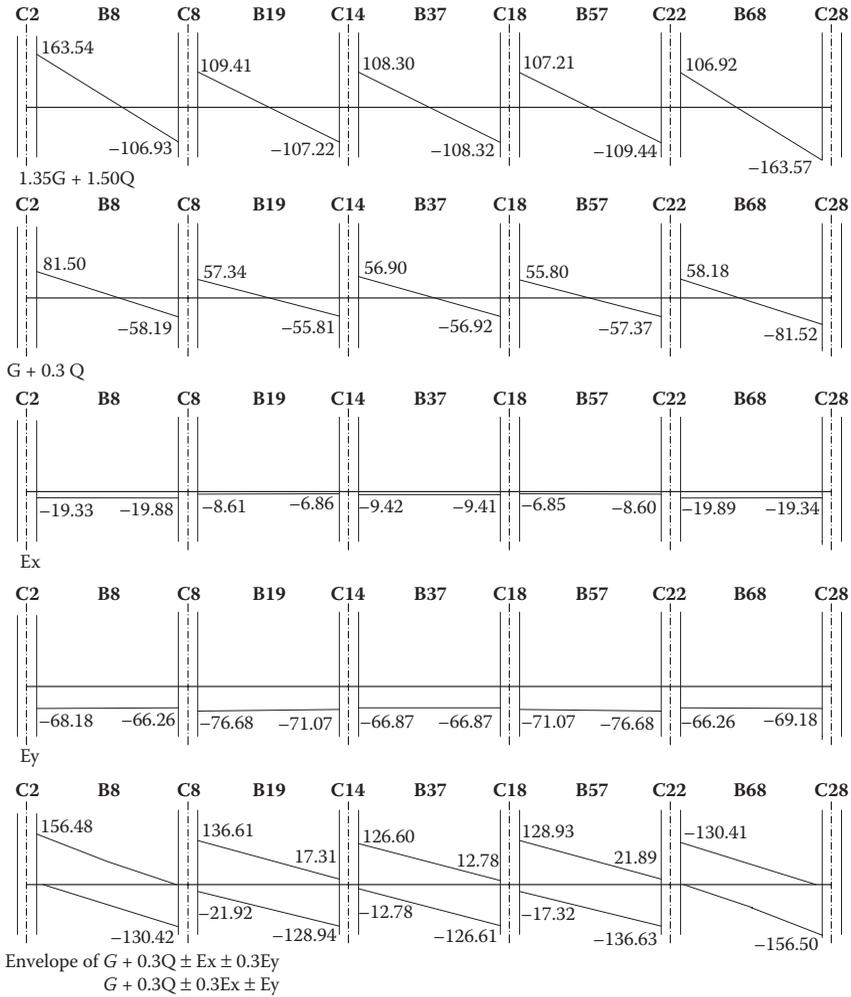
Figure 8.97 Shear diagrams for the various loading cases.

Top longitudinal reinforcement:

$$\mu_{sd} = \frac{\left|M_d^-\right|}{b \cdot d^2 \cdot f_{cd}} = \frac{222.45 \cdot 10^6}{300 \cdot 597^2 \cdot \dfrac{25}{1.5}} = 0.125 \rightarrow \omega_{req} = 0.1368 \rightarrow$$

$$A_{s,req} = \omega_{req} \cdot b \cdot d \frac{f_{cd}}{f_{yd}} = 0.1368 \cdot 300 \cdot 597 \frac{25/1.5}{500/1.15} = 9.39 \text{ cm}^2 \rightarrow 5\varnothing16 \ (10.05 \text{ cm}^2)$$

Experimental evidence has shown that after flexural yielding of a beam in negative bending (tension in the upper reinforcement), part of the slab reinforcement up to a significant distance from the web of the beam is fully activated and contributes to the beam negative flexural capacity as tension reinforcement (Fardis et al., 2005). The slab width effective as the tension flange of a beam at the support of a column is specified in paragraph 5.4.3.1.1(3.b) of EC8-Part I (2004). The effective width of the external support is shown in Figure 8.98.
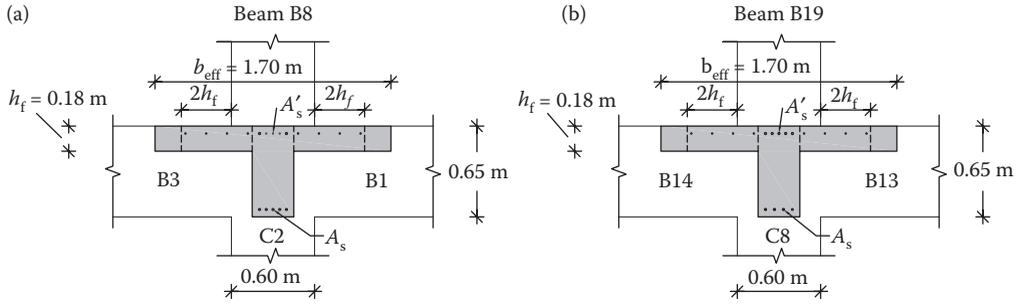
Figure 8.98 Slab effective width of the (a) external (beam 8) and (b) the internal support (beam 19).

The slab reinforcement is ∅8/150. The reinforcement of the slab within the effective width is equal to 8∅8 (4.02 cm²). The percentage of the provided tensile reinforcement, ρ_{prov}, is

$$\rho_{prov} = \frac{(4.02 + 10.05)}{300 \cdot 597} = 0.00786$$

Bottom longitudinal can be determined by

$$\mu_{sd} = \frac{\left|M_d^+\right|}{b_{eff} \cdot d^2 \cdot f_{cd}} = \frac{117.75 \cdot 10^6}{1700 \cdot 597^2 \dfrac{20}{1.5}} = 0.012 \rightarrow \omega_{req} = 0.0122 \rightarrow$$

$$A_{s,req} = \omega_{req} \cdot b_{eff} \cdot d \frac{f_{cd}}{f_{yd}} = 0.0122 \cdot 1700 \cdot 597 \frac{25/1.5}{500/1.15} = 4.76 \text{ cm}^2 \rightarrow 4\varnothing14 \text{ (6.16 cm}^2)$$

$$\rho'_{prov} = \frac{A_{s,req}}{b \cdot d} = \frac{6.16 \cdot 10^2}{300 \cdot 597} = 0.00344 < \frac{\rho_{prov}}{2} = 0.00393$$

Hence, the compressive longitudinal reinforcement has to be at least equal to 5∅14 (7.70 cm²):

$$\rho'_{prov} = 0.00430 > \frac{\rho_{prov}}{2} = 0.00393$$

Maximum reinforcement ratio of the tension zone, ρ_{lmax}, is determined by (Equation 8.69)

$$\rho_{l\max} = \rho_2 + \frac{0.0018}{\mu_{\varphi dem} \cdot \varepsilon_{sy,d}} \cdot \frac{f_{cd}}{f_{yd}}$$

For

$$T_1 = 0.82 \text{ s} \rightarrow T_1 > T_C = 0.6 \text{ s}: \mu_\varphi = 2q_o - 1 = 7.8$$

Hence,

$$\rho_{\max} = 0.00393 + \frac{0.0018}{7.8 \cdot \dfrac{(500/1.15)}{200000}} \cdot \frac{(25/1.5)}{(500/1.15)} = 0.00837 > \rho_{prov} = 0.00786$$

8.6.1.2 Internal supports on C8 and on C22 (beam B8-right, B19-left, B57-right, B68-left)

Hogging design moment for the top reinforcement: $M_d^- = -202.99$ kN m
Sagging design moment for the bottom reinforcement: $M_d^+ = 117.27$ kN m
Top longitudinal reinforcement:

$$\mu_{sd} = 0.114, \omega_{req} = 0.1237, A_{s,req} = 8.49 \text{ cm}^2, 5\varnothing16 \ (10.05 \text{ cm}^2)$$

The percentage of the provided tensile reinforcement (ρ_{prov}) is (slab reinforcement is 8Ø8): $\rho_{prov} = 0.00786$
Bottom longitudinal reinforcement:

$$\mu_{sd} = 0.0116, \omega_{req} = 0.0122, A_{s,req} = 4.74 \text{ cm}^2 \rightarrow 4\varnothing14 \ (6.16 \text{ cm}^2)$$

$$\rho'_{prov} = 0.00344 < \rho_{prov}/2 = 0.00393$$

Hence, the compressive reinforcement is taken to be equal to 5Ø14 (7.70 cm²):

$$\rho'_{prov} = 0.00430 > \rho_{prov}/2 = 0.00393$$

Maximum reinforcement ratio of the tension zone, ρ_{max}, (Equation 8.69):
For

$$T_1 = 0.82 \text{ s} \rightarrow T_1 > T_C = 0.6 \text{ s}: \mu_\varphi = 2q_o - 1 = 7.8, \rho_{max} = 0.00837 > \rho_{prov} = 0.00786$$

8.6.1.3 Internal supports on C14 and C18 (beam B19-right, B37-left, B37-right, B57-left)

Hogging design moment for the top reinforcement: $M_d^- = -189.18$ kN m
Sagging design moment for the bottom reinforcement: $M_d^+ = 110.96$ kN m
Top longitudinal reinforcement:

$$\mu_{sd} = 0.1062, \omega_{req} = 0.1145, A_{s,req} = 7.86 \text{ cm}^2, 4\varnothing16 \ (8.04 \text{ cm}^2)$$

The percentage of the provided tensile reinforcement (ρ_{prov}) is (slab reinforcement is 8Ø8): $\rho_{prov} = 0.00674$
Bottom longitudinal reinforcement:

$$\mu_{sd} = 0.0110, \omega_{req} = 0.0115, A_{s,req} = 7.49 \text{ cm}^2 \rightarrow 3\varnothing14 \ (4.62 \text{ cm}^2)$$

$$\rho'_{prov} = 0.00258 < \rho_{prov}/2 = 0.00337$$

Hence, the compressive reinforcement is taken to be equal to 4Ø14 (6.16 cm²):

$$\rho'_{prov} = 0.00334 \cong \rho_{prov}/2 = 0.00337$$

Maximum reinforcement ratio of the tension zone, ρ_{max}, (Equation 8.72): For

$$T_1 = 0.82 \text{ s} \rightarrow T_1 > T_C = 0.6 \text{ s}: \mu_\varphi = 2q_o - 1 = 7.8, \rho_{max} = 0.00751 > \rho_{prov} = 0.00674$$

8.6.1.4 Mid-span (beams B8, B68)

Sagging design moment for the bottom reinforcement: $M_d = 98.41$ kN m
  Bottom longitudinal reinforcement:

$$\mu_{sd} = 0.0097, \omega_{req} = 0.0102, A_{s,req} = 4.33 \text{ cm}^2 < A_{s,min} = 4.66 \text{ cm}^2 \rightarrow 4\varnothing14 = 6.16 \text{ cm}^2$$

  Top longitudinal reinforcement: In the case of DCH, one quarter of the maximum top reinforcement at the supports shall run along the entire beam length: $A_{s,sup} = 10.05$ cm^2 (5$\varnothing$16) $A'_{s,mid} > 1/4 \cdot A_{s,sup} = 2.51$ cm^2 2$\varnothing$16 (4.02 cm^2) is provided as top reinforcement.

8.6.1.5 Mid-span (beams B19, B37, B57)

Sagging design moment for the bottom reinforcement: $M_d = 68.89$ kN m
  Bottom longitudinal reinforcement:

$$\mu_{sd} = 0.0068, \omega_{req} = 0.0072, A_{s,req} = 3.03 \text{ cm}^2 < A_{s,min} = 4.66 \text{ cm}^2 \rightarrow 4\varnothing14 = 6.16 \text{ cm}^2$$

  Top longitudinal reinforcement:

  $A_{s,sup} = 10.05$ cm^2 (5$\varnothing$16) $A'_{s,mid} > 1/4 \cdot A_{s,sup} = 2.51$ cm^2 2$\varnothing$16 is provided as top reinforcement.
  At this stage, the maximum allowable bar diameter of beam longitudinal bar passing through beam–column joints, d_{bL}, is defined:
  Interior beam–column joints (Equation 8.81): for $N_{Ed} = 1739.99$ kN $\rightarrow v_d = 0.289$,

$$\frac{d_{bL}}{h_c} \le \frac{7.5 \cdot f_{ctm}}{\gamma_{Rd} \cdot f_{yd}} \cdot \frac{1 + 0.8 \cdot v_d}{1 + 0.75 \cdot K_D \cdot \rho'/\rho_{max}} = \frac{7.5 \cdot 2.6}{1.2 \cdot 434.78} \cdot \frac{1 + 0.8 \cdot 0.289}{1 + 0.75 \cdot 1 \cdot 0.00344/0.00751} \Leftrightarrow$$
$$d_{bL} \le 19.94 \text{ mm}$$

  Exterior beam–column joints (Equation 8.82): for $N_{Ed} = 991.21$ kN $\rightarrow v_d = 0.165$,

$$\frac{d_{bL}}{h_c} \le \frac{7.5 \cdot f_{ctm}}{\gamma_{Rd} \cdot f_{yd}} \cdot (1 + 0.8 \cdot v_d) = \frac{7.5 \cdot 2.6}{1.2 \cdot 434.78} \cdot (1 + 0.8 \cdot 0.165) \Leftrightarrow d_{bL} \le 25.4 \text{ mm}$$

8.6.2 Columns: Ultimate limit state in bending and shear

The columns selected for design are columns C2 and C8.

8.6.2.1 Column C2 (exterior column)

Ultimate limit state in bending

For all the load combinations that appear in Table 8.4 at the top and base of column C2 of storey 1 $\omega_{req} = 0$. Thus, the minimum longitudinal reinforcement is placed. The number and bar diameters selected are: 4Ø20 + 12Ø16 (36.69 cm² > $A_{s,min}$)
Minimum reinforcement: $A_{s,min} = \rho_{min} \cdot b \cdot h = 0.01 \cdot 600 \cdot 600 = 36.00$ cm²
    The minimum reinforcement is placed in all the columns of the building.
Calculation of the design values of the moments of resistance of beam 8 at the support on C2 (beam 8-left)
    → E_y: Bottom reinforcement: 5Ø14, $\omega = 0.0198$, $\mu_{Rd} = 0.019$,

$$M_{ARd} = \mu_{Rd} \cdot b_{eff} \cdot d^2 \cdot f_{cd} = 0.019 \cdot 1.700 \cdot 0.597^2 \cdot \frac{25 \cdot 10^3}{1.5} = 190.27 \text{ kN m}$$

    ← E_y: Top reinforcement: 8Ø8 + 5Ø16, $\omega = 0.2050$, $\mu_{Rd} = 0.179$,

$$M'_{ARd} = \mu_{Rd} \cdot b \cdot d^2 \cdot f_{cd} = 0.0179 \cdot 0.600 \cdot 0.597^2 \cdot \frac{25 \cdot 10^3}{1.5} = 319.50 \text{ kN m}$$

Table 8.4 Bending moments and axial forces at column C2 ends for column dimensioning – storey 1

Load combinations		N	V_x	V_y	M_x	M_y
Top of column C2						
Lc1	1.35G+1.5Q	−2831.27	−1.67	−26.26	49.27	3.34
Lc2	G+0.3Q+Ex+0.3Ey	−1268.36	47.39	4.77	52.36	88.73
Lc3	G+0.3Q+Ex−0.3Ey	−1529.94	43.22	−15.65	21.26	81.21
Lc4	G+0.3Q−Ex+0.3Ey	−1675.1	−45.13	−9.67	25.82	−77.37
Lc5	G+0.3Q−Ex−0.3Ey	−1936.68	−49.3	−30.09	−5.27	−84.89
Lc6	G+0.3Q+Ey+0.3Ex	−1105.53	19.87	23.54	79.34	39.37
Lc7	G+0.3Q+Ey−0.3Ex	−1227.55	−7.88	19.2	71.38	−10.46
Lc8	G+0.3Q−Ey+0.3Ex	−1977.49	5.97	−44.52	−24.3	14.31
Lc9	G+0.3Q−Ey−0.3Ex	−2099.51	−21.78	−48.86	−32.26	−35.52
Base of column C2						
Lc1	1.35G+1.5Q	−2884.13	−1.67	−26.26	−64.98	−3.93
Lc2	G+0.3Q+Ex+0.3Ey	−1307.51	−49.3	−30.09	−78.56	−125.74
Lc3	G+0.3Q+Ex−0.3Ey	−1569.09	−45.13	−9.67	−20.82	−115.11
Lc4	G+0.3Q−Ex+0.3Ey	−1714.25	43.22	−15.65	−42.25	110.63
Lc5	G+0.3Q−Ex−0.3Ey	−1975.83	47.39	4.77	15.48	121.26
Lc6	G+0.3Q+Ey+0.3Ex	−1144.68	−21.78	−48.86	−133.21	−55.41
Lc7	G+0.3Q+Ey−0.3Ex	−1266.7	5.97	−44.52	−122.32	15.5
Lc8	G+0.3Q−Ey+0.3Ex	−2016.64	−7.88	19.2	59.24	−19.98
Lc9	G+0.3Q−Ey−0.3Ex	−2138.66	19.87	23.54	70.13	50.94

Calculation of the design values of the moments of resistance at the ends of column C2
At the base of C2 at the second storey (Figure 8.99), using the corresponding earthquake forces from a table similar to Table 8.4

$\rightarrow E_y$: $G + 0.3Q + E_y + 0.3E_x, N = -991.21$ kN, $\nu = -0.165$
$M_y = -103.44$ kN, $\mu_y = 0.035$
$\omega = 0.2916$
$\left.\begin{array}{l}\end{array}\right\}$ $\mu_x = 0.166,$
$M_x = 498.24$ kN m

$\rightarrow E_y$: $G + 0.3Q + E_y - 0.3E_x, N = -1097.07$ kN, $\nu = -0.183$
$M_y = 30.61$ kN, $\mu_y = 0.010$
$\omega = 0.2916$
$\left.\begin{array}{l}\end{array}\right\}$ $\mu_x = 0.168,$
$M_x = 503.52$ kN m

$\leftarrow E_y$: $G + 0.3Q - E_y + 0.3E_x, N = -1743.95$ kN, $\nu = -0.291$
$M_y = -40.75$ kN, $\mu_y = 0.014$
$\omega = 0.2916$
$\left.\begin{array}{l}\end{array}\right\}$ $\mu_x = 0.179,$
$M_x = 535.78$ kN m

$\leftarrow E_y$: $G + 0.3Q - E_y - 0.3E_x, N = -1849.81$ kN, $\nu = -0.308$
$M_y = -93.30$ kN, $\mu_y = 0.031$
$\omega = 0.2916$
$\left.\begin{array}{l}\end{array}\right\}$ $\mu_x = 0.182,$
$M_x = 543.54$ kN m

The results are summarised in Table 8.5.
The same procedure is followed for calculating the design values for the moments of resistance at the top and base of storey 1. The results appear in Tables 8.6 and 8.7, respectively.

Figure 8.99 Capacity design moments for column C2.

Table 8.5 Determination of the design value of the moment of resistance M_x of column C2 at the base of storey 2

Load combination		N	M_y	μ_y	v	ω	μ_x	M_x
$\rightarrow E_y$	G+0.3Q+Ey+0.3Ex	−991.21	−103.44	0.035	−0.165	0.2916	0.166	498.24
	G+0.3Q+Ey−0.3Ex	−1097.07	30.61	0.010	−0.183	0.2916	0.168	503.52
$\leftarrow E_y$	G+0.3Q−Ey+0.3Ex	−1743.95	−40.75	0.014	−0.291	0.2916	0.179	535.78
	G+0.3Q−Ey−0.3Ex	−1849.81	93.3	0.031	−0.308	0.2916	0.182	543.54

Parameter κ_D (Equation 6.15), which accounts for the case of strong columns and weak beams, is calculated at the top of column C2 for both directions of seismic action.

$$\rightarrow E_y: \sum M_{Rb} = 190.27 \text{ kN m}, \sum M_{Rc} = 1013.55 \text{ kN m}, \kappa_D = \min\left(1, \frac{190.27}{1013.55}\right) = 0.19$$

$$\leftarrow E_y: \sum M_{Rb} = 319.50 \text{ kN m}, \sum M_{Rc} = 1111.99 \text{ kN m}, \kappa_D = \min\left(1, \frac{319.50}{1111.99}\right) = 0.29$$

Parameter κ_C at the base of column C2 is taken to be equal to 1 in order to simplify the design procedure.

Capacity design seismic shear for column C2

The shear forces are determined according to the capacity design criterion as follows (Equation 6.11):

Clear height of the column: $l_c = h_{st} - h_b = 5 - 0.65 = 4.35$ m

$$\rightarrow E_y: V_{sd,CD} = \gamma_{Rd} \frac{\kappa_C M_{CRd} + \kappa_D M_{DRd}}{l_c} = 1.30 \frac{0.19 \cdot 510.03 + 1 \cdot 511.98}{4.35} = 181.62 \text{ kN}$$

$$\leftarrow E_y: V_{sd,CD} = \gamma_{Rd} \frac{\kappa_C M_{CRd} + \kappa_D M_{DRd}}{l_c} = 1.30 \frac{0.29 \cdot 568.45 + 1 \cdot 572.35}{4.35} = 219.86 \text{ kN}$$

The checks that follow are performed for $V_{sd,CD} = 221.02$ kN.

Shear resistance in the case of diagonal concrete crushing for $\boxtimes = 21.8°$ (Equation 8.62)

$$V_{Rd,max} = \alpha_{cw} \cdot b_w \cdot 0.9d \cdot \frac{(v_1 \cdot f_{cd}) \cot\delta}{(1 + \cot^2 \delta)} = 1 \cdot 0.6 \cdot 0.9 \cdot 0.547 \cdot \frac{0.775 \cdot (25/1.5) \cdot 1000}{2.9}$$

$$= 1315.63 \text{ kN}$$

$$V_{Rd,max} = 1315.63 \text{ kN} > V_{sd,CD} = 219.86 \text{ kN}$$

Table 8.6 Determination of the design value of the moment of resistance M_x of column C2 at the top of storey 1

Load combination		N	M_y	μ_y	v	ω	μ_x	M_x
$\rightarrow E_y$	G+0.3Q+Ey+0.3Ex	−1105.53	39.37	0.013	−0.184	0.2916	0.168	503.94
	G+0.3Q+Ey−0.3Ex	−1227.55	−10.46	0.003	−0.205	0.2916	0.170	510.03
$\leftarrow E_y$	G+0.3Q−Ey+0.3Ex	−1977.49	14.31	0.005	−0.330	0.2916	0.186	556.28
	G+0.3Q−Ey−0.3Ex	−2099.51	−35.52	0.012	−0.350	0.2916	0.190	568.45

Table 8.7 Determination of the design value of the moment of resistance M_x of column C2 at the base of storey 1

Load combination		N	M_y	μ_y	v	ω	μ_x	M_x
$\rightarrow E_y$	G+0.3Q+Ey+0.3Ex	−1144.68	−55.41	0.019	−0.191	0.2916	0.169	505.90
	G+0.3Q+Ey⊠0.3Ex	−1266.7	15.5	0.005	−0.211	0.2916	0.171	511.98
$\leftarrow E_y$	G+0.3Q⊠Ey+0.3Ex	−2016.64	−19.98	0.007	−0.336	0.2916	0.187	560.18
	G+0.3Q⊠Ey⊠0.3Ex	−2138.66	50.94	0.017	−0.356	0.2916	0.191	572.35

Transverse reinforcement in the critical regions of column C2
The length of the critical region is

$$l_{cr} = \max\{1.5 h_c; l_c/6; 0.6\} = \max\{1.5 \cdot 0.6; 4.35/6; 0.6\} = 1.35 \text{ m}$$

For the factor 1.50 see EC8-1/2004 Paragraph 5.5.3.2.2(13).
The spacing of hoops shall not exceed:

$$s = \min\{b_o/3; 125; 6 \cdot d_{bL}\} = \min\{514/3; 125; 6 \cdot 16\} = 96 \text{ mm}$$

$$V_{wd} = V_{sd,CD} \Leftrightarrow s = \frac{A_{sw}}{V_{sd,CD}} 0.9 d \cdot f_{ywd} = \frac{4 \cdot (\pi \cdot 8^2/4)}{219.86} \cdot 0.9 \cdot 0.547 \cdot \frac{500}{1.15} = 195.74 \text{ mm}$$

Hence, the shear reinforcement in the critical regions of column C2 is ∅8/95.
Transverse reinforcement outside the critical regions of column C2
The spacing of hoops shall not exceed:

$$s = \min\{20\Phi_{L,min}; \min(b_c; h_c); 400\} = \min\{20 \cdot 16; 600; 400\} = 320 \text{ mm}$$

Hence, the shear reinforcement outside the critical regions of column C2 is ∅8/180.
Detailing for local ductility—confinement reinforcement in the critical region at the base of column C2.
The confinement reinforcement at the base of the column consists of a perimeter and an internal rectangular closed stirrup (4 legs). The mechanical volumetric ratio of the required confining reinforcement, ω_{wd}, should satisfy Equation 8.127. Thus,

$$\omega_{wd,req} \geq \frac{1}{\alpha}\left(30 \cdot \mu_\varphi \cdot v_d \cdot \varepsilon_{syd} \frac{b_c}{b_o} - 0.035\right) = \frac{1}{0.641}\left(30 \cdot 7.8 \cdot 0.356 \cdot 0.0022 \frac{600}{520} - 0.035\right)$$
$$= 0.27$$

This value is higher than 0.12, which is the lower limit set by the code: $\omega_{wd,req} = 0.27 > 0.12$.
The confinement effectiveness factor is Equation 8.129: $\alpha = \alpha_n \cdot \alpha_s = 0.776 \cdot 0.826 = 0.641$, where
Equation 8.130a:

$$\alpha_n = 1 - \sum_n \frac{b_i^2}{6} \cdot b_o \cdot h_o = 1 - \frac{4 \cdot 247 + 8 \cdot 123.5}{6 \cdot 522 \cdot 522} = 0.776$$

Equation 8.131a:

$$\alpha_s = (1 - s/2b_o)(1 - s/2h_o) = (1 - 95/2 \cdot 522)(1 - 95/2 \cdot 522) = 0.826$$

The provided mechanical volumetric ratio for $\varnothing 8/95$ is

$$\omega_{wd,prov} = \frac{V_o}{V_c} \cdot \frac{f_{yd}}{f_{cd}} = \frac{(4 \cdot 522 + 4 \cdot 522) \cdot \pi \cdot 8^2/4}{522 \cdot 522 \cdot 100} \cdot \frac{500/1.15}{20/1.5} = 0.212 < 0.27$$

Hence, hoops at the critical region are modified to: $\varnothing 10/90$

$$\omega_{wd,req} \geq \frac{1}{\alpha}\left(30 \cdot \mu_\varphi \cdot \nu_d \cdot \varepsilon_{syd} \frac{b_c}{b_o} - 0.035\right) = \frac{1}{0.649}\left(30 \cdot 7.8 \cdot 0.356 \cdot 0.0022 \frac{600}{520} - 0.035\right)$$
$$= 0.268$$

The confinement effectiveness factor is Equation 8.129:

$$\alpha = \alpha_n \cdot \alpha_s = 0.778 \cdot 0.834 = 0.649, \text{ where}$$

Equation 8.130a:

$$\alpha_n = 1 - \sum_n \frac{b_i^2}{6} \cdot b_o \cdot h_o = 1 - \frac{4 \cdot 245 + 8 \cdot 122.5}{6 \cdot 520 \cdot 520} = 0.778$$

Equation 8.131a:

$$\alpha_s = (1 - s/2b_o)(1 - s/2h_o) = (1 - 90/2 \cdot 520)(1 - 90/2 \cdot 520) = 0.834$$

$$\omega_{wd,prov} = \frac{V_o}{V_c} \cdot \frac{f_{yd}}{f_{cd}} = \frac{(4 \cdot 520 + 4 \cdot 520) \cdot \pi \cdot 10^2/4}{520 \cdot 520 \cdot 90} \cdot \frac{500/1.15}{20/1.5} = 0.350 > 0.268$$

8.6.2.2 Design of exterior beam–column joint

Ultimate limit state verification and design (Subsection 8.4.2)
The horizontal shear force acting on the concrete core of the exterior joint is (Equation 8.186)

$$\rightarrow E_y : V_{jh} = \gamma_{Rd} \cdot f_{yd} \cdot (0 + A_{s2}) - V_{col} = 1.2 \cdot \frac{500}{1.15} \cdot \left(0 + \frac{5 \cdot \pi \cdot 14^2}{4}\right)$$
$$- \max(112.00; 100.32) = 289.58 \text{ kN}$$

$$\leftarrow E_y : V_{jh} = \gamma_{Rd} \cdot f_{yd} \cdot (A_{s1} + 0) - V_{col} =$$
$$= 1.2 \cdot \frac{500}{1.15} \cdot \left(\left(\frac{8 \cdot \pi \cdot 8^2}{4} + \frac{5 \cdot \pi \cdot 16^2}{4}\right) + 0\right) - \max(33.20; 44.88) = 689.43 \text{ kN}$$

Table 8.8 Bending moments and axial forces at the base of the second storey for column C2

Earthquake	Load combination	N (kN)	V_x (kN)	V_y (kN)	M_x (kN m)	M_y (kN m)
$\rightarrow E_y$	G+0.3Q+Ey+0.3Ex	−991.21	−67.26	−112	−171.83	−103.44
	G+0.3Q+Ey⊠0.3Ex	−1097.07	19.37	−100.32	−153.6	30.61
$\leftarrow E_y$	G+0.3Q⊠Ey+0.3Ex	−1743.95	−26.62	33.2	52.13	−40.75
	G+0.3Q⊠Ey⊠0.3Ex	−1849.81	60.01	44.88	70.36	93.30

The shear force in the column above the joint, V_{col}, appears in Table 8.8 ($V_{col} = V_y$).
Diagonal compression induced in the joint by the diagonal strut mechanism
Equation 8.224 is applied in order to check the diagonal compression induced in the joint by the diagonal strut mechanism:

$$\rightarrow Ey: V_{jhd} \le 0.8 \cdot v_1 \cdot f_{cd} \sqrt{1 - \frac{v_d}{v_1}} \cdot b_j \cdot h_{jc} = 0.8 \cdot 0.54 \cdot \frac{25 \cdot 1000}{1.5} \sqrt{1 - \frac{0.183}{0.54}} \cdot 0.60 \cdot 0.49$$

$$= 1735.57 \text{ kN}$$

The normalised load above the joint is (Table 8.8): $N_{Ed} = 1097.07$ kN $\rightarrow v_d = 0.183$

$$\leftarrow E_y: V_{jhd} \le 0.8 \cdot v_1 \cdot f_{cd} \sqrt{1 - \frac{v_d}{v_1}} \cdot b_j \cdot h_{jc} = 0.8 \cdot 0.54 \cdot \frac{25 \cdot 1000}{1.5} \sqrt{1 - \frac{0.308}{0.54}} \cdot 0.60 \cdot 0.49$$

$$= 1397.90 \text{ kN}$$

The normalised load above the joint is (Table 8.8): $N_{Ed} = 1849.81$ kN $\rightarrow v_d = 0.308$

8.6.2.2.1 Confinement of the joint

8.6.2.2.1.1 HORIZONTAL REINFORCEMENT

The horizontal and vertical reinforcement of the joint shall be such as to limit the maximum diagonal tensile stress of concrete to the design value of the tensile strength of concrete. For this purpose, Equation 8.227 needs to be satisfied:

$$\rightarrow E_y: A_{sh} = \frac{b_j \cdot h_{jw}}{f_{ywd}} \cdot \left[\frac{\left(\frac{V_{jhd}}{b_j \cdot h_{jc}}\right)^2}{f_{ctd} + v_d \cdot f_{cd}} - f_{ctd} \right] = \frac{0.60 \cdot 0.54 \cdot 10^6}{500/1.15}$$

$$\cdot \left[\frac{\left(\frac{289.58}{0.60 \cdot 0.49 \cdot 10^3}\right)^2}{1.20 + 0.20 \cdot 25/1.5} - 1.20 \right] < 0$$

$$\leftarrow E_y : A_{sh} = \frac{b_j \cdot b_{jw}}{f_{ywd}} \cdot \left[\frac{\left(\frac{V_{jhd}}{b_j \cdot b_{jc}}\right)^2}{f_{ctd} + \nu_d \cdot f_{cd}} - f_{ctd} \right] = \frac{0.60 \cdot 0.54 \cdot 10^6}{500/1.15}$$

$$\cdot \left[\frac{\left(\frac{689.43}{0.60 \cdot 0.49 \cdot 10^3}\right)^2}{1.20 + 0.284 \cdot 25/1.5} - 1.20 \right] < 0$$

Since $A_{sh} < 0$, it means that no hoops are required and that the concrete cross section may undertake the shear force at the joint. In this case hoops and ties forseen for the column critical region are arranged also in the joint. The alternative expression given by Equation 8.229 is also applied.

$$\rightarrow E_y : A_{sh} \geq \frac{\gamma_{Rd}}{f_{ywd}} \cdot A_{s2} \cdot f_{yd} \cdot (1 - 0.8 \cdot \nu_d) = \frac{1.2}{500/1.15} \cdot \left(5 \cdot \frac{\pi \cdot 14^2}{4} \right) \cdot \frac{500}{1.15}$$

$$\cdot (1 - 0.8 \cdot 0.205) = 7.72 \text{ cm}^2$$

The normalised load below the joint is (Table 8.9): $N_{Ed} = 1227.55 \text{ kN} \rightarrow \nu_d = 0.205$

$$\leftarrow E_y : A_{sh} \geq \frac{\gamma_{Rd}}{f_{ywd}} \cdot A_{s2} \cdot f_{yd} \cdot (1 - 0.8 \cdot \nu_d) =$$

$$= \frac{1.2}{500/1.15} \cdot \left(\frac{8 \cdot \pi \cdot 8^2}{4} + \frac{5 \cdot \pi \cdot 16^2}{4} \right) \cdot \frac{500}{1.15} \cdot (1 - 0.8 \cdot 0.350) = 12.16 \text{ cm}^2$$

The normalised load below the joint is (Table 8.9): $N_{Ed} = 2099.51 \text{ kN} \rightarrow \nu_d = 0.350$
Hoop layers provided in the joint: $n = \text{int}(b_{jw}/s) + 1 = \text{int}(0.54/0.095) + 1 = 7$ layers
The total area of horizontal hoops is: $A_{sh,prov} = 7.4 \cdot \pi \cdot 10^2/4 = 21.98 \text{ cm}^2 > 12.16 \text{ cm}^2$

8.6.2.2.1.2 VERTICAL REINFORCEMENT

The vertical reinforcement of the column passing through the joint is (Equation 8.230):

$$A_{sv,1} = \frac{2}{3} \cdot A_{sh} \cdot \frac{b_{jc}}{b_{jw}} = \frac{2}{3} \cdot 12.16 \cdot \frac{0.49}{0.54} = 7.36 \text{ cm}^2$$

Table 8.9 Bending moments and axial forces at the top of storey 1 for column C2

Earthquake	Load combination	N (kN)	V_x (kN)	V_y (kN)	M_x (kN m)	M_y (kN m)
$\rightarrow E_y$	G+0.3Q+Ey+0.3Ex	−1105.53	19.87	23.54	79.34	39.37
	G+0.3Q+Ey⊠0.3Ex	−1227.55	−7.88	19.2	71.38	−10.46
$\leftarrow E_y$	G+0.3Q⊠Ey+0.3Ex	−1977.49	5.97	−44.52	−24.3	14.31
	G+0.3Q⊠Ey⊠0.3Ex	−2099.51	−21.78	−48.86	−32.26	−35.52

The provided longitudinal bars at the face of the joint are: $6\varnothing16 \rightarrow 12.06$ cm^2 > 7.36 cm^2. The flexural and shear reinforcement placed in column C2 appear in Figure 8.100.

8.6.2.3 Column C8 (interior column)

Ultimate limit state in bending

The same design procedure followed in the case of column C2 applies in column C8 as well. For all the load combinations that appear in Table 8.10 at the top and base of column C8, $\omega_{\text{req}} = 0$. Thus, the minimum longitudinal reinforcement is placed. The number and bar diameters selected are: $4\varnothing20 + 12\varnothing16$ (36.69 cm^2 > $A_{\text{s,min}}$).

Minimum reinforcement: $A_{\text{s,min}} = \rho_{\text{min}} \cdot b \cdot h = 0.01 \cdot 600 \cdot 600 = 36.00$ cm^2.

Calculation of the design values of the moments of resistance of beams 8, 19 at the supports on C8 (beam 8-right, beam 19-left).

$\rightarrow E_y$: Top reinforcement beam 8:$8\varnothing8 + 5\varnothing16$, $\omega = 0.2050$, $\mu_{\text{Rd}} = 0.179$,

$$M_{\text{ARd}} = \mu_{\text{Rd}} \cdot b \cdot d^2 \cdot f_{\text{cd}} = 0.179 \cdot 0.600 \cdot 0.597^2 \cdot \frac{25 \cdot 10^3}{1.5} = 319.50 \text{ kNm}$$
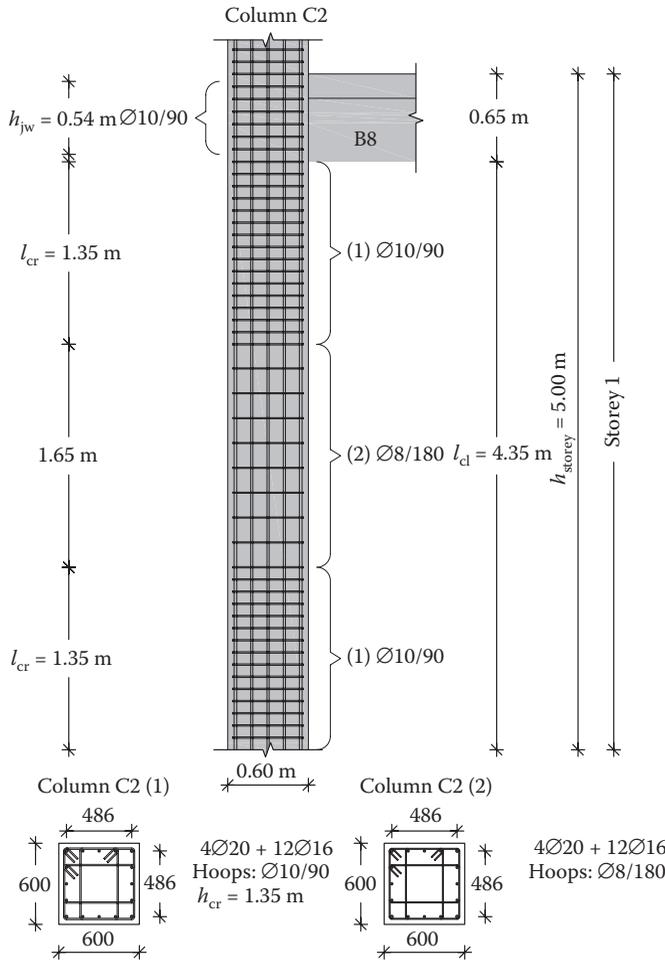
Figure 8.100 Flexural and shear reinforcement of column C2.

Table 8.10 Bending moments and axial forces at column C8 ends for column dimensioning – storey 1

Load combinations		N	V_x	V_y	M_x	M_y
Top of column C8						
Lc1	1.35G+1.5Q	−4266.45	−1.35	−4.73	9.67	3.66
Lc2	G+0.3Q+Ex+0.3Ey	−1998.25	41.1	20.88	42.38	73
Lc3	G+0.3Q+Ex⊠0.3Ey	−2156.99	38.73	−8.69	−9.1	68.57
Lc4	G+0.3Q−Ex+0.3Ey	−2605.81	−39.28	5.64	15.94	−66.08
Lc5	G+0.3Q⊠Ex⊠0.3Ey	−2764.55	−41.65	−23.93	−35.54	−70.5
Lc6	G+0.3Q+Ey+0.3Ex	−2025.71	15.73	50.04	93.19	29.48
Lc7	G+0.3Q+Ey⊠0.3Ex	−2207.97	−8.38	45.47	85.26	−12.24
Lc8	G+0.3Q⊠Ey+0.3Ex	−2554.83	7.83	−48.52	−78.41	14.74
Lc9	G+0.3Q⊠Ey⊠0.3Ex	−2737.09	−16.28	−53.09	−86.34	−26.99
Base of column C8						
Lc1	1.35G+1.5Q	−4319.3	−1.35	−4.73	−10.89	−2.18
Lc2	G+0.3Q+Ex+0.3Ey	−2037.4	41.1	−23.93	−61.7	108.3
Lc3	G+0.3Q+Ex−0.3Ey	−2196.14	38.73	5.64	15.45	102.36
Lc4	G+0.3Q−Ex+0.3Ey	−2644.96	−39.28	−8.69	−21.86	−102.26
Lc5	G+0.3Q−Ex−0.3Ey	−2803.7	−41.65	20.88	55.29	−108.2
Lc6	G+0.3Q+Ey+0.3Ex	−2064.86	15.73	−53.09	−137.77	41.53
Lc7	G+0.3Q+Ey−0.3Ex	−2247.12	−8.38	−48.52	−125.82	−21.64
Lc8	G+0.3Q−Ey+0.3Ex	−2593.97	7.83	45.47	119.4	21.74
Lc9	G+0.3Q−Ey−0.3Ex	−2776.24	−16.28	50.04	131.36	−41.43

Bottom reinforcement beam 19:5Ø14, $\omega = 0.0198$, $\mu_{Rd} = 0.019$,

$$M'_{BRd} = \mu_{Rd} \cdot b_{eff} \cdot d^2 \cdot f_{cd} = 0.019 \cdot 1.700 \cdot 0.597^2 \cdot \frac{25 \cdot 10^3}{1.5} = 190.27 \text{ kNm}$$

$\leftarrow E_y$: Bottom reinforcement beam 8:5Ø14, $\omega = 0.0198$, $\mu_{Rd} = 0.019$,

$$M'_{ARd} = \mu_{Rd} \cdot b_{eff} \cdot d^2 \cdot f_{cd} = 0.019 \cdot 1.700 \cdot 0.597^2 \cdot \frac{25 \cdot 10^3}{1.5} = 190.27 \text{ kNm}$$

Top reinforcement beam 19:8Ø8 + 5Ø16, $\omega = 0.2050$, $\mu_{Rd} = 0.179$,

$$M_{BRd} = \mu_{Rd} \cdot b \cdot d^2 \cdot f_{cd} = 0.179 \cdot 0.600 \cdot 0.597^2 \cdot \frac{25 \cdot 10^3}{1.5} = 319.50 \text{ kNm}$$

Calculation of the design values of the moments of resistance at the ends of column C8 (Figure 8.101)

The design values of the moments of resistance M_x of column C8 at the base of storey 2, and at the top and base of storey 1 appear in Tables 8.11 through 8.13.

Parameter κ_D (Equation 6.15), which accounts for the case of strong columns and weak beams, is calculated at the top of column C8 for both directions of seismic action.

$$\rightarrow E_y: \sum M_{Rb} = 509.77 \text{ kN m}, \quad \sum M_{Rc} = 1130.19 \text{ kN m}, \quad \kappa_D = \min\left(1, \frac{509.77}{1130.19}\right) = 0.45$$
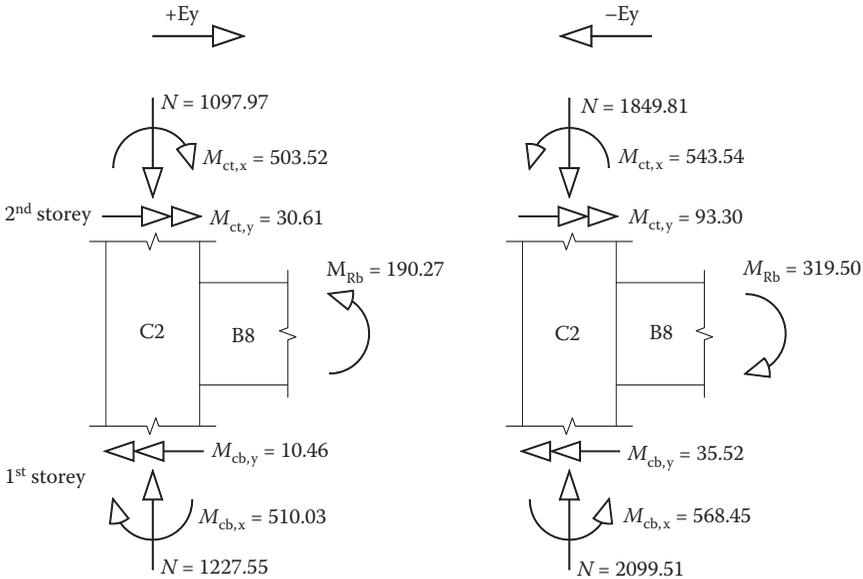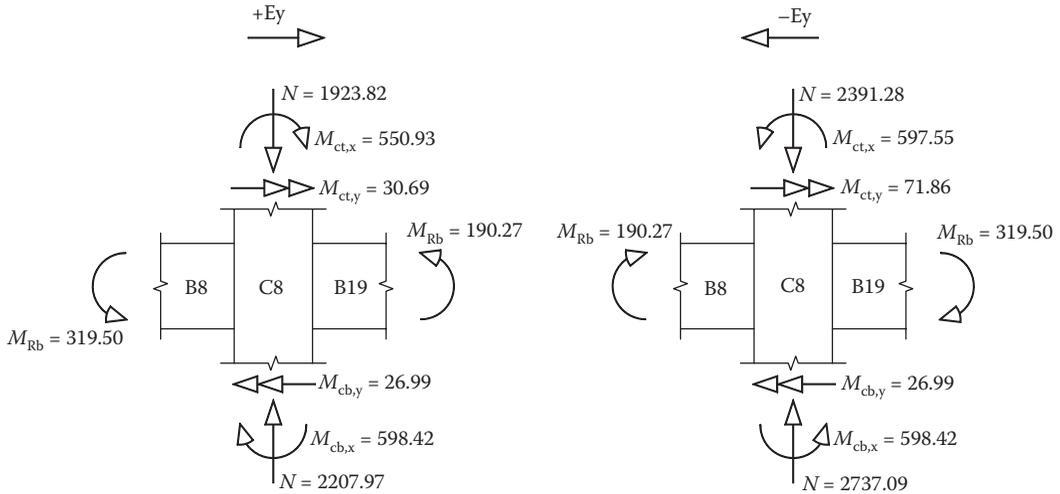
Figure 8.101 Capacity design moments for column C8.

Table 8.11 Determination of the design value of the moment of resistance M_x of column C8 at the base of storey 2

Load combination		N	M_y	μ_y	v	ω	μ_x	M_x
→ E_y	G+0.3Q+Ey+0.3Ex	−1763.46	−82.91	0.028	−0.294	0.2916	0.179	536.75
	G+0.3Q+Ey⊠0.3Ex	−1923.82	30.69	0.010	−0.321	0.2916	0.184	550.93
← E_y	G+0.3Q⊠Ey+0.3Ex	−2230.92	−41.74	0.014	−0.372	0.2916	0.194	581.55
	G+0.3Q⊠Ey⊠0.3Ex	−2391.28	71.86	0.024	−0.399	0.2916	0.200	597.55

Table 8.12 Determination of the design value of the moment of resistance M_x of column C8 at the top of storey 1

Load combination		N	M_y	μ_y	v	ω	μ_x	M_x
→ E_y	G+0.3Q+Ey+0.3Ex	−2025.71	29.48	0.010	−0.338	0.2916	0.188	561.09
	G+0.3Q+Ey⊠0.3Ex	−2207.97	−12.24	0.004	−0.368	0.2916	0.194	579.27
← E_y	G+0.3Q⊠Ey+0.3Ex	−2554.83	14.74	0.005	−0.426	0.2916	0.200	598.42
	G+0.3Q⊠Ey⊠0.3Ex	−2737.09	−26.99	0.009	−0.456	0.2916	0.200	598.42

Table 8.13 Determination of the design value of the moment of resistance M_x of column C8 at the base of storey 1

Load combination		N	M_y	μ_y	v	ω	μ_x	M_x
→ E_y	G+0.3Q+Ey+0.3Ex	−2064.86	41.53	0.014	−0.344	0.2916	0.189	564.99
	G+0.3Q+Ey⊠0.3Ex	−2247.12	−21.64	0.007	−0.375	0.2916	0.195	583.17
← E_y	G+0.3Q⊠Ey+0.3Ex	−2593.97	21.74	0.007	−0.432	0.2916	0.200	598.42
	G+0.3Q⊠Ey⊠0.3Ex	−2776.24	−41.43	0.014	−0.463	0.2916	0.200	598.42

$\leftarrow E_y$: $\sum M_{Rb} = 509.77$ kN m, $\sum M_{Rc} = 1195.97$ kN m, $\kappa_D = \min\left(1, \dfrac{509.77}{1195.97}\right) = 0.43$

Parameter κ_C at the base of column C8 is taken to be equal to 1 in order to simplify the design procedure.

Capacity design seismic shear for column 8

The shear forces are determined according to the capacity design criterion as follows (Equation 6.11):

Clear height of the column: $l_c = h_{st} - h_b = 5 - 0.65 = 4.35$ m

$\rightarrow E_y$: $V_{sd,CD} = \gamma_{Rd} \dfrac{\kappa_C M_{CRd} + \kappa_D M_{DRd}}{l_c} = 1.30 \dfrac{0.45 \cdot 579.27 + 1 \cdot 583.17}{4.35} = 252.36$ kN

$\leftarrow E_y$: $V_{sd,CD} = \gamma_{Rd} \dfrac{\kappa_C M_{CRd} + \kappa_D M_{DRd}}{l_c} = 1.30 \dfrac{0.43 \cdot 598.42 + 1 \cdot 598.42}{4.35} = 255.07$ kN

The checks that follow are performed for $V_{sd,CD} = 255.07$ kN.

Shear resistance in the case of diagonal concrete crushing for $\delta = 21.8°$ (Equation 8.62)

$$V_{Rd,max} = \alpha_{cw} \cdot b_w \cdot 0.9d \cdot \dfrac{(\nu_1 \cdot f_{cd})\cot\delta}{(1 + \cot^2\delta)} = 1 \cdot 0.6 \cdot 0.9 \cdot 0.547 \cdot \dfrac{0.775 \cdot (25/1.5) \cdot 1000}{2.9}$$
$$= 1315.63 \text{ kN}$$

$V_{Rd,max} = 1315.63$ kN $> V_{sd,CD} = 255.07$ kN

Transverse reinforcement in the critical regions of column C8

The length of the critical region is

$$l_{cr} = \max\{1.5h_c; l_c/6; 0.6\} = \max\{1.5 \cdot 0.6; 4.35/6; 0.6\} = 1.35 \text{ m}$$

The spacing of hoops shall not exceed:

$$s = \min\{b_o/3; 125; 6 \cdot d_{bL}\} = \min\{514/3; 125; 6 \cdot 16\} = 96 \text{ mm}$$

$$V_{wd} = V_{sd,CD} \Leftrightarrow s = \dfrac{A_{sw}}{V_{sd,CD}} 0.9d \cdot f_{ywd} = \dfrac{4 \cdot (\pi \cdot 8^2/4)}{255.07} \cdot 0.9 \cdot 0.547 \cdot \dfrac{500}{1.15} = 168.73 \text{ mm}$$

Hence, the shear reinforcement in the critical regions of column C8 is $\varnothing 8/95$.

Transverse reinforcement outside the critical regions of column C8.

The spacing of hoops shall not exceed:

$$s = \min\{20\Phi_{L,min}; \min(b_c; h_c); 400\} = \min\{20 \cdot 16; 600; 400\} = 320 \text{ mm}$$

Hence, the shear reinforcement outside the critical regions of column C8 is $\varnothing 8/165$.

Detailing for local ductility—confinement reinforcement in the critical region at the base of column C8

The confinement reinforcement at the base of the column consists of a perimeter and an internal rectangular closed stirrup (4 legs). The mechanical volumetric ratio of the required confining reinforcement, ω_{wd}, should satisfy Equation 8.127. Thus,

$$\omega_{wd,req} \geq \frac{1}{\alpha}\left(30 \cdot \mu_\varphi \cdot \nu_d \cdot \varepsilon_{syd}\frac{b_c}{b_o} - 0.035\right) = \frac{1}{0.641}\left(30 \cdot 7.8 \cdot 0.467 \cdot 0.0022\frac{600}{520} - 0.035\right)$$
$$= 0.371$$

This value is higher than 0.12, which is the lower limit set by the code:

$$\omega_{wd,req} = 0.371 > 0.12$$

The confinement effectiveness factor is (Equation 8.129):

$$\alpha = \alpha_n \cdot \alpha_s = 0.776 \cdot 0.826 = 0.641$$

where
Equation 8.130a:

$$\alpha_n = 1 - \sum_n \frac{b_i^2}{6} \cdot b_o \cdot h_o = 1 - \frac{4 \cdot 247 + 8 \cdot 123.5}{6 \cdot 522 \cdot 522} = 0.776$$

Equation 8.131a:

$$\alpha_s = (1 - s/2b_o)(1 - s/2h_o) = (1 - 95/2 \cdot 522)(1 - 95/2 \cdot 522) = 0.826$$

The provided mechanical volumetric ratio for $\varnothing 8/95$ is

$$\omega_{wd,prov} = \frac{V_o}{V_c} \cdot \frac{f_{yd}}{f_{cd}} = \frac{(4 \cdot 522 + 4 \cdot 522) \cdot \pi \cdot 8^2/4}{522 \cdot 522 \cdot 100} \cdot \frac{500/1.15}{20/1.5} = 0.212 < 0.371$$

Hence, hoops at the critical region are modified to: $\varnothing 12/90$

$$\omega_{wd,req} \geq \frac{1}{\alpha}\left(30 \cdot \mu_\varphi \cdot \nu_d \cdot \varepsilon_{syd}\frac{b_c}{b_o} - 0.035\right) = \frac{1}{0.650}\left(30 \cdot 7.8 \cdot 0.467 \cdot 0.0022\frac{600}{520} - 0.035\right)$$
$$= 0.370$$

This value is higher than 0.12, which is the lower limit set by the code:

$$\omega_{wd,req} = 0.370 > 0.12$$

The confinement effectiveness factor is (Equation 8.129):

$$\alpha = \alpha_n \cdot \alpha_s = 0.780 \cdot 0.834 = 0.650$$

where
Equation 8.130a:

$$\alpha_n = 1 - \sum_n \frac{b_i^2}{6} \cdot b_o \cdot h_o = 1 - \frac{4 \cdot 243 + 8 \cdot 121.5}{6 \cdot 518 \cdot 518} = 0.780$$

Equation 8.131a:

$$\alpha_s = (1 - s/2b_o)(1 - s/2h_o) = (1 - 90/2 \cdot 518)(1 - 90/2 \cdot 518) = 0.834$$

The provided mechanical volumetric ratio for $\varnothing 12/90$ is

$$\omega_{wd,prov} = \frac{V_o}{V_c} \cdot \frac{f_{yd}}{f_{cd}} = \frac{(4 \cdot 518 + 4 \cdot 518) \cdot \pi \cdot 12^2/4}{518 \cdot 518 \cdot 90} \cdot \frac{500/1.15}{20/1.5} = 0.506 > 0.370$$

8.6.2.4 Design of interior beam–column joint

Ultimate limit state verification and design (Section 8.4.2)
The horizontal shear force acting on the concrete core of the interior joint is Equation 8.186:

$$\rightarrow E_y: V_{jh} = \gamma_{Rd} \cdot f_{yd} \cdot (A_{s1} + A_{s2}) - V_{col} \Leftrightarrow$$
$$V_{jh} = 1.2 \cdot \frac{500}{1.15} \cdot \left(\frac{8 \cdot \pi \cdot 8^2}{4} + \frac{5 \cdot \pi \cdot 16^2}{4} + \frac{5 \cdot \pi \cdot 14^2}{4} \right) - \max(143.02; 131.50) = 992.87 \text{ kN}$$

$$\leftarrow E_y: V_{jh} = \gamma_{Rd} \cdot f_{yd} \cdot (A_{s1} + A_{s2}) - V_{col}$$
$$V_{jh} = 1.2 \cdot \frac{500}{1.15} \cdot \left(\frac{8 \cdot \pi \cdot 8^2}{4} + \frac{5 \cdot \pi \cdot 16^2}{4} + \frac{5 \cdot \pi \cdot 14^2}{4} \right) - \max(116.86; 128.38) = 1007.51 \text{ kN}$$

The shear force in the column above the joint, V_{col}, appears in Table 8.14 ($V_{col} = V_y$).
Diagonal compression induced in the joint by the diagonal strut mechanism
Equation 8.224 is applied in order to check the diagonal compression induced in the joint by the diagonal strut mechanism:

$$\rightarrow E_y: V_{jhd} \leq \nu_1 \cdot f_{cd} \sqrt{1 - \frac{\nu_d}{\nu_1}} \cdot b_j \cdot h_{jc} = 0.54 \cdot \frac{25 \cdot 1000}{1.5} \sqrt{1 - \frac{0.321}{0.54}} \cdot 0.60 \cdot 0.49$$
$$= 1700.22 \text{ kN}$$

Table 8.14 Bending moments and axial forces at the base of the second storey for column C8

Earthquake	Load combination	N (kN)	V_x (kN)	V_y (kN)	M_x (kN m)	M_y (kN m)
$\rightarrow E_y$	G+0.3Q+Ey+0.3Ex	−1763.46	−54.47	−143.02	−218.04	−82.91
	G+0.3Q+Ey⊠0.3Ex	−1923.82	19.26	−131.5	−200.41	30.69
$\leftarrow E_y$	G+0.3Q⊠Ey+0.3Ex	−2230.92	−27.43	116.86	179.87	−41.74
	G+0.3Q⊠Ey⊠0.3Ex	−2391.28	46.3	128.38	197.51	71.86

The normalised load above the joint is (Table 8.14): $N_{Ed} = 1923.82$ kN $\rightarrow v_d = 0.321$

$$\leftarrow E_y: \ V_{jhd} \le v_1 \cdot f_{cd} \sqrt{1 - \frac{v_d}{v_1}} \cdot b_j \cdot h_{jc} = 0.54 \cdot \frac{25 \cdot 1000}{1.5} \sqrt{1 - \frac{0.399}{0.54}} \cdot 0.60 \cdot 0.49$$

$$= 1365.31 \ \text{kN}$$

The normalised load above the joint is (Table 8.8): $N_{Ed} = 2391.28$ kN $\rightarrow v_d = 0.399$.

8.6.2.4.1 Confinement of the joint

8.6.2.4.1.1 HORIZONTAL REINFORCEMENT

The horizontal and vertical reinforcement of the joint shall be such as to limit the maximum diagonal tensile stress of concrete to the design value of the tensile strength of concrete. For this purpose, Equation 8.227 needs to be satisfied:

$$\rightarrow E_y: \ A_{sh} = \frac{b_j \cdot h_{jw}}{f_{ywd}} \cdot \left[\frac{\left(\frac{V_{jhd}}{b_j \cdot h_{jc}} \right)^2}{f_{ctd} + v_d \cdot f_{cd}} - f_{ctd} \right] = \frac{0.60 \cdot 0.54 \cdot 10^6}{500/1.15}$$

$$\cdot \left[\frac{\left(\frac{992.87}{0.60 \cdot 0.49 \cdot 10^3} \right)^2}{1.20 + 0.321 \cdot 25E1.5} - 1.20 \right] = 3.86 \ \text{cm}^2$$

$$\leftarrow E_y: \ A_{sh} = \frac{b_j \cdot h_{jw}}{f_{ywd}} \cdot \left[\frac{\left(\frac{V_{jhd}}{b_j \cdot h_{jc}} \right)^2}{f_{ctd} + v_d \cdot f_{cd}} - f_{ctd} \right] = \frac{0.60 \cdot 0.54 \cdot 10^6}{500/1.15} \cdot$$

$$\left[\frac{\left(\frac{1007.51}{0.60 \cdot 0.49 \cdot 10^3} \right)^2}{1.20 + 0.399 \cdot 25/1.5} - 1.20 \right] = 2.05 \ \text{cm}^2$$

The alternative expression given by Equation 8.228 is also applied.

$$\rightarrow E_y: \ A_{sh} \ge \frac{\gamma_{Rd}}{f_{ywd}} \cdot (A_{s1} + A_{s2}) \cdot f_{yd} \cdot (1 - 0.8 \cdot v_d) \Leftrightarrow A_{sh} \ge \frac{1.2}{500/1.15} \cdot$$

$$\left(\frac{8 \cdot \pi \cdot 8^2}{4} + 5 \frac{4 \cdot \pi \cdot 16^2}{4} + \frac{5 \cdot \pi \cdot 14^2}{4} \right) \cdot \frac{500}{1.15} \cdot (1 - 0.8 \cdot 0.329)1 = 19.42 \ \text{cm}^2$$

The normalised load below the joint is (Table 8.14): $N_{Ed} = 1923.82$ kN $\rightarrow \nu_d = 0.321$

$$\leftarrow E_y: \quad A_{sh} \geq \frac{\gamma_{Rd}}{f_{ywd}} \cdot (A_{s1} + A_{s2}) \cdot f_{yd} \cdot (1 - 0.8 \cdot \nu_d) \Leftrightarrow$$

$$A_{sh} \geq \frac{1.2}{500/1.15} \cdot \left(\frac{5 \cdot \pi \cdot 14^2}{4} + \frac{8 \cdot \pi \cdot 8^2}{4} + \frac{5 \cdot \pi \cdot 16^2}{4} \right) \cdot \frac{500}{1.15} \cdot (1 - 0.8 \cdot 0.399) = 17.80 \text{ cm}^2$$

The normalised load below the joint is (Table 8.14): $N_{Ed} = 2391.28$ kN $\rightarrow \nu_d = 0.399$.

As may be observed, the two alternative expressions suggested by EC8-Part I (2004) for determining the required horizontal reinforcement of the joint yield very different results ($A_{sh} = 2.05$ cm² vs $A_{sh} = 17.80$ cm²), which is rather confusing for the designer. Fardis (2009) suggests that the least among the steel requirements of Equations 8.227 and 8.228 may be used with some confidence. Following this approach, the hoop layers provided in the joint are:

$$n = \text{int}(h_{jw}/s) + 1 = \text{int}(0.54/0.095) + 1 = 7 \text{ layers}$$

The total area of a horizontal hoop is: $A_{sh,prov} = 7 \cdot 4 \cdot \pi \cdot 12^2/4 = 31.64$ cm² > 19.42 cm²

8.6.2.4.1.2 VERTICAL REINFORCEMENT

The vertical reinforcement of the column passing through the joint is (Equation 8.230):

$$A_{sv,1} = \frac{2}{3} \cdot A_{sh} \cdot \frac{h_{jc}}{h_{jw}} = \frac{2}{3} \cdot 17.80 \cdot \frac{0.49}{0.54} = 11.76 \text{ cm}^2$$

The horizontal reinforcement of the joint is given below:
The longitudinal bars provided at the face of the joint are: 6Ø16 $\rightarrow$ 12.06 cm² $>$ 9.75 cm².
The flexural and shear reinforcement placed in column C8 appears in Figure 8.102.

Remark: Capacity design of columns to bending (Equation 6.8) has not been carried out, since the structural system has been classified as an *uncoupled wall* system (see Subsection 5.9.7).

8.6.3 Beams: Ultimate limit state in shear

8.6.3.1 Design shear forces

The design shear forces are determined in accordance with the capacity design rule (par. 6.1.3):
$\rightarrow E_y$: Joint A:
Bottom reinforcement (beam 8-left): 5Ø14, $\omega = 0.0198$, $\mu_{Rd} = 0.019$, $M_{AR} = 190.27$ kN m

$$\sum M_{Rb} = 190.27 \text{ kN m}, \quad \sum M_{Rc} = 1013.55 \text{ kN m}, \quad \kappa_A = \min(1, \Sigma M_{Rb}/\Sigma M_{Rc}) = 1$$

$$M_{A,d} = \gamma_{Rd} \cdot M_{AR} \cdot \kappa_A = 1.20 \cdot 190.27 \cdot 1 = 228.33 \text{ kN m}$$

$\rightarrow E_y$: Joint B:
Top reinforcement (beam 8-right): 8Ø8 + 5Ø16, $\omega = 0.2050$, $\mu_{Rd} = 0.179$, $M'_{BR,l} = 319.50$ kN m

Bottom reinforcement (beam 19-left): 5Ø14, $\omega = 0.0198$, $\mu_{Rd} = 0.019$, $M_{BR,r} = 190.27$ kN m

$$\sum M_{Rb} = (319.50 + 190.27) = 509.77 \text{ kN m}, \quad \sum M_{Rc} = 1130.19 \text{ kN m}, \quad \kappa_B$$

$$= \min\left(1, \sum M_{Rb} / \sum M_{Rc}\right) = 1$$
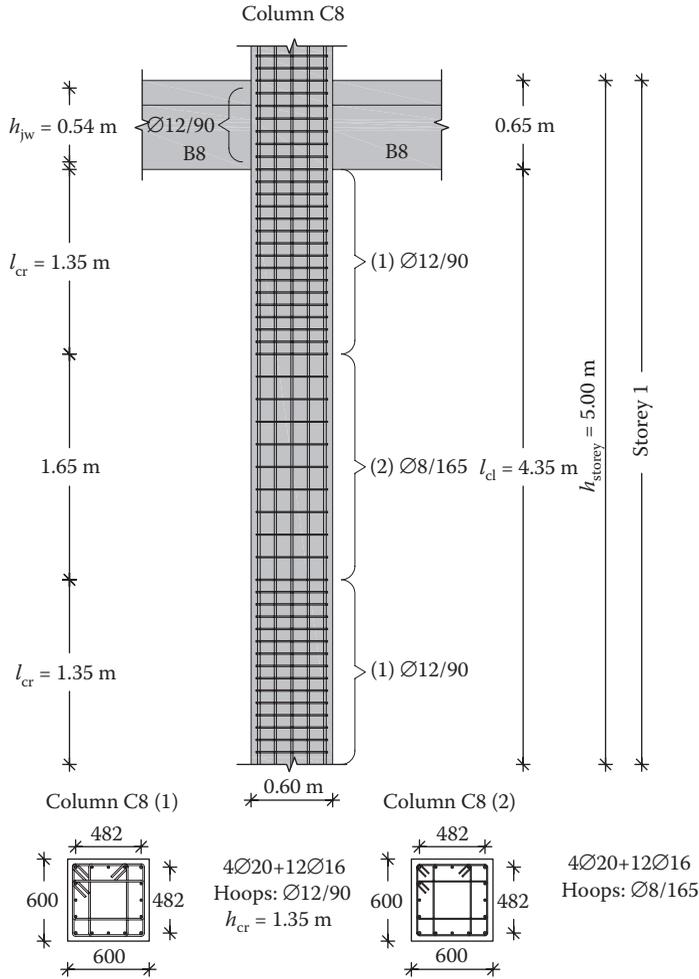
Figure 8.102 Flexural and shear reinforcement of column C8.

$$M^l_{\text{Bl,d}} = \gamma_{\text{Rd}} \cdot M^l_{\text{BR}} \cdot \kappa_A = 1.20 \cdot 319.50 \cdot 1 = 383.40 \text{ kN m}$$

$$M_{\text{Br,d}} = \gamma_{\text{Rd}} \cdot M_{\text{BR}} \cdot \kappa_A = 1.20 \cdot 190.27 \cdot 1 = 228.33 \text{ kN m}$$

$\rightarrow E_y$: Joint C:
Top reinforcement (beam 19-right):

$$8\varnothing8 + 4\varnothing16, \omega = 0.1757, \mu_{\text{Rd}} = 0.157, M^l_{\text{CR,l}} = 280.25 \text{ kN m}$$

Bottom reinforcement (beam 37-left): $4\varnothing14$, $\omega = 0.0158$, $\mu_{\text{Rd}} = 0.015$, $M_{\text{CR,r}} = 152.22$ kN m

$$\sum M_{\text{Rb}} = (280.25 + 152.22) = 432.47 \text{ kN m}, \sum M_{\text{Rc}} = 1157.83 \text{ kN m}, \kappa_B$$
$$= \min\left(1, \sum M_{\text{Rb}} \Big/ \sum M_{\text{Rc}}\right) = 1$$

$$M^l_{\text{Cl,d}} = \gamma_{\text{Rd}} \cdot M^l_{\text{CR}} \cdot \kappa_{\text{A}} = 1.20 \cdot 280.25 \cdot 1 = 336.30 \text{ kN m}$$

$$M_{\text{Cr,d}} = \gamma_{\text{Rd}} \cdot M_{\text{CR}} \cdot \kappa_{\text{A}} = 1.20 \cdot 152.22 \cdot 1 = 182.66 \text{ kN m}$$

Beam 8:

$$V_{\text{sd,AB}} = \frac{\left(M_{\text{A,d}} + M^l_{\text{Bl,d}}\right)}{l} = \frac{-(228.33 + 383.40)}{4.40} = -139.03 \text{ kN}$$

$$V_{\text{A},G+0.3Q} = 81.51 \text{ kN}, V_{\text{B},G+0.3Q} = -58.19 \text{ kN}$$

$$V_{\text{AS2}} = V_{G+0.3Q} + V_{\text{sd,AB}} = 81.51 - 139.03 = -57.52 \text{ kN}$$

$$V_{\text{BS1}} = V_{G+0.3Q} + V_{\text{sd,AB}} = -58.19 - 139.03 = -197.22 \text{ kN}$$

Beam 19:

$$V_{\text{sd,BC}} = \frac{\left(M_{\text{Br,d}} + M^l_{\text{Cl,d}}\right)}{l} = \frac{-(228.33 + 336.30)}{4.40} = -128.32 \text{ kN}$$

$$V_{\text{B},G+0.3Q} = 57.35 \text{ kN}, V_{\text{C},G+0.3Q} = -55.81 \text{ kN}$$

$$V_{\text{BS2}} = V_{G+0.3Q} + V_{\text{sd,BC}} = 57.35 - 128.32 = -70.98 \text{ kN}$$

$$V_{\text{CS1}} = V_{G+0.3Q} + V_{\text{sd,BC}} = -55.82 - 128.32 = -184.13 \text{ kN}$$

$\leftarrow E_{\text{y}}$: Joint A:
Top reinforcement (beam 8-left):

$$8\varnothing8 + 5\varnothing16, \omega = 0.2050, \mu_{\text{Rd}} = 0.179, M^l_{\text{AR}} = \mu_{\text{Rd}} \cdot b \cdot d^2 \cdot f_{\text{cd}} = 319.50 \text{ kNm}$$

$$\sum M_{\text{Rb}} = 319.50 \text{ kN m}, \sum M_{\text{Rc}} = 1111.99 \text{ kN m}, \kappa_{\text{A}} = \min\left(1, \sum M_{\text{Rb}} \Big/ \sum M_{\text{Rc}}\right) = 1$$

$$M^l_{\text{A,d}} = \gamma_{\text{Rd}} \cdot M^l_{\text{AR}} \cdot \kappa_{\text{A}} = 1.20 \cdot 319.50 \cdot 1 = 383.40 \text{ kN m}$$

$\leftarrow E_{\text{y}}$: Joint B:
Bottom reinforcement (beam 8-right):

$$5\varnothing14, \omega = 0.0198, \mu_{\text{Rd}} = 0.019, M_{\text{BR,l}} = \mu_{\text{Rd}} \cdot b_{\text{eff}} \cdot d^2 \cdot f_{\text{cd}} = 190.27 \text{ kN m}$$

Top reinforcement (beam 19-left):

$8\varnothing 8 + 5\varnothing 16$, $\omega = 0.2050$, $\mu_{Rd} = 0.179$, $M_{BR,r}^{l} = \mu_{Rd} \cdot b \cdot d^2 \cdot f_{cd} = 319.50$ kN m

$$\sum M_{Rb} = (190.27 + 319.50) = 509.77 \text{ kN m}, \sum M_{Rc} = 1195.97 \text{ kN m}, \kappa_B$$
$$= \min\left(1, \sum M_{Rb} \Big/ \sum M_{Rc}\right) = 1$$

$M_{Bl,d}^{l} = \gamma_{Rd} \cdot M_{BR,l} \cdot \kappa_A = 1.20 \cdot 190.27 \cdot 1 = 228.33$ kN m

$M_{Br,d}^{l} = \gamma_{Rd} \cdot M_{BR,r}^{l} \cdot \kappa_A = 1.20 \cdot 319.50 = 383.40$ kN m

$\leftarrow E_y$: Joint C:
Bottom reinforcement (beam 19-right):

$4\varnothing 14$, $\omega = 0.0158$, $\mu_{Rd} = 0.015$, $M_{CR,l} = 152.22$ kN m

Top reinforcement (beam 37-left):

$8\varnothing 8 + 4\varnothing 16$, $\omega = 0.0176$, $\mu_{Rd} = 0.157$, $M_{CR,r}^{l} = 280.25$ kN m

$$\sum M_{Rb} = (280.25 + 152.22) = 432.47 \text{ kN m}, \ \sum M_{Rc} = 1188.84 \text{ kN m}, \kappa_B$$
$$= \min(1, \Sigma M_{Rb}/\Sigma M_{Rc}) = 1$$
$$M_{Cl,d} = \gamma_{Rd} \cdot M_{CR} \cdot \kappa_A = 1.20 \cdot 152.22 \cdot 1 = 182.66 \text{ kN m}$$

$M_{Cr,d}^{l} = \gamma_{Rd} \cdot M_{CR}^{l} \cdot \kappa_A = 1.20 \cdot 280.25 \cdot 1 = 336.30$ kN m

Beam 8 (Figures 8.99 and 8.103):

$$V_{sd,AB} = \frac{\left(M_{A,d}^{l} + M_{Bl,d}\right)}{l} = \frac{(383.40 + 228.33)}{4.40} = 139.03 \text{ kN}$$

$V_{A,G+0.3Q} = 81.51$ kN, $V_{B,G+0.3Q} = -58.19$ kN

$V_{AS1} = V_{G+0.3Q} + V_{sd,AB} = 81.51 + 139.03 = 220.53$ kN

$V_{BS2} = V_{G+0.3Q} - V_{sd,AB} = -58.19 + 139.03 = 80.84$ kN

Beam 19 (Figures 8.101 and 8.104):

$$V_{sd,BC} = \frac{\left(M_{Br,d}^{l} + M_{Cl,d}\right)}{l} = \frac{(383.40 + 182.66)}{4.40} = 128.65 \text{ kN}$$
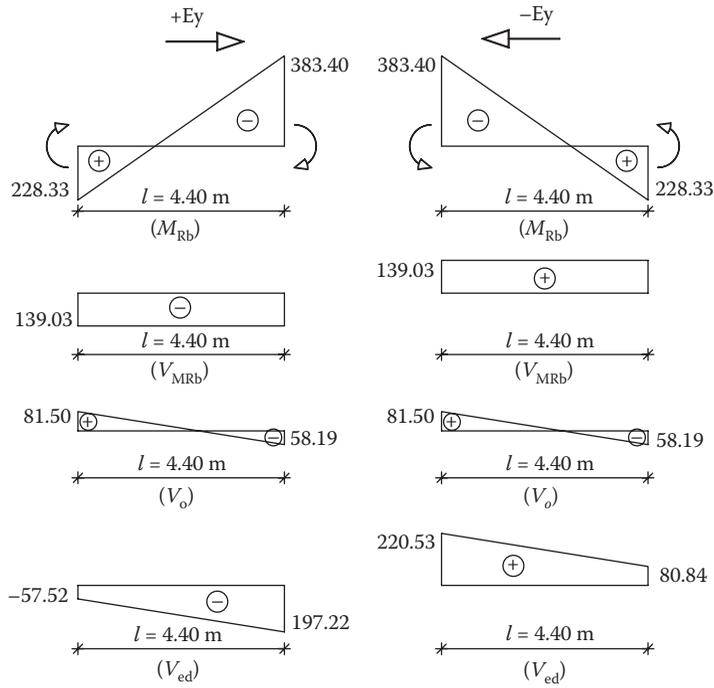
Figure 8.103 Design shear forces of beam 8.
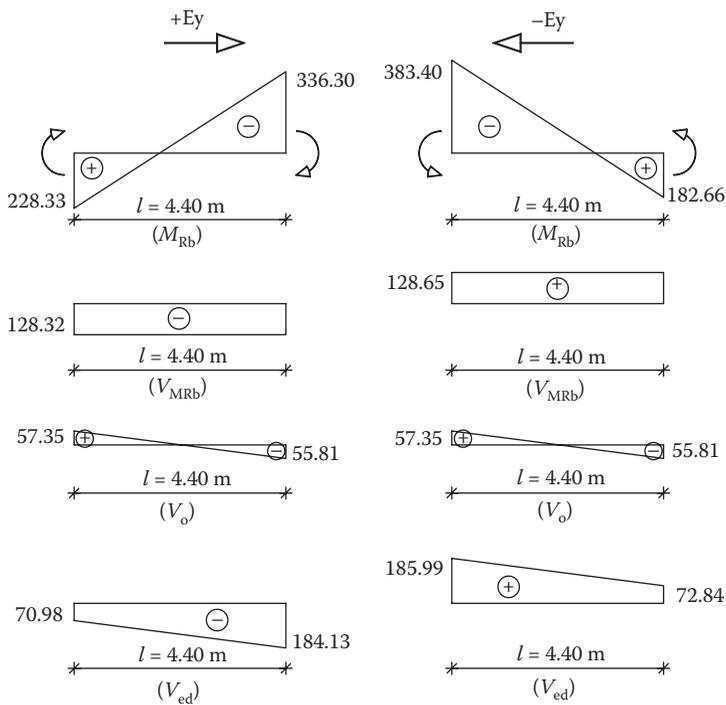
Figure 8.104 Design shear forces of beam 19.

$$V_{\mathrm{B,G+0.3Q}} = 57.35 \text{ kN}, \ V_{\mathrm{C,G+0.3Q}} = -55.82 \text{ kN}$$

$$V_{\mathrm{BS1}} = V_{\mathrm{G+0.3Q}} + V_{\mathrm{sd,BC}} = 57.35 + 128.65 = 185.99 \text{ kN}$$

$$V_{\mathrm{CS2}} = V_{\mathrm{G+0.3Q}} + V_{\mathrm{sd,BC}} = -55.82 + 128.65 = 72.84 \text{ kN}$$

Beam 8:

The algebraic value of the ratio between the minimum and maximum acting shear forces is (Equation 6.6):

$$\zeta = \frac{V_{\mathrm{AS2}}}{V_{\mathrm{AS1}}} = \frac{-57.52}{220.53} = -0.26 > -0.5; \ \zeta = \frac{V_{\mathrm{BS2}}}{V_{\mathrm{BS1}}} = \frac{80.84}{-197.22} = -0.41 > -0.5$$

Hence, shear resistance is provided by hoops only.

Beam 8-left: $V_{\mathrm{A}} = \max(|V_{\mathrm{AS1}}|; |V_{\mathrm{AS2}}|) = \max(220.53; 57.52) = 220.53 \text{ kN}$

Beam 8-right: $V_{\mathrm{B}} = \max(|V_{\mathrm{BS1}}|; |V_{\mathrm{BS2}}|) = \max(197.22; 80.84) = 197.22 \text{ kN}$

Beam 19:

The algebraic value of the ratio between the minimum and maximum acting shear forces is estimated for beam 19 as well (Equation 6.6):

$$\zeta = \frac{V_{\mathrm{BS2}}}{V_{\mathrm{BS1}}} = \frac{-70.98}{185.99} = -0.38 > -0.5; \ \zeta = \frac{V_{\mathrm{CS2}}}{V_{\mathrm{CS1}}} = \frac{72.84}{-184.13} = -0.40 > -0.5$$

Hence, shear resistance is provided by hoops only.

Beam 19-left: $V_{\mathrm{B}} = \max(|V_{\mathrm{BS1}}|; |V_{\mathrm{BS2}}|) = \max(185.99; 70.98) = 185.99 \text{ kN}$

Beam 19-right: $V_{\mathrm{C}} = \max(|V_{\mathrm{CS1}}|; |V_{\mathrm{CS2}}|) = \max(184.13; 72.84) = 184.13 \text{ kN}$

8.6.3.2 Shear reinforcement

Shear resistance in case of diagonal concrete crushing for ⊠ = 21.8o (Equation 8.62):

Beam 8:

$$\begin{aligned} V_{\mathrm{Rd,max}} &= 1 \cdot 0.3 \cdot 0.9 \cdot 0.597 \cdot 0.54 \cdot (25/1.5) \cdot 1000/2.9 = 500.24 \text{ kN} > \max(V_{\mathrm{A}}; V_{\mathrm{B}}) \\ &= 220.53 \text{ kN} \end{aligned}$$

Beam 19:

$$\begin{aligned} V_{\mathrm{Rd,max}} &= 1 \cdot 0.3 \cdot 0.9 \cdot 0.597 \cdot 0.54 \cdot (25/1.5) \cdot 1000/2.9 = 500.24 \text{ kN} > \max(V_{\mathrm{B}}; V_{\mathrm{C}}) \\ &= 185.99 \text{ kN} \end{aligned}$$

Transverse reinforcement in the critical regions

The critical region is $l_{\mathrm{cr}} = 1.5 \cdot h_{\mathrm{w}} = 1.5 \cdot 65 = 97.5$ cm.

The maximum longitudinal spacing should not exceed s_{max}:

$$s_{\mathrm{max}} = \min\left\{\frac{h_{\mathrm{w}}}{4}; 24d_{\mathrm{bw}}; 175; 6d_{\mathrm{bL}}\right\} = \min\left\{\frac{650}{4}; 24 \cdot 8; 175; 6 \cdot 14\right\} = 84 \text{ mm}$$

Ø8/84 are the minimum allowed hoops.
Beam 8:

$$V_{wd} = \max(V_A; V_B) \Leftrightarrow s = \frac{A_{sw}}{V_A} 0.9d \cdot f_{ywd} = \frac{2 \cdot \pi \cdot 8^2/4}{220.53} \cdot 0.9 \cdot 0.597 \cdot \frac{500}{1.15} = 106.49 \text{ mm}$$

Hence, the shear reinforcement in the critical regions of beam 8 is Ø8/80.
Beam 19:

$$V_{wd} = \max(V_B; V_C) \Leftrightarrow s = \frac{A_{sw}}{V_A} 0.9d \cdot f_{ywd} = \frac{2 \cdot \pi \cdot 8^2/4}{185.99} \cdot 0.9 \cdot 0.597 \cdot \frac{500 \cdot 10^3}{1.15}$$
$$= 126.27 \text{ mm}$$

Hence, the shear reinforcement in the critical regions of beam 19 is Ø8/80.
Transverse reinforcement outside the critical regions
The minimum shear reinforcement ratio is

$$\rho_{w,min} = \frac{0.08 \cdot \sqrt{f_{ck}}}{f_{yk}} = \frac{0.08 \cdot \sqrt{25}}{500} = 0.8?$$

The maximum longitudinal spacing between hoops should not exceed s_{max}:

$$s_{max} = 0.75 \cdot d = 075 \cdot 597 = 447.75 \text{ mm}$$
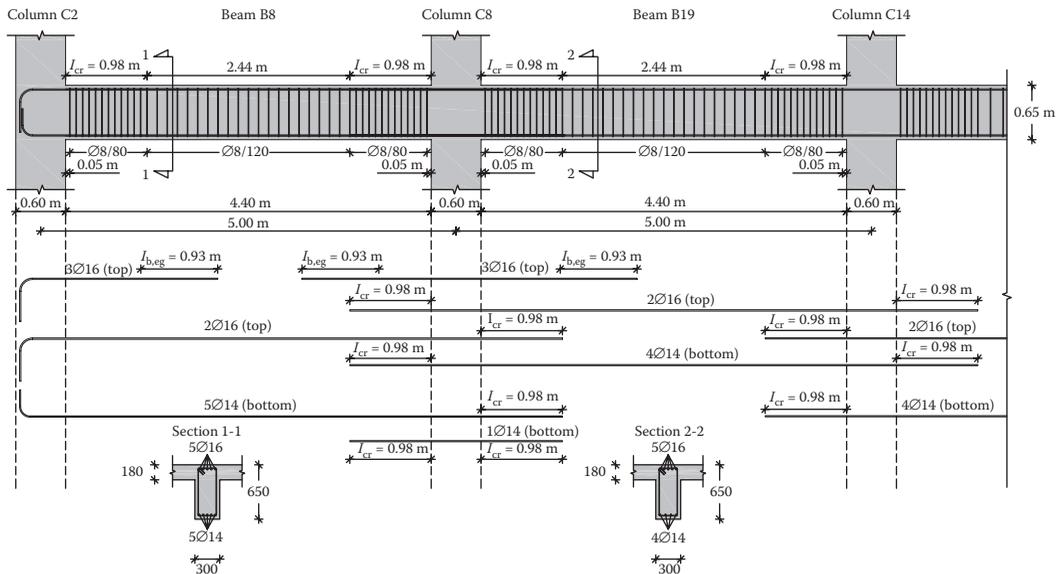
Figure 8.105 Flexural and shear reinforcement of beams 8 and 19.

In case of a two-leg 8 mm bar diameter hoops, stirrup spacing is defined as equal to

$$s = \frac{A_{sw}}{\rho_{w,min} \cdot b_w} = \frac{2 \cdot (\pi \cdot 8^2/4)}{0.0008 \cdot 300} \approx 419 \text{ mm}$$

$\varnothing 8/419$ are the minimum allowed hoops.
Beam 8:

$$V_{wd} = 189.58 \Leftrightarrow s = \frac{2 \cdot \pi \cdot 8^2/4}{189.58} \cdot 0.9 \cdot 0.597 \cdot \frac{500}{1.15} = 123.88 \text{ mm}$$

Hence, the shear reinforcement outside the critical regions of beam 8 is $\varnothing 8/120$.
Beam 19:

$$V_{wd} = 160.92 \Leftrightarrow s = \frac{2 \cdot \pi \cdot 8^2/4}{160.92} \cdot 0.9 \cdot 0.597 \cdot \frac{500}{1.15} = 145.94 \text{ mm}$$

The shear reinforcement outside the critical regions of beam 19 is taken to be equal to $\varnothing 8/120$ as in the case of B8 for simplicity in construction.

The flexural and shear reinforcement placed in beams B8–B19 appears in Figure 8.105.

Chapter 9

Seismic-resistant R/C walls and diaphragms

9.1 GENERAL

R/C walls together with frames and diaphragms constitute the main structural members in the planning and designing of the structural system of a seismic-resistant R/C building.

Thus far, many detailed references have been made to the structural behaviour of walls as members of a structural system (Paragraph 4.5.2.2) and wall structural systems (Paragraphs 4.6.3.3.4 and 4.6.3.3.5), to their behaviour factors 'q' (Section 5.4), to their modelling for structural analysis (Paragraph 5.6.3.2) and to their capacity design action effects (Subsections 6.1.5 through 6.1.7). All of the above refer to *'demand'*. In the following sections, detailed reference will be made to the *'capacity'* of R/C walls in terms of strength, ductility and energy dissipation under cyclic loading.

Before any further reference to 'capacity' issues, it will be useful to make a short summary of the main points on walls that have been presented so far.

1. 'R/C walls', according to modern Codes, are vertical structural members with an orthogonal cross-section and a ratio of a side of the cross-section

$$\frac{l_w}{b} > 4.0 \tag{9.1}$$

2. R/C walls may constitute basic structural elements in the following building structural systems:
   a. Uncoupled wall systems (Figure 4.21a)
   b. Dual systems (wall-equivalent of frame-equivalent systems; Figure 4.23)
   c. Coupled wall systems (Figure 4.22)
   d. Systems with large, lightly reinforced walls (Figure 9.2)
3. Apart from the structural system under consideration, the types of R/C walls in use may be classified into the following types:
   a. Slender ductile walls (Figure 4.21a)
   b. Squat ductile walls (Figure 9.1)
   c. Coupled walls (Figure 4.22)
   d. Large, lightly reinforced walls (Figure 9.2)

The most common walls in use are the first (slender ductile walls). In the following sections these four types of walls will be examined as far as their capacity is concerned.
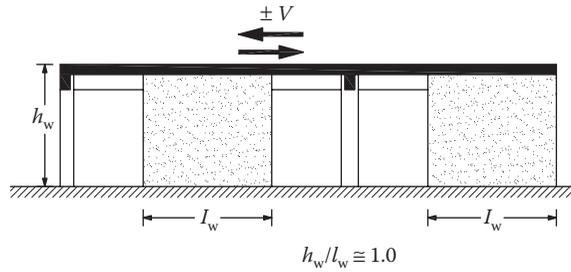
Figure 9.1 A typical structural system with squat walls under seismic action ± *V*.
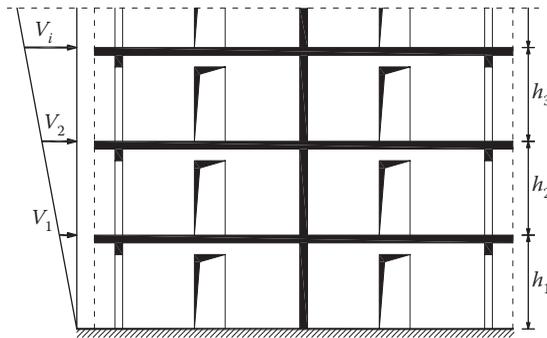
Figure 9.2 Large, lightly reinforced wall.

This chapter will also include design issues relating to diaphragms, for two reasons:

1. Diaphragms are planar elements, and in this respect their behaviour better matches that of walls.
2. The design of diaphragms in R/C buildings cast *in situ* in the form of slabs does not have any particular design concern; design issues arise only in special cases. Therefore, the presentation of the design of these special cases would not justify an independent chapter.

9.2 SLENDER DUCTILE WALLS

9.2.1 A summary on structural behaviour of slender ductile walls

1. The usual cross-section of these members is the orthogonal one. However, barbell cross-sections or T, U, L, Z and tubular cross-sections are not uncommon (Figure 9.3a–g).
2. A recommended aspect ratio α_s of these walls with an orthogonal cross-section lies between:

$$7.0 \geq \alpha_s = \frac{h_w}{l_w} \geq 2.0 \tag{9.2}$$

and

$$l_w \geq 2.00 \ m$$
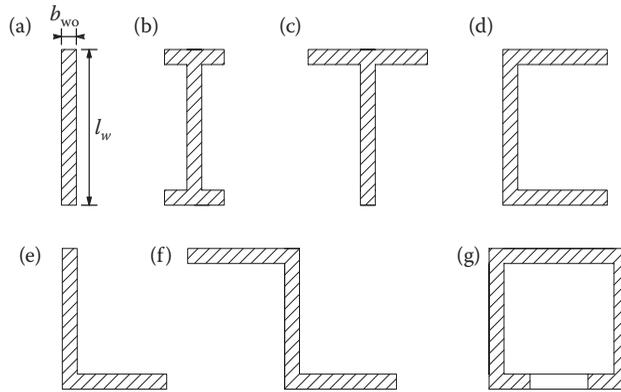
Figure 9.3 Various cross-sections of ductile slender walls: (a) orthogonal; (b) barbell; (c) T-shaped; (d) C-shaped; (e) L-shaped; (f) Z-shaped; (g) tubular.

where
l_w is the length of the cross-section
h_w is the height of the wall

3. The thickness b_{wo} of these walls should be (Figure 9.4):

$$b_{wo} \geq \max\{0.15, h_s/20\}[m] \tag{9.3}$$

where
h_s is the clear storey height in meters.

In addition, these walls should be strengthened with confined boundary elements with a minimum thickness of 200 mm. In the case that the thickness of the wall is greater than 200 mm, as we will see later, these confined boundary elements may be incorporated into the cross-section of the wall. The depth l_c of the confined boundary element determined in accordance with Paragraph 9.2.4.2(3) should not be less than $0.15\ l_w$ or less than $1.50\ b_w$, whichever is greater (Figure 9.4b). Moreover, the thickness b_w should not be less than $h_s/15$ (h_s: storey height).
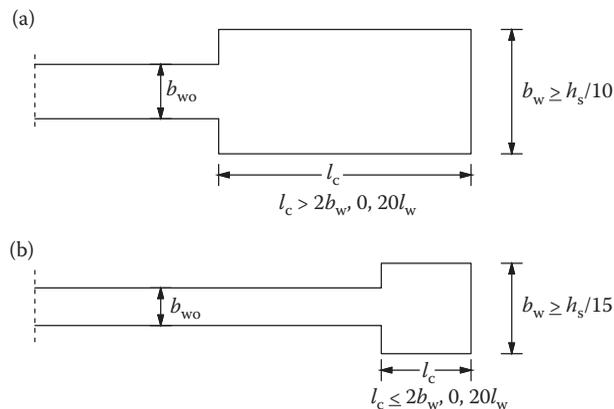
Figure 9.4 (a, b) Minimum thickness of confined boundary elements. (Adapted from E.C.8-1/EN1998-1. 2004. *Design of Structures for Earthquake Resistance: General Rules, Seismic Actions and Rules for Buildings.* CEN, Brussels, Belgium.)

If the depth of the confined part exceeds $2b_w$ or $0.20l_w$, whichever is greater, b_w should not be less than $h_s/10$ (Figure 9.4a). These requirements for confined boundary elements aim at ensuring a quantified *local ductility* in parallel with the protection of the edge of the walls from buckling (Figure 9.5).

4. The main structural characteristics of these walls are the following:
   - They are slender elements, and therefore design for bending with axial force is separated from design for shear, since the distribution of axial strains on a deformed cross-section is planar (Bernoulli concept; Figure 9.9).
   - The capacity design for shear ensures the plastic behaviour to bending at the fixed end before the failure of the wall to shear. At the same time, the form of the envelope of the capacity design moment diagram (see Paragraph 6.1.5.1) ensures that only one plastic hinge may be formed. In this respect, a robust backbone is formed in the structural system by means of the ductile walls, which minimises the hazard of a collapse in pancake form.
   - In Paragraph 9.2.1.2 the recommended values for the aspect ratio aim at the proper slenderness together with an adequate stiffness for the behaviour of the wall as a cantilever beam without change of the sign of curvature along the height of the walls.

In fact, according to what has been presented in Paragraph 4.6.3.3, the second part of the inequality (9.2) ensures that the wall is not a short one and therefore plastic formation at the fixed-end precedes the shear failure of the member $((M_{fixed-end}/V \cdot l_w) \geq 2.0)$. At the same time, the first part of the inequality (9.2) ensures that the curvature of the wall does not change sign along its height, as may be concluded from engineering practice.

9.2.2 Behaviour of slender ductile walls under bending with axial load

9.2.2.1 General

Slender walls with an orthogonal cross-section are considered to fulfill the Bernoulli concept for linear distribution of axial strains on the cross-section like beams and columns if they have an aspect ratio a_s:

$$a_s = \frac{M_{fix\text{-}end}}{V \cdot l_w} \geq 2 \tag{9.4}$$
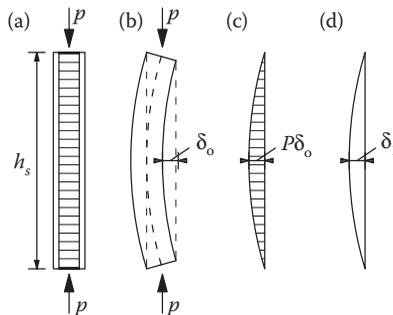
Figure 9.5 Deformations causing out-of-plane ductility: (a) compressive axial load P; (b) accidental displacement at the middle of wall height; (c) moment diagram generated by the axial compressive force; (d) additional displacement δ_l due to the moment diagram $P \cdot \delta_0$ (second order effects) if $\delta_l \geq \delta_0$ then the wall passes to instability (out-of-plane buckling).

where

$M_{\text{fix-end}}$ is the bending moment at the fixed end

V is the relevant shear force

l_w is the length of the cross-section

Having in mind that usually the axial compressive stresses of a wall due to the axial design forces are smaller than those of columns, it follows that the structural behaviour of a wall lies between that of a beam and a column. Therefore, generally speaking, the same assumptions may be used for the design of ductile walls as for beams and columns, with some necessary changes, as we will see later. As in the case for beams and columns, the failure mode of walls may be of *flexural type* or *shear type,* depending on the reinforcement of the member.

As in the case of beams, the failure mechanism under flexure may have one of the following forms:

1. Yield of tensile steel reinforcement, wide flexural cracks in tension zone near the fixed end, large defections at the top and spalling of the compression zone, that is, ductile type of failure (Figure 9.6a,b).
2. Narrow cracks at the tension zone ($\sigma_s < f_y$) crushing of concrete at the compression zone near to the fixed-end and buckling of reinforcement under compression (Figure 9.6a,c), that is, brittle failure due to over-reinforced tensile zone.

The $M-\varphi$ diagram for an orthogonal cross-section is similar to that of a beam (Chapter 8, Figure 8.12). The length of the plastic branch depends to a high degree on the confinement of the boundary elements of the wall and on the degree of the axial compression. A more detailed approach will be made later. The same holds for the $M-\theta$ diagram under cyclic loading, as can be seen in the diagram of Figure 9.7, which is similar to that of a cantilever beam (Figure 8.21) and a column (Figure 8.46). Therefore, in the case that special care has been taken in the design of the wall for ductile behaviour, the $M-\delta$ diagram exhibits a stable form under reversed cycles of loading.
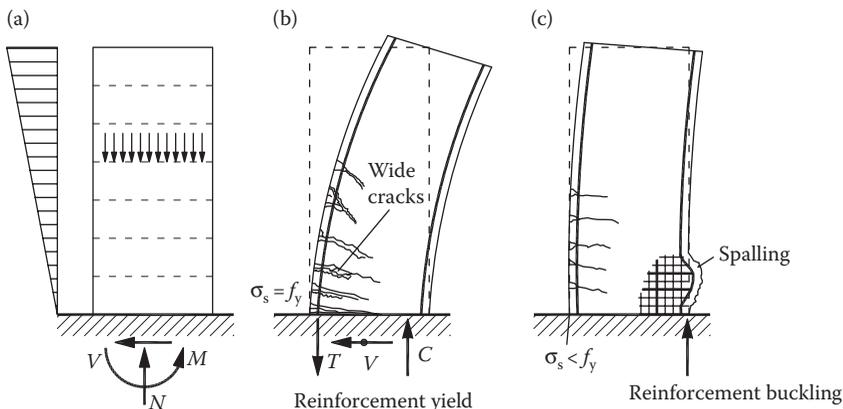
Figure 9.6 Failure mechanism of slender walls under flexure: (a) loading pattern; (b) ductile failure; (c) brittle failure.
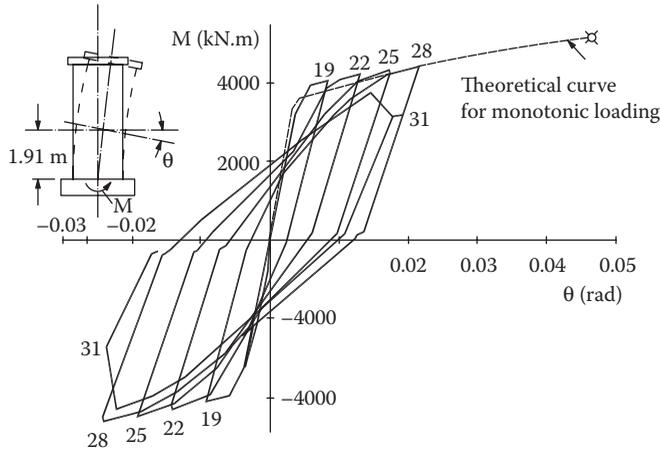
Figure 9.7 Moment–rotation hysteresis loops for slender R/C wall with barbell cross-section subjected to cyclic loading. (Oesterle et al., 1980)

Interaction *M–N* diagrams for symmetrically reinforced wall cross-sections of orthogonal form are similar to those of columns (Figure 9.8). Additionally in the case of walls, the following remarks should be made:

- Moment carrying capacity is strongly influenced by the concentration of a large percentage of longitudinal reinforcement at the confined boundary elements.
- N_{Ed} in the case of ductile walls almost always has values below N_{Rd} balanced. Therefore, ductile walls almost always enter the post-elastic region of $M–\varphi$ diagrams. This capacity is enhanced due to the proper confinement of the boundary elements.
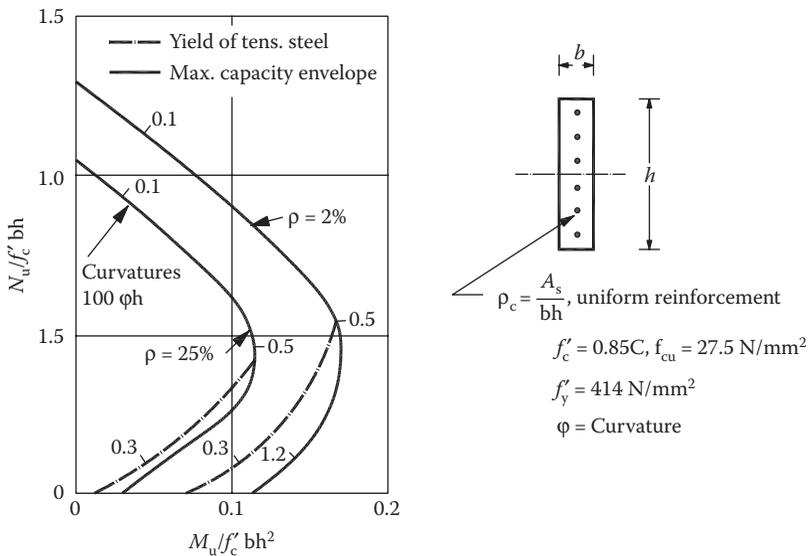
Figure 9.8 Axial load–moment interaction curves for rectangular uniformly reinforced concrete walls. (After Salse and Fintel, 1973; From Dowrick, D. 2005. *Earthquake Risk Reduction.* Copyright Wiley-VCH Verlag GmbH & Co. KGaA. Reproduced with permission.)

9.2.2.2 Dimensioning of slender ductile walls with orthogonal cross-section under bending with axial force

The dimensioning of walls under bending moment with axial force is carried out under the same assumptions as for beams and columns (see Paragraphs 8.2.2.1 and 8.3.2.1). Therefore, for *orthogonal cross-sections* where the bending moment acts mainly about a main axis perpendicular to the length of the cross-section, and therefore it is considered uniaxial bending with axial force, the dimensioning may be carried out either with the aid of design charts (e.g. Figure 9.8) or simplified expressions of a closed form (Tassios, 1984).

So, for example, in the case of a rectangular cross-section reinforced with vertical grids corresponding to a reinforcement ratio $\rho_v = A_{sv}/b_w l_w$, where b_w is the width and l_w is the length of the cross-section, and with concentrated reinforcement at the ends with an area $A_{s1} = A_{s2} = A_s$, the design moment M_{Rd} may be determined from the following expression (Figure 9.9a; Tassios, 1984).

$$M_{Rd} = \left[\left(1 - \frac{\xi}{2} \right) \frac{A_s}{b_w l_w} f_{yd} + \frac{1}{2} (1 - \xi)(\rho_v f_{yd} + \sigma_o) \right] b_w l_w^2 \tag{9.5}$$

where

$$\sigma_o = N_{Ed}/b_w l_w$$

is the average stress due to axial load alone (compression positive) and

$$\xi = \left(\frac{A_s f_y}{b_w l_w f_c} + \rho_v \frac{f_{yd}}{f_{cd}} + \frac{\sigma_o}{f_{cd}} \right) \frac{1}{1 + \rho_y f_{yd}/f_{cd}} \tag{9.6}$$

is the neutral depth ratio (x_u/l_w) at the ultimate limit state.
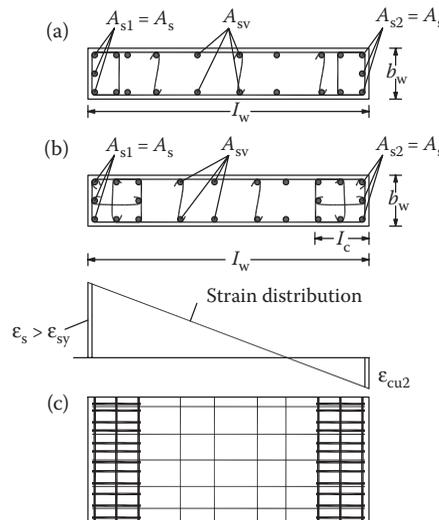
Figure 9.9 Dimensioning of slender ductile walls to bending with axial force: (a) main reinforcement A_s concentrated at the boundaries; (b) main reinforcement A_s concentrated in confined boundary elements; (c) concept of plane strain distribution.

On the other hand, for walls with barbell section or with boundary-confined elements having a width l_c as shown in Figure 9.9b,c, with the main reinforcement concentrated at the boundary elements ($A_{s1} = A_{s2} = A_s$), the design bending strength may be determined from the expression below (Tassios, 1984):

$$M_{Rd} \cong \left(A_s f_{yd} + \frac{N}{2} \right)(l_w - l_c') \qquad (9.7)$$

However, the above-mentioned methods should nowadays be considered obsolete, since various commercial computer platforms have been developed, which make possible the dimensioning of cross-sections of any shape for biaxial bending with axial force (see Figure 9.10) like ECtools, CUBUS, NOUS and so on. These platforms may be used either for columns or for walls, since the design assumptions are the same. It should not be forgotten that for the cross-sections of each vertical member and at each storey, at least 2×33 load cases should be examined at the top and bottom of the storey (see Subsection 5.8.4), a fact that makes almost impossible the use of manual calculations either with the aid of charts or simplified expressions.

9.2.2.3 Dimensioning of slender ductile walls with a composite cross-section under bending with axial force

Usually the cross-section of the ductile walls has a composite form (e.g. L, T, U, I, Z hollow tubular form, etc.). These composite wall sections, according to EC8-1/2004, should be taken as integral units in analysis and design. The dimensioning of a cross-section of this form may be carried out only with the aid of computational tools. Consider a cross-section in the form shown in Figure 9.10, loaded by a vector group M_{Eyd}, M_{Ezd}, N_{Ed} at the geometrical centre S of the cross-section. The ULS verification of bending resistance is expressed by the relation:
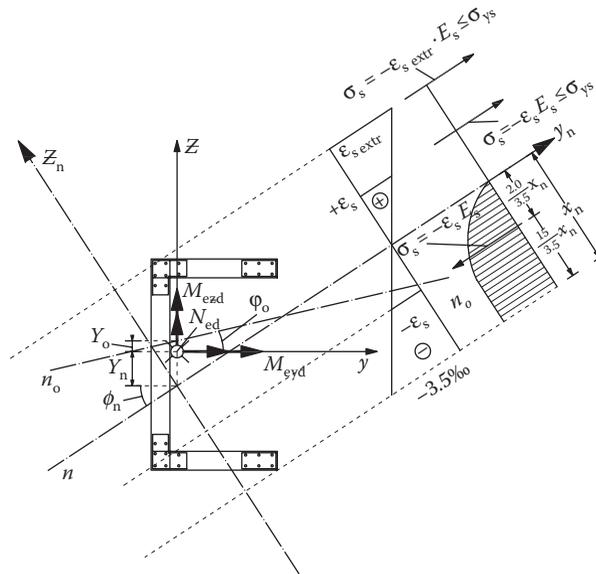
Figure 9.10 Dimensioning of a composite cross-section bending with axial force.

$$\frac{M_{\text{Ryd}}}{M_{\text{Eyd}}} = \frac{M_{\text{Rzd}}}{M_{\text{Ezd}}} = \frac{N_{\text{Rd}}}{N_{\text{Ed}}} = \gamma \geq 1.0 \tag{9.8}$$

or

$$\left.\begin{aligned}
M_{\text{Ryd}} &\geq \gamma M_{\text{Eyd}} \\
M_{\text{Rzd}} &\geq \gamma M_{\text{Ezd}} \\
N_{\text{Rd}} &\geq \gamma N_{\text{Ed}}
\end{aligned}\right\} \tag{9.8a–c}$$

If the neutral axis n–n has been determined (y_n, φ_n) the corresponding strain diagram at failure will be that given in Figure 9.10, together with the stress field of concrete and steel. Therefore, M_{Ryd}, M_{Rzd}, N_{Rd} can be determined and ULS verification of Equation 9.8a–c is easy. Starting from a first position of the neutral axis corresponding to the uncracked cross-section (Stage I) and applying a Newton–Raphson procedure already presented in Paragraph 8.2.2.4 for beams, the unknown parameters y_n, φ_n and γ can be defined very quickly via a proper commercial platform (NOUS/3P (2002) FAGUS/CUBUS-2011) or more sophisticated computer aids proper for academia purposes (Papanikolaou, 2012).

It is apparent that, at the same time, it is possible for the design of the cross-section to be carried out automatically. Having an estimated steel reinforcement pattern in advance and introducing as unknown the change ΔA_s of the steel reinforcement in predefined positions (e.g. the corners and the ends of the composite cross-section), in place of γ, which is predefined as $\gamma = 1$, the automated computer-aided design gives the required change of the reinforcement after all 33 load combinations have been checked, so that $[E_d] = [R_d]$.

9.2.2.4 Determination of M–φ diagram and ductility in terms of curvature under axial load for orthogonal cross-sections

According to what has been presented so far, ductile walls are the main vertical members of the structural system at the base of which seismic energy will be dissipated, together with the ends of the beams and the columns at their bases (see Subsection 6.1.5, Figure 6.7). Therefore, a special concern must be given to the design of walls for *local ductility at their base*.

In the case that their cross-section is orthogonal, it is self-evident that they resist bending on the long side of their cross-section. In this respect they behave like columns under uniaxial bending. Therefore, the procedure developed in Paragraph 8.3.2.2 also holds for orthogonal ductile walls.

From the above-mentioned treatment for the ductility of columns, Equations 8.99b, 8.106 and 8.107 will be recalled and modified properly for the case of walls. According to Equation 8.106, κ should be introduced in Equation 8.107 with the value $\kappa = 1.44$. Therefore,

$$\boxed{\mu_{\varphi} = \frac{\varepsilon_{\text{cu}}}{\varepsilon_{\text{y}}} \frac{0.72}{0.9\kappa(\nu + w_{\text{v}})} \cong \frac{0.80}{1.44} \frac{\varepsilon_{\text{cu}}}{\varepsilon_{\text{y}}} \frac{1}{(\nu + w_{\text{v}})}} \tag{9.9}$$

The above equations (8.99b), (8.106) and (9.9) will be used a little bit later for the design of the local ductility of orthogonal walls according to EC8-1/2004.

For composite cross-sections (L, T, U, I, Z, etc.), computer platforms have been developed that allow the determination of points A, B and C (Figure 8.12, Chapter 8.3.2.2; e.g. RCCOLA, FAGUS, NOUS/3P, etc.). Computer platform NOUS/3P (2002) has already been presented for beams and can also be used for composite wall sections and for columns.

9.2.3 Behaviour of slender ductile walls under prevailing shear

The failure modes of walls with orthogonal cross-section under prevailing shear, as in the case of beams, may be classified in the following types:

- Diagonal tension (Figure 9.11a)
- Diagonal compression (Figure 9.11b)
- Sliding shear in the region of the plastic hinge (construction joint; Figure 9.11c)

Keeping in mind that the maximum normalised axial forces in ductile walls are limited by current Codes, much lower than those in columns, as we will see a little later, it is apparent that the behaviour of ductile walls to shear lies between the behaviour of beams and columns. Therefore, the design of walls to shear follows in concept the methods developed for beams and columns with minor modifications, which will be presented in the next paragraph (Subsection 9.2.4). Here, only two particular points should be presented:

1. From extended experimental work it has been determined (Kowalski and Priestley, 2000) that in the region of the plastic hinge at the base of the wall, due to the degradation of concrete compressive strength under loading reversals, the diagonal compression strength is also degraded. Therefore, a reduction factor should be introduced in the expressions used for the determination of V_{Rdmax}. This factor, as we will see later, is on the order of 0.40 for DCH buildings.
2. Sliding shear may appear in the region of a plastic hinge and particularly at the position of a construction joint. This failure at horizontal planes can be resisted by:

   - Shear friction across the horizontal crack
   - Dowel action
   - Resistance of inclined steel bars arranged in the joint region

The main reason of this type of failure must be attributed to the low value of axial loading ($\nu_d \leq 0.35$ and therefore $\nu_\kappa \leq (0.35/1.50) \cong 0.23$)(see Paragraph 9.2.4.3(2)).
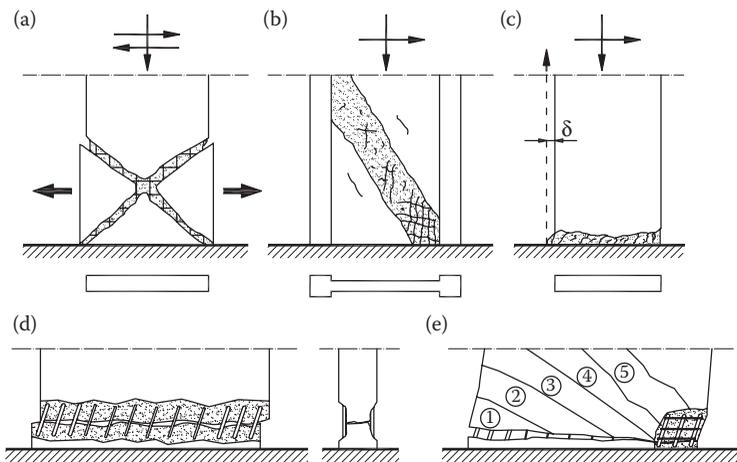
Figure 9.11 Failure modes of walls under prevailing shear: (a) diagonal tension; (b) diagonal compression; (c) sliding shear; (d) detail of sliding shear; (e) bending failure combined with sliding. (From Salonikios, T. 2007. Analytical prediction of the inelastic response of R/C walls with low aspect ratio. *ASCE Journal of Structural Engineering*, 133(6), 844–854. With permission of ASCE.)

As a consequence, the behaviour of a wall to cyclic loading after yield as far as the shear type of failure at the critical region is similar to that of beams under cyclic loading (Paragraph 8.2.4.2, Figure 8.30).

Expressions for the strength calculation to sliding shear will be given in the next Subsection 9.2.4.

9.2.4 Code provisions for slender ductile walls

9.2.4.1 General

According to EC8-1/2004, ductile walls are defined as '**slender**' if the aspect ratio h_w/l_w satisfies the known relation:

$$\boxed{h_w/l_w \geq 2} \tag{9.10}$$

where
h_w is the height of the wall
l_w is the length

The design rules for slender ductile walls under seismic actions according to EC8-1/2004 are given below, together with the required justification in terms of the theory developed in previous subsections (Chapters 8 and 9). It should be noted that, as in the case of beams and columns, the design specifications are directly related to ductility demand in consideration, that is, DCL, DCM and DCH. For a higher ductility class these requirements tend to be stricter in order to obtain a *higher local ductility* in terms of curvature.

Specifications for the design effects of ductile walls, taking into account capacity design procedure, have already been presented in Chapter 6.

Material issues have also been presented in Subsections 7.2.4 and 7.3.5 for all ductility classes.

It should also be noted here that for the design of slender walls of class DCL, Code specifications for conventional R/C structures are applied (EC2-1-1/2004), except that concrete and steel reinforcement qualities are specified by EC8-1/2004 and have already been presented in Chapter 7. For this reason, design of slender walls for DCL buildings do not require further treatment in this book.

In conclusion, it should also be noted that all rules and specifications of the corresponding Code for conventional R/C structures (EC2-1-1/2004) continue to be in effect, unless they contradict what will be presented below.

9.2.4.2 Design of slender ductile walls for DCM buildings

1. *Geometrical constraints*
   These have been given already in Subsection 9.2.1.
2. *Resistance to flexure and shear*
   a. *Flexural* and *shear* resistances will be computed in accordance with EN1992-1-1/2004 using the axial force resulting from the analysis in the seismic design situation and the gravity load combination (basic).

   It is apparent that bending and shear demand, which are introduced in ULS verification, result from the *capacity design* procedure. In this respect, for each cross-section under consideration, 33 load case combinations should be taken into account (1 basic +32 seismic combinations).

b. The value of the normalised axial load v_d should be limited to 0.40, that is:

$$\boxed{v_d \leq 0.40} \tag{9.11}$$

c. Vertical web reinforcement should be taken into account for the calculation of flexural resistance.

d. Composite wall sections, that is, wall sections of the form L, T, U, I, Z, should be taken as integral units. In any case, EC8-1/2004 allows the replacement of a composite cross-section by webs connected with flanges and distribution of the bending moments and the axial forces to these T or I elements in a uniaxial bending load case. It is the author's opinion that this simplification cannot much help the design procedure, at least in flexure, since each load combination corresponds to a biaxial bending. Therefore, the T or I models should be formed for both main directions, the moment vectors in each main direction should be distributed to the elements acting in this direction and thus the number of verifications should be a multiple of 33 (Figure 9.12). Consequently, the easiest way is to design the composite section for each group of M_{Eyd}, M_{Ezd}, N_{Ed} using a proper computer platform for biaxial bending (Paragraph 9.2.2.3). Conversely, for shear design the only realistic approach is the above simplification recommended by the Code. In this respect, shear forces V_{Eiyd} and V_i of each load combination are distributed to the webs corresponding to their direction proportional to the area of each web. From this point on these webs are dimensioned to shear as independent orthogonal cross-sections (Figure 9.13).
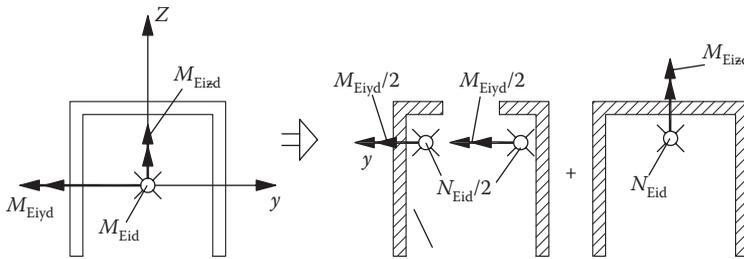
Figure 9.12 Biaxial bending of a composite cross-section: Simplified procedure replacing the composite cross-section by orthogonal cross-sections with flanges.
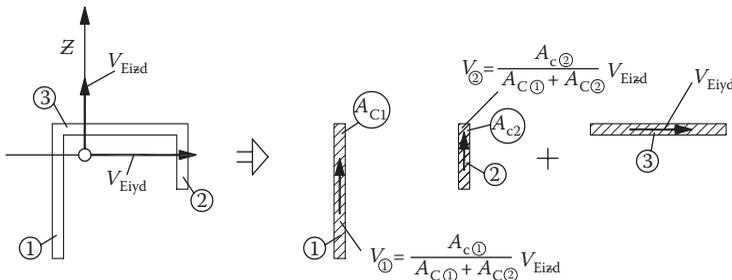
Figure 9.13 Biaxial shear of a composite cross-section: Simplified procedure replacing the composite cross-section by orthogonal elements in each direction.

3. *Detailing of slender ductile walls for local ductility*
   a. The height of the critical region h_{cr} above the base of the wall is estimated as:

$$\boxed{h_{cr} = \max\{l_w, h_w/6\}} \tag{9.12}$$

but

$$\boxed{h_{cr} \leq \begin{cases} 2l_w \\ \begin{cases} h_s & (\text{for } n \leq 6 \text{ storeys}) \\ 2h_s & (\text{for } n > 6 \text{ storeys}) \end{cases} \end{cases}} \tag{9.13}$$

where
   h_w is the total height of the wall from the base to the top
   l_w is the length of the cross-section of the wall
   h_s is the clear storey height
   base is defined as the level of the foundation (Figure 9.14) or the top of base-ment storeys with rigid diaphragms and perimeter walls (box-type foundation).

   b. In the critical region *at the base* of the slender ductile walls, a value of the curva-ture ductility factor μ_ϕ should be provided, directly related to the basic value of the behaviour factor q_o of the building via Equations 5.52a and 5.52b.
   In order for the eventual overstrength at the fixed end of the wall to be taken into account, q_o should be introduced in the above expressions reduced by the factor M_{Ed}/M_{Rd} (counter-balance between ductility and overstrength), where M_{Ed} is the seismic design combination of bending moment from the analysis and M_{Rd} is the design flexural resistance. It is obvious that M_{Ed}/M_{Rd} is always less or equal to 1.0.
   c. The above specified ductility μ_ϕ is ensured by means of a proper confinement of the edge regions of the cross-section using steel hoops and ties (Figures 9.15 and 9.16).
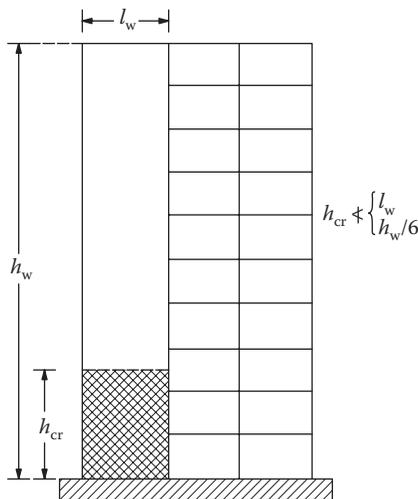
Figure 9.14 Determination of the wall critical region.
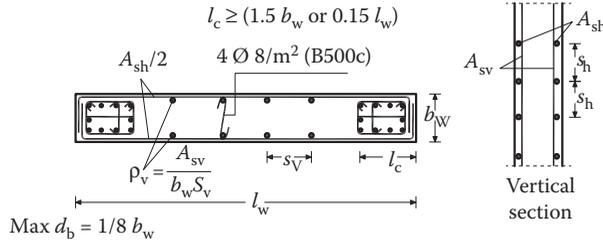
Figure 9.15 Arrangement of horizontal and vertical reinforcement in walls with a rectangular cross-section.
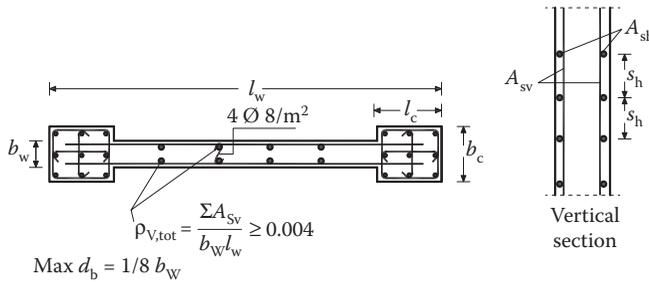
Figure 9.16 Arrangement of horizontal and vertical reinforcement in walls with a barbell cross-section.

d. For walls of a rectangular cross-section, the mechanical volumetric ratio ω_{wd} of the required confining reinforcement in boundary elements should satisfy the following expression:

$$\alpha\omega_{wd} \geq 30\mu_\varphi(\nu_d + \omega_{vd})\varepsilon_{sy,d}\frac{b_c}{b_o} - 0.035 \tag{9.14}$$

The above equation is similar to Equation 8.127, which has been introduced in the case of columns. The only difference is that in the case of walls the term ω_{vd} is introduced in addition, which expresses the mechanical volumetric ratio of the longitudinal web reinforcement.

$$\omega_{vd} = \frac{A_{sv}}{b_c d_c} \cdot \frac{f_{yd}}{f_{cd}} \tag{9.15}$$

The meaning of the above notation has been defined in Paragraphs 8.3.4.2.3 and 8.3.4.2.4 for columns. The justification of Equation 9.14 has already been presented in Paragraph 8.3.4.2.4 in the case of columns.

For the evaluation of the *safety factor of local ductility of walls*, Equation 8.106 (b) should be introduced in place of Equation 8.133, that is,

$$\varphi_y = \frac{1.44\,\varepsilon_y}{h} \tag{8.106b}$$

From that point on and following the procedure of Paragraph 8.3.4.2.4, it follows that $\alpha\omega_{wd}$ is given by the expression:

$$\alpha\omega_{wd} = \frac{1.30}{0.72} 10.0 \cdot \mu_\varphi \cdot \varepsilon_y (\nu + \omega_v) \frac{b_c}{b_o} \beta - 10.0 \cdot \varepsilon_{cu2} \tag{8.137b}$$

for

$\varepsilon_{cu2} = 0.0035$

$\beta \cong 1.15$

$⊠ = ⊠_d/1.50$

$\varepsilon_y = 1.15 \cdot \varepsilon_{yd}$

(see Paragraph 8.3.4.2.4; Equation 8.138, 8.139)
Equation 8.137b) results in

$$\alpha\omega_{wd} = \frac{1.30}{0.72} 10.0 \cdot \mu_\varphi \left(\frac{\nu_d}{1.50} + \omega_{vd} \frac{1.15}{1.50} \right) \frac{b_c}{b_o} 1.15 - 0.035$$

or

$$\boxed{\alpha\omega_{wd} \cong 14.30 \mu_\varphi (\nu_d + \omega_{vd}) \frac{b_c}{b_o} - 0.035} \tag{9.16}$$

Comparing Equations 9.16 and 9.14 and taking into account that the safety factor of μ_ϕ derived from Equations 5.52a and 5.52b in relation to q_o is of the order of 1.10 (Equation 5.52c), it may be seen that the imposed confinement by the Code via Equation 9.14 ensures a safety factor for local ductility of ductile walls on the order of

$$\gamma_{\mu\varphi} \cong 1.10 \frac{30}{14.30} = 2.30 \tag{9.17}$$

e. The above-specified confinement must extend vertically over the height h_{cr} of the critical region and horizontal along a length l_c (Figure 9.17) from the extreme compression fibre of the wall up to the point where compressive strain becomes less than $\varepsilon_{cu2} = 0.0035$. Therefore, the confined boundary element for a wall of orthogonal section is limited to a distance (Figure 9.17):

$$\boxed{l_c = x_u \left(1 - \frac{\varepsilon_{cu2}}{\varepsilon_{cu2,c}} \right)} \tag{9.18}$$

where

$$\boxed{x_u = (\nu_d + \omega_{vd}) \frac{l_w \cdot b_c}{b_o}} \tag{9.19}$$

(see Equation 8.99b)
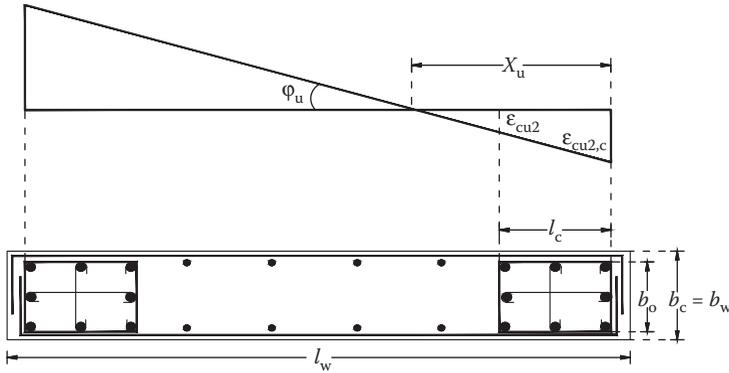
Figure 9.17 Confined boundary element of free-edge wall end (top: strains at ultimate curvature; bottom: wall cross-section). (Adapted from E.C.8-1/EN1998-1. 2004. *Design of Structures for Earthquake Resistance: General Rules, Seismic Actions and Rules for Buildings.* CEN, Brussels, Belgium.)

The extreme compressive strain $\varepsilon_{cu2,c}$ is related to the degree of confinement $\alpha\omega_{wd}$ via the following expression:

$$\varepsilon_{cu2,c} = 0.0035 + 0.1\,\alpha\omega_{wd}$$
(9.20)

(see Paragraph 8.3.4.2.4; Equation 8.136)

f. Therefore, for the determination of the required confinement in the critical regions of the wall, the following steps are followed:
  i. Step 1: Determination of the required confinement $\alpha\omega_{wd}$ using Equation 9.14
  ii. Step 2: Determination of the required $\varepsilon_{cu2,c}$ using Equation 9.20
  iii. Step 3: Determination of the neutral axis depth x_u at ultimate curvature Equation 9.19
  iv. Step 4: Determination of the depth l_c of the confined boundary using Equation 9.18
  v. Step 5: Formulation of the confinement detail and determination of $\alpha = \alpha_n \cdot \alpha_s$ Equation 8.129
  vi. Step 6: Determination of $\omega_{wd} = \rho_w(f_{yd}/f_{cd})$ using the results of steps 1 and 5.
  It should be noted that the whole issue is handled by the American Code (ACI 318M-2011) in a very simplified manner, although the procedure followed is based on the same concept as EC8-1/2004, that is, the enhancing of the extreme compressive strain via concrete confinement with steel hoops and ties.
g. The minimum dimensions of the confined boundary elements of free-edge wall ends have been specified in Paragraph 9.2.1 (3).
h. The longitudinal reinforcement ratio in the boundary element should not be less than 0.005 over all the height of the element. It is obvious that the depth l_c of the boundary element may be decreased above the critical region to the lower limit that has been specified in Paragraph 9.2.1 (3).
i. The provisions for the base of primary columns as far as the minimum value of ω_{wd} of 0.08 and the spacing of the hoops and ties should also be applied within the boundary elements of walls.
j. In the height of the wall above the critical region the rules of EN 1992-1-1/2004 regarding vertical horizontal and transverse reinforcement basically apply.

k. The required area of transverse reinforcement A_{si} within the lap zone of the longitudinal reinforcement of boundary elements in walls, no matter if they are classified as DCM or DCH, is calculated as in the case of columns (Equation 8.150; Paragraph 8.3.4.5).

l. In the case of walls with barbells or with composite cross-section (T, U, L, I, Z-shaped sections), the boundary elements should be formed in all boundaries and at the joints of the orthogonal parts (Figure 9.18). In this way, both local ductility and shear transfer at the joints between adjacent orthogonal parts is ensured. The required confinement degree $\alpha\omega_{wd}$ and the confined area in this case are defined as follows:

i. The axial force N_{Ed} and the total area of the vertical reinforcement in the web A_{sv} are normalised to the area of the barbell or the flange ($h_c b_c$)(Figure 9.19 and Figure 9.20), that is,

$$v_d = \frac{N_{Ed}}{h_c b_c f_{cd}}, \quad \omega_v = \frac{A_{sv}\, f_{yd}}{h_c b_c f_{cd}} \tag{9.21a,b}$$
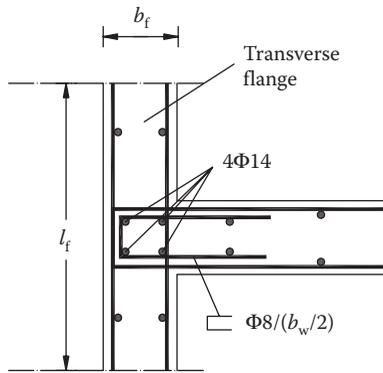
Figure 9.18 Detailing of the web-flange connection in flanged walls.
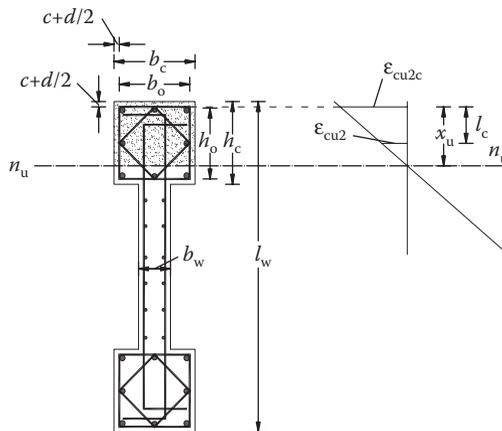
Figure 9.19 Determination of the confined boundary elements of a free-edge wall with barbells.
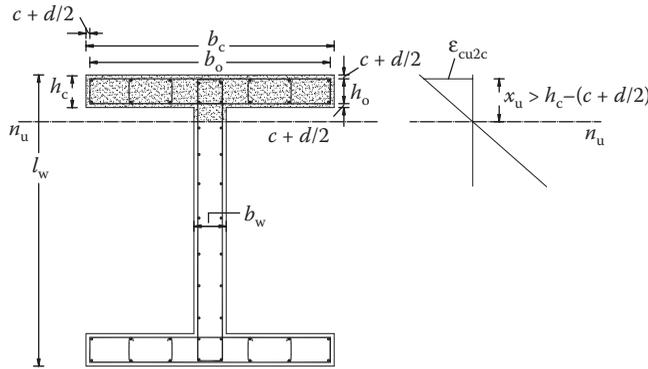
Figure 9.20 Determination of the confined region of a composite cross-section.

The neutral axis depth x_u at ultimate curvature φ_u after concrete spalling is given by expression 9.19. If the value of x_u does not exceed the depth of the barbell or the flange thickness after spalling of the cover concrete, then $\alpha\omega_{wd}$ may be defined using Equation 9.14. In this case, the flange or the barbell will be confined to their total area $b_c \cdot h_c$ (Figures 9.19, 9.20).

ii. In the case of a wall with barbells, if the value x_u exceeds the depth of the barbell, the simplest solution is to design a bigger barbell.

iii. In the case of a composite wall, if the value x_u significantly exceeds the thickness of the flange, an approach to the problem would be an increase in the thickness of the flange. A second approach more suitable for an automatic computer-aided design is to sacrifice the flange and to confine the web as an orthogonal cross-section with confined boundary elements (Fardis et al., 2005; Fardis, 2009).

Such an approach to the problem is compatible with the concept of the formation of confined boundary elements not only at the ends of the orthogonal components but also in all joints presented in a previous paragraph (Figure 9.21). However, this approach leads to very long confined boundary elements.

iv. In the case of a composite wall, if the value x_u exceeds the thickness of the flange, a computer-aided design could ensure an accurate determination of the required confinement $\alpha\omega_{wd}$ for a given local ductility μ_ϕ at curvature level. This procedure is codified by EC8-1/2004 and is outlined below:

–   The required value of μ_ϕ is determined using Equations 5.52a) and 5.52b) as a function of the basic value of the behaviour factor q_o

–   For successive values of $\alpha\omega_{wd}$ using Equation 9.20 the values of $\varepsilon_{cu2,c}$ are determined.

–   For each of these values of $\varepsilon_{cu2,c}$, the values of φ_y and φ_u^* are determined using a computer-aided iterative procedure (e.g. platform NOUS; Figure 9.22). When the ratio reaches:

$$\mu_\varphi^{avail} = \frac{\varphi_u^*}{\varphi_y} \geq \mu_\varphi^{required} \tag{9.22}$$

the procedure stops and the area with compressive strain greater than $\varepsilon_{cu2} = 3.5‰$ is confined with hoops and ties corresponding to $\alpha\omega_{wd}$, for which inequality (9.22) is fulfilled.
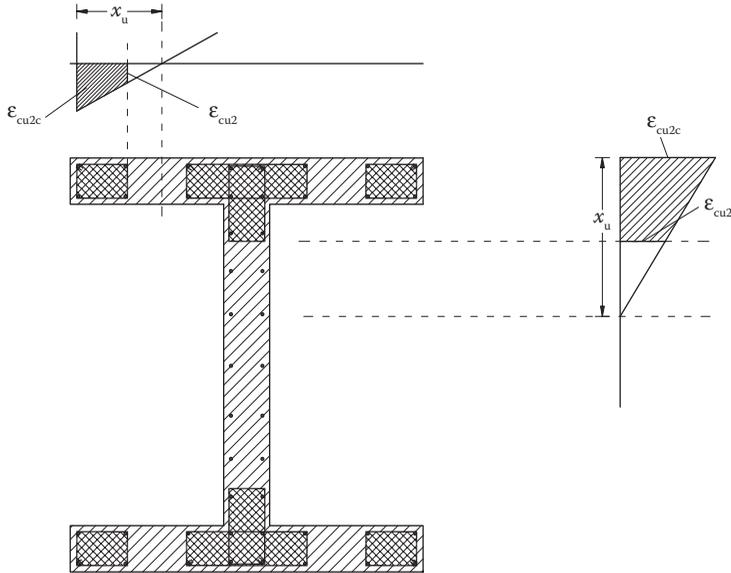
Figure 9.21 Determination of the confined regions of a composite cross-section based on the assumption of sacrificed flanges.
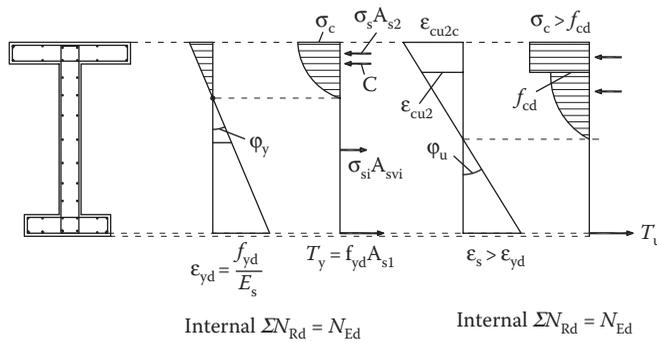
Figure 9.22 Determination of the confinement of a composite cross-section following an iterative step-by-step method.

9.2.4.3 Design of slender ductile walls for DCH buildings

1. *Geometrical constraints*
   In addition to what has been specified for ductile walls of DCM buildings, the following requirements are imposed:
   a. The minimum dimensions of barbells and flanges are given in the relevant paragraph for confined boundary elements.
   b. Random openings not regularly arranged to form coupled walls should be avoided, unless their influence is either insignificant or accounted for in the analysis dimensioning and design.
2. *Bending resistance*
   a. Flexural resistance is evaluated as for DCM walls.
   b. The value of the normalised axial load ν_d should be limited to 0.35, that is:

$$v_d \leq 0.35 \qquad\qquad (9.23)$$

3. *Diagonal compression failure due to shear*
   a. The value of V_{Rdmax} should be calculated as follows:
      i. *Outside the critical region*
         The value of V_{Rdmax} should be calculated as in the case of columns with a length of the internal lever arm z equal to $0.8l_w$ and an inclination of the compression struts to the vertical equal to $\delta = 45°$ (Figure 9.23a).
      ii. *In the critical region, shear resistance is limited to 40% of the value outside the critical region* to confront the shear degradation of concrete in the critical region under cyclic loading. It should be noted that in the corresponding American Code (ACI 318M-2011) there is not any provision for this type of reduction.
4. *Diagonal tension failure of the web due to shear*
   a. The calculation of web reinforcement for the ULS verification in shear, in the case that:

$$\alpha_s = \frac{M_{Ed}}{V_{Ed}\, l_w} \geq 2.0 \qquad\qquad (9.24)$$

   is carried out as in the case of columns, but with the values of z and $\tan \delta$ as follows (Figure 9.23b):

$$z = 0.80\, l_w \qquad\qquad (9.25a)$$

$$\tan \delta = 1.0 \qquad\qquad (9.25b)$$

   that is, the variable strut inclination concept is replaced by the Mörsh concept of 45° strut inclination, as in the case of beams of DCH buildings.
   b. It is apparent that horizontal web bars must be properly anchored at the ends of the wall sections (Figures 9.15 and 9.16).
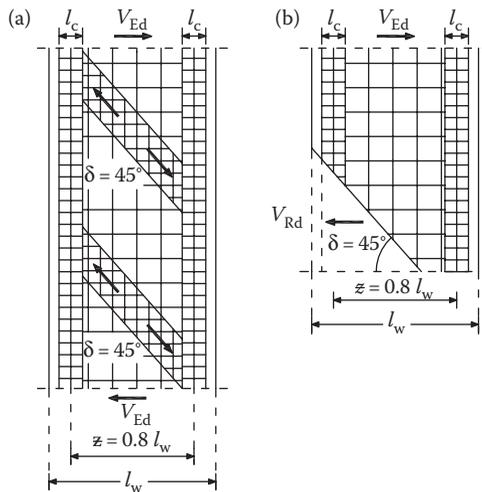
Figure 9.23 Diagonal shear resistance V_{Rd}: (a) compressive struts resistance; (b) tensile reinforcement resistance.

   c. If the mechanical aspect ratio at the base of a storey is

$$\frac{M_{Ed}}{V_{Ed}\, l_w} \leq 2.0 \qquad (9.26)$$

even in case of slender walls, the design of diagonal tension should be carried out as in the case of squat walls (par. 9.4.4.4). This rule is meaningful basically for the upper storeys of dual systems. In these systems, while M_{Ed} is given by the diagram of Figure 6.8 in Paragraph 6.1.5.2, which is linear over the entire height of the building, the relevant V_{Ed} diagram Figure 6.10, Paragraph 6.1.5.3, due to capacity design, is over-estimated at the upper storeys, and, therefore, very often, the aspect ratio $M_{Ed}/V_{Ed}l_w$ results in values less than 2. So, the web reinforcement at the upper storeys turns out to be unexpectedly high.

5. *Sliding shear failure*
   a. At potential sliding shear planes (e.g. at construction joints) within the critical region, sliding shear failure may occur only in *slender walls of high ductility*. This has been properly explained in Paragraph 9.2.3.2. As was already noted there, the shear resistance against sliding, $V_{Rd,s}$, comprises three components, that is:

$$V_{Rd,s} = V_{dd} + V_{id} + V_{fd} \qquad (9.27)$$

where

    V_{dd} is the dowel resistance of the vertical bars
    V_{id} is the shear resistance of inclined bars (at an angle φ to the potential sliding plane)
    V_{fd} is the friction resistance

The wall is deemed to be safe against sliding if the following condition is satisfied:

$$V_{Ed} \leq V_{Rd,s} \qquad (9.28)$$

   b. The above components V_{dd}, V_{id} and V_{fd} may be determined by means of the following expressions:

$$V_{dd} = \min \begin{cases} 1.3\sum A_{sj}\sqrt{f_{cd}\cdot f_{yd}} \\ 0.25 f_{yd}\cdot \sum A_{sj} \end{cases} \qquad (9.29a,b)$$

$$V_{id} = \sum A_{si}\cdot f_{yd}\cdot \cos\varphi \qquad (9.30)$$

$$V_{fd} = \min \begin{cases} \mu_f\left[\left(\sum A_{sj}f_{cd} + N_{Ed}\right)\xi + \dfrac{M_{Ed}}{z}\right] \\ 0.5n\cdot f_{cd}\cdot \xi\cdot l_w\cdot b_{wo} \end{cases} \qquad (9.31a,b)$$

where

μ_f is the concrete-to-concrete friction coefficient under cyclic action, which may be assumed to be equal to 0.6 for smooth interfaces and to 0.7 for rough ones.

z is the internal lever arm with a value equal to $0.8l_w$.

ξ is the normalised neutral axis depth at failure.

ΣA_{sj} is the sum of the cross-section areas of the vertical bars of the web and of *additional* bars arranged in the boundary elements specifically for resistance against sliding.

ΣA_{si} is the sum of the cross-section areas of all inclined bars in both directions; large-diameter bars are recommended for this purpose (Figure 9.24).

n: $0.6/(1 - f_{ck}[MP_a]/250)$

N_{Ed} is introduced with a positive sign when compressive.

c. The three mechanisms of shear resistance against sliding have been developed progressively in the past 50 years by various investigators.

The dowel effect mechanism V_{dd} (Equation 9.29a) is based on the Rasmussen (1963) reports in combination with an upper bound (Equation 9.29b) suggested by Paulay and Priestley (1992) as a reasonable limit for squat walls under cyclic loading.

The diagonal truss mechanism V_{id} is based on Mörsh and its "truss analogy model," and has thus far been used many times (mainly for shear transfer in beams and short columns).

Finally, the friction mechanism V_{fd} (aggregate interlock) is based on the assumption that friction is developed along the compression zone only. Therefore, the axial forces contributing to friction are the following (Tassios, private communication, 1994):

i. The fraction of the wall axial force corresponding to the compression zone, ξN_{Ed}

ii. The clamping action of the vertical reinforcement intersecting the joint in the compression zone when sliding is activated $(\Sigma A_{sj})f_{yd} \cdot \xi$ (Figure 9.25; Park and Paulay, 1975)

iii. The compression force caused by the bending moment M_{Ed}/z

d. The arrangement of x-shaped reinforcement intersecting the sliding joint in the critical region is not obligatory; it is in the hands of the designer to decide if he uses additional vertical web reinforcement or x-shaped rebars. It should be noted that the arrangement of x-shaped bars in the walls is not an easy task from the constructability point of view.
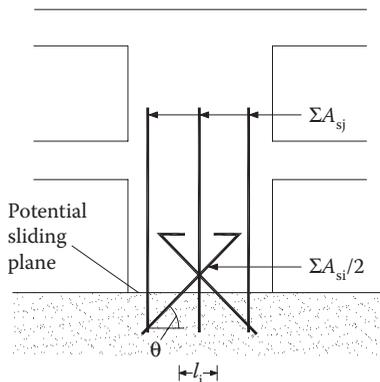
Figure 9.24 Bidiagonal reinforcement in structural walls.
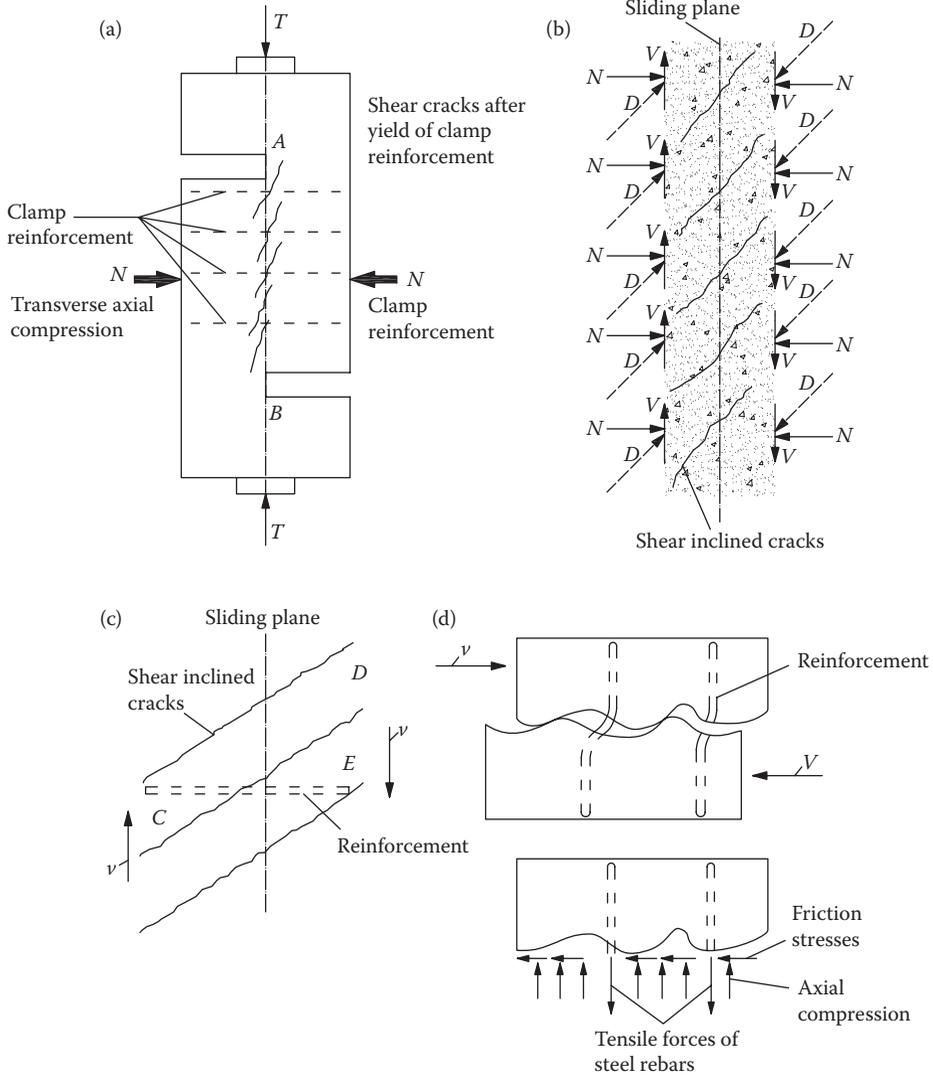
Figure 9.25 Shear transfer model at a sliding joint: (a) experimental set-up; (b) transfer model along an uncracked joint; (c) detail of (b); (d) shear sliding. Friction stresses along a pre-cracked sliding plane.

e. Inclined bars should be fully anchored on both sides of the potential sliding joint. It should also be noted that inclined bars, if arranged after the general design of the wall as a result of a local design for the wall sliding at the base joint, lead to an increase of the bending resistance of the wall there and, therefore, to an increase of the base shear resulting from the capacity design procedure. This increase of the bending moment may be estimated as follows (Figure 9.26):

$$\Delta M_{\mathrm{Rd}} = \frac{1}{2} \sum A_{\mathrm{si}} \cdot f_{\mathrm{yd}} \sin \varphi \cdot l_1 \qquad (9.32)$$
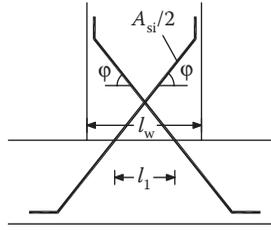
Figure 9.26 Increase of bending resistance at the base of the wall due to x-shaped rebar arrangement.

where

l_1 is the distance between the centrelines of the two sets of inclined bars at the x-shaped arrangement.

Alternatively, the shear resistance V_{id} of the inclined bars may be reduced instead of increasing of V_{Ed} due to ΔM_{Rd}. In this context, V_{id} takes the form:

$$V_{idred} = \sum A_{si}f_{yd}(\cos\varphi - 0.5l_1 \sin\varphi/\alpha_s \cdot l_w) \tag{9.33}$$

This expression results very easily from the following considerations. The increase ΔV_{Ed} of V_{Ed} due to the increase of base moments by ΔM_{Rd} may be derived from the expression:

$$\alpha_s = \frac{\Delta M_{Ed}}{l_w \Delta V_{Ed}} \cong \frac{\Delta M_{Rd}}{l_w \Delta V_{Rd}} \tag{9.34}$$

or

$$\Delta V_{Rd} \cong \frac{\Delta M_{Rd}}{l_w \alpha_s} \tag{9.35}$$

Keeping in mind that

$$V_{idred} = V_{id} - \Delta V_{Rd} \tag{9.36}$$

and introducing the values of V_{id} and ΔV_{Rd} from Equations 9.30 and 9.35, we get expression 9.33.

6. *Detailing of slender ductile walls for local ductility*
In addition to the rules for DCM buildings presented in Paragraph 9.2.4.2.3, EC8-1/2004 specifies some additional rules for DCH buildings, the most important of which are given below:
Within the boundary elements in the critical region a minimum value of ω_{wd} equal to

$$\omega_{wd\,min} = 0.12 \tag{9.37}$$

is specified.

At the same time, for the confining reinforcement of the boundary elements, that is, the hoop bar diameters, their spacing, and the distance between consecutive

longitudinal bars restrained by hoops, the rules specified for the base critical region of columns of DCH buildings are also specified in the case of DCH slender structural walls.

a. The critical region is extended for one more storey than the critical region for DCM buildings, but only with half of the confining reinforcement.

b. A minimum amount of web reinforcement:

$$\rho_{1,min} = \rho_{v,min} = 0.002$$ (9.38)

is specified to prevent premature web shear cracking. This reinforcement is provided in the form of two grids of bars, one in each face of the wall. The grids should be connected through cross-ties spaced at about 500 mm. Web reinforcement should have a diameter of those shown in Figures 9.15 and 9.16.

$$8.0 \text{ mm} \leq d_{web} \leq b_{wo}/8$$ (9.39)

and should be spaced at not more than 250 mm or 25 times the diameter of the bar, whichever is smaller.

c. For the protection of horizontal construction joints out of the critical region against cracking, a minimum amount of fully anchored vertical reinforcement should be provided across such joints.

   The minimum ratio of this reinforcement ρ_{min} is given by the expression:

$$\rho_{min} \geq \begin{cases} \left(1.3 \cdot f_{ctd} - \dfrac{N_{Ed}}{A_{sw}}\right) / \left(f_{yd}\left(1 + 1.5\sqrt{f_{cd}/f_{yd}}\right)\right) \\ 0.0025 \end{cases}$$ (9.40)

where

   A_{sw} is the total horizontal cross-sectional area of the wall and
   N_{Ed} is the design axial load of the seismic load combinations
   (N is considered positive when it is compressive)

9.3 DUCTILE COUPLED WALLS

9.3.1 General

- As was presented in Paragraphs 4.5.2.3 and 4.6.3.3, ductile coupled walls result when slender ductile walls are coupled with spandrels arranged at the level of the storeys above doors or windows. Moment diagrams of these systems are depicted in Figure 4.22.
- The main characteristic of these diagrams is that the fixed-end moment at the base of each of the coupled walls is smaller than half of the fixed-end moment that would be developed in the case that the stiffness of the spandrels was zero. This reduction of the fixed-end moment at the base is attributable to the function of the spandrels. This function has been explained in detail in Paragraph 4.5.2.3.
- The analysis of coupled walls has passed through three stages related to the development of computers. In the late 1960 s, the method of a continuous connecting medium was used, known also as 'laminar analysis', Figure 9.27 (Rosman, 1965; Penelis, 1969). Frame models were introduced in the early 1980s (see Subsection 4.5.2; Figure 4.25),
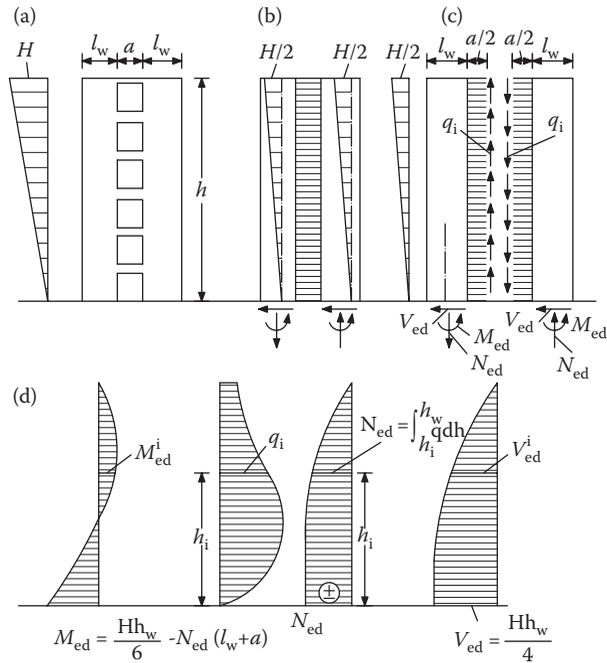
Figure 9.27 Structural behaviour of coupled walls: (a) structural system; (b) laminar analysis; (c) internal forces at the laminated spandrels; (d) diagrams of internal forces.

since their high redundancy could be dealt with by commercial computer platforms. Today, FEM discretisation is in favour, as it also may be used for any type of wall. Of course, this discretisation is supported by post-processing procedures for integration of resulting stresses to internal forces M_{Ed}, N_{Ed}, V_{Ed}, as we will see later (Subsection 9.6.1).

9.3.2 Inelastic behaviour of coupled walls

Apart from the analytical procedure for the determination of internal forces based on linear elastic procedure, it should be noted again (see Paragraph 4.6.3.3) that the yield of spandrels under horizontal loading precedes the yield at the base of the walls. In fact, from analytical investigations and experimental evidence, the following conclusions have been drawn (Park and Paulay, 1975; Aristizabal-Ochoa, 1982; Shiu et al., 1984):

- Ductility demand of the spandrels in terms of rotations $\theta\rho/\theta_y$ reaches a value of about 3.5, while the coupled walls continue to be in elastic range.
- For a ductility demand of the walls at their base on the order of 4, the ductility demand of spandrels reaches a value of about 11. Therefore, special concern is needed for ensuring high-ductility capacities for the spandrels (Figure 9.28, position 1).
- Keeping in mind that the seismic horizontal loading is counterbalanced by fixed-end moments combined with axial loads of opposite sign, it is apparent that in every half-loading cycle one of the walls is subjected to considerable tension in addition to flexure and shear. This load condition may adversely affect the diagonal tension capacity of the wall (Figure 9.28, position 2).
- Sliding of the walls at their base also constitutes an eventual failure mechanism (Figure 9.28, position 3).
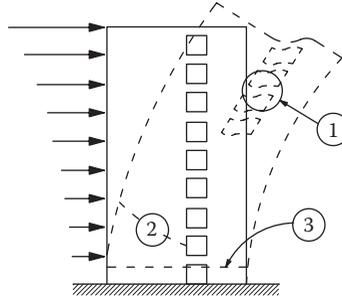
Figure 9.28 Critical areas of behaviour in coupled shear walls. (Adapted from Park, R. and Paulay, T. 1975. *Reinforced Concrete Structures*. J. Wiley & Sons, New York.)

- From all of the above it can be seen that if the ductility of the spandrels is ensured and no preemptive shear failure appears at their web, coupled ductile walls provide an effective ductile system with an additional first line of defense at the spandrels against seismic action. In this respect, spandrels act like fuses (Abrams, 1991). For this reason EC8-1/2004 classifies coupled walls in a higher 'behaviour' category than that for isolated (single) slender ductile walls (see Subsection 5.4.3). A basic condition for the characterisation of two or more ductile walls connected with beams is that their fixed-end moments are reduced by at least 25%, due to their coupling in relation to the fixed-end moments of the individual walls (see Paragraph 4.5.2.3, Figure 4.22).
- It has been verified by extensive experimental evidence that spandrels reinforced with x-shaped reinforcement (Figure 9.29) well-anchored in the walls exhibit a very high ductility in relation to spandrels reinforced conventionally (steel bars at the upper and bottom flanges and web reinforcement in the form of ties; Park and Paulay, 1975).

  This type of reinforcement has also been adopted by the Code for DCH beams in the case of shear reversals (see Subsection 8.2.4). Even in the case of squat columns where axial load prevails, this type of reinforcing has been introduced as an alternative solution (Tegos and Penelis, 1988). For this reason, x-shaped reinforcing bars arranged in the form of hidden inclined columns in the spandrel to avoid buckling have been adopted by all modern Seismic Codes.

  Contribution to shear resistance V_{Rdx} of x-shaped reinforcement is given by the following expression:

$$\boxed{V_{Rdx} = 2 \cdot A_{si} \cdot f_{yd} \cdot \sin\alpha} \tag{9.41}$$
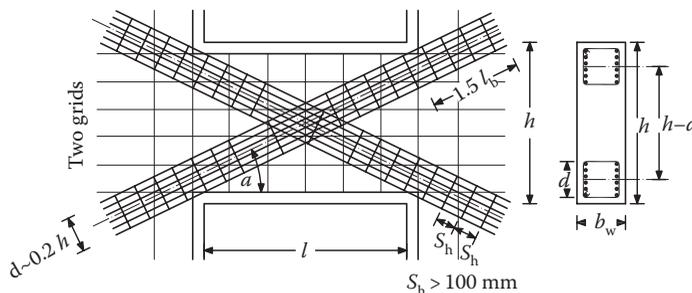
Figure 9.29 Arrangement of reinforcement in a coupling beam.

where

V_{Rdx} is the shear resistance in terms of design
A_{si} is the total area of steel bars in each diagonal direction
α is the angle between the diagonal bars and the axis of the beam

On the other hand, the contribution M_{Rdx} to moment resistance of the spandrel due to the x-shaped steel reinforcement is given by the expression:

$$\boxed{M_{Rdx} \cong (h - d) \cdot A_{si} \cdot f_{yd} \cdot \cos\alpha} \tag{9.42}$$

The notation in use in the above expressions is given in Figure 9.29.

As far as the coupled walls are concerned, two issues arise:

- The high tensile force at the base of the walls and its influence on their shear strength. From existing experimental evidence (Santhakumar, 1974; Park and Paulay, 1975; Abrams, 1991) it has been concluded that the shear design foreseen by modern Codes for slender ductile walls also provides adequate shear resistance for coupled walls.
- Design to flexure at the critical regions of the walls should take into account the sign of the axial force in relation to the sign of the corresponding moment (Figure 9.27c). This sign combination results in stronger reinforcement at the external flanges of the coupled walls than the internal ones. In the case that the analysis has been carried out using modal response spectrum analysis, this discrimination cannot be made easily, since all results have a positive sign.

9.3.3 Code provisions for coupled slender ductile walls

As was already noted, two or more walls are considered *coupled* if the connecting beams reduce the fixed-end moments of the individual walls by at least 25%. Therefore, coupling of walls by means of slabs must not be taken into account, as it is not effective.

Rules in use for ductile beams of DCH may also apply for spandrels, only in the case that *at least one* of the following conditions is fulfilled:

- Cracking in both diagonal directions is unlikely, to occur, if:

$$\boxed{V_{Ed} \leq f_{ctd} \cdot b_w (h - d)} \tag{9.43}$$

- A prevailing flexural mode of failure is ensured. An acceptable rule is

$$\boxed{l/h \geq 3.0} \tag{9.44}$$

- If neither of the above conditions is fulfilled, the resistance to seismic actions should be provided by reinforcement arranged along both diagonals of the beam (Figure 9.29).

In this case:

$$\boxed{V_{Ed} \leq 2 \cdot A_{si} \cdot f_{yd} \cdot \sin\alpha} \tag{9.45}$$

$$\boxed{M_{Ed} \leq (h - d) \cdot A_{si} \cdot f_{yd} \cdot \cos\alpha} \tag{9.46}$$

(see Subsection 9.3.2, Equations 9.41 and 9.42)

where

$$V_{Ed} = 2 M_{Ed}/l \tag{9.47}$$

- The diagonal reinforcement is arranged in column-like elements with side lengths equal at least to $0.50 \cdot b_w$, its anchorage length greater by 50% than that required by the Code for conventional R/C structures. The hoops of these elements should fulfil the provisions for the critical region of columns in DCH buildings, to prevent buckling.
- Longitudinal and transverse reinforcement is provided on both lateral faces of the spandrel according to the Code for conventional R/C structures and particularly for deep beams. The longitudinal reinforcement should not be anchored in the coupled walls and should extend into them by 150 mm, so that a change in the structural behaviour of the spandrel can be avoided.
- Slender ductile coupled walls are designed according to the rules for individual (single) walls and in accordance with their ductility class (M or H), since there is no difference in their behaviour under seismic loading in the post-elastic stage.

9.4 SQUAT DUCTILE WALLS

9.4.1 General

Squat ductile walls with a ratio of height h_w to length l_w of less than 2, that is,

$$\boxed{\alpha_s = \frac{h_w}{l_w} \le 2.0} \tag{9.48}$$

find a wide application in earthquake-resistant low-rise buildings. They are also used in high-rise buildings extending from their foundation to a number of lower storeys, contributing so significantly to the decreasing of stress and strain of the structural system extending to the whole height of the building.

As it was already noted in previous sections, squat walls are nearly two-dimensional (planar) structural elements. Therefore, the design for bending cannot be separated from the design to shear, as also happens in the case of squat columns, spandrels and so forth. However, due to low load effects that develop in squat walls for the seismic combination, as these walls are used mainly in low-size buildings, approximate simplified methods are used for their design.

The main problem of these elements is that after reaching their shear-dependent flexural capacity, as in the case of short columns (see Subsection 8.3.6), they fail in shear at relatively low values of the chord rotation θ_ρ and, therefore, their available ductility $\mu_{\theta,avall}$ in terms of rotations is limited. This is the reason why EC8-1/2004 (see Subsection 5.4.3, Equation 5.7b) introduces for the determination of the q-factor a reduction factor κ_w equal to

$$\boxed{0.5 \le \kappa_w = (1 + \alpha_o)/3 \le 1} \tag{9.49}$$

for *wall* or *wall-equivalent* systems,

where
  α_o is the prevailing aspect ratio of the walls of the structural system.
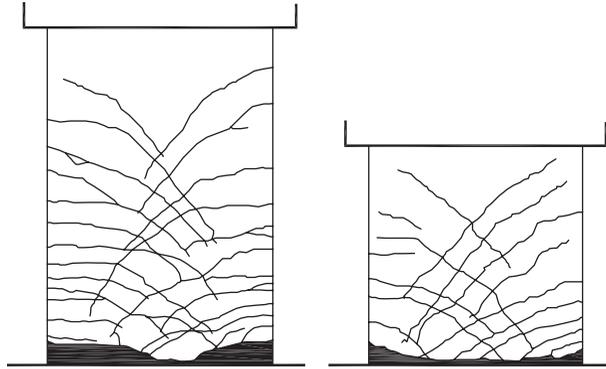
Figure 9.30 Crack patterns for Specimens MSW1 and LSW3 at the end of the experiment. (From Salonikios, T. 2007. Analytical prediction of the inelastic response of R/C walls with low aspect ratio. *ASCE Journal of Structural Engineering*, 133(6), 844–854. With permission of ASCE.)
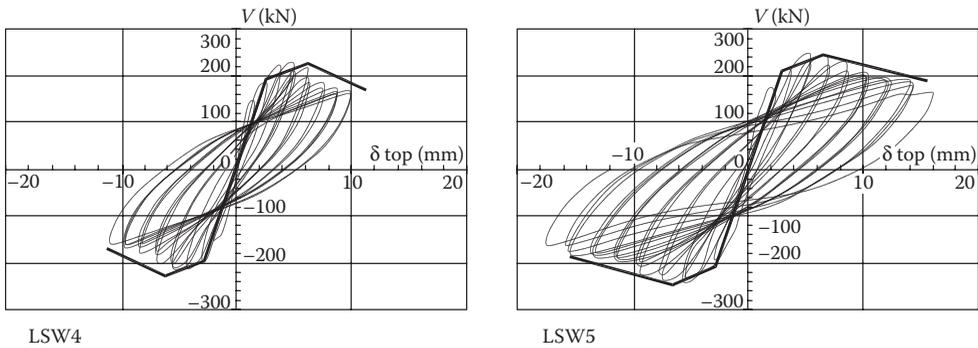
Figure 9.31 Comparative diagrams of the recorded hysteresis loops and the analytically calculated envelope curve, for Specimens LSW4 and LSW5. (From Salonikios, T. 2007. Analytical prediction of the inelastic response of R/C walls with low aspect ratio. *ASCE Journal of Structural Engineering*, 133(6), 844–854. With permission of ASCE.)

For example, for $\alpha_o = 2.0, \kappa_w = 1.0$, while for $\alpha_o = 1.0, \kappa_w = 0.66$, that is, a decrease of ductility demand of 33%.

However, from extensive experimental research it has been concluded (Salonikios et al., 2000; Salonikios, 2007) that the ductility of properly designed squat ductile walls μ_θ in terms of rotation is rather high and may range from 5.0 to 7.0 (Figures 9.30 and 9.31).

9.4.2 Flexural response and reinforcement distribution

- Although Bernoulli's concept (linear strain distribution) is significantly violated in the case of short walls due to the strong interaction of normal and shear strains, the design in bending with axial force may be carried out as in the case of slender members (beams, columns, walls), since at ULS most of the steel reinforcement bars are at yield stage and therefore the strain distribution is insignificant. Therefore, the standard procedure used in the case of slender walls for bending may also be used for squat walls. The flexural strength at the base of the wall must be carefully evaluated, taking the contribution of all vertical bars into account, so that a realistic value of shear load effect resulting from the capacity design procedure can be derived (see Subsection 6.1.6).

The same process also holds for the analytical determination of ductility factors in terms of curvature (Paragraph 9.2.2.4; Equation 9.9), although here the results usually depart more from experimental results.

- Various authors have adopted the view that evenly distributed vertical reinforcement at the base is preferable (Paulay and Priestley, 1992), because it results in an increased flexural compression zone and, therefore, in better conditions for inhibiting shear sliding, improving friction and dowel resistance.

However, Codes of Practice (EC8-1/2004 and ACI318M-2011) do not make any discrimination between slender and squat ductile walls. Therefore, the concept of strengthening their flanges *with confined boundary elements* in critical regions holds in practice also for squat ductile walls. In this regard, bending strength and ductility are mainly ensured by the flange chords, while shear resistance is ensured by the web.

9.4.3 Shear resistance

Shear failure modes of squat ductile walls are similar to those of slender ones, that is:

- Diagonal tension failure (Figure 9.11a)
- Diagonal compression failure (Figure 9.11b)
- Sliding shear failure (Figure 9.11c)

Keeping in mind that the normalised axial forces in squat ductile walls are usually very low (<0.20), their behaviour to shear is closer to the shear behaviour of spandrels.

9.4.4 Code provisions for squat ductile walls

Rules for DCM and DCH buildings will be presented together, as the differences of squat walls from slender ones are not significant.

It should also be noted that for the design of squat walls of DCL buildings, Code specifications for conventional R/C structures are applied (EC2-1-1/2004), except for requirements for concrete and steel reinforcement qualities, as in the case of slender walls.

- *Geometrical constraints*
  These are the same as those of slender walls (i.e. 9.2.4.2(1), 3(1)).
- *Bending resistance*
  As was already explained in Subsection 9.4.2, the rules in force for a slender wall hold also for squat walls.
- *Detailing for local ductility*
  Rules presented in previous paragraphs for slender walls are also in effect in the case of squat walls.
- *Shear resistance*

It should be recalled (Subsection 6.1.6) that capacity design rules for shear of squat walls require:

- For DCM buildings:

$$\boxed{V_{\text{Ed}} = 1.50\, V'_{\text{Ed}}} \tag{9.50}$$

where
  V'_{Ed} is the analysis load effect for shear force.

- For DCH buildings:

$$V_{Ed} = \gamma_{Rd}\left(\frac{M_{Rd}}{M_{Ed}}\right)V'_{Ed} \le qV_{Ed} \qquad (9.51)$$

(see Paragraph 6.1.6.1; Equation 6.23)
- From the above Equation 9.51 it can be seen that in the case of DCH buildings special care should be taken that flexural resistance M_{rd} is kept near M_{Ed}, otherwise high over-strength in bending would also lead to shear over-strength.
- Shear resistance for DCM buildings is computed in accordance with EC2-1-1/2004, that is, as in the case of conventional R/C buildings.
- Shear resistance for DCH buildings should be computed in accordance with the following rules:
  - Design for *diagonal compression failure* of the web due to shear should be carried out as in the case of slender ductile walls (Paragraph 9.2.4.3(3)).
  - Design for *diagonal tension failure* of the web due to shear should be carried out as follows:
    - Horizontal web bars should satisfy the expression:

$$V_{Ed} \le V_{Rd,c} + 0.75\rho_h \cdot f_{yd,h} \cdot b_{wo}\alpha_s l_w \qquad (9.52)$$

where
ρ_h is the reinforcement ratio of horizontal web bars ($\rho_h = A_h/(b_{wo} \cdot s_h)$)
s_h is the distance between successive horizontal web bars
b_{wo} is the web width
$f_{yd,h}$ is the design yield strength of the horizontal reinforcement
$V_{Rd,c}$ is the design shear resistance for members without shear reinforcement (see Subsection 8.2.4)

The above Equation 9.52 is in accordance with the concept for diagonal tension design followed by EC2-1-1/2004 for beams with an aspect ratio lower than 2 and by the American Code of Practice ACI M318-2011. Shear resistance of the horizontal reinforcement is based on the diagonal tension failure mode (Figure 9.32), where the strut inclination according to experimental evidence is defined by the corner-to-corner diagonal of the wall ($h_w = \alpha_s l_w$), and on the free-body equilibrium depicted in Figure 9.32. The coefficient 0.75 is introduced in accordance with EC2-1-1/2004 for beams with a short aspect ratio ≤ 2.0, where only the central 75% of the web reinforcement intersecting the inclined crack should be taken into account. In the critical region of the wall, $V_{Rd,c}$ should be taken *as zero* if the axial force N_{Ed} *is tensile*.

$$\rho_h = \frac{A_{sh}}{b_{wo}}h_w$$

$$V_{Rd} = 0.75 \; A_{sh}' f_{ydh}$$

$$= 0.75 \; \rho_h f_{ydh} \cdot b_{wo} \cdot \alpha_s l_w$$

$$\alpha_s = \frac{h_w}{l_w}$$
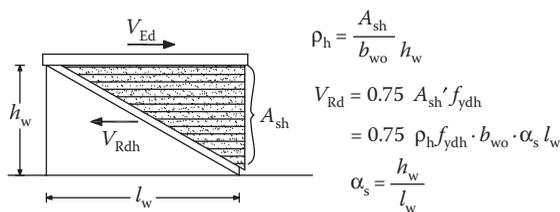
Figure 9.32 Diagonal tension failure mode on squat walls.

– Vertical web bars should be provided to satisfy the condition:

$$\boxed{\rho_h \cdot f_{yd,h} \cdot b_{wo}z \leq \rho_v \cdot f_{yd,v} \cdot b_{wo}z + \min N_{Ed}}$$ (9.53)

where

ρ_v is the reinforcement ratio of vertical web bars ($\rho_v = A_v/b_{wo} \cdot s_v$)
$f_{yd,v}$ is the design yield strength of the vertical web reinforcement
$z \cong 0.8\, l_w$
N_{Ed} is positive when compressive

The above expression (9.53) results from the condition that the distributed vertical reinforcement force $\rho_v f_{yd}$, together with the distributed axial force $v_{Ed} \leq 0.40 = N_{Ed}/b_{wo}z$ composed with the horizontal $\rho_h f_{yd}$, should give a resultant with an angle of 45° (compressive strut inclination). This condition does not comply with the assumption of the corner-to-corner diagonal compressive strut inclination adopted in the previous paragraph for the determination of ρ_h (Equation 9.52). If the assumption of corner-to-corner diagonal strut were adopted, the above expression (9.53) would take the form:

$$\rho_h \cdot f_{yd,h} \cdot b_{wo}z\alpha_s^2 \leq \rho_v \cdot f_{yd,v} \cdot b_{wo}z + \min N_{Ed}$$ (9.54)

The above design procedure, which refers mainly to squat walls, according to EC8-1/2004, should also be applied to slender DCH walls in the case that the ratio $\mathbf{M_{Ed}/V_{Ed} \times l_w}$ at the base of a storey (shear span ratio) is lower than 2 (see 9.2.4.3(4)).

• *Sliding shear failure*
Design for sliding shear failure at a base of the squat wall should be carried out in accordance with the procedure developed previously in Paragraph 9.2.4.3(5), Equation 9.27 of this chapter. In the case of squat walls, half of the design base shear VEd should be carried by the contribution of diagonally arranged reinforcement, that is:

$$\boxed{\frac{V_{Ed}}{2} \leq V_{id}}$$ (9.55)

At higher levels, V_{id} should be greater than only 25% of V_{Ed}.

9.5 LARGE LIGHTLY REINFORCED WALLS

9.5.1 General

This type of R/C structural system has already been defined in Chapter 4.4. Its capacity design has been presented in Subsection 6.1.7, while the corresponding behaviour factors and their justification have been outlined in Subsection 5.4.3. In this subsection the design of these walls will be presented and discussed in detail.

First, a short overview will be made of the main structural characteristics and seismic behaviour of these structural systems.

• The main structural system consists of large R/C walls, which carry a large part of the gravity loads and the seismic action as well, while the fundamental period T_1 of the building, assuming fixed walls at the foundations, is less than 0.5 s.
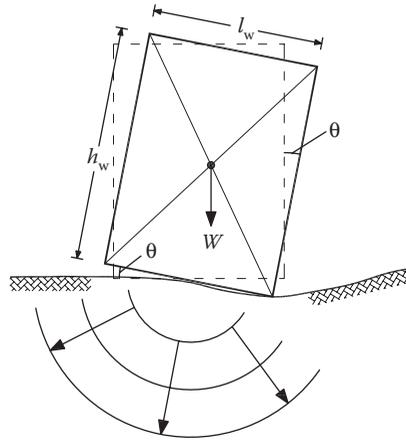
Figure 9.33 Rocking of large, lightly reinforced walls.

- The energy dissipation mechanism of these buildings is not based on the formation of plastic hinges at the base of the walls, since this is not feasible due to the large length of the cross-sections of the walls. Instead of a 'plastic hinge' dissipating mechanism, an 'uplift' mechanism of the walls from the soil or through opening and closing of horizontal cracks (Figure 9.33) is anticipated. In fact, such a wall is expected to transform seismic energy to potential energy through temporary uplift of structural masses and then to kinetic energy dissipated in the soil or in the flexural cracks through rigid body 'rocking'. In this respect the dissipation zone is not concentrated at a plastic hinge in a critical zone at the base of the wall, but it is distributed to the soil joint and a number of flexural cracks over the entire height of the building.
- So, although this dissipation mechanism is not quantitatively controlled and justified as in the case of all other structural systems in effect, EC8-1/2004 has also adopted this type of structure, *but only for DCM buildings*. Additionally, it should be noted that, due to its low construction cost, this type of structural system is very popular in southern France and has been implemented for many years with very good results in response to seismic actions. So, the design rules used in these buildings thus far have also been mostly adopted by EC8-1/2004.
- The basic design concept includes the following principles:
  - Design to bending is carried out using the moment diagram directly from the analysis, without any capacity design envelope, in contrast to all other types of wall systems. This moment diagram is combined with the gravity axial load fluctuating between $(1 \pm 0.5)N_{Ed}$ in order for the dynamic vibrating masses in the vertical direction to be taken into account.
  - Design for shear is carried out for increased shear forces (see Subsection 6.1.7) in order to ensure that flexural failure precedes shear failure.

9.5.2 Design to bending with axial force

- The ULS in bending with axial force should be verified, assuming:
  - Horizontal cracking
  - Plane strain distribution

no matter what the aspect ratio h_w/l_w. Therefore, the design for bending is carried out in accordance with the relevant provisions of EN 1992-1-1/2004.

- Due to the small thickness of the wall in relation to its other two dimensions, normal stresses in concrete should be limited to prevent out-of-plane buckling. This requirement is satisfied if the rules of EN 1992-1-1/2004 for second-order effects are satisfied. These rules are stated in:
  - Paragraph 12.6.5.2/EC2-1-1/2004: the simplified design method for walls and columns of plain or lightly reinforced structures.
  - Paragraph 5.9 (Equation 5.40b)/EC2-1-1/2004: the lateral instability of slender beams.
- In case that the dynamic axial force $(1 \pm 0.5)N_{Ed}$ must be taken into account, the limiting strain ε_{cu2} for concrete may be increased to:

$$\boxed{\varepsilon_{cu2} = 0.005} \tag{9.56}$$

This increase allows a higher efficiency of the concrete compression zone and therefore diminishes the cases where steel in tension zones does not yield at ULS.

9.5.3 Design to shear

Due to the high safety margin for shear imposed by the capacity design rules (Chapter 6.1.7), the following requirements are specified by EC 8-1/2004:

- If

$$\boxed{V_{Ed} \leq V_{Rdc}} \tag{9.57}$$

the rules for minimum web reinforcements $\rho_{w,min}$ foreseen in the Code for conventional R/C walls are not obligatory.

- If

$$\boxed{V_{Rdc} \leq V_{Ed}} \tag{9.58}$$

the web reinforcement should be calculated in accordance with EN 1992-1-1/2004 on the basis of the *variable inclination truss model* or *a strut-and-tie model,* whichever is most appropriate for the particular geometry of the wall. If a strut-and-tie model is used, the *width of the compressive strut should take into account* the presence of openings and should not exceed $0.25\ l_w$ or $4\ b_{wo}$, whichever is smaller (Figure 9.34).

The ULS against sliding shear at horizontal construction joints should be verified in accordance with EN 1992-1-1/2004 § 6.2.5, with 50% longer anchorage lengths.

9.5.4 Detailing for local ductility

- At the ends of the cross-sections of the walls, boundary elements should be formed, reinforced with vertical steel rebars combined with hoops and cross ties. These elements should have a length c in the direction of the long side of the cross-sections in the range of:

$$\boxed{\max \begin{Bmatrix} b_w \\ 3b_w\sigma_{cm}/f_{cd} \end{Bmatrix} < c} \tag{9.59}$$
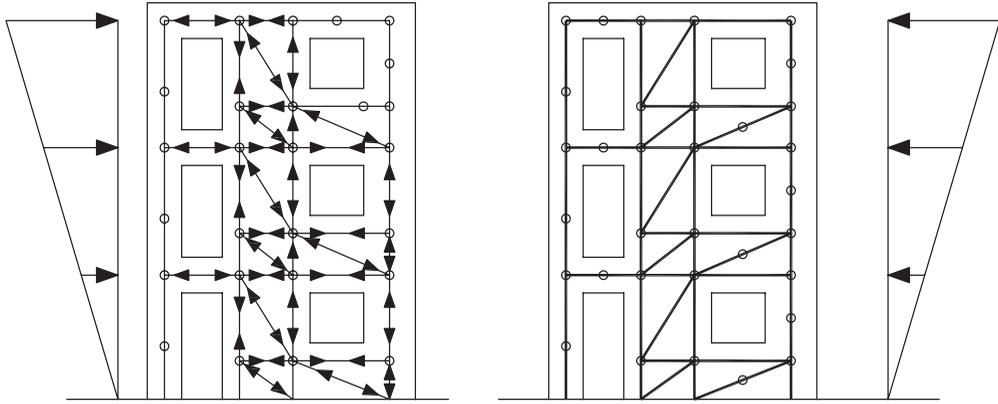
Figure 9.34 A strut-and-tie model for the shear design of a large, lightly reinforced wall.

where

σ_{cm} is the mean value of the concrete stress in the compression zone in the ULS of bending with axial force.

- The diameter of the vertical bars should *not be less than 12 mm* in the lower storey and upwards up to the storey where the length of the wall l_w is reduced by one third. From that storey on, the diameter of the vertical rebars may be reduced to 10 mm.
- The diameter of the hoops or cross-ties should *not be less than 6 mm* or one-third of the diameter of the vertical bars.
- In order for flexural failure to precede that of shear, the amount of vertical reinforcement should not exceed that which results from the design for bending with axial force at the successive storeys of the building.
- Continuous horizontal and vertical steel ties should be provided (Figure 9.35):
  - Along all intersections of walls or connections with flanges
  - At all floor levels
  - Around openings in the wall.

These ties should be designed in accordance with EN 1992-1-1/2004 9.10.

9.6 SPECIAL ISSUES IN THE DESIGN OF WALLS

9.6.1 Analysis and design using FEM procedure

From the presentation thus far it is apparent that walls, either have an orthogonal cross-section or a composite one (Γ T, I, Π, Z, etc.), and they are considered in concept for the
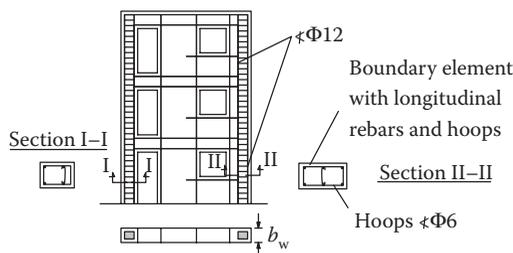
Figure 9.35 Reinforcement of a large, lightly reinforced wall.

analysis and design as linear members with an orthogonal or composite cross-section developing a planar distribution of strains under bending with axial force.

However, it is well known that most of the modern computer platforms (SAP 2000, ETABS, SCIA, etc.) allow the introduction the FEM procedure for planar members, which, of course, is not prohibited by modern Codes. In this respect, the modelling is of higher reliability than that of linear members. At the same time, modelling can proceed directly from the formwork drawings elaborated already in an Autocad or a similar platform.

Therefore, the outputs of the analysis are normal and shear-distributed forces in the middle plane of the walls combined with distributed bending moments, torsional moments and shears corresponding to their parallel behaviour *as plates* under bending. Together these two types of action constitute the *shell* function, as is well known from structural engineering (Figure 9.36).

This force pattern is proper for the design of steel walls or cores, but it is improper for the design of R/C walls for the following reasons:

1. The design of R/C members is based on the assumption of cracked tensile zones. So, the steel rebars under tension are arranged mainly at the extreme tensile chord of a cross-section under consideration. As a result, the lever arm of the internal forces in the case of bending with axial force takes its maximum value and, therefore, the required reinforcement is minimised.

   Conversely, in the case that the internal normal tensile forces are covered by distributed reinforcement, as in the case of shell design due to the smaller internal lever arms, the amount of the required reinforcement would be much more than that resulting from conventional R/C design.

   For example, in case of a wall of orthogonal cross-section loaded in its main direction (Figure 9.37a) with a lateral load P, if it is analysed as a linear member, it will be subjected at its base to a bending moment $M_{Ed} = h_w P$. Therefore, the required reinforcement in the tensile zone will be derived from the following expressions (Figure 9.37b):

$$M_{Ed} \leq M_{Rd} = z \cdot T \quad \text{or} \quad T = \frac{M_{Ed}}{0.85 \, l_w} \qquad (9.60)$$
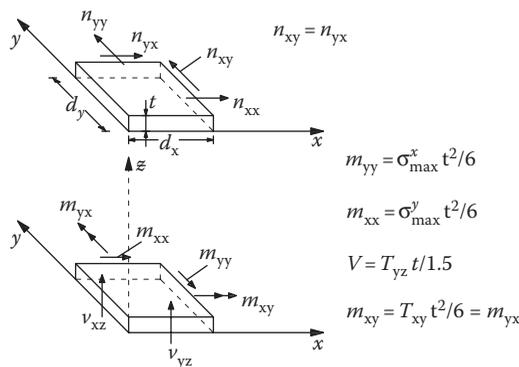
Figure 9.36 Notation for internal forces of a 'disk' and a 'shell'.
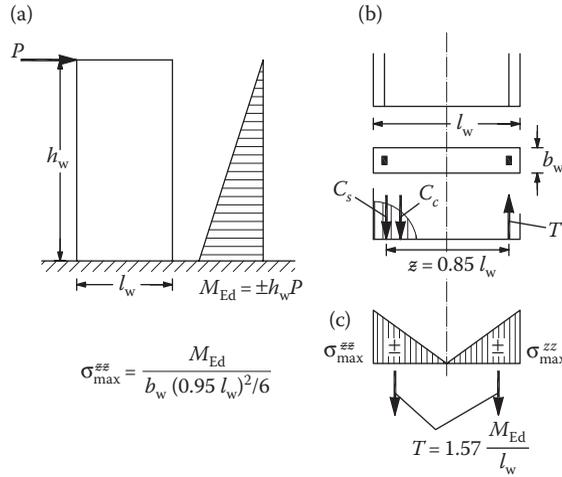
Figure 9.37 (a) Loading pattern of an orthogonal wall and bending moment diagram; (b) dimensioning of the wall as a linear member; (c) dimensioning of the wall using FEM method.

Therefore,

$$A_s = \frac{T}{f_{yd}} \cong \frac{M_{Ed}}{0.85 f_{yd} l_w} = \frac{1.18\, M_{Ed}}{f_{yd}\, l_w} \tag{9.61}$$

On the other hand, if this wall is analysed as a disc, the resulting axial stress distribution at its base is given in Figure 9.37c. Taking into account that the reinforcement is distributed in the tensile zone proportionally to the stress distribution, that is,

$$dA_s = \sigma_m b_w d_x / f_{yd} \tag{9.62}$$

and that

$$\sigma_{max}^{zz} = \frac{M_{Ed}}{b_w l_w^2 / 6} \tag{9.63}$$

It follows that

$$T = \frac{1}{2}\frac{l_w}{2} b_w \sigma_{max}^{zz} = \frac{1}{2}\frac{l_w}{2} b_w \frac{M_{Ed}}{b_w l_w^2 / 6} = 1.50 \frac{M_{Ed}}{l_w} \tag{9.64}$$

Therefore,

$$A_s = \frac{T}{f_{yd}} = \frac{1.50 M_{Ed}}{f_{yd} \cdot l_w} \tag{9.65}$$

Consecutively, 27% more reinforcement is required where dimensioning follows the procedure used in the case of shells.

2. The above calculated over-reinforcement *must be considered the minimum* that can result, and it refers to systems where the 'lateral force method' is implemented. In case of 'the modal response spectral analysis', the stress distribution is a value resulting

from the application the 'SRSS' or 'CQC' method. In this respect, this output does not correspond to any consistent state of stress of the structure, but represents the distribution of the most probable values of stresses during the seismic action. At the same time, as these stresses are the output of a square root, they are values of undefined sign and therefore might be tensile or compressive. So, in the usual case where axial load effects also act together with bending if it were decided to cover the whole diagram by reinforcement in tension, the resulting amount of reinforcement seems to be even 2.0 times more than the reinforcement that would result in the case of implementation of the 'lateral force method' or the 'time history linear dynamic analysis'.

In order to overcome the above difficulties, many computer platforms for the seismic analysis of concrete or masonry structures (SAP 2000, ETABS/2011, SCIA—ECtools), have incorporated a post-processor that proceeds for each eigenvalue (i) to the integration of the stresses corresponding to this eigenvalue to a group of M_{Ed}^i N_{Ed}^i V_{Ed}^i load effects. From these load effects of the successive eigenvalues, using the SRSS or CQC procedure, the most probable values of M_{Ed}, N_{Ed} and V_{Ed} are computed, for each cross section of course again with an undefined sign. This procedure is implemented at the walls of each storey and at eventual spandrels where 'piers' and 'spandrels' are generated accordingly. From this point on the design proceeds as in the case of linear members with a composite cross-section.

9.6.2 Warping of open composite wall sections

9.6.2.1 General

The conventional approach to the torsional effects on cross-sections of structural members is that they remain undeformed to their axial direction, and in this respect torsional loading is resisted only by shear stresses (torsion according to Saint-Venant theory). This is completely true only for members with a symmetric closed cross-section. It is well known from the technical theory of elasticity that when structural members with composite cross-sections that are also characterised as thin-walled sections are loaded by torsional external moments, they develop axial strains leading to warping of the cross-section (Figure 9.38). Therefore, when this warping is prohibited by boundary constraints it is reasonable for axial stresses to develop in addition to shear stresses due to torsion. Therefore, parallel to Saint-Venant uniform torsion, a *torsional bending* develops known as *torsion according to Vlasov theory* (Taranath, 2010).
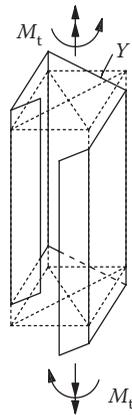
Figure 9.38 Warping of a thin-walled composite section under torsion.

This normal stress state *does not follow the assumption of plane distribution of stresses*, since it is the result of the prevention of the cross-section warping caused by the torsional moment. The resultants of these normal stresses are zero ($N_{Ed} = 0, M_{Ed} = 0$), since there is not such external loading on the structural member. This normal stress state changes along the axis of the structural member. Therefore, additional shear stresses are generated as the derivatives of normal stresses. Their sum over the section is also zero, but their torsional resistance contributes to the counterbalance of the external torsional moment together with the torsional resistance of the Saint-Venant shear stress state. In this respect, one part of the external torsional moment $T_{(z)}$ is resisted by the Saint-Venant shear $T_{v(z)}$ and the rest by the shear stresses due to warping behaviour (Vlasov stress state) $T_{w(z)}$, that is,

$$T_{(z)} = T_{v(z)} + T_{w(z)} \tag{9.66}$$

The scope of this book does not allow a detailed reference to the torsional theory of thin-walled cantilevers, since such an approach requires formation and integration of the relevant differential equations that relate the external loading torsional moment $T_{(z)}$ to the angle of twist $\theta_{(z)}$ and the geometrical and mechanical properties of the structural member and therefore the distribution of $T_{(z)}$ to $T_{v(z)}$ and $T_{w(z)}$.

However, it is useful to stay on this subject a little while longer for a thorough understanding of R/C wall behaviour. In fact, keeping in mind that R/C walls and cores in buildings usually constitute the main structural component resisting seismic action, and that analysis and design are carried out basically by means of computer-aided procedures, it is of paramount importance to know, at least qualitatively, the degree of approximation made by the conventional programming platforms and the way these results could be improved using post-processing procedures by hand or computationally so that the warping issue may be dealt with.

9.6.2.2 Saint-Venant uniform torsion

First, it is important to recall the torsional behaviour of cantilevers with circular, orthogonal and closed thin-wall cross-sections (Figure 9.39a). According to Saint-Venant theory, the total angle of twist θ for a length z measured from the base of a cantilever is given by the expression (Anastasiadis, 1989; Taranath, 2010):
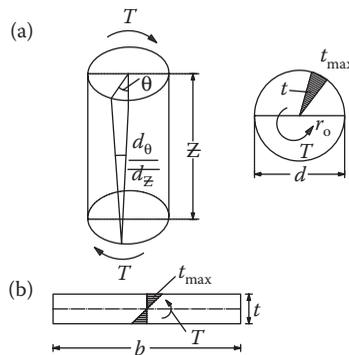
Figure 9.39 Torsion according to Saint-Venant theory (Zero axial strain of the cross-sections): (a) notation for uniform torsion, and ⊠ distribution for circular cross section; (b) ⊠ distribution for orthogonal cross section.

$$\theta_{(z)} = \frac{T}{GJ_p} z$$

(9.67)

or

$$\frac{d\theta}{dz} = \frac{T}{GJ_p} \quad \text{and} \quad T = GJ_p \frac{d\theta}{dz}$$

(9.68)

where

T is the twisting moment

z is the ordinate on the cantilever wherein to which twist $\theta_{(z)}$ is referred

G is the shear modulus of elasticity

J_ρ is the polar moment of inertia of the symmetric section (Figure 9.39a, b)

$$J_{pc} = \frac{\pi d^4}{32} = \frac{\pi r_o^4}{2} \quad \text{(circular cross section)}$$

(9.69a)

$$J_{po} = \frac{bt^3}{3} \quad \text{(long orthogonal cross section)}$$

(9.69b)

On the other hand, the maximum shear stress due to twisting moment is given by the expression:

$$\tau_{max} = \frac{T r_o}{J_{pc}} \quad \text{(for circular cross section)}$$

(9.70a)

$$\tau_{max} = \frac{2T b}{J_{po}} \quad \text{(for orthogonal cross section)}$$

(9.70b)

where

r_o is the radius of the circular cross-section

b, t are the dimensions of the orthogonal cross-section

In the case of a closed thin-wall cross-section, the shear stress (τ) developing in the wall of the cross-section is given by the expression (Figure 9.40):

$$\tau = \frac{T}{2A_c \cdot t}$$

(9.71)

(1st Bredt's formula)

where

t is the thickness of the wall

A_c is the area enclosed by the central line of the cross-section

At the same time, the angle of twist θ for a cantilever at a height z from the base is given by the expression:

$$\theta = \frac{T}{GJ_{ph}} z$$

(9.72)
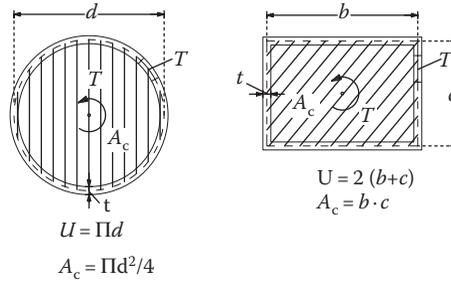
Figure 9.40 Torsional behaviour of members with symmetric tubular cross-section.

or

$$\boxed{\frac{d\theta}{dz} = \frac{T}{G J_{ph}} \quad \text{or} \quad T = G J_{ph} \frac{d\theta}{dz}}$$

(9.73)

(2st Bredt's formula)

where

$$J_{ph} = \frac{4 A_c^2}{U}$$

(9.74)

U is the perimeter of the cross-section

The above equations are based on the following assumptions:

1. Plane cross-sections in the undeformed state remain plane when torque is applied.
2. Cross-sections remain undistorted in their own plane.

The first assumption is true for *circular sections, orthogonal sections,* and *tubular sections.* As was already mentioned above, this approach to the problem is known as Saint-Venant's or *uniform torsion.* When the structural member is an open thin-walled structure, the above first assumption no longer remains true. This type of torsion is known as *warping torsion*, or as *constrained torsion* or *torsion bending.*

Being acquainted with the uniform torsion from their first contact with the classic strength of materials, designers generally encounter difficulties either with the concept of warping behaviour or with the methods of analysis and design referring to warping. Therefore, the task here is to introduce the concept of warping torsion and to give methods for taking into account the additional state of stress generated, or to ignore it in a justified way.

9.6.2.3 Concept of warping behaviour

We will try to describe the warping torsion on an I-shaped shear wall with unequal flanges as depicted in Figures 9.41 and 9.42 (Taranath, 2010). If the influence of the web is neglected, the centre of gravity (CG) of the cross-section may be estimated with a close approximation by the relations:

$$\bar{y}_1 = \frac{A_2 L}{A_1 + A_2} \quad \text{and} \quad \bar{y}_2 = \frac{A_1 L}{A_1 + A_2}$$

(9.75a,b)
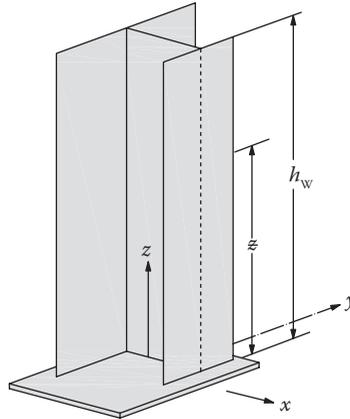
Figure 9.41 H-section core. (Adapted from Taranath, B.S. 2010. *Reinforced Concrete Design of Tall Buildings*, CRC Press (Taylor & Francis Group).)
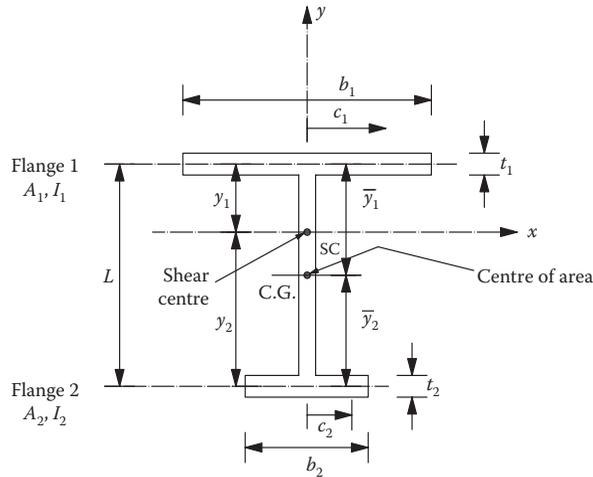
Figure 9.42 Core properties. (Adapted from Taranath, B.S. 2010. *Reinforced Concrete Design of Tall Buildings*, CRC Press (Taylor & Francis Group).)

It is well known that a horizontal load at the top of a cantilever with height h_w acting parallel to the flanges and passing through the CG of the cross-section generates normal stresses at the base, accomplishing the plane stress distribution concept of Navier, given by the expression:

$$\sigma_x = \frac{M}{J_y}x = \frac{P h_w}{J_y}x \tag{9.76}$$

At the same time, the internal shear force V_x equal to P results in shear stresses at the flanges, given by the expression (Figure 9.43):

$$\tau = \frac{V_x S_{yi}}{J_y t_i} \tag{9.77}$$

$$S_{yi} = \left(\frac{b_1}{2} - c_1\right)t_1\left(\frac{b_1}{2} + c_1\right)/2$$

$$= \left(\frac{b_1^2}{4} - b_1^2\right)t_1/2$$
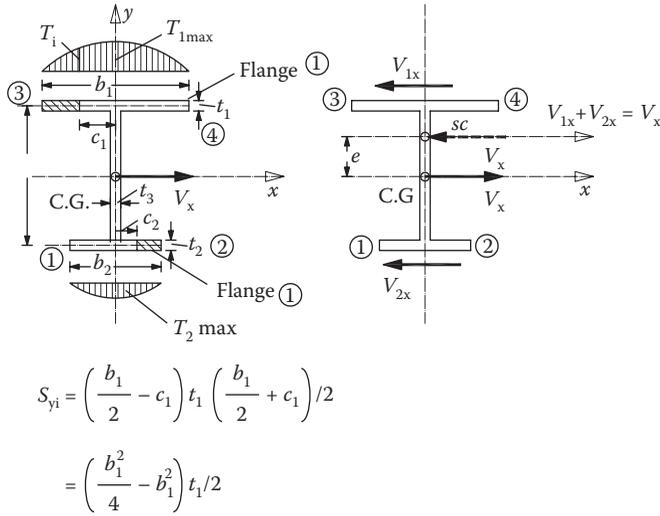
Figure 9.43 Shear diagrams due to V_X. The meaning of shear centre SC.

where

   S_{yi} is the static moment on the part of the cross-section to the left of point (i) in relation to the y–y axis (Figure 9.43)
   t_i is the thickness of the section at the point of reference (i)
   J_y is the moment of inertia of the cross-sections in relation to the y–y axis

The resultants of these stresses V_1 and V_2 of the flanges satisfy the expression:

$$V_x = V_{1x} + V_{2x} \tag{9.78}$$

and they are equal to

$$V_1 = \frac{J_1}{J_1 + J_2}V \tag{9.79}$$

$$V_2 = \frac{J_2}{J_1 + J_2}V \tag{9.80}$$

In fact, taking into account that:

$$\tau_{1max} = \frac{(b_1/2)\cdot(b_1/4)t_1}{J_y t_1}V_x = \frac{b_1^2}{8J_y}V_x \tag{9.81a}$$

$$\tau_{2max} = \frac{(b_2/2)\cdot(b_2/4)t_1}{J_y t_2}V_x = \frac{b_2^2}{8J_y}V_x \tag{9.81b}$$

It is concluded that V_{1x} and V_{2x} have the following values:

$$V_{1x} = \frac{2}{3}\tau_{1max}t_1b_1 = \frac{b_1^3 t}{12J_y}V_x \tag{9.82a}$$

$$V_{2x} = \frac{2}{3}\tau_{2\max}t_2 b_2 = \frac{b_2^3 t}{12 J_y} V_x \qquad (9.82b)$$

or

$$V_{1x} = \frac{J_1}{J_y} V_x, \quad V_{2x} = \frac{J_2}{J_y} V_x \qquad (9.83a,b)$$

The resultant of these internal forces passes through a point SC called the *shear centre* (SC), which is located at the position:

$$\bar{y}_{1s} = \frac{J_2}{J_1 + J_2} L \quad \text{and} \quad \bar{y}_{2s} = \frac{J_1}{J_1 + J_2} L \qquad (9.84a,b)$$

This means that in order for no torsional loading to exist, the horizontal load P should pass through the SC of the cross-section. Otherwise, the structural member is subjected to a twisting moment T about this centre, equal to

$$T = P \cdot e \qquad (9.85)$$

where
  e is the distance between GC and SC (Nitsiotas, 1960)

From the above equations (9.84a) and (9.84b) it may easily be concluded that in symmetric cross-sections the SC coincides with GC, and therefore for horizontal loading passing through the GC axis, no torsional effect is generated.

When a torque T is now applied at the top of the cantilever of Figure 9.44, this cantilever twists about the SC axis, causing the flanges to:

  1. Bend in opposite directions about the y–y (Figure 9.44a) axis
  2. Twist about their vertical axes (Figure 9.44b), passing through their own SC, which coincides with their GC, since their cross-section is orthogonal and therefore presents double symmetry

The effect of this flange bending, according to the Bernoulli assumption for planar distribution of strain, results in a rotation of the flange sections in an opposite direction and in this respect to a warping of the cross-section. Diagonally opposite corners 1 and 4 in Figure 9.44 displace downward, while 2 and 3 displace upward. All along the axis of the cantilever at every ordinate (z) the torque $T = T_{(z)}$ is resisted internally by a couple $T_{w(z)}$, resulting from the shears in the flanges related to their bending in plane, and a couple $T_{v(z)}$, resulting from the twisting of the flanges and the web according to Saint-Venant torsion (Equation 9.67).

The angle of twist $\theta_{(z)}$ of the cantilever about the SC axis at a height (z) from the base results in a horizontal displacement of flange (1) at this level equal to

$$u_{x1}(z) = \bar{y}_1 \theta(z) \qquad (9.86)$$
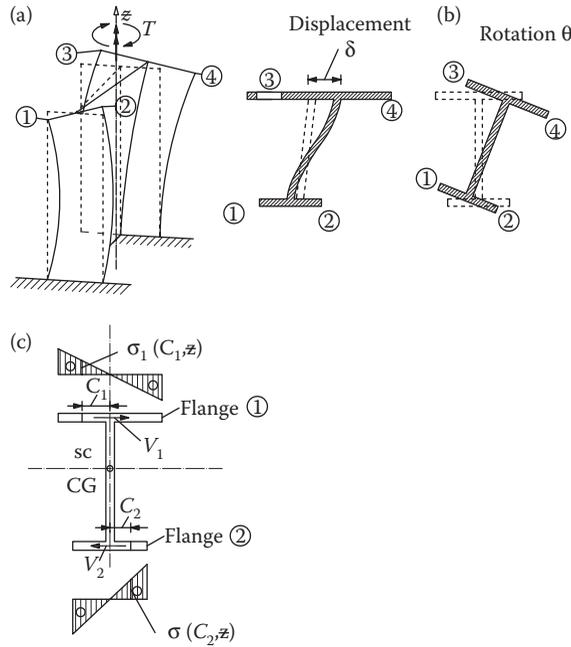
Figure 9.44 Combination of warping and uniform torsion; normal stresses due to warping: (a) the concept of warping; (b) displacements in-plane for bending in torsion; (c) normal stress distribution due to warping.

Therefore,

$$\frac{du_{x1}(z)}{dz} = \bar{y}_1 \frac{d\theta(z)}{dz} \tag{9.87}$$

$$\frac{d^2 u_{x1}(z)}{dz^2} = \bar{y}_1 \frac{d^2\theta(z)}{dz^2} \tag{9.88}$$

$$\frac{d^3 u_{x1}(z)}{dz^3} = \bar{y}_1 \frac{d^3\theta(z)}{dz^3} \tag{9.89}$$

Similar expressions are in effect for flange (2).
Shear related to the bending in flanges (1) and (2) may be expressed by the following equations:

$$V_1(z) = -EJ_1 \frac{d^3 u_{x1}(z)}{dz^3} = -EJ_1 \bar{y}_1 \frac{d^3\theta(z)}{dz^3} \tag{9.90}$$

$$V_2(z) = -EJ_2 \frac{d^3 u_{x2}(z)}{dz^3} = -EJ_2 \bar{y}_2 \frac{d^3\theta(z)}{dz^3} \tag{9.91}$$

The torsional moment of the above internal shear forces to the SC of the cross-section is the warping moment:

$$\boxed{T_{w(z)} = V_1 y_1 + V_2 y_2 = -(EJ_1 \bar{y}_1^2 + EJ_2 \bar{y}_2^2)\frac{d^3\theta(z)}{dz^3}} \tag{9.92}$$

or

$$T_{w(z)} = EJ_w \frac{d^3\theta(z)}{dz^3}$$ (9.93)

where

$$J_w = J_1\bar{y}_1^2 + J_2\bar{y}_2^2$$ (9.94)

Equation 9.94 is identical to Equation 2.87 of Chapter 2. From the development thus far, what becomes apparent is the close relationship between warping of composite open-wall sections and the torsional behaviour of a pseudospatial structure subjected to torsional action. In fact, in the second case, the main part of the external torsional loading is resisted by bending of the vertical structural elements and a smaller part by the torsional resistance of the vertical structural members. Therefore, the approach to the problem is identical to that of a pseudospatial structure, since the influence of the web of the I section has been neglected. Nevertheless, the following steps will allow the formulation of the warping differential equations in a comprehensible way. J_w, above, is a geometric property of the section similar to the moments of inertia J_1 and J_2 and is called the warping moment of inertia or warping constant.

This parameter expresses the capacity of the section to resist warping torsion, as J_1 and J_2 express the capacity of the section to resist bending moments. Neglecting the web and taking into account Equation 9.68, the torque resisted by the twisting of the cross-section according to Saint-Venant theory becomes

$$T_v(z) = GJ_p \frac{d\theta(z)}{dz}$$ (9.95)

where
 J_p is the polar moment of inertia of the section, that is:

$$J_p = \frac{b_1h_1^3}{3} + \frac{b_2h_2^3}{3}$$ (9.96)

The sum of $T_w(z)$ and $T_v(z)$ results in the external torque $T(z)$, that is,

$$-EJ_w \frac{d^3\theta(z)}{dz^3} + GJ_p \frac{d\theta(z)}{dz} = T(z)$$ (9.97)

The above differential equation (9.97) is the fundamental equation for restrained warping torsion and has been derived in a simplified inductive way, bypassing the technical theory of elasticity for torsion of open thin-wall members (Taranath, 2010). Of course, in the case of a cross-section of general form, the geometric parameter J_w cannot be expressed by Equation 9.94. Its general form will be given in the next paragraph. The integration of the above equation gives θ, and from Equations 9.93 and 9.95 $T_w(z)$ and $T_v(z)$ are determined.

The normal stresses in the flanges due to bending (Figure 9.44a, b, c) caused by V_1 and V_2 (warping action) are determined by the expression (see also Equation 9.76):

$$\sigma_1(c_1, z) = \frac{M_1(z)c_1}{J_1} \tag{9.98}$$

and

$$\sigma_2(c_2, z) = \frac{M_2(z)c_2}{J_2} \tag{9.99}$$

Keeping in mind that

$$V_1(z) = -V_2(z) = V(z) \tag{9.100}$$

and

$$M_1(z) = -M_2(z) = M(z) \tag{9.101}$$

Equation 9.98 takes the form

$$\sigma_1(c_1, z) = \frac{M(z)c_1}{J_1} \tag{9.102}$$

or

$$\sigma_1(c_1, z) = \frac{M(z)c_1}{(J_1\bar{y}_1^2 + J_2\bar{y}_2^2)} \frac{J_1\bar{y}_1^2 + J_2\bar{y}_2^2}{J_1} \tag{9.103}$$

$$\sigma_1(c_1, z) = \frac{M(z)c_1}{J_w}\left(\bar{y}_1^2 + \bar{y}_2^2 \frac{J_2}{J_1}\right) \tag{9.104}$$

Taking into account from Equations 9.84a and 9.84b that

$$\frac{J_1 + J_2}{L} = \frac{J_2}{\bar{y}_1} = \frac{J_1}{\bar{y}_2} \tag{9.105a}$$

or

$$\frac{J_2}{J_1} = \frac{\bar{y}_1}{\bar{y}_2} \tag{9.105b}$$

and introducing Equation 9.105b into Equation 9.104, the following expression is obtained:

$$\sigma_1(c_1, z) = \frac{M_{(z)}c_1}{J_w}\bar{y}_1(\bar{y}_1 + \bar{y}_2) \tag{9.106}$$

or

$$\sigma_1(c_1, z) = \frac{M_{(z)} L \, c_1 \bar{y}_1}{J_w} \tag{9.107}$$

or

$$\sigma_1(c_1, z) = \frac{B_{(z)} w_{(ci)}}{J_w} \tag{9.108}$$

where

$$B(z) = M(z)L \tag{9.109}$$

is an action effect termed by Vlasov *bimoment* and

$$w(c) = y_1 c_1 \tag{9.110}$$

is a coordinate termed *principal sectorial area* or *principal sectorial ordinate* for the point of reference of the section. Of course, in the general case of an open composite cross-section, the principal sectorial ordinate cannot be expressed by Equation 9.110, which relates to a special form of cross-section. Its general form will be given in the next paragraph.

On the other hand, bimoment $B_{(z)}$, being in the special case of an I section, the product of the two opposite directed bending moments $M_{(z)}$ of the flanges with the flanges distance L, will be given in general form in Table 9.2. This magnitude corresponds to the bending moment in case of simple bending.

Returning to differential Equation 9.97, it should be noted that this equation holds for any form of a composite open thin-walled member.

The integration of this equation takes the form (Anastasiadis, 1989):

$$\theta = \kappa_1 \cos h(\lambda z) + \kappa_2 \sin h(\lambda z) + \kappa_3 + \frac{T(z)}{GJ_p} z \tag{9.111}$$

where
$\kappa_1, \kappa_2, \kappa_3$ are constants determined by the boundary conditions and

$$\lambda = \sqrt{\frac{GJ_p}{EJ_w}} \tag{9.112}$$

If θ and its derivatives are introduced in Equations 9.93 and 9.95, $T_w(z)$ and $T_v(z)$ may be determined. This procedure exceeds the scope of this subsection. However, it will be used next to draw useful conclusions for design.

If J_p is small enough, as happens in the case of very thin walls, Equation 9.97 takes the form:

$$-EJ_w \frac{d^3\theta(z)}{dz^3} = T(z) \tag{9.113}$$

Table 9.1 Analogy between bending and warping torsion

Bending	Warping torsion
$p_x(z)$: distributed load per m	$m(z)$ = distributed moment per m
$u_x(z)$: deflection	$\theta(z)$ = rotation
$u_x'(z)$: inclination of the deformed axis	$d\theta(z)/dz$ = twist
$J_y = \int y^2\, dA$	$J_w = \int w^2\, dA$
$M_y(z) = EJ_y \cdot u_x''(z)$	$B_\kappa(z) = -EJ_w\,(d\theta^2(z)/dz^2)$
$Q_x(z) = -EJ_y \cdot u_x'''(z)$	$T_\kappa(z) = -EJ_w\,(d\theta^3(z)/dz^3)$
$\sigma = -x\,(M_y/J_z)$	$\sigma_\kappa(z) = -w_{(s)}B_\kappa(z)/J_w$

It is apparent that this differential equation, which expresses the warping torsion, exhibits a *complete formal analogy* with *simple bending*. This may easily be seen by the comparison of the corresponding values given in Table 9.1 (Anastasiadis, 1989).

9.6.2.4 Geometrical parameters for warping bending

From what has been presented so far, the following geometrical parameters of the cross-section are needed for warping torsion:

- Coordinates of SC (x_s, y_s) (Figure 9.45)
- The *principal sectarian ordinate* (w_{cs}) of the successive points of the centre line of the cross-section with reference to the SC
- The *warping moment of inertia* or warping constant J_w

$$\bar{T}_2 = t_1\,(b - t_2/2)(h - t_1)/2)\,\frac{'1'}{J_{①}}$$

$$\bar{T}_4 = \bar{T}_2$$

$$\bar{T}_3 = \bar{T}_2 + \frac{1}{4}\,(h - t_1)^2\,\frac{1}{2}\cdot\frac{'1'}{J_1}$$

$$R_{1,2} = T_2\,(b - \frac{t_2}{2})\,\frac{1}{2}$$

$$R_{2,4} = 1$$

$$R_{4,5} = -T_2(b - t_2/2)\,\frac{1}{2}$$

$$e = R_{1,2}(h - t_1)/1)$$
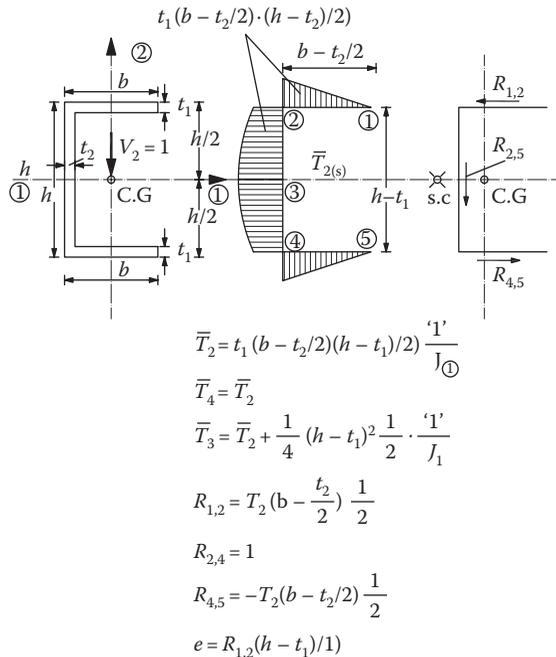
Figure 9.45 Determination of the SC of a U section.

- SC

  As has been clarified in a previous paragraph, the SC of an open section is defined as the point through which a horizontal load should pass so that no torsional effect is developed in the cross-section.

  For the determination of the coordinates of the SC, the following procedure is used (Figure 9.45):

  - Determine the CG of the cross-section, the principal axes 1 and 2 and the principal moments of inertia J_1 and J_2 of the cross-section.
  - For a vertical shear force equal to "1" parallel to axis 2 and passing through the CG, the shear flow diagram is determined by implementing the known expression:

$$\bar{\tau}_{(2)s} = \tau_{(2)s}t = \frac{\text{"1"}\, S_{(1)s}}{J_1}$$

(9.114)

  where

  $S_{(1)S}$ is the static moment at the successive points of the cross-section with respect to axis 1-1, that is:

$$S_{(1)s} = \int_{o}^{s} s \cdot t \cdot ds$$

(9.115)

  J_1 is the principal moment of inertia of the cross-section with respect to axis 1-1.
  t is the thickness of the wall element.

  - Integrate the shear flow along each wall element:

$$R_{i(1)} = \int_{i} \bar{\tau}_{(2)s} \cdot ds$$

(9.116)

  - Find the axis of the resultant of successive $R_{i(2)}$. The SC of the cross-section will lie on this axis.
  - Repeat the above steps 2–4 for a shear force equal to "1" parallel to axis 1 and passing through the CG. The new axis of the resultant of $R_{i(2)}$ will pass through the SC, and therefore its intersection with the axis defined at step 4 will determine the SC.

  In the case that the cross-section is symmetric to one principal axis, as in the example depicted is (Figure 9.45), the SC will be located on the axis of symmetry. In case of cross-sections of double symmetry, the SC coincides with the CG. In the case that all legs of the composite section pass through a common point, it is apparent that this point will be also the SC of the cross-section. For usual forms of cross-section, the position of the SC is given by closed expressions in conventional manuals (e.g. Table 9.2; Taranath, 2010).

- *Principal sectorial or warping ordinate $w_{(s)}$*

  The principal sectorial or warping coordinate at a point of the cross-section of a thin-walled member is a parameter that expresses the warping response (i.e. displacement, strain and stress) at that point relative to the response at all other points of the section. Therefore, this value is similar to the ordinate x_i of a point i of a section under plain bending in the expression $\sigma_i = M_y x_i / J_y$, where σ_i is determined.

Table 9.2 Torsion constants for open sections

Cross-section reference number	Constants

Channel

$$e = \frac{3b_2}{h + 6b}$$

$$j = \frac{t_3}{3}(h + 2b)$$

$$I_w = \frac{h2b2t}{12} \cdot \frac{2h + 3b}{h + 6b}$$

C section
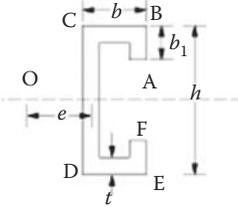
$$e = b\frac{3h2b + 6h2bl - 8bl2}{h2 + 6h2b + 6h2bl + 8bl3 - 12hbl2}$$

$$J = \frac{t_3}{3}(h + 2b + 2b_1)$$

$$I_w = I\left[\frac{h2b2}{2}\left(bl + \frac{b}{3} - e - \frac{2ebl}{b} - \frac{2bl2}{h}\right) + \right.$$

$$\left. + \frac{h2c2}{2}(b + bl + \frac{h}{6} + \frac{2bl2}{h}) + \frac{2bl2}{3}(b + e)2\right]$$

Hat section
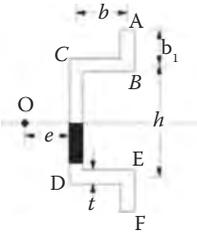
$$J = \frac{t_3}{3}(h + 2b + 2b_1)$$

$$e = b\frac{3h2b + 6h2bl - 8bl2}{h2 + 6h2b + 6h2bl + 8bl3 + 12hbl2}$$

$$I_w = I\left[\frac{h2b2}{2}\left(bl + \frac{b}{3} - e - \frac{2ebl}{b} - \frac{2bl2}{h}\right) + \right.$$

$$\left. + \frac{h2c2}{2}\left(b + bl + \frac{h}{6} + \frac{2bl2}{h}\right) + \frac{2bl2}{3}(b + e)2\right]$$

Twin channel with flanges inward
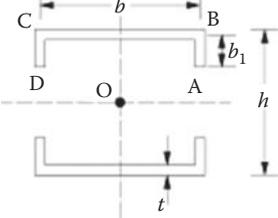
$$J = \frac{t_3}{3}(2b + 4b_1)$$

$$I_w = \frac{tb_2}{24}(8bl2 + 6h2bl + h2b + 12bl2h)$$

Twin channel with flanges outward
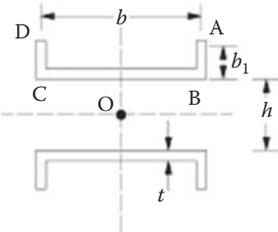
$$J = \frac{t_3}{3}(2b + 4b_1)$$

$$I_w = \frac{tb_2}{24}(8bl2 + 6h2bl + h2b + 12bl2h)$$

The principal warping coordinate is defined with respect to the SC and a point of origin p_o on the section selected in such a way that the integration of the principal warping ordinates along the cross-section give a resultant equal to zero. This is determined by the fact that the resultants of axial stresses due to warping are zero. In this respect, in the case of simple symmetric sections, the point of origin p_o is selected *on the symmetry axis*. The value of the principal sectorial coordinate at any point P on the profile is given by the area (Figure 9.46a):

$$\boxed{w_c = \int_o^s h ds}$$

(9.117)

where

$\quad$ h is the perpendicular distance of the SC to the tangent of the profile at P
$\quad$ s is the distance between p_o and p measured on the central line of the profile

In Figure 9.46b the principal warping ordinate of a C section is given as an example.

- *Warping moment of inertia*
  This parameter expresses the warping torsional resistance of the cross-section and is analogous to the moment of inertia in bending.
  The warping moment of inertia is defined by the expression:

$$\boxed{J_w = \int_o^A w_{(s)}^2 dA}$$

(9.118)

and is easily determined if the warping ordinate $w_{(s)}$ has been defined. For usual cross-sections, closed expressions are given for the determination of J_w (see Table 9.2; Taranath, 2010). Implementing Equation 9.118 in the case of the cross-section of Figure 9.42, the expression given by Equation 9.94 (Figure 9.47) is obtained.

$$W_P = \int_o^s h ds = S_P h = 2A_P \qquad W_{s\,②} = h(I - t_1)/2$$
$$W_{s\,①} = h(I - t_1)/2 - (b - t_2)/2)(I - t_1)/2$$
$$W_{s\,③} = \varnothing$$
$$W_{s\,④} = -W_{s\,(2)}$$
$$W_{s\,⑤} = -W_{s\,(1)}$$
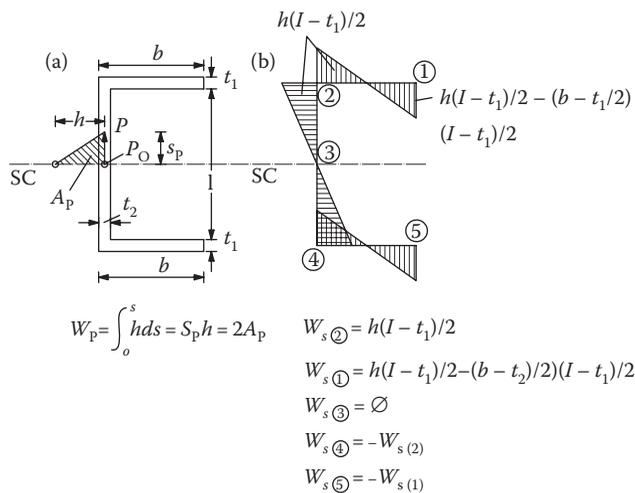
Figure 9.46 Determination of the principal warping ordinate $w(s)$: (a) definition of $w(s)$; (b) $w(s)$ diagram of a C section.
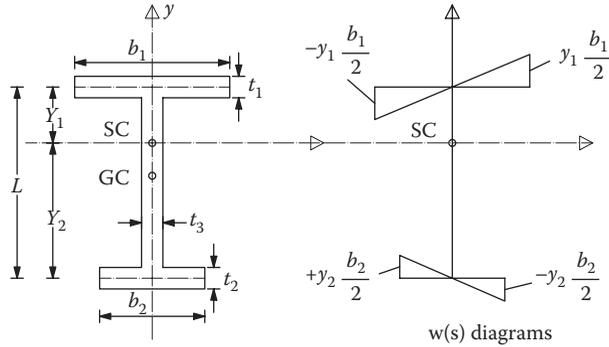
$$J_w = \int_A w^2(s)\, dA = 2\left(\frac{1}{3}\, y_1^2\, \frac{b_1^2}{4}\, \frac{b_1}{2}\, t_1\right) + 2\left(\frac{1}{3}\, y_2^2\, \frac{b_2^2}{4}\, \frac{b_2}{2}\, t_2\right) =$$

$$= y_1^2\, \frac{b_1^3 t_1}{12} + y_2^2\, \frac{b_2^3 t_2}{12} = y_1^2\, J_{1(y)} + J_{2(y)} y_2^2$$

Figure 9.47 Determination of the principal warping *moment of inertia* J_W of an I section with unequal flanges.

9.6.2.5 Implications of warping torsion in analysis and design to seismic action of R/C buildings

9.6.2.5.1 General

It has been noted many times so far that walls constitute the main backbone of the structural system of a building in resisting earthquakes. Usually they are arranged in cores of a composite open cross-section in the form of U, Γ, T, Z or similar sections. Therefore, in addition to their torsional rigidity due to bending and pure torsion, they are considered 3-D linear elements with their axes localised in the SC of their cross-section, and they develop a warping torsional rigidity that should be taken into account. However, this stiffness parameter is ignored by almost all commercial computer programs for analysis and design. At the same time, EC8-1/2004 par. 5.4.3.4.1/(1) and (4) provides that the design of bending resistances of composite wall sections should be carried out, assuming that the cross-sections are *integral units* and the strain distribution is planar, without any reference to warping torsion issues. In this respect, the analysis and design in almost all conventional commercial programs are in accordance with the Code.

However, the question remains as to how strong the influence of warping torsion on the results of the conventional approach would be in case this influence were taken into account.

This influence depends basically on the torsional stiffness of the structural system. In fact, keeping in mind that the torsional stiffness of a structural system has the form of the following expression (see 2.4.4(2)):

$$T.R. = \sqrt{\sum J_{ix} y_i^2 + \sum J_{iy} x_i^2 + \sum J_p} \qquad (9.119)$$

where

J_{ix}, J_{iy} are the moments of inertia of the resisting vertical structural members (walls and columns)

x_i, y_i are the coordinates of the axes of these members passing through their local SCs with respect to the global stiffness centre.

it is apparent, according to what has been presented in Paragraph 9.6.2.3, that *the warping stiffness of each composite section to its local SC will be a small percentage of expression (9.119)* if the global torsional stiffness results from many vertical elements distributed throughout the plan of the building. In this case, the warping torsion can be regarded as insignificant for the structural behaviour of the building. However, in the case that almost all walls are concentrated in a core while all other vertical elements are columns of low stiffness compared to the core stiffness, then warping torsion should be taken into account, since it constitutes the main part of the torsional stiffness of the building. The results included in Example 9.8.2 are indicative of the soundness of the above remark.

9.6.2.5.2 Analysis and design to warping torsion in the case of FEM modelling of the walls

In this case, warping torsion has already been taken into account in the determination of stresses, since the analysis is based on the theory of elasticity where all elastic compatibility considerations are taken into account, and not on the Bernoulli concept for planar distribution of strains. The results of the structural analysis of a U section at the level of stresses are given in Figure 9.48.

However, the axial stresses due to warping torsion cannot be taken into consideration in dimensioning and design for the following reasons. As has been noted in a previous paragraph, the normal stresses due to bimoment (warping) have a resultant axial force and bending moments with reference to the composite section equal to zero. In this respect, the integration of normal stresses on wall sections to a group of internal forces N, M_x and M_y (pier assumption) reduces to zero the influence of warping normal stresses and in this respect the influence of bimoment, too. It should be noted that a composite section is designed according to EC2-1-1/2004 as cracked, with a planar distribution of strains, and in this respect the existence of warping normal stresses contradicts the above assumptions of EC2-1-1/2004.

In the case that warping of open-wall R/C sections should be taken into account (small torsional stiffness of the structural system), the following approximate approach could be followed:

Step 1: From the static or dynamic analysis the rotation angle θ_i at the level of the successive storeys is determined.
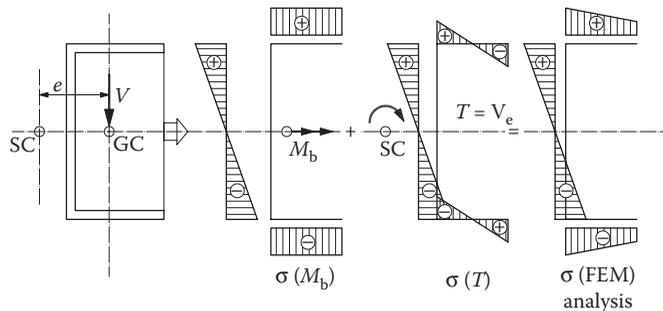
Figure 9.48 Normal stress state of a C section due to pure bending and warping torsion.

Step 2: From the diagram $z - \theta$ the diagram of $d\theta_i/d_z$ may be produced, that is,

$$\theta'_i = \frac{d\theta_i}{dz} = \frac{\Delta\theta_i}{h_{storey}} \tag{9.120}$$

and from θ'_i the diagram of the second derivative may also be derived, that is,

$$\theta''_i = \frac{d^2\theta_i}{(dz)^2} = \frac{\Delta\theta_i}{h^2_{storey}} \tag{9.121}$$

Step 3: Using the expression of Table 9.1, which relates $d^2\theta/dz^2$ to bimoment, that is,

$$\boxed{B_\kappa(z) = EJ_w \frac{d^2\theta(z)}{(dz)^2}} \tag{9.122}$$

the bimoment $B_\kappa(z)$ is determined at each storey level for every open thin-walled member. It should be noted that J_w refers to the local SC of the open composite wall section.

Step 4: Having defined the bimoments $B_\kappa(z)$ at each storey level of each composite section, the warping normal stresses are calculated using the relevant equation of Table 9.1.

$$\boxed{\sigma_\kappa(z) = -w_{(s)}B_\kappa(z)/J_w} \tag{9.123}$$

where
$w(s)$ is the principal sectorial ordinate of the point of reference of the cross-section.

Step 5: The above normal stresses are then integrated along each straight component of the composite section, and the tensile resultants are used to define the additional reinforcement at each leg due to warping torsion.

It is obvious that the above procedure ignores cracking and violates the Bernoulli concept for planar distribution of strain over the section.

The above five steps may be programmed in a conventional program (e.g. ECtools) in the form of a post-processor and be activated only in case the designer decides that warping torsion should be taken into account.

9.6.2.5.3 Analysis and design to warping torsion in the case of linear 3-D modelling of the walls

In the case that the walls are modelled as 3-D linear elements with their axes passing through their local SC, warping torsion should be taken into account for the formation of the stiffness matrix of the element. In this respect, instead of a square symmetric matrix of 12×12 elements, a matrix of 14×14 should be introduced with two extra 'displacements' at the end of the member, that is, $d\theta(z)_i/d_z$ and $d\theta(z)\kappa/d_z$ (Taranath, 2010). This means that the main computer program for the analysis and design should be drastically modified in order for warping torsion to be taken into account.

9.7 SEISMIC DESIGN OF DIAPHRAGMS

9.7.1 General

In addition to their main role in carrying gravity loads, the floor slabs of R/C buildings contribute to the formation of the structural system resisting seismic or wind actions. They act as horizontal diaphragms that transfer the inertial forces to the vertical structural system and ensure that these systems act together in carrying the seismic actions.

Very early in this book (see Subsection 2.4.4) a thorough reference was made to diaphragms and their significance in generating pseudospatial structural systems. For conventional R/C buildings, orthogonal in plan, with their dimensions l_x and l_y almost equal, and a smooth distribution of the stiffness of vertical elements over the plan of the building, there is no concern for the seismic analysis and design of the diaphragms, as they are formed automatically at the floor-level of the storeys by the cast *in situ* slabs.

On the other hand, special attention should be given to the following cases:

1. Non-compact or very elongated in-plan shapes and in the case of large floor openings, particularly if these openings are located in the vicinity of the main vertical elements, prohibiting the effective connection between the vertical and horizontal elements, or at the perimeter of the diaphragm, interrupting in this way the formation of the tension chord of the diaphragm (Figures 9.49 and 9.50).
2. Complex and/or non-uniform layout of the lateral load resisting system, such as basements with R/C walls located only in parts of their perimeter.
3. Dual systems where structural systems of different stiffness characteristics are coupled together through the floor slab. Major problems may be expected only in the case where the distribution of walls is not appropriate (e.g. cores at the opposite sides of the building in plan; Figure 9.50).

Diaphragms must have sufficient in-plane stiffness for the distribution of horizontal inertial forces to the vertical structural system in accordance with the assumptions of the
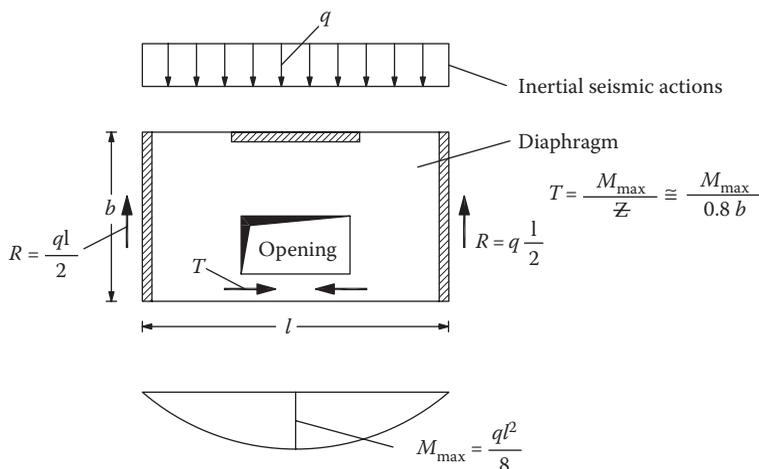
Figure 9.49 A diaphragmatic slab with an opening near the tension chord.
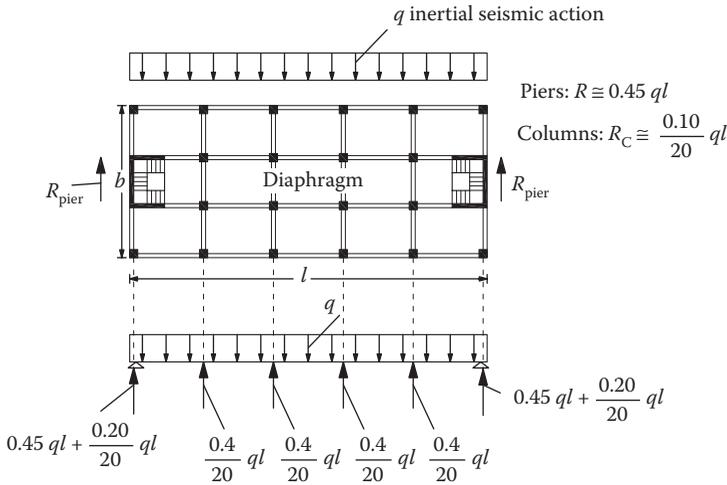
Figure 9.50 The structural behaviour of a long diaphragm with two cores at its ends.

analysis (pseudospatial system). In this respect, plan shapes of L, C, H, I and X form should be carefully examined. According to EC8-1/2004, a solid reinforced concrete slab may be considered sufficient to serve as a diaphragm for conventional structures, if it has a thickness of not less than 70 mm and is reinforced in both directions with at least the minimum reinforcement specified in EC2-1-1/2004.

9.7.2 Analysis of diaphragms

9.7.2.1 Rigid diaphragms

- Floor diaphragms are commonly assumed and modelled as rigid in-plane bodies. In this respect, the analysis of the diaphragm is separated from the analysis of the global structural system, which in this case is considered as a pseudo-structural system.
- Lateral loading of the diaphragm at any storey may result as the difference of the shear forces due to seismic action at the vertical shear-resisting elements above and below the diaphragm (Figure 9.51). The resultant of these seismic actions in each main direction will be distributed in trapezoidal form along the dimension of the diaphragm,
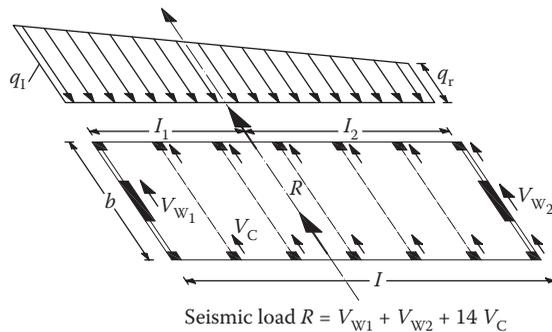
Figure 9.51 Determination of diaphragm loading due to seismic action.

perpendicularly to the seismic action, to simulate the inertial forces of the masses of the diaphragm.

In this respect, the resultant of the distributed inertial forces of the diaphragm will act on the same axis of the shear actions of the vertical elements on the diaphragm (Figure 9.51). Eurocode EC8-1/2004 makes no reference to lateral loading for the analysis of a diaphragm. American Code ASCE7-05 provides that this loading should satisfy design seismic force from the structural analysis as presented above, and additionally requires that this loading should not be less than that determined in accordance with the following equation:

$$ F_{px} = \frac{\displaystyle\sum_{i=x}^{n} F_i}{\displaystyle\sum_{i=x}^{n} W_i} W_{px} \tag{9.124} $$

where

F_{px} is the diaphragm design force at level x
F_i is the design force applied at level i (lateral force method of analysis, Chapter 5.6.4)
W_i is the weight tributary to level i
W_{px} is the weight tributary to the diaphragm at level x

- The action effects may then be estimated by modelling the diaphragm as a deep beam or a plane truss or strut-and-tie model, considered simply a supported beam with reactions at the supports almost equal to zero. (The simple supports are introduced only for avoiding the geometric redundancy of the system.) If the in-plane stiffness of the diaphragm is introduced, the deflections of the diaphragm may be calculated. If these deflections are less than 10% of the corresponding horizontal displacements of the pseudospatial structural system at that storey, the procedure is deemed to be correct. Otherwise, the diaphragm should be introduced in the overall structural system as a flexural planar member.

    For analysis of the diaphragm, Eurocode EC8-1/2004 proposes the introduction of elastic supports at the location where vertical members are connected with the diaphragms. This approach is not easily implemented, since the spring coefficients of the supports are not easily determined. A criterion for the correct choice of the spring coefficients would be the following: The spring reactions from the analysis of the diaphragm should be equal to the shear forces at those points from the analysis of the pseudospatial structure that have been taken into account from the beginning for the determination of the inertial forces of the diaphragm.

- The design values of the action effects should be derived by introducing an overstrength factor. The value of this overstrength factor recommended by EC8-1/2004 is

$$ \gamma_d = 1.3 \tag{9.125} $$

9.7.2.2 Flexible diaphragms

In the case that the diaphragm that has been modelled separately from the overall pseudospatial structural system exhibits displacements of more than 10% of the corresponding absolute horizontal displacements of the pseudospatial structural system due to seismic

action, then the structural system must be reanalysed from the beginning by introducing the diaphragms in the model with their actual in-plane stiffness.

In this respect the pseudospatial model of analysis is abandoned and diaphragms are introduced in the form of a Finite Elements Mesh (Subsection 4.2.8, Figure 4.14). It is obvious that in this case the analysis becomes very time consuming, since the number of the unknown displacements and rotations and the number of modes – if the model response spectrum analysis is followed – increases significantly. However, nowadays, with the rapid development of computer capacities, the procedure must not be considered prohibitive. It is apparent that in this case the output of the analysis is expressed in the form of stresses σ_x, σ_y, τ_{xy} in the middle plane of the diaphragm and in the form of axial forces along the beams that act as chords and collectors (Subsection 4.2.8, Figure 4.15).

9.7.3 Design of diaphragms

The seismic design of diaphragms must include ULS verifications of reinforced concrete. The design resistances should be defined in accordance with EC2-1-1/2004.

In cases of core or wall structural systems, it should be verified that the transfer of the horizontal forces from the diaphragm to the cores or walls is ensured by the following provisions:

1. The design shear stress in the interface of the diaphragm and the core or the wall should be limited to $1.5f_{ctd}$ for cracking control.
2. Shear sliding failure should be ensured (see par. 9.2.4 (3) and (5)), assuming strut inclination of 45°. In this respect, properly anchored additional bars should be provided, contributing to the shear strength of the interface between diaphragms and cores or walls.

9.7.4 Code provisions for seismic design of diaphragms

The above procedure for analysis and design of diaphragms is provided by EC8-1/2004 only for DCH R/C buildings with properties already described in Subsection 9.6.1.

9.8 EXAMPLE: DIMENSIONING OF A SLENDER DUCTILE WALL WITH A COMPOSITE CROSS-SECTION

The design of a wall of composite cross-section, wall W2, is presented here (Figure 5.44). The C-shaped wall is considered an integral unit and is modelled with shell elements (Paragraph 5.6.3.1). W2 wall comprises a web parallel to the y–y axis and two flanges normal to it. The analysis in biaxial bending is conducted according to the computational platform NOUS (NOUS/3P, 2002). The procedure described in Paragraph 9.2.2.3 is followed. The algorithm is based on the ultimate limit state design method, considering the following assumptions:

1. A parabolic-rectangular concrete stress diagram is used
2. Ultimate compressive concrete strain is taken to be $\varepsilon_{cu} = 3.5‰$
3. Ultimate tensile steel strain is taken to be $\varepsilon_{cu} = 20‰$
4. Concrete tensile strength is taken to be equal to zero

Moreover, the flexural capacity is estimated by taking into account only the vertical reinforcement of the boundary elements, whereas the shear capacity is estimated by considering only the web horizontal reinforcement and for a web length approximately equal to 0.8 l_w.

9.8.1 Ultimate limit state in bending and shear

The load combinations at the base of wall W2 appear in Table 9.3.

The design of the composite wall W2 in bending and shear is performed by using the cross-section analysis program NOUS in combination with ECtools (ECtools, 2013). An automatic iterative procedure is followed for establishing cross-section equilibrium for the applied action effects and the considered length and percentage of longitudinal reinforcement of the confined boundary elements (defined according to the provisions of EC8-Part I, 2004). The section at the base of the first storey is loaded at the centre of gravity, C, by $M_{Eyd} = -2207.69$ kNm, $M_{Exd} = 21536.22$ kNm and $N_{Ed} = -5914.55$ kN. This is considered, according to the checks performed by NOUS, to be the critical load combination, $G+0.3Q+E_y+0.3E_x$ (see Table 9.3); it is reminded that the effect of the accidental eccentricity is included in the response spectrum analysis, thus the total number of load combinations, including the gravity load combination, is limited to 9 (see Paragraph 5.9.6.1).

Five iterations are performed before reaching cross-section equilibrium. In order for the safety factor γ to become equal to 1, the required percentage of longitudinal reinforcement of the entire wall cross-section is 0.19%. Due to restrictions related to:

1. The maximum distance between consecutive longitudinal bars restrained by hoops, which is defined as equal to $s_{min} = 150$ mm for high ductility walls
2. The mechanical volumetric ratio of the required confining reinforcement in the boundary elements

the longitudinal reinforcement percentage is increased to 0.55%.

The strain and stress profiles along with the position of the neutral axis (point N) are depicted for the elastic (non-cracked) and final iteration state in Figures 9.52a and 9.52b, respectively.

The ordinates of the geometrical centre (point C) are $x = 2.650$ m, $y = 2.184$ m, whereas the neutral axis position is modified from point N, in the first iteration (uncracked cross-section; $x = 3.900$ m, $y = 1.656$ m, $r_z = 67.09$ deg), to point P, in the last (5th) iteration ($x = 2.595$ m, $y = 2.943$ m, $r_z = 49.54°$).

Table 9.3 Bending moments and axial forces for Wall W2 dimensioning

Load combinations		N	V_x	V_y	M_x	M_y
Lc1	1.35G+1.5Q	−11378.01	−86.63	0.42	4.02	−205.69
Lc2	G+0.3Q+Ex+0.3Ey	−4348.01	−1442.03	1061.81	7140.18	−7146.97
Lc3	G+0.3Q+Ex-0.3Ey	−4348.28	−1441.97	−805.91	−5645.90	−7146.75
Lc4	G+0.3Q-Ex+0.3Ey	−8824.76	1368.35	806.41	5651.47	6966.00
Lc5	G+0.3Q-Ex-0.3Ey	−8825.04	1368.41	−1061.31	−7134.61	6966.22
Lc6	G+0.3Q+Ey+0.3Ex	−5914.55	−458.47	3151.42	21536.22	−2207.69
Lc7	G+0.3Q+Ey-0.3Ex	−7257.58	384.65	3074.80	21089.61	2026.20
Lc8	G+0.3Q-Ey+0.3Ex	−5915.47	−458.27	−3074.30	−21084.04	−2206.95
Lc9	G+0.3Q-Ey-0.3Ex	−7258.50	384.85	−3150.92	−21530.65	2026.94

(a)   Elastic state

External forces	Internal forces	Neutral axis location	Centre of gravity (C)	Elastic neutral axis
N: −7258.50 kN	N_i: −28911.31 kN	(P=N)	x_o: 2.650 m	location (N)
M_x: 3472.73 kNm	M_{xi}: 87423.36 kNm	x_p: 3.900 m	y_o: 2.184 m	x_n: 3.900 m
M_y: −6513.28 kNm	M_{yi}: −15706.00 kNm	y_p: 1.656 m		y_n: 1.656 m
		a_p: 67.09 d		a_n: 67.09 d

(b)   Last iteration

External forces	Internal forces	Neutral axis location	Centre of gravity (C)	Elastic neutral axis
N: −7258.50 kN	N_i: −16184.80 kN	(P)	x_o: 2.650 m	location (N)
M_x: 13815.94 kNm	M_{xi}: 30788.39 kNm	x_p: 2.595 m	y_o: 2.184 m	x_n: 3.900 m
M_y: −16361.05 kNm	M_{yi}: −36479.92 kNm	y_p: 2.943 m		y_n: 1.656 m
		a_p: 49.54 d		a_n: 67.09 d

Figure 9.52 W2 cross-section equilibrium: (a) at the elastic state, and (b) at the final iteration step.

The internal forces developed in the concrete and the reinforcing bars at the last iteration (5th) step are equal to $N_{Rd} = −16184.80$, $M_{Rxd} = 30788.39$ kNm, $M_{Ryd} = −36479.92$ kNm relative to original coordinate system passing through print C.

The safety factor at the final iterative step is defined as equal to $\gamma = 2.23$. The length of the boundary elements is shown in Figure 9.53, while the longitudinal and transverse reinforcements of the wall are depicted in Figure 9.54.

The mechanical volumetric ratio of the required confining reinforcement $\alpha\omega_{wd,req}$ within the critical height of the wall has been defined as equal to 0.193 for web element A and 1.04
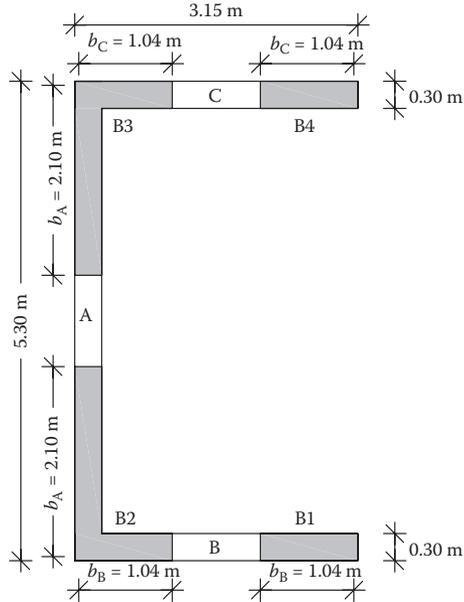
Figure 9.53 Definition of boundary elements.
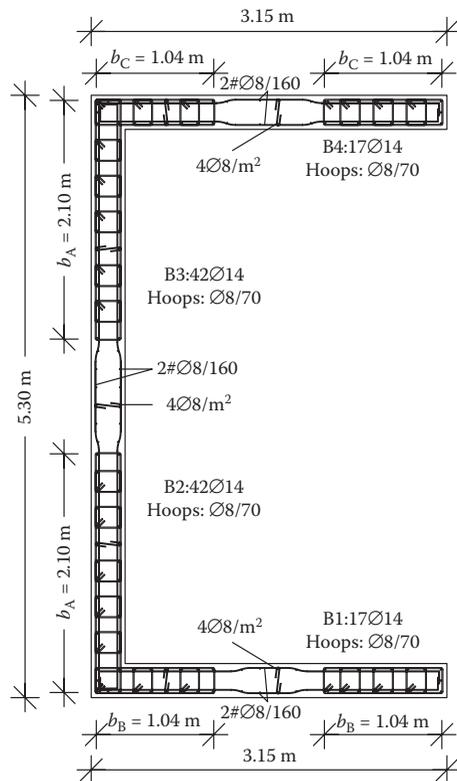
Figure 9.54 Flexural and shear reinforcement of wall W2.

for flange elements B and C (Figure 9.53). These volumetric ratio correspond to the hoop configuration shown in Figure 9.54 consisting of hoops of Φ8/70. The above computations have been carried out automatically using EC Tools (2013) and are based on the assumption of sacrificed flange (see par. 9.2.4.2(3)).

The shear actions for which the horizontal reinforcement of the web is defined are $V_{Exd} = 1442.03$ kN (load combination $G+0.3Q+E_x+0.3E_y$, Table 9.3) and $V_{Eyd} = 3151.42$ kN (load combination $G+0.3Q+E_y+0.3E_x$, Table 9.3). The same amount of horizontal and vertical reinforcement is placed in the web of the wall being equal to 2#∅8/160 (i.e. two legs of ∅8 at 160 mm).

9.8.2 Estimation of axial stresses due to warping torsion

The 8-storey RC building presented in the example of Chapter 5 has a sufficient number of vertical members distributed all over the plan of the building as well as two walls placed at the perimeter, *implying that warping torsion is insignificant and can be ignored in the structural design*. The objective of this example is to estimate the developed warping normal stresses for wall W2 (Figure 5.44) and compare them to pure bending normal stresses. Therefore, the procedure described in detail in Paragraph 9.6.2.5.2 is implemented.

9.8.2.1 Estimation of the geometrical parameters for warping bending of an open composite C-shaped wall section

9.8.2.1.1 Shear centre

The SC lies on the horizontal symmetry axis at a distance h from the central line of the vertical component of the wall (Figure 9.55). The distance h is estimated as (Table 9.2):

$$h = \frac{3 \cdot b^2}{l + 6 \cdot b} = \frac{3 \cdot 300^2}{500 + 6 \cdot 300} = 117.39\,\text{cm}$$

The CG is estimated at a distance 81.61 cm from the central line of the vertical component.

9.8.2.1.2 Principal sectorial ordinates, w_s

The determination of the principal warping ordinates of the successive points 1–5 of the central line of the cross-section of the C-shaped wall with reference to the shear centre are given at each position by (Figure 9.56)

$$w_s(1) = h \cdot \frac{(l-t)}{2} - \left(b - \frac{t}{2}\right)\frac{(l-t)}{2} = 117.39 \cdot \frac{(530-30)}{2} - \left(315 - \frac{30}{2}\right)\frac{(530-30)}{2}$$

$$= -45652.5$$

$$w_s(2) = h \cdot \frac{(l-t)}{2} = 117.39 \cdot \frac{(530-30)}{2} = +29347.5$$

$$w_s(3) = 0$$

$$w_s(4) = -w_s(2) = \boxtimes 29347.5$$

$$w_s(5) = -w_s(1) = 45652.5$$
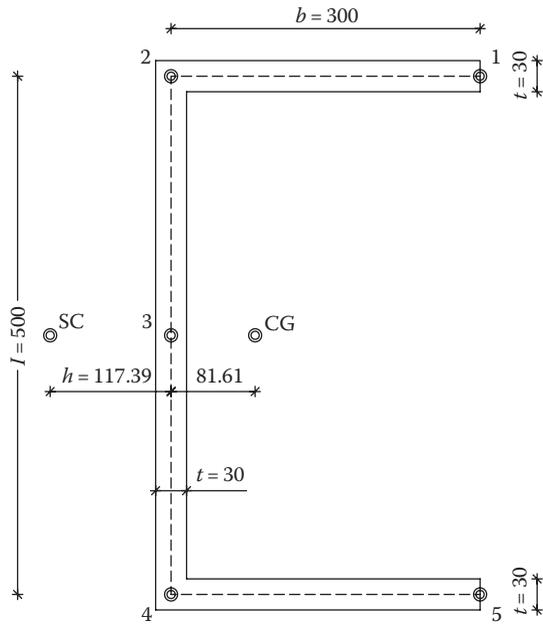
Figure 9.55 Centre of gravity (CG) and shear centre (SC) position.
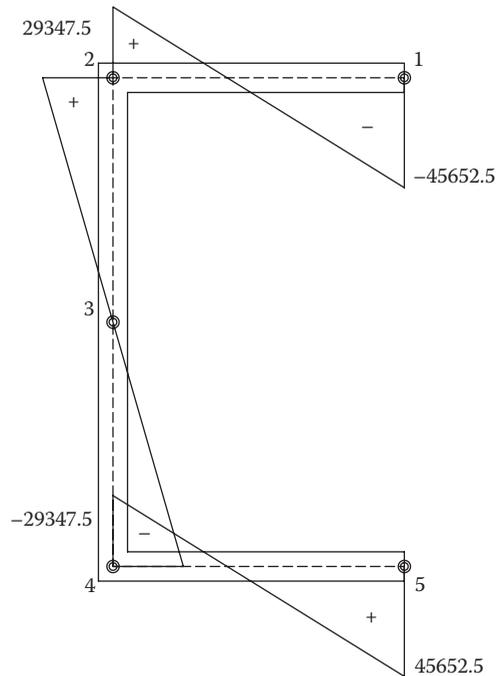
Figure 9.56 Principal sectorial ordinates, w_s, at the successive points of the central line of the cross-section.

9.8.2.1.3 Warping moment of inertia, J_w

The warping moment of inertia, J_w, is estimated as follows (Table 9.2):

$$J_w = \frac{(l-t)^2 \cdot (b-(t/2))^2 \cdot t}{12} \cdot \frac{[2 \cdot (l-t) + 3 \cdot (b-(t/2))]}{(l-t) + 6 \cdot (b-(t/2))} \Leftrightarrow$$

$$J_w = \frac{(530-30)^2 \cdot (315-(30/2))^2 \cdot 30}{12} \cdot \frac{[2 \cdot (530-30) + 3 \cdot (315-(30/2))]}{(530-30) + 6 \cdot (315-(30/2))}$$

$$= 4.64 \cdot 10^{10} \text{ cm}^6$$

9.8.2.2 Implementation of the proposed methodology for deriving the normal stresses due to warping

The normal stresses due to warping are estimated according to the following steps:

Step 1: The rotation angle θ_i at the centre of mass at each storey diaphragm for seismic loading in the x–x and y–y directions is presented in Tables 9.4 and 9.5, respectively. The rotation angle profile for each loading direction is presented in Figures 9.57 and 9.58.

Table 9.4 Estimation of the bimoment B_κ at each storey in the x–x direction

	Seismic action in the x–x direction			
Storey	θ_i (rad)	θ_i' (1/mm)	θ_i'' (1/mm²)	B_κ (N mm²)
8th	7.92E−04	2.93E−08	1.63E−15	2.35E+06
7th	7.04E−04	1.47E−08	−1.63E−15	−2.35E+06
6th	6.60E−04	2.93E−08	0.00E+00	0.00E+00
5th	5.72E−04	2.93E−08	−1.63E−15	−2.35E+06
4th	4.84E−04	4.40E−08	1.63E−15	2.35E+06
3rd	3.52E−04	2.93E−08	−1.63E−15	−2.35E+06
2nd	2.64E−04	4.40E−08	1.96E−15	2.82E+06
1st	1.32E−04	2.64E−08	1.06E−15	1.52E+06

Table 9.5 Estimation of the bimoment b_κ at each storey in the y–y direction

	Seismic action in the y–y direction			
Storey	θ_i (rad)	θ_i' (1/mm)	θ_i'' (1/mm²)	B_κ (Nmm²)
8th	1.01E−03	2.93E−08	0.00E+00	0.00E+00
7th	9.24E−04	2.93E−08	−4.04E−30	−5.83E−09
6th	8.36E−04	2.93E−08	−1.63E−15	−2.35E+06
5th	7.48E−04	4.40E−08	4.41E−30	6.35E−09
4th	6.16E−04	4.40E−08	−2.21E−30	−3.18E−09
3rd	4.84E−04	4.40E−08	0.00E+00	0.00E+00
2nd	3.52E−04	4.40E−08	−7.35E−31	−1.06E−09
1st	2.20E−04	4.40E−08	1.76E−15	2.54E+06

x–x direction of loading

3.00 m	7.92	2.93	1.63
3.00 m	7.04	1.47	−1.63
3.00 m	6.60	2.93	0.00
3.00 m	5.72	2.93	−1.63
3.00 m	4.84	4.40	1.63
3.00 m	3.52	2.93	−1.63
3.00 m	2.64	4.40	1.96
5.00 m	1.32	2.64	1.06

θ ($\times 10^{-4}$ rad) θ' ($\times 10^{-8}$ 1/mm) θ'' ($\times 10^{-15}$ 1/mm^2)
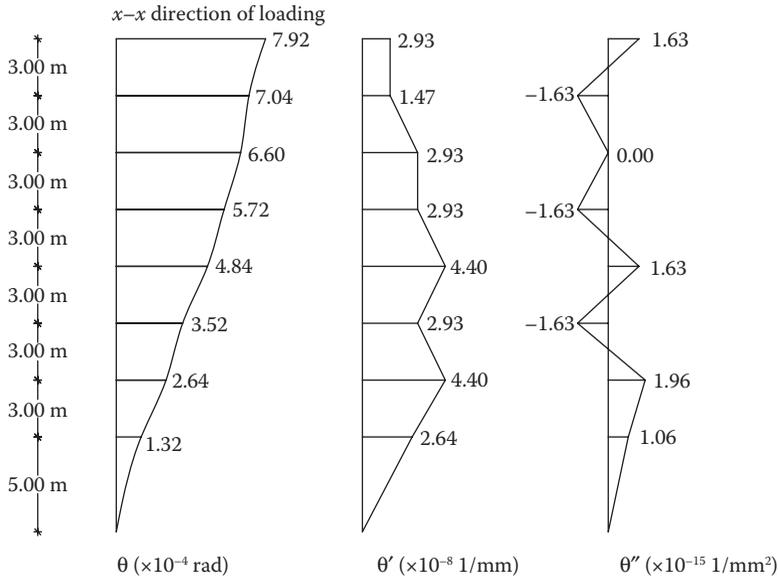
Figure 9.57 Rotation angle, θ_i, θ_i' and θ_i'' profile along building height for the x–x direction of loading.

Step 2: The profiles of the first derivative, $\theta_i' = d\theta_i/d_z = \Delta\theta_i/h_{st}$, and the second derivative, $\theta_i'' = d^2\theta_i/(d_z)^2 = \Delta\Delta\theta_i/h_{st}^2$, of the rotation angle are estimated for all the storeys in the two directions of loading (Tables 9.4 and 9.5, Figures 9.57 and 9.58).

Step 3: The bimoment $B_\kappa(z)$ is estimated at each storey via Equation 9.122 for the two loading directions, utilising the estimated warping moment of inertia, J_w, and the profile of the second derivative of the rotation angle, θ_i'' (Tables 9.4 and 9.5).

y–y direction of loading

3.00 m	10.10	2.93	0.00
3.00 m	9.24	2.93	0.00
3.00 m	8.36	2.93	−1.63
3.00 m	7.48	4.40	0.00
3.00 m	6.16	4.40	
3.00 m	4.84	4.40	
3.00 m	3.52	4.40	0.00
5.00 m	2.20	4.40	1.76

θ ($\times 10^{-4}$ rad) θ' ($\times 10^{-8}$ 1/mm) θ'' ($\times 10^{-15}$ 1/mm^2)
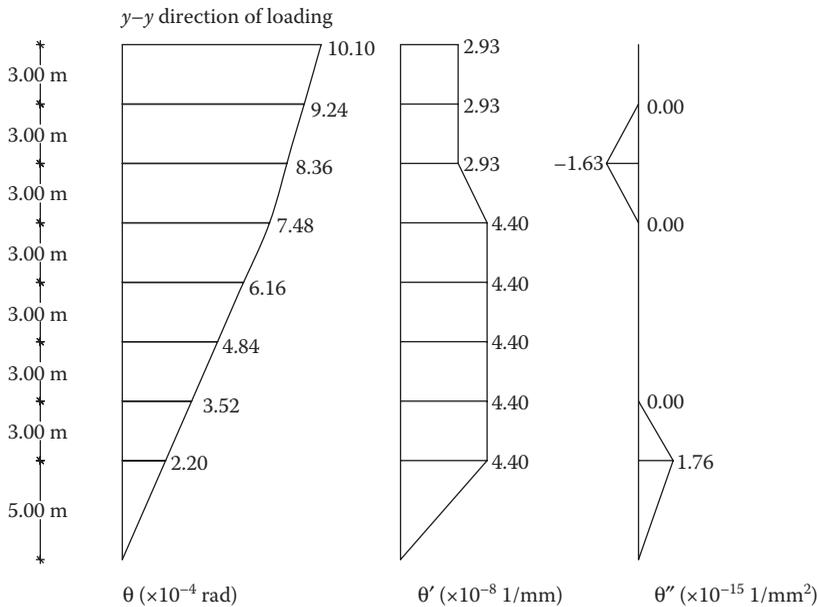
Figure 9.58 Rotation angle, θ_i, θ_i' and θ_i'' profile along building height for the y–y direction of loading.

Table 9.6 Estimation of the warping normal stresses (in MPa) for wall W2 at each storey in the *x–x* Direction

	Seismic action in the x–x direction				
Storey	$\sigma_\kappa(1)$	$\sigma_\kappa(2)$	$\sigma_\kappa(3)$	$\sigma_\kappa(4)$	$\sigma_\kappa(5)$
8th	2.31E–04	−1.48E–04	0.00E+00	1.48E–04	−2.31E–04
7th	−2.31E–04	1.48E–04	0.00E+00	−1.48E–04	2.31E–04
6th	0.00E+00	0.00E+00	0.00E+00	0.00E+00	0.00E+00
5th	−2.31E–04	1.48E–04	0.00E+00	−1.48E–04	2.31E–04
4th	2.31E–04	−1.48E–04	0.00E+00	1.48E–04	−2.31E–04
3rd	−2.31E–04	1.48E–04	0.00E+00	−1.48E–04	2.31E–04
2nd	2.77E–04	−1.78E–04	0.00E+00	1.78E–04	−2.77E–04
1st	1.49E–04	−9.61E–05	0.00E+00	9.61E–05	−1.49E–04

Table 9.7 Estimation of the warping normal stresses (in MPa) for wall W2 at each storey in the *y–y* direction

	Seismic action in the y–y direction				
Storey	$\sigma_\kappa(1)$	$\sigma_\kappa(2)$	$\sigma_\kappa(3)$	$\sigma_\kappa(4)$	$\sigma_\kappa(5)$
8th	0.00E+00	0.00E+00	0.00E+00	0.00E+00	0.00E+00
7th	−5.72E–19	3.68E–19	0.00E+00	−3.68E–19	5.72E–19
6th	−2.31E–04	1.48E–04	0.00E+00	−1.48E–04	2.31E–04
5th	6.24E–19	−4.01E–19	0.00E+00	4.01E–19	−6.24E–19
4th	−3.12E–19	2.01E–19	0.00E+00	−2.01E–19	3.12E–19
3rd	0.00E+00	0.00E+00	0.00E+00	0.00E+00	0.00E+00
2nd	−1.04E–19	6.69E–20	0.00E+00	−6.69E–20	1.04E–19
1st	2.49E–04	−1.60E–04	0.00E+00	1.60E–04	−2.49E–04

Table 9.8 Estimation of the normal stresses due to bending (in MPa) for wall W2 at the first storey for both directions of loading

	Normal stresses due to bending				
1st storey	$\sigma(1)$	$\sigma(2)$	$\sigma(3)$	$\sigma(4)$	$\sigma(5)$
x–x dir.	3.84	2.53	1.60	2.53	3.84
y–y dir.	2.71	4.02	0.62	4.02	2.71

Step 4: Having estimated the principal sectorial ordinates, $w_s(i)$, and the warping moment of inertia, J_w, the axial stresses due to warping are estimated for the C-shaped wall section $\sigma_\kappa(z)$ in Equation 9.123 and presented in Tables 9.6 and 9.7 for seismic loading in the *x–x* and *y–y* directions, respectively.

In light of the above, it may be seen that the effect of warping torsion is insignificant, with the estimated normal stresses receiving almost zero values. This is expected, since the building is not torsionally flexible due to the existence of the walls W1 and W4 at the perimeter of the building (Figure 5.44) and the vertical elements distributed throughout its plan. Hence, for buildings with similar characteristics to the 8-storey building, warping has no significant effect and can be safely ignored.

For comparison purposes, the normal stresses due to bending in the first storey at successive points 1–5 of the central line of the cross-section of the C-shaped wall (Figure 9.56) are presented in Table 9.8. Comparison with the corresponding values in Tables 9.6 and 9.7 *confirms that the increase of the normal stresses due to warping is negligible.*

Chapter 10

Seismic design of foundations

10.1 GENERAL

It is known that the foundation design of conventional buildings consists of two main components:

- The safety and service verification of the soil where the building is embedded
- The safety and service verification of the structural members of the foundation

It should be noted from the beginning that the building material of foundations has basically been reinforced concrete for almost the past 100 years, no matter what the building material of the superstructure has been.

While the analysis and design of the structural system has been gradually developed since the beginning of the nineteenth century, the study of the structural behaviour of the soil where the loads of the superstructure are transferred was delayed for almost a century. This delay must be attributed:

- To the uncertainties of soil properties
- To the soil composition of various strata with different properties
- To the difficulty of generating constitutive laws for the mechanical properties of soil analogous to those of conventional structural materials. In fact, the soil composition in particles, the cohesion among them, the existing voids among the grains, the water content in the voids and so on, generate a very complicated mixture of parameters that does not allow an easy and reliable interpretation of the behaviour of this mixture by mechanical laws for a continuous medium
- And finally, it should be attributed to the 3-D solid-state structural form of the foundation ground, since it is in fact a half 3-D continuous medium.

Therefore, a new engineering discipline was developed (soil mechanics) constituting the background of foundation design. The specialist in soil mechanics, after thorough *in situ* investigations and extended tests in the lab, gives all necessary data for strength, stiffness, damping and time-dependent properties for the soil under consideration in the form of a technical report.

The above difficulties, and particularly the 3-D solid state of the soil, had made an approach to soil–structure interaction issue, that is, the relationship among (Penelis et al., 1995) *'subsoil – foundation – superstructure'* as a structural continuum, almost impossible for many decades (Figure 10.1).
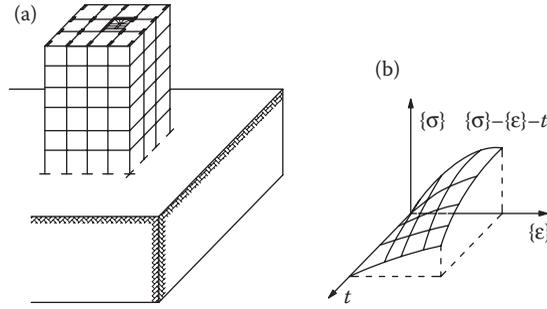
Figure 10.1 Soil–structure interaction analysis inelastic procedures: (a) structural model; (b) $\{\sigma\}$–$\{\varepsilon\}$–t relation.

To the above difficulties common for all buildings, some extra parameters should be added for buildings under seismic actions. These parameters are the following:

1. While all other loadings are transferred from the building to the ground, seismic actions are transferred from the ground to the building in the form of seismic waves (time-dependent constraints). This means that the soil during the earthquake is under dynamic excitation, and therefore its mechanical properties should be re-examined.
2. The consequences of the capacity design concept established for the superstructure should be investigated in detail with regard to foundation behaviour.
3. The ductility concept, on which the analysis, design and detailing of the superstructure is based, should be linked with the relevant procedures for the foundation members.
4. Perspectives on taking into account inelastic soil cyclic deformations due to seismic actions as a damping mechanism for the structure as a whole should be investigated thoroughly.

In the following sections, after a short overview of the mechanical properties of soil under dynamic loading, the presentation will concentrate on the design of foundations under seismic action.

10.2 GROUND PROPERTIES

10.2.1 Strength properties

According to EC8-5/2004, the value of the soil strength parameters applicable under static undrained conditions may also generally be used for soil under seismic action, taking into account that water draining of the soil during the short duration of an earthquake is not possible. However, some additional information should be given.

10.2.1.1 Clays

For cohesive soils, undrained shear strength c_u should be used. However, the value of c_u is affected both by the loading rate and by the number of cycles of loading. Rate effects may increase c_u up to 25% compared with the static strength. Conversely, the number of cycles reduces c_u, particularly in case of over-consolidated clays. For example, a normally consolidated clay (OCR = 1) can sustain 10 cycles at 90% of the undrained static shear strain c_u.

10.2.1.2 Granular soils (sands and gravels)

For cohesionless soil, the appropriate strength parameter is the undrained shear strength $\tau_{cy,u}$. This parameter relies on the friction among grains and therefore on the angle of internal friction φ', which is not influenced by cyclic loading. However, the effective stress between grains may be reduced in saturated granular soils, and more particularly in sands, if pore water pressures increase during an earthquake. This reduction leads to shear strength reduction. Pore water pressure may increase during an earthquake in the case of loose sands, where granular material tends to increase in density under the shaking actions of the earthquake. This results in an increase of pore pressure, since pore water has not had time to drain away. In due time, pore water will find paths to leak out of the voids, and in this way strength is restored. In the meantime, due to a significant temporary soil shear strength reduction, which may be drastically decreased, dramatic collapses of buildings may occur. This phenomenon is known as *soil liquefaction*. In a subsequent paragraph, more extended reference will be made to soil liquefaction, and more particularly to soils susceptible to liquefaction. EC8-5/2004 notes that this probability should be taken into consideration for the determination of $\tau_{cy,u}$.

10.2.1.3 Partial safety factors for soil

The partial safety factors for soil properties c_u, $\tau_{cy,u}$, q_u and $\tan \varphi'$, namely γ_{cu}, $\gamma_{\tau cy}$, γ_{qu} and $\gamma_{\varphi'}$, may be found according to EC8-5/2004 in the National Annex of each E.U. country. The recommended values of EC8-5/2004 are given below:

$$\boxed{\begin{aligned} \gamma_{cu} &= 1.4 \\ \gamma_{\tau cy,u} &= 1.25 \\ \gamma_{qu} &= 1.40 \\ \gamma_{\varphi'} &= 1.25 \end{aligned}} \tag{10.1}$$

10.2.2 Stiffness and damping properties

The main stiffness parameter of the ground under seismic action is the shear modulus G given by the expression:

$$\boxed{G_s = \rho V_s^2} \tag{10.2a}$$

where
  ρ is the unit mass and
  V_s is the shear wave propagation velocity of the ground.

Table 10.1 contains representative values of G_s and E_s of various soil categories. The value of G_s has been calculated by applying the well-known expression of the theory of elasticity:

$$\boxed{G_s = \frac{E_s}{2(1 + n_s)}} \tag{10.2b}$$

where
  n_s is Poisson's ratio taken to be equal to 0.40 (mean value).

Table 10.1 Typical values of E_s and G_s for soils and rocks

Soil type	E_s (MPa)	G_s (MPa)
Soft clay	Up to 15	5.3
Firm, stiff clay	10–15	3.0–18.0
Very stiff, hard clay	25–200	9.0–70.0
Silty sand	7–70	2.0–2.5
Loose sand	15–50	5.0–18.0
Dense sand	50–120	18.0–43.0
Dense sand and gravel	90–200	32.0–70.0
Sandstone	Up to 50.000	Up to 18.000
Chalk	5.000–20.000	1.800–7.000
Limestone	25.000–100.000	9.000–35.000
Basalt	15.000–100.000	5.000–35.000

Source: Adapted from Dowrick, D. 2005. *Earthquake Risk Reduction*, John Wiley and Sons, Ltd, Chichester, West Sussex, England.

Values of E_s have been taken from Dowrick (2005). Shear wave propagation velocity v_s and therefore G_s has been taken into account in EC8-1/2004 (see Paragraph 3.4.2.2) for the ground classification of various types (A to S_1) and, therefore, for the determination of the parameter S of the elastic response spectra. It should also be noted that G_s is the basic parameter for the determination of the overall foundation spring stiffness. Detailed reference will be made to this issue in the following sections.

Damping, on the other hand, should be considered as an additional ground property in the cases where the effects of soil–structure interaction should be taken into account.

From extended laboratory and *in situ* tests it has been concluded that stiffness and damping under cyclic loading are affected primarily by the shear strain amplitude (Figure 10.2). Keeping in mind that v_s measured by *in situ* tests refers to small strain values, it is apparent that for the strain values caused by the design earthquake, which are bigger, a reduction factor should be introduced. EUROCODE 8-5/2004 includes information about these reduction factors of:

- Damping ratio
- Shear wave propagation velocity V_s and
- Shear modulus G_s
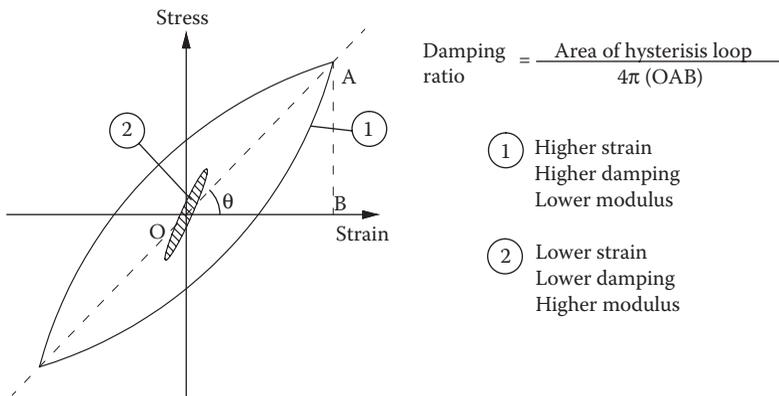
Figure 10.2 The effect of shear strain on damping and shear modulus of soils. (Adapted from Dowrick, D. 2005. *Earthquake Risk Reduction*, John Wiley and Sons, Ltd, Chichester, West Sussex. England.)

Table 10.2 Average soil damping ratios and average reduction factors (± one standard deviation) for shear wave velocity V_s and shear modulus G within 20 m depth

Ground acceleration ratio, $a.S$	0.10	0.20	0.30
Damping ratio	0.03	0.06	0.10
$\dfrac{V_s}{V_{s,max}}$	0.90 (±0.07)	0.70 (±0.15)	0.60 (±0.15)
$\dfrac{G}{G_{max}}$	0.80 (±0.10)	0.50 (±0.20)	0.36 (±0.20)

Source: Adapted from EC8-5/2004. Design of Structures for Earthquake Resistance, Part 5: Foundations, Retaining Structures and Geotechnical Aspects. European Committee of Standardization, CEN, Brussels.

Note: $V_{s,max}$ is the average V_s value at small strain ($<10^{-5}$), not exceeding 360 m/s. G_{max} is the average shear modulus at small strain.

in relation to $a_g.S$ (Table 10.2), where

- a_g is the ratio of the design ground acceleration to the acceleration of gravity, and
- S is the soil factor

For both properties, that is, shear modulus and damping, more information may be found in specialised books on soil mechanics and foundations.

10.2.3 Soil liquefaction

In the previous Paragraph 10.2.1.2, the soil liquefaction phenomenon was briefly outlined. Soil types that are susceptible to liquefaction basically have the following features:

1. They are soils that tend to be densified under induced cyclic shear strains (e.g. geologically young deposits).
2. There is water between the soil particles (e.g. the water table is not deeper than 15.0 m from foundation level; Youd, 1998).
3. A part of the shear strength of the soil is attributable to friction between soil particles (e.g. loose sands and even silts).
4. There are restrictions on the drainage of pore water from the soil (e.g. gravel is not susceptible to liquefaction).

Eurocode EC8-5/2004 makes special recommendations for the analytical assessment, of liquefaction which are beyond the scope of this book.

If soils are found to be susceptible to liquefaction to the degree that the safety of the foundation is endangered, special measures must be taken.

These measures are:

- Ground improvement or
- Piling

Ground improvement is accomplished either by soil compaction to increase soil resistance beyond the dangerous zone, or by the use of drainage.

Pile foundation makes possible the transfer of loads to layers not susceptible to liquefactions. The use of pile foundation alone should be considered with caution due to the large forces induced in the piles by the loss of soil support in the liquefiable layer or layers in combination with the uncertainties of the thickness of such layers.

10.2.4 Excessive settlements of sands under cyclic loading

Sand deposits, even if they are not under water level, are susceptible to densification and to excessive settlements under seismic-induced cyclic stresses. Therefore, when extended layers of loose unsaturated cohesionless materials exist in a small depth below the foundation, special care should be taken for the foundation and the building. The most effective method for limiting these settlements is soil improvement by compaction or grouting.

The densification and settlement potential of the previously mentioned soils should be evaluated properly using analytical models based on parameters justified by static or cyclic laboratory tests (Seed and Idriss, 1982; Kramer, 1996; Kramer and Elgamal, 2001).

The scope of this book does not allow further discussion of this issue.

10.2.5 Conclusions

From what has been presented thus far it may be concluded that the structural engineer, responsible for the analysis and design of major R/C buildings in a seismic region, must have the support of a geotechnical engineer specialised in soil dynamics. This support must cover at least the following issues:

- *In situ* and laboratory tests necessary for ground evaluation
- Soil stratification
- Soil strength parameters, including the influence of the design seismic action
- Soil deformation and damping parameters
- Soil time-dependent deformations (consolidation of clays)
- Soil classification in one of the categories specified by EC8-1/2004 or other relevant Codes
- Susceptibility of soil to liquefaction
- Susceptibility of sandy soils to settlements under seismic excitation
- Recommendations for eventual soil improvement in relation to the recommended foundation system (shallow foundations, pile foundation, pier foundations)

10.3 GENERAL CONSIDERATIONS FOR FOUNDATION ANALYSIS AND DESIGN

10.3.1 General requirements and design rules

In addition to the conceptual design requirements and rules for foundations of conventional buildings, the following should be taken into account for buildings in seismic areas:

1. Gravity loads and seismic actions from superstructures must be transferred to the ground without substantial deformations. Permanent settlements must be compatible with the design requirements of the structure and of preexisting buildings adjacent to the new one. Special care should be taken for the permanent differential settlements, which influence the service limit state of the superstructure.
2. The foundation must be stiff enough in relation to the superstructure so that the localised actions coming from the vertical members (columns—walls) to the ground are uniformly distributed to the ground. In this respect, permanent differential settlements could be minimised.
3. Usually, mixed foundations (e.g. piles with shallow foundations) should be avoided in the same structural system. In fact, the dynamic response of two different foundation parts belonging to the same structural system of the superstructure will differ, so the assumption of the analysis of the superstructure with a base that is uniformly excited is violated. Therefore, mixed foundation types may be used in dynamically independent

units that are in parts of a building separated with structural joints into more than one unit. Only in special cases, where the need of mixed foundations is proved through specific studies, such a solution may be acceptable.

4. Vertical members (columns and walls) must be tied at the level of the foundation to a diaphragmatic disk using tie-beams in the form of a grillage, foundation beams, or a raft so that the uniform seismic vibrations of the base of the building is ensured (see Subsection 4.2.12).

5. Foundations at different levels should be avoided (see Subsection 4.2.12, Figure 4.18).

6. Special care should be taken of the strain dependence of the dynamic properties of soils and of effects related to the cyclic nature of seismic loading.

10.3.2 Design action effects on foundations in relation to ductility and capacity design

10.3.2.1 General

The design action effects on foundations, according to EC 8-5/2004 and EC 8-1/2004, are strongly related to the design considerations of the superstructure in relation to *ductility* level and *capacity* design. So,

- *For dissipative buildings* the action effects for the foundations must be based on capacity design considerations. The basic principle is that the order of formation of yielding mechanisms must stop at the base of the superstructure above the foundations. *Foundation members and ground must remain in elastic range during the seismic excitation* (Figure 10.3a). Alternatively, the ductility mechanism may be extended even to the foundation structural members (Figure 10.3b), but *never to the ground level,* which must always be in elastic range. The above extension of the ductile system to the foundation members should be used with due concern because damaged foundations are retrofitted with great difficultly. The New Zealand concrete code NZS3101/1995 follows a similar concept, while this approach is uncommon in U.S. practice. As is well known, buildings of ductility class M and H (DCM, DCH) belong to the category of dissipative buildings.

- *For non-dissipative buildings* (DCL), the action effects will result from the analysis in the seismic design combination without any capacity design consideration ($q = 1.5$). The above procedure may also be followed for dissipative buildings (DCM, DCH) on
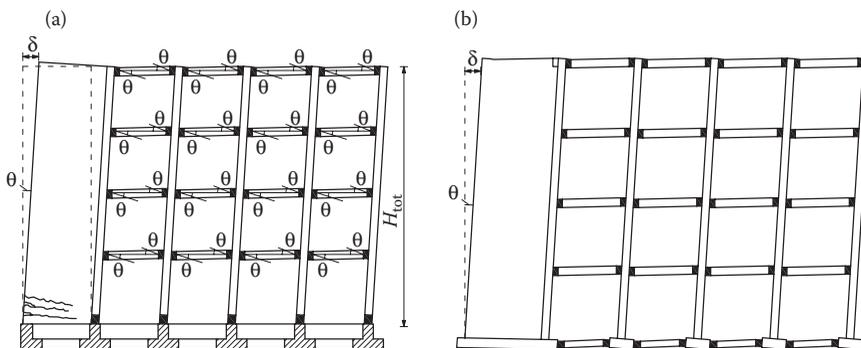
Figure 10.3 Dissipative mechanisms accepted by the Code: (a) dissipative superstructure–non-dissipative foundation mechanism (recomented); (b) dissipative superstructure–dissipative foundations mechanism. (With kind permission from Springer Science+Business Media: Fardis, M.N. 2009. *Seismic Design, Assessment and Retrofitting of Concrete Buildings.*)

the condition that a q factor equal to 1.50 is introduced for the design of foundation members and ground. This is based on the reasonable consideration that capacity design effects cannot overcome those corresponding to $q = 1.50$.

10.3.2.2 Design action effects for various types of R/C foundation members

R/C foundation members, that is, *footings, tie-beams, foundation beams, foundation slabs, pile caps* and *piles,* as well as the joints between them and the vertical structural R/C elements of the buildings, are analysed and designed according to EC8-1/2004 following rules, which result from the conceptual approach of the previous paragraph.

1. *Dissipative superstructure – non-dissipative foundation elements and foundation ground.*
   a. For dissipative buildings (DCM or DCH), foundations of structural walls or of columns of moment-resisting frames are analysed for the following design actions effects E_{Fd}:

$$\boxed{E_{Fd} = E_{F,G} + \gamma_{Rd}\, \Omega\, E_{F,E}}$$

(10.3)

where
   γ_{Rd} is the overstretch factor taken as being equal to:

$$\boxed{\begin{aligned} \gamma_{Rd} &= 1 && \text{for } q \leq 3 \\ \gamma_{Rd} &= 1.2 && \text{for } q \geq 3 \end{aligned}}$$

(10.4)

   $E_{F,G}$ is the action effect due to the non-seismic actions included in the seismic combinations.
   $E_{F,E}$ is the action effect from the analysis of the design seismic action.
   Ω is the value of $R_{di}/E_{di} \leq q$ of the dissipative zone or element of the structure.
   R_{di} is the design resistance of the zone or element i.
   E_{di} is the design value of the action effect on the zone or element i in the seismic design situation.
   b. For foundations of independent walls or columns:

$$\boxed{\Omega = \min of \left\{ \frac{M_{Rd,x}}{M_{Ed,x}}, \frac{M_{Rd,y}}{M_{Ed,y}} \right\}}$$

(10.5)

   in the two orthogonal principle directions in the seismic design situation.
   c. For common foundations of more than one vertical element (e.g. foundation beams, rafts etc.), Ω is derived from the vertical element with the largest horizontal shear force in the design seismic situation, or, alternatively, a value for $\gamma_{Rd}\Omega$ is introduced in Equation 10.3 equal to

$$\boxed{\gamma_{Rd}\Omega = 1.40}$$

(10.6)

   It is apparent that in the case that:

$$\frac{q_{design}}{\gamma_{Rd}\Omega} \leq q(DCL)$$

(10.7a)

that is,

$$\frac{q_{\text{design}}}{1.40} \leq 1.50 \tag{10.7b}$$

or

$$\boxed{q_{\text{design}} \leq 2.10} \tag{10.8}$$

the design action effects for the seismic design situation, as was also previously noted, may be derived for a q factor value equal to 1.50 for the foundation members and foundation ground.

d. The design of the above foundation elements *except for concrete piles* will be dimensioned and designed following the design rules for DCL buildings that are without any requirement for ductility or capacity design. In fact, according to what has been presented in the previous paragraph, no energy dissipation is expected in these elements.

e. The same also holds for the verification and dimensioning of the foundation ground. This is carried out under the assumption that the ground under the capacity design effects of item (1) (Equation 10.3) *responds linearly*.

2. *Dissipative superstructure and dissipative foundation elements – non-dissipative foundation ground.*

a. In the case that the alternative solution of a complete dissipative structural system (DCM or DCH) is decided on by the designer, as far as the superstructure and *the foundation elements* are concerned, the capacity coefficient $\gamma_{\text{Rd}}\Omega$ is taken in Equation 10.3 to be equal to

$$\boxed{\gamma_{\text{Rd}}\Omega = 1.0} \tag{10.9}$$

that is, the design action effects of the foundation elements are derived on the basis of the analysis of the seismic design situation. In this case, the design and dimensioning of the foundation R/C members is carried out according to the ductility and capacity rules that have been followed for the superstructure.

b. Action effects for dimensioning and design of *foundation ground* must be increased to values given by Equations 10.4 through 10.6, since ground must be kept in linear range for these action effects so that dissipative mechanisms and, therefore, inelastic deformations are not derived in the foundation ground.

3. *Non-dissipative superstructure – non-dissipative foundation elements and foundation ground.*

This case refers to DCL buildings where q factor is assumed to be equal to 1.5 for an R/C structural system. For these buildings, the action effects, as was mentioned previously (par. 10.3.2.1), will result from the analysis in the seismic design combinations without any capacity design consideration. In this case, the whole structural system will be dimensioned and designed with the procedure followed for DCL structural systems, while the ground should be considered also to respond elastically.

4. *Box-type basements of dissipative structures*

As was noted in Subsection 4.2.12 on the conceptual design of R/C buildings to seismic actions, this type of basement comprises (Figure 10.4):

a. A concrete slab at the roof of the basement

b. A foundation slab (raft foundation) or a grillage of tie-beams connecting foundation pads or pile caps or foundation beams at foundation level, and
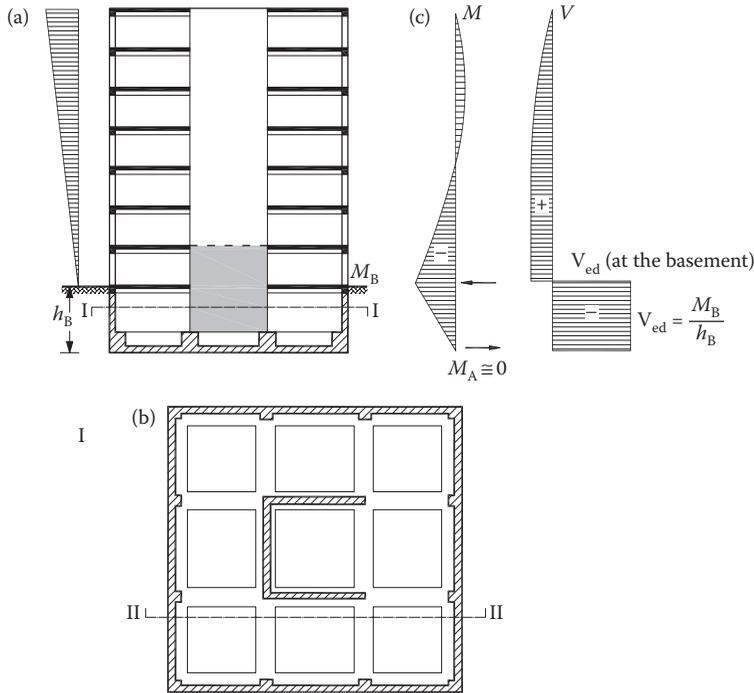
Figure 10.4 Box-type basement and its structural behaviour in relation to the superstructure (dual-system): (a) elevation; rastered area is considered to be the critical region for ductile behaviour; (b) plan view at basement; (c) M_{Ed}, V_{Ed} diagrams of the structural wall core.

    c. Perimetric and eventually interior walls, designed in the superstructure above the basement roof as dissipative structures.

This box-type basement constitutes a very robust and stiff foundation system that minimises

- Differential settlements
- The risk of overturning failure, since the integral foundation acts as a box-like structure
- Sliding risk due to the additional activation of passive resistance of the surrounding ground in the case that a small slide is tolerated.

However, special care should be taken of the uplift risk in the case that the level of underground water is expected to be above the contact surface of the foundation slab and ground.

In this system the *columns* and *beams* (including those of the basement roof) are expected to remain elastic under the seismic design situation. Therefore, they may be designed in the framework of the box as DCL structures without special measures for ductile behaviour and capacity design procedure. Conversely, *structural walls* should be designed for plastic hinge development at the level of the basement roof slab with a critical region also extending downward in the basement (Figure 10.4a).

Moreover, the full free height of these walls within the basement should be dimensioned for shear, assuming that the wall develops its flexural strength $\gamma_{Rd}M_{Rd}$ (with $\gamma_{Rd} = 1.1$ for DCM and $\gamma_{Rd} = 1.2$ for DCH) at the basement roof level and zero moment at the foundation level.

In conclusion, it should be noted that the analysis of the box-type basement must be carried out for seismic loadings magnified by $\gamma_{Rd}\Omega$ (Equation 10.6) so that its elastic behaviour is ensured.

10.4 ANALYSIS AND DESIGN OF FOUNDATION GROUND UNDER THE DESIGN ACTION EFFECTS

10.4.1 General requirements

The design action effects due to gravity loads at service and to seismic combination must be transferred to the ground without substantial permanent settlements (SLS), that is, they must be compatible with the functionality requirements of the superstructure.

At the same time, the foundation ground must be ensured against *failure* caused by the basic combination of gravity loads introduced with the codified partial safety coefficients as well as the 'seismic combination' (ULS).

It should be noted that in addition to the ground resistance at the base of the foundation, friction shear developing between the side of the foundation body and the ground in the case that the foundation body is embedded in the ground, could be taken into account.

10.4.2 Transfer of action effects to the ground

For transferring the design action effects, that is, *shear forces,* on one hand, and *normal forces combined with bending moments* on the other, to the ground, the following mechanisms may be taken into consideration. For piles, additional mechanisms are taken into account, which will be presented in an independent paragraph.

10.4.2.1 Horizontal forces

The design horizontal shear effect V_{Ed} is transferred by the following mechanisms:

1. By means of a design shear resistance F_{Rd} developed between the horizontal base of the footing of the foundation slab of foundation raft and the ground (Figure 10.5a,b).
2. By means of the design lateral shear resistance E_{pd} arising from earth pressure on the vertical sides of the foundation parallel to V_{Ed} (Figure 10.5a,b).
3. By means of the design resisting earth pressure on the other sides of the foundation transversally to V_{Ed} (passive earth resistance—earth pressures at rest).
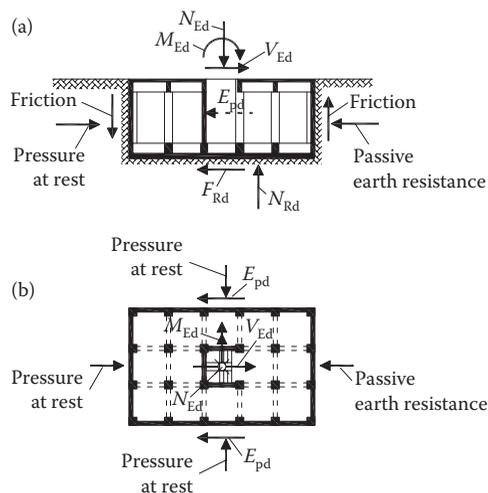
Figure 10.5 Mechanisms for transferring design action effects V_{Ed}, M_{Ed}, N_{Ed} to the ground: (a) elevation; (b) plan view.

It should be noted that a combination of the shear resistance with up to 30% of the resistance arising from fully developed passive earth pressure is allowed according to EC8-5/2004.

10.4.2.2 *Normal force and bending moment*

Normal force N_{Ed} and bending moment M_{Ed} may be transferred to the ground by means of one or a combination of the following mechanisms (Figure 10.5a,b):

1. By the design value of resisting vertical forces acting at the base of the foundation (Figure 10.5a,b).
2. By the design values of bending moments developed due to the design horizontal shear resistance between the sides of deep foundations like box-type basements and the ground (Figure 10.5a,b).
3. By the design value of vertical shear resistance between the sides of embedded deep foundation elements (box-type basements) and the ground (Figure 10.5a,b).

The last two contributions must be ensured with special measures relating to the formation of the backfill of the excavation, so that the development of shear resistance between backfill and the sides of the foundation may be ensured. The above last two contributions are taken into account only in special cases, like those of very high buildings with large aspect ratios h_w/l_w of total height h_w to horizontal length l_w, which cannot be counterbalanced easily by the reactions between the foundation base and the ground.

10.4.3 Verification and dimensioning of foundation ground at ULS of shallow or embedded foundations

10.4.3.1 *Footings*

Footings at ultimate limit state are verified and dimensioned at the level of the ground foundation against sliding and bearing capacity failure.

10.4.3.1.1 Failure by sliding

1. The design shear resistance F_{Rd} between the horizontal base of the footing or of the foundation slab and the ground above the water table may be calculated according to EC8-5/2004 from the following expression:

$$F_{Rd} = N_{Ed} \frac{\tan \delta}{\gamma_m} \qquad (10.10)$$

   where
   N_{Ed} is the design normal force on the horizontal base.
   δ is the structure–ground interface friction angle at the base of the footing.
   γ_m is the partial factor for material property equal to $\gamma'_{\varphi} = 1.25$ (Equation 10.1).
   For footings below the water table the design shear resistance is evaluated on the basis of undrained strength.
2. The design lateral resistance E_{pd} arising from earth pressure on the sides of the foundation and the ground (Figure 10.4a,b) E_{pd} may be calculated by the following expression:

$$E_{pd} = E_d \frac{\tan \delta}{\gamma_m} \qquad (10.11)$$

where

E_d is the earth pressure at rest soil state without static and hydrodynamic water force (see EC8-5/2004 ANNEX E).

It is apparent that appropriate measures must be taken on site, such as the compaction of backfill against the sides of the footing so that E_d develops.

From what has been presented above, it may be concluded that the safety verification criterion for sliding may be formed as follows:

$$V_{Ed} \leq F_{Rd} + E_{pd} \tag{10.12}$$

The mobilisation of sliding shear between foundation and ground supposes the development of a limited amount of sliding. This amount is tolerated provided those special measures are taken for the performance of lifelines connected with the building.

10.4.3.1.2 Bearing capacity of ground to failure

The bearing capacity verifications of the foundation ground under N_{Ed}, M_{Ed} and V_{Ed} for footings, raft foundations or a grillage of foundation beams are carried out by methods that have been developed for many years in soil mechanics (Hansen and Brinch, 1961; Meyerhof, 1965; Anagnostopoulos et al., 1994; Terzaghi et al., 1996). EC8-5/2004, in its Annex F, gives expressions for this verification, the detailed presentation of which exceeds the scope of this book.

It should be noted that N_{Ed}, M_{Ed} and V_{Ed} introduced to the bearing capacity verifications of ground are either the original design values derived as reactions of the foundation from the superstructure properly modified to take into account the capacity design procedure or they are reduced values derived after the subtraction of the soil shear friction resistance at the sides of the foundation in the case that these restoring forces are taken into consideration. The same applies for the weight of removed soils in case of deep excavations.

10.4.3.2 Design effects on foundation horizontal connections between vertical structural elements

10.4.3.2.1 General

As has been already noted many times, analysis reasons and good performance to seismic action require the provision of horizontal connections at the base of vertical members (columns–walls) so that relative displacements at their bases are excluded.

The above conceptual requirement is fulfilled if the foundation ground for all vertical members is positioned at the same horizontal level and a tie-beam grillage or a grillage of foundation beams or an adequate foundation slab are provided at the level of footings or pile caps (Figure 10.6). In this respect, and keeping in mind that from the analysis no action effects are derived at these ties, since the base vibrates in two main directions during the seismic action as a solid diaphragm, it is apparent that these design action effects must be defined explicitly by the Code.

10.4.3.2.2 Tie-beams

According to EC8-5/2004, tie-beams or a connecting slab may be omitted only in the following cases:

- Foundation ground Type A and
- In low seismicity cases, for foundation ground Type B
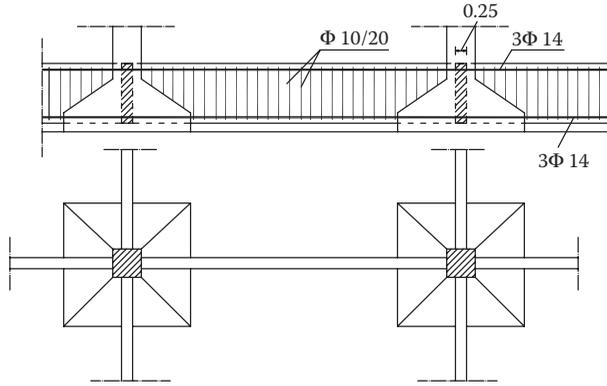
Figure 10.6 Independent footings with a tie-beams grillage.

In all other cases the tie-beams are designed to resist an axial force with reversed sign equal to

- For ground type *B*: $\pm 0.3 \cdot \alpha \cdot S \cdot N_{\text{Ed}}$
- For ground type *C*: $\pm 0.4 \cdot \alpha \cdot S \cdot N_{\text{Ed}}$
- For ground type *D*: $\pm 0.6 \cdot \alpha \cdot S \cdot N_{\text{Ed}}$ (10.13a–c)

where

N_{Ed} is the mean value of the design axial forces of the connected vertical members in the seismic design situation (see Subsection 4.2.12, Figure 4.17); Values *a* and *S* have already been defined in Paragraph 3.4.2.2.

10.4.3.2.3 Foundation slab

Tie-zones should be designed to resist axial tensile or compressive forces equal to those of tie-beams (Equation 10.13a–c). The width of these zones may be estimated at *ten times* their thickness.

10.4.3.3 Raft foundations

A raft foundation for the sliding or bearing capacity failure verification may be considered a solid footing loaded by V_{Edi}, N_{Edi}, M_{Edi} of all vertical members acting at their connection to the raft foundation. The same holds in case of a grillage of foundation beams.

It is apparent that in this case the slab of the raft foundation or the foundation beams also act as tie beams, and in this respect must be dimensioned additionally for axial load effects equal to those given by Equation 10.13a–c). The width of the connecting zone may be taken as *ten times* its thickness.

10.4.3.4 Box-type foundations

This type of foundation is considered a solid body (footing) for the verification and dimensioning of the foundation ground. It must be remembered that seismic loading should be magnified by $\gamma_{\text{Rd}}\Omega$ (Equation 10.6), so that its elastic behaviour may be ensured. It should also be noted that this type of foundation is the most proper for shear friction forces developing on the sides of the box and resulting from the earth pressure to be taken into account, so that the load effects at the horizontal base may be significantly reduced.

10.4.4 Settlements of foundation ground of shallow or embedded foundations at SLS

10.4.4.1 General

It should be remembered that the analysis and design of foundation ground is carried out under the assumption that it remains in elastic range. It is beyond the scope of this book to undertake a rigorous treatment of methods for estimating the expected settlements and rotations of the foundation ground under loading effects. However, an overview of this issue will be necessary, especially for the analysis and design of the structural members of the foundation.

10.4.4.2 Footings

Under the assumption that an orthogonal footing is a rigid body based on a homogeneous ground, the expected settlement and rotation are given by expressions that are functions of the shear modulus G, the Poisson's ratio ν and the dimensions of the foundations. These expressions are based on the 'half space' Boussinesq theory properly modified to comply with experimental results. So, for example, according to Whitman and Richart (1967):

$$\Delta_z = \frac{N_{Ed}}{K_z} = N_{Ed}\left(\frac{G}{1-\nu}\beta_z\sqrt{BL}\right)^{-1} \tag{10.14}$$

$$\Delta_x = \frac{V_{Ed,x}}{K_x} = V_{Ed,x}\left(2G(1+\nu)\beta_x\sqrt{BL}\right)^{-1} \tag{10.15}$$

$$\Delta_{\varphi y} = \frac{M_{Ed,y}}{K_{\varphi y}} = M_{Ed,y}\left(\frac{G\beta_\varphi BL^2}{1-\nu}\right)^{-1} \tag{10.16}$$

where
- B, L are the dimensions of the footing.
- β_z, β_x, β_φ are factors related to the dimensions B and L of the footing and given by the diagram depicted in Figure (10.7b).
- G, ν are the modulus of shear and the Poisson's ratio, respectively.
- K_z, K_x, $K_{\varphi y}$ are the spring constants (Figure 10.7a).
- N_{Ed}, $V_{Ed,x}$, $M_{Ed,y}$ are the design load effects on the footing.
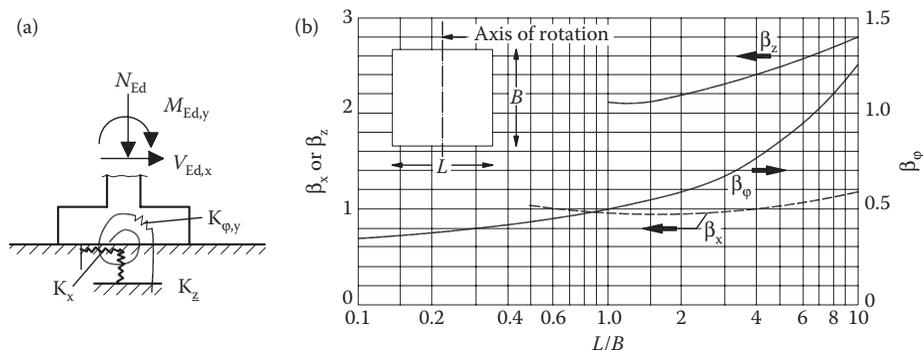
Figure 10.7 Load effects on a footing and stiffness simulation of the ground by elastic springs: (a) structural model; (b) coefficients β_x, β_z and β_φ, for estimating spring stiffness of rectangular footings. (From Dowrick, D. 2005. *Earthquake Risk Reduction.* Copyright Wiley-VCH Verlag GmbH & Co. KGaA. Reproduced with permission.)

Spring constants K_z, K_x, $K_{\varphi y}$ may be introduced as restraints in the analysis of the super-structure and the foundation, considered as an integrated system.

Representative values of G for seismic conditions are given in Table 10.1 of this chapter.

In the case that successive strata of soil underlying the foundation base have different mechanical properties, determined by lab tests, the simplest and most modern way to determine K_z, K_x, K_φ is to use a proper computer platform (e.g. PLAXIS-2D, 2012) that allows the determination of the settlement Δ_z, the sliding Δ_x and the rotation Δ_φ of the footing for a given group of loading effects N_{Ed}, M_{Ed}, V_{Ed} and then to generate the ratios N_{Ed}/Δ_z, $V_{Ed,x}/\Delta_x$, $M_{Ed,y}/\Delta_{\varphi y}$, which represent K_z, K_x, $K_{\varphi y}$. It should be noted that for many decades this procedure was carried out through extended tiresome manual calculations (Anagnostopoulos et al., 1994; Terzaghi et al., 1996).

10.4.4.3 Foundation beams and rafts

For the determination of the mean value of settlements Δ_z of the ground below a foundation beam or a raft, equations in effect for footings may be used (Equation 10.14). Keeping in mind that the lab tests output result is usually E_s instead of G_s, Equation 10.14 takes the form:

$$\Delta_z = \frac{N_{Ed}}{K_z} = N_{Ed}\left(\frac{E_s}{2(1-\nu^2)}\beta_z B\sqrt{\frac{L}{B}}\right)^{-1} \tag{10.17}$$

The above expression is used as a tool for the determination of *sub-grade modulus* or *'Winkler constant'*, which is necessary for the determination of the distribution of the soil reaction in the form of stresses on the foundation beam, so that internal forces M_{Ed} and V_{Ed} of the foundation beam may be determined (Figure 10.8).

It is well known that according to the Winkler approach, which is the most common assumption for the analysis of foundation beams or rafts, foundation ground is simulated with independent springs (Figure 10.9), the settlement Δ_z of which is given by the expression:

$$\boxed{q_o = \bar\kappa_s \Delta_z} \tag{10.18}$$
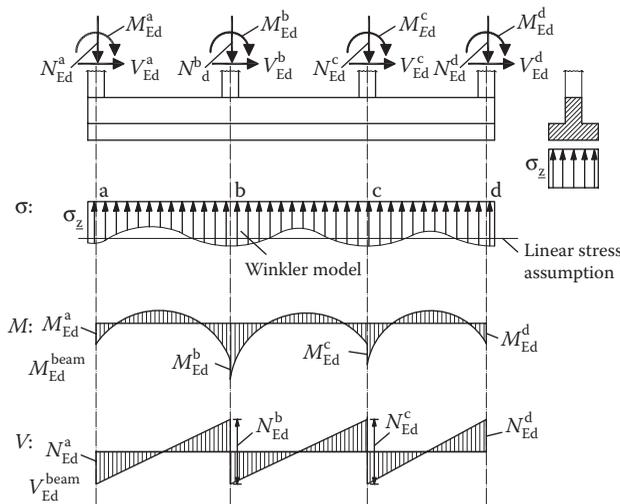
Figure 10.8 Ground reactions σ_z on a foundation beam and internal forces diagram.

where
q_o is the compression of the foundation ground expressed in [MPa].
Δ_z is the settlement in [m] of the point where q_o is induced.
$\overline{\kappa}_s$ is the *sub-grade modulus* in [MN/m³].

Using Equation 10.17 and taking into account that:

$$N_{Ed} = q_o LB \tag{10.19}$$

it follows that

$$\Delta_z = q_o LB \left(\frac{E_s}{2(1 - v^2)} \beta_z B \sqrt{\frac{L}{B}} \right)^{-1} \tag{10.20}$$

Therefore,

$$\boxed{\overline{\kappa}_s = \frac{E_s}{(1 - v^2)B} \rho} \tag{10.21}$$

where

$$\rho = \frac{0.5\beta_z}{\sqrt{L/B}} \tag{10.22}$$

For various ratios of (L/B), ρ takes the values given in Table 10.3. A very common expression for $\overline{\kappa}_s$ is given below (Anagnostopoulos et al., 1994):

$$\boxed{\overline{\kappa}_s = \frac{E_s}{B}} \tag{10.23}$$

where
B is the shorter dimension of the orthogonal foundation base.
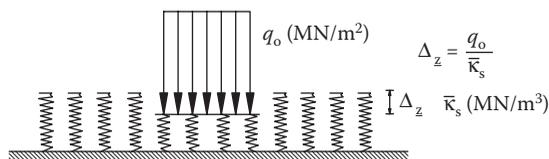
Figure 10.9 Ground simulation according to the Winkler model.

Table 10.3 ρ Values for various L/B ratios

L/B	1.0	1.50	2.0	3.0	5.0	10.0	20.0	30.0
ρ	1.05	0.86	0.78	0.66	0.56	0.44	0.39	0.33

10.4.5 Bearing capacity and deformations of foundation ground in the case of a pile foundation

10.4.5.1 General

Piles and piers are usually designed to resist the following two types of action effects:

1. *Inertia forces* due to seismic action from the superstructure combined with gravity loads (N_{Ed}, V_{Ed}, M_{Ed})
2. *Kinematic forces* caused by soil deformations during the passage of the seismic waves through the region of the foundation. This second type of forces is taken into account only in the case that all conditions mentioned below are in effect simultaneously:
   a. The ground profile is of type D, S_1 and S_2, including soil strata of sharply different stiffness
   b. The building's zone is not of low seismicity ($\alpha_g S$ is higher than 0.10 g) and
   c. The building is of importance class III or IV

In this respect, this second type of forces may be considered an unusual load case that is taken into consideration in special cases. Therefore, in this short overview of pile foundations it will not be analysed. The ultimate load resistance of the ground to vertical and horizontal loading is verified according to rules included in EC7-1/2004, which refers to foundation issues. Although pile foundations are beyond the scope of this book, a short overview will be given so that the way in which the pile restraints are introduced to the model for the analysis of the foundation and the superstructure may be clarified.

The design resistance of an R/C pile at the ULS is defined by the load capacity of the soil around the pile and by the load capacity of the body of the pile. Therefore, the action effects on the top of the pile must fulfill the following two groups of inequalities:

$$\{N_{Ed}, M_{Ed}, V_{Ed}\} \leq \begin{cases} N_{Rd}^s, M_{Rd}^s, V_{Rd}^s & \text{10.24a} \\ N_{Rd}^p, M_{Rd}^p, V_{Rd}^p & \text{10.24b} \end{cases} \qquad (10.24)$$

where symbol *s* refers to soil and *p* to piles.

10.4.5.2 Vertical load resistance and stiffness

The normal force resistance of a pile is determined analytically and in most cases there is a Code requirement to be verified by trials *in situ*. Computationally, this resistance includes two components (Figure 10.10):

1. The base resistance

$$R_{bd} = R_{b\kappa}/\gamma_b \qquad (10.25a)$$

2. The shaft resistance

$$R_{sd} = R_{s\kappa}/\gamma_s \qquad (10.25b)$$

where γ_b and γ_s are partial safety factors with recommended values given in EC7-1/2004.

For the determination of $R_d\kappa$ and $R_s\kappa$, various methods have been developed (Terzaghi et al., 1996; Anagnostopoulos et al., 1994; Dowrick, 2005).
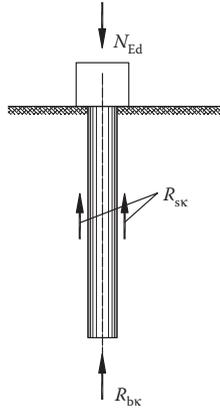
Figure 10.10 Base and shaft reactions $R_{b\kappa}$ and $R_{s\kappa}$ of a pile, respectively.

Very useful information on this issue is included in DIN 4014/1990 (B.K. 1994), the German Code for bored piles. In this Code, detailed information is given for the elaboration of $R_c - \Delta_z$ diagrams, which relate the settlements of the pile to its base and shaft resistance (Figure 10.11).

For the elaboration of these two diagrams of R_s, R_b and their resultant curve R_c, codified tables are used to relate the soil mechanical properties to the base and shaft resistance of the pile for critical settlements of the pile-head given by the Code. Thus, the $R_{c\kappa}$ is the result of the sum of $R_{b\kappa}$ and $R_{s\kappa}$ for an ultimate settlement equal to 010D, where D is the pile diameter. Thus,

$$R_{c\kappa} = R_{b\kappa} + R_{s\kappa} \tag{10.26}$$

It is obvious that after these calculations partial safety factors must be introduced. It should be noted that this diagram must be verified by tests *in situ*.

The above outlined procedure also allows the determination of the spring stiffness of the pile κ_z^p for the vertical settlements.

In fact, keeping in mind that:

$$R_c = \kappa_z^p \Delta z \tag{10.27}$$
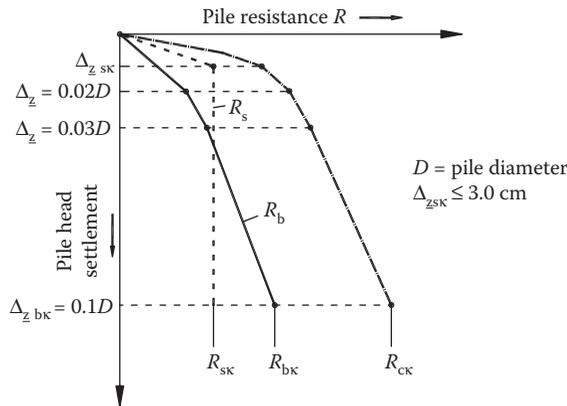
Figure 10.11 $R_c - \Delta z$ curve according to DIN 4014/1990.
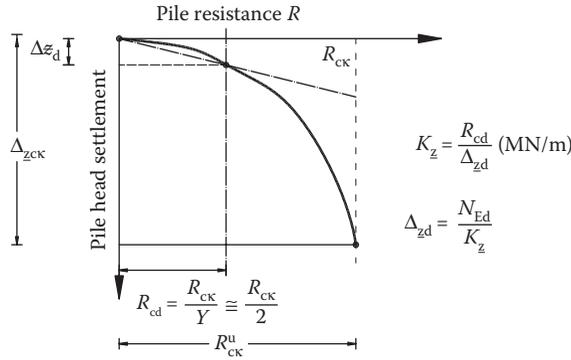
Figure 10.12 Determination of the axial spring stiffness of a pile from an $R - \Delta z$ diagram.

it follows that κ_z^p may be derived from the $R_c - \Delta z$ diagram using the relation (Figure 10.12):

$$\kappa_z^p = \frac{R_{cd}}{\Delta z_d} \tag{10.28}$$

where

R_{cd} is the design resistance of the pile.

Δz_d is the settlement of the pile corresponding to R_{cd} and taken from the diagram of Figure (10.12; secant modulus).

The above crude approach to the stiffness of piles in axial direction may be replaced by more refined computational methods using proper computer platforms (e.g. PLAXIS-2D, 2012).

10.4.5.3 Transverse load resistance and stiffness

For the analysis of the ground surrounding pile and for the analysis and design of the body of the pile, proper models are elaborated for loading of the pile-head with a bending moment M_{Ed} and a shear force V_{Ed}. The results of the analysis contain:

- Flexural stiffness of the pile-ground interaction
- Soil reactions along the pile
- Pile-to-pile dynamic interaction (dynamic pile-group)

To verify that a pile is in position to carry the design transverse load and bending moment with adequate safety according to EC7-1/2004, one of the following failure mechanisms should be considered:

- For short piles, rotation and displacements as a rigid body (Figure 10.13)
- For long piles, bending failure of the pile accompanied by local yielding and displacement of the soil near the top of the pile (Figure 10.14)

For the determination of M_{Rd}^s, V_{Rd}^s at the pile head, simplified models have been developed, accompanied by relevant diagrams and tables (Dowrick, 2005; Anagnostopoulos et al., 1994), the presentation of which exceeds the scope of this book.

At the same time, computational methods have been developed allowing the determination of M_{Rd}^s, V_{Rd}^s, the corresponding horizontal displacements Δx, bending rotations $\Delta\varphi$, the
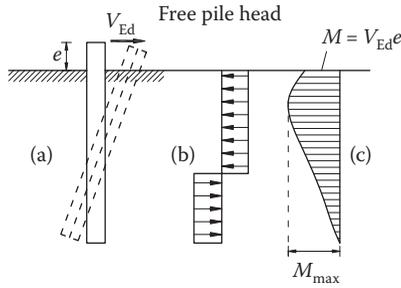
Figure 10.13 Short pile response to V_{Ed} loading in cohesive soil: (a) load pattern—deflections; (b) soil reactions; (c) pile bending moments.

horizontal soil reactions on the pile and its internal forces M_{Rd}^p and V_{Rd}^p. The most common method is that of a beam on elastic sub-grade based on the Winkler assumption already presented in the case of foundation beams. Keeping in mind that the Winkler method assumes linear soil behaviour, it is obvious that the reversal of Δx and $\Delta \varphi$ for $M_{Ed} = "1"[KNm]$ and $V_{Ed} = "1"[KN]$ gives the head stiffness of the pile that may be introduced in the analysis of the foundation of the building (Figure 10.15).
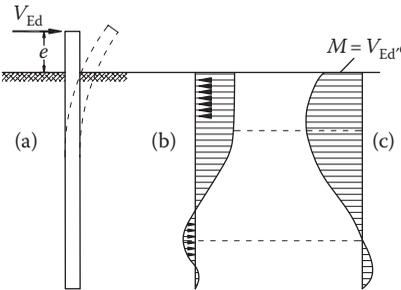
Figure 10.14 Long pile response to V_{Ed} loading in cohesive soil (a) load pattern—deflections; (b) soil reactions; (c) pile bending moments.
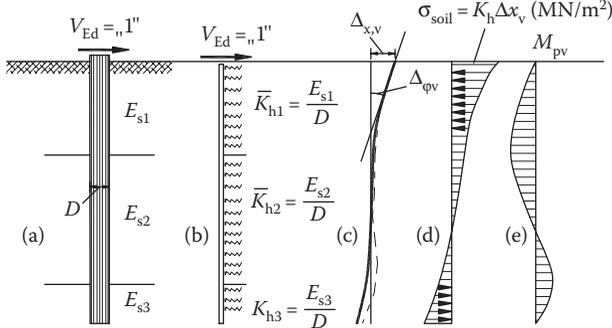
Figure 10.15 Response of a long pile to $V_{Ed} = {}_{,,}1"$ using the Winkler model: (a) soil layers and pile position; (b) 'Winkler' model; (c) soil stiffness $\bar{K}_{vv} = ({}_{,,}1"/\Delta x_v), K_{\varphi v} = ({}_{,,}1"/\Delta \varphi_v)$; (d) soil reactions $\sigma_{soil} = \bar{K}_h \Delta x_v (MN/m^2)$; (e) pile bending moments.

The *horizontal sub-grade modulus* $\bar{\kappa}_{sh}$ (Figure 10.15) along the pile axis for each soil layer may be determined by the following relation (DIN 4014/1990):

$$\bar{\kappa}_{h} = \frac{E_{sh(z)}}{D} \qquad (10.29)$$

where
  E_{sh} is the soil modulus of elasticity with a usual value equal to 50% of E_s in the vertical direction and
  D is the pile diameter.

According to DIN4014/90, the failure criterion of soil for the determination of M_{Rd}^{s} and V_{Rd}^{s} is defined by the condition that the soil reactions to the pile should not exceed the passive strength of the soil, that is,

$$\boxed{\sigma_{u} = \kappa_{p} \cdot z} \qquad (10.30)$$

where
  σ_{u} is the ultimate value of soil reaction on the pile:

$$\kappa_{p} = \tan^{2}\left(\frac{\varphi}{2} + 45^{0}\right) \qquad (10.31)$$

  φ is the angle of soil internal friction.

In case of homogeneous soil, the soil modulus of elasticity may very with the depth z from the soil surface to the pile base with one of the following expressions:

$$E_{s(z)} = E_s\, z/D \text{ (linear)} \qquad (10.32a)$$

$$E_{s(z)} = E_s \text{ (constant)} \qquad (10.32b)$$

$$E_{s(z)} = E_s\sqrt{z/D} \text{ (parabolic)} \qquad (10.32c)$$

where
  E_s is the modulus of elasticity of soil at a depth of D
  D is the pile diameter, and
  z is the depth of reference along the pile.

In this case, the *pile head stiffness* $K_{H,H}$, K_{MM} and $K_{HM} = K_{MH}$ may be found in a closed form in EC8-5/2005 Annex C.

It should be noted that in the above calculations for the determination of the bearing capacity of the foundation ground around the pile and the horizontal displacements and rotations of the pile head, the side resistance of the soil layers that are susceptible to liquefaction or to substantial strength degradation should be ignored.

10.5 ANALYSIS AND DESIGN OF FOUNDATION MEMBERS UNDER THE DESIGN ACTION EFFECTS

10.5.1 Analysis

10.5.1.1 Separated analysis of superstructure and foundation

Until recently and even nowadays the most usual method for the analysis and design of foundations has been the following:

1. The superstructure is analysed and designed under the assumption of fixed-end columns and walls at the level of foundation.
2. The action effects (N_{Ed}, M_{Ed}, V_{Ed}) of the fixed ends of vertical members are used as loads for the foundation. For these loads, ULS and SLS verification is carried out:
   a. For the foundation ground and
   b. For the structural members of the foundation

EC8-1/2004 permits the above procedure for modelling of the superstructure. However, in the case that the deformability of the foundation has an adverse overall influence on the structural response, the participation of the ground deformability in the formation of a model for dynamic analysis is obligatory.

For many decades the basic assumption for the stress distribution of the ground reaction on the foundation members was the concept of *'planar stress distribution'*. It should be noted that this stress distribution is necessary for the determination of the internal forces (M_{Ed}, V_{Ed}) of foundation members so that their dimensioning and design is possible. It is apparent that using the information presented in subsections 10.4.3 and 10.4.4 that the verification and design at ULS and SLS may be carried out for the ground and the foundation members.

After the introduction of computer techniques in analysis and design in the early 1950s, a simplified system of linear reaction springs was introduced for soil simulation, the well-known Winkler model, which has been discussed in detail in the preceding subsections.

In this respect, a more reliable model of soil reaction distribution has been introduced, which allows a more reliable determination of the internal forces of the foundation members and of the developing differential settlements than the 'planar stress distribution'.

The *sub-grade modulus* of the foundation ground, and the pile head stiffness or footing stiffness, are calculated separately using the procedures presented in subsections 10.4.4 and 10.4.5 and are introduced as restraints at the surface of the foundation. It should be noted that soil springs must have *unilateral compressive* reactions. In this respect, in the case that the analysis output includes tensile reactions in various positions, an interactive procedure should be adapted and carried out manually from step to step or automatically if a proper computer platform is available. In any case, at the successive steps the springs of tensile reactions are deactivated before the next step iteration is carried out.

In foundation modelling the following cases may be met with:

1. *Footing tied with tie-beams or a slab*
   In this case the foundation is modelled as a linear space structural system with offsets at the joints of the vertical elements to simulate the footing. In this system, spring constants κ_z, κ_x, κ_y, $\kappa_{\phi x}$, $\kappa_{\phi y}$ are introduced at the joints, simulating the ground stiffness (see Paragraph 10.4.4.2).

2. *Foundation beams or rafts*

Foundation beams are usually simulated as foundation straps using the FEM procedure supported on the ground, which is simulated by springs with a sub-grade modulus defined according to what has been presented in Paragraph 10.4.4.3 (Equations 10.21, 10.23). These straps are connected at the joints of the mesh with the beams of the foundation. It should be noted that the straps and the beam are considered to be interconnected at the centre line of the beam so that the developing bending moment of the beam is not divided in one part as bending moment and a second one as two equal internal axial forces with opposite sign, one at the centre of the beam and the other in the strap.

Depending on the available computing platform, the *sub-grade modulus* $\overline{\kappa}_s$ is introduced either as the sub-grade modulus of a continuous support system (see Paragraph 10.4.4.3) or as a concentrated spring at the joints of the FEM mesh. In this case, the concentrated spring constant $\kappa_{(z)}$ is introduced with a value equal to

$$\boxed{\kappa_{(z)} = \overline{\kappa}_s \cdot a \cdot b}$$

(10.33)

where

a, b are the dimensions of the mesh of finite elements.

The same procedure is followed in the case of a raft foundation.

3. *Pile foundation tied with tie-beams or slab*

In the case of piled foundations, their structural system is simulated as a linear space structure with offsets at the joints of the vertical elements to simulate the pile cup. In this system spring constraints K_{MM}, $K_{MH} = K_{HM}$, K_{HH} are introduced at the joints, simulating the interacting stiffness of ground and piles (see Paragraph 10.4.5.2 and 10.4.5.3) in the form of pile-head stiffness. In the case of groups of piles it is advisable to replace the stiffness of each pile group by an integrated stiffness (EC7-1/2004) for each pile group.

10.5.1.2 Integrated analysis of superstructure and foundation (soil–structure interaction)

In the past decade the rapid development of computer techniques has allowed the unification of the analysis and design of the superstructure and foundation of a building in an integrated model, also including the elastic springs of the foundation ground in the form in which they have been presented in the previous paragraph. In this respect an approximate reliable simulation of the soil–structure interaction has been accomplished, since the influence of the differential settlements of the foundation at the joints with the vertical members of the superstructure is taken into account in the analysis and design of the integrated system 'sub-grade foundation–superstructure'. At the same time, the integrated approach of the whole system has made the elaboration of input information simpler, since there is no need for using the output of the superstructure analysis as input for the foundation. EC8-1/2004 requires that the soil–structure interaction should be taken into account in the case that this parameter leads to adverse results for the structural response. On the other hand, Code *allows* this procedure, even if this approach leads to beneficial results of the structural response.

In conclusion, it should be noted that in the procedure presented thus far, the influence of soil damping has not been taken into account, nor have the ground inertial forces. In fact, in the implementation of the modal response spectrum analysis, which is according to EC8-1/2004, the 'reference method', it is not possible to introduce different damping values for the various members of the structure since a common design response spectrum is used.

Therefore, if the soil damping was going to be taken into account, a composite new viscous damping ratio $\bar{\zeta}$ should be introduced in the calculation of the design spectrum ordinates instead of the viscous damping ratio ζ of the structure (see Subsection 3.4.3). This procedure has been elaborated by Veletsos and Nair (1975) and Veletsos and Meek (1974) and is presented in detail by Dowrick (2005).

In any case, for the majority of common building structures the effects of soil–structure interaction tend to be beneficial. Only in special cases of buildings, explicitly defined in EC 8-5/2004, the soil–structure interactions derive adverse results in structural response. Some of these categories of buildings are:

1. Slender tall structures such as towers and chimneys
2. Structures supported on very soft soil
3. Structures susceptible to P–δ effects

10.5.1.3 Integrated analysis of superstructure foundation and foundation soil

Recently, the introduction of the FEM procedure for soil simulation has allowed a more reliable approach to the problem in elastic or inelastic range. In this procedure damping and vibrating masses (inertial forces) of the ground are introduced in the model. Of course, in this case time-history dynamic analysis must be implemented. It should also be noted that serious problems continue to arise with the boundary conditions of the ground that should be introduced into the model.

In any case, this procedure is rather complicated and is used in special cases such as the retaining of deep excavations or construction of underground works, for example, metro tunnels and so forth, for which special computer platforms have been developed for elastic or inelastic range (e.g. PLAXIS-2D, 2012; Figure 10.16).

Vertical phase displacements (dUy)
Extreme dUy −48.23 × 10⁻³ m
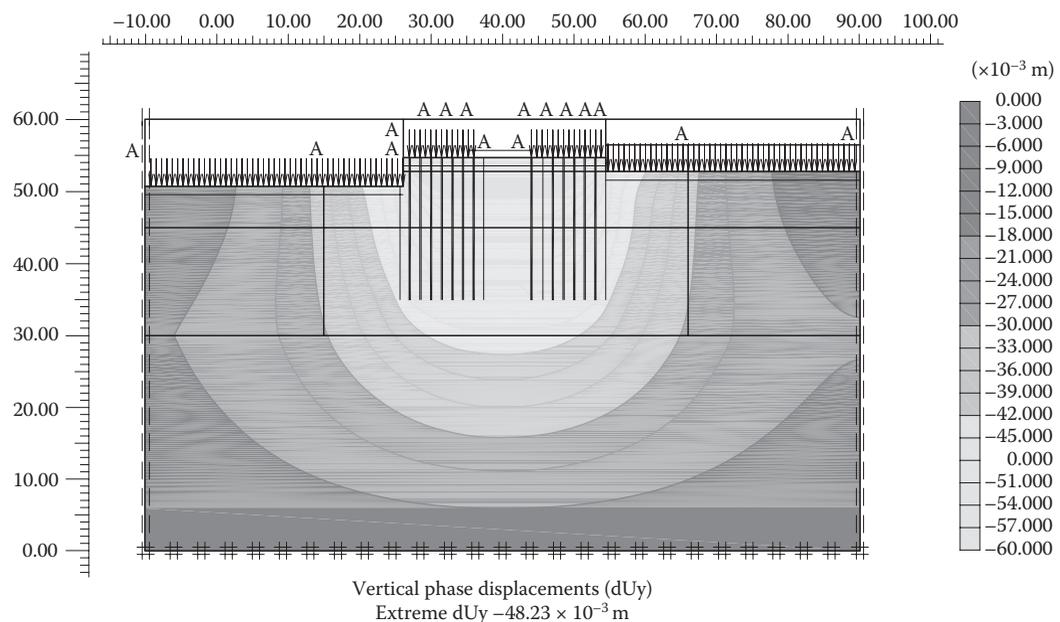
Figure 10.16 Vertical displacements of a raft foundation combined with a network of piles for the foundation of a nine-storey building in Thessaloniki, Greece. (From Penelis, S.A. 2011. Structural and seismic design of a nine storey building with one basement in Vasileos Irakliou Str. Nr. 45 (Domotechniki real estate) Thessaloniki, Greece, documents for permit issue. Penelis S.A. archives.)

10.5.2 Design of foundation members

10.5.2.1 Dissipative superstructure – non-dissipative foundation elements and foundation ground

Design action effects for this design alternative, which is the most common, have been given already in Paragraph 10.3.2.2 (1) for all types of foundation members. It should be remembered that the basic concept for this alternative is that for foundations the internal forces at the base of the vertical members (columns–walls) caused by seismic actions are multiplied by a magnifying factor $\gamma_{Rd}\Omega$ (par. 10.3.2.2) for them to be used as loads for the foundation. Of course, in the case that an integrated system of analysis for the superstructure and foundation has been used, the above-mentioned magnification factor $\gamma_{Rd}\Omega$ will be introduced for an additional group of load case combinations for the foundation design.

10.5.2.1.1 Footing with tie-beams or a slab

The modelling of this type of foundation has been described in Paragraph 10.5.1.1 (1). The reactions N'_{Ed}, M'_{Ed}, V'_{Ed} of the stiffness springs result from the analysis of this system for the corresponding loading. These values are generally reduced in relation to input values N_{Ed}, M_{Ed}, V_{Ed} from the superstructure, as the tie-beams or the foundation slab participate with their stiffness in carrying a part of the input loading. Of course in the case of an integrated model of superstructure – foundation – ground this reduction cannot be seen immediately since N_{Ed}, M_{Ed}, V_{Ed} are not loads for the foundation, but load effects at the base of columns and structural walls.

The verification of *foundation ground* and the *footing* itself is carried out for the combination of N'_{Ed}, M'_{Ed}, V'_{Ed}. This verification includes (Figure 10.17):

- Ground failure under the bending moment M'_{Ed} and axial force N'_{Ed} Sliding failure under V'_{Ed}
- Overturning according to EN1990/2003
- Footing failure to bending
- Footing failure to shear

For the determination of the internal forces in the footing, a planar stress distribution of soil reactions is assumed. Generally, for the dimensioning and design of the footings the rules for the conventional design of R/C structures (EC2-1/2004) are implemented.
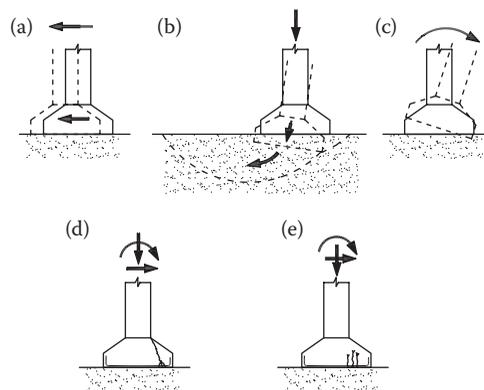
Figure 10.17 Modes of failure in pad foundations: (a) sliding failure; (b) soil-bearing capacity failure; (c) overturning; (d) shear failure in footing; (e) bending failure in footing. (Adapted from Booth, E. and Key, D. 2006. *Earthquake Design Practice for Buildings*. Thomas Telford Ltd.)

Tie-beams must have minimum cross-sectional dimensions included in the National Annex of each E.U. member state. In EC8-1/2004 the following values are recommended:

$$b_{w\,min} = 0.25 \text{ m} \tag{10.34a}$$

$$b_{w\,min} = 0.40 \text{ m} \tag{10.34b}$$

for buildings up to three storeys, or $h_{wmin} = 0.50$ m for those with four storeys and more above the basement. It is recommended by EC8-1/2004 that tie-beams have along their length a longitudinal reinforcement of at least ρ_{min} both at top and the bottom:

$$\rho_{min} = 0.4\% \tag{10.35}$$

of the area of the cross-section of the tie-beam.

On the other hand, foundation slabs should have a minimum thickness h_t. The recommended value of h_t is

$$h_t = 0.20 \text{ m} \tag{10.36}$$

and the recommended longitudinal tie-reinforcement should be ρ_{smin} at the top and the bottom, equal to

$$\rho_{smin} = 0.2\% \tag{10.37}$$

Stub columns (Figure 10.18) between the top of a footing and the soffit of tie-beams or foundation slabs *must be avoided*. In fact, the creation of a short column between the tie-beam or the slab and the footing very often leads to shear explosive cleavage failure (see Subsection 8.3.6).

The minimum axial forces for the design of the tie-beams or the slab connecting zone have already been given in Paragraph 10.4.3.2.1 (Equation 10.13a–c). However, it should
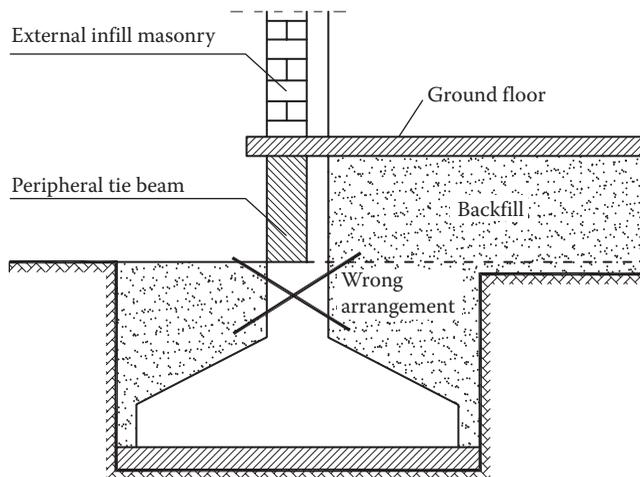
Figure 10.18 Wrong arrangement of the peripheral tie beam due to the formation of a stub column.

be noted that tie-beams or connecting slab zones should be dimensioned and designed for the combinations of the above axial forces with the bending moments and shear forces that derive from the analysis for the seismic load combinations. It should be noted that these bending moments and shear forces have high values in the case of structural walls where large overturning moments develop. Therefore, in the case of multi-storey buildings with dual structural systems, tie-beams should be replaced by grid foundation beams with large cross-sections (Figure 4.16, Subsection 4.2.12).

The dimensioning and design of tie-beams and foundation slabs are carried out according to EC2-1/2004, as in the case of conventional R/C structures.

10.5.2.1.2 Foundation beams and rafts

These are the most common foundation systems in seismic areas. This type of foundation ensures, on one hand, the mutual connection of the vertical members of the superstructure at their base, and on the other, due to their high stiffness, the uniform distribution of the loads to the ground and the safe transfer of the high-level overturning moments of structural walls to the ground. The modelling of this type of foundation has been presented in Paragraph 10.5.1.1 (2). From the analysis of this system the following output is obtained:

- The distribution of the soil reactions
- The slab moment and shear diagrams
- The beam moment shear and axial forces diagrams

Using these data, the dimensioning in bending and shear is carried out according to EC2-1/2004, that is, *without any extra provision for local ductility.*

10.5.2.1.3 Cast in place concrete piles and pile cups connected with tie-beams

The modelling of this type of foundation has been described in Paragraph 10.5.1.1 (3). From the analysis of this system for loading described at the beginning of this paragraph, the reactions N'_{Ed}, M'_{Ed}, V'_{Ed} of the stiffness springs simulating the piles result. These values are reduced in relation to input N_{Ed}, M_{Ed}, V_{Ed} from the superstructure, as the tie-beams or the foundation slab participates with their stiffness in carrying the input loading.

Next, the interaction of the pile and the foundation ground must be analysed under the reactions N'_{Ed}, M'_{Ed}, V'_{Ed} of the pile head. This analysis will be carried out in accordance with the procedure described in Paragraphs 10.4.5.2 and 10.4.5.3. From this analysis, the following output is obtained:

1. Stress distribution diagram on the surrounding ground (Figure 10.15)
2. Internal force diagrams N_{Ed}, M_{Ed}, V_{Ed} of the pile

From this point on, the safety verification may be easily carried out as follows:

1. *For the ground resistance:*
   a. The design axial loading must be less than the ground design resistance (see Paragraph 10.4.5.2)
   b. The transverse soil reactions due to M'_{Ed}, V'_{Ed} must be less than the ground design resistance to horizontal loading (see Paragraph 10.4.5.3, Equation 10.31)
2. *For pile dimensioning, EC2-1/2004 will be implemented, as in the case of columns of conventional buildings*

It should be noted that, although according to the design alternative under consideration, the structural members of the foundations and the foundation ground are considered to be in elastic range, piles under certain conditions according to EC8-5/2004 are allowed to develop plastic hinges.

In this context, according to EC8-1/2004, the top of the pile up to a distance from the underside of the cup of 2d, where d is the pile diameter, as well as the regions up to a distance of 2d on each side of an interface between two soil layers with strongly different shear stiffness (ratio of shear model greater than 6) will be detailed as a potential plastic hinge of a column, with proper confinement of reinforcement in the form of hoops and a minimum longitudinal reinforcement. The design of these critical regions will follow the rules for local ductility of columns at least of DCM (see Paragraph 8.3.4(2)). What has been presented for these members in the case of footings also holds true for the tie-beams or foundation slabs.

10.5.2.1.4 Joints of vertical elements with foundation beams

The joints of vertical elements (columns or walls) and foundation beams must be designed according to the rules in effect for joints of frame systems and according to the ductility class of the superstructure, although the foundation in this design alternative is considered to remain in non-dissipative condition. It should be remembered that joints at the foundation of DCM buildings are reinforced according to the rules described in Subsection 8.4.3 *without any analytical justification*.

Conversely, joints at the foundation of DCH buildings have to be dimensioned analytically. The shear action effect V_{jhd}, which is introduced for the ULS verifications of joints (see Subsection 8.4.3), is determined on the basis of analysis results that have been derived for the seismic action effects magnified by $\gamma_{Rd}\Omega$.

10.5.2.2 Dissipative superstructure – dissipative foundation elements – elastic foundation ground

Design action effects for this design alternative have been presented in Paragraph 10.3.2.2 (2). It should be remembered that the basic concept of this alternative is that superstructure and foundation are designed to dissipate energy, while the foundation ground is considered to remain in elastic rage during the seismic action. In this respect, all structural members of the superstructure and foundation are designed according to capacity design procedures in combination with local ductility requirements. Foundation ground on the other hand is designed at ULS for magnified seismic loading by a magnifying factor $\gamma_{Rd}\Omega$ (par. 10.3.2.2).

The structural members of various types of foundation are designed for the above seismic action effects as the members of the superstructure following all code specifications for capacity design and local ductility.

In particular, piles are designed and detailed for potential plastic hinging at the head as in Paragraph 10.5.2.1.3. In this case, the confinement length at critical regions must be increased by 50% in comparison with 10.5.2.1.3.

In addition, the ULS verification of the pile to shear must be carried out for shear seismic action magnified by $\gamma_{Rd}\Omega$. Obviously, the piles in this case will be designed for local ductility for the same ductility class as the superstructure.

Finally, the horizontal shear force V_{jhd} that should be introduced for the ULS verification of joints (see Subsection 8.4.3) in the case of DCH buildings should be determined in accordance with the capacity design procedure (see Chapter 8.4.2.1).

In closing, it should be noted that the ULS verification of the foundation ground will be carried out following the same procedure as that presented in Paragraph 10.5.2.1.

Table 10.4 An overview of the design procedures for the foundation and the ground

Parts of the structure	Ductility classes				
Superstructure	DCL	DCM		DCH	
Foundation in general	DCL	DCL	DCM	DCL	DCH
		Seismic load magnification $\gamma_{Rd}\Omega$	$\gamma_{Rd}\Omega = 1.0$	Seismic load magnification $\gamma_{Rd}\Omega$	$\gamma_{Rd}\Omega = 1.0$
Box-type basement	DCL	DCL[a]		DCL[a]	
		Seismic load magnification $\gamma_{Rd}\Omega$		Seismic load magnification $\gamma_{Rd}\Omega$	
Connections	DCL	DCM		DCL	DCH
		Confinement of critical region extended in the connection		Seismic load magnification $\gamma_{Rd}\Omega$	$\gamma_{Rd}\Omega = 1.0$
Piles and piers	DCL	DCL	DCM[b]	DCL	DCH[b]
		Seismic load magnification $\gamma_{Rd}\Omega$	$\gamma_{Rd}\Omega = 1.0$	Seismic load magnification $\gamma_{Rd}\Omega$	$\gamma_{Rd}\Omega = 1.0$
Ground	DCL	DCL		DCL	
		Seismic load magnification $\gamma_{Rd}\Omega$		Seismic load magnification $\gamma_{Rd}\Omega$	

[a]   Structural walls in the basement are designed following the rules of dissipative structures (critical region).
[b]   ULS shear verification must use V_{Ed} corresponding to DCL.

10.5.2.3 Non-dissipative superstructure – non-dissipative foundation elements and foundation ground

As it was noted in Paragraph 10.3.2.2 (3), this case refers to DCL buildings where the *q* factor is equal to 1.50. In this case, superstructure, foundation and ground are designed for seismic load effects resulting from the analysis without any measure for capacity design of local ductility.

10.5.2.4 Concluding remarks

As may be seen from the previous presentation of this subsection, various design alternatives are given to the designer by the Code, which are summarised in Table 10.4.

10.6 EXAMPLE: DIMENSIONING OF FOUNDATION BEAMS

The design of the foundation beams B9, B20, B58 and B69 along grid axis C of the foundation shown in Figure 10.19 is presented here. The procedure implemented follows EC8-Part I, paragraphs 4.4.2.6(8) and 5.8.1(5).

The foundation is considered to be of box type, since it consists of the basement slab, the perimeter walls and the foundation beams. The perimeter walls are based on strip footings, the columns on foundation beams, whereas the walls W2 and W3 are based on a mat foundation. Line and shell elements are used to model the web and the flange of the foundation beams, respectively. In order to account for soil deformability, shell elements are considered to be on elastic support by assigning area springs at their vertical direction (Figure 10.20).

The mechanical properties of the soil are: Modulus of elasticity of soil $E_s = 54$ GPa, spring constant $K_s = E_s/b = 54,000/1.8 = 30,000$ kN/m³, where $b = 1.8$ m is the width of the

foundation beam, angle of soil internal friction $\varphi = 42°$, soil weight density $\gamma = 18\ \text{kN/m}^3$ and cohesion intercept $c = 180$ MPa.

The minimum cross-section dimensions are:

- Cross-sectional width: $b_{w,min} = 0.25$ m (Equation 10.34a)
- Cross-sectional depth: $h_{w,min} = 0.50$ m for buildings with four storeys or more above the basement, Equation 10.34a).

The minimum percentage of longitudinal reinforcement is (Equation 10.35):

$$\rho_{min} = 0.4‰ \rightarrow A_{s,min} = 0.40‰ \cdot 60 \cdot 103.2 = 24.77\ \text{cm}^2$$

Details regarding the geometry of the foundation beams appear in Figure 10.19.

The design action effects considered in the analysis for the case of dissipative buildings (DCH for the building studied here) are estimated as follows (Paragraph 10.3.2.2 (1), Equation 10.3):

$$E_{Dd} = E_{F,G} + \gamma_{Rd} \cdot \Omega \cdot E_{F,E} = E_{F,G} + 1.40 \cdot E_{F,E}$$

The term $\gamma_{Rd} \cdot \Omega$ is equal to 1.40 according to the requirement of EC8-Part I (2004) for common foundations of more than one vertical element. The moment and shear envelopes that appear in Figures 10.21 and 10.22 are extracted after having been multiplied by 1.40.

10.6.1 Ultimate limit state in bending

Owing to the fact that beams B69 and B58 are symmetrical to B9 and B20, detailed design is presented only for Beams B9 and B20.

External supports on the boundary element of W4 and on C9 (Beam B9-left, B69-right):

Hogging design moment for the bottom reinforcement: $M_d^- = 184.61$ kN m

- Bottom longitudinal reinforcement:

$$\mu_{sd} = \frac{\left| M_d^- \right|}{b \cdot d^2 \cdot f_{cd}} = \frac{184.61 \cdot 10^6}{600 \cdot 1032^2 \cdot (25/1.5)} = 0.0173 \rightarrow \omega_{req} = 0.0178 \rightarrow$$

$$A_{s,req} = \omega_{req} \cdot b \cdot d \frac{f_{cd}}{f_{yd}} = 0.0178 \cdot 600 \cdot 1032 \frac{25/1.5}{500/1.15} = 4.21\ \text{cm}^2 < A_{s,min} = 24.77\ \text{cm}^2 \rightarrow$$

$$\rightarrow 8\varnothing 20\ (25.13\ \text{cm}^2)$$

- Top longitudinal reinforcement: The minimum amount of reinforcement placed at the top of the beam is $8\varnothing 20$

Internal supports on C9 and on C23 (Beam B9-right, B20-left, B58-right, B69-left):

Hogging design moment for the top reinforcement: $M_d^- = -975.19$ kN m

- Bottom longitudinal reinforcement:

$$\mu_{sd} = 0.0916 \rightarrow \omega_{req} = 0.0979 \rightarrow A_{s,req} = 23.23\ \text{cm}^2 \ < A_{s,min} = 24.77\ \text{cm}^2 \rightarrow 8\varnothing 20$$

- Top longitudinal reinforcement: The minimum amount of reinforcement placed at the top of the beam is $8\varnothing 20$

(a)

(b)

Section I–I, II–II

Section III–III, IV–IV

Section I–I, final arrangement
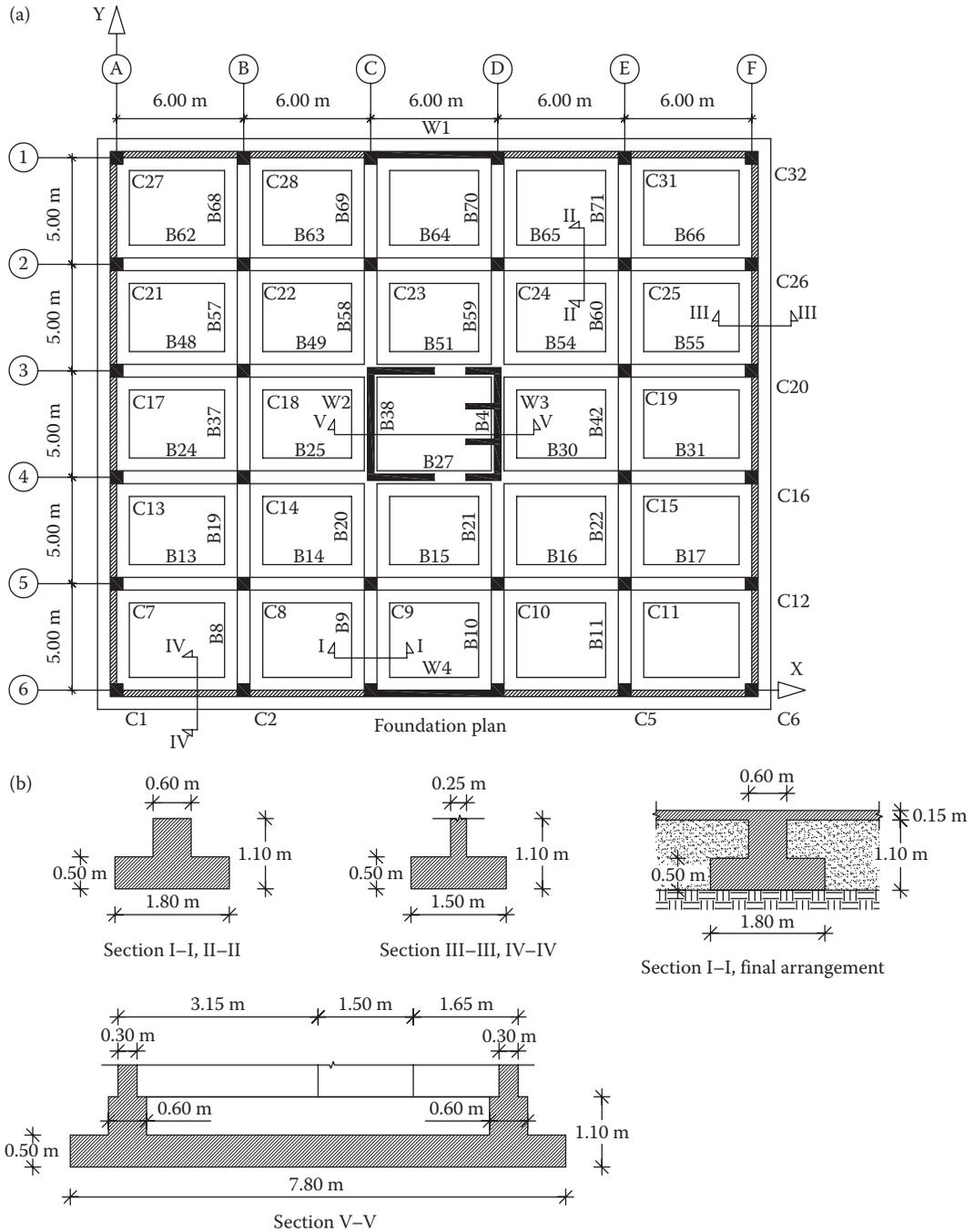
Section V–V

Figure 10.19 (a) Plan view of the foundation system; (b) characteristic cross-sections of the foundation beams.
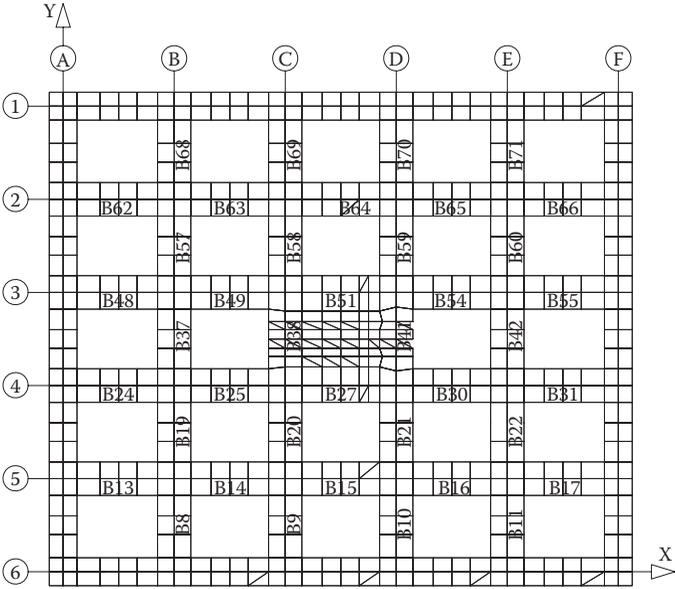
Figure 10.20 Model of the foundation by means of line and shell elements.

Envelope of 1.35G + 1.50Q, G + 0.3Q + 1.40 (±Ex ± 0.3Ey), and G + 0.3Q + 1.40 (±0.3Ex ± Ey)
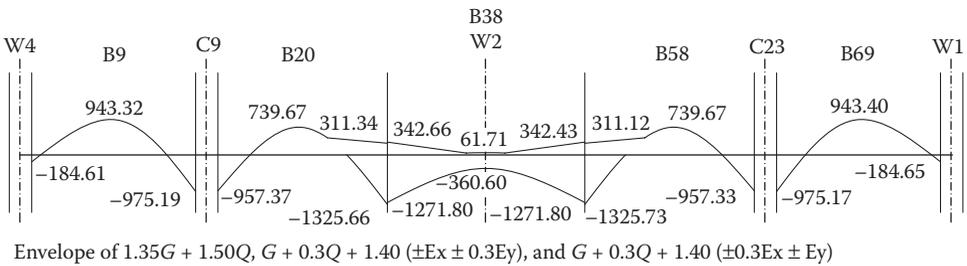
Figure 10.21 Moment envelope for the foundation beams along grid axis C.

Envelope of 1.35G + 1.50Q, G + 0.3Q + 1.40 (±Ex ± 0.3Ey), and G + 0.3Q + 1.40 (±0.3Ex ± Ey)
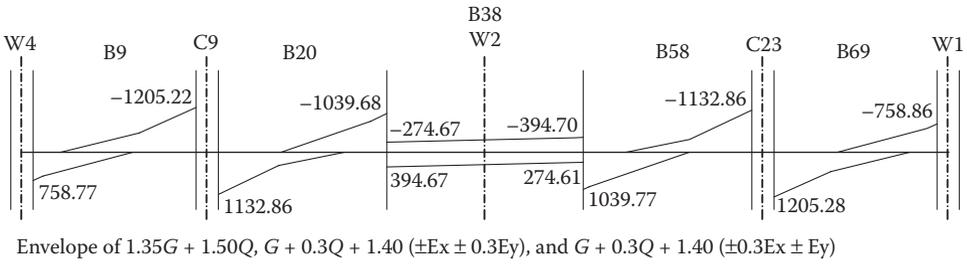
Figure 10.22 Shear envelope for the foundation beams along grid axis C.

Internal supports on the boundary elements of W2 (B20-right, B58-left):
Hogging design moment for the top reinforcement: $M_d^- = -1325.66$ kN m
Sagging design moment for the bottom reinforcement: $M_d^+ = 311.34$ kN m

- Bottom longitudinal reinforcement:

$$\mu_{sd} = 0.1245 \rightarrow \omega_{req} = 0.1364 \rightarrow A_{s,req} = 32.37\,\text{cm}^2 > A_{s,min} \rightarrow 11\varnothing20\,(34.56\,\text{cm}^2)$$

- Top longitudinal reinforcement:

$$\mu_{sd} = 0.0097 \rightarrow \omega_{req} = 0.0102 \rightarrow A_{s,req} = 7.29\,\text{cm}^2 < A_{s,min} = 24.77\,\text{cm}^2 \rightarrow 8\varnothing20$$

Mid-span (Beam B9, B69):
Sagging design moment for the bottom reinforcement: $M_d^+ = 943.32$ kN m

- Top longitudinal reinforcement:

$$\mu_{sd} = \frac{\left|M_d^+\right|}{b_{eff} \cdot d^2 \cdot f_{cd}} = \frac{943.32 \cdot 10^6}{1800 \cdot 1032^2(25/1.5)} = 0.0295 \rightarrow \omega_{req} = 0.0310 \rightarrow$$

$$A_{s,req} = \omega_{req} \cdot b_{eff} \cdot d\frac{f_{cd}}{f_{yd}} = 0.0310 \cdot 1800 \cdot 1032\frac{25/1.5}{500/1.15} = 23.53\,\text{cm}^2 < A_{s,min}$$

$$= 24.77\,\text{cm}^2 \rightarrow 8\varnothing20$$

- Bottom longitudinal reinforcement: 8⌀20 were placed according to the minimum requirements.

Mid-span (Beam B20, B58):
Sagging design moment for the bottom reinforcement: $M_d^+ = 739.67$ kN m

- Top longitudinal reinforcement:

$$\mu_{sd} = 0.0232 \rightarrow \omega_{req} = 0.0243 \rightarrow A_{s,req} = 18.45\,\text{cm}^2 < A_{s,min} = 24.77\,\text{cm}^2 \rightarrow 8\varnothing20$$

- Bottom longitudinal reinforcement: 8⌀20 were placed according to the minimum requirements.

10.6.2 Ultimate limit state in shear

Shear resistance in case of diagonal concrete crushing for δ = 21.8° (8.62):
Beam 9-left:

$$V_{Rd,max} = 1 \cdot 0.6 \cdot 0.9 \cdot 1.032 \cdot 0.54 \cdot (25/1.5) \cdot 1000/2.9 = 1729.49\,\text{kN} > 758.77\,\text{kN}$$

Beam 9-right:

$$V_{Rd,max} = 1729.49\,\text{kN} > 1205.22\,\text{kN}$$

Beam 20-left:

$$V_{\text{Rd,max}} = 1729.49\,\text{kN} > 1132.86\,\text{kN}$$

Beam 20-right:

$$V_{\text{Rd,max}} = 1729.49\,\text{kN} > 1039.68\,\text{kN}$$

Transverse reinforcement in the critical regions

The critical region is $l_{\text{cr}} = 1.5 \cdot h_{\text{w}} = 1.5 \cdot 110 = 165$ cm
The maximum longitudinal spacing should not exceed s_{max}:

$$s_{\text{max}} = \min\left\{\frac{h_{\text{w}}}{4}; 24d_{\text{bw}}; 175; 6d_{\text{bL}}\right\} = \min\left\{\frac{1100}{4}; 24 \cdot 10; 175; 6 \cdot 20\right\} = 120\,\text{mm}$$

$\varnothing$10/120 are the minimum allowed hoops (a bar diameter of 10 mm was considered as the minimum diameter for hoops).

Beam 9-left:

$$V_{\text{wd}} = 758.77 \Leftrightarrow s = \frac{A_{\text{sw}}}{V_{\text{A}}} 0.9d \cdot f_{\text{ywd}} = \frac{4 \cdot \pi \cdot 10^2/4}{758.77} \cdot 0.9 \cdot 1.032 \cdot \frac{500}{1.15} = 167.20\,\text{mm}$$

Hence, the estimated shear reinforcement in the critical region at the left end of Beam 9 is 4$\varnothing$10/120.

Beam 9-right:

$$V_{\text{wd}} = 1205.22 \Leftrightarrow s = 105.26\,\text{mm} \rightarrow 4\varnothing10/100$$

Beam 20-left:

$$V_{\text{wd}} = 1132.86 \Leftrightarrow s = 111.98\,\text{mm} \rightarrow 4\varnothing10/100$$

Beam 20-right:

$$V_{\text{wd}} = 1039.68 \Leftrightarrow s = 122.02\,\text{mm} \rightarrow 4\varnothing10/120$$

For simplicity in construction, the same number of stirrups was considered for both beams, that is, 4$\varnothing$10/100 (Figure 10.23).

Transverse reinforcement outside the critical regions

The length outside the critical regions for Beam 9 is 1.1 m, whereas for Beam 20 it is 1.25 m.
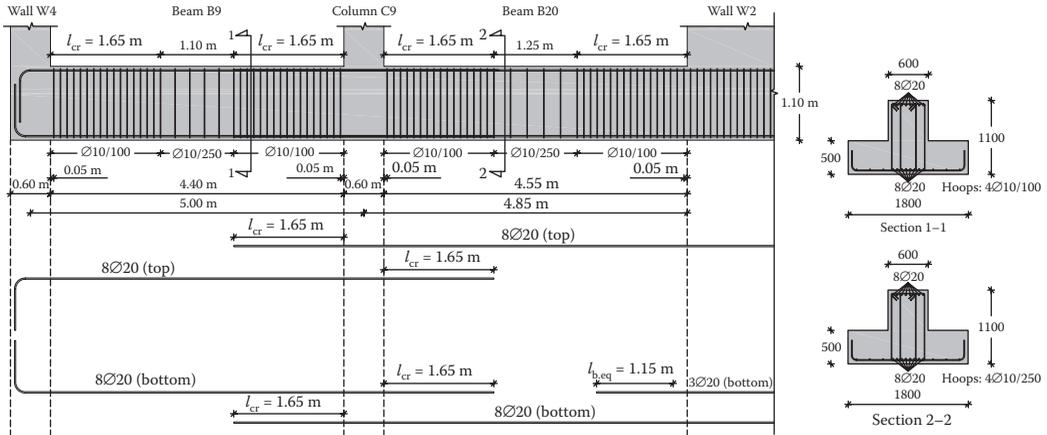
Figure 10.23 Flexural and shear reinforcement of foundation beams 9 and 20.

The minimum shear reinforcement ratio is

$$\rho_{w,min} = \frac{0.08 \cdot \sqrt{f_{ck}}}{f_{yk}} = \frac{0.08 \cdot \sqrt{25}}{500} = 0.8‰$$

The maximum longitudinal spacing between hoops should not exceed s_{max}:

$$s_{max} = 0.75 \cdot d = 0.75 \cdot 1032 = 774 \, \text{mm}$$

In the case of four-leg 10 mm bar diameter hoops, stirrup spacing is defined as equal to

$$s = \frac{A_{sw}}{\rho_{w,min} \cdot b_w} = \frac{4 \cdot (\pi \cdot 10^2/4)}{0.0008 \cdot 600} \approx 655 \, \text{mm}$$

$\varnothing 10/655$ are the minimum allowed hoops.
Beam 9:

$$V_{wd} = 468.72 \Leftrightarrow s = \frac{4 \cdot \pi \cdot 10^2/4}{468.72} \cdot 0.9 \cdot 1.032 \cdot \frac{500}{1.15} = 270.66 \, \text{mm}$$

The shear reinforcement outside the critical regions of Beam 9 was taken to be $4\varnothing 10/250$.
Beam 20:

$$V_{wd} = 345.02 \Leftrightarrow s = \frac{4 \cdot \pi \cdot 10^2/4}{318.16} \cdot 0.9 \cdot 1.032 \cdot \frac{500}{1.15} = 367.71 \, \text{mm}$$

$4\varnothing 10/250$ were also considered for Beam 20 for simplicity in construction.

Chapter 11

Seismic pathology

11.1 CLASSIFICATION OF DAMAGE TO R/C STRUCTURAL MEMBERS

11.1.1 Introduction

Seismic pathology of R/C buildings is of major importance for the assessment of their structural condition just after a strong earthquake. In fact, after a strong earthquake a large number of structural engineers are mobilised for the emergency inspection and assessment of the buildings in the affected area. Therefore, it is necessary that they must be in a position:

1. To focus their attention to the most frequent types of damage
2. To assess qualitatively the existing hazard for an eventual aftershock collapse from the damage under inspection and, therefore, to prohibit the use of certain buildings until more detailed evaluation or retrofitting actions take place
3. To proceed with temporary general or local propping of buildings in case the existing hazard of collapse is evident

At the same time, damages to the structural system constitute an excellent benchmark for the quantitative evaluation of the structural post-earthquake condition of a building, and therefore a reliable guide for an effective retrofitting.

A strong earthquake puts the whole structure through a hard test. As a result, all the weaknesses of the structure, due to either Code imperfections or analysis and design errors, or even bad construction, are readily apparent. It is not unusual that a strong earthquake leads to improvements or even drastic changes in design Codes and modifications in design methods. Similarly, it triggers liability and responsibility issues for the design and execution of construction projects.

It is difficult to classify the damage caused by an earthquake, and even more difficult to relate it in a quantitative manner to the cause of the damage. This is because the dynamic character of the seismic action and the inelastic response of the structure render questionable every attempt to explain the damages by means of a simplified structural model. Furthermore, the coincidence of more than one deficiency in the building makes the quantitative evaluation of the influence of each deficiency very difficult and sometimes even impossible.

Despite all the difficulties inherent in a damage classification scheme, an attempt will be made in this chapter to classify the damage into categories and to identify the cause of the damage in each case, according to current concepts of the behaviour of structural elements under cyclic inelastic loading, which sufficiently simulates the response of structural members to a strong earthquake.

In this section, damage classification will refer to individual structural elements (Tegos, 1979), while in the following section reference will be made to the main causes of damage to R/C buildings as a whole. In both sections, the qualitative analysis will be supplemented with statistical data for the behaviour of structural elements and buildings during strong earthquakes.

The basic source of the statistical data is the research project, 'A statistical evaluation of the damage caused by the earthquake of June 20, 1978, to the buildings of Thessaloniki, Greece', which was carried out at the Laboratory of Reinforced Concrete of Aristotle University of Thessaloniki, in collaboration with the Ministry of Environment and Public Works (Penelis et al., 1987, 1988), and also the report, 'The Earthquake of 19 September 1985 – Effects in Mexico City', by the Committee for Reconstruction of Mexico City (Rosenblueth and Meli, 1985). In addition, the technical report for the 'Evaluation of damages and their cause for the 103 near-collapse R/C buildings in Athens after the earthquake of September 07, 1999' prepared by an (OASP) committee (Kostikas et al., 2000) will be a valuable source of statistical information.

In the classification that follows, there is no reference to damage due to analysis errors, bad concrete quality, improper reinforcement detailing and so on, since the classification is based mainly on statistics. On the other hand, weaknesses of this type are always present in structures, and their frequency and severity depend on the level of technological development of a country. Of course, these weaknesses contribute to the degree of damage caused by an earthquake, and occasionally they become fatal for the stability of buildings.

Finally, it should be noted that the classification presented below is based mainly on the behaviour of R/C buildings designed and constructed according to a previous generation of Codes, since the main volume of the existing building stock was constructed before the introduction of modern Codes (before 1985). However, there are some first results for the behaviour of buildings designed and constructed recently according to modern Codes that have been affected by recent earthquakes, and therefore a first indicative reference will also be made to these cases. In any case, after future strong earthquakes an extended survey and evaluation must be carried out on the stock of buildings designed according to the modern Code philosophy that will have been stocked in the meantime, so that justified conclusions can be drawn about the effectiveness of modern building Codes.

11.1.2 Damage to columns

Damage to columns caused by an earthquake is mainly of two types:

- Damage due to cyclic flexure and low shear under strong axial compression
- Damage due to cyclic shear and low flexure under strong axial compression

The first type of damage is displayed by failures at the top and bottom of the column (Figures 11.1, 11.2 and 11.3). It occurs in columns of moderate-to-high aspect ratio. For

$$\alpha = \frac{M}{Vh} = \frac{L}{2h} \geq 5.0 \div 6.0 \tag{11.1}$$

this is the prevailing mode of failure. For

$$5.0 \div 6.0 \geq \frac{L}{2h} \geq 2.0 \tag{11.2}$$
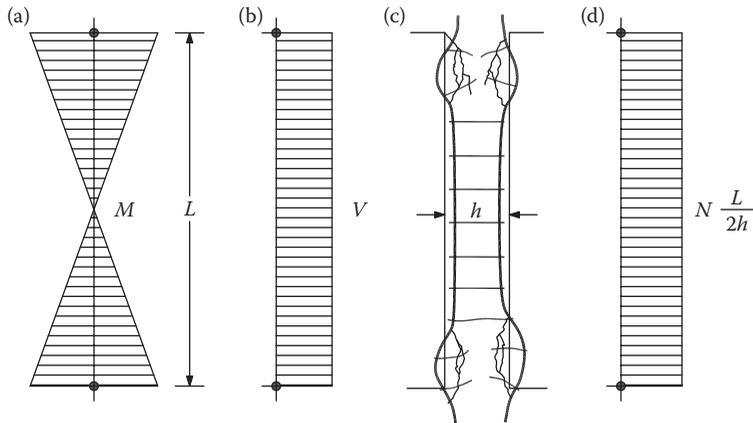
Figure 11.1 Column damage due to strong axial compression and cyclic bending moment (a) bending moment diagram; (b) shear force diagram; (c) sketch of damage; (d) axial force diagram.

mode of failure depends on the degree of shear reinforcement (transverse ties; see Subsections 8.3.3 and 8.3.4). If shear reinforcement is high, the prevailing mode of failure continues to be of flexural type at the ends of the column, otherwise shear-compression failure prevails. It should be noted that, at least in Greece, for buildings designed before 1985, where no special concern for shear reinforcement in columns existed (capacity design to shear), for columns of moderate slenderness, bending failure is combined with shear compression failure at the ends (Figures 11.4d, 11.5 and 11.6).

The high bending moment at the ends of the column, combined with the axial force, leads to the crushing of the compression zone of concrete, successively on both faces of the

Figure 11.2 Column damage due to high axial compression and cyclic bending moment: Bucharest, Romania (1977).

Figure 11.3 Column damage due to high axial compression and cyclic bending moment: Kalamata, Greece (1986).

column. The smaller the number of ties in these areas, the higher their vulnerability to this type of damage. The crushing of the compression zone is displayed first by spalling of the concrete cover to the reinforcement. Subsequently, the concrete core expands and crushes. This phenomenon is usually accompanied by buckling of bars in compression and by hoop fracture. The fracture of the ties and the disintegration of concrete lead to shortening of the column under the action of the axial force. Therefore, this type of damage is very serious, because the column not only loses its stiffness, but it also loses its ability to carry vertical loads. As a result, there is a redistribution of stresses in the structure, since the column has shortened due to the disintegration of concrete in the above-mentioned areas.

This type of damage is very common; 23.3% of R/C buildings damaged in their structural systems by the Thessaloniki earthquake of 20 June 1978 displayed damage of this type
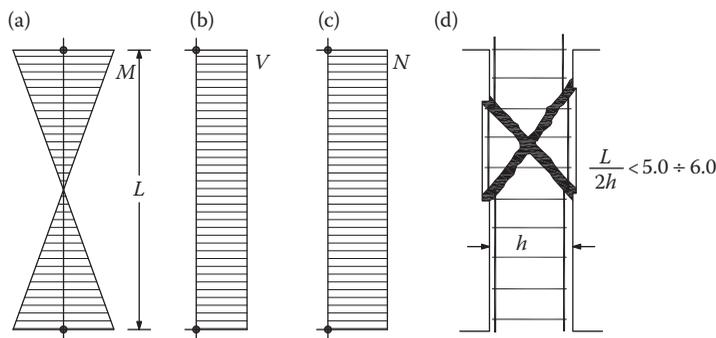
Figure 11.4 Column damage due to strong axial compression and shear (a) bending diagram; (b) shear force diagram; (c) axial force diagram; (d) sketch damage.

Figure 11.5 Column damage due to high axial compression and cyclic shear: Kalamata, Greece (1986).

(Penelis et al., 1987, 1988). The great majority of failures of buildings with frame systems during the Mexico City earthquake of 19 September 1985 were caused by column damage (Rosenblueth and Meli, 1985). As the main causes for this brittle type of failure, one should consider the low quality of concrete; the inadequate number of ties in the critical areas; the presence of strong beams, which leads to columns failing first; and finally, of course, the strong seismic excitation inducing many loading cycles in the inelastic range.

Figure 11.6 Column damage due to high axial compression and cyclic shear: Kalamata, Greece (1986).
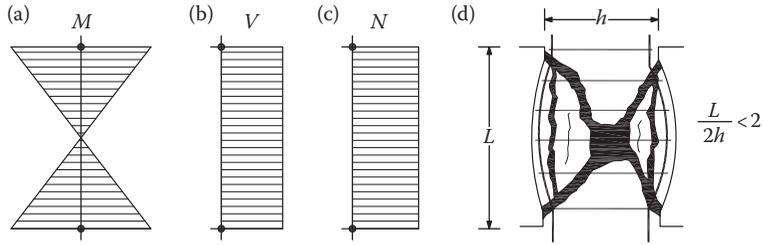
Figure 11.7 Explosive cleavage of a short column: (a) bending moment diagram; (b) shear force diagram; (c) axial force diagram; (d) sketch of damage.

The second type of damage is that of shear type and is displayed in the form of X-shaped cracks in the weakest zone of the column (Figures 11.4, 11.5 and 11.6). As was explained in the previous paragraph, this type of failure occurs in columns of moderate slenderness ratio $L/2h$ between $5.0 \div 6.0$, and 2.0 in the case that transverse shear reinforcement is inadequate.

The ultimate form of this type of damage is the explosive cleavage failure of short columns (Figures 11.7, 11.8 and 11.9), for a slenderness ratio:

$$\alpha = \frac{M}{Vh} = \frac{L}{2h} \leq 2.0 \tag{11.3}$$

(see Paragraph 8.3.6.2). This type of failure usually leads to a "spectacular" collapse of the building.

Figure 11.8 Explosive cleavage failure of a short column: Kozani, Greece (1996).

Figure 11.9 Explosive cleavage failure of a short column: Kalamata, Greece (1986).

Generally speaking, the main reason for this type of damage is that the flexural capacity of columns with moderate to small slenderness ratio is higher than their shear capacity, and as a result shear failure prevails. The frequency of this type of damage is lower than the failure at the top and bottom of the column. It usually occurs in columns on the ground floor, where, because of the large dimensions of the cross-section of the columns, the slenderness ratio is low. It also occurs in short columns, which have either been designed as short or have been reduced to short because of adjacent masonry construction that was not accounted for in the design (Subsection 4.2.5, Figure 4.8).

Finally, sometimes in the case of one-sided masonry-infilled frames, masonry failure is followed by shear failure of the adjacent columns (Figures 11.10 and 11.11; Stylianidis and Sariyiannis, 1992).
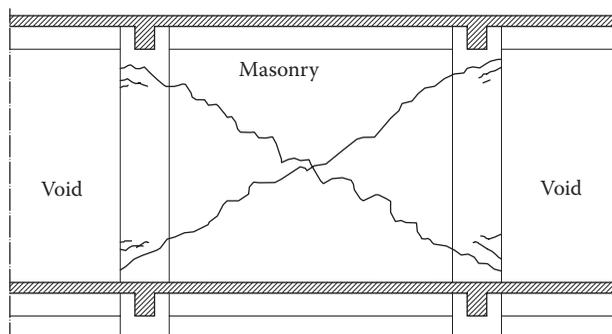
Figure 11.10 Damage in columns in contact with masonry on one side only.
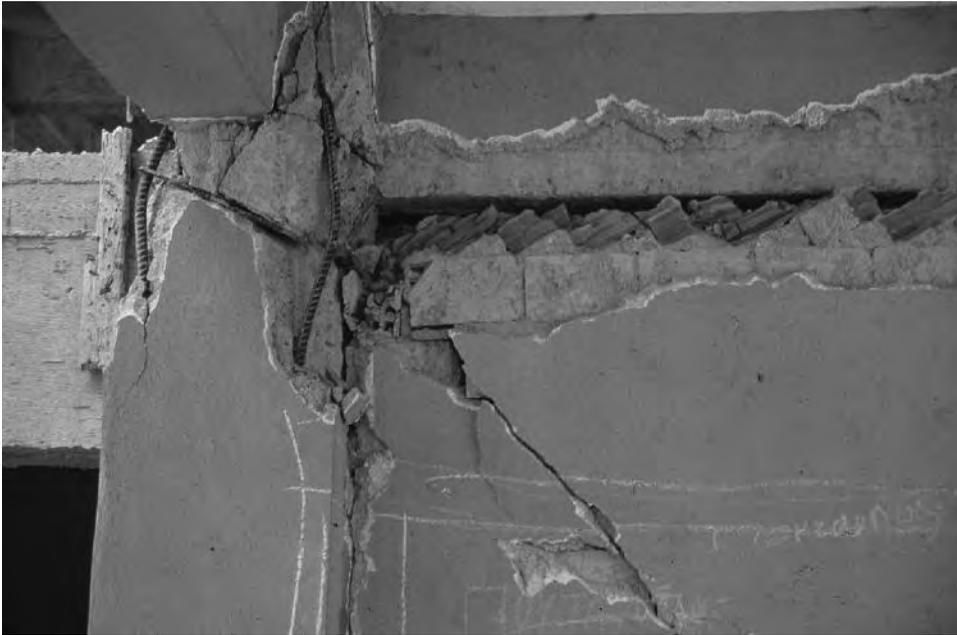
Figure 11.11 Damage of column in contact with masonry on one side only: Kalamata, Greece (1986).

From the survey and evaluation of the 103 R/C buildings most affected by the earthquake of September 07, 1999, in Athens (Kostikas et al., 2000), it was found that 27% of the affected buildings presented shear damage at their short columns. It was also ascertained that 89 out of 103 buildings presented damages in columns due to inadequate transverse hoop and tie reinforcement either in critical regions (confinement reinforcement) or along the column axis (shear reinforcement). Moreover, this was one of the main types of damage near collapse (Figure 11.51) for 55% of the cases under consideration.

In conclusion, it must be noted that column damage is very dangerous for the structure, because it alters or even destroys the vertical elements of the structural system. Thus, when damage of this type is detected, emergency measures of temporary support should be provided immediately.

11.1.3 Damage to R/C walls

The damage caused to R/C walls by earthquakes is of the following types:

- X-shaped shear cracks
- Sliding at the construction joint
- Damage of flexural character (horizontal cracks—crushing of the compression zone)

During the Thessaloniki earthquake of 20 June 1978, 28.6% of the buildings that suffered damage to their structural system displayed damage in the R/C walls (Penelis et al., 1987).

The most frequent type of damage is the appearance of cracks at the construction joint (Figures 11.12 and 11.13). Damage of this type occurred in 88% of the buildings with wall damage caused by the Thessaloniki earthquake of 20 June 1978 (Penelis et al., 1987–1988).
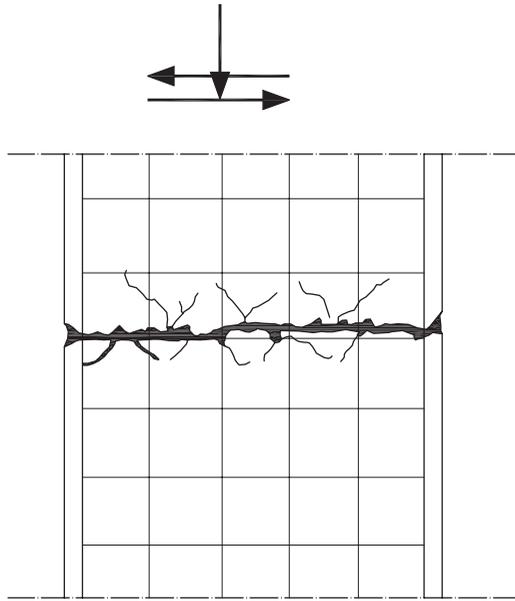
Figure 11.12 Shear wall damage at a construction joint.
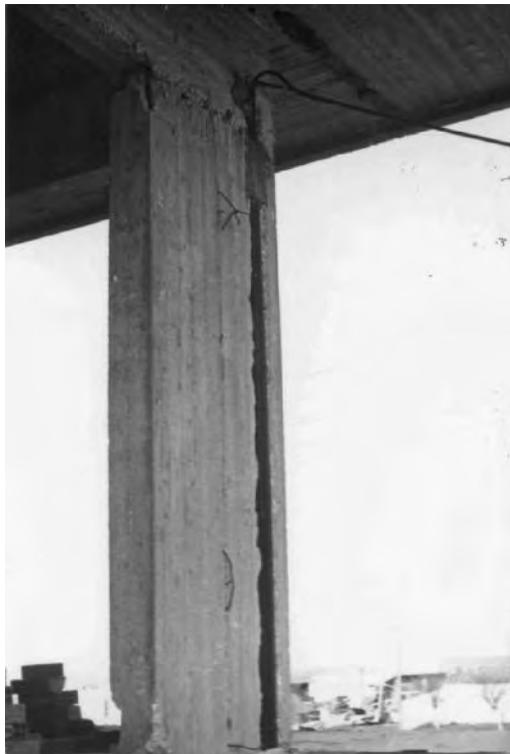
Figure 11.13 Shear wall crack at the construction joint at the top of an R/C wall, Kalamata, Greece (1986).

This damage is mainly due to the fact that fresh concrete was not properly bonded with the hardened old one. All seismic codes in effect today require that extra care is taken when construction work is discontinued in order to ensure proper bonding of concrete (rough surface, cleaning, soaking, pouring of strong cement mortar first and then concrete). In addition, placement of connecting reinforcement is also required in the form of dowels. The introduction of these requirements is the result of the high frequency of this type of damage. However, it has to be mentioned that this type of damage does not pose a threat to the stability of the building, because, with the horizontal arrangement of the cracks, the wall can still carry vertical loads. Also, from the stiffness point of view, this type of damage has only a slight effect on the entire structural system.

The appearance of X-shaped cracks in R/C walls is the next most frequent damage (Figures 11.14–11.16). During the above-mentioned Thessaloniki earthquake the frequency of this damage reached 30% of the buildings with wall damage. This is a shear type of brittle failure. Because of the arrangement of the cracks under the action of vertical loads, the isosceles triangles that form on the two sides tend to separate from the structure and therefore cause its collapse (Figure 11.14). In order to protect the structure from this type of failure, all current codes require the formation of a column at each side of the wall that will carry the vertical loads after the shear failure of the web. These columns can either be thicker than the wall and visible (barbells), or they can be incorporated into the wall (Subsection 9.2.4).

Damage of flexural type occurs very rarely (Figures 11.15 and 11.17). It is the author's opinion that this is due to the fact that the bending moments developing at the base of the wall are much smaller than those calculated for the design, because the footing rotates as the soil deforms during the earthquake (Subsection 4.5.2, Figure 4.25). On the other hand, this soil deformation does not significantly alter the shear force that is carried by the wall, and, as a result, shear failure prevails. It is hoped that for buildings designed according to the new generation of Codes, the ductile mode of failure will prevail.
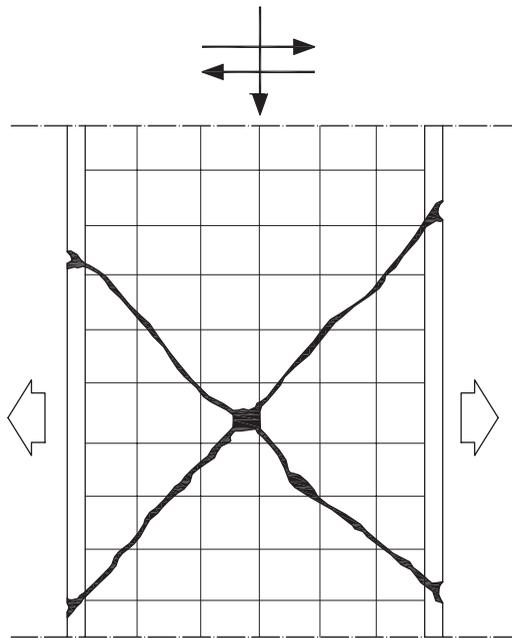
Figure 11.14 Shear wall damage due to shear (X-shaped cracks).

Figure 11.15 Shear wall failure: Kalamata, Greece (1986) failure to shear and in parallel to bending.

Figure 11.16 Shear wall failure due to shear: Kalamata, Greece (1986).
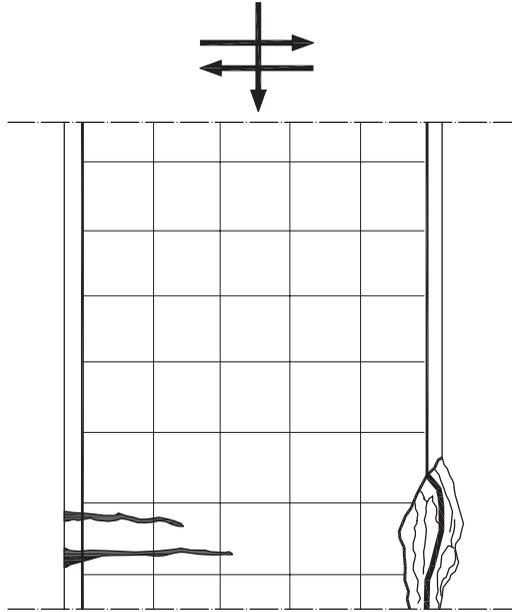
Figure 11.17 Shear wall damage due to flexure and compression.

11.1.4 Damage to beams

The damage that occurs to R/C beams due to an earthquake is as follows:

- Cracks perpendicular to the beam axis along the tension zone of the span
- Shear failure near the joints
- Flexural cracks on the upper or lower face of the beam at the joints
- Shear or flexural failure at the points where secondary beams or cut-off columns are supported by the beam under consideration
- X-shaped shear cracks in short beams that connect shear walls (coupled walls)

Although damage to beams does not jeopardise the safety of the structure, it is the most common type of damage in R/C buildings; 32.6% of the buildings that displayed structural system damages during the Thessaloniki earthquake of 20 June 1978 exhibited some type of beam damage.

Cracks in the tension zone of the span constitute the most common type of damage—83% of the structures with beam damage in Thessaloniki due to the June 1978 earthquake had damage of this type. This type of damage (Figure 11.18) cannot be explained using analytical
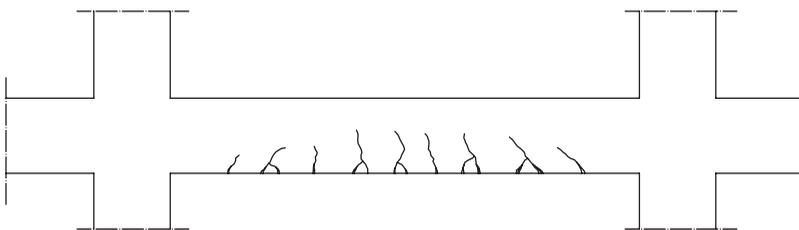
Figure 11.18 Flexural cracks at a beam span.
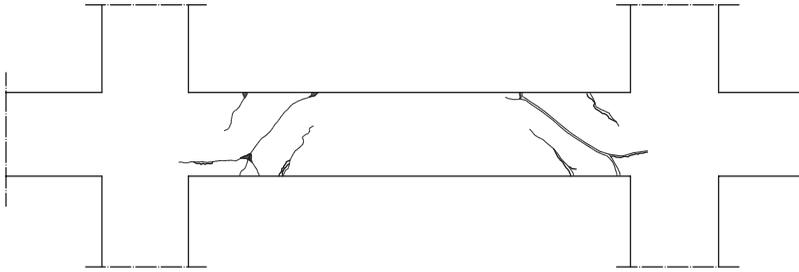
Figure 11.19 Bending-shear cracks near the joints of a beam.

evidence, given the fact that the action of the seismic forces does not increase the bending moment in the span. However, the vertical component of the seismic action, due to its cyclic character, simply makes visible the micro cracks that result from bending of the tensile zone under tension, thus creating the impression of earthquake damage. This is the reason why the large majority of the cases of beams with this type of damage do not jeopardise the overall stability of the structure. It is also understood that the high frequency of damage of this type is rather misleading, since in most cases it is just a display of already existing normal cracking rather than of earthquake damage.

The bending-shear failure near the joints (Figure 11.19) is the second most frequent type of damage (43%) in beams. Undoubtedly it constitutes a more serious type of damage than the previous one, given its brittle character. However, only in a very few cases does it jeopardise the overall stability of the structure.

The flexural cracks on the upper and lower face of the beam at the joints (Figure 11.20) can be fully explained if the earthquake phenomenon is statically approximated by horizontal forces. From the frequency point of view, this type of damage is rarer than the shear type (28%). In most cases, cracking of the lower face is due to bad anchorage of the bottom reinforcement into the supports, in which case one or two wide cracks form close to the support.

The shear or flexural failure at the points where secondary beams or cut-off columns are supported (Figure 11.21) appears quite frequently. This is due to the vertical component of the earthquake, which amplifies the concentrated load.

X-shaped shear cracks in short beams coupling shear walls also appear quite often. This is a shear failure similar to that which occurs in short columns (Figure 11.22) but not dangerous for the stability of the building (see also Subsection 9.3.3).

Figure 11.20 Flexural cracks at the lower face of the beam near the joint.
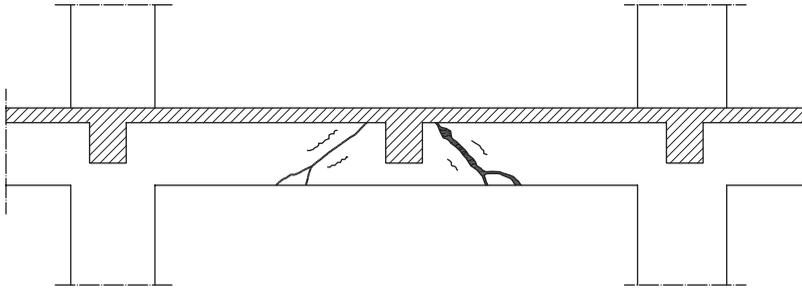
Figure 11.21 Shear failure at the location of an indirect support.
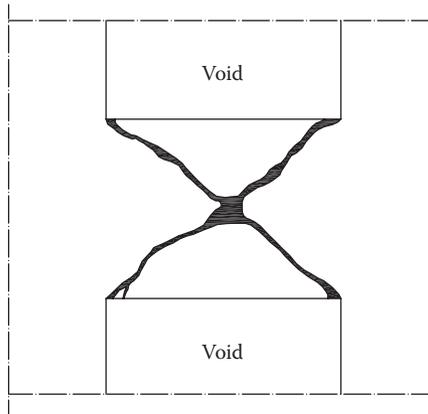
Figure 11.22 Shear failure of a shear wall coupling beam.

11.1.5 Damage to beam–column joints

Damage to beam–column joints, even at the early stages of cracking, must be considered extremely dangerous for the structure and be treated accordingly. Damage of this type reduces the stiffness of the structural element and leads to uncontrollable redistribution of load effects. Common failures of beam–column joints (corner joint, exterior joint of a multi-storey structure and interior joint) are shown in Figures 11.23 through 11.26.

The flow of internal forces in the reinforcement and the concrete during the successive phases of cyclic loading has already been explained in Subsection 8.4.2 and will not be discussed here.
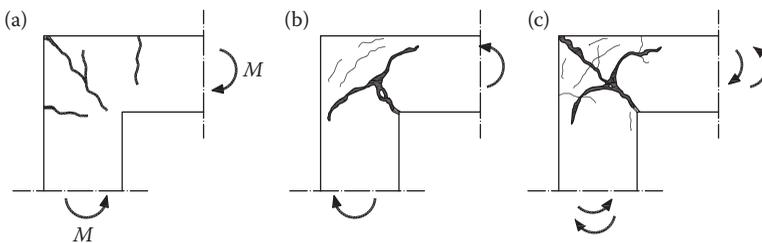
Figure 11.23 Failure of a corner joint: (a) moments subjecting the inner fibre to compression; (b) moments subjecting the inner fibre to tension; (c) cyclic bending moment loading.
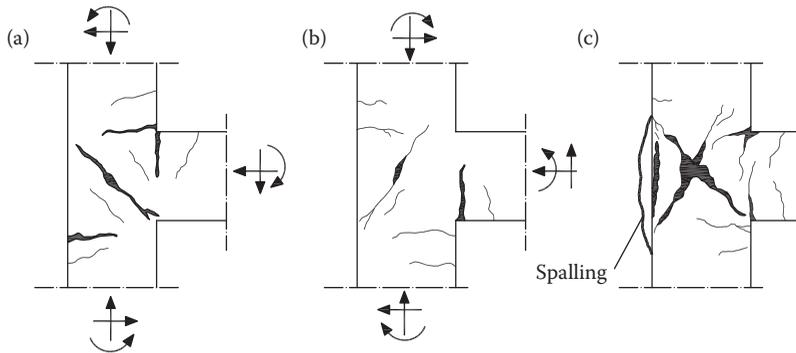
Figure 11.24 Failure of exterior joint in a multi-storey building: (a) moments inducing compression at the lower fibre of the beam; (b) moments inducing compression at the upper fibre of the beam; (c) cyclic bending moment loading.
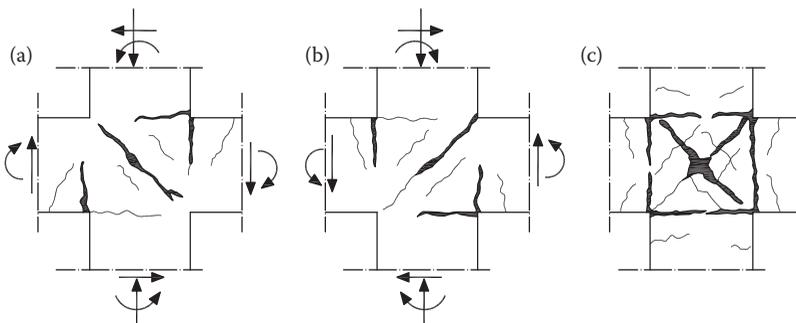
Figure 11.25 Failure of a cross-shaped interior joint: (a) seismic action in the right to left direction; (b) seismic action in the left to right direction; (c) cyclic seismic action.

11.1.6 Damage to slabs

The most common types of damage that occur in slabs are the following:

- Cracks parallel or transverse to the reinforcement at random locations
- Cracks at critical sections of large spans or large cantilevers, transverse to the main reinforcement
- Cracks at locations of floor discontinuities, such as the corners of large openings accommodating internal stairways, light shafts and so on
- Cracks in areas of concentration of large seismic load effects, particularly in the connection zones of slabs to shear walls (diaphragmatic action) or to columns in flat slab systems

With the exception of the last type, damage to slabs cannot generally be considered dangerous for the stability of the structure. However, it creates serious aesthetic and functional problems, so it must be repaired. Moreover, the creation of such damage leads to the reduction of the available strength, stiffness and energy dissipation capacity of the structure in the case of a future earthquake, and this is an additional reason for repair.

The first type of damage is the most frequent. Most cases are due to the widening of already existing micro cracks that are formed either because of bending action, temperature changes or shrinkage, and they become visible after dynamic seismic excitation. Rarely they

Figure 11.26 Failure of an exterior joint in a multistorey building Kalamata, Greece (1986).

are due to differential settlement of columns. In such cases, however, the phenomenon is accompanied by extensive cracking of the adjacent beams and masonry infills, and in this context it is detectable.

The second and third types of damage are typically due to the vertical component of the earthquake action (Figures 11.27 and 11.28).

The fourth type of damage is usually related to punching shear failure, aggravated by the cyclic bending caused by the earthquake (Figure 11.29). It has already been stressed in Chapter 4 that slabs on columns are seismically vulnerable structures, and they must be
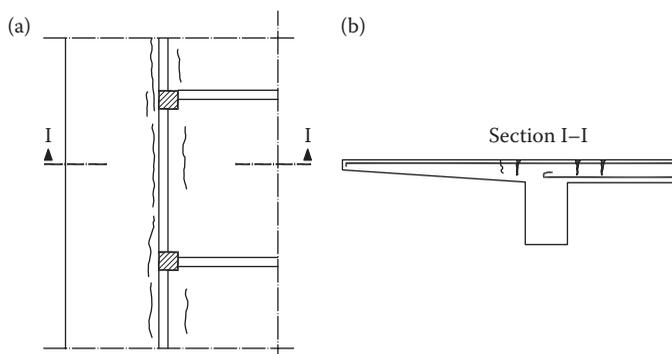
Figure 11.27 Slab damage at the critical area of a cantilever: (a) floor plan of the slab (upper side); (b) section I–I.
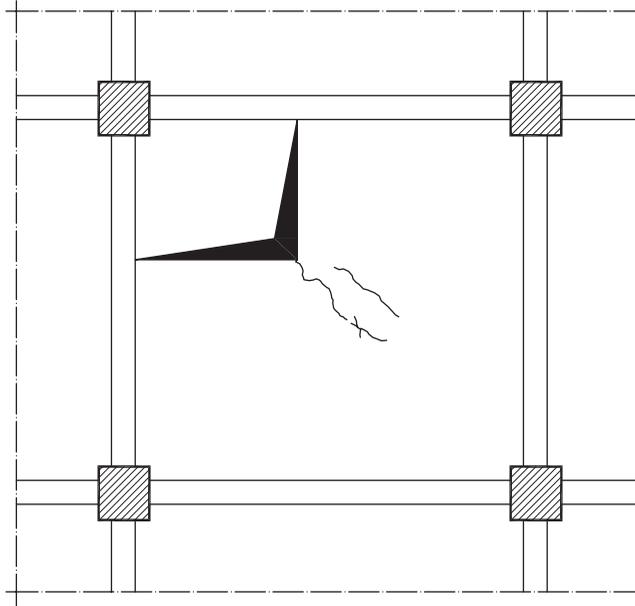
Figure 11.28 Slab damage at the corner of a large opening (down side of the slab).
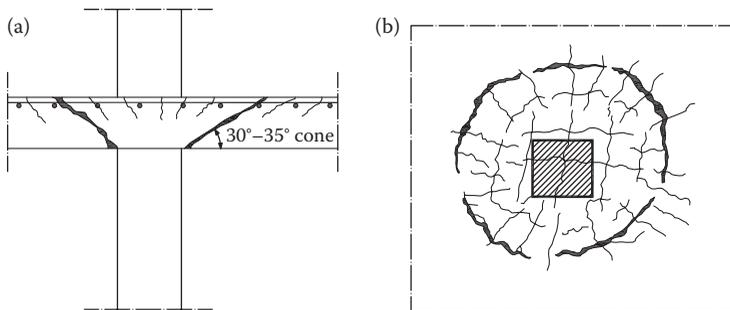
Figure 11.29 Damage at a slab-to-column connection: (a) section; (b) top side of the slab.

avoided, as they are not covered by the Codes in effect unless they are combined with other seismic-resistant systems (i.e. shear walls or ductile frames).

11.1.7 Damage to infill walls

As discussed earlier, almost all the infill walls in southern Europe are constructed with masonry in contact with the surrounding structural members of the frame. Since these infills are constructed with materials (bricks, mortar and plaster) of lower strength and deformability than the structural members, they are the first to fail. Thus, the failure of the infills starts before damage to the frame occurs, and therefore, if not accompanied by damage to the structural members, the infills cannot be considered dangerous for the stability of the structure. However, the largest portion of the repair cost is usually attributable to damage to the infills, because they involve extensive repair of installations and of finishes, such as plastering, painting, tiling, plumbing, electric installations and so on.
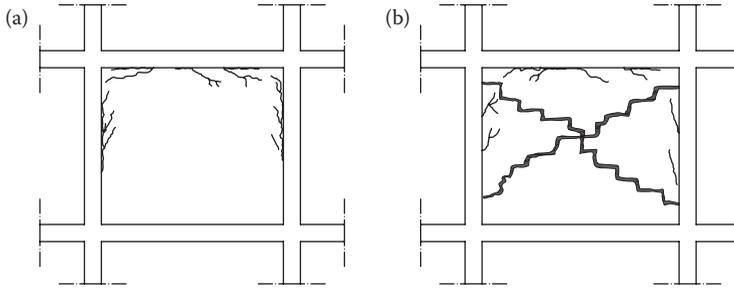
Figure 11.30 Damage in the infill panels: (a) detachment from the frame; (b) X-shaped through cracks.

The damage in the infills occurs in the following sequence: during the excitation of the structure due to an earthquake, the R/C frame starts to deform, and at this stage the first cracks appear on the plastering along the lines of contact of the masonry with the frame. As the deformation of the frame becomes larger, the cracks penetrate into the masonry, and this is displayed by the detachment of the masonry from the frame (Figures 11.30a). Subsequently, X-shaped cracks appear, small at first and becoming larger later, in the masonry itself, in a stepwise pattern following the joint lines (Figures 11.30b, 11.31 and 11.32). When the cracks do not penetrate the whole thickness of the wall, the damage is characterised as 'light', otherwise it is 'serious' damage (X-shaped cracks).

From the above discussion one can conclude that the damage in the infill panels must be the first in frequency of occurrence, since they usually precede damage in the R/C structural system (Tiedemann, 1980; Penelis et al., 1987, 1988; Stylianidis, 2012).

During the Thessaloniki earthquake of 20 June 1978, while damage occurred in 7.4% of the beams, in 5.3% of the columns and in 6.5% of the shear walls of R/C buildings, damage

Figure 11.31 Damage to masonry walls: Kalamata, Greece (1986).

Figure 11.32 Damage to masonry walls: Kozani, Greece (1996).

in infill panels occurred in 22.9% of the buildings with an R/C structural system. It should also be noted that out of the R/C buildings that suffered damage at the infill panels, 96% exhibited detachment from the surrounding frame, 79% exhibited X-shaped full-depth cracks and 12% exhibited out-of-plane collapse of the masonry wall.

11.1.8 Spatial distribution of damage in buildings

At this point it would be useful to discuss the distribution of damage in buildings.

Along the vertical direction, the most serious damage occurs on the ground floor. The frequency and intensity of damage is gradually reduced in the upper floors. This distribution has been observed in most recent earthquakes: the Bucharest, Romania, earthquake of 1977; the Thessaloniki, Greece, earthquake of 1978; the Alkyonides, Greece, earthquake of 1981; the Montenegro, Former Yugoslavia, earthquake of 1980; the Kalamata, Greece, earthquake of 1986; and the Athens (Parnitha) earthquake of 1999. The Mexico City earthquake of 1985 constitutes an exception to the above observation and will be discussed later.

The methodology for analysis and design of earthquake-resistant structures cannot explain this phenomenon. In fact, the lower storeys, particularly the ground storey, due to the higher inertial forces, are subjected to larger seismic effects. However, their structural elements are also designed for these higher seismic effects according to rules that apply to the whole building, and therefore they conform to common partial safety factors. Thus, damage is expected to be uniformly distributed throughout the building. Dynamic inelastic analysis of multi-storey buildings (Figure 11.33; Kappos and Penelis, 1987) also supports the notion of uniform
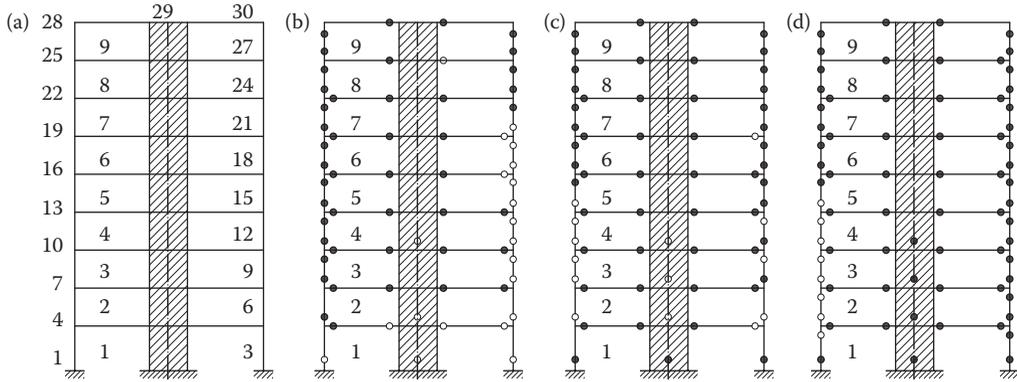
Figure 11.33 Distribution of plastic hinges in a dual nine-storey building, subjected to an El Centro (1940) excitation scaled by 0.75, 1.0 and 1.5, respectively; • = yielding of reinforcement on both ends (top and bottom); o = yielding of reinforcement on one end (top and bottom). (a) Geometry of the struct. system; (b) El Centro (1940) excitation scaled by 0.75; (c) scaled by 1.0; (d) scaled by 1.50.

distribution of damage. It is the author's opinion that the higher degree of damage in the ground floor is due to the fact that the infills contribute with the same amount of additional strength to all floors (given the fact that the masonry layout is the same on every floor), which is not taken into account when analysing the structure. Indeed, if the masonry did not exist and the required strength for the earthquake were higher than that available by a given percentage, the same for all storeys, there would be a uniform vertical distribution of damage. The addition of the strength of masonry to that of the R/C structural system exceeds the required strength in the upper storeys but not in the lower ones, and that is where damage occurs (Figure 11.34).

In the case of a flexible ground floor (shops with glass panels or the pilotis system with an open ground floor), the damage to this floor is much more severe and usually occurs only there (Figure 11.35). This subject will be discussed in detail in Subsection 11.2.5.
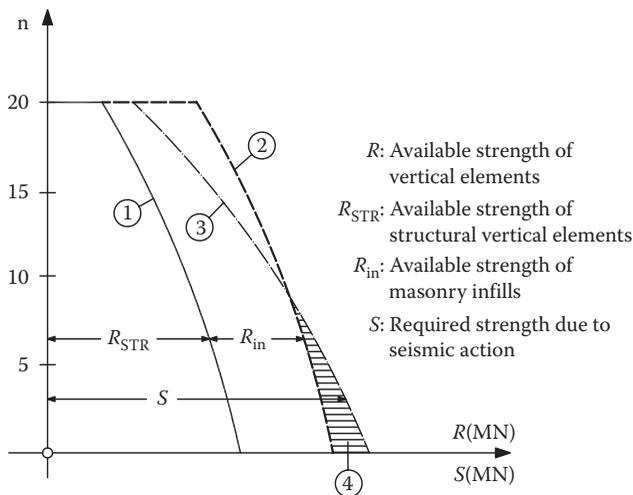
Figure 11.34 Explanation of the higher sensitivity of the lower storeys of a building: (1) shear-strength curve of the vertical structural elements of a building; (2) additional shear strength due to masonry, constant for all storeys; (3) required strength (seismic action) per storey, almost proportional to R_{STR} (e.g. 1.5 R_{STR}); (4) shaded area—storeys with damage.

Figure 11.35 Column damage of the open ground storey (pilotis system), Kalamata, Greece (1986).

As far as the horizontal distribution is concerned, most of the damage occurs in areas that are far from the stiffness center of the building and mainly on the perimeter of the building.

The Mexico City earthquake (1985) was the first during which a large percentage of collapses and large-scale damage occurred in the upper floors of buildings (38%; Figure 11.36). This can be fully explained, considering the fact that the damaged buildings were very tall (with more than 12–15 storeys), with very flexible structural systems (flat slabs), wherein higher modes generate large seismic effects in the upper floors. Furthermore, the same types of damage occur in masts or tower-like structures (e.g. bell-towers, minarets, chimneys).

11.1.9 Stiffness degradation

Strong earthquakes induce inelastic deformations to buildings accompanied in most cases by visual damage. As a result, the buildings sustain a stiffness degradation that is displayed by an increase in their fundamental period. Site investigations on actual buildings before and after an earthquake (Ogawa and Abe, 1980) have shown that there is a strong correlation between the extent of damage and the value of the ratio of the fundamental period of the building after the earthquake to that before the event. Shear cracks can be found by visual observation of buildings in which the value of the fundamental periods ratio is more than 1.3, that is,

$$\frac{T_2}{T_1} \geq 1.30 \tag{11.4}$$

Figure 11.36 Large-scale damage at the upper floors of a flexible high building, Mexico City (1985).

where
  T_1 is the fundamental period before the earthquake and
  T_2 is the fundamental period after the earthquake.

  Taking into account the fact that:

$$\frac{T_2}{T_1} = \left(\frac{K_1}{K_2} \right)^{1/2} \tag{11.5}$$

where
  K_1 is the equivalent stiffness of the building before the earthquake and
  K_2 is the equivalent stiffness of the building after the earthquake

it follows that where visual damage is observed in the building, the stiffness degradation is on the order of 40%.

$$\frac{K_1}{K_2} \geq \approx 0.60 \tag{11.6}$$

11.2 FACTORS AFFECTING THE DEGREE OF DAMAGE TO BUILDINGS

11.2.1 Introduction

In the subsections that follow, there will be an attempt to present systematically the most important factors that seem to affect the degree of damage to buildings. The presence of one

of these factors does not necessarily mean that it is the only reason for the damage. In most cases there is more than one adverse factor in a structure; therefore, the determination of how much each of the factors contributes to the damage is not feasible, even after a systematic statistical analysis of the damages.

11.2.2 Deviations between design and actual response spectrum

The first and most important reason for damage to structures is the inaccurate estimation of the characteristics of the expected earthquake excitation during the design of the structure. As is well known, in every city there are still buildings up to 100 years old in use—besides the monuments, which have survived millennia. Thus, a strong earthquake acts upon a variety of structures, some built with no structural design at all, others designed only for gravity loads, others designed for static earthquake horizontal loads with no consideration of ductility requirements, and still others, the most recent ones, designed according to the current knowledge of seismic design. It is therefore reasonable to expect that this spectrum of structures, the great majority of which do not conform to design specifications based on the current state of knowledge, will experience some damage. Furthermore, it is not impossible for damage to occur in engineered structures designed according to the current Codes, mainly for the following three reasons:

1. Even though there has been significant progress in the design of earthquake-resistant structures during the last few decades, this does not mean that the seismic protection problem has been solved. Every generation believes that it has taken important steps towards the advancement of an area of interest; future developments, though, usually come to prove this belief wrong. Thus, it is not impossible that structures built today according to the most recent advances in earthquake engineering will not conform to the specifications in effect in a few years' time.
2. Contemporary structures are designed in such a way that when the design earthquake occurs, they should respond inelastically, that is, they are expected to sustain a controllable degree of damage.
3. Quite often, the design spectrum, scaled according to the behaviour coefficient and the safety factor, does not correlate with the actual response spectrum. The Mexico City (1985) earthquake, the Kalamata (1986) earthquake and the Athens (Parnitha, 1999) earthquake can be cited as examples (Figures 11.37–11.39). Therefore, before rushing into conclusions about the contribution of each damage factor, one should first study carefully the actual response spectrum of the earthquake that has caused the damage in relation to the provisions of the Code according to which most of the structures in the area were built (Rosenblueth and Meli, 1985; Anagnostopoulos et al., 1986; Penelis et al., 1986, 2000; Kostikas et al., 2000).

Independent of the characteristics of the exciting force, a number of the structure's own characteristics, which will be discussed subsequently, are factors that contribute to the vulnerability of the structures.

11.2.3 Brittle columns

In Section 11.1, which refers to the typology of damage in structural elements, the types of column failure have been discussed in detail. The vast majority of failures in buildings with R/C structural systems are due to column failure, caused by bending and axial load, or by shear under strong axial compression. There are clear indications that in buildings
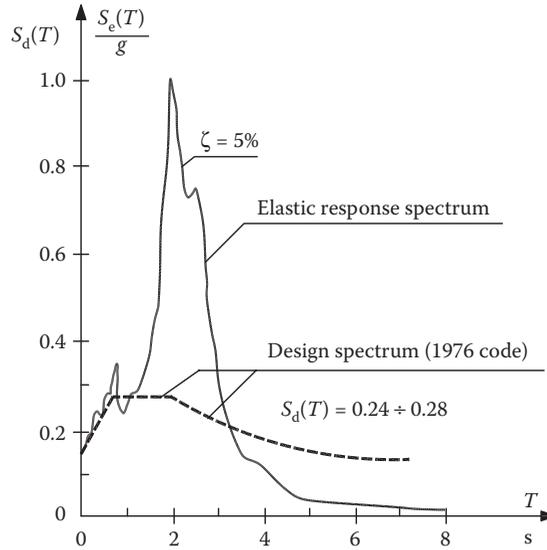
Figure 11.37 The 1985 Mexico City earthquake: comparison of the actual response spectrum with the design spectrum.

designed during recent decades, due to high axial loading level, most of the time the column reinforcement does not reach the yield point. Column failures must be attributed to the degradation of the mechanical properties of the concrete due to high inelastic strains under cyclic loading (low cycle fatigue). Quite often, the main reason for failure is the large spacing of ties at the critical regions of the column.

It should be noted that the main cause for 55% of the 103 most affected buildings in the Athens earthquake (1999) must be attributed to poor hoop and tie reinforcement of columns either at critical regions of confinement or along the axis of the column for shear (Figure 11.51).
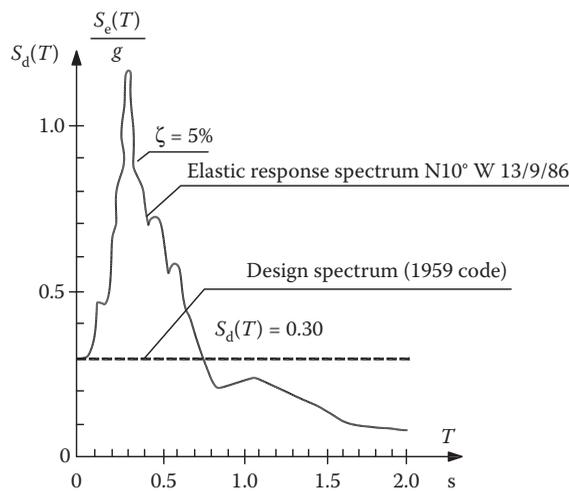
Figure 11.38 The Kalamata, Greece, earthquake of 13 September 1986: comparison of the elastic response spectrum with the design spectrum.

Athens E/Q7/9/1999
Elastic spectra
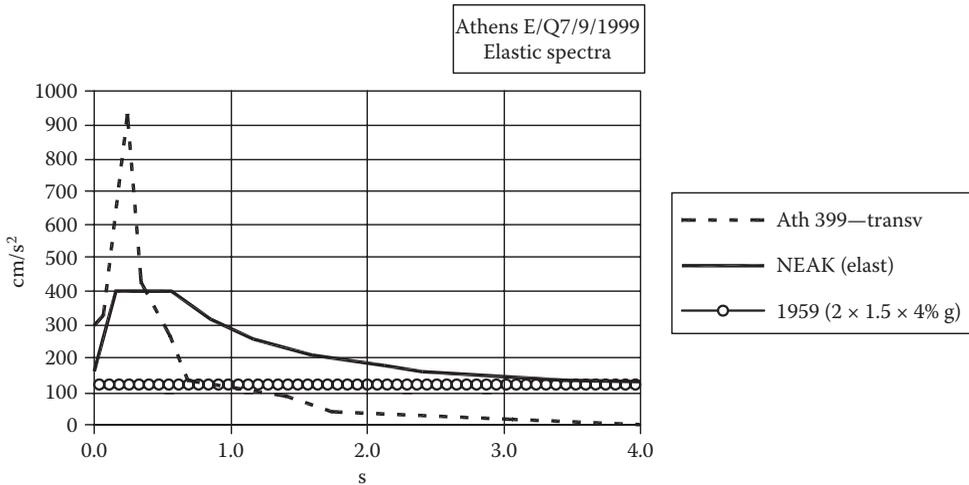
Figure 11.39 The Athens (Parnitha) 1999 earthquake, comparison of the elastic response spectrum with the design spectrum.

11.2.4 Asymmetric arrangement of stiffness elements in plan

It is well known that the core of the staircase and elevators is the basic stiffness element in the structural system of a building; therefore, according to what has been discussed in the chapter on the analysis of structures, its central or eccentric position should be of major importance for the behaviour of the building in an earthquake (Figure 11.40). However, a statistical evaluation of the damage that the 1978 earthquake caused to the buildings of Thessaloniki (Penelis et al., 1987, 1988) shows that this factor affected only by 6% the mean value of the percentage of the damaged structures (Figure 11.41). This phenomenon must be mainly attributed to the fact that the infills drastically change the stiffness distribution in the building, and, as a result, the effect of eccentricities due to asymmetric arrangement of R/C stiffness elements is reduced. In contrast, asymmetric arrangement of masonry causes markable inferior behaviour. This asymmetric arrangement of masonry is usually observed in the ground floors of structures located at the corners of building blocks, where the two sides of the perimeter are not filled with masonry because of their usage as shops (Figure 11.42). This is one of the topics that will be discussed next.

It should be noted that according to the survey and evaluation of damages for the 103 most affected buildings in Athens (1999), the asymmetric arrangement of structural stiffness elements in plan covered 15% of the cases, while the asymmetric arrangement of masonry infills in plan corresponded to 7% of cases (Figure 11.51).

11.2.5 Flexible ground floor

The sudden reduction of stiffness at a certain level of the building, typically at one of the bottom floors, results in a concentration of stresses in the structural elements of the flexible floor, which causes damage to those elements. An illustrative example of this fact is the distribution of shear forces that are developed on the R/C staircase core of a 20-storey building with no masonry at the four lower floors (Figure 11.43; Dowrick, 2005). The shear force distribution has been determined using dynamic inelastic analysis. This example makes obvious the fact that, for the floors with masonry, the shear force acting on the staircase core

Figure 11.40 Torsional collapse of a building in Mexico City (1985).
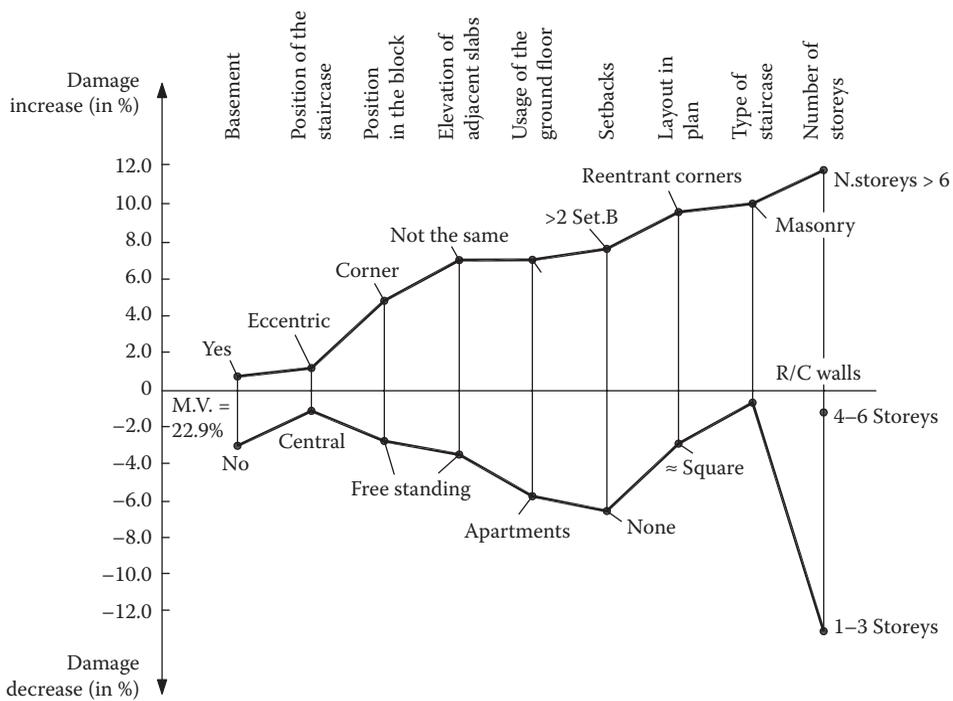
Figure 11.41 Statistical evaluation of the damage in Thessaloniki, Greece (1978).
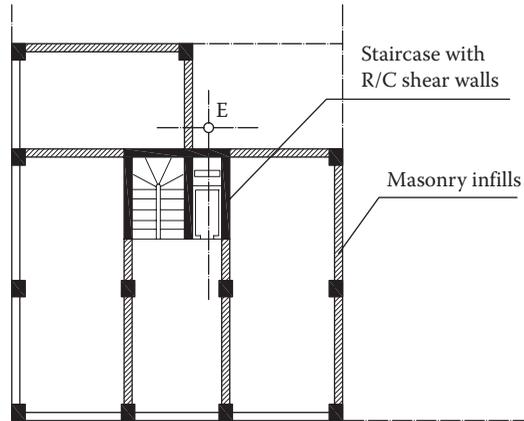
Figure 11.42 Stiffness centre location of a corner structure, when masonry infills are taken into account (approximately).

is much smaller if the infills are taken into account for the analysis, while for the four lower floors without masonry, the resulting shear force is much higher. For this reason the Seismic Codes in effect today require an increase in the design shear for the storey with reduced stiffness compared to that of upper floors (see Paragraph 8.5.3.2). They also require a high degree of confinement through closely spaced ties or in the form of spirals, throughout the height of the columns of the weak floor, in order to increase their ductility.

The most common case of a flexible floor is the open ground floor (pilotis system) or the ground floor used as a commercial area. In such a case, while the upper floors have high stiffness due to the presence of masonry infills, the ground floor has a drastically reduced stiffness because the vertical structural members contribute almost exclusively to it. In these buildings almost all the damage occurs in the vertical structural elements of the ground floor, while the rest of the building remains almost unaffected (Figure 11.44). In contrast, in buildings with masonry infills in the ground floor, the damage spreads throughout the structure with usually decreasing intensity from the ground to the upper floors. The 1978
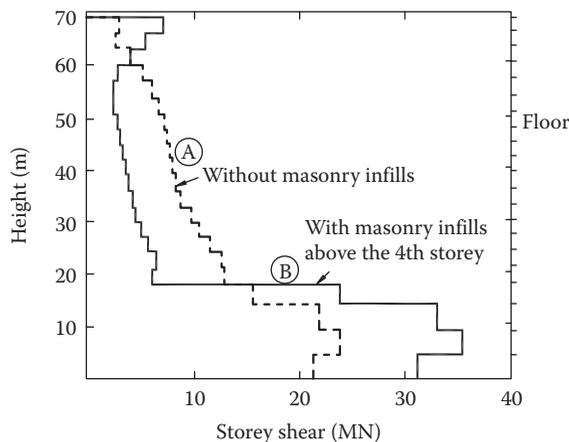
Figure 11.43 Shear force diagram of the staircase core of a 20-storey building, which is indicative of the effect of masonry infills on the storeys above the fourth floor.

Figure 11.44 Collapse of a building with a flexible ground floor: Bucharest, Romania (1977).

Thessaloniki earthquake caused damage to only 16.4% of the buildings with masonry infills in the ground floor, while damaged buildings having the pilotis system or shops on the ground floor reached 29.8% of the total number of this type of building. During the Mexico City earthquake of 1985, 8% of the buildings that collapsed or exhibited severe damage had a flexible ground floor.

Finally, during the Athens earthquake (1999) one of the main causes of damage for 22% of the 103 most affected R/C buildings was the 'pilotis effect' (Figure 11.51).

11.2.6 Short columns

It has already been noted (see also Subsection 8.3.6) that short columns can experience an explosive shear failure that can lead to a spectacular collapse of the building. This phenomenon, however, appears to be rarer than the failure of regular columns.

In the case of the Athens earthquake (1999), the failure of short columns was one of the main causes of damage near collapse for almost 16% of the 103 most affected R/C buildings (Figure 11.51).

11.2.7 Shape of the floor plan

Buildings with a square-shaped floor plan have the best behaviour during an earthquake, while buildings with divided shapes such as +, I, X or with re-entrant corners have the worst. During the 1978 Thessaloniki earthquake, among the damaged buildings (with damage in the R/C system), 19.5% had a square-shaped floor plan, while 32.5% had non-convex shapes of floor plan. This is the reason why EC8 and the CEB/MC-CD/85 do not allow simplified methods of analysis for earthquake actions when the building under consideration does not have a regularly shaped floor plan.

11.2.8 Shape of the building in elevation

Buildings with upper storeys in the form of setbacks have markedly inferior behaviour than buildings with regular form in elevation. During the 1978 Thessaloniki earthquake, among the total number of damaged buildings, 15.9% were buildings regular in elevation, while 29.9% were buildings with three or more successive setbacks (see also Figure 11.41).

11.2.9 Slabs supported by columns without beams (flat slab systems)

This type of failure has been discussed in the section on slab failures. In seismically active southern Europe, this type of structure is rather recent and therefore there are no statistical data regarding this failure mode. Experimental data, however, as well as statistical data from the 1985 Mexico City earthquake, suggest that this is a very vulnerable type of structure. Indeed, in Mexico City, where this kind of structural system is widely used, 41% of collapses or serious damage occurred in buildings of this type. Structures with such slabs are very flexible and with low ductility. Most of the failures in Mexico City occurred in columns. However, in more than 10% of the cases the columns punched through the slab, under the action of a combination of both vertical and horizontal seismic loads. Moreover, the small thickness of the slab did not allow the development of the required bond stresses around the longitudinal reinforcement of the columns, and, therefore, after a few loading cycles, the joints failed due to the failure of bond mechanisms along the thickness of the slabs (Figure 11.45). For this reason, EC 8-1/2004 does not cover this type of structural system if it is not combined with other seismic-resistant systems (i.e. shear walls, ductile frames).

11.2.10 Damage from previous earthquakes

Buildings that have sustained damage during a previous earthquake and have been repaired usually exhibit the same type of damage in the next earthquake, to a larger extent. This
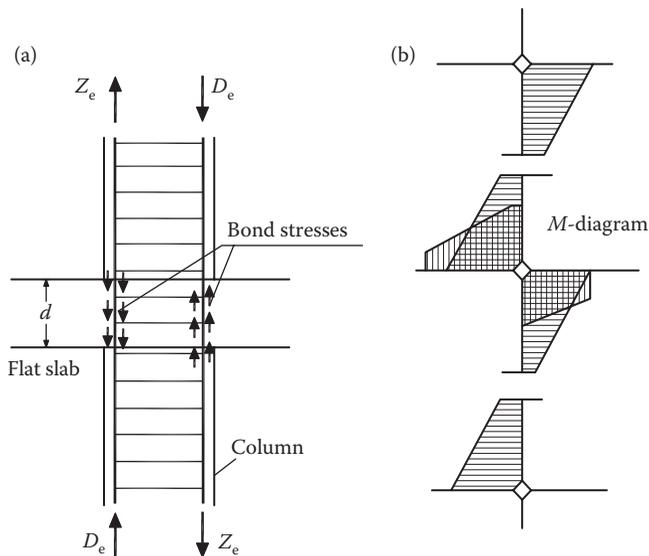
Figure 11.45 Degradation of bond between concrete and column reinforcement within the small thickness d of the slab: (a) sketch of the flow of forces; (b) corresponding bending moment diagram.

Figure 11.46 Collapse of a building in Bucharest during the 1977 earthquake. The building, as depicted in the illustration, had been repaired after the 1940 earthquake.

phenomenon was observed in Bucharest during the 1977 earthquake, where many of the buildings repaired after the 1940 earthquake collapsed (Figure 11.46), and also more recently in Mexico City. The main reason for this phenomenon is that the repair work was not carried out carefully enough, and also the fact that 60 to 70 years ago the repair technology of earthquake damage was in the early stages of development.

In the case of the Athens earthquake (1999), only 3% of the 103 most affected buildings exhibited damages due to poor repair or strengthening from the previous earthquake of 1981 (Alkyonides earthquake).

11.2.11   R/C buildings with a frame structural system

Frame systems, not inferior to dual systems as far as strength is concerned, but superior with regard to available ductility, have lower stiffness than dual systems. As a result, during a seismic excitation, large inter-storey drifts develop, which cause extensive damage in the infill system. Given that the repair of this damage is a very costly procedure, it is understood why the 'frame system' constitutes a source of vulnerability for buildings. Therefore, although with frame systems ductile behaviour can be achieved more easily than with dual ones, and although this had led to extensive use of the frame systems in the 1960s, since about 1975 the idea that shear-wall systems are more suitable for R/C buildings has become more widely accepted. Comparative studies of building behaviour during the earthquakes of Managua (1972), San Fernando (1971), Caracas (1967) and Skopje (1963) support the

above opinion (Fintel, 1974). From the Thessaloniki earthquake (1978), among the damaged buildings (damage in the structural system), 22% were buildings with shear walls and 32.9% were buildings without shear walls. Finally, one of the main observations of the research team from the University of Thessaloniki, which visited and studied the earthquake damage in Kalamata, Greece, in 1986, was the large extent of masonry damage in most multi-storey buildings with a frame structural system (Penelis et al., 1986). It is important here to note again that this type of structural system is susceptible to collapse in a pancake mode (Figure 11.51) in the case of poor design of columns or joints.

11.2.12 Number of storeys

The number of storeys is directly related to the fundamental period T of the structure, as discussed in previous chapters. Therefore, at least theoretically, the vulnerability of the structure to an earthquake depends on the ordinate of the acceleration spectrum of that specific earthquake corresponding to T, in relation to that of the design response spectrum of the building. In this context, the vulnerability of the building should be independent of the number of storeys. However, the existing statistical data from earthquakes show that the vulnerability increases with the height of the buildings. As typical examples, one can cite Bucharest (1977), where damage and collapse were focused mainly in buildings with more than six storeys, Mexico City (Table 11.1; Rosenblueth and Meli, 1985) and Thessaloniki (1978), where among the damaged buildings, 10.9% were low-rise buildings (one to three storeys), while 34.9% were high-rise buildings (over six storeys). In Bucharest and Mexico City the concentration of damage in high-rise buildings is compatible with the response spectrum of the corresponding earthquake, since large acceleration values correspond to high natural periods, corresponding to high-rise buildings. In the case of Thessaloniki, however, this correlation does not exist. The author's opinion on this issue is that the infill system drastically increases the stiffness as well as the strength of the structure. Given the fact that the masonry layout is more or less the same in every floor and independent of the height of the building, the percentage of additional stiffness and strength due to the presence of masonry is higher in low-rise buildings than in high-rise ones. As a result, the behaviour of low-rise buildings appears to be better (Figure 11.47).

11.2.13 Type of foundations

The form of the foundation of the structure has two types of effects on the extent of damage in the building: direct and indirect.

Direct effects are displayed in the following characteristics:

- Failure of the foundation members (e.g. fracture of a foundation beam)
- Fracture of the foundation soil

Table 11.1 Percentages of collapses and serious damage in Mexico City (1985)

Number of storeys	Percentages of collapses and serious damage (% of every building category)
1–2	0.9
3–5	1.3
6–8	8.4
9–12	13.6
>12	10.5
Total	1.4
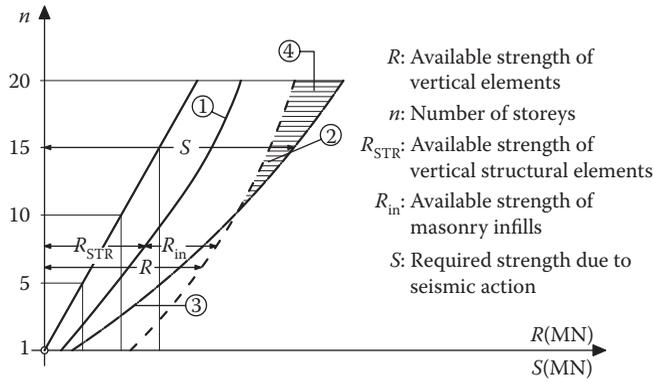
Figure 11.47 Explanation of the seismic vulnerability of high-rise buildings: (1) shear-strength curve of vertical structural elements; (2) additional strength due to masonry, constant for all floors; (3) required shear strength (seismic action), almost proportional to R_{STR}; (4) shaded area—buildings with damage.

- Soil liquefaction
- Differential settlements of the ground
- Partial or general landslide of the foundation soil

The most usual form of the effects listed above is the differential settlements of the ground, especially in soft soils. Failures due to soil liquefaction are seldom seen, but spectacular (Figure 11.48).

Figure 11.48 Consequences of soil liquefaction on a high building in Mexico City (1985).

The *indirect effects* are related to the out-of-phase motion of the bases of the individual columns, when their footings are not interconnected (see Subsection 4.2.12, Figure 4.17), or when the existing connection is too flexible. These differential displacements in both the horizontal and the vertical directions subject the structure to additional strains. As a result, buildings with isolated footings suffer more under seismic action than others. A characteristic example of the above is the fact that in the 1986 Kalamata, Greece, earthquake, the damage to the buildings on the sea-front avenue, where the foundations had great stiffness, was limited. The same did not happen in Thessaloniki, Greece, however: although the foundations of the buildings in the coastal zone were either mat foundations or grids of foundation beams, the percentage of damage was high. The interference of other factors irrelevant to the type of the foundation, such as the amplification factor of the seismic excitation that is applied to soft soil deposits, and the shift of the prevailing period of the exciting force toward higher values when such soils are present, does not allow a clear statistical evaluation of how the presence of a good foundation indirectly affects the vulnerability of structures.

11.2.14 Location of adjacent buildings in the block

The location of adjacent buildings on the block has a great effect on the behaviour of the structure in response to an earthquake. More particularly, corner buildings are much more sensitive to earthquakes than free-standing ones. In the 1977 Bucharest earthquake, 35 out of the 37 buildings that collapsed were located at the corner of the block (Figures 11.41 and 11.49). In the 1985 Mexico City earthquake, 42% of the buildings that suffered serious damage or collapsed were corner structures (Rosenblueth and Meli, 1985; Table 11.2). In the 1978 Thessaloniki earthquake (Figures 11.41 and 11.49), among the damaged buildings (with damage to the R/C structural systems), only 19.9% were free-standing buildings, while

Figure 11.49 Collapse of an eight-storey corner building in Thessaloniki, Greece (1978).

27.9% were corner ones. As sources of the higher vulnerability of corner structures, the following can be mentioned:

- Asymmetric distribution of stiffness elements on the floor plan due to the lack of masonry on two sides of the perimeter of the ground floor, where the space is usually occupied by stores.
- Transfer of kinetic energy to the corner buildings during the seismic interaction of adjacent buildings (Figure 11.50) through pounding. This transfer of energy causes a substantial increase of the inertial forces acting on the end structures (Anagnostopoulos, 1988; Athanassiadou et al., 1994).

11.2.15 Slab levels of adjacent structures

The impulse loading that a building receives from an adjacent structure during an earthquake is a major source of damage. The problem becomes even more serious when the floor slab levels of adjacent buildings do not coincide. In this case, the slabs of one structure

Table 11.2 Causes of failure in Mexico City (1985)

Reason for failure	Percentage
Asymmetric stiffness	15
Corner structure	42
Weak ground floor	8
Short columns	3
Exceeded vertical design load	9
Pre-existing ground settlement	2
Pounding of adjacent structures	15
Damage from previous earthquakes	5
Punching failure of flat slabs	4
Failure of upper floors	38
Failure of lower floors	40
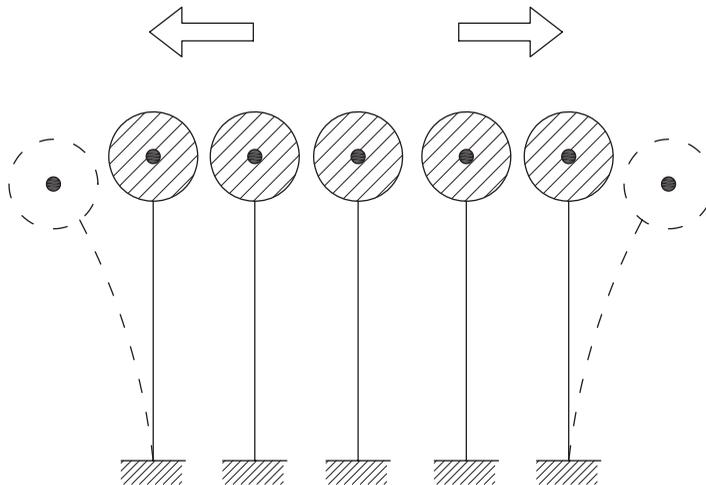
Figure 11.50 Transfer of energy at the end of SDOF oscillators in a series of adjacent systems.

during the oscillation pound on the columns of the adjacent building, and this results in fracture of the columns. In the 1978 Thessaloniki earthquake, among the damaged structures, the percentage of free-standing buildings or buildings that had the same floor slab levels as adjacent ones was only 19%, while the percentage of buildings with slab levels different from those of adjacent ones was 30.5%. In the 1985 Mexico City earthquake, in more than 40% of the structures that collapsed or suffered serious damage, pounding of adjacent structures took place (Table 11.2).

In the Athens earthquake of 1999, 21% of the most affected 103 R/C buildings had pounding from adjacent buildings as a main cause of damage.

11.2.16 Poor structural layout

This category includes buildings with asymmetric arrangement of stiffness elements in plan and elevation, irregularities of form in plan and elevation, cut-offs of columns, setbacks and so forth. Most of these categories have already been examined in previous items. However, as a whole they reflect the result of poor collaboration of the architect and the structural engineer during the phase of conceptual design.

From the evaluation of the 103 most affected R/C buildings in Athens (1999), it has been concluded that almost 29% of them had poor structural layout as a main cause of failure (Figure 11.51). This, together with poor transverse column reinforcement, the 'pilotis effect', and the pounding of adjacent buildings on the block *were the four main reasons for collapse*

	Main cause of damage	Frequency in %										
		5	10	15	20	25	30	35	40	45	50	55
②	Poor layout of the structural system						29%					
④	'Pilotis effect'					22%						
⑤	Irregularities in plan of masonry infill	7%										
⑥	Irregularities in plan of vertical stiffness elements			15%								
⑦	Short columns				16%							
⑧	Adverse foundation conditions	8%										
⑫	Pounding from adjacent buildings				21%							
⑬	Inadequate longitudinal reinforcement in columns		9%									
⑮	Inadequate transverse reinforcement (hoops) in columns											55%
⑱	Inadequate column cross sections			13%								
㉔	Inadequate anchorage of longitudinal reinforcement		11%									

Figure 11.51 Frequency (in %) of appearance of various main cases of damage in the 103 most affected R/C buildings in Athens after the earthquake of 1999. (Adapted from Kostikas, Ghr. et. al. 2000. *Evaluation of damages and their cause for 103 near to collapse R/C buildings in Athens after the earthquake of September 7, 1999*, Report of the OASP (Seismic Risk Management Agency of Greece).)

or damage near to collapse of the 103 most affected buildings in the Athens earthquake (1999; Figure 11.51).

11.2.17 Main types of damage in buildings designed on the basis of modern codes

The earthquake of Athens, 1999, was a chance for a preliminary evaluation of damages displayed in R/C buildings constructed after 1985, which is the *'benchmark year'* in Greece for new generation Seismic Codes.

In fact, out of 103 of the most affected R/C buildings, 12 were designed and constructed according to these Codes. Although the number is limited and, therefore, statistically justified conclusions cannot be drawn, some initial remarks can be made:

1. The main causes of heavy damage continued to be the following:
   - Poor confinement and poor shear reinforcement of columns
   - 'Pilotis effect'
   - Short columns
   - Pounding of adjacent buildings
   - Poor structural layout
2. The ratio of the number of heavily affected R/C buildings of the period between 1985 and 1999 (14 years) to the total number of heavily affected buildings (12/103) did not display any improvement in relation to the ratio of the building stock of this period to the total stock (0.12–0.14). In the author's opinion, this must be attributed to the fact that there is always a lag between establishment and implementation of a new Code in practice.
3. The above explanation is based on the findings *in situ*, that is, poor structural layout, inadequate confinement in critical regions, inadequate joints between adjacent buildings and so on, although there was detailed reference in the Codes after 1985 for special concern on these points. In any case, the above remarks must be considered of limited credibility since they refer to a transient period of 14 years with a limited number of new buildings under consideration.

Chapter 12

Emergency post-earthquake damage inspection, assessment and human life protection measures

12.1 GENERAL

The aim of this chapter is to present a reliable procedure that should be followed for the emergency inspection of buildings after an earthquake so that all the structures of the affected area will be inspected in a credible way. The data collected by such inspections assist the State in achieving the following goals (UNIDO/UNDP, 1985, Penelis and Kappos, 1997):

- Reduce the number of casualties and injuries to occupants of damaged buildings, which might be caused by collapses due to subsequent aftershocks;
- Help people of the affected area gradually return to a normal way of life, which presupposes a reliable characterisation of the dangerous buildings and full knowledge of the extent of hazardous structures;
- Develop a database for a uniform assessment of risk in economic, social, political and other terms;
- Record and classify earthquake damage, so that the repair of damaged buildings will follow a priority order;
- Improve earthquake-resistant design, based on the recorded damage.

It should be obvious from this brief introduction that after a destructive earthquake, two levels of building inspection follow. The first level of inspection is performed by the State, during which there is a recording of damage, characterisation of hazardous (for usage) structures, demolition of buildings close to collapse, and propping for those that need it. This is an operation that needs to be carried out quickly, in order to gradually restore the normal way of life in the affected area.

During the second level of inspection, which will be discussed in detail in Chapter 13, the residual strength of every affected structure is estimated and the degree of intervention is decided. This is a laborious procedure that starts as soon as the first level of inspection is completed and the frequency and intensity of the aftershocks have diminished. It is also a procedure that is directly related to the decision about the repair and/or strengthening of the structures (EC8-3, CEN, 2005).

12.2 INSPECTIONS AND DAMAGE ASSESSMENT

12.2.1 Introductory remarks

The purpose of this section is a brief treatment of the problems related to the evaluation of damage to structures after an earthquake. A strong earthquake, like every other hazard,

puts on trial not only the citizens, but also the State. The authorities have to face chaotic situations due to lack of information, delays in locating the affected areas, eventual interruption of communications and multiple requests for assistance and for inspections of damaged buildings. In the first tragic hours, even days sometimes, the affected area stands almost alone, and it is during this initial period when good construction, good communications, good decision-making and good planning pay off in terms of lives and properties saved. The credibility of the State in its citizens' eyes depends on what the State can or cannot do during this early period. These are the views of government officials in charge of disaster relief, who have experienced the situations and problems that arise after a strong earthquake (Office of Emergency Preparedness, 1972; Penelis, 1984, 2008).

The foregoing remarks aim at depicting the environment in which the structural engineer is called upon to do an assessment; this should be the prevailing element for the design of the entire operation (see Chapters 13 and 14). Indeed, since damage evaluation sometimes refers to thousands of buildings, which have to be assessed in a short period of time in order for the affected area to return to a normal way of life, a special procedure has to be followed, completely different form that used for the assessment of the structural resistance of an individual building. In this context, procedures developed for '*seismic evaluation of buildings*' for the pre-earthquake period (FEMA 154-158-178, FEMA 310; see Chapter 14) cannot be implemented in post-earthquake emergency conditions. After a strong earthquake, only *damage-oriented evaluation* may be implemented.

In the subsections that follow, there is systematic reference to organisational matters of an operation for damage assessment, and also to matters of inspection, as well as to problems that the structural engineers face during evaluation of individual cases. At the same time, reference is made to propping measures that are taken in case of serious damage susceptible to collapse. This presentation is based on experience from the organisation and implementation of such an operation in the Thessaloniki (Greece) metropolitan area in 1978, for which one of the co-authors was the person in charge. Since then, this procedure, with minor modifications, has been implemented for various strong earthquakes that have affected Greece (Alkionides earthquake 1981, Kalamata earthquake 1986, Grevena earthquake 1989, Aigion earthquake 1990, Athens (Parnitha) earthquake 1999, etc.). It is also based on publications of several international organisations and national committees on the same subject (ATC, 1978; Greek National Report, 1982; Yugoslav National Report, 1982).

12.2.2 Purpose of the inspections

The main purpose of the inspection procedure for the structures after a destructive earthquake is to minimise the probability of casualties or injuries for the occupants. The hazard of such an event in buildings where damage has occurred in the main shock is serious enough, because it is possible for some of them to partly or completely collapse due to repeated aftershocks, as happened with the Alkyonides, Greece, earthquake (1981), and also with the Kalamata, Greece, earthquake (1986).

There are also other reasons for the inspections, beyond the above-mentioned, which are also of great importance. Thus, after the classification of those damaged buildings which are hazardous to use, life gradually returns to normal, given the fact that the rest of the buildings – as soon as the first psychological reactions begin to disappear – gradually return to their normal usage. Also, based on the first damage assessment, an approximate idea of the magnitude of the disaster in economic terms may be obtained. These data are needed by all levels of administration almost immediately for them to be able to start a

proper planning of aid. Of course, the development of fragility curves in the pre-earthquake period in relation to the seismic action intensity of the seismic event allows the cost estimate of retrofitting activities that will follow (see Chapter 16).

Finally, the statistical data from such an operation are very useful, not only for short-term decision-making regarding temporary housing but also in the long run on matters of evaluation of the construction procedures followed in the past and the factors that could affect them positively.

In closing, it should be noted that in the case that the affected area includes a large city, the whole procedure should be managed very carefully, as this becomes a large-scale operation with very high cost and organising requirements, accompanied by long-term implications. Indeed, the classification of a building as 'damaged' by the State leads to a long-term degradation of its market value, even though strengthening interventions after the earthquake could make it stronger than other non-damaged buildings.

12.2.3 Damage assessment

12.2.3.1 Introduction

It has already been mentioned that the main concern during damage inspection in structures after an earthquake is to minimise the probabilities of accidents to occupants, caused by partial or total post-earthquake collapses. Therefore, the problem that the structural engineer has to face in every case is to estimate the residual strength, ductility and stiffness of the structure, and decide whether or not they are sufficient to allow the use of the building at an acceptable level of risk.

It is understood that this evaluation, based on the existing evidence, is probably the most difficult problem for the structural engineer – much more difficult than the design of a new building. Extensive site inspections are required, first of all for a damage survey, and then to check the geometry of the structural system, the quality of the construction materials, the placement of reinforcement at critical structural elements compared to the original drawings, the vertical loads of the structure and the quality of the foundation soil. Subsequently, extensive calculations are needed, using the information collected from site observations, in order to determine the residual strength, stiffness and ductility of the structure. Finally, it has to be estimated whether or not the seismic excitation under consideration did not exceed the level of seismic hazard adopted by the code for the particular zone, as expressed by the design response spectrum.

Such a procedure is time-consuming and requires the full involvement of specialised personnel with a variety of technical means at their disposal. It is therefore obvious that such a procedure cannot be activated during the phase of emergency classification of structures as usable or not, since it is not feasible due to time and cost constraints.

Thus, engineers come face to face with buildings struck by the earthquake, without being able to use the scientific tools that they possess for the quantitative evaluation of the structure, which are the *in-situ* measurements, the tests, and the analysis. They are compelled by the circumstances to restrict themselves to qualitative evaluations and make decisions based solely on visual observation of damage, using of course their knowledge and experience and good engineering judgment. This last statement is extremely important because it shows that these evaluations are very subjective. Notwithstanding its weaknesses, according to international practice, damage assessment is based on the above procedure (ATC 3-06, 1978; Greek National Report, 1982; Yugoslav National Report, 1982; UNDP/UNIDO, 1985).

12.2.3.2 General principles of damage assessment

Although damage assessment and decision making regarding the degree of usability of a structure are very subjective, there are some general principles that structural engineers must keep in mind when they have to make a decision concerning a building damaged by an earthquake. These are as follows

1. They must have clearly in mind that their judgment must be limited to the evaluation of the risk of partial or total collapse in case of an aftershock, which is an earthquake of smaller magnitude than the main earthquake that comes from the same tectonic fault, therefore having characteristics similar to the main one (similar acceleration spectrum with smaller maxima). Thus, if the building does not exhibit damage to the structural system from the main shock, it means that it has not exceeded the elastic range, therefore the probability of damage, and, even more, the probability of collapse caused by aftershocks is statistically insignificant.

2. The risk of partial or total collapse of a structure damaged by the main earthquake comes from failure of vertical structural members (columns, structural walls, load-bearing masonry) under the action of vertical loads in combination with the horizontal seismic loads from aftershocks, which are expected to be smaller than the loads from the main event. The engineer should keep in mind that if damage appears in the structural system of a building, it means that the elastic range has been exceeded and therefore the resistance of the structure to seismic loading has been reduced by the main seismic event.

3. According to the above, engineers who perform the inspection first have to find out the layout of the structural system of the building, at least in the cases when it is damaged. If necessary, in the absence of drawings, they should use hammer and chisel in order to determine the location of the vertical structural elements of the building. No reliable damage assessment is possible without a clear understanding of the structural system of the building.

4. In order to estimate the residual strength, stiffness and ductility of a structure, the engineer has to trace out the damage to the structural system as well as to the infill panels. Particularly hazardous is damage to the vertical elements, especially at the ground floor. Crushing of concrete at the top or the bottom of a column accompanied by buckling of the longitudinal reinforcement, X-shaped cracks in shear walls with significant axial loading, and X-shaped cracks in short columns are some of the types of damage that should seriously worry the engineer who performs the inspection. Extensive X-shaped cracks in the infills accompanied by permanent deviation of the structure from the vertical are also alarming indications. In contrast, cracks in horizontal structural elements, caused by either flexure or shear, are not particularly alarming. The same holds for limited spalling of vertical elements or flexural cracks. However, it has to be stressed that the familiarity of the engineer with the various types of earthquake damage is very useful, if not indispensable, for damage evaluation.

5. Before concluding the final evaluation, the engineer should pay particular attention to the following:
   a. The configuration of the structure. Buildings with symmetric or approximately symmetric floor plans have better seismic behaviour than asymmetric ones.
   b. The location of the vertical stiffness members on the floor plan. Symmetrically located stiffness members drastically reduce the consequences of eccentric loading.

   c. The existence of a flexible storey. The open ground floor (pilotis system) or ground floor occupied by stores make the building vulnerable to seismic actions.
   d. The quality of the construction material. *In situ* tests with hammer and chisel, or, better, with special hammer testing equipment, constitute a very good relative indicator for the engineer, who can draw very useful conclusions after a few repetitions.
   e. The location of the structure in the block. It should not be forgotten that the vast majority of total collapses worldwide have occurred in corner structures.
 6. The conclusion of the foregoing discussion is that the engineer can make one of the following decisions:
   a. Allow use of the building without any restriction, provided it does not exhibit any visible damage to the structural system (classification with, say, the color *green*);
   b. Classify it as temporarily unusable and limit access to it (shifting the responsibility to the occupant) because of limited damage, until it is repaired (classification with, say, the color *yellow*);
   c. Classify it as out of use because of extensive damage, until based on a detailed study, it is decided either to repair or demolish it (classification with, say, the color *red*);
   d. Classify it as a *near-collapse building* and activate propping measures together with prohibition of any approach to the area around the building.

It is obvious that buildings that fall into the first and last categories can easily be distinguished from buildings of the other two categories, for which capacity to resist an earthquake has been reduced because of damage, but they do not exhibit signs of a near-collapse condition. In contrast, the distinction between the 'yellow' and 'red' categories is not always easy; therefore, in case of doubt, the more conservative decision should be made.

12.3 ORGANISATIONAL SCHEME FOR INSPECTIONS

12.3.1 Introduction

The earthquake damage assessment – a job greatly affected by subjective judgment – requires hundreds and sometimes even thousands of engineers, each with a different level of knowledge, experience, and engineering judgment. Therefore, prior to the earthquake, an appropriate organisational scheme should be developed, which would ensure the following:

- Immediate start of the inspections just after the earthquake and the main aftershocks, and the completion of the entire operation in a short time;
- Damage assessment in a uniform and in as objective as possible way, so that mistakes are statistically minimised;
- Detection of possible mistakes made during the first inspection and damage evaluation;
- Timely notification of the authorities about buildings in need of propping or demolition.

The basic features of such a scheme are discussed in the sections that follow.

12.3.2 Usability classification–inspection forms

For an objective and uniform damage evaluation, the inspection must be performed by teams consisting of at least two engineers, so that a judgment that is as objective as possible is formulated. Also, it is necessary to prepare ahead of time special forms for damage

description, strength evaluation and usability classification of structures, which should be based on the following principles:

- Easy completion of the data of the structure and the degree of damage, based on visual inspection as already mentioned.
- Assignment of the damage degree into a few clearly defined categories.
- Assessment of the usability of the building on the basis of clearly defined categories. International practice (ATC 3-06, 1978; Yugoslav National Report, 1982; UNIDO/UNDP, 1985; FEMA, 1986) has adopted the three levels of usability mentioned in the preceding section, each one of which is characterised by the color of the sticker posted on the buildings, the already mentioned green, yellow and red stickers, which were also used after the 1978 Thessaloniki, Greece, earthquake.
- Codification of data for future statistical processing.

It has to be mentioned that most countries currently have standard inspection forms (ATC 3-06, 1978; Yugoslav National Report, 1982; FEMA, 1986). In the framework of the UNIDO/UNDP-funded program 'Earthquake-Resistant Structures in the Balkan Region', such an inspection form was developed (Anagnostopoulos, 1984) as a result of cooperation of the Balkan countries (Figure 12.1) supported by international experts.

In Greece, between 1978 and 1981, simple inspection forms were used, which partly fulfilled the requirements given above. An attempt was made to use a form similar to that used by UNIDO (Constantinea and Zisiadis, 1984) in Kalamata (1986). However, the attempt failed for the following reasons:

1. In most of the buildings some apartments were locked, hence detailed recording of damage was not possible.
2. The engineers were not trained to complete the forms in a uniform way.
3. The requirement for quick completion of the inspections did not allow a systematic and detailed description of the situation.

The author's opinion is that the forms for the preliminary (emergency) inspection must be as simple as possible, while for the statistical evaluation of the consequences of the earthquake, the engineer who has the responsibility for the repair should submit a detailed form to the authorities, along with the repair design, after performing a second detailed inspection aiming at designing the repair of the building.

12.3.3 Inspection levels

In order to locate probable mistakes made during the first (emergency) inspection, a second degree of inspection must be carried out, performed by two-member teams of engineers with high qualifications and experience. In both ATC 3-06 (1978) and the final manual of UNIDO/UNDP (1985), such an inspection is suggested for buildings that have been classified as red, as well as for buildings with owners or occupants that hindered the evaluation of the first inspection. This procedure was also followed in Thessaloniki in 1978.

The timely notification of the authorities about buildings in need of *immediate propping* or *demolition* is one of the first priorities of the inspection teams, during both the first- and second-degree inspection.

Finally, it has to be emphasised that for the inspection of buildings that are of vital importance for post-earthquake life in the affected area, committees of highly qualified engineers must be formed to inspect these buildings first. In Figure 12.2, the chart of the successive

EARTHQUAKE DAMAGE INSPECTION FORM

SKETCH OF THE BUILDING

PLAN   CROSS SECTION

```
    4     3
  2   ⊕   2
    3     4
      5
```

ADDRESS :
OWNER :

1. TOWN (NAME)   1 ☐☐☐☐☐ 5
2. BUILDING IDENTIFICATION :
    2.1 SECTION NUMBER OF CONSIDERED
    TOWN AREA OR SE TTLEMENT :   6 ☐☐ 7
    2.2 WORKING TEAM NUMBER :   8 ☐☐ 9
    2.3 NUMBER OF THE BUILDING: 10 ☐☐☐ 12

10. TYPE OF STRUCTURE (SEE DESCRIPTION ON
    BACK PAGE) :   33 ☐☐☐ 35
11. FLOORS:
    1.R.C., 2. STEEL. 3.WOOD. 4.OTHER   36 ☐
12. 1.R.C., 2. STEEL. 3.WOOD. 4.OTHER   37 ☐
13. ROOF COVERING: 1.TILES, 2.METAL SHEETS,
    3.LIGHTWEIGHT ASBESTOS CEMENT,
    4.ASPHALT PAPER, 5.HEAVY INSULATION,
    6. LIGHT INSULATION, 7.OTHER   38 ☐

18. DEGREE OF DAMAGE
    STRUCTURAL ELEMENTS (SEE DESCRIPTION ON
    BACK PAGE):
    1.NONE, 2.SLIGHT, 3.MODERATE, 4.HEAVY, 5.SEVERE
    18.1.BEARING WALLS: 44 ☐
    18.2.COLUMNS: 45 ☐
    18.3.BEAMS: 46 ☐
    18.4.FRAME JOINTS: 47 ☐
    18.5.SHEAR WALLS: 48 ☐
    18.6.STAIRS: 49 ☐
    18.7.FLOORS: 50 ☐
    18.8.ROOF: 51 ☐

19. DAMAGE OF ENTIRE BUILDING :
    1.1 NONE,1.2 SLIGHT,2.1 MODERATE,2.2 HEAVY
    3.1 SEVERE,3.2 TOTAL   57 ☐☐ 58
20. INDIRECT DAMAGE (FIRE,SLAMMING,ETC.)
    1.NO, 2.YES   59 ☐

3. ORIENTATION OF THE BUILDING PRINCIPAL AXIS(X)
    1.NS, 2.EW. 3.N45E 4.N45W   13 ☐
4. POSITION OF BUILDING IN THE BLOCK:
    1. CORNER, 2. MIDDLE, 3. FREE   14 ☐
5. NUMBER OF STOREYS
    5.1 STOREYS   15 ☐☐ 16
    5.2 APPENDAGES   17 ☐
    5.3 MEZZANINES   18 ☐
    5.4 BASEMENTS   19 ☐
6. GROSS AREA OF THE BUILDING (m²):   20 ☐☐☐ 22
7. USAGE (SEE DESCRIPTION ON BACK PAGE).
    7.1 BUILDING   23 ☐☐☐ 25
    7.2 GROUND FLOOR   26 ☐☐☐ 28
8. NUMBER OF APARTMENTS: 29 ☐☐ 30
9. CONSTRUCTION PERIOD (TO BE DEFINESD BY EACH
    COUNTRY):
    1.   2.   3.   31 ☐

14. QUALITY OF WORKMANSHIP:
    1.GOOD , 2. AVERAGE, 3.POOR   39 ☐
15. TYPE OF LOAD CARRYING SYSTEM(SEE
    DESCRIPTIONON BACK PAGE):
    1.BEARING WALLS, 2. FRAMES, 3.FRAMES WITH   40 ☐
    INFILL WALLS, 6.MIXED, 7.OTHER (SPECIFY)
16. FIRST FLOOR-STIFFNESS RELATIVE TO OTHERS:
    1. LARGER, 2. ABOUT EQUAL, 3. SMALLER   41 ☐
17. REPAIRS FROM PREVIOUS EARTHQUAKES:
    1. NO, 2. YES, 3. UNKNOWN   42 ☐

NONSTRUCTURAL ELEMENTS AND INSTALLATIONS
(SEE DESCRIPTION IN THE MANUAL)
1.NONE,2.SLIGHT,3.MODERATE,4.HEAVY,5.SEVERE
18.11 INTERIOR WALLS: 52 ☐
18.12 PARTITIONS: 53 ☐
18.13 EXTERIOR WALLS (FACADE):   54 ☐
18.14 ELECTRICAL INSTALLATIONS: 55 ☐
18.15 PLUMBING: 56 ☐

21. OBSERVED SOIL INSTABILITIES AND GEOLOGICAL PROBLEMS
    1.NONE, 2.SLIGHT SETTLEMENTS, 3.INTENSIVE
    SETTLEMENTS, 4.LIQUWFACTION, 5.LANDSLIDE,   60 ☐
    6.ROCKFALLS, 7.FAULTING, 8.OTHER (SPECIFY)

22. USABILITY CLASSIFICATION AND POSTING:
    POSTED: 1.GREEN, 2.YELLOW, 3.RED
    NOT POSTED: 4 TO BE POSTED GREEN AFTER REMOVAL OF LOCAL HAZARD, 5.SOIL AND GEOLOGICAL PROBLEMS,
    REINSPECTION REQUIRED, 6.UNABLE TO CLASSIFY, REINSPECTION NECESSARY, 7.BUILDING INACCESSIBL E   62 ☐

GREEN	1 ORIGINAL SEISMIC CAPACITY HAS NOT BEEN DEGREASED	UNLIMITED USAGE
YELLOW	2 ORIGINAL SEISMIC CAPACITY HAS BEEN DEGREASED	TEMPORARILY UNUSABLE LIMITED ENTRY
RED	3 BUILDING DANGEROUS AS SUBJECT TO SUDDEN COLLAPSE	ENTRY PROHIBITED

MAIN REASONS FOR YOUR CLASSIFICATION AND POSTING:

23. RECOMMENDATIONS FOR EMERGENCY MEASURES:
    1.NONE, 2.REMOVE LOCAL HAZARD, 3.PROTECT
    BUILDING FROM FAILURE, 4.URGENT DEMOLITION   64 ☐
24. ADDITIONAL DATA (PHOT/SKETCHES AND COMMENTS):
    1. NONE, 2.PHOTOS ONLY, 3.SKETCH AND COMM.ONLY
    4. PHOTOS AND SKETCH AND COMM.   65 ☐

25. ESTIMATED PRESENT VALUE OF BUILDING
    (MILLIONS OF............)   66 ☐☐☐ 68
26. ESTIMATED LOSS (% OF ESTIMATED VALUE)   69 ☐☐☐ 71
27. HUMAN LOSSES (DEATHS AND INJURIES)
    (1) NO; (2)POSSIBLY; (3)YES (4)IF INFORMATION
    AVAILABLE PLEASE INDICATE: 72 ☐
                        NO . OF DEATHS   73 ☐☐ 74
    OPTIONAL   NO. OD INJURIES   75 ☐☐ 76

28. DATE OF INSPECTION: MONTH/DAY   77 ☐☐☐ 80
    NAMES OF INSPECTION ENGINEERS: SIGNATURES
    1.
    2.
    3.

Figure 12.1 Inspection form of the first-level committee proposed by UNIDO/UNDP, project RER/79/015/
volume 4.
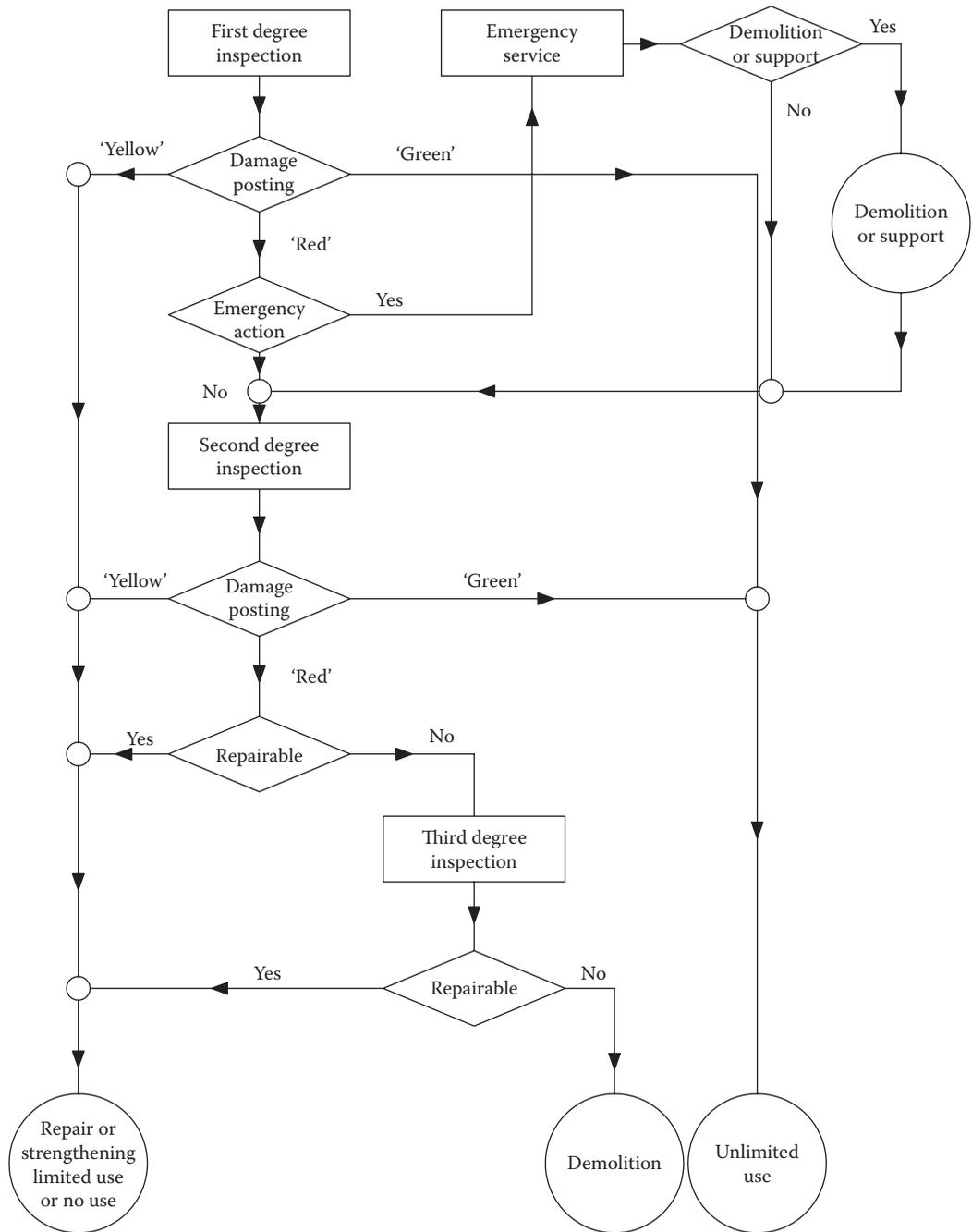
Figure 12.2 Chart of inspection procedure in Thessaloniki 1978.

inspection levels of structures in the Thessaloniki earthquake is shown, the application of which did not exhibit any particular problem.

12.4 ACTION PLAN

12.4.1 Introduction

It has become clear, from what has been said so far, that such an operation constitutes a large-scale mobilisation, from which the State expects a great deal. Obviously, there must be a detailed action plan developed before an earthquake occurs, in order to have immediate and effective mobilisation of such a mechanism. This action plan must be part of the nationwide general emergency plan for earthquakes. Some basic features of such a plan are presented in the following sections.

12.4.2 State agency responsible for the operation

The existence of a public agency with well-defined responsibilities for the operation in every prefecture (or country) from the pre-earthquake period is extremely important for the immediate start and implementation of the programme of inspection of structures after an earthquake. The selection of the public agency must be done in advance, so that its staff will have the time to review the action procedure and prepare all the orders and decisions that must be implemented, as well as the materials and equipment needed for the operation. Obviously, this responsibility must be assigned to an already existing technical service with good organisation and the necessary personnel and means to become the core of the entire operation. Given the fact that in large urban areas there are several such services, belonging to several ministries, the coordination and the duties of each one of them must be clearly defined from the pre-earthquake period in the action plan.

12.4.3 Inspection personnel

In principle, the inspection personnel should consist of structural engineers organised in two-member teams so that they can have a better engineering judgment during the inspections. The high degree of subjectivity in the decision about the usability of structures does not permit the use of scientists with other specialties at this phase. It has already been mentioned that a large number of engineers will be needed to carry out the inspection.

For example, in the case of Thessaloniki in 1978, about 1000 engineers worked for 45 days for the first- and second-degree inspections of about 250,000 apartments located in about 60,000 buildings, while in California in 1971, after the San Fernando earthquake, about 250 engineers were involved for one month with the inspection of 12,000 buildings. These two examples give an idea of the scale of mobilisation that would probably be needed.

Given the fact that the required number of personnel cannot be covered by the State agency in charge of the operation, there must be a recruiting plan for additional personnel in every area of the country, which must provide successive levels of reserves. These personnel, with proper annual training, will know in advance the meeting points in case of an emergency. Recourse to civil conscription should not be ruled out in the case that after a call the number of personnel gathered is not adequate. In Thessaloniki, the entire operation started on a voluntary basis, but no more than 150 to 200 engineers form the private sector volunteered. Therefore, after the first week the government was forced to conscript all civil engineers of the region for a 2-month period.

12.4.4 Pre-earthquake organising procedures

The public agency in charge of the inspections should also have the responsibility of organising the whole operation during the pre-earthquake period. This organising procedure should cover the following:

- Preparation of inspection personnel lists, providing for several levels of reserves, on the basis of experience and qualifications.
- Determination of local mobilisation centres (e.g. police stations).
- Distribution of inspection personnel depending on qualifications to first-level teams, second-level teams, committees for checking buildings of special usage and so forth.
- Listing of buildings of vital importance for the after-shock operation of the area, such as hospitals, schools, communication buildings, police stations and public buildings, which must be inspected first, and formation of inspection teams of highly qualified engineers for inspection of these buildings immediately after the earthquake.
- Acquisition of all materials and equipment needed for the inspections, such as inspection forms, notebooks, measuring tapes, hammers, chisels, helmets, flashlights, batteries and so forth.
- Acquisition of means of communication, given the fact that it is not unusual for telecommunications to be interrupted after an earthquake. It is interesting at this point to mention the report on the San Fernando earthquake, which estimates that if the telecommunication system had been down, the effectiveness of the entire operation would have been limited to 10%. This is similar to the authors' assessments for the recent earthquakes in Greece.
- Organising short courses for the inspection personnel on the subject of damage assessment.

Figure 12.3 shows the organising diagram that was implemented in the case of Thessaloniki, while Figure 12.4 shows the organising diagram suggested by the ATC 3-06 for the United States at the state level (ATC 3-06, 1978).

Finally, it is the author's opinion that the inspection personnel should not be held personally liable for any damage that may occur to persons or property as a result of any act or any omission in carrying out their duties. This is because these inspection procedures are conducted under the pressure of time in emergency situations, and, therefore, since engineers are not able to use their main scientific tools, that is, measurements, tests and analysis, they should not be held liable for any mistakes that could occur during the first emergency evaluation. A similar reasoning is followed in ATC 3-06 (1978) and also in the Presidential order for the pre-earthquake seismic evaluation of public buildings in the United States (presidential order 12941, 1994).

12.4.5 Post-earthquake organising procedures

Right after of an earthquake, in order for the inspection mechanism to be set in motion, a series of actions is necessary, the most important of which are the following:

1. Determination of the affected areas in order to estimate the scale of the operation. Characteristic of the difficulty of this task is the fact that for the San Fernando, California, earthquake of 1971, it took 12 h to localise the boundaries of the affected area. In the 1978 Thessaloniki, Greece, earthquake, it took 2 days to localise the boundaries of the effected area.
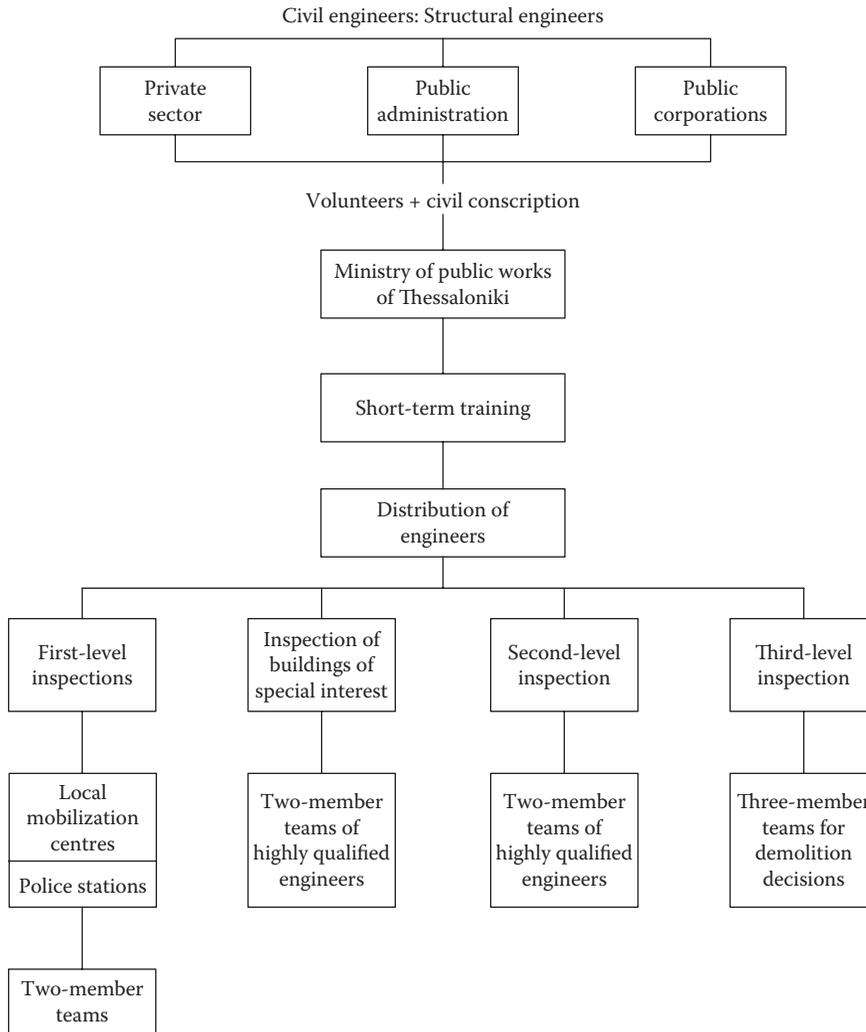
Figure 12.3 Organisational chart for the inspection service in Thessaloniki after the earthquake of 20 June 1978.

2. Establishment of the operational headquarters. This centre should be housed, if possible, in the same building as the disaster relief services, so that easy communication and coordination will be possible. In Thessaloniki, the whole operation was housed in the Ministry of Northern Greece, while in Kalamata (1986) the operational headquarters were housed together with the disaster relief headquarters in the telecommunications building. The operation headquarters should perform the following duties:
   a. Coordinate its actions with the activities of the other services for disaster relief
   b. Mobilise the personnel of inspections and local centres
   c. Establish top priorities for inspections of critical facilities such as hospitals, police and fire stations and so forth
   d. Set up central and local offices
   e. Establish and maintain communications
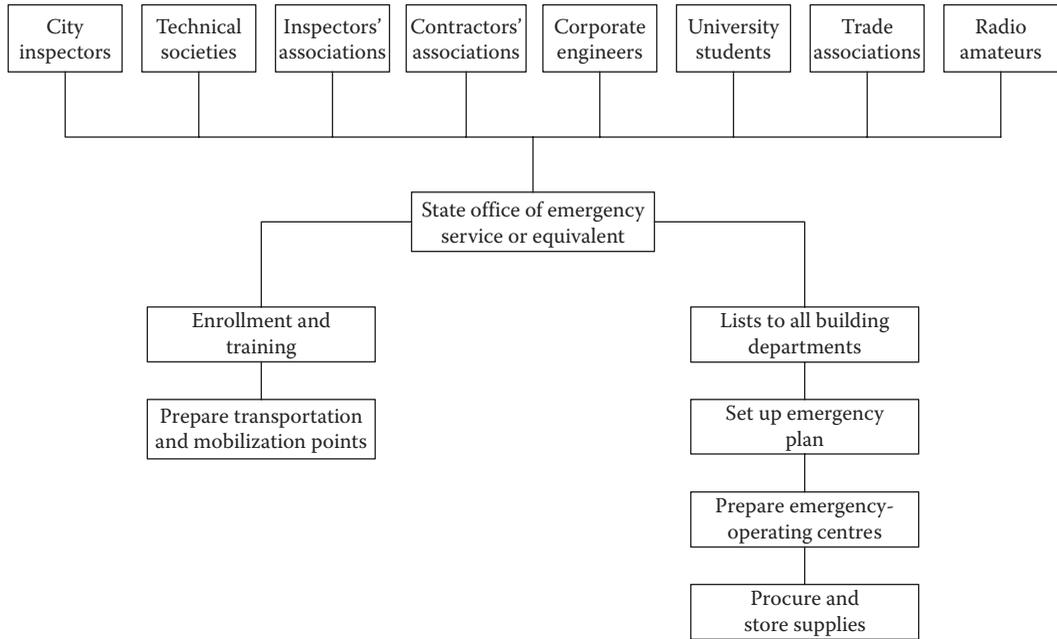
Figure 12.4 Organisational chart for the pre-earthquake preparation period (ATC 3-06 proposal, USA).

    f. Provide transportation for inspection personnel
    g. Distribute equipment and supplies to local mobilisation centres
    h. Provide food and housing for inspection personnel
    i. Process inspection reports
    j. Provide statistical data where necessary
    k. Coordinate the local mobilisation centres
    l. Establish and maintain a demolition and temporary propping centre
    m. Coordinate the immediate flow of information for demolition or propping works
        from the inspection teams to the demolition and propping centre
  3. Establishment of local mobilisation centres. In Greece, for example, the most appro-
     priate places have proved to be police stations, where a lot of data about the area
     around the station are available.
  4. Distribution of the inspection personnel to the local centres with the proper authorisa-
     tion for inspections.

12.5 EMERGENCY MEASURES FOR TEMPORARY PROPPING

12.5.1 General

Immediate shoring (temporary propping) is recommended for buildings with serious damage
in the vertical structural elements (columns, walls) or serious inclination from the vertical.
By using shoring, the damaged elements are relieved of their loads by temporary additional
structures, and therefore the danger of collapse, due to aftershocks, is mitigated.
    Propping must take place *initially* at the floor where the damage of the vertical element
occurred. It is necessary, however, to estimate the ability of adjacent beams to carry the ver-
tical load of the damaged element, and if this is not adequate, support must be extended to
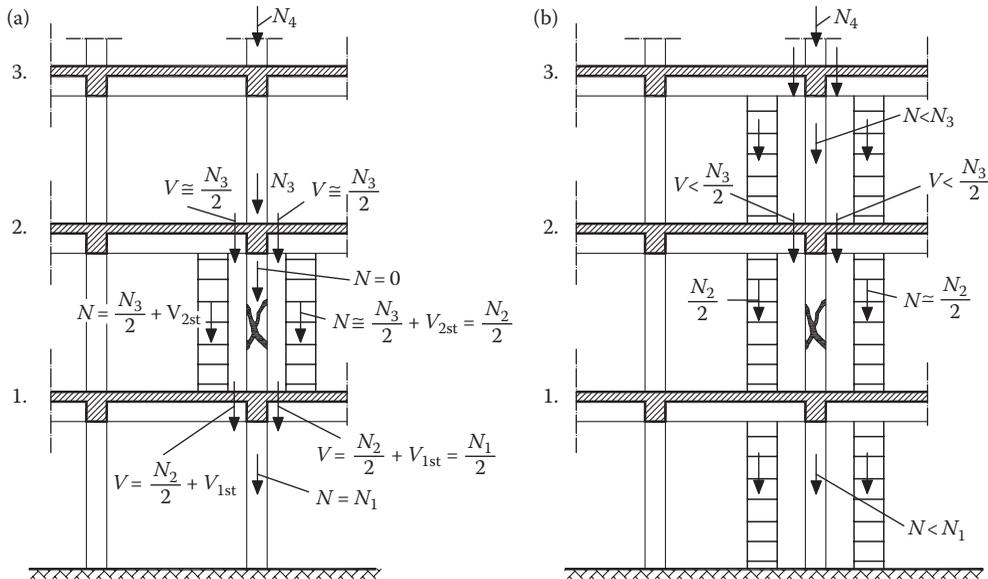
Figure 12.5 Shoring (temporary supporting) of a multi-storey building with a damaged column: (a) shoring of only one floor; (b) shoring of more floors.

other floors as well (Figure 12.5). The support system must be placed at a certain distance from the damaged element so that enough room is left for the repair work that will follow.

When there are problems of lateral instability in a structure, displayed mainly by vertical inclination, lateral support is provided either in the form of ribs or diagonal braces between the frames formed by beams and columns, and even internal tension ties can be used for supporting buildings close to collapse.

The design of temporary supports must be done promptly, with the aid of approximate analysis and design, performed to determine only the order of magnitude of actions and action effects (stresses). The materials and techniques foreseen must be readily available, for instance, metal scaffolds, timber, steel profiles, timber grillage and so on.

Given the fact that the shoring of damaged structures is very hazardous work for the people involved, the time these people spend in the building must be kept to a minimum. Therefore, it is recommended that the preparation of all the supporting elements be done away from the damaged structure (based on the dimensions measured on site), so that the work of shoring will be limited to the installation of these elements in the damaged building. It is recommended that extensiometers in the form of glass pieces bonded through gypsum plaster on critical cracks should be established before any propping work on site to safeguard the stability of the structure and therefore the life safety of the personnel involved in propping activities.

12.5.2 Techniques for propping vertical loads

12.5.2.1 Industrial-type metal scaffolds

In the case of small loads, independent industrial-type metal tube shores are used (Figure 12.6), having a load-bearing capacity of about 20 kN and a height of about 3.00 m.

For the shoring of beams or slabs, prefabricated metal towers are used (Figure 12.7), which are wedged to the surface to be shored with the aid of the special screw-type bolts with which all industrial-type scaffolds are equipped.
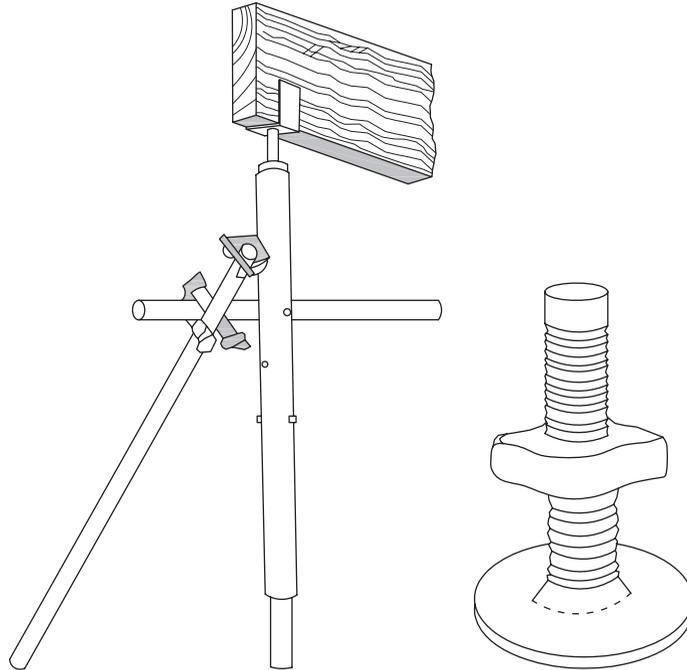
Figure 12.6 Independent industrial-type metal supports.

12.5.2.2 Timber

Timber elements can also be used for carrying vertical loads, either in the form of logs or telephone poles, or in the form of timber grillages. For every damaged column at least one 250-mm diameter log should be used on each side of the column. The allowable (service) load for this diameter and for floor heights about 3.00 m is estimated at 300 kN per pole for timber of good quality. If the height is greater than 3.00 m or the diameter smaller than 250 mm, the pole must be checked for buckling (EC 5/2004).

In the case where two or more supporting elements are used on each side, they must be connected to each other with X-shaped braces. If no logs are available, shoring can be achieved with timber grillage (Figure 12.8).

12.5.2.3 Steel profiles

Steel profiles can be used either in the same manner as timber or as an immediate strengthening means of the damaged column (Figure 12.9). In this case, they can be incorporated later into the concrete jacket. In the first case there should always be a buckling verification. In the second case the key to success is the tightening of the vertical steel angles to the column with the aid of transverse angles and prestressed ties before the transverse connecting straps are welded to the vertical angles.

12.5.3 Techniques for resisting lateral forces

12.5.3.1 Bracing with buttresses

Bracing with buttresses is the most common way of resisting lateral forces. These forces are due to the deviation of the building from the vertical axis either because of failure of vertical

Support

Frame

Diagonals

Connector

Mechanical jack

1.50

1.20

20–35 kN*

1.20

1.80

Frame 1.20 × 1.80

20–35 kN*

1.20

1.20

Frame 1.20 × 1.20

* For a free height
of $\cong$ 3.00 m
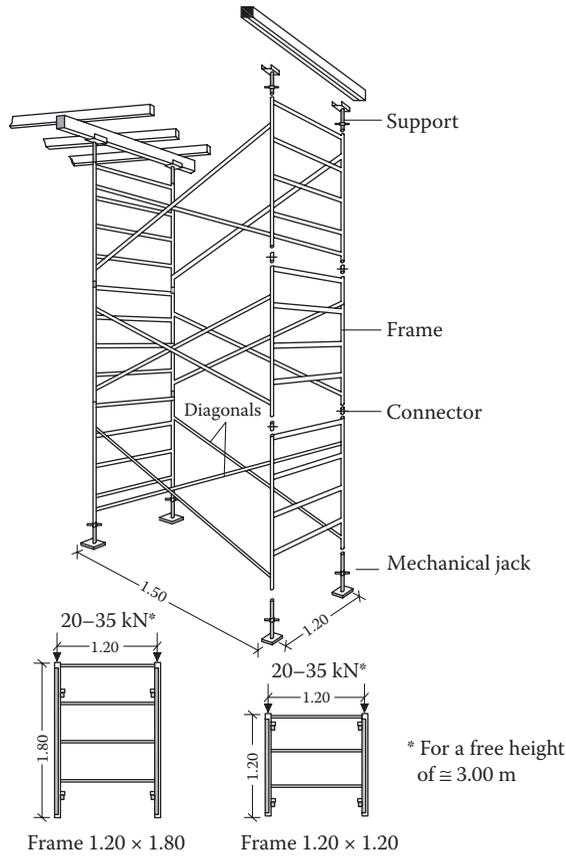
Figure 12.7 Industrial-type metal towers.

structural elements or because of settlement of the foundations (Figure 12.10). Some critical points of such a bracing system are the following:

- Anchoring of the bracings to the ground, so that they may resist horizontal thrusts;
- Attachment of the vertical member to the building so that it prevents relative slipping;
- Limiting the unbraced length of the inclined member of the lateral bracing to low values, to avoid in-plane or out-of-plane buckling.

For this type of shoring, usually timber and rarely steel members are used. It should be noted that the horizontal forces that such a system is assumed to resist, for small deviations

Wedges   Wedges
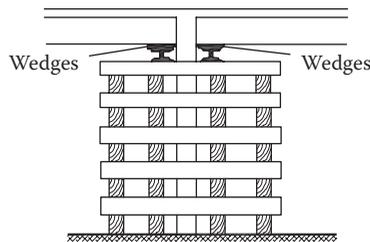
Figure 12.8 Shoring with timber grillage.
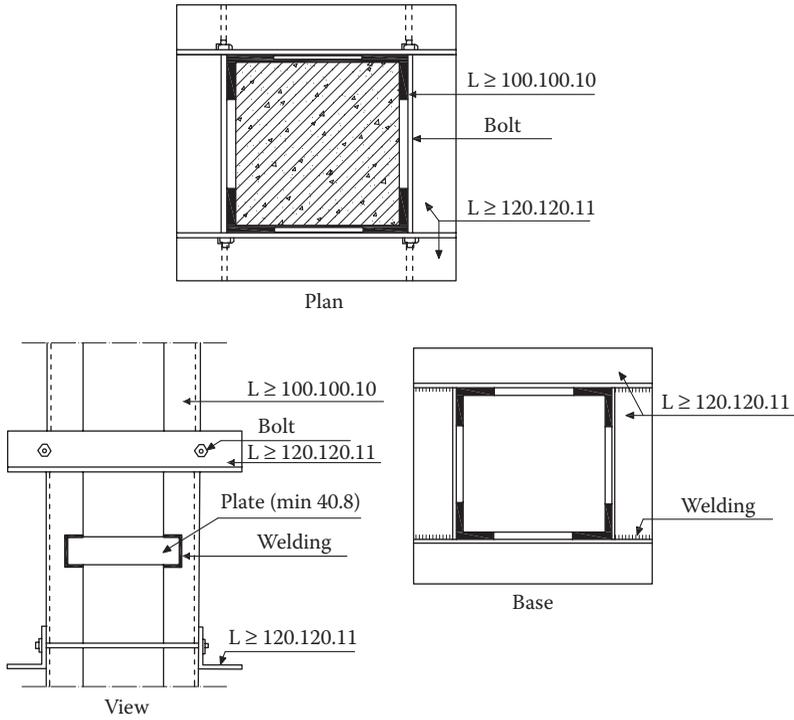
Figure 12.9 Immediate tying of a column with steel profiles.

from the vertical axis, are not very large and can easily be estimated approximately, using the relationship (Figure 12.11):

$$\Delta H = \frac{\delta}{h} G \qquad (12.1)$$
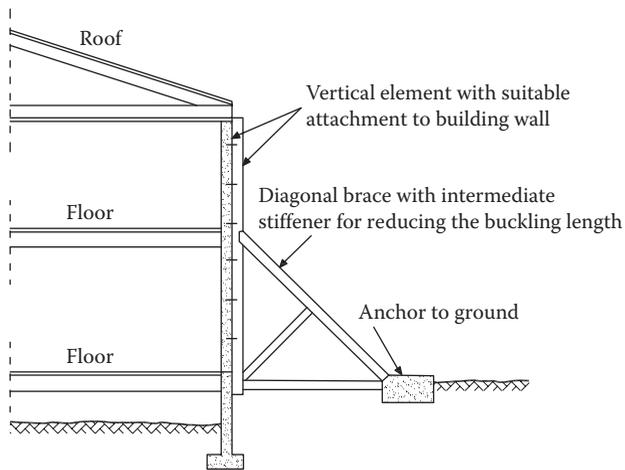
Figure 12.10 Bracing with buttresses.
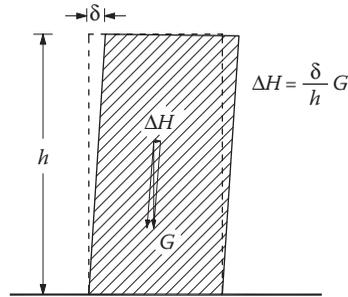
Figure 12.11 Estimate of the horizontal forces due to deviation from the vertical axis.

where δ/h is the deviation from the vertical axis and G is the total vertical load of the structure, which for normal buildings is estimated to be $10.0–12.0$ kN/m^2 of floor area.

12.5.3.2 Bracing with diagonal X-braces

On the one hand, the use of diagonal timber or steel members in the plane of R/C frames allows the partial transfer of gravity loads to undamaged vertical elements, and on the other, prevents lateral deformation (Figure 12.12).

Frame bracing can consist of timber, tree logs or steel profiles of sufficient strength considering their tendency for buckling. This method is used when external bracing with buttresses cannot be easily installed.

12.5.3.3 Bracing with interior anchoring

In the case of hybrid structures consisting of R/C slabs supported by masonry, in order to retain external walls that have been detached and deviate from the vertical axis, metal tensioners are often used, which are prestressed with the aid of tensioner couplers (Figure 12.13).

12.5.3.4 Bracing with tension rods or rings

In the case of deviation from the vertical axis due to arch thrusts, prestressed metal rings or prestressed rods are used, depending on whether the structure is a dome or an arch.
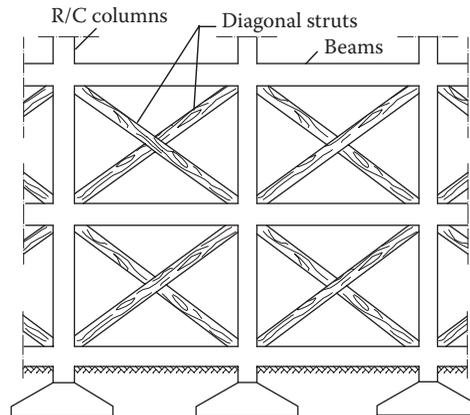
Figure 12.12 Bracing with diagonal struts.
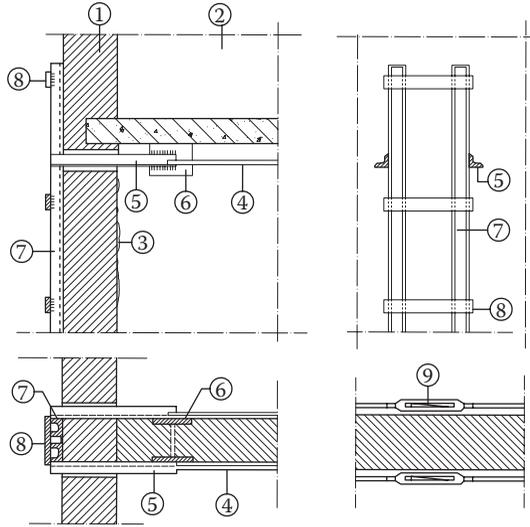
Figure 12.13 Bracing with internal tension ties: 1 = exterior wall; 2 = interior wall; 3 = crack; 4 = steel tensioner; 5 = angle 50.50.5 mm; 6 = steel plates; 7 = steel profiles; 8 = steel plates; 9 = tensioner coupler.

12.5.4 Wedging techniques

The wedging procedure is a crucial part of every supporting or bracing procedure, because the transfer of the loads of a damaged element to the shoring or bracing system is accomplished through wedging. Wedging can be achieved by the following means:

- Wooden twin wedges (Figure 12.14)
- Mechanical jacks (screws; Figure 12.7)
- Hydraulic jacks (Figure 12.15)
- Couplers (Figure 12.13)

12.5.5 Case studies

In the following figures (Figures 12.16 through 12.19), various propping case studies have been depicted from post-earthquake shoring measures.

$$P = H \frac{1 - f \tan \alpha}{2f + \tan \alpha}$$

$$\alpha \cong 5° \div 15°$$

$$f_{\text{wood}} \simeq 0.30$$
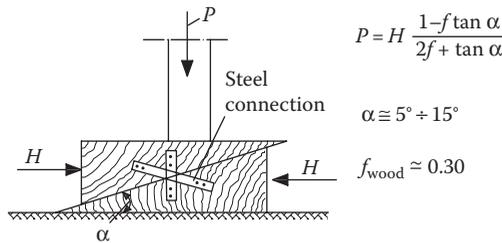
Figure 12.14 Wedging with twin wooden wedges (f is the friction coefficient).
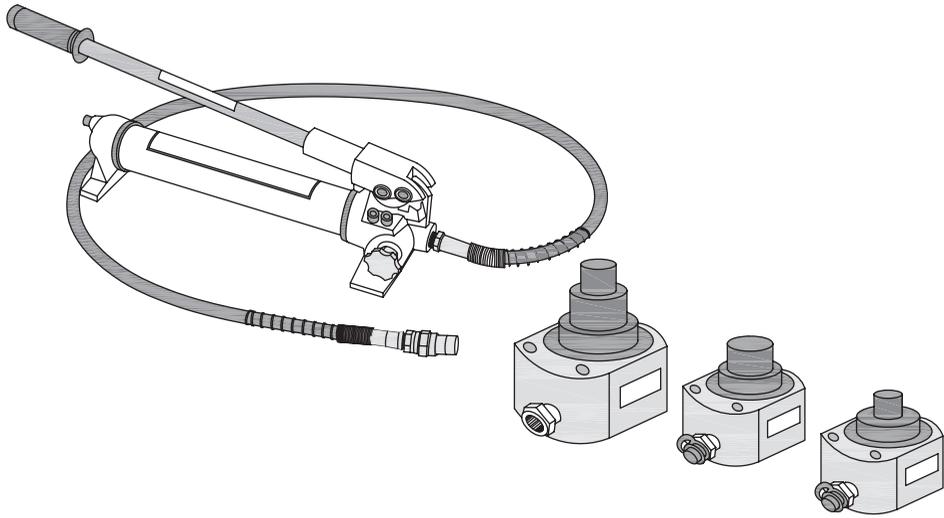
Figure 12.15 Wedging with hydraulic jacks.

12.6 FINAL REMARKS

The main conclusion of this chapter is that emergency damage inspection and assessment after an earthquake is a completely different procedure from that followed for the evaluation of residual seismic resistance of a structure in the pre- or post-earthquake period. This is because in the case of an earthquake, very often thousands of buildings must be inspected and evaluated in a short period of time, so that the affected area can return to normal life.

Therefore, given the fact that hundreds and sometimes even thousands of engineers must be engaged in damage evaluation, each with a different level of knowledge, experience and

Figure 12.16 Timber propping of a damaged column; Bucharest, Romania (1977).

Figure 12.17 Timber propping of a damaged column; Kalamata, Greece (1986).

Figure 12.18 Steel profile props for the repair of a damaged column; Kalamata, Greece (1986).

Figure 12.19 Confinement of an R/C wall using external profiles, for temporary propping and in parallel final repair.

engineering judgment, the main task is the creation of the appropriate organising scheme before the earthquake, which will ensure the following:

- A damage evaluation that is uniform and as objective as possible, so that statistical mistakes will be minimised.
- Quick detection of any serious mistakes in evaluation from the first inspection.
- Timely notification about buildings in need of immediate support or demolition.

It is understood that such operations, which require a high degree of staff organisation and are directly associated with public security, should be undertaken by the central or regional government.

For the uniform and objective evaluation of the degree of hazard, it is necessary to prepare in advance special forms for damage description, residual seismic resistance evaluation and usability classification of structures, which must be based on the following principles:

- Easy completion with the data of the structure and the damage level, based on visual inspection.
- Assignment of the damage degree into a few clearly defined categories.
- Assessment of the usability of the building, on the basis of clearly defined categories.
- Organisation of data for future statistical processing.

For the effective completion of the engineers' mission, there is a need to organise short training courses, accompanied by visual aids (powerpoint, DVDs, etc.) on the expected damage classified into categories, and on the procedure of completion of the inspection forms.

For the detection of serious errors and for inspection of special buildings, there is a need for a second-level inspection by experienced, highly qualified structural engineers.

For timely notification for emergency action on buildings needing propping or demolitions, the development of an appropriate coordination mechanism is required.

Chapter 13

Seismic assessment and retrofitting of R/C buildings

13.1 GENERAL

The seismic evaluation of existing buildings has as its main objective decision-making about the need for rehabilitation of each individual building. On the other hand, any retrofitting activity aims at upgrading the seismic performance of the building to a level similar to that of new buildings designed and constructed in accordance with the Seismic Codes now in effect. Keeping in mind that the retrofitting cost (structural–non-structural) is very high, ranging around a mean value of 10–12% of the original cost of construction, it is apparent that an evaluation procedure must be established for screening the buildings under consideration in successive steps of accuracy and, until the number of buildings designated for eventual intervention has been minimised. At the same time, the reduction of the number of buildings from step to step also reduces the cost of evaluation of the whole procedure. For these buildings a detailed quantitative evaluation is implemented and eventually a retrofitting design is applied.

National programmes for seismic risk mitigation (see Section 16.7), through seismic assessment and retrofitting, may differentiate between *'pre-earthquake'* and *'post-earthquake'* programmes. The first category is triggered by 'political decisions' and in this respect may be characterised as 'active' programmes, while the second is triggered by a strong earthquake or, rather, the damages caused by the earthquake, and in this respect they may be characterised as 'passive' programmes (EC8-3/2005).

Buildings for which the owners have decided to intervene mainly for commercial reasons, such as a change in use that increases occupancy or importance class, remodelling above certain limits and so forth, must be classified in an independent category. In fact, in these cases the 'screening' procedure is omitted and the building is evaluated and retrofitted in detail directly, since the decision for intervention has already been taken for operational reasons.

It is reasonable that in the main two categories, since the trigger is different, the methods of seismic evaluation at the stage of screening display differences, while at the final stage of quantitative detailed seismic evaluation and retrofitting design, the procedure that is implemented is the same for both (Figure 13.1). In the following sections, the above two cases will be presented in detail, that is,

- Pre-earthquake seismic evaluation of R/C buildings
- Post-earthquake seismic evaluation of R/C buildings
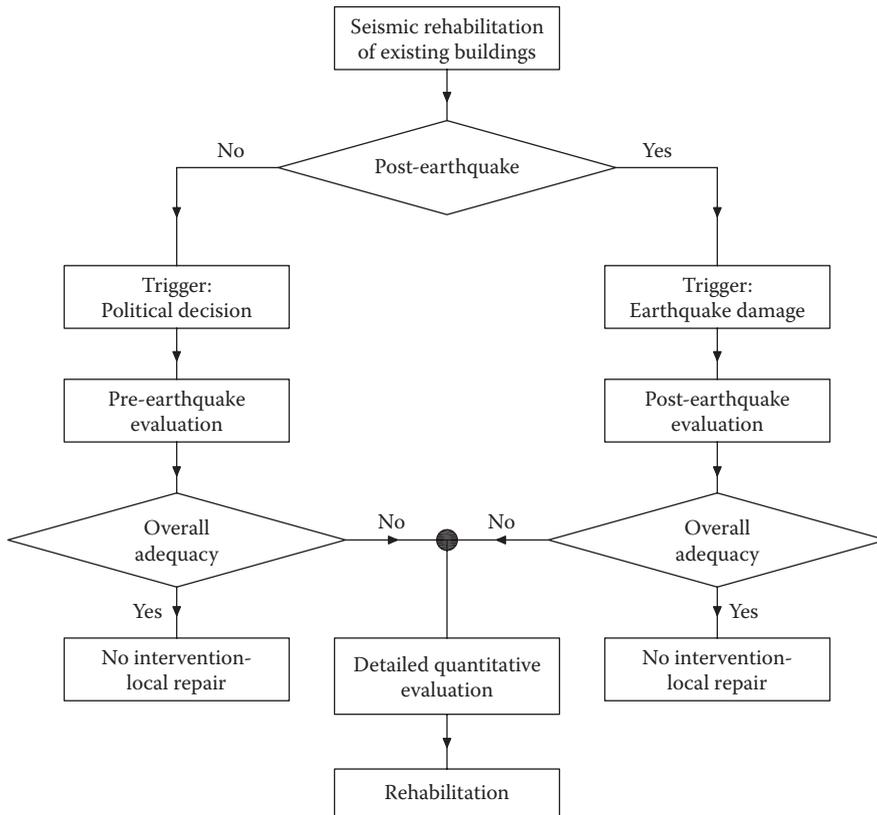
Figure 13.1 Flow chart for pre- and post-earthquake evaluation and rehabilitation.

13.2 PRE-EARTHQUAKE SEISMIC EVALUATION OF R/C BUILDINGS

13.2.1 Introduction

For many decades the main tool for seismic risk reduction was considered to be the design and construction of earthquake-resistant buildings based on modern Codes into which new knowledge on earthquake engineering and engineering seismology had been incorporated. However, as engineering seismology and earthquake engineering have been passing through a transitional period of development over the past 100 years, buildings designed and constructed in the past based on Codes then in effect are no longer compatible with modern Codes. These buildings constitute the majority of the building stock of a region and therefore they also constitute the main problem in case of a strong earthquake. For example, in the case of the Athens earthquake of 1999, the number of buildings constructed in the most affected area (Karabinis, 2002 Figure 13.2) during the 14 years after the benchmark year of establishment of a modern Seismic Code (1985) was only 17 out of 214 R/C buildings. Collapses of buildings constructed during this 14-year period were only 4 out of 93 in total.

   In this context it has been realised, particularly in the United States since the early 1980s, that a drastic reduction of seismic risk could be achieved only by an 'active' intervention in the existing building stock, where the most damages and collapses take place in case of a strong earthquake.
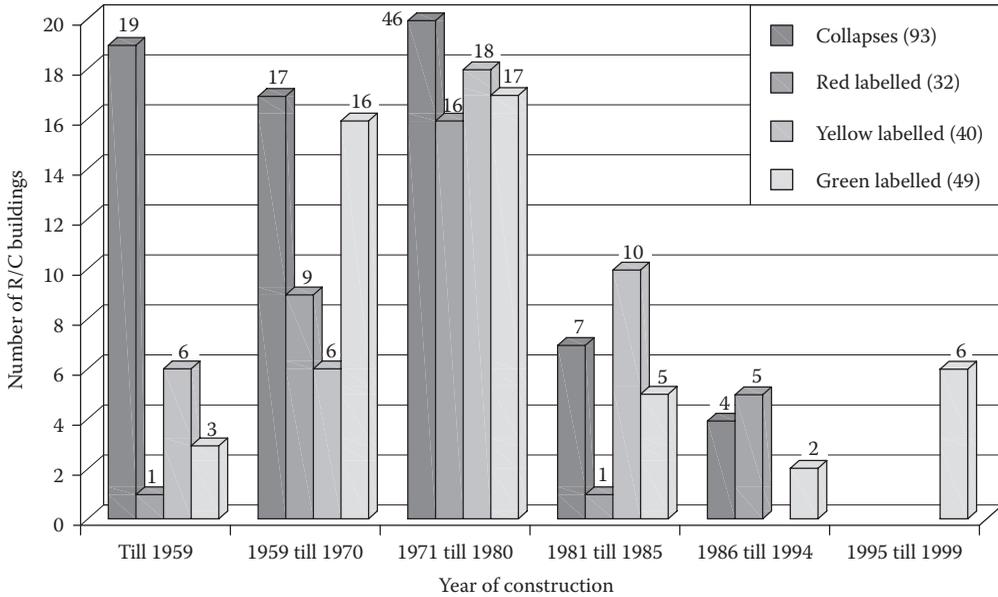
Figure 13.2 Distribution of vulnerability of R/C buildings in the most affected area of Athens in the 1999 earthquake, by year of construction. (Adapted from Karabinis, A. 2002. Validation of the pre-earthquake assessment procedure of R/C buildings in Greece, Technical Report (O.A.S.P.) Athens, Greece.)

Therefore, systematic initiatives were undertaken for the development of a framework of procedures for seismic evaluation of buildings and retrofitting of those with critical deficiencies. These initiatives were mainly developed in the United States (ATC-3-06/1978, FEMA 154/ATC-21/1988, FEMA 178/1992, ICSSC PR-4/1994, FEMA 273-274/1997, ASCE 31-02/FEMA 310/1998, FEMA 356/2000, ASCE/SEI 41-06).

At the same time, similar procedures have been developed to a degree in other countries (e.g. UNIDO/UNDP, 1985; Japan, 1990; New Zealand, 1996; Italy, 1998; Greece, 2000). In most cases the procedure is articulated in three successive steps of higher detail and accuracy, from the first step to the third.

Nowadays, the U.S. framework of standards in effect for pre-earthquake seismic evaluation and rehabilitation of existing buildings comprises:

- FEMA 154/ATC-21/1988
  Rapid visual screening of buildings for potential seismic hazards.
- ASCE 31-02/FEMA 310/1998
  'Seismic evaluation of buildings' articulated in three successive steps of higher detail and accuracy.
- ASCE/SEI 41-06/FEMA 356/2000
  Seismic rehabilitation of buildings is the third step of FEMA 310, together with detailed procedures for rehabilitation

The European framework of standards includes only EC8-3/2005, which is relevant to ASCE/SEI 41-06/FEMA 356 and refers to a detailed quantitative seismic assessment and retrofitting of buildings, leaving to the member states the initiative for development of standards for the preliminary seismic evaluation of buildings.

In the following subsection a brief reference will be made to the U.S. system of the seismic evaluation of buildings, which may be considered the most integrated system in effect the world over.

13.2.2 Rapid visual screening procedure

This first approach includes a rapid visual screening of all buildings included in the evaluation programme (e.g. schools, hospitals and so on of a region). All of these buildings are ranked according to the adopted procedure with a Structural Score S ranging from 0 to 6, with higher scores corresponding to an expected better seismic performance.

The structural score takes into account:

- Vulnerability of the building
- Seismic hazard of the region
- Occupancy status

Buildings with a Structural Score less than 2 are considered to be of low seismic performance and, therefore, have to undergo a further more detailed evaluation. A flow chart of the procedure together with the typology of the buildings and the specified ranking are given in the tables of Figures 13.3 through 13.5. Each type of building is ranked with a score depending on the seismicity of the region where it is located. This score is modified downwards by
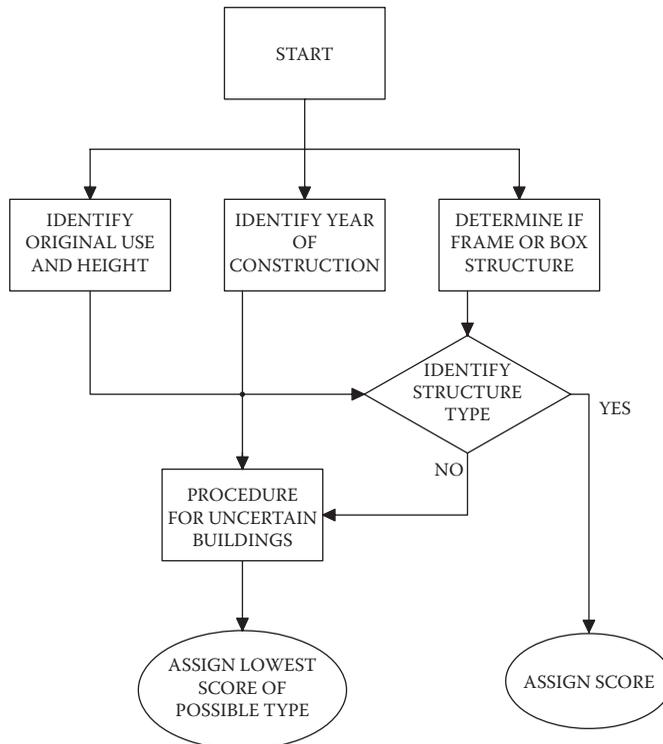
Figure 13.3 Flow chart for the RVSP identification procedure. (From FEMA-154/1988. *Rapid Visual Screening of Buildings for Potential Seismic Hazards: A Handbook*. Federal Emergency Management Agency, Washington, DC. With permission.)

STRUCTURAL TYPE: Benchmark year

W	wood frame	_____
S1	steel moment resisting frame	_____
S2	steel brace frame	_____
S3	light metal frame	_____
S4	steel frame with concrete shear wall	_____
C1	concrete moment resisting frame	_____
C2	concrete shear wall	_____
C3/S5	steel or concrete frame with masonry infill	_____
PC1	tilt-up	_____
PC2	precast frame	_____
RM	reinforced masonry	_____
URM	unreinforced masonry	_____

OCCUPANCY LOAD:	sq. ft. per person
residential	100-300
commercial	50-200
office	100-200
industrial	200-500
public assembly	varies, 10 minimum
school	50-100
goverment bldg	100-200
emergency service	100

MODIFIERS:

High-Rise -	8 stories and taller except URM, URM above 4 stories
Poor Condition -	showing cracks, damage, settlement, etc
Vertical Irregularity-	steps in elevation, inclined walls,discontinuities in load path, building on hill
Soft Storey-	open on all sides of building, tall ground floor, discontinuous shear walls
Torsion-	eccentric stiffness in plan (e.g. corner building, wedge shaped building with one or two solid walls and all other walls open)
Plan Irregularity-	"L" ,"U","E","T" or other irregular building shape
Pounding-	floor levels of adjacent buildings not aligned and less than 4* of separation per story
Large Heavy Cladding-	many large heavy stone or concrete panels, glass panels and masonry veneer do not qualify
Short Columns-	some columns restrained by half walls or spandrel beams
Post Benchmark Year-	building designed after certain key year when Code requirement was increased - different for each building type and municipality
Soil Profile: SL1-	rock, or stiff clay less than 200 feet overlying rock
Soil Profile: SL2-	cohesionless soil or stiff clay greater than 200 feet deep
Soil Profile: SL3-	30 or more feet of soft or medium stiff clays (use if do not know soil profile)
SL3 & 8 TO 20 Storeys-	8-to 20- storey building on SL3 soil profile
Non-structural Falling Hazard-	masonry cornices, veneer, small cladding, overhangs especially on older structures. wood and sheet metal ornaments do not qualify

Figure 13.4 Rapid visual screening – quick reference. (From FEMA-154/1988. *Rapid Visual Screening of Buildings for Potential Seismic Hazards: A Handbook*. Federal Emergency Management Agency, Washington, DC. With permission.)

modifiers related to building negative characteristics (e.g. high rise, vertical irregularity, etc.; Figure 13.4). The ranking above has been based on the evaluation of 55,000 cases.

In Greece, the above procedure has been adapted to the characteristics of Greek buildings typology, and the Structural Score benchmark for R/C buildings was validated to $S = 1.75$ based on the results of the Thessaloniki (1978) and Athens (1999) earthquakes (Penelis, 2001; Karabinis, 2002). This validation was based on comparative studies of post-earthquake evaluation results of buildings against the results of ranking of the same buildings using the RVSP procedure (Figures 13.6 and 13.7).

ATC-21/ (NEHRP Map Areas 5.6.7 High)

Rapid Visual Screening of Seismically Hazardous Buildings

Scale:

Address _____
_____ Zip _____
Other Identifiers _____
No. Storeys _____ Year Built _____
Inspector _____ Date _____
Total Floor Area (sq. ft.) _____
Building Name _____
Use _____

(Peel-off label)

INSTANT PHOTO

OCCUPANCY			STRUCTURAL SCORES AND MODIFIERS											
Residential Commercial	No. Persons	BUILDING TYPE	W	S1 (MRF)	S2 (BR)	S3 (LM)	S4 (RC SW)	C1 (MRF)	C2 (SW)	C3/S5 (URM INF)	PC1 (TU)	PC2	RM	URM
Office Industrial Pub. Assem. School Govt. Bldg. Emer. Serv. Historic Bldg.	0 - 10 11 - 100 1000+	Basic Score	4.5	4.5	3.0	5.5	3.5	2.0	3.0	1.5	2.0	1.5	3.0	1.0
		High Rise	N/A	-2.0	-1.0	N/A	-1.0	-1.0	-1.0	-0.5	N/A	-0.5	-1.0	-0.5
		Poor Condition	-0.5	-0.5	-0.5	-0.5	-0.5	-0.5	-0.5	-0.5	-0.5	-0.5	-0.5	-0.5
		Vert. Irregularity	-0.5	-0.5	-0.5	-0.5	-0.5	-1.0	-0.5	-0.5	-1.0	-1.0	-0.5	-0.5
		Soft Story	-1.0	-2.5	-2.0	-1.0	-2.0	-2.0	-2.0	-1.0	-1.0	-2.0	-2.0	-1.0
		Torsion	-1.0	-2.0	-1.0	-1.0	-1.0	-1.0	-1.0	-1.0	-1.0	-1.0	-1.0	-1.0
		Plan Irregularity	-1.0	-0.5	-0.5	-0.5	-0.5	-0.5	-0.5	-0.5	-1.0	-1.0	-1.0	-1.0
		Pounding	N/A	-0.5	-0.5	N/A	-0.5	-0.5	N/A	N/A	N/A	-0.5	N/A	N/A
		Large Heavy Cladding	N/A	-2.0	N/A	N/A	N/A	-1.0	N/A	N/A	N/A	-1.0	N/A	N/A
Non Structural Falling Hazard ☐		Short Columns	N/A	N/A	N/A	N/A	N/A	-1.0	-1.0	-1.0	N/A	-1.0	N/A	N/A
		Post Benchmark Year	+2.0	+2.0	+2.0	+2.0	+2.0	+2.0	+2.0	N/A	+2.0	+2.0	+2.0	N/A
DATA CONFIDENCE		SL2	-0.3	-0.3	-0.3	-0.3	-0.3	-0.3	-0.3	-0.3	-0.3	-0.3	-0.3	-0.3
* = Estimated Subjective or Unreliable Data		SL3	-0.6	-0.6	-0.6	-0.6	-0.6	-0.6	-0.6	-0.6	-0.6	-0.6	-0.6	-0.6
DNK = Do Not Know		SL3 & 8 to 20 stories	N/A	-0.8	-0.8	N/A	-0.8	-0.8	-0.8	-0.8	N/A	-0.8	-0.8	-0.8
		FINAL SCORE												

COMMENTS

ATC87HI
30032.01

Detailed Evaluation Required ?

YES   NO

Figure 13.5 Data collection form. (From FEMA-154/1988. *Rapid Visual Screening of Buildings for Potential Seismic Hazards: A Handbook*. Federal Emergency Management Agency, Washington, DC. With permission.)

Percentage (%) of R/C buildings with repair cost more than
0%, 3.3%, 10%, 20% and 30% of construction cost
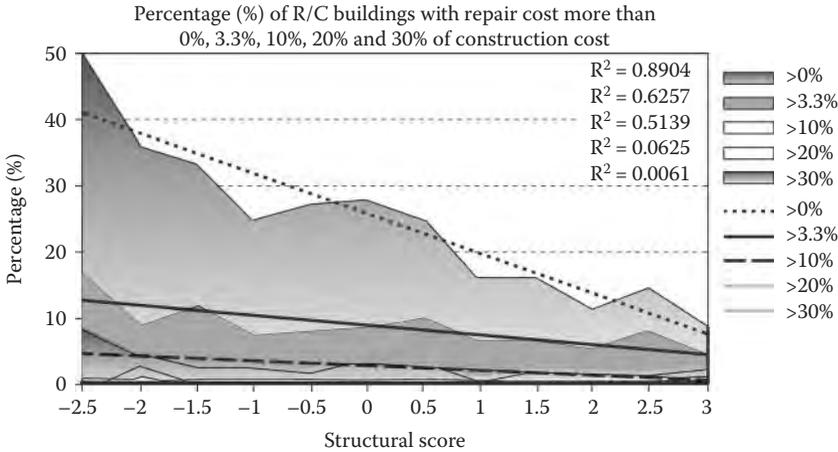
Figure 13.6 Relation between structural score and percentage of R/C buildings with predefined repair cost. (From Penelis, G.G. 2001. Pre-earthquake assessment of public buildings in Greece. *Greek-Turkish Conference on Seismic Assessment*, Istanbul, Technical Chambers of Greece and Turkey.)

13.2.3 Seismic evaluation of buildings according to ASCE 31-02/ FEMA 310/1998

This standard provides a *three-tiered procedure* for seismic evaluation of existing buildings for any level of seismicity. It is apparent that the main task of seismic evaluation is the identification of buildings that might be hazardous after a strong earthquake for the safety

Total number of R/C buildings: 463
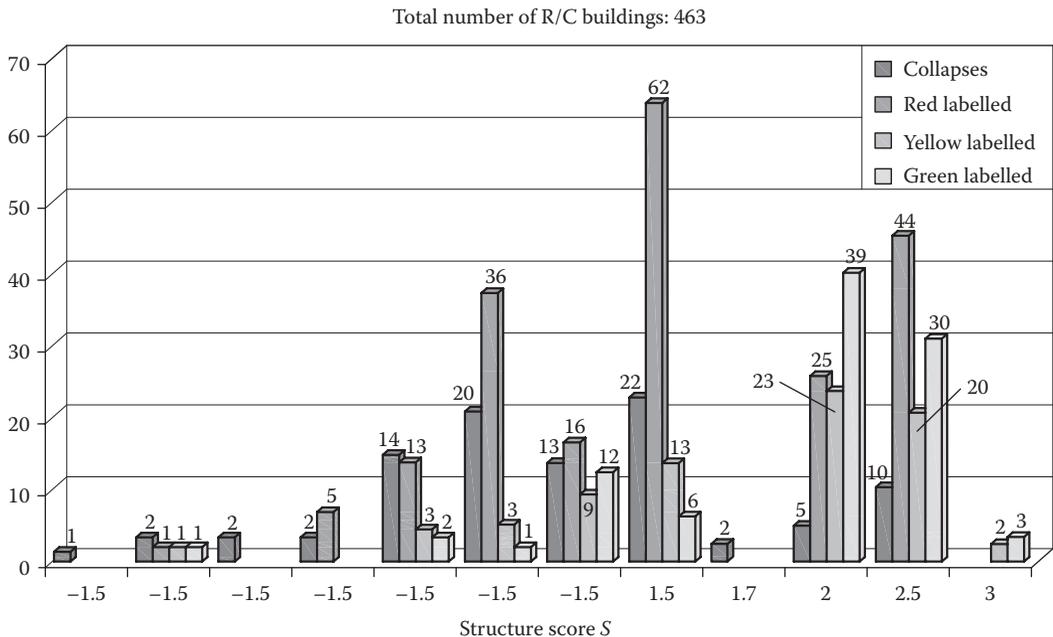
Figure 13.7 Distribution of the structural score to the R/C buildings of the most affected area of Athens due to the earthquake of 1999. (From Karabinis, A. 2002. Validation of the pre-earthquake assessment procedure of R/C buildings in Greece, Technical Report (OASP) Athens, Greece.)

of life, or buildings intended to be used for immediate occupancy that they might fail to comply with this purpose. Therefore, buildings are evaluated according to this standard to either *Life Safety* or *Immediate Occupancy* Performance Level (see Subsections 3.5.1 and 14.4.1). All aspects of building performance are considered and defined in terms of structural, nonstructural, and foundation/geologic hazard issues. Prior to using this standard, a rapid visual screening of the building may be performed to determine if an evaluation is needed.

The evaluation procedure specified in this standard consists of the following *three tiers* shown in Figure 13.8.

- Screening Phase (Tier 1)
- Evaluation Phase (Tier 2)
- Detailed Evaluation Phase (Tier 3)

The screening phase, Tier 1, consists of three sets of checklists that allow a rapid seismic evaluation of the building. The level of analysis required at this Tier is minimal. If deficiencies are identified the designer may proceed to Tier 2 and conduct a more detailed evaluation of the building. Otherwise, the evaluation may be finalised at the end of the first tier.

For *Tier 2*, a complete analysis of the building will be performed that addresses all of the deficiencies identified in Tier 1.

Analysis in Tier 2 is limited to *simplified linear analysis methods*. Evaluation in Tier 2, as in Tier 1, is intended to identify buildings not requiring rehabilitation. If deficiencies are identified during a Tier 2 evaluation, the designer may choose either to conclude the evaluation, proposing repair of the deficiencies, or proceed to Tier 3.

Tier 3 includes a detailed seismic evaluation using even non-linear analysis procedures. Usually, Tier 3 seismic evaluation is carried out, implementing ASCE SEI 41-06/FEMA 356/2000.

In all three steps the relevant report includes:

- Analytical checking of capacity adequacy of strength or deformation in relation to the corresponding demand at all critical regions
- Detailing deficiencies in geometry and reinforcement
- Identified damages for any reason
- Designer's decision about terminating the evaluation or proceeding to the next step

The final report of seismic evaluation usually includes at least the following items:

1. A list of the tier(s) followed and level of investigation conducted
2. Site and building data
3. List of assumptions on material properties and site conditions
4. List of identified deficiencies
5. Appendix with references and preliminary calculations

The above procedure properly adapted for Greek conditions has been implemented in a pilot programme for the R/C buildings of the University of Thessaloniki (Kappos et al., 2006). The main adaptation related to the distinction of deficiencies between those posing a risk to life safety and those not posing such risks. This approach has given the opportunity to design professionals, based on a semi-automatic procedure, to establish priorities for retrofitting actions, which are known to be of high cost and therefore cannot all be carried out at the same time.
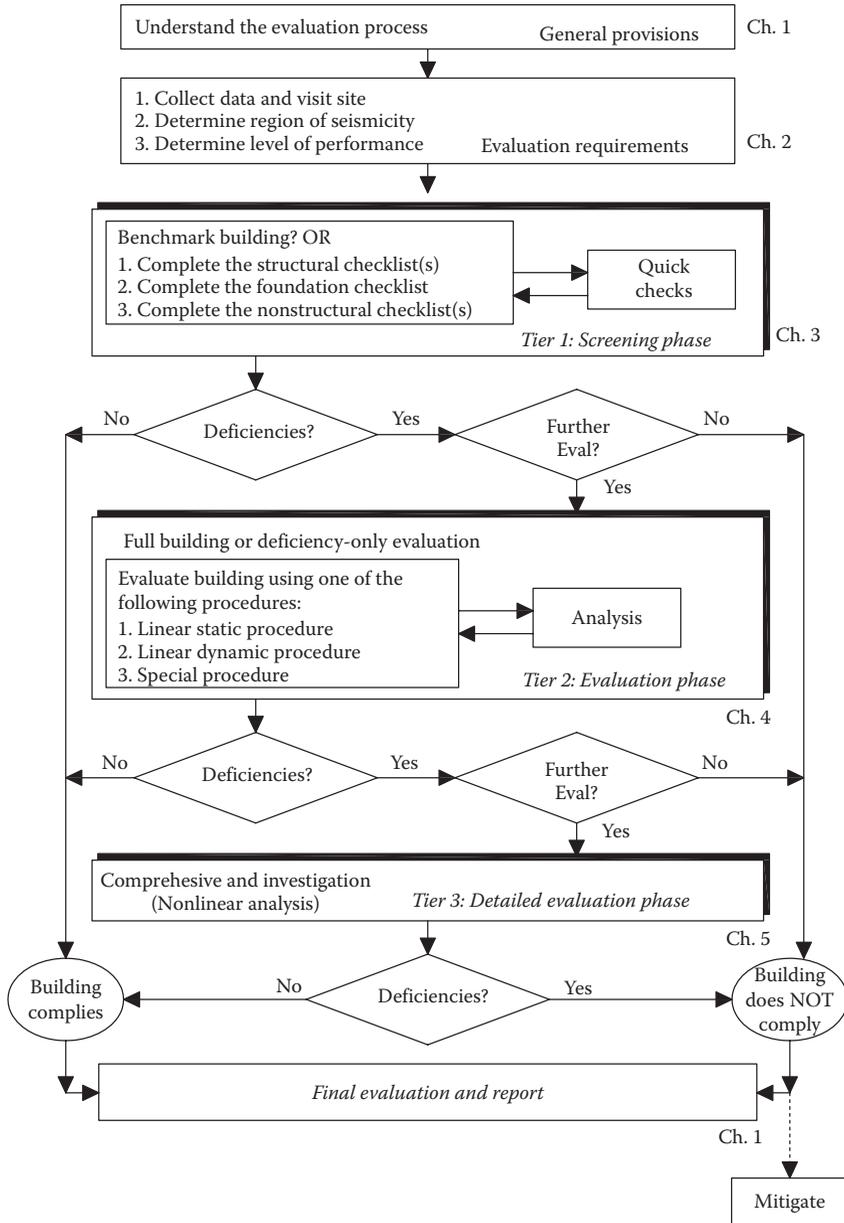
Figure 13.8 Evaluation process according to ASCE 31-02/FEMA 310/1998. (From FEMA-310/1998/ASCE 31-02. *Handbook for the Seismic Evaluation of Buildings*—A standard prepared by the ASCE for the Federal Emergency Management Agency, Washington, DC. With permission.)

13.2.4 Concluding remarks

1. As was noted in Section 13.1, *'pre-earthquake'* seismic risk mitigation programmes are activated for categories of buildings that have been selected according to criteria depending on:
   - Seismicity and ground conditions
   - Importance class and occupancy (e.g. school, hotels, hospitals, etc.)

- Perceived vulnerability of the building influenced by the type of material and construction, number of storeys, age of the building with respect to benchmark year of the various Codes and so on

Therefore, seismic evaluation and the eventual retrofitting that follows *are triggered* by political decisions, based, of course, on seismic risk reduction criteria like those noted above.

In this context this type of seismic evaluation is based mainly on the technical characteristics of the building category under consideration, the seismic hazard of the region, and the occupancy status. Damages caused by earthquakes in the past are only occasionally taken into account in the cases where such information exists.

2. As was noted at the beginning of this chapter, the mean cost for seismic rehabilitation, including all by-costs of evaluation and design, ranges between 10% and 12% of the cost of a corresponding new building. However, keeping in mind that the percentage of buildings with deficiencies may be considerable and that it is very difficult to specify among them for rehabilitation only those which are near collapse, *a decision for a general pre-earthquake evaluation and retrofitting* has not so far been undertaken, to the authors' knowledge, anywhere in the world. For example, in Greece, according to a recent survey carried out by the Technical Chamber of Greece in 2001, 32% of the building stock preexists the first Greek Seismic Code of 1959, 46% has been constructed according to the Code of 1959 in effect until 1985, while only the remaining 22% was constructed between 1985 and 2001, according to the new Greek Seismic Code reflecting modern earthquake engineering considerations. Therefore, a campaign for a general seismic evaluation of buildings would lead to an unaffordable cost.

3. For the above reasons, pre-earthquake rehabilitation programmes have been activated only for special categories of buildings and in countries of high gross national product. Among them, the pre-earthquake seismic evaluation programme of government-owned or leased buildings in the United States (Presidential Order 12941, 1994) and eventual future rehabilitation may be considered the most extended and significant one.

13.3 POST-EARTHQUAKE SEISMIC EVALUATION OF R/C BUILDINGS

13.3.1 Introduction

As was noted in Section 13.1, strong earthquakes and the damage that they cause are the trigger for post-earthquake assessment and retrofitting actions. In this context, the main criterion for seismic evaluation and the degree of retrofitting should be the extent of damage and its seriousness.

However, most of the methods developed so far do not make any distinction in evaluation procedure between pre- or post-earthquake cases. In this respect, methods that have been presented in the previous section could also be implemented in the case of post-earthquake seismic evaluation. Keeping in mind that damage due to earthquakes may extend from plaster detachment to heavy damage of structural elements or overall structural degradation to a near-collapse situation or even collapse, it is obvious that the implementation of methods that are applied in pre-earthquake conditions need to have a well-defined limit of the level of damage, above which the evaluation process is activated. For example, in the case of the Thessaloniki earthquake (1978), which is a typical case study, buildings with severe damage corresponded only to 4.5% of the building stock of the city, buildings with intermediate damage corresponded to 21%, and buildings with damage only at partition walls corresponded

to 22.9%. In this context, it is apparent that the cost of seismic evaluation and retrofitting increases rapidly in relation to the level above which evaluation is activated (Penelis, 2008).

In practice, in most cases, the degree and extent of seismic evaluation, and therefore the consecutive retrofitting actions, are strongly related to the seismic damage (Penelis and Kappos, 1997). *This approach radically decreases the rehabilitation cost of an affected region and the time required for the whole campaign.*

Two tendencies usually appear after a catastrophic earthquake. The first one is known worldwide as 'cover-up' of the damage that the structural system and the infills exhibit. It is a quick solution of low cost, but extremely dangerous. A commonly expressed opinion is that 'since the building withstood the earthquake only with some cracks, there is no problem', which leads into ignoring the extent and pattern of damage, as well as its influence on a possible future seismic loading, which could be fatal for a structurally degraded building and its inhabitants.

The second tendency, which is the exact opposite of the first one, comes from people who are terrified by the destruction and suggest a large-scale strengthening of all buildings, damaged or not, disregarding the economic consequences of such a decision.

It is obvious that the best solution can be reached if the problem is approached in a cool and scientifically rational manner, at the same time using international practice on the subject.

13.3.2 Terms and definitions related to post-earthquake evaluation

Before proceeding to the objectives and to the principles of structural post-earthquake evaluation, it is necessary to clarify some terms and definitions in use in post-earthquake evaluation and retrofitting (Penelis and Kappos, 1997).

13.3.2.1 Seismic demand

Seismic demand E_d, as already explained in Chapter 3, is expressed quantitatively by the seismic effects at all critical cross sections expressed as internal forces or strains. The seismic action for the determination of E_d is defined by the design spectrum S_d for elastic analysis (Paragraph 3.4.3.7). As is well known (Equation 3.43), this value at the spectrum plateau is given by the expression:

$$\boxed{S_d(T) = a_g S \frac{2.5}{q}} \tag{13.1}$$

The *base seismic demand* V_B according to the 'lateral force method of analysis' is given by the expression:

$$V_d = S_d(T_1)W \tag{13.2}$$

where

$$W_d = \sum G_{\kappa i} \text{'+'} \sum \Psi_{Ei} Q_i \tag{13.3}$$

and is used as seismic demand in post-earthquake assessment considerations.

Given the fact that damaged structures have been built in different time periods, they have a different behaviour factor q, which depends to a certain degree on the available ductility of the building (Subsection 5.4.3). Thus, in Greece, for example, R/C structures built before 1985 may roughly be classified in DC 'L', those built after 1985 in DC 'M', while those built after 1995 are classified in DC 'H' in respect to their available ductility.

The seismic demand is a value that is defined by the authorities after every catastrophic earthquake. The decision about this value is a function of economic and social parameters on the one hand and the safety of the buildings on the other. The basic criterion of this decision is the actual elastic response spectrum of the earthquake that caused the damage, as well as the degree of damage. Thus, in the Thessaloniki, Greece, earthquake (1978), the required seismic resistance was kept at the same value as that specified by the Code applicable at the time of the earthquake. In the Bucharest, Romania, earthquake (1977), the same response spectrum was used for the repairs as the one in effect before the earthquake. In the Mexico City earthquake (1985), the ordinates of the design spectrum were increased by 60% in the area mostly affected (Jirsa, 1994). In the Kalamata, Greece, earthquake (1986), the required seismic demand was kept at the same levels as before the earthquake.

13.3.2.2 Seismic capacity

For the post-earthquake assessment considerations, seismic capacity is expressed by the base shear V_c, for which the first of the columns or R/C walls of the ground floor level reaches its ultimate limit state, provided that the structure is in the elastic range. Seismic capacity refers to the condition of the building prior to earthquake damage. At the same time, for the determination of V_c, the concrete quality and reinforcement of the vertical structural elements must be known. It should be pointed out that this definition does not cover the case of very flexible structures where damage may first appear at the top rather than the bottom of the structure (e.g. the Mexico City case).

Usually, V_c is less than V_B for several reasons, such as:

1. The design provisions have not been fully implemented during the construction of the building as far as the quantity of reinforcement and the quality of concrete and detailing are concerned.
2. The structure was designed and built on the basis of design seismic actions different from those specified by the authorities after the earthquake.
3. The usage of the building has changed, and therefore the gravity loads have been increased or its importance factor has changed.
4. Environmental attacks, such as corrosion of the reinforcing steel bars, have caused a decrease in the load-carrying capacity of members.

13.3.2.3 Residual seismic resistance

The residual seismic resistance V_D of a damaged structure is expressed quantitatively by the base shear under which, assuming an elastic behaviour of the structure, at least one of the (undamaged) columns or walls of the ground floor reaches its ultimate strength. For the estimation of V_D the decrease in the stiffness of the damaged structural elements is taken into account. If a structure exhibits damage due to an earthquake, V_D is always less than V_c (Figure 13.9; Anagnostopoulos, 1986).
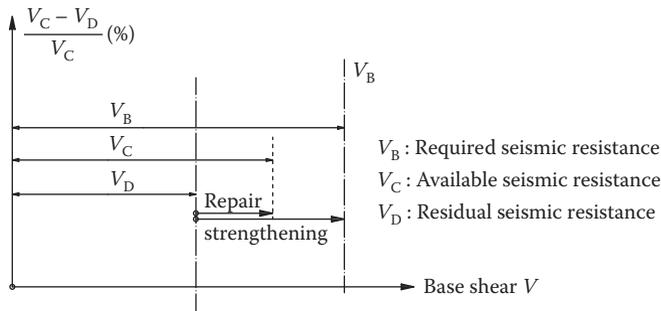
Figure 13.9 Schematic presentation of V_B, V_C, V_D.

13.3.2.4 Loss of seismic resistance

The difference

$$V_C - V_D \tag{13.4}$$

is defined as loss of seismic resistance.

13.3.2.5 Repair

The term 'repair' means that the damaged structural or non-structural members again reach the minimum strength, stiffness and ductility they ought to have before the earthquake. This means that 'repair' is limited only to the damaged elements, and in this sense 'repair' must be considered a *local intervention*. V_D is increased with the repair at least up to the value of V_c (Figure 13.9).

13.3.2.6 Strengthening

The term 'strengthening' is used to express the increase of the seismic resistance of the structure with interventions beyond repair, so that the available seismic resistance becomes equal to V_B, or to a predefined percentage of it (Figure 13.9). This means that in addition to the local interventions to the damaged elements, interventions of *global type* will be carried out, so that the overall structural behaviour of the building is improved.

13.3.2.7 Strength index

By this term, two different quantities can be defined:

1. In the literature (ATC 3-06,1978; UNIDO/UNDP, 1985), the strength index is determined as:

$$R_C = \frac{V_C}{V_B} \tag{13.5}$$

2. In practice, for post-earthquake intervention this index is usually replaced (Tassios, 1984; Chronopoulos, 1984; EC 8/Part 1.4/Draft-CEN, 1993) by

$$R_D = \frac{V_D}{V_C} \tag{13.6}$$

As we will see later, R_C and R_D are strongly interrelated; however, as we will also see later, the second index is much more reliable than the first. These two indices constitute a decisive criterion for the level of intervention, that is, whether simple repair or strengthening of the structure is required.

13.3.3 Objectives and principles of retrofitting

The main objectives of intervention in an earthquake-damaged building are to protect the structure from collapse in a future strong earthquake, to keep damage at tolerable levels in earthquakes of moderate intensity, and to eliminate damage in earthquakes with a relatively short return period. In other words, the objectives of an intervention more or less coincide with those set for the design of a new structure.

In this sense, the only rehabilitation action that can guarantee the above objectives is strengthening, that is, the repair of damaged structural elements and the increase of the seismic resistance of the structure up to the value of the required seismic resistance by the Code in effect, using additional strengthening measures. However, such an approach must be considered to be unrealistic.

In fact, taking into account that the buildings with severe seismic damage are limited to 4.5–5.0% of the building stock of a city (see subsection 13.3.1), it is obvious that strengthening actions cannot be extended to all buildings with any degree of damage, even only to the partition walls, because in this case, the strengthening activities would be extended to almost 50% of the building stock, and, in this context, the intervention cost would be multiplied by almost 10. In other words, it is not reasonable to transform in practice the post-earthquake repair and strengthening intervention to a pre-earthquake rehabilitation activity having as trigger the seismic event and not a thorough cost-benefit analysis, which might activate such a rehabilitation action for a special category of buildings in case of a pre-earthquake intervention and of course without the panic of the consequences of an earthquake.

In view of the foregoing, the most realistic approach appears to be the repair of the damaged building to pre-earthquake condition. This is based on the notion that if the damaged elements, structural and non-structural, are repaired, the structure more or less regains its pre-earthquake seismic resistance and therefore will behave similarly in a future earthquake with the same characteristics. However, this approach has a weak point: the extent and the seriousness of damage caused by an earthquake constitute the most reliable criterion regarding the difference of the available seismic resistance V_C and the required one, V_B. Therefore, in the case of serious damage with an existence that proves the structure came near to collapse, we cannot consider repair to be enough. The structure should be strengthened to a degree so that in a future earthquake it will behave like buildings with no or only light damage (Holmes, 1994).

Based on the above, the recommended approach to the intervention procedure may be stated as follows:

1. In buildings with light damage, of local nature, intervention should be limited to repair.
2. In buildings with extensive or heavy damage, of global type, intervention should include strengthening of structure.

Extended discussion accompanied by divergent opinions on this issue may be found in the literature (Anagnostopoulos et al., 1989; Freeman, 1993).

In conclusion, it should be noted that in post-earthquake rehabilitation practice the trigger for structural repair or strengthening is damage to the structural system. Therefore, only buildings labeled as 'yellow' or 'red' by the post-earthquake inspecting of the affected region are further evaluated for *repair* or *strengthening.*

In this context the post-earthquake inspection of the buildings and their labeling as 'green', 'yellow' or 'red' plays the role of the 'rapid visual screening of buildings for potential seismic hazards' in the case of pre-earthquake evaluation.

13.3.4 Criteria for repair or strengthening

To comment on the criteria specified by several agencies and organisations for the choice between repair and strengthening, review of Figure 13.10 is useful. The *x*-axis represents the seismic demand and resistance expressed according to the definitions of Subsection 13.3.2 as the base shear *V*, and the *y*-axis represents the loss of seismic resistance (Section 13.2), expressed as the percentage of the available seismic resistance. Curve V_C represents the seismic capacity and V_D the residual capacity after the earthquake.

Theoretically speaking, if V_C equals V_B, no damage should be expected and V_C should intersect the *x*-axis at the same point as V_D and V_B. As the ordinate increases, that is, as damage becomes more severe, the distance between curves V_C, V_D and V_B increases, and finally for $(V_C - V_D)/V_C = 100\%$, that is, in the case of collapse, curve V_D intersects the *y*-axis.

If a reliable value of V_C could be determined analytically, the ratio V_C/V_B would be a safe indication of the expected damage, or in other words, there would be a quantitative correlation between the two ratios V_C/V_B and V_D/V_C; therefore, it would not be significant to determine which of the two ratios was to serve as 'index' for the kind of intervention required. However, the reliability of the value of V_C is questionable because of the dynamic character of the problem, the inelastic behaviour of the structure, the materials, the infills and so on. For this reason, although the structure does not exhibit serious damage, the ratio V_C/V_B often has a very small value or, in contrast, in structures with serious damage, this ratio displays a very large value. Therefore, the most reliable index for the choice of intervention level seems to be the ratio V_D/V_C, residual over seismic capacity, because it expresses undeniable facts, that is, the degree of damage to the structure.
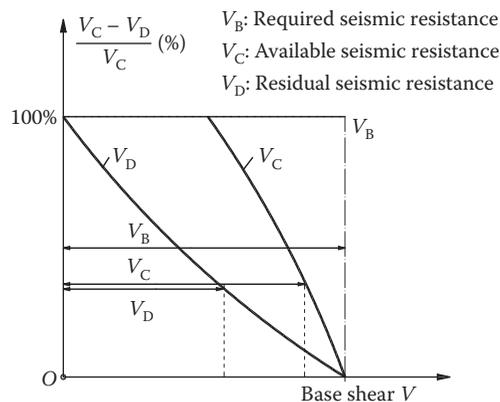
Figure 13.10 Correlation between the indices V_C/V_B and V_D/V_C.

Of course, in the case of a pre-earthquake assessment of important or socially sensitive buildings, such as schools, hospitals, or hotels where there is no damage indication, the available index is the ratio V_C/V_B, and this is the one usually used. In the manual Post-Earthquake Damage Evaluation and Strength Assessment of Buildings of UNIDO/UNDP (1985), the ratio V_C/V_B is used as an index of seismic resistance for both pre-earthquake and post-earthquake assessment.

Greek practice for post-earthquake interventions since 1978 and up to the recent Athens (1999) earthquake has used the ratio V_D/V_C as the index of seismic resistance (Chronopoulos, 1984; Penelis, 1979; Tassios, 1984). The values of this index are estimated in practice. Of course, in the case of very important structures, highly sophisticated approaches are used.

13.3.5 UNIDO/UNDP procedure

The procedure suggested in the UNIDO/UNDP/PR.RER/79/015 (1985) manual takes into account four factors for a preliminary determination of the type of intervention, that is:

- Arrangement of the structural elements
- Strength of the structure
- Flexibility of the structure
- Ductility of the structure

A brief summary of the method will follow.

13.3.5.1 Arrangement of the structural elements

The structural system of the building, depending on the layout of the structural members, can be classified as:

- *Good* – the arrangement of the structural members is clear, without any irregularities in plan or elevation, and the horizontal forces are carried by clearly defined structural systems of frames or walls in both main directions (Figure 13.11).
- *Acceptable* – the building in general has a good structural system except for some weaknesses, such as large stiffness eccentricity, discontinuity of stiffness in elevation (e.g. open ground floor) and so on (Figure 13.12).
- *Unclear* – the horizontal forces are carried by systems of structural elements that are not clearly defined (Figure 13.13).

13.3.5.2 Strength of the structure

Three levels of the index of seismic resistance $R_C = V_C/V_B$ are adopted for decision-making needs. Of course, the limit values adopted are to be considered as guidelines and not as strict limit conditions.
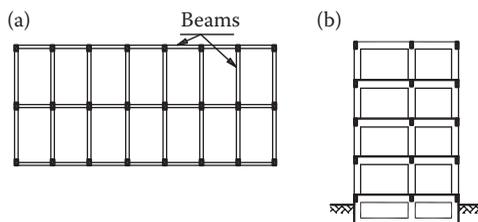
Figure 13.11 Example of 'good' structural layout.
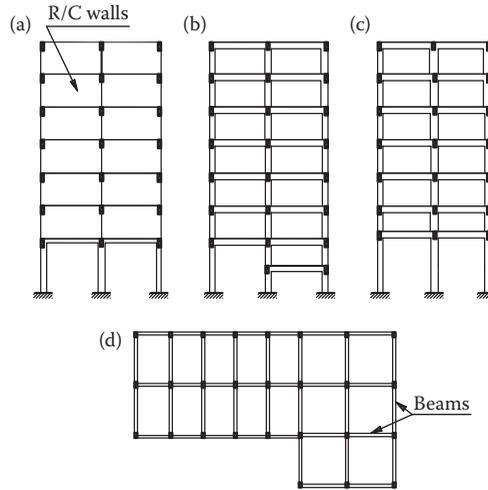
Figure 13.12 Examples of 'acceptable' structural layout.

$R_C > 0.8$: seismic resistance is considered satisfactory with the probability of somewhat deeper incursions into the inelastic range, without approaching the failure limits. Therefore, *repair* is adequate.

$0.8 > R_C > 0.5$: despite the diminished strength, if enough ductility exists, the building can be secured against collapse in a strong earthquake, although this type of structure can reach the failure limits. Therefore, the structure must be strengthened.

$0.5 > R_C$: the safety of the structure is clearly unsatisfactory.

Combining the estimation for the layout of the structural system with that for the strength index, five categories of the actual structural quality are defined, from A to E, given in Table 13.1.
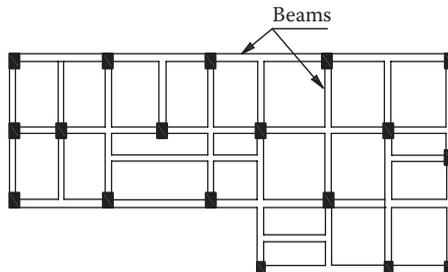
Figure 13.13 Example of 'unclear' structural layout.

Table 13.1 Five building categories based on structural layout and strength index

	Structural layout		
Strength index	Good	Acceptable	Unclear
$R_c > 0.8$	A	B	C
$0.8 > R_c > 0.5$	B	C	D
$0.5 > R_c$	C	D	E

13.3.5.3 Flexibility of the structure

The flexibility of the structure expressed as the inter-storey drift ratio δ_B/h for loading equal to V_B is compared with two quantities:

- With the deformation limit of the structure itself:

$$\frac{d_C}{h} = \frac{0.01 \text{ to } 0.015}{q} \tag{13.7}$$

- With the deformation limit of the infill system:

$$\frac{d_D}{h} = \frac{0.007 \text{ to } 0.0075}{q} \tag{13.8}$$

where
q is the behaviour factor of the building.

13.3.5.4 Ductility of the structure

The ductility requirements specified by modern Codes are met only by a very small number of recently built structures. Indeed,

- Strong columns – weak beams
- Adequate shear reinforcement (ties) so that bending mode of failure is secured
- Confined compression zones with closely spaced hoops or ties

are requirements that were established for the first time in the late 1960s. Thus, in most cases, ductility requirements for DC 'M' or 'H' are not met, and the engineer has to choose between large-scale interventions to increase ductility, something that is unrealistic in most cases, or to accept DC 'L'. In this case, V_B must be increased, since q corresponding to DC 'L' is lower, and the structure must be strengthened.

13.3.5.5 Decision for the degree and type of intervention

As has already been mentioned, four factors are considered for the degree and type of intervention, that is:

- Layout of the structural system
- Strength of the structure
- Flexibility of the structure
- Ductility of the structure

The type of intervention can either be *repair* or *strengthening*.

The type of strengthening, depending on the seriousness of the situation, may be one of following:

- Type I: improvement of the ductility and the energy-dissipation mechanism (Figure 13.14) through upgrading of existing structural elements (e.g. using thin jackets on columns with closely spaced ties).
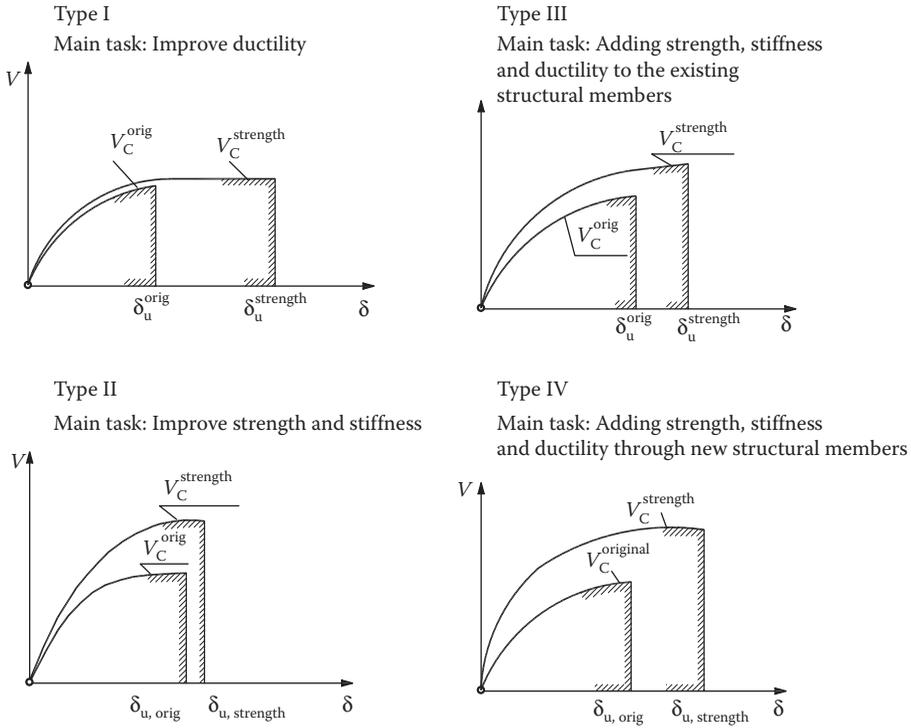
Figure 13.14 Diagrams illustrating the four strengthening types.

- Type II: increase of strength and stiffness through strengthening of existing structural elements (Figure 13.14; e.g. increase of the thickness of walls).
- Type III: increase of strength, stiffness and ductility through strengthening of existing structural elements (e.g. increase of the thickness of walls and jackets on columns; Figure 13.14).
- Type IV: increase of strength, stiffness, and ductility through the addition of new structural elements (e.g. addition of new walls, jackets on columns, jackets or one-sided strengthening of walls; Figure 13.14).

The type of intervention can be chosen in every case with the aid of Table 13.2.

The strengthening level (R_{req}) can be determined through probabilistic relationships of seismic risk, which take into account the remaining life of the building in relation to the design life as determined by the Code (UNIDO/UNDP, 1985). Thus, the design base shear for the strengthening V_{str} can be derived from the relationship:

$$V_{str} = \left(\frac{T_{rem}}{T_{des}}\right)^{0.50 \div 0.67} \cdot V_B \tag{13.9}$$

where

V_{str} is the base shear for the reanalysis and redesign of the building under strengthening.
T_{rem} is the remaining lifetime of the building.
T_{des} is the design lifetime of the building.
V_B is the Code-specified base shear for new buildings of the same ductility class.

Table 13.2 Selection of the degree and type of intervention

Structural category	Satisfactory ductility (DC 'M' or 'H')		
	$\delta_R < \delta_D$	$\delta_D < \delta_R < \delta_C$	$\delta_C < \delta_R$
A	R[a]	R or II	III
B	R or II[b]	R or II or IV	III or IV
C	R or II[c] or IV	R or II or IV	IV
D	IV[d]	IV	IV
E	IV[d]	IV	IV
	Unsatisfactory ductility (DC 'L')		
A	R or I	R or III	III
B	I or II or III	III or IV	III or IV
C	IV	IV	IV
D	IV	IV	IV
E	IV	IV	IV

[a] R = Repair.
[b] Category B is strengthened in order to be upgraded to A.
[c] Category C is strengthened in order to be upgraded to A or B, depending on the means available.
[d] Categories D and E are strengthened in order to be upgraded to A or B, depending on the means available.

For some cases in Table 13.2, two or three alternatives appear. In these cases the choice is made based on the cost of intervention.

13.3.5.6 Concluding remarks

The authors' opinion is that the weak point of the method is the use of the ratio V_C/V_B as an index for the choice of degree of intervention, instead of the ratio V_D/V_C. The reasons for this have been explained in the previous subsection.

Another weakness of the method is the attempt to introduce a standard algorithm through Tables 13.1 and 13.2 for the choice of the type of intervention, something that cannot be standardised due to the special problems arising in each case.

While the method gives the impression that the procedure for the choice of the degree and type of intervention is quantitative and therefore objective, it is still highly subjective with regard to the following points:

- Modelling of the structural system for the determination of V_C
- Classification of the layout of the structural system
- Choice of the type of strengthening

As far as the computational work is concerned, analysis of the system along both main directions is required, in order to determine V_C based on the available sections and reinforcement. This analysis may be avoided with the application of the simplified approximate approaches that are given in UNIDO/UNDP (1985).

The above procedure should be considered as a preliminary step for the decision-making for *repair* or *strengthening* and for the preliminary choice of the strengthening type.

In the case that the ratio V_D/V_C is used as a *strength index,* most buildings characterised as 'yellow' will need only to be repaired and not strengthened. The determination of ratio V_D/V_C may be accomplished by using very simplified and fast procedures. More particularly, in Greece, empirical indices of seismic resistance are introduced for various types of

damage to each vertical structural element (columns—shear walls). Based on these indices a general index of seismic resistance of each storey is calculated as the mean value of indices of damaged and undamaged elements. From that point on, and having the ratio V_D/V_C determined as presented above, the UNIDO/UNDP procedure is followed (Penelis, 1979; Chronopoulos, 1984; Tassios, 1984).

Buildings for *repair* are approached as cases with *local damage*. The method of design for these cases will be given in the next section. Buildings for *strengthening* must be evaluated and retrofitted quantitatively in detail following the procedure in Chapter 14.

13.4 DESIGN OF REPAIR OF R/C BUILDINGS (LOCAL INTERVENTION)

13.4.1 Repair of the structural system

In the case of repair, the procedure followed is considerably simpler than that followed in the case of strengthening (Chapter 14), and is given below.

13.4.1.1 Information necessary for the final structural assessment

1. The original structural drawings and the original structural analysis must be found. If this is not possible, sketches of the structural system should be prepared by the professional who is responsible for the repair.
2. A detailed presentation of the damage pattern in plan and elevations should be prepared, including photos indicative of the damaged elements.

13.4.1.2 Analysis and design in case of repair

As has often been previously observed, repair is limited only to the retrofitting of damaged elements.

1. The load effects for this intervention may be taken from the original analysis if there are not obvious mistakes. These values should be properly modified to take into account stiffness changes due to additional material (e.g. jacketing).
2. The materials and techniques are then selected, depending on their availability in the market.
3. Based on the load effects derived, as described previously, and on the type of repair, the design resistances are calculated and used for the safety verifications.
4. Techniques, materials and design of the damaged members follow the same procedures as with strengthening, which will be described in detail in Chapter 15.

13.4.2 Repair of the masonry infills

At this point it is necessary to consider the repair of the infill system. It is obvious that if the infill system is not taken into account in the original analysis and design of the building, it is not reasonable to carry out analytical checks on the strength and ductility of the masonry infill in a way similar to that of the structural system. However, the importance of the infill system for the stiffness and strength of a structure has already been adequately stressed, as well as its importance for energy dissipation. Therefore, the retrofitting of masonry walls, especially if they have suffered serious damage, is of vital importance for the safety of the building,

probably of greater importance than the repairing of a single column or a wall. Masonry walls with full-depth cracks should be carefully retrofitted, so that they can again become the first line of defense against a new earthquake, not only through the strength they contribute and the energy they dissipate, but also to restore the initial stiffness of the structure. It should be stressed that the foregoing refers not only to buildings with structural damage, but also to those with no structural damage at all but extensive damage to their masonry infills.

Chapter 14

Detailed seismic assessment and rehabilitation of R/C buildings

14.1 GENERAL

As was clarified in Section 13.1, detailed seismic assessment and retrofitting of buildings is activated after a seismic evaluation procedure has been completed and buildings designated for detailed investigation and eventual rehabilitation have been identified. Whether the designation of these buildings is the result of a pre-earthquake or a post-earthquake procedure, the method for this detailed assessment or retrofitting is the same.

It should be noted in advance that detailed assessment and retrofitting is basically governed by the *'displacement-based design concept'* in all modern guidelines and Codes. Therefore, the next section will be devoted to the presentation of this method, before any reference to Code specifications is made.

The core of this method is the elaboration of the *capacity curve* of the structure, that is, the implementation of an inelastic static analysis, for a lateral force or displacement pattern (see Subsection 5.7.3) and the transformation of the MDOF structural system to an *equivalent SDOF* one, for which target displacement can easily be determined using relevant response spectra reduced to proper ductility or damping level (Subsection 5.7.5).

It should be noted that in the United States detailed seismic evaluation and rehabilitation is specified by ASCE/SEI41-06/(FEMA 356/2000). In Europe it is specified by EC8-3/2005. In the sections that follow, a detailed analysis of this procedure will be presented based mainly on EC8-3/2005, as has been done thus far in this book. Additionally, an overview will be made of methods used in the United States.

14.2 OVERVIEW OF DISPLACEMENT-BASED DESIGN FOR SEISMIC ACTIONS

14.2.1 Introduction

As explained in Subsection 3.2.3, new buildings are analysed and designed according to all modern Seismic Codes, in effect following the *force-based design* procedure.

The basic concept of this procedure is the *reduction* of the elastic inertial seismic forces by a *q-factor* and counterbalancing this reduction by providing adequate *ductility* at all critical regions of the structural members capable of ensuring the overall *q*-factor for the structural system.

For seismic loads reduced by *q*, linear analysis is implemented. Additionally, capacity-design procedures are introduced to postpone any early brittle failure of various structural members or an early overall collapse due to the creation of a soft storey.

The above procedure, which is followed for new buildings, presents serious problems for implementation in the case of existing buildings because the *q*-factor cannot be codified, since the ductility of the structural members of existing buildings built in various periods in the past do not comply with the provisions of modern Codes for local ductility and capacity design requirements.

Therefore, a reliable approach to the problem would be to calculate the capacity curve of the structural system, taking into account the inelastic deformation capacities (θ_p) at the ends of the structural members (Figure 3.22a and b), and therefore the implementation of the displacement-based design *in the form of an inelastic static analysis,* as presented in concept in Subsection 3.2.2 and in detail in Subsection 5.7.3.

In the next section this method will be presented in detail together with various simplifications that also allow the use of elastic procedures for the analysis and design of existing R/C buildings.

14.2.2 Displacement-based design methods

The most rigorous displacement-based design is based on the complete non-linear dynamic time history analysis, which even today is considered very complex and impractical for general use (see Subsections 2.5.3, 3.2.2.1 and 5.7.2). So, simplified nonlinear methods have been developed based on a nonlinear static analysis procedure known as '*pushover analysis*' (see Subsections 3.2.2.2 and 5.7.3). This method, developed in the last 20 years, is implemented mainly for the assessment, verification and retrofitting of existing buildings.

Various approaches to the problem have been developed that have been adopted by various Codes of Practice. An overview of the following methods will be presented below:

- N2 Method (EC8-1/2004)
- Capacity-Spectrum Method (ATC 40-1996)
- Coefficient Method (ASCE/SEI 41-06; FEMA 356/2000)
- Direct Displacement-Based Design (DDBD; Priestley et al., 2007)

14.2.2.1 N2 method (EC8-1/2004)

This method has been adopted by Eurocode EC8-1/2004 and is recommended in Annex B as an informative procedure (Fajfar, 1996).

The steps for the implementation of this method may be summarised as follows (see Paragraph 3.2.2.2):

Step 1. Determination of the capacity curve of the MDOF model

Consider the structural system of (Figure 14.1a) and its eigen mode Φ_i corresponding to its fundamental period T_1. For a lateral load pattern F_i normal to Φ_i ($\Phi_n = 1$), that is:

$$F_i = \Phi_i \cdot m_i \tag{14.1}$$

increasing from zero values stepwise to collapse or at least to 150% of the target displacement (see Paragraph 14.2.2.1.5), the *capacity curve* $V-\delta$ of the structure is derived, where V_b is the base shear and δ_n is the displacement of the top storey *n* (Figure 14.1c).

For the calculation of the coordinates of the above curve it is necessary to know:

- The geometry of the structure
- The quality of the construction materials (concrete-steel)
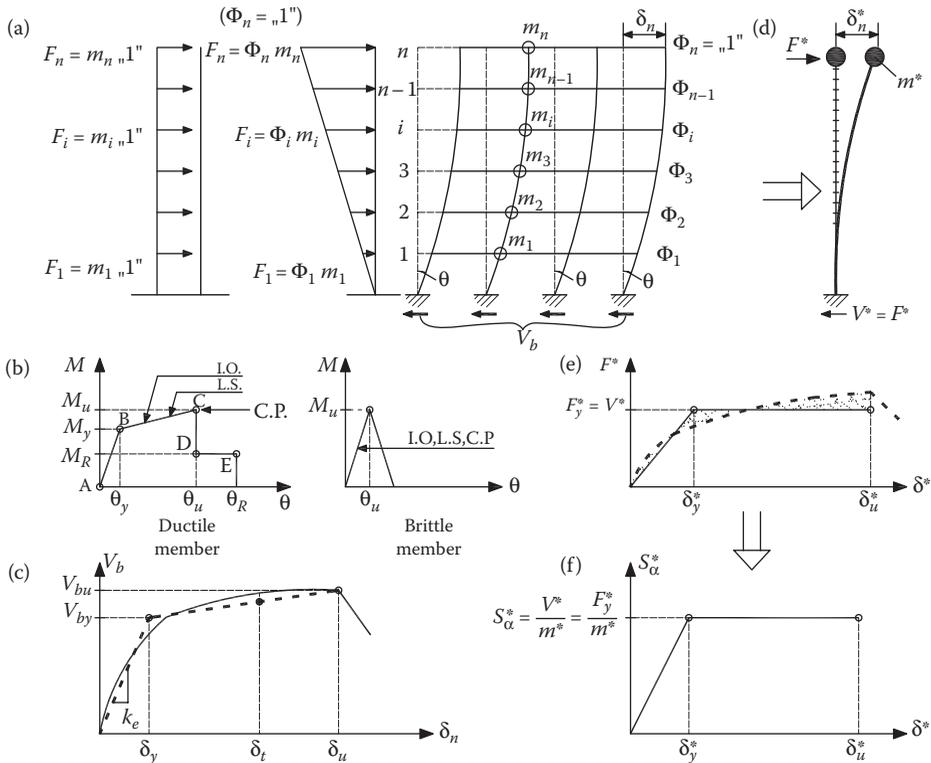
Figure 14.1 Procedure to obtain capacity curves of a structural system: (a) structural system (MDOF) loaded laterally by two different load patterns (eigen modes) for the implementation of a 'push-over' analysis; (b) input data ($M-\theta$ curves) for the member rotations at their ends; (c) capacity curve of the MDOF system; (d) equivalent SDOF model; (e) capacity curve of the equivalent SDOF model transformed to an EPP curve; (f) EPP capacity curve of the SDOF model normalised to a 'capacity spectrum'.

- The reinforcement of the structure in detail (bending-shear)
- Gravity loads of the system

This information makes possible the elaboration of $M-\theta$ diagrams for the ends of each structural member (beams, columns, shear walls; Figure 14.1b), which are input data required for the capacity curve calculation. It should be noted that these diagrams may have the form depicted in Figure 14.1b, depending on the member *ductility*. It should also be noted that the length of the plastic plateau ($\theta_u \boxtimes \theta_y$ depends on the axial load of the member (see Chapters 8 and 9). Therefore, an analysis of the structural system for gravity loads must precede any other calculation so that an approximate value of normal forces of the columns is determined, which is necessary for the elaboration of $M-\theta$ curves.

From the above it may easily be concluded that the calculation of the capacity curve presumes the structural system to be known in detail. That is why inelastic static or dynamic analysis basically suits the assessment procedure of existing buildings. It may also be concluded that the capability of calculating the capacity curve is the core of the displacement-based design method.

It is important to note here that the adoption of the first eigen mode Φ_i of the elastic spectral dynamic analysis (e.g. inverted triangle) as a load pattern is not an indisputable

assumption. It has been found through inelastic dynamic analysis that the results of the displacement δ_n (or building inter-storey drift) at various levels of deformation may be satisfied only if various load patterns are adopted (Figure 14.2; Elnashai and Di Sarno, 2008). So, in recent years, various methods have been developed for adapting the force distribution to the non-elastic state. These modified methods are known as "adaptive push-over methods" (Bracci et al., 1997; Gupta and Kunnath, 2000; Elnashai, 2002). Research to refine adaptive pushover methods is still in progress; for example, modal pushover analysis (Antoniou and Pinho, 2004; Chopra and Chintanapakdee, 2004). Eurocode 8-1/2004 specifies two vertical distributions of the lateral loads (Figure 14.1a):

- A 'uniform' pattern, and
- A 'modal' pattern ('inverted triangle')

Step 2. Equivalent SDOF elastoplastic model

The capacity curve of the MDOF system is transformed, then, to the capacity curve of an equivalent SDOF model (Figure 14.1d,e; Fajfar, 1996; Fajfar and Dolšek, 2000).

As explained in Subsection 5.7.5, this transformation is achieved by introducing the following transformed quantities corresponding to the SDOF model:

$$m^* = \sum m_i \Phi_i = \sum F_i \tag{14.2}$$

$$V^* = V_b/\Gamma \tag{14.3}$$

$$F_i^* = \frac{F}{\Gamma}, \quad V^* = \frac{\sum F_i}{\Gamma} \tag{14.4}$$

$$\delta_n^* = \frac{\delta_n}{\Gamma} \tag{14.5}$$
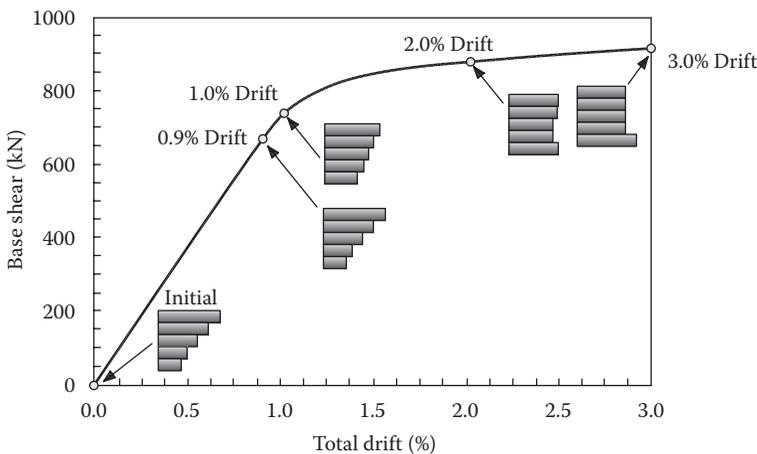
Figure 14.2 Changes of the distribution of an inertially framed building (adaptive force distribution). (From Elnashai, A.S. and Di Sarno, L. 2008. *Fundamentals of Earthquake Engineering.* Copyright Wiley-VCH Verlag GmbH & Co. KGaA. Reproduced with permission.)

where

$$\Gamma = \frac{m^*}{\sum m_i \Phi_i^2} = \frac{\sum F_i}{\sum (F_i^2 / m_i)} \tag{14.6}$$

is the '*transformation factor*' (see Subsection 5.7.5, Equation 5.92).

Thereafter, the corresponding capacity curve may be transformed to that (Figure 14.1e) of an idealised elasto-perfectly plastic (EPP) force–displacement diagram.

For the SDOF model in EPP form, the original stiffness K^* and the fundamental period T^* result from the following relations (Figure 14.1e):

$$K^* = F_y^* / \delta_y^* = V^* / \delta_y^* \tag{14.7}$$

and

$$T^* = 2\pi \sqrt{\frac{m^*}{K^*}} = 2\pi \sqrt{\frac{m^* \delta_y^*}{F_y^*}} \tag{14.8}$$

Thereafter, this EPP capacity curve of the SDOF model may be normalised in terms of acceleration, that is,

$$S_a^* = \frac{V^*}{m^*} \tag{14.9}$$

This curve is known as the '*capacity spectrum*' (Figure 14.1f).

Step 3. Demand spectra

For the next step of the procedure the acceleration elastic response spectrum must be known (demand spectrum; Figure 14.3a). From this spectrum the elastic acceleration–displacement response spectrum (ADRS) is determined using the relation (Figure 14.3b; see Paragraph 2.2.4.5):

$$\boxed{S_{ae} = \left(\frac{4\pi^2}{T^2}\right) S_{de}} \tag{14.10}$$

From the above expression for various values of T and for the corresponding values of S_{ae}, the relevant values of S_{de} may be determined, and therefore the ADRS graph may be easily plotted.

In this respect, radial lines correspond to constant periods T. From the family of the successive graphs, each corresponds to *a given ductility μ* and expresses for this ductility the corresponding inelastic response spectrum of the SDOF model.

The successive graphs may result from the elastic spectrum $S_{ae} - S_{de}$ if the following expressions are used:

$$S_a = S_{ae} / q_0, \quad S_d = \left(\frac{\mu_\delta}{q_0}\right) S_{de} \tag{14.11}$$
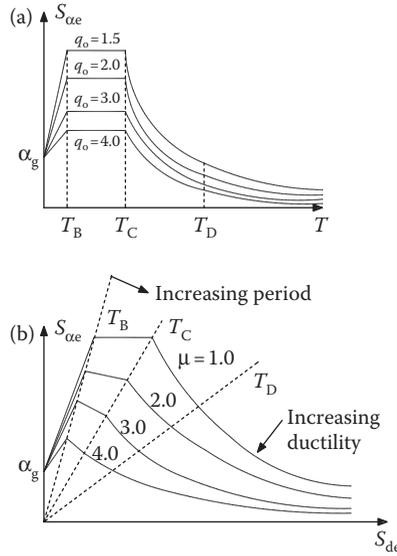
Figure 14.3 Demand spectra for various ductility μ values: (a) traditional acceleration response spectrum in relation to period T; (b) acceleration–displacement response spectra (ADRS) for various ductility μ values.

where

$$q_0 = \mu_\delta \quad \text{for } T > T_c \tag{14.12}$$

$$q_0 = (\mu_\delta - 1)\left(\frac{T}{T_c}\right) + 1 \quad \text{for } T < T_c \tag{14.13}$$

(see Paragraph 5.4.4.1, Equation 5.17). This form of design loading, as we will see next, can be compared directly with the non-linear capacity curve of the equivalent SDOF model.

Step 4. Target displacement of the equivalent SDOF model

Having calculated the capacity spectrum (Figure 14.1f), it may then be plotted upon the corresponding ADRS demand spectrum curve, the ordinates of which give the maximum acceleration of the elastic SDOF system in relation to the corresponding relative displacement S_e (Figure 14.4).

The target displacement demand of the SDOF model with period T^* and *unlimited elastic behaviour* is given by the following expression:

$$\frac{\delta^*_{et}}{\delta^*_y} = \frac{S_e(T^*)}{S^*_\alpha} \tag{14.14a}$$

or

$$\delta^*_{et} = S_e(T^*)\frac{\delta^*_y}{S^*_\alpha} = S_e(T^*)\left(\frac{T^*}{2\pi}\right)^2 \tag{14.14b}$$
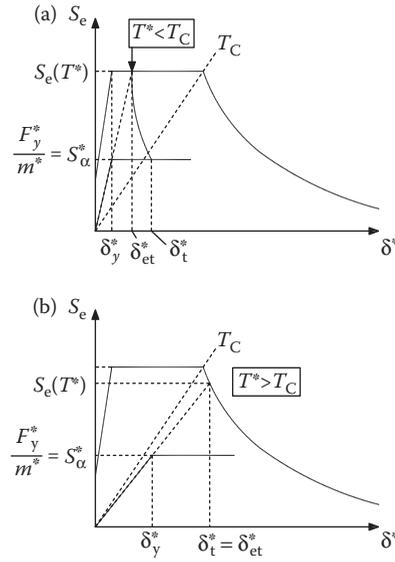
Figure 14.4 Determination of the target displacement for the equivalent SDOF system: (a) short period; (b) medium and long period.

where

$S_e(T^*)$ is the elastic acceleration response spectrum at the period T^* (Figure 14.4).

Equation 14.14b is obtained by substituting Equation 14.10 into Equation 14.14a.

For the determination of the target displacement δ_t^* for inelastic behaviour, different expressions are used depending on the period T^* of the structure in relation to the corner period T_c of the plateau of the ADRS demand spectrum (Figure 14.4a,b).

- *Short period range (Figure 14.4a)*

$$T^* < T_c \tag{14.15}$$

In this case, if

$$S_a^* = \frac{F_y^*}{m^*} \geq S_e(T^*) \tag{14.16}$$

it means that the yield point of the capacity curve is higher than the corresponding elastic response spectrum, and therefore the response is elastic. Therefore,

$$\delta_t^* = \delta_{et}^* \tag{14.17}$$

Otherwise, if

$$S_a^* = \frac{F_y^*}{m^*} < S_e(T^*) \tag{14.18}$$

it means that the response is non-linear. Therefore (see Chapter 5, Equation 5.17),

$$\delta_t^* = \frac{\delta_{et}^*}{q_0}\left(1 + (q_0 - 1)\frac{T_c}{T}\right) \geq \delta_{et}^* \tag{14.19}$$

where

q_0 is the ratio between the acceleration of the structure with unlimited linear behaviour $S_e(T^*)$ and the structure with limited strength $F_y^*/m^* = S_a^*$, that is,

$$q_0 = \frac{S_e(T^*)}{S_a^*} = \frac{S_e(T^*)m^*}{F_y^*} \tag{14.20}$$

It is recommended that δ_t^* should be limited to values less than $3\delta_{et}^*$

- *Intermediate or long period*

$T^* > T_c$

In this case (Figure 14.4b):

$$\delta_t^* = \delta_{et}^* \tag{14.21}$$

Step 5. Global target displacement

Then, target displacement δ_t^* of the SDOF model is transformed to top target displacement of the MDOF model using the expression:

$$\delta_t = \Gamma\delta_t^* \tag{14.22}$$

This value is compared with δ_u (near collapse global displacement), that is,

$$\frac{\delta_u}{\delta_t} \geq \gamma_d \tag{14.23}$$

(see Paragraph 3.2.2.2, Equation 3.13)
where

γ_d is the safety factor in terms of displacements.

This factor is specified in EC8-1/2004 to 1.50, that is,

$$\frac{\delta_u}{\delta_t} \geq 150\% \tag{14.24}$$

Step 6. Local seismic demands

For the defined target displacement δ_t, the local deformation quantities (e.g. θ_{dem}) of the ductile members, and the local strength demands (V_{dem}, M_{dem}) of the brittle elements, as well, are determined using the output of the push-over analysis of the system.

Step 7. Performance evaluation

Having the target displacement δ_t as the output of the 'pushover' analysis completed at a previous step, performance evaluation is carried out at the level of global and local performance, as well, according to Code specifications. These specifications refer to

- *Global deformation performance* (e.g. $\delta_{target}/\delta_{collapse}$, global drift, distribution of the plastic hinges over the structure for the control of eventual premature collapse)
- *Local deformation performance for ductile members* (e.g. capacity rotation θ_u to rotation demand θ_p at the plastic hinges of the ductile members, inter-storey drifts, etc.)
- *Local strength performance for brittle members* (e.g. bending strength M_u to output moments for the target displacement or shear strength verification)

14.2.2.2 Capacity-spectrum method ATC 40-1996

This method was developed by the Applied Technology Council (ATC) in the framework of the 'Seismic Retrofit Practices Improvement Program' that was initiated by the 'Seismic Safety Commission of California'. It basically refers to R/C buildings. The steps for the implementation of this method maybe summarised as follows:

Step 1. Determination of the capacity curve of the MDOF model
This procedure is the same as that developed in the previous Paragraph 14.2.2.1.

Step 2. Equivalent SDOF model
The capacity curve of the MDOF system is transformed into the capacity curve of an equivalent SDOF model using the same procedure as in the previous Paragraph (14.2.2.1). The only difference from the previously presented method is that this capacity curve is not transformed further into an EPP diagram, but is used in the next step (Step 4) in a *bilinear form (BI)*, as it will be presented next.

Consider the capacity curve of an equivalent single-degree-of-freedom model transformed to a *capacity spectrum* in Figure 14.5. If the target displacement point were $a_{pl} - d_{pl}$, then the curve of the capacity spectrum could be transformed into a bilinear diagram of equivalent

E_D = Energy dissipated by damping
     = Area enclosed by hysteresis loop
     = Area of parallelogram

E_{So} = Maximum strain energy
     = Area of hatched triangle
     = $a_{pi}\, d_{pi}/2$

ζ_o = Equivalent viscous damping associated with full hysteresis loop area

     = $\dfrac{1}{4\pi} \dfrac{E_D}{E_{So}}$
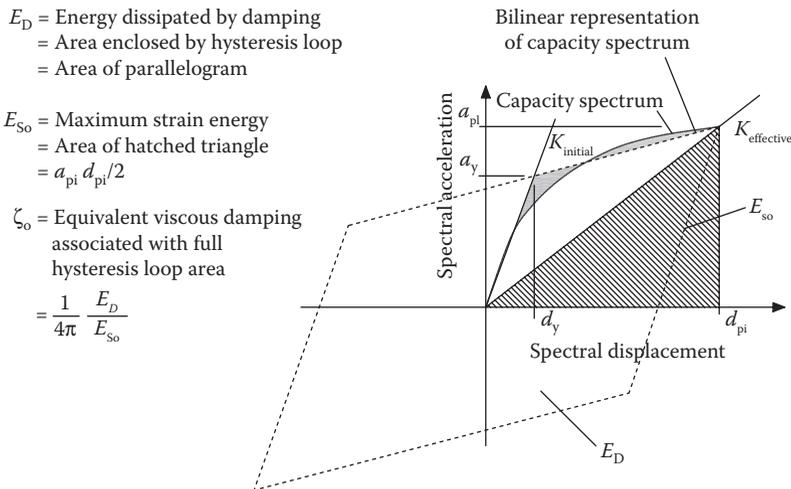
Figure 14.5 Derivation of damping for spectral reduction. (From ATC 40. 1996. *Seismic Evaluation and Retrofit of Concrete Buildings*. Applied Technology Council, Redwood City, California. With permission.)

energy dissipation, as shown in Figure 14.5. The damping that occurs when seismic action drives the structure to point $a_{pl} \boxtimes d_{pl}$ may be given as a combination of viscous damping equal to 0.05 for R/C structures and hysteretic damping ζ_o, that is:

$$\zeta_{eq} = 0.05 + \zeta_o \tag{14.25}$$

Hysteretic damping ζ_o may be given by the relation (see Subsection 2.3.3, Equation 2.38):

$$\zeta_o = \frac{1}{4\pi} \frac{E_D}{E_{SO}} \tag{14.26}$$

Values of ζ_{eq} may be taken from Table 14.1 (ATC 40-96) for various slope ratios $((a_{pl}/a_y) - 1)/(d_{pl}/d_y - 1)$ and ductilities d_{pl}/d_y. The notation above is explained in Figure 14.5.

Step 3. Demand spectra

A family of successive demand spectra is plotted, each for a given *damping ratio ζ* (Figure 14.6), in standard S_{ea} versus T format, following the same procedure as in the previous paragraph (14.2.2.1). Successive ARDS spectra may result, then, by combining the above spectra with a family of successive standard S_d (displacement) versus T spectra given by Equations 3.39, 3.40 and 3.41 (Paragraph 3.4.3.6; EC8-1/2004). The value of n in these equations is determined using the expression (see Chapter 3.4.3.4, Equation 3.33):

Table 14.1 Effective damping, ζ_{eff}, in per cent – structural behaviour type B

d_{pi}/d_y	Slope ratio: $[(a_{pi}/a_y) \boxtimes 1]/[(d_{pi}/d_y) \boxtimes 1]$						
	0.5	0.4	0.3	0.2	0.1	0.05	0
10	9	10	12	16	23	27	29
8	9	11	13	17	24	27	29
6	10	12	15	19	25	27	29
4	11	14	17	21	25	27	29
3	12	14	17	21	25	27	29
2	12	14	16	19	22	24	25
1.5	11	12	14	15	17	18	18
1.25	9	10	10	11	12	13	13

Source: From ATC 40. 1996. *Seismic Evaluation and Retrofit of Concrete Buildings.* Applied Technology Council, Redwood City, California. With permission.
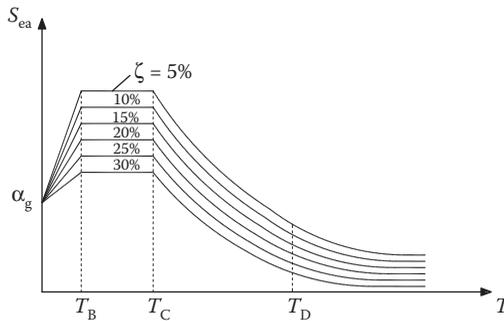
Figure 14.6 Family of demand spectra in standard S_{ea} versus T format.
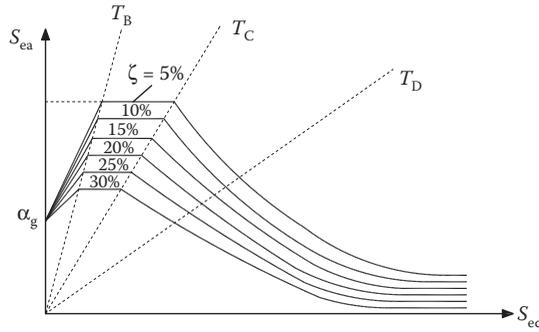
Figure 14.7 Family of demand spectra in ADRS format.
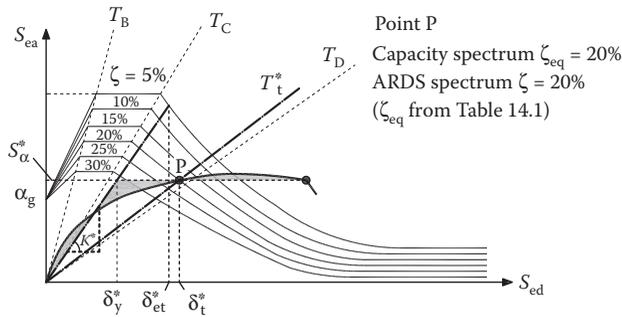
Figure 14.8 Determination of the target displacement implementing iterative procedure.

$$n = \sqrt{10/(5 + \zeta)} \le 0.55 \tag{14.27}$$

with ζ [%] values ranging from 5.0 (%) to 30 (%). A family of such spectra is depicted in Figure 14.7.

Step 4. Target displacement of the equivalent SDOF model

Demand spectra and the capacity spectrum are plotted on the same diagram (Figure 14.8). The intersection point of the capacity spectrum with a demand spectrum for which ζ_{eq} of the capacity spectrum is equal to the damping ζ of the demand spectrum presents the target displacement δ_t^* of the SDOF system. It is apparent that this point is determined by an iterative procedure.

Next steps for the determination of:

- Global target displacement
- Local seismic demands
- Performance evaluation

follow the same procedure as in the previous Paragraph 14.2.2.1.

14.2.2.3 Coefficient method/ASCE/SEI 41-06 (FEMA 356/2000)

This method was originally developed by ATC in the framework of the FEMA 273-274/1997 report of 'Guidelines for the Seismic Rehabilitation of Buildings'. Soon thereafter

the American Society of Civil Engineers (ASCE) prepared the FEMA 356/2000 report, which was later issued as a national standard (ASCE/SEI 41-06). This is the most often used method in practice, at least in the United States.

This method allows the estimate of the target displacement of the system by applying a series of approximate inelastic displacement modifiers (i.e. coefficients) to the *elastic spectral displacement* of the system.

According to this method, the target displacement δ_t, which corresponds to the displacement at roof level, can be estimated by the expression:

$$\delta_t = C_0 \cdot C_1 \cdot C_2 \cdot C_3 \cdot S_\alpha \frac{T_e^2}{4\pi^2} g \tag{14.28}$$

where

C_0 is the modification factor to relate spectral displacement of an equivalent SDOF system to the roof displacement of the building MDOF system. It can be calculated as developed in Paragraph 14.2.2.1 or it may be taken from Table 14.2 (FEMA 356).

C_1 is the modification factor to relate the expected maximum displacements of an *inelastic SDOF oscillator with EPP hysteretic properties to* displacements calculated for *the linear elastic response.*

$$C_1 = 1.0 \quad \text{for } T_e > T_c \tag{14.29a}$$

or

$$C_1 = \frac{1.0 + ((R - 1) / T_e)T_c}{R} \quad \text{for } T_e < T_c \tag{14.29b}$$

Values for C_1 need not exceed values:

$$C_1 = 1.50 \quad \text{for } T_e < 0.10 \text{ s} \tag{14.30}$$

$$C_1 = 1.0 \quad \text{for } T_e > T_c \text{ s} \tag{14.31}$$

In no case may C_1 be taken as less than 1.0.

T_c is the characteristic period corresponding to the end of the plateau of the elastic acceleration response spectrum (Chapter 3.4.3.3, Figure 3.16).

Table 14.2 Values for modification factor C_0[a]

| Number of stories | Shear buildings[b] | | Other buildings |
	Triangular load pattern (1.1, 1.2, 1.3)	Uniform load pattern (2.1)	Any load pattern
1	1.0	1.0	1.0
2	1.2	1.15	1.2
3	1.2	1.2	1.3
5	1.3	1.2	1.4
10+	1.3	1.2	1.5

Source: From FEMA 356. 2000. *Prestandard and Commentary for the Seismic Rehabilitation of Buildings*, Washington, DC. With permission.

[a] Linear interpolation shall be used to calculate intermediate values.
[b] Buildings in which, for all stories, interstorey drift decreases with increasing height.

Table 14.3 Values for modification factor C_2

Structural performance level	$T \leq 0.1\ s^a$		$T \geq T_S\ s^a$	
	Framing Type 1[b]	*Framing Type 2[c]*	*Framing Type 1[b]*	*Framing Type 2[c]*
Immediate occupancy	1.0	1.0	1.0	1.0
Life safety	1.3	1.0	1.1	1.0
Collapse prevention	1.5	1.0	1.2	1.0

Source: From FEMA 356. 2000. *Prestandard and Commentary for the Seismic Rehabilitation of Buildings*, Washington, DC. With permission.

[a] Linear interpolation shall be used for intermediate values of *T*.
[b] Structures in which more than 30% of the story shear at any level is resisted by any combination of the following components, elements or frames: ordinary moment-resisting frames, concentrically-braced frames, frames with partially-restrained connections, tension-only braces, unreinforced masonry walls, shear-critical, piers and spandrels of reinforced concrete or masonry.
[c] All frames not assigned to Framing Type 1.

T_e is the effective period of the structural system (Figure 14.1c). This means that the capacity curve of the MDOF system must have been determined before the estimate of the target displacement.

R is the ratio of elastic strength demand to calculated yield strength coefficient. See below for additional information.

C_2 is the modification factor to represent the effect of hysteresis shape on the maximum displacement response. Values for C_2 are given in Table 14.3 (FEMA 356).

C_3 is the modification factor to represent increased displacements due to dynamic p–Δ effects. For buildings with positive post-yield stiffness, it takes the value:

$$C_3 = 1.0 \tag{14.32}$$

S_α is the elastic response spectrum acceleration at the effective fundamental period T_e and damping ratio ζ for concrete 5.0%.

The strength ratio R is equal to

$$R = \frac{S_\alpha}{V_{by}/W} \cdot \frac{1}{C_0} = \frac{q_o}{C_0} \tag{14.33}$$

where
V_{by} is the yield strength of the MDOF system (Figure 14.1c).
W is the total gravity loads that have been taken into account for the deformation of inertial seismic forces.

14.2.2.4 Direct displacement-based design

This method has been developed in the last 25 years (Moehle, 1987) and it is still in progress. Basically, it aims at mitigating the deficiencies in the current force-based design of *new buildings*. It is based on the substitution of an MDOF building by the equivalent SDOF model already presented in Paragraph 14.2.2.1 and the use of displacement design spectra developed for various levels of damping. Below, this method, which is presented in detail elsewhere (Priestley et al., 2007), will be presented in concept.

The method is illustrated in Figure 14.9. A multi-storey building is replaced by an SDOF model (Figure 14.9a). The capacity curve of the SDOF model is transformed to a bilinear elastic–plastic diagram for a predefined displacement (target displacement) δ_t (Figure 14.9b). Therefore, the ductility demand μ_D of the model is predefined. For this ductility, μ_D, the
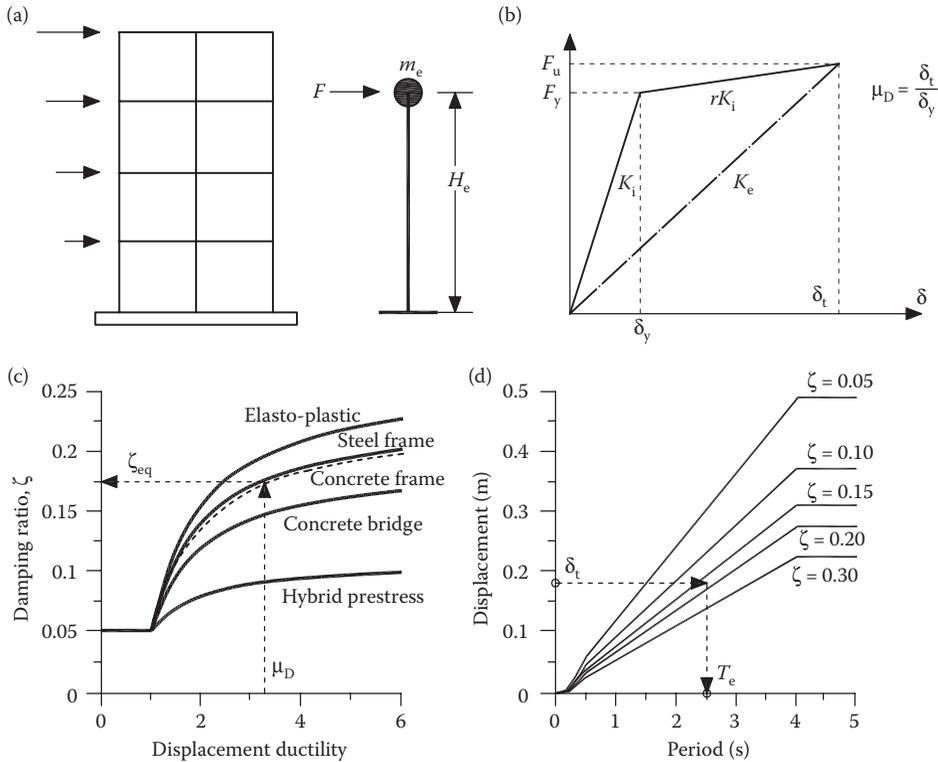
Figure 14.9 Fundamentals of direct displacement-based design. (a) SDOF simulation; (b) Effective stiffness K_C; (c) Equivalent damping vs. ductility; (d) Design displacement spectra. (From Preistley, M.J., Calvi, G.M. and Kowalsky, M.J. 2007. *Displacement-Based Seismic Design of Structures*. IUSS Press, Pavia. With permission.)

corresponding damping ratio ζ_{eq} is determined based on existing relations between the ductility μ_D and damping ratio ζ_{eq} (see Chapter 2.3.3, Equation 2.45, Figure 14.9c).

For the damping ratio determined above, and using displacement spectra directly (e.g. the displacement spectra of EC8-1/2004), the effective period T_e may be determined (Figure 14.9d). Thereafter, using the well-known equation:

$$K_e = 4\pi^2 m^* / T_e^2 \tag{14.34}$$

the effective stiffness K_e of the SDOF model may also be determined. So, the base shear of the SDOF model is given by the relaton:

$$V_{base} = F_u = K_e \delta_t \tag{14.35}$$

Base shear of the SDOF model is then transformed into the corresponding base shear of the MDOF structure. This value is distributed between the mass elements of the real structure as inertial forces, and then the structure is analysed for these forces to determine the design moments at locations of potential plastic hinges.

From what has been presented so far, the above method more or less follows the same steps as N2 and capacity-spectrum methods with some modifications relating, mainly, to the direct introduction of the displacement design spectra versus period T elaborated for various damping ratios (see Paragraph 14.2.2.2).

The main question is how to define a series of the structural information necessary for the assessment of the base shear V_b of the building before it has been designed and detailed.

In particular, the following structural information is needed:

- The design displacement δ_t (target displacement)
- Displacement eigen modes
- Yield displacement δ_y
- Effective height H_e
- Distribution of the design-base shear

Thus, the main contribution of this method is the systematic elaboration of methodologies for the determination of the above-noted necessary information for various types of structures, taking into account their overall behaviour from the elastic range to collapse. More particularly, this information is given for:

- Frame buildings
- Structural wall buildings
- Dual systems
- Masonry buildings
- Timber buildings
- Structures with isolation

The scope of this book does not allow for further development, for which a detailed presentation is made in the book *Displacement-Based Seismic Design of Structures* (Priestley et al., 2007).

14.2.2.5 Concluding remarks

From what has been presented thus far, the following conclusions may be drawn:

1. Methods N2 and Capacity-Spectrum are quite similar
   a. They use the capacity curve of the MDOF system.
   b. They transform this curve and all relevant mechanical properties of the system into those of an SDOF model.
   c. They both use ADRS demand spectra in the form of a family of curves, the N2 method for successive ductilities μ_B and the capacity-spectrum for successive damping ratios ζ.
   d. The capacity-spectrum method makes use of the demand and the capacity spectra of the SDOF model plotted on the same diagram for the iterative estimate of the target displacement of the equivalent SDOF model.
   e. The N2 method, simplifying the capacity-spectrum of the SDOF to an EPP-equivalent diagram, makes possible the direct determination of the target displacement. In this context it must be considered a more simplified method for easy computer programming.
   f. From that point on (determination of target displacement of the SDOF model), they both follow the same procedure for the quantitative evaluation of the MDOF system.
2. The 'Coefficient Method' seems to be the most easily applicable in practice and computerised for the following reasons:
   a. After the elaboration or the capacity curve of the MDOF system there is no need to transfer the procedure to an equivalent SDOF system.

   b. Target displacement is determined using a direct method of coefficients without any iterative procedure.
3. In the last 10 years, extended efforts have been made for the evaluation of the above methods, and for their improvement on the basis of extended inelastic dynamic analyses, which are used, as is well known, as a benchmark. It is worth referring, at this point, to the FEMA 440/2005 publication 'Static Seismic Analysis Procedures' (FEMA 440, 2005) and to the National Institute of Standards and Technology (NIST) GCR 10-917-9/2010 publication on the 'Applicability of MDOF Modeling for Design' (NIST GCR 10-917-9/2010, 2010).
4. Displacement-based design may also be used for new buildings. From what has been presented so far, the building must have been analysed, dimensioned and detailed using the traditional codified procedures, so that all necessary input for the nonelastic static analysis has been set down. In this context, the already designed new building may be evaluated for the following purposes:
   a. To verify or revise the overstrength ratio values α_u/α_1 (see Subsection 5.4.3).
   b. To estimate the expected plastic mechanisms and distribution of damage.
   c. As an alternative to the design based on linear-elastic analysis, which uses the behaviour factor q. In this case, the q-factor is verified using the target displacement and the capacity curve of the MDOF model (Figure 14.1c).
5. Finally, it should be noted that significant efforts have been recently made for the development of a DDBD of new buildings without a previous force-based design, as specified by contemporary Codes (Priestley et al., 2007). It is the author's opinion that this is a very promising approach to the seismic design of structures, with high prospects for further development at the level of applications in codified form.

14.3 SCOPE OF THE DETAILED SEISMIC ASSESSMENT AND REHABILITATION OF R/C BUILDINGS

After the detailed presentation in the previous section (Section 14.2) of the basic procedure for a quantitative seismic assessment of an existing building and for redesign of its rehabilitated form in the case that an intervention has been decided upon, it is necessary to give in concept the scope of seismic assessment and rehabilitation. This scope is described in EC8-3/2005 as follows:

- Provide criteria for the seismic performance of existing individual R/C buildings.
- Describe procedures for the selection of necessary corrective measures.
- Display methods and procedures for structural analysis and design, taking into account the corrective measures that have been chosen.
- Examine the degree of uncertainty of the partial safety factors of materials, taking into account that R/C buildings have been built in various periods in the past and probably contain hidden malfunctions. In this respect, the introduction of *confidence factors* (CFs) should be examined, in addition to the original partial safety factors.

In closing, it should be noted that in the case of listed (historical) R/C buildings, these may be assessed and retrofitted using the framework that will be presented below; however, additional considerations have to be taken into account, having to do with the obligation for retaining the authenticity of the building and avoiding the falsifying of its original characteristics. All these rules are included in restoration charts (e.g. Chart of Venice) and are beyond the scope of this book.

14.4 PERFORMANCE REQUIREMENTS AND COMPLIANCE CRITERIA

14.4.1 Performance requirements

Performance levels introduced in EC8-3/2005 do not comply with those introduced for new R/C buildings in EC8-1/2004. Rather, they are much closer to performance levels in effect in US codes and guidelines (FEMA 273-274/1997, FEMA 356/2000). They are characterised as limit states and are listed below:

- *LS of Near Collapse (NC).* The structure is heavily damaged with low residual lateral strength and stiffness.
- *LS of Significant Damage (SD).* The structure is significantly damaged with some residual lateral strength and stiffness.
- *LS of Damage Limitation (DL).* The structural system is only lightly damaged, with structural elements kept below or at the limit of yielding.

Detailed relations between limit states and structural damage are given in Table 14.4 (Elnashai and Di Sarno, 2008).

The appropriate levels of protection are achieved by selecting for each of the limit states a return period for the seismic action. Values recommended by EC8-3/2005 are given below:

- *For NC*: 2475 years return period (2% probability of exceedance in 50 years); very rare earthquake, equal to 150% of design seismic action (DSA) earthquake.
- *For SD*: 475 years return period (10% probability of exceedance in 50 years); rare earthquake DSA.
- *For DL*: 225 years return period (20% probability of exceedance in 50 years); occasional earthquake, equal to 70% of DSA earthquake.

The above presented performance levels and the relevant seismic excitation levels are coupled in the matrix of Figure 14.10). The above return periods of the seismic action are given in the form of a note in EC8-3/2005 as 'recommended values'.

The authors agree with the position of Professor Fardis on this issue (Fardis, 2009), namely that this return period of DL is very high, near to DSA, and therefore may prevail in design. Therefore, this level should be decreased in NA to the level of 95 years, that is, to a

Table 14.4 Correlation of engineering limit states and performance levels

Engineering limit states	Performance levels		
	Damage limitation	Significant damage	Near collapse
Cracking	▒		
First yielding	▒		
Spalling		▒	
Plastification		▒	
Local buckling		▒	
Crushing			▒
Fracture/fatigue			▒
Global buckling			▒
Residual drift			▒

Source: Adapted from Elnashai, A.S. and Di Sarno, L. 2008. *Fundamentals of Earthquake Engineering*, Wiley, West Sussex, UK.

Note: Main symptoms at each limit state are in grey boxes.
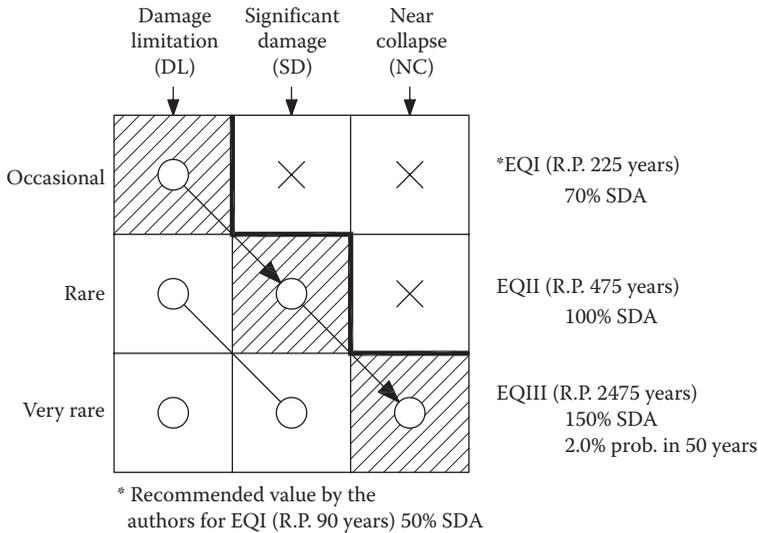
Figure 14.10 Relationship between performance level and earthquake design level (according to EC8-3/2005).

seismic action equal to 50% of DSA, and in this respect to coincide with the DL of new R/C buildings specified in EC8-1/2004.

If this change is introduced in the matrix of Figure 14.10, then the relevant matrices of parts 1 and 3 of EC8 take the same form (cf. Figure 3.24 with Figure 14.10).

In addition, it should be noted that the limit state of *no (local) collapse* requirement of EC 8-1 corresponds to the limit state of *SD,* and both correspond to *Life Safety* level of FEMA 273-274/1997 (FEMA 356/2000).

The limit states of EC8-3/2005 correspond to the following levels of the diagram of Figure 3.22:

- *LS of NC*: Level 4
- *LS of SD*: Level 3
- *LS of DL*: Level 2 or Level 1

depending on the adopted return period.

In closing, it should be noted that EC8-3/2005 allows the national authorities of each member state to decide whether all three limit states should be checked or two of them or just one of them. It is the author's opinion that the limit states of DL and of SD should be the two obligatory limit states, so that the procedure of assessment and rehabilitation complies with that of the design of new R/C buildings.

14.4.2 Compliance criteria

14.4.2.1 Seismic actions

1. For all methods of analysis except that of the *q*-factor method, *elastic response spectra* are introduced, that is, spectra not reduced by *q*-factor.
2. For the *q*-factor method, the design spectra in use for new buildings, which are elastic acceleration response spectra reduced by the *q*-factor, are also used for existing ones.

14.4.2.2 Safety verification of structural members

1. A distinction is made between *'ductile'* and *'brittle'* elements (see Paragraph 14.2.2.1, Figure 14.1b).
2. For all methods of analysis except the *q*-factor method, the safety verifications are carried out according to the following procedure:
   a. For 'ductile' elements, safety is verified by checking that demands do not exceed the corresponding capacities in terms of deformation (Figure 14.1b).
   b. For 'brittle' elements, the above verifications are carried out *in terms of strength* (Figure 14.1b).
3. For the *q*-factor method, the safety verification is carried out for all types of elements *in terms of strength,* as in the case of new buildings, with some additional measures that will be examined later.

14.4.2.3 'Primary' and 'secondary' seismic elements

Some of the existing structural elements may be designated as *'secondary seismic elements',* like those of new buildings. These elements are verified with the same compliance criteria as primary ones, but using less conservative estimates of their capacity than for the 'primary' ones.

  The introduction of the concept of 'secondary' seismic elements is particularly significant for rehabilitation procedures, because it allows the designer to limit the intervention only to a number of vertical elements, and therefore to decrease the extent of the rehabilitation.

14.4.2.4 Limit state of NC

1. Analysis may be carried out using any elastic or non-elastic method of analysis, except the *q*-factor method, which is considered to be unsuitable for this limit state. The reason is obvious, since the *q*-factor method has been developed for new buildings (EC8-1/2004) for the ultimate limit state compliance criterion, which for existing buildings corresponds to the SD limit state (Figure 14.10) and not to the NC limit state.
2. Seismic action for which the analysis of this level must be carried out is *150% of the seismic actions for DSA of EC8-1/2004* corresponding to the ultimate limit state.
3. Demands will be based on the results of the analysis for the above seismic actions.
4. Capacities will be based on proper ultimate deformations for ductile elements and on ultimate strengths for brittle ones.

14.4.2.5 Limit state of SD

1. As explained previously, this limit state corresponds to the ultimate limit state of new buildings. Therefore, the seismic action for which the analysis of this level will be carried out is that of EC 8-1/2004 for the ultimate limit state of new buildings.
2. This limit state is the most important, as it corresponds to the ultimate limit state of new buildings and to the 'Life Safety' of the U.S. codes. *Therefore, verifications based on this limit state must be considered obligatory.*
3. All methods of analysis may be used, including the *q*-factor method approach. However, a critical point is the value of the *q*-factor that is introduced in the design, since the design and detailing of existing buildings usually do not comply with the specifications of modern seismic Codes.
4. Except when using the *q*-factor approach, capacities will be based on damage-related deformations for ductile elements and on strengths for brittle ones.

5. In the *q*-factor method, demands shall be based on the seismic actions reduced by *q*. Capacity verifications in this case will be made in *strength terms,* no matter if the members are ductile or brittle.

14.4.2.6 Limit state of DL

1. Analysis may be carried out using any one of the accepted methods (elastic, inelastic, *q*-factor approach).
2. Seismic actions for this limit state must be considered at 50% of DSA of EC8-1/2004 corresponding to ultimate limit state. This seismic action corresponds, as known, to the level of 95 years of return period.
3. Except when using *q*-factor capacities, it should be based *on yield strengths* either for ductile or brittle members. Capacities of infills must be based on mean inter-storey drift capacity of the infills.
4. In the case of the *q*-factor approach, demands and capacities will refer to mean inter-storey drift.

14.5 INFORMATION FOR STRUCTURAL ASSESSMENT

14.5.1 General

The selection and evaluation of input data necessary for quantitative seismic assessment of an R/C building may be considered the most significant part of the assessment procedure. For this reason, all modern codes of quantitative evaluation of buildings pay special attention to this issue, since all subsequent steps of evaluation are based on this information. Besides keeping in mind that the level of knowledge of this information cannot always be equally reliable, Codes usually introduce in codified form three *knowledge levels* for the building under examination and thereafter relevant *CFs*, increasing the partial safety factors of materials.

At the same time, the selection and evaluation of input data constitutes the bigger part of the assessment cost, as will be clear from the presentation below.

Eurocode 8-3/2005 specifies in detail the procedure for the selection of information and for the validation of the knowledge level. The input data according to EC8-3/2005 will be collected from a variety of sources, including:

- Available documentation of the building (e.g. structural drawings, structural analyses, technical reports referring to the structure and the soil, etc.).
- Relevant generic data sources (e.g. Codes and standards contemporary with the time of the building design).
- Field investigations (e.g. survey of the geometry of the structural system, arrangement of reinforcement detailing, etc.).
- *In situ* and laboratory measurements and tests (destructive and non-destructive tests of concrete and steel, soil investigations, etc.).

14.5.2 Required input data

The information for structural evaluation must basically cover the following issues:

14.5.2.1 Geometry of the structural system

This information is collected from the existing structural drawings of the building under evaluation (formwork drawings). This information must be cross-checked by *in situ* survey

of the main critical general dimensions and of the crucial cross-sections as well (e.g. large spans, column cross-sections, main beams, shear walls, etc.).

In the case that the structural drawings cannot be found, which is a very usual case for buildings of the past, a detailed survey must be carried out so that new formwork drawings of the structural system of the building can be elaborated on, accompanied by proper detail drawings. It is obvious that in order for such an effort to be reliable, scaffoldings must be erected and plasters and finishes at various critical positions must be removed so that the structural engineer in charge is in a position to identify the structural system and the credibility of the survey.

Special concern must be given to the foundation of the building. In the case that the structural drawings are available, limited local excavations should be carried out just for a cross-check on the existing drawings. Otherwise, these excavations should be extended to the degree that using a back analysis (see below) the foundation layout may be at least estimated. Infill masonry should also be surveyed.

In the case of a post-earthquake quantitative assessment, a detailed survey of damage at structural elements and infill masonry should be carried out, accompanied by sketches and illustrations. Damage pattern in post-earthquake cases constitutes a high-level tool for the structural system identification, that is, the assessment that will follow must be in a position to justify the damage pattern in order to be considered a reliable result.

14.5.2.2 Detailing

This includes the number of bars in the cross-section and their arrangement in the structural members (longitudinal and stirrup reinforcement, rebar overlapping) and reinforcement detailing in the joints.

This information is collected basically from the existing structural drawings (i.e. general reinforcement drawings, detailing drawings, barbending schedules, etc.). This information must be cross-checked with *in situ* investigation using destructive (DT) or non-destructive (NDT) tests at selected critical positions. If the *in situ* findings do not comply with the existing drawing information, then a statistical evaluation of the total information must be carried out based on the information collected by the *in situ* investigations.

In the case that the reinforcement drawings cannot be found, an extended investigation procedure is necessary, destructive and non-destructive, at a statistically reliable number of critical positions.

Of course, these data cannot cover all of the structural system, for which reinforcement detail is necessary for a quantitative assessment. So, a back analysis of the structural system must be carried out according to the Codes in effect at the time of original design, and the reinforcement output must be cross checked against the *in situ* findings. This is a time-consuming job and must be accompanied by a statistical elaboration of the back-analysis results based on the *in situ* findings.

This procedure has been implemented extensively by the authors at the complex of buildings of the Army Pension Fund in Athens, Greece, a complex of nine structurally independent eight-storey buildings with a total useful surface of 80.000 m² (Figure 14.11). For this complex, designed and constructed between 1930 and 1939, fewer than 35% of the structural drawings were found, and therefore an extended investigation program was needed for the quantitative evaluation and retrofitting of the complex (Penelis and Penelis, 2001).

14.5.2.3 Materials

Points of reference for the materials (concrete-steel) that were used for the construction of a building are the structural drawings – if they exist – because, as usual, the specifications

Figure 14.11 Complex of buildings of the army pension fund in Athens Greece.

for the materials in use have been clearly defined on them for many decades past. However, an extended investigation on the construction materials (steel-concrete) must be carried out using *in situ* non-destructive tests (hammer tests, ultrasonic tests, electromagnetic detectors, etc.; Figures 14.12, 14.13) and cross-checked by destructive ones (Figure 14.14; core-taking, rebar extraction for tests, etc.) executed in the lab.

Figure 14.12 Hammer tests at MELISSARI Complex (Thessaloniki).

Figure 14.13 Electromagnetic steel detecting (MELISSARI Complex, Thessaloniki).

It should be noted that on the core samples carbonation tests should be also carried out for checking the degree of rebar protection against corrosion, particularly in older buildings. This information is very important in the case that rehabilitation is planned, which will undoubtedly prolong the life of the structure and will upgrade its operational status. It should also be noted that the hammer testing results on old concrete surfaces may mislead

Figure 14.14 Core taking (Papanikolaou Hospital, Thessaloniki).

the engineer in charge to wrong conclusions, since carbonation hardens the concrete and in this respect increases the strength indication of the equipment. Therefore, in this case, hammer testing must always be accompanied by a core taking test so that hammer testing results may be reduced properly.

In order to give a sense of the extent of an investigation program for materials, we note that in the case study of the Pension Army Fund Complex in Athens, to which reference was made above, the material tests included (Penelis and Penelis, 2001):

- NDT
  - Schmidt hammer testing: 320 test groups
  - Steel detecting: 300 positions
- DT
  - Core taking of 400 cores
  - Dismantling of rebars at R/C members: 600 positions
  - Bore holes for soil investigation: 3

14.5.2.4 Other input data not related to the structural system

In addition to the above three categories of input data that are related exclusively to the structural system, a series of input data must be clarified, that is:

- Ground conditions
  - Geotechnical soil properties based on bore holes and laboratory or *in situ* tests
  - Classification of the ground conditions as categorised in EC 8-1/2004
  - Information on the seismic design criteria used in the original design. This information is necessary for an eventual back-analysis as mentioned above
- Description of the present and the planned use of the building. This information will include:
  - Changes in dead loads (partition walls, floors, etc.)
  - Changes in live loads (change of the use of the building, for example, from residence to department store)
  - Changes in the importance class

14.5.3 Knowledge levels and confidence factors

For the purpose of choosing the *admissible type of analysis* and the appropriate *CF values*, EC8-3/2005, like the relevant U.S. Code, classifies knowledge about the structural system of the existing building into *three levels*, that is:

- *KL1*: Limited knowledge
- *KL2*: Normal knowledge
- *KL3*: Full knowledge

The factors determining the appropriate knowledge level focus on:

- Geometry
- Details
- Materials

Table 14.5 Knowledge levels and corresponding methods of analysis (LF: lateral force procedure, MRS: modal response spectrum analysis) and confidence factors (CF)

Knowledge level	Geometry	Details	Materials	Analysis	CF
KL1		Simulated design in accordance with relevant practice *and* from *limited in-situ* inspection	Default values in accordance with standards of the time of construction *and* from *limited in-situ* testing	LF-MRS	CF_{KL1}
KL2	From original outline construction drawings with sample *visual* survey *or* from *full* survey	From incomplete original detailed construction drawings with *limited in-situ* inspection *or* from *extended in-situ* inspection	From original design specifications with *limited in-situ* testing *or* from *extended in-situ* testing	All	CF_{KL2}
KL3		From original detailed construction drawings with *limited in-situ* inspection *or* from *comprehensive in-situ* inspection	From original test reports with *limited in-situ* testing *or* from *comprehensive in-situ* testing	All	CF_{KL3}

Source: From EC8-3/2005. *Design of Structures for Earthquake Resistance. Part 3: Assessment and Retrofitting* of Buildings. European Committee for Standardization, BSI, CEN, Brussels. With permission.

Note: The values ascribed to the confidence factors to be used in a country may be found in its National Annex. The recommended values are $CF_{KL1} = 1.35$, $CF_{KL2} = 1.20$, $CF_{KL3} = 1.00$.

that is, the input data relating to the structural system of the building. EC8-3/2005 specifies rules in a descriptive form for this classification. At the same time, it recommends the extent of inspections, details, and testing of materials for each type of primary element (beams, columns, walls) that should be carried out for each knowledge level (see Table 14.5). The knowledge level adopted determines:

- The admissible method of analysis, and
- The CFs

The above relation, along with the values recommended by EC8-3/2005, is given in Table 14.5. Confidence factors are used as *denominators* for the determination of the material properties to be used in the calculation of the force capacity (strength), when capacity is to be compared with demand for safety verification. As *nominators* in the above relations, the mean values obtained from *in situ* or laboratory tests will be used. In other words, in the case of existing buildings *the mean values of in situ*-defined strengths play the role of characteristic strength, and the CFs play the role of partial safety factors of materials for new buildings.

14.6 QUANTITATIVE ASSESSMENT OF SEISMIC CAPACITY

14.6.1 General

Assessment is a quantitative procedure for checking whether an existing undamaged or damaged R/C building will satisfy the required limit state appropriate to the seismic actions under consideration (see Subsections 14.4.1 and 14.4.2).

This procedure includes:

1. Selection of seismic actions
2. Structural modelling
3. Structural analysis
4. Safety verification

These issues will be examined in detail below.

14.6.2 Seismic actions

For all admissible methods of analysis—except that of the *q*-factor procedure—no matter if they are based on elastic or non-elastic models, *the elastic response spectra* of EC8-1/2004 are used *without any reduction by a q-factor.*

In the case of the *q-factor approach*, the *design factors* of EC8-1/2004 are used with a q_o-factor for R/C buildings equal to 1.50:

$$q_o = 1.50 \tag{14.36}$$

However, higher values of *q* may be adopted if this could be justified in reference with the local and global available ductility. This may be accomplished with a sufficient accuracy if a pushover analysis of the structural system is carried out. Alternatively, as will be explained next, simplified approximate methods may be used for the determination of the *q*-factor of the structural system (Tassios, 2009).

What is specified by EC8-1/2004 for new buildings also holds for load combinations in the case of retrofitting.

14.6.3 Structural modelling

Structural modelling is based on the input data information presented in a previous subsection. For the material properties, the *mean values* of the data that have been determined are used. All provisions of EC 8-1/2004 regarding modelling and accidental torsional effects may be applied here, also without modification.

The strength and stiffness of secondary seismic elements against lateral actions may in general be neglected in the analysis. However, in no case could the selection of secondary elements be made in such a way that the irregularities of the structure disappear.

In the case of post-earthquake assessment, special care should be paid to the evaluation of the residual stiffness and strength of damaged structural members (Tassios, 2009).

14.6.4 Methods of analysis

14.6.4.1 *General*

Seismic action effects may be evaluated using one of the following methods:

- Lateral force (LF) analysis (linear)
- Multi-modal response spectrum (MRS) analysis (linear)
- Non-linear static (push-over) analysis
- Non-linear time-history dynamic analysis
- *q*-factor approach

It should be noted that the most easily applicable of the above methods are the non-linear static (pushover) analysis and the *q*-factor approach, since both may be implemented directly without the risk that by the end of the analysis the method that has been implemented is prohibited for the particular structural system (see the following paragraphs).

14.6.4.2 Lateral force elastic analysis

Conditions for the applicability of this method according to EC 8-1/2004 have been presented in Subsection 5.6.4.

These conditions aim at ensuring a smooth fundamental eigen mode and a limited influence of the higher eigen modes, so that an inverted triangular load distribution results in reliable seismic load effects. In this context, regularity in elevation and limited value of the fundamental period *T* constitute the conditions for applicability of this method. In addition to the above conditions, a further one is specified for the applicability of the method to existing buildings. The aim of this new *basic condition* is ensuring that the inelastic deformations at the plastic joints are distributed smoothly throughout the structural system, so that local or storey chord plastic deformations (inter-storey drifts) do not present serious irregularities in relation to the overall structural deformation (Figure 14.15).

The above additional condition is quantified as follows:

1. The structural system is analysed using the lateral force method according to what has been presented in Chapter 5.6.4 for a base shear V_b, resulting from the codified *elastic response* acceleration spectrum (without any reduction due to *q*-factor).
2. For each member *i* of the system under bending, the *demand* D_i in terms of strength is determined (M_{iD}, N_{iD}) from the preceding analysis. At the same time, the capacity C_i of the member is determined, that is, the bending moment M_{iR} for an axial load equal to N_{iD}.
3. For the ends of each member, the magnitudes:

$$\rho_i = \frac{D_i}{C_i} \tag{14.37}$$

are computed. The above value ρ_i indicates approximately the *ductility demand* μ_D at each critical region (see Figure 14.16). Usually μ_D resulting from the above procedure is higher than 1.0, since the analysis has been carried out for the elastic base shear, which is 3.0–4.0 times higher than the design base shear, for which the *q*-factor has been taken into account at the derivation of the design acceleration response spectrum. If, for example, this demand is very high at a soft storey in relation to the other storeys
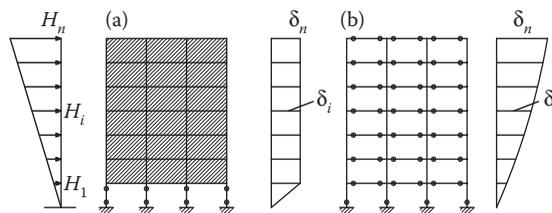
Figure 14.15 Storey displacements under a triangular lateral loading (a) irregular distribution of inter-storey drifts due to masonry infills (generation of a soft storey); (b) regular distribution of inter-storey drifts in the case of a frame with strong columns-weak beams.
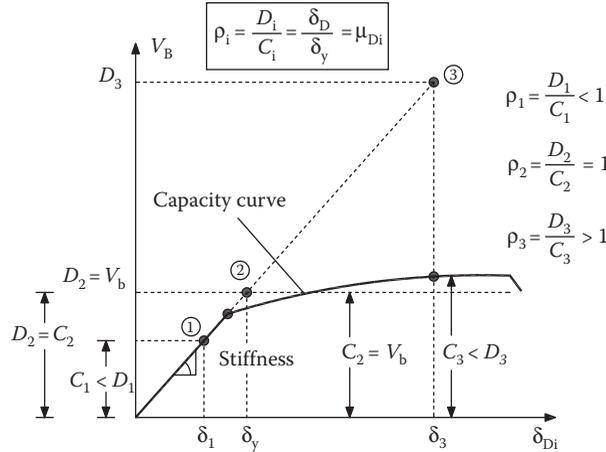
Figure 14.16 Concept for the lateral force elastic analysis.

(Figure 14.5), it is obvious that the fundamental eigen mode, at the inelastic stage, stops being a smooth inverted triangle, and so the lateral load distribution assumed in the analysis is no longer valid. Therefore, the method is not permitted to be used for the analysis.

4. From the above members, those for which:

$$\rho_i < 1.0 \qquad (14.38)$$

it is anticipated that even for the target displacement expressed by the ρ_{imax} (Figure 14.16), they remain in the elastic region and therefore do not contribute to the plastic deformation of the system.

For those for which

$$\rho_i > 1.0 \qquad (14.39)$$

it is anticipated that they enter in the plastic region. Among them ρ_{imax} and ρ_{imin} (>1.0) are selected, and the ratio ρ_{imax}/ρ_{imin} is determined. If

$$\boxed{\frac{\rho_{imax}}{\rho_{imin}} \leq 2.5 \quad \text{(recommended value)}} \qquad (14.40)$$

the use of the method is permitted. It should be noted that the ratio $\rho_i = D_i/C_i$ may be replaced by the ratio of the reinforcement demand A_{siD} in the tensile zone to the available reinforcement A_{siav} at the same zone of the cross-section, that is,

$$D_i/C_i \cong A_{siD}/A_{siav} \qquad (14.41)$$

The above acceptability criterion requires that the structural system will be first analysed, the ratios ρ_i will be determined, and then a decision will be made if the method is acceptable or not.

In closing, it should be clarified that the above procedure is a criterion for the acceptance of the method and has nothing to do with the *safety verification procedure* to which reference will be made later.

14.6.4.3 Multi-modal response spectrum analysis

The conditions of the applicability of this method have been given in Subsection 5.6.5. In addition, the condition above (Equation 14.40) for the ratio of ρ_{imax}/ρ_{imin} must also be in effect.

It must also be remembered here that the seismic input for this method is the *elastic* acceleration response spectrum and not the design spectrum, which is reduced by the *q*-factor.

14.6.4.4 Non-linear static analysis

14.6.4.4.1 General

Non-linear static (pushover) analysis has already been presented in Subsection 5.7.3, while the use of this method for the seismic assessment of the structural response of a building has been set forth in detail in Section 14.2.2.

As is well known, it is a non-linear static analysis under constant gravity loads and monotonically increasing loads.

14.6.4.4.2 Lateral loads

As was mentioned and explained in Subsection 14.2.2, at least two vertical distributions of lateral loads should be applied (Figure 14.1a).

- A 'uniform' pattern, based on lateral forces that are proportional to mass distribution at height.
- A 'triangular' pattern corresponding to the fundamental eigen mode of the structural system.

These two patterns of lateral forces are applied at the centres of masses of the storeys.

At the same time, accidental eccentricities should be taken into account, as was presented for new buildings ($e_{xi}, e_{yi} = 5\% L_x, L_y$). These patterns of lateral loads are applied successively in two main directions perpendicular to each other, as in the case of new buildings.

14.6.4.4.3 Capacity curve – target displacement – torsional effects

As explained in Subsection 14.2.2, the relation between base shear and the displacement at a control point at the roof results in the capacity curve of the system. The control displacement is taken *at the centre of mass at the top storey* of the building. It is obvious that for each lateral load pattern two such capacity curves are generated, one for each main direction of the building. The target displacement is defined following one of the procedures presented in Subsection 14.2.2.

Pushover analysis performed with the force patterns presented above may significantly underestimate deformations at the stiff/strong side of a *torsionally flexible structure*. In fact, the static approach to the eccentricities between the centre of mass and the centre of rigidity (see Sections 2.4.4 and 5.3) underestimates the torsional deformations φ_i of the space structural system, *even in the case of elastic static analysis*, in comparison with the corresponding multimodal response spectrum analysis (dynamic amplification of torsional deformations).

For such structures, EC 8-1/2004 specifies that displacements at the stiff/strong side should be increased by applying an *amplification factor* to the displacements of the stiff/strong side based on the results of an elastic modal analysis of the spatial model, meaning that the amplification factor for the inelastic static response would result in the ratio $\varphi_{idynamic}/\varphi_{istatic}$ of the elastic system.

It is apparent that this procedure requires:

- Non-linear static analysis
- Linear static analysis
- Multimodal response spectrum analysis

for the determination of the amplification factors for each direction at the stiff/strong side of the structural system. During the past 10 years efforts have been made for a reliable simulation of the torsional effects on spatial systems designed by means of non-linear static analysis. One of them, developed by the authors, has already been presented in Paragraph 5.7.5.2 (Penelis and Kappos, 2005; Penelis and Papanikolaou, 2010).

14.6.4.5 Non-linear time–history analysis

The procedure developed for new buildings in Subsections 2.5.2 and 5.7.6 may also be implemented for the assessment of existing buildings. It should be remembered, however, that this procedure is proper only for the evaluation of all the others and the results are used as benchmarks for such evaluations.

14.6.4.6 The q-factor approach

The *q*-factor approach, as is well known, is the "reference method" of the design of new buildings adopted by EC 8-1/2004 and the relevant U.S. standards. This has been presented in detail in Chapters 2 through 10 of this book, and in the same way it is also implemented for the seismic assessment of existing buildings.

Taking into account that the global and the local ductility of an existing building is not controlled by rules that are taken into account in the design of new buildings, for existing R/C buildings EC8-3/2005 specifies a low value of *q*-factor equal to

$$q = 1.50 \tag{14.42}$$

It has already been explained in Subsection 5.4.3 that this value corresponds to R/C buildings designed according to Codes for conventional R/C structures.

However, as noted above, higher values of *q* may be adopted if they were suitably justified with reference to the local and global available ductility. This justification may be based either on approximate procedures (Tassios, 2009) or on the implementation of a push-over procedure up to failure (δ_u) for the generation of the capacity curve of the system.

From this curve, the upper limit of available ductility $\mu_{\alpha v}$ is easily determined (Figure 14.17) by the expression:

$$\mu_{\alpha v} \cong \frac{\delta_{u,\alpha v}}{1.50\delta_y} \tag{14.43}$$

Keeping in mind that there is a direct relation between $\mu_{\alpha v}$ and $q_{\alpha v}$ (e.g. for $T_1 > T_C$, $q = \mu$), it follows that the *q*-factor can then be determined very easily (Figure 14.17).

From this point on, the *q*-factor approach is implemented as in the case of new buildings.

$$\mu_{av} = \frac{\delta_{u,av}}{1.5\,\delta_y} \cong q_{av} \geq q_{\text{demand}}$$
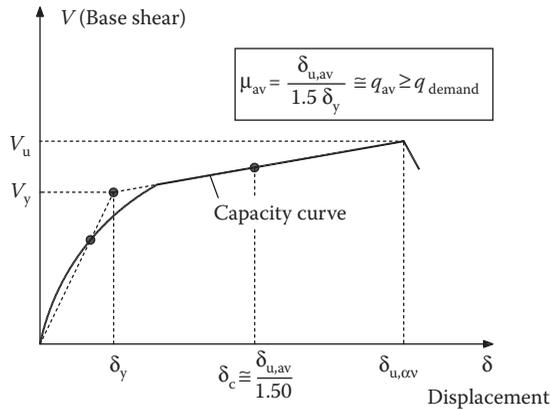
Figure 14.17 Determination of the *q*-factor value using the push-over capacity curve.

14.6.4.7 Additional issues common to all methods of analysis

For the following issues:

- Combination of the components of the seismic actions
- Additional measures for masonry infills
- Combination coefficients for variable actions
- Importance classes

the rules in effect for new buildings included in EC8-1/2004 are also adopted by EC8-3/2005 for existing buildings.

14.6.5 Safety verifications

14.6.5.1 General

As is well known, structural elements are classified in two main categories:

- Ductile ones
- Brittle ones

In the first category, failure is caused in the case of bending moments with low axial force presenting plastic deformations, so that the element is *deformation-controlled*.

In the second category, failure is caused either by low bending moment with high axial force or by prevailing shears presenting brittle failures, so the element is *force-controlled*.

14.6.5.1.1 Ductile elements

(Moment–rotation) M–θ diagrams at critical regions of ductile members have the form of Figure 14.1b left and are defined by the coordinates of the following points:

Point B: yield stage, $M_y\ \theta_y$
Point C: failure stage, $M_u\ \theta_u$
Point D: residual strength stage, $M_R\ \theta_R$

They constitute the capacity curves of the critical regions of ductile members and are introduced as input data for capacities in inelastic methods. It should be noted that the residual resistance from D to E may be non-zero in some cases and zero in others. Many computer programs for the Nonlinear Static Procedure can have only a bilinear capacity curve as input (points A, B, C).

As was thoroughly explained in Chapters 5, 8 and 9, end rotations θ at plastic hinges may be determined by the relevant cross-section curvatures φ_u and the length L_{pl} of the plastic hinge. Both magnitudes have been examined in detail in the above chapters and closed expressions have been formulated for *beams*, *columns* and *ductile walls*. Therefore, curves $M-\theta$ may be generated easily up to point C (Figure 14.1b). EC 8-3/2005 includes in Annex A (Concrete Structures) in the form of information, closed expressions for θ_y and θ_u. In ATC 40-1986 and FEMA 356-2000 the coordinates of points B, C and D of Figure 14.1b are given in a normalised form in tables, which can be easily used as an input in computer programs for non-elastic analysis.

The plateau length between B and C depends basically on the axial force and on the reinforcement in the tension and compression zones of the member. It should be noted that the slope of branch B–C according to FEMA 356 and ATC 40 ranges between 5% and 10% of the initial slope (effective stiffness of the member).

14.6.5.1.2 Brittle members

$M-\theta$ diagrams (moment–rotation) at the critical regions of brittle members have the form of Figure 14.1b right. The critical point B of this diagram is defined either by the bending strength at the end of the brittle member or by its shear strength. In both cases, as explained in Chapters 8 and 9, in the diagrams of beams, columns and walls there is no ductility plateau, so the element is *force-controlled*. Ultimate moment or shear force at failure may be calculated using procedures presented in Chapters 8 and 9. At the same time, EC 8-3/2005 in Annex A includes information for the evaluation of the above strength for beams, columns and shear walls in the form of closed expressions similar to those presented in Chapters 8 and 9 of this book.

14.6.5.2 Linear methods of analysis

For the lateral force method or for modal response spectrum analysis, the following principles and rules for safety verifications are adopted by EC 8-3/2005.

14.6.5.2.1 Ductile members

- These are members under bending with low axial force (beams, shear walls, columns with low axial force). They are verified in terms of deformations, that is, chord rotation θ_E at the ends of the members.
- Demand θ_E results from the linear analysis.
- Capacities θ_u result according to what has been presented in a previous paragraph for *mean values* of the material properties divided by the *CF* of the structural system.

14.6.5.2.2 Brittle members

- Safety verification of these members is carried out in *terms of strength*.
- Demands V_E result either from the analysis or from a *capacity design* as presented in Chapter 6. More particularly (Figure 14.18):
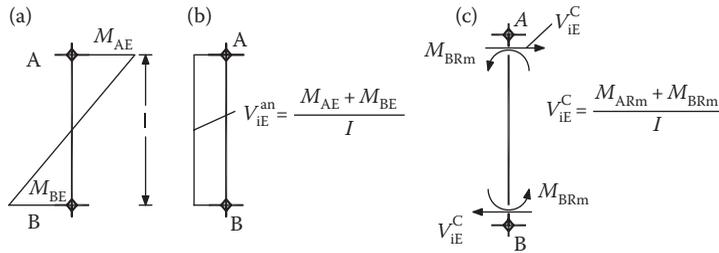
If $V_{iE}^{an}/V_{iRm} \leq 1.0$: for safety verification $V_{iE} = V_{iE}^{an}$

If $V_{iE}^{an}/V_{iRm} \geq 1.0$: for safety verification $V_{iE} = V_{iE}^{C}$

V_{iRm}: capacity of the column to shear

M_{ARm}, M_{BRm}: capacity of the ends of the column to bending

Figure 14.18 Determination of V_{iE} for the safety verification of a column to shear (brittle failure): (a) and (b) moment and shear diagrams from the analysis for seismic lateral loads; (c) shear force V_{iE}^{C} from the capacity design procedure.

- If the ratio:

$$\rho_i = D_i/C_i = V_{iE}/V_{iRm} \leq 1.0 \qquad (14.44)$$

demand D_i (e.g. V_{iE}) resulting from the analysis is introduced in the safety verification inequities.

Capacity C_i (e.g. V_{iRm}) of the ductile component (to shear) is evaluated using mean values of the material properties and introducing the relevant CF.
- If the ratio:

$$\rho_i = D_i/C_i = V_{iE}/V_{iRm} \geq 1.0 \qquad (14.45)$$

the capacity design value V_{iE}^{C} is introduced in the safety verification inequities.
- Capacity design values V_{iE}^{C} introduced in the above equations are calculated for overstrengths:

$$\gamma_{Rd} = 1.0 \qquad (14.46)$$

- In the above equations, bending moments M_{Rm} at the ends of the columns, which are introduced for the determination of capacity design shear $D_i = V_{iE}^{C}$, may be calculated for an axial load due to the gravity loads only.

14.6.5.3 Non-linear methods of analysis (static or dynamic)

- In this case the demands for both 'ductile' or 'brittle' components result from the analysis, performed in accordance with Paragraphs 14.6.4.4 and 14.6.4.5, using mean value properties of the material.
- The values of the capacity of both ductile or brittle components to be compared to demand in safety verifications are determined in accordance with Paragraphs 14.6.5.1.1 and 14.6.5.1.2 of this subsection for *mean values* of the material properties divided by the *CF* of the structural system.

14.6.5.4 The q-factor approach

The values of both the demand and capacity of ductile and brittle members should be in accordance with what has been set forth in Paragraph 14.4.2.2 for the *q*-factor procedure.

14.6.5.5 Acceptance criteria

- It is obvious that the acceptance criteria vary according to:
  - The limit state under consideration
  - The type of control mechanism of the member ("ductile" or "brittle")
  - The structural contribution of the member (primary or secondary) to the seismic resistance.
- It should be remembered that for each limit state from DL to NC limit, the seismic action for which the structure is examined has been gradually increased (see Subsection 14.4.2), and therefore demand is also enhanced.
- Chord rotation capacities θ_{um} at the end of ductile members, according to EC 8-3/2005 recommendations at its Annex A (concrete structures), must be reduced by one standard deviation σ for *primary members*. This reduction is estimated at:

$$\theta_{u,m-\sigma} = \frac{\theta_{um}}{1.50} \qquad (14.47)$$

For the secondary members, the denominator of the above expression (14.47) is taken to be equal to 1.0. Therefore, rotation chord capacity of secondary members is taken to be equal to θ_{um}.

- In ATC 40-1996 and FEMA 356-2000 these capacities are tabulated in a normalised form and therefore may be easily incorporated as general type input in a computer program. However, the concept of these tables is the same as that of the procedure followed by EC 8-3/2005.
- For all methods of analysis (elastic or non-elastic)—except for the *q*-method procedure—the following safety verifications are specified by EC 8-3/2005 in its informative Annex A (concrete structures).

1. Primary ductile members (deformation controlled; Figure 14.19a)

$$\text{Limit States:} \quad \begin{cases} Damage\ Limitation\ (DL) \\ M_E \leq M_y,\ or\ \theta_E \leq \theta_y \\ Significant\ Damage\ (SD) \\ \theta_E \leq 0.75\theta_{u,m-\sigma} \\ Near\ Collapse\ (NC) \\ \theta_E \leq \theta_{u,m-\sigma} \end{cases} \qquad (14.48a\text{--}c)$$

2. Primary brittle members (force-controlled; Figure 14.19b)
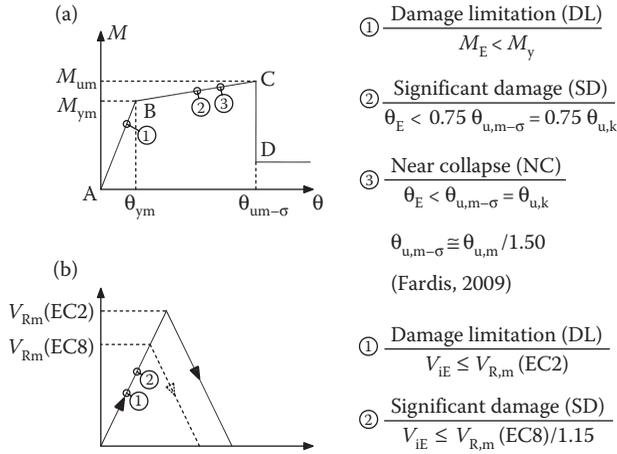
Figure 14.19 Safety verifications for primary elements: (a) ductile elements; (b) brittle elements.

$$\text{Limit States:} \begin{cases} \textit{Damage Limitation (DL)} \\ V_E \leq V_{Rm,EC2} \\ \textit{Significant Damage (SD)} \\ V_E \leq V_{Rm,EC8/1.15} \\ \textit{Near Collapse (NC)} \\ \text{joints: } V_{CD,j} \leq V_{Rm,jEC8} \end{cases}$$
(14.49a–c)

3. Secondary ductile members

$$\text{Limit States:} \begin{cases} \textit{Damage Limitation (DL)} \\ M_E \leq M_y, \text{ or } \theta_E \leq \theta_{y,ef} \\ \textit{Significant Damage (SD)} \\ \theta_E \leq 0.75\theta_{um} \\ \textit{Near Collapse (NC)} \\ \theta_E \leq \theta_{um} \end{cases}$$
(14.50a–c)

4. Secondary brittle members

$$\text{Limit States:} \begin{cases} \textit{Damage Limitation (DL)} \\ V_E \leq V_{Rm,EC2} \\ \textit{Significant Damage (SD)} \\ V_E \leq V_{Rm,EC8/1.15} \\ \textit{Near Collapse (NC)} \\ \text{Joints: } V_{CD,j} \leq V_{Rm,jEC8} \end{cases}$$
(14.51a–c)

- For the *q-factor approach*, safety verification checks are carried out as in the case of new structures *in terms of strength*, taking into account in addition the following remarks that have been already noted.
  - For the three limit states (LD, SD, NC), relevant design acceleration spectra should be introduced increasing accordingly from DL to NC (see Subsection 14.4.1) for the determination of relevant seismic effects.
  - For the NC limit state, *q*-factor may be increased by one-third of its value for SD (corresponding to the no [local] collapse requirement for new buildings)
- In Table 5.5, EC 8-3/2005 are summarised:
  - The values of the material properties to be adopted in evaluating both the demand and capacities of the elements for all types of analysis.
  - The criteria that should be followed for the safety verification of both ductile and brittle elements for all types of analysis.

14.7 DECISIONS FOR STRUCTURAL RETROFITTING OF R/C BUILDINGS

14.7.1 General

As has been presented in Chapter 13, a preliminary seismic evaluation comes first, both in the case of post- or pre-earthquake decisions for evaluation and eventual intervention. A detailed quantitative evaluation follows only in the case that serious damages have been identified or serious deficiencies have been revealed during the preliminary evaluation.

Therefore, after the quantitative seismic evaluation of an R/C building, one of the following two types of intervention may be decided:

- Repair, or
- Strengthening

The effects of rehabilitation on *stiffness, strength* and *deformability* must be taken into account in an analytical model of the rehabilitated structure.

Keeping in mind the definitions given in Chapter 13.3.2, for these types of interventions and taking into account the quantitative approach to seismic evaluation at global (general) as well local level (Figure 14.1c and 14.1b), the above definitions may be quantified as follows:

Seismic repair refers to cases where the global stability is satisfied (the target displacement δ_t for SD Limit does not exceed $\delta_u/1.50$), that is:

$$1.50\delta_t(SD) \leq \delta_u(NC) \tag{14.52}$$

However, some members exhibit deficiencies or damages (i.e. local demand in terms of deformation (θ_E) or strength (V_E) exceed the limits defined by the safety verification). Therefore, in these cases intervention is limited only to the *local retrofitting* of these members, so that their stiffness, strength and ductility cover the safety verification checks.

Conversely, *seismic strengthening* refers to cases where the global stability mentioned above is not satisfied. In this case, a *general type intervention* is required (strengthening). This intervention may aim at one or more of the following improvements of the structural behaviour, which have already been mentioned in Paragraph 13.3.5.5, that is:

- Increasing the overall structural ductility (e.g. confinements of columns in frame systems).

- Increasing strength and stiffness (e.g. by strengthening existing structural members and particularly vertical ones, or by adding shear walls in the spans of existing frames).
- Increasing stiffness, strength and ductility by strengthening and confining existing vertical members.
- Drastically increasing stiffness, strength and ductility by adding new seismic-resisting members like R/C cores, new structural walls, jacketing successive frame columns and filling their span with structural walls.

Many times the general type intervention may be limited to one or two storeys to improve 'soft storey' vulnerability (irregularities in elevation) or to a region in the plan view of the building to improve its irregularities in plan.

Seismic risk is radically reduced in the fourth case above, particularly when new R/C cores or structural walls are added. In this case, if a significant part of the seismic action is resisted, say 70%, by these new members, then the intervention presents a high degree of reliability, since there are no uncertainties about the effectiveness of the intervention. These new elements can be designed, constructed and supervised as for a new structure, and therefore the professional who is responsible for the intervention feels safe enough.

This type of intervention is extended to the foundation, where special concern should be given to resistance to the overturn moments newly appearing there, due to the high stiffness of the new elements that concentrate a large percentage of the base shear. The above type of intervention is proper for pre-earthquake interventions in buildings with a usage that is changing and, therefore, where there is high flexibility due to the high degree of architectural modifications. In case of post-earthquake interventions of a general type (strengthening) where broad constraints exist due to building operation, particularly in the case of residential buildings, and where the intervention cost plays a considerable role, these types of interventions are questionable.

14.7.2 Criteria governing structural interventions

Criteria governing structural interventions in R/C buildings may be classified into two categories, namely, *general* and *technical* ones, according to generally accepted Codes of Practice (e.g. EC 8-3/2005 FEMA 396/ASCE/SEI 41-06).

14.7.2.1 General criteria

The retrofitting scheme should consider the following points:

- Costs, both initial and future. This parameter is particularly crucial after a destructive earthquake when the intervention is obligatory by undisputable needs based on damage exhibited.
- Durability of original and new elements, particularly their *compatibility* (e.g. position of new R/C cores ensuring the diaphragmatic action of the floors), existing carbonation or corrosion of steel reinforcement below new concrete jacketing and so on.
- Available skilled personnel, equipment and materials. For example, in the case of the Thessaloniki earthquake (1978), issuing of permits for new buildings was postponed for one year to ensure the availability of skilled personnel for retrofitting works.
- Existing means for quality control (e.g. proper labs for testing materials and techniques).
- Occupancy (impact on the building) both during and after the work.
- Aesthetics of the building.
- Preservation of the historical and architectural identity of historical buildings.
- Duration of the work in relation to the needs of the occupants (occupancy disruption).

14.7.2.2 Technical criteria

The following technical aspects should be taken into account:

- All identified deficiencies or damages should be appropriately repaired, implementing local modification of the damaged members.
- High irregularities in stiffness and strength should be improved as much as possible, both in plan and elevation.
- Increase in the local ductility should be effected, where required.
- Overall strength increase of the structure should not lead to a reduction of the overall ductility of the structural system.
- All strength requirements of the relevant Code should be fulfilled after the intervention, taking into account the provisions of Chapter 15 for the redesign of elements.
- Spreading the areas of potential inelastic behaviour as much as possible across the entire structure should be one of the tasks of the intervention.

14.7.2.3 Types of intervention

Bearing in mind the above general and technical criteria, an intervention may be selected from the following representative types individually or in combination:

- Restriction or change of use of the building
- Local or global modification (repair or strengthening) of damaged or undamaged elements
- Possible upgrading of existing non-structural elements into structural ones
- Modification of the structural system aiming at stiffness regularity, elimination of vulnerable elements or a beneficial change of the natural period of the structure
- Mass reduction
- Addition of new structural elements (e.g. bracings, infill walls)
- Full replacement of inadequate or heavily damaged elements
- Redistribution of action effects, for example, by means of re-levelling (bringing columns back to their original position) of supports, or by adding external pre-stressing
- Addition of a new structural system to carry the seismic action
- Addition of damping devices at appropriate parts of the structure
- Partial demolition

In Figure 14.20 typical strengthening methods used in Japan are given in a schematic form (Sugano, 1981; Rodriguez and Park, 1991).

14.7.2.4 Examples of repair and strengthening techniques

Finally, to give a clearer picture of the frequency of implementation of the various techniques, some statistics on R/C building repair and strengthening techniques in Japan and Mexico are given.

In the case of the 1966 Tokachi-Oki earthquake, the strengthening methods used for the rehabilitation of 157 R/C buildings are listed in Figure 14.21 (Endo et al., 1984; Rodriguez and Park, 1991). In general, more than one method was used for a building, and the most common method of strengthening (in 85% of cases) was the addition of shear walls cast into existing frames. Column jacketing was used in 35% of cases.
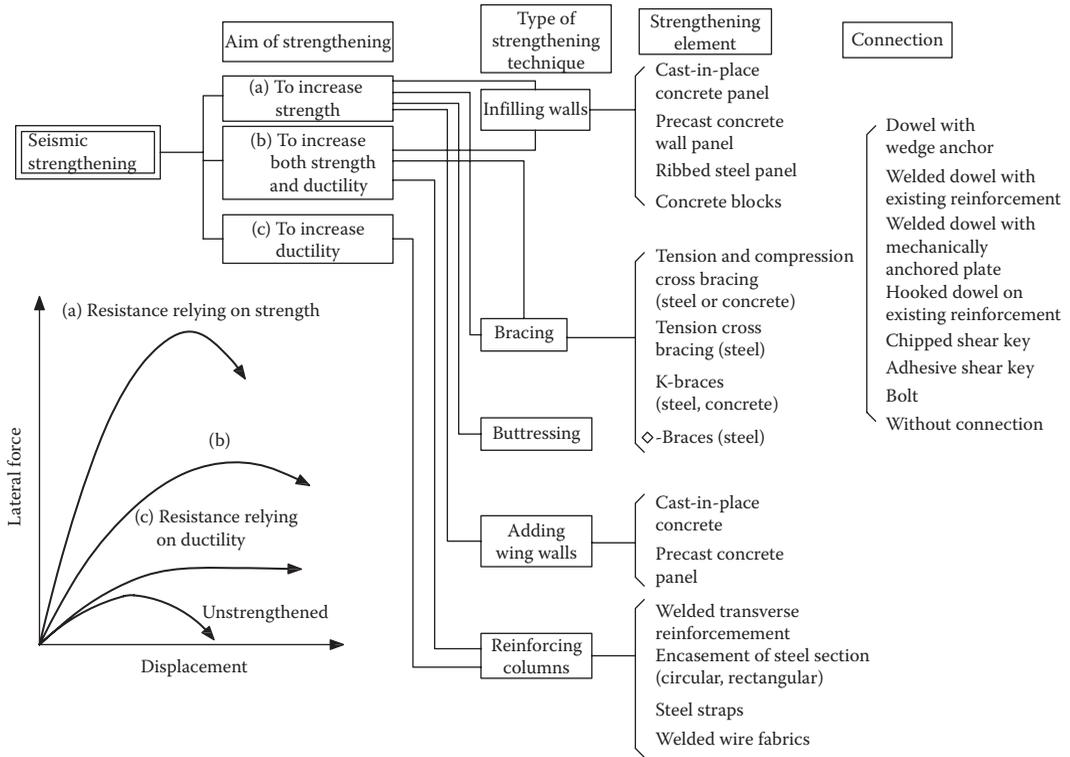
Figure 14.20 Typical strengthening methods used in Japan.

In the case of the 1985 Mexico City earthquake, the various strengthening methods used for 114 R/C buildings are listed in Table 14.6, in relation to the number of floors of the structures. According to these data, jacketing of columns (designated as concrete JC in Table 14.6) was the most commonly used technique for buildings with 12 storeys or fewer (Aguilar et al., 1989; Rodriguez and Park, 1991).
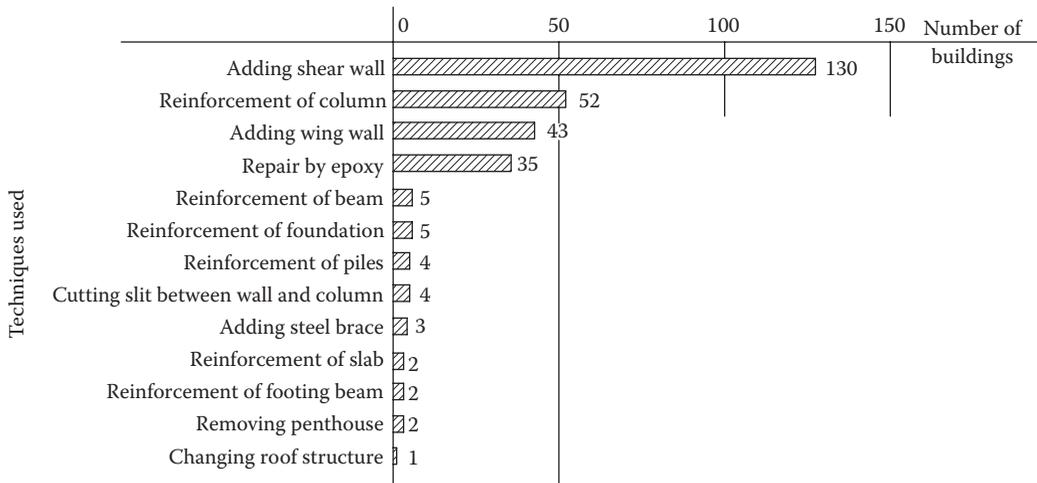
Figure 14.21 Repair and strengthening techniques used for 157 buildings in Japan.

Table 14.6 Repair and strengthening techniques for 114 reinforced concrete buildings in Mexico versus number of floors

Repair and strengthening techniques	Number of floors			
	<5	6–8	9–12	>12
Sealing	1	1	0	0
Resins	2	2	3	2
Replacement	7	8	5	6
Hydraulic jacks	1	1	1	0
Concrete JC[a]	11	18	26	5
Steel JC	2	7	10	2
Concrete JB[b]	4	7	14	2
Steel JB	1	0	3	1
Shear wall	8	12	16	9
Infill wall	4	9	2	2
Steel diagonals	0	7	7	2
Concrete frames	1	3	3	3
Additional elements	3	3	4	2
Straightening	0	1	2	2
New piles	2	4	8	3

[a] JC = Column jacketing.
[b] JB = Beam jacketing.

14.8 DESIGN OF STRUCTURAL REHABILITATION

14.8.1 General

The retrofit design procedure includes the following steps:

- Conceptual design
- Analysis
- Verifications
- Drawings
- Technical reports

14.8.2 Conceptual design

Conceptual design usually covers the following issues:

1. The type and configuration of the retrofit scheme
2. Selection of intervention techniques and materials
3. Preliminary estimation of dimensions of additional structural components
4. Preliminary estimation of the modified stiffness of the retrofitted elements

14.8.3 Analysis

All methods accepted for use at the stage of assessment (see Subsection 14.6.4) may also be used at the stage of analysis for retrofitting. Of course, modified or repaired structural members will be modelled, taking into account their modified characteristics. It is apparent that

in both stages the same method is selected, since in this case the remodelling at the stage of retrofitting usually needs minor modification relative to that used for assessment.

It should be remembered that of all methods permitted by EC 8-3/2005, the non-linear static (push-over) analysis and the *q*-factor approach are the most easily applied in practice. For both of them, the computational determination of the corresponding $M-\theta$ diagrams for all new or repaired elements is a prerequisite. For new elements the procedure is well known and is similar to that followed at the assessment stage. For the elements for which a repair is foreseen, the $M-\theta$ diagram depends on the method of repair that will be followed (e.g. R/C jacketing, FRPs, etc.). This issue will be presented in Chapter 15.

14.8.4 Safety verifications

According to EC 8-3/2005, safety verifications are carried out in general as in the stage of assessment (see Section 14.7) for all types of members, modified or repaired as well as new ones. For existing members, mean values from *in situ* tests and any additional sources of information will be used for the determination of local capacities, as explained in detail in the case of assessment. These values will also be reduced by the CF, as in the case of assessment. For new elements or added materials for repair or strengthening of existing members, nominal design values are used without reduction by CF. The remarks of the previous Subsection (14.8.3) in regard to the capacity diagrams $M-\theta$ of repaired members also hold in the case of safety verifications.

A more detailed approach to safety verifications for the non-linear static analysis method and for the *q*-factor approach will be made below.

14.8.4.1 Verifications for non-linear static analysis method

In this case, the following verifications must be carried out:

1. *Global safety verification*
   Target displacement (δ_t) for loading at DL limit state (e.g. ULS for new buildings) should not be bigger than NC displacement (δ_u) reduced by 1.50 (Figure 14.1), that is,

$$\boxed{\delta_t = \frac{\delta_u}{1.50}}$$

   (14.53)

2. *Local safety verification of ductile members*
   This category includes members under prevailing bending with or without axial force, at the end of which plastic joints may be formed (beams, columns, walls).
   In rehabilitation stage, three cases may appear:
   a. Existing members without any intervention
   b. Existing members modified through repair or strengthening
   c. New members
      Safety verification in this case is carried out in terms of deformation, as in the case of assessment.
      In the case that some of the members under consideration do not comply with the safety verification requirements presented in Section 14.6.5, one of the following alternatives may be implemented.
   d. For new elements, the most convenient way is enhancing of the ductility of the new member.

M_{ud}, θ_{ud}, θ_{yd}: Design capacities

M_{ud}^{ov}: Increased capacity
to balance demand θ_E
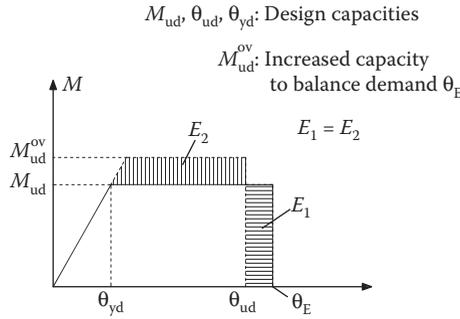
Figure 14.22 Strength of a member increased to balance the deformation θ_{ud} inefficiency to cover the deformation demand θ_E.

e. For existing or modified members, the easiest way is to increase their strength. In this case, if the required end rotation θ_E exceeds θ_{ud} (Figure 14.21), then, based on the concept of 'energy balance' (see Chapter 3.2), M_{ud} should be increased by an overstrength factor γ_{ov} (Figure 14.22) equal to

$$\gamma_{ov} = \frac{M_{ud}^{ov}}{M_{ud}} \cong \frac{\mu_E - 1}{\mu_{ud} - 1} \tag{14.54}$$

In this respect, the required extra energy capacity E_1 due to θ_E, which is greater than θ_{yd}, is balanced by extra energy capacity E_2 due to overstrength γ_{ov}. In fact, referring to the diagram of Figure 14.21, it may be seen that:

$$E_1 = (\theta_E - \theta_{ud})M_{ud} \tag{14.55}$$

$$E_2 = (M_{ud}^{ov} - M_{ud})(\theta_{ud} - \theta_{yd} \tag{14.56}$$

Expression (14.54) results from the condition that $E_1 = E_2$ where:
μ_E is the ductility demand θ_E/θ_{ud}
μ_{ud} is the design ductility θ_{ud}/θ_{yd}
It should be noted that θ_{ud} refers to the specified limit for the limit state for which the design is carried out.
Another way to approach the problem is to characterise these elements as 'secondary', and in this respect to increase the specified deformation limit θ_{ud}.

3. *Local safety verification of brittle members or mechanisms*
This category basically includes members under prevailing shear that fail in a brittle way before plastic hinges can be formed at their ends due to bending. It may also include columns with high axial load, which can develop a very low plasticification at their ends and, therefore, they function as brittle elements.

   In rehabilitation stage the same cases of characteristic members may appear, as in the case of ductile ones, that is: new members, existing unmodified members and strengthened or repaired ones.

   Safety verification in this case is carried out in terms of *strength,* as in the case of assessment.

   In the case that some of the members under consideration do not comply with the safety verification parameters presented in paragraph 14.6.5.5, strengthening of the member is the only way to improve its response.

14.8.4.2 Verifications for the q-factor approach

It is obvious that similar safety verifications with the non-linear static method must also be carried out in the *q*-factor approach.

1. *Global safety verification*

   This safety verification has the objective of verifying that:

   $$q_{\text{Dem}} \leq q_{\text{cap}} \tag{14.57}$$

   where

   q_{Dem} is the *q*-factor introduced in the design acceleration response spectrum for the force-based design of the system.

   q_{cap} is the available global *q*-factor of the system. Of course, this value should by no means exceed values of the *q*-factor codified for new buildings.

   The verification of q_{Dem}-factor that is introduced in the design spectrum of new R/C buildings is ensured explicitly by design Code requirements for local ductility of the members of the new building and by the capacity design requirements. In the case of the rehabilitation of an existing R/C building, it comprises new members, existing unmodified members and those under repair or strengthening. Therefore, for the determination of the available *q*-factor, a reliable method must be mobilised.

   The safest procedure is to determine the capacity curve of the system using a pushover static analysis procedure. Having this curve, the *q*-factor can easily be determined. A reduction factor of about 1.50 should be introduced to this value. The resulting final q_{Dem}-factor should by no means be bigger than *q*-factors recommended by Code for new R/C buildings.

   In the case that the main structural system carries the seismic actions by means of new structural elements (e.g. R/C cores, R/C walls, R/C jacketed columns), the existing structural elements might be designated as 'secondary'. In this case, the building is designed as a new one, with values of *q*-factor those recommended by the Code.

   An alternative approach could be the design of the new structural system using the *q*-factor recommend by Code, while for an existing system for which the R/C members do not comply with the rules of the Code for local ductility, a value of $q = 1.50$ should be implemented. In this case, neither local ductility rules nor capacity design rules would be obligatory for the existing members. It should be noted that in this case the analysis of the overall structural system is carried out for a *q*-factor corresponding to a new building. In this respect, the seismic effects of the existing structural system must be increased by $q/1.50$, and as a consequence they will exhibit very high values.

2. *Local safety verifications*

   Local safety verifications at ULS or DLS are carried out for all structural members, new or existing, using the force-based design that has been presented for new buildings.

   In the case that the existing elements are considered 'secondary', or in the case that a *q*-factor equal to 1.50 is introduced for these members, nothing new should be added here in relation to the procedure specified by EC 8-1/2004 for new buildings.

   In the case that a common *q*-factor is determined by means of the capacity curve of the building, overload factors γ_{ov} for the existing elements should be introduced to the seismic effects resulting from the common *q*-factor given by expression (14.54).

   It should be noted that the mobilisation of the capacity curve as an additional tool for the *q*-factor approach is a very effective means for the reduction of the degree of strengthening of existing R/C members.

14.8.5 Drawings

Drawings for rehabilitation may be classified in three groups, namely:

- Demolitions
- Temporary propping
- Rehabilitation

1. Demolitions

   Demolition drawings display
   a. The regions of the structural system that should be demolished
   b. The order in which the various members should be demolished so that local or total collapse is avoided
   c. The equipment that might be used for the demolition
   d. Life protection measures that should be taken during the demolition.

2. Temporary propping

   These drawings must comply with those of demolitions. They must include information:
   a. About supporting systems of dead loads
   b. About bracing systems to protect the building from lateral inclination and therefore from significant second-order effects that might lead to pancake collapse
   c. About stabilising systems of weakened diaphragms due to demolition of broader regions for passing new R/C shafts or staircase cores and so forth.
   d. About the order of installation of the supporting systems
   e. About details of connections of these systems to the structural system
      It should be noted that temporary propping is one of the most significant actions of rehabilitation procedures, because during the demolition the structural system is weakened or sometimes loses its robustness and integrity. If it is not well propped, the building may collapse. The most common accidents with fatalities happen during demolition activities.
      In closing, it should be noted that propping drawings should be accompanied by the relevant technical report, including necessary structural design of the various parts of the propping system.

3. Rehabilitation drawings

   Rehabilitation drawings include, as do the drawings of new buildings, the following:
   a. General layout drawings in plan, also including characteristic cross-sections in elevation. In these drawings must be displayed:
   b. All new members
   c. All repaired or modified members with detailed information about the material and the degree of repair (e.g. dimensions of R/C jackets with the new reinforcement, etc.)
   d. General information about:
      i. Dead loads
      ii. Live loads
      iii. Seismic loads
      iv. Ground conditions
      v. Construction materials of the existing system
      vi. Construction materials of new parts or repaired members and so on.
   e. Detailing drawings of all new elements, repaired elements, connections of new to old parts of the building and so on.

It should be noted that for all drawings of the above three groups (demolitions, temporary propping and rehabilitation) various colours should be used to differentiate the existing parts from the new ones and the interventions to existing elements.

4. *Technical report*

Technical reports should accompany the design of the rehabilitation scheme. These reports should include:

   a. Justification of the structural intervention
   b. Technical description of the intervention
   c. Quantity estimates
   d. Bill of quantities
   e. Cost estimates

14.9 FINAL REMARKS

From what has been presented so far, it can be concluded that very few structural problems are as challenging for a professional as confronting the consequences of an earthquake.

From the scientific point of view, the main tool available to the engineer, that is, the analysis, has often been proved to be inadequate to explain the damage patterns, possibly because the assumptions on which it is based are over-simplified (static loading, elastic response of the system, not taking into account the infill system, etc.). Thus, there is always doubt regarding the effectiveness of whatever intervention has been decided upon. This doubt is much higher in case of a pre-earthquake rehabilitation, since in this case there is no damage pattern for system identification.

From a practical point of view, the determination of the 'available' and the 'residual' seismic resistance of existing members, damaged or not, involves a high degree of uncertainty because of the subjectivity involved in the determination of the seismic resistance of the structural elements.

Referring to conceptual design, the various types of intervention that are decided upon are not always feasible. For example, structures that were built without respecting the provisions of modern Codes (most existing structures fall into this category) cannot meet ductility DC 'M' requirements, and possibly not even ductility DC 'L' requirements. On the other hand, a large increase in base shear V_B creates the need for additional strength and stiffness elements, which leads to foundation problems, as well as to functional problems when the structure is in use again.

Based on the above, the legal framework that is set every time after a destructive earthquake for the rehabilitation of damage cannot withstand strictly scientific criticism. This is because this framework attempts to establish a balance between the desirable and the feasible. In other words, it is a political decision within the broader meaning of the term, which tries to optimise the combination of scientific knowledge with the technological and financial possibilities in order to face the acute social problem of the safe retrofitting of damaged structures.

Of course, in the case of pre-earthquake assessment and rehabilitation, the above controversial parameters, that is, cost and safety, are not so acute, since the rehabilitation procedure is not as urgent as in the case of post-earthquake rehabilitation activities.

Independently of the previous general remarks, in summarising, reference should be made to the following special points:

1. The rehabilitation of a seismically damaged building is a much more difficult task than the original design and construction of the building. The same holds for an intervention in the pre-earthquake period.

2. The difficulties arise during the design, as well as during the supervision and execution of the intervention works.
3. A basic factor for the successful outcome of the whole operation is the correct diagnosis of the causes of damage or the deficiencies, in the case of a pre-earthquake intervention. It is on this diagnosis that the level of intervention depends, that is, the repair or strengthening of the structure.
4. The design of the rehabilitation must aim at:
   a. Providing the structure with the stiffness, strength and ductility that it had before the earthquake by means of repair in the case of local damage.
   b. Providing the structure with the strength, stiffness and ductility required by the current Codes in the case of damage of global character (strengthening). The same holds for structures in pre-earthquake conditions, for which a global instability is verified.
5. Independent of the local or global character of the damage, the structural elements must be repaired in such a way that they regain the strength and ductility required by the current Codes.
6. For the choice of the repair technique, the market conditions and the feasibility of application of the chosen techniques in every particular case must be taken into account.
7. The rehabilitation is usually accompanied by the removal of many structural members, and therefore special care should be taken of the temporary support of the structure.
8. The outcome of the intervention depends to a large extent on the quality control of the design and construction. Therefore, very careful supervision is necessary during the execution of the rehabilitation works.
9. Intervention in heavily damaged infills is very important for the structure, and for this reason appropriate care should be taken.
10. Finally, it has to be stressed once again that structural rehabilitation must have as its point of reference the proper combination of strength, stiffness and ductility.

Technology of repair and strengthening

15.1 GENERAL

The purpose of this chapter is to present in brief the technological problems associated with interventions in structures damaged by earthquakes or at pre-earthquake stage in the case of an active seismic retrofitting.

In the preceding chapters detailed reference has been made to the procedure followed for decision-making about the extent and the type of interventions. At the same time, the successive steps for the design of the interventions were discussed in detail. In this chapter, reference will be made to the materials and techniques of interventions and to the dimensioning of the structural elements for various types of intervention. However, given the fact that several manuals, specifications and Codes have been published to date (UNDP, 1977; NTU, 1978; AUTH, 1978, 1979; GMPW, 1978; UNIDO/UNDP, 1983; Penelis and Kappos, 1997; OASP, 2001; Dritsos, 2004) where numerous technical details are given, the focus here will be mainly on some typical repair and strengthening techniques and on the dimensioning of the relevant structural elements.

Particularly on the subject of dimensioning, there are many reservations with regard to the reliability of the proposed methods, for the following reasons:

- There is no adequate experimental verification of these methods.
- Most of them are based on rough and/or simplified models, since analytical models based on experimental and theoretical knowledge have not yet been developed to a degree suitable for practical use.
- The quality of execution of the repair and strengthening works on site influences the results significantly.
- The evaluation of the redistribution of stresses from the old element to its strengthening presents reliability problems.

It should be stressed here that the main issues concerning repair and strengthening, which are materials, techniques and redesign considerations, exhibit different degrees of development in regard to research, implementation and codification level. Table 15.1 gives a qualitative picture of this development (Zavliaris, 1994).

Before the individual topics of this chapter are addressed, it will be useful to summarise the intervention procedure as given in the previous chapters.

After a destructive earthquake, an inspection operation is usually organised by the state, aiming at locating the buildings that are unsuitable for use on the one hand, and on the other, carrying out the necessary demolitions or shorings. After this first phase and once the aftershocks have attenuated, the procedure for the design of the intervention in every individual damaged building to be retrofitted begins.

Table 15.1 Development in materials, techniques and redesign considerations

	Materials	*Techniques*	*Redesign considerations*
Research and development (R&D)	◯	◯	◯
Implementation	○	○	○
Codification	∘	∘	∘

Note: The diameter of the circles represents the degree of development (qualitatively).

A similar procedure is followed in the case of a pre-earthquake active rehabilitation. After successive tiers of evaluation and screening of the buildings that are susceptible to damage or even collapse in the case of a strong earthquake, a detailed quantitative assessment is carried out, which, most of the time, is followed by a rehabilitation procedure. This second phase, that is, the quantitative assessment and retrofitting, is much more systematic than the first, more laborious and more effective, and it requires much time and expenses. The preceding chapter, as well as the present one, cover the approach to problems associated with this second phase.

In closing, in this brief introduction, it must be mentioned that the main reference for the intervention techniques for individual structural members presented here was the UNIDO/UNDP manual, *Repair and Strengthening of Reinforced Concrete, Stone and Brick-Masonry Buildings* (*UNIDO/UNDP, 1983*), which represents a synthesis of experience and expert knowledge at an international level. By this choice it is felt that some contribution is being made to the realisation of one of the UNIDO/UNDP goals, that is, the dissemination of this widely accepted up-to-date knowledge on intervention techniques to the international scientific community with special interest in the subject.

15.2 MATERIALS AND INTERVENTION TECHNIQUES

In this section, reference will be made to the materials and intervention techniques that are frequently encountered in the repair or strengthening of structures after an earthquake. Given the fact that these special materials, as well as their application techniques, are governed by detailed specifications that are typically related to the know-how that accompanies them, the designer, before including any of these materials in a rehabilitation project, must be fully informed about them. In the following, a general presentation of the materials and techniques is given, and some critical points related to their advantages, disadvantages and successful application are discussed.

15.2.1 Conventional cast-in-place concrete

Conventional concrete is very often used in repairs as a cast-in-place material. In many cases the results are not satisfactory because of the shrinkage of conventional cement, which causes reduced bonding between old and new concrete. In order to improve bonding conditions and cover additional uncertainties in construction operations, the use of concrete having a strength higher than that of the element to be repaired is recommended ($f_{c_{rep}} \geq f_{c_{exist}} + 5$ MPa), as well as a low slump and water/cement ratio. Such a choice, however, renders compaction very difficult, especially when thin jackets are forseen, thus making necessary the use of super-plasticisers to increase slump up to 200 mm with the standard method of Abram's cone. The maximum size of aggregates should not exceed 20 mm, so

Figure 15.1 Dedusting and wetting of the old concrete and reinforcement at the complex of the Army Pension Organization (Athens).

that the mix will be able to pour through the narrow space between the old concrete and the forms.

   The procedure of casting the concrete is critical for the success of the intervention. Old surfaces should be made as rough as possible and cleaned in order to increase the adhesion between old and new concrete. After the placement of the reinforcement, the forms are placed, which have special lateral openings for casting of concrete. Before concreting, there should be a final dedusting of the surfaces with compressed air, as well as extensive wetting of the old concrete and the forms. Concrete should be thoroughly vibrated to ensure a high degree of compaction (Figure 15.1).

15.2.2 High-strength concrete using shrinkage compensating admixtures

For the construction of cast-in-place concrete jackets, very often special dry-packed mortar is used, which is available in the market under several commercial names. This mortar consists of cement, fine sand (up to 2.0 mm), super-plasticisers and expansive admixtures in the appropriate proportions, so that mixing with water of about 15% of weight produces fluid mortar that attains high strength in a very short time (e.g. 30 MPa in a 24-h period, 70 MPa in 28 days), while at the same time it does not shrink. The attainment of high strength in a short period of time is due to the formation of a special silica calcium hydrate from the reaction between the expansive admixture and the cement. Therefore, very satisfactory repairs are accomplished, without voids and shrinkage cracks, using very thin jackets, for example, 40 mm. In order for these products to be used, they must be accompanied by a quality control certificate. As far as the rest of the procedure is concerned, it is the same as for conventional concrete.

15.2.3 Shotcrete (gunite)

If the appropriate equipment and trained personnel are available, shotcrete is considered to be a very good repair solution. Indeed, due to the fact that forms are not needed, it can be applied on surfaces of any inclination, even on ceilings. Its use is more common on extended surfaces such as R/C and masonry walls, but it can also be used for the construction of jackets around columns or beams.

As far as strength is concerned, a strength higher than that of the repaired element is always specified ($f_{c_{rep}} \geq f_{c_{exist}} + 5\,\text{MPa}$).

The main advantages of the method are the absence of forms, the very good adhesion between old and fresh concrete due to the high degree of compaction energy during shotcreting and high strength due to the low water/cement ratio.

Two different processes have been developed so far for gunite application, namely:

- Dry process
- Wet process

15.2.3.1 Dry process

This process requires the following equipment for production and application (NTU, 1978):

- Concrete mixer for dry mixing
- Water tank
- Centrifugal water pump
- High-capacity compressor
- Gun with one or two chambers
- High-pressure hoses
- Nozzle

The production procedure is as follows (Figure 15.2):

1. A mixture of 0.5 kN of cement and about 2.0 kN of aggregates with maximum grain size of 7,12 or 16 mm, depending on the case, is dry-mixed in the concrete mixer.
2. The mixture is fed into the gun and still in dry form, in suspension, reaches the nozzle through a hose with the aid of compressed air.
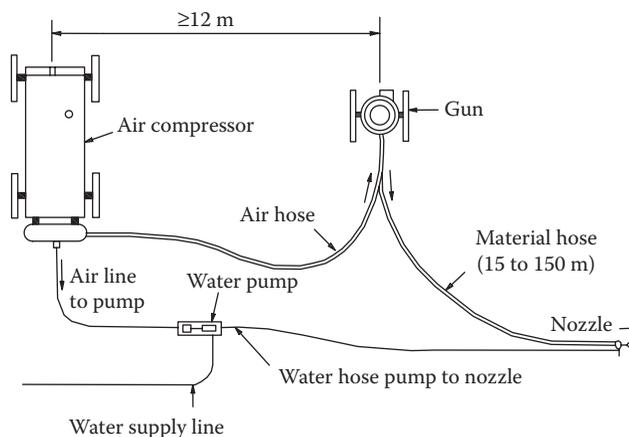

Figure 15.2 Typical arrangement of equipment for shotcreting.

3. At the nozzle, water is injected into the material. From there the mixture is forcefully shot onto the surface to be repaired, which has been previously roughened, wetted and appropriately reinforced. Every layer has a maximum thickness of 30–40 mm. If larger thickness is required, a second layer should be applied.

4. The resulting surface is very rough; therefore, after hardening it must be covered with plain plaster or mortar.

15.2.3.2 Wet process

This process was introduced rather recently, in late 1970s. The required equipment includes the following:

- Concrete mixer for wet mixing ready for use. This mixer may be avoided in case of the use of ready-mixed wet concrete
- High-capacity compressor
- Gun of continuous supply (open)
- High-pressure hoses
- Nozzle

The production procedure is as follows:

Ready-mixed concrete of aggregates with maximum grain size of 7–12 mm, depending on the case, is fed into the gun (Figure 15.3); it reaches the nozzle through a hose with the aid of compressed air and is forcefully shot onto the surface to be repaired.

15.2.3.3 Final remarks

- As disadvantages of the dry procedure may be considered, (1) the fact that the water/cement ratio cannot be quantitatively controlled, given the fact that the fluidity of the mix is controlled only visually by the operator; (2) the waste of a large fraction of the material due to reflection on the surface of application; and (3) the cement dust sprayed in the space, which makes application in close spaces difficult.
- Flexibility and fluidity must be considered the main advantage of the material, as it is controlled visually by the operator who attends the shooting of the material onto the old surface.
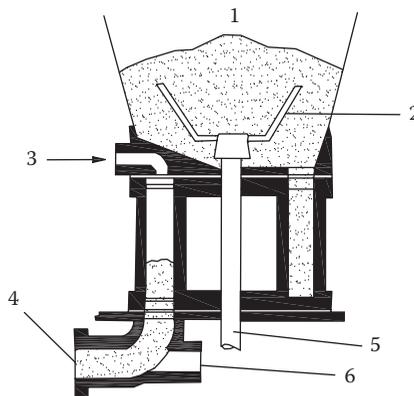

Figure 15.3 The principle of functioning of a shotcreting machine: 1 = wet material supply; 2 = mixer; 3 = compressed air; 4 = material exit under compression; 5 = rotor; 6 = compressed air.

Table 15.2 Dry-mix shotcrete on old concrete

Sample no.	Compressive strength of shotcrete cores, psi (MPa)	Bond strength in shear, psi (MPa)
1	5850 (40.3)	720 (5.0)
2	7140 (49.2)	598 (4.1)
3	5900 (40.7)	422 (2.9)
4	5410 (37.3)	520 (3.6)
5	7060 (48.7)	874 (6.0)
6	4620 (31.9)	411 (2.8)
7	4580 (31.6)	508 (3.5)

Source: From ACI 506 R-90. 1995. Guide to shotcrete. ACI Manual of Concrete Practice, Part 5. Farmington Hills, MI, USA. With permission of ACI.

Data are from a single project. It is presented for illustrative purposes only.

All tests on 6 in (150 mm) diameter cores.

Shotcrete placed by dry method.

Shear test conducted by 'guillotine' method where load is applied parallel to the bonded surface.

Table 15.3 Wet-mix shotcrete on old wet-mix shotcrete

Sample no.	Compressive strength of shotcrete core, psi (MPa)	Bond strength in shear, psi (MPa)
11	4810 (33.2)	131 (0.9)
12		181 (1.3)
13	4420 (30.5)	243 (1.7)
14		220 (1.5)
15	4860 (33.5)	336 (2.3)

Source: From ACI 506 R-90. 1995. Guide to shotcrete. ACI Manual of Concrete Practice, Part 5. Farmington Hills, MI, USA. With permission of ACI.

Data are from a single project. It is presented for illustrative purposes only.

All tests on 6 in (150 mm) diameter cores.

Shotcrete placed by wet method.

Shear test conducted by 'guillotine' method where load is applied parallel to the bonded surface.

- The above disadvantages are eliminated in the case of wet process. However, the advantage of flexibility in controlling fluidity does not exist in this case.
- In Tables 15.2 and 15.3 (ACI-506, 1995), below, representative values of experimental results for dry and wet processes are displayed. From the comparative evaluation, the following conclusions may be drawn:
  - The scattering of compression strength in dry process is higher than that of the wet one.
  - The bond strength of dry process is almost twice as high as that of the wet process.

15.2.4 Polymer concrete

Polymer-modified concrete is produced by replacing part of the conventional cement with certain polymers that are used as cementatious modifiers. The polymers, which are normally supplied as water dispersants, act in several ways. They function as water-reducing plasticisers, they improve the bond between old and new elements, they improve the strength of the hardened concrete and so on. However, it should be noted that polymer concrete also

has several disadvantages. It is vulnerable to fire conditions and, due to its lower alkalinity, presents inferior resistance against carbonation compared to conventional concrete.

15.2.5 Resins

Resins are usually used for grouting injections into cracks in order to glue together cracked concrete or for bonding thin metal or fibre reinforced plastic (FRP) sheets onto concrete surfaces. These are materials made up of two components that react and harden after they are mixed together. More specifically, one component is the resin in fluid form (epoxy, polyester polyurethane, acrylic, etc.), while the second is the hardener (NTU, 1978; AUTH, 1978; AUTH, 1979). There is a great variety of such products with different properties depending on the chemical composition of the components, the mixing ratios and the possible additives such as fillers or sand. Therefore, the engineer must have a good knowledge of the properties of such a material before selecting the proper one for a specific use.

Epoxy resins are the most common type of these materials in use today.

Resins must have an adequate *pot life* so that a usual dosage can be used before it hardens. Curing requirements should be compatible with the temperature and moisture conditions of the structure. The resin must have excellent bonding and adhesion to concrete and steel and must present small to negligible shrinkage. Also, its modulus of elasticity must be generally compatible with that of the concrete to be glued. Resins lose their strength at temperatures higher than 100°C, and therefore such repairs are not fireproof without fire protection (e.g. plaster). Resins used in the form of injections must have a viscosity appropriate for the crack width to which the injection is applied. Resins used for bonding metal or FRP sheets usually have high viscosity. Table 15.4 shows comparative data for strength and deformability of conventional concrete and of epoxy resins (AUTH, 1978).

There are several techniques for the application of resin injections. In the simplest case the resin is mixed with the hardener in a separate receptacle and a gun with an injection nozzle is filled with the mixture (Figure 15.4). Sometimes the mixing is done within the gun with

Table 15.4 Comparison between mechanical properties of concrete and epoxy resins

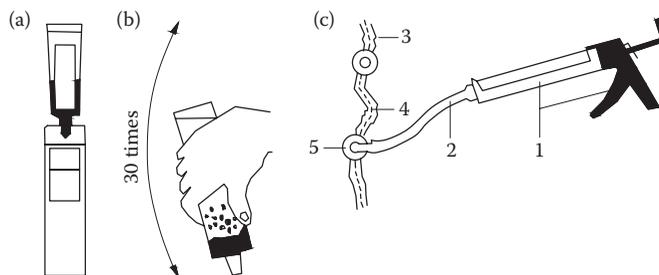| Property	Concrete	Epoxy resin
Compressive strength (MPa)	20–90	Up to 250
Tensile strength (MPa)	2–6	3.5–35
Flexural strength (MPa)	3.5–9.0	10–35
Elongation (%)	0.01	0.2–50

Figure 15.4 Procedure for the application of resin injections: (a) mixing of resin with the hardening agent; (b) shaking of the mixture for it to become homogeneous; (c) application of the resin injection: 1 = injection gun, 2 = plastic hose, 3 = crack, 4 = sealer, 5 = nipples.

separately controlled supply of the two components. The injection is applied with low pressure (up to 1 MPa), in which case it is done by hand, or with high pressure (up to 20 MPa), in which case it is done with a pump. The gun is equipped with a pressure gauge. Since epoxy resins are materials that cause irritation to skin, eyes and lungs, the appropriate means of personnel protection are required when working with them (gloves, protective eyeglasses, masks). When the crack width is small (0.3–0.5 mm), pure resin is used. In the case of wider cracks it is useful to mix the resin with filler, having a grain diameter not larger than 50% of the crack width or 1.0 mm, whichever is smaller. The ratio of resin to filler is usually about 1:1 in weight.

Before the application of resin injections the crack is cleaned with compressed air. Then holes of 5–10 mm in diameter are opened with a drill at certain distances along the length of the crack and nipples or ports of the appropriate diameter are placed on the mouths of the holes to facilitate the execution of the resin injections. The crack is then sealed on the surface with a quick-hardening resin paste and the injections are applied. On vertical surfaces the procedure starts from the lowest nipple or port, and as soon as the resin leaks from the mouth of the next nipple the procedure is discontinued, the mouth is sealed, and the same process is repeated for the next nipple. The next day, when the epoxy resin hardens, the resin paste is removed from the surface with an emery wheel.

15.2.6 Resin concretes

Resin concretes are concretes in which the cement has been replaced by resin. They are mainly used for replacing pieces of concrete that have been cut off. In order to make sure that there will be enough bonding between the old and the new parts, it is recommended that the old concrete be well cleaned and its surface coated with pure resin before the new resin concrete is cast in the place of the cut-off piece. Resin concretes require not only a special aggregate mix to produce the desired properties, but also special working conditions, since all two-component systems are sensitive to humidity and temperature.

15.2.7 Grouts

Grouts are often used for the filling of voids or cracks with large openings on masonry or concrete. The usual grouts consist of cement, water, sand, plasticisers and expansive admixtures in order to obtain high strength and minimum shrinkage during hardening. Details on the composition of conventional grouts can be found in all prestressed concrete manuals where they are used for bonding of post-tensioned tendons. Grouts are mainly used for the repair of structural masonry. In the case of traditional or monumental buildings, the grouts that are used must be compatible with the original construction materials as far as strength and deformability are concerned. Therefore, a large percentage of the cement is replaced in this case by pozzolans or fly ash and calcium hydroxide (UNIDO/UNDP, 1984; Penelis et al., 1984).

For application, the same procedure is followed, as in the case of resin injections. Figure 15.5 shows the general set-up for the application of grouts.
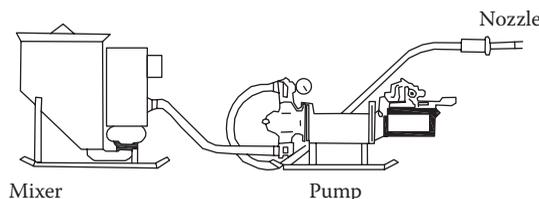

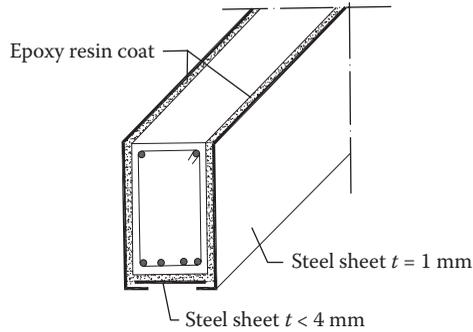Figure 15.5 Arrangement for application of cement grouts.

Figure 15.6 Strengthening of a beam with resin bonded metal sheets.

15.2.8 Epoxy resin-bonded metal sheets on concrete

In this method of intervention (Figure 15.6) the bonding is carried out with epoxy resin spread on the lower face of beams, on the vertical faces of beams, or on the joints. The sheets are made of stainless steel (usually 1.00–1.50 mm thick) so that they can be fitted well and bonded on the surface of the element to be strengthened (NTU, 1978; AUTH, 1979).

The intervention procedure includes the following phases: careful smoothing of the concrete surface with an emery wheel or emery paper; washing and drying of the concrete surface; roughening up the sheet surface using the process of sandblasting; coating of the concrete surface with an epoxy resin of high viscosity; covering the steel sheet with an epoxy resin layer; and putting it up and keeping it in place with tightening screws for 24 h, so that it will be glued onto the concrete. Repeat this procedure if a second sheet is necessary. Finally, cover up the sheets with wire mesh and cement plaster or shotcrete. The introduction of FRPs has minimised the use of the above method.

15.2.9 Welding of new reinforcement

The most usual way to strengthen regions under tension is the use of new reinforcement. The force transfer from the old reinforcement to the new is accomplished through welding (Figure 15.7). New bars are welded onto the old ones with the aid of connecting bars (bar pieces of the same diameter, but not smaller than 16 mm, and of at least 5ø length, spaced about 500 mm apart).
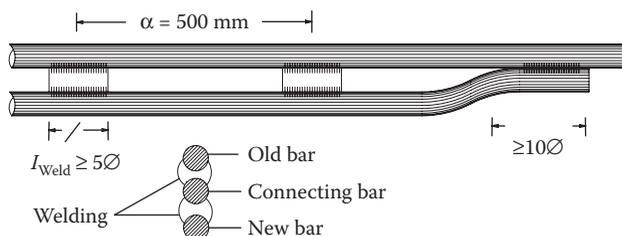

Figure 15.7 Welding of a new reinforcement bar.

15.2.10 Fibre-reinforced plastic (FRP) laminates and sheets bonded on concrete with epoxy resin

15.2.10.1 General

The strengthening of R/C structural members (e.g. beams, slabs, walls, columns, joints) with externally bonded FRP systems is a relatively new method of intervention that has to a large extent replaced the use of externally bonded steel sheets. FRPs exhibit the following advantages compared to steel sheets:

- They are light in weight
- They do not corrode
- They are available in large dimensions
- They have very high strength accompanied by a linear elastic behaviour up to failure (Figure 15.8)

On the other hand, they exhibit a series of disadvantages:

- They have a brittle type of failure (Figure 15.8). Therefore, they must be considered materials of low ductility. However, they may be used in the form of sheets for external confinement of concrete, which, as is well known, positively influences the ductility of columns (see Subsection 15.5.4).
- They are susceptible to fire.
- They lose a large percentage of their initial strength under permanent loading, ranging from 15% to 60% (Table 15.5).

FRPs are formed by embedding continuous fibres into a resin matrix that binds the fibres together.
The common fibres are:

- Carbon fibres (CFRP)
- Glass fibres (GFRP)
- Aramid fibres (AFRP)
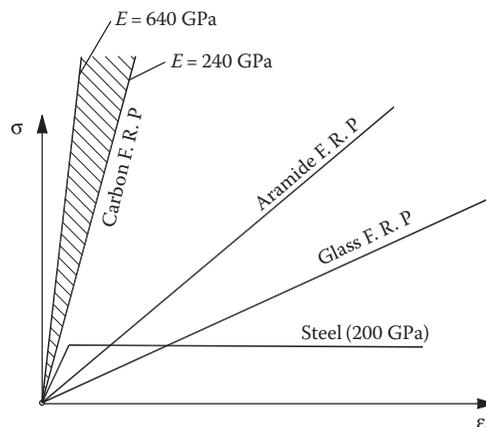
The most usual resins in practice are the epoxy ones.

Figure 15.8 Constitutive laws of FRP.

Table 15.5 Mechanical properties of FRP

Material	Elastic modulus (GPa)	Tensile strength (MPa)	Failure deformation (%)	Loss of strength under permanent load (%)
Glass-FRP	50	1700–2100	3	60
Aramid-FRP	65–120	1700–2100	2–3	50
Carbon-FRP	165–600	1400–3000	0.5–1.7	15
Steel	200	220–400	0.2[a]	

[a] Yield deformation.

15.2.10.2 Technical properties of FRPs

All three types of FRPs, that is, CFRP, GFRP and AFRP, used for strengthening of R/C structures exhibit a wide variety of tensile strength and stiffness, as depicted in Table 15.5.

On the other hand, the comparison of their σ–ε diagrams to that of mild steel shows that some of them, and particularly the CFRPs, have a high *E*-modulus equal or 2–3 times higher than that of steel (Figure 15.8).

At the same time, it can easily be concluded that their strength is much higher—5–10 *times*—than the strength of steel. However, their brittle behaviour and debonding problems, which will be examined later, do not allow an exploitation of this strength to a high degree.

For the choice of the proper type of FRP for an intervention, various parameters should be taken into account. In Table 15.6, a series of properties is evaluated for each of the three main types of FRPs in use (Meier and Winistorfer, 1995), taking into consideration the integrated behaviour of the type of FRP and the resin matrix.

15.2.10.3 Types of FRP composites

Two common methods of forming FRP composites have been used so far in strengthening R/C members:

- The wet lay-up method
- The use of prefabricated laminates

The first one involves the *in-situ* application of resin to a woven fabric or a unidirectional woven sheet applied on the R/C surface (Teng et al., 2002). These sheets are applied in successive layers until the proper resistance is ensured. The wet lay-up method is more versatile for *in-situ* applications in case of bonding to curved surfaces and wrapping around corners.

Table 15.6 Holistic evaluation of FRPS

Criteria	Behaviour		
	CFRP	GFRS	AFRP
Tensile strength	Very good	Very good	Very good
Compressive strength	Very good	Poor	Very good
E-module	Very high	Medium	Low
Fatique	Excellent	Good	Acceptable
Creep	Good	Acceptable	Poor
Resistance to alkaline enviroment	Very good	Good	Poor
Durability	Very good	Good	Acceptable
Resistance to fire	Poor	Poor	Poor

It is basically used for the confinement of R/C columns, for shear strengthening of beams, and for shear strengthening of R/C or masonry walls.

In the second method, prefabricated laminates are industrially produced. In this procedure, fibres are embedded in an epoxy resin matrix, and then laminates are thermically cured until hardening. With this procedure, laminates may contain a percentage of up to 70% of fibres. Laminates are produced with various cross-sections, varying from 50×1.2 to 120×1.4 mm. These laminates are bonded on-site with epoxy resin on a concrete surface, which has been properly prepared. Prefabricated laminates are used basically for strengthening R/C members against bending.

The most common FRP material in practice for seismic repair and strengthening of R/C members is CFRP. It may be found in markets either in the form of laminates or in the form of sheets.

Laminates are produced in three different degrees of E-modulus, namely soft, medium and high. The mechanical properties of these three types are given in Table 15.7.
Type H is not used very often due to the inability of effective exploitation of its high stiffness.

CFRP sheets are basically used for:

- Confinement of columns
- Shear strengthening of beams
- Shear strengthening of walls

They are usually found in two main categories, namely, C sheets with unidirectional fibres and *low* or *high* modulus of elasticity. The mechanical properties of these two types are displayed in Table 15.8.
CFRP sheets of low modulus of elasticity are used for column confinement, while sheets of high E-modulus are used basically for shear strengthening.

Figures 15.9 through 15.11a,b exhibit the application of CFRPs for R/C member strengthening. Producers' manuals give in detail all necessary information on technical properties

Table 15.7 Mechanical characteristics of CFRP laminates (indicative values)

Properties	Type S	Type M	Type H
Modulus of elasticity	>165.000 N/mm²	>210.000 N/mm²	>300.000 N/mm²
Tensile strength	>2.800 N/mm²	>2.400 N/mm²	>1.350 N/mm²
Mean tensile strength at failure	>3.050 N/mm²	>2.900 N/mm²	>1.450 N/mm²
Failure deformation/design strain	>1.7% 0.6–0.8%	>1.2% 0.6–0.8%	>0.45% 0.6–0.8%
Colour		Black	
Fibre content (volumetric)		≈68–70%	

Table 15.8 Mechanical characteristics of CFRP sheets (indicative values)

Properties	Low E-modulus	High E-modulus
Modulus of elasticity	>240.000 N/mm²	>640.000 N/mm²
Tensile strength	>3.500 N/mm²	>3.500 N/mm²
Failure deformation	1.55%	0.4%
Weight	200 g/m²	400 g/m²
Mean thickness	0.117 mm	0.190 mm
Design strain	0.4–0.6%	0.2%
Safety coefficient S	1.2	1.2

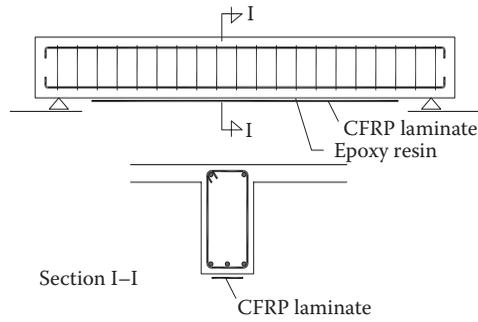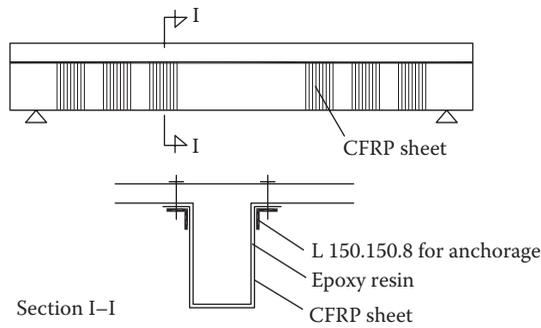*Figure 15.9* Strengthening of a T beam against bending by applying CFRP laminates.

Figure 15.10 Strengthening of a T beam against shear by applying CFRP sheets.
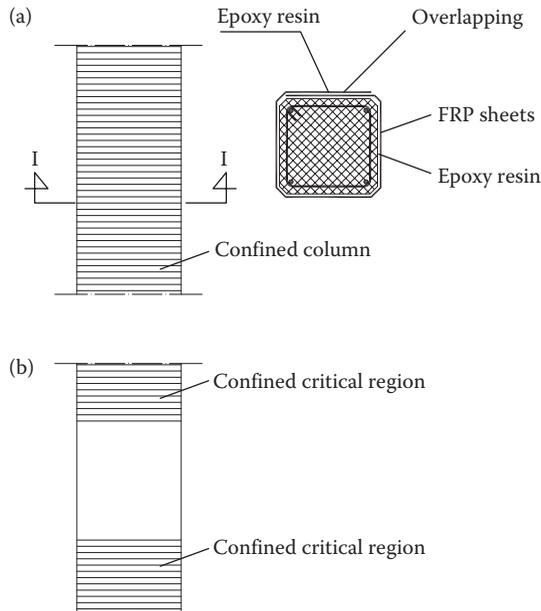

Figure 15.11 Confinement of an orthogonal R/C column by applying CFPR sheets: (a) wrapping with FRP sheets for axial strength enhancement; (b) wrapping with FRP sheets at the plastic joints for increasing ductility capacity of the plastic joints.

of the available materials, their application techniques and the specifications with which they comply.

In closing, it should be noted that C laminates or C sheets may be used in successive layers.

15.3 REDIMENSIONING AND SAFETY VERIFICATION OF STRUCTURAL ELEMENTS

15.3.1 General

Repair and strengthening have to do mainly with several interface issues, which are due to the damage itself or are created by the intervention. New materials are added to the existing structural elements, for example, concrete to concrete, epoxy resin to concrete, steel to concrete, steel acting through welding and so on. Consequently, load transfer from the original element to the additional 'reinforcing' materials is carried out through discontinuities, by means of unconventional mechanisms like friction, dowel action, large pull-out action, adhesion and so on. The systematic study of these mechanisms constituting a kind of new mechanics of the non-continuum appears to be a fundamental prerequisite for the rational design of repaired and strengthened structural elements (Tassios, 1983; Tassios and Vintzeleou, 1987; CEB, 1991). However, besides the independent study of these force transfer mechanisms, the proper combination of several of them in integrated physical and mathematical models is needed for the safety verification of the structural elements, since the various repair or strengthening techniques may activate several force transfer mechanisms simultaneously. In this context, extensive research is needed to bridge the existing gaps in knowledge in this area until this process is applicable to practical problems.

Therefore, at present, redimensioning and safety verification follow in interventions practice a semi-empirical procedure based on practical rules supported by experimental evidence. In subsequent subsections these two methods will be presented in detail.

15.3.2 Revised γ_m-factors

No matter which one of the two methods mentioned above is followed for the redimensioning and safety verification, it should be stressed that special attention should be given to the γ_m-factors introduced in the calculation.

Original materials will be factored by the *confidence factor* (see Chapter 14) applied to the mean values of their mechanical properties, as specified in EC 8-3/2005. The strengths of additional materials bonded to the original structural elements must be divided by increased γ_m-factors in recognition of the additional uncertainties in reconstruction operations. Keeping in mind the above considerations, particularly in the case of cast-in-place new concrete, the use of concrete with a strength of 5 MPa higher than that of the original elements has already been recommended (Section 15.2). Thus, the designer may retain the same γ_m-factor for both the original and the new element, on the condition that the strength introduced in the redesign calculations will be that of the original concrete.

15.3.3 Load transfer mechanisms through interfaces

In the following paragraphs the most common transfer mechanisms along the several discontinuities or interfaces between existing and additional material will be presented as they were grouped in EC8/Part 1.4/Draft (CEN, 1993). A separate section will be devoted next

(Section 15.5) to load transfer mechanisms between FRPs and concrete due to the significant importance of this mechanism for repair and strengthening of R/C members using FRPs.

15.3.3.1 Compression against pre-cracked interfaces

During reloading after cracking due to tension, compressive forces may be carried prior to full recovery of the previous extensional deformation, since the protruding elements constituting the rough surface at both faces of a crack may come into earlier contact due to their transversal microdisplacement (uneven bearing). Consequently, it is allowed to account for this phenomenon by means of an appropriate model (Figure 15.12; Tassios, 1983; Gylltoft, 1984). The quantitative evaluation of such a model needs extensive experimental support.

15.3.3.2 Adhesion between non-metallic materials

Local adhesion versus local slip between old and new materials may be accounted for by means of appropriate models, but taking into account their sensitivity to curing conditions and the characteristics of possible bonding agents. Taking into account that the value of the slip needed to mobilise adhesion is very low, it is permissible to consider that the entire adhesion resistance is developed under almost zero displacement (Figure 15.15; Hanson, 1960; Ladner and Weber, 1981; Tassios, 1983).

15.3.3.3 Friction between non-metallic materials

In several cases, friction resistance may be accounted for as a function of relative displacement (slip) along the discontinuity or along the interface. A constitutive law must be formulated for this purpose based on experimental data (Figure 15.13).

In some cases, when the slip needed to activate the maximum friction resistance (τ_u) is relatively low, the concept of a 'friction coefficient', that is,

$$\tau_u = \mu\sigma_u \tag{15.1}$$
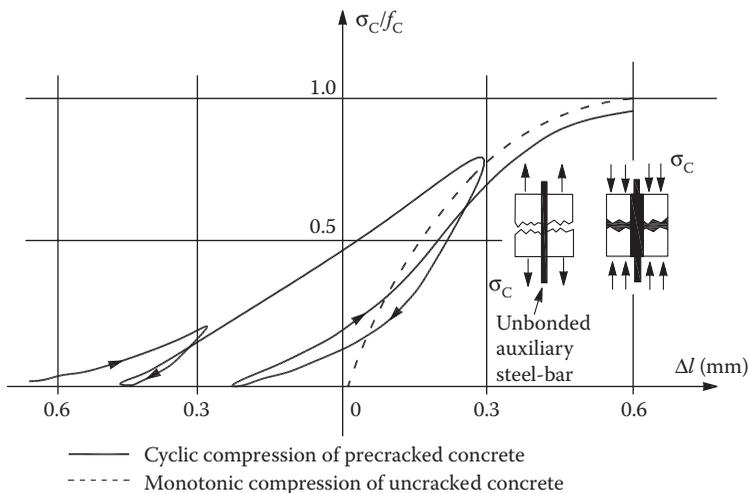
Figure 15.12 Monotonic and cyclic compression of cracked concrete.
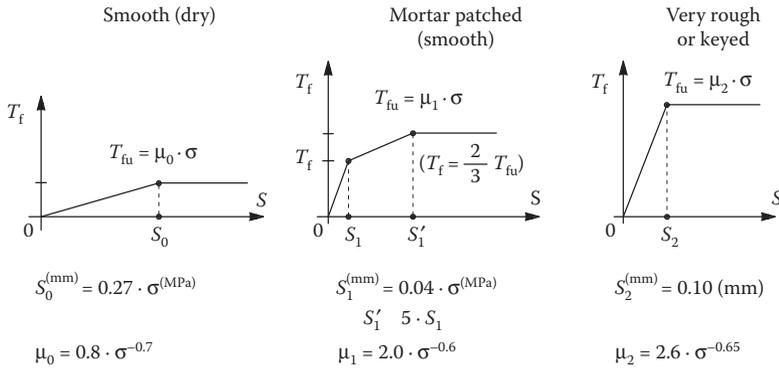
Figure 15.13 Formalistic models for concrete-to-concrete friction as a function of normal compressive stress σ.
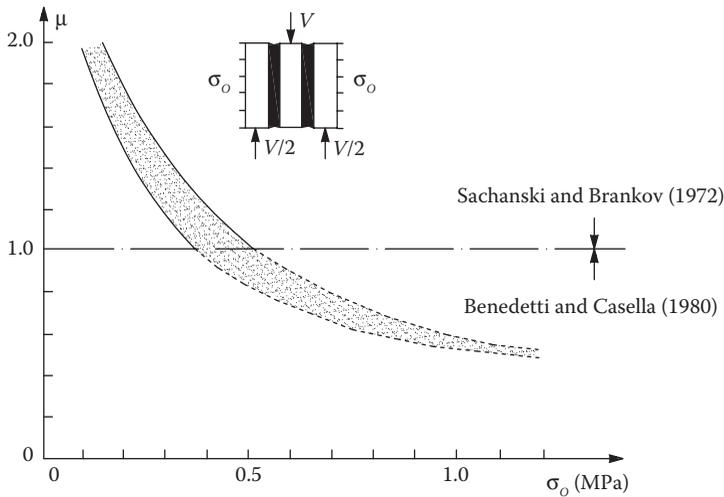
Figure 15.14 Friction coefficients for masonry as a function of the average normal stress.
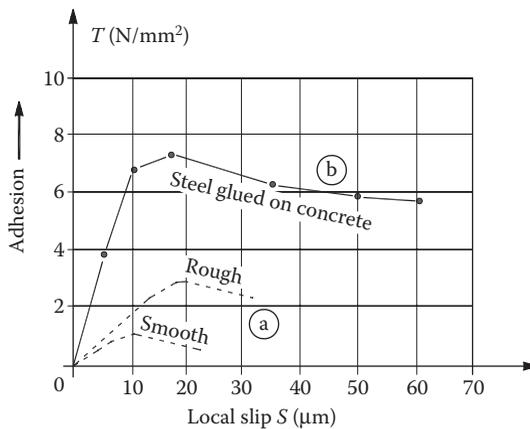
Figure 15.15 Constitutive law of adhesion: (a) concrete-to-concrete through bonding agent (Hanson, 1960); (b) steel sheets glued to concrete by means of epoxy resin (Ladner and Weber, 1981).

may be used. However, for relatively low σ-values, the strong relation between 'μ' and 'σ' values must be taken into account (Figure 15.14; Tassios, 1983, 2009).

15.3.3.4 Load transfer through resin layers

The tensile strength of the contact interface between a resin layer and a given material (e.g. concrete) may be taken as equal to the tensile strength of the weaker of the two. Therefore, in the case of concrete, its tensile strength f_{ctm} must be introduced in all calculations related to the load transfer through this interface. Of course this value must be divided by a γ_m at least equal to 1.5. The local shear resistance generated along such an interface is a function of the local slip and the normal stress acting on the area under consideration. Figure 15.15 gives the constitutive law of the shear resistance as a function of the slip for σ-equal to zero (adhesion).

15.3.3.5 Clamping effect of steel across interfaces

The friction generated across a sheared interface transversely reinforced by well-anchored steel bars may be evaluated as follows (Figure 15.16; Chung and Lui, 1978):

1. In the case of an expected large relative displacement along the interface, the ultimate friction resistance may be estimated as

$$\tau_R = \mu\sigma_{tot} \not> \tau_{um} \qquad (15.2)$$

   Where μ denotes the friction coefficient available under normal stress (Figure 15.13) and

$$\sigma_{tot} = \rho f_y + \sigma_o \qquad (15.3)$$

   f_y is the yield strength of steel.
   σ_o is the external normal stress across the interface.
   ρ is the effective steel ratio along the interface.
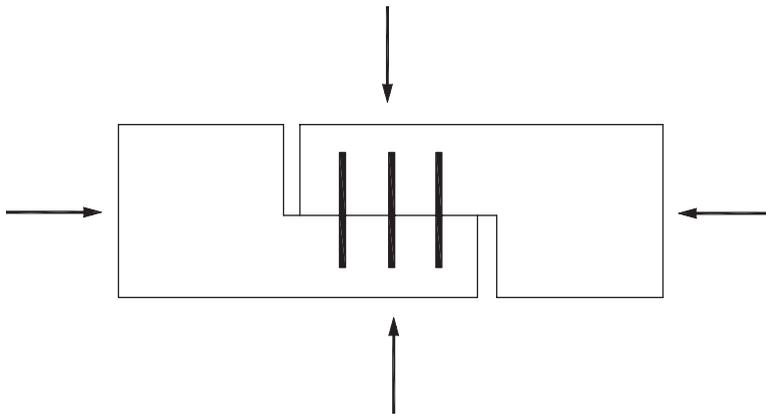 $\tau_{u,m}$ is the shear resistance of the material itself.

Figure 15.16 Clamping effect of steel across interfaces.

2. If large slips along the interface are not tolerated, the generated friction resistance is evaluated, taking into account the displacement compatibility on both faces of the interface.

15.3.3.6 Dowel action

The design value of the maximum shear force that may be transferred by a bar crossing an interface may be calculated, taking into account the strength and deformability of the dowel and the connected material as well as the distance of the dowel from the edges. According to Rasmussen (1963), for the plastic compressive stage:

$$D_u \cong 1.3 d_b^2 \sqrt{f_c f_y} \qquad (15.4)$$

while according to Vintzeleou and Tassios (1986) for the post-cracking stage:

$$\frac{D}{D_u} \cong 0.7 \sqrt[4]{s}(\text{mm}) \quad \text{for } d_b \cong 12 - 22\,\text{mm} \qquad (15.5)$$

where
D_u is the ultimate capacity of a dowel embedded in uncracked concrete.
f_c is the unconfined strength of concrete.
f_y is the yield strength of steel.
d_b is the dowel diameter.
s is the local slip at the interface (in mm).
D is the dowel action for slip equal to s.

15.3.3.7 Anchoring of new reinforcement

1. Anchorage lengths of steel bars in new concrete must follow the criteria of relevant codes such as EC2. In the case of bar anchorages in holes bored in old concrete where special grouts are used (e.g. high-strength concrete with shrinkage compensating admixtures, resin concretes, etc.), shorter anchorage lengths are needed. These are specified in the manuals of the material used and must be verified by pull-out tests performed by an authorised laboratory.
2. In most cases, the anchoring of additional steel bars is accomplished by welding them onto the existing bars directly or by means of additional welded spacers (Figure 15.7); such force transfers may be considered rigid. In such cases it is necessary to verify that the bond ensured by the existing bar is sufficient to anchor the total force acting on both bars.

15.3.3.8 Welding of steel elements

In designing steel-to-steel connections by means of welding, in addition to the checks of welding resistance, the following mechanical behaviour should be considered, since the activation of force transfer depends on the concept of the connections:

- Direct welding of additional bars or steel profiles on existing ones ensures a complete generation of force transfer with almost zero slip.
- Intermediate deformable steel elements necessitate the introduction of proper models so that compatibility of deformations may be ensured (Tassios, 1983).

15.3.3.9 Final remarks

From the preceding presentation the following conclusions may be drawn:

a. The constitutive laws of the transfer mechanisms need to be supported by additional experimental evidence covering several parameters related to the intervention techniques.

b. It should be stressed that in designing the repair or strengthening of a structural element, several force transfer mechanisms are generated, so that only an integrated model based on the finite element method (FEM) may take all of them into account, the interrelations among them, and the level at which each of them is activated during loading, as happens with the analysis of original R/C elements or masonry walls (Ignatakis et al., 1989, 1990).

c. Furthermore, even if such models based on the FEM were available, they would have to be verified through experimental evidence on repaired or strengthened structural subassemblages.

d. From the foregoing follows that at present the formation of integrated analytical models cannot yet lead to dimensioning or safety verification methods for general use, suitable for practical applications. However, it is hoped that in the near future this procedure will lead to the derivation of reliable models.

e. For the time being, the approach to the problem is based on a simplified estimation of resistances originating from practical rules that are verified by laboratory tests. Sometimes this approach is combined with oversimplified models of force transfer mechanisms, as will be seen later. In the next subsection the basic concept of this semi-empirical method used in practice will be given in detail.

15.3.4 Simplified estimation of the resistance of structural elements

1. The basic concept in developing any repair or strengthening technique is to ensure that failure of the repaired structural element as a monolithic unit will precede any failure at the interfaces between old and new material. This is verified by tests, and where failure at the interfaces occurs first, extra connecting means are provided on an empirical basis (e.g. closer-spaced dowels, a resin layer between old and new concrete). In order for this basic concept to be accomplished, the specifications referring to each intervention technique should be rigorously followed during the execution of the work.

2. With the above concept as a prerequisite, specimens of the repaired or strengthened structural elements are tested in the laboratory under monotonic or cyclic loading to failure, and relevant displacement versus resistance diagrams are plotted. From these diagrams the basic values of ultimate strength $R_{u,rep}$, stiffness K_{rep} and energy dissipation $E_{u,rep}$ are determined.

3. At the same time, the above values are calculated based on the assumption that the structural element under consideration was constructed as a monolithic unit, including the initial element and its additional elements in the form of repair (e.g. R/C jackets). It is obvious that the respective values of $R_{u,monol}$, K_{monol} and $E_{u,monol}$ will be greater or at least equal to those of the repaired element due to the fact that interface deficiencies are not taken into account in the calculation of $R_{u,monol}$, K_{monol}, $E_{u,monol}$. Therefore, *'model reduction factors'* are introduced (EC8 Part 1.4/ENV draft, EC8-3/2005 Annex A [informative]), that is,

$$\varphi_R = \frac{R_{u,rep}}{R_{u,monol}} \quad \varphi_K = \frac{K_{rep}}{K_{monol}} \quad \varphi_E = \frac{E_{u,rep}}{E_{u,monol}} \tag{15.6}$$

The index 'monol' refers to a monolithic element consisting of the initial element and the repair. These factors allow the redimensioning and safety verification of the repaired element to be carried out as if it were a monolithic unit. In fact, the results of the calculation of the resistance of a repaired or strengthened element that is based on monolithic considerations are multiplied by the model reduction factors, in order to comply with the capacity expected for the repaired or strengthened element. These reduced results of the resistance are introduced in the design verification at ULS. The whole procedure is accomplished with some additional simplified force transfer checks at the critical interfaces, as will be discussed later.

4. From the preceding presentation it may be concluded that *'model reduction factors'* have reliable values only for the special cases for which laboratory tests have been performed. If the geometrical data of the original and the added sections are different, or the span or the height of the structural element changes, there is no evidence that these values will still be valid. Therefore, it is clear that additional experimental and analytical research is urgently required to provide information about the seismic behaviour of structures repaired or strengthened using different techniques (Rodriguez and Park, 1991).

15.4 REPAIR AND STRENGTHENING OF STRUCTURAL ELEMENTS USING CONVENTIONAL MEANS

15.4.1 General

Structural elements, depending on the desirable seismic resistance, the damage level and the type of their joints, may be repaired or strengthened with resin injections, replacement of broken-off parts, R/C jackets, metal cages or FRPs.

As mentioned in Subsection 15.3.3, the key to the success of the repair or strengthening procedure is to attain a high degree of bonding between the old and the new concrete. This can be accomplished as follows:

- By roughening the surface of the old concrete
- Coating the surface with epoxy or another type of resin before concreting
- Welding reinforcement bars
- Using steel dowels

The ductility of the repaired element is improved by proper confinement with closely spaced hoops, steel jackets, composite materials (FRP) jackets and so on.

It should be kept in mind that changes in the sectional area of the structural elements lead to a redistribution of stress due to resulting changes in the stiffness of the various structural elements.

Metal cages made of steel angles and straps are used exclusively for column repair. However, the repair of the joint between column and beam is not possible.

The bonding of metal plates or FRP laminates on concrete is in general a technique easy to apply, whereby zones under tension can be strengthened without altering the stiffness.

The last two methods require special means of fire protection, which is not the case with R/C jackets.

Repair and strengthening of R/C members using FRP sheets or laminates will be examined separately in the next Section 15.5 because their safety verification requires a detailed examination of the load transfer mechanisms between FRPs and concrete, and because in the last 15 years this technique has been gaining more ground every day.

15.4.2 Columns

Damage to columns appears at different levels, such as:

- Fine cracks (horizontal or diagonal) without crushing of concrete or failure of reinforcement.
- Surface spalling of concrete without damage to the reinforcement.
- Crushing of concrete, breaking of the ties and buckling of the reinforcement.

Depending on the degree of damage, different techniques may be applied, such as resin injections, and removal and replacement or jacketing.

15.4.2.1 Local interventions

Resin injections and resin mortars are applied only for the repair of columns with small cracks or peelings, without crushing of concrete or damage to the reinforcement. The degree of retrofit can be checked by comparing the force–displacement (H–δ) diagrams of the original column and the repaired one with epoxy resins (Figure 15.17; Sariyiannis and Stylianidis, 1990; Sariyiannis, 1990). The results from such comparisons are very encouraging, with regard to the effectiveness of the repair.

Removal and replacement are applied in columns with a high degree of damage, that is, crushing of concrete, breaking of ties and buckling of longitudinal reinforcement. Of course, before carrying out such work, a temporary support system is always provided to carry the column loads. Then, if concrete failure is only superficial, partial removal and repair are carried out (Figure 15.18). Otherwise, in the case of a total failure, there is a complete removal of the material, placement of new longitudinal reinforcement with welding, placement of new closely spaced ties and concreting (Figure 15.19). It should be mentioned that, in the first case, good bonding between old and new concrete is absolutely necessary. In the second case, most of the time the construction of an R/C jacket follows the retrofit.
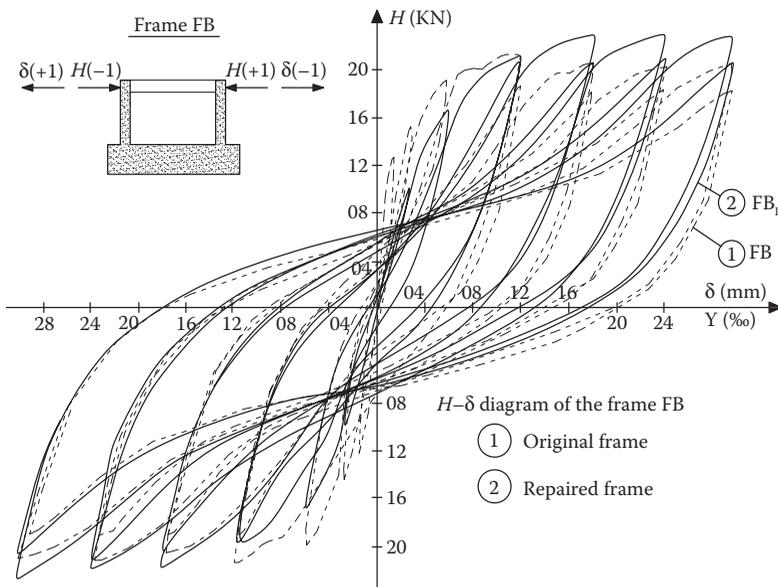

Figure 15.17 H–δ diagram of the original frame and then when repaired with epoxy resin injections.
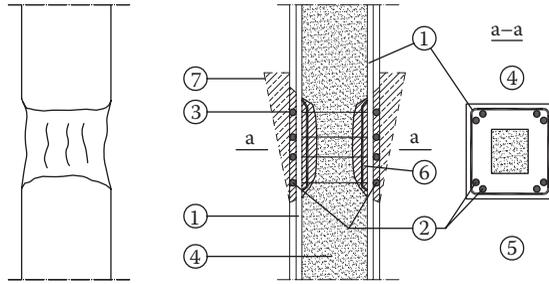
Figure 15.18 Column repair in the case of superficial damage: 1 = existing reinforcement; 2 = added new reinforcement; 3 = added new ties; 4 = existing concrete; 5 = new concrete; 6 = welding; 7 = temporary cast form.
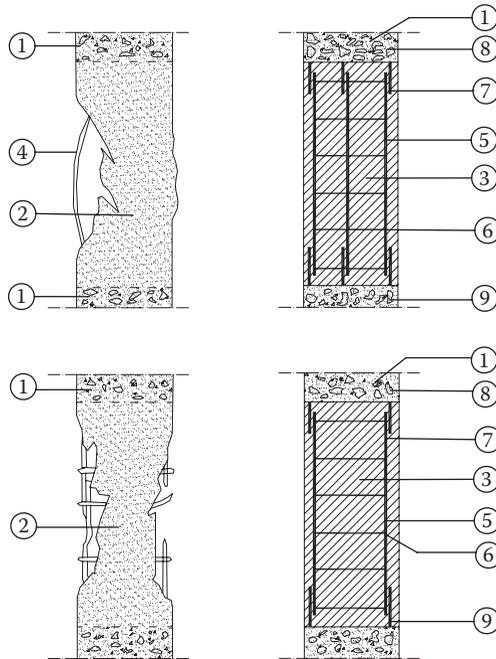
Figure 15.19 Repair of a seriously damaged column: 1 = existing undamaged concrete; 2 = existing damaged concrete; 3 = new concrete; 4 = buckled reinforcement; 5 = added new reinforcement; 6 = added new ties; 7 = welding; 8 = existing ties; 9 = existing reinforcement.

15.4.2.2 R/C jackets

R/C jackets are applied in the case of serious damage or inadequate seismic resistance of the column. Jackets are applied basically at all sides of the perimeter of the column, which is the ideal case. However, sometimes, depending on the existing local conditions, jackets are applied on one or more sides (Figure 15.20). In cases where the jacket is limited to the storey height, an increase in the axial and shear strength of the column is achieved with no increase in flexural capacity at the joints. Therefore it is recommended that the jackets extend beyond the ceiling and the floor slabs of the storey where column repair is necessary (Figure 15.21).

Figure 15.20 R/C column jacketing arrangement: 1 = existing column; 2 = jacketing concrete.

Figure 15.21 Column jackets: (a) jacket along the height of one storey; (b) jacket extended to the upper and lower storey; 1 = slab, 2 = beam, 3 = existing column, 4 = jacket, 5 = added longitudinal reinforcement, 6 = added ties.

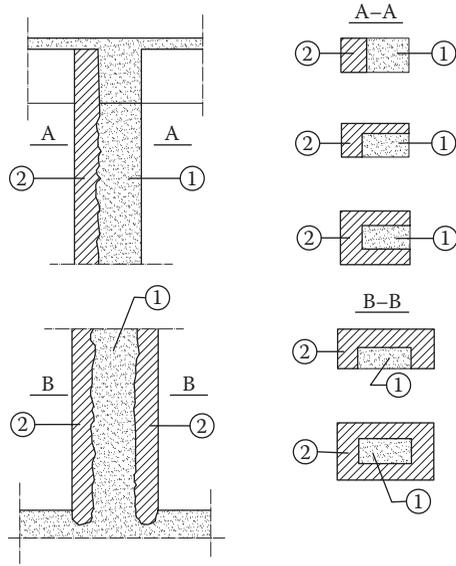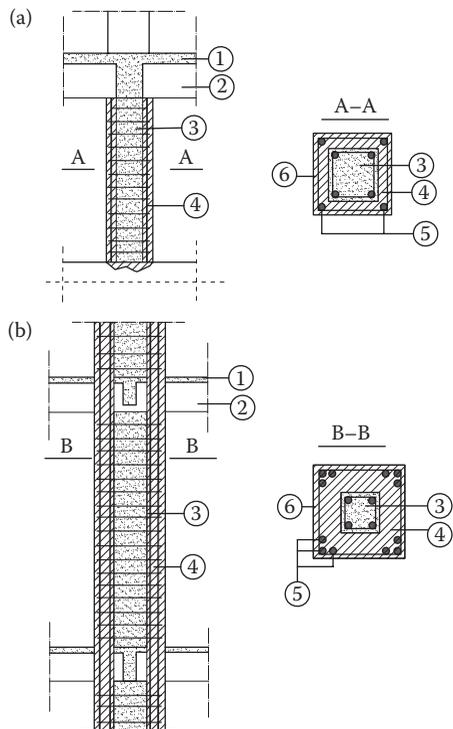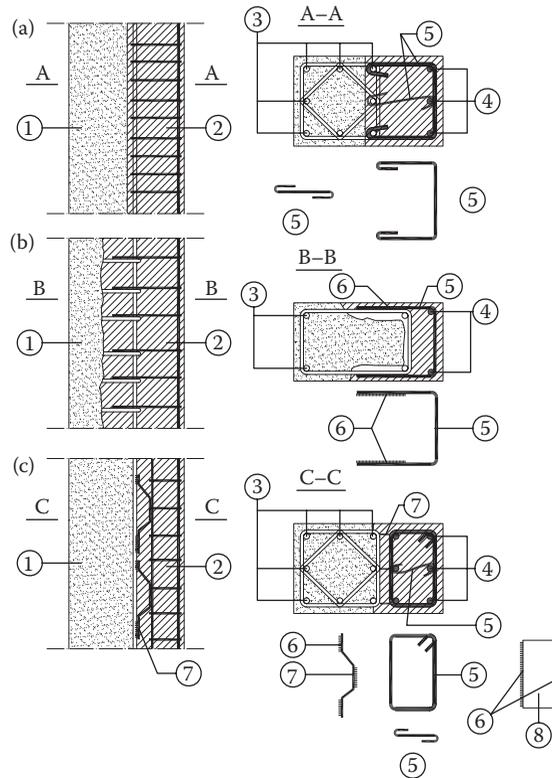*Figure 15.22* One-sided strengthening of a column: (a) use of hooks for reinforcement connection; (b) use of welding of ties for reinforcement connection; (c) use of welded bent bars for reinforcement connection. 1-existing column; 2 = jacket; 3 = existing reinforcement; 4 = added longitudinal reinforcement; 5 = added ties; 6 = welding; 7 = bent bars; 8 = metal plate.

In the case of one-sided jackets, special care should be taken to connect the old with the new part of the section; this can be accomplished by welding closely spaced ties to the old reinforcement (Figure 15.22).

In the usual case of full jackets, the composite action of the old and new concrete is sometimes left solely to the natural bonding of the two materials, which can be strengthened with roughening of the old surface. It is also sometimes strengthened by welding some bent-up bars between the old and new longitudinal reinforcement (Figure 15.23). This connection is necessary when the column has completely deteriorated or when its height is too great, in which case there is a danger of buckling of the new longitudinal reinforcement. However, laboratory tests have shown that, in general, the degree of composite action obtained is very satisfactory even without the strengthening of force transfer by welding the longitudinal reinforcement (Zografos, 1987).

15.4.2.3 Steel profile cages

In general, this is a technique not widely used. The cage consists of four steel angles of minimum dimensions L 50.50.5, which are connected to each other with welded blades of minimum dimensions 25.4 mm (see Paragraph 12.5.2.3, Figure 12.9). Prior to welding, the angles are held tight on the column with the aid of transverse angles and pre-stressed ties. The voids between the angles and the concrete are filled with non-shrinking mortar (EMAKO,
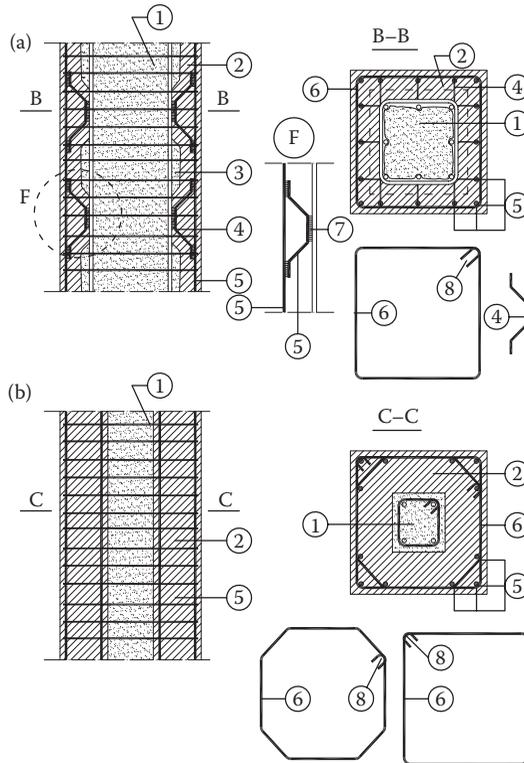
Figure 15.23 Connection of the old to the new reinforcement of the jacket: (a) protection of new bar against buckling with welding; (b) protection of new bars against welding with octagonal ties. 1 = existing column; 2 = jacket; 3 = key; 4 = bent bars; 5 = added reinforcement; 6 = ties; 7 = welding; 8 = alternating corners.

EMPECO, etc.) or resin grout, and then the column is covered with gunite or cast-in-place concrete reinforced with welded wire fabric. It is obvious that, with this arrangement, increase in the flexural capacity of the column at the joints with the top and bottom is impossible, due to the fact that the cage is not extended into the floors above and below.

15.4.2.4 Steel or FRP encasement

Steel or FRP encasement is the complete covering of an existing column with thin steel or FRP sheets. This type of intervention offers the possibility of only a small increase in column size. Steel sheets (with 4–6 mm thickness) are welded together throughout their length and located at a distance from the existing column. The voids between the encasement and the column are filled with non-shrinking cement grout.

The strengthening with FRP can be accomplished basically with encasement using FRP sheets bonded on the concrete surface. Unidirectional fibres of the sheet are arranged transversally to the column axis.

In this context, strengthening may aim at improving:

- Ductility through confinement
- Shear resistance
- Lap splice resistance of the original reinforcement

Bending enhancement of the column may also be achieved by bonding of FRP laminates parallel to the column axis. However, the flexural strength of the frame structure cannot be improved because it is impossible to pass the encasement through the floors.

15.4.2.5 Redimensioning and safety verifications

Experimental results (Sariyiannis and Stylianidis, 1990; Sariyiannis, 1990; French et al., 1990; Stylianidis, 2012) regarding the dimensioning of repaired columns have shown the following:

1. In the case of repair with resin injections, the ratio of the strength of the repaired element to that of the original one is about 1. In general, the epoxy-repaired cracks do not reopen in tests; new cracks tend to develop adjacent to the repaired ones. The stiffness of the repaired column appears to exceed 85% of the original one, and the same happens with the energy dissipation capacity, that is:

$$\frac{R_{d,rep}}{R_{d,orig}} \cong 1 \quad \frac{K_{rep}}{K_{orig}} \cong 0.85 \quad \frac{E_{rep}}{E_{orig}} \cong 0.85 \qquad (15.7a)$$

The bond between reinforcement and concrete also appears to be restored, even for high inter-storey drifts exceeding 4%.

Similar results have been incorporated in FIB state-of-the-art-report Bulletin 24 Seismic assessment and retrofit of R/C buildings (2003). According to this document the statistical evaluation of 33 experimental tests of repaired columns and R/C walls injected with epoxy resins has given the following results:

$$\frac{M_{y,exp}}{M_{y,pred}} = 1.04, \quad \frac{K_{ef,exp}}{K_{ef,pred}} \cong 0.89, \quad \frac{\theta_{u,exp}}{\theta_{u,pred}} \cong 0.95 \qquad (15.7b)$$

Predicted capacity values have resulted from the design of the original member.

2. In the case of repair with reinforced cast-in-place jackets, the experimental results have shown (Zografos, 1987; Bett et al., 1988; Bush et al., 1990) that the lateral capacity of the strengthened column can be reliably predicted, assuming complete compatibility between the jacket and the original column. For jackets with gunite concrete, despite all the contrary estimation (NTU, 1978), the results fall slightly below those of conventional R/C jackets cast in forms. However, given the fact that field conditions are not as ideal as those of a laboratory, the author's opinion is that, on the one hand, the new concrete must have a strength 5 M Pa greater than that of the original element, and on the other, a model correction factor $\varphi \cong 0.90$ for the strength and the stiffness of the repaired element should be introduced.

$$\frac{R_{d,rep}}{R_{d,monol}} \cong 0.90, \quad \frac{K_{rep}}{K_{monol}} \cong 0.90 \qquad (15.8a)$$

The index 'monol' refers to a monolithic element consisting of the initial element and the jacket.

Similar results have been presented in the above-mentioned FIB Bulletin 24 (2003) document as a result of the statistical evaluation of 15 experimental tests of jacketed columns, as follows:

$$\frac{M_{\mathrm{y,exp}}}{M_{\mathrm{y,monol}}} = 0.97, \quad \frac{K_{\mathrm{ef,exp}}}{K_{\mathrm{ef,monol}}} \cong 1.02, \quad \frac{\theta_{\mathrm{u,exp}}}{\theta_{\mathrm{u,monol}}} \cong 1.08 \tag{15.8b}$$

3. In the case of repair with metal cages of straps and angles (Arakawa, 1980; Tassios, 1983), redimensioning may be carried out according to what was suggested in (2).
4. In the case of repair with bonded steel sheets, the additional shear resistance V_{fc} of the column may be estimated by the following expression:

$$V_{\mathrm{fc}} = 2tf_{\mathrm{y}}h\cot\delta \tag{15.9}$$

where
   f_{y} is the yield strength of the steel sheet.
   t is the thickness of the plate.
   h is the dimension of the column cross-section parallel to V_{fc}.
   δ is the angle between the column axis and diagonal cracks. It may be considered that $\delta = 30°$ (Priestley and Seible, 1991).

   The coefficient 2 has been introduced to take into account that the plates are bonded on both sides over the shear crack. In both cases a load transfer verification control is necessary on the bond interface between concrete and sheet (Subsection 15.3.3).
5. Safety verification of strengthening with FRPs will be examined in Section 15.5 collectively for all cases of strengthening with FRPs.

15.4.2.6 Code (EC 8-3/2005) provisions

Eurocode EC 8-3/2005 gives the following recommendations in its Annex A in the form of information:

1. *Concrete jacketing*
   a. For the purpose of evaluating strength and deformation capacities of jacketed members, the following approximate assumptions may be made.
      • The jacketed member behaves monolithically
      • The fact that axial dead load is originally applied to the original column alone is disregarded
      • The concrete properties of the jacket may be assumed to apply over the full section
   b. The following relations may be assumed to hold between the values V_{R}, M_{y}, θ_{y} and θ_{u} calculated under the assumptions above and the values V_{R}^*, M_{y}^*, θ_{y}^* and θ_{u}^* to be adopted in the capacity verifications:

$$\frac{V_{\mathrm{R}}^*}{V_{\mathrm{R}}} = 0.9, \quad \frac{M_{\mathrm{y}}^*}{M_{\mathrm{y}}} = 1.0, \quad \frac{\theta_{\mathrm{y}}^*}{\theta_{\mathrm{y}}} = 1.05, \quad \frac{\theta_{\mathrm{u}}^*}{\theta_{\mathrm{u}}} = 1.0 \tag{15.8c}$$

2. *Steel jacketing*
   a. Steel jackets are mainly applied to columns for the purpose of:
      • Increasing shear strength
      • Increasing ductility through confinement
      • Improving the strength of deficient lap-splices
   b. Shear strength

The contribution of the jacket to shear strength given by Equation 15.9 is recommended by EC 8-3/2005 to be reduced to 50% of its value so that the jacket remains in elastic stage and in this respect is able to control the width of internal cracks.

15.4.3 Beams

As in the case of columns, depending on the degree of damage to the beams, several techniques are applied, such as resin injections, bonded metal or FRP sheets, FRP laminates, and removal and replacement of concrete and R/C jackets.

15.4.3.1 Local interventions

Resin injections are applied only for the repair of beams with light cracks without crushing of concrete.

Removal and replacement are applied to beams with a high degree of damage such as crushing of concrete or failure of reinforcement, loss of bonding and spalling due to dowel action. Propping with temporary supports always precedes repair work of this type. The procedure that is then followed is similar to that described for column repair. However, at this point it has to be stressed that difficulties may arise regarding the compaction of concrete if it is not possible for casting to be carried out from the upper side of the beam with special openings in the slab.

15.4.3.2 R/C jackets

Reinforced concrete jackets can be applied by adding new concrete to three or four sides of the beam. In the same technique one should also include the strengthening of the tension or compression zone of a beam through concrete overlays. In order to accomplish force transfer between old and new concrete, roughening of the surface of the old concrete is required, as well as welding of connecting bars to the existing bars and new reinforcement.

Reinforced overlays on the lower face of the beam (Figure 15.24) can only increase its flexural capacity. Existing reinforcement is connected to the new reinforcement by welding. Jacketing on all four sides of the beam is the most effective solution. The thickness of the concrete that is added to the upper face is such that it can be accommodated within the floor thickness (maximum: 50–70 mm). The placement of the ties is achieved through holes, which are opened in the slab at closely spaced distances and are also used for pouring the concrete. The longitudinal reinforcement bars of the jacket are welded to those of the old concrete (Figure 15.25).

Jackets on three sides of the beam are used to increase the flexural and shear capacity of the beam for vertical loading, but not for seismic actions, given that strengthening of the load-bearing capacity of the section near the supports is impossible. The key to the success of such an intervention is the appropriate anchorage of the stirrups at the top of the sides of the jacket (Figure 15.26). Due to the fact that using forms and pouring the concrete from the top is not possible, the only feasible solution is gunite concrete.

15.4.3.3 Bonded metal sheets

The technique for bonding metal sheets onto concrete was described in detail in a previous section. These sheets arc bonded either on the lower face of the beam under repair, for strengthening of the tension zone, or on the vertical sides of the beam near the supports, for
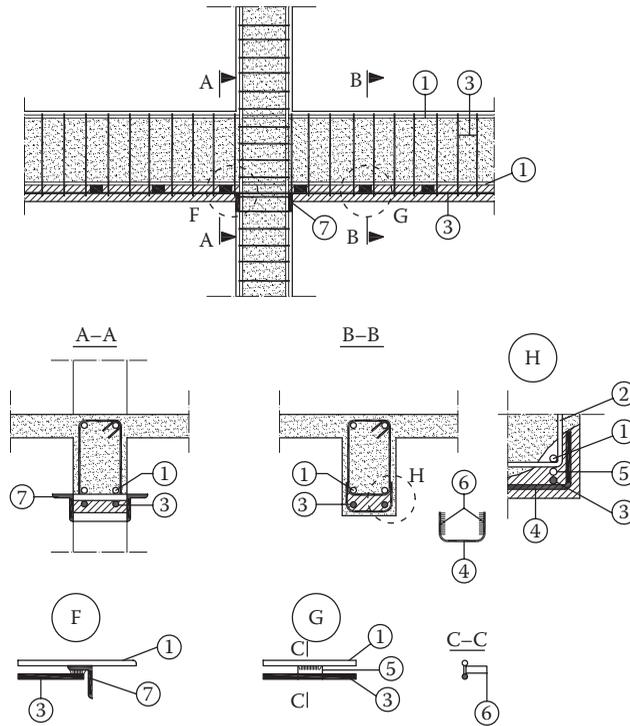
Figure 15.24 Strengthening of a beam on the lower face: 1 = existing reinforcement; 2 = existing stirrups; 3 = added longitudinal reinforcement; 4 = added stirrups; 5 = welded connecting bar; 6 = welding; 7 = collar of angle profiles.

shear strengthening. This procedure should be preceded by crack repair with epoxy resin. The bonded plates must be protected by welded wire mesh and cement plaster or shotcrete.

15.4.3.4 Redimensioning and safety verification

1. *Resin injections.* Extensive laboratory tests (Popov and Bertero, 1975; French et al., 1990; Economou et al., 1994) have shown that if there is no concrete degradation, epoxy resin injections are very effective. The repaired beam is capable of resisting several loading cycles, the initial strength is completely restored, while stiffness and energy dissipation appear to be somewhat lower than those of the original beam. Consequently, *'the model correction factor'* φ may be considered equal to 1 in this case:

$$\frac{R_{d,rep}}{R_{d,orig}} \cong 1.0, \quad \frac{K_{rep}}{K_{orig}} \cong 1.0, \quad \frac{E_{rep}}{E_{orig}} \cong 1.0 \tag{15.10}$$

2. *R/C overlays or jacketing.* Extensive experimental results have shown (Vassiliou, 1975; Tassios, 1983; Abdel-Halim and Schorn, 1989; Saiidi et al., 1990) that concrete overlays or jacketing are an effective technique for repair or strengthening. The additional layers and the parent concrete remain bonded throughout loading until failure, provided that construction specifications given in the previous paragraphs are met. The reduction in strength of the repaired beam varies between 8% and 15% of the strength
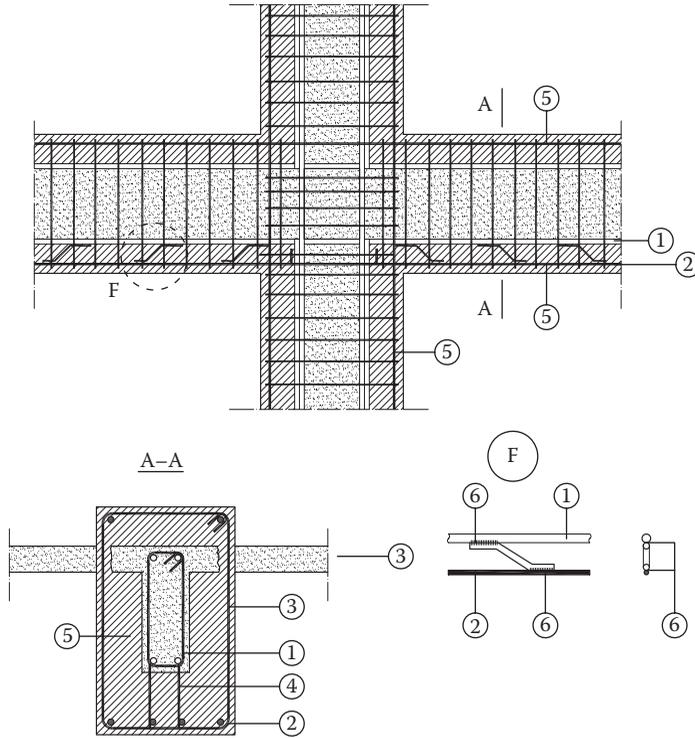
Figure 15.25 Jacket on four sides of a beam: 1 = existing reinforcement; 2 = added longitudinal reinforcement; 3 = added stirrups; 4 = welded connecting bar; 5 = concrete jacket; 6 = welding.

of the monolithic beam (initial + jacket). The reduction in stiffness of the repaired beam is somewhat higher (10–20%) with respect to the stiffness of the monolithic beam. Consequently, 'the model correction factor' φ may be considered as follows:

$$\frac{R_{d,rep}}{R_{d,monol}} \cong 0.85, \quad \frac{K_{rep}}{K_{monol}} \cong 0.80 \tag{15.11}$$

EC 8-3/2005 makes no reference to jacketed beams, nor does FIB Bulletin 24 (2003). It is anticipated that the recommendations for the reduction factor of jacketed R/C columns and walls might also be adopted for jacketed beams on all their sides.

In addition to the general strength and stiffness verifications described previously, specific verifications for the force transfer mechanisms along the several interfaces between existing and additional material should be performed. In the case where adhesion between old and new concrete is proved to be inadequate, the transfer mechanism should be ensured with extra connectors on the interface. Two such cases can be identified:

a. *Interface of connection in the tension zone* (Figure 15.27a). The shear stresses developing on the interface between old and new concrete are given, according to the theory of strength of materials applied to reinforced concrete, by the approximate relationship (Tassios, 1984):

$$\tau_{02} = V_d / \left[b_w z \left(1 + \frac{A_{s1}}{A_{s2}} \frac{(d_1 - x)}{(d_2 - x)} \frac{z_1}{z_2} \right) \right] \tag{15.12}$$
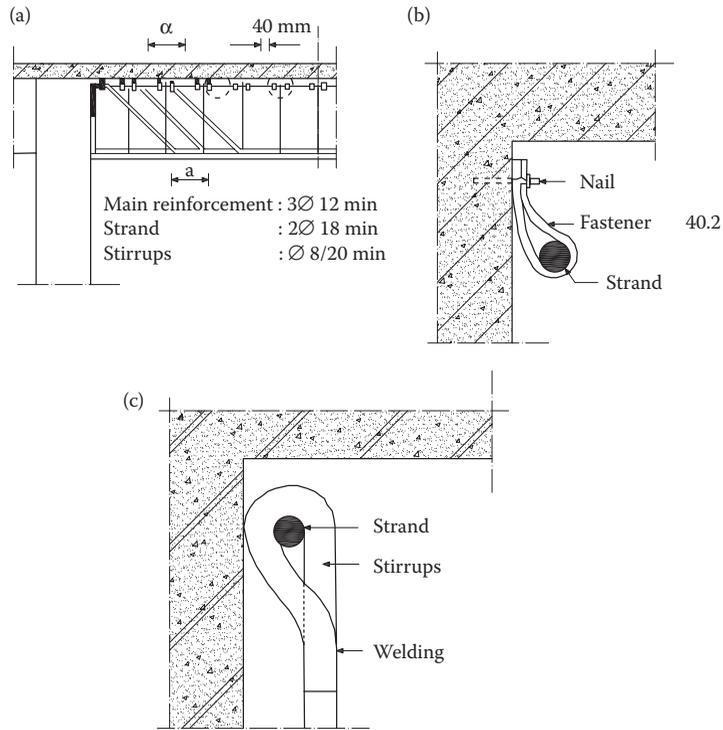
Figure 15.26 Jacket on three sides of a beam: (a) general reinforcement pattern; (b) detail of fixing of the strand; (c) detail of anchoring the ties on the strand.
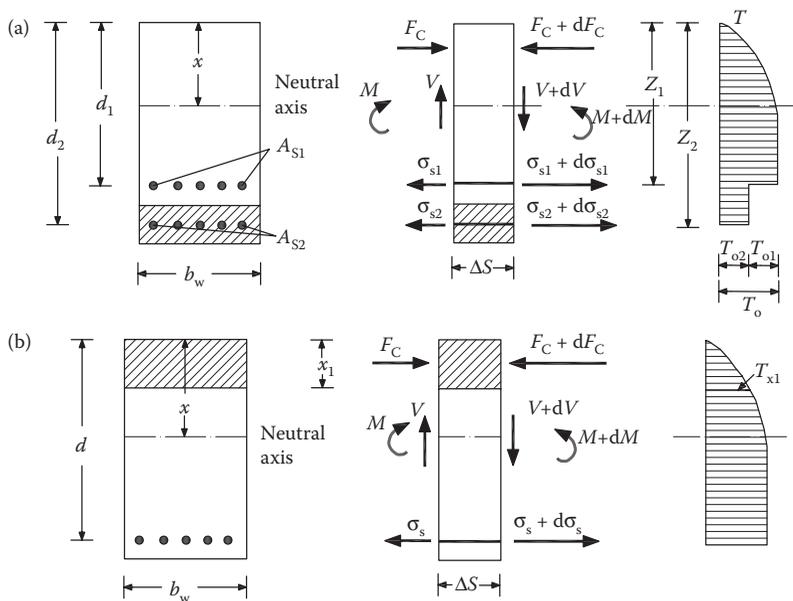

Figure 15.27 Shear stress between old and new concrete: (a) intervention in the tension zone; (b) intervention in the compression zone.

where

$$z = \frac{A_{s1}z_1 + A_{s2}z_2}{A_{s1} + A_{s2}} \tag{15.13}$$

Bearing in mind that special care is taken in ensuring the adhesion of the new to the old concrete through resin coats of higher strength than that of concrete, the value resulting from the above relationship at the interface must be compared with the basic concrete shear strength (see Paragraph 15.3.3.4).
Therefore, if τ_{02} is greater than

$$\tau_{Rdc} = \frac{V_{Rdc}}{b_w d_2} \tag{15.14}$$

(see EC2-1/2004, Chapter 8.2.5)
where
V_{Rdc} is design capacity for shear without reinforcement in (N).
$b_w d_2$ are the dimensions of the cross-section in (mm).
τ_{Rdc} is the shear stress capacity of a beam without shear reinforcement in (N/mm^2).
That is,

$$\tau_{02} \geq \tau_{Rdc} \tag{15.15}$$

    or

$$\tau_{02} \geq \tau_{Rdl} \tag{15.16}$$

then the total shear flow ($T = \tau_{02}b$) must be carried by welding of the new reinforcement to the old one.
Therefore, for a distance α between successive weldings, welding thickness t and number η of new bars, the welding length l_{wel} must be equal to (Figure 15.7)

$$l_{weld} = \frac{\tau_{02} \cdot b_w \cdot \alpha}{t \cdot n \cdot 0.8 f_{yd}} \tag{15.17}$$

where $f_{yd} = f_{yk}/1.15$ is the yield stress of the welding steel divided by the safety factor γ_s of the material (design strength). It is understood that a *'model correction'* factor equal to 0.8 has been introduced in Formula 15.17.

b. *Interface of connection in the compression zone* (Figure 15.27b). The shear stresses developing at the interface between the old and the new concrete are again given according to the classic theory of strength of materials by the approximate relationship:

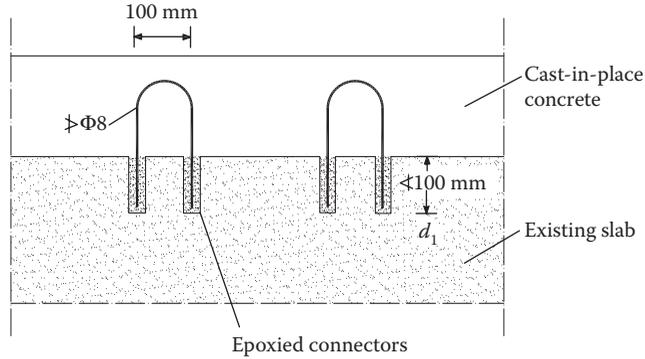$$\tau_{x1} = \frac{V_d}{b_w z} \frac{x_1}{x} \left(2 - \frac{x_1}{x} \right) \tag{15.18}$$

Figure 15.28 Shear connectors between old and new concrete in the compression zone.

If the resulting value of τ_{x1} is greater than τ_{Rdc}, as defined above, the total shear flow ($T = \tau_{x1}b$) must be carried by shear connectors (Figure 15.28). The ultimate shear carried by the two legs of such a connector is equal to (Tassios, 1984):

$$D_u \cong 2d^2\sqrt{f_{cd}f_{yd}} \tag{15.19}$$

where d is the diameter of the connector, f_{cd} the design strength of concrete and f_{yd} is the design strength of the connector's steel. In Equation 15.19, a model correction factor $\varphi = 1.30$ has been introduced (Paragraph 15.3.3.6).

3. *Bonded metal sheets.* The required section b_t of a sheet in a flexural area is expressed by the relationship:

$$\Delta M_d \leq (bt)zf_{yd}$$

and hence,

$$(bt)_{req} \geq \frac{\Delta M_d}{zf_{yd}} \tag{15.20}$$

(model correction factor equal to 1) where ΔM_d is the additional moment (strengthening) beyond the ultimate M_{du} carried by the original section (ΔM_d should not be greater than $0.5M_{du}$ for construction reasons), z is the lever arm of the internal forces and f_{yd} is the design strength of the sheet.

The required anchorage length of the sheet is given by the relationship:

$$l_a = \varphi\left(\frac{f_{yd}}{r \cdot \tau_u}t\right) \tag{15.21}$$

where φ is the model correction factor ($\varphi \cong 1.3$), f_{yd} the design strength of the sheet, t is the thickness of the sheet and τ_u the maximum local adhesion strength between concrete and the steel sheet. For sheet thickness $t < 1$ mm, the recommended value for $\tau_u \cong 2f_{ctd}$, while for $t = 3$ mm, the recommended value for $\tau_u \cong f_{ctd}$ (Figure 15.15). Note that f_{ctd} is the tensile design strength of concrete and r is the correction factor to take

into account the non-uniform distribution of τ_u over the bonding area due to the different slippage from point to point, from the crack to the end of the sheet. Recommended value: $r = 0.40$ (Tassios, 1983).

The required thickness t of the sheets that are bonded on both sides of a beam over shear cracks to carry additional shear forces may be given by the relationship (Tassios, 1984):

$$\Delta V_d \leq 2t \cdot z \cdot f_{yd} \cot \delta$$

$$t_{req} \geq \frac{1}{2} \frac{\Delta V_d}{2z \cdot f_{yd} \cot \delta} \qquad (15.22)$$

For the meaning of the symbols included in the above relationships see Paragraph 15.4.2.5, item (4).

The safety verification of the force transfer through the bonded interface may be carried out with the aid of the following expressions (Figure 15.29; Tassios, 1983):

$$\frac{\Delta V_d}{2} \leq F_s = \left(\frac{1+\xi}{2}\right) d \cdot l_o \cdot r \cdot \tau_u \qquad (15.23)$$

taking into account that:

$$l_o = (1 - \xi) d \cot \delta$$

the Equation 15.23 takes the form:

$$\frac{\Delta V_d}{2} = \frac{1 - \xi^2}{2} d^2 \cdot r \cdot \tau_u \cdot \cot \delta \qquad (15.24)$$

For $\xi \cong 0.30$ and $\delta \cong 30^0$ Equation 15.24 takes the form:

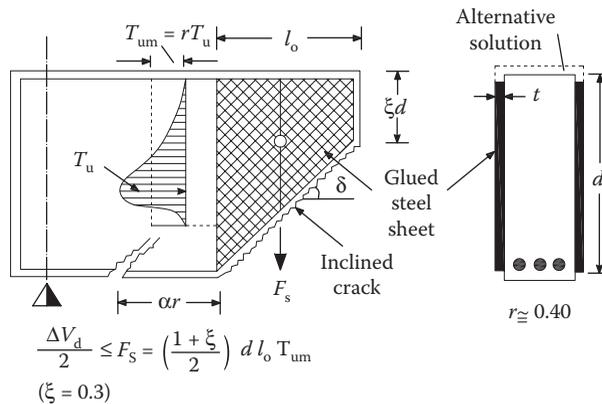$$\Delta V_d \leq 0.7 \tau_u d^2 \qquad (15.25)$$

Figure 15.29 Shear force transfer through epoxy resin glued steel sheet.

15.4.4 Beam–column joints

Depending on the degree of damage, the following techniques are applied for the repair of beam to column joints:

- Resin injection
- X-shaped prestressed collars
- Bonded steel plates or FRP sheets
- R/C jackets

A very interesting report on 'Repair and Strengthening of Beam-Column R/C Joints' is the state-of-the-art report No. 04-4 of the Georgia Institute of Technology (Engindeniz et al., 2004).

15.4.4.1 Local repairs

Resin injections are applied in the case of fine and moderate cracks, without degradation of concrete or buckling of the reinforcement bars. However, restoration of bonds between steel and concrete with the aid of epoxy resin is questionable, since contradictory results appear in the international literature (Popov and Bertero, 1975; French et al., 1990; Karayannis et al., 1998). Therefore, the joint should be strengthened at the same time with one of the techniques that will be presented next, especially in the case of frame structural systems without R/C walls.

15.4.4.2 X-shaped prestressed collars

After the cracks have been filled in with resin injections, or after the decomposed concrete is removed and the voids are filled with epoxy or non-shrinking mortar, the joint is strengthened with external ties (collars), which are prestressed with tensioner couplers (Figure 15.30). Then the joint is covered with welded wire fabric and a jacket of gunite concrete. When four beams are framing into the joint, the application of this technique is not feasible because the X-shaped collars cannot pass through the joint (NTU, 1978).

15.4.4.3 R/C jackets

The construction of R/C jackets to a damaged joint is the safest method for strengthening. This is generally a difficult technique, given the fact that a jacket must usually be constructed for every structural element framing into the joint. It is obvious that roughening of the surfaces is required, as well as punching of the slabs, in order for the ties to go through; injecting of the damaged joint area with resins must precede the construction of the R/C jackets (Figure 15.31; Alcocer and Jirsa, 1993; Tsonos A., 1999, 2002).

15.4.4.4 Bonded metal plates

Bonded metal plates can only be applied to plane joints, as in the case of X-shaped collars. This is a technique that provides strengthening to the joint without altering its dimensions. Local repair precedes the bonding of the plates, then the plates are tied with prestressed bolts (Figure 15.32). The thickness of the plates in this case must be at least 4.0 mm, which does not create any problems with the bonding process, since the plates are kept tight to the concrete surface with the aid of prestressed bolts (Corazao and Durruni, 1989; Beres et al., 1992; Hoffschild et al., 1995).

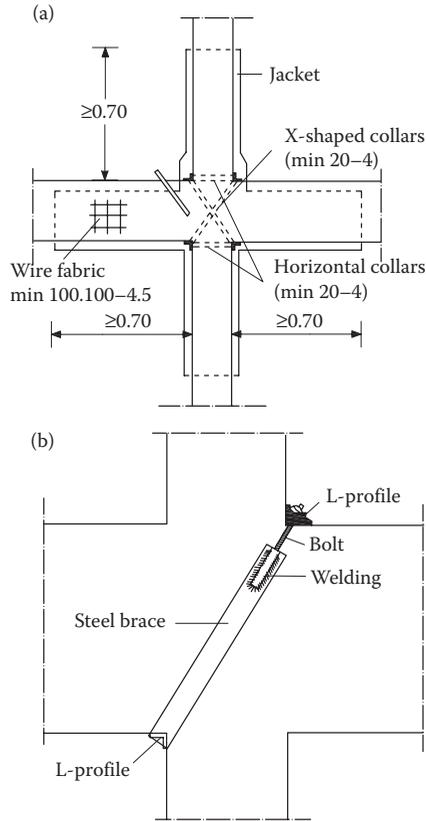*Figure 15.30* Strengthening of a joint with prestressed collars: (a) general arrangement of the strengthening; (b) detail of the prestressed collar.
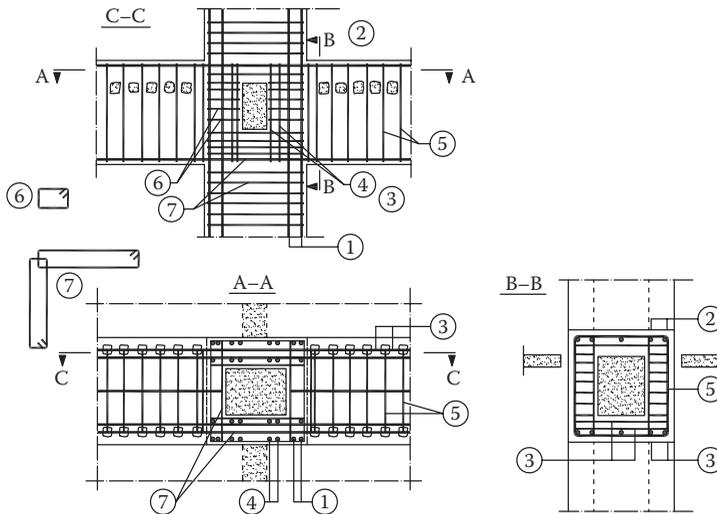
Figure 15.31 Strengthening of a joint with a jacket: 1 = column reinforcement; 2 = beam top reinforcement; 3 = beam bottom reinforcement; 4 = joint vertical stirrups; 5 = beam stirrups; 6 = column ties; 7 = column ties in joint.
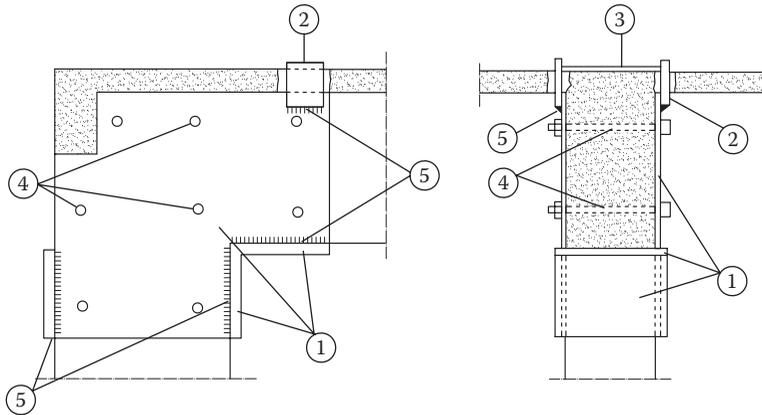
Figure 15.32 Bonded metal plates on a joint: 1 = steel plate; 2 = steel plate; 3 = steel strap; 4 = prestressed bolts; 5 = welding.
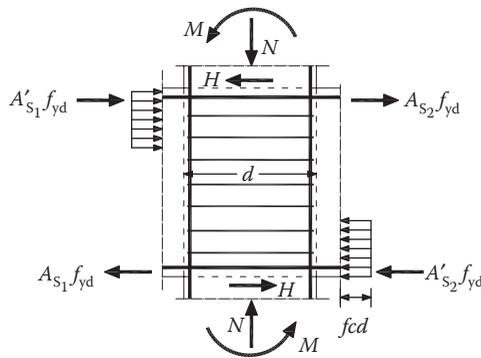
Figure 15.33 Schematic representation of the internal forces in a joint.

15.4.4.5 Redimensioning and safety verification

The redimensioning of the joint is carried out under the assumption that complete compatibility has been achieved between the original element and the added material, as happens with columns. The internal force distribution is given in Figure 15.33. However, given the fact that the field conditions are not as ideal as those in a laboratory, the author's opinion is that a model correction factor φ should be introduced, equal to

$$\frac{R_{d,rep}}{R_{d,monol}} \cong 0.80, \quad \frac{K_{rep}}{K_{monol}} \cong 0.80 \tag{15.26}$$

15.4.5 R/C walls

It is well known that R/C walls, due to their high stiffness and strength, are the most effective seismic-resistant elements of a structure. Therefore, the repair and strengthening of a damaged R/C wall can drastically improve the seismic resistance of a building.

15.4.5.1 Local repairs

If a properly reinforced wall exhibits cracks of small width, without bond deterioration or concrete crushing, it can be repaired with epoxy resins. Laboratory tests have shown that such an intervention fully restores the strength of the wall, but not its stiffness and energy dissipation capacity, due to the fact that resin cannot penetrate into the capillary cracks that accompany cracks with larger openings (Tassios, 1983; Lefas et al., 1990; Lefas and Kotsovos, 1990).

It should be mentioned here that most of the walls in older buildings have inadequate reinforcement due to the Code requirements of earlier years. Thus, a simple repair with resin injections is very often not enough. It needs to be combined with R/C jackets to strengthen the wall.

15.4.5.2 R/C jackets

R/C jackets can have one of the forms shown in Figure 15.34. In the case of a jacket on both sides of the wall, the connection of the two layers with through-thickness ties is necessary (at least 3 bars $d = 14$ mm/m^2).

At the points where the wall passes from one storey to the other it is necessary to punch holes in the slab and place diagonal reinforcements through them (Figure 15.35).
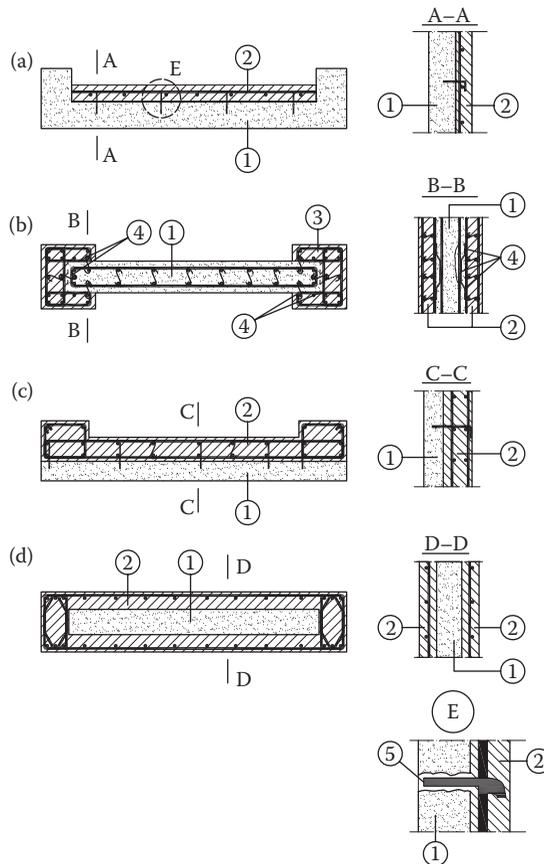
Figure 15.34 Strengthening of a wall with a jacket: (a) one sided jacket; (b) thickenings at the ends of the existing wall; (c) one sided jacket with end-thickenings; (d) jackets, on both sides of the existing wall. 1 = existing wall; 2 = added wall; 3 = added columns; 4 = welding; 5 = epoxied bar.
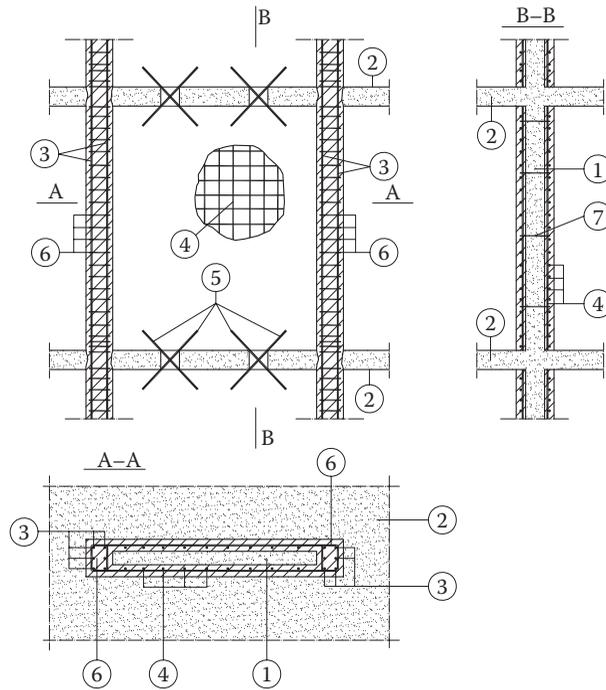
Figure 15.35 General arrangement for the strengthening of a wall: 1 = existing wall; 2 = existing slab; 3 = added longitudinal reinforcement; 4 = added wire fabric; 5 = diagonal connecting bars; 6 = added ties, 7 = connecting ties.

In the construction of the R/C jackets the following rules apply:

- The strength of the new concrete must be at least 5 MPa greater than that of the old concrete.
- The minimum thickness of the jacket should be 50 mm on each side.
- The minimum horizontal and vertical reinforcement should be 0.25% of the section of the jacket.
- The minimum reinforcement of the strengthening ends of the wall should be 0.25% of the section of the jacket end.
- The diameter of the ties at the wall ends should not be less than 8 mm, with a maximum spacing not exceeding 150 mm.
- The jacket must be anchored to the old concrete, with dowels spaced at no more than 600 mm in either direction (NTU, 1978; AUTH, 1978).

15.4.5.3 Redimensioning and safety verification

1. In the case of repair with resin injections, the ratio of the strength of the repaired element to the strength of the original may be taken to be equal to 1, as discussed earlier, while the ratio of the stiffness and energy dissipation capacity may be taken to be equal to 0.85, that is:

$$\frac{R_{d,rep}}{R_{d,orig}} \cong 1, \quad \frac{K_{rep}}{K_{orig}} \cong 0.85 \quad \frac{E_{rep}}{E_{orig}} \cong 0.85 \tag{15.27}$$

2. In the case of repair with jackets, provided that the damaged wall was repaired earlier either with resins or resin mortars or non-shrinking cement mortars, the behaviour of the repaired element does not differ from that of the monolithic one (original + jacket), as far as both strength and stiffness are concerned. Therefore, as in the case of columns, walls are dimensioned based on the relationships:

$$\frac{V_{R\,rep}}{V_{R\,monol}} = 0.9, \quad \frac{M_{y\,rep}}{M_{y\,monol}} = 1.0, \quad \frac{\theta_{y\,rep}}{\theta_{y\,monol}} = 1.05, \quad \frac{\theta_{u\,rep}}{\theta_{u\,monol}} = 1.0 \tag{15.28}$$

The required number of dowels between the original wall and the jacket can be estimated by the relationship (Tassios, 1984):

$$n_d = \frac{\left[(V_d - V_{R,orig}) - l_w h_w \tau_{adh}\right]}{D_u} \tag{15.29}$$

where
   V_d is the shear strength of the repaired wall (wall + jacket; MN).
   $V_{R,orig}$ is the shear strength of the original wall after it is repaired, estimated to be 0.80 of the strength of the original undamaged wall (MN).
   $l_w h_w$ are the dimensions of the wall under repair (m).
   τ_{adh} is the average adhesion design strength of the new to the old concrete estimated to be equal to τ_{Rdl} (section 15.4.3.4, item 2).
   D_u is the dowel strength equal to

$$D_u = d^2 \sqrt{f_{cd} f_{yd}} \, (MN) \tag{15.30}$$

where
   d is the diameter of the dowel (m).
   f_{yd} is the design strength of the dowel (MPa).
   f_{cd} is the design strength of concrete (MPa).

15.4.6 R/C slabs

It was stated in Chapter 11 that slab damage mainly appears in the form of cracks in the middle of large spans, above thier supports, near discontinuities such as corners of large openings, at the connections of stairs to the slabs and so on. Depending on the extent and the type of damage, a different degree of intervention can be applied.

15.4.6.1 Local repair

If a properly reinforced slab exhibits cracks of small width without crushing of the concrete or bond deterioration, it can be repaired with epoxy resins. In the case of local failure accompanied by crushing or degradation of concrete, there can be a local repair for the full thickness of the slab (Figure 15.36). However, the need for such a repair is typically accompanied by the need to increase the slab thickness or to add new reinforcement.

15.4.6.2 Increase of the thickness or the reinforcement of a slab

Where the computational verification indicates that the slab resistance is insufficient, the slab can be strengthened either by increasing its thickness from the upper side with cast-in-place
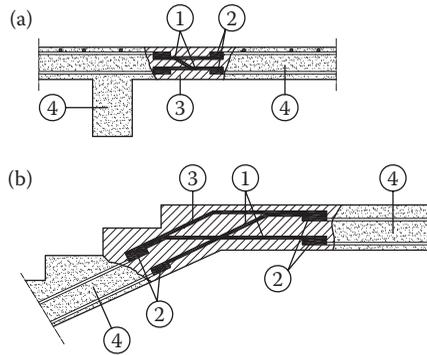
Figure 15.36 Local repair through the thickness of a slab: (a) repair in the span; (b) repair on the connection of a stair to the slab; 1 = added reinforcement; 2 = welding; 3 = added concrete; 4 = existing slab.
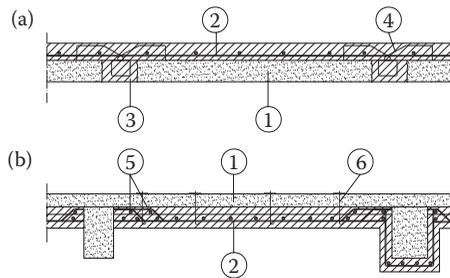
Figure 15.37 Increase of the thickness of the slab and addition of new reinforcement: (a) increase of the thickness on the upper face; (b) increase of the thickness on the lower face with the addition of new reinforcement; 1 = existing slab; 2 = added reinforcement; 3 = dowel; 4 = anchoring bent bars; 5 = welded connecting bars; 6 = hanging ties.
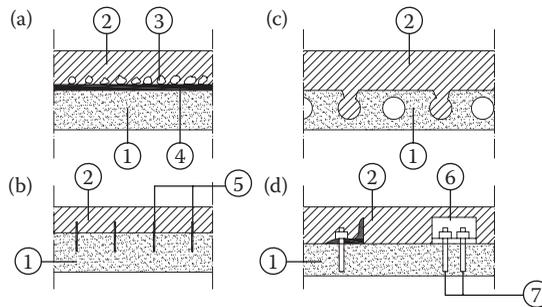
Figure 15.38 Details of connection of a new layer to the old concrete on a slab: (a) connection of new to old concrete using epoxy resin; (b) connection using epoxy bolts; (c) connection using existing voids of a voided slab; (d) connection using angle profiles; 1 = existing slab; 2 = new slab; 3 = sand corner; 4 = epoxy resin; 5 = epoxied bolts; 6 = angle profile; 7 = anchor bolts or shoot nails.

concrete or by increasing its thickness and placing additional reinforcement on its lower side with gunite concrete (Figure 15.37). The force transfer between the old and the new concrete is the key to the success of the intervention. This can be accomplished by other means in addition to roughening the old surface or resin coatings on the interface, such as anchors, dowels and so on (Figure 15.38).

15.4.6.3 Redimensioning and safety verifications

The dimensioning of slabs that have been strengthened with additional reinforcement and increase of thickness is carried out based on the assumption of a monolithic section (original + additional layer). The results are multiplied by the model *correction factor* φ, which is taken to be equal to 1.0 if the thickness of the new layer h is less than $h_o/3$ and $\varphi = 0.65$ if h is equal or larger than $h_o/3$ (Tassios, 1983, 1984), that is,

$$\frac{M_{rep}}{M_{monol}} = 1.0 \quad \text{for } h < \frac{h_o}{3} \tag{15.31}$$

$$\frac{M_{rep}}{M_{monol}} = 0.65 \quad \text{for } h \geq \frac{h_o}{3} \tag{15.32}$$

The proposed values for the stiffness ratio are

$$\frac{K_{rep}}{K_{monol}} = 0.90 \quad \text{for } h < \frac{h_o}{3} \tag{15.33}$$

$$\frac{K_{rep}}{K_{monol}} = 0.40 \quad \text{for } h \geq \frac{h_o}{3} \tag{15.34}$$

However, in addition to the general safety verifications there should be specific considerations for the force transfer mechanism through adhesion between the old and the new concrete, similar to those that were explained for the dimensioning of beams.

15.4.7 Foundations

The methods of repair or strengthening of foundations fall beyond the scope of this book, given the fact that they are related to interventions that belong to the field of foundation engineering. Indeed, when damage related to foundations occurs, it is not unusual for the need to arise for construction of retaining walls with anchorages to resist landslides, for construction of piles, for strengthening the soil with cement groutings and so on. Therefore, only the technique of connecting the column jacket to the footing will be dealt with here, as well as eventual strengthening of the footing itself.

15.4.7.1 Connection of column jacket to footing

Given the fact that the critical area of a column to flexure is at its top and bottom, the column jacket must continue beyond the point where the column frames into the footing, so that reinforcement bars will have the required anchorage length. This can be accomplished either with the arrangement of Figure 15.39 or with that of Figure 15.40.

15.4.7.2 Strengthening of footings

An increase in the area of a footing is decided on either because of inadequate bearing surface due to poor original estimation of the soil-bearing capacity, or because larger axial forces are transferred to the foundation due to the addition of new structural elements. In these cases the increase in the area of the footing is carried out according to the arrangements shown in Figures 15.41 and 15.42.
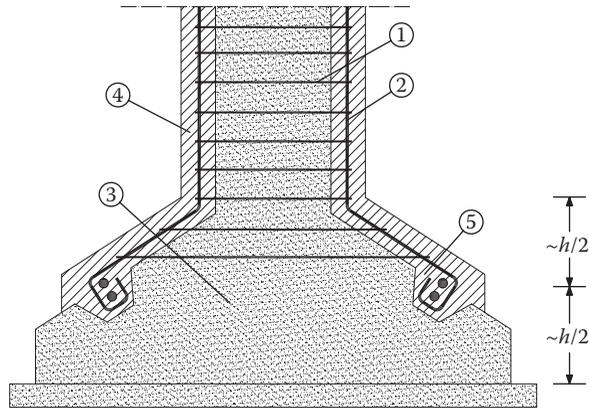
Figure 15.39 The end of a column jacket in the footing: 1 = new ties Φ12/100 mm; 2 = longitudinal reinforcing bars; 3 = existing concrete; 4 = added concrete; 5 = dowel in old concrete.
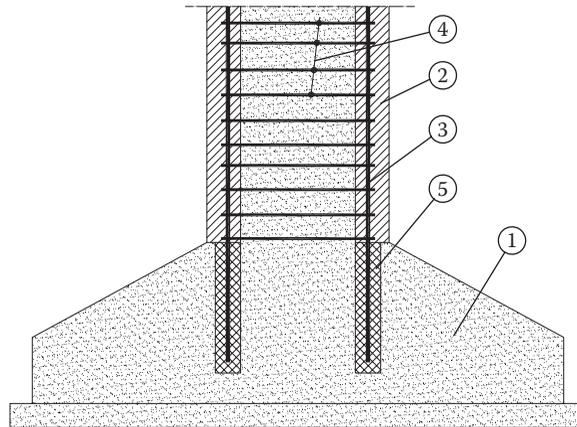
Figure 15.40 Anchorage of the column jacket reinforcement in the footing: 1 = old concrete; 2 = jacket; 3 = long reinforcement; 4 = new ties; 5 = epoxied connections.

The first arrangement, which is simpler than the second, is applied when the strengthening of the footing is extended to the column in the form of a jacket. In this case, the inclined forces for the transmission of the soil pressure to the column jacket (Figure 15.41) are carried by rectangular closed reinforcement rings, which are formed either with large overlaps or welding.

The second arrangement is much more difficult because excavation under the existing footing is required. In this case, a temporary support is usually required, and special attention should be paid to avoiding settlement due to undermining.

15.4.8 Infill masonry walls

In previous chapters there was systematic reference to the significance of the infill system to the seismic behaviour of structures, and the importance of its repair was explained (Bertero and Brokken, 1983; Sarigiannis et al., 1990; Stylianidis, 2012).
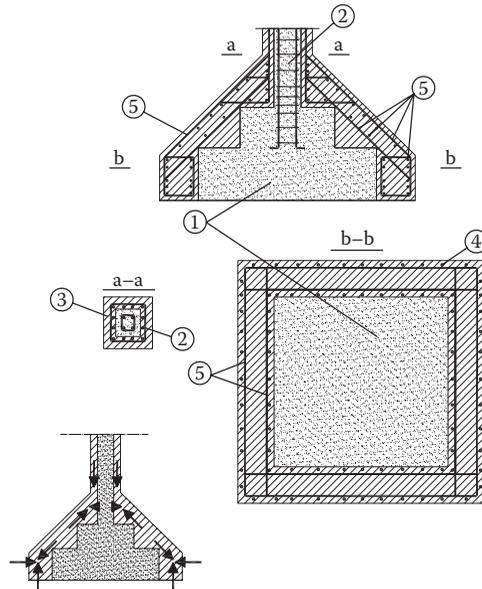
Figure 15.41 Strengthening of footing – column: 1 = existing foundation; 2 = existing column; 3 = reinforced jacket; 4 = added concrete; 5 = added reinforcement.

15.4.8.1 Light damage

Cracks that do not go through the thickness of the wall but appear only on the plaster have already been characterised as 'light damage' (Subsection 11.1.7). To repair this kind of damage a band of plaster of a width equal to 100–150 mm on each side of the crack is removed
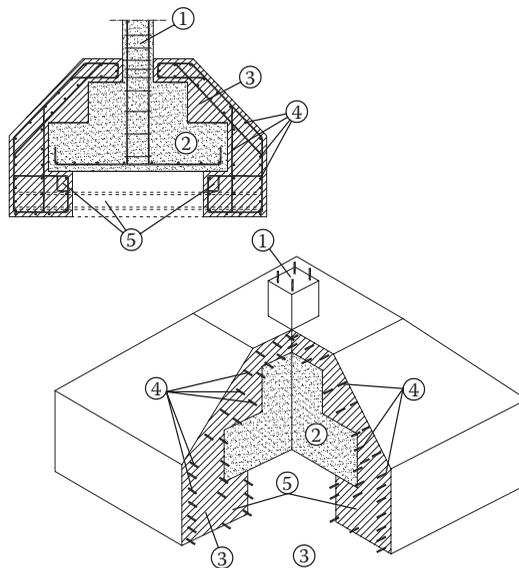
Figure 15.42 Strengthening of a footing without strengthening of the column: 1 = existing column; 2 = existing foundation; 3 = added concrete; 4 = added reinforcement; 5 = steel profile.

and it is replaced by new plaster after the wall is moistened with water. Very often, a band of light wire mesh or a suitable FRP sheet is used as reinforcement underneath the new plaster.

15.4.8.2 Serious damage

This term refers to open (full-thickness) cracks in the infill wall, independently of the crack width. In this case, the strength, the stiffness, as well as the ability of the infill to dissipate energy have obviously been reduced, and therefore an intervention more extended than the previous one is required. Therefore, if the crack is only a few millimetres wide, after the plaster is removed in a band of 100–150 mm on each side, the crack is widened on the surface of the wall, it is washed using a water jet and filled with cement mortar of high cement content, pushing the mortar as deep as possible inside the crack with a thin trowel and smoothing the surface. Then a wire mesh or an FRP band is nailed on the area where the plaster has been removed and new plaster is applied (Figure 15.43).

If the cracks are wider, two solutions are possible: either the wall is removed and reconstructed, or the plaster on the whole surface of the wall is removed and the procedure of the previous paragraph is followed. The wire mesh or the FRP sheet in this case is placed on the whole surface of the wall and a plaster consisting of cement mortar of 20 mm thickness or a thin layer (about 30–40 mm) of gunite concrete is shotcreted. It is understood that interventions
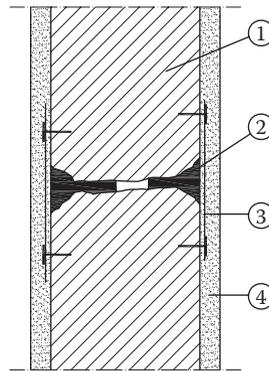
Figure 15.43 Repair of a through-thickness crack in an infill wall: 1 = existing masonry walls; 2 = sealing of the crack with cement mortar; 3 = wire mesh; 4 = plaster.
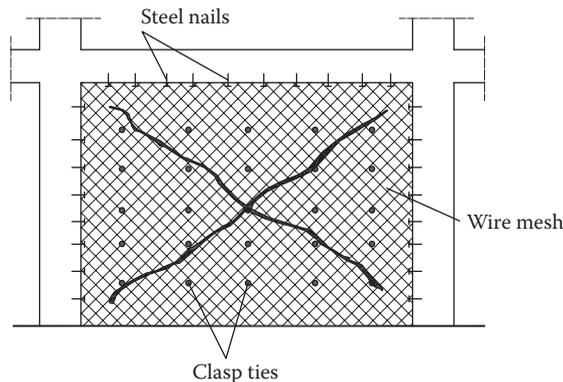
Figure 15.44 Repair of a seriously damaged infill masonry wall.

of this type lead to strengths and stiffnesses of the masonry wall higher than the original ones (Figure 15.44). Therefore, there should be a verification of the relative strength and stiffness of the adjacent columns in order to avoid shear failure in the columns due to a new earthquake (Sariyiannis, 1990), in case the repaired masonry is not extended into the next span.

15.5 REPAIR AND STRENGTHENING OF STRUCTURAL ELEMENTS USING FRPs

15.5.1 General considerations

Summarising the main properties of FRP sheets and laminates that have been presented in Subsection 15.2.10, we should recall the following key points:

1. Carbon FRPs (CFRPs) in the form of sheets or laminates are the most suitable for the repair and strengthening of R/C members than all other FRP categories.
2. The *E*-modulus of CFRPs is almost equal to or higher than that of steel ($E_{cf} \cong 165 - 640$ GPa compared to $E_{steel} = 200$ GPa).
3. Tensile strength at failure is very high, ranging between 1.450 and 3.500 MPa.
4. Deformation at failure ranges between 0.45% and 1.7%.
5. Constitutive law $\sigma–\varepsilon$ is linear without a plastic plateau at all (brittle behaviour).
6. Load transfer from an R/C member to an FRP sheet or laminate is accomplished through adhesive epoxy resins.
7. Taking into consideration remarks 5 and 6 above, it follows that the design strength of FRP is defined by two limits:
   a. The first is FRP tensile strength reduced by a rather high safety factor on the order of 2.0 due to the brittle failure character of FRP.
   b. The second is shear (bond) stress developing at the contact surface by which *delamination* of the FRP from the concrete may be caused. This value is related to the strain that develops on FRPs at the delamination stage.
   The second limit is usually the parameter defining the design strength of FRPs.
8. The fire resistance of an FRP intervention is very low. Therefore,
   a. The original member must be in a position to carry all dead loads with its original steel reinforcement at least with the safety factor specified for fire resistance. This implies that the strengthening degree with FRPs cannot exceed the original strength of the member by 100%.
   b. Protection measures against fire should be taken (e.g. mortar protective coatings).
9. Interventions based on FRPs cannot substantially change the stiffness of the member since they are flexible materials.
10. FRPs may be used for the following types of intervention:
    a. Strengthening to bending
    b. Strengthening to shear
    c. Strengthening to axial compression through confinement
    d. Ductility increase of columns through confinement at their ends
    e. Clamping of lap-splices
    f. Strengthening of joints

15.5.2 Bending

Main failure modes of an R/C beam additionally reinforced by CFRP laminates to flexure are the following (Teng et al., 2002):
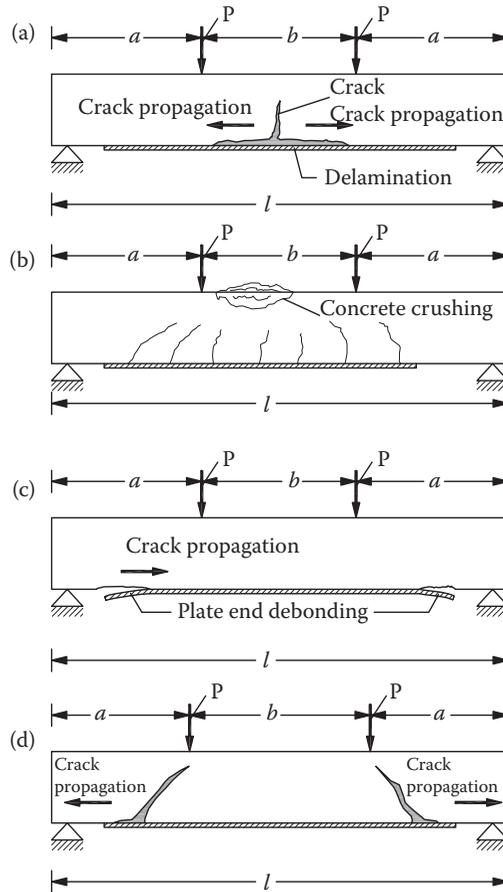
Figure 15.45 Failure modes of FRP-plated R/C beams: (a) intermediate flexural crack-induced delamination; (b) crushing of compressive zone; (c) plate-end debonding; (d) intermediate shear crack-induced debonding.

1. Intermediate flexural crack-induced debonding (Figure 15.45a)
2. Crushing of concrete under compression (Figure 15.45b)
3. Plate-end debonding (Figure 15.45c)
4. Shear failure (Figure 15.45d)

FRP design must cover all of the above failure modes.

15.5.2.1 Intermediate flexural crack-induced debonding

In order for the strengthening of the beam to be ensured against crack-induced debonding, FRP elongation must be limited to a specified value defined as *'effective strain'*. If this value is exceeded, cover delamination or FRP debonding may occur, since the force in the FRP cannot be sustained by the concrete substrate. For that value of the 'effective strain', there are strong deviations among various standards and specifications.

• According to the Swiss prenorm SIA 166/2004, design elongation is specified to

$$\varepsilon_{fe} = 0.6\%$$

Therefore, design strength f_{fd} may by derived from the expression:

$$f_{fd} = \frac{1}{\gamma_{fd}} E_f \cdot \varepsilon_{fe} = \frac{1}{\gamma_{fd}} 0.6\% \cdot E_f \tag{15.35}$$

where
γ_{fd} is the partial safety factor for FRP laminates or sheets. The usually recommended value for $\gamma_{fd} = 1.2$

- According to the Japanese standards (JBDPA, 1999), effective strain is specified to

$\varepsilon_{fe} \le 0.7\%$

- According to FIB (2003):

$\varepsilon_{fe} \le 0.6\%$

- According to ACI 440.2R-02/2002: (SI units)

$$\varepsilon_{fe} \le \kappa_m \cdot \varepsilon_{fu} \tag{15.36}$$

where
ε_{fu} is strain at failure, and:

$$\kappa_m = \begin{cases} \dfrac{1}{60\varepsilon_{fu}} \left(1 - \dfrac{nE_f \cdot t_f}{300.000}\right) \le 0.6, & \text{for } nE_{FRP} \cdot t_f \le 180.000 \\[3mm] \dfrac{1}{60\varepsilon_{fu}} \left(1 - \dfrac{90.000}{nE_f \cdot t_f}\right) \le 0.6, & \text{for } nE_{FRP} \cdot t_f > 180.000 \end{cases} \tag{15.37a,b}$$

The meaning of the above notation is the following:
E_f is the modulus of elasticity of the FRP.
n is the number of plies.
t_f is the thickness of each CFRP laminate.
Application of the above two equations (15.37) results in a value for κ_m ranging between 0.35% and 0.60% ε_{fu}.
- In closing, it should be noted that according to EC 8-3/2005 Annex A, the following value is recommended for ε_{fe}:

$$\varepsilon_{fe} = \sqrt{\frac{0.6 \cdot f_{ctm} \cdot \kappa_b}{E_f \cdot t_f}} \quad \text{and } \sigma_{fe} = \sqrt{\frac{0.6 \cdot f_{ctm} \cdot \kappa_b \cdot E_f}{t_f}} \tag{15.38}$$

where
f_{ctm} is concrete mean tensile strength.

$$\kappa_b = \sqrt{1.50(2 - w_f/s_f)/(1 + w_f/100 \text{ mm})} \tag{15.39}$$

(known as the 'covering coefficient')
w_f is the width of the FRP laminate.

s is the spacing of the FRP laminates.

E_f is the modulus of elasticity of the FRP.

t_f is the thickness of the FRP.

EC 8-3/2005 recommends a partial safety factor for debonding equal to $\gamma_{fd} = 1.50$, since this mode of failure depends on the concrete tensile strength. Therefore,

$$f_{td} = \frac{1}{\gamma_{fd}} \sqrt{0.6 \frac{E_f \cdot f_{ctm} \cdot \kappa_b}{t_f}} \qquad (15.40)$$

This basic value is reduced further for the various types of applications (full warping, U-shaped [i.e. open] jackets and side-bonded sheets/strips).

It should be noted that although the provisions of EC 8-3/2005 Annex A (informational) are based on sound theoretical, experimental, and statistical research (Biskinis, 2007), they are very conservative in relation to other standards and specifications in effect and, therefore, in the opinion of the authors, they should be reconsidered, because they almost overturn the capability of using FRPs in practice.

From what has been presented above it may be concluded that the design strength to flexure is determined by the relation:

$$f_{fd} = \frac{1}{\gamma_{fd}} \varepsilon_{fe} \cdot E_f \qquad (15.41)$$

since this value is always, at least for CFRPs, lower than:

$$f_{fu}/\gamma_{fm} = f_{fu}/2.0 \qquad (15.42)$$

The design may be carried out using existing computer platforms for the case. An approximate estimate is given below.

Consider the R/C cross-section depicted in Figure 15.46, loaded by a bending moment:

$$M_{Ed} = M_{0E} + M_{1E} \qquad (15.43)$$
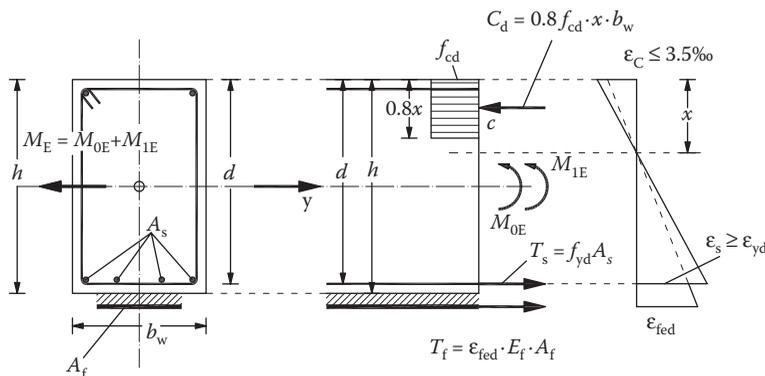
Figure 15.46 Strengthening of a beam under flexure using FRP laminates.

where

M_{0E} is the original bending moment for which the cross-section was designed and reinforced through steel rebars.

M_{1E} is the additional bending moment for which FRP reinforcement will be used.

The equilibrium condition of the moments of the internal forces with reference to point c balancing M_E result in

$$M_{Rd} \cong 0.9d \cdot T_s + 0.9h \cdot T_f \geq M_E \tag{15.44}$$

or

$$0.9d \cdot f_{yd} \cdot A_s + 0.9h \cdot \varepsilon_{fed} \cdot E_f \cdot A_f \geq M_{Ed} \tag{15.45}$$

or

$$\boxed{A_f \geq \frac{M_{Ed} - 0.9d \cdot f_{yd} \cdot A_s}{0.9h \cdot \varepsilon_{fed} \cdot E_f}} \tag{15.46}$$

15.5.2.2 Crushing of concrete under compression before tension zone failure

The condition that the depth x of the compressive zone of the beam should fulfill in order for concrete crushing to precede steel yielding is given by the following expression:

$$\xi = \frac{x}{h} = \frac{\varepsilon_c}{\varepsilon_{fe} + \varepsilon_c} \geq \frac{3.5\%_0}{f_{fd}/E_f + 3.5\%_0} = \xi_{bal} \tag{15.47}$$

(balanced section, see Paragraph 8.2.2.2)

Bearing in mind that:

$$C_d \cong 0.8 f_{cd} \, x \, b_\omega \tag{15.48}$$

and that

$$C_d = T_d \tag{15.49a}$$

or

$$0.8 f_{cd} \, x \, b_\omega = f_{yd} \cdot A_s + \varepsilon_{fed} \cdot E_f \cdot A_f \tag{15.49b}$$

it may be concluded that

$$\boxed{x = \frac{f_{yd} \cdot A_s + \varepsilon_{fed} \cdot E_f \cdot A_f}{0.8 \cdot f_{cd} \cdot b_w}} \tag{15.50}$$

The value of A_f in Equation 15.50 has already been determined by Equation 15.46 and therefore the right term of Equation 15.50 is completely determined. So if

$$\xi = \frac{x}{h} \leq \xi_{bal} = \frac{3.5\%_0}{f_{fd}/E_f + 3.5\%_0} \tag{15.47a}$$

the condition for failure of the tensile zone at yield is fulfilled. Otherwise the design must be revised, because crushing of the compressive zone prevails.

15.5.2.3 Plate-end debonding

- In order for a laminate to be ensured against plate-end debonding, the laminate should extend a distance l_b past the point along the span corresponding to the cracking moment M_{cr} given by the following expression (Figure 15.47):

$$l_e = l_b = \sqrt{\frac{E_f \cdot t_f}{2.5 \cdot f_{ctm}}} \text{ (mm)} \tag{15.51}$$

l_e is defined as *'effective length'*, the meaning of which will be explained later. (Triandafillou, 1998; Tassios, 2009).

- For this value EC 8-3/2005 recommends the following expressions:

$$l_e = l_b = \sqrt{\frac{E_f \cdot t_f}{\sqrt{4 \cdot \tau_{max}}}} \text{ (units N, mm)} \tag{15.52}$$

where

$$\tau_{max} = 1.8 \cdot f_{ctm} \cdot \kappa_b \tag{15.53}$$

is the maximum bond strength influenced basically by the concrete average tensile strength f_{ctm} and by the covering coefficient κ_b, already defined in Paragraph 15.5.2.1, Equation 15.39.

- ACI 440.R2-02 specifies for l_b a value:

$l_b = \max(d, 150 \text{ mm})$

where
  d is the effective height of the cross-section (Figure 15.48).

In the case of successive plies, l_b refers to each ply from the end of the one above.
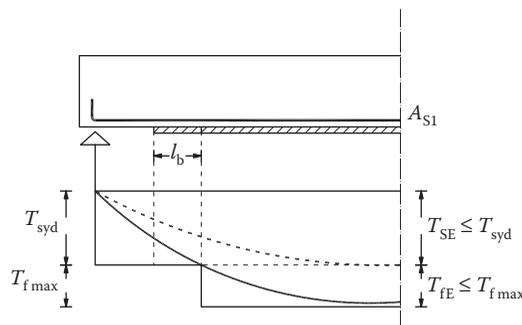
Figure 15.47 Graphic representation of the plate-end extension to avoid plate-end debonding.
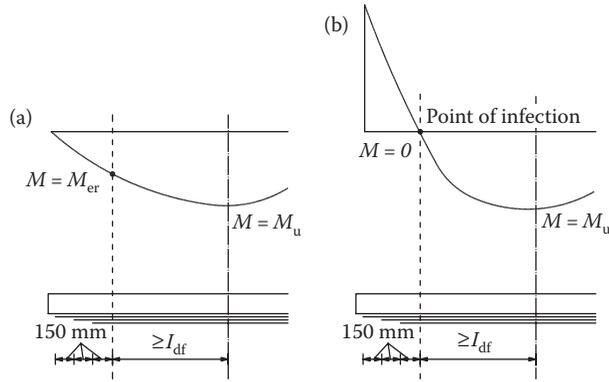
Figure 15.48 Graphic representation of the guidelines for allowable termination points of a three-ply FRP laminate. (a) Simply supported beam; (b) continuous beam. (From ACI 440-2R-02. With permission.)

15.5.2.4 Theoretical justification of debonding length l_b and strain ε_{fe}

Debonding strain and length has been the subject of extended analytical, experimental, and statistical investigations in the last 15 years, since they constitute the main parameters for the design of FRPs in R/C structures (Hollaway and Leeming, 1999; Concrete Society, 2000; Teng et al., 2002; Tassios, 2009).

A simplified conceptual approach to this issue will be made below so that an in-depth understanding of the relations presented above may be achieved.

Consider in Figure 15.49 a laminate bonded externally to a beam under bending. From two successive intermediate hairline cracks of the concrete, debonding starts to propagate in both directions as the loading and, therefore, the developing bending moment at the crack positions along the beam increases. The debonding mechanical model, together with the stresses and strains developing on the laminate and the bonding stresses developing at the interface, are given conceptually in Figure 15.50a,b,c. Stresses and strains of the laminate are considered as a linear function along the effective length l_e, while bonding stresses are considered to be uniform along the same length.
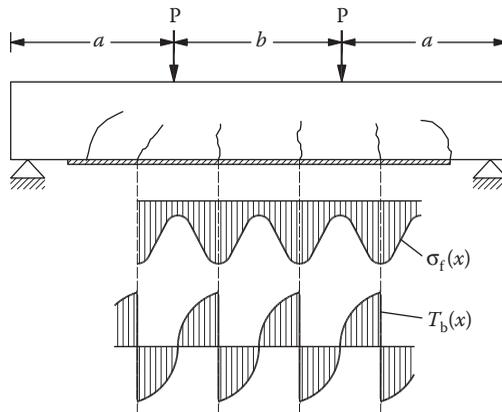
Figure 15.49 Load transfer from the beam to the bonded laminate.
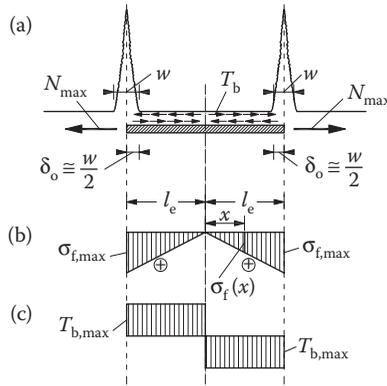
Figure 15.50 Intermediate crack-induced debonding: (a) stress–displacement pattern; (b) assumption for axial stress–strain distribution along the FRP laminate axis; (c) assumption for bond stress distribution along the contact surface.

Under the above assumptions at 'debonding stage', the following relations are in effect:

$$\sigma_{f(x)} = \frac{x}{l_e}\sigma_{f\,max}, \quad \varepsilon_{f(x)} = \frac{x}{l_e}\varepsilon_{f\,max} \tag{15.54a,b}$$

$$\varepsilon_{f(x)} = \frac{\sigma_{f(x)}}{E_f} = \frac{x}{l_e}\frac{\sigma_{f\,max}}{E_f} \tag{15.55}$$

The laminate elongation at the boundary of the crack will be equal to

$$\delta_o = \int_0^{l_e} \varepsilon_{f(x)}\mathrm{d}x \tag{15.56}$$

or

$$\delta_o = \int_0^{l_e} \frac{x}{l_e}\varepsilon_{f\,max}\mathrm{d}x = \frac{l_e}{2}\varepsilon_{f\,max} \tag{15.57}$$

Therefore,

$$\boxed{\varepsilon_{max} = \frac{2\delta_o}{l_e}} \tag{15.58}$$

and

$$\boxed{N_{max} = \varepsilon_{f\,max}E_f \cdot t_f \cdot b_f = \frac{2E_f \cdot t_f \cdot b_f}{l_e}\delta_o} \tag{15.59}$$

On the other hand, according to the above assumption, the maximum bonding action balancing N_{max} is equal to

$$\boxed{T_{max} = \tau_{b\,max} b_f l_e}$$ (15.60)

Bearing in mind that $\tau_{b\,max}$ is a function of the mean tensile strength of concrete f_{ctm}, since this strength is usually much lower than the shear strength of the adhesive bonding epoxy resin and of the covering coefficient κ_b, that is,

$$\tau_{b\,max} = \lambda \cdot \kappa_b \cdot f_{ctm}$$ (15.61)

it follows that

$$T_{max} = \lambda \cdot \kappa_b \cdot f_{ctm} \cdot b_f \cdot l_e$$ (15.62)

At the debonding stage:

$$\boxed{N_{max} = T_{max}}$$ (15.63)

Therefore, by introducing in Equation 15.63 the values of N_{max} and T_{max} given by Equations 15.59 and 15.62, the result is

$$\frac{2E_f \cdot t_f \cdot b_f}{l_b}\delta_o = \lambda \cdot \kappa_b \cdot f_{ctm} \cdot b_f \cdot l_e$$ (15.64)

or

$$\boxed{l_e = \sqrt{\frac{2E_f \cdot t_f \cdot \delta_o}{\lambda \cdot \kappa_b \cdot f_{ctm}}}}$$ (15.65)

$$\boxed{\varepsilon_{f\,max} = \frac{2\delta_o}{l_e} = \sqrt{\frac{2\lambda \cdot \kappa_b \cdot f_{ctm} \cdot \delta_o}{E_f \cdot t_f}}}$$ (15.66)

For a reasonable crack width w equal to 0.4 mm it follows that:

$$\delta_o = \frac{w}{2} \cong 0.2\,\text{mm}$$

Consequently, the above two equations (15.65) and (15.66) take the following form:

$$\boxed{l_e = \sqrt{\frac{0.4\,E_f \cdot t_f}{\lambda \cdot \kappa_b \cdot f_{ctm}}}}$$ (15.67)

and

$$\boxed{\varepsilon_{f\,max} = \varepsilon_{fe} = \sqrt{\frac{0.4\lambda \cdot \kappa_b \cdot f_{ctm}}{E_f \cdot t_f}}}$$ (15.68)

It is obvious that l_e also represents the debonding length l_b beyond the final crack before the end of the laminate.

It should be noted also that κ_b and λ may take various values as the result of a best-fit procedure with experimental results. At the same time, the original assumptions of linear distribution of strains and uniform distribution of bond stresses on the conduct surface may be modified, leading to a similar expression.

15.5.3 Shear

Additional shear capacity due to FRP sheets or laminates may be estimated using similar expressions, like those for steel stirrup rebars.

- So, according to EC 8-3/2005 recommendations, $V_{\mathrm{Rd,f}}$ is given by the following expressions (Figure 15.51):
  - For side FRP stirrups or sheets (e.g. T beams):

$$V_{\mathrm{Rd,f}} = 0.9\,d \cdot f_{\mathrm{fd,e}} \cdot 2\,t_{\mathrm{f}}\,\frac{\sin\beta}{\sin\delta} \cdot \frac{w_{\mathrm{f}}}{s_{\mathrm{f}}} \tag{15.69}$$

  - For full warping with FRP or for U-shaped FRP strips or sheets:

$$V_{\mathrm{Rd,f}} = 0.9\,d \cdot f_{\mathrm{fd,e}} \cdot 2\,t_{\mathrm{f}}\left(\frac{w_{\mathrm{f}}}{s_{\mathrm{f}}}\right)^{2} (\cot\delta + \cot\beta)\sin\beta \tag{15.70}$$

where
   d is the effective depth.
   δ is the strut inclination angle.
   β is the angle between the strong fibre direction in the FRP sheet or fabric and the axis of the member, usually $\beta = 90^{0}$.
   w_{f} is the width of the FRP strip or sheet orthogonally in the main direction of the fibres.
   (for sheets $w_{\mathrm{f}} = \min(0.9d, h_{\mathrm{w}})\sin(\theta + \beta)/\sin\theta$
   s_{f} is the spacing of the FRP strips ($=w_{\mathrm{f}}$ for sheets).
   $f_{\mathrm{fd,e}}$ is the design FRP effective debonding strength, which depends on the strengthening configuration (fully wrapped FRP, U-shaped FRP, side bonded FRP). The main parameter in these expressions for $f_{\mathrm{fd,e}}$ is the effective maximum strain and the effective debonding, to which extended reference has been made in the previous subsection.
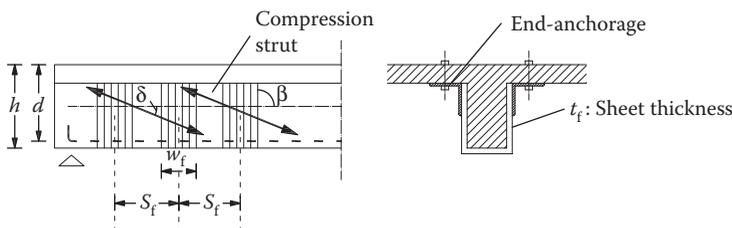
Figure 15.51 Additional shear capacity due to FRP wrapping strips.

- According to ACI 440.2R-02, effective strain in FRP laminates or sheets is specified in the following simple form.
  - For completely wrapped members:

$$\varepsilon_{fr} = 0.004 \leq 0.75\,\varepsilon_{fu} \tag{15.71}$$

The same value for *bonded U wraps* or bonded *face plies* is limited to

$$\varepsilon_{fr} = \kappa_r \cdot \varepsilon_{fu} \leq 0.004 \tag{15.72}$$

where
κ_r is computed from Equations 15.73 to 15.76 (Khalifa et al., 1998)

$$\kappa_r = \frac{\kappa_1 \cdot \kappa_2 \cdot l_e}{11.9\,\varepsilon_{fu}} \leq 0.75 \tag{15.73}$$

$$l_e = \frac{23.3}{(n \cdot t_f \cdot E_f)^{0.58}} \quad \text{(SI units)} \tag{15.74}$$

n is the number of successive plies

$$\kappa_1 = \left(\frac{f_d}{27}\right)^{2/3} \quad \text{(SI units)} \tag{15.75}$$

$$\kappa_2 = \begin{cases} \dfrac{d_f - l_e}{d_f} & \text{for } U - \text{wraps} \\[2ex] \dfrac{d_f - 2l_e}{d_f} & \text{for two sides bonded} \end{cases} \tag{15.76}$$

d_f is the effective depth of the FRP sheet or stirrup

15.5.4 Axial compression and ductility enhancement

15.5.4.1 Axial compression

- FRP systems can be used to increase the axial compression strength of a concrete member by providing confinement with FRP jackets (Teng et al., 2002; Fardis, 2009; Tassios, 2009). Apparently, in this case the fibres are oriented transversally to the axis of the R/C member (column) in the form of hoops (Figure 15.11a,b). The concept of concrete confinement with FRPs is similar to that of the confinement with continuous steel spiral rebars (see Subsections 7.4.3 and 8.3.4). However, due to the different constitutive law of steel and FRPs (Figure 15.8) and to the different bond action of embedded steel rebars and externally bonded FRP sheets or laminates through adhesive epoxy resins, extended experimental and analytical research has been made for the establishment of design rules in the case of FRP concrete confinement (Pantazopoulou, 1995; Teng et al., 2002; Biskinis, 2007; Fardis, 2009; Tassios, 2009).

- The model of Lam and Teng (2003a,b) has been proven to be the most reliable among many others for the determination of the apparent confined strength f_c^* of concrete and its corresponding ultimate strain ε_{cu}^* (Vintzeleou and Panagiotidou, 2007). These two values for full jacketing of a rectangular column with FRP sheets are given in the following expressions (Fardis, 2009):

$$\frac{f_c^*}{f_c} = 1.0 + 3.3 \left(\frac{b}{h}\right)^2 \alpha_n \frac{\rho_f f_{fe}}{f_c} \tag{15.77}$$

$$\frac{\varepsilon_{cu}^*}{\varepsilon_{c2}} = 1.75 + 12\sqrt{\frac{h}{b}} \, \alpha_n \frac{\rho_f f_{fe}}{f_c} \left(\frac{\varepsilon_{su}}{\varepsilon_{co}}\right)^{0.45} \tag{15.78}$$

where
b and h are the shorter and longer of the two sides of a rectangular section. In the case of a circular section $b = h =$ diameter of the section
α_n is the confinement effectiveness factor equal to $\alpha_n = 1$, for circular sections, and

$$\alpha_n = 1 - \frac{(b - 2R)^2 + (h - 2R)^2}{3b \cdot h} \tag{15.79}$$

for rectangular sections,
where
R is the radius of rounded corners (Figure 15.52)

$$f_{fe} = E_f \varepsilon_{se} \tag{15.80}$$

$\varepsilon_{fe} \cong 0.60 \varepsilon_{fu}$ (for CFRP)

$\varepsilon_{fe} \cong 0.85 \varepsilon_{fu}$ (for GFRP, AFRP)

$\varepsilon_{c2} = 2‰$ (EC2-1-1/2004)
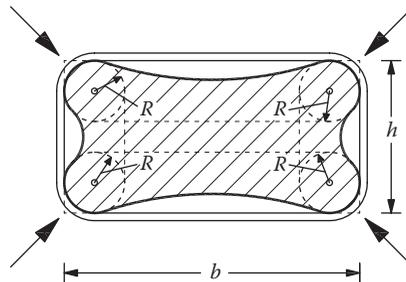
Figure 15.52 Confinement effectiveness factor for orthogonal cross-section depending on rounded corner radius R.

ρ_f is the geometric ratio of FRP to the wrapped concrete, that is,

$$\boxed{\rho_f = \frac{\pi D\, t_f}{\pi D^2 / 4} = \frac{4t_f}{D}} \quad \text{(circular cross-section)} \tag{15.81}$$

or

$$\boxed{\rho_f = \frac{2(b + h)t_f}{bh}} \quad \text{(orthogonal cross-section)} \tag{15.82}$$

t_f is the sheet thickness.

It should be noted that in the case of a circular section (Figure 15.53), value:

$$\boxed{f_1 = \frac{1}{2}\rho_f\, f_{de} = \frac{1}{2}\rho_f\, \varepsilon_{de}\, E_f} \tag{15.83}$$

expresses the lateral pressure applied by the FRP sheet to the concrete core at the stage of bonding failure of the FRP. In fact, at this stage:

$$f_1 D = 2t_f \cdot f_{de} \tag{15.84}$$

or

$$\boxed{f_1 = \frac{2t_f\, f_{de}}{D}} \tag{15.85}$$

Taking into account that the volumetric content of the FRP sheet to concrete is

$$\rho_f = \frac{\pi D\, t_f}{\pi D^2 / 4} = \frac{4t_f}{D} \tag{15.86}$$

It follows that

$$t_f = \frac{\rho_f\, D}{4} \tag{15.87}$$
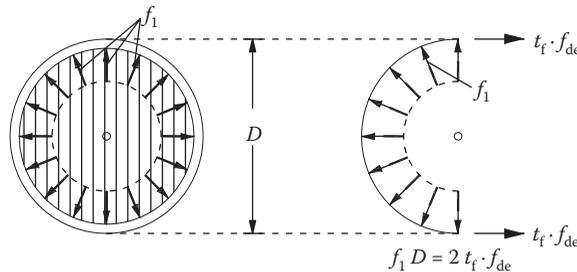
Figure 15.53 Confinement of a circular cross-section by wrapping with FRP sheets.

Introducing Equation 15.87 into Equation 15.85 results in

$$f_1 = \frac{1}{2}\rho_f \, f_{de} = \frac{1}{2}\rho_f \, \varepsilon_{de} \, E_f \tag{15.88}$$

Equation 15.77 enables the design of an existing R/C column for an axial load for which dimensions and reinforcement of the column are inadequate. In fact, the design capacity N_{ed} of an R/C column with a cross-section A_c and longitudinal reinforcement A_s in the case of confinement is given by the expression:

$$N_{Rd} = \frac{f_c^*}{\gamma_c} A_c + \frac{f_{y\kappa}}{\gamma_s} A_s \tag{15.89a}$$

where
 f_c^* is the apparent strength of confined concrete given by Equation 15.77.
 γ_c is the partial safety factor for concrete ($\gamma_c = 1.5$).
 $f_{y\kappa}$ is the characteristic yield strength of steel.
 γ_s is the partial safety factor for steel ($\gamma_s = 1.15$).
Capacity N_{Rd} must be bigger than demand N_{Ed}. Therefore, Equation 15.89a takes the form:

$$N_{Ed} \leq N_{Rd} = \frac{f_c^*}{\gamma_c} A_c + \frac{f_{y\kappa}}{\gamma_s} A_s \tag{15.89b}$$

Equation 15.89b results in f_c^* and then Equation 15.77 results in ρ_f. Finally, from Equation 15.81 or 15.82 the thickness of the wrapping sheet or the number of the successive sheets of a sheet of a given thickness may be calculated.
- EC8-3/2005 does not make any reference to strengthening of columns under axial loading using FRPs, since such an action does not refer directly to seismic retrofitting. However, the case of existing column inadequacy to axial loading in the framework of safety verifications for seismic loading is not infrequently encountered.
- ACI 440.2R-02 guidelines for 'the design and construction of externally bonded FRP systems for strengthening concrete structures' provide the following for the apparent strength of concrete f_c^* confined with FRPs:

$$\frac{f_c^*}{f_c} = 2.25\sqrt{1 + 7.9\frac{f_1}{f_c}} - 2\frac{f_1}{f_c} - 1.25 \tag{15.90}$$

where

$$f_1 = \frac{\kappa_\alpha \, \rho_f}{2} f_{f\,max} = \frac{\kappa_\alpha \, \rho_f \, \varepsilon_{fe} \, E_f}{2} \tag{15.91}$$

$$\varepsilon_{fe} = 0.004 \leq 0.75\varepsilon_{fu} \quad \text{(effective strain)} \tag{15.92}$$

κ_α is the 'efficiency factor' equal to

$$\kappa_\alpha = 1.0 \quad \text{(for circular sections)}$$

$$\rho_f = \frac{4\,n\,t_f}{D} \text{ (for circular sections)} \tag{15.93}$$

and

n is the number of jacketing plies.

The above approach is based on the Spoelstra and Monti (1999) model.

15.5.4.2 Ductility enhancement

- Ductility enhancement of an R/C member may be achieved by wrapping the critical regions where plastic hinges are potentially developed with FRP sheets. Obviously, these sheets are arranged with their fibres transversal to the axis of the member in the form of hoops (Figure 15.11b). This type of strengthening causes an increase of the strain capacity ε_u^* of the member due to confinement (Equation 15.78).
- According to EC8-3/2005, the necessary amount of confinement pressure f_1 to be applied depends on the ratio:

$$I_x = \mu_{\varphi,tar}/\mu_{\varphi,avail} \tag{15.94}$$

of the target curvature ductility $\mu_{\varphi,tar}$ to the available curvature ductility $\mu_{\varphi,ava}$ and may be evaluated as

$$\boxed{f_1 = 0.4\,I_x^2\,\frac{f_c\,\varepsilon_{cu}^2}{\varepsilon_{fe}^{1.5}}} \tag{15.95}$$

where
  f_1 is the confinement pressure.
  f_c is the concrete strength.
  ε_{cu} is the concrete ultimate strain.
  ε_{fe} is the adopted FRP jacket effective strain, which is lower than the ultimate strain of FRP ε_{fu}.

In the case of a circular cross-section, f_1 is given by Equation 15.88, from which ρ_f results if the value of f_1 derived from Equation 15.85 is introduced into Equation 15.88.

In the case of rectangular cross-sections in which the corners have been rounded to allow wrapping, the confinement pressure demand f_1' is given by Equation 15.95 after it has been multiplied by $\kappa_s = 2R/D$, where D is the larger section width.

- ACI 440.2R-2 specifies that the maximum usable compressive strain in concrete for FRP-confined circular R/C members may be evaluated by the following equation (15.96) (Mander et al., 1988):

$$\boxed{\varepsilon_{cu}^* \cong \frac{1.71(5f_{cu}^* - 4f_c)}{E_c}} \tag{15.96}$$

However, this specification does not make any reference to orthogonal cross-sections.

15.5.4.3 Clamping of lap-splices

In its Annex A, EC8-3/2005 also makes recommendations for the strengthening design of existing lap-splices by means of clamping, using FRP wrapping of the region in question.

15.5.5 Strengthening of R/C beam–column joints using FRP sheets and laminates

- Since 1998 efforts for upgrading existing beam–column joints have been focused on the use of FRPs in the form of epoxy-bonded sheets and laminates, since they are attractive for their flexibility. The fibre orientation in each ply can be adjusted so that specific strengthening objectives can be achieved (Engindeniz et al., 2004).
  The literature on FRP-strengthened joints mainly consists of simplified two-dimensioned tests, while three-dimensional tests are rather rare due to the difficulties of application. Below two successful proposals are presented, the first for a two-dimensional joint arrangement (Figure 15.54; Clyde and Pantelides, 2002) and the second for a three-dimensional one (Tsonos, 2008; Figure 15.55).
- The additional shear capacities of the strengthened columns and beam–column joints due to FRPs may be evaluated by the following equation (Tsonos, 2002):

$$\boxed{V_f = 0.9\, \varepsilon_{fe}\, E_f\, \rho_f\, b_w\, d} \tag{15.97}$$

where
  d is the effective depth of the cross-section.
  b_w is the minimum width of the cross-section over the effective depth.
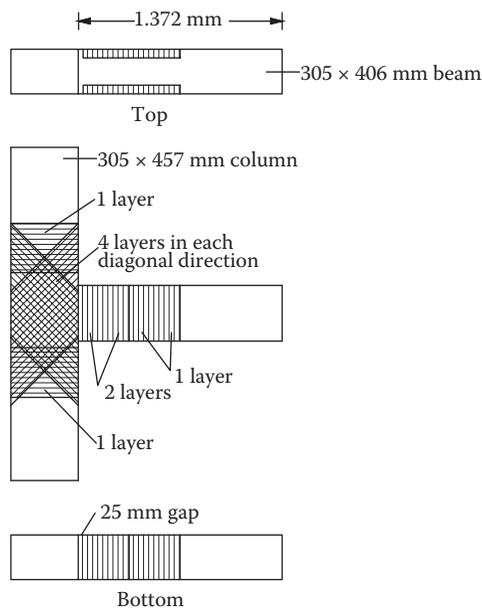
Figure 15.54 CFRP-strengthened specimen tested by Clyde and Pantelides. (Adapted from Clyde, C. and Pantelides, C.P. 2002. Seismic evaluation and rehabilitation of R/C exterior building joints. *Proceedings of the Seventh U.S. National Conference on Earthquake Engineering*, Georgia Institute of Technology, Boston, USA.)
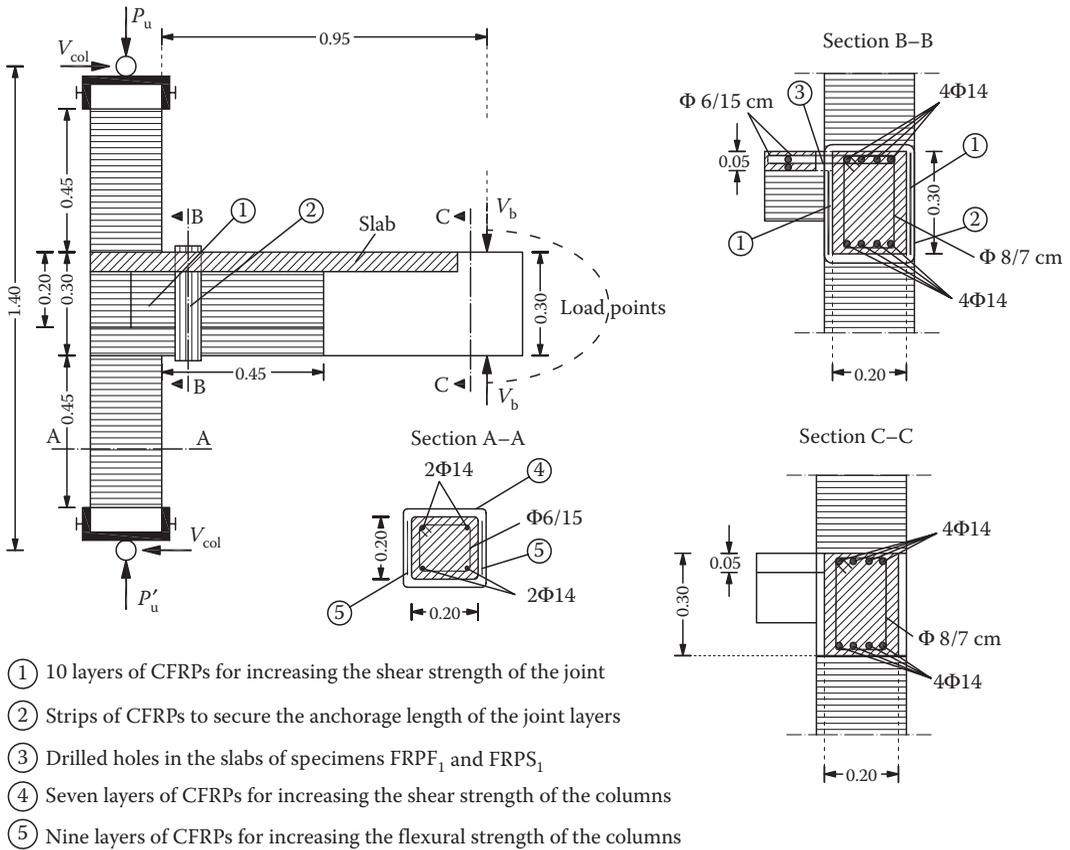
Figure 15.55 Jacketing of column and beam–column connection of subassemblages FRPF1 and FRPS1 (dimensions in m). (From Tsonos, A. 2008. Effectiveness of CFRP-jackets in post-earthquake and pre-earthquake retrofitting of beam-column subassemblages. *Engineering Structures*, 30, 777–793. Copyright 2008, with permission from Elsevier.)

ρ_f is the volumetric ratio of the FRP equal to $2t_f/b_w$ for continuously bonded shear reinforcement of thickness t_f.
E_f is the elastic modulus of elasticity of the FRP.
ε_{fe} is the effective FRP strain given by the following expression for fully wrapped or properly anchored FRPs (FIB, 2003):

$$\varepsilon_{f,e} = \left[0.17\varepsilon_{fu}\left(\frac{f_{cm}^{\frac{2}{3}}}{E_f \cdot \rho_f} \right) \cdot 0.006 \right] \tag{15.98}$$

where
f_{cm} is the mean value of the concrete *compressive* strength.

15.6 ADDITION OF NEW STRUCTURAL ELEMENTS

The seismic resistance of a structure is drastically improved by the addition of new structural elements of great stiffness able to carry horizontal forces.

Added shear walls
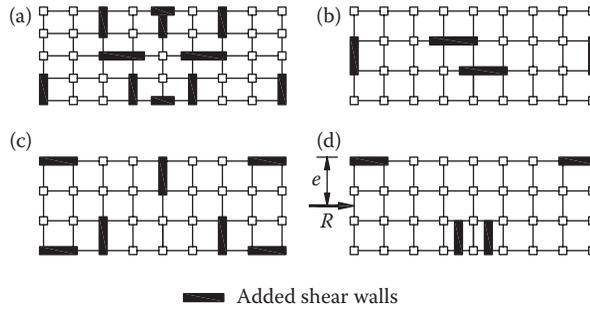
Figure 15.56 Addition of new R/C walls inside a frame or skeleton structure: (a), (b), (c) favourable layout (symmetric); (d) unfavourable layout (eccentric walls).

The new structural elements could be (Sugano, 1981; Bertero and Brokken, 1983; Bush et al., 1991; Rodriguez and Park, 1991; Penelis, 2001):

- R/C walls inside the frames that are formed by beams and columns (Figure 15.56). In this case, usually the columns at the ends of the wall are also jacketed with R/C jackets.
- Additional R/C walls outside the frames (Figure 15.56d).
- New frames.
- Truss systems (made of metal or R/C) in the R/C frame (Figure 15.57).

The choice of type, number and size of the new elements depends on the characteristics of each structure. The most common type is the addition of R/C walls. Since interventions of this type alter the stiffness of the structure as well as its dynamic characteristics, they must
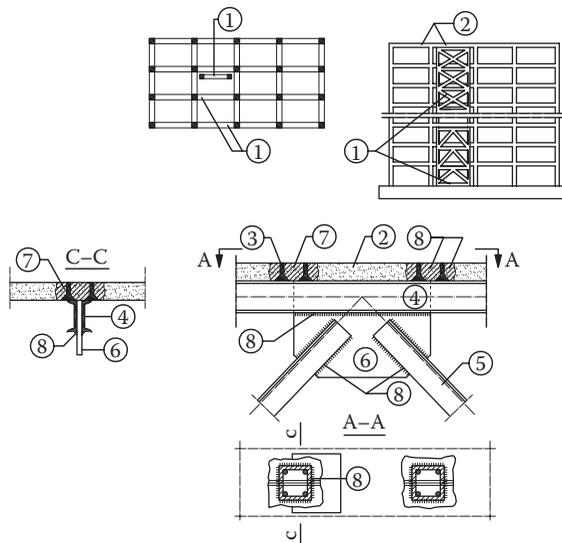
Figure 15.57 Addition of truss systems inside R/C frames: 1 = added steel truss; 2 = existing structure; 3 = steel dowel; 4 = horizontal steel rod; 5 = diagonal steel rod; 6 = steel joint plate; 7 = added concrete; 8 = welding.

Existing shear walls
Added shear walls
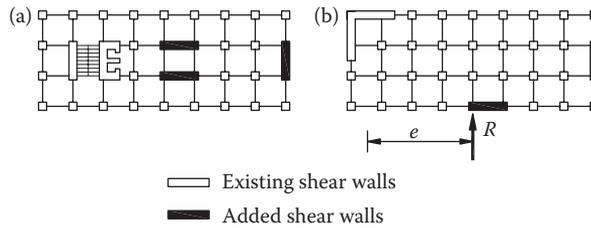
Figure 15.58 Improvement of stiffness eccentricities with the addition of new R/C walls.
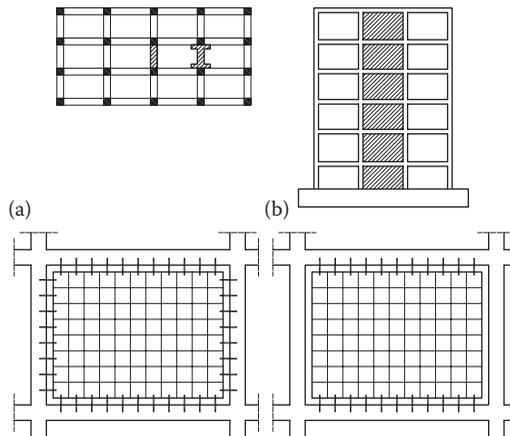
Figure 15.59 Addition of new R/C walls inside a frame: (a) connection along the four sides; (b) connection only with the beams.

be introduced into the original structure with special care. In this case, re-evaluation of the structural response of the building is necessary based on a rigorous new analysis and design. This re-evaluation must also be extended to the foundations, since the addition of new stiffness elements (e.g. multi-storey walls) leads to a concentration of large shear forces and moments at the base of these elements, which requires an appropriate strengthening of their foundation with widened footings or additional connecting beams, new foundation beams or even micropiling. Finally, it has to be stressed that very often the addition of new elements is carried out not only to increase the stiffness or the strength of the structure but mainly to alleviate some of the existing stiffness eccentricities that led to damage (Figure 15.58).

In the case of the addition of new elements, special care should be taken to ensure their connection with the existing elements so that force transfer is secured. Especially in the case of the addition of new R/C walls, the connection with the frame is made with dowels anchored with epoxy mortar or with reinforcement bars welded to the existing bars (Figure 15.59; Bertero and Brokken, 1983; Bush et al., 1991).

15.7 QUALITY ASSURANCE OF INTERVENTIONS

15.7.1 General

For a successful structural intervention, additional measures are needed in order to ensure quality of design and construction. Quality assurance of the design includes a thorough

review by an independent reviewer so that it is made sure that the design criteria and solutions are the proper ones and that the computational work and structural details have been properly prepared. Quality assurance of construction includes inspection and testing of materials, elaboration of method statements for construction, and assurance that the design is properly implemented during construction. While quality control is important for all constructions affecting the safety of the occupants, it is particularly important for seismic repair or strengthening due to the fact that these activities require a high degree of engineering judgment and careful attention to detail.

15.7.2 Quality plan of design

Seismic repair and strengthening projects require an appropriate scheme of counter-checking of design documents. When the design has been completed and the project manager has thoroughly reviewed the work, an additional check should be performed by an independent engineer. This may be a governmental or private agency responsible for verifying the criteria and checking the calculations and drawings to make sure that they conform to the criteria and regulations of the building codes.

15.7.3 Quality plan of construction

Construction inspection is carried out by an individual agency or firm, similar to conventional construction. However, an experienced engineer, with an extensive knowledge of repair materials and techniques, should be appointed as construction inspector of repair and strengthening projects. The design engineer should continue to be involved with the inspection process and provide answers to questions arising during the implementation of the design details in the construction. This is extremely important for such projects, as many unexpected situations will be encountered during the construction, related mainly to hidden damage discovered after the finishes have been removed.

The quality of materials is verified by sampling and testing as in a conventional project. The differences involve only the verification of existing conditions and the testing of special materials such as resins, non-shrinking mortars, shotcrete and so forth.

The design documents should include a detailed description of the work schedule related to the repair and strengthening, as well as detailed specifications for the materials and construction techniques.

15.8 FINAL REMARKS

From the preceding presentation the following final remarks can be made:

1. During the process of repairing damage caused by an earthquake or reforming the structural system in a pre-earthquake period, due to demolition works on the structure, a strong temporary shoring system is required to avoid collapse.
2. During the repair process additional materials and techniques are used that are very rarely applicable to new structures. Therefore, a detailed study of their characteristics is required, as well as very careful supervision during their application.
3. The form and extent of repairs cannot be completely foreseen during the design phase. The engineer is often compelled to improvise in order to adjust the materials and techniques to the needs of the existing special conditions.

4. Those interventions that drastically alter the original dynamic characteristics of the building must be applied with extreme care.
5. The redimensioning and safety verification of the repaired elements is achieved by more or less approximate procedures, firstly because no reliable analytical models based on laboratory tests have yet been developed for the variety of cases met with in a damaged structure, and secondly because there is a high degree of uncertainty with regard to the achieved degree of composite action of the old element and the new materials.
6. Finally, the repair cost of an element is much higher than the cost of its original construction, due to the fact that, on the one hand, repair involves complicated works such as demolition, supports, welding, injections and so on, and on the other, the original construction inhibits the unobstructed use of mechanical equipment. Therefore, the cost estimate of such an operation is to an extent unpredictable.

Chapter 16

Seismic risk management

16.1 GENERAL

In simple terms, seismic risk management may be defined as the framework of activities for the most effective use of available financial resources in an effort to reduce the consequences of earthquakes in a region. It is apparent that this framework constitutes the strategic plan of the government of a country for seismic risk reduction in its seismic regions. Earthquakes, as natural phenomena, in very few cases pose a direct threat to humans (e.g. landslides, tsunamis). Earthquakes generally become hazardous only when they are considered in relation to the built environment. In this respect, the built environment as a whole (buildings, bridges, dams, motorways, lifelines, etc.) contributes to the formation of the 'seismic risk'. However, since buildings, and particularly those with R/C structural systems, constitute the basic core of the built environment, it was decided to include a chapter on seismic risk management in this book, although it does not relate only to R/C buildings.

Before proceeding to the presentation of the main issues involving seismic risk management, it will be useful to give a short glossary of terms that will be used in the following sections (UNIDO/UNDP, 1985; FEMA 366, 2008).

1. *Seismic hazard*: The probability of occurrence within a specified period of time, in a given area, of a potentially damaging seismic action, quantified by its intensity or other characteristics (e.g. spectral characteristics, duration, accelerograms, etc.).
2. *Vulnerability*: The degree of damage resulting from the occurrence of a seismic action with specified characteristics to a type of building expressed both in *qualitative* and *quantitative* terms.
3. *Specific risk*: the expected degree of *loss* due to earthquakes during a specified period of time, given as a function of both *seismic hazard* and *vulnerability*.
4. *Elements at risk*: The population, property, and economic activities, including public services, *at risk* due to the seismic action in a given area.
5. *Seismic risk*: The damage and/or losses expected (in a probabilistic sense) to affect the elements at risk together with related structures during a specified period of time and as a result of a seismic action.
6. *Annualised earthquake loss (AEL)*: The estimated long-term value of earthquake losses in any given single year in a specified geographic area.
7. *Annualised earthquake loss ratio (AELR)*: The ratio of average AEL to the replacement value of the building inventory.

16.2 CONCEPTUAL APPROACH TO THE STEPS OF SEISMIC RISK MANAGEMENT

In a broad sense, 'seismic risk' is a product of a system of random factors, that is:

1. Seismic hazard of the region of reference
2. Vulnerability of the structures of the region under examination
3. Elements at risk exposed in the structures under consideration

Therefore, quantification techniques for risk analysis rely on probabilistic concepts.
   The procedure of seismic risk management basically includes three steps:

1. *Step one:* Specific risk evaluation.
   The interrelation of *seismic hazard* characteristics of the geographic area under consideration with the *seismic vulnerability* characteristics of the buildings results in the *specific risk* characteristics of the region (Figure 16.1).
2. *Step two:* Evaluation of elements at risk.
   The interrelation of *specific risk* characteristics with the *exposure* of *elements at risk* results in the *seismic risk* characteristics (Figure 16.2) of the region.
3. *Step three*: Cost–benefit analysis, or risk–benefit analysis.
   Seismic risk characteristics expressed by expected cumulative losses in monetary terms for a period of time are examined in relation to *alternative mitigation programmes*. Expected *cost* for the implementation of each programme under consideration is then compared with expected *benefits* in monetary terms. The ratio of benefit to cost in monetary terms is the final criterion for decision making for the acceptance or rejection of the alternative mitigation programme under consideration (Figure 16.3).
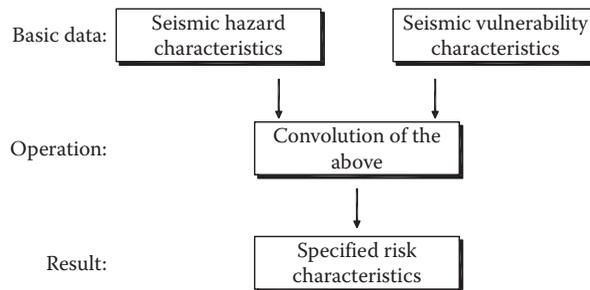
Figure 16.1 Evaluation of specific seismic risk.
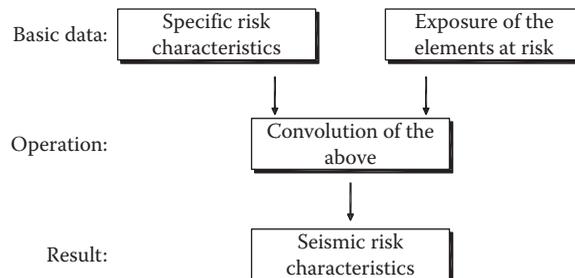
Figure 16.2 Evaluation of seismic risk.
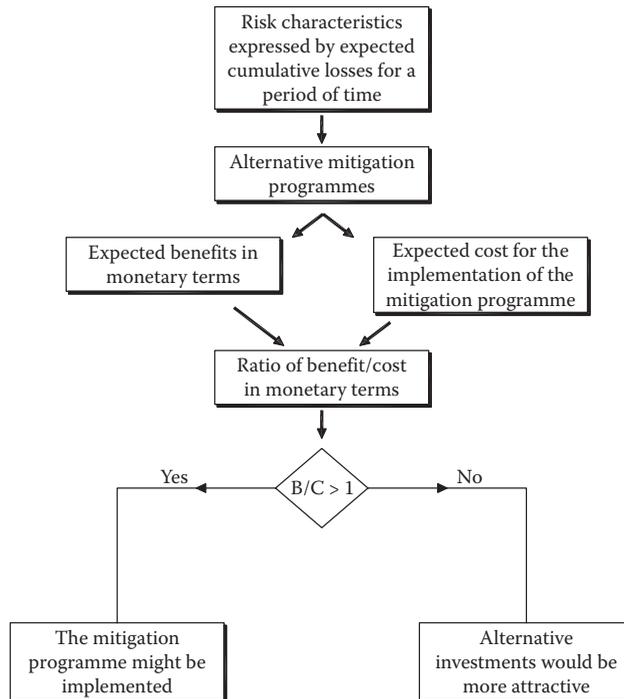
Figure 16.3 Cost–benefit analysis procedure.

   Alternatively, expected *reduction of life losses* for a period of time is estimated in relation to *alternative mitigation programmes*. Expected *cost* for the implementation of each programme under consideration is then divided by the number of casualties averted. Then the *cost* per death averted is used as a criterion for decision making for the implementation of the programme in comparison with other corresponding actions.

16.3 SEISMIC RISK ASSESSMENT IN THE UNITED STATES AND EUROPEAN UNION

In the last 15 years, after a long elaboration of the above ideas and research activities on the subject, integrated tools for seismic risk analysis were developed first in the United States (1999) and soon after (2000) in the European Union. It is worth making a short reference here to both of them.

 1. HAZUS-MH: (Hazards U.S. – Multi Hazard) Version MR2 (FEMA/NIBS/2006).
    Six modules are included, namely:
    Module 1: Potential earth-science hazard (PESH)
    Module 2: Inventory and exposure data
    Module 3: Direct damage
    Module 4: Induced damage
    Module 5: Indirect losses (short term)
    Module 6: Indirect losses (long term)
    HAZUS-MH is a tool that local, state and federal governments in the United States can use for seismic mitigations, emergency preparedness, response and recovery planning

and disaster response operations. The methodology of HAZUS-MH incorporates state-of-the-art approaches for characterisation of hazard, estimating damage and losses to buildings and lifelines, estimating casualties, and estimating direct and indirect economic losses. It is an integrated system that has already been implemented in the United States with very interesting results (FEMA/HAZUS-MH/MR1, 2002). HAZUS-MH allows decision makers to base their decisions on seismic risk and not on seismic hazard anymore, which was considered for many decades the reference point for seismic losses.

2. RISK-UE (2001–2004)

This procedure includes seven basic working packages and seven working packages of application of the procedure to seven European cities. The basic work packages are the following:

- WP1: European distinctive features, inventory database and typology
- WP2: Basis of a handbook of earthquake ground motion scenarios
- WP3: Methodology on Urban System Exposure (USE) assessment for natural disasters
- WP4: Vulnerability of current buildings
- WP5: Vulnerability assessment of historical and monumental buildings
- WP6: Vulnerability assessment of lifelines and essential facilities
- WP7: Seismic risk scenarios handbook

The rest of the seven working packages include an implementation of RISK-UE procedure to seven characteristic European cities, namely Barcelona (Spain), Bitola (FYROM), Bucharest (Romania), Catania (Italy), Nice (France), Sofia (Bulgaria) and Thessaloniki (Greece). RISK-UE is a risk analysis tool similar to HAZUS-MH. However, it mirrors the characteristics of the European building stock and particularly the buildings of European cultural heritage, that is, monumental buildings and urban nuclei.

It was elaborated in the framework of a European seismic risk reduction programme by the following Agencies or Universities Partners:

- Spain ICC and CIMNE (Barcelona)
- Italy POLIMI (Milano) and UNIGE (Genova)
- Greece AUTH (Thessaloniki)
- FYROM: IZIIS (Skopje)
- Bulgaria CLSMEE (Sofia)
- Romania UTCB (Bucharest)
- France DRGM and GeoTer (Marseille)

The whole structure of RISK-UE in large part complies with the HAZUS-MH computer platform. In this respect, this platform may also be used for RISK-UE analysis for input related to the characteristics of the European-built environment.

In the next sections a closer approach will be made to the quantification procedure of *hazard, vulnerability, specific risk, elements at risk* and *seismic risk*. A reference will also be made to the techniques for their interrelation for the determination of seismic risk in the form of monetary losses in the case of an expected seismic action, which is a basic step for the seismic risk management. Finally, an overview will be made to the mitigation programmes that have been adopted nowadays by various countries for seismic risk reduction.

16.4 SEISMIC HAZARD

This is the primary source of seismic risk analysis and is defined basically in terms of macrozonation and also microzonation maps and studies. Macrozonation maps define broad

zones or contours assumed to be homogeneous in regard to the hazard (maximum intensities in regard to a given return period). Until recently they had the form of qualitative empirical intensity scales (e.g. MM scale or MSK scale-EMS-98), while nowadays they are expressed by the expected peak ground acceleration (PGA) and a normalised elastic acceleration response spectrum. Seismic hazard, elastic and inelastic spectra, and their probabilistic character have already been examined in detail in Subsections 2.2.4, 2.2.6, 3.3.2 and 3.4.3, and further reference to the issue should therefore be superfluous. Here it should be noted that all this information must be classified and filed using a well-organised geographic information system (GIS) common for all other steps of seismic risk management.

Microzonation maps or studies refer to restricted areas that are densely built and populated, or else refer to the locations for some particularly important structures. These maps provide detailed zones and specify the expected spectral content of expected strong earthquakes (Figure 16.4; Faccioli and Pessina, 2003; Pitilakis et al., 2006).

16.5 SEISMIC VULNERABILITY

16.5.1 Fundamentals

The main aim of the seismic vulnerability analysis of a region is the generation of *seismic vulnerability curves* for a series of model building types into which the buildings of the region have been classified. Each of these curves relates the earthquake intensities expressed either in the form of a qualitative scale (EMS-98 scale) or in the form of PGA or spectral displacements S_d, with the corresponding damage indices D_r defined as

$$D_r = \frac{\text{Cost of damage to an item}}{\text{Value of that item}} \qquad (16.1)$$
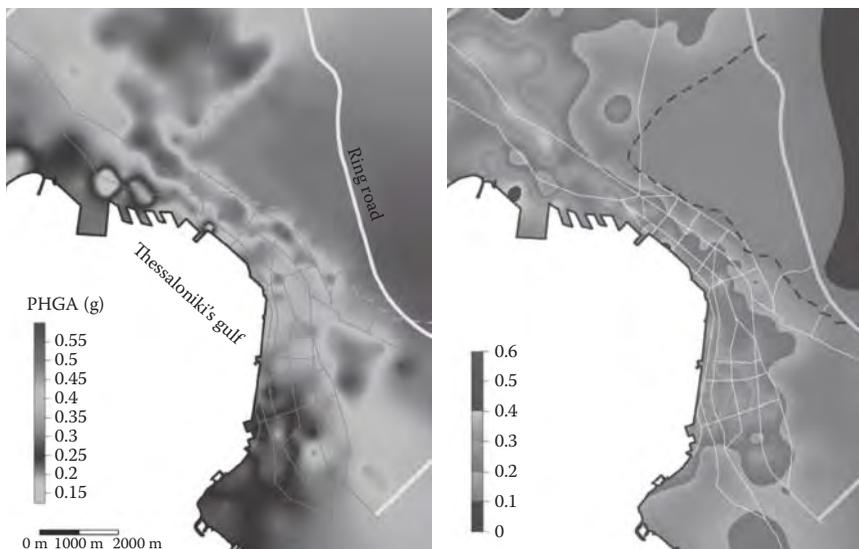
Figure 16.4 Spatial distribution of mean peak horizontal acceleration for $T = 0$ s (left) and $T = 1$ s (right) for the city of Thessaloniki. (With kind permission from Springer Science+Business Media: Pitilakis, K. 2006. Earthquake risk assessment of lifelines. *Bulletin of Earthquake Engineering* 4(4).)
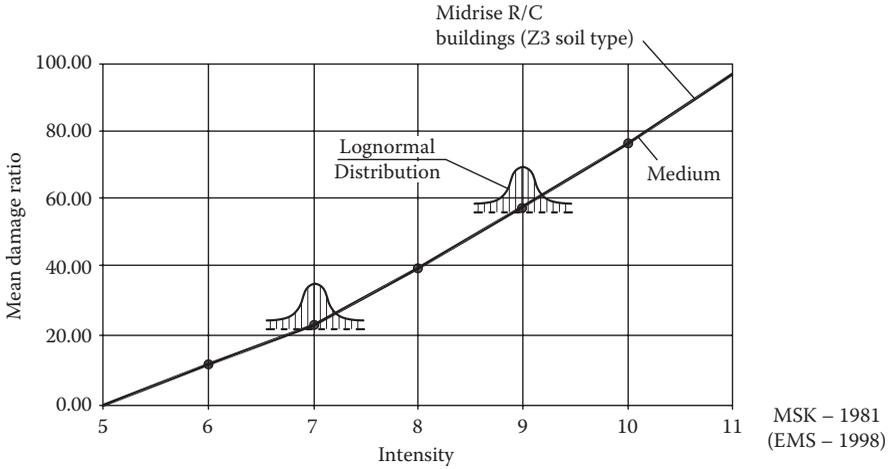
Figure 16.5 Mean damage ratio at different intensity levels of midrise R/C buildings after CAR and BU. (Adapted from Erdik, M. and Aydinoğlu, N. 2000. *Earthquake vulnerability of buildings in Turkey.* Internal report, Boğaziçi University, Istanbul.)

where Value is expressed best in terms of Replacement Value and D_r is a function of the seismic intensity and the physical nature (vulnerability) of the item considered (Dowrick, 2005).

It is apparent that this vulnerability curve has a probabilistic character in the sense that all buildings of the same model type in the same region will present scattered values around a medium value. Therefore, the vulnerability curves of Figure 16.5 (Erdik and Aydinoğlu, 2000) and Figure 16.6 (Kappos et al., 2006b) represent the medium of the scattered values of D_r. Based on statistical analyses of damages caused by various earthquakes, it has been found that the statistical distribution of the results fits better with a *lognormal* distribution (Kappos et al., 2006; FEMA/HAZUS-MH/MR1, 2002).
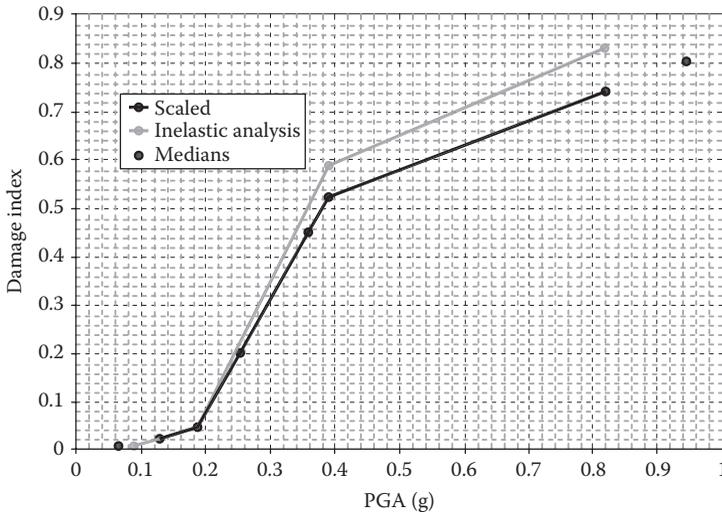
Figure 16.6 PGA – damage index relationship for an R/C building type (moderate height infilled). (With kind permission from Springer Science+Business Media: Kappos, A. et al. 2006b. A hybrid method for the vulnerability assessment of R/C and URM buildings. *Bulletin of Earthquake Engineering*, 4, 391–413.)
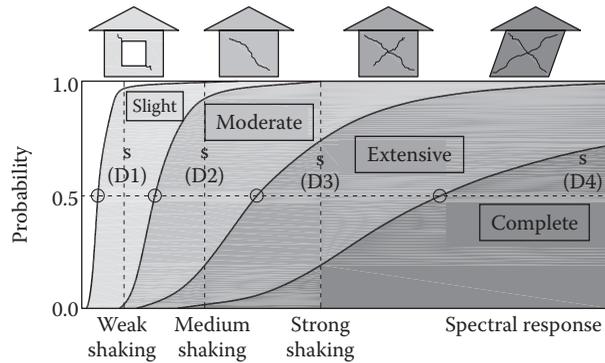
Figure 16.7 Examples of fragility curves for slight, moderate, extensive and complete damage. (From FEMA/ HAZUS-MH/MR1. 2002. *Multi-Hazard Loss Estimation Methodology: Earthquake Model*, Federal Emergency Management Agency (FEMA), Washington, DC. With permission.)

Taking the vulnerability curve of a building model type as a basis, a suite of probabilistic curves can be developed, known as '*fragility curves*'. These curves are very useful for specific risk assessment (losses of buildings in economic terms). They are depicted in diagrams where the horizontal axis represents successive steps of earthquake excitations expressed in the form of a qualitative scale, or in the form of PGA, or in the form of spectral displacement S_d, and the vertical axis the probability of a building of the category under consideration of overcoming a predefined *damage threshold* DS (Figures 16.7 and 16.8) (FEMA/HAZUS-MH/MR1, 2002).

This predefined damage threshold DS is directly related to an empirical scale of '*apparent vulnerability*' (Table 16.1; Mouroux and Le Brun 2006). This damage scale refers to slight, moderate, extensive and complete damage states (DS). As it emerges from Table 16.1, this table is similar for RISK-UE and HAZUS-MH.

For the generation of the fragility curves of a building category, the successive values of spectral displacements $\bar{S}_{d,\mathrm{DS}}$ corresponding to the successive DS are depicted in the diagram
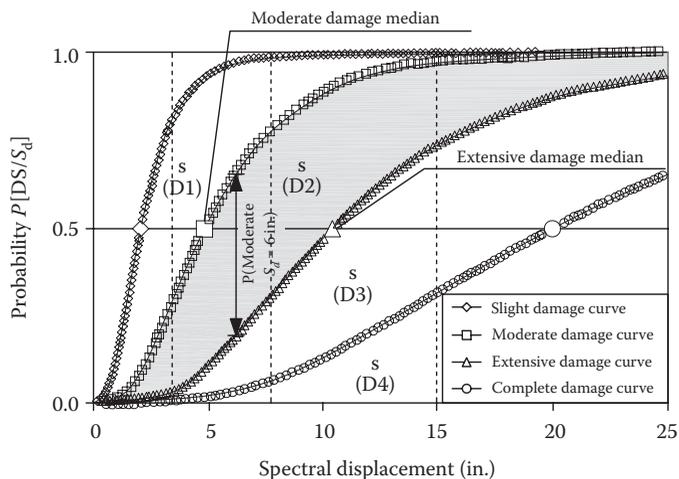
Figure 16.8 Examples of fragility curves – calculation of damage state probability. (From FEMA/HAZUS-MH/ MR1. 2002. *Multi-Hazard Loss Estimation Methodology: Earthquake Model*, Federal Emergency Management Agency (FEMA), Washington, DC. With permission.)

Table 16.1 Damage grading and loss indices

| Damage grade/DS | Damage grade label | | | Description | Loss indices | | | |
| | RISK-UE | | | | AUTH | IZIIS | | |
	LM1 method	LM2 method	FEMA/NIBS (HAZUS)			RC	Masonry	UNIGE
(DS0)	None	None	None	No damage	0.0	0.0	0.0	0.0
(DS1)	Slight	Minor	Slight	Negligible to slight damage	0–0.05	<0.15	<0.2	0.1
(DS2)	Moderate	Moderate	Moderate	Slight structural, moderate nonstructural	0.05–0.2	0.15–0.25	0.20–0.30	0.2
(DS3)	Substantial to heavy	Severe	Extensive	Moderate structural, heavy nonstructural	0.2–0.5	0.25–0.35	0.30–0.40	0.35
(DS4)	Very heavy	Collapse	Complete	Heavy structural, very heavy nonstructural	0.5–1.0	0.35–0.45	0.40–0.50	0.75
(DS5)	Destruction			Very heavy structural, total or near total collapse	—	>0.45	>0.50	1.00

Source: With kind permission from Springer Science+Business Media: Mouroux, P. and Le Brun, B. 2006. An advanced approach to Earthquake risk scenarios with applications to different European Towns. *Assessing and Managing Earthquake Risk*.

at the probability ordinate 0.50. *This value* $\bar{S}_{d,DS}$ *is taken from the vulnerability curve*, which represents, as already noted, the medium values of the successive thresholds DS (Figure 16.8). Taking each of these points as a point of reference, the corresponding fragility curves may be formulated. For structural damage corresponding to a given spectral displacement DS, the probability of being in or exceeding a damage state DS is modelled as (Figures 16.7 and 16.8):

$$p[DS/S_d] = \Phi\left[\frac{1}{\beta_{DS}}l_n\left(\frac{S_d}{\bar{S}_{d,DS}}\right)\right]$$

(16.2)

(lognormal function)
where

$\bar{S}_{d,DS}$ is the medium value of spectral displacement at which the building reaches the threshold of the damage state DS.

β_{DS} is the standard deviation of the natural logarithm of spectral displacement of damage state DS (lognormal deviation).

Φ is the standard normal cumulative distribution function.

Lognormal deviation β_{DS} for buildings varies from 0.4 to 1.2 (HAZUS-MH MR1, Chapter 6) and depends on the variability associated with the discrete threshold of each damage state, the variability of the capacity of each structural type, and, finally, the variability of the demand.

Fragility curves of Figure 16.8 are cummulative and may be interpreted as follows: The probability of moderate damage at a given level of spectral demand, for example, 6.0 in. ($\approx$15.2 cm) is calculated as the difference of probability of moderate (or greater) damage minus the probability of extensive (or greater) damage, that is, 0.40.

In Figure 16.9a,b the fragility curves are given in terms of DS of infilled R/C buildings for medium-rise frames for low design requirements (left) and for high design requirements (right) according to the Greek Seismic Code (Kappos et al., 2006b).
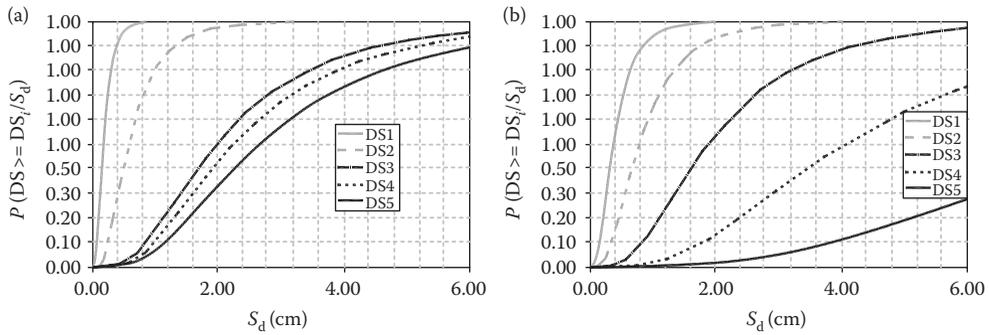
Figure 16.9 S_d-based fragility curves for medium-rise infilled frames, low (a) and high (b) code design. (With kind permission from Springer Science+Business Media: Kappos, A. et al. 2006b. A hybrid method for the vulnerability assessment of R/C and URM buildings. *Bulletin of Earthquake Engineering*, 4, 391–413.)

It is apparent that for the generation of fragility curves of various building categories, an immense volume of information must be gathered and classified in a proper way using a well-organised GIS.

16.5.2 Inventory of the building stock-classification

16.5.2.1 Inventory of the building stock

For the building stock under consideration an inventory must be developed. This inventory must be filed in the GIS in use for the seismic risk management of the region or the country.

This inventory must include at least the following information for the buildings:

1. Construction material
2. Number of storeys
3. Structural system (e.g. framed or dual)
4. Usage (elements at risk)
5. Number of occupants (elements at risk)
6. Characteristic period of construction in relation to Codes in force at that period
7. Replacement cost
8. Seismic zone
9. Construction quality

This information may be gathered by a census campaign at the local or country level.

16.5.2.2 Building classification based on the structural system and its material

Furthermore, these buildings are classified both in terms of their use, or occupancy class, and in terms of their structural system or model building type. Damage is predicted based on model building type, since the structural system is considered the key factor in assessing overall building performance, loss of function and casualties (Figure 16.10) (FEMA/HAZUS-MH/MRI, 2002).

In RISK-UE, the general building stock is classified into nine categories, namely (Table 16.2, Lungu et al., 2001):

- B1: Residential
- B2: Commercial
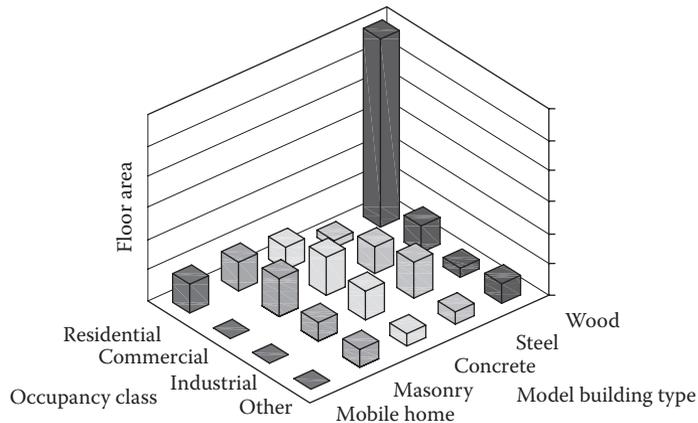
Figure 16.10 Examples of inventory relationship of model building type and occupancy class. (From FEMA/ HAZUS-MH/MR1. 2002. *Multi-Hazard Loss Estimation Methodology: Earthquake Model*, Federal Emergency Management Agency (FEMA), Washington, DC. With permission.)

- B3: Cultural
- B4: Multiple use
- B5: Monuments and historical heritage
- B6: Religious
- B7: Industrial
- B8: Agricultural
- B9: Temporary buildings

Each of these is divided into sub-categories. At the same time, they are classified in a matrix form according to their importance or exposure category (three categories).

Next, the *building typology matrix* (BTM) is developed according to building material, number of storeys and the Code level for which each building has been designed.

In HAZUS-MH, buildings have been classified into 36 categories based on the building material and the structural system. Furthermore, for each of these categories an additional classification has been made based on the construction period and their macrozoning distribution.

In Greece, R/C buildings with or without infills and with or without a ground soft storey (pilotis) have been classified into 72 model building types. For 36 of them, fragility curves have been generated (Kappos et al., 2006b).

16.5.2.3 Classification of non-structural systems and contents

The non-structural system and building's contents (e.g. mechanical installations) tend to dominate economic loss. Typically, the structural system represents about 20% of the building's value. To better estimate different types of loss due to building damage, functions separate from the structural system have been established to predict damage to non-structural components. These functions are separated into:

1. Drift-sensitive components such as building partition walls
2. Acceleration-sensitive non-structural elements, such as suspended ceilings. Table 16.3 gives typical drift-sensitive and acceleration-sensitive components in the HAZUS classification system.

Table 16.2 Classification of buildings occupancy (indicative) according to RISK-UE-WP1

Name	Occupancy category	Importance/exposure category		
		1	*2*	*3*
B	**General building stock**			
B1	**Residential**			
1.1	Single-family dwelling (house)			x
1.2	Multi-family dwelling (apartment bldg.)			
1.3	Low-rise (1–2)			x
1.4	Mid-rise (3–7)			x
1.5	High-rise (8+)		x^a	x
…	…	…	…	…
B2	**Commercial**			
2.1	Supermarkets, malls		x^b	x
2.2	Offices		x^b	x
2.3	Services			x
2.4	Hotels, motels		x^b	x
…	…	…	…	…
B3	**Cultural**			
3.1	Museums		x^c	x
3.2	Theatres, cinemas		x^b	x
3.3	Public event buildings		x^b	x
3.4	Stadiums		x^b	x
…	…	…	…	…
B4	**Multiple use**		x^a or x^b	x
B5	**Monuments and historical heritage**			
5.1	Palaces, mansion houses	x^d	x	
5.2	Tower			x
5.3	Castles		x	
…	…	…	…	…

Source: Adapted from Lungu, D. et al. 2001. *RISK-UE, WP 1: European distinctive features, inventory database and typology*. EVK4-CT-2000-00014.

[a] Buildings with capacity greater than 150 people.
[b] Buildings with capacity greater than 300 people or where more than 300 people congregate in one area.
[c] Museums housing very important cultural values.
[d] Buildings with essential functions and possibility of crowding.

Table 16.3 HAZUS classification of drift-sensitive and acceleration-sensitive non-structural components and building contents (indicative)

System type	Component description	Drift-sensitive	Acceleration-sensitive
Architectural	Nonbearing walls/partitions	•	
	Cantilever elements and parapets		•
	Exterior wall panels	•	
Mechanical and electrical	General mechanical (boilers, etc.)		•
	Manufacturing and process machinery		•
	Piping systems		•
	Storage tanks and spheres		•
Contents	File cabinets, bookcases, etc.		•
	Office equipment and furnishings		•
	Computer/communication equipment		•

Source: From FEMA/HAZUS-MH/MR1. 2002. *Multi-Hazard Loss Estimation Methodology: Earthquake Model*, Federal Emergency Management Agency (FEMA), Washington, DC. With permission.

16.5.2.4 Damage states

As was noted before, damage is described by one of four discrete *damage states* (DS):

- Slight (DS1)
- Moderate (DS2)
- Extensive (DS3)
- Complete (Collapse; DS4)

These DS must be related on one hand with *loss indices*, and on the other with structural characteristic limits of the *spectral lateral load–displacement diagram*.

The first relation has already been given in Table 16.1. This relation has been based on information resulting from statistical analyses of post-earthquake damages and their repair cost. For example, in Greece, for almost all relevant studies, the report on the post-earthquake damage evaluation of the Thessaloniki earthquake of June 20, 1978 has been used as the main source of information (Penelis et al., 1987).

The second relation is depicted schematically in Figure 16.11, while the relevant values for High Code R/C buildings are given in Table 16.4 (Milutinovic and Trendafilovski, 2003). This information is the result of inelastic push-over analysis related to experimental results and statistical analyses of post-earthquake damage evaluation.

16.5.2.5 Relation of seismic intensity and the damage index

16.5.2.5.1 Statistical procedure

For many years, the relation between seismic intensity and the damage index has been based on statistical damage evaluation of the results of strong earthquakes in a region (see Table 16.5; Penelis et al., 1988a). The information in these tables was transformed to vulnerability curves (Dowrick, 2005).

It is apparent that this is a very tiresome procedure and that the findings for one strong earthquake were not enough, because in the influence zone of a strong earthquake where various intensities were exhibited (e.g. MM V–XII), buildings of all classified categories were not located in every distinct intensity area.

Thus, in the last 15 years this method has tended to be replaced *by hybrid procedures* where the results of inelastic static or dynamic analyses are combined with damage indices
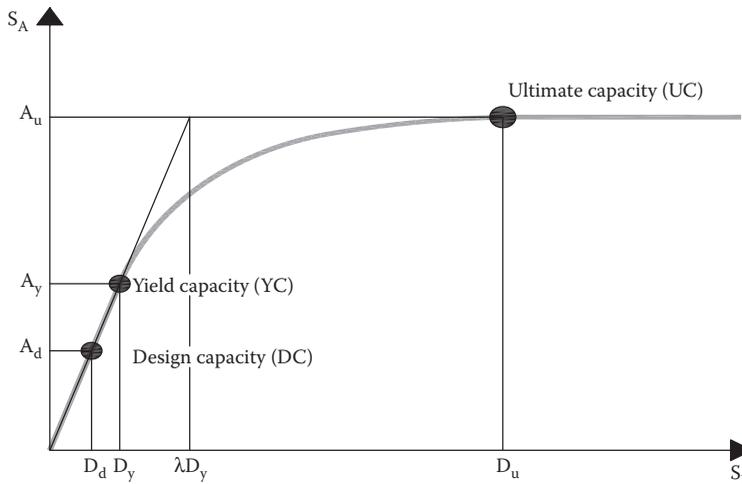
Figure 16.11 Building capacity spectrum. (Adapted from RISK-UE. 2001–2004. *An advanced approach to earthquake risk scenarios with applications to different European towns*, Contract: EVK4-CT-2000–00014, European Commission, Brussels.)

of the structural system that have resulted from the statistical evaluation of post-earthquake damage surveys (Penelis et al., 1988a; Kappos et al., 1991; Penelis et al., 1988b).

16.5.2.5.2 Hybrid procedures

According to this procedure, for each building category a typical structural system is selected that may be considered to be a representative model of this category. This structural system is designed according to the Seismic Codes of the successive reference periods of building construction and for the successive Seismic Zones where this building category was in use.

For each of these typical structural systems (e.g. three successive Codes × three Seismic Zones makes nine different design alternatives for the same structural type), an inelastic static or dynamic analysis is carried out.

In the Lab of R/C structures of AUTH, Greece, inelastic dynamic analysis has been used (Kappos et al., 1991, 2006; Penelis et al., 1988b). Seismic excitations have been introduced in the form of proper accelerograms proportional to each other and with successively increasing PGA. For this excitation, the response time history of the structural system was determined and particularly the developing plastic hinges and the percentage of their available plastic rotation, consumed as seismic demand during the seismic excitation. These 'structural damage' indices have been correlated with 'apparent damages' and the cost of their repair in economic term derived from an extended post-earthquake rehabilitation programme in Thessaloniki. This programme included repair activities of epoxy resin injections, R/C or FRP jacketing according to the degree of damage, and the correlation of degree of damage to the structural damage indices are used in the hybrid procedure (see RISK-UE WP04). The repair costs for each damaged element were summed up for the whole structural system, and by applying Equation 16.1 the damage index of the structure in economic terms was determined. So, for each PGA and the relevant accelerogram, a 'medium' value for the damage index was concluded, and therefore the *vulnerability curve* for the model building of the category under consideration plotted.

From these curves the corresponding fragility curves as derivatives were generated according to what has been noted in a previous subsection. In these diagrams the horizontal axis

Table 16.4 Parameters of the fragility curves for high code RC buildings

Bldg. properties		Height (m)		Interstorey drift at threshold of damage slate				Spectral displacements (cm)							
								Slight		Moderate		Extensive		Complete	
BTM	Institution	Roof	Modal	Slight	Moderate	Extensive	Complete	Median	Beta	Median	Beta	Median	Beta	Median	Beta
RCIL	3							0.12	0.40	0.19	0.50	0.26	0.60	0.53	0.70
	5	570	342	0.18	0.39	0.59	1.40	0.63	0.65	1.32	0.75	2.01	0.85	4.78	0.95
RCIM	3							2.11	0.40	3.31	0.50	4.52	0.60	9.35	0.70
	5	1710	1026	0.15	0.32	0.49	1.17	1.58	0.65	3.32	0.75	5.06	0.85	12.03	0.95
RCIH	3							7.40	0.40	11.64	0.50	15.87	0.60	32.82	0.70
	5	2850	1710	0.21	0.44	0.67	1.60	3.59	0.65	7.55	0.75	11.51	0.85	27.35	0.95

Table 16.5 Repair cost per unit volume (in drachmas 1978, 1$ = 36 drachmas 1978)

Type of structural system	Non-structural elements (drach/m³)	Structural elements (drach/m³)	Total cost (drach/m³)	Economic losses (% of the construction cost)
R/C	12.87	17.07	29.94	1.00
Mixed	78.55	65.49	144.04	4.81
Masonry	132.00	155.68	287.68	9.59
Total	21.05	26.09	47.14	1.57

represents the successive steps of PGA, while the vertical one represents the probabilities of exceedance of one of the given fragility curves, which correspond to the four or five damage thresholds. These curves are transformed into the damage probability matrix (DPM) of the building category for input into the GIS system.

The above procedure has been used for the production of the fragility curves of R/C and unreinforced masonry (URM) buildings in Greece, and it is incorporated in RISK-UE (WP 04 and UP 14) Figure 16.12 (Kappos et al., 2006b).

This method was used first in its original form for the damage prediction of the city of Thessaloniki for an earthquake scenario of 7.0 on the Richter scale from the same source of the earthquake of June 20, 1978 of magnitude 6.5 on the Richter scale. Having the accelerogram of this earthquake at a seismic station in the center of the city, this record using 'top-to-bottom one-degree site response analysis' was estimated at the bedrock. Then, following the 'bottom-to top-procedure', it was estimated at the surface of ten positions in the city where the geotechnical information was well documented from borehole and crosshole tests. For these artificial accelerograms and for the four main types of buildings given in Table 16.6, the damage index for the earthquake of June 20, 1978 was determined, and it was correlated to the repair cost in the various positions under consideration (Figure 16.13). The correlation coefficient was found to be astonishingly high ($r^2 = 0.92$). However, the ratio of analytically estimated cost to the real one was found to be $\kappa = 2.80$ (Figure 16.13). This high value was attributed to the contribution of masonry infills to the response of the buildings on site, which had been taken into account in the analytical model only as loads without their contribution to strength, stiffness and ductility. For this reason, in Greece, buildings with well-constructed infill masonries have been considered as separate categories from the bare R/C structures in the procedure for preparation of the DPMs. Thereafter, the accelerograms of the characteristic positions were increased accordingly to simulate a scenario of an earthquake of 7.0 on the
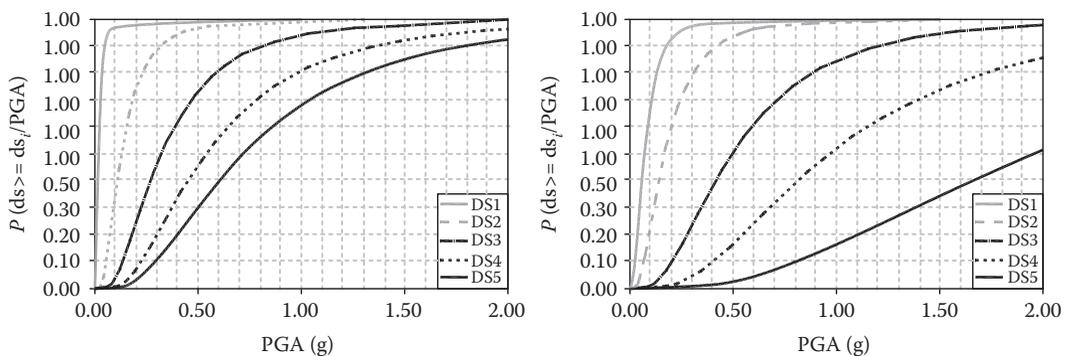
Figure 16.12 Fragility curves (in terms of PGA) for medium-rise dual infilled systems, low (left) and high (right) code design. (With kind permission from Springer Science+Business Media: Kappos, A. et al. 2006b. A hybrid method for the vulnerability assessment of R/C and URM buildings. *Bulletin of Earthquake Engineering*, 4, 391–413.)

Table 16.6 Types of structural systems used for the prediction of damage losses in Thessaloniki for an earthquake of 7.0 grades in Richter scale
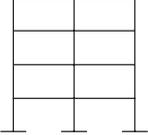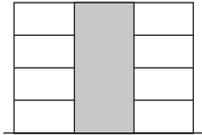
Figure 16.13 Correlation of the actual with the analytically determined repair cost. (Adapted from Penelis, G.G., Stylianidis, K. and Kappos, A. 1988b. *Analytical prediction of the response of the building stock of Thessaloniki to future earthquakes*, invited lecture at the 1st Conference on Engineering Seismology in Greece, Department of Geophysics, Aristotle University of Thessaloniki, Greece.)

Table 16.7 Predicted tagging of buildings of Athens (MASSIVE damage assessment approach) versus On-site reported (validation) data by YAS

Municipality	ITSAK/AUTH (MASSIVE) damage assessment approach			YAS damages reported on site		
	Green (%)	Yellow (%)	Red (%)	Green (%)	Yellow (%)	Red (%)
Ag. Paraskevi	92.9	7.1	0.0	99.0	1.0	0.0
Ano Liosia	71.9	26.8	1.3	77.1	17.0	5.9
Acharnes	76.6	23.0	0.4	78.8	17.1	4.1
Zefyri	71.4	28.0	0.6	73.8	23.5	2.7
Kamatero	70.4	29.0	0.6	87.1	11.4	1.5
Kifisia	89.3	10.2	0.5	92.7	6.5	0.8
Metamorfosi	79.2	20.6	0.2	82.1	16.2	1.6
Chalandri	89.0	10.9	0.1	95.4	4.5	0.2
Thrakomakedones	81.8	18.2	0.0	58.5	36.3	5.1
Total	80.6	19.0	0.5	85.0	12.4	2.6

Source: Adapted from Karakostas, Ch. et al. 2012. Evaluation of seismic vulnerability of buildings in Athens and L'Aquila in the framework of the MASSIVE seismic mitigation system. *Proceedings of 15th World Conference of Earthquake Engineering (WCEE)*, Lisbon.

Richter scale. The predicted damage in comparison to that of the earthquake of June 20, 1978 was higher, estimated to be 2.0–2.5 times that of 1978 (Penelis et al., 1988b).

However, having used the damage cost of the earthquake of Thessaloniki June 20, 1978 for the transformation of structural damage (plastic rotations) into repair costs, there was a reservation that the resulting correlation coefficient between analytical and statistical results was not objective enough. The validation of the fragility curves elaborated for Greek R/C buildings in the earthquake of November 7, 1999 in Athens (Parnitha earthquake) by Karakostas et al. (2012) gave reliable results (Table 16.7).

In the HAZUS-MH system and in many EU countries the inelastic static method (pushover analysis) is used for the generation of hybrid vulnerability curves and then the derivative fragility ones. After the structural type has been chosen as the representative building model of a building category, this structure is designed for a suite of codes and seismic zones that might refe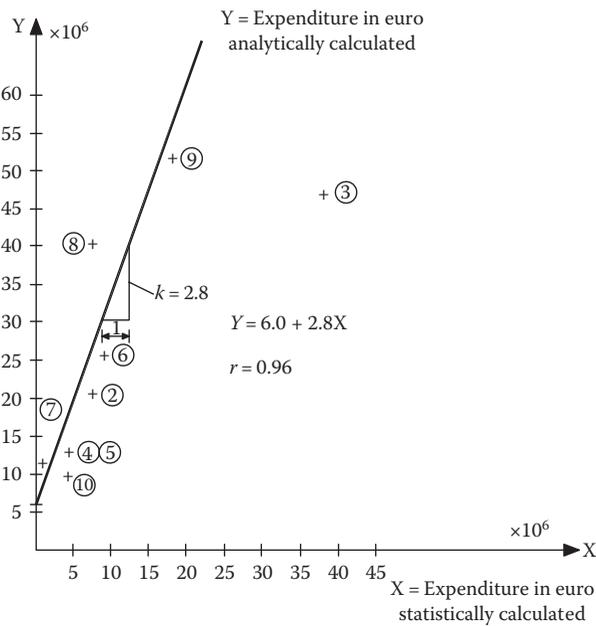r to this structural type. For each of these design alternatives the P–δ curve is calculated (capacity curve). For a given PGA and a 5% damping ratio the acceleration-displacement response spectrum (ADRS) is generated. From this point on the capacity spectral procedure (see Paragraph 14.2.2.2) is implemented, from which the spectral target displacement S_d is defined (Figure 16.14).

For this target displacement the damage index is estimated using methods similar to those that have been used in Greece. For example, Table 16.4 presents the spectral displacement limits for high Code R/C buildings (RISK-UE WP 04). So, the medium vulnerability curve results, and from this curve the relevant fragility curves are generated as derivatives using Equation 16.2.

It should be noted here that relevant fragility curves have been developed for bridges and for various lifelines as well.

16.5.2.6 *Relation of structural damage to non-structural damage and contents*

While damage to the structural system is the most important index of building damage, affecting casualties and catastrophic loss of function, damage to the non-structural system and contents tends to dominate economic loss, since the structural system represents about 20% of building value.
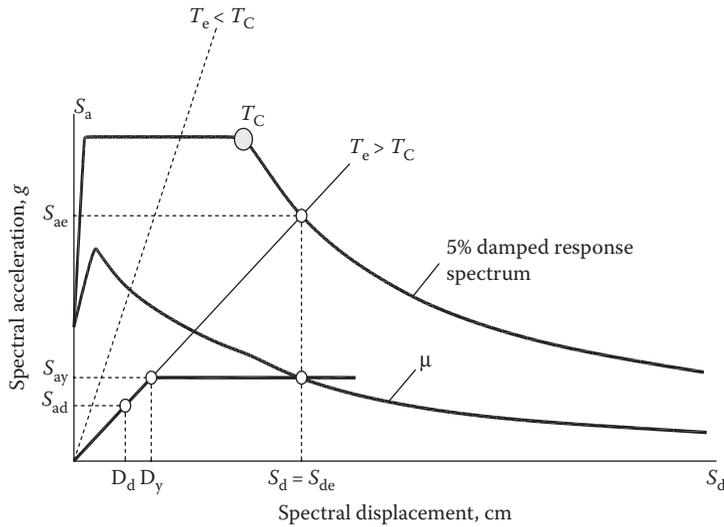
Figure 16.14 Capacity spectrum procedure for bilinear capacity model. (Adapted from RISK-UE W.P. 04, 2003.)

For the determination of the damage index of non-structural elements and contents, these are grouped in two main categories, those that are sensitive to inter-storey drifts (first category) and those sensitive to inertial forces due to their high dead weight (second category).

The thresholds of failure of the first category are defined by the inter-storey drifts that are considered common for all buildings. The thresholds of failure of the second category are defined by the accelerations that develop at these elements during a catastrophic earthquake. The threshold values for both categories of non-structural elements and contents are given in Table 16.8 (HAZUS-MR1).

In the case of well-constructed infill masonry, the structural system should be classified in a separate category from the bare one, because, as noted previously, infill systems strongly influence the stiffness, strength, ductility and energy dissipation of the building. In Greece, masonry infilled structures have even been separated into two subcategories, one with uniform distribution of masonry infills over the height of the building and another with a soft ground storey with pilotis.

Table 16.8 HAZUS damage-state criteria for non-structural systems and contents

	Non-structural damage states – all building types			
Design level	*Slight*	*Moderate*	*Extensive*	*Complete*
Interstorey drift ratio (Δ_{ds}) – drift-sensitive components				
All	0.004	0.008	0.025	0.05
Peak floor acceleration (A_{max},ds) – acceleration-sensitive components/contents (g's)				
Special high code	0.45	0.9	1.8	3.6
High code	0.30	0.6	1.2	2.4
Moderate code	0.25	0.5	1.0	2.0
Low code	0.20	0.4	0.8	1.6
Pre-code	0.20	0.4	0.8	1.6

Source: From FEMA/HAZUS-MH/MR1. 2002. *Multi-Hazard Loss Estimation Methodology: Earthquake Model*, Federal Emergency Management Agency (FEMA), Washington, DC. With permission.

16.6 SEISMIC RISK ANALYSIS

16.6.1 General

As noted in Section 16.2, *specific risk*, which refers to the built environment and particularly to buildings, is the 'convolution' of the seismic hazard and the seismic vulnerability of the built environment. If we consider the 'simplistic' approach that 'risk' is the 'product' of hazard and vulnerability, it follows that (Figure 16.15):

$$Rs = `H` \cdot `V` \tag{16.3}$$

where
   H is the hazard.
   V is the vulnerability as consequences of the hazard to the built environment.
   Rs is the specific risk.

   In this respect seismic risk is the area of the orthogonal of Figure 16.15. Since for the time being the seismic hazard cannot be diminished, the only way to reduce specific seismic risk is to diminish the seismic vulnerability of the built environment.

   The seismic risk of the built environment is expressed in economic terms by direct losses, which include damages to:

- Building stock
- Critical facilities
- The transportation system (mainly bridges, tunnels, etc.)
- Utilities (lifelines)

   A similar conceptual approach may be used for the convolution of the *specific seismic risk*, with the losses of *elements at risk* to produce the *final risk* (Figure 16.2). The losses of elements at risk may be classified in the following categories (HAZUS-MH/MR1):

- Induced physical damage
  - Fire following the earthquake
  - Debris generation
  - Release of hazardous materials
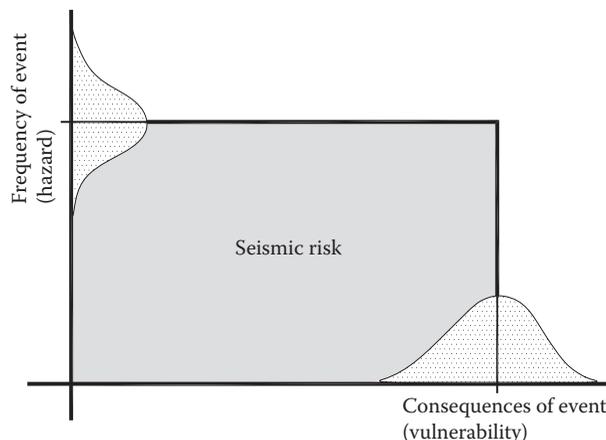
Figure 16.15 Simplified presentation of risk as a product of hazard and consequences (vulnerability).

- Direct economic losses
  - Business interruption
  - Damage to building contents
- Direct social losses
  - Casualties
  - Need for shelters
- Indirect economic losses
  - Employment
  - Income changes
  - Influence on main economic sections, for example, agriculture, commerce, building materials industry and so forth.

The analysis and quantification of the above categories exceeds the scope of this book and the capacities of a structural engineer. However, it was considered useful to make reference to them so that an integrated picture of *'risk analysis'* can be formed by the reader. From the above it may be concluded that seismic risk analysis is a multidisciplinary activity. Items that are of interest to a structural engineer are included in the shaded frames in Figure 16.16.

A more detailed approach will be made below to seismic risk analysis for the built environment expressed in terms of monetary losses (absolute values) or as a percentage of losses in relation to the replacement cost of the built environment.
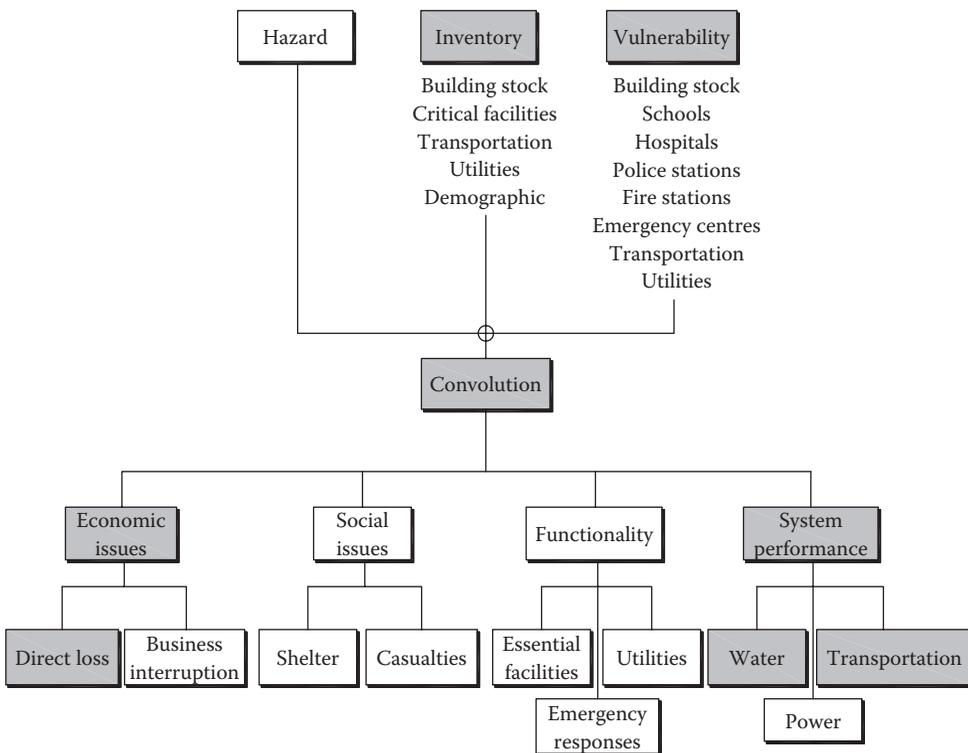
Figure 16.16 Detailed flow chart of risk analysis.

16.6.2 Specific seismic risk analysis

The technique of assessing the specific seismic risk aims at the evaluation in economic terms of losses to the built environment due to a seismic action. To carry this out, the following steps are followed:

Step 1

The intensity of the seismic action is determined in predefined districts of the region (e.g. city) where the analysis will be carried out, using microzoning information. Intensity is expressed by the PGA of each district and the expected spectral intensities for the predefined earthquake. This procedure presumes that seismic hazard and the geotechnical properties from the bedrock to the surface are known in the distinct districts, that is, that there exists microzonation mapping of the region under examination.

Step 2

Based on the *inventory* of the region and the *classification* of the buildings and the rest of the constructions into separate categories for which *fragility curves* have been generated in advance, the probable loss is calculated in economic terms for a region or a country.

In particular, for each building or other construction category, the percentage of the buildings that will be found between the successive fragility curves is determined.
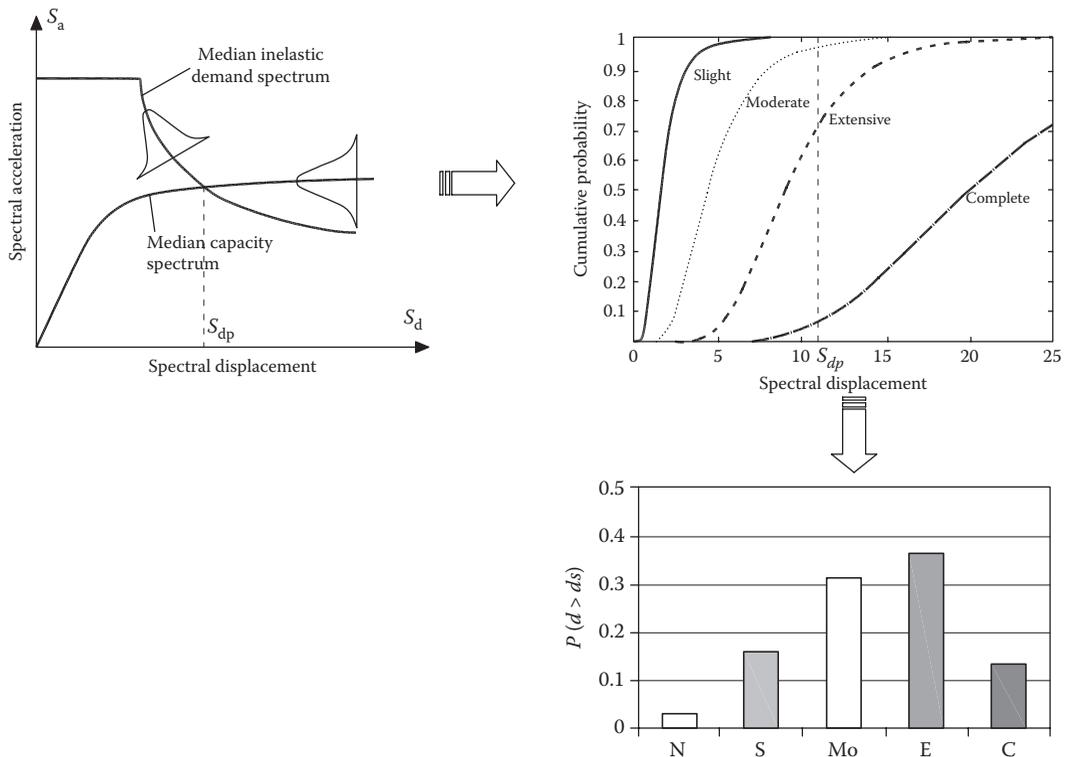
Figure 16.17 Damage estimate process. N, none; Mi, minor; Mo, moderate; S, severe; C, collapse. (With kind permission from Springer Science+Business Media: Erdik et al., 2010.)

To this end, the following steps are made (Figure 16.17, Erdik et al., 2010):

Step 2.1

Select the model building from the inventory BTM, define the capacity model, and convert it into a capacity spectrum.

Step 2.2

Model the building's site-specific demand spectrum (ADRS).

Step 2.3

Model the expected building response (performance) by intersecting capacity and demand spectra and determining the intersection (performance) point.

Step 2.4

From the corresponding fragility curves of the building category, estimate conditional probabilities that for the determined performance point the building category will exhibit certain DS.

Step 3

Now knowing from the inventory of the building stock the total built area E_i in m^2 of the building category under consideration, it is easy to determine the area in a district in m^2 that will be found most probably in one of the five DS of Table 16.1. In fact,

$$\begin{aligned}
E_{i0} &= p_{i0}E_i \\
E_{i1} &= p_{i1}E_i \\
&\vdots \\
\underline{E_{i5}} &= \underline{p_{i5}E_i} \\
E_i &= \left[\sum_{j=1}^{5}(p_j)\right]E_i
\end{aligned} \tag{16.4}$$

The damage index d_{ij} for each damage state (Table 16.1) of the building category under consideration being known, it may be concluded that:

$$\begin{aligned}
D_{i0} &= p_{i0}d_{i0}E_i \\
D_{i1} &= p_{i1}d_{i1}E_i \\
&\vdots \\
D_{ij} &= p_{ij}d_{ij}E_i \\
&\vdots \\
\underline{D_{i5}} &= \underline{p_{i5}d_{i5}E_i} \\
D_i &= \left[\sum_{j=1}^{5}(p_{ij}d_{ij})\right]E_i
\end{aligned} \tag{16.5}$$

The total loss of the built environment of the district is therefore given by the expression:

$$L_d = \sum_{i=1}^{n}D_i = \sum_{i=1}^{n}\left[\sum_{j=1}^{5}(p_{ij}d_{ij})\right]E_i \tag{16.6}$$

where:

    j is the damage state (1–5).

    i is the building category.

    n is the number of building categories in the inventory.

    E_i is the built area of building category i.

    p_{ij} is the percentage of area in damage state j for the building category i.

    d_{ij} is the damage index of building category i for damage state j.

    D_{ij} is the damage index of the percentage of building category i in damage state j.

    L_d is the loss of the district expressed as a percentage of the total value of the district.

This procedure in this or in a similar form setting forth the damage in the form of monetary loss is carried out for buildings, bridges, tunnels, lifelines and generally for all built environments for each district of a region, and the results are summed up for each type of damage loss of the region.

16.6.3 Losses for elements at risk

The loss for elements at risk in a region in economic terms for a given earthquake is a function of the *specific risk* of the region and particularly of:

- The number of elements at risk
- The time of exposure
- The value of the elements at risk
- The number of occupants
- The time of occupants' exposure

Special models have been developed for this by specialists for various loss sources.

16.6.4 Casualties

An exceptionally sensitive category is *'casualties'*. These are classified in two main categories:

- Casualties caused by partial or complete collapse of a building
- Casualties caused by falling objects of sensitive elements of buildings like chimneys, parapets, plasters and so forth

About 70% of fatalities and nearly 100% of injuries attributable to earthquakes are caused by collapse of buildings (Vacareanu et al., 2004; Coburn and Spence, 2002).

When a high-rise building collapses completely, about 70% of its occupants are likely to be killed. In low-rise buildings, more than 75% of occupants may escape, having apparently 20 to 30 s available time until collapse.

There is a wide range in the severity of injuries caused by an earthquake, mainly by falling objects and small parts of the building.

The ratio of killed to hospitalised and to outpatient hospitalisation is about

    1:3:60

(Vacareanu et al. RISK-UE/WP7, 2004; Coburn and Spence, 2002).

Coburn and Spence (2002) have given an interesting expression for the determination of the fatalities per building collapse presented in detail in RISK-UE WP 07. Similar procedures are given in HAZUS-MH/MR1.

In closing, it should be noted that the category of social losses and particularly that of casualties is usually not expressed in economic terms neither in the United States nor in Europe. A more detailed reference to this issue will be made in Section 16.7 in cost–benefit analysis.

16.6.5 Seismic risk outputs

The sum of losses of specific risk and that of losses of elements at risk expressed in monetary or general economic terms gives the seismic risk caused by a given earthquake in a region under consideration. This loss estimate may be used as an absolute value in monetary terms, or as a percentage of the value of the built environment of the region. It may be used for the estimate of the AEL or the AELR of the region. In the last two cases the probable catastrophic earthquakes of a long period, for example, 50 years, are taken into account for the evaluation of the losses of the region. These losses are summed up and the output is reduced to a period of 1 year. In the diagrams of Figures 16.18 and 16.19 the AEL and AELR of the United States are given per U.S. state in the form of total losses per year and in the form of percentages (HAZUS-2003).

It is obvious that such a tool in the hands of the proper staff offers a very useful framework of results for the quantitative assessment of the seismic risk caused by a single event or on an annual basis for the various regions of a country. These results are summarised as follows:

- Direct physical damage
- Induced physical damage
- Direct economic losses
- Direct social losses
- Indirect economic losses
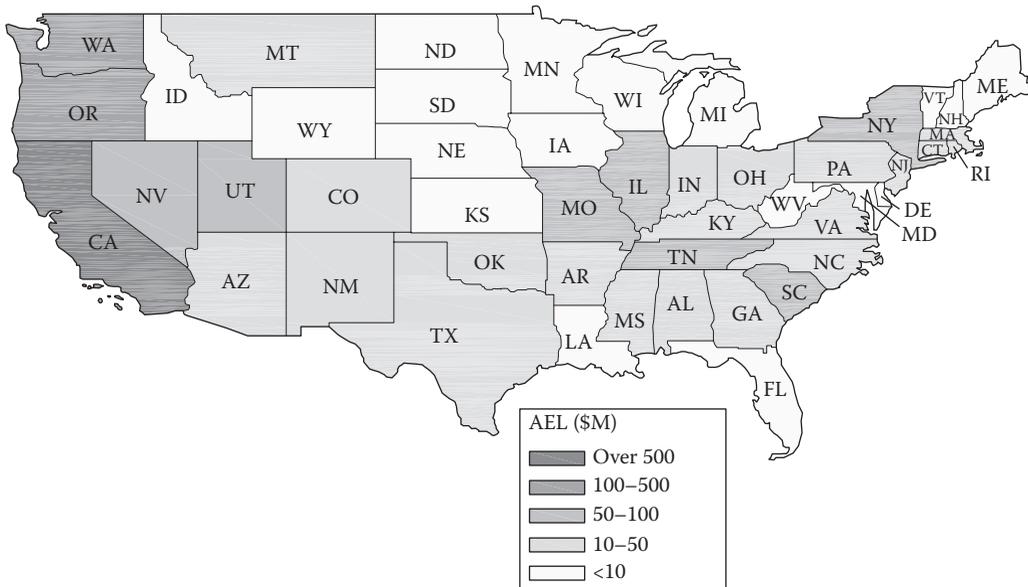
Figure 16.18 AELs in the United States by state. (From FEMA 366. 2008. HAZUS-MH: *Estimated Analyzed Earthquake Losses for the United States*, Federal Emergency Management Agency (FEMA), Washington, DC. With permission.)
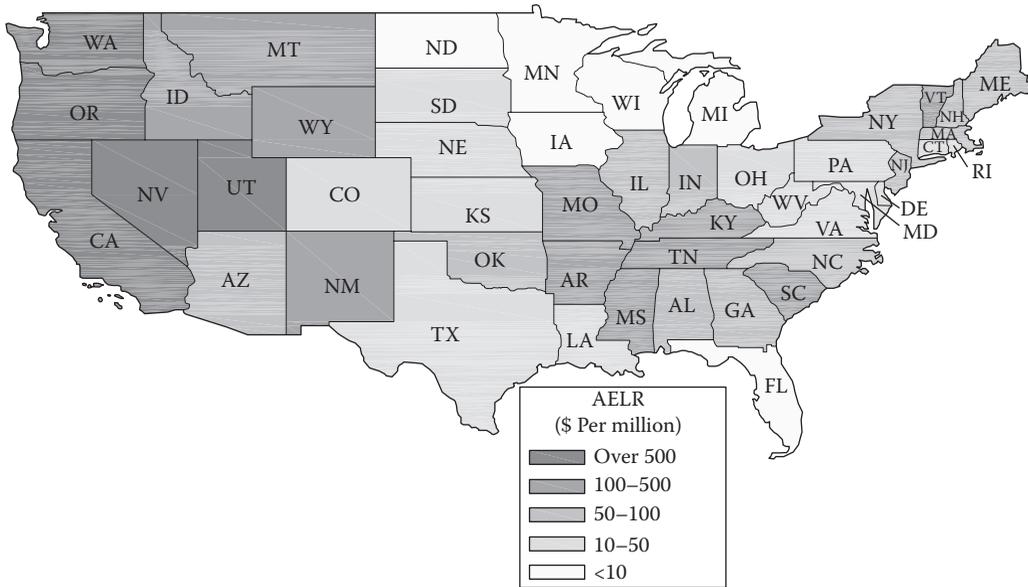
Figure 16.19 AELRs in the United States by state. (From FEMA 366. 2008. HAZUS-MH: *Estimated Analyzed Earthquake Losses for the United States*, Federal Emergency Management Agency (FEMA), Washington, DC. With permission.)

These results are used for the management of the seismic risk at a regional or national level. It should be noted that they prove to be of particular significance for the distribution of funds allocated for seismic risk reduction in various regions of a country in a reasonable way.

In closing, it is worth summarising the whole procedure for the determination of the seismic risk of a region, exhibited in Figure 16.20 (SCEEP/FEMA).
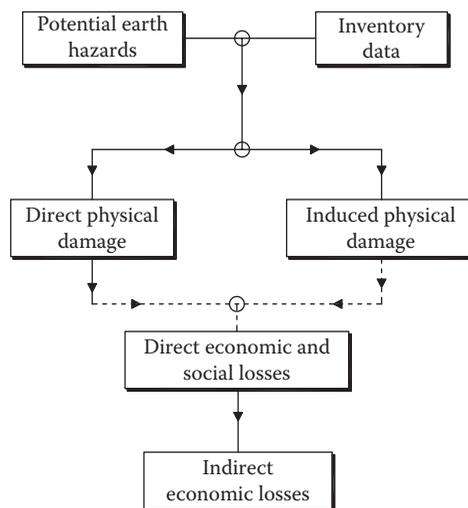
Figure 16.20 General flow chart of seismic risk analysis.

16.7 COST–BENEFIT ANALYSIS

16.7.1 General

Having the results of the seismic risk analysis of a region or a country expressed in the form of losses, various alternative schemes of seismic risk mitigation are examined in relation to the results of the seismic risk analysis. For each of these alternatives, two parameters have to be defined.

1. The implementation cost
2. The expected seismic risk reduction and the benefits resulting from this reduction

This seismic reduction is estimated in economic terms for everything, except casualties. For these, the reduction is estimated as a percentage of casualties to the population of the region under consideration that may be expected if the mitigation programme is not implemented.

In this context, two main categories of values that may be estimated in economic terms must be calculated, that is:

1. Loss reduction (B) caused by the implementation of the mitigation programme under consideration.
   This category includes the reduction of the following losses:
   • Direct physical damage
   • Induced physical damage
   • Direct economic losses
   • Indirect economic losses
2. The implementation cost (C) of the mitigation programme includes:
   • The cost of the preliminary study of buildings, bridges, tunnels, lifelines and the like is included in the assessment and rehabilitation programme. In the case of buildings this cost refers to the implementation of the procedure specified by FEMA 310-ASCE 31-02, which includes, as is well known (see Chapter 13), a three-step procedure for screening buildings in successive levels of intervention depending on the degree of deficiencies certified in them:
   • Design cost for the buildings that will be rehabilitated
   • Rehabilitation cost
   • Cost due to interruption of the buildings usage during the rehabilitation activities

The ratio B/C is a reasonable criterion for decision making about the adoption or rejection of a mitigation programme.

In fact, if:

$$B/C > 1.0$$

the proposed programme might be approved for implementation; otherwise, other alternatives must be examined. It is apparent that in trying various alternatives of mitigation programmes, a series of B/C ratios result. The alternative with the highest value of B/C is considered the most proper for implementation.

In the above procedure the reduction of casualties has not been taken into consideration, since U.S. and European ethics do not accept evaluating human life in economic terms. In this respect, the reduction of casualties is evaluated only qualitatively.

The attempt made by various insurance organisations to assess human life (fatalities and injuries) in economic terms on the basis of compensension paid for other types of casualties (i.e. in traffic accidents, etc.) seems, beyond the ethical considerations, that it cannot estimate the psychological impact of group deaths and injuries caused by collapses during an earthquake on the economic, social and political issues.

In fact, it is difficult to estimate the above consequences from, say, 40 fatalities in a school due to its collapse during an earthquake, while this is an expected number of traffic fatalities during a three-day holiday in a small country like Greece. It is also impossible to estimate the induced indirect losses due to the collapse of a hotel full of tourists in a country of high tourism like Greece. So, for the correlation of the cost of a mitigation programme with casualties, another procedure may be followed, known as the *'risk–benefit method'*. The only difference of this method from the cost–benefit procedure is that it does not specify explicit monetary value placed on lives. Instead, various actions are evaluated *based on costs per life saved*. Once a cost per life criterion is adopted, various levels can be set at which an activity is deemed very worthwhile, acceptable, tolerable, or unacceptable. For purposes of evaluating earthquake safety programmes, the following value was suggested in a UNIDO/UNDP document some years ago (1985).

$$V = 40 \text{ GNP/per. cap/life saved}$$

where a 40-year social average lifetime has been considered.

16.7.2 Basic seismic risk mitigation alternatives

From what has been presented so far it may be concluded that seismic risk is a function of:

- Seismic hazard
- Elements exposed to risk
- Vulnerability of the built environment

Keeping in mind that the first parameter cannot be mitigated, at least for the time being, seismic risk management is limited to two areas:

- Reduction of the exposure of elements and occupants at risk
- Reduction of the vulnerability of the built environment

The first direction of actions is of rather limited value, and it mainly includes restrictions issued by the authorities on the use of buildings of high vulnerability. For example, buildings of this type with high vulnerability such as schools, hospitals, department stores and so forth cannot have a permit for use due to their high occupancy in terms of the number of occupants and time of occupancy. This procedure is a common practice in almost all seismically affected countries. These restrictive rules are usually combined with financial incentives for intervention to reduce the vulnerability of buildings of this type.

In this respect, the reduction of the vulnerability of the built environment is the most effective way for the reduction of seismic risk.

This may be accomplished mainly through three basic procedures:

1. By using modern Seismic Codes in the design and construction of new buildings, and applying a high level of quality control onsite.

2. By post-earthquake rehabilitation of the built environment following modern regulations for repair and strengthening (see Chapters 13, 14 and 15) and modern techniques in construction. At the same time, a high level of quality control should be established onsite.

3. By implementation of pre-earthquake mitigation programmes to the total building stock of a region or to special building categories.

The two first alternatives are the oldest and more usual in seismically affected countries. They have long-term consequences for the seismic vulnerability of a region, since the transformation of the building stock and therefore the reduction of seismic risk are both very slow, taking many decades. They may be considered procedures of a *'passive character'* in the sense that the seismic protection of the building is a consequential action of the main decision for the construction of a new building or the reuse of a damaged one. The third alternative may be considered as an action of *'active character'* and seems to be the most effective, since the results on seismic vulnerability are *'direct'*.

A prerequisite for reliable management of this type is the existence of reliable information on seismic hazard, and on the vulnerability and exposure of the elements and occupants at risk. The limited reliability of this input in the analytical models that have been developed so far makes their results of rather limited value for the implementation. The reason for this is that the decision for any pre-earthquake intervention on the building stock for the reduction of seismic risk has a tremendous and factual cost, while the results remain in the framework of probabilities. So, it is not strange that up to now this type of intervention has been implemented only on buildings of special social sensitivity like schools, hospitals, public buildings and so on.

The effort undertaken in the United States for the seismic safety of existing federally owned or leased buildings (ICSSC RP4-NISTIR 5382/1994) beginning with the seismic evaluation of these buildings on a national level, within a horizon of 6 years, is worth mentioning here. The already completed seismic rehabilitation programme of schools in Cyprus should also be mentioned. In conclusion, mention should also be made to the seismic evaluation programme for schools implemented in Greece five years ago.

16.7.3 Semi-empirical seismic risk management

The approach to the problem presented below, although semi-empirical, is much broader and covers what the policy-making agencies understand in the sense of the reduction of the seismic risk for an area or a country. This management includes the following components (Penelis, 1996):

1. Actions for the reliable determination of the seismic hazard.
2. Actions for the continuous improvement of the quality of new construction (Codes—Quality Control) as it will constitute part of the building stock when put in use.
3. Actions for the determination of the vulnerability of the building stock and lifelines, with verification after strong earthquakes.
4. Actions for the reduction of seismic risk, in the sense of the previously developed approach, of buildings with special social interest (schools, hospitals, etc.)
5. Actions for the reduction of the seismic risk in a whole district through interventions of minor cost but high effectiveness for the security of the users (chimneys, parapets, interior finishings such as hanging mirrors, air condition units, high furniture, etc.).
6. Preparation of realistic emergency plans for post-earthquake interventions for disaster relief and verification of their feasibility through training carried out periodically.

7. Preparation of standard documents for post-earthquake management of the building stock (damage estimates, vulnerability, repair and strengthening).
8. Continuous education and training of specific social groups related to the management of the problem (engineers, physicians, firemen, etc.).
9. Public awareness of the problem (special brochures, social media, adds, apps, special posters for schools, etc.).
10. Studies of the post-earthquake social behaviour of the population.

It is the authors' opinion that an integrated and well-balanced approach to the above items must be the main task of a national agency responsible for the management of the seismic risk in a country. In other words, beyond the reduction of the seismic risk through pre-earthquake interventions in the building stock—an action with a tremendous cost—a series of other actions of much lower cost may radically reduce the seismic risk in the sense of the security of users by stopping the chain effects or side effects that follow a strong earthquake.

References

Abdel-Halim, M.A.H. and Schorn, H. 1989. Strength evaluation of shotcrete-repaired beams. *ACI Structural Journal,* 86(3), 272–276.

Abrams, D.P. 1991. Laboratory definitions of behaviour for structural components and building systems, in ACI SP-127: *Earthquake-resistant Concrete Structures-Inelastic Response and Design.* ACI, Detroit, Michigan, 91–152.

ACI 318 M. 2011. *Building Code Requirements for Structural Concrete.* American Concrete Institute, Farmington Hills, Michigan.

ACI 440.2R-02. 2002. *Guide for the design and construction of externally bonded FRP systems for strengthening concrete structures.* ACI, Detroit, Michigan, USA.

ACI 506 R-90. 1995. *Guide to shotcrete. ACI Manual of Concrete Practice*, Part 5. Farmington Hills, MI, USA.

ACI Committee 408. 1991. *Splice and Development Length of High Relative Rib Area Reinforcing Bars*. American Concrete Institute, Farmington Hills, Michigan.

ADAPTIC. 2012. *User Manual.* Department of Civil and Environmental Engineering, Imperial College, London SW7 2BU.

Aguilar, J., Juarez, H., Ortega, R. and Iglesias, J. 1989. The Mexico earthquake of September 19, 1985: Statistics of damage and retrofitting techniques in R/C buildings affected by the 1985 earthquake. *Earthquake Spectra*, EERI, 5(1), 145–152.

AIJ. 1994. S*tructural Design Guidelines for Reinforced Concrete Buildings*. Architectural Institute of Japan, Tokyo.

Alcocer, S.M. and Jirsa, J.O. 1993. Strength of reinforced concrete frame connections rehabilitated by jacketing. *ACI Structural Journal*, 90(3), 249–261.

Ambraseys, N.N and Bommer, J.J. 1991. The attenuation of ground accelerations in Europe. *Earthquake Engineering and Structural Dynamics*, 20(12), 1179–1202.

Ambraseys, N.N., Smit, P., Douglas, J., Margaris, B., Sigbjornsson, R., Olafson, S., Suhadolc, P. and Costa, G. 2000. Dissemination of European strong motion data, CD ROM edition, European Council, Environment and Climate Research Programme.

Ambraseys, N.N., Douglas, I., Sarma, S.K. and Smit, P.M. 2005. Equations for the estimation of strong ground motions from shallow crustal earthquakes using data from Europe and the Middle East. Horizontal peak ground acceleration and spectral acceleration. *Bulletin of Earthquake Engineering,* 3(1), 1–53.

Ambraseys, N.N., Simpson, K.A. and Bommer, J.J. 1996. Prediction of horizontal response spectra in Europe. *Earthquake Engineering and Structural Dynamics*, 25(4), 371–400.

Anagnostopoulos, C., Georgiadis, M. and Pitilakis, K. 1994. *Foundation-Retaining Works* (in Greek). Civil Engineering Department, Aristotle University of Thessaloniki.

Anagnostopoulos, S. 1988. Pounding of buildings in series during an earthquake. *Earthquake Engineering Structural Dynamics,* 16, 443–456.

Anagnostopoulos, S. et al. 1986. *The Kalamata earthquake of September 1986*. Report of the Institute of Engineering Seismology and Earthquake Engineering, Thessaloniki, Greece (in Greek).

Anagnostopoulos, S.A. 1984. Listing of earthquake damage of buildings and building characterization in emergency situations. *Proceedings* of *the Conference on Earthquakes and Structures,* EPPO, Athens, I, pp. 550–561 (in Greek).

Anagnostopoulos, S.A. 1986. Proposals on the framework for rehabilitation of Kalamata, Greece, *Report of the Institute of Engineering Seismology and Earthquake Engineering*, Thessaloniki (in Greek).

Anagnostopoulos, S.A., Petrovski, J. and Bouwkamp, J.G. 1989. Emergency earthquake damage and usability assessment of buildings. *Earthquake Spectra*, 5(3), 461–476.

Anastasiadis, K. 2001. 'Aseismic structures', Ziti Editions, Thessaloniki, Greece, p. 397 (in Greek).

Anastassiadis. K. 1993. Directions sismiques défavorables et combinaisons défavorables des efforts. *Annales de l' ITBTP*, No. 512.

Anastasiadis, K.K. 1983. *Structural Dynamics* (in Greek). Ziti, Thessaloniki, Greece.

Anastasiadis, K.K. 1989. *Earthquake Resistant Structures* (in Greek). Computer Technics, Thessaloniki, Greece.

Anastasiadis, K.K. and Athanatopoulou, A. 1996. Torsional flexibility of buildings and seismic Codes (in Greek). *12th Greek Conference for Concrete Structures*, Technical Chamber of Greece, Limasol, Cyprus.

Antoniou, S. and Pinho, R. 2004. Advantages and limitations of adaptive and non-adaptive force-based pushover procedures. *Journal of Earthquake Engineering*, 8(4), 497–522.

Antoniou, S., Rovithakis, A. and R. Pinho. 2002. Development and verification of a fully adaptive pushover procedure. *Proceedings of the 12th European Conference on Earthquake Engineering*, London. Paper No. 882.

Aoyama, H. and Noguchi, H. 1979. Mechanical properties of concrete under load cycles idealizing seismic actions. *Bulletin d'Information*, CEB, 131, 29–63.

Arakawa, T. 1980. Effect of welded bond plates on seismic characteristics of R/C columns. *Proceedings of the 7th World Conference on Earthquake Engineering* Istanbul, 7, pp. 233–240.

Aristizabal-Ochoa, J.D. 1982. Dynamic response of coupled wall systems, *ASCE Journal of the Structural Division,* 108(ST8), 1846–1857.

ASCE/SE17-10, 2010. *Minimum Design Loads for Buildings and Other Structures*. American Society of Civil Engineers, Reston, Virginia.

ATC 13-06. I978. *Tentative Provisions for the Development of Seismic Regulations for Building.* US Government Printing Office, Washington, DC.

ATC 40-1996. *Seismic Evaluation and Retrofit of Concrete Buildings*. Applied Technology Council, Redwood City, California.

Athanassiadou, C.J., Penelis, G.G. and Kappos, A.J. 1994. Seismic response of adjacent buildings with similar or different dynamic characteristics. *Earthquake Spectra*, 10(2), 293–317.

AUTH (Aristotle University of Thessaloniki). 1978 *Earthquake Damage Repair in Buildings,* Thessaloniki (in Greek).

AUTH (Aristotle University of Thessaloniki). 1979 *A Seminar for Earthquake Damage Repair in Buildings,* Thessaloniki (in Greek).

Baden Württemberg Innenministerium. 1985. *Erdbebensicher Bauen*, Stuttgart.

Balázs, G.L. 1989. Bond softening under reversed load cycles. *Studie Ricerche, Politecnico di Milano,* Milano, No. 11, 503–524.

Bett, B.J., Klingner, R.E. and Jirsa, J.O. 1988. Lateral load response of strengthened and repaired concrete columns. *ACI Structural Journal,* 85(5), 499–508.

Beres, A., El-Borgi, S., White, R.N. and Gergely, P. 1992. *Experimental results of repaired and retrofitted beam-to-column joint tests in lightly reinforced concrete buildings.* Technical report NCEER-92-0025, SUNY/Buffalo, USA.

Bertero, V. and Brokken, S.I. 1983. Landfills in seismic resistant buildings. *Journal of Structural Engineering ASCE,* 109(6), 1337–1361.

Bertero, V.V. 1979. Seismic behaviour of structural concrete linear elements (beams, columns) and their connections. *CEB Bulletin d'Information,* 131, Paris.

Bertero, V.V. and Popov, E.P. 1977. Seismic behaviour of ductile moment resisting reinforced concrete frames, *in ACI SP 53: Reinforced Concrete Structures in Seismic Zones,* ACI, Detroit Michigan, pp. 247–291.

Bigs, J.M. 1964. *Introduction to Structural Dynamics*. McGraw-Hill, New York.

Biskinis, D.E. 2007. Resistance and deformation capacity of concrete members with or without retro-fitting. (in Greek). *Doctoral Thesis*, Civil Engineering Department, University of Patras, Patras, Greece.

Blakeley, R.W.G. 1971. *Ductility of prestressed concrete frames under seismic loading*. PhD thesis, University of Canterbury, Christchurch.

Blume, J.A. 1960. Structural dynamics in earthquake resistant design. *Transactions of ASCE*, USA, 125, 1088–1139.

Bommer, J.J. and Elnashai, A.S. 1999. Displacement spectra for seismic design. *Journal of Earthquake Engineering*, 3(4), 1–32.

Boore, D.M. 2005. Erratum: Equations for estimating horizontal response spectra and peak acceleration from western North American earthquakes. A summary of recent work. *Seismological Research Letters*, 76(3), 368–369.

Booth, E. and Key, D. 2006. *Earthquake Design Practice for Buildings*. Thomas Telford Ltd, London.

Borzi, B. and Elnashai, A.S. 2000. Refined force reduction factors for seismic design. *Engineering Structures*, 22(10), 1244–1260.

Bousias, S.N., Panagiotakos, T.B. and Fardis, M. 2002. Modelling of R/C members under cyclic biaxial flexure and axial force. *Journal of Earthquake Engineering* 6(3), 213–238.

Bracci, J.M., Kunnath, S.K. and Reinborn A.M. 1977. Seismic performance and retrofit evaluation of R/C structures. ASCE *Journal of Structural Engineering*, 123(1), 3–10.

BSSC. 2003. NEHRP. *Recommended provisions for seismic regulations for new buildings and other structures*. Building Seismic Safety Council (FEMA Rep. 368, 369). Washington D.C.

Bush, T.D., Tallon, R. and Jirsa, J.O. 1990. Behaviour of a structure strengthened using reinforced concrete piers. *ACI Structural Journal,* 87(5), 557–563.

Bush, T.D., Wyllie, L.A. and Jirsa, J.O. 1991. Observations on two seismic strengthening schemes for concrete frames. *Earthquake Spectra*, *EERI Journal*, 7(4), 511–527.

Cairns, J. 2006. *Proposals of fib TG 4.5 for bond anchorage in the new fib Model code*, Fib, Lausanne.

CEB. 1970 CEB-FIP. *International Recommendations for the design and construction of concrete structures: 1 Principles and recommendations*, Bulletin No. 72. Comité Euro-international du Beton (CEB), Paris.

CEB. 1985. *Model Code for Seismic Design of Concrete Structures*. Bulletin d'Information CEB, 165, Lausanne.

CEB. 1991. *CEB-FIP Model Code 1990*, *Bulletin d'Information*, Nos. 203/204/205, Comité Euro-International du Béton, Lausanne.

CEB. 1991. *Behaviour and Analysis of Reinforced Concrete Structures under Alternate Actions Including Inelastic Response*, Vol. 1. *CEB, Bul. d'Inf. 210.*

CEB. 1993. CEB-FIP Model Code 1990, *Bulletin d'Information*, CEB, 213/214, Lausanne.

CEB. 1996. *R/C frames under earthquake loading*. T. Telford, London for Comité Euro international du Beton, Lausanne.

CEN Techn. Comm. 250/SC8. 1993. *Eurocode 8: Earthquake Resistant Design of Structures, Part 1 4 (Draft): Repair and Strengthening,* CEN, Berlin.

CEN Techn. Comm. 250/SC8. 1994. *Eurocode 8: Earthquake Resistant Design of Structures-Part 1: General Rules and Rules for Buildings* (ENV 1198-1-1), CEN, Berlin.

CEN Technical Committee 250/SC2. 1991. *Eurocode 2: Design of Concrete Structures—Part 1: General Rules and Rules for Buildings (ENV 1992-1-1)* CEN, Berlin.

Chopra, A.K. 2001. *Dynamics of Structures: Theory and Application in Earthquake Engineering*, 2nd Edition. Prentice-Hall, New Jersey.

Chopra, A.K. and Chintanapakdee, C. 2004. Evaluation of modal and FEMA pushover analyses. Vertically 'regular' and irregular generic frames. *Earthquake Spectra*, 20(1), 255–271.

Chopra, A.K. and Goel, R.K. 2002. A modal pushover analysis procedure for estimating seismic demands for buildings. *Earthquake Engineering and Structural Dynamics*, 31, 561–582.

Chronopoulos, M. 1984. Damage and rehabilitation cost, *Proceedings of the Conference on Earthquakes and Structures*, EPPO, Athens, I, pp. 459–469 (in Greek).

Chung, H.W. and Lui, L.M. 1978 Epoxy-repaired concrete joints under dynamic loads. *Journal of ACI*, 75(7), 313–316.

Clough, R.W. 1970. *Earthquake Response of Structures, Earthquake Engineering*. Prentice-Hall, New Jersey.

Clough, R.W. and Johnston, S.B. 1966. Effects of stiffness degradation on earthquake ductility requirements. *Proceedings of Japan Earthquake Engineering Symposium*, Tokyo, pp. 227–232.

Clough, R.W. and Penzien, J. 1975. *Dynamics of Structures*. McGraw-Hill, New York.

Clyde, C. and Pantelides, C.P. 2002. Seismic evaluation and rehabilitation of R/C exterior building joints. *Proceedings of the Seventh U.S. National Conference on Earthquake Engineering*, Georgia Institute of Technology, Boston, USA.

Coburn, A. and Spence, R. 2002. *Earthquake Protection*, 2nd ed. John Wiley and Sons, Chichester.

Collier, C.J. and Elnashai, A.S. 2001. A procedure for combining horizontal and vertical seismic action effects. *Journal of Earthquake Engineering*, 5(4), 521–539.

Concrete Society. 2000. *Design guidance for strengthening concrete structures using FRP materials*. Concrete Society Technical Report No. 55, Crownthorne, Berkshire, UK.

Constantinea, A.M. and Zisiadis, N.A. 1984. A proposal for inspection procedure after an earthquake. *Proceedings* of *the Conference on Earthquakes and Structures,* EPPO, Athens. I, 574–594 (in Greek).

Corazao, M. and Durrani, A.J. 1989. *Repair and strengthening of beam-to-column connections subjected to earthquake loading. Technical Report* NCEER-89-0013, SUNY/Buffalo, USA.

Cosenza, E., Manfredi, G. and Realfonzo, R. 2000. Torsional effects and regularity conditions in R/C buildings. *Proceedings of the 12th World Conference on Earthquake Engineering*, Auckland.

Darwin, D., McCabe, S.L., Browning, J.-A., Mutumoros, A. and Zuo, J. 2002b. Evaluation of development length design expressions. In: Balázs GL et al. (eds.) *3rd International Symposium: Bond in Concrete—from Research to Standards*, Budapest, 747–754.

Darwin, D., Zuo, J. and McCabe, S.L. 2002a. Descriptive equations for development and splice strength of straight reinforcing bars. In Balázs GL et al. (eds.) *3rd International Symposium: Bond in Concrete—from Research to Standards*, Budapest, 501–508.

Der Kiureghian, A. 1981. A response spectrum method for random vibration analysis of MDOF systems. *Earthquake Engineering and Structural Dynamics*, 9, 419–435.

DIN 4014/1990. *Bohrpfähle, Herstellung, Bemessung, Tragverhalten, Beton Kalender*, Band II, 1994, Ernst & Sohn, Berlin.

Dowrick, D. 2005. *Earthquake Risk Reduction*, John Wiley and Sons, Ltd, Chichester, West Sussex. England.

Drakopoulos, J. and Makropoulos, K. 1983, *Seismicity and Hazard Analysis Studies in the Area of Greece*, Athens, Greece.

Dritsos, S. 2004. *Repair and Strengthening of R/C structures (in Greek)*. Patras, Greece.

Dwairi, H.M., Kowalsky and Nau, J.M., 2007. Equivalent viscous damping in support of Direct Displacement-Based Design. *Journal of Earthquake Engineering*, 11(4), 512–530.

EAK (Greek Seismic Code). 2000. *Seismic Risk Management and Protection Organisation (ΟΑΣΠ)*. Athens, Greece.

E.C.8-1/EN1998-1. 2004. *Design of Structures for Earthquake Resistance: General Rules, Seismic Actions and Rules for Buildings*. CEN, Brussels, Belgium.

EC2-1-1/EN1992-1-1. 2004. *Design of Concrete Structures—Part 1-1: General Rules and Rules for Buildings*. BSI, CEN, Brussels, Belgium.

EC7-1/2004. *Geotechnical Design. Part 1: General Rules*. The European Committee for Standardization, CEN, Brussels.

EC8-3/2005. *Design of Structures for Earthquake Resistance. Part 3: Assessment and Retrofitting of Buildings*. European Committee for Standardization, BSI, CEN, Brussels.

EC8-5/2004. *Design of Structures for Earthquake Resistance, Part 5: Foundations, Retaining Structures and Geotechnical Aspects*. European Committee of Standardization, CEN, Brussels.

Economou, C., Karayiannis, C. and Sideris, K. 1994. Epoxy repaired beams under cyclic loading. *Proceedings of the 11th Hellenic Conf. on Concrete,* Techn. Chamber of Greece, Corfu, 3, pp. 26–37 (in Greek).

ECtools 2013. *User Manual*. 3Pi Software Ltd, Thessaloniki, Greece, www.ectools.eu, 2013.

EERI Committee on Seismic Risk. 1984. Glossary of terms for probabilistic seismic risk and hazard analysis. *Earthquake Spectra*, 1, 33–40.

Eibl, J. and Keintzel, E. 1988. Seismic shear forces in R/C cantilever shear walls. *Proceedings of the 9th World Conference on Earthquake Engineering*, Tokyo-Kyoto, Aug. 1988, Maruzen, VI, pp. 5–10.

Eligehausen, R. and Lettow, S. 2007. *Formulation of Application Rules for Lap Splices in the New Fib Model Code,* Stuttgart.

Eligehausen, R., Popov, E.P. and Bertero, V.V. 1983. Local bond stress–slip relationships of deformed bars under generalized excitations. *Report EERC-83/23*, University of California, Berkeley.

Elnashai, A.S. 1998. *Use of real earthquake time-history in analytical seismic assessment of structures*. HM Nuclear Installations Directorate (NH) Report.

Elnashai, A.S. 2000. Advanced inelastic static analysis for seismic design and assessment. *G. Penelis International Symposium on Concrete and Masonry Structures*, Aristotle University of Thessaloniki, Greece.

Elnashai, A.S. 2002. Do we really need inelastic dynamic analysis? *Journal of Earthquake Engineering*, 6(1), 123–130.

Elnashai, A.S. and Di Sarno, L. 2008. *Fundamentals of Earthquake Engineering*, Wiley, West Sussex, UK.

Elnashai, A.S. and Papazoglou, A.J. 1997. Procedure and spectra for analysis of R.C. structures subjected to strong vertical earthquake loads. *Journal of Earthquake Engineering*, 1(1), 121–155.

Elnashai, A.S. and Mwafy, A.M. 2000. Static pushover versus dynamic to collapse analysis of RC buildings. ESEE Research Report, No 00-1, Imperial College, Jan.

Elnashai, A.S., Papanikolaou, V.K. and Lee, D.H. 2002–2005. Zeus NL A Program for Inelastic Dynamic Analysis of Structures, Mid-America Earthquake Center, University of Illinois at Urbana-Champaign, 2005.

EN1990. 2002. *Eurocode—Basis of Structural Design*. CEN, Brussels, Belgium.

Endo, T. et al. 1984. Practices of seismic retrofit of existing concrete structures in Japan. *Proceedings of the 8th World Conference on Earthquake Engineering,* San Francisco, USA, I, pp. 469–476.

Engindeniz, M., Kahn, L. and Zureick, A. 2004. Repair and strengthening of non-seismically designed R/C beam-column joints. Georgia Institute of Technology: State-of-the-art report 04-4.

Erdik, M. and Aydinoğlu, N. 2000. *Earthquake vulnerability of buildings in Turkey*. Internal report, Boğaziçi University, Istanbul.

Erdik, M. et al. 2010. Rapid earthquake hazard and loss assessment for Euro-mediteranean region. *Acta Geophysica,* 58(5), 855–892.

Etabs. 2013. *Integrated Building Design Software*. Computers and Structures Inc, Berkeley, California.

Faccioli, E. and Pessina, V. 2003. RISK-UE, EP2-*Basis of a Handbook of Earthquake Ground Motions Scenarios* 99, (57 Figures, 12 Tables, 3 Appendices).

FAGUS/Cubus. 2011. *R/C Cross Sections Definition and Analyses*, Zurich.

Fajfar, P. 1996. *Towards a New Seismic Design Methodology for Buildings*. University of Ljubljana, Faculty of Civil Engineering and Geodesy Ljubljana, Slovenia.

Fajfar, P. and Dolšek, M. 2000. A transparent nonlinear method for seismic performance evaluation. *Collective Edition Entitled 'Implications of Recent Earthquakes on Seismic Risk*, A.S. Elnashai and S. Antoniou (eds.), pp. 165–176, Imperial College Press, London.

Fajfar, P., Marusic, D. and Perus, I. 2005. The extension of the N2 method to asymmetric buildings, *Proceedings of the 4th European Workshop on the Seismic Behaviour of Irregular and Complex Structures*, CD ROM, Thessaloniki.

Fardis, M.N. 2009. *Seismic Design, Assessment and Retrofitting of Concrete Buildings*, Springer, Heidelberg.

Fardis, M., Carvalho, E., Elnashai, A., Faccioli, E., Pinto, P. and Plumier, A. 2005. *Designer's Guide to EN 1998-1 and EN 1998-5*. Thomas Telford Ltd, London.

FEMA (Federal Emergency Management Agency). 1986. *NEHRP: Recommended Provisions for the development of seismic regulations for new building,* Part III (App: Existing Buildings), Washington, DC.

FEMA 356. 2000. *Prestandard and Commentary for the Seismic Rehabilitation of Buildings*, Washington, DC.

FEMA 366. 2008. HAZUS-MH: *Estimated Annual Earthquake Losses for the United States*, Federal Emergency Management Agency (FEMA), Washington, DC.

FEMA/HAZUS-MH/MR1. 2002. *Multi-Hazard Loss Estimation Methodology: Earthquake Model*, Federal Emergency Management Agency (FEMA), Washington, DC.

FEMA-154/1988. *Rapid Visual Screening of Buildings for Potential Seismic Hazards: A Handbook*. Federal Emergency Management Agency, Washington, DC.

FEMA-172/NEHRP. 1992. *Handbook of Techniques for Seismic Rehabilitation of Existing Buildings*, Federal Emergency Management Agency, Washington, DC.

FEMA-179/NEHRP. 1992. *Handbook for the Seismic Evaluation of Existing Buildings*. Federal Emergency Management Agency, Washington, DC.

FEMA-274/1997, NEHRP. Commentary on the Guidelines for seismic rehabilitation of buildings, prepared by the Building Seismic Safety Council for the Federal Emergency Management Agency, Washington, DC.

FEMA-273/1997, NEHPR. Guidelines for the seismic rehabilitation of buildings prepared by the Building Seismic Safety Council for the Federal Emergency Management Agency, Washington, DC.

FEMA-310/1998/ASCE 31-02. *Handbook for the Seismic Evaluation of Buildings*—A standard prepared by the ASCE for the Federal Emergency Management Agency, Washington, DC.

FEMA-356. 2000. Prestandard and Commentary for the seismic rehabilitation of buildings, prepared by the SAC Joint Venture for the Federal Emergency Management Agency, Washington, DC.

FEMA-356/2000/ASCE SEI 41-06. *Standard and Commentary for the Seismic Rehabilitation of Buildings*, Federal Emergency Management Agency, Washington, DC.

FEMA-440/2005. *Static Seismic Analysis Procedures*. Report prepared by the A.T.C. for the Federal Emergency Management Agency, Washington, DC.

Fib. 2003. Seismic assessment and retrofit of reinforced concrete buildings, Bulletin 24: State-of-the-art report. International Federation for Structural Concrete (fib), Lausanne, Switzerland.

Filippou, F.C., Popov, E.P. and Bertero, V.V. 1993. Modeling of R/C joints under cyclic excitations. *Journal of Structural Engineering*, ASCE, 109(11), 2666–2684.

Fintel, M. 1974a. *Multistorey Structures: Chapter 10 of Handbook of Concrete Engineering*, Van Nostrand Reinhold Co., New York.

Fintel, M. 1974b. Ductile shear walls in earthquake-resistant multistory buildings. *Journal of the ACI,* 71(6), 296–304.

Fischinger, M. and Fajfar, P. 1994. Seismic force reduction factors. *Proceedings of the 17th Regional European Seminar on Earthquake Engineering*, Haifa, Israel, Sep. 1993 (Ruttenber A. ed.) Balkema, Rotterdam, pp. 279–296.

Freeman, S.A. 1993. Assessment of structural damage and criteria for repair. *Proceedings of the 3rd US/Japan Workshop on Urban Earthquake Hazard Reduction*, Publication No.93-B, EERI, Oakland, California.

French, C.W., Thorp, G.A. and Tsai, W.J. 1990. Epoxy repair techniques for moderate earthquake damage. *ACI Structural Journal,* 87(4), 416–424.

Gasparini, D.A. and Vanmarcke, E.H. 1976. *Simulated Earthquake Motion Compatible with Preselected Response Spectra*. Department of Civil Engineering Research Report R76-4, MIT, Cambridge, MA.

GMPW (Greek Ministry of Public Works). 1978. *Recommendations for the Repair of Buildings with Earthquake Damage,* Thessaloniki (in Greek).

Grant, D.N., Blandon, C.A. and Priestley, M.J. 2005. *Modelling inelastic response in Direct Displacement-Based Design*. Report 0.3, IUSS Press, Pavia.

Greek National Report. 1982. *On Damage Evaluation and Assessment of Earthquake Resistance of Existing Buildings*, Pr. Rep. 13/05 UNIDO/UNDP, Thessaloniki.

Gupta, A.K. 1990. *Response Spectrum Method in Seismic Analysis and Design of Structures*. Blackwell Scientific Publishing, Cambridge, Mass.

Gupta, A.K. and Chu, S.L. 1977. Probable simultaneous response by the response spectrum method of analysis. *Nuclear Engineering and Design,* 44, 93–97.

Gupta, A.K. and Singh, M.P. 1977. Design of column sections subjected to three components of earthquakes. *Nuclear Engineering and Design,* 41, 129–133.

Gupta, B. and Kunnath, S.K. 2000. Adaptive spectra-based pushover procedure for seismic evaluation of structures. *Earthquake Spectra* 16(2), 367–391.

Gutenberg, B. and Richter, C.F. 1942, 1956. Earthquake magnitude, intensity, energy and acceleration. *Bulletin of the Seismological Society of America*, 32, 163 and 46, 105.

Gylltoft, K. 1984. Fracture mechanics model for fatigue in concrete. *Materials and Structures*, RILEM, 17(97), 55–58.

Haisen, J. Brinch. 1961. A general formula for bearing capacity. *Ingeniören*, 5, 38–46.

Hanson, N.W. 1960. Precast-prestressed concrete bridges. 2. Horizontal shear connections. *JPCA Research and Development Laboratories*, 2(2).

Hassoun, M.N. and Al-Manaseer, A. 2008. *Structural Concrete*. John Wiley & Sons Inc., Hoboken, New Jersey.

Hoffschild, T.E., Prion, H.G.L. and Gherry, S. 1995. Seismic retrofit of beam-to-column joints with grouted steel tubes, '*Thomas Paulay Symposium, Recent Developments in Lateral Force Transfer in Buildings*, SP-157', pp. 397–425. ACI, Detroit, Michigan, USA.

Hollaway, L.C. and Leeming, M.B. 1999. *Strengthening of Reinforced Concrete Structures Using Externally-Bonded FRP Composites in Structural and Civil Engineering*, Woodhead Publishing, Cambridge, UK.

Holmes, T.W. 1994. Policies and standards for reoccupancy repair of earthquake-damaged buildings. *Earthquake Spectra*, 10(1), 197–208.

Housner, G.W. et al. 1953. Spectral analysis of strong-motion earthquakes. *Bulletin of the Seismological Society of America*, 43(2).

IBC. 2012. *International Building Code*, International Code Consortium, 2012.

ICONS Project. 2012, Center for International Development and Conflict Management Department of Government & Politics, University of Maryland.

ICSSC PR-4/1994. *Standards of seismic safety for existing federally owned or leased buildings*. National Institute of Standards and Technology (NISTIR 5382), Gaithersburg, Maryland.

IESEE (Institute of Engineering Seismology and Earthquake Engineering, Greece). 2003. *Strong Motion Data Base of Greece 1978–2003*, Thessaloniki, Greece.

Ignatakis, C. 2011. Reinforcement detailing for R/C structures according to EC2–1–1/2004 and EC8-1/2004 (in Greek). *Seminar of Hellenic Steel Industry on European Codes for R/C structures*, Herakleion, Crete.

Ignatakis, C., Stavrakakis, E. and Penelis, G. 1989. Parametric analysis of R/C columns under axial and shear loading using the finite element method. *ACI Structural Journal*, 86(4), 413–418.

Ignatakis. C., Stavrakakis, E. and Penelis, G. 1990. Analytical model for masonry using the finite element method. *Software for Engineering Work Stations, International Journal* 6(2), 90–96.

Jacobsen, L.S. 1960. Damping in composite structures. *Proceedings of the 2nd World Conference on Earthquake Engineering*, Tokyo and Kyoto, 1029–1044.

JBDPA. 1999. *Seismic retrofit design and construction guidelines for existing reinforced concrete and steel encased R/C buildings using continuous fibre reinforcing materials*. Japan Buildings Disaster Prevention Association, Tokyo.

Jirsa, J.O. 1974. Factors influencing behaviour of reinforced concrete members under cyclic overloads. *Proceed of 5th World Conf. on Earthq. Eng.* June 1973, Rome, Italy, pp. 1198–1204.

Jirsa, J.O. 1994. Divergent issues in rehabilitation of existing buildings. *Earthq. Spectra*, 10(1), 95–112.

Jirsa, J.O., Maruyama, K. and Ramirez, H. 1980. The influence of load history on the shear behaviour of short RG columns. *Proceedings of the 7th World Conference on Earthquake Engineering*, Istanbul, 6, 339–146.

Kaku, T. and Asakusa, H. 1991. *Bond and Anchorage of Bars in Reinforced Concrete Beam-Column Joints*. ACI Special Publication SP123, American Concrete Institute, Detroit. Michigan, 401–124.

Kanaan, A.E. and Powell, G.H. 1973. DRAIN-2D: *A General Purpose Computer Program for Dynamic Analysis of Inelastic Plane Structures*, Rep. EERC-73/6 and EERC-73/22, Univ. of California, Berkeley.

Kappos, A. and Penelis, G.G. 1987. Investigation of the inelastic behaviour of existing R/C buildings in Greece. *Journal of Engineering*, TCG, 7(3), 53–86.

Kappos, A.J. 1991. Analytical prediction of the collapse earthquake for R/C buildings: Suggested methodology. *Earthquake Engineering and Structural Dynamics*, 20(2), 167–176.

Kappos, A.J. and Penelis, G.G. 1986. Discussion of influence of concrete and steel properties on calculated inelastic seismic response of reinforced concrete frames. *ACI Journal,* 83(1), 167–169.

Kappos, A.J. and Penelis, G.G. 1989. Evaluation of the inelastic seismic behaviour of R/C buildings designed using CEB model code, *Proceedings of the 9th World Conference on Earthquake Engineering,* Tokyo-Kyoto, 1988, Maruzen, **V**, 1137–1142.

Kappos, A.J., Stylianidis, K.C. and Penelis, G.G. 1991. Analytical prediction of the response of structures to future earthquakes. *Proceedings of European Earthquake Engineering*, 5(1), 10–21.

Kappos, A., Mergos, P., Penelis. G.G. and Stylianidis, K. 2006a. Second step seismic evaluation of the R/C buildings of Aristotle University of Thessaloniki, *Proceedings of the 15th National Conference on R/C Structures*, Technical Chamber of Greece.

Kappos, A., Panagopoulos, G., Panagiotopoulos, C. and Penelis, Gr. 2006b. A hybrid method for the vulnerability assessment of R/C and URM buildings. *Bulletin of Earthquake Engineering*, 4, 391–413.

Kappos, A., Panagopoulos, G. and Penelis, Gr. 2008. Development of a seismic damage and loss scenario for contemporary and historical buildings in Thessaloniki. *Soil Dynamics and Earthquake Engineering,* 28, 836–850, Elsevier, Amsterdam.

Kappos, A.J. 1990. Sensitivity of calculated inelastic seismic response to input motion characteristics. *Proceedings of 4th US National Conference on Earthquake Engineering, Palm Springs*, Calif., **2**, pp. 25–34.

Kappos, A.J. 1991. Analytical prediction of the collapse earthquake for R/C buildings: Case studies. *Earthquake Engineering and Structural Dynamics*, 20(2), 177–190.

Kappos, A.J. and Kyriakakis, P. 2001. A re-evaluation of scaling techniques for natural records, *Soil Dynamics and Earthquake Engineering*, 20, 111–123.

Karabinis, A. 2002. *Validation of the pre-earthquake assessment procedure of R/C buildings in Greece*, Technical Report (O.A.S.P.) Athens, Greece.

Karakostas, Ch., Lekidis, V., Kappos, A., Panagopoulos, G., Kontoes, C. and Keramitsoglou, I. 2012. Evaluation of seismic vulnerability of buildings in Athens and L'Aquila in the framework of the MASSIVE seismic mitigation system. *Proceedings of 15th World Conference of Earthquake Engineering (WCEE)*, Lisbon.

Karayannis, C.G., Chalioris, C.E. and Sideris, K.K. 1998. Effectiveness of R/C beam-column connection repair using epoxy resin injections. *Journal of Earthquake Engineering,* 2(2), 217–240.

Karsan, I.D. and Jirsa, J.O. 1969. Behaviour of concrete under compressive loading. *Journal of the Structural. Division*, ASCE 95(ST 12), 2543–2563.

Kent, D.C. and Park, R. 1971. Flexural members with confined concrete. *Journal of the American Concrete Institute*, Proceedings, 67(3), 243–248.

Khalifa, A., Gold, W., Nanni, A., Abel-Aziz, M. 1998. Contribution of externally bonded FRP to the Shear Capacity of R/C Flexural Members. *Journal of Composites in Construction*, 2(4), 195–203.

Kitayama, K., Otani, S. and Aoyama, H. 1989. Behaviour of reinforced concrete beam-column-slab subassemblies subjected to bi-directional load reversals. *Proceedings of the 9th World Conference on Earth*quakes, Tokyo-Kyoto, 1988, Maruzen, VIII, 581–586.

Kitayama, K., Otani, S. and Aoyama, H. 1991. *Development of Design Criteria for R/C Interior Beam-Column Joints*, ACI Special Publication SP123, American Concrete Institute, Detroit, Michigan, 97–124.

König, G. and Liphardt, S. 1990. *Hochhäuser aus Stahlbeton*, Beton Kalender, Teil II, 457–539. John Wiley and Sons (in German).

Kostikas, Ghr. et. al. 2000. *Evaluation of damages and their cause for 103 near to collapse R/C buildings in Athens after the earthquake of September 7, 1999*, Report of the O.A.S.P. (Seismic Risk Management Agency of Greece) (in Greek).

Kowalsky, M.J. and Priestley, M.J.N. 2000. Improved analytical model for shear strength of circular reinforced concrete columns in seismic regions. *ACI Structural Journal* 97(3), 388–396.

Kramer, S.L. 1996. *Geotechnical Earthquake Engineering*, Prentice-Hall, Upper Saddle River, New Jersey.

Kramer, S.L. and Elgaral, A.W. 2001. Modelling soil liquefaction hazards for performance-based earthquake engineering. *Pacific Center for Earthquake Engineering*. Report PEER 2001/13, Berkeley, California.

Krawinkler, H. and Nassar, A.A. 1992. Seismic design based on ductility and cumulative damage demand and capacities, in *Nonlinear Seismic Analysis and Design of R.C. Buildings,* P. Fajfar and H. Krawinkler, eds., Elsevier Applied Science, New York, N.Y.

Kupfer, H., Hilsdorf, H.K. and Ruesch, H. 1969. Behaviour of concrete under biaxial stresses. *Journal of the ACI*, 66(8), 656–666.

Ladner, M. and Weber, C. 1981 *Geklebte Bewehrung im Stahletondau,* EMPA, Düsseldorf.

Lam, L. and Teng, J.G. 2003b. Design oriented stress-strain model for FRP-confined concrete in rectangular columns. *Journal of Reinforced Plastic Composites* 22(13), 1149–1186.

Lam, L. and Teng, J.G. 2009a. Design oriented stress-strain model for FRP confined concrete *Construct-Build. Mater.* 17(627), 471–489.

Leblond, L. 1980. Calcul sismique par la méthode modale. Utilisation des réponses pour le dimensionnement, *Annales de l' ITBTP*, No. 380.

Lefas, I., Tsoukis, D. and Kotsovos, M. 1990. Behaviour of repaired R/C walls to monotonic and cyclic loading. *Proceedings of the 9th Greek Conf. on Concrete,* TCG, Kalamata, **2**. pp. 231–8 (in Greek).

Leonhardt, F. 1977. *Vorlesungen uber massivbau, Vierter teil*, Springer-Verlag, Berlin.

Leonhardt, F. and Mönnig, E. 1973. *Vorlesungen über Massivbau, Erster Teil*, Springer-Verlag, Berlin.

Leonhardt, F. and Walther, R. 1962. *Schubversuche an einfeldrigen Stahlbetonbalken mit und ohne Schubbewehrung*. DA für Stahlbeton Heft 151, W. Ernst und Sohn, Berlin.

Lolas, I.D. and Kotsovos, M.D. 1990. Strength and deformation characteristics of reinforced concrete walls under load reversals. *ACI Struct. Journal,* 87(6), 716–726.

Luft, R. 1989. Comparisons among earthquake codes. *Earthquake Spectra,* 5(4), 767–789.

Lungu, D. et al. 2001. *RISK-UE, WP 1: European distinctive features, inventory database and typology*. EVK4-CT-2000-00014.

Mahaney et al. 1993. The capacity spectrum method for evaluating structural response during the Loma Pietra Earthquake, *Proceedings of the National Earthquake Conference*, Memphis Tennessee.

Makarios, T. and Anastasiadis, K. 1997. The real and the 'plasmatic' axis of centres of stiffness (in Greek). *Journal of Engineering,* Vol. 17, Issue 3, pp. 97–120, Technical Chamber of Greece, Athens, Greece.

Mander, J.B., Priestley, M.J.N. and Park, R. 1988. Theoretical stress-strain model for confined concrete. *ASCE Journal of Structural Engineering*, 114(8), 1804–1826.

Martinez-Rueda, J.E. 1997. *Energy dissipation devices for seismic upgrading of R.C. strucures*, Ph.D. thesis, University of London.

Meier, U. and Winistorfer, A. 1995. Retrofitting of structures through external bonding of CFRP sheets. Non-metallic (FRP) reinforcement for concrete structures. *Proceedings of the 2nd International RILEM Symposium*, Ghent, Belgium, ed. L. Tuerwe, pp. 509–516, E&FN Spon London, UK.

Meyerhof, G.G. 1965. Shallow foundations. *ASCE Journal of Soil Mechanics*, 91(SM2), 21–31.

Michailidis, C.N., Stylianidis, K.C. and Kappos, A.J. 1995. Analytical modeling of masonry infilled R/C frames subjected to seismic loading, *Proceedings of the 10th European Conference on Earthquake Engineering*, Vienna, 1994, Balkema, **3**, 1519–1524.

Milutinovic, Z. and Trendafilovski, G. 2003. RISK-UE, WP4-*Vulnerability of current buildings*, Contract: EVK4-CT-2000-00014, European Commission, Brussels.

Minami, K. and Wakabayashi, M. 1980. Seismic resistance of diagonally reinforced concrete columns, *Proceedings of the 7th World Conference on Earthquake Engineering*, Istanbul.

Ministry for Environment and Public Works. 1992. *Greek Code for Earthquake Resistant Structures,* Athens.

Moehle, J.P. 1987. Displacement-based design of R/C structures subjected to earthquakes. *Earthquake Spectra*, 4, 403–428.

Moore, Gordon E. 1965. 'Cramming more components onto integrated circuits' (PDF). *Electronics Magazine*. p.4.

Mouroux, P. and Le Brun, B. 2006. An advanced approach to Earthquake risk scenarios with applications to different European Towns. *Assessing and Managing Earthquake Risk*. Eds. Oliveira, Roca and Goula, Springer.

Mutsumura, K. 1992. On the intensity measure of strong-motions related to structural failures. *Proceedings of the 10th World Conference on Earthquake Engineering*, 1, 375–380.

Nau, J.M. and Hall W.J. 1984. Scaling methods for earthquake response spectra. *Journal of Earthquake Engineering ASCE*, 110(7), 1533–1548.

Newman, K. and Newman, J.B. 1971. *Failure Theories and Design Criteria for Plain Concrete*, *Solid Mechanics and Engineering Design*. J. Wiley-Interscience, New York.

Newmark, N.M. and Hall, W.J. 1982. *Earthquake spectra and design*, *EERI Monograph Series,* EERI, Oakland, California.

NIST GCR 10-917-9/2010. *Applicability of MDOF Modeling for Design*. Prepared by the National Institute of Standards and Technology, Gaithersburg , Maryland.

Nitsiotas, G. 1960. *Technical Theory of Elasticity* (in Greek). Konstardopoulos Pb., Thessaloniki, Greece.

NOUS/3P. 2002. *RC Section Designer*, 3P Penelis Logismica Ltd., Thessaloniki, Greece.

NTU (National Technical University). 1978. *Recommendations on the Repair of Earthquake Damaged Buildings,* Athens (in Greek).

NZS 3101. 1995. *The Design of Concrete Structures*. New Zealand Standards parts 1 and 2, Wellington.

O.A.S.P. (Seismic Risk Management and Protection Agency). 2000. *Causes of damage to the 103 most affected buildings (near collapse) in Athens after the earthquake of Parnitha (7-9-1999)*, Report (Coordinator Kostikas C.), OASP, Athens.

OASP. 2001. *Recommendations for pre and post earthquake retrofitting of buildings* (in Greek). Seismic Risk Management Agency of Greece, Athens, Greece.

Oesterle, R.G., Fiorato, A.E., Aristizabal–Ochoa, J.D. and Corley, W.G. 1980. Hysteretic response of reinforced concrete structural walls, in *ACI SP-63: Reinforced Concrete Structures Subjected to Wind and Earthquake Forces*, American Concrete Institute, Detroit, pp. 243–273.

Office of Emergency Preparedness. 1972. *Disaster Preparedness*. Report to the Congress, Vols. 1–3, Washington, DC.

Ogawa, J. and Abe, Y. 1980. Structural damage and stiffness degradation of buildings caused by severe earthquakes. *Proceedings of the 7th World Conf. on Earthquake Engineering,* Istanbul, VII, pp. 527–34.

Otani, S. and Sozen, M.A. 1972. *Behaviour of Multistorey Reinforced Concrete Frames during Earthquakes*, Civil Engineering Studies, Structural Research Series No. 392, Univ. of Illinois, Urbana.

Pantazopoulou, S. 1995. Role of expansion on mechanical behaviour of concrete. *ASCE Journal of Structural Engineering*, 121(12), 1795–1805.

Papaioannou, C.A., Kiratzi, A.A., Papazachos, B.C. and Theoduiidis, N.P. 1994. Scaling of normal faulting earthquake response spectra in Greece. *Proceedings of the 7th Congress of the Hellenic Geological Society*, Thessaloniki, May 1994.

Papapetrou, A. and A. 1934. Dynamics in earthquake engineering (in Greek). *Journal of Engineering Technical Chamber of Greece*, 1.1.34.

Papazoglou, A.J. and Elnashai, A.S. 1996. Analytical and field evidence of the damaging effect of vertical earthquake ground motion. *Earthquake Engineering and Structural Dynamics*, 25(10), 1109–1137.

Park, R. 1973. Theorization of structural behaviour with a view to defining resistance and ultimate deformability. *Symposium on Resistance and Ultimate Deformability of Structures Acted on by Well-Defined Repeated Loads*. IABSE, Lisboa.

Park, R. 1986. Ductile design approach for reinforced concrete frames. *Earthquake Spectra, Earthquake Engineering. Research Institute*, 2(3), 565–619.

Park, R. and Paulay, T. 1975. *Reinforced Concrete Structures*. J. Wiley & Sons, New York.

Park, R., Priestley, M.J.N and Gill, W.D. 1982. Ductility of square confined concrete columns. *Journal of the Structural. Division*, ASCE, 108(4), 929–950.

Park, Y.-J. et al. 1985. Mechanistic seismic damage model for reinforced concrete. *Journal of Engineering, ASCE*, 111(4), 722–739.

Paulay, T. 1986a. A critique of the special provisions for seismic design of the Building Code Requirements for Reinforced Concrete (ACI 318-83). *Journal of the ACI*, 83(2), 274–283.

Paulay, T. 1986b. The design of ductile reinforced concrete structural walls for earthquake resistance. *Earthquake Spectra, Earthquake Engineering. Research Institute* 2(4), 783–823.

Paulay, T. 1996. Seismic design for torsional response of ductile buildings. *Bulletin of the New Zealand National Society for Earthquake Engineering*, 29(3).

Paulay, T. 1997. Seismic torsional effects on ductile structural wall systems. *Journal of Earthquake Engineering*, 1(4).

Paulay, T. and Bull, I.N. 1979. Shear effects on plastic hinges of earthquake resisting reinforced concrete frames. CEB *Bulletin d'Information*, Paris, 132, 165–172.

Paulay, T. and Priestley, M.J.N. 1992. *Seismic Design of Reinforced Concrete and Masonry Buildings*. J. Wiley & Sons, New York.

Paulay, T., Bachmann, H. and Moser, K. 1990. *Erdbebenbemessung von Stahlbeton Hochbauten,* Birkhäuser, Berlin.

Paulay, T., Park, R. and Priestley, M.J.N. 1978. Reinforced concrete beam-column joints under seismic actions. *Journal of the ACI,* 75(11), 585–593, also Discussion by D.F. Meinheit and Authors' closure, *Journal of the ACI,* 76(5), May 1979, 662–667.

Penelis, G.G. 1969. Design of R/C cross sections under biaxial bending combined with axial force using inelastic stress-stain laws for concrete and steel. *Habilitation Thesis* (in Greek), Thessaloniki, Greece.

Penelis, G.G. 1969. Eine Verbesserung der R. Rosman - H. Beck Methode, *Der Bauingenieur* H. 12.

Penelis, G.G. 1979. *Rehabilitation of Buildings Damaged by Earthquakes*. Ministry of Public Works, Thessaloniki (in Greek).

Penelis, G.G. 1984. Problems after earthquake: inspections and damage assessments. *Proceedings of the EPPO Conference on Earthquakes and Structures,* OASP, Athens, I, 521–537 (in Greek).

Penelis, Gr. G. et al. 1995. Reinforced concrete structures (University Notes) Aristotle University of Thessaloniki, Thessaloniki (in Greek).

Penelis, G.G. 1996. An overview of seismic risk management, *Proceedings of the 1st Japan-U.K seismic risk forum*, London.

Penelis, G.G. 2001. Pre-earthquake Assessment of public buildings in Greece. *Greek-Turkish Conference on seismic assessment*, Istanbul, Technical chambers of Greece and Turkey.

Penelis, G.G. 2008. The earthquake of Thessaloniki, in 1978: Turning point for seismic risk management in Greece (in Greek). *Special Publication of the Engineering Faculty of Aristotle University of Thessaloniki on the occasion of the 30th anniversary of the Earthquake of Thessaloniki in 1978.*

Penelis, G.G. and Kappos, A.J. 1997. *Earthquake-Resistant Concrete Structures*. SPON E&FN (Chapman & Hall), London.

Penelis, G.G. and Penelis, Gr. 2001. *Structural design for rehabilitation of the buildings of the Army Pension Organization, Athens,* Technical report attached to the design permit, Athens, Greece.

Penelis, G.G. et al. 1984. Case study: the Rotunda, Thessaloniki, in *Repair and Strengthening of Historical Monuments and Buildings in Urban Nuclei*, 6, UNIDO/UNDP, Vienna, pp.165–188.

Penelis, G.G. et al. 1986. *Technical Report on the September 13 and 15, 1986 Kalamata Earthquake,* Lab of R/C, Dept. of Structural Engineering, University of Thessaloniki, Thessaloniki (in Greek).

Penelis, G.G. et al. 1987. *A statistical evaluation of damage caused by the 1978 earthquake to the buildings of Thessaloniki*, Technical Report of the Laboratory of R/C, Aristotle University of Thessaloniki (in Greek).

Penelis, G.G. et al. 1988a. A statistical evaluation of damage to buildings in the Thessaloniki, Greece, earthquake of June 20, 1978. *Proceedings of the 9th World Conference on Earthquake Engineering.* Tokyo-Kyoto, VII, pp. 187–192.

Penelis, G.G., Papagiannidou, C. and Penelis Gr. 2000. Response of buildings designed according to the old and new Greek Seismic Code to 7.9.99 Athens earthquake. *Proceedings of the Japan-U.K. seismic risk forum, 3rd Workshop, Imperial College*, London, Imperial College Press.

Penelis, G.G., Stylianidis, K. and Kappos, A. 1988b. *Analytical prediction of the response of the building stock of Thessaloniki to future earthquakes,* invited lecture at the 1st Conference on Engineering Seismology in Greece, Department of Geophysics, Aristotle University of Thessaloniki, Greece.

Penelis, Gr. and Kappos, A. 2005. Inelastic Torsional Effects in 3D pushover analysis of buildings, *Proceedings of the 4th European Workshop on the Seismic Behaviour of Irregular and Complex Structures*, CD ROM, Thessaloniki.

Penelis, Gr., Papanikolaou. 2010. Nonlinear static and dynamic behaviour of a 16-storey torsionally sensitive building designed according to Eurocodes. *Journal of Earthquake Engineering*, 14(5), 2010.

Penelis, S.A. 2011. Structural and seismic design of a nine storey building with one basement in Vasileos Irakliou Str. Nr. 45 (Domotechniki real estate) Thessaloniki, Greece, documents for permit issue. Penelis S.A. archives.

Pitilakis, K., Alexoudi, M., Argyroudis, S., Monge, Ol. and Martin, Chr. 2006. Earthquake risk assessment of lifelines, *Bulletin Earthquake Engineering*, 4(4), 365–390.

PLAXIS-2D. 2012. *User Manual*. Plaxis bv P.O. Box 572, 2600 AN DELFT, Netherlands

PLAXIS-2D. 2012. *Finite Element Package for Geotechnical Engineering*. Plaxis bv, Delft.

Polyakov, S. 1974. *Design of Earthquake-Resistant Structures*. Mir Publications, Moscow.

Popov, E.P. 1977. Mechanical characteristics and bond of reinforcing steel under seismic conditions. *Proceedings of Workshop on Earthquake Resistant Reinforced Concrete Buildings Construction,* Univ. of California, Berkeley, II, 658–662.

Popov, F.P. and Bertero, V.V. 1975 Repaired R/C members under cyclic loading. *Earthquake Engineering and Structural Dynamics*, 4(2), 129–144.

Priestley, M.J., Calvi, G.M. and Kowalsky, M.J. 2007. *Displacement-Based Seismic Design of Structures*. IUSS Press, Pavia.

Presidential Order 12.941. 1994. *Seismic Safety of existing federally owned or leased buildings*, Executive Order of December 1, 1994, The White House, Washington, DC.

Priestley, M.J.N. and Calvi, E.M. 1991. Towards a capacity-design assessment procedure of reinforced concrete frames. *Earthquake Spectra*, 7(3), 413–438.

Priestley, M.J., Calni, M.G. and Kowalsky, M.J. 2007. *Displacement-Based Seismic Design of Structures*. IUSS Press, Pavia.

Priestley, M.J.N. and Park, R. 1987. Strength and ductility of concrete bridge columns under seismic loading. *ACI Structural Journal*, 84(1), 61–76.

Priestley, M.J.N. and Seible, F. 1991. Design of retrofit measures for concrete bridges, in *Seismic Assessment and Retrofit of Bridges,* Struct. Syst. Res. Rep., No. SSRP 91/03, Univ. of California, San Diego.

Priestley, M.J.N. and Wood, J.H. 1977. Behaviour of a complex prototype box girder bridge. *Proceedings of the RILEM International Symposium on Testing In-Situ of Concrete Structures*, Budapest, I, 140–153. John Wiley and Sons.

Rasmussen, B.H. 1963. *Betonindstobte Tvaer Belastede Boltes og Dornes Baereevne*, Bygningstatiske Meddelser. Copenhagen.

RCCOLA 90/1977. *A computer program for R/C column analysis*, NISEE, Pacific Earthquake Engineering Research (PEEP) Center, University of California, Berkeley.

Reid, H.F. 1911. The elastic-rebound theory of earthquakes. *Bulletin of Geology*, 6, 413.

Richter, C.F. 1958. *Elementary Seismology*. San Francisco, W.H. Freeman.

Richart, F.E., Woods, R.D. and Hall, J.R. 1970 *Vibrations of Soils and Foundations*. Prentice-Hall, New Jersey.

Riddell, R. and Newmark, N.M. 1979. Force-deformation models for nonlinear analysis (technical note). *Journal of the Structural. Division*, ASCE, 105(12), 2773–2778.

RISK-UE. 2001–2004. *An advanced approach to earthquake risk scenarios with applications to different European towns*, Contract: EVK4-CT-2000–00014, European Commission, Brussels.

Rodriguez, M. and Park, R. 1991. Repair and strengthening of reinforced concrete buildings for seismic resistance. *Earthquake Spectra*, Journal of EERI, 7(3), 439–460.

Rosenbluth, E. and Meli, R. 1985. The 1985 earthquake: Causes and effects in Mexico City. *Concrete International (ACI)*, 8(5), 23–36.

Rosenblueth, E. and Contreras, H. 1977. Approximate design for multicomponent earthquakes. *Journal of Engineering Mechanics*, ASCE, 103, EM5.

Rosman, R. 1965. *Zahlentafeln für die Schnittkräfte von Windscheiben mit Öffnungsreihen*. Bauhingenier-Praxis, Heft 65, W. Ernst and Sohn, Berlin.

Rowe, R.E. 1970. Current European views on structural safety. *Journal of Structural Division,* ASCE, 96(ST3), 461–467.

Saiidi, M. and Sozen, M.A. 1981. Simple nonlinear seismic analysis of R/C structures. *Proceedings of ASCE*, 107(ST5).

Saiidi, M., Vrontinos, S. and Douglas, B. 1990. Model for the response of reinforced concrete beams strengthened by concrete overlays. *ACI Structural Journal,* 87(6), 687–695.

Sakai, K. and Sheikh, S.A. 1989. What do we know about confinement in reinforced concrete columns? *ACI Structural Journal*, 86(2), 192–207.

Salonikios, T. 2007. Analytical prediction of the inelastic response of R/C walls with low aspect ratio. *ASCE Journal of Structural Engineering*, 133(6), 844–854.

Salonikios, T., Kappos, A.J., Tegos, I. A. and Penelis, G.G. 2000. Cyclic load behaviour of low slenderness R/C walls. Failure modes, strength and deformation analysis and design implications. *ACI Structural. Journal*, 97(1), 132–141.

Salse, E.A.B. and Fintel, M. 1973. Strength, stiffness and ductility properties of slender shear walls. *Proc. 5th World Conf. of Earthquake Eng.*, Rome Vol. 1, pp. 919–928.

Santhakumar, A.R. 1974. The ductility of coupled shear walls. PhD thesis, University of Canterbury, Christchurch.

SAP2000. *Three Dimensional Static and Dynamic Finite Element Analysis and Design of Structures*. Computers and Structures Inc., 1999, Berkeley, California.

SAP2000 V-14. 1999. *Integrated Software for Structural Analysis and Design*, Computers and Structures, Inc. Berkeley, California.

Sariyiannis, D. 1990. *Seismic Behaviour of R/C Frames Filled with Masonry After Repair.* Reports of the R/C Lab, AUTH, Thessaloniki (in Greek).

Sariyiannis, D. and Stylianidis, K. 1990. Experimental investigation of R/C one storey frames repaired with resins under cyclic shear, *Proceedings of the 9th Hellenic Conf. on Concrete. TCG, Kalamata,* 2, pp. 223–230 (in Greek).

SCEEP/HAZUS-MH/FEMA. 2008. *Overview of Hazus-MH: The Earthquake Module*. South Carolina Earthquake Education & Preparedness Program.

SCIA Engineer 2013. *User Manual*. Nemetschek Scia nv, Industrieweg 1007, 3540, Herk-de-Stad, Belgium.

Scott, B.D., Park, R. and Priestley, M.J.N. 1982. Stress–strain behaviour of concrete confined by overlapping hoops at low and high strain rates. *ACI Structural Journal*, 79(1), 13–27.

Scribner, C.F. and Wight, J.K. 1980. Strength decay in R/C beams under load reversals. *ASCE Journal of the Structural Division,* 106(ST4), 861–876.

SEAOC. 1978. *Recommended Lateral Force Requirements and Commentary*. Structural Engineers Associations of California, Sacramento, California.

SEAOC. 1995. *Performance Based Seismic Engineering of Buildings: Vision 2000,* Structural Engineering Association of California, Sacramento, California.

SEAOC. 1999. *Recommended Lateral Force Requirements and Commentary*, Seismology Committee, Structural Engineers Association of California, Sacramento, California.

SEAOC 09. 2009. IBC *Structural/Seismic Design Manual,* SEAOC, 2009.

Seed, H.B. and Idriss, I.M. 1982. *Ground Motions and Soil Liquefaction During Earthquakes*, Earthquake Engineering Research Institute, Oakland, California.

Seismostruct. 2013. *User Manual, Seismosoft Ltd*, Via Boezio 10, 27100 Pavia, Italy.

Sextos, A., Pitilakis, K. and Kappos, A. 2003. Inelastic dynamic analysis of R/C bridges accounting for spatial variability of ground motion, site effects and soil-structure interaction phenomena. Part 1: Methodology and Analytical tools. *Earthquake Engineering and Structural Dynamics*, V, 32(4), 607–627.

Sheikh, S.A. and Uzumeri, S.M. 1982. Analytical model for concrete confinement in tied columns. *Journal of the Structural Division*, ASCE, 108(ST12), 2703–2722.

Shiu, K.N., Takayanagi, T. and Corley, W.G. 1984. Seismic behaviour of coupled wall systems. *ASCE Journal of the Structural Division*, 110(5), 1051–1066.

Shohara, R. and Kato, B. 1981. Ultimate strength of reinforced concrete members under combined loading. *IABSE Colloquium*, Advanced mechanics of R/C, Delft.701–716.

SIA 166. 2004. Schweizerische Vornorm Klebebewehrungen. Schweizerische Normenvereinigung, Zürich, Schweiz.

Sinha, B.P., Gerstle, K.H. and Tulin, L.C. 1964. Response of simply reinforced beam to cyclic loading. *Journal of the American Concrete Institute*, Proceedings, 61(8), 1021–1038.

Soroushian, P., Obasaki, K. and Marikunte, S. 1991. Analytical modelling of bonded bars under cyclic loads. *Journal of Structural. Engineering* ASCE, 117(1), 48–60.

Spoelstra, M.R. and Monti, G. 1999. FRP-confined concrete model. *Journal of Composites for Construction*, 3(3), 143–150.

Strobach, K.L. and Heck, H. 1980. Von wegeners kontinental verschiebung zur modernen Plattentektonik. *Bild der Wissenschaft*, 11, 99–109.

Stylianidis, C.K. 1985. Experimental Investigation of the behaviour of single-storey infilled R/C frames under cyclic quasi-static horizontal loading – parametric analysis. *Ph.D. thesis* (in Greek), Aristotle University of Thessaloniki, Greece.

Stylianidis, K. 2012. Experimental investigation of masonry infilled R/C frames. *Journal of O.C.B.T.*, 6, 194–212.

Stylianidis, K. and Sariyiannis, D. 1992. Design criterion to avoid column shear failure in infilled frames due to seismic action. *Proceedings of the 1st National Conference on Engineering Seismology and Earthquake Engineering*, Athens, Greece, 2, 220–230 (in Greek).

Sugano, S. 1981. Seismic strengthening of existing concrete buildings in Japan. *Bulletin of the New Zealand Society for Earthquake Engineering*, 14(4), 209–222.

Takahashi, T., Kobayashi, S., Fukushima, Y., Zhao, J.X., Nakamura, H. and Somerville, P.G. 2000. A spectral attenuation model for Japan using strong motion database, *Proceedings of the 6th International Conference on Seismic Zonation; Managing Earthquake risk in the 21st century*, Earthquake Engineering Research Institute, Oakland, California.

Takeda, T., Sozen, M.A. and Nielsen, N.N. 1970. Reinforced concrete response to simulated earthquakes. *Journal of the Structural. Division,* ASCE, 96(12), 2557–2573.

Taranath, B.S. 2010. *Reinforced Concrete Design of Tall Buildings*, CRC Press (Taylor & Francis Group).

Tassios, T.P. 1979. Properties of bond between concrete and steel under loads idealizing seismic actions. CEB *Bulletin d'Information*, 131, Paris, 67–122.

Tassios, T.P. 1983. Physical and mathematical models for redesign of damaged structures. *Introductory Report, IABSE Symposium,* Venice, pp. 29–77.

Tassios, T.P. 1984a. Repairs after an earthquake. *Proceedings of the Conf. on Earthquake and Struct.* EPPO, Athens, 1, pp. 595–636 (in Greek).

Tassios, T.P. 1984b. Masonry infill and R/C walls under cyclic actions, *CIB Symposium on Wall Structures*, Warsaw, 1984.

Tassios, T.P. 1984c. Post-earthquake interventions. *Proceedings of the Conference on Earthquakes and Structures*, EPPO, Athens, I, 595–636 (in Greek).

Tassios, T.P. 1989. Specific rules for concrete structures-justification note no. 6: Required confinement for columns, in *Background Document for Eurocode 8-Part 1, Vol. 2-Design Rules*, CEC DG III/8076/89, 23–49.

Tassios, T.P. and Vintzeleou, E.N. 1987 Concrete-to-concrete friction. *Journal of Structural Engineering, ASCE.*, 113(4), 832–849.

Tassios, Th. 2009. *Theory for the Design of Repair and Strengthening.* Symmetry Publishers, Athens (in Greek).

Tegos, I. 1984. *Contribution to the study and improvement of earthquake-resistant mechanical properties of low slenderness structural elements*, PhD thesis, Aristotle University of Thessaloniki (in Greek).

Tegos, I. and Penelis, G.G. 1988. Seismic resistance of short columns and coupling beams reinforced with inclined bars. *ACI Structural Journal,* 85(1), 82–88.

Tegos, I.A. 1979. A *Systematic Analysis of Damage in R/C Buildings,* a Seminar for the Repair of Buildings with Earthquake Damage, Ministry of Public Works, Thessaloniki (in Greek).

Teng, J.G., Chen, J.F., Smith, S.T. and Lam, L. 2002. *FRP Strengthened R/C Structures.* Wiley, Chichester, West Sussex, UK.

Terzaghi, K., Peck, B.R. and Mesri, Gh. 1996. *Soil Mechanics in Engineering Practice, (third edition),* John Wiley and Sons Inc., New York.

Tiedemann, H. 1980. Statistical evaluation of the importance of non-structural damage to buildings. *Proceedings of the 7th World Conference on Earthquake Engineering,* Istanbul, VI, pp. 617–624.

Tolis, S.V. and Faccioli, E. 1999. Displacement design spectra. *Journal of Earthquake Engineering*, 3(1), 107–125.

Triantafillou, T.C. 1998. Strengthening of structures with advanced FRPs. *Progress in Structural Engineering and Materials*, 1(2), 126–134.

Tsamkirani, A. 1982. *Structural Dynamics* (in Greek), Ziti, Thessaloniki, Greece.

Tsonos, A.G., Tegos, I.A. and Penelis, G.G. 1992. Seismic resistance of type 2 exterior beam-column joints reinforced with inclined bars. *ACI Structural Journal*, 89(1), 3–12.

Tsonos, A. 1999. Lateral load response of strengthened reinforced concrete beam-to-column joints. *ACI Structural Journal Proceedings,* V 96(1), 46–56.

Tsonos, A. 2001. Seismic retrofit of R/C beam-to-column joints using local three-sided jackets. *Journal of European Association for Earthquake Engineering,* I, 48–64.

Tsonos, A. 2008. Effectiveness of CFRP-jackets in post-earthquake and pre-earthquake retrofitting of beam-column subassemblages. *Engineering Structures*, 30, 777–793.

Tsonos, A.G. 2002. Seismic repair of exterior R/C beam-to-column joints using two-sided and three-sided jackets. *Structural Engineering and Mechanics*, 13(1), 17–34.

Tsonos, A.G., Tegos, I.A. and Penelis, G.G. 1995. Influence of axial force variations on the seismic behaviour of exterior beam-column joints. *European Earthquake Engineering*, IX(3), 51–63.

Uang, C.-M. and Bertero, V. 1991. UBC seismic serviceability regulations: Critical review. *Journal of Structural Engineering.* ASCE, 117(7), 2055–2068.

Umehara, H. and Jirsa, J.O. 1984. Short rectangular R/C columns under bidirectional loading. *Journal of Struct. Engng. ASCE*, 110(3), 605–618.

UNDP. 1977. *Repair of Buildings Damaged by Earthquakes,* New York.

UNIDO/UNDP. 1975. *Post-earthquake damage evaluation and strength assessment of buildings under seismic conditions,* Vol. 4 of 'Building construction under seismic conditions in the Balkan Region', United Nations Development Programme, Vienna.

UNIDO/UNDP. 1983. *Repair and Strengthening of Reinforced Concrete. Stone and Brick Masonry Buildings,* 5, Vienna.

UNIDO/UNDP. 1984. *Repair and Strengthening of Historical Monuments and Buildings in Urban Nuclei,* 6, Vienna.

UNIDO/UNDP PR. RER/79/015. 1985. *Post-Earthquake Damage Evaluation and Strength Assessment of Buildings under Seismic Conditions,* Vol. 4, Chap. 2, Vienna.

Vacareanu, R., Lungu, D., Aldea, A. and Arion, C. 2004. RISK-UE WP7-report, *Seismic Risk Scenarios Handbook*.

Valiasis, N.T. 1989. Experimental investigation of the behaviour of R/C frames infilled with masonry panels subjected cyclic horizontal load-analytical modeling of the masonry panel. *Ph.D. thesis* (in Greek), Aristotle University of Thessaloniki, Greece.

Valiasis, N.T. and Stylianidis, C.K. 1989. Masonry infilled R/C frames under horizontal loading. *Experimental results. European Earthquake Eng.* Vol. 3, pp. 10–20.

Valiasis, N.T., Stylianidis, C.K. and Penelis, Gr.G. 1993. Hysteresis model for weak brick masonry infills in R/C frames under lateral reversals. *European Earthquake Eng.* Vol. 1, pp. 3–9.

Vamvatsikos, D. and Cornell, C.A. 2002. Incremental dynamic analysis. *Earthquake Engineering and Structural Dynamics* 31(2), 491–514.

Vassiliou, G. 1975. *Behaviour of repaired R/C elements*. PhD thesis, NTU, Athens (in Greek).

Veletsos, A.S. and Meek, J.W. 1974. Dynamic behaviour of building – foundation systems. *Earthquake Engineering Structural Dynamics,* 3(2), 121–138.

Veletsos, A.S. and Nair, V.V.D. 1975. Seismic interaction of structures on hysteretic foundations. ASCE, *Journal of Structural Division*, 101(ST1), 109–129.

Vidic, T., Fajfar, P. and Fischinger, M. 1994. Consistent inelastic design spectra. Strength and displacement. *Earthquake Engineering and Structural Dynamics*, 23(5), 507–521.

Vintzeleou, E. and Panagiotidou, E. 2007. An empirical model for predicting the mechanical properties of FRP-confined concrete, in Triantafillou T.C. (ed.) *8th International Symposium on FRP Reinforcement of Concrete Structures*, paper 6-4, Patras, Greece.

Vintzeleou, E.N. and Tassios, T.P. 1986. Mathematical models for dowel action under monotonic and cyclic conditions. *Magazine of Concrete Research,* 38(134), 13–22.

Vinzeleou, E. 1987. *Behaviour of Infilled Frames Subjected to Lateral Actions. A State-of-the-Art report* EC8 Editing Panel, Brussels.

Walraven, J.C. 2002. Delft, University of Technology, Background document for EN1992-1-1. Eurocode 2: Design of Concrete Structures-Chapter 6.2: Shear, Delft.

Warburton, G.B. 1976. *The Dynamical Behaviour of Structures*, 2nd ed. Pergamon Press, Oxford.

Whitman, R.V. and Richart, F.E. 1967. Design procedures for dynamically loaded foundations. *Journal of Soil Mechanics and Foundation Division, 93*(SM6): 169–91.

Wiegel, L.R., ed. 1970. *Earthquake Engineering*. Prentice-Hall, New Jersey.

Wight, J.K. and Sozen, M.A. 1975. Strength decay of R/C columns under shear reversals. *Journal of the Structural Division, ASCE*, Vol. 101, No. STS Proc. Paper 11311, pp. 1053–1065.

Wilson, E.L. 2002. *Three Dimensional Static and Dynamic Analysis of Structures*. Computers and Structures Inc. (CSI), Berkeley, California.

Wilson, E.L. and Button, M.R. 1982. Three-dimensional dynamic analysis for multicomponent earthquake spectra. *Earthquake Engineering and Structural Dynamics*, 10, 471–476.

Wilson, E. and Habibullah, A. 1987. Static and dynamic analysis of multistory buildings including ρ-δ effects. *Earthquake Spectra*, 3(2), 289–298.

Wilson, L.E. 1985. A new method of dynamic analysis for linear and nonlinear systems. *Finite Elements in Analysis and Design*, 1(1), 21–23.

Youd, T.L. 1998. *Screening Guide for Rapid Assessment of Liquefaction Hazard at Highway Bridge Sites*, National Center for Earthquake Engineering Research, Buffalo, New York, Technical Report MCEER-98-0005.

Yugoslav National Report. 1982. *On damage Evaluation and Assessment of Earthquake Resistance of Existing Buildings*, Pr. Rep. 13/05 UNIDO/UNDP, Skopje.

Zararis, P. 2002. *Design Methods of Reinforced Concrete* (in Greek). Kyriakides Bros. Ltd, Thessaloniki.

Zavliaris, K. 1994. Repairs in R/C structures. General report. *Proceedings of the 11th Hellenic Conf. on Concrete,* Techn. Chamber of Greece, Corfu (in Greek).

Zografos, P. 1987. *Repair of columns with R/C jackets*. Reports of the R/C Lab, AUTH, Thessaloniki (internal report).

Concrete Buildings in Seismic Regions

"This book is arguably the most comprehensive and accessible book on the subject. It pulls together the wide range of tools and procedures for a complete treatment of structural earthquake engineering, from building components to regional impact assessment, including foundations. The book will be invaluable for practicing engineers, students, researchers, and emergency managers."

—**Amr S. Elnashai, FREng,** Dean, College of Engineering, Pennsylvania State University

"This is a comprehensive and excellent book covering all aspects of seismic design and seismic assessment including post-earthquake retrofitting and repair. The latest analysis and design concepts are explained with a focus on RC structures, and it is highly recommended."

—**Jean-Pierre Rammant,** CEO, Nemetschek Scia nv

Concrete Buildings in Seismic Regions combines current approaches to seismic analysis and design with a particular focus on reinforced concrete structures, and includes

- An overview of structural dynamics
- Analysis and design of new R/C buildings in seismic regions
- Post-earthquake damage evaluation, pre-earthquake assessment of buildings and retrofitting procedures
- Seismic risk management of R/C buildings within urban nuclei
- Extended numerical example applications

It covers the last two decades of analysis, design and earthquake engineering, and especially the nonlinear analysis of R/C structures with an emphasis on practical applications. It also includes recent developments in structural intervention pre- or post-earthquake, an aspect which is rarely found in the current literature. It complies with the last edition of the European Codes of Practice for R/C buildings in seismic regions, and includes references to the American Standards in effect for seismic design, and should suit not only practising engineers but also graduate students.

Gregory G. Penelis, MSc, DIC, PhD, runs Penelis Consulting Engineers S.A., and has been involved in the design/review of more than 100 buildings throughout Europe.

George Gr. Penelis is Emeritus Professor at the Aristotle University of Thessaloniki, Greece, and has served as Greek national representative in the Eurocode 2 drafting committee.